

Sept-Oct.
1960
Vol. 64 D.
No. 5

Volume 64D

D.
Radio
Propagation

Number 5

Sept.-Oct. 1960

SCIENCE
St. 2



Journal of Research

of the

NATIONAL BUREAU OF STANDARDS

SEP 20 1960



D. RADIO
PROPAGATION

Journal of Research

of the

National Bureau of Standards

D. RADIO PROPAGATION

SEPT.-OCT. • 1960

VOLUME • 64D

NUMBER • 5



Editor: James R. Wait

Central Radio Propagation Laboratory,
National Bureau of Standards, Boulder,
Colo.

Associate Editors: T. N. Gautier, J. W.
Herbstreit, R. C. Kirby, C. G. Little, A. G.
McNish, R. A. Helliwell, W. E. Gordon,
A. D. Wheelon, S. Silver

IRE Advisors: D. G. Fink, K. M. Siegel

Publication dates:

Jan. 15; Mar. 15; May 15; July 15; Sept. 15; Nov. 15, 1960

JOURNAL OF RESEARCH

The National Bureau of Standards Journal of Research reports research and development in the fields of activity shown at right. Also included from time to time are survey articles of information on topics closely related to the Bureau's scientific and technical program.

The Journal is published in four separate sections as follows:

A. Physics and Chemistry

Contains papers of interest primarily to scientists working in these fields. Issued six times a year. Annual subscription: domestic, \$4.00; foreign, \$4.75.

B. Mathematics and Mathematical Physics

Presents studies and compilations designed mainly for the mathematician and the theoretical physicist. Issued quarterly. Annual subscription: domestic, \$2.25; foreign, \$2.75.

C. Engineering and Instrumentation

Reports research and development results of interest chiefly to the engineer and the applied scientist. Issued quarterly. Annual subscription: domestic, \$2.25; foreign, \$2.75.

D. Radio Propagation

Reports research in radio propagation, upper atmospheric physics, and communications. Issued six times a year. Annual subscription: domestic, \$4.00; foreign, \$4.75.

Functions and Activities

The functions of the National Bureau of Standards are set forth in the Act of Congress, March 3, 1901, as amended. These include the development and maintenance of the national standards of measurement and the provision of means and methods for making measurements consistent with these standards; the determination of physical constants and properties of materials; the development of methods and instruments for testing materials, devices, and structures; advisory services to government agencies on scientific and technical problems; invention and development of devices to serve special needs of the Government; and the development of standard practices, codes, and specifications. The work includes basic and applied research, development, engineering, instrumentation, testing, evaluation, calibration services, and various consultation and information services. The Bureau also serves as the Federal technical research center in a number of specialized fields. The scope of activities of the National Bureau of Standards is suggested in the following listing of the divisions and sections engaged in technical work.

Washington, D.C.

Electricity and Electronics. Resistance and Reactance. Electron Devices. Electrical Instruments. Magnetic Measurements. Dielectrics. Engineering Electronics. Electronic Instrumentation. Electrochemistry.

Optics and Metrology. Photometry and Colorimetry. Optical Instrument Photographic Technology. Length. Engineering Metrology.

Heat. Temperature Physics. Heat Measurement. Cryogenic Physics. Rheology. Molecular Kinetics. Free Radicals Research. Equation of State. Statistical Physics. Molecular Spectroscopy.

Radiation Physics. Neutron Physics. Radiation Theory. Radioactivity. X-ray. High Energy Radiation. Nucleonic Instrumentation. Radiological Equipment.

Chemistry. Organic Coatings. Surface Chemistry. Organic Chemistry. Analytical Chemistry. Inorganic Chemistry. Electrodeposition. Molecular Structure and Properties of Gases. Physical Chemistry. Thermochemistry. Spectrochemistry. Pure Substances.

Mechanics. Sound. Mechanical Instruments. Fluid Mechanics. Engineering Mechanics. Mass and Scale. Capacity, Density, and Fluid Meters. Combustion Controls.

Organic and Fibrous Materials. Rubber. Textiles. Paper. Leather. Testing and Specifications. Polymer Structure. Plastics. Dental Research.

Metallurgy. Thermal Metallurgy. Chemical Metallurgy. Mechanical Metallurgy. Corrosion. Metal Physics.

Mineral Products. Engineering Ceramics. Glass. Refractories. Enameled Metals. Constitution and Microstructure.

Building Technology. Structural Engineering. Fire Protection. Air Conditioning, Heating, and Refrigeration. Floor, Roof, and Wall Coverings. Codes and Safety Standards. Heat Transfer. Concreting Materials.

Applied Mathematics. Numerical Analysis. Computation. Statistical Engineering. Mathematical Physics.

Data Processing Systems. SEAC Engineering Group. Components and Techniques. Digital Circuitry. Digital Systems. Analog Systems. Applications Engineering.

Atomic Physics. Spectroscopy. Radiometry. Mass Spectrometry. Solid State Physics. Electron Physics. Atomic Physics.

• Office of Basic Instrumentation. • Office of Weights and Measures.

Boulder, Colorado

Cryogenic Engineering. Cryogenic Equipment. Cryogenic Processes. Properties of Materials. Gas Liquefaction.

Radio Propagation Physics. Upper Atmosphere Research. Ionosphere Research. Regular Prediction Services. Sun-Earth Relationships. VHF Research. Radio Warning Services. Airglow and Aurora. Radio Astronomy and Arctic Propagation.

Radio Propagation Engineering. Data Reduction Instrumentation. Radio Noise. Tropospheric Measurements. Tropospheric Analysis. Propagation-Terrain Effects. Radio-Meteorology. Lower Atmosphere Physics.

Radio Standards. High-Frequency Electrical Standards. Radio Broadcast Service. Radio and Microwave Materials. Electronic Calibration Center. Microwave Circuit Standards.

Radio Communication and Systems. Low Frequency and Very Low Frequency Research. High Frequency and Very High Frequency Research. Modulation Research. Antenna Systems. Navigation Systems. Systems Analysis. Field Operations.

U.S. DEPARTMENT OF COMMERCE

Frederick H. Mueller, Secretary

NATIONAL BUREAU OF STANDARDS

A. V. Astin, Director

Order all publications from the Superintendent of Documents,
U.S. Government Printing Office, Washington 25, D.C.

Use of funds for printing this publication approved by the Director of the Bureau of the Budget (June 24, 1958).

ELF Electric Fields From Thunderstorms^{1,2}

A. D. Watt

(April 28, 1960; revised May 6, 1960)

The varying electromagnetic fields produced by thunderstorms and associated lightning discharges are examined. Calculated field variations produced by an assumed typical cloud to ground discharge model are found to agree well with observed fields. The magnitude of these vertical electric field changes are observed to decrease very slowly with distance from the source for values comparable to discharge channel heights. From 4 to 20 kilometers a $1/d^3$ relation is observed, and beyond 30 kilometers the field variations appear to follow a $1/d$ relation.

The expected radiation field frequency spectra from 1 cycle per second to 100 kilocycles per second are calculated employing models assumed to be typical of "long" and "short" discharges. The radiation spectra obtained from 1 to 100 kilocycles per second for observed cloud to ground discharge field variations normalized to 1 kilometer are seen to agree within expected limits with calculated values.

The models employed indicate that below 300 cycles per second "long" discharges produce much more energy than "short" discharges, and that inter- and intra-cloud discharges may produce as much energy as cloud to ground discharges.

Anticipated variations of total vertical electric field frequency spectra as a function of distance, based on the work of Wait, are shown for the frequency range from 1 cycle per second to 100 kilocycles per second.

1. Introduction

It is well known that the natural background radio noise field in the region from 3 kc/s to 30 Mc/s is largely produced by lightning discharges. Although the natural noise level above 30 Mc/s is largely due to cosmic sources, Atlas [1]³ has shown that lightning sources are observable at frequencies as high as 3,000 Mc/s.

Below 3 kc/s, the noise spectra produced by lightning discharges is not well known, although it is generally believed that below 1 c/s the background noise fields are produced largely by ionospheric currents or extraterrestrial sources rather than by lightning discharges.

In view of the somewhat limited information available regarding the ELF electromagnetic fields produced by thunderstorm and lightning activity, it is the purpose of this paper to consider the mechanism by which time varying electric and magnetic fields and their associated frequency spectra are likely to be produced by thunderstorms and lightning discharges.

2. Observed Vertical Electric Field Variations

The vertical electric field at the surface of the earth has a fair weather field potential of approximately 100 v/m with a diurnal variation, which appears to be well correlated with worldwide thunder-

storm activity, having approximate plus or minus 20 percent variation about this mean value, as shown by Pierce [2]. The fair weather field is negative since the potential increases with height above the surface of the earth.⁴ This means that a vertical rod antenna will have a positive potential with respect to ground.

During a thunderstorm or disturbed weather, the vertical electric field in the vicinity of such a storm can become quite great and usually changes sign from the negative fair weather field to a positive value which, as has been shown by Smith [4], can become quite large, i.e., values in the order of 4,000 v/m. These changes in the vertical electric field caused by motion of clouds and charged volumes are at a relatively slow rate. The magnitude of the change is, however, great and the possible contribution by this mechanism to the total observed vertical electric field spectrum must be considered for frequencies in the order of several cycles per second.

Tamura [5] has observed that, even with thunderstorms 10 to 20 km from the observing point, the field intensity can become several hundred volts positive. In some cases the field slowly varies to a relatively large negative value, although the general trend during storms is for a positive field with rather abrupt negative direction changes during cloud to ground lightning discharges. These negative field changes soon recover (in about a minute) to an average positive field of several hundred volts per meter. The general mechanism involved in a typical cloud to ground discharge can be seen from figure 1

¹ Contribution from Central Radio Propagation Laboratory, National Bureau of Standards, Boulder, Colo.; paper presented at Conference on the Propagation of ELF Radio Waves, Boulder, Colo., Jan. 26, 1960.

² The studies contained in this paper were sponsored by the Office of Naval Research under contract NR 371-291.

³ Figures in brackets indicate the literature references at the end of this paper.

⁴ Since $E = -d\phi/dz$, the vertical electric field considering up in a positive sense is actually a negative quantity as shown by Clark [3]. Considerable care must be taken when reading the literature on atmospheric electricity. Most workers have plotted observed potential gradient which is sometimes referred to as the observed field without the appropriate change in sign.

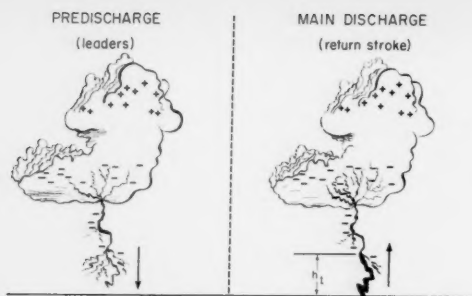


FIGURE 1. Lightning discharge.

(a) PredischARGE (leaders), $v_l \approx 80$ m/ μ sec. (during each step), $I_l \approx 300$ amp (avg) (b) Main discharge (return stroke), $v_r \approx 80$ m/ μ sec., $I_r \approx 30$ kiloamp (avg peak value).

where it is apparent that the negative charge on the bottom of the cloud will produce a positive electric field beneath it. The buildup of charge in the thunderstorm cloud cell produces an increase in potential gradient. When this gradient exceeds the break down potential of the air, the step leader is initiated along a path which generally follows the direction of maximum gradient. Although the instantaneous direction may be quite variable and can contain various "false start" trials as shown, the general trend must be to the ground for this type of discharge. The process of the leader or pilot streamer as it advances in spurts of 10 to 100 m has been described in detail by Schonland [6], and the total period during which it is progressing downward in a cloud to ground discharge can vary appreciably about some average value in the order of 500 to 1,000 μ sec.

It is apparent from figure 1 that if the point of observation is beneath the cloud cell in which the lightning discharge is forming that the field will increase positively as the leader lowers negative charge. It is well known that the leader mechanism contributes appreciably to the spectrum of the electric field at frequencies above 20 kc/s [7]; however, aside from the contribution due to the positive field increase during formation and those cases where the leader lowers a substantial part of the total charge, the leader mechanism is not likely to appreciably contribute to the spectrum below about 5 kc/s.

3. Return Stroke Current Moment Characteristics

Once the step leader reaches the earth's surface, the main return stroke is initiated which travels upward with an initial velocity in the order of 80 m/ μ sec. It should be observed that this vertical upward travel which actually slows down at higher altitudes is really a growth vertically in the downward acceleration of negative charge (in almost all cloud to ground strokes) which has been deposited during the leader process of the lightning discharge. This downward flow of negative charge causes a

positive⁵ (upward) vertical electric current. Employing well-known concepts, we see that the main return stroke in practically all cases constitutes a positive vertical electric moment which can be obtained by integrating the current times differential height along the discharge path.

The height of various discharge paths differ appreciably, and it is obvious when one visualizes the mechanism involved that the shape of the moment curve as a function of time as well as the relative amounts of vertical and horizontal moment will vary appreciably from one discharge to another. A typical base current versus time for a single stroke is shown in figure 2a. Figure 2b shows the manner in which the return stroke length varies with time, and the effective vertical moment and its differential and integral as a function of time are shown in figure 2c.

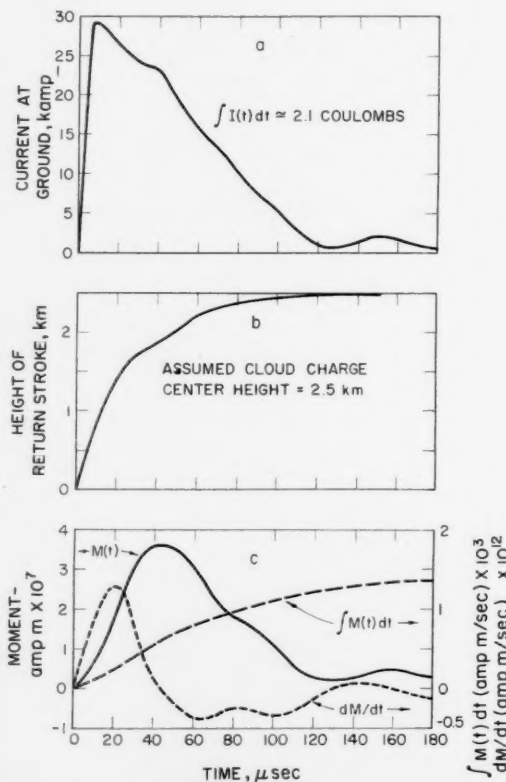


FIGURE 2. Cloud to ground lightning stroke—estimated median characteristics.

4. Electric and Magnetic Fields Produced by a Time Varying Vertical Current

A vertical electric monopole on the surface of a flat perfectly conducting earth as shown in figure 3

⁵ Schonland, Hodges, and Collins [8] observed only one apparent negative current in more than 350 cloud to ground discharges.

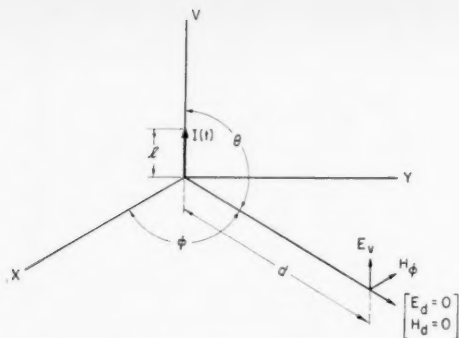


FIGURE 3. Current monopole field geometry.

produces both electric and magnetic fields which, on the surface neglecting ionospheric effects, can be written as ⁶

$$E_v = \frac{-1}{2\pi\epsilon_0} \left[\int \frac{M(t')dt}{d^3} + \frac{M(t')}{cd^2} + \frac{dM(t')/dt}{c^2d} \right] \quad (1)$$

(electrostatic) (induction) (radiation)

$$H_\phi = \frac{1}{2\pi} \left[\frac{M(t')}{d^2} + \frac{dM(t')/dt}{cd} \right] \quad (2)$$

(induction) (radiation)

where:

- E_v ⁷ is the vertical electric field in volts/meter,
- H_ϕ is the tangential magnetic field in ampere turns/meter,
- ϵ_0 is the permittivity of free space = $[36\pi \times 10^9]^{-1}$ in farads/meter,
- $M(t)$ ⁸ is the changing vertical electric moment, $I \times l$, in ampere meters,
- $I(t)$ is the dipole antenna current in amperes,
- l is the dipole length in meters,
- d is the distance from the source to the point of observation in meters where $d \gg l$,
- c is the velocity of light = 3×10^8 m/sec, and
- t' = $(t - d/c)$.

If the current is chosen as $I(t) = I \cos \omega t$, we can write

$$E_v = \frac{-Il}{2\pi\epsilon_0} \left[\frac{\sin \omega t'}{\omega d^3} + \frac{\cos \omega t'}{cd^2} - \frac{\omega \sin \omega t'}{c^2d} \right] \quad (3)$$

and

$$H_\phi = \frac{Il}{2\pi} \left[\frac{\cos \omega t'}{d^2} - \frac{\omega \sin \omega t'}{cd} \right] \quad (4)$$

It is interesting to observe the effects of distance upon the various terms of the electric field produced

⁶ See for example Jordan [9] or Walt [10].

⁷ Note that with respect to the conventional spherical coordinates, $E_\theta = -E_\phi$ when $\theta = 90^\circ$.

⁸ It is noted that $\int_0^T M(t) dt = q_t l_{eff}$ where q_t is the total charge lowered in coulombs and l_{eff} is the average effective length of the discharge in meters.

by an oscillating electric dipole [11]. Beyond one wavelength E_v and H_ϕ decay as $1/d$. In figure 4, obtained from Norton, it can be seen that between $d/\lambda = 0.1$ and 1, all three terms are contributing to E_v , while for distances less than 0.1 the $(1/d)^3$ term predominates.

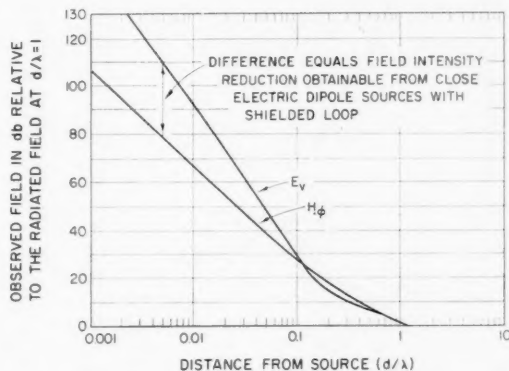


FIGURE 4. Electric fields versus distance for oscillating electric or magnetic dipoles.

5. Effective Discharge Moment Field Relations

From eq (1) we obtain the three components for an electric monopole. The radiation field term, E_r , can be shown to be

$$E_r = \frac{-2dM(t')/dt}{10^7d}, \quad (5)$$

the induction field term is

$$E_i = \frac{-60M(t')}{d^2} \quad (6)$$

and the electrostatic term is

$$E_e = \frac{-1.8 \times 10^{10} \int M(t') dt}{d^3}. \quad (7)$$

It should be emphasized that the monopole fields shown hold only as long as d is large compared to the monopole length, and reasonably small compared to the height of the ionosphere whose effects have thus far been neglected.

Before attempting to examine fields produced by actual discharges, it is important to note that the peak currents observed at the ground vary appreciably about the average 30-kamp value shown in figure 2a. Cloud to ground stroke data obtained from Robertson, Lewis, and Faust [12] are shown in figure 5 along with radiated field data from Taylor and Jean [13] where it is seen that the currents have a somewhat greater dynamic range than a Rayleigh

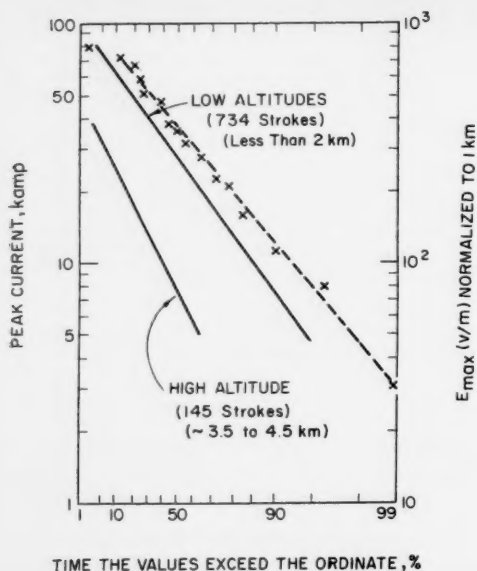


FIGURE 5. Cumulative distribution of cloud to ground lightning stroke current amplitudes at the earth's surface, and E_{max} of radiated waveform normalized to one km.

— Peak current from Robertson, Lewis, Faust [12]. — Peak fields from Taylor and Jean [13].

distribution which has a slope of (-1) on this graph. It should also be noted that the high altitude strokes have much lower peak current amplitudes which may result from the lower break down potential of air at high altitudes or the lower ground conductivity high in the mountains. The slope of the distribution of normalized peak radiated fields is similar to that for low altitude (below 2 km at the ground) currents as would be expected.

6. Variation With Distance of Field Strength Changes During Lightning Discharges

Observed changes in the vertical electric field near to thunder storms obtained from Hatakeyama [14], Tamura [5], Florman [15], and Taylor and Jean [13] are plotted on figure 6 where it appears that the $1/d^3$ relation is valid for distances of about 4 to 20 km. This agrees with Morrison [16] who indicated that $E_e = E_r$ at $d = 26$ km. Beyond 30 km the observed points group around the $1/d$ line with an amount of scatter expected from the variations in peak radiated field.

The peak negative swing of the radiation field assuming a median stroke from figure 5 is seen to be

$$E_r \approx 300/d(\text{km}). \quad (8)$$

The peak field calculated for the example in figure 2 is $E_r \approx 260/d(\text{km})$ which would indicate that it is typical of a median return stroke.

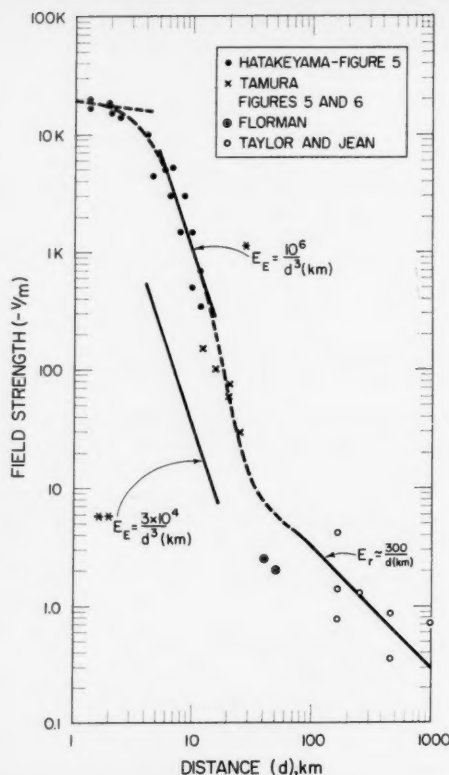


FIGURE 6. Peak electric field variation from lightning discharges.

*for a complete discharge, assuming $q \times 1 = 5.6 \times 10^4$ amp meter sec. **for a single return "short" stroke (current flow from 0 to 150 μ sec.)

When the electrostatic term is calculated with eq (7) and a value of $\int M(t')/dt \approx 1.5 \times 10^3$ amp meter-seconds, we obtain

$$E_e \approx 3 \times 10^4/d^3(\text{km}). \quad (9)$$

(single stroke)

It is obvious that this line shown on figure 6 is far below the observed values. This relation takes into account only the charge lowered during the first 180 μ sec which, for the example in figure 2a, is 2.1 coulombs assuming that the current ceased to flow after this time. This assumption, which is allowable for the VLF radiation spectra considerations, is certainly not valid as far as the total electrostatic field change is concerned.

Typical "long" cloud to ground discharges contain several multiple strokes each lasting about 100 μ sec and separated by an average time of about 40 millise. The median peak current is about 30 kA, and after each stroke a relatively small amount

⁹ A long discharge occurs when a small ($I \approx 500$ – 1000 A) current continues to flow for several hundred milliseconds, and $q \geq 10$ coulombs. Short discharges also occur where the current flow stops after about 4 millise and $q \approx 2$ to 10 coulombs.

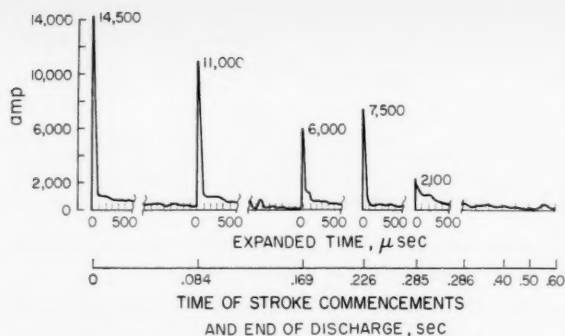


FIGURE 7. Lightning stroke, complete discharge current.

Record 208 7-31-42 smokestack of Anaconda Copper Mining Co., Great Falls, Montana (From McCann).

of current (around 500 to 1,000 amp) continues to flow between these strokes. A typical long discharge from McCann [17] is shown in figure 7. Although the peak currents are less than the expected median value, it is instructive to note that 81 coulombs of charge were lowered to the earth in this complete discharge as compared to only 2.1 during the single "short discharge" stroke of figure 2a. This means that a large portion of the charge is actually lowered between and after the main strokes.

Since the change in the electrostatic field is proportional to the charge lowered times the effective height, it is obvious that the actual field change observed for a complete discharge will be much greater than that indicated by (9) for a typical single stroke. It should also be noted that during the high currents of the return stroke, not only is the total charge lowered small, but in addition the effective height is likely less than during the between stroke current flow. The charge of 81 coulombs is larger than the average value of about 10 to 20 shown by McCann [17]. Assuming an average value of 20 coulombs and an average effective height of 2.5 km, we obtain

$$E_s \approx 10^6/d^3 \text{ (km)} \quad (10)$$

(total discharge)

which is seen from figure 6 to agree very well with observed field changes.¹⁰

When the field is observed at a distance, comparable or short compared to the discharge length, eq (7) no longer is valid. In close where $d \ll l$, it is shown by Wait [10] that the length of the column is no longer a factor. The field is now a function of I and d , and we can write

$$H_\phi = \frac{I}{2\pi d} \quad (11)$$

$$E_s \approx \frac{\mu\omega I}{\pi^2} \log_e \left(\frac{2\pi d}{\lambda} \right) \quad (12)$$

¹⁰ This relation obtained from independent data is the same as that given by Pierce [18]. Reference [18] and its companion paper [19] contain a large amount of useful information relative to the characteristics of lightning discharges.

where μ is the permeability of the medium $= 4\pi \times 10^{-7} \text{ h/m}$ for free space, and λ is the free space wavelength in meters. For these relations to hold $d \ll l$, and $d/\lambda \ll 1$. Thus it is seen that the magnitude of E_s will vary slowly with d . For example, if d varies from 4 to 1 km and we assume λ in the order of $6 \times 10^4 \text{ km}$ ($f=10 \text{ c/s}$), the log function varies by about 1 to 1.2. A dotted line with this slope is drawn at the top of figure 6 where it appears that the observed fields are varying in about this manner from 1 to 4 km.

7. Frequency Spectra of Individual Return Strokes

It is instructive to consider the frequency spectrum of an individual return stroke such as shown in figure 2 where the complete event is considered as being consummated in approximately 180 μsec . The frequency spectrum of the induction field term will first be considered because of the ease with which it can be obtained.

The induction field produced, E_t , from eq (6) and figure 2c is seen to be an unidirectional pulse with an area in (v/m). The frequency spectrum of the induction field can be obtained by means of the Fourier transform

$$G(f)_i = \int_{-\infty}^{\infty} E(t)_i e^{-j\omega t} dt$$

$$= \frac{-60}{d^2} \int_{-\infty}^{\infty} M(t') e^{-j\omega t} dt. \quad (13)$$

When the frequency spectrum is obtained from the response of narrow band filters, the relations described in the appendix must be employed.

It is well known [20] that for a pulse of length τ , the frequency spectrum is essentially constant for $f \leq 1/3\tau$ and that $G(f) = A$ where A is the area of the pulse. Since $\tau \approx 180 \mu\text{sec}$, we can write for the single isolated stroke

$$|G(f)_i| = \frac{60}{d^2} \int_0^\tau M(t') dt \quad (14)$$

$$200 \text{ c/s} \leq f \leq 2,000 \text{ c/s.}$$

If $M(t)$ actually became and remained zero beyond 180 μsec , eq (14) would be valid for all frequencies below 2,000 c/s. Since in a typical "long discharge" the channel continues to carry some 500 to 1,000 amp until the next stroke or for a time in the order of a hundred milliseconds, the value of $\int M(t) dt$ given in figure 2c is no longer valid beyond about 20 millisecc and a lower limit of around 200 c/s must be placed on f in eq (14).

The radiation spectrum in this frequency range can be obtained by observing from eq (3) that

$$G(f)_r = \frac{2\pi f d G(f)_i}{3 \times 10^8} \quad (15)$$

and as a result combining (14) and (15)

$$|G(f)|_r = \frac{4\pi f}{10^7 d} \int_0^{\tau} M(t) dt \quad (16)$$

$$200 \text{ c/s} \leq f \leq 2,000 \text{ c/s.}$$

Assuming a typical average value of 1.4×10^3 for $\int M(t) dt$ for the first 180 μsec , we can write

$$|G(f)|_r \approx \frac{2f}{10^3 d} \quad (17)$$

typical avg long discharge, $200 \text{ c/s} \leq f \leq 2,000 \text{ c/s}$;
typical avg short stroke, $f \leq 2,000 \text{ c/s}$.

The spectrum below 100 c/s for a long discharge can be obtained by observing the shape of the $\int M(t) dt$ for the complete discharge as shown in figure 8. This function is seen to be essentially a ramp function with a linear slope $m \approx 1.7 \times 10^6$ amp meters out to the end of the complete discharge which may be in the order of 100 to 500 millise. From the end of the discharge, the electrostatic field recovers to its initial value in a period of the order of 100 sec.

A ramp function with a slope "m" is known to have a spectrum

$$G(f) = \frac{-m}{4\pi^2 f^2} \quad (18)$$

Combining eq (3), (7), and (18) we obtain

$$|G(f)|_r \approx \frac{2m}{10^7 d} \quad (19)$$

$$10 \leq f \leq 100 \text{ c/s.}$$

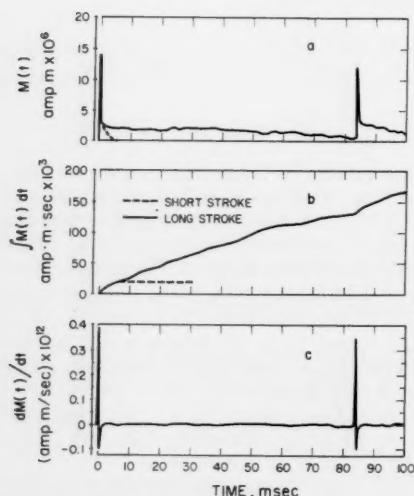


FIGURE 8. Typical long discharge moment relationships.

Employing an assumed typical $\int M(t) dt$ with an m of 1.7×10^6 amp meters

$$|G(f)|_r \approx \frac{0.3}{d} \quad (20)$$

$$10 \leq f \leq 100 \text{ c/s typical avg discharge.}$$

It is interesting to observe that the radiated spectrum in this region is independent of frequency.

For frequencies in the order of 1 c/s, the $\int M(t) dt$ looks like a saw-tooth wave where the important contributions come from the leading edge which approximates a step function. The step function has the well known spectrum

$$G(f) = \frac{h}{2\pi f} \quad (21)$$

where h is the height of the step.

Combining eqs (3), (7), and (21) we obtain

$$|G(f)|_r = \frac{4\pi f}{10^7 d} \int M(t) dt (\text{max}) \quad (22)$$

$$0.2 \text{ c/s} \leq f \leq 2 \text{ c/s.}$$

If we employ the maximum moment integral value shown in figure 8 as 1.5×10^5 amp meter seconds, we obtain

$$|G(f)|_r \approx \frac{0.2f}{d} \quad (23)$$

The radiation spectrum obtained for an assumed average complete cloud to ground discharge is shown in figure 9 where the straight line sections are obtained from the preceding simplified relationships

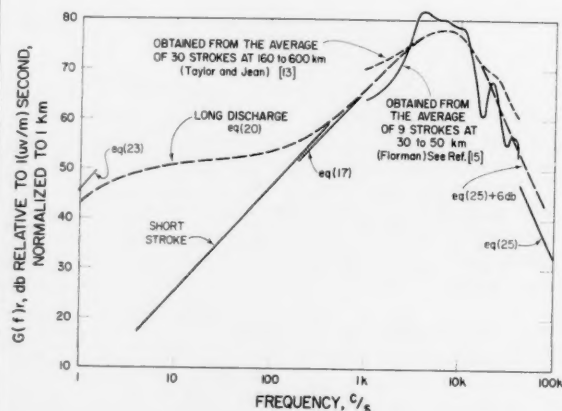


FIGURE 9. Calculated and observed frequency spectrum of the radiation component of field strength from an average cloud to ground discharge, normalized to a distance of 1 km. (precursor fields have been neglected).

over the frequency range where they are expected to be valid. The solid and dotted curves represent the average spectra obtained by Fourier transforms of observed fields of individual cloud to ground strokes. The solid straight line with a 12 db/octave slope near 50 kc/s was calculated employing the ramp function transform and the initial slope of the dM/dt curve in figure 2c. The general expression is

$$G(f) = \frac{m}{2\pi^2 10^7 f^2 d} \quad (24)$$

If we employ a slope $m = 8 \times 10^{16}$ amp meters/sec²

$$G(f) = \frac{4 \times 10^8}{f^2 d} \quad (25)$$

$$f > 50 \text{ kc/s.}$$

This line appears to lie about 6 db below the observed spectral values in the 40-kc/s region. If the waveform in figure 2c is closely observed, it is apparent that the reversal in slope at 20 μ sec will contribute almost an equal amount to the frequency spectrum in the 30- to 50-kc/s region. Adding 6 db to the values from eq (25) gives good agreement with the observed spectra.

It should be emphasized that individual spectra will vary appreciably since the moment time functions of individual discharges are quite variable. The maximums and minimums observed in the 15- to 40-kc/s region of the radiation spectra obtained from Florman are caused by the different lengths of the + and - half cycles of the moment differential, and each individual discharge is likely to have this type of structure above 15 to 20 kc/s.

The average frequency spectra shown by the dashed lines in figure 9 are based on assumed average cloud to ground discharges where the low frequency portion for the long discharge include the effects of normal multiple strokes. The actual spectrum of any particular cloud to ground discharge may vary appreciably from the spectra shown. There is also a possibility that discharges from tropical types of storms may differ appreciably from the results shown here which are based on a model believed to be fairly typical of the discharges occurring in temperate zone thunderstorms. It is instructive to observe that in the frequency range from roughly 10 to 100 c/s that the radiation spectrum for a long discharge appears to be essentially constant. This results from the appreciable current flow between multiple strokes which may last for periods up to several hundred milliseconds. For short discharges where the current ceases to flow relatively soon after the initial stroke, the frequency spectral components continue to decrease with decrease in frequency as indicated by eq (17). Since the frequency spectrum components in the 1- to 200-c/s region are seen to be primarily generated by the relatively low amplitude current flow between strokes, it would appear that inter- and intracloud strokes with appreciable vertical travel may be as effective as cloud to ground

strokes in producing ELF energy. The importance of the initial slope of the dM/dt curve in producing energy in the 3- to 30-kc/s region indicates that cloud to cloud discharges are not likely to produce large VLF fields.

8. Variation of Frequency Spectra With Distance

The frequency spectra shown in figure 9 would not be observable at any given location because of the wide frequency range covered. The actual observed field would vary according to eqs (3) and (4) if the ionosphere could be neglected and the earth were a perfectly conducting flat plane. For distances short compared to the height of the ionosphere, this assumption is relatively valid provided of course that the distance is large compared to the height of the discharge channel.

Wait [21] has treated the waveform variations at short ranges, and also given the relationships anticipated at longer ranges for the observed electric and magnetic fields relative to the plane earth radiation field from calculations based on the waveguide concept [21, 22]. The results obtained are shown in figure 10 in terms of the W function which is the ratio (expressed in decibels) of the vertical electric field to the radiation component of the vertical electric field for an assumed infinitely conducting plane. The frequency spectra expected at 10 and 100 km from a typical average discharge have been calculated with the aid of figures 9 and 10 and the results shown in figure 11. For longer ranges the appropriate W function values can be obtained from Wait [21 to 23].

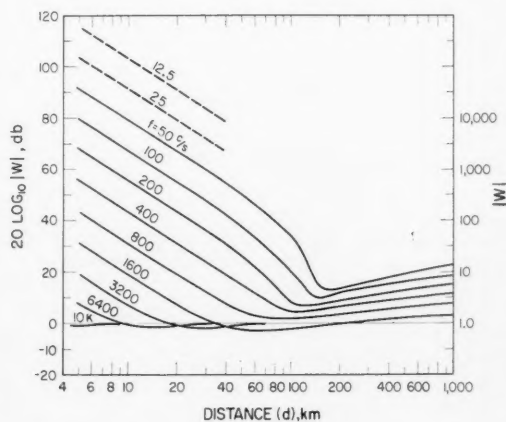


FIGURE 10. Ratio of actual vertical electric field to the radiation component over an infinitely conducting plane, $|W| = E_v/E_r$ (from Wait).

Calculations based on ionospheric:
height = 90 km
parameter, $\omega_p = 5 \times 10^3$ rad/sec } night.

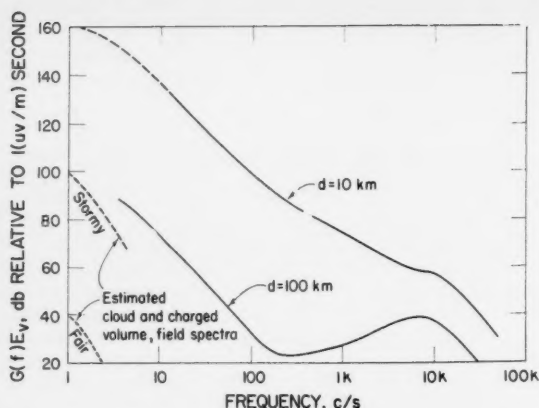


FIGURE 11. Calculated spectrum of the vertical electric field for an assumed average long discharge cloud to ground lightning discharge, d km from the observing point.

9. Spectra From Fields Produced by Motions of Clouds

The motion of clouds and charged volumes produces relatively large vertical electric field changes. The magnitude and rate of change in these fields suggest that a very rough approximation of the spectra for $f < 1$ c/s might be obtained by considering portions of $E_v(t)$ which appear as ramp functions. Typical slopes are in the order of 4 and 0.004 (v/m)/sec for stormy and fair weather fields. Employing eq (18) we obtain

$$G(f)E_v \simeq \frac{1}{10f^2}$$

stormy clouds

$$f \simeq 1 \text{ c/s}$$

and

$$G(f)E_v \simeq \frac{1}{10^4 f^2}$$

fair weather

$$f \simeq 1 \text{ c/s.}$$

For frequencies above 1 c/s the spectrum is likely to decrease as $1/f^3$ since the field appears not to have discontinuity in slope for $f \geq 1$ c/s. These fields are included in figure 11 to give a rough estimate of possible contributions from this mechanism. Loop antennas will of course be much less subject than whips to effects of this kind.

The author acknowledges the assistance received from: J. R. Wait, E. L. Maxwell, A. G. Jean, and W. L. Taylor during many helpful discussions, as well as permission to use material prepared by them; and from Winifred Mau during the preparation of the manuscript.

10. Appendix. Filter Impulse Response

It should be observed that the frequency spectrum as defined has the dimensions of $E(t)$ multiplied by time which in this case is (volts/meter) seconds. The frequency spectrum amplitude observed with a spectrum analyzer is dependent on the characteristics of the filter employed. The impulse function response of a circuit is given by

$$v_0(t) = \frac{A}{\pi} \int_0^\infty A(\omega) \cos[\omega t - B(\omega)] d\omega$$

where A is the area of the impulse function, $A(\omega)$ and $B(\omega)$ are the amplitude and phase functions of the circuit. If we assume an idealized loss-less rectangular filter with a linear phase $B(\omega) = S\omega$, the output is

$$v_0(t) = 4AF_c \left[\frac{\sin \omega_c(t-S)}{\omega_c(t-S)} \right] \cos \omega_0(t-S)$$

where the peak transient response is $2Ab$ which means that peak output of this filter is $2bg(\omega)$ provided of course that $g(\omega)$ is constant over the 6-db bandwidth b . In actual practice $A(\omega)$ is not rectangular and the peak response of a physical filter with unity gain at the center frequency is given as

$$V_0(\text{peak}) = kg(\omega) b \\ = kG(f) b$$

where k is dependent on filter configuration, and varies from values of about 1.5 to 3 for typical filters.

11. References

- [1] D. Atlas, Radar lightning echoes in atmospheres in vertical cross section, Recent Adv. Atmos. Elec., pp. 441 to 459 (Pergamon Press, Inc., New York, N.Y., 1958).
- [2] E. T. Pierce, Some topics in atmospheric electricity, Recent Adv. Atmos. Elec., pp. 5 to 16 (Pergamon Press, Inc., New York, N.Y., 1958).
- [3] J. F. Clark, The fair-weather atmospheric electric potential and its gradient, Recent Adv. Atmos. Elec., pp. 61-74 (Pergamon Press, Inc., New York, N.Y., 1958).
- [4] L. G. Smith, Electric field studies of Florida thunderstorms, Recent Adv. Atmos. Elec., pp. 299 to 308 (Pergamon Press, Inc., New York, N.Y., 1958).
- [5] Y. Tamura, Investigations on the electrical structure of thunderstorms, Recent Adv. Atmos. Elec., pp. 269 to 276 (Pergamon Press, Inc., New York, N.Y., 1958).
- [6] B. F. Schonland, The pilot streamer in lightning and the long spark, Proc. Roy. Soc. (London) [A] **220**, pp. 25 to 28, (1953).
- [7] A. D. Watt and E. L. Maxwell, Characteristics of Atmospheric noise from 1 to 100 kc, Proc. I.R.E. **45**, No. 6, pp. 787 to 794, (1957).
- [8] B. F. J. Schonland, D. B. Hodges, H. Collens, Progressive lightning V, A comparison of photographic and electrical studies of the discharge process, Proc. Roy. Soc. (London) [A] **166**, pp. 56 to 75 (1938).
- [9] E. C. Jordan, Electromagnetic waves in radiating systems (Prentice Hall, Inc., New York, N.Y., 1950).
- [10] J. R. Wait, Electromagnetic radiation from cylindrical structures (Pergamon Press, Inc., New York, N.Y., 1959).

- [11] J. R. Wait and James Householder, Mixed-path ground-wave propagation: 2. Larger distances, *J. Research NBS* **59**, 19 (1957) RP2770; also K. A. Norton, private communication.
- [12] L. M. Robertson, W. W. Lewis, and C. N. Faust, Lightning investigation at high altitudes in Colorado, *Trans. AIEE* **61**, pp. 201 to 208 (1942).
- [13] W. L. Taylor and A. G. Jean, Very-low-frequency radiation spectra of lightning discharges, *J. Research NBS* **63D**, pp. 199 to 204 (1959).
- [14] H. Hatakeyama, The distribution of the sudden change of electric field on the earth's surface due to lightning discharge, *Recent Adv. Atmos. Elec.*, pp. 269 to 276 (Pergamon Press, Inc., New York, N.Y., 1958).
- [15] E. F. Florman, Private communication.
- [16] R. B. Morrison, The variation with distance in the range zero-100 km of atmospheric wave-forms, *Phil. Mag.* **44**, pp. 980 to 986 (1953).
- [17] G. D. McCann, The measurement of lightning current in direct strokes, *Trans AIEE* **63**, pp. 1157 to 1164 (1944).
- [18] E. T. Pierce, Electrostatic field-changes due to lightning discharges, *J. Roy. Met. Soc.* **81**, 229 (1955).
- [19] E. T. Pierce, The development of the lightning discharge, *J. Roy. Met. Soc.* **81**, pp. 229 to 240 (1955).
- [20] Reference Data for Radio Engineers, Intern. Telephone and Telegraph Corp., p. 1012 (1956).
- [21] J. R. Wait, On the waveform of a radio atmospheric at short ranges, *Proc. I.R.E.* **44**, No. 8, p. 1052 (1956).
- [22] J. R. Wait, Mode theory and the propagation of ELF radio waves, *J. Research NBS* **64D**, 387 (July 1960).
- [23] J. R. Wait and N. F. Carter, Field strength calculations for ELF radio waves, *NBS Tech. Note* 52 (March 1960).

(Paper 64D5-77)



Field Strength Measurements in Fresh Water¹

Gurdip S. Saran² and Gedalia Held³

(February 26, 1960; revised April 5, 1960)

Experiments were performed to measure field strength at a frequency of 18.6 kilocycles per second in fresh water of conductivity 2.66×10^{-3} mhos/meter down to depths of 1,000 feet using monopole and loop antennas. The experimental results verify the theoretical values of field strength attenuation with depth for all antennas and of the ratio of vertical to horizontal field strength for the monopole antennas.

1. Introduction

The theoretical relationships of field strength in air and in the conducting medium for different antennas imbedded in the semi-infinite conducting medium have been presented by different authors [1 to 7].⁴ M. B. Kraichman [8] has presented experimental results of the measurements of magnetic field strength in air for the various dipoles and loops immersed in a concentrated sodium chloride solution, which are in agreement with the above-referenced theoretical work. His experimental results, however, are limited in the horizontal range to a distance of over a wavelength in the conducting medium but a fraction of wavelength in air. Experiments are now in progress at Boeing Airplane Company to verify the theoretical results of electric field strength in air and in the conducting medium for the horizontal electric dipole in salt water for distances of several wavelengths in air.

Unfortunately the model-scale experiments performed in a laboratory are generally limited in scope due to the small dimensions of the tank, lead lengths, and the scaling factors that are introduced to fit the experiments to the limited space. Therefore full-scale experiments were performed. They are described briefly in this paper.

The experiments were performed at Lake Chelan in the State of Washington during the summer of 1959. The attenuation of field strength for different antennas down to depths of 1,000 feet was measured, and the field strength relationship between the horizontal and vertical monopoles was established experimentally. The conductivity of the water was 2.66×10^{-3} mhos/meter, which is comparable to that of the ground. The large size and great depth of the lake simplify considerably the experiments with regard to configurations and orientations of the antennas.

The signals were received from the U.S. Navy Radio Station (T) Jim Creek, Oso, Washington, at a frequency of 18.6 kc/s. The field strength at different places on the surface of the lake was nearly 40 millivolts per meter.

The antennas tested were a 10-ft loop with 15 turns, a 6-ft loop with 15 turns, and a 36-ft short-circuited coaxial antenna with 88-ft bare wire for grounding to the water. The short-circuited coaxial antenna consists of an insulated section and a bare-wire section for grounding to the water [2]. All antennas were made of wire gage No. 4 with neoprene insulation.

2. Theoretical Results

The theoretical results of field strength for the electric and magnetic dipole antennas imbedded in the conducting medium are of the following general form:

$$\psi = CPg(f, \sigma) \exp. \{-z/\delta\} h(f, r, \phi).$$

C = a constant,

P = electric or magnetic dipole moment,

σ = conductivity in mhos/meter,

z = sum of depths for the transmitting and the receiving antennas,

$\delta = [2/\omega\mu_0\sigma]^{1/2}$, skin depth,

f = frequency,

r, ϕ = range and azimuth.

While the theoretical results involve different assumptions in the solution, they all suggest that the field strength attenuates exponentially with depth for the different antennas in the conducting medium. The exponential variation, furthermore, is invariant to the mode of excitation and reception for the antennas, as long as the distances involved are much greater than a skin depth [5]. The behavior of appropriate electromagnetic waves, therefore, is similar to that of a plane wave propagating in the conducting medium. For attenuation measurements in the lake water, therefore, only the relative amplitude of the electromagnetic wave was measured and is of importance.

¹ Contribution from Boeing Airplane Company, Seattle, Wash., paper presented at Conference on the Propagation of ELF Radio Waves, Boulder, Colo., January 25, 1960.

² Present address, Space Sciences Laboratory, Missile and Space Vehicle Dept., General Electric Co., 3750 D St., Philadelphia, Pa.

³ Present address, Space Technology Laboratories, Inc., P. O. Box 95001, Los Angeles 45, Calif.

⁴ Figures in brackets indicate the literature references at the end of this paper.

The ratio of vertical to horizontal component of the electric field strength in the conducting medium for a plane wave propagating along the interface is:

$$\eta = E_v/E_h = [\omega\epsilon_0/i\sigma]^{1/2}.$$

For a wave propagating in water, the vertical component is negligible compared to the horizontal component of electric field strength. The index of refraction of water is determined by the conductivity and is large compared to that of air. The direction of propagation of a wave in the water, therefore, is nearly vertical [9].

3. Experimental Apparatus and Procedure, and Results

3.1. Apparatus and Procedure

The apparatus consisted of a wooden raft, a small boat, a tank, antennas, and the receiving equipment consisting of batteries, converter, recorder, and a timer. The metal tank was used to accommodate the receiving equipment and could withstand pressure down to water depth of 1,500 ft. The test antennas were kept at a distance of nearly 12 ft from the tank. The tank and antennas were supported by a nylon rope from a wooden raft. A barge was used only to handle the weight of the tank when the latter was out of the water. During the experiments, however, the barge was taken away and kept at a distance of at least 2,000 ft from the test site. The timer inside the tank was set to start the receiving equipment approximately 12 min before the end of each hour and to shut off the equipment a few minutes past the hour. During the equipment-on period, the signals from the Naval Radio Station followed this sequence: a period of a few minutes with no signal followed by a period of approximately 5 min with cw power. During the cw signals, the antenna depth was varied with the rope on the wooden raft. The signals were also monitored in the air with another receiver on the raft to notice possible variation in field strength and to check the period of cw power from the radio station.

3.2. Experimental Results

The attenuation of field strength with depth for the monopole and the loop antennas are presented in figure 1. The field strength follows an exponential law as $E=E_0 \exp. \{-z/\delta\}$. At one skin depth (72 meters for this case), for example, the field strength decreases to $1/e$ of its value at the interface of air and water. The field strength, furthermore, decreases to $1/10$ and $1/100$ of its interface value at the depths of 164 and 329 meters respectively.

The vertical component is smaller than the horizontal component of the field strength. The experimental ratio of vertical to horizontal components is 0.0141, 0.0138, and 0.0149 for the respective depths of 3, 10, and 50 meters.

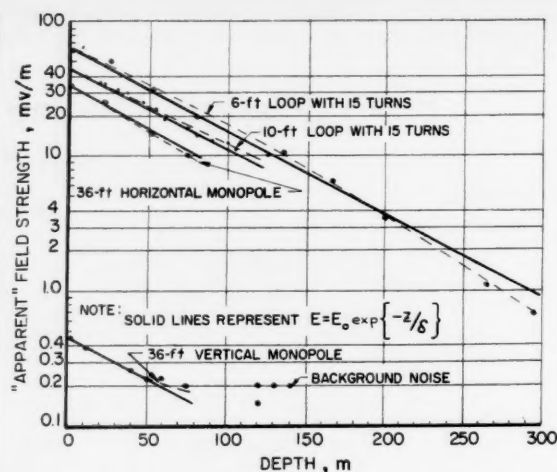


FIGURE 1. Attenuation of field strength with depth for the electric and magnetic dipole antennas.

4. Discussion of Results

The experimental values of field strength with depth correlated closely with those of theoretical values represented by $E=E_0 \exp. \{-z/\delta\}$. Precautions were taken to keep metal objects, including the barge, at least a few thousand feet away from the test site and the wooden raft. In order to avoid any questions about the transmission of the signal over lines or wire, only nylon rope (no wires) was used to lower, raise, or handle the receiving equipment in the water.

The theoretical ratio of vertical to horizontal components of the field strength in the conducting medium is 0.0197 for the frequency of 18.6 kc/s and conductivity of 2.66×10^{-3} mhos/meter. The experimental values are lower than the theoretical results and are presented in table 1.

TABLE 1.— η , Ratio of vertical to horizontal component of E in water

Depth in meters	Experimental η	Theoretical η
3	0.0141	0.0197
10	.0138	.0197
50	.0149	.0197

The discrepancy of 20 to 30 percent could have been caused by the change of azimuth angle and test site during experiments. The strong winds, particularly during these tests, on the lake could easily have moved the raft at least a mile away from the original test site. The change in both the azimuth angle and test site can influence results; the former because of transmitter location and the latter because of the variation of field strength with location at the surface of the lake.

5. Conclusions

The experimental results for the attenuation of field strength with depth for the different antennas correlate with the theoretical results. The experiments, furthermore, verified the theoretical results that the horizontal electric antennas are superior to the vertical antennas for reception, and also for radiation (by reciprocity theorem), in the conducting medium.

6. References

- [1] C. T. Tai, Hertzian dipole immersed in a dissipative medium, Cruft Lab. Rept. No. 21, Harvard Univ. (1947).
- [2] R. K. Moore, The theory of radio communication between submerged submarines, Ph. D. Thesis, Cornell Univ. (1951).
- [3] W. VonAulock, Low frequency electromagnetic dipole fields in a semi-infinite conductor, Navy Dept., Bureau of Ships, Minesweeping Sec., Tech. Rept., No. 104 (1952).
- [4] J. R. Wait, Magnetic dipole antenna in a conducting medium, *Proc. IRE* **40**, 1244 (1952).
- [5] J. R. Wait and L. L. Campbell, The fields of an oscillating magnetic dipole immersed in a semi-infinite conducting medium, *J. Geophys. Research* **58**, 167 (1953).
- [6] R. H. Lien and J. R. Wait, Radiation from a horizontal dipole in a semi-infinite dissipative medium, *J. Appl. Phys.* **24**, 1 to 5, 958 to 959 (1953).
- [7] A. Baños, Jr., and J. P. Wesley, The horizontal electric dipole in a conducting half-space, Pt. I, Univ. Calif., Marine Phys. Lab., Scripps Inst. Oceanography, SIO Ref. 53-33 (Sept. 1953); Pt. II, SIO Ref. 54-31 (Aug. 1954).
- [8] M. B. Kraichman, Basic experimental studies of the magnetic field from electromagnetic sources immersed in a semi-infinite conducting medium, *J. Research NBS* **64D**, 21 (1960).
- [9] H. A. Wheeler, Fundamental limitations of a small VLF antenna for submarines, *IRE Trans. on Antennas and Propagation*, **Ap-6**, 123 (1958).

(Paper 64D5-78)

h
re
an
n
th
co
us
pi
pi
co

m
su
S
G
th
A
pi
be
is
an

A
A
B
m
8,
T
gl
hu
re
th

at
25,

Electrical Resistivity Studies on the Athabasca Glacier, Alberta, Canada¹

G. V. Keller and F. C. Frischknecht

(May 3, 1960)

The use of electrical methods for measuring ice thickness and properties on the Athabasca Glacier, Alberta, Canada, has been studied by the U.S. Geological Survey. Two methods for measuring resistivity were tried: (1) a conventional resistivity method in which current was introduced galvanically into the glacier through electrodes, and (2) the other an electromagnetic method in which a wire loop laid on the ice was used to induce current flow. Results of the galvanic measurements showed large variations in the resistivity of the ice; in a surface layer several tens of feet thick the resistivity is between 0.3 and 1.0 megohm-meters, and under this layer, the resistivity of the ice is more than 10 megohm-meters. The resistivity of the surface ice is determined by its water content rather than by molecular resonance loss. The ice had no effect on the mutual coupling measurements in the frequency range from 100 to 10,000 cycles per second. As a consequence the electromagnetic data could be interpreted simply in terms of ice thickness and bedrock resistivity.

1. Introduction

Geological exploration in polar areas is often hampered by the presence of thick ice sheets covering rock outcrops. Geological studies in ice-covered areas are facilitated by the use of geophysical techniques to provide information about the rocks under the ice. Seismic, magnetic, and gravity methods are commonly used, but electrical methods have been used only rarely [1, 2], despite the fact that ice probably has more significantly different electrical properties than any rock with which it may be in contact.

An opportunity for studying the use of electrical methods over glacial ice came about during the summer of 1959, when the U.S. National Bureau of Standards planned a field study on Athabasca Glacier in Alberta Province, Canada, [3] and invited the U.S. Geological Survey to participate. The Athabasca Glacier was an attractive location for preliminary studies because of its accessibility and because an extensive program of glaciological work is being carried on there by the Universities of Alberta and British Columbia.

2. Description of Athabasca Glacier

The Columbia Ice Field, which is the source of the Athabasca Glacier, lies astride the British Columbia-Alberta border, about 110 mi north of the town of Banff, Alberta. Athabasca Glacier extends approximately $2\frac{1}{2}$ mi from the névé line at an elevation of 8,000 ft, to the toe at an elevation of 6,300 ft (fig. 1). There are two ice falls in the first $\frac{1}{4}$ mi after the glacier leaves the ice field, each with a drop of several hundred feet. The lowermost step of the glacier is relatively flat and smooth for more than a mile before the ice surface drops off to the terminal lake.

¹ Contribution from U.S. Geological Survey, Denver 25, Colo.; paper presented at Conference on the Propagation of ELF Radio Waves, Boulder, Colo., January 25, 1960.

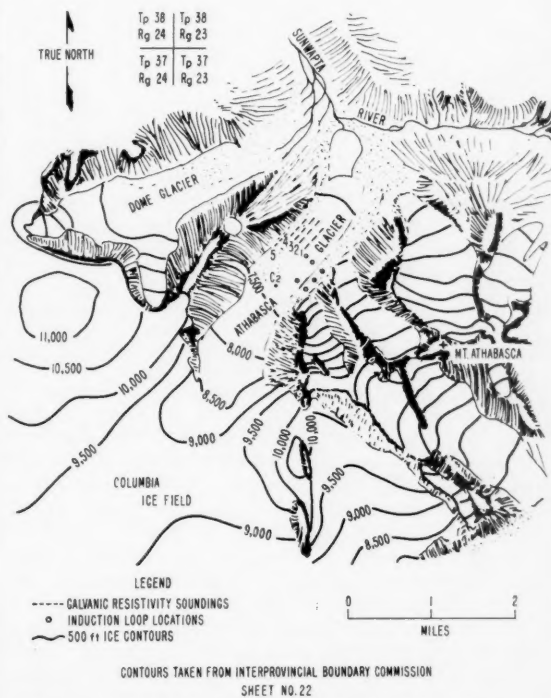


FIGURE 1. Sketch map showing the Athabasca Glacier.

The lower step is only slightly crevassed, though during the melt season parallel hummocks 3 to 5 ft high, spaced at 10 ft intervals, develop over most of the surface. Commonly, the valleys between these hummocks provide drainage for melt water. Drainage streams usually end in moulins, or melt holes, several hundred feet deep.

All of the electrical studies were carried out on the lower step, as indicated on figure 1.

3. Field Work With Electrical Methods

Two methods of measuring resistivity were used; one, a conventional method in which current was fed galvanically into the ice through electrodes, and the other, an electromagnetic method in which the mutual coupling between two wire loops laid on the ice was measured.

3.1. Galvanic Method

The galvanic measurements consisted of five depth soundings made at 300-ft intervals across the glacier from the midpoint to the northwest margin, and a resistivity profile along this line (fig. 1). A four-terminal electrode system was used to make the depth soundings, with three of the four electrodes being fixed in position, and the fourth electrode (P_1) being moved to increase the effective depth of the resistivity measurements (fig. 2). The electrodes (C_1 and C_2) used to supply current to the ice were separated a distance of 2,500 ft, while the fixed voltage-measuring electrode (P_2) was located 2,500 ft further down the glacier. The other voltage-measuring electrode was placed at distances ranging from 5 to 1,600 ft from the middle electrode.

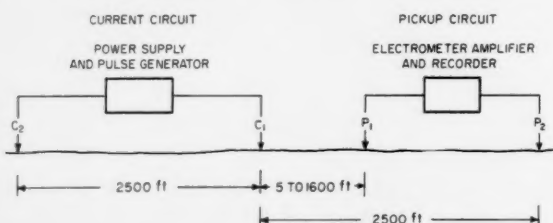


FIGURE 2. Block diagram of the single moving electrode array used in measuring ice resistivity.

Electrode P_1 is the only electrode moved in making a depth sounding.

The steel pins or lead rods used for electrode contacts in the ice, were usually placed in shallow melt ponds. Contact resistance which varied from location to location, was within the range 0.5 to 5 meg. Pulsed direct current, with a period of 0.1 to 3 sec, was used to energize the current spread, with the plateau current being approximately $\frac{1}{2}$ ma.

The voltage between the pickup electrodes was recorded on a hot-stylus oscillograph. Examples of some typical recordings are shown in figure 3. Ideal voltage forms (fig. 3a) were recorded only at short spacings: the signal was large compared to background noise, and the transient rise and fall of the signal due to capacitance in the ice may be detected in spite of the switching transient. With large electrode separations the recorded signal was comparable in amplitude to the noise level (fig. 3b). Frequently, the recorded voltage form showed the effect of the capacitive surge of current from the wire connecting the current electrodes (fig. 3c). This surge became larger as the current cable melted into the ice, and the capacity between the cable and the ice increased.

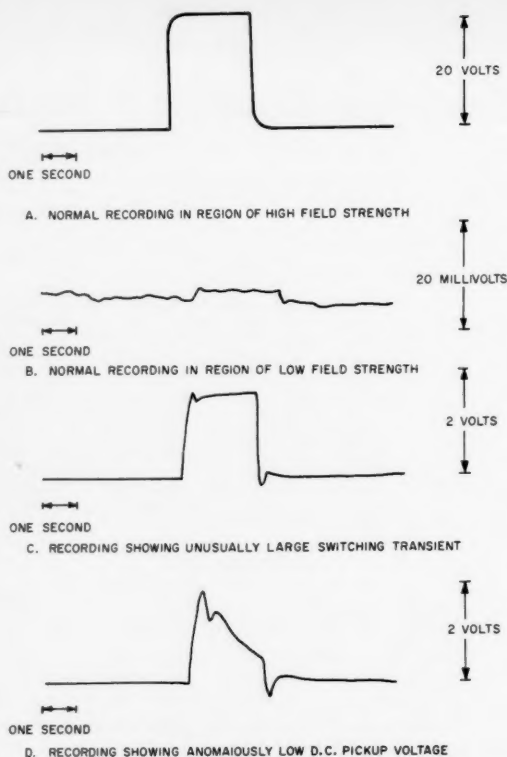


FIGURE 3. Examples of voltages recorded at the pickup electrodes during current pulses.

In a few cases, the recorded voltage form fell to a very low plateau value after the initial capacity surge (fig. 3d). It is possible that this type of voltage form occurred when the pickup electrode was located over a zone of highly resistant ice causing a very large source impedance to be in series with the recorder. Such high source impedances could not be detected by connecting an ohmmeter across the pickup terminals because the resistance measured in this way is that of a conducting surface film of water.

Both the apparent resistivity and the apparent dielectric constant of the ice can be calculated from the recorded voltages. Resistivity is calculated directly from the voltage, current and electrode geometry:

$$\rho_a = 2\pi \frac{E}{I} \left(\frac{1}{\frac{1}{d_1} - \frac{1}{d_2} - \frac{1}{d_3} + \frac{1}{d_4}} \right) \quad (1)$$

where

ρ_a = the apparent resistivity for d-c current
 E = the plateau voltage

I = the current

d_1 and d_2 = the distances between the moving electrode and the near and far current electrodes, respectively,

d_3 and d_4 = the distances from the fixed pickup electrode to the near and far current electrodes, respectively.

The dielectric constant may be calculated from a Fourier analysis of the pickup-voltage form. The Fourier analysis gives the phase shift for the harmonics comprising the square wave pulse transmitted through the current electrodes. The apparent dielectric constant, is

$$\epsilon = \frac{\tan \delta}{\rho_a \omega \epsilon_0} \quad (2)$$

where

- δ = the phase shift determined by Fourier analysis.
- ρ_a = the apparent resistivity calculated from the same data.
- ϵ_0 = the dielectric constant for free space, 8.854×10^{-12} f/m.
- ω = the angular frequency for which the phase shift is determined.

3.2. Interpretation of Galvanic Resistivity Measurements

The resistivities measured at one depth-sounding point near the northwest edge of the glacier are shown in figure 4, plotted as a function of the current-

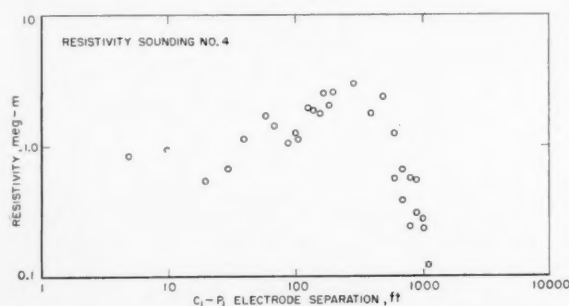


FIGURE 4. Example of resistivity depth sounding recorded on the Athabasca Glacier.

electrode pickup-electrode (C_1-P_1) separation. The most striking feature of these data is the large amount of scatter, more than can be accepted if the data are to be used for quantitative interpretation. In spite of this scatter, the general form of the sounding is evident: it represents a surface layer with a resistivity of the order of 1 meg-m, a second layer with a much higher resistivity, and a bottom layer of low resistivity.

Resistivity departure curves were prepared from tables given by Mooney and Wetzel [4] for this sequence of resistivities. An example of a family of such curves is shown in figure 5 for the case in which the resistivity of the second layer is 100 times that of the first layer and the resistivity of the third layer is 1/100 that of the first layer. Each curve represents a different thickness for the second layer. Such

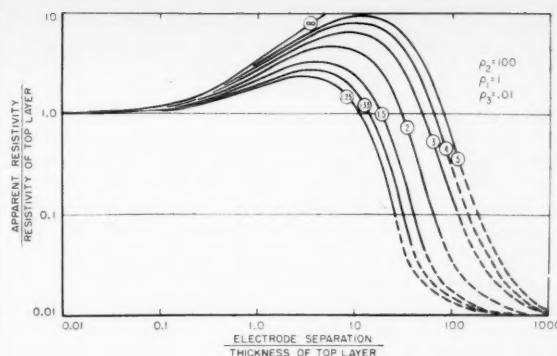


FIGURE 5. Theoretical curves of apparent resistivity as a function of electrode separation (computed from Wetzel [4]).

families of curves were prepared also for resistivity ratios between the three layers of 1:10:1/100 and 1:3:1/100.

It is difficult to compare the field measurements directly with these families of departure curves because of the large scatter in the data. The field data were smoothed by taking a running harmonic average of each consecutive set of six resistivity values. The five smoothed sounding curves are shown on figure 6. Sounding 1, which was made

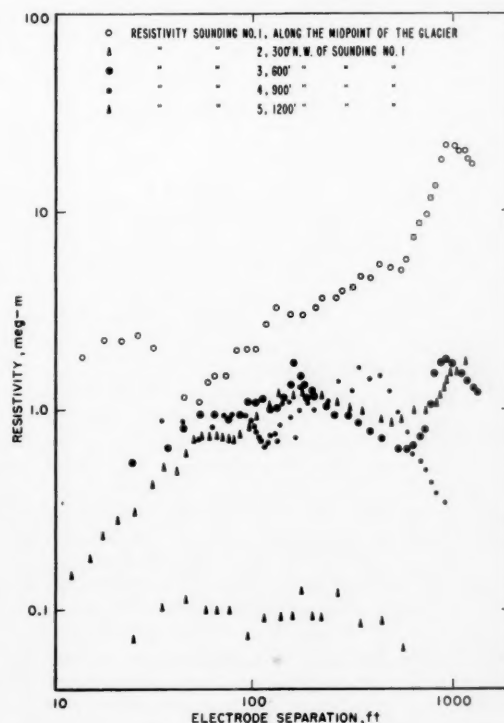


FIGURE 6. Resistivity sounding curves after forming a running average of each six consecutive resistivity values.

along the center line of the glacier, showed much higher resistivities than any of the other soundings, with values ranging from 1.1 meg-m for relatively short spacings to 21 meg-m for relatively large spacings. Soundings 2, 3, and 4 show similar values of resistivity, one to another, though the resistivities recorded for sounding 4 (the closest of the three to the edge of the glacier), are significantly lower than for the other two soundings for the largest electrode separations. Sounding 5, which was recorded along the rubble-covered edge of the glacier, shows the lowest resistivities, approximately 0.1 meg-m.

Field measurements which indicate a medium-high-low sequence of resistivities may be interpreted in the following manner. The initial portion of the sounding curve is matched with the initial portion of a family of three-layer curves, as shown in figure 5. The shape of this initial portion of the curve is independent of the resistivity of the third layer, and if the thickness and resistivity of the second layer are greater than some threshold value, the initial shape is also independent of these parameters. By fitting only the first part of the field data, we may obtain values for the resistivity and thickness of the surface layer:

Sounding	Resistivity of surface layer	Thickness of surface layer
1	1.8×10^6 ohm-m	60 ft
2	0.070 or 0.70×10^6	18 or 140
3	$.70 \times 10^6$	60
4	$.75 \times 10^6$	70
5	$.070 \times 10^6$	50

The form of sounding 2 indicates a very low resistivity in a thin surface layer which was not apparent in the other soundings. The other four soundings suggest the surficial layer of low resistivity is approximately 60 ft thick and varies in resistivity from a high value of 1.8 meg-m at the center line of the glacier to a low value of 0.070 meg-m in the rubble-strewn margin of the glacier.

This variation in the resistivity of the surface ice in the glacier is further demonstrated by a resistivity profile which was measured along a line running from the midpoint of the glacier to the northwest edge (fig. 7). A constant electrode separation of 80 ft was used, so the measured resistivity is controlled mainly by the thickness and resistivity of the surface layer. It is apparent that sounding 1 (fig. 6) was located in an area of high-surface resistivity, soundings 2, 3, and 4 in an area of low-surface resistivity, and sounding 5 in an area of very low surface resistivities.

The resistivity and thickness of the second layer indicated by the soundings were determined from the position and value of the maximum observed resistivity for each sounding. The spacing for which the maximum resistivity is observed is related to the thickness of the second layer (fig. 8). If the resis-

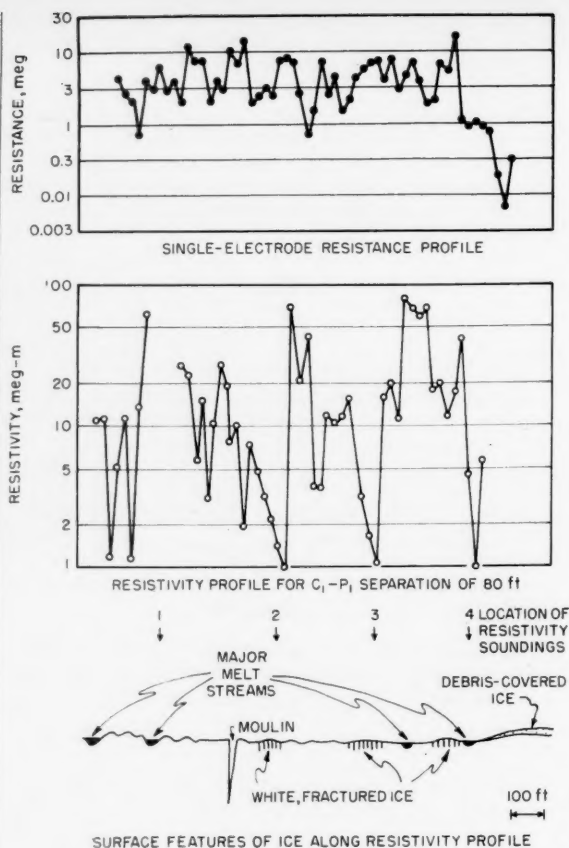


FIGURE 7. Resistivity profile from the midpoint of Athabasca Glacier to the northwest edge, measured with a fixed electrode separation of 80 ft.

tivity of the second layer is very high, the maximum will be observed with electrode separations as much as three times greater than the combined thickness of the first and second layers. If the resistivity of the second layer is only 10 to 20 times greater than the resistivity of the first layer, then the maximum will be observed at an electrode separation about equal to the combined thicknesses of the first two layers.

The maximum observed resistivity will always be less than the true resistivity of the second layer for the sequence of resistivities observed on the Athabasca Glacier. Curves showing the relation between the maximum observed resistivity and the true resistivity of the second layer are presented in figure 9.

The ragged shape of the observed sounding curves makes the selection of maximum values somewhat

arbitrary. One set of reasonable values is:

From field data		
Sounding	Maximum resistivity	Spacing at which maximum resistivity is measured
	Surface resistivity	
1	7.2	1,000 to 1,500
2	2.9	900 to 1,200
3	2.9	800
4	2.1	400
5	1.7	250

Interpretation		
Sounding	Resistivity of second layer	Depth to bottom of second layer
1	22×10^6 ohm-m	1,000 ft
2	11×10^6	900
3	15×10^6	800
4	21×10^6	400
5	3.5×10^6	250

These measurements are in agreement with seismic determinations of the thickness of the glacier near the midpoint, where depths of approximately 1,000 ft were recorded (oral communication, P. J. Savage, Univ. of British Columbia). The bulk of the glacier appears to have a high resistivity, approximately 10 or 20 meg-m.

The electrode separations used were not large enough to determine the resistivity of the third, or

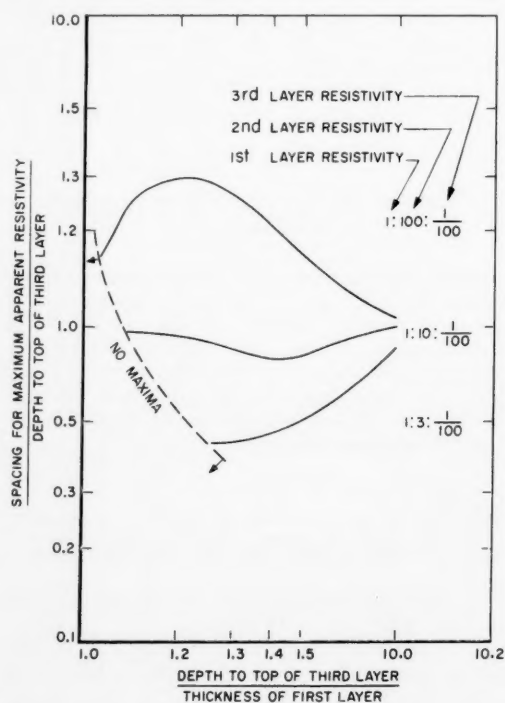


FIGURE 8. Relationship between the spacing for which maximum apparent resistivity is measured and the depth to the third layer for several ratios of resistivities.

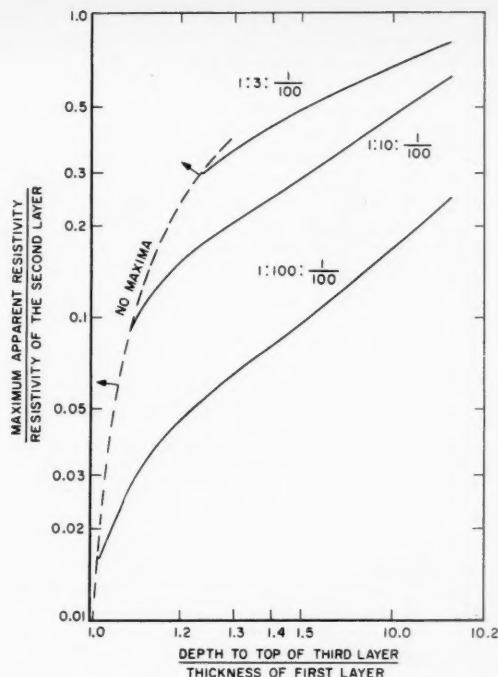


FIGURE 9. Maximum measured apparent resistivity as a function of the depth to the third layer for several sets of resistivity ratios.

bottom layer. However, the rate at which measured resistivity decreased at very large spacings indicates that the resistivity is 1/100 (or less) than that of the surface layer. Resistivity of the bottom layer is, therefore, thought to be 7,000 ohm-m or less.

In summary, the data show that the glacier has a surface layer 60 ft thick which is highly variable in resistivity, ranging from 0.07 to 80 meg-m. Beneath this surface layer, the ice has a resistivity of 10 to 20 meg-m. The lowermost layer has a resistivity of 7,000 ohm-m or less, and so, is probably bedrock.

The apparent dielectric constants for a depth sounding located at the middle of the glacier are shown in figure 10, plotted as a function of the C_1-P_1 separation. No theoretical curves are available for interpreting these data for an insulator over a conductor. However, data presented by Zablocki [5] suggest that if the surface layer in a section is much more resistant than the underlying medium, as electrode separations are increased, the apparent dielectric constant will first increase over the true value for the top layer and then decrease to the true value for the lower medium.

The lowest value of dielectric constant calculated from field data is approximately 140. The higher values indicated on figure 10 for C_1-P_1 separations of 100 to 1,000 ft are probably caused by resistivity layering, which results in large interfacial polarization.

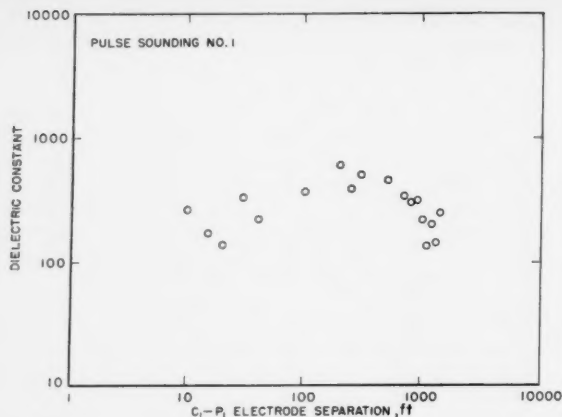


FIGURE 10. Apparent dielectric constant as a function of electrode separation.

3.3. Electromagnetic Methods

Electromagnetic soundings were made at five locations near the southeast edge of the glacier, as indicated by the pairs of small circles on the map in figure 1. The procedure consisted of measuring the mutual coupling between two loops of wire laid on the ice as a function of frequency in the range 100 to 10,000 c/s (fig. 11). An oscillator and a 70-w audio

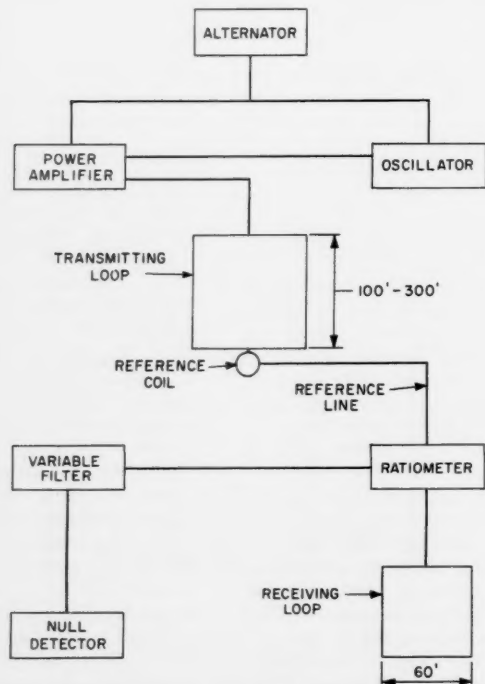


FIGURE 11. Block diagram of variable frequency electromagnetic apparatus.

amplifier were used to supply several amperes of current to the transmitting loop, which consisted of 1 to 3 turns of wire, 100 to 300 ft on a side. The receiving coil consisted of eight turns of wire with a braided shield and was 60 ft on a side. The loops were separated by a fixed distance in the range from 500 to 1,820 ft for each sounding. Neither loop was tuned.

A reference voltage, induced in a small coil placed at one side of the transmitting loop, was carried to the measuring apparatus over a two-conductor cable. The phase and amplitude of the received signal were compared with the reference voltage using a ratiometer and null detector. A variable-frequency bandpass filter was used to reduce interference from sferics and signals from a low-frequency radio station at Jim Creek, Wash.

The amplitude ratios and phase differences observed at different frequencies are a function of the impedances of the receiving and reference coils and of the reference line. This dependence was determined by measuring the frequency response of the system with the coils very close together and with the reference line extended to its full length. All subsequent measurements were corrected for the frequency-dependence determined in this way.

Instrumentally, the only problem in making the field measurements was the difficulty in obtaining a sharp null at frequencies below about 300 c/s and above 3,000 c/s. The difficulty at low frequencies was caused by low signal strength, and at high frequency by the high noise level from sferics and signals from the Jim Creek station. Amplitude ratios were measured with an accuracy of about ± 2 percent at low frequencies. The phase angles and, above 3,000 c/s, the amplitude ratios are of doubtful accuracy.

3.4. Theoretical Curves for Electromagnetic Sounding

Equations for the mutual coupling between horizontal loops lying on the surface of a homogeneous flat earth are given by Wait [6] for the case in which both the dielectric constant and the conductivity of the earth are important. The family of curves presented by Wait are plotted with the mutual impedance ratio, Z/Z_0 as a function of the parameter B , for various values of b , where

$$B = \sqrt{\frac{\mu_0 \omega I^2}{2\rho}}$$

Z_0 = mutual coupling between loops in free space

$$b = \omega \rho e$$

Z/Z_0 = complex mutual coupling between these loops with the earth present

$|Z|$ = amplitude of the coupling with the earth present

θ = phase angle of the coupling with the earth present

μ_0 = magnetic permeability of free space = $4\pi \times 10^{-7}$ h/m

ω = angular frequency

r =spacing between the loops
 ϵ =dielectric constant of the earth
 ρ =the resistivity of the earth=reciprocal of conductivity.

These theoretical curves may be compared with field curves of mutual coupling measured as a function of loop separation, but with the frequency held constant. In the present work, mutual coupling was measured as a function of frequency with the loop spacing held constant. In order to plot coupling curves, which vary with frequency rather than spacing, we permit b to vary proportionally with B^2 :

$$b = AB^2 \quad (3)$$

where A is an arbitrarily selected constant, instead of holding b constant. Referring to the definitions of b and B , we see that this is equivalent to:

$$\frac{2\rho^2\epsilon}{\mu_0} = Ar^2 \quad (4)$$

and since ρ , ϵ , μ_0 , and A are constants, this means r must be constant for this particular curve relating coupling to the ratio B . Figure 12 shows two families of coupling curves, one calculated for constant values of the ratio b , and the other calculated for sets of values of b proportional to B^2 . These sets of curves are valid only if the coil spacing, r , is larger than the height of the loops above bedrock.

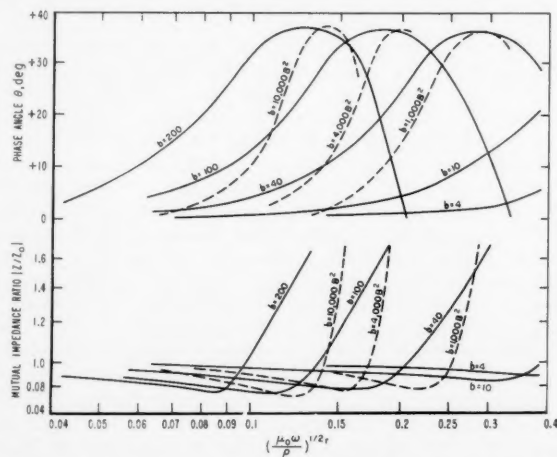


FIGURE 12. Mutual impedance plotted as a function of the conductivity parameter for two horizontal loops on a lossy dielectric earth (calculated from Wait [7]).

In reference [7] Wait gives equations and some computations and curves for the case in which the loops are raised above a conducting homogeneous earth, but with the effect of dielectric constant neglected. Slichter and Knopoff [8] have presented equations and computations for the case in which loops are placed on the surface of a conducting two layer earth. This case degenerates into the preceding

case, considered by Wait, if the conductivity of the upper layer is zero. In both cases, the mutual coupling is presented as a function of loop separation rather than of frequency. They may be replotted as a function of frequency, but they do not cover adequately the range of interest.

Wait [9] has derived equations for the coupling of loops raised above a two-layer earth. This equation has been evaluated for a large number of cases by the Computations Branch, U.S. Geological Survey. The results are plotted as families of curves with mutual impedance Z/Z_0 plotted as a function of B , for various parametric values of the ratios h/r , d/r , and $K = \rho_1/\rho_2$ where

h =height of the loops above the earth

d =thickness of the upper layer

ρ_1 and ρ_2 =resistivities of the upper and lower layers, respectively.

A family of curves for horizontal loops raised above homogeneous earth ($K=1$) is shown in figure 13.

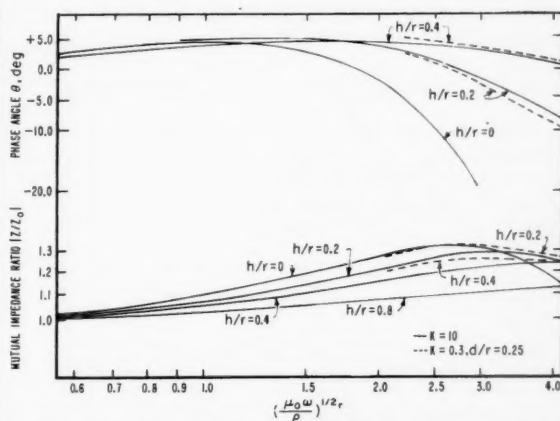


FIGURE 13. Mutual impedance plotted as a function of the conductivity parameter for two horizontal loops raised above a two-layer conducting earth (calculated from Wait [9]).

Portions of curves for loops raised above a two-layered earth with $K=0.3$ and $d/r=0.25$ are also shown in figure 13 as dashed lines. If it can be assumed that the ice is an insulator, then the measurements made on Athabasca Glacier can be treated as a case in which the loops are raised over a conducting earth by a distance equal to the thickness of the ice. The field data then could be compared with the families of curves shown in figure 13. Neither the curves in figure 12 or figure 13 apply to the case of a lossy dielectric over a conducting earth, but each set is an approximation to the two limiting cases, one where the ice is very thick, and the other where the loss in the ice is very small.

Relative to the theoretical curves, both the abscissa and the ordinate of the measured curves contain undetermined constant multipliers. In normalizing the field curves by making measurements with the loops close together, the free-space mutual coupling, Z_0 , is determined. However, since Z_0

varies as the cube of the separation between the loops, it is not possible to calculate an accurate value of Z_0 for a large spacing from the value determined at a small spacing. Therefore, the ordinate of the field curve is $\psi_1 Z/Z_0$, where ψ_1 is undetermined. Similarly, the abscissa of the field curves is f rather than B , so $B = \psi_2 \sqrt{f}$, where ψ_2 is not known.

In interpretation, the field curves and the theoretical curves are plotted on separate sheets of log-log graph paper. The field curve is laid over a family of theoretical curves until a good match is found with one of the theoretical curves. If a valid fit between curves is found, ψ_1 , ψ_2 and the other parameters are readily determined. The position of the ordinate of the field curve relative to the theoretical curve determines ψ_1 ; the position of the abscissa determines ψ_2 , from which ρ may be calculated. The particular theoretical curve which is matched specifies $\omega \rho \delta$ or h/r , depending on which type of curve is used. If the field curve can be extrapolated to zero frequency, ψ_1 may be determined from the relationship $\psi_1(Z/Z_0) = 1$. If ρ is known by some independent measurement, ψ_2 and B can be determined without curve matching.

3.5. Results of Electromagnetic Soundings

The first two soundings were made with a 500-ft coil separation over a section of the glacier where the ice is known to be at least 800 ft thick. The data from one of these soundings is shown as curve *a*, in figure 14. The maximum change in coupling with

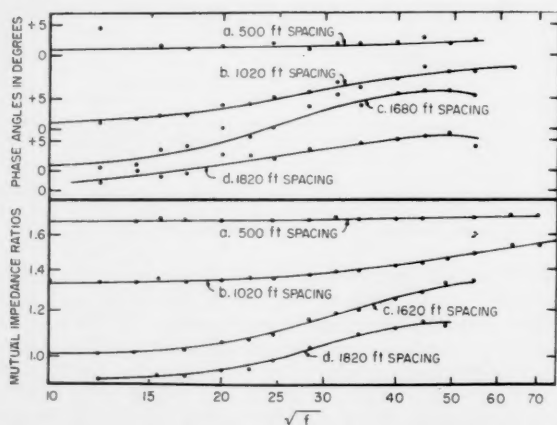


FIGURE 14. Changes in mutual impedance (as a function of the square root of frequencies) measured on the Athabasca Glacier.

change in frequency is about one-half percent, which is the approximate range of scatter of the data. The soundings with relatively close spaced loops showed that the ice had a negligible effect on coupling, so that it would be impossible to use the curves in figure 13 for interpretation.

The rest of the measurements were made with larger loop separations with the loops aligned along the length of the glacier near the southeast edge

(fig. 1). The data are shown as curves *b*, *c*, and *d*, in figure 14. Soundings *b* and *c* were made at the same distance from the edge of the glacier.

The data for soundings *b* and *c* are superimposed on theoretical curves for horizontal loops raised above a conducting earth in figure 15. Only the amplitude

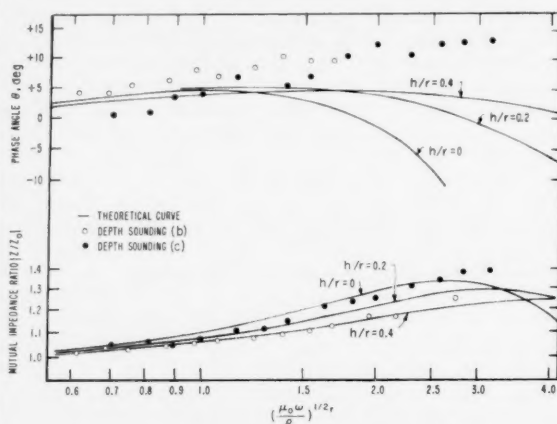


FIGURE 15. Comparison of data from Athabasca Glacier with theoretical curves (calculated from Wait [9]) for horizontal loops raised above a two-layer conducting earth.

curve for sounding *b* matches the theoretical curves well; the amplitude curve for sounding *c* and the phase curves for both soundings do not fit the theoretical curves.

Three possible explanations for the departure of these sounding curves from the theoretical curves have been considered: (1) layering within the bedrock, (2) a dipping surface at the bottom of the glacier, and (3) response from the ice. It is likely that the dipping contact at the base of the glacier is the most important of the three factors. This dip may be as much as 30 or 40 deg, so the approximation of horizontal loops raised over the horizontal surface of a conducting earth is in error. A better approximation may be obtained by replacing the horizontal loops with two sets of component loops, one set with their axes parallel to the bedrock surface and the other set with their axes perpendicular to the bedrock surface. Figure 16 shows the soundings *b* and *c* superimposed on theoretical curves for loops inclined at 45 deg to the surface of the earth. The measured and theoretical amplitude curves match well, and while the match with the phase curves is not perfect, it is better than that shown in figure 14.

The amplitude curves may be interpreted as follows: for sounding *b*, we find that $h/r \approx 0.50$, and since $r = 1,020$ ft, $h \approx 510$ ft. The abscissa position gives a value for the resistivity of the bedrock as 670 ohm-m. For sounding *c*, we find that $h/r \approx 0.27$, and since $r = 1,680$ ft, $h \approx 454$ ft and $\rho = 530$ ohm-m. These values for soundings *b* and *c* compare reasonably well, particularly, since observation of the edge of the glacier indicates that the bottom surface is irregular.

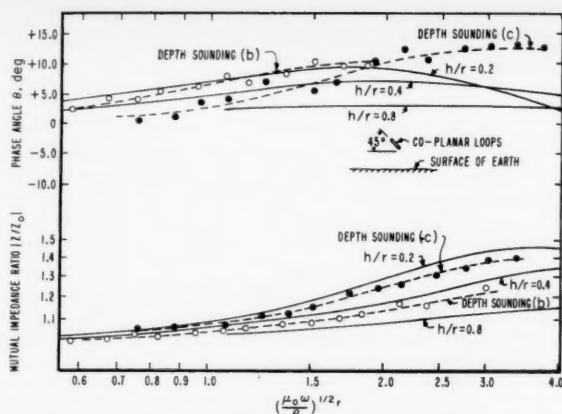


FIGURE 16. Comparison of data from Athabasca Glacier with theoretical curves (calculated from Wait [9]) for coplanar inclined loops raised above a homogeneous conducting earth.

4. Summary of Electrical Properties of Athabasca Glacier

Extensive laboratory studies of the electrical properties of ice have been reported in the literature (see, for example, Smythe and Hitchcock [10]). The ice molecule is polar, and exhibits molecular resonance at audio and lower frequencies at subzero centigrade temperatures. The relationships between dielectric constant and frequency and between resistivity and frequency as found by Smythe and Hitchcock for ice near the melting point are shown by the two solid curves in figure 17. At low fre-

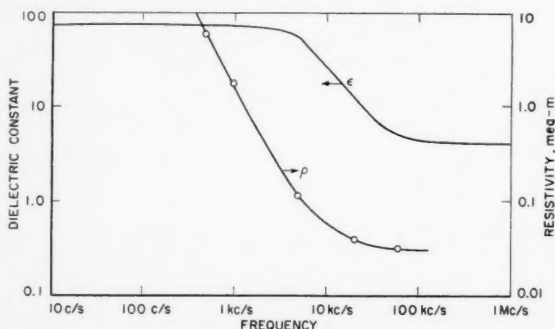


FIGURE 17. Summary of the electrical properties of ice slightly below the freezing point (data from Smythe and Hitchcock, 1932).

quencies, the dielectric constant is 73.7, while at high frequencies, it is 4.0. The relaxation frequency of the dispersion is 15.5 kc/s.

As in any case of molecular resonance, the relaxation frequency is also the frequency at which the highest loss is observed. At high frequencies, the resistivity of the ice approaches a constant value, 0.0335 meg-m. At frequencies below the relaxation frequency, the resistivity increases as the inverse

square of the frequency. At zero frequency, the resistivity is infinitely large.

In the measurements on Athabasca Glacier, it was found that the resistivity of the ice at low temperatures is finite and for the surface layer ranges from 0.3 to 1.0 meg-m. This can be attributed to the fact that glacial ice has a different genesis than the ice usually studied in the laboratory. For the most part, glacial ice is compacted snow rather than frozen water. In this respect, glacial ice resembles any other detrital rock. In general, glacial ice will have considerably more pore space than crystalline ice, and during the melt season, these pores may contain water.

There are three types of porosity apparent in glacial ice: (1) crevasse porosity, (2) vugular or melt cavity porosity, and (3) microporosity. An open crevasse might be expected to increase the resistivity of the ice greatly. On the lower part of the Athabasca Glacier, most of the fractures are not open, and are probably filled with a thin film of water, affording a path for conduction. Even if the glacier is slightly below the melting point, these fractures may contain water. Since the fractures absorb the downward motion of the glacier, there may be pressure melting of ice where irregularities on either side of a fracture bear the brunt of the down-glacier pressure.

In many respects, the porosity of glacial ice resembles the porosity in limestones, which also have three types: (1) intercrystalline microporosity, (2) vugs or solution cavities, and (3) joints. It seems reasonable that the equation relating water content and resistivity in limestones might be applied to ice:

$$\rho = 1.4 \rho_w S^{-1.8} \quad (5)$$

where ρ_w is the resistivity of the water contained in the rock and S is the volume fraction of water in the rock.

Samples of water taken from the runoff streams on the glacier were found to have a resistivity of 650 ohm-m at 0° C. Assuming eq (3) applies to glacial ice, we may calculate that ice with a resistivity of 0.3 meg-m has a water content of 4.0 percent by volume.

Fine-grained detrital rock material in ice can lower the resistivity considerably, because such impurities can retain water in a liquid state even well below freezing. Parts of the Athabasca Glacier appear to include high concentrations of rock, particularly along the lateral moraines where landslides have covered the margins of the glacier with rock. These zones were found to be 10 to 100 times more conductive than the clean ice, but this conductivity extended only a few inches or few feet into the ice.

At low frequencies, it is apparent that the resistivity of the ice is determined by the moisture content rather than by molecular resonance. At some frequency, the molecular loss must become more important than conduction through the water, since at high frequencies, the conduction caused by molecular losses is ten times greater than the conduction through the water.

5. Conclusions

Resistivity studies on Athabasca Glacier indicate that electrical methods may be useful in studying the thickness and texture of temperate-glacial ice. Electromagnetic methods are probably preferable to galvanic methods if the primary interest is in the thickness of the ice and the nature of the underlying material.

The electromagnetic method described here can probably be used over thicker glaciers or ice caps with equal success. The limiting factor in using the method over very thick ice will be the response from the ice itself. It would be possible to calculate coupling curves taking into account the loss in the ice, but probably the effect of the loss in the ice would mask the small response from the conductive earth under the ice for those ice thicknesses where loss in the ice becomes important.

In order to use this electromagnetic method on an ice cap four times as thick as the Athabasca Glacier, the coil separation would have to be increased by a factor of 4 to maintain a favorable ratio, h/r . The frequency range would have to be lowered by a factor of 16 to stay in the same range of values for the parameter B . Therefore, the product $\rho\omega\epsilon$ for the ice could be 16 times larger than on the Athabasca Glacier and yet cause no more distortion of the observed data.

In many areas, bedrock resistivities may be larger than 600 ohm-m. The frequencies used in sounding must be increased in a direct ratio to the bedrock resistivity in order to stay in the same range of values of B . If the bedrock resistivity were too large, such high frequencies might be required that some response would be obtained from the ice itself.

If primary interest is in the properties of the glacial ice rather than bedrock, galvanic resistivity measurements are preferable. In this study, it was found that resistivity measurements could distinguish between zones of massive ice and zones of compacted névé, and so, may be helpful in tracing structure in a glacier. Resistivity measurements may be used to detect the depth to which a glacier contains

liquid water. As corollary, it may be possible to measure thermal layering in a glacier by measuring the resistivity layering.

The authors are indebted to James Wait and Donald Watt, of the National Bureau of Standards, for suggesting the work on Athabasca Glacier; to George Garland of the University of Alberta, for his invitation and offer of assistance; and to the Department of Northern Affairs and National Parks of the Commonwealth of Canada for permission to work in Jasper National Park. We especially appreciate the assistance given by W. R. Ruddy of Snowmobile Tours, Ltd., in providing transportation on the glacier.

6. References

- [1] C. Lefevre, P. Albertinoli, A. Bauer, A. Blum, L. Cagnaird, and H. Fournier. Mesures electriques et telluriques sur le grand Glacier D'aletsch, *Ann. de geophys.*, **13**, 54 (1957).
- [2] C. Queille-LeFevre, A. Bauer, Girard, Premier essai de mesure electrique d'epaisseur d'un glacier, *Ann. de geophys.*, **15**, 564 (1959).
- [3] A. D. Watt, and E. L. Maxwell. Measured electrical properties of snow and glacial ice, *J. Research NBS*, (in print).
- [4] H. M. Mooney, and W. W. Wetzel. The potentials about a point electrode and apparent resistivity curves for a two-, three-, and four-layer earth, p. 146 (Univ. of Minn. Press, Minneapolis, Minn., 1956).
- [5] C. Zablocki. Analog studies of induced polarization over a layered earth, *Geophysics*, **22**, 502 (1957).
- [6] J. R. Wait. Mutual coupling of loops lying on the ground, *Geophysics*, **19**, 290 (1954).
- [7] J. R. Wait. Mutual electromagnetic coupling of loops over a homogeneous ground, *Geophysics*, **20**, 630 (1955).
- [8] L. B. Slichter and L. Knopoff. Field of an alternating dipole on the surface of a layered earth, *Geophysics*, **24**, 77 (1959).
- [9] J. R. Wait. Induction by an oscillating magnetic dipole over a two-layered earth, *Appl. Sci. Research*, **7**, 73 (1958).
- [10] C. P. Smythe, and C. S. Hitchcock. Dipole rotation in crystalline solids, *J. Am. Chem. Soc.*, **54**, 4631 (1932).

(Paper 64D5-79)

Amplitude Distribution For Radio Signals Reflected by Meteor Trails. I¹

Albert D. Wheelon

(March 22, 1960; revised May 2, 1960)

The probability distribution for the envelope of the received signal composed of reflections from many meteor trails is derived theoretically. Both the effects of numerous, small meteors and the residual reflections from infrequent, large meteors are treated simultaneously. For the particular example of exponential decay of initial spikes which are themselves distributed as the inverse square of their amplitudes, we find that the probability that the composite residual signal amplitude exceeds a prescribed level r is given by

$$P(R > r) = \frac{1}{\left[1 + \frac{r^2}{(\nu\eta Q)^2}\right]^{1/2}}$$

This function behaves as a Rayleigh distribution for small amplitude margins r . For the larger, less likely amplitudes it agrees with the result predicted by elementary analysis of isolated meteor reflections. Possible refinements of these results are also discussed. A second paper will discuss time correlation of composite meteor signals at different times.

1. Introduction

Backscattering of radiowaves by meteor trails in the E region of the ionosphere is a valuable direct means for studying meteors. VHF signals are also propagated obliquely to as far as 1,500 km by oblique reflections from the same meteor trails. Signals reflected from the largest meteors are easily recognized as individual spikes in amplitude records. There are also overlapping signal contributions from much smaller meteors which cannot be so distinguished.

The smaller meteors have been suggested as a possible source of the continuous background signal observed on the VHF scatter circuits. To distinguish between the signal due to turbulence and that due to small meteors, the cumulative probability distribution for signal amplitudes has been measured for narrow beams directed both on and off a great circle path. However, a theoretical distribution for overlapping meteors does not seem to have been developed thus far, and this paper is addressed to that problem.

The very small meteors can be analyzed if one considers only the meteor signals which arrive at the precise instant of signal evaluation. A vector combination of many randomly oriented (phased) signal vectors is known to follow a Rayleigh distribution. The corresponding probability that the echo signal lies in the range R to $R+dR$ is:

$$\text{Small: } W(R)RdR = \frac{RdR}{\sigma^2} e^{-R^2/(2\sigma^2)} \quad (1.1)$$

where

$$\sigma^2 = \frac{1}{2} \langle R^2 \rangle \quad (1.2)$$

is the mean square voltage in the ensemble of meteor echoes. Although this description does recognize a distribution of meteor signals, it is deficient in that it ignores the residual effect of meteor signals created prior to the measuring instant. Even though such signals may have experienced appreciable decay, their combined effect may make a significant contribution to the distribution. This is especially true of the larger meteors, which have a poorer chance of occurring precisely at the instant of measurement, although their residual signal may still be comparatively large.

The very large meteors can be treated as isolated random events. The probability of receiving such an echo signal with an initial pulse height lying between p and $p+dp$ (volts) is experimentally found to follow a distribution of the form

$$D(p)dp = \frac{Q}{p^{2+\epsilon}} dp, \quad (1.3)$$

where the parameter ϵ is commonly taken to be zero for analytical convenience. The residual signal left after t seconds is adequately described by an exponential decay of the initial spike p .

$$R = pe^{-t/\eta}, \quad (1.4)$$

where η is the characteristic (diffusion) decay time of the meteor trail itself. The probability that the residual signal exceeds a prescribed level r is thus an interlocking marginal average over the distribution of observing a signal of exactly strength p and the probability of having received an echo at all. Since the echoes are found to occur at random at an average rate ν ,

$$P(R > r) = \int_0^\infty dt \nu \int_{r/e^{-t/\eta}}^\infty dp D(p) = \nu \eta \frac{Q}{r} \quad (1.5)$$

¹ Contribution from Space Technology Laboratories, Inc., P.O. Box 95001, Los Angeles 45, Calif.

The distribution $W(R)$ for the signal produced by large isolated meteor echoes is obtained from this result by differentiation.

$$\text{Large: } W(R)dR = \nu\eta Q \frac{dR}{R^2} \quad (1.6)$$

This form is evidently quite different in nature from the Rayleigh distribution (1.1) ascribed to the smaller meteor contributions. However, these two results will emerge as asymptotic behaviors of a distribution which accounts for the effect of both the large and small meteors simultaneously. This distribution is derived in section 3, after the basic probabilistic expressions are developed in section 2. The bivariate probability density function for observing two meteor echo signals within prescribed ranges at different times will be discussed in a second paper on the subject.

2. General Amplitude Distribution Expressions

To derive the statistical distribution of the fading signal amplitude produced by a variety of meteor signals, one must recognize a spectrum of echo signal strengths in various stages of decay. It is convenient to tabulate the random occurrence of each meteor echo according to the envelope amplitude p with which the echo first appears. A typical sequence of meteor echoes is so separated in figure 1. The individual signals are randomly phased as they arrive, but figure 1 plots only the envelope magnitudes, independent of phase. The larger, less frequent signals are plotted on the top line as they might occur in time; with the smaller, more frequent echoes plotted on the lower scales. Actually, we shall wish to deal with a continuum of initial echo amplitudes p , and one should really show an infinite number of traces to handle each signal size interval p to $p+dp$.

At any given time, the total measured signal is the vector summation of the individual residual signals produced by each meteor in all size classes. Of

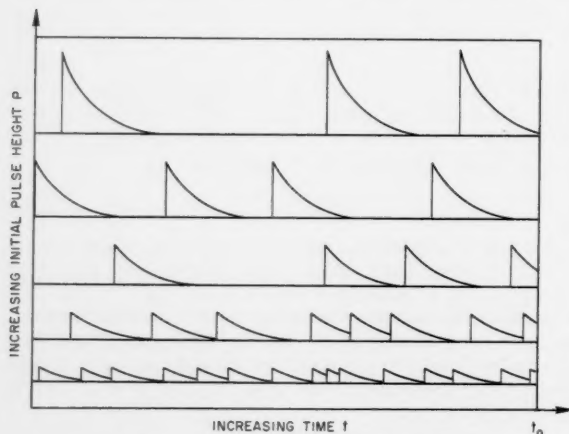


FIGURE 1. Typical occurrence history of individual meteor echoes arranged according to increasing initial pulse height.

course, the pulses which occur closest to the measuring instant produce the greatest remnant signals. On the other hand, there are an infinite number of very small signal remnants in the receiver from all previous meteors which may well contribute significantly to the composite total signal. To calculate the precise distribution in which both effects take their balanced roles, we use the Markoff method. The application of this method to the meteor echo problem follows closely Chandrasekhar's derivation of the Holtzmark distribution¹ for stellar attractive forces.

Consider first a finite time interval T prior to the time of measurement. The number of meteors which are likely to have occurred during this fixed interval is, of course, a random variable. Let us suppose, however, that exactly N meteor echoes occur in this interval. Since the meteor echoes form a Markoff process of small probability, one can argue that the probability of observing exactly N echoes in a fixed interval T should follow a Poisson distribution.

$$P(N|T) = \frac{(\nu T)^N}{N!} e^{-\nu T}, \quad (2.1)$$

The average number of meteors to be expected in an interval T is νT , and this estimate becomes sharper as this interval is lengthened. Let us assume that N is fixed for the moment, and label the individual meteor echoes by a subscript i . The residual vector signal S_i remaining at the measuring instant t_0 produced by an initial pulse \vec{p}_i at time t_i becomes:

$$\vec{S}_i = \vec{p}_i F(t_0 - t_i), \quad 1 \leq i \leq N, \quad (2.2)$$

where $F(\tau)$ is the form factor which describes the temporal decay of the initial pulse. The composite signal at t_0 is the vector sum of all N residual signals.

$$\vec{R} = \sum_{i=1}^N \vec{S}_i, \quad (2.3)$$

According to Markoff's method, the probability distribution for the total measured vector \vec{R} at time t_0 is the two-dimensional Fourier transform of a finite product taken over the set of initial echoes.

$$W(\vec{R}) = \frac{1}{(2\pi)^2} \int d^2k e^{i\vec{k} \cdot \vec{R}} A(k), \quad (2.4)$$

where

$$A(k) = \left\langle \prod_{i=1}^N \exp i\vec{k} \cdot \vec{p}_i F(t_0 - t_i) \right\rangle. \quad (2.5)$$

In the definition of $A(k)$, the averaging brackets must sum over all possible: (1) times of echo occurrence t_i , (2) initial echo vector pulse amplitude \vec{p}_i , and (3) total number of echoes N in the interval

¹ S. Chandrasekhar, Stochastic problems in physics and astronomy, Rev. Mod. Phys. 15, 1 (1943).

T . The initial pulses \vec{p}_i are independent of one another, since multiple (i.e., trail-to-trail) scattering is apparently unimportant, and there is insignificant gravitational interaction between the meteors. The infinite product thus becomes:

$$A(k) = \left\langle \left[\int_0^T d^2 p \int_0^T dt \gamma(\vec{p}, t) e^{i\vec{k} \cdot \vec{p} F(t_0 - t)} \right]^N \right\rangle, \quad (2.6)$$

where $\gamma(\vec{p}, t)$ is the probability that a *single* meteor echo occurs at time t and produces a vector signal \vec{p} in the receiver.

The average over N can be performed by multiplying with the probability (2.1) of observing exactly N echoes in the interval T and summing over all N .

$$\begin{aligned} A(k) &= \sum_{N=0}^{\infty} \frac{(\nu T)^N}{N!} e^{-\nu T} \\ &\quad \left[\int_0^T d^2 p \int_0^T dt \gamma(\vec{p}, t) e^{i\vec{k} \cdot \vec{p} F(t_0 - t)} \right]^N \\ &= \exp -\nu T \left[1 - \int_0^T d^2 p \int_0^T dt \gamma(\vec{p}, t) e^{i\vec{k} \cdot \vec{p} F(t_0 - t)} \right]. \end{aligned} \quad (2.7)$$

To proceed further, one must examine the probability density function $\gamma(\vec{p}, t)$ for a single echo pulse. If we were to examine the interval T in an a priori fashion, we could estimate that $N = \nu T$ echoes would most probably occur somewhere in the interval. However, their actual time of occurrence could not be predicted at all accurately, and one could only say that an individual meteor is equally likely to occur anywhere in the interval, viz,

$$\gamma(\vec{p}, t) = \frac{1}{T} \gamma(\vec{p}). \quad (2.8)$$

One can exploit this form in equation (2.7) by noting that

$$\frac{1}{T} \int_0^T d^2 p \int_0^T dt \gamma(\vec{p}) = 1,$$

since $\gamma(\vec{p})$ itself must be normalized to unity. Substituting this expression for the one in the exponent of (2.7) allows one to cancel off the arbitrary finite time interval T .

$$A(k) = \exp -\nu \int_0^T d^2 p \int_0^T dt \gamma(\vec{p}) [1 - e^{i\vec{k} \cdot \vec{p} F(t_0 - t)}] \quad (2.9)$$

At this stage one can safely take the limit of infinite sample length, $T \rightarrow \infty$, since the exponential term's unit value for large time displacements (i.e., F small) is now cancelled in the integrand.

One can further reduce expression (2.9) by recalling that the initial echo pulses are randomly phased,

since the distance from the transmitter to each meteor (and back) is a random variable, when expressed in wavelength units.

$$\int d^2 p \gamma(p) = \int_0^\infty dp p \int_0^{2\pi} d\phi \frac{D(p)}{2\pi p}, \quad (2.10)$$

Here $D(p)$ is the distribution of initial pulse heights, and ϕ is the angle between \vec{p} and a convenient reference, which we choose as the transform vector \vec{k} . One can now use the integral definition of the zero-order Bessel function to carry out the angular ϕ integration in (2.9).

$$A(k) = \exp -\nu \int_0^\infty dt \int_0^\infty dp D(p) \{1 - J_0[kpF(t_0 - t)]\} \quad (2.11)$$

This expression, in conjunction with the Fourier transform (2.4), represent the formal solution to the problem at hand. To proceed further with the calculation of the probability density, one must assume explicit forms for the temporal decay function $F(\tau)$ and the pulse height distribution $D(p)$.

3. Meteors Which Decay Exponentially

Most of the smaller, underdense meteor echo signals are found to decay exponentially, viz,

$$F(t) = e^{-t/\eta}, \quad (3.1)$$

corresponding to molecular diffusion of reflecting electrons in the ionized column of the meteor trail itself. The decay time constant η is related to the diffusion constant D at the height of reflection and the wavelength λ of the radiation employed.

$$(\eta)^{-1} = \frac{16\pi^2 D}{\lambda^2}. \quad (3.2)$$

There are, of course, overdense meteor echoes² which do not obey the simple decay law (3.1), and one must treat them separately.

In evaluating $A(k)$ from eq (2.11), it is convenient to take the reference or measuring time t_0 to be zero and to run the time backward in a positive sense.

$$A(k) = \exp -\nu \int_0^\infty dp D(p) \int_0^\infty dt [1 - J_0(kpe^{-t/\eta})]. \quad (3.3)$$

One can simplify the calculation by settling $u = kp \exp -t/\eta$ and reversing the order of integration.

$$A(k) = \exp -\nu \eta \int_0^\infty \frac{du}{u} [1 - J_0(u)] \int_{u/k}^\infty dp D(p). \quad (3.4)$$

² L. A. Manning and V. R. Eshelman, Meteors in the Ionosphere, Proc. IRE 47, 186 (1959).

The cumulative integral of $D(p)$ expresses the probability that the initial pulse height equals or exceeds the lower limit. As noted earlier, measurements of individual echo pulse heights show that

$$\int_r^\infty dp D(p) = \frac{Q}{r^{1+\epsilon}}, \quad (3.5)$$

and it is presumed that this same law extends down to the smaller meteors which cannot be distinguished as individual echoes. The fractional exponent ϵ has been variously reported to lie between 0 and 0.3.

The case $\epsilon=0$ is analytically important, since all of the required integrations can be performed for this case and it serves as a good working example. Combining (3.4) and (3.5), we find for this special case,

$$A(k) = \exp - \nu\eta \int_0^\infty \frac{du}{u} [1 - J_0(u)] \left(\frac{Qk}{u} \right),$$

or since the definite integral has unit value.

$$A(k) = \exp - \nu\eta Qk. \quad (3.6)$$

One may now compute the probability distribution for the resultant signal by introducing (3.6) into expression (2.4).

$$\begin{aligned} W(R, \phi) &= \frac{R}{4\pi^2} \int_0^\infty dk k \int_0^{2\pi} d\omega e^{ikR \cos(\omega - \phi)} e^{-\nu\eta Qk} \\ &= \frac{R}{2\pi} \int_0^\infty dk k J_0(kR) e^{-\nu\eta Qk} \end{aligned}$$

or

$$W(R, \phi) = \frac{R}{2\pi} \frac{\nu\eta Q}{[R^2 + (\nu\eta Q)^2]^{3/2}} \quad (3.7)$$

This distribution is independent of the phase angle ϕ , expressing the fact that the vector sum of a large number of randomly phased vectors is itself randomly oriented. The probability density for R alone is obtained by integrating over ϕ .

$$W(R) dR = \frac{(\nu\eta Q) R dR}{[R^2 + (\nu\eta Q)^2]^{3/2}}. \quad (3.8)$$

It is important to note that this distribution does not possess finite moments of any order, although it is properly normalized to unity. This means that one cannot define an RMS signal level for describing the cumulative probability as suggested in eqs (1.1) and (1.2). The root of the problem, of course, lies in the initial pulse height distribution assumption of eq (3.5). The integrals of $W(R)$ diverge for large amplitudes, which, in turn, are produced by the very large individual echoes. The assumed distribution (3.5) does not suppress these large echoes rapidly enough to insure convergence, although most workers agree that the form (3.5) must eventually change its rate of decrease with r so as to properly represent the rarity of really large meteors.

The function which is commonly measured experimentally is the cumulative probability that the total signal amplitude R exceeds a prescribed level r .

$$P(|R| > r) = \int_r^\infty dR W(R) = \frac{1}{\left[1 + \left(\frac{r}{\nu\eta Q}\right)^2\right]^{1/2}} \quad (3.9)$$

This result is plotted on Rayleigh graph paper versus the ratio $r/\nu\eta Q$ in figure 2. The Rayleigh cumulative distribution $P = \exp -(r^2/2\sigma^2)$ plots as a straight line with slope minus one on this paper. The probability of observing very small signals r is seen to follow the straight line Rayleigh behavior with slope minus one. This is because the small argument expansion of eq (3.9)

$$\lim_{r \rightarrow 0} (P) = 1 - \frac{1}{2} \frac{r^2}{(\nu\eta Q)^2} \quad (3.10)$$

is essentially identical to that for the Rayleigh distribution (1.1) with $\sigma = (\nu\eta Q)$. On the other hand, we have already noted that the meteor distribution (3.8) does not possess a finite variance, so that $\nu\eta Q$ cannot be identified with an RMS signal level. Note, however, that the curve in figure 2 is displaced upward from the normal Rayleigh curve by a factor of $\sqrt{2} = 0.707$, since $P(r)$ is plotted versus $\nu\eta Q$, not $\sqrt{2}\nu\eta Q$ which would be the root mean square signal level of a Rayleigh distribution with the same small amplitude asymptotic behavior.

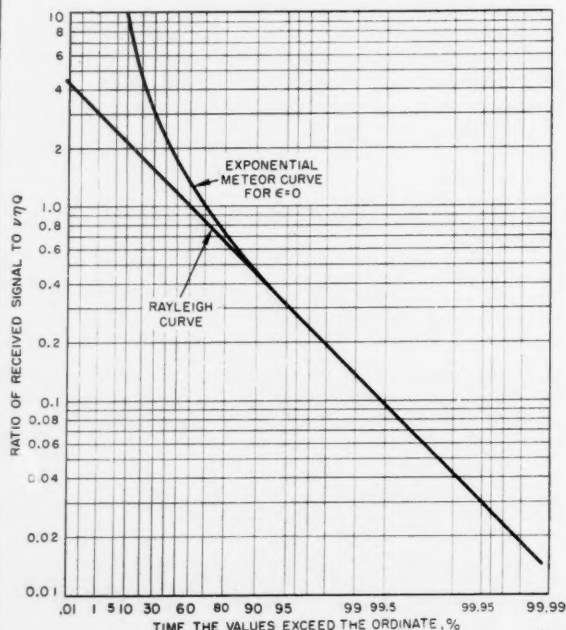


FIGURE 2. Probability that signal exceeds prescribed level for exponential meteors with $\epsilon=0$, compared with Rayleigh curve.

The cumulative probability distribution for the very large, unusual signals is markedly different than a Rayleigh distribution, reflecting the unique character of meteor echoes. One may expand (3.9) for large r to find

$$P(R > r) \simeq \frac{\nu \eta Q}{r}$$

in agreement with the qualitative result (1.5). This also agrees in form with the basic assumption (3.5) for the cumulative probability that an individual meteor echo amplitude exceeds the level r . The important difference is that eq (3.5) assumes that a meteor signal has just been received, whereas eq (3.11) calculates the residual large meteor signal at any time. The additional factor $\nu \eta$ in (3.11) is the average rate of occurrence times the half life of individual meteors, and is a measure of the fraction of time that the large, isolated meteor signals are greater than e^{-1} of their initial value.

The simplified theoretical result of eq (3.9) was compared with experimental data gathered by Bowles³ on the Havana, Ill., to Boulder, Colo., VHF scatter link operated by the National Bureau of Standards. Totalizer outputs obtained with rhombic antennas directed off path were employed, so as to accentuate the meteoric signal contribution. The experimental points follow a Rayleigh distribution above the 50 percent level, but indicate a higher probability of observing the very large signals produced by combinations of strong echoes than is predicted by the Rayleigh distribution. This is in qualitative agreement with the theoretical result plotted in figure 2, although the quantitative agreement is not as precise as one would like. It is believed that the residual discrepancy can be traced to the three basic assumptions used in deriving eq (3.9):

1. The large meteors do not decay exponentially, as assumed in eq (3.1), especially if they are strong enough to produce overdense echoes.

2. The assumption $\epsilon = 0$ in applying eq (3.5) is not consonant with some meteor radar experiments, which suggest small fractional values.

3. The initial pulse height cumulative distribution (3.5) is almost certainly not correct for the very large meteor end of the spectrum.

The second possibility was checked numerically by rederiving the transform function $A(k)$ for arbitrary ϵ .

$$\begin{aligned} A_\epsilon(k) &= \exp -\nu \eta \int_0^\infty \frac{du}{u} [1 - J_0(u)] \frac{Q k^{1+\epsilon}}{u^{1+\epsilon}} \\ &= \exp -\nu \eta Q k^{1+\epsilon} \xi \end{aligned} \quad (3.12)$$

where

$$\xi = \frac{1}{1+\epsilon} \frac{1}{2^{1+\epsilon}} \frac{\Gamma\left(\frac{1-\epsilon}{2}\right)}{\Gamma\left(\frac{3+\epsilon}{2}\right)}$$

³K. L. Bowles, private communication.

However, the coefficient of $k^{1+\epsilon}$ which appears in the polar integration for computing $W(R)$ may be removed by renormalizing k itself.

$$\begin{aligned} W(R) R dR &= R dR \int_0^\infty dk k J_0(kR) e^{-\gamma k^{1+\epsilon}} \\ &= d\rho \left[\rho \int_0^\infty dz z J_0(z\rho) e^{-z^{1+\epsilon}} \right], \end{aligned} \quad (3.13)$$

with

$$\rho = \frac{R}{\gamma^{1/(1+\epsilon)}} \text{ and } z = k \gamma^{1/(1+\epsilon)}.$$

The function given by the bracketed integral in (3.13) was tabulated numerically on a digital computing machine for the following values: $\epsilon = 0.1, 0.2, 0.25, 0.3$, and the results are plotted in figure 3.

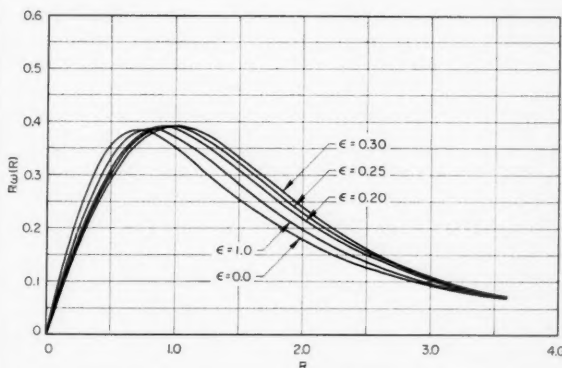


FIGURE 3. Plots of the probability that the instantaneous signal lies in the range R to $R+dR$ for various values of the parameter ϵ which determines the distribution of initial pulse heights for individual meteors.

The cumulative probability corresponding to the various ϵ -fractional distributions (3.13) was also computed numerically using the analytical equivalence

$$\begin{aligned} P(\rho) &= \int_\rho^\infty d\rho \rho \int_0^\infty dz z J_0(\rho z) e^{-z^{1+\epsilon}}, \\ &= 1 - \rho \int_0^\infty dz J_1(\rho z) e^{-z^{1+\epsilon}}, \end{aligned} \quad (3.14)$$

which follows by reversing the order of integration, and treating the limits cautiously. The second form is plotted in figure 4 for various values of ϵ on Rayleigh paper. The various curves in this figure do not have the same asymptotic behavior because of different normalizations of the vertical scale for each ϵ . However, one can imagine the signal levels adjusted for each case so that all approach the same Rayleigh limit. This would show that the $P(r)$ curves all fall between the $\epsilon = 0$ curve shown in figure 2 and the Rayleigh distribution straight lines. Insofar as the present data of Bowles suggests

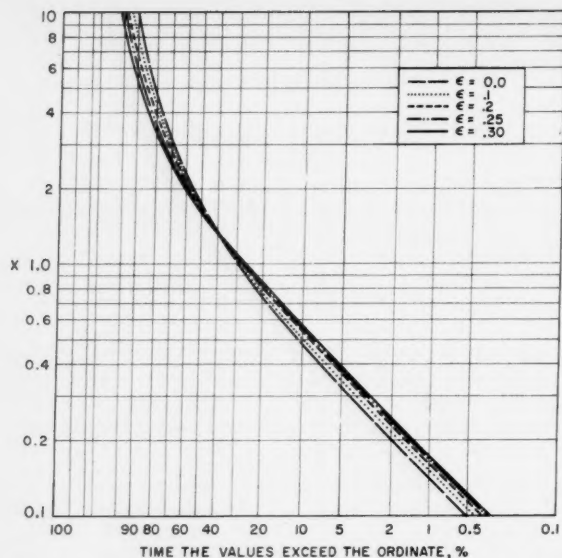


FIGURE 4. Plots of the cumulative probability that the instantaneous signal exceeds a prescribed level for various values of the parameter ϵ which determines the distribution of initial pulse heights for individual meteors.

that the departure from Rayleigh is not as marked as that predicted in eq (3.9), this would seem to indicate that values of ϵ near 0.2 may give better agreement. On the other hand, the data sample now available is certainly too limited to pronounce final judgment.

The first two objections raised above also deserve further attention in a careful comparison of the theory with experiment. The approximate descriptions developed by Manning and Eshelman (see footnote 3) for overdense echoes were examined briefly, but unfortunately the split (p) integrations were not found to be tractable analytically.

Valuable discussions of the problem with V. R. Eshelman and T. A. Magness are acknowledged. K. L. Bowles kindly made his experimental data available prior to publication. B. A. Troesch and L. Stohler computed the numerical results displayed in figures 3 and 4.

(Paper 64D5-8C)

Computation and Measurement of the Fading Rate of Moon-Reflected UHF Signals¹

S. J. Fricker, R. P. Ingalls, W. C. Mason, M. L. Stone, and D. W. Swift²

(April 29, 1960)

A method is described for predicting the fast fading rate of moon-reflected signals. It is based entirely upon considerations of the observer-moon positions and relative motions. Experimental results which are in good agreement with the computed fading rates have been obtained from a moon-reflection experiment at a frequency of 412 megacycles per second. Some possible implications of this method of interpreting fading rates are given.

1. Introduction

The effect on UHF signals of transmission through the ionosphere and into space is becoming a problem of increasing importance. At present the characteristics of the transmission medium are not known in detail, and the effects upon transmitted signals remain questionable.³ It is known that under certain conditions, e.g., auroral activity, the disturbances are such that radar returns may be obtained from them. While this provides valuable information about the backscatter which may be expected, it does not give a direct measure of the effect upon the transmitted signal. Some information may be obtained by making use of the signals received from radio stars; the scintillation rates of such signals have been observed to increase at times of disturbed ionospheric conditions. However, a more controllable extra-terrestrial signal source has some advantages compared with radio stars. Prior to the advent of artificial satellites, it appeared that use of the moon as a reflector was a reasonable means of obtaining such a signal. Moon-reflected signals have been reported for some years [2],⁴ and the use of moon relay circuits for communications purposes is developing, but most of the measurements reported have not been directly applicable to the problem of ionospheric transmission effects upon UHF signals. The results reported in this paper were obtained in the course of a moon-reflection experiment carried out between South Dartmouth, Mass., and Alpha, Md. [3]. The procedures established in this test formed the basis for a later transmission experiment carried out between College, Alaska, and Westford, Mass. It is hoped to publish a full account of this latter experiment at a later date.

Among the results of the test was the direct correlation between the fading rate of the received signal and the predicted calculations of the total libration rate of the moon. The spectral broadening

of the lunar signal was thus shown to be an effect of the motion of the moon. The major portion of this paper is concerned with an outline of these calculations and a demonstration of their agreement with measured values.

2. System Used in the Experiment

The transmitter and 60-ft diam parabolic antenna were located at the M.I.T. field station at Round Hill, South Dartmouth, Mass. (41.5395° N, 70.9512° W). The receiving site was at Alpha, Md. (39.3224° N, 76.9258° W), about 350 miles from South Dartmouth. The receiving system used a 28-ft diam parabolic antenna with two orthogonal feeds. Two identical receiving systems were used with common local oscillators. With a transmitted power of 40 kW at 412 Mc/s and a final receiver bandwidth of 50 c/s, a signal-to-noise ratio of 25 to 30 db was obtained. Paper tape records were made of the detected signals, and periodic magnetic tape recordings were made of the signals at an intermediate frequency of 2,500 c/s. Observations were made from moonrise to moonset each day from 6 August until 29 August 1957.

3. Paper-Tape Recording for Fading-Rate Measurements

Typical recordings of the detected signals are shown in figures 1, 2, and 3. The frequency of the "fading" shown is a prominent feature, and during

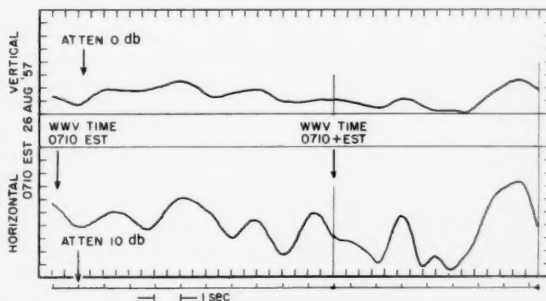


FIGURE 1. Fast recording of detected signal, slow fading rate.
(Traced from original recording chart.)

¹ Contribution from Lincoln Laboratory, Massachusetts Institute of Technology, Lexington 73, Mass. The Lincoln Laboratory is operated with support from the U.S. Army, Navy, and Air Force.

² Present address of D. W. Swift: Avco Research and Advanced Development Division, Wilmington, Mass.

³ A summary of the work in this area through 1956 is given in reference [1].

⁴ Figures in brackets indicate the literature references at the end of this paper.

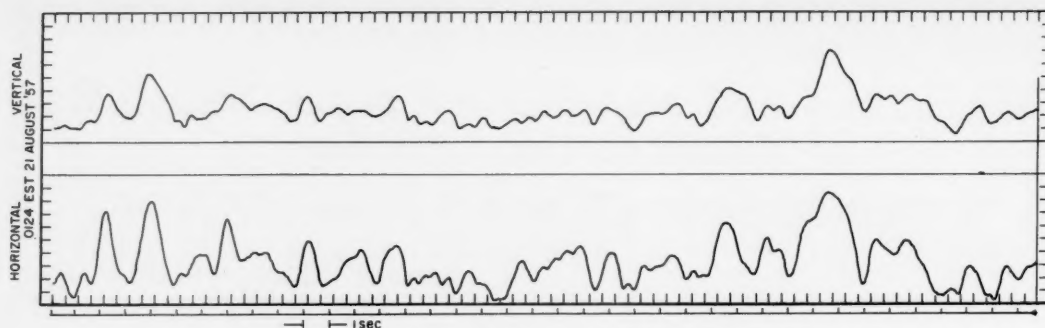


FIGURE 2. Fast recording of detected signal, medium fading rate.
(Traced from original recording chart.)

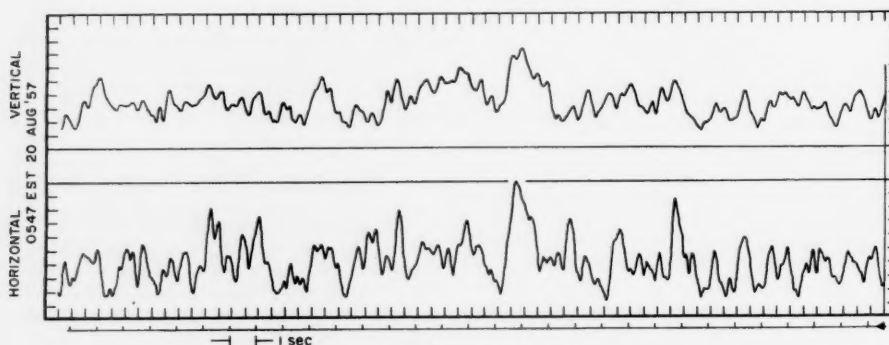


FIGURE 3. Fast recording of detected signal, fast fading rate.
(Traced from original recording chart.)

the test it was found to vary within fairly wide limits. At times the rate appeared to be several cycles per second, at other times the signal level remained almost constant for several minutes. Figure 1 shows a typical section of a recording taken at a relatively slow fading rate period, figure 2 shows an average fading rate, and figure 3 shows one of the faster fading rates. All of these were taken during the test with a detector time constant of 0.15 sec. The magnetic-tape recordings of the 2,500 c/s IF signals formed a convenient stored source of signals to be played back through a detector with an adjustable time constant. Some experimentation was needed to determine a suitable time constant which, it was felt, produced a record that showed up most of the signal variations without being too affected by noise. A value of 0.015 sec for the time constant was chosen as a suitable compromise, and many of the recorded 2,500 c/s IF signals were replayed with this modified detector system. Typical results obtained on a Brush recorder are shown in figures 4 (a) and (b). The paper-tape recordings thus obtained were used to measure the fading rate in a rather arbitrary but consistent manner. This was done simply by counting the number of detected signal maximums occurring over an interval of approximately 1 min at any given period. Results varied from 3 to 4 fades/sec to approximately 0.005 fades/sec. The higher frequencies were observed most of the time, while the very low fading rates

were comparatively infrequent, and lasted for only a short time in any case. Some of the measurements are shown plotted as fading rate versus time of day in figures 11 (a) to (g).

4. Libration-Rate Computations

It seemed to be a reasonable assumption that the effective libration of the moon had a large part to play in producing the varying fading rates of the moon-reflected signals [2]. (The computations to be described first determine what is termed here the "total libration rate" of the moon, and thus proceed to calculate the resulting "Doppler spread." This can then be interpreted as a fading rate, and compared with the measured fading rate.)

An overall view of the geometry involved in the calculation may be useful. Figure 5 shows a simplified sketch of the earth-moon system. In effect, the moon presents a slightly varying face to the earth, due to the dynamics of its motion. This means that an observer on earth looking toward the center of the moon does not always see the same surface point (A in fig. 5), but rather a changing point on the surface. The motion involved is described by the selenographic latitude and longitude figures listed in the *American Ephemeris and Nautical Almanac*. The axes about which these positions are measured are shown in figure 5. In general, the axis for the selenographic latitude variations is inclined to the celestial equator.

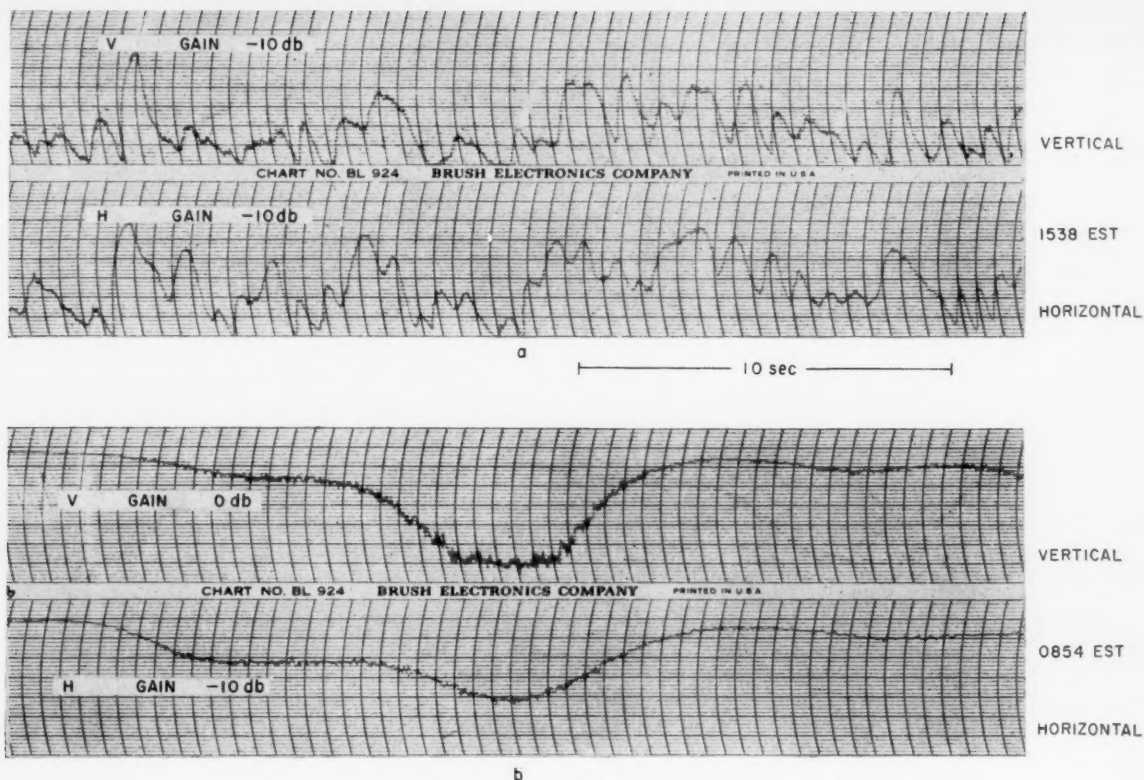


FIGURE 4 a, b. Fast recordings of detected signals with 0.015-sec. time constant.

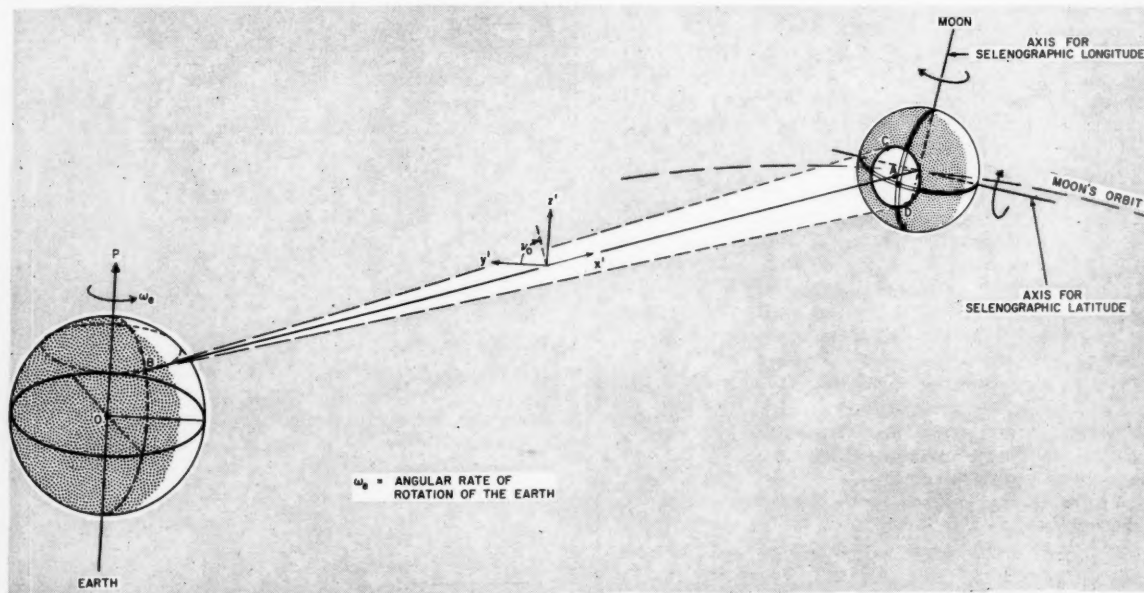


FIGURE 5. Geometry for fading rate computations.

An observer on earth, at point B, must look in the direction BA in order to see the moon. Then, due to the earth's rotation about the axis OP, the ray BA sweeps across the moon's surface. On addition, the combination of these two effects give rise to what is termed the "total libration" of the moon. A system of axes can be set up, and the motion of the moon can be resolved along the same set of axes. Combination of the two sets of components is then a simple matter. In effect, expressions are derived for the total libration rates in latitude and longitude, $l_{T\beta}$ and l_{TL} , respectively, of the form

$$l_{T\beta} = (l'_{\beta} + f_1),$$

and

$$l_{TL} = (l'_L + f_2),$$

where l'_{β} and l'_L are libration rates due to the moon's motion, and f_1 and f_2 are equivalent functions due to the earth's motion. All the functions, of course, are time-dependent. The total libration rate is given by the square root of the sums of the squares of $l_{T\beta}$ and l_{TL} . Hence, both of these quantities must become small in order to give a low value for the total effective libration rate.

With the libration rate computed, the next step is to transform it into an effective fading rate. Suppose that instantaneously the moon had only one strongly reflecting region located centrally at point A, so that a cw signal reflected from this region would show only the main Doppler shift in frequency. If now two additional reflecting portions are assumed to exist at C and D, toward the rim of the moon and symmetrically located with respect to the center portion, then each of these regions would be in motion due to the effective libration of the moon. The component of this motion resolved along the direction to the observer would give rise to a small additional "Doppler spread," so that an incident cw signal would be reflected with two Doppler sidebands. Reception and detection of this signal would then show a signal of varying level, with the Doppler spread in effect producing the "fading rate." Now actually a large portion of the moon must be effective in giving rise to appreciable reflections, and each small contributing area gives rise to its own particular Doppler spread. Integration over the whole surface is difficult, since the reflection mechanism is by no means well understood, and the moon is a rough body. However, it is possible to examine the moon's surface to determine the maximum extent of the Doppler spread. Consider a circle drawn on the moon's surface, the radius of this circle being specified as a given fraction of the actual full radius of the moon. All points on this circle can then be examined to determine that point which gives rise to the maximum magnitude of Doppler spread. If the point C on the moon's surface is considered to be the point in question, then its position on the circle is specified by the angle ν_0 , measured from the y' axis. It is apparent that major emphasis in the calculation must be given to a careful consideration of the geometry involved.

4.1. Moon's Position

Figure 6 shows a sketch of the celestial sphere with the celestial equator in the same plane as the earth's equator. The ecliptic has its ascending node on the celestial equator at the point γ , the vernal equinox, while the ascending node of the moon's orbit on the celestial equator is marked by the point γ' . The moon is assumed to be at the point B, so that the right ascension of the moon, RA_m , is given by the arc γC , and the declination, δ_m , by CB .

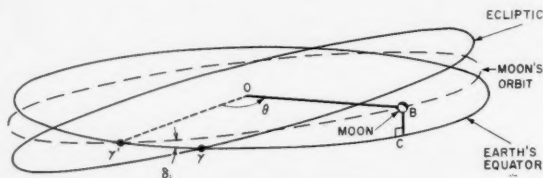


FIGURE 6. Moon-position geometry.

The angle θ is measured in the plane containing the radii $O\gamma'$ and OB , and is taken to be positive in the direction from $O\gamma'$ to OB . The angle δ_i is the inclination angle of the great circle, centered at O , and passing through the points γ' and B .

At any particular time the position of the point γ' is given by noting the value of the moon's right ascension during the preceding month when its declination is zero, and when it is changing from negative to positive values. Hence, with this value of right ascension RA_0 in degrees, $\gamma'\gamma$ is given by

$$\gamma'\gamma = 360^\circ - RA_0,$$

and

$$\gamma'C = \gamma'\gamma + RA_m \quad (2)$$

Thus, from the triangle $\gamma'CB$, the angle θ is specified by

$$\cos\theta = \cos(\gamma'\gamma + RA_m) \cos\delta_m, \quad (3)$$

and

$$\delta_i = 2 \arcsin \sqrt{\frac{\sin(S - \theta) \sin(S - \gamma'\gamma - RA_m)}{\sin\theta \sin(\gamma'\gamma + RA_m)}} \quad (4)$$

where

$$S = [\theta + \gamma'\gamma + RA_m + |\delta_m|]/2.$$

4.2. Orientation of Moon in its Orbit

Figure 7 shows the moon's equatorial plane, with its ascending node on the celestial equator designated as γ'' . The angle Ω' is defined as the distance along the celestial equator from the true equinox to the ascending node of the moon's mean equator, so that the arc $\gamma'\gamma''$ is given by

$$\gamma'\gamma'' = \Omega' + \gamma'\gamma \quad (5)$$

Consider two vectors \bar{A}_1 , \bar{A}_2 , where the vector \bar{A}_1 is parallel to the equatorial plane of the moon and perpendicular to OB , while \bar{A}_2 is orthogonal to \bar{A}_1

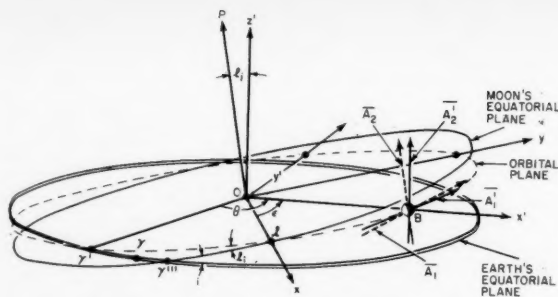


FIGURE 7. Moon orientation geometry.

and normal to the equatorial plane and directed upward. These vectors describe the axes about which the moon's selenographic latitude and longitude are measured. For computational purposes, it is convenient to transform these two vectors into two vectors \bar{A}_1' , \bar{A}_2' , where \bar{A}_1' is in the moon's orbital plane, perpendicular to OB , and \bar{A}_2' is orthogonal to \bar{A}_1' and OB . Let three unit vectors be defined as follows:

\bar{i}_x = unit vector in direction OB ,

\bar{i}_z = unit vector in direction OZ (OZ perpendicular to orbital plane),

\bar{i}_p = unit vector in direction OP (OP perpendicular to equatorial plane).

Consider an xyz -axis system, with the x -axis coincident with Ol and with the y -axis in the orbital plane. Then the angle ϵ is defined as the angle from the x -axis to OB , measured in the orbital plane. The angle l_i is the included angle $\gamma'l\gamma''$ (see fig. 7). Unit vectors \bar{i}_a , \bar{i}_p , in the direction of \bar{A}_1 and \bar{A}_1' respectively, are given by

$$\bar{i}_a = \frac{\bar{i}_p \times \bar{i}_x}{|\bar{i}_p \times \bar{i}_x|} \quad (6)$$

and

$$\bar{i}_p = \bar{i}_z \times \bar{i}_x. \quad (7)$$

The vectors \bar{A}_1 , \bar{A}_2 can be described with the aid of unit vectors as

$$\bar{A}_1 = A_1 \bar{i}_a, \quad (8)$$

and

$$\bar{A}_2 = A_2 (-\bar{i}_y \sin l_i + \bar{i}_z \cos l_i). \quad (9)$$

The relations between the two sets of vectors \bar{A}_1 , \bar{A}_2 and \bar{A}_1' , \bar{A}_2' give the following expressions for the magnitudes A_1 and A_2 :

$$A_1' = (\bar{A}_1 + \bar{A}_2) \cdot \bar{i}_y = \frac{A_1}{\sqrt{1 + \cos^2 \epsilon \tan^2 l_i}} - A_2 \sin l_i \cos \epsilon \quad (10)$$

$$A_2' = (\bar{A}_1 + \bar{A}_2) \cdot \bar{i}_z = \frac{A_1 \cos \epsilon \tan l_i}{\sqrt{1 + \cos^2 \epsilon \tan^2 l_i}} + A_2 \cos l_i \quad (11)$$

The angle i is defined as the inclination of the moon's mean equator to the earth's true equator. With knowledge of $\gamma'\gamma''$, i and δ_i , the triangle $\gamma'\gamma''l$ can be solved for l_i to give

$$l_i = \arccos [\cos \delta_i \cos i + \sin \delta_i \sin i \cos (\gamma'\gamma'')] \quad (12)$$

and

$$\gamma'l = \arccos \left[\frac{\cos \delta_i \cos l_i - \cos i}{\sin \delta_i \sin l_i} \right]. \quad (13)$$

With the angle θ obtained from (3) and $\gamma'l$ from (13), the angle ϵ is given by

$$\epsilon = \theta - \gamma'l. \quad (14)$$

4.3. Effect of Nonspherical Earth

If a meridional cross section of the earth is assumed to be elliptical in shape, then each point on the surface has a geocentric latitude that is slightly different from its normal geographic latitude. In addition, of course, the radius from the center point of the earth to the observer varies with latitude. The relations among the following parameters:

a_{eq} = equatorial radius of earth,

r = radius to point at geocentric latitude ϕ_c ,

e = ellipticity,

ϕ_c = geocentric latitude,

ϕ = geographic latitude,

are given by

$$r^2 = \frac{a_{eq}^2 (1 - e^2)}{1 - e^2 \cos^2 \phi_c}, \quad (15)$$

$$\tan \phi_c = (1 - e^2) \tan \phi, \quad (16)$$

$$e^2 = 0.006768658.$$

4.4. Doppler Shift of Moon-Reflected Signal

The sketch shown in figure 8 demonstrates the geometry involved. In essence, for an observer at position A , it is necessary to calculate the rate of change of the distance D . The moon's position is given by the distance D_0 and the coordinates shown in figure 9. It is necessary to note the distinction between the two sets of coordinates shown in this figure. The unprimed set is related to the earth's equatorial plane, while the primed system is related to the moon's orbital plane. The following parameters are shown in figures 8 and 9.

D_0 =distance from center of earth to center of moon,

D =distance from observer at A to moon's center,

a_a =distance between earth's center and observer at A ,

ψ =angle between D_0 and a_a ,

δ_i =angle between earth's equatorial plane and the moon's orbital plane,

$\gamma'C$ =right ascension of moon $+\gamma'\gamma$,

δ_m =declination of moon,

ϕ_a =geocentric latitude of observer,

$\gamma'D$ =right ascension of observer $+\gamma'\gamma$.

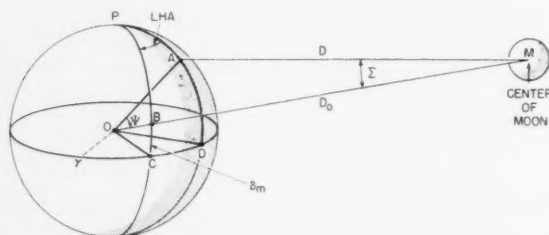


FIGURE 8. Geometry for distance from observer to moon.

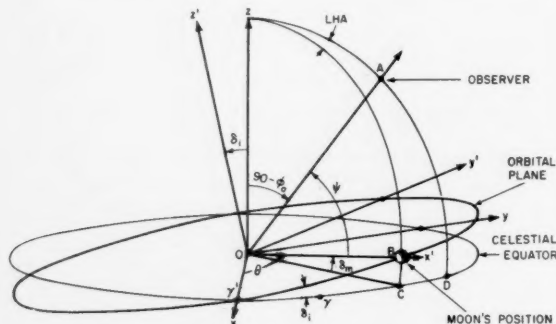


FIGURE 9. Geometry for positions of observer and moon.

In order to express the angle ψ in terms of the position parameters two unit vectors are introduced. A unit vector \bar{i}_a is defined in the direction OA , while \bar{i}_z' is defined as a unit vector in the direction of D_0 in figure 8 (OB in fig. 9). These vectors may be expressed as

$$\bar{i}_a = \bar{i}_z \sin \phi_a + \bar{i}_x \cos \phi_a \cos (\gamma'D) + \bar{i}_y \cos \phi_a \sin (\gamma'D), \quad (17)$$

and

$$\bar{i}_z' = \bar{i}_z \sin \delta_m + \bar{i}_x \cos \delta_m \cos (\gamma'C) + \bar{i}_y \cos \delta_m \sin (\gamma'C) \quad (18)$$

The angle ψ is given by

$$\cos \psi = \bar{i}_z' \cdot \bar{i}_a$$

$$\therefore \cos \psi = \sin \delta_m \sin \phi_a + \cos \phi_a \cos \delta_m \cos (LHA) \quad (19)$$

where LHA is the local hour angle of the moon, and may be expressed as

$$LHA = (\gamma'D) - (\gamma'C) = (\gamma D) - (\gamma C)$$

Now the rate of change of the distance D is given by

$$\dot{D} = \frac{d}{dt} \sqrt{D_0^2 + a_a^2 - 2a_a D_0 \cos \psi}$$

$$\dot{D} = \frac{\dot{D}_0(D_0 - a_a \cos \psi) - D_0 a_a \frac{d}{dt} (\cos \psi)}{D} \quad (20)$$

The values of horizontal parallax, Π , listed in the *American Ephemeris* may be used to compute D_0 , giving

$$D_0 = \frac{a_{eq}}{\sin \Pi},$$

and

$$\dot{D}_0 = -\frac{a_{eq} \cos \Pi}{\sin^2 \Pi} \frac{d\Pi}{dt}$$

It is also necessary to differentiate $\cos \psi$ from eq (19), which in turn involves the rate of change of the local hour angle. In this manner the angular rotation rate of the earth and the rate of change of right ascension of the moon are brought into the computations. Thus

$$\frac{d}{dt} (\cos \psi) = \delta_m [\cos \delta_m \sin \phi_a - \sin \delta_m \cos \phi_a \cos (LHA)]$$

$$- \cos \phi_a \cos \delta_m \sin (LHA) \frac{d}{dt} (LHA)$$

and

$$\frac{d}{dt} (LHA) = \omega_e - \frac{d}{dt} (RA_m),$$

where ω_e is the angular velocity of the earth, and $d/dt (RA_m)$ is the major component of the angular velocity of the moon about the earth.

The above expressions enable \dot{D}_a and \dot{D}_b to be derived for the transmitting and receiving stations, so that the total Doppler shift f_d is given by

$$f_d = -\frac{f_e}{c} (\dot{D}_a + \dot{D}_b) \quad (21)$$

where D_a and D_b now represent the distances between the transmitter and the moon and the receiver and the moon, respectively.

4.5. Libration-Rate Computation

The essence of this computation lies in the description of the motion of a point on the moon's surface as seen by an observer on earth. Part of this motion is due to the actual libration of the moon, and part is due to the movement of the observer. Thus the computations involve the rates of change of the selenographic latitude and longitude, plus the rate of change of some quantity which describes the geometrical earth-moon relationship. The effects of these two physically distinct processes, when added appropriately, then give the total libration rate. It is convenient to use the sign convention used in the *American Ephemeris*. Thus, the selenographic longitudes are measured in the plane of the moon's equator, positive toward the west, the axis of reference being the radius of the moon which passes through the mean center of the visible disk. Latitudes are measured from the moon's equator, positive toward the north.

In section 4.2, two vectors \bar{A}_1, \bar{A}_2 were considered. Now, let \bar{A}_1 become the axial vector \bar{S}_β and \bar{A}_2 become the axial vector \bar{S}_L , where \bar{S}_β and \bar{S}_L represent axes about which the selenographic latitudes and longitudes are measured. The time derivatives of the scalar values of these quantities are given by

$$l_\beta = \frac{dS_\beta}{dt},$$

and

$$l_L = \frac{dS_L}{dt}.$$

Also, in sections 4.2 and 4.4 primed quantities were used with reference to the moon's orbital plane. The same significance again is attached to primed quantities here. Equations (10) and (11) can be rewritten to give S'_β and S'_L , and the resulting expressions differentiated to give

$$\begin{aligned} \frac{dS'_\beta}{dt} = l'_\beta = & \frac{l_\beta}{\sqrt{1 + \cos^2 \epsilon \tan^2 l_i}} - l_L \sin l_i \cos \epsilon \\ & - \left[\frac{S_\beta \cos^2 \epsilon \tan^2 l_i \sec^2 l_i}{(1 + \cos^2 \epsilon \tan^2 l_i)^{3/2}} + S_L \cos \epsilon \cos l_i \right] \frac{dl_i}{dt} \\ & + \left[\frac{S_\beta \cos \epsilon \tan^2 l_i \sin \epsilon}{(1 + \cos^2 \epsilon \tan^2 l_i)^{3/2}} + S_L \sin \epsilon \sin l_i \right] \frac{d\epsilon}{dt}, \end{aligned} \quad (22)$$

and

$$\begin{aligned} \frac{dS'_L}{dt} = l'_L = & \frac{l_L \cos \epsilon \tan l_i}{\sqrt{1 + \cos^2 \epsilon \tan^2 l_i}} + l_\beta \cos l_i \\ & + \left[\frac{S_\beta \cos \epsilon \sec^2 l_i}{(1 + \cos^2 \epsilon \tan^2 l_i)^{3/2}} - S_L \sin l_i \right] \frac{dl_i}{dt} \\ & - \left[\frac{S_\beta \sin \epsilon \tan l_i}{(1 + \cos^2 \epsilon \tan^2 l_i)^{3/2}} \right] \frac{d\epsilon}{dt} \end{aligned} \quad (23)$$

The effect of the observer's motion may be introduced through use of the parallax angle \sum , shown in figure 8. Consider \sum to be an axial vector representing a small rotation when the magnitude of \sum represents the angle between D and D_0 . Hence for small \sum , \sum is given by

$$\sum = (\bar{i}_x \cdot \bar{i}_a) \frac{a_a}{D_1} \quad (24)$$

where

$$D_1 = D_0 - a_a \cos \psi \quad (25)$$

In general, the observer's motion will give contributions to both the longitudinal and the latitudinal libration rates. Bearing in mind the association of the primed coordinates with the moon's orbit, and the fact that the selenographic latitudes and longitudes were adjusted to this set of coordinates, it is apparent that the projections of \sum on the y' and z' axes are required. The component in the z' direction is given by

$$\sum_L = (\bar{i}_x \times \bar{i}_a) \cdot \bar{i}_z \frac{a_a}{D_1} = \frac{a_a}{D_1} \bar{i}_a \cdot \bar{i}_y, \quad (26)$$

and in the y' direction by

$$\sum_\beta = (\bar{i}_x \times \bar{i}_a) \cdot \bar{i}_y \frac{a_a}{D_1} = -\frac{a_a}{D_1} \bar{i}_a \cdot \bar{i}_z, \quad (27)$$

From figure 9, it is seen that

$$\bar{i}_{z'} = \bar{i}_z \cos \delta_i - \bar{i}_y \sin \delta_i \quad (28)$$

and the unit vector $\bar{i}_{y'}$ is given by

$$\bar{i}_{y'} = \bar{i}_z \times \bar{i}_{z'}$$

with $\bar{i}_{z'}$ and \bar{i}_x described by eqs (28) and (18) respectively. The dot products in eqs (26) and (27) may now be expanded to give the components of \sum as,

$$\begin{aligned} \sum_L = \frac{a_a}{D_1} \{ & \cos \delta_i \cos \delta_m \cos \phi_a \sin (LHA) \\ & - \sin \delta_i [\sin \delta_m \cos \phi_a \cos \gamma' D - \cos \delta_m \cos (\gamma' C) \sin \phi_a] \} \end{aligned} \quad (29)$$

and

$$\sum_\beta = \frac{a_a}{D_1} [\sin \delta_i \cos \phi_a \sin (\gamma' D) - \cos \delta_i \sin \phi_a] \quad (30)$$

The above two equations can be differentiated to give their rates of change. This involves a number of terms, as most of the parameters are time dependent. However γ' and δ_i change so slowly that negligible error is introduced by assuming them to be constant. The terms thus involve the rate of change of the distance, \dot{D}_1 ; the angular rotation rate of the earth ω_e ; and the rates of change of the moon's right ascension and declination. Hence \sum_L and \sum_β

may be expressed as

$$\begin{aligned}\dot{\Sigma}_L = & -\frac{\dot{D}_1}{D_1} \Sigma_L + \omega_e \frac{a_a}{D_1} \cos \varphi_a [\cos \delta_i \cos \delta_m \cos (LHA) + \sin \delta_i \sin \delta_m \sin (\gamma'D)] \\ & - \frac{d}{dt} (RA_m) \cos \delta_m \frac{a_a}{D_1} [\cos \delta_i \cos \varphi_a \cos (LHA) + \sin \delta_i \sin \varphi_a \sin (\gamma'C)] \\ & - \frac{a_a}{D_1} \dot{\delta}_m \{ \sin \delta_m \cos \delta_i \cos \varphi_a \sin (LHA) \\ & + \sin \delta_i [\cos \delta_m \cos \varphi_a \cos (\gamma'D) + \sin \delta_m \cos (\gamma'C) \sin \varphi_a] \} \quad (31)\end{aligned}$$

and

$$\dot{\Sigma}_\beta = -\frac{\dot{D}_1}{D_1} \Sigma_\beta + \omega_e \frac{a_a}{D_1} \sin \delta_i \cos \varphi_a \cos (\gamma'D), \quad (32)$$

where

$$\dot{D}_1 = \dot{D}_0 - a_a \frac{d}{dt} (\cos \psi).$$

In obtaining the sum of the effects of the moon's motion and the earth's motion, it must be remembered that a rotation in one sense on earth appears as the opposite sense on the moon. That is, an increase of the parallax angle toward the west or north appears as a rotation of the moon toward the east or south. Hence, the components of the total libration rate for a two-station system are

$$l_{T\beta} = \left\{ l'_\beta - \frac{1}{2} \dot{\Sigma}_{\beta a} - \frac{1}{2} \dot{\Sigma}_{\beta b} \right\} \quad (33)$$

$$l_{TL} = \left\{ l'_L - \frac{1}{2} \dot{\Sigma}_{La} - \frac{1}{2} \dot{\Sigma}_{Lb} \right\} \quad (34)$$

where the subscripts *a* and *b* refer to the transmitting and receiving stations. The total libration rate, l_T , is thus given by

$$l_T = \sqrt{l_{T\beta}^2 + l_{TL}^2}. \quad (35)$$

4.6. Doppler Spread of Moon-Reflected Signal

So far, when considering the geometry of the earth-moon system, the reference point on the moon has been its center. The corresponding point seen on the surface of the moon may be imagined to be the main reflecting point. However, as mentioned previously, many other points on the moon's surface are effective as reflectors. Any one such point will be in motion due to the libration of the moon, and in consequence of the fact that its line-of-sight velocity is different from that of the central point, its Doppler frequency will be slightly shifted with respect to that of the central point, i.e., with respect to the main computed Doppler frequency. This shift in Doppler frequency is referred to as the "Doppler spread." Obviously, this will depend upon the position of the offset region as well as on the angular velocities involved. Consequently, in order to obtain an idea of the maximum Doppler spread that may occur over

a given portion of the moon's surface, it is convenient to specify a ring whose radius is a given fraction of the radius of the moon, and to examine this ring from 0° to 360° in order to pick out the maximum value of the Doppler spread.

This method of computing the Doppler spread allows a number of approximations to be made. The choice of which approximations to make can be based upon the magnitude of the total libration rate. When this is not too small, the Doppler spread is of the order of cycles per second, and any refinement in the computation would have a relatively small effect. As the libration rate decreases, so does the magnitude of the Doppler spread, and at some point the errors introduced by the approximate computations may become significant. The overall accuracy depends, of course, upon the accuracy of the input information and, if this is not very precise, any small differences carried in the computations may not show up.

Figure 10 shows a sketch of the geometry involved. The moon's center is at 0 and the observer at 0'. Although only one observer's position is shown, the computations are carried out for two separated stations, i.e., transmitter at station *a* and receiver at station *b*. The axes shown at the moon's position refer to the moon's orbit, as mentioned previously, and the quantities l_{TL} and $l_{T\beta}$ are used to describe the moon's apparent rotation about these axes. The circle to be examined is shown as *GLCH* with radius *FL*, or kR_m , where R_m is the moon's radius and *k* is the fractional moon's radius. The position of the point *L* is specified by giving the value of *k* and the angle ν , where ν is measured positively upwards from a line parallel to the axis of $l_{T\beta}$.

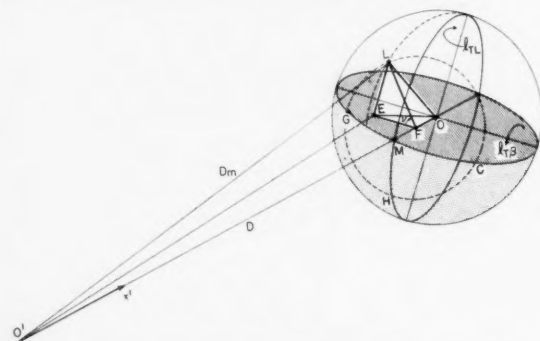


FIGURE 10. Geometry for Doppler-spread computations.

Due to the apparent rotation of the moon about the $l_{T\beta}$ axis, the point L has a component of velocity directed towards $0'$. The approximation is made that station a may be assumed to be at $0'$, so that an observer sees the incremental velocity of point L as

$$v_{a\beta} = kR_m \sin \nu (l'_{\beta} - \dot{\Sigma}_{\beta a}).$$

Rotation about the l_{TL} axis gives a similar component

$$v_{aL} = -kR_m \cos \nu (l'_L - \dot{\Sigma}_{La}).$$

The Doppler spread for each station is due to these incremental velocities. The Doppler spread of the transmitted signal plus the Doppler spread of the reflected signal is the total observed Doppler spread. Thus, the Doppler spread due to the moon's libration is

$$\Delta f'_d = f_c \frac{kR_m}{c} [\sin \nu (2l'_{\beta} - \dot{\Sigma}_{\beta a} - \dot{\Sigma}_{\beta b}) - \cos \nu (2l'_L - \dot{\Sigma}_{La} - \dot{\Sigma}_{Lb})].$$

Hence with the use of eqs (33) and (34) this may be expressed as

$$\Delta f'_d = 2f_c \frac{kR_m}{c} (\sin \nu l_{T\beta} - \cos \nu l_{TL}). \quad (36)$$

There is a small additional Doppler spread term which arises from the fact that the observer is approaching the general point L on the moon's surface, rather than its center. The original main Doppler shift, given by eq (21), was developed for the center point of the moon. Actually it is the rate of change of D_m in figure 10 which should be considered, i.e., $\dot{D}_m = \dot{D} +$ small correction, and this correction will be different for the transmitting and receiving stations. Now $\dot{D}_m \cong \dot{D}$ may be expressed as $\dot{D}_m = \dot{D} \sqrt{1 - (k^2 R_m^2 / D_m^2)}$. The first term expansion of \dot{D}_m is sufficiently accurate for our purposes, so that with D substituted for D_m in the expansion term the correction is given by

$$\dot{D}_m \cong \dot{D} - \frac{1}{2} \dot{D} \frac{k^2 R_m^2}{D^2}.$$

Thus the additional Doppler spread term is

$$\Delta f''_d = \frac{1}{2} \frac{f_c}{c} k^2 R_m^2 \left[\frac{\dot{D}_a}{D_a^2} + \frac{\dot{D}_b}{D_b^2} \right] \quad (37)$$

where the subscripts a and b refer to the two stations. The total Doppler spread is now given by

$$\Delta f_d = 2f_c \frac{kR_m}{c} [\sin \nu l_{T\beta} - \cos \nu l_{TL}] + \frac{1}{2} \frac{f_c}{c} k^2 R_m^2 \left[\frac{\dot{D}_a}{D_a^2} + \frac{\dot{D}_b}{D_b^2} \right]. \quad (38)$$

The maximum (or minimum) value of the Doppler

spread occurs at the angle ν_0 given by

$$\nu_0 = \arctan [-(l_{T\beta}/l_{TL})]. \quad (39)$$

In order to obtain the maximum Doppler spread value, the positive value of (36) is chosen and added to the absolute magnitude of (37).

When the libration rates are not too small in magnitude (for example, not less than 10^{-7} rad/sec) a number of approximations can be made in the computations. In eqs (31) and (32), terms involving δ_m and $D_1/D_2 \Sigma_{\beta, L}$ can be ignored. The term $\Delta f_d^{(7)}$ (eq (37)) also may be neglected. Check calculations show that in general a negligible effect is produced by these approximations. For small libration rates their effect needs to be included.

However, it is to be noted that the calculations for the Doppler spread involve the daily values of selenographic latitude and longitude. *The American Ephemeris and Nautical Almanac* lists these to only three significant figures, so that at some point it is to be expected that lack of accuracy in these data will affect the computations. This appears to be the case at periods of very low libration rate.

4.7. Relationship of "Fading Rate" and "Maximum Doppler Spread"

The "fading rate" of the detected signal was determined as outlined in section 3, i.e., by counting the number of maximums in a given time interval. This obviously gives some measure of the form of the returned signal spectrum. It is apparent, physically, that the total signal is due to reflections taking place over much of the moon's surface, probably with a larger weighting factor attached to the central regions. If the spectrum is regarded as similar to that obtained when Gaussian noise is passed through a narrow Gaussian bandpass filter, then work by Rice [4] indicates that the expected number of maximums per second is

$$N \cong 2.52 \sigma$$

where σ is the standard deviation of the Gaussian filter. Suppose the noise bandwidth, B c/s, is defined as that bandwidth containing half the total power passed by the filter, then

$$B \cong 1.35 \sigma$$

or

$$B \cong 0.54 N \text{ c/s.}$$

This gives a relationship between the bandwidth and fading rate that may be useful as applied to the lunar signal. The maximum Doppler spread $(\Delta f_d)_{\max}$ is a measure of the change in Doppler experienced at the limb of the moon due to libration. The maximum band limits of the signal, if its spreading were entirely due to libration effects, would be $2\Delta f_d$ corresponding to the range of signal returns from opposite limbs of the moon.

The fading rate of the lunar signal was found to be proportional to the libration rate and hence to the value of $(\Delta f_d)_{\max}$. The best fit to the data was found to be given with $k=0.67$ by the empirical formula

$$N = k (\Delta f_d)_{\max} = 0.67 (\Delta f_d)_{\max}. \quad (40)$$

If our assumed relationship between fading rate and bandwidth is correct, then

$$B = 0.54 \times k (\Delta f_d)_{\max} = 0.36 (\Delta f_d)_{\max}. \quad (41)$$

The bandwidth obtained is $0.36/2=0.18$ of the maximum possible band limits due to the libration spreading. Since the change in Doppler Δf_d is proportional to the distance from the center of the moon's disk, then it is apparent that most of the signal energy is reflected from a portion of the moon about the center of the face with a fractional radius of only about 0.2.

4.8. Actual Computations

As results were required at intervals of a few minutes over a period of months, the computations were programmed for the IBM 704 and 709 Electronic Data-Processing Machines. Much of the astronomical input data for the program was obtained on standard IBM cards from the U.S. Naval Observatory. Other input quantities were prepared from the American Ephemeris. The machines also were used for additional computations concerned with the antenna orientations.

5. Results Obtained

Figures 11 (a) to (g) show plots of some of the measured fading rates. The computed curves are based on a value of 0.67 in the empirical relationship of (40). The agreement in general is excellent, except at periods of very low fading rate of the order of 0.05 to 0.005 c/s.

In general, the computed values for August 1957 did not fall below approximately 0.1 c/s for either the approximate or the more accurate methods of computation. The approximations involved in the method of computation are capable of allowing a better resolution than this, and it appears that the limiting factor probably is due to the 3-figure accuracy of the published daily values of selenographic latitude and longitude given in the *American Ephemeris and Nautical Almanac*.

The value of k used, 0.67, when inserted in eq (41) for the "noise bandwidth" B , gives

$$B = 0.36 (\Delta f_d)_{\max} \text{ c/s.}$$

On this basis the major portion of the reflected signal is obtained from a central disk on the moon, the fractional radius of this disk being approximately 0.2. A different approach is afforded by the results of experiments carried out at the Naval Research

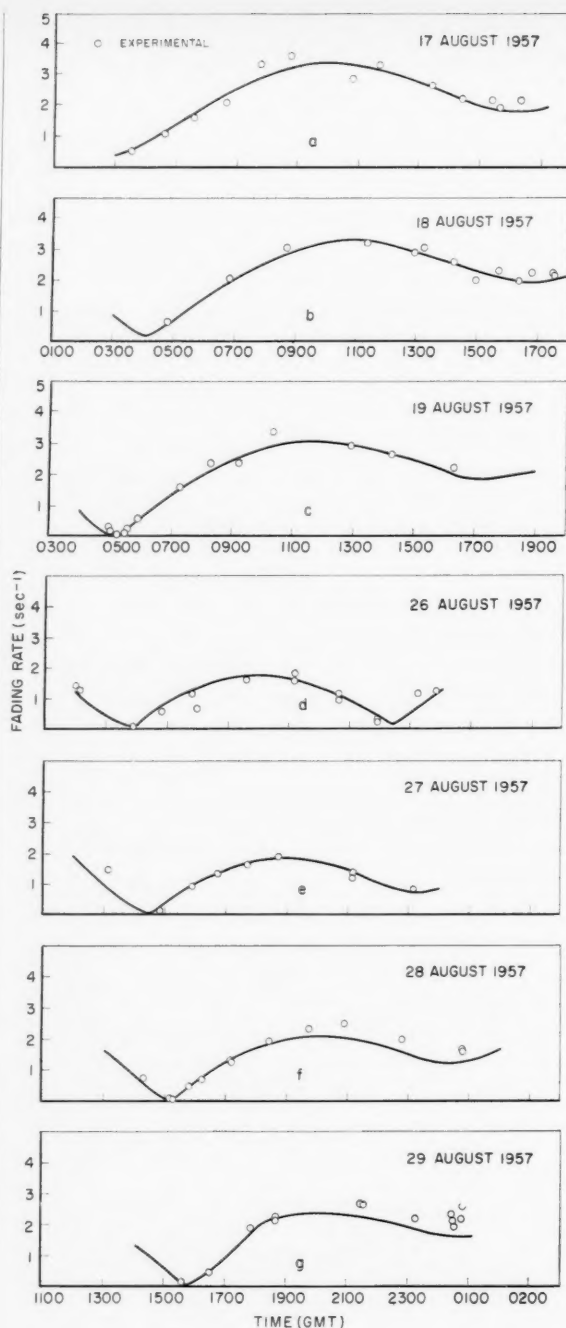


FIGURE 11 a, b, c, d, e, f, g. Comparison of measured and computed fading rates.

Laboratory [5, 6], in which the interpretation of the form of reflected pulsed signals was that only a relatively small central portion of the moon's surface was effective as a reflector.

Although not described here, it is of interest to note that the measured total signal levels showed no evidence of any slow fades. The Faraday rotation was observed, but the total received signal level, after correction for the varying earth-moon distance, was essentially constant.

6. Conclusions

Calculation of the rapid fading rate of moon-reflected signals, in the manner described, has been shown to give results which agree very well with measured values. It appears as if most of the reflected signal may be obtained from a central disk on the moon with a fractional radius of approximately 0.2.

The variation of the position of the region on the moon's surface which gives the maximum Doppler spread is of interest. Table 1 lists values of the angle ν_0 for a typical day, together with the angles of elevation and azimuth. The angle ν_0 depends upon the rates of change of the moon's selenographic latitude and longitude, so that the figures given in table 1 vary from day to day. However, the variation is typical; values of approximately 200° to 300° during moonrise, an increase to values of 10° to 30° while going through transit, and then a further increase to 70° to 130° during moonset. It is apparent that whatever the value of the fractional radius of the moon is taken to be, a considerable portion of the moon's surface is covered during the course of a day. Since the agreement between the computed and measured fading rates is so striking, it would seem that, in its behavior as a reflector or scatterer at 400 Mc/s, the moon's surface is reasonably uniform over quite a large region.

TABLE 1. Variation of angle ν_0 with time for 21 August 1957

Time (21 August 1957) (G.m.t.)	Angle of maximum Doppler spread ν_0 degrees	Moon direction at South Dartmouth	
		Elevation degrees	Azimuth degrees
0600	196	3.9	67.8
0700	229	14.4	76.8
0800	316	25.0	85.9
0900	349	33.9	95.7
1000	359	46.7	107.3
1100	005	56.6	123.0
1200	010	64.5	146.1
1300	016	67.6	179.5
1400	021	64.5	213.1
1500	029	56.5	236.4
1600	038	46.6	252.2
1700	053	36.0	263.5
1800	074	25.0	273.4
1900	102	14.2	282.4
2000	128	3.8	291.3

From the measured signal levels and a knowledge of the parameters of the system, the usual radar equation was applied to give an estimate of the

cross section of the moon. This was

$$\sigma = 7 \times 10^{11} \text{ m}^2.$$

The projected area of the moon is approximately $0.95 \times 10^{13} \text{ m}^2$, so that the radar cross section, at 412.85 Mc/s, represents 0.074 of the projected area. The manner in which the effective cross section of the moon may be proportioned between "gain" and "reflectivity" figures has been the subject of some discussion [2, 7, 8]. If an element of surface is assumed to scatter in a fairly directional manner, for example according to $(\cos \theta)^k$, where typical k values may be 30, 40, 50, etc., then most of the return is given by the central portion of the moon, and the "gain" of the moon as a reflector, relative to its cross sectional area, approaches 4. With this sort of model, which is not critical at all, the power reflectivity must be of the order of 0.02. Values of 0.1 have been quoted, which appear to be high, even allowing for a possible 3-db error in the measurements.

The predictability of the rapid fading rate of a moon-reflected signal is of interest when considering the effects of the ionosphere upon transmission of a UHF signal. The signal is fairly well described when its average amplitude is known, the Faraday rotation allowed for, the Doppler shift computed, and the fading rate predicted to within a constant factor. Changes in the transmission medium, for example, auroral effects, then may be investigated by measuring their effects upon the known characteristics of the undisturbed signal. As mentioned in the introduction, such an experiment has been carried out between Alaska and Massachusetts. This experiment will be described in a forthcoming article.

The authors thank the members of Lincoln Laboratory who contributed to this experiment. They are particularly indebted to S. C. Wang for his discussion of the libration calculations, and to J. C. James for his assistance in reading and correcting the manuscript.

7. References

- [1] C. G. Little, W. M. Thayton, and R. B. Root, Review of ionospheric effects at VHF and UHF, Proc. IRE **44**, 992 (1956).
- [2] I. C. Browne et al., Radio echoes from the moon, Proc. Phys. Soc. B **69**, 901 (1956).
- [3] S. J. Fricker, R. P. Ingalls, W. C. Mason, M. L. Stone, and D. W. Swift, Characteristics of moon-reflected UHF signals, Tech. Rept. 187, Lincoln Lab., M.I.T. (Dec. 1958).
- [4] S. O. Rice, Mathematical Analysis of Random Noise, Bell System Tech. J. **23**, 282 (1944); **24**, 46 (1945).
- [5] J. H. Trexler, Lunar radio echoes, Proc. IRE **46**, 286 (1958).
- [6] B. S. Yaplee et al., Radar echoes from the moon at a wavelength of 10 cm, Proc. IRE **46**, 293 (1958).
- [7] J. V. Evans, Research on Moon Echo Phenomena, Tech. Note No. 1 (1 May 1956 to 30 Apr. 1957) Univ. Manchester, England.
- [8] D. D. Grieg, S. Metzger, and R. Waer, Considerations of moon-relay communication, Proc. IRE **36**, 652 (1948).

(Paper 64D5-81)



On the Theory of Wave Propagation Through a Concentrically Stratified Troposphere With a Smooth Profile¹

H. Bremmer

(February 1, 1960)

Part I. Discussion of the Extended W.K.B. Approximation

The W.K.B. approximation for the solution of the height-gain differential equation for a curved stratified troposphere is discussed in detail. The approximation depends mainly on a variable $u_l(r)$ which can be interpreted as the height dependent contribution of the phase for a field solution obtained by separation of variables. An expansion of $u_l(r)$ with the aid of partial integrations leads to further approximations which facilitate the determination of the eigenvalues, and of the amplitudes of the modes connected with the propagation problem. The influence of the refractive-index profile, if assumed as smooth, then appears to be restricted to a dependence on the surface values of this index and of its gradient insofar as propagation over the ground is concerned. Further, all height effects of elevated antennas can be expressed in terms of the distance to the corresponding radio horizon. This results in simple relations between the fields connected with two different refractive-index profiles, provided both profiles coincide near the earth's surface.

1. Introduction

The propagation theory of a concentrically stratified atmosphere usually concerns a discussion of the corresponding height-gain differential equation. The W.K.B. approximation of the latter has amply been discussed, but little attention has been paid to its corrections. Some material on the form of these corrections has been presented by Pekeris [1]² while applying an earth-flattening approximation. This paper concerns (in part II) an expansion of the solution for a curved stratified atmosphere which starts with an "extended W.K.B. approximation." By the latter we understand a well-known modification of the W.K.B. approximation, in terms of Hankel functions of order 1/3; it is determined such as to remain finite at a turning point of the geometrical optics trajectory associated with the solution. The discussion of this extended W.K.B. approximation (in part I) shows the dominating role of the refractive-index profile near the earth's surface, provided that this profile and all its derivatives are continuous functions of the height throughout the troposphere.

2. Reduction to a Scalar Problem

We start from Maxwell's equations for time-harmonic solutions (time factor $e^{-i\omega t}$) for a medium with spherical symmetry, the refractive index $n(r)$ of which only depends on the distance r to the center of symmetry. We further assume a permeability 1; the equations in question then read as follows in Gaussian cgs units:

$$\text{Curl } \mathbf{e} - i \frac{\omega}{c} \mathbf{h} = 0, \quad (1)$$

$$\text{Curl } \mathbf{h} + i \frac{\omega}{c} n^2(r) \mathbf{e} = 0. \quad (2)$$

¹ Contributions from Philips Research Laboratories, N. V. Philips' Gloeilampenfabrieken, Eindhoven, Netherlands.

² Figures in brackets indicate the literature references at the end of this paper.

The two standard solutions, known as the electric and the magnetic solution respectively, can be represented by:

$$\left. \begin{aligned} \mathbf{e}_e &= \frac{ic}{\omega} \frac{1}{n^2(r)} \text{curl curl } \{n(r)\Pi_e \mathbf{r}\}, \\ \mathbf{h}_e &= \text{curl } \{n(r)\Pi_e \mathbf{r}\}, \end{aligned} \right\} \quad (3)$$

and

$$\left. \begin{aligned} \mathbf{e}_m &= \frac{i\omega}{cn^2(r)} \text{curl } \{n^2(r)\Pi_m \mathbf{r}\}, \\ \mathbf{h}_m &= \text{curl } \left[\frac{1}{n^2(r)} \text{curl } \{n^2(r)\Pi_m \mathbf{r}\} \right]. \end{aligned} \right\} \quad (4)$$

The symbol \mathbf{r} represents the radial vector of length $(x^2 + y^2 + z^2)^{1/2}$.

The Maxwell eq (2) is verified at once for the electric solution (3); the same holds with respect to the other Maxwell eq (1) for the magnetic solution (4). The remaining Maxwell equations can be checked by deriving the following relations with the aid of a tedious analysis based on vector-field identities:

$$\begin{aligned} \text{Curl } \mathbf{e}_e - \frac{i\omega}{c} \mathbf{h}_e &= -\frac{ic}{\omega} \text{curl } \left[\mathbf{r} \left\{ \frac{1}{n} \Delta \Pi + \left(\frac{\omega^2}{c^2} n - \frac{d^2}{dr^2} \frac{1}{n} \right) \Pi \right\} \right], \\ \text{Curl } \mathbf{h}_m + \frac{i\omega}{c} n^2 \mathbf{e}_m &= -\text{curl } \left[\mathbf{r} \left\{ \Delta \Pi + \left(\frac{\omega^2}{c^2} n^2 \Pi \right) \right\} \right]. \end{aligned}$$

Therefore, both Maxwell equations are satisfied, for the electric as well as the magnetic solution, if the scalar Π does satisfy a wave equation of the form,

$$\Delta \Pi + \frac{\omega^2}{c^2} n_{\text{eff}}^2(r) \Pi = 0; \quad (5)$$

the effective refractive index then has to be defined as follows:

$$\begin{aligned} n_{\text{eff}}^2(r) &= n^2 - \frac{c^2}{\omega^2} n \frac{d^2}{dr^2} \frac{1}{n} \quad \text{for the electric solution,} \\ n_{\text{eff}}^2(r) &= n^2 \quad \text{for the magnetic solution.} \end{aligned} \quad (6)$$

3. Height-Gain Differential Equation and Its Extended W.K.B. Approximation

We are particularly interested in the solutions corresponding to a vertical electric or magnetic dipole. In the system of spherical coordinates r, θ, φ ($x+iy=r \sin \theta e^{i\varphi}$, $z=r \cos \theta$) this dipole may be situated at $r=b, \theta=0$. The field then becomes independent of φ , and particular solutions Π_l of (5) are found by a separation of variables according to

$$\Pi_l = f_l(r) P_l(\cos \theta). \quad (7)$$

The corresponding height-gain differential equation for $f_l(r)$ can be put in the form

$$\left\{ \frac{d^2}{dr^2} + \frac{\omega^2}{c^2} m_l^2(r) \right\} \{r f_l(r)\} = 0, \quad (8)$$

if

$$m_l^2(r) \equiv n_{\text{eff}}^2(r) - \frac{l(l+1)}{k_0^2 r^2}, \quad (9)$$

$k_0 = \omega/c$ being the wave number in vacuum.

The W.K.B. approximation of (8) consists of a linear combination of the functions

$$\frac{e^{\pm i k_0 \int^r m_l(s) ds}}{\{m_l(r)\}^{1/2}};$$

it therefore breaks down at a so-called turning point, that is a zero $r=r_l$ of $m_l(r)$. In the case of a single turning point a better approximation is obtained, as is well known, by approximating $m_l^2(r)$ near $r=r_l$ by a linear profile; the equation can then be solved there rigorously with the aid of Hankel functions of order $1/3$. This procedure leads to the following "extended W.K.B. approximation:"

$$rf_l(r) \sim A_l \frac{\left\{ \int_{r_l}^r m_l(s) ds \right\}^{1/2}}{\{m_l(r)\}^{1/2}} H_{1/3}^{(1)} \left\{ k_0 \int_{r_l}^r m_l(s) ds \right\}; \quad (10)$$

it reduces to the conventional W.K.B. approximation if the Hankel function is replaced by the first term of its asymptotic expansion for large arguments.

In (10) we assume $\text{Im } m_l \geq 0$, which guarantees an exponential decrease for $r \rightarrow \infty$ if $\text{Im } m_l$ differs from zero; the function (10) then represents an approximation in accordance with the radiation condition at infinity. In part II of this paper (10) will appear as the first term of a complete expansion for the solution Π_l .

4. Position of a Turning Point for a General Profile of the Refractive Index

The significance of a turning-point level $r=r_l$ is obvious when r_l is a real quantity larger than the earth's radius a . We then consider the relation

$$n_{\text{eff}}(r) \cdot r \cdot \sin \tau(r) = \frac{\{l(l+1)\}^{1/2}}{k_0}; \quad (11)$$

it determines a ray trajectory in a stratified troposphere with refractive index n_{eff} , if $\tau(r)$ represents the angle, at any level r , between the tangent to the trajectory and the radius vector towards the center of the earth. On the other hand, the turning-point relation $m_l(r_l)=0$ can be written as follows in view of (9):

$$n_{\text{eff}}(r_l) \cdot r_l = \frac{\{l(l+1)\}^{1/2}}{k_0}. \quad (12)$$

Therefore, $r=r_l$ characterizes the level at which the trajectory in question becomes horizontal ($\tau=\pi/2$). In other words, the turning-point level constitutes an altitude at which this trajectory passes continuously from a rising branch into a descending branch.

In the absence of a turning point in the physical space $a < r < \infty$, a zero r_l of $m_l(r)$ might occur in the interval $r < a$ outside the troposphere (in accordance with some extrapolation there of $n(r)$), or also at some complex value of r . The "extended W.K.B. approximation" (10), defined with the aid of such a nonphysical turning-point level, will still be important when the latter proves to be situated near the section $a < r < \infty$ of the real axis in the complex r -plane.

As a matter of fact zeros r_l of this type occur for the most important modes (7), since all these modes correspond to complex l values situated near l_0 defined by

$$\frac{\omega}{c} a n_{\text{eff}}(a) = \{l_0(l_0+1)\}^{1/2}. \quad (13)$$

According to (12) l_0 itself is connected with a ray trajectory tangential the earth's surface, r_l then assuming the value a . Hence we expect for all eigenvalues l near l_0 (to be discussed in part II) a corresponding turning point r_l near a .

The exact position of this turning point can be derived from an expansion to be obtained as follows. We replace (12) by the equivalent equation:

$$M_{\text{eff}}^2(r_l) = \frac{l(l+1)}{k_0^2 a^2} = C_l^2, \text{ say,} \quad (14)$$

in which

$$M_{\text{eff}}(r) = \frac{r}{a} \cdot n_{\text{eff}}(r) \quad (15)$$

denotes a modified refractive index which includes the effects of both the curvature and the profile of the effective refractive index n_{eff} . We consider the following Taylor expansion of (14):

$$M_{\text{eff}}^2(a) + \sum_{j=1}^{\infty} \frac{\Lambda_j}{a^j j!} (r_l - a)^j = \frac{l(l+1)}{k_0^2 a^2}, \quad (16)$$

in which the dimensionless parameters

$$\Lambda_j \equiv a^j \left\{ \frac{d^j (M_{\text{eff}}^2)}{dr^j} \right\}_{r=a} \quad (17)$$

characterize the complete tropospheric profile. In view of (14), (15), and (9) we may replace (16) by

$$\sum_{j=1}^{\infty} \frac{\Lambda_j}{a^j j!} (r_l - a)^j = C_l^2 - n_{\text{eff}}^2(a) = -m_l^2(a).$$

We next assume the possibility of inverting this latter relation. The inverted series can be represented as follows:

$$\frac{r_l - a}{a} = -\frac{m_l^2(a)}{\Lambda_1} - \frac{\Lambda_2}{2\Lambda_1^3} m_l^4(a) + \left(\frac{\Lambda_3}{6\Lambda_1^4} - \frac{\Lambda_2^2}{2\Lambda_1^5} \right) m_l^6(a) + \left(\frac{5}{12} \frac{\Lambda_2 \Lambda_3}{\Lambda_1^6} - \frac{5}{8} \frac{\Lambda_2^3}{\Lambda_1^7} - \frac{\Lambda_4}{24\Lambda_1^5} \right) m_l^8(a) + \dots \quad (18)$$

It shows how the turning point can easily be evaluated for modes with small values of $m_l^2(a) = n_{\text{eff}}^2(a) - C_l^2$, which, however, are the only modes of practical interest.

5. Dependence of the Extended W.K.B. Approximation on the Profile

In view of (10) this approximation can be represented by the expression

$$r f_l(r) \sim A_l \frac{\{u_l(r)\}^{1/2}}{\left\{ \frac{d}{dr} u_l(r) \right\}^{1/2}} \cdot H_{\frac{1}{2}}^{(1)} \{u_l(r)\}, \quad (19)$$

which depends uniquely on the variable:

$$u_l(r) = k_0 \int_{r_l}^r m_l(s) ds = k_0 a \int_{r_l}^r \frac{ds}{s} \{M_{\text{eff}}^2(s) - C_l^2\}^{1/2}. \quad (20)$$

This variable constitutes, apart from the factor i , the exponent in the asymptotic approximation of (19) for large values of $|u_l(r)|$. Therefore, u_l may be interpreted as the radial contribution to the phase of the complete wave function $f_l(r) P_l(\cos \theta)$.

Unfortunately, the definition (20) of u_l involves the turning point r_l ; hence, the expansion (18) should be substituted in order to show the complete dependence of $u_l(r)$ on the profile $M_{\text{eff}}(r)$. Under practical circumstances, however, this dependence can also be established without having to resort to the turning point at all. In fact, by applying partial integrations to (20) we obtain an expansion in which the turning point disappears in all but the last term, such in consequence of (14). The expansion in question reads:

$$u_l(r) = k_0 a \left[\sum_{j=0}^{p-1} \frac{2 \cdot 2 \cdot 2 \cdots 2}{3 \cdot 5 \cdot 7 \cdots (2j+3)} (-1)^j \{M_{\text{eff}}^2(r) - C_l^2\}^{j+3/2} \cdot \frac{d^j}{d(M_{\text{eff}}^2)^j} \left\{ \frac{1}{r \frac{dM_{\text{eff}}^2}{dr}} \right\} \right. \\ \left. + \frac{2 \cdot 2 \cdot 2}{3 \cdot 5 \cdot 7} \cdots \frac{2}{(2p+1)} (-1)^p \int_{s=r_l}^{s=r} \{M_{\text{eff}}^2(s) - C_l^2\}^{p+1/2} \cdot \frac{d^p}{d(M_{\text{eff}}^2(s))^p} \left\{ \frac{1}{s \frac{d(M_{\text{eff}}^2)}{ds}} \right\} dM_{\text{eff}}^2(s) \right].$$

This expression suggests the infinite series

$$u_i(r) = k_0 a \sum_{j=0}^{\infty} \frac{2}{3} \frac{2}{5} \frac{2}{7} \cdots \frac{2}{(2j+3)} (-1)^j \{M_{\text{eff}}^2(r) - C_l^2\}^{j+3/2} \cdot \frac{d^j}{d\{M_{\text{eff}}^2(r)\}^j} \left\{ \frac{1}{r} \frac{dM_{\text{eff}}^2}{dr} \right\}. \quad (21)$$

In the case of convergence of this series, we can verify, differentiating term by term, the relation

$$\frac{du_i(r)}{dr} = \frac{k_0 a}{r} \{M_{\text{eff}}^2(r) - C_l^2\}^{1/2};$$

this proves the correctness of (21) when taking into account the property $u_i(r_i) = 0$.

As an example we consider the magnetic solution in the case of the "Eckersley profile." The refractive index $n(r)$ of the latter is defined by

$$n^2(r) = n^2(a) \left\{ \frac{a}{a_{\text{eff}}} + \left(1 - \frac{a}{a_{\text{eff}}}\right) \frac{a^2}{r^2} \right\}, \quad (22)$$

a_{eff} being the effective earth radius. The corresponding effective modified refractive index, viz

$$M_{\text{eff}}(r) = n(a) \left\{ \frac{r^2}{a \cdot a_{\text{eff}}} + \left(1 - \frac{a}{a_{\text{eff}}}\right) \right\}^{1/2},$$

leads to the following series for (21):

$$\{u_i(r)\}_{\text{Eck}} = \frac{k_0 a r}{2} \sum_{j=0}^{\infty} j! \frac{2}{3} \frac{2}{5} \cdots \frac{2}{(2j+3)} \left\{ \frac{a \cdot a_{\text{eff}}}{n^2(a)} \right\}^{j+1} \left\{ \frac{n^2(a)}{a \cdot a_{\text{eff}}} + \frac{n^2(a)(1 - a/a_{\text{eff}}) - C_l^2}{r^2} \right\}^{j+3/2}.$$

The convergence condition here amounts to:

$$\left| 1 + \frac{a \cdot a_{\text{eff}}}{r^2} \left\{ 1 - \frac{a}{a_{\text{eff}}} - \frac{C_l^2}{n^2(a)} \right\} \right| < 1;$$

in view of the smallness in practice of the quantities $(r-a)/a = h/a$ and $\delta C_l = C_l - n(a)$ this reduces to the following approximative condition

$$\left| \frac{2h}{a} - \frac{2a_{\text{eff}}}{a} \frac{\delta C_l}{n(a)} \right| < 1,$$

which is satisfied for all relevant values of the height h and the parameter C_l . The actual smooth profiles, excluding ducts and so on, deviate only slightly from the Eckersley profile; this suggests the validity of the corresponding expansion (21) in all practical cases.

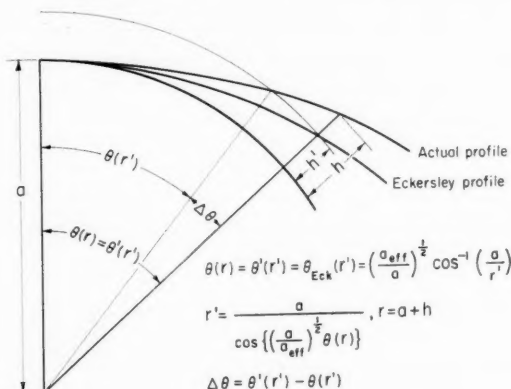


FIGURE 1. Geometry of radio ray bending.

6. Formulation of the Eigenvalue Problem

It is now well established [2] that our propagation problem concerning the two media of the spherical earth and its surrounding stratified atmosphere can be reduced approximatively to a one-medium problem by introducing a proper boundary condition at the earth's surface. This condition is arrived at by considering the surface impedance

$$Z = \frac{4\pi}{c} \frac{E_{\parallel}}{H_{\parallel}},$$

which depends on the ratio of the horizontal components E_{\parallel} and H_{\parallel} of the electric and the magnetic field at the earth's surface. The factor $4\pi/c$ is such that Z represents the ratio of the tangential electric field at the earth's surface, and of the density of a properly chosen two-dimensional current distribution on this surface; the effect of this fictitious current distribution is identical with that of the actual field inside the earth.

The value of Z depends on the field solution under consideration. In the case of a flat boundary, and a plane incident wave arriving from the atmosphere, e.g., Z depends on the direction of arrival τ of the incident wave. The assumption which enables us to leave out of consideration the medium inside the earth altogether is that Z may be replaced by its special value for a plane wave at grazing incidence ($\tau = \pi/2$). The corresponding boundary condition, viz

$$E_{\parallel} = \frac{c}{4\pi} Z_{\tau=\pi/2} H_{\parallel} \quad \text{at } r=a,$$

can be worked out with the aid of (3) and (4) for the electric and magnetic solution respectively. It results in a relation of the following form for the scalar Π describing these solutions:

$$\frac{\partial}{\partial r} (r\Pi) = \frac{\Gamma}{a} r\Pi \quad \text{at } r=a. \quad (23)$$

The parameter Γ is then given, respectively, by

$$\Gamma_e = \frac{i\omega}{4\pi} a n^2(a) Z_{e1} - a \frac{n'(a)}{n(a)} = ik_0 a n(a) \frac{(n_e^2 - 1)^{1/2}}{n_e^2} - a \frac{n'(a)}{n(a)}; \quad \Gamma_m = \frac{4\pi a \omega}{ic^2 Z_m} = -ik_0 a n(a) (n_e^2 - 1)^{1/2};$$

in these expressions $n(a)$ denotes the atmospheric refractive index at the earth's surface, and n_e the refractive index associated with a refraction from the atmosphere towards the earth.

The boundary condition (23) can only be fulfilled for a discrete set of modes (7). Henceforth the parameter l will refer to a special complex eigenvalue fixing the order of the Legendre function $P_l(\cos\vartheta)$ that constitutes a factor of the field of such a mode. The amplitudes of the modes depend on the source of the field. In the case of a vertical electric or magnetic-dipole point source at $r=b$, $\vartheta=0$ the expansion in terms of these modes becomes as follows [3]:

$$\Pi = \frac{\pi B}{ca^2 b} \sum_l \frac{(2l+1)}{\frac{\partial}{\partial \lambda} \left\{ \frac{d}{dr} (r f_{\lambda}) \right\}_{r=a; \lambda=l}} \frac{f_l(b) f_l(r)}{f_l^2(a)} \frac{P_l\{\cos(\pi - \vartheta)\}}{\sin(\pi l)}. \quad (24)$$

The constant B represents the moment of the dipole. Each function $f_l(r)$ constitutes a solution of the height-gain differential equation, that has to satisfy the radiation condition at infinity.

7. Logarithmic Derivative of the Height-Gain Function at the Earth's Surface

The boundary condition (23) can be put in the following form for the individual modes:

$$\left\{ \frac{\partial}{\partial r} (rf_\lambda) \right\}_{r=a; \lambda=l} = \frac{\Gamma}{a}. \quad (25)$$

Hence the quantity

$$\left\{ \frac{\partial}{\partial r} (rf_\lambda) \right\}_{r=a}$$

proves to be important in connection with the evaluation of both the eigenvalues l , and of the denominator of the amplitude factor in (24). Its approximation for small values of h/a and of $\delta C_l = C_l - n(a)$ (see the end of section 5) will be discussed now.

We start from the extended W.K.B. approximation (19) for rf_λ . Its logarithmic derivative becomes:

$$\frac{\partial}{\partial r} (rf_\lambda) = \frac{1}{6} \frac{u'_\lambda}{u_\lambda} - \frac{1}{2} \frac{u''_\lambda}{u'_\lambda} - e^{-i\pi/3} u'_\lambda \frac{H_{2/3}^{(1)}(u_\lambda)}{H_{1/3}^{(1)}(u_\lambda)}. \quad (26)$$

Another logarithmic derivation of the expression

$$u'_\lambda = \frac{k_0 a}{r} \{M_{\text{eff}}^2(r) - C_l^2\}^{1/2} \sim k_0 \{M_{\text{eff}}^2(r) - C_l^2\}^{1/2} \quad (27)$$

results in:

$$\frac{u''_\lambda}{u'_\lambda} \sim \frac{M_{\text{eff}}(r) \cdot M'_{\text{eff}}(r)}{M_{\text{eff}}^2(r) - C_l^2}. \quad (28)$$

We next introduce a definition for the effective-earth radius for any profile, viz:

$$a_{\text{eff}} = \left[\frac{r n_{\text{eff}}(r)}{\frac{d}{dr} \{r n_{\text{eff}}(r)\}} \right]_{r=a} = \frac{M_{\text{eff}}(a)}{M'_{\text{eff}}(a)}. \quad (29)$$

This definition involves the following value of (28) at $r=a$:

$$\left(\frac{u''_\lambda}{u'_\lambda} \right)_{r=a} \sim \frac{n_{\text{eff}}^2(a)}{a_{\text{eff}} \{n_{\text{eff}}^2(a) - C_l^2\}}. \quad (30)$$

On the other hand, the expansion (21) may be approximated for small h/a and δC_l by its first term. Its value for $r=a$ reduces to:

$$u_\lambda(a) \sim \frac{k_0 a_{\text{eff}}}{3} \frac{\{n_{\text{eff}}^2(a) - C_l^2\}^{3/2}}{n_{\text{eff}}^2(a)}. \quad (31)$$

A comparison of (30), (31), and of the special value of (27) at $r=a$ then proves the vanishing (for the approximations under consideration) of the quantity

$$\frac{1}{6} \frac{u'_\lambda}{u_\lambda} - \frac{1}{2} \frac{u''_\lambda}{u'_\lambda}$$

at $r=a$. Further, when evaluating the remaining term in the right-hand side of (6) for $r=a$, we may substitute, applying (27) and (31)

$$u'_\lambda(a) \sim k_0 \{n_{\text{eff}}^2(a) - C_l^2\}^{1/2} \sim k_0 \left\{ \frac{3n_{\text{eff}}^2(a)}{k_0 a_{\text{eff}}} \right\}^{1/3} \{u_\lambda(a)\}^{1/3}. \quad (32)$$

The following final approximation thus results from (26) for $r=a$:

$$\left\{ \frac{\partial}{\partial r} (rf_\lambda) \right\}_{r=a} \sim -e^{-i\pi/3} \left\{ \frac{3k_0^2 n_{\text{eff}}^2(a)}{a_{\text{eff}}} \right\}^{1/3} u_\lambda^{1/3}(a) \frac{H_{2/3}^{(1)}\{u_\lambda(a)\}}{H_{1/3}^{(1)}\{u_\lambda(a)\}}. \quad (33)$$

8. Equation for the Eigenvalues

According to (5) and (33) the eigenvalues are to be determined from the equation:

$$u_l^{1/3}(a) \frac{H_{2/3}^{(1)}\{u_l(a)\}}{H_{1/3}^{(1)}\{u_l(a)\}} = -\frac{\Gamma}{a} e^{i\pi/3} \left\{ \frac{a_{\text{eff}}}{3k_0^2 n_{\text{eff}}^2(a)} \right\}^{1/3}. \quad (34)$$

The resulting roots $u_l(a)$ fix in succession the corresponding values of C_l and l (see (31) and (14)).

The only profile parameters entering in the equations (34), (31), and (14) for the eigenvalues are $n(a)$, and the effective earth's radius a_{eff} defined by (29). Hence the conventional diffraction theory for a homogeneous atmosphere with refractive index $n(a)$ can be applied at once, provided that the actual earth's radius a is replaced by a_{eff} . This simple result depends on the smallness of $\delta C_l = C_l - n(a)$ which will be proved later on in the rigorous theory of part II. It then appears that the eigenvalues do only depend, in the approximations under consideration, on profile properties of the refractive index near the earth's surface; these properties concern $n(a)$ and the derivative $n'(a)$, both of which determine the parameter a_{eff} . However, we emphasize the assumption of a *smooth* profile $n(r)$ without any discontinuity of a derivative of any order; such a discontinuity would involve higher-order terms in the expansion (21) for $u_l(r)$ which are not negligible with respect to the first term.

9. Approximate Expansion in Terms of Modes

In order to obtain a final approximation replacing (24) we have to evaluate, among others, the derivative of (33) with respect to λ . This can be facilitated with the aid of two relations, to be derived as follows. First we obtain from a differentiation of (31):

$$\frac{\partial u_\lambda(a)}{\partial \lambda} \sim -\frac{3^{1/3}}{2} \left\{ \frac{k_0 a_{\text{eff}}}{n_{\text{eff}}^2(a)} \right\}^{2/3} u_\lambda^{1/3}(a) \frac{\partial(C_\lambda^2)}{\partial \lambda}. \quad (35)$$

The last factor can further be reduced, with the aid of the approximation $C_l \sim l/k_0 a$ of (14). We find:

$$\frac{\partial(C_\lambda^2)}{\partial \lambda} = \frac{2\lambda+1}{k_0^2 a^2} \sim \frac{2\{\lambda(\lambda+1)\}^{1/2}}{k_0^2 a^2} \sim \frac{2C_\lambda}{k_0 a}. \quad (36)$$

On the other hand, we shall make use of the identity

$$\frac{d}{du} \left\{ \frac{u^{1/3} H_{2/3}^{(1)}(u)}{H_{1/3}^{(1)}(u)} \right\} = e^{i\pi/3} u^{1/3} \left[1 + \left\{ e^{-i\pi/3} \frac{H_{2/3}^{(1)}(u)}{H_{1/3}^{(1)}(u)} \right\}^2 \right]. \quad (37)$$

The application of (35), (36) and (37) to the determination of the λ derivative of (33) results in an expression which can further be simplified for λ equaling an eigenvalue l . In fact, we then have $C_\lambda = C_l \sim n_{\text{eff}}(a)$; this latter zero-order approximation [which is equivalent to $l \sim k_0 a n_{\text{eff}}(a)$] is well known from the diffraction theory for a homogeneous atmosphere. Moreover, we may then also eliminate the Hankel functions with the aid of (34). The procedure outlined here results in:

$$\frac{\partial}{\partial \lambda} \left\{ \frac{\partial}{\partial r} (rf_\lambda) \right\}_{r=a; \lambda=l} \sim \frac{3^{2/3} k_0^{1/3} a_{\text{eff}}^{1/3} n_{\text{eff}}(a)}{a} \left[u_l^{2/3}(a) + \frac{\Gamma^2}{a^2} \left\{ \frac{a_{\text{eff}}}{3k_0^2 n_{\text{eff}}^2(a)} \right\}^{2/3} \right]. \quad (38)$$

We further substitute in (24):

$$2l+1 \sim 2l \sim 2k_0 a n_{\text{eff}}(a) \quad (39)$$

as well as the well-known approximation for Legendre functions with large complex order having a positive imaginary part. The latter reads:

$$\frac{P_l\{\cos(\pi-\vartheta)\}}{\sin(\pi l)} \sim -(2i)^{1/2} \frac{e^{i l \vartheta}}{(\pi l \sin \vartheta)^{1/2}}. \quad (40)$$

In view of the approximate value $l \sim k_0 a n_{\text{eff}}(a)$ we introduce the representation

$$l = k_0 a n_{\text{eff}}(a) + \delta l, \quad (41)$$

whereas the correction δl may be omitted in the factor $l^{1/2}$. The substitution of (38), (39), (40), and (41) into (24) leads to:

$$\Pi \sim - \frac{2^{3/2} (i\pi)^{1/2} B k_0^{1/6} e^{i k_0 a n_{\text{eff}}(a) \vartheta}}{c b a_{\text{eff}}^{1/3} \{a n_{\text{eff}}(a) \sin \vartheta\}^{1/2}} \sum_i \frac{f_i(b) f_i(r)}{f_i^2(a)} \left[\frac{e^{i \delta l \vartheta}}{\{3 u_i(a)\}^{2/3} + \frac{\Gamma^2}{a^2} \left\{ \frac{a_{\text{eff}}}{k_0^2 n_{\text{eff}}^2(a)} \right\}^{2/3}} \right] \quad (42)$$

We are interested first of all in the field strength attenuation that is due to the atmospheric refraction and the diffraction by the earth. Therefore, we next pass to the ratio of $|\Pi|$ and the modulus $|\Pi_{pr}|$ of the scalar determining the primary unattenuated field. The latter modulus reads [4]:

$$|\Pi_{pr}| = \frac{B}{c b} \frac{1}{TP} \sim \frac{B}{c b a \vartheta}, \quad (43)$$

TP being the distance from the transmitter to the receiver.

We thus obtain from (42) and (43):

$$\left| \frac{\Pi}{\Pi_{pr}} \right| \sim \frac{2^{3/2} k_0^{1/6}}{a_{\text{eff}}^{1/3}} \left\{ \frac{\pi a \vartheta}{n_{\text{eff}}(a)} \right\}^{1/2} \sum_i \frac{f_i(b) f_i(r)}{f_i^2(a)} \left[\frac{e^{i \delta l \vartheta}}{\{3 u_i(a)\}^{2/3} + \frac{\Gamma^2}{a^2} \left\{ \frac{a_{\text{eff}}}{k_0^2 n_{\text{eff}}^2(a)} \right\}^{2/3}} \right]. \quad (44)$$

The effects of the elevations $b-a$ of the transmitter, and $r-a$ of the receiver, are contained, for each individual mode, in the height-gain factors

$$\frac{f_i(b)}{f_i(a)} \text{ and } \frac{f_i(r)}{f_i(a)}.$$

These factors depend, according to (19) and (20), on the *complete* profile between the earth's surface and the levels of the transmitter and receiver. On the other hand, these factors can be left out of consideration when considering propagation along the ground. In this case the field is completely determined by $n_{\text{eff}}(a)$, a_{eff} and Γ ; the dependence on the profile of the refractive index (if assumed as smooth), then only concerns its properties at the vicinity of the earth's surface.

10. Connection of the Height-Gain Factors With Horizon Distances

For an investigation of the height-gain effects we can restrict ourselves to an elevated receiver, the dependence on the height being completely similar for an elevated transmitter. Substitution of the extended W.K.B. approximation (19) in both $f_i(r)$ and $f_i(a)$ yields:

$$\frac{f_i(r)}{f_i(a)} \sim \frac{a}{r} \left\{ \frac{u_i(r) \cdot u_i'(a)}{u_i(a) \cdot u_i'(r)} \right\}^{1/2} \frac{H_{1/3}^{(1)}\{u_i(r)\}}{H_{1/3}^{(1)}\{u_i(a)\}}. \quad (45)$$

The effect of the height $h=r-a$ enters implicitly through the variable $u_i(r)$, and also in the factor

$$\frac{1}{r\{u_i(r)\}^{1/2}} = \frac{1}{(k_0 a r)^{1/2} \{M_{\text{eff}}^2(r) - C_1^2\}^{1/4}}.$$

The dependence on the height can therefore be expressed by:

$$\frac{f_i(r)}{f_i(a)} \sim \frac{F\{u_i(r)\}}{r^{1/2} \{M_{\text{eff}}^2(r) - C_1^2\}^{1/4}} \quad (46)$$

The variable $u_i(r)$ can be connected with a geometric property of the profile, viz the angular distance $\vartheta(r)$ from the elevated receiver to its horizon point. This distance can be evaluated with the aid of Snell's law for the curved ray trajectory that passes through the receiver, and meets the earth tangentially. For our spherically symmetric medium this law amounts to the relation (11), if its refractive index is given by $n_{\text{eff}}(r)$ instead of $n(r)$ [thus differing slightly from the actual refractive index in the case of the electric solution, see (6)]. We have:

$$r' n_{\text{eff}}(r') \sin \tau(r') = a n_{\text{eff}}(a), \quad (47)$$

if $\tau(r')$ represents the angle, at an arbitrary point (r', ϑ') of the trajectory, between the tangent of the latter and the vertical through this point. Hence $\tan \tau = r' d\vartheta/dr'$.

The relation (47), or the equivalent one

$$M_{\text{eff}}(r') \sin \tau(r') = M_{\text{eff}}(a),$$

can also be put in the form:

$$\frac{d\vartheta'}{dr'} = \frac{\tan \tau(r')}{r'} = \frac{M_{\text{eff}}(a)}{r' \{M_{\text{eff}}^2(r') - M_{\text{eff}}^2(a)\}^{1/2}}.$$

An integration along the trajectory, from the horizon point at $r'=a$ up to the receiver at $r'=r$, yields the following formula for the angular horizon distance $\vartheta(r)$ of the receiver:

$$\vartheta(r) = M_{\text{eff}}(a) \int_a^r \frac{dr'}{r' \{M_{\text{eff}}^2(r') - M_{\text{eff}}^2(a)\}^{1/2}}. \quad (48)$$

We also need the derivative of this function, viz

$$\frac{d\vartheta}{dr} = \frac{M_{\text{eff}}(a)}{r \{M_{\text{eff}}^2(r) - M_{\text{eff}}^2(a)\}^{1/2}}. \quad (49)$$

The connection between r and $\vartheta(r)$ is unique for the smooth troposphere profile (excluding, e.g., "ducts") under consideration. Therefore, all functions of r may also be considered as functions of $\vartheta(r)$, in particular the variable $u_i(r)$. In order to determine the explicit dependence of $u_i(r)$ on $\vartheta(r)$, we first derive, with the aid of (49), the relation:

$$\frac{d\{M_{\text{eff}}^2(r) - M_{\text{eff}}^2(a)\}^{1/2}}{d\vartheta} = \frac{r \frac{d(M^2)}{dr}}{2n(a)}.$$

We can deduce similar relations for the higher-order derivatives of $\{M_{\text{eff}}^2(r) - M_{\text{eff}}^2(a)\}^{1/2}$ with respect to ϑ , again using (49); for instance we find:

$$\frac{d^2}{d\vartheta^2} \{M_{\text{eff}}^2(r) - M_{\text{eff}}^2(a)\}^{1/2} = \frac{r}{2M_{\text{eff}}^2(a)} \cdot \frac{d}{dr} \left\{ r \frac{dM_{\text{eff}}^2(r)}{dr} \right\} \cdot \{M_{\text{eff}}^2(r) - M_{\text{eff}}^2(a)\}^{1/2}.$$

The special values of these derivatives at $r=a$ can be expressed in terms of the coefficients Λ_j defined by (17). These latter derivatives determine the coefficients of the Taylor expansion

of $\{M_{\text{eff}}^2(r) - M_{\text{eff}}^2(a)\}^{1/2}$, with respect to ϑ , taken at the point $r=a$, that is $\vartheta(r)=0$. The expansion in question starts as follows:

$$M_{\text{eff}}^2(r) = M_{\text{eff}}^2(a) + \frac{\Lambda_1^2}{4n_{\text{eff}}^2(a)} \vartheta^2(r) + \frac{\Lambda_1^2(\Lambda_1 + \Lambda_2)}{24 n_{\text{eff}}^4(a)} \vartheta^4(r) + \dots; \quad (50)$$

moreover, the definition (29) implies the relation

$$\Lambda_1 = 2n_{\text{eff}}^2(a) \frac{a}{a_{\text{eff}}}. \quad (51)$$

We next consider the approximation of $u_i(r)$ by the first term of (21), viz

$$u_i(r) \sim \frac{2}{3} k_0 a \frac{\{M_{\text{eff}}^2(r) - C_1^2\}^{3/2}}{r \frac{d(M_{\text{eff}}^2)}{dr}} = \frac{2}{3} \frac{k_0 a}{n_{\text{eff}}(a)} \frac{\{M_{\text{eff}}^2(r) - C_1^2\}^{3/2} \{M_{\text{eff}}^2(r) - M_{\text{eff}}^2(a)\}^{1/2}}{d(M_{\text{eff}}^2)/d\vartheta} \quad (52)$$

Each factor can be expanded with the aid of (50), but we shall only retain terms up to the first one depending on ϑ . This requires the validity of the relation

$$(\Lambda_1 + \Lambda_2) \cdot \vartheta^2(r) \ll n^2(a). \quad (53)$$

Moreover we substitute [compare (14) and (41)]:

$$C_1^2 = \{n_{\text{eff}}(a) + \delta C_1\}^2 \sim n_{\text{eff}}^2(a) + 2n_{\text{eff}}(a) \cdot \delta C_1 \sim n_{\text{eff}}^2(a) + 2n_{\text{eff}}(a) \frac{\delta l}{k_0 a}. \quad (54)$$

The corresponding evaluation of (52) results in:

$$u_i(r) \sim \frac{k_0 a_{\text{eff}}}{3 \{n_{\text{eff}}(a)\}^{1/2}} \cdot \left\{ -\frac{2 \delta l}{k_0 a} + n_{\text{eff}}(a) \frac{a^2}{a_{\text{eff}}^2} \cdot \vartheta^2(r) \right\}^{3/2}. \quad (55)$$

Apart from the inequality (53) this approximation depends on the neglect of the higher-order terms of (21). This neglect proves to be justified in view of the smallness of $\delta l/k_0 a$ and ϑ^2 compared to unity, remembering also the order of magnitude of unity for $n_{\text{eff}}(a)$ and a/a_{eff} . Moreover, (53) is even satisfied automatically for all $\vartheta(r) \ll 1$ provided that we have $|\Lambda_2| \ll \Lambda_1$. Under such circumstances $u_i(r)$ only depends on the eigenvalue δl , the horizon distance $\vartheta(r)$, and the profile properties $n_{\text{eff}}(a)$ and a_{eff} ; on the other hand, the eigenvalues δl merely depend on $n_{\text{eff}}(a)$ and a_{eff} (see section 8). As a consequence $n_{\text{eff}}(a)$, a_{eff} and $\vartheta(r)$ may be considered as the only quantities determining $u_i(r)$. The same then holds for $F\{u_i(r)\}$ in (46), as well as for the quantity [compare (50) and (54)],

$$\{M_{\text{eff}}^2(r) - C_1^2\}^{1/4} = \left\{ -2n_{\text{eff}}(a) \frac{\delta l}{k_0 a} + \frac{\Lambda_1^2}{4n_{\text{eff}}^2(a)} \vartheta^2(r) \right\}^{1/4}.$$

The still remaining factor $r^{-1/2}$ of (46) can be approximated by $a^{-1/2}$. We thus finally conclude that the height-gain factor does depend, in the approximations under consideration [the most restrictive one being (53)], on no other quantities than $n_{\text{eff}}(a)$, a_{eff} and $\vartheta(r)$.

11. Asymptotic Approximation of the Height-Gain Factors

We might substitute the approximations of the preceding section into the height-gain factors (45) for both the transmitter and the receiver, and next the values of the latter into the mode expansion (44). This would show the explicit dependence of the attenuation factor $|\Pi/\Pi_{pr}|$ on the four quantities $n_{\text{eff}}(a)$, a_{eff} , $\vartheta(r_1)$ and $\vartheta(r_2)$; $\vartheta(r_1)$ and $\vartheta(r_2)$ here represent the angular distances from the transmitter and receiver to their horizon point. The complicated final expression depends, among other things, on Hankel functions of order 1/3. The latter can be simplified considerably by replacing them by their asymptotic approximation. This can be justified in the case of an argument with modulus well above unity. Unfortunately, the argument $u_i(a)$ of the Hankel functions in the denominator of (45) proves to be of the order of unity, but the other argument $u_i(r)$ of the Hankel functions in the numerator of (45) may be much larger for elevated transmitters and receivers.

Let us consider, once again, the height-gain function for the receiver, and estimate the order of magnitude of $|u_i(r)|$. When leaving out of consideration the term with ϑ^2 in (55) we find an order of unity for $|u_i(r)|$, remembering (from the case of a homogeneous atmosphere) the order of $(k_0 a)^{1/3}$ for δl . Therefore, $|u_i(r)| \gg 1$ will certainly hold provided we have

$$n_{\text{eff}}(a) \frac{a^2}{a_{\text{eff}}^2} \vartheta^2(r) \gg \frac{|2\delta l|}{k_0 a} \approx \frac{1}{(k_0 a)^{2/3}}. \quad (56)$$

Hence, a sufficient condition for applying the asymptotic expression for $H_{1/3}^{(1)}\{u_i(r)\}$ reads very roughly $[n_{\text{eff}}(a)$ and a/a_{eff} being of the order of unity]:

$$\vartheta(r) \gg \frac{1}{(k_0 a)^{1/3}}. \quad (57)$$

This inequality holds for altitudes $h=r-a$ above some critical value, h_{cr} say.

Let us now assume $h > h_{cr}$ for the receiver in question. We may then also replace the expression between braces in (55) by the first two terms of its binomial expansion with respect to δl , so as to obtain:

$$u_i(r) \sim \frac{k_0 n_{\text{eff}}(a) a^3}{3a_{\text{eff}}^2} \vartheta^3(r) - \delta l \cdot \vartheta(r). \quad (58)$$

The substitution of the asymptotic expression for $H_{1/3}^{(1)}\{u_i(r)\}$ into (44) first results in:

$$\frac{f_i(r)}{f_i(a)} \sim \frac{a}{r} \left\{ \frac{2}{\pi} \frac{u_i'(a)}{u_i(a) \cdot u_i'(r)} \right\}^{1/2} \frac{e^{i\left\{ \frac{u_i(r)}{12} - \frac{5}{12} \pi \right\}}}{H_{1/3}^{(1)}\{u_i(a)\}}.$$

In the exponent we must take into account both terms of (58), but the dominating first term suffices in the nonexponential factors. We shall substitute, moreover, the relations (31) and (32) for evaluating $u_i(a)$ and $u_i'(a)$ [applying also (54)], the approximation $a/r \sim 1$, and finally the following relation based on (20), (50), (54), (51) and (56):

$$\begin{aligned} u_i'(r) &= \frac{k_0 a}{r} \{M_{\text{eff}}^2(r) - C_i^2\}^{1/2} \sim k_0 \left\{ M_{\text{eff}}^2(a) - C_i^2 + \frac{\Lambda_i^2}{4n_{\text{eff}}^2(a)} \vartheta^2(r) \right\}^{1/2} \\ &= k_0 \left\{ -2n_{\text{eff}}(a) \frac{\delta l}{k_0 a} + \frac{n_{\text{eff}}^2(a) a^2}{a_{\text{eff}}^2} \vartheta^2(r) \right\}^{1/2} \sim k_0 n_{\text{eff}}(a) \frac{a}{a_{\text{eff}}} \vartheta(r). \end{aligned}$$

We then find:

$$\frac{f_i(r)}{f_i(a)} \sim \left(\frac{6}{\pi} \right)^{1/2} \frac{e^{i\left\{ \frac{k_0 n_{\text{eff}}(a) a^3}{3a_{\text{eff}}^2} \cdot \vartheta^3(r) - \delta l \cdot \vartheta(r) - \frac{5}{12} \pi \right\}}}{\left\{ -2\delta l \cdot \vartheta(r) \right\}^{1/2} \cdot H_{1/3}^{(1)} \left[\frac{a_{\text{eff}} (-2\delta l)^{3/2}}{3 \{k_0 n_{\text{eff}}(a)\}^{1/2} a^{3/2}} \right]}. \quad (59)$$

12. Mode Expansion for Transmitter and (or) Receiver Above the Critical Altitude

We first assume a receiver at an elevation $h_2=r_2-a$ above the critical height h_{cr} given by (57), and a transmitter on the ground. When evaluating the mode expansion (44) we can then substitute (59) for the height-gain factor of the receiver, that of the transmitter being unity. The term proportional to ϑ^3 in the exponent of (59) drops out, it being real and independent of l ; it therefore has no effect on the modulus $|\Pi/\Pi_{pr}|$. The use of this substitution results in:

$$\left| \frac{\Pi}{\Pi_{pr}} \right| \sim \frac{2^{3/2} k_0^{1/6}}{a_{\text{eff}}^{1/3}} \left\{ \frac{3a\vartheta}{n_{\text{eff}}(a)\vartheta(r_2)} \right\}^{1/2} \left| \sum_l \frac{e^{i\delta l \{ \vartheta - \vartheta(r_2) \}}}{(\delta l)^{1/2} \left[\left\{ 3u_i(a) \right\}^{2/3} + \frac{\Gamma^2}{a^2} \left\{ \frac{a_{\text{eff}}}{k_0^2 n_{\text{eff}}^2(a)} \right\}^{2/3} \right] \cdot H_{1/3}^{(1)}\{u_i(a)\}} \right|, \quad (60)$$

in which

$$u_l(a) = \frac{a_{\text{eff}} (-2\delta l)^{3/2}}{3 \{k_0 n_{\text{eff}}(a)\}^{1/2} a^{3/2}}.$$

We next consider a transmitter and receiver at elevations $h_1 = r_1 - a$ and $h_2 = r_2 - a$ which are both above the critical height. We may then apply (59) to each of the two height-gain factors $f_l(r_1)/f_l(a)$ and $f_l(r_2)/f_l(a)$ occurring in (44). It leads to the expression:

$$\left| \frac{\Pi}{\Pi_{pr}} \right| \sim \frac{6k_0^{1/6}}{a_{\text{eff}}^{1/3}} \frac{(2a\vartheta)^{1/2}}{\{\pi n_{\text{eff}}(a)\vartheta(r_1)\vartheta(r_2)\}^{1/2}} \times \left| \sum_l \frac{e^{i\delta l \{ \vartheta - \vartheta(r_1) - \vartheta(r_2) \}}}{\delta l \left[\{3u_l(a)\}^{2/3} + \frac{\Gamma^2}{a^2} \left\{ \frac{a_{\text{eff}}}{k_0^2 n_{\text{eff}}^2(a)} \right\}^{2/3} \right]} \cdot [H_{1/3}^{(1)}\{u_l(a)\}]^2 \right|. \quad (61)$$

13. Final Expressions for the Vertical Field Component

So far we have derived expressions for the scalar quantity Π . The transition to the field components is conditioned by (3) and (4). In the case of the electric solution this transition is effected for the vertical component E_r of the electric field by multiplying the coefficient of each individual mode by [5] $il(l+1)/(k_0 r)$. In view of our approximations this quantity can be simplified to

$$\frac{il^2}{k_0 a} \sim ik_0 a n_{\text{eff}}^2(a).$$

By combining this quantity with the expression (43), that is

$$|\Pi_{pr}| \sim \frac{B}{c b a \vartheta} \sim \frac{B}{c a^2 \vartheta},$$

we deduce the following converting factor for passing from the attenuation factor $|\Pi/\Pi_{pr}|$ to $|E_r|$:

$$k_0 a \cdot n_{\text{eff}}^2(a) \frac{B}{c a^2 \vartheta} = \frac{k_0 B n_{\text{eff}}^2(a)}{c a \vartheta}.$$

A similar factor proportional to ϑ^{-1} applies to the reduction of $|\Pi/\Pi_{pr}|$ to the vertical magnetic field component $|H_r|$ in the case of the magnetic solution.

With the aid of this factor we find the following representation replacing (44):

$$|E_r| \sim \frac{2^{3/2} k_0^{7/6} B n_{\text{eff}}^{3/2}(a)}{c a_{\text{eff}}^{1/3}} \left(\frac{\pi}{a \vartheta} \right)^{1/2} \times \left| \sum_l \frac{f_l(b) f_l(r)}{f_l^2(a)} \frac{e^{i \delta l \vartheta}}{\left[\{3u_l(a)\}^{2/3} + \frac{\Gamma^2}{a^2} \left\{ \frac{a_{\text{eff}}}{k_0^2 n_{\text{eff}}^2(a)} \right\}^{2/3} \right]} \right|. \quad (62)$$

We also mention the field representations corresponding to (60) and (61) for a transmitter and (or) receiver well above the critical height:

$$|E_r| \sim \frac{2^{3/2} k_0^{7/6} B n_{\text{eff}}^{3/2}(a)}{c a_{\text{eff}}^{1/3}} \left\{ \frac{3}{a \vartheta \cdot \vartheta(r_2)} \right\}^{1/2} \times \left| \sum_l \frac{e^{i \delta l \{ \vartheta - \vartheta(r_1) - \vartheta(r_2) \}}}{(\delta l)^{1/2} \left[\{3u_l(a)\}^{2/3} + \frac{\Gamma^2}{a^2} \left\{ \frac{a_{\text{eff}}}{k_0^2 n_{\text{eff}}^2(a)} \right\}^{2/3} \right]} \cdot H_{1/3}^{(1)}\{u_l(a)\} \right|, \quad (63)$$

$(h_1 = 0; h_2 > h_{cr})$

and

$$|E_r| \sim \frac{6k_0^{7/6} B n_{\text{eff}}^{3/2}(a)}{c a_{\text{eff}}^{1/3}} \left\{ \frac{2}{\pi a \vartheta \cdot \vartheta(r_1) \cdot \vartheta(r_2)} \right\}^{1/2} \times \left| \sum_l \frac{e^{i \delta l \{ \vartheta - \vartheta(r_1) - \vartheta(r_2) \}}}{\delta l \left[\{3u_l(a)\}^{2/3} + \frac{\Gamma^2}{a^2} \left\{ \frac{a_{\text{eff}}}{k_0^2 n_{\text{eff}}^2(a)} \right\}^{2/3} \right]} \cdot [H_{1/3}^{(1)}\{u_l(a)\}]^2 \right|. \quad (64)$$

$(h_1 > h_{cr}; h_2 > h_{cr})$

All these expressions contain the quantity $H_{1/3}^{(1)}\{u_t(a)\}$ either explicitly, or implicitly in the height-gain factors. This quantity can not be reduced any further for the most general soil conditions of the earth. However, a convenient expression may be obtained in the two limiting cases of very long and very short waves. The latter case corresponds to an infinite value of the right-hand side of (34). Let us denote this right-hand side by $-e^{i\pi/3}N$. The solution of (34) can then be expanded with respect to N^{-1} , a method well known in the diffraction theory for a homogeneous atmosphere [6]. A corresponding expansion then exists for $H_{1/3}^{(1)}\{u_t(a)\}$. Its leading term for large $|N|$ reads:

$$H_{1/3}^{(1)}\{u_t(a)\} \sim -\frac{e^{-i\pi/3}H_{2/3}^{(1)}(u_{l,\infty}) \cdot u_{l,\infty}^{1/3}}{N},$$

$u_{l,\infty}$ here marks a zero of $H_{1/3}^{(1)}(u)$.

14. Comparison Between the Fields Corresponding to Two Different Profiles

As stated above (end of section 9), the influence of the refractive-index profile is restricted to that on the parameters $n_{\text{eff}}(a)$ and a_{eff} for propagation over the ground. Moreover, the height-gain effects reduce to an additional dependence on the angular horizon distances $\vartheta(r_1)$ and $\vartheta(r_2)$ of the elevated transmitter and receiver (see section 10). This involves an extremely simple relation between the fields corresponding to two profiles having identical values of $n_{\text{eff}}(a)$ and a_{eff} . Such two profiles show the same surface values of the refractive index and its gradient, but they may differ noticeably at high altitudes. According to section 8 the eigenvalues l , too, prove to be identical for these profiles; therefore, the same then holds for all parameters occurring in expansions such as (62), (63) and (64).

We shall compare the actual profile with some reference profile, the quantities of which will be marked by a dash (see fig. 1 in which the Eckersley profile (22) is assumed to be the reference profile); both profiles are assumed to have coincident values of a and a_{eff} . In view of the above remarks, raising of an antenna (transmitter or receiver) to an elevation $h=r-a$ will produce the same field as an elevated antenna at a height $h'=r'-a$ in the reference profile, provided that we have $\vartheta(r)=\vartheta'(r')$.

This may be applied to atlases of propagation curves, such as edited by the C.C.I.R. [7] and by the Japanese Ministry of Postal Services [8]. The data of these atlases are essentially based on the Eckersley profile (22) with $a_{\text{eff}}=(4/3)a$. The evaluation of (48) for the angular horizon distance results for this profile in the expression:

$$\vartheta_{\text{Eck}}(r) = \left(\frac{a_{\text{eff}}}{a}\right)^{1/2} \arccos\left(\frac{a}{r}\right).$$

Therefore, the curves of the mentioned atlases can also be used for other profiles with the same value of a_{eff} [the value of $n_{\text{eff}}(a)$ is irrelevant, since $n_{\text{eff}}(a) \sim 1$]. The antenna heights $h=r-a$, corresponding to a horizon distance $\vartheta(r)$, are then to be replaced by an effective height $h'=r'-a$ for which

$$r' = \frac{a}{\cos\left\{\left(\frac{a}{a_{\text{eff}}}\right)^{1/2} \cdot \vartheta(r)\right\}}.$$

Examples of the use of such corrections are given in two recent publications by Norton [9, 10].

15. Concept of the Effective or "Angular" Distance

The most striking feature of the expressions (63) and (64) concerns the presence of the angular distances $\vartheta-\vartheta(r_2)$ and $\vartheta-\vartheta(r_1)-\vartheta(r_2)$ in the exponent. The effect of the antenna heights is mainly contained in the corresponding exponential, the influence of the nonexponential factors $\{\vartheta(r_1)\}^{1/2}$ and $\{\vartheta(r_2)\}^{1/2}$ being much smaller. The importance of the distances in

question has been emphasized in particular by Norton, Rice, and Vogler [11]. These authors have introduced the term "angular distance" with an extension to the cases of propagation over irregular terrain. For propagation over a smooth spherical earth beyond the line of sight the "angular distance" represents simply the actual distance between the radio horizons of the transmitter and the receiver divided by the radius of the sphere.

For a smooth earth the expansions (63) and (64) justify the reduction of the height dependence to that on the "angular" distance, under the following conditions: (a) the elevated antennas are to be situated above the critical height h_{cr} fixed by (57); and (b) the effect of the square roots $\{\vartheta(r_1)\}^{1/2}$ and $\{\vartheta(r_2)\}^{1/2}$ should be negligible.

Let us abstract from the factor $\vartheta^{1/2}$ in (63) and (64) which is not very critical. The dependence on the "angular distance" then combines both the influence of the antenna elevations and of the horizontal distance. The influence of the former simply amounts to a reduction of the actual distance $d=a\vartheta$ to that of the radio horizons, that is to $a\{\vartheta-\vartheta(r_1)\}$ or $a\{\vartheta-\vartheta(r_1)-\vartheta(r_2)\}$. The comparison with a reference profile (see the preceding section) can be expressed here in terms of a shift $\Delta\vartheta$ of the "angular" distance. In fact, let an antenna height $h=r-a$ in the actual profile produce the same field, at a distance $d=a\vartheta$, as the reference profile at a distance $d+\Delta=a(\vartheta+\Delta\vartheta)$, the antenna elevation being kept constant. The unique dependence on the "angular" distance, assumed here for both profiles, then involves the relation:

$$\vartheta-\vartheta(r)=\vartheta+\Delta\vartheta-\vartheta'(r).$$

Hence

$$\Delta\vartheta=\vartheta'(r)-\vartheta(r).$$

The corresponding linear distance shift is given, according to (48), by

$$\Delta=a\Delta\vartheta=aM_{\text{eff}}(a)\int_a^r \frac{dr'}{r'} \left[\frac{1}{\{M_{\text{eff}}'^2(r')-M_{\text{eff}}^2(a)\}^{1/2}} - \frac{1}{\{M_{\text{eff}}^2(r')-M_{\text{eff}}^2(a)\}^{1/2}} \right].$$

The derivative with respect to the antenna elevation $h=r-a$, reading

$$\frac{d\Delta}{dh} \sim M_{\text{eff}}(a) \left[\frac{1}{\{M_{\text{eff}}'^2(r)-M_{\text{eff}}^2(a)\}^{1/2}} - \frac{1}{\{M_{\text{eff}}^2(r)-M_{\text{eff}}^2(a)\}^{1/2}} \right],$$

can be reduced for small altitudes with the aid of the expansions:

$$M_{\text{eff}}^2(r)-M_{\text{eff}}^2(a)=\frac{\Lambda_1}{a}h+\frac{\Lambda_2}{2a^2}h^2+\dots,$$

$$M_{\text{eff}}'^2(r)-M_{\text{eff}}^2(a)=\frac{\Lambda_1}{a}h+\frac{\Lambda_2'}{2a^2}h^2+\dots$$

This leads to the following approximation for Δ itself for small heights:

$$\Delta \sim \frac{n_{\text{eff}}(a)(\Lambda_2-\Lambda_2')}{6a^{1/2}\Lambda_1^{3/2}} h^{3/2} = \frac{(\Lambda_2-\Lambda_2')a_{\text{eff}}^{3/2}}{12.2^{1/2}n_{\text{eff}}^2(a)a^2} h^{3/2}.$$

Equivalent expressions have been derived by Millington [12] and Wait [13] in a simplified derivation of the effective-distance concept.

16. References and Notes

- [1] C. L. Pekeris, Asymptotic solutions for the normal modes in the theory of microwave propagation, *J. Appl. Phys.* **17**, 1108 (1946).
- [2] J. R. Wait, Radiation from a vertical antenna over a curved stratified ground, *J. Research NBS* **56**, 237 (1956); see eq (6).
- [3] H. Bremner, Mode expansion in the low-frequency range for propagation through a curved stratified atmosphere, *J. Research NBS* **63D**, 75 (1959); see eq (15).

- [4] See reference [3], eq (5).
- [5] This follows from a comparison of the amplitude factors of the expansions (15) and (16) in reference [3].
- [6] Compare H. Bremmer, *Terrestrial radio waves*, p. 45 (Elsevier Publishing Co., New York, N.Y., 1949); the quantities $\mu_1(a)$ and $(\Gamma/a)\{a_{eff}/3k_0^2 n_{eff}^2(a)\}^{1/3}$ of the present paper correspond to $(-2\tau_e)^{3/2}/3$ and $1/(3^{1/2}\delta)$ in this reference.
- [7] Atlas of ground-wave propagation curves for frequencies between 30 Mc/s and 300 Mc/s, published by the International Telecommunications Union, Geneva, Switzerland (1955).
- [8] Atlas of radio wave propagation curves for frequencies between 30 and 10,000 Mc/s, prepared by the Radio Research Laboratory, Tokyo, Japan (January 1958).
- [9] K. A. Norton, Transmission loss in radio propagation—II, NBS Tech. Note **12** (1959).
- [10] K. A. Norton, System loss in radio wave propagation, J. Research NBS **63D**, 53 (1959).
- [11] K. A. Norton, P. L. Rice, and L. E. Vogler. The use of angular distance in estimating transmission loss and fading range for propagation through a turbulent atmosphere over irregular terrain, Proc. IRE **43**, 1488 (1955). See in particular p. 1491.
- [12] G. Millington, Propagation at great heights in the atmosphere, Marconi Rev. **21**, 143 (1958).
- [13] J. R. Wait, On the propagation of radio waves in an inhomogeneous atmosphere, NBS Tech. Note **24** (1959).

(Paper 64D5-82)

Polarization and Depression-Angle Dependence of Radar Terrain Return¹

I. Katz and L. M. Spetner

(March 25, 1960; revised May 2, 1960)

A study of recent experimental results on radar back scattering from land and sea surfaces indicate: (a) The polarization dependence of the normalized radar cross section, σ_0 , of ocean surfaces cannot be explained by the usual "interference phenomenon," and (b) there is a distinct difference in the form of the depression-angle dependence in that σ_0 for "smooth" surfaces follows a negative exponential whereas σ_0 for "rough" surfaces drops off as the sine of the depression angle.

1. Introduction

In order to progress toward a better understanding of back-scattering from natural surfaces a large amount of radar-return data from various sources has been studied.

For the first time in the history of the radar terrain-return problem, large volumes of data have become available. The data which have been studied include experimental results from the Naval Research Laboratory and Goodyear Aircraft Corp. under sponsorship of the Applied Physics Laboratory, Ohio State University, and the Admiralty Signal and Radar Establishment and the Royal Radar Establishment in Great Britain. As a whole, these data include radar return from various kinds of terrain as well as from the ocean in various sea states, several wave lengths, and in general both polarizations. In most of these cases, a wide range of depression angles has been covered. As a result of these studies certain features of radar terrain back-scattering are becoming clear. In this paper the polarization and depression-angle dependence of radar return are discussed.

2. Polarization Dependence

The polarization dependence of sea return is more striking than that of land return and the present discussion of polarization dependence will be confined to sea return. Herbert Goldstein [1]² has postulated a droplet theory to explain the fact that the radar return for horizontal polarization is less than that for vertical polarization. In his theory, it is the droplets or spray particles that are cast up by the water which do most of the reflecting or back-scattering of the radar energy. Since these droplets are illuminated within the interference pattern

formed by the direct ray from the radar and the reflection from the ocean surface, horizontally polarized radiation which has a higher reflection coefficient for forward scattering has a deeper first null and hence, gives weaker illumination on the scattering droplets. This leads to a smaller radar return. Katzin [2] has postulated surface scatterers in the place of Goldstein's droplets, which are also illuminated within the interference pattern of the radar.

There is now evidence that the polarization dependence of sea return cannot be explained by an interference pattern in the illumination. Results on forward scattering of energy by the ocean surface [3] indicate that for microwave frequencies and for depression angles above a few degrees in most sea conditions the interference pattern may be negligible even for horizontal polarization. In figure 1 are shown experimental values of the normalized radar cross section, σ_0 , plotted against depression angle using an L-band radar. Although the sea state in this experiment is unknown, the water surface was subjected to a 30-knot wind which would normally result in 8 ft rms wave heights in a fully developed sea. Interference effects, at depression angles above 10 deg, can account for less than 3 db difference between the reflected power for horizontal and vertical polarization even if one assumes only a root mean square wave height of 1 ft. Yet the difference between the powers returned on the two polarizations is greater than 6 db between 10 and 25 deg.

It is only at the very low angles that significant interference effects can arise, usually at angles substantially smaller than 1 deg, depending, of course, upon the sea state and the wave length. Note, again in figure 1, that at the lower depression angles it appears that the curve for vertical polarization is tending to cross the one for horizontal polarization. Figure 2 [4] shows that this trend continues and crossover does take place,³ i.e., for depression angles

¹ Contribution from Applied Physics Laboratory, The Johns Hopkins University, Silver Spring, Md. This work was supported by the Bureau of Naval Weapons, Department of the Navy under Contract NOrd-7386.

² Figures in brackets indicate the literature references at the end of this paper.

³ Although figures 1 and 2 refer to different sea states and different radar frequencies they do tend to establish the existence of crossover at least for some frequencies and for some sea states.

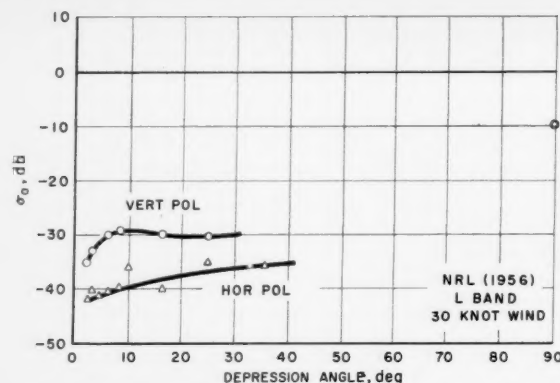


FIGURE 1. Normalized radar cross section of sea surface for vertical and horizontal polarizations as a function of depression angle.

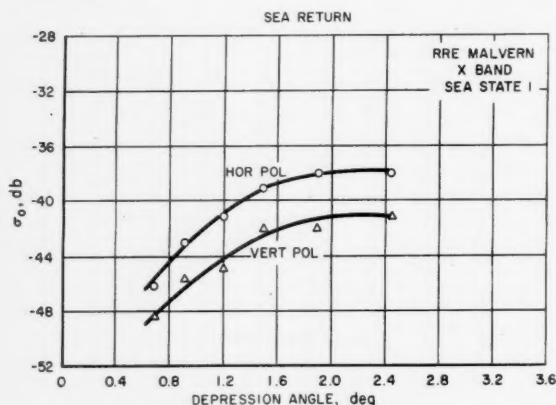


FIGURE 2. Normalized radar cross section of sea surface for vertical and horizontal polarizations as a function of depression angle for very small depression angles.

less than 2.5 deg the normalized radar cross section for vertical polarization is smaller than that for horizontal polarization.

Thus the interference pattern explanation of the polarization dependence of sea return is faced with the following dilemma. It serves as an explanation of the fact that σ_0 for vertical polarization is greater than that for horizontal polarization but a non-negligible interference pattern obtains only at extremely low depression angles. At these low angles, however, experimental evidence is quite to the contrary in that σ_0 for vertical polarization is smaller than that for horizontal polarization. Where the experimental data show σ_0 for vertical polarization greater than that for horizontal polarization, interference theory is at a loss for an explanation.

The interference theory has a further unsatisfactory feature. It is not clear how a scatterer on the surface can be illuminated in an interference pattern which includes a ray reflected from the same surface. If the scatterers on the surface of a homogeneous sea are sufficiently illuminated to enable them to scatter in the forward direction a ray which is strong enough

to produce a deep null in the interference pattern, then the scatterers should be illuminated strongly enough to reflect back to the radar.

Since the interference phenomenon cannot reasonably explain the polarization dependence of sea return one must look elsewhere; it is possible that the correct explanation will come by examining the fundamental properties of electromagnetic scattering from an ocean-type surface. Katzin suggested in his paper an array of circular disks as a model for the ocean surface. The exact theory of electromagnetic scattering off a circular disk has recently been worked out by Flammer [5] and by Meixner and Andrejewski [6]. The results of these calculations are difficult to evaluate numerically. Calculations have been made, however, from Flammer's results for a disk of diameter of the order of a wavelength. These results show that a disk has a larger back-scattering cross section for horizontal than for vertical polarization. This agrees with the results of Copson [7] for scattering from an extremely small disk. In applying these results to interpretation of the data it is tacitly assumed that effects of multiple scattering are negligible. It is interesting to note that single scattering off small circular disks is consistent with the experimental results available at the extremely low angles, because at the very low angles one expects only the small and rather isotropic scatterers to be effective. At the higher angles, one can expect larger, more directive, scatterers to contribute the bulk of the radar return; an examination of the back-scattering from a large circular disk may suggest an appropriate explanation for the experimental results.

3. Depression-Angle Dependence

Data from Ohio State University [8] on radar return from various kinds of land surfaces show that for the case of rough surfaces with only a few exceptions, there seems to be no significant difference between horizontal and vertical polarization, but for smooth surfaces and for angles larger than 10 deg, σ_0 for vertical polarization is larger than that for horizontal polarization just as in the case of the ocean.

This leads to a plausible explanation for the depression angle dependence of sea return. At extremely large depression angles, near 90 deg, the radar return arises largely from specular reflections off the very large and almost horizontal facets of the ocean surface. At the very small depression angles, radar return is in large part caused by the isotropic scattering off the extremely small scatterers. In the intermediate range of depression angles from about 20 to 70 deg, lies an interesting region which may also hold the key to the polarization dependence.

A study of the curves of normalized radar cross section versus depression angle, θ , brings out clearly the difference in form between "rough" and "smooth" surfaces. For the most part the curves taken over rough surfaces show that σ_0 varies as θ or $\sin \theta$ between 10 and 80 deg. Figure 3 is an example of

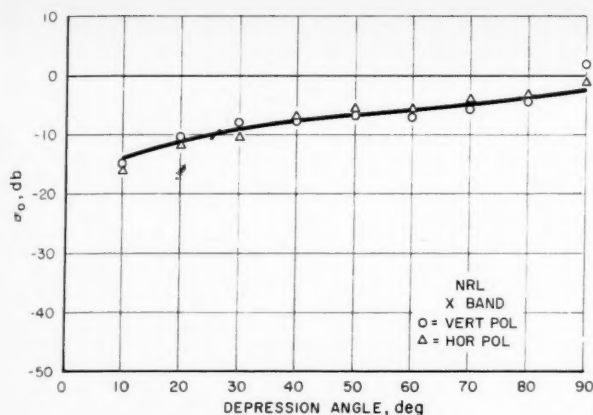


FIGURE 3. Normalized radar cross section of forest.

The solid line represents a linear variation of σ_0 with θ .

radar return from a forested area using an X-band radar. These measurements were made over New Jersey woods which consisted of trees about 50 ft high. The important feature of the radar return from rough terrain appears to be the flatness of the σ_0 versus θ curves.

For smoother surfaces the cross section curves increase more sharply with increasing depression angle as illustrated in figure 4. In this figure are presented radar-return data from three surfaces with different degrees of smoothness characterized as: (1) concrete road, (2) concrete road with 2 in. of smooth snow, and (3) concrete road with 2 in. of rough snow; clearly, the smoother the surface the steeper is the σ_0 curve.

In a previous paper [9] theoretical results were reported based on a facet model with specular reflection to explain radar return from smooth-type surfaces. There it was suggested that if the probability distribution of the slopes were Gaussian one might expect that the radar cross section would be proportional to $\exp(-k \cot^2 \theta)$. An examination of the experimental results that have since become

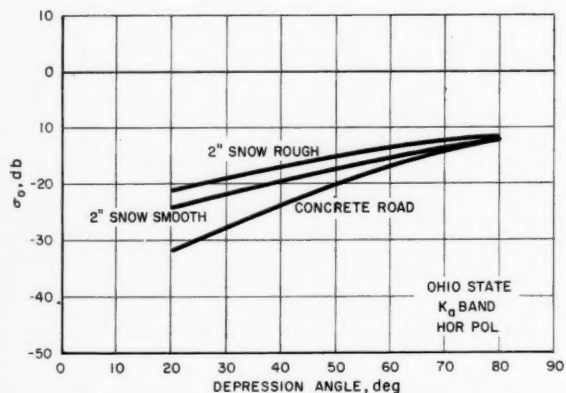


FIGURE 4. Normalized radar cross section showing the transition from rough to smooth surfaces.

available indicates that a better description of the radar cross section would be given by $\exp(-k \cot \theta)$ instead. This suggests that if the model of a random distribution of facet slopes is to be preserved then the probability distribution of the slope, x , is of the form $\exp(-kx)$ rather than a Gaussian. Figure 5 is an example of data taken over Lake Michigan using both polarizations which show the depression angle regions where the form $\exp(-k \cot \theta)$ for σ_0 holds.

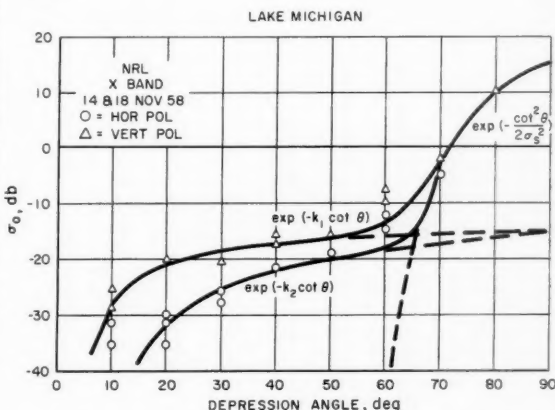


FIGURE 5. Normalized radar cross section of the surface of Lake Michigan for horizontal and vertical polarizations.

In the case of extremely low angles over land a mechanism was previously suggested [10] that would lead to an increase in σ_0 as θ approaches very close to zero. This mechanism was based on more efficient scattering from vertical structures as the depression angle approaches zero. It is noteworthy that data for extremely small angles between 1 and 4 deg show there is an upturn in the curves with decreasing θ . An example of this is shown in figure 6.

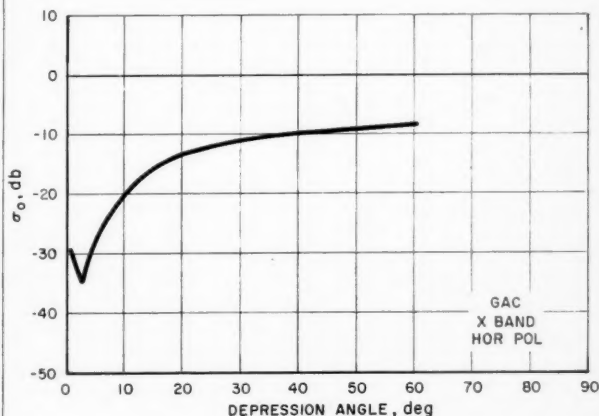


FIGURE 6. Normalized radar cross section of cultivated terrain illustrating the increase of σ_0 with decreasing θ for very small values of depression angle.

4. Conclusion

Another mechanism must be found to explain the polarization dependence of sea return. It would be instructive to calculate the back scattering from disks having diameters of a wavelength and greater. The non-Gaussian nature of the reflecting facets in the ocean surface is somewhat surprising. This fact may point to a clearer understanding of radar reflectivity, if pursued.

5. References

- [1] D. E. Kerr, *Propagation of Short Radio Waves*, pp 481-527 (McGraw-Hill Book Co., Inc., New York, N.Y., 1951).
- [2] M. Katzin, On the mechanisms of radar sea clutter, *Proc. IRE* **45**, 44 (1957).
- [3] C. I. Beard, I. Katz, L. M. Spetner, Phenomenological vector model of microwave reflection from the ocean, *IRE Trans.* **AP-4**, 162 (1956).
- [4] Private communication from M. H. Oliver, (Oct. 6, 1959).
- [5] C. Flammer, The vector wave function solution of the diffraction of electromagnetic waves by circular disks and apertures, *J. Appl. Phys.* **24**, 1218 (1953).
- [6] J. Meixner and W. Andrejewski, Exact theory of the diffraction of plane electromagnetic waves from a perfectly conducting circular disk and from a circular aperture in a perfectly conducting plane screen (in German), *Ann. Phys.* **7**, 157 (1950).
- [7] E. T. Copson, An integral-equation method of solving diffraction problems, *Proc. Roy. Soc. (London)* [**A**] **186**, 100 (1946).
- [8] R. C. Taylor, Terrain return measurements at X-, K_u-, K_a-band, *IRE Conv. Rec.* **1** (1959).
- [9] L. M. Spetner and I. Katz, Two statistical models for radar terrain return, *IRE Trans.* **AP-8**, (May 1960).
- [10] I. Katz and L. M. Spetner, A program to investigate radar terrain return, The Johns Hopkins Univ. Appl. Phys. Lab. Rept. CF-2700 (1958).

(Paper 64D5-83)

Methods of Predicting the Atmospheric Bending of Radio Rays¹

B. R. Bean, G. D. Thayer, and B. A. Cahoon

(March 3, 1960; revised March 22, 1960)

Three methods for predicting the bending of radio rays when the refractive index profile above the surface layer is unknown have been developed recently by the authors. These methods are: a statistical technique for refraction at high initial elevation angles, estimation of bending from an exponential model of atmospheric refractive index, and a modification of the exponential model to account for the heavily weighted effects of anomalous initial refractive index gradients at small initial elevation angles. Each model is dependent upon the value of the refractive index at ground level or, in the case of superrefraction, the additional knowledge of the refractive index gradient next to the earth's surface. Each method works best in a particular range of initial elevation angles or meteorological conditions. The height and angular ranges of application of each method are checked by comparison with values obtained from 77 diverse refractive index profiles representative of wide climatic variation. It is found that the use of the best of the three methods will always result in a prediction of the total atmospheric bending within 10 percent for initial elevation angles from zero to 10 milliradians and to within 4 percent for initial elevation angles greater than 17 milliradians (~ 1 deg).

Glossary of Terms

- n = the radio refractive index.
- n_s = the value of n at the earth's surface.
- N = the radio refractivity, $N \equiv (n-1) \times 10^6$.
- N_s = value of N at the earth's surface.
- ΔN = difference between N_s and the N value at one km above the surface, $-\Delta N \equiv N_s - N_1$.
- $(dN/dh)_0$ = gradient of N with respect to height, dN/dh , evaluated at the earth's surface.
- r = vector radius from the center of the earth.
- r_0 = radial distance from the center to the earth's surface.
- h = height above the surface, $h \equiv r - r_0$.
- θ = elevation angle of a radio ray, the (acute) angle between the tangent to the ray path and the local horizontal (i.e., perpendicular to the radius vector.)
- θ_0 = the value of θ at the ray path origin (transmitting or receiving point).
- θ_p = the angle of penetration for a radio duct, i.e., the smallest value of θ_0 for which the radio ray will *not* be trapped, or conversely, the largest θ_0 for which the ray *will* be trapped.
- τ = the angular refraction, or bending, of a radio ray.
- ϵ = elevation angle error, the angular difference between θ_0 and the true elevation angle to a target at a given point on the ray path.

1. Introduction

Recent years have seen considerable activity in the evaluation of refraction effects in the troposphere. Schulkin [1]² outlined a simple method for refraction calculations and applied it to determine the mean refraction expected in arctic, temperate, and tropical climates. Fannin and Jehn [2] made an extensive analysis of elevation angle errors expected in various air masses and geographic locations for initial elevation angles in excess of 3 deg above the horizontal. In a series of papers [3,4,5,6] the present authors have examined atmospheric refractive index structure, the effect of this structure upon radio-ray refraction and have evolved methods of estimating the refraction of radio rays for *all* initial elevation angles. These methods are unique in that they depend only upon a knowledge of the refractive index at the earth's surface or, in the case of superrefraction, the gradient of the refractive index in the earth-boundary layer. Thus distributions of elevation angle error, angular bending, and other refraction effects may be determined for the majority of practical applications by simple reference to distributions of the surface value of the refractive index such as those for the United States [7]. It is assumed of course, that these various methods will be applied only when either details of the actual refractive index profile are unknown or it is impractical to obtain these details. It is under this assumption that this paper tests the relative accuracy of these various prediction methods to arrive at a delineation of conditions under which each method works best.

¹ Contribution from Central Radio Propagation Laboratory, National Bureau of Standards, Boulder, Colo.

² Figures in brackets indicate the literature references at the end of this paper.

2. Theory and Background

A basic measure of atmospheric refraction effects on high frequency radio propagation is the bending, or angular refraction, of individual rays. By assuming the refractive index to be a function only of height above the surface of a smooth, spherical earth rays can be traced using Snell's law in the following form [1]:

$$nr \cos \theta = n_s r_0 \cos \theta_0. \quad (1)$$

The geometry is shown in figure 1. The equation for the ray bending, τ , can be obtained from eq (1) as [1, 9]

$$\tau_{s,1} = - \int_{n_s}^{n_1} \frac{dn}{n} \cot \theta \quad (2)$$

where
$$\theta = \cos^{-1} \left\{ \frac{n_s r_0 \cos \theta_0}{n_1 r} \right\},$$

and $\cot \theta$ is given to a very high degree of approximation by:

$$\cot \theta = \sqrt{\frac{\cos \theta_0}{\sin^2 \theta_0 + \frac{2h}{r_0} - 2(N_s - N) \times 10^{-6} \cos^2 \theta_0}} \quad (3)$$

It can be seen from inspection of eq (2) and (3) that in order to evaluate τ directly it is necessary to know the refractive index of the atmosphere, n as a function of height, h .

How one evaluates eqs (2) and (3) depends upon the availability of data and computing facilities. If details of the refractive index profile are available

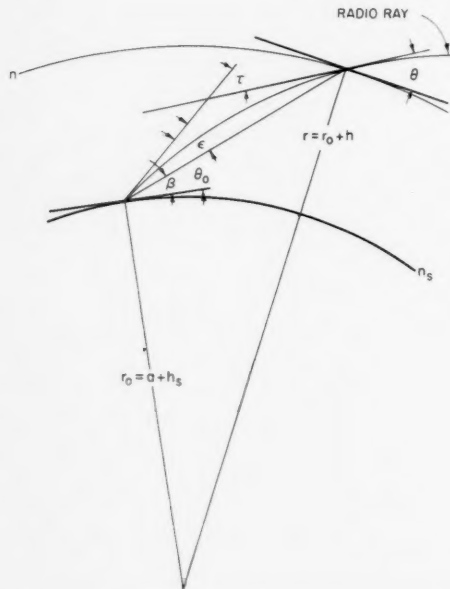


FIGURE 1. Geometry of radio-ray refraction.

from either refractometer or radiosonde ascents, then one could evaluate refraction effects with the aid of of an electronic computer or simplified graphical techniques [9]. However, frequently the desired refractive index profile data are simply not available and one must fall back upon less exact methods of estimating τ . One may use average values of τ such as given by Schulkin or the distributions of refraction effects given by Fannin and Jehn. However, simple, standard measurements of pressure, temperature, and humidity at the earth's surface are almost always available and may be used to estimate tropospheric refraction effects. In the sections that follow, the evaluation of the integral for τ will be examined from three different viewpoints:

1. Simplification of eqs (2) and (3), to permit evaluation of τ without knowledge of details of the actual refractive index profile.

2. Evaluation of τ for actual observed refractive index profiles and the statistical reduction of the data so derived into a function of some observable parameter (e.g., N_s).

3. Construction of an analytic model of $n(r)$ for normal conditions, thus yielding expected values of τ by direct integration of the model.

3. τ as a Function of N_s

As a first approximation towards evaluation of τ without detailed knowledge of $n(r)$, consider the integration by parts of eq (2):

$$\begin{aligned} \tau_{s,1} = & - \int_{n_s}^{n_1} \frac{dn}{n} \cot \theta = - \ln \{n\} \cot \theta \Big|_{n_s}^{n_1} \\ & + \int_{\cot \theta_0}^{\cot \theta_1} \ln \{n\} d(\cot \theta) \end{aligned}$$

or:

$$\tau_{s,1} = \ln \{n_s\} \cot \theta_0 - \ln \{n_1\} \cot \theta_1 - \int_{\theta_0}^{\theta_1} \ln \{n\} \csc^2 \theta d\theta$$

Now since $n = 1 + N \times 10^{-6}$ and $N \times 10^{-6} < 5 \times 10^{-4}$

then

$$\ln \{n\} = N \times 10^{-6} \{1 - \frac{1}{2}(N \times 10^{-6}) + \dots\} \cong N \times 10^{-6}$$

with this approximation (i.e., a maximum error of less than 0.2%) the above equation becomes

$$\begin{aligned} \tau_{s,1} \cong & N_s \times 10^{-6} \cot \theta_0 - N_1 \times 10^{-6} \cot \theta_1 \\ & - \int_{\theta_0}^{\theta_1} N \times 10^{-6} \csc^2 \theta d\theta \text{ for } \theta_0 \pm 0. \quad (4) \end{aligned}$$

The integral in eq (4) has been found to contribute no more than 3 percent to the value of $\tau_{s,\infty}$ for an initial elevation angle of 10 deg or greater [1] while the second term is zero due to $N_\infty \equiv 0$. Thus the first term of (4) forms an approximation to $\tau_{s,\infty}$ which is asymptotic to the true value of $\tau_{s,\infty}$ as θ_0

approaches 90 deg. It may be shown that for normal conditions and all heights the integral in (4) is essentially independent of N_s for $\theta_0 > 17$ mr (~ 1 deg); the term $N_1 \cot \theta_1$ tends to be constant; thus (4) reduces to a linear equation

$$\tau_{s,1} \cong b_1 N_s + a_1. \quad (5)$$

The form of eq (5) is very attractive, since it implies two things:

1. $\tau_{s,1}$ may be predicted with some accuracy as a function only of N_s (h_1 and θ_0 constant), a parameter which may be observed from simple surface measurements of the common meteorological elements of temperature, pressure, and humidity.

2. The simple linear form of the equation indicates that, given a large mass of observed $\tau_{s,1}$ versus N_s for many values of h and θ_0 , the expected (or best estimate) values of b and a can be obtained by the standard method of statistical linear regression.

The method of attack indicated by implication number two has, in fact, been carried out by the authors [3]. The results show that for $h_1 = \infty$ the method is accurate to within ± 3 percent of the true value (as an rms error) for initial elevation angles as small as 1 deg. The accuracy of this method and the following methods, will be examined for $0.1 \text{ km} \leq h \leq \infty$ in the following sections.

4. Exponential Model

The development of a model of $N(h)$ to describe the normal behavior of atmospheric N as a function of N_s and height has received a considerable amount of treatment in the past. One of the simplest, and, at the same time, most accurate models which has emerged from these studies is that in which $N(h)$ has an exponential decrease with height [4, 5, 10],

$$N(h) = N_s \exp \{-c_s h\}. \quad (6)$$

One of the earliest applications of this particular model has been attributed by Garfinkel to Sir Isaac Newton, who used the exponential form in a study of astronomical refraction [11].

If it is assumed that $N(h)$ is indeed an exponential function of height, then the gradient of $N(h)$ would also be an exponential function of height. The most extensive source of data with which to evaluate the coefficients in the exponential is that of ΔN (the value of N at 1 km minus the surface value, N_s) which has received wide application in radio propagation problems [12]. Thus we would expect

$$\frac{\Delta N}{\Delta h} = k_1 \exp \{-k_2 h\} \quad (7)$$

to take the form

$$\Delta N = k_1 \exp \{-k_2 h\}$$

for our special case of $\Delta h = h = 1 \text{ km}$. Examination of the ΔN data soon revealed that k_2 was dependent upon N_s , i.e., the higher the surface value of N the greater the expected drop in N over 1 km. Examination of the data indicated that

$$k_2 = k_3 N_s$$

and the resultant equation,

$$\Delta N = k_1 \exp \{-k_3 N_s\} \quad (8)$$

was solved by least squares. The least squares determination was facilitated by converting (8) to the form

$$\ln |\Delta N| = -k_3 N_s + \ln k_1 \quad (9)$$

or, in words, expressing the natural logarithm of ΔN as a linear function of N_s . The values of k_1 and k_3 were established from some 888 sets of 8-year means of ΔN and N_s from 45 U.S. weather stations. The results of this study are shown graphically in figure 2 where the least squares exponential fit of $\overline{\Delta N}$ and \overline{N}_s is given by:

$$-\overline{\Delta N} = 7.32 \exp \{0.005577 \overline{N}_s\}. \quad (10)$$

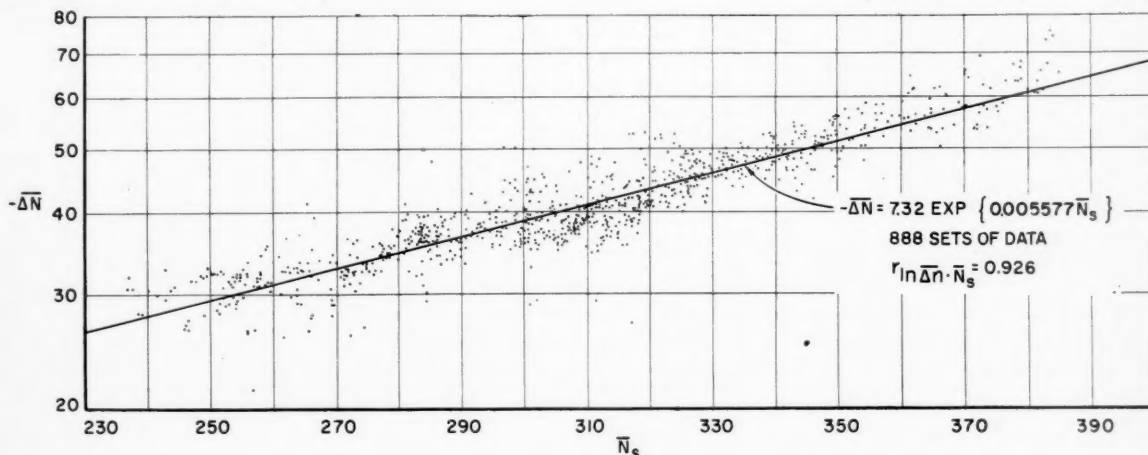


FIGURE 2. Regression of $\ln |\Delta N|$ upon N_s .

From this equation the CRPL Exponential Reference Atmosphere [5] was determined, the profiles being defined by the following equations:

$$N = N_s \exp \{-c_e h\}$$

$$c_e = \ln \left\{ \frac{N_s}{N_s + \Delta N} \right\} \quad (11)$$

Ray tracings have been computed for this model covering more than the normal range of N_s , and the results may be used, either in tabular or graphical form, to predict τ for any normal combination of N_s , θ_0 , and height [5].

5. Initial Gradient Correction Method

The importance of the initial gradient in radio propagation where the initial elevation angle of a ray path is near zero has long been recognized. For example, if $dN/dh = 1/r_0$ then $\Delta\tau = \infty$, an expression of the fact that the ray path will travel at a constant height above the earth's surface. This is called ducting, or trapping of the radio ray. The effect of anomalous initial N -gradients on ray propagation at elevation angles near zero, and for gradients less than ducting, ($|dN/dh| < 157/\text{km}$, or $dn/dh > -157/\text{km}$), may also be quite large. A method has been presented [4] for correcting the predicted refraction (from the exponential reference atmosphere) to account for anomalous initial N -gradients, assuming that the actual value of the initial gradient is known. The result is,

$$\tau_h = \tau_h(N_s, \theta_0) + [\tau_{100}(N_s^*, \theta_0) - \tau_{100}(N_s, \theta_0)] \quad (12)$$

where $\tau_h(N_s) = \tau$ at height h , for the exponential reference atmosphere corresponding to N_s and N_s^* is the N_s for the exponential reference atmosphere having the same initial gradient as that observed; τ_{100} is τ at 100 meters height.

This procedure has the effect of correcting the predicted bending by assuming that the observed initial gradient exists throughout a surface layer 100 meters thick, calculating the bending at the top of the 100-meter-thick layer, and assuming that the atmosphere behaves according to the exponential reference profile corresponding to the observed value of N_s for all heights above 100 meters. This approach has proven quite successful in predicting τ for initial elevation angles under 10 mr, and will, of course, predict ducting when it occurs.

6. Analysis of the Accuracy of the Prediction Methods

A test sample of ray bendings for the range of N -profiles likely to be encountered was prepared from 77 refractivity profiles derived from radiosonde observations. These 77 profiles represent both normal and extreme refractivity profiles for 13 climatically diverse locations in the United States and are actually representative of a nearly worldwide range of conditions [13]. Values of τ were calculated by

numerical integration for values of θ_0 from 0 to 900 mr. (For a thorough discussion of the ray-tracing techniques employed see reference [5].) The results of this general refraction study provided a large mass of data for checking the accuracy of each of the prediction methods.

The relative accuracy of the exponential model and the initial gradient correction method were tested by predicting the bending at particular heights and initial elevation angles for the 77 sample profiles and finding the rms error of prediction for each case. Since 13 of the 77 profiles had surface ducts they could be used only for elevation angles greater than the angle of penetration for each case, given by:

$$\theta_p = \sqrt{0.2[156.9 - (dN/dh)_0] \times 10^6} \text{ radians} \quad (13)$$

where $(dN/dh)_0$ is the observed initial gradient of N per km, assumed to extend over 100 m. Thus there were only 64 profiles analyzed at $\theta_0 = 0$, and 77 at $\theta_0 = 10$ mr. These same data were also used to derive the regression of τ upon N_s for various heights and initial elevation angles. The scatter of points about the regression line was then used as an estimate of the minimum rms error that would be expected from any of the three prediction methods. Note carefully, however, that the regression lines are a "best fit" to the test data. Although a future sample of data would presumably yield similar rms deviations, the possibility exists that the present sample data are systematically biased, in this case there would be an additional error encountered in practice due to this bias.

The primary purpose of the present analysis is to determine over which regions of height and θ_0 each method will give the best results. It was found that the statistical correlation method is more accurate from 1 deg to vertical incidence and that for all altitudes in this range of θ_0 it is the most accurate of the three methods. At θ_0 smaller than 1 deg, and especially at $\theta_0 < 10$ mr, the methods based on the exponential reference atmosphere, particularly the corrected exponential reference atmosphere, are more accurate. Figure 3 illustrates these conclusions by

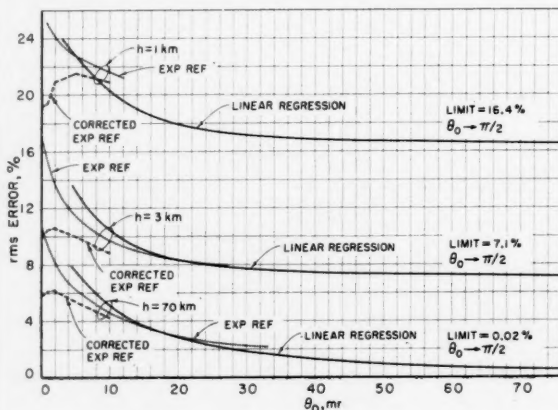


FIGURE 3. RMS error of predicting τ at various heights as a percent of mean τ , excluding superrefractive profiles.

comparing the rms error of prediction as a percent of mean τ for all three methods at three different heights and over a large range of θ_0 , excluding all superrefractive profiles. A superrefractive profile is here defined as one with an initial gradient of N in excess of 100 N -units per km, i.e., $(dN/dh)_0 < -100/\text{km}$.

It is evident from figure 3 that the percentage error of predicting τ decreases with increasing thickness of the atmosphere through which the ray passes. This is as one would expect since the value of the refractive index becomes less variable with increasing height and, one might say, the upper limit of integration of (2) becomes more a function of the lower limit, N_s . Further, the sensitivity of refraction effects to low-level profile anomalies for small values of θ_0 is reflected by the relatively small percentage error of the corrected exponential model for $\theta_0 < 10$ mr.

It must be remembered that the statistical regression technique is only *apparently* superior to methods using the exponential reference atmosphere since, by definition, it must have a minimum rms error provided that τ is a linear function of N_s . Although the difference in the percentage rms error between these two methods appears quite large, the actual rms error of the exponential reference atmosphere is either less than or within 0.1 mr of that of the statistical correlation technique for $\theta_0 \geq 7$ mr, thus, for practical considerations, indicating no clear-cut superiority of one technique over the other; this is illustrated in figure 4.

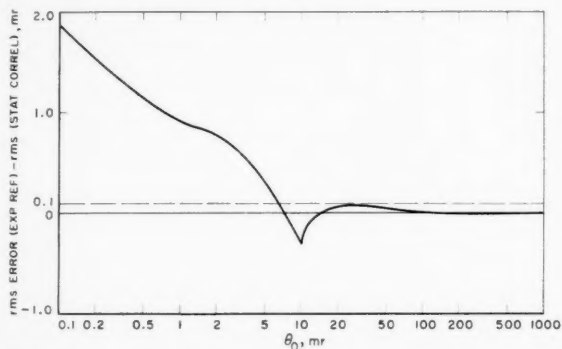


FIGURE 4. Difference between rms error of predicting τ at 70 km for the exponential reference atmosphere and the statistical correlation method.

One may evaluate the minimum rms error expected in predicting τ by these three methods by defining a composite prediction method that utilizes the best of the three methods in each range of θ_0 and height to yield a minimum overall error.

The numerical value of the rms deviations for the optimized composite of the three methods is shown on figure 5 for heights of 1, 3, and 70 km and all profiles. It is seen that the maximum error for any case is about 2 mr and decreases to 1 mr or less for $\theta_0 \geq 10$ mr for all height increments. The error for the total bending case, $h=70$ km, drops below an rms value of 1 mr for $\theta_0 \geq 5$ mr.

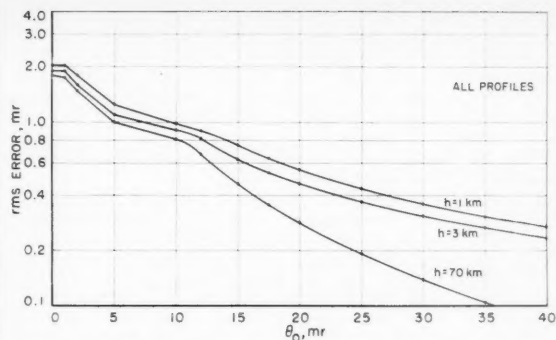


FIGURE 5. RMS error of predicting τ , composite prediction method.

7. Conclusions

The present study appears to indicate that:

1. The statistical regression technique is an adequate solution to the bending problem for all θ_0 larger than about 10 mr, and all heights from 1 km up.
2. The exponential reference atmosphere is equally as good as the statistical technique over the same range of θ_0 and height.
3. The initial gradient correction method is very useful for $\theta_0 < 10$ mr, and can be used to extend predictions of τ down to a θ_0 of 0 for any model which yields N as a function of height.

These conclusions indicate that the reader who desires the quick evaluation of some refraction effect should consult the rather extensive tables of the CRPL Exponential Reference Atmosphere [5]. These tables would allow, for instance, the determination of the elevation angle error as a function of θ_0 , N at the earth's surface, and the radar range. The reader desiring the convenience of the statistical regression technique for estimating either τ or the elevation angle error may obtain the necessary statistical parameters from the literature [14].

The authors express their gratitude to Mrs. B. J. Weddle, Mrs. M. A. Fischer, and Mrs. G. M. Richmond for their aid in the calculations of this study.

8. References

- [1] M. Schulkin, Average radio-ray refraction in the lower atmosphere, Proc. IRE **40**, 554 (1952)
- [2] B. M. Fannin and K. H. Jehn, A study of radar elevation-angle errors due to atmospheric refraction, IRE Trans. AP-5, 71 (1957).
- [3] B. R. Bean and B. A. Cahoon, The use of surface weather observations to predict the total atmospheric bending of radio waves at small angles, Proc. IRE **45**, 1545 (1957).
- [4] B. R. Bean and G. D. Thayer, On models of the atmospheric radio refractive index, Proc. IRE **47**, 740 (1959)
- [5] B. R. Bean and G. D. Thayer, CRPL exponential reference atmosphere, NBS Monograph 4 (1959).

- [6] B. R. Bean and B. A. Cahoon, Effect of atmospheric horizontal inhomogeneity upon ray tracing, *J. Research NBS* **63D**, 287 (1959).
- [7] B. R. Bean, J. D. Horn, and A. M. Ozanich, Jr., Climatic charts and data of the radio refractive index for the United States and the world, NBS Monograph (in press).
- [8] W. M. Smart, Spherical astronomy, chap. 3 (Cambridge University Press, London, 1931).
- [9] S. Weisbrod and L. J. Anderson, Simple methods for computing tropospheric and ionospheric refractive effects on radio waves, *Proc. IRE* **47**, 1770 (1959).
- [10] J. R. Bauer, W. C. Mason, and F. A. Wilson, Radio refraction in a cool exponential atmosphere, Lincoln Laboratory, MIT, Tech. Rpt. 186 (27 Aug. 1958).
- [11] Boris Garfinkel, An investigation in the theory of astronomical refraction, *The Astronomical Journal* **50**, 169 (1944).
- [12] B. R. Bean and F. M. Meaney, Some applications of the monthly median refractivity gradient in tropospheric propagation, *Proc. IRE* **43**, 1419 (1955).
- [13] B. R. Bean and G. D. Thayer, Comments on the limits to the utilization of the refractive index at ground level as a radio-meteorological parameter, To be published in *Proc. IRE* in reply to a letter by P. Misme.
- [14] B. R. Bean, B. A. Cahoon, and G. D. Thayer, Tables for the statistical prediction of radio ray bending and elevation angle error using the surface values of the radio refractive index, NBS Tech. Note 44 (in press).

(Paper 64D5-84)

Loss in Channel Capacity Resulting From Starting Delay in Meteor-Burst Communication

George R. Sugar

(March 25, 1960; revised April 25, 1960)

The loss in channel capacity of a meteor-burst communication system is computed as a function of the time required to initiate control of the system. The result is compared with various experimental data and appears to be applicable for signal bursts up to one-half second in duration. It is noted that in the very high frequency range the loss should increase with frequency.

1. Introduction

It appears that in any practical meteor-burst communication system, there will always be a brief time interval, after the meteor trail is formed, before the channel is used for message transmission. In the case of the familiar controlled two-way systems, this interval consists of one delay associated with the round-trip propagation time, a second associated with the recognition and identification of the distant transmitter, and sometimes a third associated with delays in starting the apparatus itself or in synchronizing one unit with another. In the case of a one-way or broadcast-type system, the propagation delay is not a factor but the other two delays can be significant. Some experimental data on these effects have already been reported by Forsyth et al. [1].² It is the purpose of this paper to show how the message capacity of a meteor-burst channel is related to a system's initiation time.

2. Estimation From Detailed Measurements of Burst Statistics

The loss in channel capacity for a specific system can be estimated directly from measurements of the distribution of signal durations above threshold. The distribution required is not the distribution of meteor-burst lengths in the usual sense but is, rather, the distribution of fading-cycle durations. Each signal excursion above the chosen threshold is assumed to be equivalent to a separate transmission. It is then assumed that signals with durations less than the initiation time are useless for message transmission and that the useful duration of each other signal is reduced by the initiation time. Once the signal duration distribution has been obtained the desired result can be readily computed. As an example, the relation between useful transmission time and system initiation time

obtained from one set of experimental data³ is shown in figure 1.

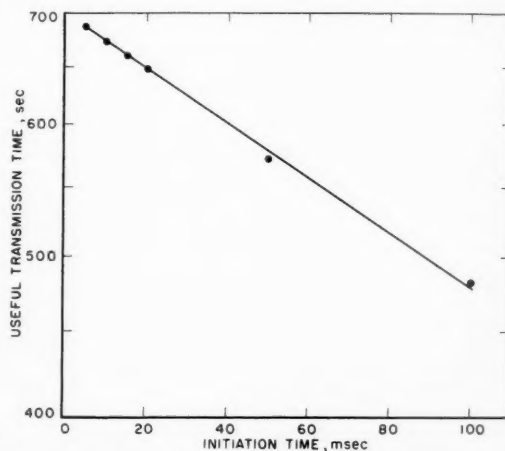


FIGURE 1. Reduction in effective channel capacity as a function of system initiation time.

3. Estimation From Theory

An accurate theoretical estimate for the general case appears to be quite complex and will not be attempted at present. Instead only the case for specular underdense trails is considered.

Assume that the signal amplitude for a burst is given by

$$\begin{aligned} S &= 0 & \text{for } t < t_0, \\ S &= S_0 \exp(-t/\tau) & \text{for } t \geq t_0, \end{aligned} \quad (1)$$

and that the number N of bursts with peak amplitudes greater than some amplitude S_1 is given by

$$N(S_0 > S_1) = CS_1^{-\alpha}. \quad (2)$$

¹ Contribution from Central Radio Propagation Laboratory, National Bureau of Standards, Boulder, Colo.

² Figures in brackets indicate the literature references at the end of this paper.

³ The data used were taken over the transmission path from Long Branch, Ill., to Boulder, Colo., at a frequency near 50 Mc/s. The observing interval was 1 hr.

A burst with duration t at threshold S_1 then has a peak value $S_0 = S_1 \exp(t/\tau)$, and the number of bursts having peak values between S_0 and $S_0 + dS_0$ is

$$dN = aC S_0^{-a-1} dS_0.$$

The cumulative duration of these bursts is

$$dT = t dN = taC S_0^{-a-1} dS_0.$$

Upon substituting for S_0 this becomes

$$dT = taC [S_1 \exp(t/\tau)]^{-a-1} (S_1/\tau) \exp(t/\tau) dt.$$

The total duration T above threshold S_1 is then

$$T = \int t dN = C S_1^{-a} \int_0^{\infty} (a/\tau) t \exp(-at/\tau) dt, \quad (3)$$

and

$$T = (\tau/a) C S_1^{-a} \quad (4)$$

Since this can be written as $T = (\tau/a)N$, the factor (τ/a) is just the average duration of a burst.

If an initiation time t_i is now assumed the useful duration of each burst is decreased and the effective time-above-threshold T' becomes

$$T' = \int (t - t_i) dN \quad \text{for } t \geq t_i$$

$$T' = 0 \quad \text{for } t < t_i.$$

Upon integration this becomes

$$T' = (\tau/a) C S_1^{-a} \exp(-at_i/\tau),$$

or

$$T' = T \exp(-at_i/\tau), \quad (5)$$

which is the desired result.

It is seen that in a system with an initiation time t_i the time available for message transmission is reduced to $\exp(-at_i/\tau)$ times that available in a system having an initiation time of zero.

4. Discussion

We first compare the theoretical relation (5) with two published curves depicting system efficiency in terms of initiation time. Forsyth et al. [1] have published a curve of normalized effective duty cycle versus initiation time, derived partially from operating experience with the JANET system and partly from extrapolation of measurements of signal duration. Their data corresponds nearly exactly (within a few percent) to the relation

$$T' = T \exp(-t_i/0.160) \text{ for } t_i \text{ in seconds.}$$

The second curve of interest is that given by Rach [2] for system efficiency versus number of teletype characters omitted (in starting). His curve is based on an experimentally determined distribution of burst durations as applied to a system with a 16.3 msec character length. This curve is nicely described by the relation

$$T' = T \exp(-t_i/0.39).$$

A further comparison can be made with data published by Forsyth et al. [ref. 1, fig. 11(c)], giving the distribution of the duration of signal excursions above

a fixed threshold. We find that for durations of less than one-half second their curve is of the form $\exp(-t/0.24)$.

Similar data has been published by Vincent et al. [3] and it is found that for durations of 0.06 sec to 0.6 sec their data are of the form $\exp(-t/0.20)$. (Data for durations less than 0.06 sec are of the form $\exp(-t/0.04)$. The reason for this discrepancy is not apparent.)

It appears from the above comparisons that for signal durations above threshold of one-half second or less the duration distribution is exponential in form. Therefore, eq (5) is applicable in computing efficiency as a function of initiation time. Since the theory was based entirely on idealized underdense trails, it is not surprising that the exponential law does not apply for durations longer than one-half second. However, since the experimental data considered the duration of individual excursions above threshold, rather than the total duration of signals from a single trail, it is certain that the fading signals from overdense trails have contributed to the net result. Further study is needed to define the role of the overdense trail in communications applications.

It is interesting to note that the theory predicts a loss in transmission time as the operating frequency increases. Since the conventional form of the time variation of signal amplitude is $S \propto \exp(-16\pi^2 Dt/\lambda^2 \sec^2 \phi)$, then $\tau \propto \lambda^2 \sec^2 \phi / 16\pi^2 D$. Therefore τ should vary as λ^2 . From this it would be expected that the loss would increase rapidly with increase in operating frequency. For example, if we choose $\tau/a = 0.2$ sec as a representative value at 50 Mc/s and the initiation time is 40 msec, then the channel capacity is reduced to 82 percent of its nominal value. If however the operating frequency were 100 Mc/s, then we would have $\tau/a = 50$ milliseconds and the channel capacity would be reduced to 45 percent of its nominal value.

In practice the loss may not be as great as this since, according to Eshleman [4], as the frequency increases the decay constant τ for underdense trails first decreases and then increases again. However, for a typical communications case, the minimum value appears to occur at frequency of the order of 300 Mc/s and thus the λ^2 relation should be applicable at frequencies below 100 Mc/s.

5. References

- [1] P. A. Forsyth, E. L. Vogan, D. R. Hansen, and C. O. Hines, The principles of JANET—a meteor-burst communication system, see figure 16, Proc. IRE **45**, 1642 (1957).
- [2] R. A. Rach, An investigation of storage capacity required for a meteor-burst communications system, see figure 1, Proc. IRE **45**, 1707 (1957).
- [3] W. R. Vincent, R. T. Wolfram, B. M. Sifford, W. E. Jaye, and A. M. Peterson, A meteor-burst system for extended range vhf communications, see figure 13, Proc. IRE **45**, 1693 (1957).
- [4] V. R. Eshleman, Short-wavelength radio reflections from meteoric ionization. Part I: Theory for low-density trails, Scientific Report No. 5 (Radio Propagation Laboratory, Stanford Electronics Laboratories, Stanford Univ., Stanford, Calif., Aug. 30, 1956).

(Paper 64D5-85)

Elementary Considerations of the Effects of Multipath Propagation in Meteor-Burst Communication¹

George R. Sugar, Robert J. Carpenter, and Gerard R. Ochs

(April 14, 1960; revised April 25, 1960)

Three mechanisms likely to regularly produce multipath propagation are examined. These are: (1) The simultaneous existence of two meteor trails; (2) the existence of a Rayleigh-fading background continuum; and (3) the existence of two first-Fresnel zones along a single meteor trail.

An analysis of the first mechanism indicated that in a typical meteor-burst communication system two-trail propagation would cause transmission errors at a rate directly proportional to the system duty cycle. Satisfactory agreement was obtained between predicted and observed error rates for such a system. An examination of the significance of interference from the continuum in some wide-band transmission tests indicated that this source of multipath could be responsible for a significant fraction of the errors observed. The third mechanism was examined to determine the magnitude of the multipath delays it could produce. It was found that the effect of this single-trail multipath was likely to be significant only for transmission rates in excess of 2×10^4 bauds. However, the results of measurements at a rate of 10^5 bauds indicated that even at this high rate over one-half of the transmissions were error free and that this latter type of multipath may not be of much importance in system design.

1. Introduction

One of the important results of the first theoretical studies of meteor-burst communication [1,2]² was that the average channel capacity could be increased by raising the signaling rate. It is likely that this result, more than any other, led to the extensive study and development of meteor-burst systems. However, when experimental systems were tested it was found that the channel capacity observed fell far short of that predicted by theory. (For example, in one set of measurements [3], at a signaling rate of 10^5 bauds the predicted channel capacity was 10^4 bauds at an error rate of 10^{-5} . The measured capacity, however, was 10^3 bauds at an error rate near 10^{-3} .) This discrepancy between theory and experiment has led to a search for ways of modifying or extending previous theoretical results so that practical channel capacities could be accurately predicted. One aspect under study at NBS has been an examination of the deleterious effects of multipath propagation.

Multipath propagation is one source of transmission error and this fact, although recognized, was neglected in the development of the meteor-burst communication theory. In this paper three likely sources of multipath propagation will be considered. The first arises from the possibility that two meteor trails can exist simultaneously. The second arises because a secondary signal is propagated by the background continuum (the so-called "ionospheric scatter" mode of propagation). The third situation

to be considered arises as a consequence of the existence of single long-enduring meteor trails which have been distorted by winds in the ionosphere.

It has not been practical, as yet, or even desirable to consider the practical effects of these three classes of multipath propagation from a unified viewpoint. In each case the analysis has been carried only to the point where some results of practical value were obtained, and no attempt has been made to consider the effects in combination rather than separately.

For the two-trail case a general relation between error rate, duty cycle, and the statistical parameters of meteor-burst propagation is developed and then applied to a hypothetical fsk communication system. In the case of multipath interference from the continuum the interference is treated as being a noise-like signal which reduces the effective signal-to-noise ratio at the receiver.³ For the case of multipath propagation from a single trail the analysis is limited to a computation of the maximum delay which is likely to be produced. The application of the computational techniques is illustrated by using them to compute error rates for two experimental meteor-burst communication systems and comparing these with the error rates actually observed.

No consideration is given to the frequently-observed signal fading which can result from quite short multipath delays, since the equipment techniques for combating such fading are well known and readily available. Consideration is limited instead to those multipath conditions which are likely to result in receiving strong but badly-distorted signals for systems utilizing conventional modulation techniques such as fsk or ppm.

¹ Contribution from Centra Radio Propagation Laboratory, National Bureau of Standards, Boulder, Colo.

² Figures in brackets indicate the literature references at the end of this paper.

³ This is similar to the treatment by Montgomery and Sugar [1].

2. Two-Trail Multipath Propagation

The binary error rate for a meteor-burst system is now computed under the assumption that the only source of error is the multipath propagation which results from the simultaneous existence of two suitably-oriented meteor trails. Three conditions must be met. First, there must be two trails present at the same time with the amplitude of the signal from one of them above the operating threshold of the system. Second, the signal from the second trail, the interfering signal, must be comparable in amplitude to that from the first trail. Third, the interfering signal must be sufficiently delayed so as to cause errors (rather than just causing fading). The exact details of the latter two requirements will depend on the characteristics of the particular communications system under study. The error for an fsk radiotelegraph system is computed since experimental results from two such systems are available for comparison with the theory. However, the same general procedure can be followed in predicting the error for any system.

Assume that meteoric particles enter the earth's atmosphere at random times and that the radio properties of trails are statistically independent of the time when the trail was formed. Let the distribution function $F(S)$ represent the probability that the signal amplitude is greater than S , and let $f(S)$ represent the associated probability density. Then for a system threshold S_t , the duty cycle or probability that the signal will be above S_t is just $F(S_t)$. The probability that signals from trails 1 and 2 will be simultaneously present and contribute amplitudes S_1 and S_2 respectively is

$$f(S_1)f(S_2)dS_1dS_2.$$

Assume that the error rate for a binary signaling system can be given by a function $p(S_1, S_2, \tau)$ where τ is the multipath delay. Thus the error for signals S_1, S_2 , and multipath delay τ is

$$p(S_1, S_2, \tau)f(S_1)f(S_2)dS_1dS_2d\tau.$$

The average error rate P for the interval T is then given by

$$P(S_t) = \frac{\int_{\tau=0}^{\infty} \int_{S_1=S_t}^{\infty} \int_{S_2=0}^{S_1} p(S_1, S_2, \tau)f(S_1)f(S_2)dS_1dS_2d\tau}{F(S_t)}.$$

(S_t is chosen here as the amplitude of the stronger signal and it is assumed that during each binary digit S_1, S_2 , and τ are constant.) It remains now only to put in the functions p and f for a given system and evaluate the integral. Since experimental data for two fsk radiotelegraph systems is available the error will be computed for such a system.

Assume that all signals result from specular reflections from underdense trails, that the decay param-

eter k (in $S=S_{\max}e^{-kt}$) is fixed over the observing interval, that the system uses fsk and that the receiver has an effective capture ratio R . (R is defined as the amplitude ratio of the stronger signal to the weaker signal required to achieve error-free reception.) Then

$$P(S_t) = \frac{\int_{S_1=S_t}^{\infty} \int_{S_2=0}^{S_1} \frac{1}{2} f(S_1)f(S_2)dS_1dS_2}{F(S_t)}$$

if $1 < S_1/S_2 < R$, $\tau > \tau_0$, and $P(S_t) = 0$ otherwise. If the distribution function is assumed to be given by $F(S) = (S_0/S)^a$ where S_0 and a are constants, then $f(S) = (a/S)(S_0/S)^a$.

For the present assume that any multipath delay is sufficient to cause system errors.⁴ This implies that $\tau_0 = 0$ and

$$P(S_t) = \frac{\int_{S_1=S_t}^{\infty} \int_{S_2=S_1/R}^{S_1} \frac{a^2}{2} S_0^a S_1^{-a-1} S_2^{-a-1} dS_1dS_2}{F(S_t)}.$$

After integration the result becomes

$$P(S_t) = \frac{1}{4}(R^a - 1)(S_0/S_t)^a.$$

Then, since the duty cycle for any threshold is just

$$F(S_t) = (S_0/S_t)^a,$$

in terms of duty cycle

$$P(S_t) = \frac{1}{4}(R^a - 1)F(S_t).$$

The error rate is therefore proportional to duty cycle. Figure 1 is a plot of the factor $\frac{1}{4}(R^a - 1)$ for various values of the parameters R and a .

Some results obtained from the NBS Meteor-Burst Communication System [5] are now compared with those predicted by the above theory. The operating data available for the system gives character error rate and duty cycle as a function of the system parameters. The first step is to relate binary error to character error. When the system is operated at low error rates, it is estimated that each binary transmission error will produce an average of 1.35 character errors on the teleprinter. (This estimate should not be considered generally applicable to other radio-teletype systems since it is based on a specific set of rules for counting errors and also includes a consideration of control errors in the system.) Through the use of this factor the character error rate can be predicted and compared with the measured error rate. This has been done for various values of R and the comparison is shown in figure 2. Each point represents the average error rate and duty cycle for $\frac{1}{2}$ hr of system operation.

⁴ At present some data is available which can be interpreted to give multipath delays. Bailey, Bateman, and Kirby [4] give delays of meteor bursts relative to the continuum at 40.7 Mc/s and these can be interpreted as indicating that the most probable multipath delay in the two-trail case is of the order of 200 μ sec or less. Delays up to 2 msec were observed occasionally.

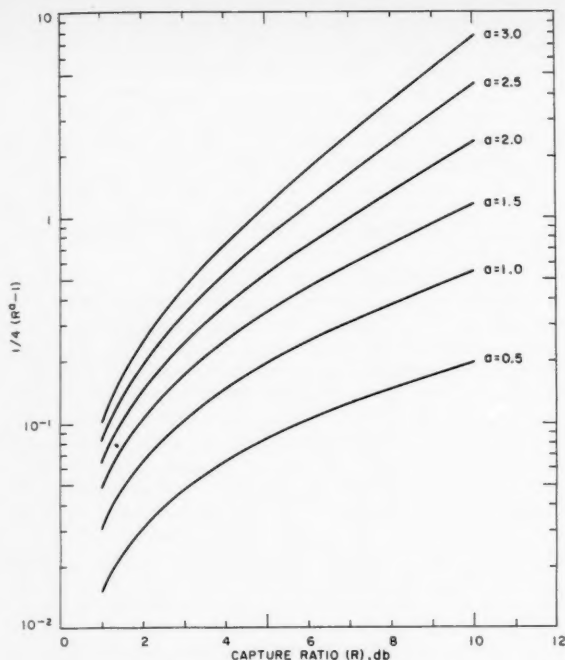


FIGURE 1. Error rate factor for fsk transmission.

Error rate = ordinate \times duty cycle.

Unfortunately, the capture ratio R was not measured for the system and an exact comparison between predicted and observed error rates is not possible. However, measurement in similar systems has indicated that capture ratios of 2 to 3 db are readily attainable. It therefore appears that the theoretically predicted results are not inconsistent with the observations and there may in fact be good agreement. The slope of the experimental data is quite close to that predicted and the magnitude is representative of that predicted for a system with an effective capture ratio of 3 to 4 db.

3. Multipath Interference From the Continuum

The effect of interference from the continuous background signal on an idealized meteor-burst communication system is now considered and the predicted error rates are compared with some experimental results. For the burst system itself, error-free performance in the absence of the continuum is assumed. In addition it is assumed that all of the multipath delays involved are at least comparable to the bit length and therefore can cause transmission errors. The signal from the continuum can then be considered as being a type of *Gaussian noise* which sets the effective signal-to-noise ratio for the system. This assumption is justified since the continuum exhibits a Rayleigh fading characteristic [6]. Moreover for large signaling bandwidths the continuum signal is not phase coherent over the

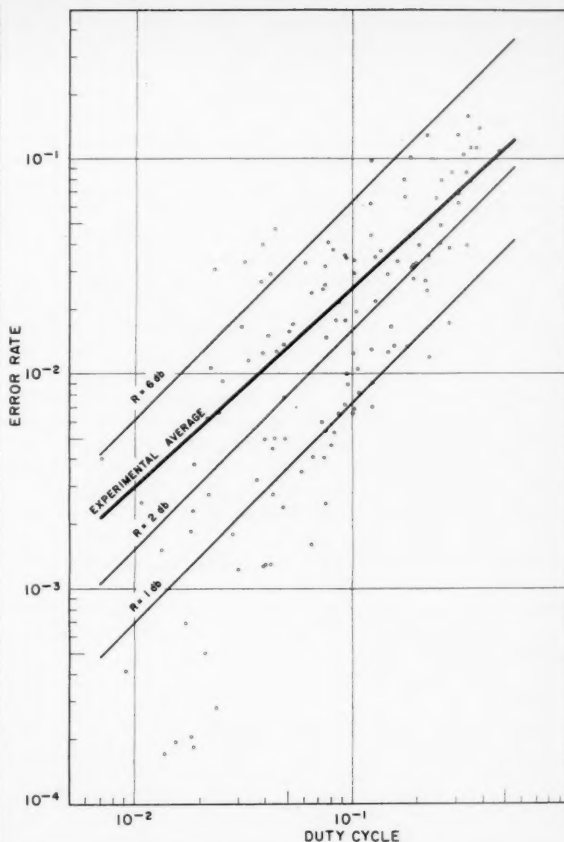


FIGURE 2. Computed and observed error rates for two-trail multipath.

The 3 light lines give computed error rates. The points and heavy line are experimental data.

band [4, 7]. Thus to a first approximation the continuum signal is not correlated with the meteor-burst signal and can therefore be analyzed as if it were random noise.

Under these assumptions, the error rate for a system can readily be predicted since the signal-to-noise-ratio performance of most modulation systems has been worked out and is available in the literature. For simplicity the signal level can be taken to be the signal threshold at which the burst system is operated. The more complex procedure of using the actual meteoric signal distribution could be followed, but at present there seems to be little to be gained by using this more difficult approach since even it is highly idealized and neglects many restrictions present in actual systems.

For a comparison between theory and experiment the results from some wide-band meteor-burst transmission studies performed at NBS⁵ are utilized. The signaling rate was 10^5 bauds using fsk, and

⁵ These studies were a continuation of the work reported by Montgomery and Sugar [1].

binary error was measured. The continuum was measured during the experiment by use of a strip-chart recorder operated from the agc circuits of the fsk receiver. For the theoretical relation between error and signal-to-noise ratio, that given by Montgomery [8] for fsk is used. This is plotted in figure 3, as the curve labelled 0 db, along with the experimental data. Each small circle represents the error rate observed over a 15-min interval. (The large circles represent averages of the 15-min points. The points plotted with an x, the apparatus capability, indicate the performance of the equipment as measured in the laboratory using a nonfading signal and Gaussian noise. The additional curves indicate the performance to be expected if the system is 5, 10, or 15 db poorer than the theoretical prediction.) It is seen that at high error rates the experimental results fall within a few decibels of the predicted values. However, at low error rates the agreement is poor and there are discrepancies of up to 15 db between theory and experiment. These observations are interpreted as indicating that at high error rates the observed error can almost wholly be accounted for in terms of multipath interference from the continuum whereas at low error rates some other sources of error are controlling. It is useful to now consider two-trail multipath as another possible source of error here.

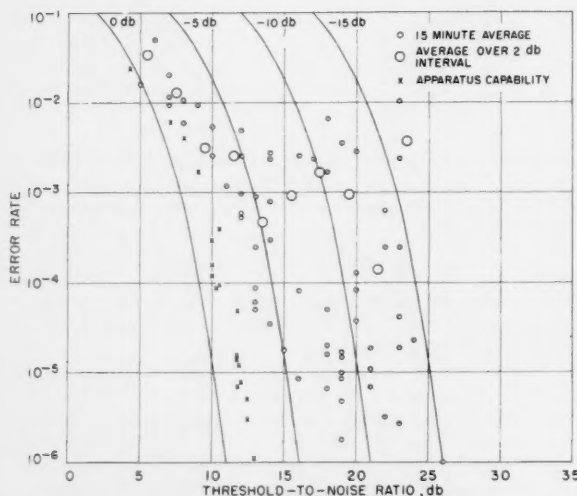


FIGURE 3. Computed and observed error rates for a system subjected to multipath interference from the continuum.

The apparatus capability as indicated in figure 3 is about 2 db poorer than the theoretical prediction. It is therefore assumed that this represents a receiver capture ratio of 2 db. For the distribution we take the value $a=1.2$ as used before. It is found then from figure 1 that the predicted error rate is 0.08 times the duty cycle. When this is applied to the data given in figure 3, it is found that the predicted

error rate varies from about 10^{-4} for low threshold-to-noise ratio data to about 10^{-5} for high threshold-to-noise ratio data. The observed error rates are 10 to 200 times these values. Thus it appears that two-trail multipath does not contribute significantly to the observed error rate, and therefore, that still another source of error is important.

4. One-Tail Multipath Propagation

The last possibility to be considered is that of having two distinct transmission paths result from the entry of a single meteoric particle into the earth's atmosphere. This will occur when, through the action of wind shears in the ionosphere, a single, overdense trail becomes distorted into an irregular column and as a result has two (or more) "first" Fresnel zones. These could be separated as much as the whole length of the trail and thus produce two distinct transmission paths. The multipath delays to be expected from this mechanism are, as will be shown, quite small and therefore of importance only in very high signaling rate systems. The computation of error for this case appears to be substantially more complex than either of the two previous cases and we have not attempted it. However, some of the factors involved in such a computation can be indicated.

First consider the magnitude of the multipath delay. It has been shown that for a trail which originally gives a specular reflection, the action of the wind shears is to produce "glints" (local first Fresnel zones) which first form near the original first Fresnel zone and later form further out along the trail [9, 10]. The maximum delay results when there is a glint at each end of the trail, and therefore the delays produced by two glints separated by a distance L are computed. Several trail orientations are possible and for each of these a different delay will result from a given L . The limiting cases are given below. (All of these are for long oblique paths with one end of the trail formed at the path midpoint.)

(a) Trail normal to plane of propagation

$$\text{delay} \sim L^2/(cD)$$

where L =glint separation,
 D =slant range to path midpoint,
 and
 c =velocity of propagation.

(b) Horizontal trail in the plane of propagation

$$\text{delay} \sim (L^2 \cos^2 \theta)/(cD)$$

where θ is $\frac{1}{2}$ the angle between the incident and reflected rays at the path midpoint.

(c) Vertical trail in the plane of propagation⁶

$$\text{delay} \sim (2L \cos \theta)/c.$$

⁶ Trails oriented in this manner are of minor practical importance. They do not have first Fresnel zones at the time of formation and will have glints only if they endure long enough to be severely distorted by wind shears.

For trail lengths the values published by Eshleman [11] are taken. These data indicate that the most probable trail length is about 15 km, with trails 40 to 50 km long occurring about 5 percent of the time. (The ends of a trail are defined here as being the points with a specific electron density.) As the limiting case, it is assumed that the separation L between glints is equal to the trail length. (The delays experienced in any experiment would be expected to be less than those predicted by this method.) Table 1 gives the delays predicted for the three cases. These delays are likely to produce transmission distortion in fsk systems operating at speeds of 20,000 bauds or greater.

TABLE 1. Maximum multipath delay expected from an irregular overdense trail

($D=1277$ km)

Trail orientation	Trail length	
	15 km	40 km
Normal to propagation plane	11 μ s	82 μ s
Horizontal, in plane	0.5	3.4
Vertical, in plane	20	54

It would be desirable to calculate error rate in this case as was done in section 2. However, we see no straightforward way to do so. Consideration of the error associated with overdense trails requires that we know the distribution of glint separations, how these are related to the length of the meteor trail, and the relative contribution of overdense trails to the total channel capacity. The latter, of course is closely associated to system design parameters such as sensitivity, operating frequency, antenna directivity, and control system design philosophy. Since the signal from a specular overdense trail is likely to exhibit fading long before producing transmission distortion, a system can be arranged to stop signaling before any significant delays can occur, and thus this case may be of little practical importance. For the nonspecular overdense case, again similar data on burst statistics are required and these are not available. Therefore we have stopped here with only a computation of delays and hope to extend this work at a later time.

5. Discussion

As is often the case there is a significant question whether the experimental results presented were taken under the conditions assumed, implicitly or explicitly, in the theory. Some discussion of this point seems desirable.

In the two-trail case, it was assumed that multipath distortion was the only source of error and satisfactory agreement was obtained between theory and experiment. One can ask, however, if the same experimental result would have been obtained even if two-trail multipath were not present. This result might be possible if all errors resulted from noise interference instead of multipath. The data plotted

in figure 2 were taken at several thresholds and thus might reflect primarily the effect of changing the threshold-to-noise ratio rather than any multipath phenomena. This does not appear to be the case, however, since data for a single threshold show the same relation as that shown in figure 2, and it is concluded that the correlation between theory and experiment is meaningful and not fortuitous. A second question arises in regard to the scatter of data in figure 2 both above and below the theoretical curve. It could be argued that the observed error rate should always be greater than the predicted value (as indeed it was in fig. 3) since some sources of error have been ignored. However, this does not seem to be a valid objection when we consider that the data for figure 2 were taken from an operating communication system in which a variety of special techniques were being used to stop transmissions at times when high error rates were likely. This control of transmission will, of course, bias the results so that error rates less than those predicted will be observed. (No such devices were used in the system represented by the data of fig. 3.)

A third question to ask is why the second kind of multipath distortion was not considered in relation to the data shown in figure 2, and was considered in relation to figure 3. The difference here lies in the difference in antenna systems used in the two experiments. In the NBS Meteor-Burst Communication System, the antennas were arranged with a null along the great circle path and data were taken during normal working hours. This results in the suppression of the continuum relative to the meteoric bursts and nearly all of the data shown in figure 2 correspond to threshold-to-noise ratios of 12 db or greater. It therefore seems reasonable to ignore the effect in this case. For the 10⁵-baud measurements, however, the situation was reversed, for the antennas were high-gain rhombics directed along the great-circle path. This, of course, enhances the continuum and suppresses meteoric burst signals. Thus, in the second case the continuum was of greater importance.

A final item for discussion is the total effect of the various kinds of multipath distortion on error rate in high rate systems. Data from the 10⁵-baud system are plotted in figure 4 so as to show the relation between the information capacity and error rate for single bursts. Each point represents one transmission. The data have been divided into class intervals and are plotted opposite the lower bound of the interval. (In the experiment the data were transmitted in groups of 4,000 binary digits, each group lasting 1/25 sec.) Data for threshold-to-noise ratios less than 12 db have not been plotted since it is unlikely that an fsk system would be operated in that region. It can be seen from figure 4 that many transmissions are error-free and that there is a tendency for the longer transmissions to have higher error rates than the shorter ones. The data show that 57 percent of the transmissions, carrying 32 percent of the channel capacity, are error-free.

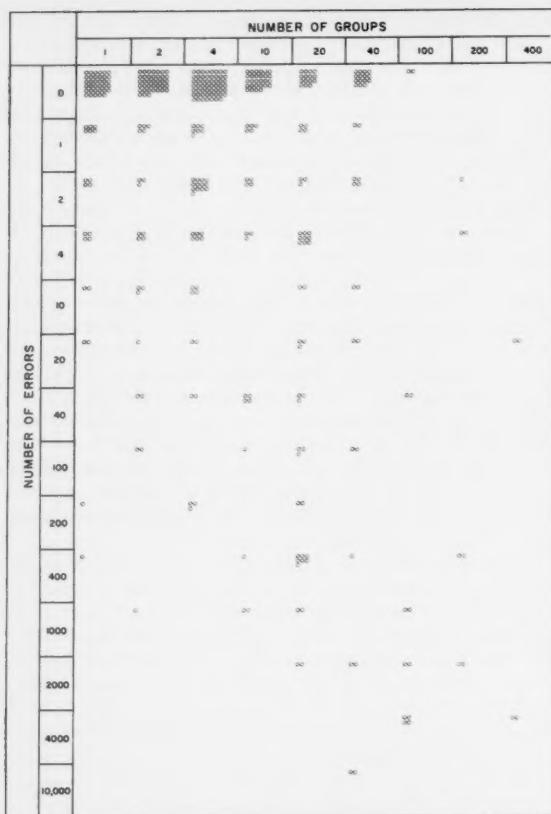


FIGURE 4. Errors observed for individual transmissions in a 10^5 -baud fsk system.

Each point gives the transmission length and number of errors observed. (One group equals 4,000 binary digits.)

For 86 percent of the transmissions, carrying 64 percent of the channel capacity, the error rate is less than 10^{-3} . It therefore appears that a signaling rate of 10^5 bauds is not so high as to be rendered useless by transmission distortion. Whether or not such systems will have the practical utility of low rate systems will depend on the ingenuity of the designing engineers.

6. Summary

Some aspects of multipath transmission and the transmission distortion which can result from it have been considered. For the two-trail case, the relation between error rate and duty cycle for fsk transmission have been computed. In applying this result to a specific system, fair agreement is found. However, there are a number of known factors which would be expected to increase the spread of the experimental data. The agreement is considered satisfactory, and it is concluded that the assumptions involved are reasonably valid and applicable to the specific system examined.

For the second case, the interference from the continuum was examined, and error rate was computed assuming that the interference could be considered as being of the nature of random noise. When the result was compared with data from the 10^5 -baud system (one where the assumptions seemed applicable), good agreement between theory and experiment for low values of threshold-to-continuum ratio was found. At high values of this ratio, the observed error rates were 10 to 200 times higher than would be predicted from either two-trail or continuum-multipath theory.

The multipath delays expected from a single trail were estimated to be as great as 82 μ sec and these delays may account for the above discrepancy. However, insufficient data are available to permit any reasonable estimate of the likelihood of error arising from this source.

Some overall results of the 10^5 -baud transmission experiment were examined, and these indicated that most of the individual transmissions had low error rates and that these low-error-rate bursts accounted for more than half of the signaling capacity of the system. It therefore appears that signaling rates of 10^5 bauds or higher can be used by devising special circuitry to reject (or repeat) transmissions having high error rates.

7. References

- [1] G. F. Montgomery and G. R. Sugar, The utility of meteor bursts for intermittent radio communication, *Proc. IRE* **45**, 1684 (1957).
- [2] L. L. Campbell and C. O. Hines, Bandwidth consideration in a JANET system, *Proc. IRE* **45**, 1658 (1957).
- [3] G. F. Montgomery and G. R. Sugar, unpublished report, National Bureau of Standards, September 1955. Most of this material has been published [1].
- [4] D. K. Bailey, R. Bateman, and R. C. Kirby, Radio transmission at VHF by scattering and other processes in the lower ionosphere, *Proc. IRE* **43**, 1181 (1955). See fig. 63.
- [5] R. J. Carpenter and G. R. Ochs, The NBS meteor-burst communication system, *IRE Trans. PGCS* **CS-7**, 263 (1959).
- [6] G. R. Sugar, Some fading characteristics of regular VHF ionosphere propagation, *Proc. IRE* **43**, 1432 (1955).
- [7] J. W. Koch, Factors affecting modulation techniques for VHF scatter studies, *IRE Trans. PGCS* **CS-7**, 77 (1959).
- [8] G. F. Montgomery, A comparison of amplitude and angle modulation for narrow-band communication of binary-coded messages in fluctuation noise, *Proc. IRE* **42**, 447 (1954).
- [9] L. A. Manning, Air motions and the fading, diversity, and aspect sensitivity of meteoric radio echoes, *J. Geophys. Research* **64**, 1415 (1959).
- [10] J. S. Greenhow and E. L. Neufeld, Turbulence at altitudes of 80-100 km and its effects on long-duration meteor echoes, *J. Atmospheric and Terrest. Phys.* **16**, 384 (1959).
- [11] V. R. Eshleman, The theoretical length distribution of ionized meteor trails, *J. Atmospheric and Terrest. Phys.* **10**, 57 (1957).

Use of Logarithmic Frequency Spacing in Ionogram Analysis¹

G. A. M. King²

(April 7, 1960)

The use of logarithmic frequency spacing brings several advantages to the reduction of ionograms to electron density profiles. Among them is the fact that, when computing factors for the analysis, one need not determine the group refractive index. Formulas involving only the phase refractive index are presented; for the ordinary component one exact and one approximate formula are given, while for the extraordinary component there is an approximate formula valid over a wide range of geomagnetic latitudes. There is a brief discussion of quasi-longitudinal approximations to the extraordinary phase refractive index.

1. Introduction

In his important paper on obtaining electron density profiles, Budden [1]³ used for illustration a linear sampling of the frequency scale of the ionogram. He also mentioned the possibility of other samplings, including logarithmic. At about the same time, King [2] presented an illustration based on logarithmic sampling, and later [3] showed that this spacing simplifies inclusion of the earth's magnetic field in the analysis, by the use of an accurate approximation.

The methods of real height analysis using summation of spaced ordinates due to Kelso [4], Shinn (described by Thomas [5]), and Schmerling [6], are much easier to apply if the ionograms have a logarithmic frequency scale, for then overlays can be used. This derives from the fact that the properties of the propagation equation depend mainly on f_N/f , the ratio of the plasma frequency to the exploring frequency, and to a much less extent on the absolute frequencies (determined by f_H/f , where f_H is the gyro-frequency. As is usual in treating this subject, the effects of electron collisions are neglected.)

The purpose of this note is to inquire more closely into the advantages of logarithmic spacing and to present an approximation using it for analysis of the extraordinary ionogram trace.

2. General Equations

The basic equation relating the virtual height, h' , and the real height, h_r , at the reflection point (assuming geometrical optics) is, [2]

$$h' = \int_0^{h_r} \mu' dh, \quad (1)$$

where μ' is the group refractive index. This can be rewritten

$$h' = \int_{\Phi_0}^{\Phi_r} \mu' \frac{dh}{d\Phi} d\Phi, \quad (2)$$

where Φ is any single valued function of the electron density. The integration can now be divided into a series of steps within which $dh/d\Phi$ is varying sufficiently slowly to be taken out of the integral sign.

$$h'_m = \sum_m \left(\frac{\Delta h}{\Delta \Phi} \right)_m \int_{\Delta \Phi_m} \mu' d\Phi \quad (3)$$

The integral $\int_{\Delta \Phi_m} \mu' d\Phi$, which we shall denote by F_m , defines constant factors used in the analysis of the ionograms to obtain h . Once the table of factors is prepared, the reduction to real heights is simply a matter of solving a set of simultaneous equations in $(\Delta h/\Delta \Phi)_m$.

If now Φ is identified with the logarithm of f_N , a simplification results. (The natural logarithm, \ln , will be discussed here to simplify the presentation, although common logarithms may be used in practice.)

For, at fixed f_N ,

$$\begin{aligned} \mu' &= \left[\frac{\partial(\mu f)}{\partial f} \right]_{f_N} \\ &= \mu + \left[\frac{\partial \mu}{\partial \ln f} \right]_{f_N}, \end{aligned} \quad (4)$$

where μ is the phase refractive index; it is a function of both f and f_N .

Using the theorem

$$\left[\frac{\partial \mu}{\partial \ln f} \right]_{f_N/f} = \left[\frac{\partial \mu}{\partial \ln f} \right]_{f_N} + \left[\frac{\partial \mu}{\partial \ln f} \right]_f \quad (5)$$

¹ Contribution from Central Radio Propagation Laboratory, National Bureau of Standards, Boulder, Colo.

² Guest worker at Central Radio Propagation Laboratory and the High Altitude Observatory, Boulder, Colo., from the Geophysical Observatory, Christchurch, New Zealand.

³ Figures in brackets indicate the literature references at the end of this paper.

relating the partial differential at fixed f_N/f to partial differentials at fixed f_N and at fixed f , we get

$$\mu' = \mu - \left[\frac{\partial \mu}{\partial \ln f_N} \right] + \left[\frac{\partial \mu}{\partial \ln f} \right]_{f_N/f} \quad (6)$$

The factors used in the ionogram analysis then become

$$\begin{aligned} \int_{\Delta \Phi} \mu' d\Phi &= \int_{\Delta \ln f_N} \mu' d \ln f_N \\ &= \bar{\mu} \Delta \ln f_N - [\Delta \mu]_f + \left[\frac{\partial \mu}{\partial \ln f} \right]_{f_N/f} \Delta \ln f_N \end{aligned} \quad (7)$$

where the "bars" denote mean values of the quantities over the interval.

All terms of eq (7) can be evaluated from a table of $\mu(\ln f, \ln f_N)$, so that one can avoid the tedious calculation of the group refractive index. In a recent paper, Titheridge [7] has given an expression with the same advantage.

3. Ordinary Component

While one would normally use the complete eq (7), it is worth noting that, for routine analysis of the ordinary component, the last term can be dropped [3]. Experience shows that the heights deduced from the ionograms are not seriously affected

The assumption here is

$$\left[\frac{\partial \mu}{\partial \ln f} \right]_{f_N/f} \doteq 0 \quad (8)$$

4. Extraordinary Component

While eq (7) applies formally to either the ordinary or the extraordinary component its use with the latter is made difficult by the rapid change of the last term near the gyrofrequency. By making the transformation

$$\xi^2 = f^2(1-y), \quad (9)$$

where $y = f_H/f$, one can adopt an assumption similar to eq (8),

$$\left[\frac{\partial \mu}{\partial \ln \xi} \right]_{f_N/\xi} \doteq 0, \quad (10)$$

and so simplify the computations.

The approximation of eq (10) will be considered in the next section where it will be shown to hold extremely well down to geomagnetic latitudes as low as 30° (where the propagation angle, θ , between the earth's magnetic field and the vertical is as large as 50°).

When eq (7) is put in terms of ξ and eq (10) is applied, one obtains

$$F_{xm} = \int_{\Delta \ln f_N} \mu' d \ln f_N = \bar{\mu} \Delta \ln f_N - \frac{d \ln \xi}{d \ln f} [\Delta \mu]_{\xi} \quad (11)$$

where the subscript x in F_{xm} denotes the extraordinary component.

As constant ξ implies constant f , and

$$\frac{d \ln \xi}{d \ln f} = \frac{1-y/2}{1-y}, \quad (12)$$

the factors for analysis of the extraordinary component become

$$F_{xm} = \bar{\mu} \Delta \ln f_N - \frac{1-y/2}{1-y} [\Delta \mu]_f \quad (13)$$

5. Phase Refractive Index for the Extraordinary Mode

In order to justify use of the approximation (10), a few remarks on quasi-longitudinal approximations to the phase refractive index of the extraordinary mode are appropriate.

Common approximations are [8],

$$\frac{1}{1-\mu^2} \doteq \frac{f^2}{f_N^2} (1-y \cos \theta) \quad (14)$$

and [9],

$$\frac{1}{1-\mu^2} \doteq \frac{f^2}{f_N^2} (1-y) = \xi^2/f_N^2 \quad (15)$$

The exact expression is

$$\frac{1}{1-\mu^2} = \frac{f^2}{f_N^2} \left(1 - y \cos \theta \cot \frac{\psi}{2} \right), \quad (16)$$

where

$$\tan \psi = \frac{2(f^2 - f_N^2) \cos \theta}{f f_H \sin^2 \theta} \quad (17)$$

Equations (14), (15), and (16) can be compared as follows: For the extraordinary trace, the *least* value of $\tan \psi$ occurs at the reflection point, where it is $2 \cos \theta / \sin^2 \theta$, so that the greatest value of $\cot \psi/2$ is $1/\cos \theta$.

That is to say,

$$1 < \cot \frac{\psi}{2} < \frac{1}{\cos \theta} \quad (18)$$

Therefore the exact value for $1/(1-\mu^2)$ (16) always lies between those given by the two approximate expressions (14) and (15), except at the reflection point, where (15) is exact.

Now if we let A represent the ratio of (16) to (14) and B the ratio of (16) to (15), i.e.,

$$A = \frac{1-y \cos \theta \cot \frac{\psi}{2}}{1-y \cos \theta}, \quad (19)$$

and

$$B = \frac{1-y \cos \theta \cot \frac{\psi}{2}}{1-y}, \quad (20)$$

the following table compares the ratios for $y=\frac{1}{2}$ and various values of $(f_N/f)^2$, at different geomagnetic latitudes.

Latitude	$(\frac{f_N^2}{f})=$	0.5	0.4	0.3	0.2	0.1	0.0
14°	A	0.644	0.714	0.762	0.797	0.823*	0.844*
	B	1.000	1.109	1.184	1.238	1.278	1.310
23½°	A	0.743	0.792	0.825	0.850	0.868*	0.883*
	B	1.000	1.065	1.110	1.143	1.168	1.187
30°	A	0.804	0.840	0.864	0.883	0.897*	0.908*
	B	1.000	1.045	1.075	1.098	1.116	1.129
45°	A	0.904	0.921	0.933	0.941	0.948	0.954*
	B	1.000	1.018	1.031	1.041	1.048	1.054
60°	A	0.962	0.969	0.973	0.977	0.979	0.982*
	B	1.000	1.007	1.011	1.015	1.018	1.020

Only in those positions of the table marked by an asterisk is A closer to unity than B. Clearly, then, the approximation (15) is the better, especially near the reflection point $[(f_N/f)^2=1-y]$ where the need for accuracy is greatest. Accepting eq (15), eq (10) follows.

Writing the exact expression, using eqs (16), (20), and (9), as

$$\frac{1}{1-\mu^2} = \frac{\xi^2}{f_N^2} B, \quad (21)$$

it can be shown that, because of the slow rate of change of B with $(f_N/f)^2$ (and hence with ξ^2/f_N^2), eq (10) is applicable to ionogram analysis over a wider range of latitudes than eq (15). Rydbeck [9] used a relation equivalent to eq (15) in a method of ionogram analysis for $\theta < 20^\circ$ (latitudes greater than 54°), where it certainly holds within the accuracies to which the ionograms can be read. Use of eq (10) extends the range of application down to geomagnetic latitude 30° .

6. A Numerical Example

The following tables illustrate the computation of the factors F_{zm} for analyzing the extraordinary ionogram trace.

The first table gives μ as a function of $\log_{10} f_N$ and $\log_{10} \xi$. This was calculated using eq (16).

Table of $\mu \times 10^4$			$f_N = 1.4753 \text{ Mc/s}$				$\theta = 21^\circ 53'$			
f Mc/s	$\log \xi$	$\log f_N$								
		0.32	0.28	0.24	0.20	0.16	0.12	0.08	0.04	0.00
2.95	0.32	0000	4209	5658	6610	7302	7827	8236	8500	8821
2.78	0.28	-----	0000	4210	5660	6613	7305	7830	8239	8562
2.63	0.24	-----	-----	0000	4211	5662	6616	7308	7833	8242
2.48	0.20	-----	-----	-----	0000	4212	5664	6619	7311	7836
2.36	0.16	-----	-----	-----	-----	0000	4214	5667	6622	7314
2.25	0.12	-----	-----	-----	-----	-----	0000	4215	5669	6625
2.15	0.08	-----	-----	-----	-----	-----	-----	0000	4217	5672
2.06	0.04	-----	-----	-----	-----	-----	-----	-----	0000	4219
1.98	0.00	-----	-----	-----	-----	-----	-----	-----	-----	0000

Lines parallel to the diagonal in the table define values of μ for constant values of the ratio f_N/ξ . Differences between the values along such a line, therefore, give $[\partial\mu/\partial \log \xi]_{f_N/\xi}$; and as this is very small compared with $[\partial\mu/\partial \log \xi]_{f_N}$ and $[\partial\mu/\partial \log f_N]_{\xi}$, the assumption made in section 4 (eq (10)) is quite satisfactory.

From this table one can obtain the components $\mu \Delta \log f_N$ and $M[(1-y/2)/(1-y)] [\Delta\mu]_r$, of the factors F_{zm} (eq (13)). Here, $M=0.4343$ is the conversion factor to change from natural logarithms to common logarithms. Thus for $\log \xi=0.24$, we obtain the factor for the interval $\Delta \log f_N$ (0.16-0.12) by adding $\mu \log f_N$ (0.0246) and $-M \frac{1-y/2}{1-y} [\Delta\mu]_r$ (0.0680) giving a value of 0.0926.

The table of $F_{zm} \times 10^4$ is then,

log ξ	Interval of log f_N											
	0.28 to 0.32	0.24 to 0.28	0.20 to 0.24	0.16 to 0.20	0.12 to 0.16	0.08 to 0.12	0.04 to 0.08	0.00 to 0.04	-0.04 to 0.00	-0.08 to -0.04	-0.12 to -0.08	
0.32	2855	1142	866	730	645	587	574	518	494	476	462	
.28	-----	2976	1184	894	749	660	599	556	525	500	481	
.24	-----	-----	3117	1233	926	772	677	613	566	534	506	
.20	-----	-----	-----	3280	1290	964	799	697	628	579	544	
.16	-----	-----	-----	-----	3470	1356	1006	830	721	646	593	
.12	-----	-----	-----	-----	-----	3692	1434	1058	867	749	688	
.08	-----	-----	-----	-----	-----	-----	3954	1525	1117	910	780	
.04	-----	-----	-----	-----	-----	-----	-----	4262	1631	1187	960	
.00	-----	-----	-----	-----	-----	-----	-----	-----	4625	1757	1269	

This example is taken from part of a table prepared for testing methods of ionogram analysis which use both the ordinary and extraordinary traces to give information on the unobserved parts of the ionosphere [10], [11], [12].

7. Conclusions

The use of logarithmic frequency spacing allows easy computation of factors for the real height analysis of ionograms, using tables of phase refractive index; the group refractive index need not be calculated.

For the ordinary wave component, there is an exact formula for the factors eq (7), and an approximate formula good enough for most work. The formula for the extraordinary wave component eq (13) contains an approximation, but it can be used with negligible error for analysis of ionograms from any but the lowest latitudes.

In the justification of the extraordinary wave approximation it was shown that the simplest quasi-longitudinal approximation to the phase refractive index eq (15) is better than one in common use eq (14).

The work described in this paper was partly supported by the International Geophysical Year program of the National Academy of Sciences.

8. References

- [1] K. G. Budden, A method for determining the variation of electron density with height, Rept. Cambridge Conf. Ionospheric Phys., Phys. Soc. London, p. 332 (1955).
- [2] G. A. M. King, Electron distribution in the ionosphere, *J. Atmospheric and Terrest. Phys.* **5**, 245 (1954).
- [3] G. A. M. King, Electron distribution in the ionosphere, *J. Atmospheric and Terrest. Phys.* **8**, 184 (1956).
- [4] J. M. Kelso, A procedure for the determination of the vertical distribution of the electron density in the ionosphere, *J. Geophys. Research* **57**, 357 (1952).
- [5] J. O. Thomas, The distribution of electrons in the ionosphere, *Proc. IRE*, **47**, 162 (1959).
- [6] E. R. Schmerling, An easily applied method for the reduction of h'-f records to N-h profiles, *J. Atmospheric and Terrest. Phys.* **12**, 8 (1958).
- [7] J. E. Titheridge, Calculation of real and virtual heights in the ionosphere, *J. Atmospheric and Terrest. Phys.* **17**, 96 (1959).
- [8] J. A. Ratcliffe, *The magneto-ionic theory* (Cambridge 1959).
- [9] O. E. H. Rydbeck, On the propagation of electromagnetic waves in an ionized medium and the calculation of the true heights of the ionized layers of the atmosphere, *Phil. Mag.* **30**, 282 (1940).
- [10] J. E. Jackson, A new method of obtaining the electron density profiles from h'-f records, *J. Geophys. Research* **61**, 107 (1956).
- [11] J. E. Titheridge, The use of the extraordinary ray in the analysis of ionospheric records, *J. Atmospheric and Terrest. Phys.* **17**, 110 (1959).
- [12] L. R. O. Storey, The joint use of the ordinary and extraordinary virtual height curves in determining ionospheric layer profiles, *J. Research NBS* **64D**, 111 (1960).

(Paper 64D5-87)

Guiding of Whistlers in a Homogeneous Medium

R. L. Smith

(May 4, 1960)

The velocity of energy flow of whistlers in a homogeneous medium is computed as a function of wave-normal angles. The maximum allowable cone of ray angles approaches $19^{\circ}29'$ at very low frequencies, decreases with frequency to a minimum of 11° at a wave frequency of one-fifth the gyrofrequency, then increases to 90° at the gyrofrequency. The velocity of energy flow departs markedly from the longitudinal value except at very low frequencies or very small wave-normal angles.

1. Introduction

Part of the energy from a lightning stroke can penetrate the lower ionosphere and be guided approximately along the earth's magnetic field in the outer ionosphere. The energy is dispersed as it travels in this region, causing the original signal, which can be considered an impulse, to be stretched or dispersed into a gliding tone, typically lasting about a second. This gliding tone is called a whistler. The dispersion is a measure of the electron content along the path.

Storey [1]² has analyzed the properties of whistler propagation for the case of wave frequency very low compared to the local electron plasma frequency and gyrofrequency. Briefly, his results show that (a) the direction of energy flow lies within a limiting cone of $19^{\circ}29'$ around the magnetic field direction; (b) the longitudinal expression for group velocity can be used to describe the velocity of the energy flow with an error less than 8 percent for wave normal angles up to 70° ; (c) if the initial wave normal angles for the different frequency components are identical, the path of energy flow is independent of frequency; and (d) the time delay T from the causative lightning stroke is given by $T = D f^{-1/2}$, where f is the frequency and D is a constant for a particular whistler. This relation is sometimes called "Eckersley's law". Storey found good agreement between this relation and data he obtained at Cambridge, England.

From recordings made at high latitudes, a new phenomenon, called the nose whistler, was discovered by Helliwell et al. [2] in 1955. These whistlers exhibited simultaneous rising and falling tones starting at the frequency of minimum time delay called the "nose". The nose whistler occurs when the wave frequency of the whistler becomes comparable to the local gyrofrequency at the top of a field line. Even at the lowest frequencies of most nose whistlers the departures from Eckersley's law

are significant. Other whistlers, though they may not exhibit a nose, often show similar departures from Eckersley's law. These deviations are important in determining the location of the path of propagation [3]. Without the high-frequency information, it is usually necessary to assume that whistler energy follows a field line terminating at the receiver. The diameter of the effective area of whistlers has been shown by Storey [1] and Crary et al. [4] to be approximately 1,000 km. Consider two possible whistler paths terminating at 55° and 60° geomagnetic latitude, well within the effective area of a whistler. The calculated average electron density for a whistler of given dispersion will differ by 2:1 for these two paths. Clearly the path needs to be defined more precisely. Before we use the high-frequency information however, we must re-examine the equations used to determine the dispersion and path.

The present paper is an extension of Storey's work, removing the restriction that the wave frequency be small compared to the gyrofrequency. As frequency increases, the analysis shows that the limiting cone of rays first decreases to 11° at about one-fifth the gyrofrequency, then increases to 90° at the gyrofrequency. The error in the quasi-longitudinal approximation for group velocity increases with frequency and wave normal angle.

2. Refractive Index for Whistlers

Experimental evidence shows that the attenuation of whistlers in the outer ionosphere is very low. There are estimates of attenuation of the order of 10 db and lower over paths which are roughly 10,000 km long. The attenuation will therefore be neglected. The square of the wave refractive index for the ordinary mode, as defined by Booker, is then given from the Appleton-Hartree equation as:

$$\mu^2 = 1 - \frac{X}{1 - \frac{Y_H^2 \sin^2 \theta}{2(1-X)} - Y_H \cos \theta \left[1 + \frac{Y_H^2 \sin^4 \theta}{4 \cos^2 \theta (1-X)^2} \right]^{\frac{1}{2}}} \quad (1)$$

¹ Contribution from Radioscience Laboratory, Stanford University, Stanford, Calif. The main results of this paper were presented at the Symposium on VLF Radio Waves held in Boulder, Colo., January 1957.

² Figures in brackets indicate the literature references at the end of this paper.

where

$$X = \frac{f_0^2}{f^2},$$

$$Y_H = \frac{f_H}{f},$$

θ = angle between the wave normal and magnetic field,

f = wave frequency,

$$f_0 = \sqrt{\frac{Ne^2}{4\pi^2 m \epsilon_0}} = \text{plasma frequency},$$

$$f_H = \frac{\mu_0 e H}{2\pi m} = \text{gyrofrequency},$$

N = density of electrons,

e = charge of the electron,

m = mass of the electron,

H = magnetic field strength,

ϵ_0 = permittivity of free space.

If we assume that $\tan \theta \sin \theta \ll 2 (X-1)/Y_H$, i.e., if we assume quasi-longitudinal propagation, then eq (1) is simplified to:

$$\mu^2 = 1 - \frac{X}{1 - Y_H \cos \theta}. \quad (2)$$

For most cases of interest in whistler propagation it can be assumed that the square of the refractive index is large compared to unity. Equation (2) can then be further simplified to:

$$\mu^2 = \frac{X}{Y_H \cos \theta - 1} = \frac{f_0^2}{f(f_H \cos \theta - f)}. \quad (3)$$

The phase velocity is then

$$v = \frac{c}{\mu} = \frac{c(Y_H \cos \theta - 1)^{1/2}}{X^{1/2}} = \frac{c(\cos \theta - \lambda)^{1/2}}{\lambda^{1/2} X^{1/2}}, \quad (4)$$

where $\lambda = 1/Y_H = f/f_H$ = normalized wave frequency. This relation defines the wave surface.

Equation (4) shows that for a given value of λ , the angle θ between the wave normal and the field direction must be less than that given by $\cos \theta_{\max} = \lambda$ for a propagating wave. The condition of validity of the quasi-longitudinal assumption at the maximum angle can easily be shown to be:

$$f_H^2 \ll (2f_0^2 - f^2). \quad (5)$$

Assuming the wave refractive index is given by eq

(3), then the group refractive index, from which we determine the group velocity, is:

$$\begin{aligned} \mu' = \frac{d}{df}(\mu f) &= \frac{d}{df} \frac{f_0 f^{1/2}}{(f_H \cos \theta - f)^{1/2}} \\ &= \frac{f_0 f_H \cos \theta}{2f^{1/2} (f_H \cos \theta - f)^{3/2}} \quad (6) \end{aligned}$$

The error in the group velocity as derived from eq (3) instead of eq (2) is negligible at $\lambda = 0, 0.75$, and 1.0. The greatest error occurs at $\lambda = 0.283$ and is approximately

$$0.11 \frac{f_H^2 \cos^2 \theta}{f_0^2}.$$

3. Behavior of the Ray

The direction of the ray is the direction of constructive interference of phase fronts for infinitesimal changes in the wave normal direction. If the direction of the ray with respect to the wave normal is α , and α is positive when the wave normal lies between the ray and the field direction, then α is given by

$$\tan \alpha = -\frac{1}{\mu} \frac{\partial \mu}{\partial \theta} = -\frac{\sin \theta}{2(\cos \theta - \lambda)} \quad (7)$$

This relation has been shown by Bremmer [5], Storey [1], and others.

The total angle between the ray direction and the field is $\theta + \alpha$. A sketch of $(\theta + \alpha)$ as a function of θ and parametric in λ is shown in figure 1.

The diagonal line represents the ray direction when the wave normal is at its maximum value. The greatest negative value of $(\theta + \alpha)$ is given by

$$|\theta + \alpha|_{\max} = \sin^{-1} \lambda \quad (8)$$

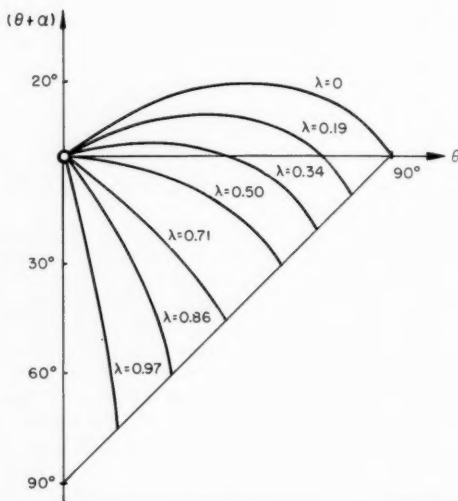


FIGURE 1. The ray direction as a function of the wave direction.

The greatest positive value of $(\theta + \alpha)$ is determined by setting

$$\begin{aligned}\frac{\partial(\theta + \alpha)}{\partial\theta} &= 0 \\ \frac{\partial(\theta + \alpha)}{\partial\theta} &= 1 + \frac{\partial}{\partial\theta} \tan^{-1} \left[-\frac{\sin\theta}{2(\cos\theta - \lambda)} \right] \\ &= \frac{3\cos^2\theta - 6\lambda\cos\theta + 4\lambda^2 - 1}{2(\cos\theta - \lambda)^2 + \sin^2\theta} = 0.\end{aligned}\quad (9)$$

Solving eq (7) for $\cos\theta$, we find

$$\cos\theta = \lambda + \frac{(1 - \lambda^2)^{1/2}}{3^{1/2}} \quad (10)$$

The maximum positive value is then easily shown to be

$$\tan(\theta + \alpha)_{\max} = \frac{[(1 - \lambda^2)^{1/2} - \sqrt{3}\lambda]^{3/2}}{2^{3/2}(1 - \lambda^2)^{3/4}} \quad (11)$$

The maximum ray direction for any given normalized frequency is given by the larger of the values determined from eqs (8) and (11). Figure 2 shows the results graphically.

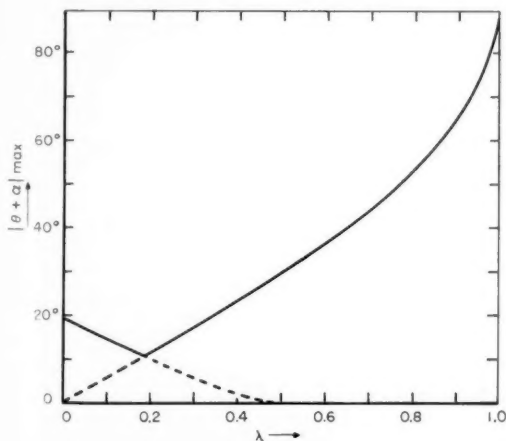


FIGURE 2. Maximum possible ray direction as a function of λ .

The minimum ray cone of 11° occurs at $\lambda = 0.189$. The value at $\lambda = 0$ is found to be $19^\circ 29'$ in accordance with Storey. The half beamwidth lies between these two values for all λ between 0 and 0.33.

The group ray refractive index is given by $M' = \mu' \cos \alpha$. The group ray velocity is the velocity of propagation of a point on a wave packet limited in both length and width where the phase is stationary with respect to independent variations of both frequency and wave normal direction. From eq (6),

we can obtain

$$\mu' = \frac{X^{1/2}\lambda^{1/2}}{2\left(1 - \frac{\lambda}{\cos\theta}\right)^{3/2}(\cos\theta)^{1/2}} \quad (12)$$

and from eq (7) we can obtain

$$\cos \alpha = \frac{2\left(1 - \frac{\lambda}{\cos\theta}\right)}{\left[\tan^2\theta + 4\left(1 - \frac{\lambda}{\cos\theta}\right)^2\right]^{1/2}} \quad (13)$$

Combining (12) and (13), we obtain

$$M' = \frac{X^{1/2}\lambda^{1/2}}{2(1 - \lambda)^{3/2}} \Phi(\theta, \lambda) = \mu_L' \Phi(\theta, \lambda) \quad (14)$$

where

$$\Phi(\theta, \lambda) = \frac{(1 - \lambda)^{3/2}}{\left[\frac{1}{4}\tan^2\theta(\cos\theta - \lambda) + \frac{(\cos\theta - \lambda)^3}{\cos^2\theta}\right]^{1/2}} \quad (15)$$

and μ_L' = group ray refractive index of a longitudinal wave. The factor Φ is plotted in figure 3 as a function of θ , with λ as a parameter. The curves show to what extent the group ray refractive index is independent of wave normal direction.

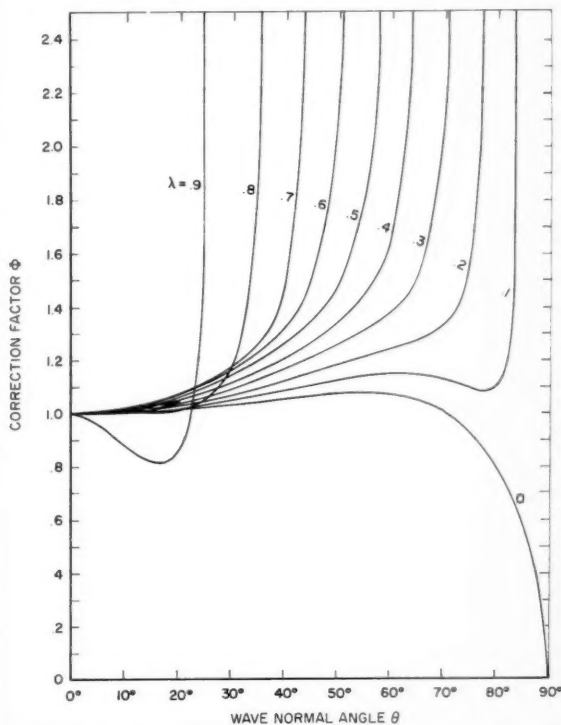


FIGURE 3. Correction factor Φ as a function of wave normal direction, with λ as a parameter.

4. Conclusion

The spread of allowable ray angles approaches $19^{\circ}29'$ as the normalized frequency $\lambda=f/f_H$ tends toward zero. The limiting cone reaches a minimum of 11° at about one-fifth of the gyrofrequency, then rapidly increases with increasing frequency. The energy near and above the nose frequency of whistlers ($\lambda \approx 0.25$) would then be expected to diverge considerably in the outer ionosphere unless an additional confining mechanism is postulated.

Furthermore, the group ray refractive index may depart markedly from the longitudinal value. Even for wave-normal angles less than one-half the limiting angle the correction factor may exceed unity by more than 10 percent. Evidence for the spread in group ray refractive index should be found in the time delay spreading of received whistlers. Since this spread is observed to be less than 1 percent in most nose whistler traces, a mechanism for confining the wave normal angles to small values is indicated. Such a mechanism might be enhanced columns of ionization aligned along the magnetic field as discussed by Helliwell [3] and Smith et al. [6].

5. References

- [1] L. R. O. Storey, An investigation of whistling atmospheres, *Phil. Trans. Roy. Soc. [A]*, **246**, 113 to 141 (July 9, 1953).
- [2] R. A. Helliwell, J. H. Crary, J. H. Pope, R. L. Smith, The "nose" whistler—a new high latitude phenomenon, *J. Geophys. Res.* **61**, 139 to 142 (Mar. 1956).
- [3] R. A. Helliwell, Low frequency propagation studies, part I: Whistlers and related phenomena. Final report, Contract AF 19 (604) 795. June 15, 1953 to Sept. 30, 1956. (Revised May 28, 1958.) AFCRC-TR-56-189, ASTIA Document No. AD110184.
- [4] J. H. Crary, R. A. Helliwell, R. F. Chase, Stanford-Seattle whistler observations, *J. Geophys. Res.*, **61**, No. 1 (Mar. 1956).
- [5] H. Bremmer, *Terrestrial radio waves* (Amsterdam: Elsevier, 1949).
- [6] R. L. Smith, R. A. Helliwell, I. W. Yabroff, A theory of trapping of whistlers in field-aligned columns of enhanced ionization, *J. Geophys. Res.*, **65**, No. 3 (Mar. 1960).

(Paper 64D5-88)

Propagation of Microwaves Through a Magneto-Plasma, and a Possible Method for Determining the Electron Velocity Distributions

A. L. Cullen

(March 1, 1960)

Sagdeyev and Shafranov have shown that the absorption of microwaves in a hot plasma in a steady magnetic field can be calculated in simple closed form with the help of the Boltzmann equation, provided that the effect of collision can be ignored.

The present paper is restricted to the special case of propagation of circularly polarized waves parallel to the magnetic field, and the extraordinary ray, in magneto-ionic terminology, is given special attention. It is shown that the formula given by Sagdeyev and Shafranov for this case can be deduced by considering the motions of individual electrons by elementary dynamical methods, using the concepts of Doppler shift and velocity distribution functions to obtain a macroscopic conductivity formula for a high-temperature plasma. From this, the absorption is easily calculated.

It is emphasized that the calculation in no way depends upon the assumption of a Maxwellian velocity distribution function. The absorption can in fact be obtained in closed form for any arbitrary velocity distribution function.

This suggests that a diagnostic technique for the determination of velocity distribution could be based on measurements of absorption of the extraordinary ray, and the potentialities and limitations of this proposal are briefly discussed.

1. Introduction

Sagdeyev and Shafranov² have shown that the absorption of microwave energy in a hot plasma can be calculated in simple closed form from the Boltzmann equation provided that the effect of collisions can be ignored.

In the present paper, the same formula is obtained from a simple dynamical-collisional argument, and it is shown that if the collision frequency is small in comparison with the Doppler frequency shift due to thermal motions of the electrons, the value of the collision frequency has only a second-order effect on the absorption coefficient. Furthermore, the results of Sagdeyev and Shafranov are extended to cover the case of an arbitrary, rather than a Maxwellian, velocity distribution function, and a microwave diagnostic technique for determining the distribution functions in low density hot plasmas is proposed.

2. Equations of Motion

In these equations, the effect of the radiofrequency magnetic field will be ignored. The electric field is assumed in the first instance to have the form

$$\left. \begin{aligned} E_x &= E_0 \sin \omega t \\ E_y &= E_0 \cos \omega t \end{aligned} \right\} \quad (1)$$

It is also assumed that there is a constant magnetic field along the z -axis of value B_0 . If the strength of this field is expressed in terms of the cyclotron frequency for electrons $\omega_c = eB_0/m$, the equations of motion can be written

$$\left. \begin{aligned} \frac{dv_x}{dt} &= -\frac{eE_0}{m} \sin \omega t \mp \omega_c v_y \\ \frac{dv_y}{dt} &= -\frac{eE_0}{m} \cos \omega t \pm \omega_c v_x \end{aligned} \right\} \quad (2)$$

The upper sign corresponds to a magnetic field directed along the positive z -axis. Looking in this direction, the electric vector described by (1) rotates *anticlockwise*. The natural direction of rotation of electrons in this magnetic field is *clockwise*. Thus if (1) described the electric field of a circularly polarized wave traveling along the z -axis in the positive direction, the upper sign will correspond to the *ordinary* ray, and the lower sign to the *extraordinary* ray, in ionosphere theory terminology.

The *extraordinary* ray is the case of interest here, for this wave can be heavily absorbed by synchronous acceleration of the electrons by a cyclotron-type mechanism. In what follows, the lower sign will be taken. To use the equations for the ordinary ray, it is only necessary to change the sign of ω_c .

From eq (2) we find

$$\left. \begin{aligned} \frac{d^2 v_x}{dt^2} + \omega_c^2 v_x &= -\frac{eE_0}{m} (\omega + \omega_c) \cos \omega t \\ \frac{d^2 v_y}{dt^2} + \omega_c^2 v_y &= +\frac{eE_0}{m} (\omega + \omega_c) \sin \omega t \end{aligned} \right\} \quad (3)$$

¹ Contribution from Microwave Laboratory, W. W. Hansen Laboratories of Physics, Stanford University, Stanford, Calif., while author was on leave from the Department of Electrical Engineering, The University of Sheffield, Sheffield, England. The research reported in this paper was sponsored by the Air Force Cambridge Research Center, Air Research and Development Command, Bedford, Mass., 1959.

² Sagdeyev and Shafranov, Absorption of high-frequency electromagnetic field energy in the high-temperature plasma. Proceedings of the Second International Conference on Peaceful Uses of Atomic Energy, Geneva, September 1958. Paper P/2215.

3. Collisions and Boundary Conditions

For our present purpose the details of the collision process are not important, since it will emerge that the collision frequency does not enter into the final formula for absorption.

We shall assume that an electron is brought to rest at each collision. Thus, for an electron which makes a collision at time t' , its motion until the next collision takes place can be found by solving the eq (3) subject to the conditions

$$\left. \begin{aligned} v_x &= v_y = 0 \\ \frac{dv_z}{dt} &= -\frac{eE_0}{m} \sin \omega t' \\ \frac{dv_y}{dt} &= -\frac{eE_0}{m} \cos \omega t' \end{aligned} \right\} \quad (4)$$

The last two formulas follow by substituting the first in (2). The solution of (3) appropriate to the boundary conditions (4) is given by

$$v_z = \frac{eE_0}{m(\omega - \omega_c)} [\cos \omega t - \cos \{\omega_c t + (\omega - \omega_c)t'\}] \quad (5)$$

$$v_y = -\frac{eE_0}{m(\omega - \omega_c)} [\sin \omega t - \sin \{\omega_c t + (\omega - \omega_c)t'\}]. \quad (6)$$

Equations (5) and (6) can be expressed more compactly thus

$$v_x - jv_y = \frac{eE_0}{m(\omega - \omega_c)} [e^{j\omega t} - e^{j\{\omega_c t + (\omega - \omega_c)t'\}}]. \quad (7)$$

Equation (7) gives the x and y components of velocity at time t of an electron which was at rest at time t' .

Assuming that n , the number of electrons per unit volume, is sufficiently large, we can assume that, on the average, at any time t the number of electrons per unit volume whose most recent collision occurred between t' and $t' + dt'$ is given by

$$dn = n\nu e^{-\nu(t-t')} dt'. \quad (8)$$

Using this formula, which in fact defines the collision frequency ν , we can calculate the current density at any time t . The contribution to J_x from the electrons whose most recent collision was in the interval t' to $t' + dt'$ is $dJ_x = -nev_x dn$, where v_x is given by (5). Hence, using (7), we find

$$J_x - jJ_y = \frac{-n\nu e^2 E_0}{m(\omega - \omega_c)} \int_{-\infty}^t [e^{j\omega t} - e^{j\{\omega_c t + (\omega - \omega_c)t'\}}] e^{-\nu(t-t')} dt'. \quad (9)$$

Carrying out the integrations in (9) and separating the real and imaginary parts, we find

$$J_x = \frac{ne^2 E_0}{m} \left[\frac{\nu \sin \omega t - (\omega - \omega_c) \cos \omega t}{\nu^2 + (\omega - \omega_c)^2} \right] \quad (10)$$

$$J_y = \frac{ne^2 E_0}{m} \left[\frac{\nu \cos \omega t + (\omega - \omega_c) \sin \omega t}{\nu^2 + (\omega - \omega_c)^2} \right]. \quad (11)$$

4. Effect of Velocity Distribution

So far, the formulas we have derived are familiar in magneto-ionic theory. We now consider the effect of thermal velocities of the electrons. If the electric field we have been discussing is associated with a wave of frequency ω_0 traveling in the direction of increasing z , with phase constant β , then an electron traveling in the same direction with velocity v_z will be subjected to a field of angular frequency $\omega_0 - \beta v_z = \omega$ say.

If dn_0 electrons/unit volume have a z -component of velocity between v_z and $v_z + dv_z$, and if the velocity distribution is Maxwellian, we have

$$dn_0 = n_0 \left(\frac{m}{2\pi kT} \right)^{1/2} e^{-mv_z^2/2kT} dv_z. \quad (12)$$

Equations (10) and (11) can be used to calculate the contribution to the current density components J_x and J_y in a frame of reference traveling with the electrons, i.e., with velocity v_z along the original z -axis, if we substitute dn_0 for n , and interpret ω as $\omega_0 - \beta v_z$. Thus

$$dJ_x = \frac{n_0 e^2 E_0}{m} \left(\frac{m}{2\pi kT} \right)^{1/2} e^{-mv_z^2/2kT} \left[\frac{\nu \sin \omega t - (\omega - \omega_c) \cos \omega t}{\nu^2 + (\omega - \omega_c)^2} \right] dv_z. \quad (13)$$

Transforming this contribution to the current back to the original frame of reference does not affect its amplitude but restores the frequency to the original value ω_0 . Thus, summing all such contributions

$$J_x = \frac{n_0 e^2 E_0}{m} \left(\frac{m}{2\pi kT} \right)^{1/2} \int_{-\infty}^{+\infty} e^{-mv_z^2/2kT} \left[\frac{\nu \sin \omega_0 t - (\omega - \omega_c) \cos \omega_0 t}{\nu^2 + (\omega - \omega_c)^2} \right] dv_z. \quad (14)$$

Similarly,

$$J_y = \frac{n_0 e^2 E_0}{m} \left(\frac{m}{2\pi kT} \right)^{1/2} \int_{-\infty}^{+\infty} e^{-mv_z^2/2kT} \left[\frac{\nu \cos \omega_0 t + (\omega - \omega_c) \sin \omega_0 t}{\nu^2 + (\omega - \omega_c)^2} \right] dv_z. \quad (15)$$

Note that parts of J_x and J_y which are in phase with the electric field components E_x and E_y are equal, and correspond to a transverse conductivity σ_{\perp} given by

$$\sigma_{\perp} = \frac{n_0 e^2}{m} \left(\frac{m}{2\pi kT} \right)^{1/2} \int_{-\infty}^{+\infty} e^{-mv_z^2/2kT} \left[\frac{\nu}{\nu^2 + (\omega_0 - \omega_c - \beta v_z)^2} \right] dv_z. \quad (16)$$

Similarly, the transverse permittivity ϵ_1 is

$$\epsilon_1 = \epsilon_0 - \frac{n_0 e^2}{\omega_0 m} \left(\frac{m}{2\pi k T} \right)^{1/2} \int_{-\infty}^{+\infty} e^{-m v_z^2 / 2kT} \left[\frac{(\omega_0 - \omega_c - \beta v_z)}{v^2 + (\omega_0 - \omega_c - \beta v_z)^2} \right] dv_z. \quad (17)$$

The effect of collisions on the v_z component of velocity has not been considered, since the absorption phenomenon is not affected by this process. We do not need to have detailed knowledge of v_z for each electron, we only need to know the number of electrons in any given small range of velocities.

5. Wave Propagation in a Hot Plasma

We assume now that the plasma temperature T is large³ and the collision frequency small, so that

$$v \ll \beta \sqrt{\frac{kT}{m}}. \quad (18)$$

In this case the bracketed factor in the integrand of (16) is small unless v_z is such that

$$\omega_0 - \omega_c - \beta v_z < v. \quad (19)$$

Within this small range of values of v_z the exponential factor can be given the value corresponding to $v_z = (\omega_0 - \omega_c)/\beta$, and taken outside the integral sign. It is then a simple matter to evaluate the integral, and the resulting formula for the conductivity is

$$\sigma = \frac{\pi n_0 e^2}{\beta m} \left(\frac{m}{2\pi k T} \right)^{1/2} e^{-m/2kT [(\omega_0 - \omega_c)/\beta]^2}. \quad (20)$$

If the conductivity is small, the absorption coefficient κ can be calculated very simply from the formula

$$\kappa = \frac{\alpha}{\beta} = \frac{\sigma_1}{2\omega\epsilon_1} = \frac{\sigma_1}{2\omega\epsilon_0 p^2}. \quad (21)$$

where α and β are the attenuation and phase constants respectively, and p is the real part of the refractive index. If, in accordance with Sagdeyev and Shafranov, we define $v_{||}$ by the equation

$$v_{||} = \sqrt{\frac{2kT}{m}} \quad (22)$$

we find

$$\kappa = \frac{\sqrt{\pi}}{2} \cdot \frac{c}{v_{||}} \cdot \frac{\omega_p^2}{\omega_0^2 p^3} \exp \left\{ -\frac{c^2}{v_{||}^2 p^2} \left(\frac{\omega_0 - \omega_c}{\omega_0} \right)^2 \right\}. \quad (23)$$

Here ω_p is the plasma frequency ($\omega_p^2 = ne^2/m\epsilon_0$), and ω_0 and ω_c are the frequency of the wave and the electron cyclotron frequency respectively.

This formula agrees exactly with the result of Sagdeyev and Shafranov, as stated in eq (13) of their paper (see footnote 2).

The calculation of ϵ_1 from (17) is carried out in

³ Since this is the only temperature involved, we use T for $T_{||}$, the effective temperature associated with thermal motion of electrons parallel to the magnetic field line.

the appendix. When this is done, we find

$$p^2 = 1 - \frac{2c}{v_{||}} \cdot \frac{\omega_p^2}{\omega_0^2 p} e^{-c^2/v_{||}^2 p^2 [(\omega_0 - \omega_c)/\omega_0]^2} \left\{ \frac{c}{v_{||} p} \left(\frac{\omega_0 - \omega_c}{\omega_0} \right) - \frac{1}{3} \frac{c^3}{v_{||}^3 p^3} \left(\frac{\omega_0 - \omega_c}{\omega_0} \right)^3 + \dots \right\}. \quad (24)$$

This also agrees with the form given by Sagdeyev and Shafranov, although their result is expressed in terms of an error integral. (The lower limit of this integral, which is missing, is presumably zero.) There is also an error in the sign of the second term in their formula.

6. A Microwave Diagnostic Technique for Determining the Electron Velocity Distribution in a Hot Plasma

It is easy to see that the method employed for integrating (16) does not depend in any way on the velocity distribution. This need not be Maxwellian, but can be quite arbitrary.

Let the velocity distribution parallel to the magnetic field be defined by formulas

$$dn_0 = n_0 f(v_z) dv_z; \quad \int_{-\infty}^{+\infty} f(v_z) dv_z = 1 \quad (25)$$

in place of the Maxwellian distribution formula eq (12).

We find for the conductivity of the plasma the very simple expression

$$\sigma_1 = \frac{\pi n_0 e^2}{\beta m} f \left(\frac{\omega_0 - \omega_c}{\beta} \right).$$

The attenuation coefficient can be written

$$\alpha = \frac{\pi e^2 \mu_0}{2m} \cdot \frac{\omega_0}{\beta^2} n_0 f \left(\frac{\omega_0 - \omega_c}{\beta} \right).$$

Thus the distribution function can be expressed in terms of experimentally observable quantities as follows

$$n_0 f \left(\frac{\omega_0 - \omega_c}{\beta} \right) = \frac{2m}{\pi e^2 \mu_0} \cdot \frac{\alpha \beta^2}{\omega_0}. \quad (26)$$

If the right-hand side of (26) is plotted as a function of $(\omega_0 - \omega_c)/\beta$, the electron velocity distribution parallel to the magnetic field is obtained. The area under this curve will give the electron density. In practical applications, the distribution function may depend on z . If this is the case, the total attenuation measured is approximately $\int \alpha dz$ along the transmission path, provided that the rate of change of attenuation per wavelength of path is not too great. Thus from the total attenuation we can determine, using (26), the average distribution function, the average being taken along the microwave path.

7. Wave Propagation in a Cold Plasma

Formulas for σ_{\perp} and ϵ_{\perp} in a cold plasma, in which $\nu \gg \beta \sqrt{kT/m}$, are easily obtained from (16) and (17) if the collision frequency can be assumed independent of ν . The familiar magneto-ionic theory formulas are obtained:

$$\left. \begin{aligned} \sigma_{\perp} &= \frac{ne^2}{m} \cdot \frac{\nu}{\nu^2 + (\omega_0 - \omega_c)^2} \\ \epsilon_{\perp} &= 1 - \frac{ne^2}{\epsilon_0 m} \cdot \frac{(\omega_0 - \omega_c)}{\nu^2 + (\omega_0 - \omega_c)^2} \end{aligned} \right\} \quad (27)$$

Note that if $\nu \gg (\omega_0 - \omega_c)$, σ_{\perp} is proportional to $1/\nu$, whilst if $\nu \ll (\omega_0 - \omega_c)$, σ_{\perp} is proportional to ν .

8. Discussion

The purpose of this section is to contrast the behavior of the conductivity of hot and cold plasmas with respect to variation of collision frequency.

Consider first the cold plasma conductivity as described by (27). For a large collision frequency, the conductivity is proportional to $1/\nu$. The physical meaning is clear. It is easy to show from (7) that an electron starting from rest at time $t=0$ acquires in time t a kinetic energy given by

$$W = \frac{1}{2} \frac{e^2 E_0^2}{m} \left\{ \frac{\sin \left[\left(\frac{\omega - \omega_c}{2} \right) t \right]}{\frac{\omega - \omega_c}{2}} \right\}^2 \quad (28)$$

assuming that no collisions take place. Differentiating, we find

$$\frac{dW}{dt} = \frac{e^2 E_0^2}{m} \frac{\sin(\omega - \omega_c)t}{(\omega - \omega_c)} \quad (28a)$$

If the collision frequency ν is large, in comparison with $(\omega_0 - \omega_c)$, the time interval t , during which the gain in kinetic energy described by (28a) can take place before the process is interrupted by another collision, is small, and $(\omega_0 - \omega_c)t \ll 1$. Hence, (28a) can be replaced by

$$\frac{dW}{dt} = \frac{e^2 E_0^2}{m} \cdot t \quad (29)$$

The average rate of absorption per electron is given by

$$\overline{dW} = \frac{e^2 E_0^2}{m} \cdot \frac{1}{\nu} \quad (30)$$

Thus the physical significance of the inverse variation of conductivity with collision frequency, when the collision frequency is large in comparison with the frequency difference, $\omega_0 - \omega_c$ becomes clear.

When the collision frequency is small in comparison with $(\omega_0 - \omega_c)$, the amplitude of oscillation, and hence the mean kinetic energy acquired by the electrons, is not limited by collisions, but by the lack of synchronism between the frequency of the alternating force by the wave and the natural frequency of gyration of the electrons. If $\omega_0 > \omega_c$, the amplitude of oscillation is limited mainly by electron inertia, while if $\omega_0 < \omega_c$, it is limited by the obstructing effect of the magnetic field. If (28) is averaged over the long time which elapsed between collision, we find

$$\overline{W} = \frac{e^2 E_0^2}{m(\omega_0 - \omega_c)^2}$$

If it is assumed that, on the average, this energy, or a definite fraction of it, is given up by an electron at each collision, the average rate of absorption of energy per electron is given by

$$\nu \overline{W} = \frac{e^2 E_0^2}{m(\omega_0 - \omega_c)^2} \cdot \nu, \quad (31)$$

and is clearly directly proportional to ν , the collision frequency. Thus the reason for the variation of conductivity with collision frequency predicted by (27) is clear, and the physical mechanism by which the energy is absorbed has been exhibited. Energy extracted from the wave appears first as kinetic energy of the electron, and is then transferred to molecules or ions of the gas by collisions. This absorption process is called *collisional absorption*, and as we have seen, depends strongly on the collision frequency.

In direct contrast to this situation, the absorption by a "hot" plasma, in which $\nu \ll \beta \sqrt{kT/m}$, is independent of ν to first order, as eq (20) shows. The reason for this is that in a hot plasma, the effective frequency seen by an electron depends on its velocity in the direction of the propagation of the wave, due to the Doppler shift. Since the electron velocities vary widely in a hot plasma, a wide range of effective frequencies exists, and the hot conductivity is essentially an average of the cold conductivity over all frequencies. That this is independent of ν can be easily seen using (27)

$$\begin{aligned} \int_{-\infty}^{+\infty} \sigma_{\perp} d\omega &= \frac{ne^2}{m} \int_{-\infty}^{+\infty} \frac{\nu}{\nu^2 + (\omega - \omega_c)^2} d\omega \\ &= \frac{ne^2}{m} \int_{-\infty}^{+\infty} \frac{\nu}{\nu^2 + \omega_1^2} d\omega_1 = \frac{\pi ne^2}{m} \end{aligned} \quad (32)$$

Provided that ν is small enough, the integrand is very small except when $(\omega - \omega_c) \sim \nu$, so that a very small range of effective frequencies (and electron velocities) contributes significantly to the absorption. Provided that the plasma temperature is high enough, the variation of the distribution function over this small range of significant electron velocities may be neglected, and the distribution function can be regarded as constant as was done in obtaining eq (20).

Further, if ν depends on v_z , the analysis is still valid, provided that the dependence is not strong in the small range of significant velocities.

The case of no collisions at all can be regarded as the limiting case $\nu \rightarrow 0$; the "cold conductivity" term in the integrand of (16) then has the character of a delta function, and eq (10) is exact.

Thus, the agreement of our analysis with that of Sagdeyev and Shafranov is to be expected, in spite of the fact that in their treatment it was assumed a priori that no collisions occurred, whereas the present analysis necessarily involves the consideration of collisions.

9. Conclusions

Summarizing, the present analysis has shown:

(a) That in the absorption of microwaves by a hot plasma in a magnetic field, collisions have a second-order effect only;

(b) That the results of Sagdeyev and Shafranov, obtained by solving the Boltzmann equations for the distribution functions by a perturbation technique, neglecting collisions at the outset, can be obtained by a direct ballistic analysis of the motion of individual electrons;

(c) That the assumption of a Maxwellian velocity distribution function made by Sagdeyev and Shafranov is not necessary to the analysis, and that a closed-form solution for conductivity can be obtained for any arbitrary distribution function;

(d) That a study of the variation with frequency of the attenuation and phase constant of a circularly polarized electromagnetic wave in an ionized plasma in a magnetic field can in principle yield the velocity distribution function for the thermal motion of electrons parallel to the magnetic field lines. There may be considerable difficulty in applying this technique in some cases. For example, the extraordinary ray only must be employed, and a high degree of discrimination against the ordinary ray in the launching and/or receiving antennas will be necessary if errors due to the ordinary ray, which is attenuated much less strongly, are to be negligible. Also diffraction effects will be serious except at microwave frequencies, so that the method can only be applied in the simple form suggested here if the magnetic field strength is of the order of 3,000 gauss or more, so that the cyclotron frequency falls in the microwave-frequency band.

As an alternative to attempting to eliminate the ordinary ray entirely, one could start with a linearly polarized wave and measure the ellipticity of the received signal. This would have some practical advantages, and the necessary theory could be developed very simply from the equations given here.

A more serious limitation arises when the order of magnitude of the attenuation at resonance is estimated. For $n=10^{11}$ electrons/cm³, $T=10^6$ °K, and $\omega=10,000$ Mc/s, the attenuation coefficient at cyclotron resonance has a value of about 100 db/cm or the attenuation length is about 1 mm. For densities of 10^8 electrons/cm³ under the same conditions, however, the attenuation coefficient is about

0.1 db/cm, and for such a low density plasma the method might be feasible.

It should be noted that the effect of the radio-frequency magnetic field has not been considered in the present analysis. While this seems unlikely to lead to serious errors at electron temperatures of a million degrees or so, these effects might be appreciable for temperatures of the order of a hundred million degrees, when the electron velocity is only one order of magnitude less than the velocity of light.

No comparison has been made with the more elaborate theory of Drummond⁴, which starts from the Boltzmann equation but retains the collision term, for which a suitable approximation is later introduced. It would be very desirable to make such a comparison, which would probably shed further light on the significance of collisions in a practical situation.

10. Appendix

We have to evaluate

$$I = \int_{-\infty}^{+\infty} e^{-m^2/2kT} \frac{(\omega_0 - \omega_c - \beta v_z)}{v_z^2 + (\omega_0 - \omega_c - \beta b_z)^2} dv_z. \quad (1)$$

Let $t = \sqrt{m/2kT} v_z$; $t_0 = \sqrt{m/2kT} [(\omega_0 - \omega_c)/\beta]$. Let us also put $\nu=0$. We get

$$I = \frac{1}{\beta} \int_{-\infty}^{+\infty} \frac{e^{-t^2} dt}{t_0 - t}. \quad (2)$$

Now put $z = t - t_0$.

$$I = -\frac{1}{\beta} \int_{-\infty}^{+\infty} \frac{e^{-(z+t_0)^2}}{z} dz. \quad (3)$$

Because of the singularity at $z=0$, we interpret I in the following way

$$-\beta I = e^{-t_0^2} \lim_{\epsilon \rightarrow 0} \left\{ \int_{-\infty}^{-\epsilon} e^{-z^2 - 2t_0 z} \frac{dz}{z} + \int_{+\epsilon}^{+\infty} e^{-z^2 - 2t_0 z} \frac{dz}{z} \right\}.$$

Replacing z by $-z$ in the first integral, and combining the two integrals gives

$$+\frac{\beta I}{2} = e^{-t_0^2} \int_0^{\infty} \frac{e^{-z^2}}{z} \sinh 2t_0 z dz. \quad (4)$$

This integral is easily evaluated by expanding $\sinh 2t_0 z$ and integrating term by term. This leads to the result given in eq (24).

This work was done during a period spent at the Microwave Laboratory, Stanford University, and the author expresses his gratitude for this opportunity. He is particularly indebted to Dr. G. S. Kino and Dr. P. Sturrock for helpful discussions.

⁴ J. E. Drummond, Basic microwave properties of hot magnetoplasma, Phys. Rev. **110** (April 15, 1958).



On Electromagnetic Radiation in Magneto-Ionic Media¹

Herwig Kogelnik

(January 12, 1960; revised April 5, 1960)

A method of treating radiation problems in magneto-ionic (anisotropic) media is presented. A "wave matrix" is defined, the zeros of whose determinant are the propagation constants of the ordinary and the extraordinary plane waves. A derivation of the dyadic Green's function for the unbounded medium is given, which is also based on this matrix. A formula is arrived at, which gives the power radiated by any distribution of alternating current in terms of the wave matrix and the spatial Fourier transforms of the currents. The method is illustrated by a discussion of the power radiated by an elementary dipole.

1. Introduction

An ionized gas in a permanent magnetic field is an anisotropic dielectric medium. Two well known examples are the ionosphere and the plasma investigated in controlled thermonuclear fusion research. We shall call this medium a "magneto-ionic medium," but other names, like "magneto-plasma," are also used in the literature.

The dielectric properties of a magneto-ionic medium can be described by a dielectric permittivity tensor [1,2,3,4]² and the propagation of plane electromagnetic waves in such a medium has been subject to many investigations [3, 5]. The purpose of this paper is to present a general treatment of electromagnetic radiation in magneto-ionic media. (The radiation properties of antennas and moving charged particles are, of course, modified by the anisotropic properties of the surrounding medium.) The method proposed avoids the introduction of vector potentials, Hertz vectors, anisotropic potentials, and the like. The computation of the fields excited by a known distribution of oscillating current will be reduced to elementary matrix operations and the evaluation of integrals. We are particularly interested in the (complex) power radiated by a current distribution and shall illustrate the method by discussing in detail the power radiated by an elementary dipole.

We would also like to direct the reader's attention to other published methods [6, 7, 8, 9, 10, 11, 12], most of which have been applied to special radiation problems, like Cerenkov Radiation, in magneto-ionic media.

2. Background

To simplify the analysis, we assume the medium to be homogeneous, of infinite extension, and nonmagnetic ($\mu_{rel}=1$). All a-c quantities shall be described by their complex amplitude. If the factor $\exp(j\omega t)$ is dropped and MKS units are used, Maxwell's equations take the form

$$\nabla \times \mathbf{E} = -j\omega\mu_0 \mathbf{H} \quad (1a)$$

$$\nabla \times \mathbf{H} = j\omega\epsilon_0 \hat{\epsilon} \mathbf{E} + \mathbf{J}, \quad (1b)$$

¹ Contribution from Engineering Laboratory, 19 Parks Road, Oxford, England.

² Figures in brackets indicate the literature references at the end of this paper.

where \mathbf{J} is the external current density—as produced by antennas or moving charged particles—which we assume to be known. The usual matrix formalism is used, and vectors are regarded as column matrices. The permittivity tensor is represented by the matrix $\hat{\epsilon}$, whose components are in general complex numbers, to include conducting (i.e., lossy) media. For most applications a matrix $\hat{\epsilon}$ of the simple form

$$\hat{\epsilon} = \begin{bmatrix} \epsilon_1 & -j\epsilon_2 & 0 \\ j\epsilon_2 & \epsilon_1 & 0 \\ 0 & 0 & \epsilon_3 \end{bmatrix} \quad (2)$$

can be used (see e.g., [2, 3]). Here the z -axis of the coordinate system is orientated in the direction of the applied permanent magnetic field. It can occur, however, that more complicated matrices have to be used, in order to describe the medium's physical behavior correctly [4].

We now rewrite eq (1a)

$$\mathbf{H} = \frac{j}{\omega\mu_0} \nabla \times \mathbf{E} \quad (3)$$

and eliminate the a-c magnetic field \mathbf{H} from eq (1b) to obtain the wave equation

$$\left(\nabla \nabla - \Delta \hat{1} - \frac{\omega^2}{c^2} \hat{\epsilon} \right) \mathbf{E} = -j\omega\mu_0 \mathbf{J}, \quad (4)$$

where $\hat{1}$ is the unit matrix, $\Delta \equiv \nabla^2$ the Laplacian operator, and the dyade $\nabla \nabla$ is standing for a matrix, whose elements are the differential operators $\partial^2 / \partial x_i \partial x_k$. We have to solve this wave equation to obtain the amplitudes $\mathbf{E}(\mathbf{r})$ of the a-c electric field in every point of space produced by a given distribution of current. The solutions shall satisfy the condition that at great distances from the sources the fields represent divergent traveling waves.

3. Plane Waves

A set of simple solutions of the homogeneous wave equation ($\mathbf{J}=0$) describe plane electromagnetic waves, which we propose to discuss in this chapter. The planes of equal phase are specified by the wave normal

$$\mathbf{n} = (n_1, n_2, n_3)$$

whose components are the direction cosines

$$n_1 = \sin \alpha \cos \beta,$$

$$n_2 = \sin \alpha \sin \beta,$$

$$n_3 = \cos \alpha.$$

Let $\mathbf{r} = (x, y, z) = (x_1, x_2, x_3)$ be the radius vector, drawn from the origin to any point in space, then

$$n_1 x + n_2 y + n_3 z = \mathbf{n} \cdot \mathbf{r} = \text{const} \quad (5)$$

is the equation of a plane, and the amplitude of a plane wave with the wave normal \mathbf{n} will vary as

$$\mathbf{E}(\mathbf{r}) = \mathbf{E}_0 e^{-jk\mathbf{n} \cdot \mathbf{r}}. \quad (6)$$

With k being any complex number, it is convenient to define the vector

$$\mathbf{k} = k\mathbf{n}.$$

We note that

$$\frac{\partial}{\partial x_i} e^{-j\mathbf{k}\cdot\mathbf{r}} = -jk_i e^{-j\mathbf{k}\cdot\mathbf{r}}, \quad (7)$$

and, operating the matrices of the wave equation on the same exponential

$$\left(\nabla \nabla - \Delta \hat{1} - \frac{\omega^2}{c^2} \hat{\epsilon} \right) e^{-j\mathbf{k}\cdot\mathbf{r}} = -\hat{\lambda}(\mathbf{k}) e^{-j\mathbf{k}\cdot\mathbf{r}}, \quad (8)$$

we get the "wave matrix"

$$\hat{\lambda} = \mathbf{k}\mathbf{k} - k^2 \hat{1} + k_0^2 \hat{\epsilon}, \quad (9)$$

Here is introduced the propagation constant of electromagnetic waves in vacuum

$$k_0 = \frac{\omega}{c}$$

The electric field of eq (6) has to satisfy the homogeneous wave equation. Using eq (8) and dropping the exponential, this condition can be written

$$\hat{\lambda}(\mathbf{k}) \mathbf{E}_0 = 0. \quad (10)$$

As we look for nonvanishing fields, this condition can only be fulfilled if

$$\det \hat{\lambda}(\mathbf{k}) = 0. \quad (11)$$

Equation (11) determines the propagation constants of possible plane waves with given wave normal \mathbf{n} .

If $\hat{\epsilon}$ has the form as in eq (2), an elementary computation shows that

$$\det \hat{\lambda}(\mathbf{k}) = k_0^2 (\epsilon_1 \sin^2 \alpha + \epsilon_3 \cos^2 \alpha) (k^2 - k_I^2) (k^2 - k_{II}^2), \quad (12)$$

with

$$k_{I,II}^2/k_0^2 = \frac{(\epsilon_1^2 - \epsilon_3^2) \sin^2 \alpha + \epsilon_1 \epsilon_3 (1 + \cos^2 \alpha) \pm \sqrt{(\epsilon_1^2 - \epsilon_3^2 - \epsilon_1 \epsilon_3)^2 \sin^4 \alpha + 4 \epsilon_1^2 \epsilon_3^2 \cos^2 \alpha}}{2(\epsilon_1 \sin^2 \alpha + \epsilon_3 \cos^2 \alpha)}. \quad (13)$$

These relations show that in a magneto-ionic medium, as is well known, two types of plane waves are possible for a given wave normal. They are called the "ordinary" and the "extraordinary" wave, and their (complex) propagation constants are k_I and k_{II} respectively, whose values depend on the angle α between wave normal and permanent magnetic field. The quantities $k_{I,II}/k_0$ are known as the "refractive indices" of the corresponding waves.

4. Dyadic Green's Function

In this chapter we propose to present a solution of the wave eq (4) for any known current-distribution $\mathbf{J}(\mathbf{r})$ (confined to a finite region of space). Because of the linearity of Maxwell's equations there must be a linear relation between the components of a current *element* and the components of the electric field produced by the latter at a point \mathbf{r} . We can, therefore write for the electric field $\mathbf{E}(\mathbf{r})$ produced by the *entire* distribution $\mathbf{J}(\mathbf{r}')$

$$\mathbf{E}(\mathbf{r}) = \int d\mathbf{r}' \hat{G}(\mathbf{r}, \mathbf{r}') \mathbf{J}(\mathbf{r}'), \quad (14)$$

where $\int d\mathbf{r}'$ stands for $\int_{-\infty}^{+\infty} \int_{-\infty}^{+\infty} \int_{-\infty}^{+\infty} dx' dy' dz'$. The matrix \hat{G} is called "dyadic Green's function."

It has proved a powerful tool in treating other problems of electrodynamics and is well known for an unbounded isotropic medium [13, 14]. In the following we shall derive \hat{G} for an unbounded anisotropic medium. An alternative derivation has been described by Bunkin [6].

We use the following identities holding for Dirac's δ -function

$$\int_{-\infty}^{+\infty} f(x') \delta(x-x') dx' = f(x) \quad (15)$$

$$\delta(x) = \frac{1}{2\pi} \int_{-\infty}^{+\infty} e^{-jk_1 x} dk_1, \quad (16)$$

and the abbreviation

$$\delta(\mathbf{r}) = \delta(x)\delta(y)\delta(z).$$

Because of eq (15) the electric field \mathbf{E} of eq (14) satisfies the wave equation if \hat{G} satisfies

$$(\nabla\nabla - \Delta\hat{1} - k_0^2\hat{\epsilon})\hat{G}(\mathbf{r}, \mathbf{r}') = -j\omega\mu_0\hat{1}\delta(\mathbf{r}-\mathbf{r}'). \quad (17)$$

We note that $\nabla\nabla$ and Δ operate on the variables \mathbf{r} only and not on \mathbf{r}' , and we have to assume that the interchange of these two operators with the integration $\int d\mathbf{r}'$ is permitted.

To find a suitable matrix \hat{G} we multiply eq (8) by the inverse of the wave matrix from the right to get

$$(\nabla\nabla - \Delta\hat{1} - k_0^2\hat{\epsilon})\hat{\lambda}^{-1}e^{-j\mathbf{k}\cdot\mathbf{r}} = -\hat{1}e^{-j\mathbf{k}\cdot\mathbf{r}}. \quad (18)$$

We can do this for all real k_1 , k_2 , and k_3 , if we assume the medium to be at least slightly lossy. Then, the zeros of $\det \hat{\lambda}(\mathbf{k})$, k_1^2 , and k_2^2 , will have imaginary parts (i.e., plane waves are attenuated). But as shown later the results are also valid for lossless media.

We finally multiply eq (18) by $e^{j\mathbf{k}\cdot\mathbf{r}'}$ and perform the integrations $\int d\mathbf{k} = \int_{-\infty}^{+\infty} dk_1 \int_{-\infty}^{+\infty} dk_2 \int_{-\infty}^{+\infty} dk_3$ to find that the matrix

$$\hat{G} = \frac{j\omega\mu_0}{8\pi^3} \int d\mathbf{k} \hat{\lambda}^{-1} e^{-j\mathbf{k}\cdot(\mathbf{r}-\mathbf{r}')} \quad (19)$$

satisfies eq (17). We have thus found the dyadic Green's function for the unbounded anisotropic medium. To this solution, of course, we can add any solution of the homogeneous wave equation, if required by the behavior of the fields "at infinity." It can be shown, however, that the result given in eq (18) satisfies the required condition that no incoming waves shall occur.

The inverse of $\hat{\lambda}$ can be computed by using Cramer's rule

$$\hat{\lambda}^{-1} = \frac{\hat{\Lambda}}{\det \hat{\lambda}}, \quad (20)$$

where the matrix $\hat{\Lambda}$ is the "adjoint" of $\hat{\lambda}$. For a magneto-ionic medium with a dielectric tensor, as in eq (2), we find

$$\hat{\Lambda}(\mathbf{k}) = k^4 \mathbf{n} \mathbf{n} - k^2 k_0^2 \hat{L} + k_0^4 \hat{E}, \quad (21)$$

where \hat{E} is the adjoint of $\hat{\epsilon}$

$$\hat{E} = \begin{bmatrix} \epsilon_1 \epsilon_3 & j\epsilon_2 \epsilon_3 & 0 \\ -j\epsilon_2 \epsilon_3 & \epsilon_1 \epsilon_3 & 0 \\ 0 & 0 & \epsilon_1^2 - \epsilon_2^2 \end{bmatrix} \quad (22)$$

and

$$\hat{L} = \begin{bmatrix} \epsilon_1(n_1^2 + n_2^2) + \epsilon_3(n_1^2 + n_3^2); & j\epsilon_2(n_1^2 + n_2^2) + \epsilon_3 n_1 n_2; & \epsilon_1 n_1 n_3 + j\epsilon_2 n_2 n_3 \\ -j\epsilon_2(n_1^2 + n_2^2) + \epsilon_3 n_1 n_2; & \epsilon_1(n_1^2 + n_2^2) + \epsilon_3(n_2^2 + n_3^2); & \epsilon_1 n_2 n_3 - j\epsilon_2 n_1 n_3 \\ \epsilon_1 n_1 n_3 - j\epsilon_2 n_2 n_3; & \epsilon_1 n_2 n_3 + j\epsilon_2 n_1 n_3; & \epsilon_1(1 + n_3^2) \end{bmatrix}. \quad (23)$$

The equivalence of \hat{G} and Bunkin's Green's function can be shown by using eq (7) to replace each k_i in $\hat{\Lambda}$ by the operation $j\partial/\partial x_i$ and interchanging the latter with the integration $\int d\mathbf{k}$.

In this chapter the problem of finding the fields, produced by a known distribution of current, has been reduced to the problem of evaluating integrals. The methods of integration will have to be adapted to the particular problem. For example, the method of steepest descents has been employed to find the dipole fields at great distances [6].

5. Power Radiated by a Distribution of Current

The mean complex power radiated by the current distribution $\mathbf{J}(\mathbf{r})$ is given by

$$P = -\frac{1}{2} \int d\mathbf{r} \mathbf{J}^+(\mathbf{r}) \cdot \mathbf{E}(\mathbf{r}), \quad (24)$$

where the row matrix \mathbf{J}^+ is the Hermite conjugate of \mathbf{J} . For some purposes it is convenient to rewrite this expression in terms of the wave matrix and the spatial Fourier transform $\mathbf{J}_{\mathbf{k}}$ of the current density

$$\mathbf{J}(\mathbf{r}) = \int d\mathbf{k} \mathbf{J}_{\mathbf{k}} e^{-j\mathbf{k} \cdot \mathbf{r}}. \quad (25)$$

Using eqs (14), (19), and (25) we get

$$P = -\frac{j\omega\mu_0}{16\pi^3} \int d\mathbf{k} d\mathbf{k}' d\mathbf{k}'' d\mathbf{r} d\mathbf{r}' \mathbf{J}_{\mathbf{k}'}^+ \hat{\lambda}^{-1}(\mathbf{k}) \mathbf{J}_{\mathbf{k}''} e^{-j[\mathbf{r} \cdot (\mathbf{k} - \mathbf{k}') - \mathbf{r}' \cdot (\mathbf{k} - \mathbf{k}'')]} \quad (26)$$

With the help of the relations (15) and (16) these 15 integrals can be reduced to 3, and we obtain the relatively useful formula

$$P = -4j\pi^3\omega\mu_0 \int d\mathbf{k} \mathbf{J}_{\mathbf{k}}^+ \hat{\lambda}^{-1} \mathbf{J}_{\mathbf{k}}. \quad (27)$$

One can, of course, rewrite eq (24) in this form almost immediately, if Parseval's equation is used.

An application of formula (27) is given in the next section.

6. Power Radiated by an Elementary Dipole

To simplify the problem, we assume here that the medium is lossless. Let an elementary electric dipole with moment \mathbf{p} be placed at the origin of our coordinate system. The spatial distribution of current is then

$$\mathbf{J}(\mathbf{r}) = j\omega\mathbf{p}\delta(\mathbf{r}). \quad (28)$$

For the calculation of many physical quantities, like the fields at great distances or the real power radiated, many current configurations $\mathbf{J}'(\mathbf{r})$, which are concentrated in an electrically small region, can be considered equivalent to an elementary dipole (see e.g. [15]). The equivalent moment is given by

$$j\omega\mathbf{p} = \int d\mathbf{r} \mathbf{J}'(\mathbf{r}). \quad (29)$$

Certain quantities, however, like the fields in the immediate neighborhood or the reactive power, depend very strongly on the dimensions of this region. We are, therefore, mainly interested in the real power, radiated by the dipole. In an anisotropic medium the power is expected to be different for different orientations and polarizations of the dipole.

As we want to apply formula (27), we need the Fourier transform of $\mathbf{J}(\mathbf{r})$, which is

$$\mathbf{J}_k = \frac{j\omega\mathbf{p}}{8\pi^3} \quad (30)$$

Putting this into the formula, we see that the complex power can be written as a bilinear form

$$P = \frac{\omega^2}{2} \mathbf{p}^+ \hat{z} \mathbf{p}, \quad (31)$$

where the components of the matrix

$$\hat{z} = -\frac{j\omega\mu_0}{8\pi^3} \int d\mathbf{k} \hat{\lambda}^{-1} \quad (32)$$

are measured in Ωm^{-2} (impedance units per unit area). This complex matrix \hat{z} can be split into a Hermitian and an anti-Hermitian part

$$\hat{z} = \hat{r} + j\hat{x}, \quad (33)$$

that is to say, the matrices \hat{r} and \hat{x} are both Hermitian ($\hat{r} = \hat{r}^+$, $\hat{x} = \hat{x}^+$). With the help of these two matrices the bilinear form of eq (31) splits up into two Hermitian forms (which are real numbers) thus separating real and reactive power. The real power P_r is therefore given by

$$P_r = \frac{\omega^2}{2} \mathbf{p}^+ \hat{r} \mathbf{p}. \quad (34)$$

The reactive power produced by a region filled with current increases without limit as the region contracts. It has, therefore, no physical meaning for an elementary dipole.

In the following we would like to sketch the steps of the computation of \hat{r} for an $\hat{\epsilon}$ as in eq (2). That means, we have to pick the Hermitian part of \hat{z} , given by eq (32), which is possible after performing two steps of the integration of $\int d\mathbf{k} \hat{\lambda}^{-1}$.

For this purpose we introduce polar coordinates in \mathbf{k} -space, with the volume element

$$d\mathbf{k} = k^2 \sin \alpha dk d\alpha d\beta. \quad (34)$$

We choose the intervals of integration from $-\infty$ to $+\infty$ for k , from 0 to $\pi/2$ for α , and from 0 to 2π for β , to cover all \mathbf{k} -space. Equations (12) and (20) are used to substitute for $\hat{\lambda}^{-1}$, and eq (21) to rewrite

$$\frac{k^2 \hat{\Lambda}(k)}{(k^2 - k_I^2)(k^2 - k_{II}^2)} = k^2 \mathbf{n} \mathbf{n} + (k_I^2 + k_{II}^2) \mathbf{n} \mathbf{n} - k_0^2 \hat{L} + \frac{1}{k_I^2 - k_{II}^2} \left[\frac{k_I^2}{k^2 - k_I^2} \hat{\Lambda}(k_I) - \frac{k_{II}^2}{k^2 - k_{II}^2} \hat{\Lambda}(k_{II}) \right]. \quad (35)$$

As k_I and k_{II} are independent of β , the integration with respect to this variable can be performed. As a result of this, we introduce two new matrices, \hat{N} and \hat{M} ,

$$\hat{N} = \frac{1}{\pi} \int_0^{2\pi} \mathbf{n} \mathbf{n} d\beta = \begin{bmatrix} \sin^2 \alpha & 0 & 0 \\ 0 & \sin^2 \alpha & 0 \\ 0 & 0 & 2 \cos^2 \alpha \end{bmatrix} \quad (36)$$

$$\hat{M} = \frac{1}{\pi} \int_0^{2\pi} \hat{L} d\beta = \begin{bmatrix} 2\epsilon_1 \sin^2 \alpha + \epsilon_3(1 + \cos^2 \alpha); & 2j\epsilon_2 \sin^2 \alpha; & 0 \\ -2j\epsilon_2 \sin^2 \alpha; & 2\epsilon_1 \sin^2 \alpha + \epsilon_3(1 + \cos^2 \alpha); & 0 \\ 0; & 0; & 2\epsilon_1(1 + \cos^2 \alpha) \end{bmatrix}. \quad (37)$$

We have postulated a lossless medium. Therefore, ϵ_1 , ϵ_2 , and ϵ_3 have to be real numbers and the matrices \hat{M} and \hat{N} are Hermitian. k_I^2 and k_{II}^2 are also real but k_I and/or k_{II} can be real or imaginary ("cut off" plane wave) because negative values of ϵ_1 and/or ϵ_3 can occur in magneto-ionic media.

The next step is to perform the integration $\int_{-\infty}^{+\infty} dk$. From (35) we notice that the two last terms of the integrands have poles if k_I and k_{II} are real. As a consequence of this, the values of the corresponding integrals are not uniquely determined. And it is here that we have to remember the medium is regarded as at least slightly lossy (see sec. 4). The poles are then removed from the path of integration, and, we obtain with the help of Cauchy's formula and the residue concept

$$\int_{-\infty}^{+\infty} \frac{dk}{k^2 - k_I^2} = -\frac{\pi j}{k_I}, \quad (38)$$

where the sign of the root of k_I^2 has been chosen such that $\text{Im } k_I \leq 0$ and $\text{Re } k_I > 0$, and similarly for k_{II} . The result of the integration is now uniquely determined and can also be used for the lossless case.

The first three terms of the integrand contribute to the anti-Hermitian part of \hat{z} only, and can be dropped. Their integral does not exist (see remarks on reactive power).

With $u = \cos \alpha$, the vacuum characteristic impedance $Z_0 = \sqrt{\mu_0/\epsilon_0}$, and the vacuum wave length $\lambda_0 = 2\pi/k_0$ we obtain finally

$$\hat{r} = -\frac{\pi Z_0}{2 \lambda_0^2} \int_0^1 \frac{du}{k_0^2 \epsilon_1 + (\epsilon_3 - \epsilon_1) u^2} \frac{\hat{F}}{(k_I^2 - k_{II}^2)}, \quad (39)$$

where

$$\hat{F} = \text{Herm} \{ (k_I^5 - k_{II}^5) \hat{N} - k_0^2 (k_I^3 - k_{II}^3) \hat{M} + 2(k_I - k_{II}) k_0^3 \hat{E} \}.$$

The symbol "Herm" stands for "Hermitian part of." As \hat{N} , \hat{M} , and \hat{E} are Hermitian, this simply means that all terms with an imaginary k_I or k_{II} have to be dropped. k_I and k_{II} vary with $u (= \cos \alpha)$ according to eq (13) and can be real for some regions of integration and imaginary for others. The latter is the case for angles α between wave normal and permanent magnetic field where the corresponding plane wave is "cut-off" and cannot transmit power.

Because of the particular structure of \hat{N} , \hat{M} , and \hat{E} the matrix \hat{r} has the form

$$\hat{r} = \begin{bmatrix} r_1 & -jr_2 & 0 \\ jr_2 & r_1 & 0 \\ 0 & 0 & r_3 \end{bmatrix}, \quad (40)$$

from which the power P_r , radiated by dipoles of any orientation and polarization, can be computed.

To discuss two special cases of polarization let us consider:

(a) A linearly polarized dipole moment \mathbf{p} , as produced by an oscillating charged particle or an electrically small linear antenna. In this case the terms with r_2 cancel in the bilinear form and the dependence of P_r on the orientation of the dipole can be computed from

$$P_r = \frac{\omega^2}{2} \mathbf{p}^+ \begin{bmatrix} r_1 & 0 & 0 \\ 0 & r_1 & 0 \\ 0 & 0 & r_3 \end{bmatrix} \mathbf{p}; \quad (41)$$

which gives, if plotted in a polar diagram, an ellipsoid of revolution for $1/\sqrt{P_r}$. For the special orientation perpendicular to the magnetic field the power radiated is

$$P_{r\perp} = \frac{\omega^2}{2} r_1 |p_\perp|^2$$

and for parallel orientation we find

$$P_{r\parallel} = \frac{\omega^2}{2} r_3 |p_\parallel|^2;$$

(b) A circularly polarized moment, as produced by a charged particle on an electrically small circular orbit or two crossed linear antennas with a difference of $\pi/2$ in phase. We propose to discuss two particular orientations only. The first is such that $p_z=0$, and $p_y=\pm jp_x$ (for left- or right-hand polarization respectively) where we obtain

$$P_r = \omega^2 |p_x|^2 (r_1 \pm r_2)$$

which is a characteristic result for magneto-ionic media. It shows that the two crossed antennas are "coupled" by the medium. The power they radiate is not the sum of the powers that each individual antenna would radiate, if the other one were not excited.

The second orientation is one where $p_y=0$ and $p_z=\pm jp_x$. Here the total power

$$P_r = \frac{\omega^2}{2} |p_x|^2 (r_1 + r_3)$$

is equal to the sum of the powers that would be radiated by the individual antennas.

The values of r_1 , r_2 , and r_3 are determined by the corresponding integrals of eq (39), which have yet to be evaluated. For the special case of an isotropic medium ($\epsilon_2=0$, $\epsilon_1=\epsilon_3$)

$$r_2=0; \quad r_1=r_3=\frac{2\pi}{3} \frac{Z_0}{\lambda_0^2} \sqrt{\epsilon_0} = r_0$$

if $\epsilon_1=\epsilon_3 \geq 0$, and $r_1=r_2=r_3=0$ if $\epsilon_1=\epsilon_3 < 0$, which is the case in an isotropic plasma at frequencies below the plasma frequency. If $\epsilon_2=0$ and $\epsilon_1, \epsilon_3 > 0$, which occurs in magneto-ionic media with a very high gyrofrequency or in an uniaxial crystal, the integration yields

$$r_1/r_0 = \frac{1}{4}(3 + \epsilon_3/\epsilon_1);$$

$$r_3/r_0 = 1; \quad r_2=0.$$

With the exception of these and a few other special cases, the integrals have to be evaluated numerically. Some plots of an evaluation of r_1/r_0 and r_3/r_0 by means of an electronic computer can be found in [16].

If the power radiated and the current distribution of an antenna is known, the radiation resistance (which is defined by them) can be easily computed. Take for example a short linear antenna of length l and with a constant distribution of current I , which is orientated perpendicular to the permanent magnetic field. It produces a moment with the components $p_x=Il/j\omega$, $p_y=p_z=0$, and its radiation resistance is $R=l^2 r_1$.

The author thanks H. Motz for encouragement and valuable discussion.

7. References

- [1] H. W. Nichols, J. C. Schelleng, B.S.T.J. **4**, 215 (1925).
- [2] W. P. Allis; Motions of electrons and ions, Handb. Phys. **21**, 383 (1956).
- [3] J. A. Ratcliffe, The magneto-ionic theory and its application to the ionosphere (Cambridge Univ. Press, Cambridge, England, 1959) (with further references).
- [4] J. E. Drummond, Basic microwave properties of hot magneto-plasmas, Phys. Rev. **110**, 293 (1958) (with further references).
- [5] M. Born, Optik, pp. 413-420 (Berlin, Germany, 1933).
- [6] F. V. Bunkin; On radiation in anisotropic media, J. Exptl. Theoret. Phys. (USSR) **32**, 338 (1957).
- [7] A. A. Kolomenskii; Radiation from a plasma electron in uniform motion in a magnetic field, Doklady Akad. Nauk S.S.S.R. **106**, 982 (1956) (with further references).

- [8] A. G. Sitenko, A. A. Kolomenskii, Motion of a charged particle in an optically active anisotropic medium, *J. Exptl. Theoret. Phys. (USSR)* **30**, 511 (1956).
- [9] K. A. Barsukov, On the Doppler effect in an anisotropic and gyrotropic medium, *J. Exptl. Theoret. Phys. (USSR)* **36**, 1485 (1959).
- [10] G. A. Begiashvile, E. V. Gedalin, Cerenkov radiation of a magnetic dipole in an anisotropic medium, *J. Exptl. Theoret. Phys. (USSR)* **36**, 1939 (1959).
- [11] V. L. Ginzburg, V. Ya. Eidman, The radiation reaction in the motion of a charge in a medium, *J. Exptl. Theoret. Phys. (USSR)* **36**, 1823 (1959).
- [12] A. D. Bresler, The far fields excited by a point source in a passive dissipationless anisotropic uniform waveguide; *Trans. I.R.E. MTT-7*, 282 (1959).
- [13] F. E. Borgnis, Ch. H. Papas, *Randwertprobleme der Mikrowellenphysik*, p. 251-60 (Springer, Berlin, Germany, 1955) (with further references).
- [14] P. M. Morse, H. Feshbach, *Methods of theoretical physics*, Pt. II, Ch. 13 (McGraw-Hill Book Co., Inc. New York, N.Y., 1953).
- [15] J. A. Stratton, *Electromagnetic theory*, p. 432 (McGraw-Hill Book Co., Inc., New York, N.Y., 1941).
- [16] H. Kogelnik, The radiation resistance of an elementary dipole in anisotropic plasmas, *Fourth Intern. Conf. on Ionization Phenomena in Gases*; (Uppsala, Sweden (North-Holland Publishing Co., Amsterdam, Aug. 1960).

(Paper 64D5-90)

F
A

in
ch
va
th
P
in

ca
an
m
th
c
n
tr
sp

m
sp
tr

sp
u
si
to
a
v
n
in
es
ti
fo

—
D
Sp
m

Radiation and Admittance of an Insulated Slotted-Sphere Antenna Surrounded by a Strongly Ionized Plasma Sheath¹

John W. Marini

(February 29, 1960; revised April 1, 1960)

Given the voltage distribution along the slot, expressions for the radiation pattern, input admittance, and the external efficiency of an insulated slotted-sphere antenna surrounded by a homogeneous, isotropic, strongly ionized sheath are obtained.

At low frequencies the input impedance is proportional to the sum of the intrinsic impedance of the sheath and an equivalent inductance due to the insulating coating; the radiation pattern reduces to that of a small loop, while the external efficiency is the product of three factors arising because of the power dissipated in the sheath by higher order modes that contribute little to the radiation field, attenuation through the sheath of the modes that do radiate, and reflection loss of these modes at the outer surface of the sheath.

Since the reflection loss decreases with increasing frequency while the attenuation increases, there exists an optimum frequency of operation. At this frequency, the ionized sheath has a thickness equal to two-and-one-half skin depths.

1. Introduction

In connection with the re-entry of a space vehicle into the earth's atmosphere, a knowledge of the characteristics of a transmitting antenna in its prevailing environment is important in order to achieve the most effective design for efficient radiation. Particularly important is the behavior of an antenna in a strongly ionized medium.

To study the behavior of such an antenna analytically, it is natural to represent the vehicle, antenna, and surrounding mediums by means of simple geometric surfaces leading to mathematical expressions that can be handled readily. One such surface is the cylinder, which has been used by Wait to study a number of radiating structures including the dielectric-clad slotted-cylinder antenna radiating into free space [1].²

The spherical surface also yields simple, tractable models for initial studies of the subject. The slotted-sphere antenna radiating into free space has been treated by Mushiake and Webster [2].

The model used in this paper is an insulated slotted-sphere antenna surrounded by an homogeneous, uniform, strongly ionized plasma sheath. Expressions for the input admittance and radiation characteristics of the antenna are derived. While the model adopted does not duplicate the shape of the space vehicle and the surrounding sheath, the analysis nevertheless sheds light on the physical processes involved and provides approximate formulas for estimating some quantities of interest. The assumption that the sheath is homogeneous is not a good one for the physical situation under consideration, but

was made for the sake of mathematical simplicity and in the absence of information about the gradients existing in the sheath.

The conditions existing in the sheath surrounding a space vehicle during re-entry are not well known at present. If one assumes, however, that a temperature of 5,000° K, a particle density of 10^{23} per cubic meter and an electron density N of 10^{19} per cubic meter are representative [3], then simple calculations [4] give a collision frequency $\nu \sim 10^9$ per second and a plasma frequency $\omega_N \sim 10^{11}$ per second. The gyromagnetic frequency due to the earth's magnetic field is roughly $2\pi \times 10^6$ radians per second, which is much less than the value calculated for the collision frequency. Inspection of the usual formula for the index of refraction given in magneto-ionic theory [5] shows that the effect of the earth's magnetic field on the values obtained for the index of refraction is very small in such cases. Consequently it will be assumed that the sheath can be regarded as an isotropic medium with an index of refraction given by $n^2 \approx 1 - (\omega_N/\omega)^2 / (1 - i\nu/\omega)$ where ω is the radian frequency of the signal emitted by the antenna.

If the transmitted frequency $\omega/2\pi$ can be made sufficiently large, n reduces to unity and the operation of the antenna is not affected by the presence of the sheath. On the other hand, over a wide range of frequencies, both ν/ω and $\omega_N^2/\omega\nu$ are much greater than unity and the index of refraction is given by $n \approx \omega_N^2/i\omega\nu$. In this case the medium behaves like a good conductor with a conductivity $\sigma = \epsilon_0\omega_N^2/\nu = 9\pi \times 10^{-9}N/\nu$. The treatment here is confined to this range of frequencies.

In the frequency range considered, then, it is to be expected that much of the power supplied to the antenna will be dissipated through ohmic losses in the conducting sheath. The electromagnetic field established by the spherical antenna can be decom-

¹ Contribution from Electromagnetic Research Corporation, Washington 5, D.C. The research reported in this paper was supported by the Missile and Space Vehicles Department of the General Electric Company under a Department of the Air Force contract.

² Figures in brackets indicate the literature references at the end of this paper.

posed into the sum of spherical waves corresponding to various spherical modes. Because of the conductivity of the ionized sheath, these spherical waves are attenuated as they progress through the sheath. When the waves reach the outer boundary of the sheath, reflection takes place, and the amplitudes of the waves transmitted into free space are further reduced.

It is important to compare the magnitudes of the effects of attenuation and reflection on the transmitted waves. The attenuation of all lower order modes is essentially equal to that of a plane wave propagating through a medium having the same electromagnetic properties as the sheath and the same thickness. Being exponential, it is the more significant loss over most of the frequency range under consideration. Measured in decibels, the attenuation is directly proportional to the square root of the transmitter frequency. It follows that attenuation loss is reduced by lowering the frequency, at least in the range in which the sheath acts like a good conductor.

In contrast, reduction in amplitude of the transmitted waves due to poor transmission through the outer boundary of the sheath increases as the frequency is lowered. Eventually, then, an optimum frequency is reached which represents the best compromise between attenuation and reflection loss.

In view of the necessity to operate at a fairly low frequency to minimize attenuation loss, it is logical to consider the case where the frequency is so low that the sphere is a small antenna, i.e., that it has a radius that is small compared to the free-space wavelength. In this case, simple expressions are obtained for the input impedance of the slot, the radiation pattern, the external efficiency of the antenna, and the optimum frequency of operation.

In fact, for a small antenna, the reflection of a given mode at the outer boundary of the sheath increases strongly with the order of the mode, so that the radiation pattern is due only to the lowest order mode and is essentially the pattern of a small current loop. Since the higher order modes contribute little to the radiation field in this case, the expression obtained for the ratio of power radiated by the slot to that delivered to the slot turns out to be the product of three factors, one representing the ratio of power supplied to the lowest order mode to that supplied to all modes, the second representing attenuation of the lowest order mode in its passage through the sheath, and the third representing the transmission coefficient for the latter mode at the outer boundary of the sheath.

In all cases it is necessary that the antenna be provided with an insulating cover in the immediate vicinity of the feed in order that the assumed voltage or current distribution is realized and that conduction losses in the ionized medium not be exorbitant. The case treated here is that of an insulating layer which covers the entire spherical surface. A criterion is established for the thickness of this insulating layer.

2. Formulation of the Problem

Consider a perfectly conducting sphere of radius a covered with a dielectric coating of outer radius b , which in turn is surrounded by an ionized sheath of outer radius c . On the sphere, a narrow slot of length $2l$ (measured along the surface of the sphere) and of width $2s$ is located with its center at $\theta = \pi/2$, $\phi = 0$ and its ends at $\theta = \pi/2$, $\phi = \pm l/a$ as shown in figure 1.

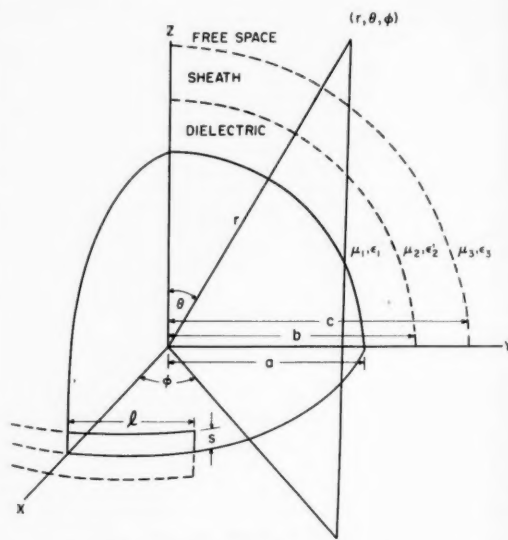


FIGURE 1. Insulated slotted-sphere antenna.

The problem under consideration is to determine the exterior admittance of the slot, assuming that it is fed at the center, and to obtain the radiation field.

The outer medium is assumed to be free space. The electromagnetic properties of the dielectric coating will be characterized by its permeability μ_1 , and its complex dielectric constant ϵ'_1 . Since the coating is assumed to have no conductivity, the complex dielectric constant is real and equal to the ordinary dielectric constant, $\epsilon'_1 = \epsilon_1$. The properties of the ionized sheath are characterized by the constants μ_2 and ϵ'_2 . In this case, however, the medium has finite conductivity, and the complex dielectric constant ϵ'_2 is equal to $\epsilon_2 + (\sigma/i\omega)$ where ϵ_2 is the equivalent dielectric constant and σ the equivalent conductivity of the ionized layer. The permeability, μ_2 , of the ionized region is the same as that of free space, μ_0 . It has been assumed that the ionized sheath acts like a good conductor. Thus σ is large compared to $\omega\epsilon_2$, so that $\epsilon'_2 \approx \sigma/i\omega$.

Use will be made of the constants $k = \omega\sqrt{\mu\epsilon}$ and $\eta = \sqrt{\mu/\epsilon'}$, ik being the complex propagation constant and η the complex impedance of the medium to plane waves. In the dielectric and in free space

both of these constants will be real, while in the ionized sheath $k_2 \approx \sqrt{\omega\mu_2\sigma} e^{-i\pi/4}$ and $\eta_2 \approx \sqrt{\omega\mu_2/\sigma} e^{i\pi/4}$. Rationalized MKS units and a time variation $e^{+i\omega t}$ are employed.

A formal solution of the exterior electromagnetic boundary value problem for a sphere has been given by Bailin and Silver [6]. Written below is a formal solution obtained using their procedure under the assumption that the impressed electric intensity $E_\theta(a, \theta, \phi)$ on the surface of the sphere is an even function of ϕ (since the slot is fed at the center) and that the impressed electric intensity $E_\phi(a, \theta, \phi)$ is negligible. The functions employed differ from those used by Bailin and Silver, however, and the constants obtained differ by a common factor.

Using the index $\lambda=1,2,3$ to refer to the dielectric, the sheath, and free space, respectively, the formal solution for the electromagnetic field is

$$\left. \begin{aligned} E_r^\lambda &= \left(\frac{\partial^2}{\partial r^2} + k_\lambda^2 \right) \Pi^{E\lambda} \\ E_\theta^\lambda &= \frac{1}{r} \frac{\partial^2}{\partial r \partial \theta} \Pi^{E\lambda} - i\omega\mu_\lambda \frac{1}{r \sin \theta} \frac{\partial}{\partial \phi} \Pi^{H\lambda} \\ E_\phi^\lambda &= \frac{1}{r \sin \theta} \frac{\partial^2}{\partial r \partial \theta} \Pi^{E\lambda} + i\omega\mu_\lambda \frac{1}{r} \frac{\partial}{\partial \theta} \Pi^{H\lambda} \\ H_r^\lambda &= \left(\frac{\partial^2}{\partial r^2} + k_\lambda^2 \right) \Pi^{H\lambda} \\ H_\theta^\lambda &= i\omega\epsilon'_\lambda \frac{1}{r \sin \theta} \frac{\partial}{\partial \phi} \Pi^{E\lambda} + \frac{1}{r} \frac{\partial^2}{\partial r \partial \theta} \Pi^{H\lambda} \\ H_\phi^\lambda &= -i\omega\epsilon'_\lambda \frac{1}{r} \frac{\partial}{\partial \theta} \Pi^{E\lambda} + \frac{1}{r \sin \theta} \frac{\partial^2}{\partial r \partial \phi} \Pi^{H\lambda} \end{aligned} \right\} \quad (1)$$

with

$$\left. \begin{aligned} \Pi^{E\lambda} &= \sum_{n=1}^{\infty} \sum_{m=0}^n A_{nm}^E Z_n^{E\lambda}(k_\lambda r) \bar{P}_n^m(\cos \theta) \cos m\phi \\ \Pi^{H\lambda} &= \sum_{n=1}^{\infty} \sum_{m=0}^n A_{nm}^H Z_n^{H\lambda}(k_\lambda r) \bar{P}_n^m(\cos \theta) \sin m\phi \end{aligned} \right\} \quad (2)$$

and

$$\left. \begin{aligned} A_{nm}^E &= -\frac{1}{(1+\delta_{om})n(n+1)} \frac{a}{k_1\pi} \frac{1}{Z_n^{E1'}(k_1 a)} \\ &\cdot \int_{-\pi}^{\pi} \int_0^\pi E_\theta(a, \theta, \phi) \bar{P}_n^{m'}(\cos \theta) \sin^2 \theta \cos m\phi d\theta d\phi \\ A_{nm}^H &= -\frac{1}{(1+\delta_{om})n(n+1)} \frac{a}{\pi i\omega\mu_1} \frac{1}{Z_n^{H1}(k_1 a)} \\ &\cdot \int_{-\pi}^{\pi} \int_0^\pi m E_\phi(a, \theta, \phi) \bar{P}_n^m(\cos \theta) \cos m\phi d\theta d\phi. \end{aligned} \right\} \quad (3)$$

The superscripts E and H refer to electric and magnetic type modes, respectively. The constant $\delta_{0m}=1$ if $m=0$; $\delta_{0m}=0$ if $m \neq 0$. The functions $\bar{P}_n^m(\cos \theta)$ are normalized associated Legendre polynomials [7] while the radial functions $Z_n^{E\lambda}(k_\lambda r)$ and $Z_n^{H\lambda}(k_\lambda r)$ are linear combinations of the functions

$$\begin{aligned} j_n(z) &= \sqrt{\pi z/2} J_{n+1/2}(z) \\ h_n^{(1)}(z) &= \sqrt{\pi z/2} H_{n+1/2}^{(1)}(z) \\ h_n^{(2)}(z) &= \sqrt{\pi z/2} H_{n+1/2}^{(2)}(z) \end{aligned} \quad (4)$$

where $J_{n+1/2}(z)$, $H_{n+1/2}^{(1)}(z)$ and $H_{n+1/2}^{(2)}(z)$ are the usual Bessel and Hankel functions of order $n+1/2$ [8].

The voltage distribution across the slot is assumed to be known. Since the slot is fed at the center, the distribution is an even function of the azimuthal angle ϕ , and can be expanded in a Fourier cosine series

$$V(\phi) = \sum_{p=0}^{\infty} V_p \cos p\phi. \quad (5)$$

The electric intensity tangent to the surface of the sphere is, then,

$$\begin{aligned} E_\theta^1(a, \theta, \phi) &= \begin{cases} \sum_{p=0}^{\infty} \frac{V_p \cos p\phi}{2s}, & \frac{\pi}{2} - \frac{s}{a} < \theta < \frac{\pi}{2} + \frac{s}{a} \\ 0, & \text{otherwise} \end{cases} \quad (6) \\ E_\phi^1(a, \theta, \phi) &= 0. \end{aligned}$$

3. Formal Solution

The equations given in section 2 above can be used to derive formal expressions for the input admittance and radiation field of the slotted-sphere antenna of figure 1. In this section, the procedure for obtaining these expressions is given.

3.1. Input Admittance

To obtain a formal expression for the input admittance is a fairly straightforward procedure, Equation (6) is substituted into (3) to obtain A_{nm}^E and A_{nm}^H :

$$A_{nm}^E = -\frac{V_m}{k_1 Z_n^{E1'}(k_1 a)} \frac{\bar{P}_n^{m'}(0)}{n(n+1)} \cdot I_E \quad (7a)$$

where

$$I_E = \frac{a}{2s} \int_{\pi/2-s/a}^{\pi/2+s/a} \frac{\bar{P}_n^{m'}(\cos \theta)}{\bar{P}_n^m(0)} \sin^2 \theta d\theta$$

and

$$A_{nm}^H = -\frac{V_m}{i\omega\mu_1 Z_n^{H1}(k_1 a)} \frac{m \bar{P}_n^m(0)}{n(n+1)} \cdot I_H \quad (7b)$$

where

$$I_H = \frac{a}{2s} \int_{\pi/2-s/a}^{\pi/2+s/a} \frac{\bar{P}_n^m(\cos \theta)}{\bar{P}_n^m(0)} d\theta.$$

I_E and I_H are approximately equal to unity for narrow slots and values of n that are not too large.

Equations (7a) and (7b) now are substituted into (2) to obtain Π^{E1} and Π^{H1} , and these in turn are used to obtain H_ϕ from (1). The input admittance is obtained by equating the conjugate of the complex power supplied to the slot to that radiated by the slot.

$$Y|V(0)|^2 = \int_{-\pi}^{\pi} \int_0^{\pi} E_\theta^*(a, \theta, \phi) H_\phi(a, \theta, \phi) a^2 \sin \theta d\theta d\phi.$$

Here the integration can be taken over the entire sphere since this must give the same result as integration over the face of the slot alone (E_θ being zero elsewhere). E_θ^* is the complex conjugate of E_θ , and is obtained from eq (6). This procedure gives a double series expansion for the input admittance.

$$Y = \sum_{n=1}^{\infty} \sum_{m=0}^{\infty} i \left| \frac{V_m}{V(0)} \right|^2 \frac{(1 + \delta_{im})\pi}{\eta_1} \left\{ \frac{Z_n^{H1'}(k_1 a)}{Z_n^{H1}(k_1 a)} \frac{m^2 \bar{P}_n^m(0)^2 I_H^2}{n(n+1)} - \frac{Z_n^{E1}(k_1 a)}{Z_n^{E1'}(k_1 a)} \frac{P_n^m(0)^2 I_E^2}{n(n+1)} \right\}. \quad (8)$$

Equation (8) is exact if the impressed voltage distribution given by (6) is realized and if the radial functions are known.³

3.2. Determination of the Radial Functions

Since the voltage distribution across the slot is assumed known, the only quantities left to determine in eq (8) are the radial functions, $Z_n^{E1}(k_1 r)$ and $Z_n^{H1}(k_1 r)$. They are determined from the boundary conditions of continuity of the tangential components of the electric and magnetic intensities at the inner and outer boundaries of the sheath, and by the radiation condition at infinity. If the sheath is sufficiently thick, it may be assumed that waves reflected from the boundary c between the sheath and free space can be neglected at the boundary b between the sheath and the dielectric. This assumption is not necessary, but it is a good one for the physical situation considered, and it simplifies the expressions obtained. Under this assumption, the input admittance is the same as if the ionized sheath were of infinite thickness.

a. Determination of Z_n^{E1} and Z_n^{H1}

Treating the electric type modes first, in the dielectric let

$$Z_n^{E1}(k_1 r) = H_n^{(2)}(k_1 r) - R_n^{E1} j_n(k_1 r) \quad (9a)$$

which represents the superposition of an outgoing and a standing wave⁴ resulting from reflection, and

³ In the case treated by Muskiak and Webster of an uninsulated slotted sphere antenna radiating into free space these functions are simply the functions $h_n^{(2)}$ defined in eq (4).

⁴ The function $h_n^{(2)}(k_1 r)$ which represents a reflected wave can, of course, be used instead of $j_n(k_1 r)$, but the latter turns out to be more convenient when the functions are approximated for small values of the argument since it turns out that only one term in the series expansion for $j_n(k_1 r)$ needs to be retained, while two are needed if $h_n^{(2)}(k_1 r)$ is used.

in the sheath let

$$Z_n^{E2}(k_2 r) = T_n^{E1} h_n^{(2)}(k_2 r) \quad (9b)$$

which represents an outgoing wave only, in accordance with the assumption above that waves reflected from the boundary at c may be neglected at b . R_n^{E1} and T_n^{E1} are constants which must be chosen to satisfy the boundary conditions at the interface between the insulating layer and the ionized sheath. The boundary conditions will be met if $k_\lambda Z_n^{E\lambda}(k_\lambda r)$ and $\epsilon'_\lambda Z_n^{E\lambda}(k_\lambda r)$ are continuous at the boundary. Therefore we have

$$\begin{aligned} k_1 h_n^{(2)'}(k_1 b) - R_n^{E1} k_1 j_n'(k_1 b) &= T_n^{E1} k_2 h_n^{(2)'}(k_2 b) \\ \epsilon_1 h_n^{(2)}(k_1 b) - R_n^{E1} \epsilon_1 j_n(k_1 b) &= T_n^{E1} \epsilon_2 h_n^{(2)}(k_2 b). \end{aligned}$$

Solving for R_n^{E1} and T_n^{E1}

$$\begin{aligned} R_n^{E1} &= \frac{k_1 \epsilon_2' h_n^{(2)'}(k_1 b) h_n^{(2)}(k_2 b) - k_2 \epsilon_1 h_n^{(2)}(k_1 b) h_n^{(2)'}(k_2 b)}{k_1 \epsilon_2' j_n'(k_1 b) h_n^{(2)}(k_2 b) - k_2 \epsilon_1 j_n(k_1 b) h_n^{(2)'}(k_2 b)} \\ T_n^{E1} &= \frac{k_1 \epsilon_1 [j_n'(k_1 b) h_n^{(2)}(k_1 b) - j_n(k_1 b) h_n^{(2)'}(k_1 b)]}{k_1 \epsilon_2' j_n(k_1 b) h_n^{(2)}(k_2 b) - k_2 \epsilon_1 j_n(k_1 b) h_n^{(2)'}(k_2 b)}. \end{aligned} \quad (10)$$

The expression above for T_n^{E1} may be simplified by using the Wronskian,

$$j_n'(k_1 b) h_n^{(2)}(k_1 b) - j_n(k_1 b) h_n^{(2)'}(k_1 b) = i.$$

The radial functions $Z_n^{H1}(k_1 r)$ and $Z_n^{H2}(k_2 r)$ for the magnetic type modes may be determined in the same manner. Thus let

$$\begin{aligned} Z_n^{H1}(k_1 r) &= h_n^{(2)}(k_1 r) - R_n^{H1} j_n(k_1 r) \\ Z_n^{H2}(k_2 r) &= T_n^{H1} h_n^{(2)}(k_2 r). \end{aligned} \quad (11)$$

In this case the boundary conditions are satisfied if $k_\lambda Z_n^{H\lambda'}(k_\lambda r)$ and $\mu_\lambda Z_n^{H\lambda}(k_\lambda r)$ are continuous at the boundary. Comparing the boundary conditions for the electric and magnetic cases, it is evident that the expressions for R_n^{H1} and T_n^{H1} are the same as those for R_n^{E1} and T_n^{E1} given in eq (10) but with μ_λ replacing ϵ'_λ (or ϵ_λ where $\epsilon_\lambda = \epsilon'_\lambda$) throughout.

With the radial functions Z_n^{E1} and Z_n^{H1} given by eq (9), (10), and (11), eq (8) provides a formal solution to the problem of an insulated slotted sphere antenna radiating into an electrically thick conducting layer.

b. Determination of $Z_n^{E3}(k_3 r)$ and $Z_n^{H3}(k_3 r)$

In order to obtain the radiation field from (1), (2), and (3), the functions $Z_n^{E3}(k_3 r)$ and $Z_n^{H3}(k_3 r)$ must be determined. Let

$$\begin{aligned} Z_n^{E2}(k_2 r) &= T_n^{E1} [h_n^{(2)}(k_2 r) - R_n^{E2} h_n(k_2 r)] \\ Z_n^{E3}(k_3 r) &= T_n^{E1} [T_n^{E2} h_n^{(2)}(k_3 r)]. \end{aligned} \quad (12)$$

The first term in the upper equation represents the outgoing wave given in (9b). The second term represents the reflected wave which was neglected in (9b). The lower equation represents an outgoing wave only, in order to satisfy the radiation condition at infinity. The procedure for determining T_n^{E2} is the same as that used to determine T_n^{E1} , except that the function $h_n^{(1)}$ replaces the function j_n . Consequently

$$T_n^{E2} = \frac{k_2 \epsilon_2' [h_n^{(1)'}(k_2 c) h_n^{(2)}(k_2 c) - h_n^{(1)}(k_2 c) h_n^{(2)'}(k_2 c)]}{k_2 \epsilon_2 h_n^{(1)'}(k_2 c) h_n^{(2)}(k_3 c) - k_3 \epsilon_2' h_n^{(1)}(k_2 c) h_n^{(2)'}(k_3 c)} \quad (13)$$

The Wronskian in the numerator in this case is equal to $2i$. T_n^{H2} can be obtained from (13) by substituting μ_λ for ϵ_λ .

3.3. Radiation Field

With the radial functions in free space determined from (12) and (13) and from the corresponding expressions for the magnetic case, the radiation field can be derived from (1), (2), (3), and (4). The θ and ϕ components of the electric intensity in free space are

$$E_\theta^{(3)} = \sum_{n=1}^{\infty} \sum_{m=0}^n \left\{ -k_3 A_{nm}^E T_n^{E1} T_n^{E2} \frac{h_n^{(2)'}(k_3 r)}{r} \right. \\ \times \left[\bar{P}_n^{m'}(\cos \theta) \sin \theta \cos m\phi - i\omega\mu_3 A_{nm}^H T_n^{H1} T_n^{H2} \right. \\ \left. \times \frac{h_n^{(2)}(k_3 r)}{r} \frac{\bar{P}_n^m(\cos \theta)}{\sin \theta} m \cos m\phi \right] \} \\ E_\phi^{(3)} = \sum_{n=1}^{\infty} \sum_{m=0}^n \left\{ -k_3 A_{nm}^E T_n^{E1} T_n^{E2} \frac{h_n^{(2)'}(k_3 r)}{r} \right. \\ \times \frac{\bar{P}_n^m(\cos \theta)}{\sin \theta} m \sin m\phi - i\omega\mu_3 A_{nm}^H T_n^{H1} T_n^{H2} \\ \left. \times \frac{h_n^{(2)}(k_3 r)}{r} \bar{P}_n^{m'}(\cos \theta) \sin \theta \sin m\phi \right\}. \quad (14)$$

The radiation field is obtained from the expressions above by replacing $h_n^{(2)}(k_3 r)$ and $h_n^{(2)'}(k_3 r)$ by their asymptotic expansions for large r :

$$h_n^{(2)}(k_3 r) \sim e^{-i\left(k_3 r - \frac{n+1}{2}\pi\right)}; \quad h_n^{(2)'}(k_3 r) \sim -ie^{-i\left(k_3 r - \frac{n+1}{2}\pi\right)}.$$

Also, for large r , $H_\theta^{(3)} \approx -E_\phi^{(3)}/\eta_3$ and $H_\phi^{(3)} \approx E_\theta^{(3)}/\eta_3$.

The radiation field so determined is exact for an insulated slotted sphere antenna radiating through an electrically thick sheath.

4. Approximate Solution

The expressions for the input admittance and the radiation field can be greatly simplified in the case where the sphere is a small antenna. If the frequency is sufficiently low, then the distance b is small

compared to the wavelength in the dielectric, and c is small compared to the wavelength in free space. The conductivity of the sheath has already been assumed large so that b is a large number of skin depths. Then $k_1 a$, $k_1 b$, and $k_3 c$ are small while $k_2 b$ and $k_2 c$ are large. Functions of $k_1 a$, $k_1 b$ and $k_3 c$ consequently can be replaced by their approximations for small arguments, while functions of $k_2 b$ and $k_2 c$ can be replaced by their asymptotic expansions for large arguments. It will be assumed that the insulating layer is thin, i.e., that $(b-a)/b \ll 1$.

4.1. Input Admittance

When these approximations are made the input admittance eventually reduces [9] to

$$Y \approx \sum_{n=0}^{\infty} \sum_{m=0}^n (1 + \delta_{om}) \pi \left\{ \frac{1}{n_2 + i\omega\mu_1(b-a)} \frac{m^2}{n(n+1)} \bar{P}_n^m(0)^2 \right. \\ \left. + \frac{1}{\eta_2 + \frac{n(n+1)(b-a)n(n+1)}{i\omega\epsilon_1 ab}} \frac{\bar{P}_n^{m'}(0)^2}{n(n+1)} \right\} \left| \frac{V_m}{V(0)} \right|^2. \quad (15)$$

In form, eq (15) represents the total admittance of two types of circuits in parallel, one circuit corresponding to each mode. The first type of circuit contains the surface impedance η_2 of the ionized sheath in series with an equivalent inductance $\mu_1(b-a)$. This circuit apparently is associated with the currents flowing on the surface of the sphere together with those induced on the interface between the dielectric and ionized layers. The second type of circuit also contains the surface impedance η_2 , this time, however, in series with an equivalent capacitance $C = \epsilon_1 ab/n(n+1)(b-a)$ between the sphere and the interface. This circuit is associated with displacement currents flowing between the sphere and the interface.

If $b-c$ is made extremely small, the properties of the first medium disappear from eq (5), which reduces to the admittance of a sphere with no dielectric coating. The admittance would then be very large because of the low impedance η_2 of the ionized medium, so that the slot would be virtually short-circuited.⁵ This makes evident the need for an insulating covering of the sphere. We shall consider, therefore, only the case where the dielectric coating is thick enough to be completely effective in reducing the shunting effect of the ionized sheath across the slot; that is, we assume that $|k_2|(b-a) \gg (\mu_2/\mu_1)k_1^2 ab$. This is equivalent to

$$|\eta_2| \ll \frac{b-a}{\omega\epsilon_1 ab}. \quad (16)$$

⁵ Also, the assumed voltage distribution might not be realized in this case.

The requirement above on the size of $b-a$ can be interpreted as requiring that this spacing between the plates of the equivalent capacitor be large enough so the capacitive reactance is large compared to the complex impedance of the ionized medium. In other words, we require the spacing to be large enough to prevent the surface currents on the sphere from being short-circuited by displacement currents flowing to the ionized sheath.

Under this stipulation, which is given quantitatively by eq (16), the final expression for Y becomes

$$Y \approx \frac{1}{\eta_2 + i\omega\mu_1(b-a)} \sum_{n=1}^{\infty} \sum_{m=1}^n \pi \frac{m^2}{n(n+1)} \bar{P}_n^m(0)^2 \left| \frac{V_m}{V(0)} \right|^2. \quad (17)$$

This was obtained under the assumptions that

$$\begin{aligned} k_1 b &\ll 1 \\ |k_2| b &\gg 1 \\ \frac{b-a}{\omega\epsilon_1 a b} &\gg |\eta_2| \\ \frac{b-a}{a} &\ll 1. \end{aligned} \quad (18)$$

Since the slot length is small compared to the wavelength, a triangular voltage distribution will be assumed. In this case the coefficients in the Fourier cosine series expansion of $V(\phi)$ are

$$V_c = \frac{l}{2\pi a} V(0) \quad (19)$$

$$V_m = \frac{4a}{\pi l} \frac{\sin^2 \frac{ml}{2a}}{m^2} V(0).$$

Using this distribution, the summation in eq (17) is dependent only on the ratio l/a (through the factor $V_m^2/V^2(0)$), where l is the half-length of the slot and a is the radius of the sphere. The double summation converges approximately as $1/n^2$ and $1/m^2$ (since $V_m^2/V^2(0)$ varies as $1/m^4$ for the assumed triangular voltage distribution), so the series may be evaluated numerically without retaining an extreme number of terms. For a slot of length $l/a = \pi/2$, the results are roughly

$$\begin{aligned} Y|_{l/a=\pi/2} &\approx 0.38 \frac{1}{\eta_2 + i\omega\mu_1(b-a)} \\ Z &\approx 0.26[\eta_2 + i\omega\mu_1(b-a)] \\ &\approx 0.26 \left\{ \frac{|\eta_2|}{\sqrt{2}} + i \left[\omega\mu_1(b-a) + \frac{|\eta_2|}{\sqrt{2}} \right] \right\}. \end{aligned} \quad (20)$$

4.2. Radiation Field

When the various approximations listed in (18) are used, and in addition, when it is assumed the outer radius, c , of the plasma sheath is small compared to a wavelength, the radiation field is found to be due only to the TE_{11} (H -type) mode. Other

modes can be neglected because they all contain higher powers of the quantity $k_3 c$ as factors. The radiation field due to the TE_{11} mode has the form

$$E_{\theta}^{(3)} \approx -\frac{3}{4} i k_3 c \frac{\eta_2 V_1}{\eta_2 + i\omega\mu_1(b-a)} e^{-ik_2(c-b)} \frac{e^{-ik_3 r}}{r} \cos \phi \quad (21)$$

$$E_{\phi}^{(3)} \approx \frac{3}{4} i k_3 c \frac{\eta_2 V_1}{\eta_2 + i\omega\mu_1(b-a)} e^{-ik_2(c-b)} \frac{e^{-ik_3 r}}{r} \cos \theta \sin \phi.$$

The electric field has components in both the θ and ϕ directions. These differ only in their dependence on the θ and ϕ coordinates. If a transformation is made to new coordinates θ' , ϕ' , as shown in figure 2, where the new polar angle θ' is measured from the y -axis, and the new azimuthal angle ϕ' is measured from the z -axis, then the electric field has only a single component, given by

$$E_{\phi'}^{(3)} = -\frac{3}{4} i k_3 c \frac{\eta_2 V_1}{\eta_2 + i\omega\mu_1(b-a)} e^{-ik_2(c-b)} \frac{e^{-ik_3 r}}{r} \sin \theta'. \quad (22)$$

The field pattern is now given by the factor $\sin \theta'$. This is exactly the pattern of a loop lying in the xz -plane with center at the origin. This is the meridian plane of the currents which flow from one edge of the slot around the sphere to the opposite edge of the slot.

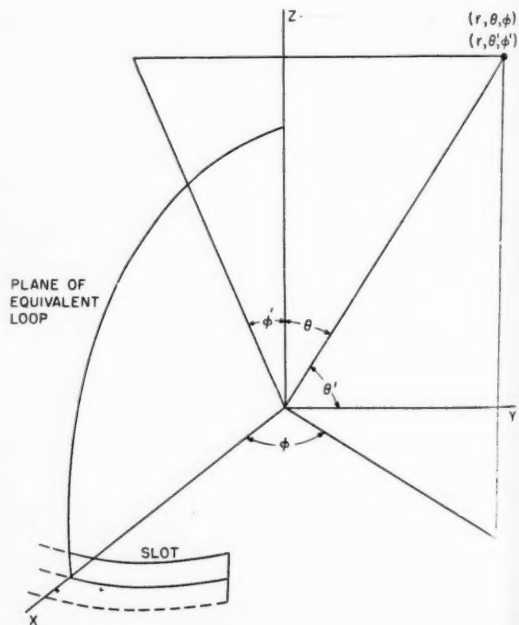


FIGURE 2. Slotted-sphere antenna and equivalent loop.

4.3. Radiation Intensity and Input Power

From eq (22), it is easy to calculate the power radiated per unit solid angle, or the radiation intensity.

The radiation intensity is

$$r^2 \frac{|E_{\phi'}|}{2\eta_3} = \left(\frac{3}{4} k_3 c \right)^2 \left| \frac{\eta_2}{\eta_2 + i\omega\mu_1(b-a)} \right|^2 \frac{V_m^2}{2\eta_3} e^{-\sqrt{2}|k_2|(c-b)} \sin^2 \theta'. \quad (23)$$

The total input power, P , which includes both the power radiated and the power absorbed by the sheath, is given by the real part of $YV(0)^2/2$. From eq (17) this is found to be

$$P = \frac{1}{2\sqrt{2}} \frac{|\eta_2|}{|\eta_2 + i\omega\mu_1(b-a)|^2} \sum_{n=1}^{\infty} \sum_{m=1}^n \pi \frac{m^2}{n(n+1)} \bar{P}_n^m(0)^2 V_m^2. \quad (24)$$

4.4. External Efficiency

A measure of the efficiency of the antenna can be obtained by calculating the external efficiency, or ratio of the radiated power to the input power supplied to the slot. This ratio then can be examined for an optimum choice of the design parameters. This, however, is only a partial optimization procedure, since it does not consider all the factors which determine the overall efficiency of the antenna. In particular, it does not include the losses in the matching networks necessary to feed the slot from the source of power. These losses will depend on the Q of the matching network and the input impedance. This latter problem, however, can be evaluated since the input impedance of the slot already has been determined.

Denoting the external efficiency by ξ ,

$$\xi = \int_{-\pi}^{\pi} \int_0^{\pi} \frac{|E_{\phi'}|^2}{2\eta_3 P} r^2 \sin \theta' d\theta' d\phi'. \quad (25)$$

Substituting (23) and (24) into (25), and integrating

$$\xi = \frac{\left[\pi \frac{m^2}{n(n+1)} \bar{P}_n^m(0)^2 \frac{V_m^2}{V(0)^2} \right]_{n=1}^{m=1}}{\sum_{n=1}^{\infty} \sum_{m=1}^n \pi \frac{m^2}{n(n+1)} \bar{P}_n^m(0)^2 \frac{V_m^2}{V(0)^2}} \times \left[(k_3 c)^2 \frac{4\sqrt{2}|\eta_2|}{\eta_3} e^{-\sqrt{2}|k_2|(c-b)} \right]. \quad (26)$$

Each of the brackets in (26) has physical significance. The first bracket is the ratio of the power delivered to the magnetic type mode $n=m=1$ (TE_{11}) (which is the only mode contributing significantly

to the radiation field) to that delivered to all the modes. The second bracket is the overall power transmission coefficient for this mode (i.e., the ratio of power of this mode that is radiated to that entering the sheath). It consists of an exponential factor representing attenuation through the sheath, and a second factor due to reflection at the outer surface of the sheath. The latter is the product of $(k_3 c)^2$ and the factor $4\sqrt{2}|\eta_2|/\eta_3$ which in turn is the power transmission coefficient for a plane wave progressing across a plane surface from a medium of intrinsic impedance η_2 to one whose intrinsic impedance is η_3 (with $|\eta_2| < \eta_3$).

5. Optimization Procedures

The expression above is proportional to the efficiency (ratio of radiated power to total input power) of the slot antenna if it is assumed that feeding losses are not important compared to losses in the sheath. Therefore, it is desirable to consider the means for maximizing the expression given in eq (26). In the first place, if the size of the vehicle is given, the quantities b and c are fairly well fixed. Since the outer medium is free space, η_3 will be equal to 377 ohms. The quantity $k_3^2 = \omega^2 \mu_3 \epsilon_3$ varies as the square of the frequency while $|\eta_2| = \sqrt{\omega\mu_2/\sigma}$ and $|k_2| = \sqrt{\omega\mu_2\sigma}$ vary as the square-root of the frequency. Consequently ξ varies as $\omega^{5/2} \exp[-\sqrt{2}\mu_2\sigma(c-b)\omega^{1/2}]$. The latter expression is maximized by setting the exponent equal to -5 :

$$\sqrt{2}\mu_2\sigma(c-b)\omega_{opt}^{1/2} = 5.$$

The optimum frequency then is

$$f_{opt} = \frac{25}{4\pi} \frac{1}{\mu_2\sigma(c-b)^2}. \quad (27)$$

This is the frequency that makes the sheath thickness, $c-b$, equal to two-and-one-half skin depths in the ionized medium.

The only other quantity in (26) besides the frequency that can be varied to make the expression a maximum is the ratio

$$\frac{\pi \frac{m^2}{n(n+1)} \bar{P}_n^m(0)^2 \frac{V_m^2}{V(0)^2} \Big|_{n=1}^{m=1}}{\sum_{n=1}^{\infty} \sum_{m=1}^n \pi \frac{m^2}{n(n+1)} \bar{P}_n^m(0)^2 \frac{V_m^2}{V(0)^2}}. \quad (28)$$

The magnitude of this can be varied by changing the length of the slot. In general, the efficiency is increased by increasing the slot length.

The thickness, $b-a$, of the dielectric layer does not appear in the expression (26) for the efficiency provided condition (16) is met. It does, however, appear in (20) where it is present as a term representing an additional series inductance.

6. Appendix

A situation that is possibly of greater practical interest than the entirely insulated spherical antenna treated above is the case of the partially insulated slotted sphere, one octant of which is illustrated in figure 3. The angular width of the dielectric cover is the same as the angular width of the slot and is equal to $2\psi_0$. The angular height of the slot is $2\phi_0$. The outer surface of the dielectric is flush with the surface of the conducting sphere. The input impedance of this configuration was estimated [9] (for low frequencies) by calculating the input admittance of a rectangular parallelepiped obtained by straightening the curved dielectric slab. The result was

$$Y = \begin{cases} \frac{1}{3} \frac{1}{\eta_2 + i\omega\mu_1(b-a)} \frac{1 + \left(\frac{\psi_0}{\phi_0}\right)^2 - 0.23 \left(\frac{\psi_0}{\phi_0}\right)^3}{\left(\frac{\psi_0}{\phi_0}\right)}; & 0 < \frac{\psi_0}{\phi_0} < 1.5 \\ \frac{1}{3} \frac{1.63}{\eta_2 + i\omega\mu_1(b-a)} & ; 1.5 < \frac{\psi_0}{\phi_0} \end{cases}$$

The external efficiency resulting in this case was also derived. The attenuation and reflection losses are given in db by

$$10 \log \left[(k_3 c)^2 \frac{4\sqrt{2}|\eta_2|}{\eta_3} e^{-\sqrt{2}|k_2|(c-b)} \right]$$

where the bracket is, of course, the same as the second one in eq (26). The loss to higher order modes is given by a different expression, however, and is plotted in figure 4.

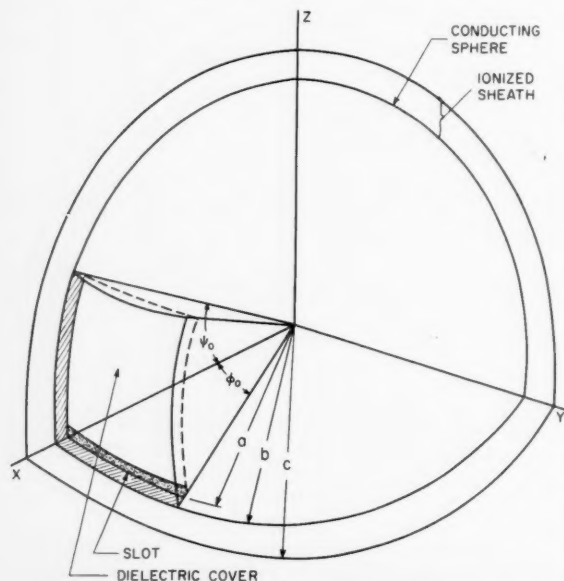


FIGURE 3. Partially insulated slotted-sphere antenna.

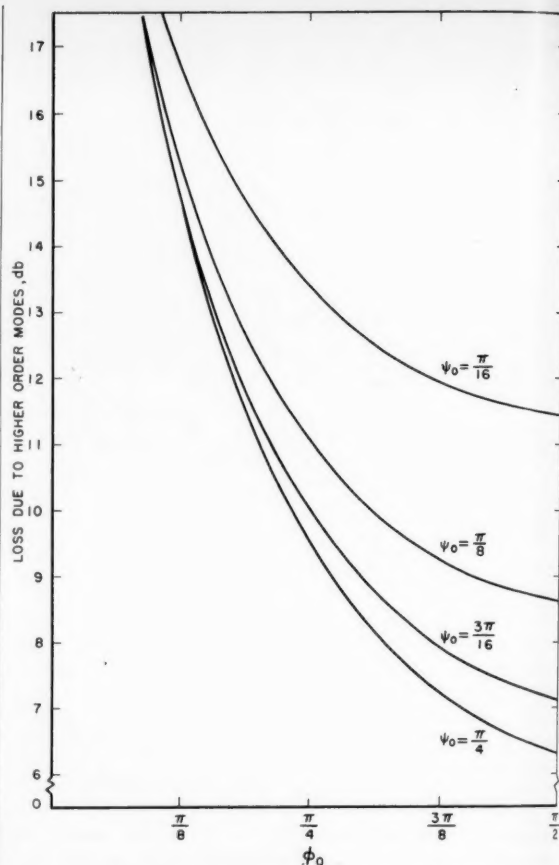


FIGURE 4. Higher order mode loss for the partially insulated slotted-sphere antenna.

7. References

- [1] J. R. Wait, *Electromagnetic radiation from cylindrical structures* (Pergamon Press, Inc., New York, N.Y., 1959).
- [2] Y. Mushiake and R. E. Webster, Radiation characteristics with power gain for slots on a sphere, *IRE Trans. on Antennas and Propagation* **AP-5**, 47 (1957).
- [3] Martin Katzin, Radiation of an electric dipole into an ionized sheath, *Electromagnetic Research Corp., Rept. 60175-7* (15 Dec. 1957).
- [4] J. A. Ratcliff, The magneto-ionic theory and its application to the ionosphere, eq 4.2.6, and para. 1.5 (Cambridge University Press, Cambridge, England, 1959).
- [5] J. A. Ratcliff, *op. cit.*, eq 4.4.1.
- [6] L. I. Bailin and S. Silver, Exterior electromagnetic boundary value problems for spheres and cones, *IRE Trans. on Antennas and Propagation* **AP-4**, 5 (1956).
- [7] Jahnke and Emde, *Tables of functions*, ch. VII, para. 7, p. 116 (Dover Publications, New York, N.Y., 1951).
- [8] S. A. Shelkunoff, *Electromagnetic waves*, para. 3.5 (D. Van Nostrand Co., Inc., New York, N.Y., 1943).
- [9] J. W. Marini, B. Y.-C. Koo, and M. Katzin, Radiation and impedance of antennas surrounded by an ionized sheath, *Electromagnetic Research Corporation, Report ERC 60301-6* (25 Aug. 1958).

(Paper 64D5-91)

A Contribution to the Theory of Corrugated Guides¹

G. Piefke

(January 25, 1960)

The transmission characteristics of certain structures belonging to the class of corrugated guides are calculated by means of a new method. It is assumed that the guide wavelength always is much greater than the corrugation constant ($D_1 + D_2$ in fig. 1). The periodical structure of the guide is therefore replaced by a quasi-homogeneous, but anisotropic medium.

The following structures are studied: The "ring-element guide," which consists of an axial stack of insulated metallic rings with arbitrary surrounding medium; the "disk guide," which is a ring-element guide with infinite radial extension of the rings; the "disk loaded waveguide," and the "corrugated waveguide."

As a rule guides can propagate modes with a phase velocity $v_p > c$ (c = velocity of light) and modes with $v_p < c$. The capability of existence of the various modes depends on the losses of the guide. The ring-element guide is well suited for transmission with the H_{01} -mode since, except the H_{0n} -modes, all modes may be highly attenuated (mode filters). As delay lines ($v_p < c$), all guides have band pass characteristics.

1. Introduction

Many periodic structures can be classified under the heading "corrugated guides." In this class are, for instance, the "disk guide," the "disk loaded waveguide," the "corrugated waveguide," the wire fitted with annular grooves and the "ring-element guide" (figs. 1 to 5). These types of guide have many potentialities in communications.

The disk guide (fig. 1) which consists of an axial stack of insulated metallic rings of such radial dimension that no electromagnetic field can exist outside the rings, can be used as a transmission path for the H_{01} -mode. Of the H_{01} -mode in the circular waveguide, it is known that its attenuation decreases with increasing frequency. An attenuation sufficiently low for communication purposes is obtained, however, only for a wavelength small with respect to the guide diameter. With an inner diameter of the circular waveguide of 5 cm and a wavelength $\lambda_0 = 6$ mm the attenuation of the H_{01} -mode is 0.134 N/km. With sufficiently small attenuation of the H_{01} -mode many other modes are capable of existence in the waveguide, however. These undesired modes can be excited by the H_{01} -mode, if at any place the waveguide deviates from its round and straight form. Such undesired modes, however, have a velocity other than the H_{01} -mode and the next inhomogeneity of the waveguide converts part of them back to the H_{01} -mode so that signal distortion comes about. By strong attenuation of the parasitic modes such reconversion and resultant signal distortion can be avoided. With transmission by means of the H_{01} -mode a guide is thus desired along which the H_{01} -mode has the same propagating properties as in a circular homogeneous waveguide and where the undesired modes are strongly attenuated. This is possible with the disk guide.

The disk loaded waveguide (fig. 2) is used as a linear accelerator. The corrugated waveguide (fig. 3) is used as a flexible waveguide. The wire with annular grooves (fig. 4) presents, if the groove depth is small with respect to the wavelength, similar properties as the Goubau guide and, if it is large, it can likewise serve as a delay line. Like the disk guide the ring-element guide (fig. 5) consists of an axial stack of insulated metallic rings, but it has another arbitrary outer medium and therefore an electromagnetic field is possible also outside the rings.

The ring-element guide is thus a generalization of the disk guide and the disk loaded waveguide, and it can likewise be used for transmission with the H_{01} -mode.

¹ Contribution from the Central Laboratories of the Siemens & Halske AG, Munich, Germany.

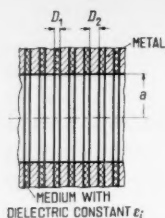


FIGURE 1. Disk guide.

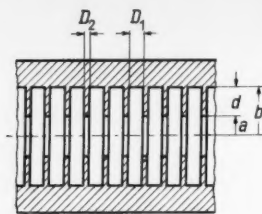


FIGURE 2. Disk loaded waveguide.

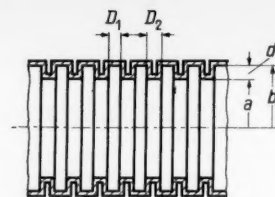


FIGURE 3. Corrugated waveguide.

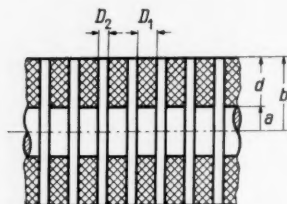


FIGURE 4. Wire with annular grooves.

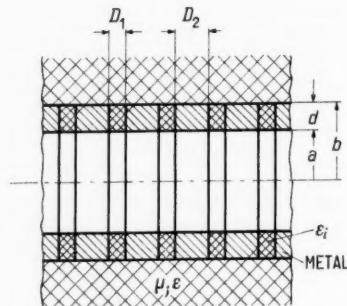


FIGURE 5. Ring-element guide.

The paper [1]² gives a good review of the principal theories known so far concerning corrugated guides. The papers [2] to [5] deserve to be mentioned in particular as individual articles. Because of the complicated boundary conditions an exact solution of Maxwell's equations is very difficult with corrugated guides.

For the case that the corrugation constant is far smaller than the guide wavelength ($D_1 + D_2 \ll \lambda$), the author has used in the papers [6] to [8] a new method of calculating the transmission characteristics of corrugated guides. It introduces a quasi-homogeneous, but anisotropic medium and offers the advantage that in each region Maxwell's equations can be solved easily and the boundary conditions can be met with ease.

In this paper the mathematical method shall be briefly recapitulated and the results of the papers [6] to [8] summarized.

2. Mathematical Approach

Let us consider the disk guide of figure 1. For the disk separation $D_1 + D_2$, the thickness D_1 of the dielectric, and the axial thickness D_2 of the disks there shall hold the inequalities

$$D_1 + D_2 \ll \lambda, \quad (1)^3$$

$$D_1 \ll \frac{1}{2} \lambda_0 \sqrt{|\epsilon_0 / \epsilon_i|}, \quad (2)$$

$$D_2 \gg \vartheta. \quad (3)$$

The medium in the region $a < r < \infty$, which is termed medium 1 herein has a periodic structure with respect to the axial coordinate z and therefore is inhomogeneous. Besides the medium has a different structure in the direction z than in the directions φ and r . The medium is therefore anisotropic as well.

² Figures in brackets indicate the literature references at the end of this paper.

³ A list at the end of this paper explains the symbols.

If a mode is excited in the region $0 < r < a$ (medium 0), the medium 1 can be considered as quasi-homogeneous because of the inequality (1). Dielectric constant and permeability of this quasi-homogeneous, but anisotropic medium 1 are found from the following consideration (see also [6] and [9]).

If the mode excited in medium 0 has an electric field only in a circular direction and a magnetic field in the axial and radial directions (H_{0n} -mode), no energy will be capable of propagating in the direction r , because of the inequality (2). At the place $r=a$ current will flow in a circular direction. For this current, i.e., in parallel to the disk, the medium 1 is a conductor with the conductivity

$$\kappa_p = \kappa \frac{D_2}{D_1 + D_2} \quad (4)$$

or the dielectric constant

$$\epsilon_p = \kappa_p / j\omega. \quad (5)$$

The permeability in the direction z , i.e., perpendicularly to the disks, is given by the permeability of the dielectric and that of the metal. If dielectric and metal have the permeability μ_0 of space, there holds accordingly

$$\mu_z = \mu_0. \quad (6)$$

If the mode excited in medium 0 has a magnetic field only in a circular direction, and an electrical field in axial and radial directions (E_{0n} -mode), energy is capable of propagating between the disks in the direction r . Because of inequality (3), the metal is field-free. Perpendicularly to the disks the medium 1 therefore has the dielectric constant

$$\epsilon_z = \epsilon_t \frac{D_1 + D_2}{D_1}, \quad (7)$$

and in parallel to them the permeability

$$\mu_p = \mu_0 \frac{D_1}{D_1 + D_2}. \quad (8)$$

Since medium 1 has the same structure in the directions φ and r , the dielectric constant ϵ_p and the permeability μ_p hold also for the directions φ and r . In the coordinate system r, φ, z , the dielectric constant and the permeability in medium 1 are thus tensors as follows

$$\epsilon_1 = \begin{pmatrix} \epsilon_p & 0 & 0 \\ 0 & \epsilon_p & 0 \\ 0 & 0 & \epsilon_z \end{pmatrix}, \quad (9)$$

$$\mu_1 = \begin{pmatrix} \mu_p & 0 & 0 \\ 0 & \mu_p & 0 \\ 0 & 0 & \mu_0 \end{pmatrix}. \quad (10)$$

In medium 0 the solution of Maxwell's equations is generally known. Because of the eqs (4) to (10) Maxwell's equations can be easily solved also in the medium 1, as shown in [6]. In the same way the boundary conditions at the point $r=a$ can now be satisfied with ease.

In calculating the transmission properties of the ring-element guide, the approach is exactly the same as with the disk guide. The difference is merely the limited extension of the quasi-homogeneous anisotropic medium which in turn is surrounded by an arbitrary outer medium. The ring-element guide thus is the more general case. The disk-loaded waveguide develops from the ring-element guide, if the outer medium is a conductor.

Because of the general importance of the ring-element guide the equation set up in [7] for calculating the propagation constants of the individual modes has been stated once more in the eqs (83) and (84) of the annex.

3. General Considerations

With all forms of guide shown in figs. 1 to 5, unlike waveguides, each mode type is a combination of an E -mode and an H -mode, even when losses are neglected. An exception is merely the rotation-symmetrical modes. Accordingly the modes with $m \neq 0$ are here termed HE -modes or EH -modes. The first letter identifies always the mode type that prevails. With the HE -modes the H -type thus prevails and with the EH -modes the E -type.

Only the rotation-symmetrical H -modes have thus no axial electric field. As mentioned above, no energy can thus be transported by these modes between the rings in the direction r ; energy will penetrate into medium 1 merely corresponding to the conductivity κ_p .

With the other modes, however, plenty of energy can penetrate into medium 1 because of the presence of the axial electric field. If the dielectric between the rings has no losses and if those of the metal are neglected, modes will propagate between the rings in a radial direction without attenuation. With the disk guide these modes receive power from the mode traveling in the region $0 < r < a$, as figure 6 shows. In medium 1 the connecting line of the points of equal phase is oblique with respect to the axis z . There exists an axial and a radial phase velocity. This fact corresponds also to the solution of Maxwell's equations in the anisotropic medium 1, where a mode propagating in the directions r and z is obtained although the thickness of the metallic disks has been assumed as very large with respect to that of the equivalent conducting layer. With the lossless disk guide all modes with an axial electric field thus are attenuated by radiation.

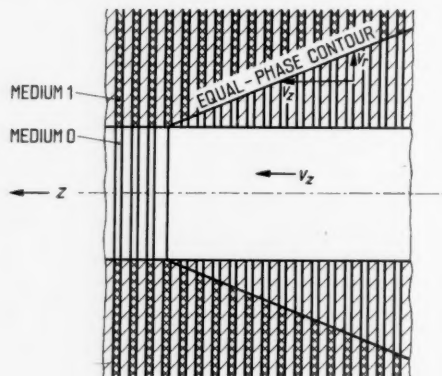


FIGURE 6. Generation of the radial modes in the disk guide with a mode propagating in the z -direction (schematic; v_z is the axial, v_r the radial phase velocity in medium 1).

It is advisable to classify the mode types in the here considered guide forms by phase velocities, for there exist as well mode types whose phase velocity v_p exceeds the velocity of light c , as others whose phase velocity v_p is less. Modes with a phase velocity $v_p > c$ are termed herein as a rule "waveguide modes" and may be HE_{mn} -modes as well as EH_{mn} -modes. In the same way as with circular waveguides, the subscript m here refers to the circular, and the subscript n to the radial dependence of the field. Modes with a phase velocity $v_p < c$ give the guide the character of a delay line and can be only EH_m -modes. The subscript n is here dropped as a rule, for in this case, unlike the waveguide modes, there exists for each m only one mode with a particular field configuration. In exceptional cases $v_p > c$ is possible even with the EH_m -modes.

An essential point with the modes is their capability of existence; with the modes with $v_p > c$ it differs from that with the modes with $v_p < c$. With some types of guides it turns out, for instance, that waveguide modes are capable of existence only if the total loss exceeds a certain limit which depends on frequency, mode type, material constants, and dimensions of the respective guide.

As an example for the existence capability of the modes let us now consider the ring-element guide. Neglecting, for instance, the losses due to the rings and the insulation between rings,

only such waveguide modes can exist, with the exception of the H_{0n} -modes, for which

$$(\beta_0 a)^2 \left| \operatorname{Im} \left(\frac{\mu \epsilon}{\mu_0 \epsilon_0} \right) \right| > \left| \operatorname{Im} ([k_0 a]^2) \right|. \quad (11)$$

The eigenvalue $k_0 a$ can be taken from the eqs (13), (18), and (22) to (24).

If the inequality (11) holds, the negative sign must always be chosen with the radial propagation constant in the outer medium that is given by

$$k_2 = \pm \sqrt{\beta_0^2 \frac{\mu \epsilon}{\mu_0 \epsilon_0} + \gamma^2} = \pm \sqrt{\beta_0^2 \left(\frac{\mu \epsilon}{\mu_0 \epsilon_0} - 1 \right) + k_0^2}. \quad (12)$$

The energy then propagates into the outer medium.

If the inequality (11) does not hold, the losses of the rings and the insulation must be also considered, followed by checking whether there results a value k_0 with positive real and imaginary parts and in addition a value k_2 with positive imaginary part. If such is not the case, the respective waveguide mode is not capable of existence. With high losses of the outer medium the inequality (11) is always met and the losses of the rings can be neglected with all waveguide modes except the H_{0n} -modes. Their losses are given by those at the inside of the guide (see eq (31)).

If the outer medium and the dielectric between the rings are free of losses, hence are air for instance, the losses of the rings must be taken into account for checking the existence of the waveguide modes and calculating their losses. The existence of the waveguide modes then depends in turn upon whether the aforementioned conditions for k_0 and k_2 are satisfied. At any rate the positive sign must now be chosen in eq (12), i.e., k_2 has a positive real part and energy flows into the rings from all sides. As a rule, however, the losses of the rings will not suffice to secure the existence of waveguide modes. An exception is merely the H_{0n} -modes which are capable of existence, even if all losses are neglected. Apart from the H_{0n} -modes the loss-free ring-element guide thus has merely modes with $v_p < c$, i.e., E_0 or EH_m -modes ($m \neq 0$) and therefore is a delay line as a rule.

Like waveguide modes, modes with $v_p < c$ are not capable of existence with any outer medium. Examples in point are the disk loaded waveguide and the corrugated waveguide, which develop from the ring-element guide, if the outer medium is metal. In these guides no modes are possible except waveguide modes, if the corrugation depth is small with respect to wavelength λ_0 . Only with a corrugation depth that is large with respect to the wavelength λ_0 waveguide modes are possible as well as modes with $v_p < c$ (see section 6).

If with the ring-element guide the losses of the dielectric between the ring are so large that the fields cannot penetrate beyond the rings, the regions $0 < r < a$ and $b < r < \infty$ are decoupled with respect to each other. For an excitation in the region $0 < r < a$ the ring-element guide acts now as a disk guide. With an excitation in the space $b < r < \infty$ surface modes are obtained on the ring-element guide. Either mode can be calculated from the general eqs (83) and (84). With high losses of the insulation between the rings the ring-element guide thus will act as waveguide or surface mode guide, depending on the excitation. Let us now proceed to a study of the various guide varieties.

4. Ring-Element Guide

4.1. Formulas for the Propagation Constants of the Waveguide Modes

As mentioned above, the ring-element guide is a generalization of the disk guide, disk loaded waveguide, and corrugated waveguide. For this reason let us begin by stating the formulas for the propagation constants of the modes in the ring-element guide. The formulas for the propagation constants of the modes in the other guide types are then obtained as specific cases.

With the ring-element guide no generally valid closed formulas exist for the propagation constants of the modes, but such formulas can be calculated under certain assumptions and the essential properties of the guide can so be explained, as was done in detail in [7].

Under the assumptions

$$k_0 a = \chi + \Theta, \quad |\Theta| \ll 1, \quad (13), (13a)$$

$$\left| \frac{2\chi\Theta}{(\beta_0 a)^2} \right| \ll \left[1 - \left(\frac{\chi}{\beta_0 a} \right)^2 \right] \quad (14)$$

$$\left| \beta_0 b \sqrt{\left(\frac{\mu\epsilon}{\mu_0\epsilon_0} - 1 \right) + \left(\frac{k_0 a}{\beta_0 a} \right)^2} \right| \left\{ \begin{array}{l} 1 \\ m \end{array} \right\} \gg \left\{ \begin{array}{l} 1 \\ m \end{array} \right\} \quad (15)$$

$$m=0, 1, 2, \text{ etc.},$$

there is according to [7]

$$\beta = \beta_0 \sqrt{1 - \left(\frac{\chi}{\beta_0 a} \right)^2} - \frac{\chi}{\beta_0 a^2 \sqrt{1 - \left(\frac{\chi}{\beta_0 a} \right)^2}} \operatorname{Re}(\Theta), \quad (16)$$

$$\alpha = \frac{\chi}{\beta_0 a^2 \sqrt{1 - \left(\frac{\chi}{\beta_0 a} \right)^2}} \operatorname{Im}(\Theta), \quad (17)$$

where

$$\chi = \begin{cases} \sigma_{mn} & \text{for } H\text{- and } HE\text{-modes with } |\Theta_H| \ll 1 \\ \chi_{mn} & \text{for } E\text{- and } EH\text{-modes with } |\Theta_E| \ll 1 \\ \sigma_{mn} & \text{for } E\text{- and } EH\text{-modes with } |\bar{\Theta}_E| \ll 1 \end{cases} \quad (18)$$

$$\Theta = \begin{cases} \Theta_H & \text{for } HE\text{-modes} \\ \Theta_E & \text{for } EH\text{-modes} \\ \bar{\Theta}_E & \text{for } EH\text{-modes for very large } a/\lambda_0. \end{cases} \quad (18a)$$

There denote

$$\Theta_H = j \frac{\sigma_{0n}}{\beta_0 a} \frac{Z_H}{Z_0}, \quad (19)$$

$$\Theta_E = j \frac{\beta_0 a}{\chi_{0n}} \frac{Z_a}{Z_0}, \quad (20)$$

$$\bar{\Theta}_E = j \frac{\sigma_{0n}}{\beta_0 a} \frac{Z_0}{Z_a}, \quad (21)$$

for $m=0, n=1, 2, 3, \text{ etc.}$

$$\Theta_H = j \frac{\sigma_{mn} Z_0 [1 - \sqrt{1 - F_a(\sigma_{mn})}]}{2\beta_0 a Z_a \left[1 - \left(\frac{m}{\sigma_{mn}} \right)^2 \right]}, \quad (22)$$

$$\Theta_E = j \frac{2\beta_0 a Z_a}{\chi_{mn} Z_0 [1 + \sqrt{1 - F_a(\chi_{mn})}]}, \quad (23)$$

$$\bar{\Theta}_E = j \frac{\sigma_{mn} Z_0 [1 + \sqrt{1 - F_a(\sigma_{mn})}]}{2\beta_0 a Z_a \left[1 - \left(\frac{m}{\sigma_{mn}} \right)^2 \right]}, \quad (24)$$

for $m=1, 2, 3, \text{ etc.}; n=1, 2, 3, \text{ etc.}$

The quantities $F_a(\sigma_{mn})$ and $F_a(\chi_{mn})$ are calculated from

$$F_a(\chi) = 4 \left(\frac{Z_a}{Z_0} \right)^2 \left\{ \left(\frac{m}{\chi} \right)^2 \left[\left(\frac{\beta_0 a}{\chi} \right)^2 - 1 \right] + \frac{Z_H}{Z_a} \right\} \quad (25)$$

by replacing χ by the quantities σ_{mn} or χ_{mn} .

There denote further in the eqs (19) to (25)

$$\frac{Z_H}{Z_0} = (1+j) \sqrt{\frac{\beta_0(D_1+D_2)}{2Z_0\kappa D_2}}, \quad (26)$$

$$\frac{Z_a}{Z_0} = \frac{Z_A}{Z_0} \frac{1+j \frac{Z_E}{Z_A} \tan p_E d}{1+j \frac{Z_A}{Z_E} \tan p_E d}, \quad (27)$$

$$\frac{Z_E}{Z_0} = \sqrt{\frac{\epsilon_0}{\epsilon_i}} \frac{D_1}{D_1+D_2}, \quad (28)$$

$$\frac{Z_A}{Z_0} = -\frac{\epsilon_0}{\epsilon} \frac{k_2}{\beta_0} = \frac{\epsilon_0}{\epsilon} \sqrt{\left(\frac{\mu\epsilon}{\mu_0\epsilon_0} - 1\right) + \left(\frac{\chi}{\beta_0 a}\right)^2}. \quad (29)$$

In calculating β and α of the H_{0n} -modes and HE_{mn} -modes with $|\Theta_H| \ll 1$ set $\chi = \sigma_{mn}$ in all equations. The same holds in calculating β and α of the E_{0n} -modes and EH_{mn} -modes with $|\Theta_E| \ll 1$. At very high frequencies, i.e., for large a/λ_0 , the E_{0n} -modes and EH_{mn} -modes thus have the eigenvalue σ_{mn} or rather $\sigma_{m(n-1)}$ ($n \neq 1$) and accordingly a phase constant approaching that of the HE_{mn} -modes or rather $HE_{m(n-1)}$ -modes ($n \neq 1$) (cf. eq (16)), viz, at very high frequencies the electrical field configuration of the E_{0n} -modes and EH_{mn} -modes is practically the same as that of the magnetic field with the corresponding $H_{0(n-1)}$ -modes and $HE_{m(n-1)}$ -modes ($n \neq 1$). In calculating β and α of the customary E_{0n} -modes and EH_{mn} -modes with $|\Theta_E| \ll 1$ there must be set $\chi = \chi_{mn}$ in all equations. Z_H/Z_0 and Z_a/Z_0 give the influence of the wall and the outer medium onto the waveguide modes, for Z_H/Z_0 is the ratio of the radial field characteristic impedance of the wall to that of space with the H_{0n} -modes (see eq (19)). Since these modes have only a circular electric field in parallel to the rings, no field penetrates between the rings, and with Z_H/Z_0 there appears as dielectric constant merely $\epsilon_p = \kappa_p/j\omega$, the outer medium having no influence. According to eq (27) Z_a/Z_0 is the input impedance of a guide terminated into the impedance Z_A , as referred to the field characteristic impedance Z_0 . This guide has here the characteristic impedance Z_E and the electrical length $\sqrt{\epsilon_i/\epsilon_0}d$, if ϵ_i is real. The magnitude Z_a/Z_0 can thus be calculated with the aid of the known Smith chart, where, as a function of d , the aforescribed input impedance lies always on a circle, if ϵ_i is real and the losses in the metal are neglected. In the same way as the quantity Z_H/Z_0 appears with the H_{0n} -modes, the quantity Z_a/Z_0 shows up with the E_{0n} -modes, since they have an axial electric field perpendicularly to the rings and the field therefore can issue between the rings into the outer region (see eqs (20) and (21)). The E_{0n} -modes can thus be affected very heavily by the outer medium. From the eqs (16), (17), and (19) to (21) there results thus for the phase and attenuation constants with the H_{0n} -modes

$$\beta_H = \beta_0 \sqrt{1 - \left(\frac{\sigma_{0n}}{\beta_0 a}\right)^2} + \alpha_H, \quad (30) \quad \alpha_H = \sqrt{\frac{D_1+D_2}{D_2}} \alpha_{Hn} \quad (31)$$

and with the E_{0n} -modes

$$\beta_E = \beta_0 \sqrt{1 - \left(\frac{\chi_{0n}}{\beta_0 a}\right)^2} + \frac{1}{a \sqrt{1 - \left(\frac{\chi_{0n}}{\beta_0 a}\right)^2}} \operatorname{Im} \left(\frac{Z_a}{Z_0} \right), \quad (32)$$

$$\alpha_E = \frac{1}{a \sqrt{1 - \left(\frac{\chi_{0n}}{\beta_0 a}\right)^2}} \operatorname{Re} \left(\frac{Z_a}{Z_0} \right), \quad (33)$$

$$\bar{\beta}_E = \beta_0 \sqrt{1 - \left(\frac{\sigma_{0n}}{\beta_0 a}\right)^2} + \frac{1}{a} \left(\frac{\sigma_{0n}}{\beta_0 a}\right)^2 \frac{\operatorname{Im} \left(\frac{Z_0}{Z_a} \right)}{\sqrt{1 - \left(\frac{\sigma_{0n}}{\beta_0 a}\right)^2}}, \quad (34)$$

$$\bar{\alpha}_E = \frac{1}{a} \left(\frac{\sigma_{0n}}{\beta_0 a}\right)^2 \frac{\operatorname{Re} \left(\frac{Z_0}{Z_a} \right)}{\sqrt{1 - \left(\frac{\sigma_{0n}}{\beta_0 a}\right)^2}}, \quad (35)$$

In eq (31) there denotes

$$\alpha_{Hn} = \sqrt{\frac{\beta_0}{2Z_0\kappa}} \frac{1}{a\sqrt{1 - \left(\frac{\sigma_{0n}}{\beta_0 a}\right)^2}} \left(\frac{\sigma_{0n}}{\beta_0 a}\right)^2 \quad (36)$$

the attenuation constant of the H_{0n} -modes in the homogeneous waveguide. The phase and attenuation constants β_E and α_E refer to the E_{0n} -modes with $|\Theta_E| \ll 1$. The quantities $\bar{\beta}_E$ and $\bar{\alpha}_E$ relate to the E_{0n} -modes with $|\bar{\Theta}_E| \ll 1$.

With

$$F_a(x) \ll 1 \quad (37)$$

the root in the eqs (23) to (25) can be expanded into a series and after insertion of eqs (22) to (24) into eq (17) there is found

$$\alpha_{HE} = \frac{1}{a} \left(\frac{\sigma_{mn}}{\beta_0 a}\right)^2 \frac{\operatorname{Re} \left(\frac{Z_a}{Z_0} \left\{ \left(\frac{m}{\sigma_{mn}}\right)^2 \left[\left(\frac{\beta_0 a}{\sigma_{mn}}\right)^2 - 1 \right] + \frac{Z_H}{Z_a} \right\} \right)}{\left[1 - \left(\frac{m}{\sigma_{mn}}\right)^2 \right] \sqrt{1 - \left(\frac{\sigma_{mn}}{\beta_0 a}\right)^2}} \quad (38)$$

$$\alpha_{EH} = \frac{1}{a\sqrt{1 - \left(\frac{\chi_{mn}}{\beta_0 a}\right)^2}} \operatorname{Re} \left(\frac{Z_a}{Z_0} \right), \quad (39)$$

$$\bar{\alpha}_{EH} = \frac{1}{a} \left(\frac{\sigma_{mn}}{\beta_0 a}\right)^2 \frac{\operatorname{Re} \left(\frac{Z_0}{Z_a} \right)}{\left[1 - \left(\frac{m}{\sigma_{mn}}\right)^2 \right] \sqrt{1 - \left(\frac{\sigma_{mn}}{\beta_0 a}\right)^2}}, \quad m=0, 1, 2, \text{ etc.} \quad (40)$$

where α_{HE} the attenuation constant with the HE_{mn} -modes, α_{EH} that with the EH_{mn} -modes ($|\Theta_E| \ll 1$) and $\bar{\alpha}_{EH}$ that with the EH_{mn} -modes with $|\bar{\Theta}_E| \ll 1$.

From the eqs (38) to (40) one obtains also the well-known attenuation formulas of the modes in the homogeneous waveguide, equating $Z_a = Z_H$ and $D_1 = 0$.

An example is to show, when the phase and attenuation constants with horizontal stroke on top hold, hence when the eqs (34), (35), and (40) are valid. With the homogeneous waveguide there is $Z_a = Z_H$ and $D_1 = 0$, as mentioned. There results accordingly from the eqs (20), (21), and (26) $|\Theta_E| = 15.4$ and $|\bar{\Theta}_E| = 0.045$ for the E_{02} -mode in the homogeneous waveguide, i.e., $\chi_{02} = 5.52$ and $\sigma_{01} = 3.83$, with $a = 2.5$ cm, $\lambda_0 = 0.01$ mm, $\kappa = 57 \times 10^4$ mho/cm (copper), i.e., the eqs (34) and (35) are valid. Since Z_a/Z_0 will mostly be greater than Z_H/Z_0 , the eqs (34) and (35) will hold with the ring-element guide even with a wavelength in excess of $\lambda_0 = 0.01$ mm. From the eqs (39) and (40) the following interesting function of the attenuation of the E_{0n} -modes ($n \neq 1$) and EH_{mn} -modes ($n \neq 1$) in the homogeneous waveguide results thus: ($Z_a = Z_H$, $D_1 = 0$). Initially, according to eq (39), starting at a very high value at the cutoff frequency the attenuation decreases with increasing frequency, subsequently it passes through a minimum and rises again. Thereafter the attenuation must pass through a maximum, since, according to eq (40), it decreases again for sufficiently high frequencies. With the ring-element guide the attenuation/frequency curve is basically the same, but additional variations will come about because of the quantity Z_a/Z_0 which, according to eq (27), is approximately periodical as a function of frequency. With respect to the attenuation constants of the H_{0n} -modes of eq (31) there can further be stated that the root term in a certain way takes into account the penetration of the field between the rings and that, because of the inequality (2), the radiation damping can mostly be neglected with the thicknesses d encountered in practice.

As mentioned above, an essential point is the capability of existence of the modes. Inserting eq (13) into the inequality (11) yields that with a real ϵ_i and neglecting of the ring losses there are capable of existence only the E_{0n} -modes, HE_{mn} -modes, and EH_{mn} -modes ($m \neq 0$) for which

$$(\beta_0 a)^2 \left| \operatorname{Im} \left(\frac{\mu \epsilon}{\mu_0 \epsilon_0} \right) \right| > \begin{cases} 2\sigma_{mn} \operatorname{Im}(\Theta_H) \\ 2\chi_{mn} \operatorname{Im}(\Theta_E) \\ 2\sigma_{mn} \operatorname{Im}(\bar{\Theta}_E). \end{cases} \quad (41)$$

4.2. Application of the Ring-Element Guide as a Mode Filter in Transmission With the H_{01} -Mode

The influence of the outer medium onto the waveguide modes is the greater, the stronger the axial electric field of the waveguide modes, i.e., an outer medium with high losses will attenuate the EH_{mn} -modes far more than the HE_{mn} -modes. With use of the ring-element guide as a mode filter in transmission with the H_{01} -mode the attenuation of the EH_{mn} -modes is always sufficient. It is, therefore, important so to design the guide that also the HE_{mn} -modes are attenuated as strongly as possible. In calculating the loss of the HE_{mn} -modes the losses of the rings and the dielectric between them can be neglected, if the outer medium has high losses, i.e., it is possible to set $\kappa = \infty$ and thus $Z_H/Z_0 = 0$. From the eqs (17) and (22) maximum attenuation results then for $F_a(\sigma_{mn}) = 1$, i.e., if Z_a/Z_0 is real and has a certain value. For a real ϵ_i one obtains therefore from the eqs (25), (27), (28), and (29) the following design rules for maximum attenuation of the HE_{mn} -modes:

$$\frac{Z_E}{Z_0} = \sqrt{R(U - \frac{V^2}{R-U})}, \quad (42)$$

$$\tan\left(\beta_0 \sqrt{\frac{\epsilon_i}{\epsilon_0}} d\right) = \frac{R-U}{VR} \frac{Z_E}{Z_0}, \quad (43)$$

$$\frac{Z_a}{Z_0} = R = \frac{\sigma_{mn}}{2m \sqrt{\left(\frac{\beta_0 a}{\sigma_{mn}}\right)^2 - 1}}, \quad m, n = 1, 2, 3, \text{ etc.} \quad (44)$$

The quantities U and V are the real and imaginary parts of Z_A/Z_0 and therefore calculated according to eq (29) from

$$\frac{\epsilon_0}{\epsilon} \sqrt{\left(\frac{\mu \epsilon}{\mu_0 \epsilon_0} - 1\right) + \left(\frac{\sigma_{mn}}{\beta_0 a}\right)^2} = U + jV. \quad (45)$$

From the eqs (17) and (22) the maximum attenuation results then as

$$(\alpha_{HE})_{\max} = \frac{m}{\beta_0 a^2 \left[1 - \left(\frac{m}{\sigma_{mn}}\right)^2\right]}, \quad m, n = 1, 2, 3, \text{ etc.} \quad (46)$$

Equation (46) shows that the maximum attenuation is inversely proportional to the square of the inner radius of the ring-element guide and inversely proportional to frequency. The higher thus the frequency, the lower the maximum attenuation. Neglecting the term $(m/\sigma_{mn})^2$ the maximum attenuation is proportional to m ($m=1, 2, 3$, etc.). It should here be noted that the material constants of the outer medium do not appear in eq (46). Since with the eqs (42) to (44) ϵ_i was assumed as real and the losses due to the rings were not taken into account, the inequality (41) must, of course, always be satisfied.

Equation (44) shows that always only for one σ_{mn} , i.e., for one mode, the conditions for maximum attenuation can be satisfied. The condition eq (44) can be interpreted as kind of a matching condition.

An example may show the application of eqs (42) to (46). Let us assume that a ring-element guide is to be found with maximum attenuation of the HE_{12} -mode. This mode is excited with particular ease by the H_{01} -mode in a homogeneous waveguide whenever it deviates from its straight circular shape and it has a relatively low attenuation.

Given are the following data: Frequency $f = 50$ kMc/s ($\lambda_0 = 6$ mm); $a = 2.5$ cm, hence $\beta_0 a = 26.2$. With the HE_{12} -mode there is $\sigma_{mn} = \sigma_{12} = 5.33$. From eq (46) there results then the maximum attenuation of the HE_{12} -mode as $\alpha_{12} = 0.0158$ N/cm, i.e., 3,180 times the attenuation

in the homogeneous circular copper waveguide. It is further assumed that a dielectric with $\epsilon/\epsilon_0=10(1-j)$ and $\mu=\mu_0$ is available for constructing the ring-element guide. The attenuation of the fields in the outer medium is then $\text{Im}(\beta_0 \sqrt{\epsilon/\epsilon_0})=15 \text{ N/cm}$. Besides it is assumed that $D_2=D_1$. Find now the quantities ϵ_i/ϵ_0 and d .

With the given values there results from the eqs (42) to (45): $U=0.242$; $V=0.093$; $R=0.553$; $Z_E/Z_0=0.344$; $\tan(\beta_0 \sqrt{\epsilon_i/\epsilon_0} d)=2.08$, i.e., $\epsilon_i/\epsilon_0=2.11$; $d=0.74 \text{ mm}$. Because of $D_2=D_1$ the attenuation of the HE_{01} -mode, according to eq (31) in this case exceeds that in the homogeneous waveguide by the factor $\sqrt{2}$.

While in the above example the increase in attenuation over the homogeneous waveguide is very high with the HE_{12} -mode, this holds no longer for the other HE_{1n} -modes. If, however, maximum attenuation of a specific mode is no longer demanded, an appropriate dimensioning of the ring-element guide allows a design that the attenuation values of a number of HE_{mn} -mode approach more closely their maximums.

Another interesting point is the basic attenuation/frequency curve of a HE_{mn} -mode. For the dimensions calculated in the example, the figure 7 shows the attenuation of the HE_{12} -mode as a function of $\sqrt{\epsilon_i/\epsilon_0} d/\lambda_0$ with a fixed $\sqrt{\epsilon_i/\epsilon_0} d$, i.e., as a function of frequency. Here, however, there must be $D_1=D_2<0.2 \text{ mm}$, to have inequality (1) satisfied for all frequencies stated in figure 7. With the maximum attenuation attainable the curve plotted in figure 7 presents a pointed peak at $\sqrt{\epsilon_i/\epsilon_0} d/\lambda_0=0.179$ ($f=50 \text{ kMc/s}$). The other extremities of the curve are no such peaks, but ordinary maximums. They are all lower than this peak, since according to eq (22) $\beta_0 a$ and thus the frequency is in the denominator of the attenuation constant. On the frequency axis the first maximum is away from the peak by 0.25. The subsequent maximums are spaced 0.5 from each other. Since the losses of the rings were neglected, the attenuation at the cutoff frequency is here zero.

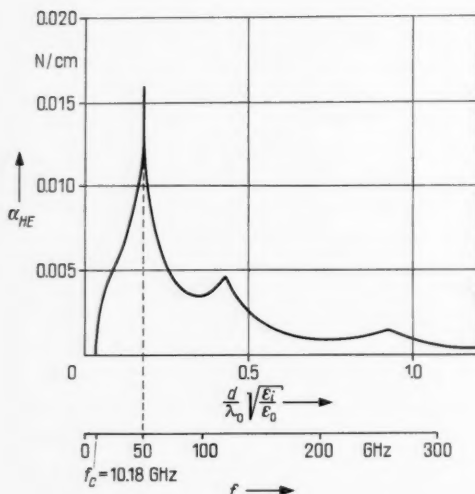


FIGURE 7. Attenuation of the HE_{12} -mode as a function of frequency with a ring-element guide with $\epsilon/\epsilon_0=10(1-j)$, $\mu=\mu_0$, $\epsilon_i/\epsilon_0=2.11$, $d=0.74 \text{ mm}$, $a=2.5 \text{ cm}$, $D_1=D_2$.

At this point let us also make some statements concerning the capability of existence of the waveguide modes. If the outer medium and the dielectric between the rings are free of losses, the quantity Z_a/Z_0 is in the left half-plane of the complex number plane when the ring losses are neglected, according to eq (27). Only with a consideration of the ring losses and a very large thickness d the quantity Z_a/Z_0 lies in the right-hand half of the complex number plane, so that $\text{Re}(Z_a/Z_0)>0$, and a sufficient condition is so satisfied for the capability of existence of waveguide modes.

4.3. Properties of the EH_m -Modes

a. General Considerations

The term EH_m -modes ($m=0, 1, 2$, etc.) is understood herein as comprising modes of E -character whose fields disappear in the region $0 \leq r \leq a$ in the axis ($r=0$) or at the point $r=a$ at most (the Bessel functions have then no zeros in $0 < r < a$). For $r > b$ the fields disappear only in the infinite. The subscript n therefore can be dropped with these modes. The surface modes, i.e., modes most of whose fields are outside the guide, hence in the region $r > b$, are counted as a rule as EH_m -modes. As will be shown below, the surface modes with H -character have no practical significance because of their high attenuation. As a rule the phase velocity of the EH_m -modes is less than the velocity of light. With the EH_m -modes the ring-element guide thus is, as a rule, a delay line. The principal characteristics of the EH_m -modes are obvious already from the special case of the rotation-symmetrical modes ($m=0$). Let us thus consider above all these modes. With

$$\left. \begin{array}{l} |p_E a| \\ |k_0 a| \\ |k_2 b| \\ |\beta_2 b| = \beta_0 b \sqrt{\frac{\mu \epsilon}{\mu_0 \epsilon_0}} \end{array} \right\} \gg 1, \quad (47)$$

$$\text{Im}(k_0 a) > 2 \quad (48)$$

there results from eq (87)

$$\frac{k_0}{\beta_0} = \frac{Z_a}{Z_0} = \frac{Z_A}{Z_0} \frac{1 + j \frac{Z_E}{Z_A} \tan p_E d}{1 + j \frac{Z_A}{Z_E} \tan p_E d}, \quad \text{for } m=0. \quad (49)$$

Insertion of eq (29) into eq (49) and resolution for $\tan p_E d$ yields

$$\tan p_E d = -j \frac{\frac{k_0}{\beta_0} \frac{\epsilon}{\epsilon_0} \pm \sqrt{\left(\frac{\mu \epsilon}{\mu_0 \epsilon_0} - 1\right) + \left(\frac{k_0}{\beta_0}\right)^2}}{\frac{Z_E}{Z_0} \frac{\epsilon}{\epsilon_0} \pm \frac{Z_0}{Z_E} \frac{k_0}{\beta_0} \sqrt{\left(\frac{\mu \epsilon}{\mu_0 \epsilon_0} - 1\right) + \left(\frac{k_0}{\beta_0}\right)^2}} \quad \text{for } m=0. \quad (50)$$

The root in eq (50) is k_2/β_0 . If $|\text{Im}((k_0/\beta_0)^2)| > |\text{Im}(\mu \epsilon / (\mu_0 \epsilon_0))|$ the upper sign of eq (50) holds. If, however, $|\text{Im}((k_0/\beta_0)^2)| < |\text{Im}(\mu \epsilon / (\mu_0 \epsilon_0))|$ the lower sign holds in eq (50).

With

$$\left. \begin{array}{l} \left| \frac{m}{k_0 a} \right| \\ \left| \frac{4m^2}{(\beta_0 a)^2} \left[\left(\frac{\beta_0 a}{k_0 a} \right)^2 - 1 \right] \right| \end{array} \right\} \ll 1 \quad m=1, 2, 3, \dots \quad (51)$$

equation (50) holds approximately also for $m \neq 0$. With use of eq (50) it should always be borne in mind, however, that the inequality (47) must be satisfied.

Because of the losses of the guide the eigenvalue $k_0 a$ is complex and there is set accordingly

$$\frac{k_0}{\beta_0} = \xi + j\eta. \quad (52)$$

The quantity k_0/β_0 is imaginary, i.e.,

$$\frac{k_0}{\beta_0} = j\eta \quad (53)$$

and there holds the upper sign in eq (50). The quantity k_0/β_0 must also be imaginary, i.e.

$$\left| \left(\frac{k_0}{\beta_0} \right)^2 \right| > \frac{\mu\epsilon}{\mu_0\epsilon_0} - 1. \quad (54)$$

For a real $\mu\epsilon/(\mu_0\epsilon_0) \neq 1$ the ring-element guide is a delay line with a periodic band pass character, because of the imaginary k_0/β_0 and the condition of the inequality (54). Apart from the H_{0n} -modes no wave guide modes are capable of existence. The limit of the pass band and stop band of the delay line is found from eq (54) with $|(k_0/\beta_0)^2| = \mu\epsilon/(\mu_0\epsilon_0) - 1$ and lies at

$$\left(\frac{2\pi}{\lambda_0} \sqrt{\frac{\epsilon_i}{\epsilon_0}} d \right)_g = \arctan \frac{Z_0}{Z_E} \sqrt{\frac{\mu\epsilon}{\mu_0\epsilon_0} - 1}. \quad (55)$$

For $\mu\epsilon \rightarrow \infty$ there is $\sqrt{\epsilon_i/\epsilon_0} d/\lambda_0 = 0.25 + \nu 0.5$; $\nu = 0, 1, 2$, etc.

In the special case $\mu\epsilon/(\mu_0\epsilon_0) = 1$ there is $k_2 = k_0$ and eq (50) yields

$$\frac{k_0}{\beta_0} = j \frac{Z_E}{Z_0} \tan \left(\frac{\pi}{\lambda_0} \sqrt{\frac{\epsilon_i}{\epsilon_0}} d - \left\{ \frac{0}{2} \right\} \right). \quad (56)$$

Also in this case the ring-element guide is a delay line, but without band pass character.

As an example, figure 8 shows the relative eigenvalue η with the E_0 -mode as a function of $\sqrt{\epsilon_i/\epsilon_0} d/\lambda_0$ for $\mu = \mu_0$, but different ϵ_i and ϵ . Figure 8 is to be thought of as continued periodically in the direction of increasing $\sqrt{\epsilon_i/\epsilon_0} d/\lambda_0$, the period amounting to 0.5. The mode will travel the slower, the higher the dielectric constant of the outer medium and the closer Z_E approaches Z_0 , i.e., if D_2/D_1 is small. With a high D_2/D_1 , e.g., for $D_2/D_1 = 5$, the relative eigenvalue at the beginning of the pass band is almost independent of d/λ_0 , but increases the more steeply later on.

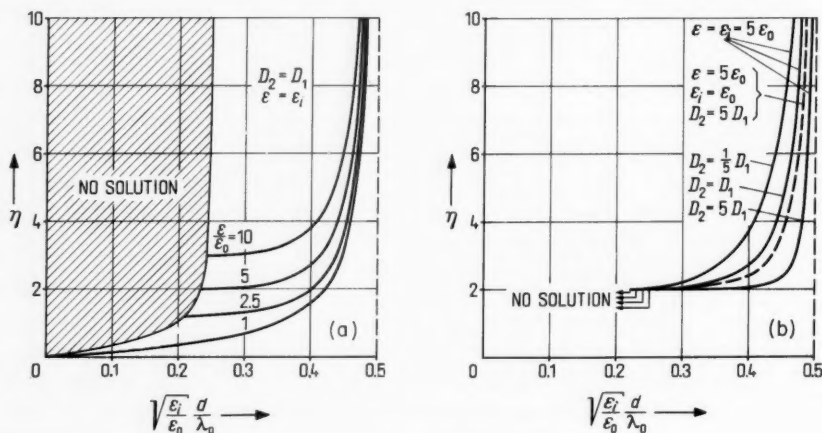


FIGURE 8. The relative eigenvalue $k_0/\beta_0 = j\eta$ with the E_0 -mode in the ring-element guide as a function of $\sqrt{\epsilon_i/\epsilon_0} d/\lambda_0$ for various ϵ , ϵ_i and D_2/D_1 .

The presentation is to be thought of as periodically continued with the period 0.5 in the direction of increasing $\sqrt{\epsilon_i/\epsilon_0} d/\lambda_0$.

For the special case $d=0$ there results from eq (50)

$$\frac{k_0}{\beta_0} = j \sqrt{\frac{\frac{\mu\epsilon}{\mu_0\epsilon_0} - 1}{\left(\frac{\epsilon}{\epsilon_0}\right)^2 - 1}} \quad (57)$$

It should here be noted that the inequality (48) must always be satisfied and k_0 must have a positive real and imaginary part. With a real ϵ the eq (57) thus yields no solution even if μ complex. From the propagation constant γ there results with $|k_0^2| \gg \beta_0^2$ in the case $d=0$ a maximum attenuation for $\tan \delta = 1 + \epsilon_0/\epsilon_a$, if $\epsilon/\epsilon_0 = \epsilon_a/\epsilon_0(1 - j \tan \delta)$.

In the special case $\sqrt{\epsilon_i/\epsilon_0}d/\lambda_0 = 0.25$ eq (50) yields

$$\frac{k_0}{\beta_0} = j \sqrt{\frac{1}{2} \left(\frac{\mu\epsilon}{\mu_0\epsilon_0} - 1 \right) + \sqrt{\frac{1}{4} \left(\frac{\mu\epsilon}{\mu_0\epsilon_0} - 1 \right)^2 + \left(\frac{Z_E}{Z_0} \right)^4 \left(\frac{\epsilon}{\epsilon_0} \right)^2}} \quad (58)$$

Unlike eq (57) the eq (58) holds for real $\mu\epsilon/(\mu_0\epsilon_0)$ as well.

Setting $\mu = \mu_a(1 - j \tan \delta_a)$ and $\epsilon = \epsilon_a(1 - j \tan \delta_e)$, and if the outer medium has but small losses, there holds $\tan \delta_a + \tan \delta_e \ll 1$. In such case the imaginary part of the eigenvalue, i.e., η of eq (52) practically agrees with the solution for a real $\mu\epsilon$. Figure 9 shows under these assumptions for $\mu = \mu_0$ and $\tan \delta_e = \tan \delta$ the quantity $\xi/\tan \delta$ as a function of $\sqrt{\epsilon_i/\epsilon_0}d/\lambda_0$ with the E_0 -mode. The dielectric constant ϵ_i and the real part of ϵ agree with figure 8. The quantity η can be taken from figure 8. A comparison with this diagram shows that with an increasing η the quantity ξ increases correspondingly. The periodic band pass character has been retained.

If the outer medium is very lossy, the real part of the eigenvalue and accordingly the quantity ξ will be larger than in figure 9. As an example the figure 10 shows the relative eigenvalue k_0/β_0 with the E_0 -mode as a function of d/λ_0 for $\epsilon_i = \epsilon_0$ and $\epsilon/\epsilon_0 = 5; 5(1 - j 0.3); 5(1 - j)$. The periodic band pass character remains also in this case, but in the pass bands there exist as a rule for each d/λ_0 two different eigenvalues which are plotted in the figures 10a and 10b. Only with a real ϵ there results only one eigenvalue for each d/λ_0 . According to figure 8 it is imaginary, and therefore it is on the imaginary axis in figure 10b. In figure 10a there is $|k_0| < \beta_0$ and in figure 10b $|k_0| > \beta_0$.

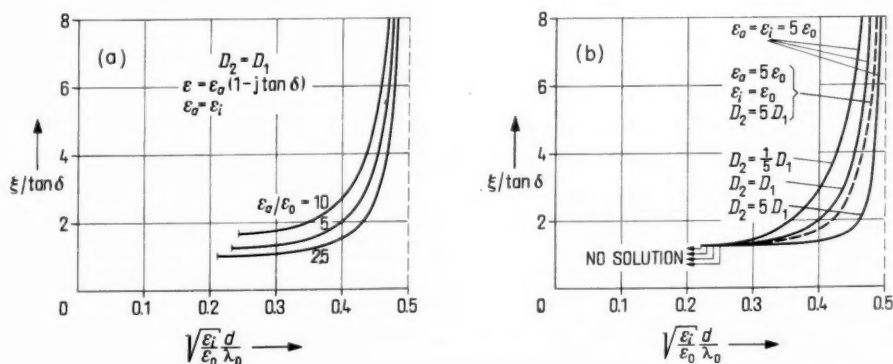


FIGURE 9. The real part ξ of the relative eigenvalue $k_0/\beta_0 = \xi + j\eta$ with the E_0 -mode in the ring-element guide as a function of $\sqrt{\epsilon_i/\epsilon_0}d/\lambda_0$ for various ϵ , ϵ_i , and D_2/D_1 under the assumption $\tan \delta \ll 1$ (δ loss angle of the dielectric outside the rings).

Because of $\tan \delta \ll 1$ η is to be taken from figure 8. The presentation is to be thought of as periodically continued with the period 0.5 in the direction of increasing $\sqrt{\epsilon_i/\epsilon_0}d/\lambda_0$.

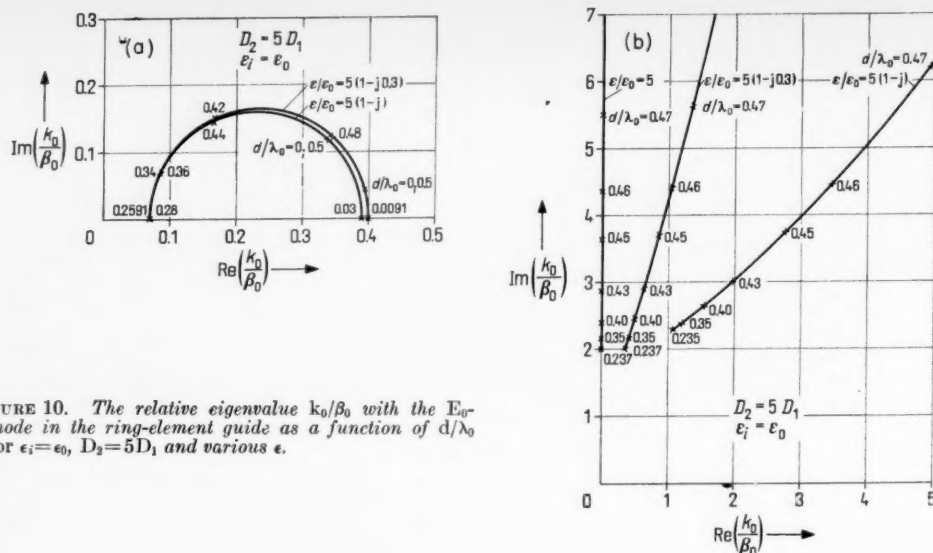


FIGURE 10. The relative eigenvalue k_0/β_0 with the E_0 -mode in the ring-element guide as a function of d/λ_0 for $\epsilon_i = \epsilon_0$, $D_2 = 5D_1$ and various ϵ .

The eigenvalue in figure 10b corresponds to that in figure 8. The pass bands of figures 10a and 10b differ slightly. With $\epsilon/\epsilon_0 = 5(1-j)$ for example, the pass band is given in figure 10a by $0 < d/\lambda_0 < 0.03$ and $0.28 < d/\lambda_0 < 0.5$. In figure 10b the pass band is given in this case by $0.235 < d/\lambda_0 < 0.5$. In either case the pass bands recur with the period $d/\lambda_0 = 0.5$.

The solution in figure 10a is very easily found, since the quantity k_0^2 can here be neglected with respect to $\beta_0^2(\mu\epsilon/(\mu_0\epsilon_0) - 1)$. The relative eigenvalues k_0/β_0 lie therefore on a circle of which only the part in the first quadrant of the complex number plane ($\text{Im}(k_0) > 0$) gives a physically reasonable solution.

The solution in figure 10b is more difficult to find (see [7]). With $\epsilon/\epsilon_0 = 5(1-j)$ the solution in figure 10b practically agrees with the values η and ξ resulting from the dashed curves of the figures 8b and 9b.

Besides the EH_m -modes and the H_{0n} -modes which are always capable of existence, even waveguide modes can propagate, if the inequality (41) holds (see sec. 4.1 and 4.2).

4.4. Special Case $a=0$, E_0 -Mode

For $a \rightarrow 0$ the ring-element guide changes into the guide discussed in [10] (fig. 11, in [10] there has indeed been assumed $\mu = \mu_0$ and $\epsilon = \epsilon_0$). With this guide most of the wave energy travels outside indeed, hence in the region $r > b$, and these modes thus are typical surface modes. The quantity k_2 and thus the propagation constants of these modes are obtained from equation (89). There results that with an outer medium consisting of a dielectric (in particular with $\epsilon = \epsilon_0$ and $\mu = \mu_0$) only the E_0 -mode is of practical interest. The H_0 , HE_{mn} , and EH_m -modes ($m \neq 0$) have very high attenuation and correspond to the spurious modes on the Sommerfeld guide. Compare hereto also the statements in [9].

For the E_0 -mode one obtains with $\beta_2 = \beta_0 \sqrt{\mu\epsilon/(\mu_0\epsilon_0)}$ from the eq (89) to (92) for the calculation of k_2

$$\frac{\beta_2}{k_2} \frac{H_1^{(1)}(k_2 b)}{H_0^{(1)}(k_2 b)} = \sqrt{\frac{\mu\epsilon}{\mu_0\epsilon_0}} \frac{D_1 + D_2}{D_1} \frac{J_1(p_E b)}{J_0(p_E b)} \quad (59)$$

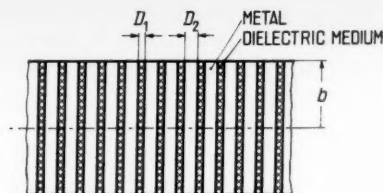


FIGURE 11. Ring-element guide with $a=0$.

Also the ring-element guide with $a=0$ has practically a periodic band pass character. Since k_2 always must have a positive imaginary part, there result from eq (59) with the lossless guide the stop bands:

$$\chi_{0n} < \beta_0 \sqrt{\frac{\epsilon_t}{\epsilon_0}} b < \sigma_{0n}, \quad (60)$$

and pass bands:

$$\sigma_{0n} < \beta_0 \sqrt{\frac{\epsilon_t}{\epsilon_0}} b < \chi_{0(n+1)} \quad n=1, 2, 3, \text{ etc.}$$

For $\epsilon=\epsilon_0$ and $\mu=\mu_0$ the eqs (59) and (60) have been stated already in [10].

With

$$\left. \begin{aligned} |k_2 b| \\ |p_E b| \end{aligned} \right\} >> 1 \quad (61)$$

one obtains from eq (59)

$$\frac{k_2}{\beta_2} = j \sqrt{\frac{\mu_0 \epsilon}{\mu \epsilon_t}} \frac{D_1}{D_1 + D_2} \tan \left(p_E b + \frac{\pi}{4} \right). \quad (62)$$

Without consideration of the losses there are then the stop bands:

$$n\pi - \frac{\pi}{4} < \beta_0 \sqrt{\frac{\epsilon_t}{\epsilon_0}} b < n\pi + \frac{\pi}{4} \quad (63)$$

and the pass bands:

$$n\pi + \frac{\pi}{4} < \beta_0 \sqrt{\frac{\epsilon_t}{\epsilon_0}} b < (n+1)\pi - \frac{\pi}{4} \quad n=1, 2, 3, \text{ etc.}$$

A comparison between the inequalities (60) and (63) shows that the inequality (63) is sufficiently accurate for practical purposes.

After inserting eq (62) into eq (12) one obtains with

$$\frac{\epsilon_t}{\epsilon_0} = \frac{\epsilon_{t1}}{\epsilon_0} (1 - j \tan \delta_t), \quad (64)$$

$$\tan \delta_t \ll 1, \quad (65)$$

$$\beta_1 b = \beta_0 \sqrt{\frac{\epsilon_{t1}}{\epsilon_0}} b, \quad (66)$$

$$|\operatorname{Re}(k_2)| \ll |\operatorname{Im}(k_2)| \quad (67)$$

for the phase and attenuation constants with $\epsilon=\epsilon_0$ and $\mu=\mu_0$

$$\beta = \beta_0 \sqrt{1 + \left[\sqrt{\frac{\epsilon_0}{\epsilon_{t1}}} \frac{D_1}{D_1 + D_2} \tan \left(\beta_1 b + \frac{\pi}{4} \right) \right]^2} \quad (68)$$

$$\alpha = \beta_0 b \frac{D_1}{D_1 + D_2} \frac{\frac{\beta_0}{2} \tan \delta_t + \frac{1}{D_1} \sqrt{\frac{\beta_0}{2Z_0 \kappa}}}{\cos^2 \left(\beta_1 b + \frac{\pi}{4} \right) \sqrt{1 + \left[\sqrt{\frac{\epsilon_{t1}}{\epsilon_0}} \frac{D_1 + D_2}{D_1} \cot \left(\beta_1 b + \frac{\pi}{4} \right) \right]^2}} \quad (69)$$

The eq (68) shows that the phase velocity of the E_0 -mode as a rule is less than the velocity of light. In eq (69) the minute losses of the metal at the surface of the guide, i.e., for $r=b$ have been neglected. The attenuation-versus-frequency response is analogous to the one shown in figure 8 of [9]. Compare hereto also [10].

If

$$|\operatorname{Im}(p_E b)| > 2 \quad (70)$$

with $\epsilon = \epsilon_0$ and $\mu = \mu_0$ eq (62) can be written as the simple formula

$$\frac{k_2}{\beta_2} = \frac{k_0}{\beta_0} = \sqrt{\frac{\epsilon_0}{\epsilon_i}} \frac{D_1}{D_1 + D_2} = \frac{Z_E}{Z_0} \quad (71)$$

Equation (71) yields the special case that, under the condition of the inequality (70), the E_0 -mode as a surface mode has a phase velocity higher than the velocity of light. See hereto also the examples at the end of section 5.

5. Disk Guide (Ring-Element Guide With $d = \infty$)

For calculating the propagation constants of the modes in the disk guide (fig. 1) the formulas for the ring-element guide are used, replacing Z_a/Z_0 by Z_E/Z_0 . With the waveguide modes the eqs (13) to (40) hold accordingly, i.e., the H_{0n} -modes have the same attenuation as with the ring-element guide. With the E_{0n} -modes there is under the assumption

$$\left| \frac{Z_E}{Z_0} \right| < \frac{\chi_{0n}}{\beta_0 a} \quad n=1,2,3, \text{ etc.} \quad (72)$$

the attenuation

$$\alpha_E = \frac{1}{a \sqrt{1 - \left(\frac{\chi_{0n}}{\beta_0 a} \right)^2}} \operatorname{Re} \left(\frac{Z_E}{Z_0} \right) \quad n=1,2,3, \text{ etc.} \quad (73)$$

The phase constant practically equals that in the lossless homogeneous waveguide.

Corresponding to the eqs (48) and (49) there appears under the assumption

$$\operatorname{Im} \left(\frac{Z_E}{Z_0} \right) > \frac{2}{\beta_0 a} \quad (74)$$

the equation

$$\frac{k_0}{\beta_0} = \frac{Z_E}{Z_0} \quad (75)$$

Because of the inequality (74) the Bessel functions have no zeros in $0 < r < a$ and the subscript n is therefore not needed. The E_{0n} -mode has changed into an E_0 -mode. Note that eq (75) agrees with eq (71). With

$$\left| \frac{Z_E}{Z_0} \right| > \frac{1}{\beta_0 a} \quad (76)$$

there is then

$$\gamma = \pm j \beta_0 \sqrt{1 - \left(\frac{Z_E}{Z_0} \right)^2} \quad (77)$$

Some examples are to show the applications of the eqs (73) and (77) for the E_{01} -mode and E_0 -mode. There is $\chi_{01} = \chi_{01} = 2.41$. The frequency is always assumed as $f = 50$ kMc/s, hence $\lambda_0 = 0.6$ cm and the inner radius is $a = 2.5$ cm.

For $D_2 = 50 D_1$ and $\epsilon_i/\epsilon_0 = 3$ the inequality (72) is satisfied and there results from eq (73) the attenuation $\alpha_E = 4.54 \times 10^{-3}$ N/cm. This attenuation comes about merely by radiation into the inhomogeneous medium and is 72.5 times larger than the attenuation of the E_{01} -mode in the homogeneous circular copper waveguide.

For $D_2=50 D_1$ and $\epsilon_i/\epsilon_0=3(1-j)$ the eq (72) can be used as well and there results $\alpha_E=3.52 \times 10^{-3}$ N/cm. Despite the lossy dielectric the attenuation is now lower, since Z_E deviates from Z_0 more heavily than with $\epsilon_i/\epsilon_0=3$ (poorer matching of the radial impedance).

With $D_2=D_1$ and $\epsilon_i/\epsilon_0=3(1-j)$ the inequalities (74) and (76) are satisfied and there results from eq (77) an attenuation $\alpha_E=0.223$ N/cm, i.e., 3.55×10^3 times as much as the attenuation of the E_{01} -mode in the homogeneous circular copper waveguide. The phase constant is 1.8 percent less than that in the homogeneous waveguide. Compared to the case $D_2=50 D_1$ the propagation constant thus has changed much more strongly relative to that in the homogeneous waveguide. In particular the attenuation has increased very heavily (superior matching of Z_E to Z_0).

With $D_2=D_1$ and $\epsilon_i/\epsilon_0=2.5(1-j)$ there results then an even higher attenuation, i.e., $\alpha_E=0.269$ N/cm, since Z_E has approached Z_0 even more. In this case the phase constant is 2.1 percent less than that in the homogeneous waveguide.

With the examples for the E_0 -mode the fact is remarkable that the phase velocity is not only greater than the velocity of light, but also greater than the phase velocity of the E_{01} -mode in the homogeneous waveguide. This is in contrast to the general behavior of the E_0 -mode which is characterized by $v_p < c$ (see notes in sec. 4).

6. Disk Loaded Waveguide and the Corrugated Waveguide (Ring-Element Guide With $\epsilon=\kappa/j\omega$ and $\mu=\mu_0$). E_{0n} -mode and E_0 -mode with $\epsilon_i=\epsilon_0$ and $\kappa=\infty$

The eigenvalues for the modes in the disk-loaded waveguide and corrugated waveguide are obtained from the eqs (83) and (84) by setting $\epsilon=\kappa/j\omega$ and $\mu=\mu_0$. All formulas derived in discussing the ring-element guide can thus here be used as well. To bring out clearly the fundamentals of the disk loaded waveguide and the corrugated waveguide, let us here consider merely the E_{0n} and E_0 -modes with $\epsilon_i=\epsilon_0$, neglecting the losses ($\kappa=\infty$).

As a first step there results quite generally that for $\beta_0 b \ll 1$ no propagating modes exist in the disk loaded waveguide and corrugated waveguide, but merely statically attenuated fields of the type of the waveguide fields.

With $\beta_0 a \ll 1$ and $\beta_0 b \gg 1$, however, the disk loaded waveguide is a delay line with filter character and very narrow pass bands. For the E_0 -mode there result the eigenvalues $k_0 a$ and the pass bands from

$$k_0 a \frac{J_0(k_0 a)}{J_1(k_0 a)} = (\beta_0 a)^2 \frac{D_1}{D_1 + D_2} \frac{\pi}{2} \frac{1}{\beta_0 b - \frac{\pi}{4} - k \frac{\pi}{2}} \geq 2 \quad k=1,3,5, \text{ etc } \dots \quad (78)$$

The pass bands are given accordingly by

$$k \frac{\pi}{2} + \frac{\pi}{4} \leq \beta_0 b \leq k \frac{\pi}{2} + \frac{\pi}{4} + (\beta_0 a)^2 \frac{D_1}{D_1 + D_2} \frac{\pi}{4} \quad k=1,3,5, \text{ etc.} \quad (79)$$

Particularly interesting is the behavior of the line with $\beta_0 a \gg 1$. This case shall be considered alone hereinafter. The eigenvalues $k_0 a$ are now obtained from

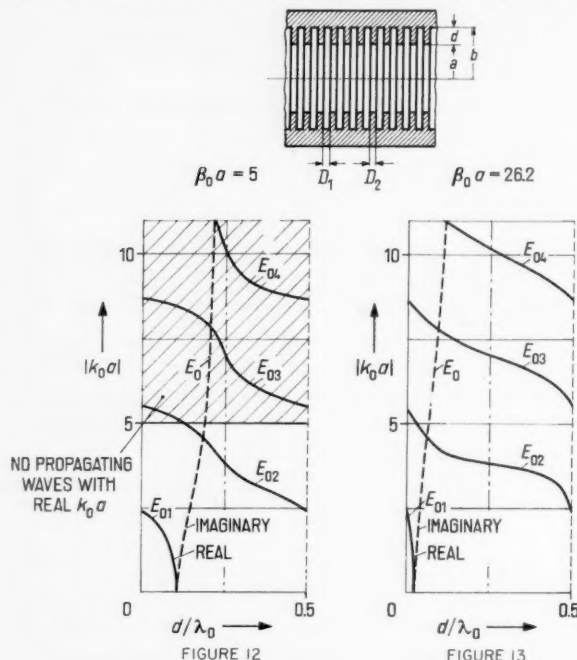
$$k_0 a \frac{J_0(k_0 a)}{J_1(k_0 a)} = \beta_0 a \frac{D_1}{D_1 + D_2} \tan \beta_0 d. \quad (80)$$

With $d=0$, the solutions of eq (80) are the zeros of $J_0(k_0 a)$. There result the E_{0n} -modes for the homogeneous waveguide.

With $d/\lambda_0=0.25$ the solutions of eq (80) are the zeros of $J'_1(k_0 a)$ and the $E_{0(n+1)}$ -modes have the same phase velocity as the H_{0n} -modes. (The notation $E_{0(n+1)}$ derives from the fact that with $d \rightarrow 0$ the waveguide mode $E_{0(n+1)}$ comes about, see also figs. 12 and 13.) Physically, this can be explained as follows. With $d/\lambda_0=0.25$ the input impedance for $r=a$ is infinite for a mode in the radial direction. This means that no current flows at this point and $H_\phi=0$ accord-

ingly. Since, however, with the E -modes H_ϕ follows the same function as E_ϕ with the H -modes, and since with these the field strength $E_\phi=0$ for $r=a$, the same phase constant results with $d/\lambda_0=0.25$ for the $E_{0(n+1)}$ -modes as for the H_{0n} -modes. The figures 12 to 15 show a further evaluation of eq (80).

The figures 12 and 13 present the eigenvalues $k_0 a$ of the E_{0n} -modes and the E_0 -mode as a function of d for a given $\beta_0 a$, i.e., for a given frequency. The figures 12 and 13 must be thought of as periodically continued in the direction of increasing d/λ_0 with the period 0.5, corresponding to the period of $\tan \beta_0 d$. With $d=0$ one obtains the solutions for the homogeneous waveguide. With increasing d the real $k_0 a$ decreases with the E_{0n} -modes and the imaginary $k_0 a$ increases with the E_0 -mode, i.e., the mode travels the slower, the higher d .



FIGURES 12 and 13. The eigenvalues $k_0 a$ with the E_{0n} -modes ($n=1,2,3,4$) and with the E_0 -mode ($k_0 a$ imaginary) in the disk loaded waveguide as a function of d for $D_2 = D_1$ and fixed $\beta_0 a$.

The presentation is to be thought of as periodically continued with the period 0.5 in the direction of increasing d/λ_0 .

As an example let us once more consider figure 12. All values $k_0 a > \beta_0 a = 5$ give no propagating modes, only statically attenuated fields. This is shown in figure 12 by cross-hatching.

Let us now study more closely the curve marked E_{01} . For $d=0$ there results $k_0 a = 2.4$, i.e., the eigenvalue of the E_{01} -mode in the homogeneous waveguide. With increasing d the quantity $k_0 a$ decreases (the mode travels more slowly) to reach finally zero for $d/\lambda_0 = 0.11$. The phase velocity of the mode now equals the velocity of light. The curve marked E_{01} can now be thought of as continued by the curve marked E_0 , i.e., the more d increases, the more the E_{01} -mode changes into the E_0 -mode whose phase velocity is less than the velocity of light. The guide now is for this mode a delay line, the eigenvalue $k_0 a$ is imaginary and increases with increasing d . With $d/\lambda_0 = 0.25$ the quantity $k_0 a = j\infty$. In the range $0.25 < d/\lambda_0 < 0.5$ no E_{01} -mode and no E_0 -mode are present. For $d/\lambda_0 > 0.5$ this repeats itself periodically with the period 0.5.

Let us now study closely the curve marked E_{02} . With $d=0$ there results $k_0 a = 5.52$, i.e., the eigenvalue for the E_{02} -mode in the homogeneous waveguide. With $k_0 a > \beta_0 a$ no propagating mode is possible, however. With increasing d the quantity $k_0 a$ decreases to attain finally the value 5 for $d/\lambda_0 = 0.12$ so that a propagating mode exists for $d/\lambda_0 > 0.12$. For $d/\lambda_0 = 0.25$ the quantity $k_0 a$ is 3.83 . The E_{02} -mode now has the same phase velocity as the H_{01} -mode. With a further increase of d the quantity $k_0 a$ finally changes for $d/\lambda_0 = 0.5$ into the eigenvalue of the E_{01} -mode in the homogeneous waveguide, i.e., $k_0 a = 2.4$. For $d/\lambda_0 > 0.5$ it is the E_{01} -curve shifted by $d/\lambda_0 = 0.5$ in a horizontal direction that continues the curve.

The curve marked E_{03} is of a similar shape; for $d=0$ there results from it the eigenvalue 3.65 of the E_{03} -mode, for $d/\lambda_0=0.5$ the eigenvalues 5.52 of the E_{02} -mode, and for $d/\lambda_0=1$ the eigenvalue 2.4 of the E_{01} -mode in the homogeneous waveguide. For $0.5 < d/\lambda_0 < 1$ the curve E_{02} shifted horizontally by $d/\lambda_0=0.5$ thus continues the curve. For $d/\lambda_0 > 1$ there follows subsequently the E_{01} -curve shifted by $d/\lambda_0=1$. The curve E_{04} , etc. runs correspondingly, and so on.

Fig. 13 shows the behavior of the guide for $\beta_0 a = 26.2$. Because of the large $\beta_0 a$, the E_{03} and E_{04} -modes are here capable of existence, in contrast to figure 12. Besides the E_{01} -mode changes into the E_0 -mode already for $d/\lambda_0=0.025$. With a waveguide radius $a=2.5$ cm a delay line thus comes about already for $d > 0.15$ mm. Such a depth of $d=0.15$ mm may result already by circular furrows due to roughing.

The figures 14 and 15 show the eigenvalues $k_0 a$ of the E_{0n} -modes and of the E_0 -mode as a function of the frequency (d/λ_0). The associated $\beta_0 a$ is also shown for each frequency. This gives a straight line through the origin. The higher the slope of this line, the smaller the ratio d/a (see the figs. 14 and 15). Above this straight line the real eigenvalues $k_0 a$ are greater than $\beta_0 a$ so that no propagating modes with real $k_0 a$ are here possible. The curves do not hold for any desired small values d/λ_0 , for the condition $\beta_0 a \gg 1$ is then no longer satisfied. Since $\beta_0 a$ here is a function of d/λ_0 , the figures 14 and 15 are no longer periodical, unlike the figures 12 and 13. This is most distinct with the values $k_0 a = 0$. The higher d/λ_0 , the more these values lie at $d/\lambda_0 = p \cdot 0.5$ ($p=1, 2, 3$, etc.).

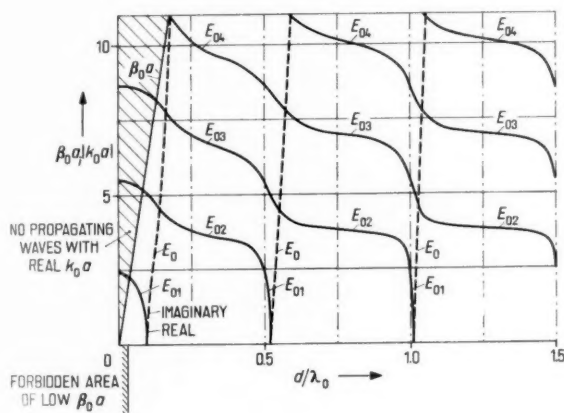
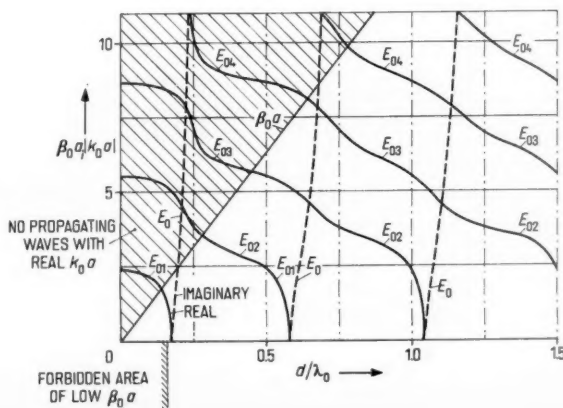


FIGURE 14. The eigenvalues $k_0 a$ with the E_{0n} -modes ($n=1,2,3,4$) and with the E_0 -mode ($k_0 a$ imaginary) in the disk loaded waveguide as a function of the frequency (d/λ_0) in the range $0.03 < d/\lambda_0 \leq 1.5$. Here $D_2 = D_1$; $d = a/10$; $a = 2.5$ cm.

FIGURE 15. The eigenvalues $k_0 a$ with the E_{0n} -modes ($n=1,2,3,4$) and with the E_0 -mode ($k_0 a$ imaginary) in the disk loaded waveguide as a function of the frequency (d/λ_0) in the range $0.16 < d/\lambda_0 \leq 1.5$. Here $D_2 = D_1$; $d = a/2$; $a = 2.5$ cm.



If we consider the range of validity of the curves in the figures 14 and 15, it is evident that d/λ_0 can always be so chosen that only one E_{0n} -mode is capable of existence. For example, in figure 14 ($d=a/10$) only the E_{01} -mode is capable of existence with $d/\lambda_0=0.08$. In figure 15 ($d=a/2$) only the E_{02} -mode is capable of existence for $0.28 < d/\lambda_0 < 0.45$.

If d/λ_0 is so chosen that the E_0 -mode is capable of existence, the ranges of validity of the figures 14 and 15 yield that in addition at least the E_{02} -mode is capable of propagation. This holds, for instance in figure 14, for the range $0.095 < d/\lambda_0 < 0.13$ and in figure 15 for $0.58 < d/\lambda_0 < 0.64$. For larger d/λ_0 the E_{03} -mode comes to these as well.

The figures 16 to 21 show in the region $0 \leq r \leq a$ the field configurations of the modes capable of existence at $\beta_0 a = 5$, $a = 2.5$ cm ($\lambda_0 = \pi$ cm), $D_2 = D_1$ for a number of d/λ_0 .

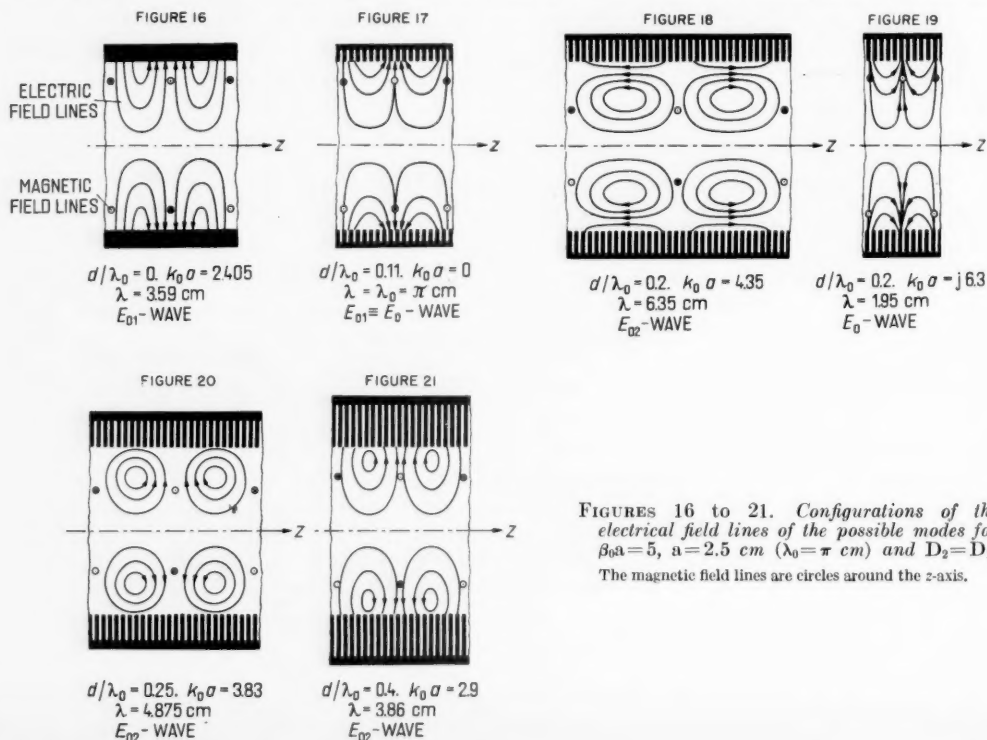
Figure 16 shows the well-known field configuration of the E_{01} -mode in the homogeneous waveguide. The guide wavelength λ exceeds the wavelength λ_0 in space. The electrical field is perpendicular to the surface $r=a$.

In figure 17 there is $d/\lambda_0 = 0.11$ and $\lambda = \lambda_0$. The electrical field is not perpendicular to the surface $r=a$.

The figures 18 and 19 show the field configurations with $d/\lambda_0 = 0.2$. Two solutions exist here for $k_0 a$, i.e., one for the E_{02} -mode and one for the E_0 -mode. With the E_{02} -mode there is $\lambda = 6.35$ cm, hence more than λ_0 (fig. 18) and with the E_0 -mode there is $\lambda = 1.95$ cm, hence less than λ_0 (delay line, fig. 19). Figure 18 does not represent the full field configuration of the E_{02} -mode in the homogeneous waveguide; the electrical field is here not perpendicular to the surface $r=a$. Figure 19 is similar to figure 17, but the wavelength is smaller.

Figure 20 shows the field configuration with $d/\lambda_0 = 0.25$. The eigenvalue $k_0 a$ is again associated with the E_{02} -mode and is 3.83. The wavelength is therefore $\lambda = 4.88$ cm and thus greater than λ_0 . Since the eigenvalue here agrees with that of the H_{01} -mode in the homogeneous waveguide, the electrical field configuration is here the same as that of the magnetic field with the H_{01} -mode.

Figure 21 shows the field configuration with $d/\lambda_0 = 0.4$. The wavelength is $\lambda = 3.86$ cm.



FIGURES 16 to 21. Configurations of the electrical field lines of the possible modes for $\beta_0 a = 5$, $a = 2.5$ cm ($\lambda_0 = \pi$ cm) and $D_2 = D_1$. The magnetic field lines are circles around the z -axis.

The electrical field is perpendicular to the surface $r=0.83a$, but no longer perpendicular to the surface $r=a$.

With the corrugated waveguide, which is often used in practice as a flexible guide section, $\beta_0 d$ always is very small. The eigenvalues $k_0 a$ therefore are near the eigenvalues χ_{0n} .

Corresponding to eq (13) there is then equated $k_0 a = \chi_{0n} + \Theta_E$. With $\epsilon_t = \epsilon_0$ and $\kappa \rightarrow \infty$ eq (20) yields

$$\Theta_E = -\frac{\beta_0 a}{\chi_{0n}} \frac{D_1}{D_1 + D_2} \tan \beta_0 d. \quad (81)$$

This reveals that a corrugated waveguide with the inner radius a has for the E_{0n} modes the same propagating constant and therefore the same field characteristic impedance as a homogeneous waveguide with the inner radius a^* , if

$$a = a^* \left(1 - \frac{\beta_0 a}{\chi_{0n}^2} \frac{D_1}{D_1 + D_2} \tan \beta_0 d \right). \quad (82)$$

If, for instance, $a = 2.5$ cm, $d = 0.1$ cm, $\lambda_0 = 4$ cm ($\beta_0 a = 3.93$), $D_1 = D_2$ there results for the E_{01} -mode $a = 0.946a^*$.

7. Appendix. Equation for Calculation of the Eigenvalue $k_0 a$

According to [7] part B, eqs (18) to (20) the following equation results with the ring-element guide for calculation of the eigenvalue $k_0 a$

$$\frac{k_E \epsilon_0}{k_0 \epsilon_z} \frac{J'_m(k_0 a)}{J_m(k_0 a)} + \frac{k_E \left[\frac{m\gamma}{a} \left(\frac{1}{k_0^2} - \frac{\mu_0}{\mu_p k_H^2} \right) \right]^2}{\omega^2 \mu_0 \epsilon_z \left[\frac{1}{k_0} \frac{J'_m(k_0 a)}{J_m(k_0 a)} + \frac{j}{k_H} \right]} = \frac{H_m^{(2)'}(p_E a) [PH_m^{(1)}(p_E b) - H_m^{(1)'}(p_E b)] + H_m^{(1)'}(p_E a) [H_m^{(2)'}(p_E b) - PH_m^{(2)}(p_E b)]}{H_m^{(2)}(p_E a) [PH_m^{(1)}(p_E b) - H_m^{(1)'}(p_E b)] + H_m^{(1)}(p_E a) [H_m^{(2)'}(p_E b) - PH_m^{(2)}(p_E b)]}, \quad (83)$$

$$P = \frac{k_E \epsilon}{k_2 \epsilon_z} \frac{H_m^{(1)'}(k_2 b)}{H_m^{(1)}(k_2 b)} + \frac{k_E \left[\frac{m\gamma}{b} \left(\frac{1}{k_2^2} - \frac{\mu_0}{\mu_p k_H^2} \right) \right]^2}{\omega^2 \mu \epsilon_z \left[\frac{1}{k_2} \frac{H_m^{(1)'}(k_2 b)}{H_m^{(1)}(k_2 b)} - \frac{j}{k_H} \frac{\mu_0}{\mu} \right]} \quad m=0, 1, 2, \text{ etc.} \quad (84)$$

where

$$k_H = (1-j) \sqrt{\frac{\omega \mu_0 \kappa_p}{2}}. \quad (85)$$

In the following the quantities $\mu_0/(\mu_p k_H^2)$ are neglected with respect to $1/k_0^2$ and $1/k_2^2$. With

$$|p_E a| \gg \begin{cases} 1 \\ m, \end{cases} \quad m=0, 1, 2, \text{ etc.} \quad (86)$$

there results then from the eqs (83) and (84)

$$\left(\frac{m\gamma}{k_0^2 a} \right)^2 = - \left[\frac{\beta_0}{k_0} \frac{J'_m(k_0 a)}{J_m(k_0 a)} + j \frac{Z_H}{Z_0} \right] \left[\frac{\beta_0}{k_0} \frac{J'_m(k_0 a)}{J_m(k_0 a)} + j \frac{Z_0}{Z_a} \right] \quad m=0, 1, 2, \text{ etc.} \quad (87)$$

where

$$\frac{Z_a}{Z_0} = j \frac{Z_E}{Z_0} \frac{P \tan p_E d - 1}{P + \tan p_E d}. \quad (88)$$

Under the assumption of the inequality (15) eq (27) is obtained from eq (88).

The eqs (83) and (84) yield

$$\left(\frac{m\gamma}{k_2 b}\right)^2 = -\left[\frac{\beta_2}{k_2} \frac{H_m^{(1)'}(k_2 b)}{H_m^{(1)}(k_2 b)} - j \frac{Z_H}{Z}\right] \left[\frac{\beta_2}{k_2} \frac{H_m^{(1)'}(k_2 b)}{H_m^{(1)}(k_2 b)} - j \frac{Z}{Z_i}\right] \quad \text{for } a \rightarrow 0, m=0, 1, 2, \text{ etc.} \quad (89)$$

where

$$\beta_2 = \beta_0 \sqrt{\frac{\mu \epsilon}{\mu_0 \epsilon_0}}, \quad (90)$$

$$Z = \sqrt{\frac{\mu}{\epsilon}} \quad (91)$$

$$Z_i = j Z_E \frac{J_m(p_E b)}{J'_m(p_E b)}. \quad (92)$$

A very similar equation may be obtained from the results of Wait [11] for a corrugated cylinder excited by a dipole.

8. Principal Symbols

ϵ_0 = dielectric constant of space,

μ_0 = permeability of space,

$Z_0 = \sqrt{\mu_0/\epsilon_0}$ = field impedance of space,

ϵ_i = dielectric constant of the dielectric in the corrugations,

ϵ = dielectric constant of the surrounding medium (can be complex),

μ = permeability of the surrounding medium (can be complex),

κ = conductivity of the metal,

a = inner radius of the guide,

b = outer radius of the guide,

$d = b - a$ = depth of the corrugations,

D_1 = width of the corrugations,

D_2 = spacing of the corrugations,

$D_1 + D_2$ = corrugation constant (analog to optics),

λ_0 = wavelength of a plane wave in space,

λ = wavelength of the guide modes,

$\beta_0 = \frac{2\pi}{\lambda_0}$ = phase constant of a plane wave in space,

$\gamma \equiv \pm j(\beta - j\alpha) = \pm j\beta_0 \sqrt{1 - (k_0/\beta_0)^2}$ = axial propagation constant of the waves on the guide,

$\beta = \frac{2\pi}{\lambda}$ = phase constant,

α = attenuation constant,

f = frequency,

$\omega = 2\pi f$ = angular frequency,

ϑ = equivalent thickness of the conducting layer of the metal,

r, φ, z = cylindrical coordinates,

v_p = phase velocity,

c = velocity of light,

$k_0 a$ = eigenvalue associated with the respective mode,

χ_{mn} =eigenvalue associated with the E_{mn} -mode in a lossless circular waveguide, i.e.,
 n -th not disappearing root of $J_m(\rho)$,

σ_{mn} =eigenvalue associated with the H_{mn} -mode in a lossless circular waveguide, i.e.,
 n -th not disappearing root of $J'_m(\rho)$,

J_m =Bessel function of m -th order,

J'_m =derivative of the Bessel function with respect to the argument,

$H_m^{(1)}$ =Hankel function of first kind and m -th order,

$H_m^{(2)}$ =Hankel function of second kind and m -th order,

$H_m^{(1)'}$, $H_m^{(2)'}$ =derivatives, with respect to the argument, of the Hankel functions of 1st and 2d kind,

$$p_E = k_E - js_E,$$

$$k_E = \beta_0 \sqrt{\epsilon_i / \epsilon_0},$$

$$s_E = \frac{1}{Z_0 D_1} \sqrt{\frac{\omega \mu_0}{2\kappa}} \sqrt{\frac{\epsilon_i}{\epsilon_0}}.$$

$$1N = \text{neper} = 8.7 \text{ db}.$$

9. References

- [1] F. E. Borgnis and C. H. Papas, Electromagnetic waveguides and resonators in encyclopedia of physics, edited by S. Flügge, Vol. XVI, Electric fields and waves, Springer-Verlag, Berlin-Göttingen-Heidelberg, p. 380-389 (1958).
- [2] C. C. Cutler, Bell Telephone Lab. Rept. No. M M 44-160-218 (1944).
- [3] E. L. Chu and W. W. Hansen, The theory of disk-loaded wave guides, J. Appl. Phys. **18**, 996 (1947).
- [4] L. Brillouin, Wave guides for slow waves, J. Appl. Phys. **19**, 1023 (1948).
- 5a) W. Rotman, A study of single-surface corrugated guides, Proc. IRE **39**, 952 (1951).
- 5b) J. R. Wait, Excitation of surface waves on conducting, stratified, dielectric-clad, and corrugated surfaces, J. Research NBS **59**, 365 (1957) RP 2807.
- [6] G. Piefke, Wellenausbreitung in der Scheiben-Leitung, Arch. elektr. Übertrag. **11**, 49 (1957).
- [7] G. Piefke, Die Übertragungseigenschaften einer Leitung aus axial angeordneten, voneinander isolierten Metallringen, Arch. elektr. Übertrag. **11**, 423 and 449 (1957).
- [8] G. Piefke, Wellenausbreitung in einem Blenden-Hohlleiter und einem gesickten Hohlleiter, Arch. elektr. Übertrag. **12**, 26 (1958).
- [9] G. Piefke, The transmission characteristics of a corrugated guide, IRE Trans. PGAP, **AP-7**, 183 (1959).
- [10] D. Marcuse, Über eine neuartige Oberflächen-Wellenleitung mit Bandpasseigenschaften, Arch. elektr. Übertrag. **11**, 146 (1957).
- [11] J. R. Wait, Radiation from an electric dipole in the presence of a corrugated cylinder, Appl. Sci. Research, **B6**, 117 (1955).

(Paper 64D 4-92)

Hi

Op
cation
requi
trans
inter
scatt
desig
lobe
meas
siting
arise
as a
radio
woul
which
for t

Th
beca
ards
comm
meas
desig
lobe-
be u
high
isties
dipol

At
butic
been

¹ Con
of Stan
² The
under s
Install
³ Fig

High-Gain, Very Low Side-Lobe Antenna With Capability for Beam Slewing^{1,2}

Alvin C. Wilson

(October 8, 1959; revised March 21, 1960)

A corner-reflector antenna having reflecting surfaces ten wavelengths wide and two wavelengths long was constructed, adjusted, and tested. The driven element was a collinear array of ten half-wave dipoles. Dolph-Chebyshev current distribution designed for side-lobe suppressions to -45 decibels was computed. The currents in the dipoles were adjusted as nearly as possible to this distribution. The phase of the dipole currents was graded so as to slew the main beam 10° off the forward direction. The radiation patterns were measured and found to be quite close to the computed.

Check of pattern stability with time and with changes in temperature and weather conditions showed it to be quite stable. Measurements of radiation pattern at frequencies departing from design frequency showed the operating bandwidth (determined by the preservation of the pattern) to be adequate for the applications likely to be considered for such antennas.

The half-power beam widths of the main lobe were 9.8° in the *E*-plane and 32° in the *H*-plane. On the basis of the measured beamwidths, the gain was calculated to be approximately 21.2 decibels relative to an isotropic radiator. The gain was experimentally measured to be 21.2 decibels.

1. Introduction

Operation of VHF ionospheric scatter communication services at frequencies below the *F*2 MUF requires, especially for high speed binary data transmission, special means to avoid long range interference, including self-interference from backscatter [1].³ The use of narrow beam antennas designed to suppress the radiation outside the main lobe by at least 40 db has been indicated as one measure for reducing such interference. In special siting situations, severe requirements occasionally arise for suppression of radiation outside the main lobe as a means of avoiding interference to neighboring radio services. Under some circumstances, there would be an advantage in having an antenna in which the main beam could be slewed to either side for taking advantage of meteor reflections.

The performance of corner-reflector antennas became of interest to the National Bureau of Standards because they appeared to be well suited to communication via ionospheric scatter. Previous measurements have shown that this antenna can be designed to have a high gain with very low secondary lobe-levels [2, 3]. A collinear array of dipoles may be used in a corner-reflector antenna to obtain higher gain and more desirable directive characteristics than are obtainable by the use of a single dipole in a corner reflector.

A method of determining the optimum current distribution in a collinear array of isotropic radiators has been described by C. L. Dolph [4]. The resultant

current distribution across the array is based on the properties of Chebyshev polynomials. When a Dolph-Chebyshev current distribution is used, the main beamwidth will be as narrow as possible for a predetermined side-lobe level; or, if the main beamwidth is specified, the side-lobe level will be a minimum.

When a collinear array of dipoles is used in a corner reflector, the resultant pattern is more directive than the array pattern for the collinear dipoles alone, and further reduction in levels of side lobes is achieved.

Computations were made to obtain the Dolph-Chebyshev current distributions to limit the side lobes 40 db below the main beam level and the resultant half-power beamwidth for collinear arrays of 6, 8, 10, 12, 14, and 16 half-wave dipoles spaced 0.5 and 0.8 wavelengths apart. Table 1 shows the relative current distribution and resultant main beam half-power beamwidth.

TABLE 1. Computed dipole current distribution and resultant half-power beamwidth of main lobe for Dolph-Chebyshev current distribution to limit all side lobes 40 db below main beam level

Number of dipoles in collinear array	Half-power beamwidth in degrees		Current distribution, decibels of attenuation relative to center elements							
	0.5λ spacing between dipole centers	0.8λ spacing between dipole centers	Dipole right and left from array center							
			1	2	3	4	5	6	7	8
6	23.6	15.0	0	4.2	14.0					
8	18.0	11.4	0	2.4	7.6	16.7				
10	14.5	9.2	0	1.5	4.7	10.0	18.1			
12	12.1	7.6	0	1.05	3.2	6.7	11.8	18.6		
14	10.3	6.4	0	0.76	2.3	4.8	8.3	13.1	18.9	
16	9.0	5.6	0	.58	1.8	3.6	6.2	9.6	14.2	18.9

¹ Contribution from Central Radio Propagation Laboratory, National Bureau of Standards, Boulder, Colo.

² The work reported herein was carried out on behalf of the U.S. Air Force, under support extended by U.S. Air Force Ground Electronics Engineering and Installation Agency, Rome, N.Y.

³ Figures in brackets indicate the literature references at the end of this paper.

In order to slew the main beam of a collinear array away from the forward direction, a change in the phase of current in the dipoles may be calculated for the desired amount of slewing.

The phase advance Φ_p of the current in a dipole p required to produce a slew angle β_0 off the broadside direction is given in degrees by

$$\Phi_p = -360 \frac{dp}{\lambda} \sin \beta_0$$

where dp is the distance of the dipole from the center of the array, taken as zero reference for phase. The negative sign signifies that the phase is retarded when the slew angle is in the direction of positive p .

Computations were made to obtain the radiation patterns for a collinear array of 16 half-wavelength dipoles, spaced a half-wavelength apart with the main beam slewed 0° , 10° , and 20° off from the forward direction. It was noted that, even with the beam slewed as much as 20° , the side lobes were still nearly 40 db down from the main beam level. Figure 1 presents these computed patterns.

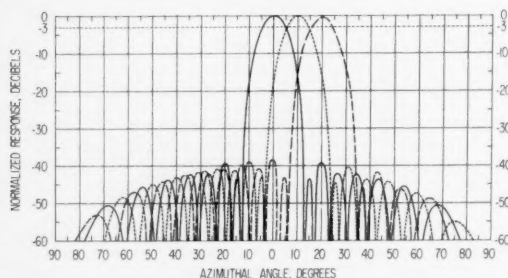


FIGURE 1. Computed radiation patterns in the E-plane of a collinear array of 16 half-wavelength dipoles spaced half-wavelength apart with a Dolph-Chebyshev current distribution computed to limit the side lobes below 40 db.

— Maximized in forward direction.
 --- Beam maximum 10° off forward direction.
 - · - Beam maximum 20° off forward direction.

The radiation patterns for a collinear array of 10 half-wavelength dipoles spaced 0.8λ apart in a corner reflector was computed. The aperture angle of the corner reflector was assumed to be 90° for purposes of computation, and the dipole position, distance to apex, 0.3 wavelength. Using a dipole current distribution to limit the side lobes 40 db below the main beam level, a main beamwidth at the half-power points of 9.2° was obtained. When the beam of this corner-reflector antenna is slewed by grading the phase of the dipole currents, the side lobes will not all be 40 db below the main beam level. With the beam slewed 10° , a high side lobe occurs at an azimuth of 68° in the direction opposite from slew; its level is 37 db below the main beam level. With the beam slewed 20° , the corresponding side lobe occurs at 56° with the response 17 db down from the main beam level. The high side lobes are actually secondary main lobes due to the dipole spacing being greater than a half-wavelength. Figure 2 shows the computed patterns for 0° , 10° , and 20° slew.

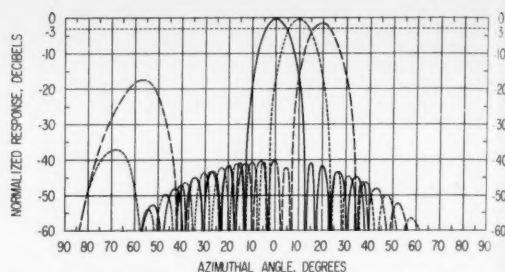


FIGURE 2. Computed radiation patterns of a 90° corner-reflector antenna using a collinear array of 10 half-wavelength dipoles as the driven element.

Dipoles spaced 0.8λ apart and 0.3λ from the apex. The dipole currents follow a Dolph-Chebyshev distribution computed to limit the side lobes below 40 db.

— Maximized in forward direction.
 --- Beam maximum 10° off forward direction.
 - · - Beam maximum 20° off forward direction.

A corner-reflector type of antenna with a Dolph-Chebyshev dipole current distribution was constructed, adjusted, and tested by the Boulder Laboratories of the National Bureau of Standards. The adjustments and tests were performed in two phases. The work performed in phase I consisted of the adjustments and measurements necessary to obtain side-lobe suppressions below -40 db. The work performed in phase II consisted of the adjustments and measurements necessary to slew the main beam 10° in addition to side-lobe suppressions below -40 db. Gain measurements were made for the antenna in both test phases.

The terminology employed here conforms to common usage. The width of the reflecting surfaces, W , is the dimension parallel to the apex line. The length, L , is measured along the direction normal to the apex line. The aperture angle, θ , is that formed by the two reflecting surfaces. The dipole position, S , is the distance of the driven element from the apex. The dipole spacing is measured between the dipole centers.

2. Experimental Procedure

On the basis of gains and radiation patterns obtained with corner-reflector structures having various combinations of lengths and widths of reflecting surfaces [2, 3] and on the basis of the computed radiation patterns for collinear arrays, a corner-reflector structure with reflecting surfaces 2 wavelengths long and 10 wavelengths wide and an aperture angle of 72° was constructed, adjusted, and tested with a Dolph-Chebyshev dipole current distribution to limit the side-lobe level.

The driven element was a collinear array of 10 half-wave dipoles spaced 0.8 wavelength center-to-center from each other and 0.45 wavelength from the apex of the corner-reflector structure.

The currents in the dipoles were initially adjusted to conform to the values determined for a Dolph-Chebyshev current distribution to limit the side lobes to -40 db. It was found, however, that small departures in current values, unavoidable in exper-

mental practice, would make the radiation pattern exceed this level by several decibels. The current distribution was then recomputed for -45-db level and the currents readjusted accordingly. These dipole currents, progressing right and left from array center, were 0, -1.7, -5.3, -11.1, and -20.4 db, respectively.

A main beam slew of 10° off from the forward direction was chosen for these measurements. For a slew angle of 10° and for 0.8λ dipole spacing, the progressive phase difference between adjacent dipoles comes to be equal to 50° . The phase of the dipoles to the right from center were progressively advanced 50° while those to the left were progressively retarded 50° .

Measurements of gain and radiation pattern were carried out using the antenna as a receiving antenna and observing precautions against antenna tilt and other sources of error as described in NBS Circular No. 598 [5].

3. Results

Figure 3 presents the radiation patterns of the antenna in the *E*- and *H*-planes for the tests performed in phase I. The *E*-plane patterns can be seen to have a half-power beamwidth of 9° and a -40-db beamwidth of 28° . Except for one point,

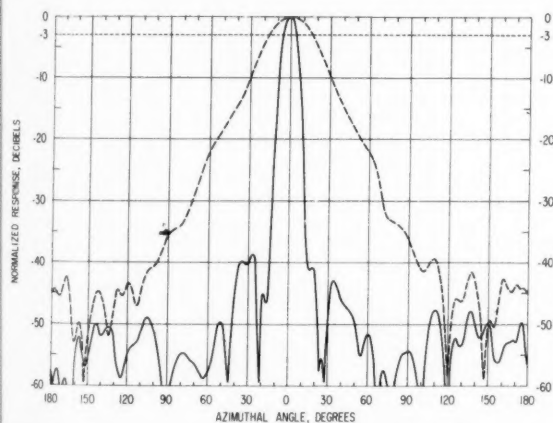


FIGURE 3. Radiation patterns in the *E*- and *H*-planes of a corner-reflector antenna using a collinear array of 10 half-wavelength dipoles as the driven element with a Dolph-Chebyshev current distribution to limit the side lobes.

Width of reflecting surfaces, $W/\lambda = 10$.
Length of reflecting surfaces, $L/\lambda = 2$.
Aperture angle, $\theta = 72^\circ$.
Dipole position, $S/\lambda = 0.45$.
Dipole spacing, 0.8λ .
— *E*-plane.
--- *H*-plane.

the secondary lobe level is everywhere below -40 db. At an azimuth angle of -26.5° , the level of one secondary lobe reached -39 db. The departures of experimental adjustments from theoretical could be maintained sufficiently small to remain within the -40-db level.

The radiation pattern of this antenna in the *H*-plane agrees very closely, as it should, with that

obtained using the same corner-reflector structure and a single half-wave dipole as the driven element (fig. 11 of ref. [3]). It should be noted that the radiation intensity in the 180° direction for the patterns in the two planes is not identical. This is explained by the fact that in making the measurement of the *H*-plane, due to the large width of the structure, one end of the corner reflector had to be suspended relatively close to the ground. The increase in the back radiation for the *H*-plane pattern is attributed to the resulting unbalance. Radiation levels of the order of -50 db are equivalent in intensity to 0.001 percent of those in the forward direction, and a small degree of unbalance is readily detectable at these levels.

Figure 4 presents the radiation pattern of the antenna in the *E*-plane after the adjustments described in phase II were completed. The main lobe is slewed 10° , as desired. The main beamwidth at the half-power points is approximately 9.8° .

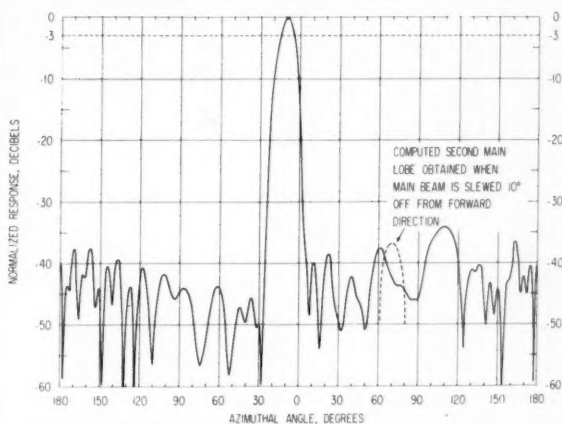


FIGURE 4. Radiation pattern in the *E*-plane of the corner-reflector antenna with the main beam slewed 10° off the forward direction.

Width of reflecting surfaces, $W/\lambda = 10$.
Length of reflecting surfaces, $L/\lambda = 2$.
Aperture angle, $\theta = 72^\circ$.
Dipole position, $S/\lambda = 0.45$.
Dipole spacing, 0.8λ .

The effect of the dipole factor and the use of the corner reflector aids in suppression of the side lobes, but not sufficiently to keep all of the side lobes below -45 db. A relatively high side lobe occurs at an approximate azimuth of 60° in the opposite direction from slew with a response 37 db down from maximum. This side lobe is actually another main lobe due to the dipole spacing used. It is believed that this lobe causes the high side lobe which appears in the back direction at an azimuth of approximately 110° due to the limited width of the corner-reflector structure. The computed second main lobe obtained from slewing the main beam 10° from the forward direction is shown as the dashed line in figure 4. This lobe was computed for a corner-reflector aperture angle of 90° instead of 72° and for a -40-db side-lobe level instead of -45-db level. Other high side lobes which occur near 180° are

probably a function of the corner-reflector structure. No further attempt was made to reduce these back-radiation lobes since they were already below the secondary lobe level at 110° . Except for a small side lobe at the base of the main lobe, all lobes in the vicinity of the main beam are below -40 db and even approach -45 db.

Measurements were carried out to determine the degree of cross polarization. Figure 5 presents these results. The curve shown as the solid line is a normal E -plane radiation pattern. The curve shown

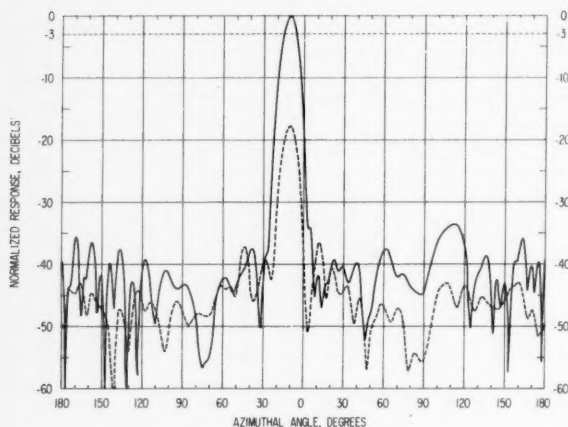


FIGURE 5. Radiation pattern in the E -plane and the cross polarization pattern in the same plane with the main beam slewed 10° off the forward direction.

— Normal E -plane pattern.
- - - Cross polarization pattern.

as the dashed line shows the cross polarization in the same plane. The main lobe of the cross polarization pattern is seen to be approximately 18 db below that of the normal pattern.

Measurements were made of the frequency sensitivity of the radiation pattern by taking patterns at 0.2-Mc/s intervals above and below the design frequency of 400 Mc/s. Figure 6 presents these patterns. As the frequency deviation became greater, the level of the side lobes near the base of the main beam increased. There was no measurable change in the back radiation or in the degree of beam slew.

Of considerable importance is the problem of electrical stability of the system with time. While the experimental measurements described were not designed with stability as the prime objective, measurements have been made on the antenna with adjustments left unchanged with time. Figure 7 shows radiation patterns recorded on three different days with adjustments not disturbed. The slight day-to-day changes appeared to be caused by weather conditions and temperature differences.

On the basis of the half-power beamwidths obtained for the H -plane from the radiation patterns of phase I and the E -plane from radiation patterns of phase II, the gain of the antenna over an isotropic radiator may be computed from the following [6]:

$$\text{Gain (db)} = 10 \log_{10} \frac{41,253}{W_E W_H}$$

$$\text{gain (db)} = 10 \log_{10} \frac{41,253}{9.8 \times 32}$$

$$\text{gain (db)} = 21.2.$$

This method of estimating the gain is most accurate when the main beam is narrow and the side lobes are minimum as is the case for this antenna. The gain was experimentally measured relative to a half-wave dipole. These measurements indicate a gain of 21.2 db over an isotropic radiator. This gain measurement was an average of three experimental measurements with maximum deviation ± 0.5 db.

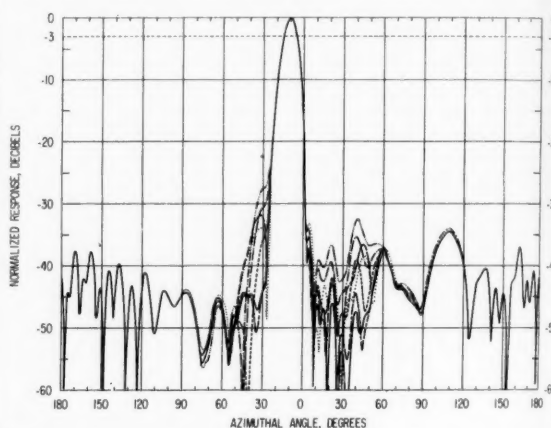


FIGURE 6. Effect of frequency changes on the radiation pattern.

— 400.60 Mc/s.
- - - 400.40 Mc/s.
- - - 400.20 Mc/s.
- - - 400.00 Mc/s.
- - - 399.80 Mc/s.
- - - 399.60 Mc/s.
- - - 399.40 Mc/s.

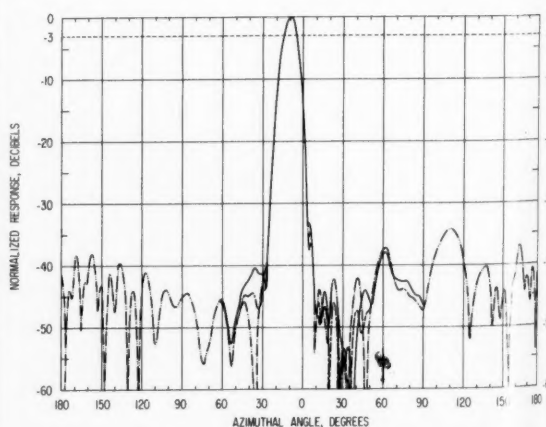


FIGURE 7. Stability of radiation pattern with time.

— Radiation pattern taken December 16, 1958.
- - - Radiation pattern taken December 17, 1958.
- - - Radiation pattern taken December 18, 1958.

4. Conclusions

The experimental work described shows that it is possible to approach in practice the results obtained theoretically for side-lobe suppression and beam slewing by using an array of collinear dipoles in a corner-reflector antenna. Compensation can be made for deviations of actual dipole currents from the theoretical currents by using a current distribution for -45 db to obtain in practice -40-db side-lobe suppression.

The corner-reflector antenna using a collinear array of dipoles as the driven element has been found to be a suitable antenna type for applications requiring a high gain, low secondary radiation levels, and a capability for beam slewing.

Beam slewing of more than 10° is practical, depending upon the tolerance for a secondary lobe at a large angle from the main lobe. To reduce this difficulty, the dipole spacing may be reduced. At 0.5λ dipole spacing, the secondary lobe is effectively eliminated, but mutual coupling between dipoles increases the problems of adjustment of current distribution and phase.

Full-scale operational antennas of this type are practical to construct and maintain. The desired

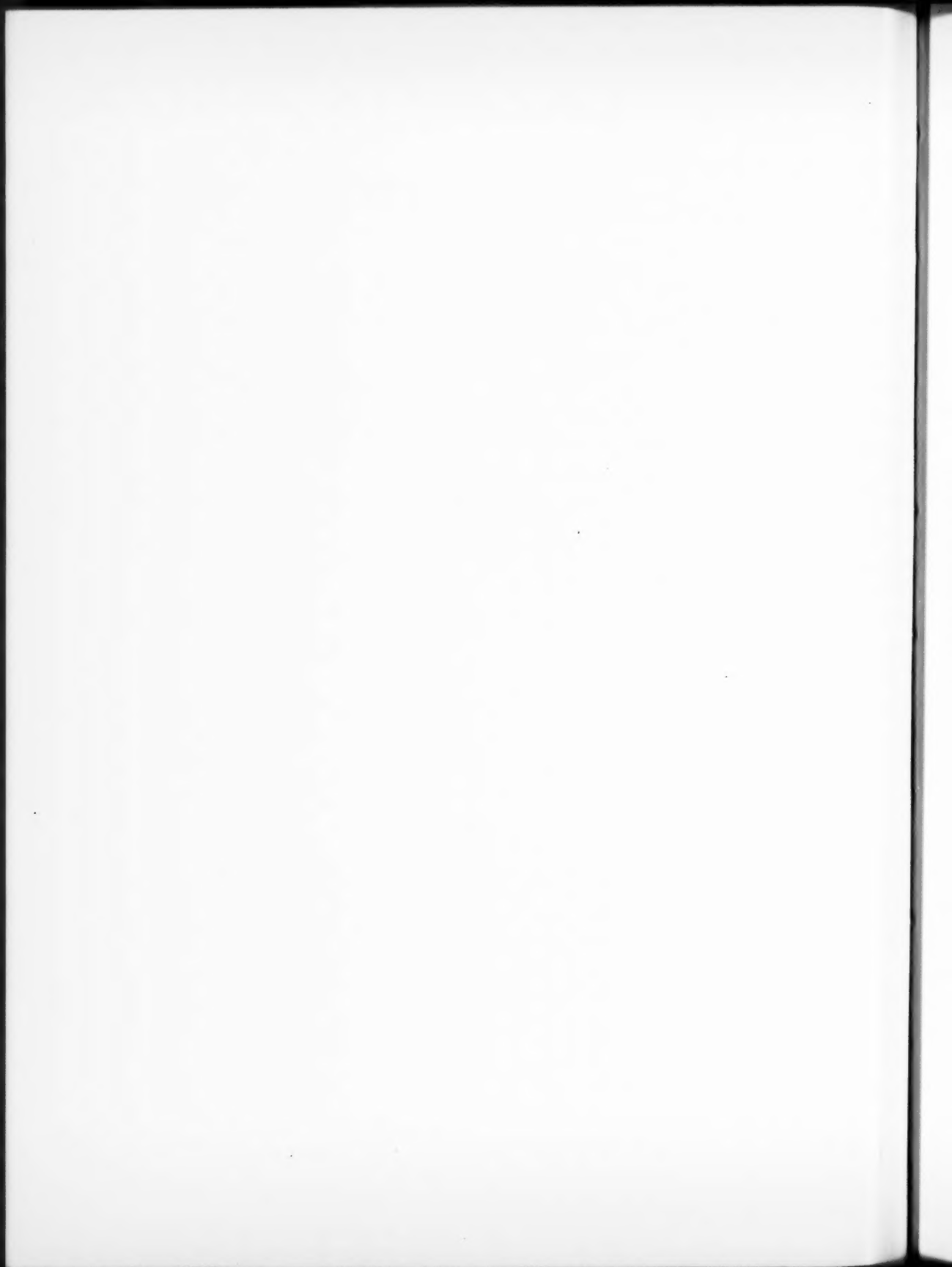
degrees of beam slew can be obtained by the use of properly adjusted plug-in current distribution networks. For purposes of initial adjustment and subsequent monitoring, a current sampling loop should be built into each dipole.

The measurements were carried out with the assistance of W. L. Martin.

5. References

- [1] R. C. Kirby, 1958 critique of VHF ionospheric scatter communication, Symp. Record, IRE-GWU Natl. Symp. on Extended Range and Space Commun. (1958).
- [2] H. V. Cottony and A. C. Wilson, Gains of finite-size corner-reflector antennas, IRE Trans. on Antennas and Propagation **AP-6**, 336 (1958).
- [3] A. C. Wilson and H. V. Cottony, Radiation patterns of finite-size corner-reflector antennas, IRE Trans. on Antennas and Propagation **AP-8**, 144 (1960).
- [4] C. L. Dolph, A current distribution for broadside arrays which optimize the relationship between beam width and side-lobe level, Proc. IRE **34**, 335 (1946).
- [5] H. V. Cottony, Techniques for accurate measurement of antenna gain, NBS Circ. 598 (1958).

(Paper 64D5-93)



Shielding of Transient Electromagnetic Signals by a Thin Conducting Sheet¹

N. R. Zitron²

(March 2, 1960)

The shielding effect of a thin, horizontal imperfectly conducting sheet against the transient field of a vertical magnetic dipole when excited by a ramp function is investigated. The results are calculated by taking Laplace transforms of the frequency spectrum functions for the steady-state problem. The response to the ramp function is calculated and the significance of the results in shielding against surges is discussed.

1. Introduction

The problem of shielding electrical equipment from transient signals emitted by high-powered radio transmitters is of practical interest. The response of a physical system to a transient electromagnetic excitation is usually in the form of a surge which decays after some time, leaving the steady fields. This paper deals with the shielding effect of a thin, infinite sheet of imperfectly conducting material against such surges.

Wait [1]³ has considered this problem in terms of a magnetic dipole excited by a step function. The purpose of this paper is to simulate more closely the building up of a surge by considering an excitation in the form of a ramp function. The ramp function takes into account the rise time of the signal, that is, the time required for the signal to rise from its initial value of zero to its peak value.

Wait [1] has calculated the response to a step function by taking Laplace transforms of the frequency spectrum functions obtained previously by a low-frequency approximation. He then suggested that the response to an arbitrary excitation may be obtained by means of the superposition theorem. Although the superposition theorem is elegant, it does not appear to offer any practical advantage over the transform method in the present problem, so the transform method is employed here.

2. Statement of the Problem

The situation considered is the excitation by a ramp function of a vertically oriented magnetic dipole above a thin, imperfectly conducting sheet. The object is to calculate the transient fields on the opposite side of the sheet with the aid of the frequency spectrum functions obtained previously by Wait [2, 3].

The magnetic dipole source is a loop antenna situated at the origin of a cylindrical coordinate system (ρ, ϕ, z). The axis of the loop of area dA (and of the dipole) is oriented in the z direction and has a total current I . The conducting sheet is centered in the plane $z = -a$ (fig. 1). Its thickness is d and its conductivity is σ .

The spectrum functions employed here are based upon a low-frequency approximation and, therefore, the distances a, ρ , and z , are assumed to be small compared to the wavelength. It is assumed also that $d \ll a$.

The low-frequency approximation, which restricts these considerations to thin, conducting sheets, was employed by Wait [2] to obtain the electric and magnetic fields as functions of frequency in order to simplify some extremely complicated expressions [3]. Once these

¹ Contribution from Gordon McKay Laboratory, Harvard University, Cambridge, Mass. This work was supported by AFWSP under Contract Nonr 1866(26) between the Office of Naval Research and Harvard University.

² Present address: Division of Engineering, Brown University, Providence 12, R.I.

³ Figures in brackets indicate the literature references at the end of this paper.

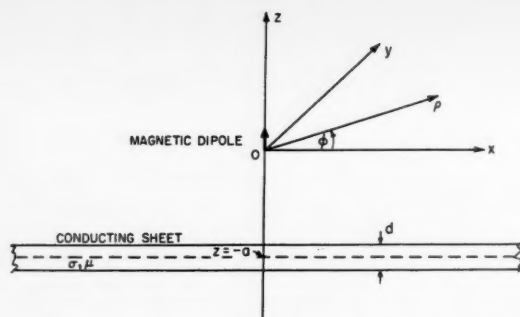


FIGURE 1. Shielded region.

fields have been obtained in the frequency domain, they are in accord with the material conditions and they may then be transformed into the time domain.

The spectrum functions for a harmonic dipole source having time dependence $e^{i\omega t}$ have been obtained by Wait [1]. The spectrum of the magnetic field is expressed as

$$H(i\omega) = -\text{grad } \psi(i\omega) = [H_\rho(i\omega), 0, H_z(i\omega)] \quad (1)$$

where the magnetic potential $\psi(i\omega)$ is given by

$$\psi(i\omega) = b \left[\frac{I(i\omega)z}{(z^2 + \rho^2)^{3/2}} + I(i\omega)i\omega \frac{\partial}{\partial z} \int_0^\infty \frac{e^{\lambda z} J_0(\lambda \rho)}{\lambda/\alpha + i\omega} d\lambda \right] \quad (2)$$

where $b = dA/4\pi$ and $\alpha = \sigma\mu d/2$ where $\mu = 4\pi \times 10^{-7}$ h/m.

It is appropriate at this point to differentiate under the integral sign in eq (2) in order to avoid the subsequent occurrence of an integral that does not exist. Equation (2) then becomes

$$\psi(i\omega) = b \left[\frac{I(i\omega)z}{(z^2 + \rho^2)^{3/2}} + I(i\omega)i\omega \int_0^\infty \frac{\lambda e^{\lambda z} J_0(\lambda \rho)}{\lambda/\alpha + i\omega} d\lambda \right]. \quad (3)$$

The frequency spectrum of the electric field is

$$E_\phi(i\omega) = -b u I(i\omega) i\omega \left[\frac{\rho}{(z^2 + \rho^2)^{3/2}} + i\omega \frac{\partial}{\partial \rho} \int_0^\infty \frac{e^{\lambda z} J_0(\lambda \rho)}{\lambda/\alpha + i\omega} d\lambda \right]. \quad (4)$$

The frequency spectrum of the current $I(i\omega)$ is the Laplace transform of the excitation $j(t)$. It is desirable for many applications to study the excitation occurring in a radio transmitter. When a transmitter is switched on, the signal is initially zero. It rises to its peak value after a certain time which will be called the rise time of the signal. It is convenient to simulate this excitation by means of a ramp function (fig. 2) which is defined as

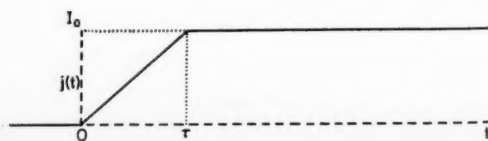
$$j(t) = \frac{I_0}{\tau} [tu(t) - (t-\tau)u(t-\tau)] \quad (4)$$

where $u(t)$ is the unit-step function

$$u(t) = \begin{cases} 0 & t < 0 \\ 1 & t > 0 \end{cases}$$

I_0 is the peak value of the current and τ is the rise time.

FIGURE 2. The ramp function.



The current spectrum of the ramp function is

$$I(i\omega) = \int_0^\infty j(t) e^{-i\omega t} dt = \frac{I_0}{\tau} \left[\frac{1}{(i\omega)^2} (1 - e^{-i\omega\tau}) \right]. \quad (6)$$

The spectrum functions of the magnetic potential (eq (3)) and the electric field (eq (4)) can now be written explicitly in terms of the frequency as follows:

$$\psi(i\omega) = b \frac{I_0}{\tau} (1 - e^{-i\omega\tau}) \left[\frac{1}{(i\omega)^2} \frac{z}{(z^2 + \rho^2)^{3/2}} + \frac{1}{i\omega} \int_0^\infty \frac{\lambda e^{\lambda z} J_0(\lambda \rho)}{\lambda/\alpha + i\omega} d\lambda \right] \quad (7)$$

and

$$E_\phi(i\omega) = b u \frac{I_0}{\tau} (1 - e^{-i\omega\tau}) \left[\frac{1}{i\omega} \frac{z}{(z^2 + \rho^2)^{3/2}} + \frac{\partial}{\partial \rho} \int_0^\infty \frac{e^{\lambda z} J_0(\lambda \rho)}{\lambda/\alpha + i\omega} d\lambda \right]. \quad (8)$$

The transient response to the ramp function is calculated by taking the inverse Laplace transform of the frequency spectrum. The transform over the frequency domain yields the behavior of the fields in the time domain. The inverse transforms $\psi(t)$ and $e_\phi(t)$ are defined by

$$\psi(t) = \frac{1}{2\pi i} \int_{c-i\infty}^{c+i\infty} \psi(i\omega) e^{i\omega t} d(i\omega), \quad (9)$$

and

$$e_\phi(t) = \frac{1}{2\pi i} \int_{c-i\infty}^{c+i\infty} E_\phi(i\omega) e^{i\omega t} d(i\omega), \quad (10)$$

The spectrum functions (eqs (7) and (8)) are transformed respectively into

$$\psi(t) = b I_0 \left[\frac{z}{(z^2 + \rho^2)^{3/2}} \frac{1}{\tau} (tu(t) - (t-\tau)u(t-\tau)) + \frac{1}{\tau\alpha} \left\{ \frac{u(t) - u(t-\tau)}{(z^2 + \rho^2)^{3/2}} - \frac{u(t)}{((-z + t/\alpha)^2 + \rho^2)^{3/2}} + \frac{u(t-\tau)}{((-z + \frac{t-\tau}{\alpha})^2 + \rho^2)^{3/2}} \right\} \right] \quad (11)$$

and

$$e_\phi(t) = -b \mu \frac{I_0}{\tau} \left[\frac{\rho}{(z^2 + \rho^2)^{3/2}} (u(t) - u(t-\tau)) - \frac{\rho u(t)}{((-z + t/\alpha)^2 + \rho^2)^{3/2}} + \frac{\rho u(t-\tau)}{((-z + \frac{t-\tau}{\alpha})^2 + \rho^2)^{3/2}} \right]. \quad (12)$$

It should be noted that the calculation of eq (11) is facilitated by the use of the shifting theorem [4]. The components of the magnetic field may be calculated from eqs (1) and (11). They are:

$$h_\phi(t) = b \frac{I_0}{\tau} \left[\frac{3\rho z(tu(t) - (t-\tau)u(t-\tau))}{(z^2 + \rho^2)^{5/2}} + \frac{\alpha\rho}{2} \left\{ \frac{u(t) - u(t-\tau)}{(z^2 + \rho^2)^{3/2}} - \frac{u(t)}{((-z + t/\alpha)^2 + \rho^2)^{3/2}} + \frac{u(t-\tau)}{((-z + \frac{t-\tau}{\alpha})^2 + \rho^2)^{3/2}} \right\} \right] \quad (13)$$

$$h_z(t) = b \frac{I_0}{\tau} \left[\frac{3z^2(tu(t) - (t-\tau)u(t-\tau))}{(z^2 + \rho^2)^{5/2}} + \frac{\alpha}{2} \left\{ \frac{-zu(t) - u(t-\tau)}{(z^2 + \rho^2)^{3/2}} - \frac{(-z + t/\alpha)u(t)}{((-z + t/\alpha)^2 + \rho^2)^{3/2}} + \frac{u(t-\tau)(-z + \frac{t-\tau}{\alpha})}{((-z + \frac{t-\tau}{\alpha})^2 + \rho^2)^{3/2}} \right\} \right]. \quad (14)$$

The components of the electric and magnetic fields, eqs (12), (13), and (14) may be decomposed into more elementary units whose physical significance will be explained. In particular,

$$h_p(t) = A_p(t) + B_p(t) + C_p(t) + D_p(t)$$

$$h_z(t) = A_z(t) + B_z(t) + C_z(t) + D_z(t)$$

$$e_\phi(t) = B_\phi(t) + C_\phi(t) + D_\phi(t)$$

where

$$A_p(t) = b \frac{I_0}{\tau} \frac{3\rho z}{(z^2 + \rho^2)^{5/2}} [tu(t) - (t-\tau)u(t-\tau)]$$

$$B_p(t) = b \frac{I_0 \alpha \rho}{\tau} \frac{u(t) - u(t-\tau)}{(z^2 + \rho^2)^{3/2}}$$

$$C_p(t) = -b \frac{I_0 \alpha \rho}{\tau} \frac{u(t)}{((-z + t/\alpha)^2 + \rho^2)^{3/2}}$$

$$D_p(t) = b \frac{I_0 \alpha \rho}{\tau} \frac{u(t-\tau)}{\left(\left(-z + \frac{t-\tau}{\alpha}\right)^2 + \rho^2\right)^{3/2}}$$

$$A_z(t) = b \frac{I_0}{\tau} \frac{3z^2}{(z^2 + \rho^2)^{5/2}} [tu(t) - (t-\tau)u(t-\tau)]$$

$$B_z(t) = b \frac{I_0 \alpha}{\tau} \frac{(-z)[u(t) - u(t-\tau)]}{(z^2 + \rho^2)^{3/2}}$$

$$C_z(t) = -b \frac{I_0}{\tau} \frac{(-z + t/\alpha)u(t)}{((-z + t/\alpha)^2 + \rho^2)^{3/2}}$$

$$D_z(t) = b \frac{I_0}{\tau} \frac{u(t-\tau)\left(-z + \frac{t-\tau}{\alpha}\right)}{\left(\left(-z + \frac{t-\tau}{\alpha}\right)^2 + \rho^2\right)^{3/2}}$$

$$B_\phi(t) = -\mu b \frac{I_0}{\tau} \frac{\rho}{(z^2 + \rho^2)^{3/2}} [u(t) - u(t-\tau)]$$

$$C_\phi(t) = \mu b \frac{I_0}{\tau} \frac{\rho u(t)}{((-z + t/\alpha)^2 + \rho^2)^{3/2}}$$

$$D_\phi(t) = -\mu b \frac{I_0}{\tau} \frac{\rho u(t-\tau)}{\left(\left(-z + \frac{t-\tau}{\alpha}\right)^2 + \rho^2\right)^{3/2}}$$

The significance of these terms may be explained as follows:

The $A(t)$ terms may be regarded as primary field terms. They represent the fields that would be produced in the absence of the conducting sheet. Their time behavior is the same as that of the source.

The $B(t)$, $C(t)$, and $D(t)$ terms represent surges resulting from the presence of the sheet. A closer examination of $B(t)$, $C(t)$, and $D(t)$ reveals the following:

$B(t)$ and $D(t)$ have the same signs but act in different time intervals. $B(t)$ acts in the interval $0 \leq t \leq \tau$, i.e., during the rise of the excitation, while $D(t)$ acts in the interval $\tau \leq t < \infty$, i.e., after the excitation has reached its peak value.

The $C(t)$ terms are opposite in sign to the $B(t)$ and $D(t)$ terms and are smaller in magnitude for $t > 0$. They may be regarded as cancellation terms which modify the surge terms $B(t)$ and $D(t)$. An examination of eqs (12), (13), and (14) shows that the $C(t)$ terms decrease monotonically in the interval $0 \leq t \leq \tau$. Since the $B(t)$ terms are constant in the interval $0 \leq t \leq \tau$, the cancellation becomes progressively weaker during the rise of the excitation. The surges reach their maxima at time $t = \tau$, since the cancellation is weakest here. At this time the total fields are

$$h_p(\tau) = bI_0 \left[\frac{3\rho z}{(\rho^2 + z^2)^{5/2}} + \frac{\alpha\rho}{2} \left\{ \frac{1}{(z^2 + \rho^2)^{3/2}} - \frac{1}{((-z + \tau/\alpha)^2 + \rho^2)^{3/2}} \right\} \right] \quad (15)$$

$$h_z(\tau) = bI_0 \left[\frac{3z^2}{(\rho^2 + z^2)^{5/2}} + \frac{\alpha}{2} \left\{ \frac{-z}{(z^2 + \rho^2)^{3/2}} - \frac{(-z + \tau/\alpha)}{((-z + \tau/\alpha)^2 + \rho^2)^{3/2}} \right\} \right] \quad (16)$$

$$e_\phi(\tau) = -\mu bI_0 \left[\frac{\rho}{(z^2 + \rho^2)^{3/2}} - \frac{\rho}{((-z + \tau/\alpha)^2 + \rho^2)^{3/2}} \right] \quad (17)$$

After $t = \tau$, $B(t)$ is replaced by $D(t)$. $C(t) \rightarrow 0$ and $D(t) \rightarrow 0$ in such a way that the surge fields die out and only the primary fields remain.

An examination of eqs (15), (16), and (17) shows that the surge in h_p is opposite in sign to the primary field (for $z < 0$) and thus serves to reduce it. The surge in h_z , on the other hand, is the same as that of the primary field and thus increases the total field. The electric field term e_ϕ consists only of a surge. The primary field is zero. It can be seen, in terms of the parameter τ/α , that the cancellation term $C(t)$ will be reduced for large values of τ/α and thus the surge will have a greater effect for longer rise times and for thinner or more poorly conducting sheets. The low-frequency approximation on which these results are based restricts these considerations to values $\tau/\alpha \gg z$ and does not permit a discussion of small rise times or thick conducting sheets.

Attempts to deal with thicker sheets have led to complicated integrals. Other authors such as Wait [3], Lowndes [5], Bhattacharyya [6], Gordon [7], and Price [8] have attempted to integrate expressions involving rational functions and exponential arising in such problems. They have been forced to make highly restrictive assumptions. Further work in this direction would appear to be desirable.

The transient response of a horizontal dipole is similar to that of the loop.

The author thanks Professor R. W. P. King for calling this problem to his attention and for many helpful discussions.

3. References

- [1] J. R. Wait, Shielding of a transient electromagnetic dipole field by a conducting sheet, *Can. J. Phys.* **34**, 890 (1956).
- [2] J. R. Wait, Induction in a conducting sheet by a small current-carrying loop, *Appl. Sci. Research* **B3**, 230 (1953).
- [3] J. R. Wait, The magnetic dipole over the horizontally stratified earth, *Can. J. Phys.* **29**, 577 (1951).
- [4] B. van der Pol and H. Bremmer, *Operational calculus* (Cambridge University Press, Cambridge, England, 1950).
- [5] J. S. Lowndes, A transient magnetic dipole source above a two-layer earth, *Quart. J. Mech. Appl. Math.* **10**, 79 (1957).
- [6] B. K. Bhattacharyya, Electromagnetic induction in a two-layer earth, *J. Geophys. Research* **60**, 279 (1955).
- [7] A. N. Gordon, The field induced by an oscillating magnetic dipole outside a semi-infinite conductor, *Quart. J. Mech. Appl. Math.* **4**, 106 (1951).
- [8] A. T. Price, Electromagnetic induction in a semi-infinite conductor with a plane boundary, *Quart. J. Mech. Appl. Math.* **3**, 385 (1950).

(Paper 64D5-94)

E
for
fall
1.
tion
point
in t
quin
gral
not
radi
tive
men
cess
seco
beco
2.
vert
with
as u
Stor
not
able
Stor
equ
ture
rath
proc
elen
ous
Nei
serie
W
whi
don
as 8
with

¹ C
This
² F

Cylindrical Antenna Theory¹

R. H. Duncan and F. A. Hinchey

(February 15, 1960; revised May 2, 1960)

A partial survey of cylindrical antenna theory pertaining to a tubular model with a narrow gap is presented. The survey includes discussion of the theories of Hallén, King and Middleton, Storm, and Zuhrt. A conceptual relation between theory and experiment is described. The latter part of the article is concerned with a new Fourier series solution of the Hallén equation. This solution is developed in such a way that the expansion coefficients are the unknowns of a system of linear equations. The elements of the coefficient matrix are given by a highly convergent series. Numerical results are given for half and full wavelength antennas with half length to radius ratios of 60 and 500π . These results compare quite closely with those obtained from King-Middleton theory.

1. Introduction

Existing solutions to Hallén's integral equation for the current distribution on cylindrical antennas fall into two main categories [1, 2]:²

1. Iterative solutions which use an approximation to cylindrical antenna current as a starting point. Successive iterations generate improvements in the original assumption. Approximations are required at some stage in the process if tractable integrals are to be obtained. The approximations are not severe if h/a , the ratio of antenna half length to radius, is large. Impedances obtained from iterative solutions are in good agreement with experiments performed on thin antennas. Although successful, iterative solutions become laborious beyond second or third order, and the approximations become suspect in the case of thick structures.

2. Solutions in which the integral equation is converted into a set of linear simultaneous equations with Fourier coefficients of the current distribution as unknowns. Typical of these are the theories of Storm and Zuhrt. (Strictly speaking, Zuhrt did not solve Hallén's integral equation, but one derivable from a somewhat different point of view.) Storm approximated matrix elements in his set of equations so that his theory is limited to thin structures. In addition, Storm's theory contains two rather fundamental errors which, acting in concert, produce fortuitous results. Zuhrt obtained matrix elements by graphical integration, a sufficiently tedious process to limit his calculations to low order. Neither of these solutions fully exploits the Fourier series technique for obtaining the current distribution.

We have obtained a solution similar to Storm's in which computation of matrix elements can be easily done with high accuracy even for h/a ratios as low as 8 or 10. Matrix inversion is easily accomplished with modern digital computers so that solutions of

high order are feasible. We have carried out calculations to 25th order for half and full wavelength antennas with h/a ratios of 60 and 500π . Results from the King-Middleton iterative solution compare favorably to ours so that their work for $h/a \geq 60$ has been checked by comparison with an exact theory.

Although this paper is principally concerned with developing a Fourier series solution, a reasonably complete treatment of iterative solutions is included in an attempt to provide a self-contained account of cylindrical antenna theory. Even with this aim in mind, the treatment of iterative solutions, as well as the theories of Storm and Zuhrt, is sufficiently involved that the reader is referred to the original work for many of the details.

2. Statement of the Problem

Vector potential as a function of position, $\vec{A}(\vec{r})$, is given in terms of a current distribution, $\vec{J}(\vec{r})$, by the expression

$$\vec{A}(\vec{r}) = \frac{\mu}{4\pi} \iiint \vec{J}(\vec{r}_0) \frac{e^{-jk|\vec{r}-\vec{r}_0|}}{|\vec{r}-\vec{r}_0|} dV_0 \quad (2.1)$$

The vector integration in (2.1) must be taken over all sources of the vector potential field and it is this requirement that causes a direct solution of a realistic antenna problem to be exceedingly difficult. In the case of a cylindrical antenna the integration would have to include currents in the antenna, the feeding transmission line, and the oscillator which supplies power to the antenna-transmission line assembly. Every possible combination of antenna, transmission line and driving generator would have to be treated as a special case and a mathematical solution of any given case would by itself be formidable. An idealized problem can be extracted from this situation by consideration of an extremely thin walled tube of infinite conductivity with a narrow circumferential gap corresponding to the antenna terminal zone.

¹ Contribution from New Mexico State Univ., University Park, N. Mex. This work was carried out under P.O. 15-0079 from Sandia Corp.

² Figures in brackets indicate the literature references at the end of this paper.

Choosing the conventional cylindrical coordinates, (ρ, ϕ, z) , the antenna is defined by $\rho = a$ and $|z| \leq h$.

A purely hypothetical generator is assumed such that the electric field in the gap is azimuthally symmetric. The voltage across the gap is defined by

$$V = - \int_{\text{gap}} E_z dz, \quad (2.2)$$

where E_z is the z -component of electric field at $\rho = a$. E_z is zero outside the gap since the simplifying assumption of perfectly conducting tube walls has been made. If the gap width is decreased as V is held constant, we must express E_z by

$$E_z = -V\delta(z) \text{ for } |z| \leq h, \quad (2.3)$$

where $\delta(z)$ is the usual delta function. Center-fed models will be considered here although this restriction can be removed.

The value of electric field anywhere in space is given by

$$E = -\text{grad } \Phi - j\omega\bar{A}, \quad (2.4)$$

where Φ is the scalar potential. (Time dependence proportional to $e^{j\omega t}$ is assumed in all of the relationships used here.) Scalar potential can be found from the Lorentz condition

$$\Phi = \frac{j}{\omega\mu\epsilon} \text{div } \bar{A}. \quad (2.5)$$

The combination of a tubular model without end caps and the assumption of a symmetric field leads to the conclusion that only the z -component of \bar{A} is different from zero since all of the current sources on the tubular surface will be in the z -direction. Equations (2.4) and (2.5) can be combined to give

$$E_z = -\frac{j}{\omega\mu\epsilon} (\partial^2 A / \partial z^2 + k^2 A), \quad (2.6)$$

where the symbol A without the vector bar simply stands for A_z , and $k^2 = \omega^2\mu\epsilon$. In general A is a function of both z and ρ . If the operator $(\partial^2 / \partial z^2 + k^2)$ is applied to $A(z, \rho)$ and then ρ is taken at the antenna surface, we obtain

$$\partial^2 A_s / \partial z^2 + k^2 A_s = \frac{\omega\mu\epsilon}{j} V\delta(z), \quad (2.7)$$

an equation for the surface value of vector potential valid for $|z| \leq h$. Solutions of the homogeneous equation, $\partial^2 A_s / \partial z^2 + k^2 A_s = 0$, are simply $\cos kz$, $\sin kz$, e^{jkz} or e^{-jkz} . Linear combinations of these solutions may be used to build a solution to (2.7). Thus,

$$A_s = C_1 \cos kz + D_1 \sin k|z|, \quad (2.8)$$

or

$$A_s = C_2 \cos kz + D_2 e^{-jk|z|}. \quad (2.9)$$

These solutions are completely equivalent. How-

ever, we prefer (2.9) as a basis for studying certain properties of the infinite cylinder. D_1 and D_2 are evaluated by substituting these solutions into (2.7) and performing the indicated operations with due account being taken of the discontinuous derivatives of $\sin k|z|$ and $e^{-jk|z|}$. The results are $D_1 = (\omega\mu\epsilon V)/2jk$ and $D_2 = (\omega\mu\epsilon V)/2k$. Then

$$A_s = C_1 \cos kz + \frac{\omega\mu\epsilon V}{jk} \frac{1}{2} \sin k|z|, \quad (2.10)$$

$$A_s = C_2 \cos kz + \frac{\omega\mu\epsilon V}{k} \frac{1}{2} e^{-jk|z|}. \quad (2.11)$$

Since $e^{-jk|z|}$ can be written as $\cos kz - j \sin k|z|$, it is easily shown that $C_1 = C_2 + \omega\mu\epsilon V/2k$. Either expression may be used, the choice between them being only a matter of taste.

Under the assumptions being made, the current distribution of the general formula (2.1) degenerates to a surface distribution, $K(z_0)$. It must be borne in mind that the tube has both inner and outer surfaces, and $K(z_0)$ is the sum of current densities on both surfaces. The field point, \bar{r} , can be taken at the surface of the cylinder $\rho = a$ so that an alternate formula for A_s is

$$A_s = \frac{\mu}{4\pi} \int_{-h}^{+h} \int_{-\pi}^{\pi} K(z_0) \frac{e^{-jk|\bar{r}_s - \bar{r}_0|}}{|\bar{r}_s - \bar{r}_0|} a dz_0 d\phi_0, \quad (2.12)$$

where \bar{r}_0 ranges over the antenna surface during the course of the integration.

Several changes in notation are convenient at this point. The field point is (a, z, ϕ) and the source point has the coordinates (a, z_0, ϕ_0) . Only the difference $\phi - \phi_0$ is of any significance because of the azimuthal symmetry. Therefore, we may set ϕ to zero, change ϕ_0 to ϕ and indicate the angular integration as already performed. The quantity z_0 is changed to ζ so that the subscripts may be avoided in future formulas. Total current is given by $I(\zeta) = 2\pi a K(\zeta)$. The quantity $|\bar{r}_s - \bar{r}_0|$ is replaced simply by R . With these changes

$$A_s = \frac{\mu}{4\pi a} \int_{-h}^{+h} I(\zeta) g(z - \zeta) d\zeta, \quad (2.13)$$

where

$$g(z - \zeta) = \frac{1}{2\pi} \int_{-\pi}^{\pi} \frac{e^{-jkR}}{R} d\phi \quad (2.14)$$

and

$$R = [4a^2 \sin^2 \phi / 2 + (z - \zeta)^2]^{1/2}. \quad (2.15)$$

We now have two formulas for the surface value of vector potential. One has been derived from the generic formula for vector potential in terms of current sources by specializing to the geometry of the problem under consideration. As such it is a general formula for vector potential generated by a ϕ -symmetric current in the z -direction on a tubular conductor no matter what other conditions are to be imposed on the problem. On the other hand, (2.10) provides a vector potential which leads to the

boundary values of electric field desired in the present problem. If these expressions are equated, an integral equation for the current distribution associated with the chosen boundary conditions results:

$$\frac{\mu}{4\pi} \int_{-h}^{+h} I(\xi) g(z-\xi) d\xi = C_1 \cos kz + \frac{\omega\mu\epsilon}{jk} \frac{V}{2} \sin k|z|. \quad (2.16)$$

It is convenient to multiply the previous equation through by $jk/\omega\mu\epsilon$ and make the following definitions:

$$C = \frac{jkC_1}{\omega\mu\epsilon}, \quad \frac{jk}{\omega\mu\epsilon} \frac{\mu}{4\pi} = \frac{j}{4\pi} (\mu/\epsilon)^{1/2} = \frac{jZ_0}{4\pi}$$

and

$$\frac{jZ_0}{4\pi} I(\xi) = f(\xi).$$

No generality is lost by letting $V=1$. This completes the mathematical formulation of the problem. We are to consider the solution of

$$\int_{-h}^{+h} f(\xi) g(z-\xi) d\xi = C \cos kz + \frac{1}{2} \sin k|z|, \quad |z| \leq h. \quad (2.17)$$

The constant C must be determined by the boundary condition $f(\pm h)=0$.

There is no doubt that the integral equation corresponds exactly to the chosen model. It has already been pointed out that the model does not correspond to any physically realizable antenna. Physical antennas may be either solid or tubular conductors, and they may or may not be fed in such a way as to preserve ϕ -symmetry. Lack of symmetry (as exemplified by a linear antenna fed by a two wire line) can be rationalized to some extent if ka is small. However, the most serious point is the highly idealized nature of the generator region of the mathematical model. The infinitesimal gap is really a short circuit across which a hypothetical but finite voltage has been impressed. Thus, the input current and admittance of the model are certainly infinite.

It is not immediately clear that an infinite admittance model can be managed mathematically in such a way as to yield a physically significant finite result. Wu and King have discussed this point in a recent paper [3]. They have shown that the singularity in $I(z)$ near $z=0$ is logarithmic and of very short range. Thus, according to Wu and King, "since . . . the singularity actually gives a contribution to the current distribution only in an exceedingly small and physically meaningless distance of the order of magnitude $h \exp(-1/ka)$, it may, in principle simply be subtracted out." According to this line of reasoning iterative solutions of the integral equation are successful because they are started with a continuous approximating function and are carried to such low order that the singularity does not develop.

An important aspect of any theory is its relationship to experiment. It is possible to avoid the inherent singularity in the current distribution which

is a solution to Hallén's integral equation and obtain a finite answer for the theoretical input admittance to a cylindrical antenna. The finiteness of the result does not, however, guarantee that it is physically significant. Experimental antennas must be provided with a realistic terminal zone which is connected to a transmission line of some sort. Measured impedances are then complex combinations of antenna and terminal zone effects. One way of extricating these effects is to make a theoretical correction for terminal zone effects on a sequence of experimental impedances and extrapolate the corrected data to the limit of a small terminal zone. The residual impedance is then supposed to be characteristic of the antenna itself and it is this idealized inference from experiment rather than raw data which is to be compared with theory.

An outline of a feasible experimental program will be helpful at this point. Consider the experimental arrangement shown in figure 1. Symmetry allows

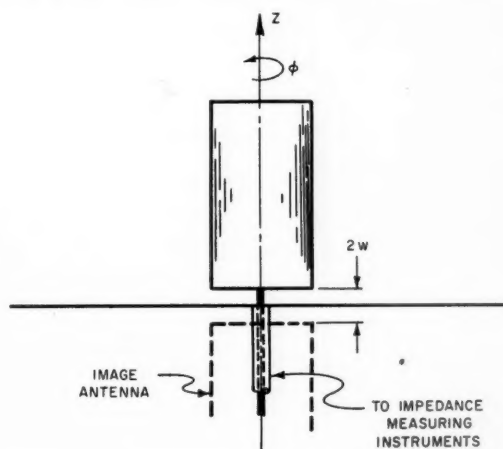


FIGURE 1. Experimental model of a cylindrical antenna.

us to place a large ground plane at $z=0$ and simulate half of a center fed antenna. Measuring instruments are located below the ground plane so that the antenna is shielded from extraneous interaction with the apparatus. Appropriate measurements are made so that the experimenter can determine Z_T , the equivalent impedance terminating the coaxial line. It should be possible to relate Z_T to parameters of the radial transmission line and to $Z_a(w)$, the input impedance of a cylindrical antenna with gap width $2w$. If so, one should be able to calculate $Z_a(w)$ given measurements of Z_T . $Z_a(w)$ can be extrapolated to obtain $Z_a(0)$. $Z_a(0)$ obtained in this way is independent of the terminal configuration actually used. We will not attempt to give a mathematical treatment of the experimental situation. It is sufficient for our purposes to establish a conceptual foundation for relating theory to experiment as a prelude to subsequent theoretical development.

Consider now the sense in which a Fourier series solution for $I(z)$ "subtracts the singularity." Since

the unknown function in (2.17) is even, it is developed to finite order as

$$f_N(\xi) = \frac{F_0}{2} + \sum_{n=1}^{n=N} F_n \cos n\pi\xi/h. \quad (2.18)$$

A procedure for determining the F_n will be exhibited later. At this point it is sufficient to recall that the sum of a finite number of terms of a Fourier series fits the function being described in a least squares sense. Specifically,

$$Q^2 = \int_{-h}^{+h} |f_N(\xi) - f(\xi)|^2 d\xi \quad (2.19)$$

is a minimum when the coefficients of $f_N(\xi)$ are Fourier coefficients. Intense, short range variations cannot contribute appreciably to $f_N(\xi)$ unless N is made so large that even the singular behavior of $f(\xi)$ begins to develop.

A numerical estimate of the range of the singularity is worthwhile at this point. Consider an antenna for which $kh = \pi/2$ and $h = 60a$. Then $ka \sim .025$ and $1/ka \sim 40$. Substitution of these numbers into the range estimate of Wu and King leads to the conclusion that a continuous function can fit the current distribution except in a small distance equal to about he^{-40} . Even if the thickness is increased until $h = 10a$ the singularity is important only over a range of about $he^{-6.5} \sim .0015h$. Thus it can be seen that $f(0)$ as given by

$$f(0) = \frac{F_0}{2} + \sum_{n=1}^{n=N} F_n \quad (2.20)$$

will be apparently well-behaved in calculations of practically feasible order even though theoretical considerations indicate that the infinite series must diverge.

An extraneous feature of the theoretical model becomes apparent when it is compared to a proposed experimental model. Current on the inner surface of the theoretical model near the feed point is replaced by current associated with a realizable terminal zone in the experimental model. If ka is less than 2.61a, tube modes are below cutoff and are rapidly damped out [4]. Formulas for removing the inner current near $z=0$ from the total current, which is a solution to the integral equation, will be presented later. As might be expected, the correction makes a small difference in theoretical antenna admittance.

Once the singularity near $z=0$ and the tube current are understood and properly removed from the theory the remaining possibilities for refinement are somewhat limited and consist, for the most part, of removing the assumption of an infinitesimally thin, perfectly conducting tube. Such considerations would be supererogatory in view of the many successes of infinite conductivity models in electromagnetic theory.

3. Solution for the Infinite Cylinder

In subsequent work the current distribution on a finite antenna is expanded in a Fourier series. Such an expansion cannot be valid for a function containing a singularity unless the singularity is integrable. One expects that $I(z)$ is singular in the neighborhood of the delta generator and that the nature of the singularity is independent of antenna length. It can be imagined that the current on a finite antenna is composed of waves emanating from the feedpoint and waves reflected from the ends of the antenna. Only the outgoing waves are expected to be singular at $z=0$ since they are directly associated with the delta generator. It is instructive to consider the case of the infinite cylinder before proceeding with the solution for a finite antenna. This case can be solved exactly in integral form and the Fourier transform of the current identified from the solution. Asymptotic behavior of the transform gives a clue to the nature of $I(z)$ near $z=0$ even for the finite antenna.

Consider now the integral equation formed by equating (2.11) and (2.13),

$$\frac{\mu}{4\pi} \int_{-h}^{+h} I(\xi) g(z-\xi) d\xi = C_2 \cos kz + \frac{\omega\mu\epsilon}{k} \frac{V}{2} e^{-jk|z|}. \quad (3.1)$$

If h becomes infinite there is no mechanism for the formation of standing waves on the cylinder. In that event C_2 may be set to zero. The integral equation becomes

$$\frac{Z_0}{2\pi} \int_{-\infty}^{+\infty} I(\xi) g(z-\xi) d\xi = V e^{-jk|z|}; |z| < \infty. \quad (3.2)$$

Solution of this equation is easy if we are armed with the identities

$$g(z-\xi) = -\frac{j}{2} \int_{-\infty}^{+\infty} J_0(\beta a) H_0^{(2)}(\beta a) e^{j\alpha(z-\xi)} d\alpha, \quad (3.3)$$

and

$$e^{-jk|z|} = \frac{j}{2\pi} \int_{-\infty}^{+\infty} \frac{2ke^{j\alpha z}}{(\alpha+k)(\alpha-k)} d\alpha. \quad (3.4)$$

The parameter β is given by

$$\beta = (k^2 - \alpha^2)^{1/2}. \quad (3.5)$$

Each integral is taken in the complex plane of α along the real axis from $-\infty$ to $+\infty$ with a downward indentation at $\alpha = -k$ and an upward indentation at $\alpha = +k$.

The Fourier transform of $I(z)$ is

$$\hat{I}(\alpha) = \frac{1}{\sqrt{2\pi}} \int_{-\infty}^{+\infty} I(\xi) e^{-j\alpha\xi} d\xi. \quad (3.6)$$

This definition and the identities for $g(z-\xi)$ and

$e^{-jk|z|}$ lead to

$$\int_{-\infty}^{+\infty} J_0(\beta a) H_0^{(2)}(\beta a) \hat{I}(\alpha) e^{j\alpha z} d\alpha = \frac{4kV}{\sqrt{2\pi}Z_0} \int_{-\infty}^{+\infty} \frac{e^{-j\alpha z} d\alpha}{\beta^2} \quad (3.7)$$

If (3.7) is to be true for all z ,

$$\hat{I}(\alpha) = \frac{4kV}{\sqrt{2\pi}Z_0} \frac{1}{\beta^2 J_0(\beta a) H_0^{(2)}(\beta a)} \quad (3.8)$$

Then the solution of (3.2) is

$$I(z) = \frac{2kV}{\pi Z_0} \int_{-\infty}^{+\infty} \frac{e^{j\alpha z}}{\beta^2 J_0(\beta a) H_0^{(2)}(\beta a)} d\alpha \quad (3.9)$$

Since $e^{j\alpha z}$ is the only factor in the integrand containing an odd part, (3.9) becomes

$$I(z) = \frac{4kV}{\pi Z_0} \int_0^{+\infty} \frac{\cos \alpha z}{\beta^2 J_0(\beta a) H_0^{(2)}(\beta a)} d\alpha \quad (3.10)$$

We have defined β as follows:

$$\begin{aligned} \beta^2 &= k^2 - \alpha^2, \\ \beta &= |\beta| \text{ for } \alpha < k \text{ and} \\ \beta &= -j|\beta| \text{ for } \alpha > k. \end{aligned} \quad (3.11)$$

Therefore, for large α

$$\beta = -j\alpha. \quad (3.12)$$

Certain identities involving cylindrical functions are required:

$$\begin{aligned} J_0(-j\alpha a) &= I_0(-\alpha a) = I_0(\alpha a), \\ H_0^{(2)}(-j\alpha a) &= -H_0^{(1)}(j\alpha a) = -\frac{2}{j\pi} K_0(\alpha a), \end{aligned} \quad (3.13)$$

$$I_0(\alpha a) \rightarrow \frac{e^{\alpha a}}{(2\pi\alpha a)^{1/2}}, \text{ and}$$

$$K_0(\alpha a) \rightarrow (\pi/2\alpha a)^{1/2} e^{-\alpha a}.$$

For the definition of cosine transforms we take

$$I_c(\alpha) = \sqrt{\frac{2}{\pi}} \int_0^{+\infty} I(z) \cos \alpha z dz. \quad (3.14)$$

Equations (3.10) through (3.14) imply that, for large α

$$\hat{I}_c(\alpha) \rightarrow 2j \frac{\sqrt{2\pi}kaV}{Z_0} \frac{1}{\alpha}. \quad (3.15)$$

Inspection of tables of cosine transforms [5] reveals that when a function behaves as $\ln z$ for small z , its cosine transform behaves as $-\sqrt{\pi/2} \alpha^{-1}$ for large α . It follows that for small enough z

$$I(z) \simeq -j \frac{4kaV}{Z_0} \ln kz. \quad (3.16)$$

In the above expression k has been selected as a multiplier for $|z|$ to make the argument of the logarithmic function a pure number. The asymptotic behavior of $\hat{I}_c(\alpha)$ is of no help in deciding whether or not k is a proper choice for this parameter. However, k seems attractive since it is given by $k=2\pi/\lambda$, and the wavelength is a natural unit of length in radiation problems.

There is also a somewhat obscure reason for choosing k as a parameter to convert $|z|$ to nondimensional form. Consider another version of (3.15) in which the parameter k is retained as α is allowed to become large. As soon as α becomes greater than k , $\hat{I}_c(\alpha)$ becomes a pure imaginary, $J_0(\beta a)$ and $H_0^{(2)}(\beta a)$ go over to $I_0(|\beta|a)$ and $(-2/j\pi) K_0(|\beta|a)$. Then using asymptotic forms,

$$\hat{I}(\alpha > k) \rightarrow j \frac{2\sqrt{2\pi}kaV}{Z_0} \frac{1}{(\alpha^2 - k^2)^{1/2}}. \quad (3.17)$$

$\hat{I}_c(\alpha)$ can now be regarded as having been separated into two parts: $\hat{I}_c(\alpha < k)$ which is zero if $\alpha > k$ and $\hat{I}_c(\alpha > k)$ which is zero if $\alpha < k$. Only $\hat{I}_c(\alpha > k)$ is of interest at present since it is responsible for the singularity in $I(z)$. Now $\hat{I}_c(\alpha > k)$ is asymptotically proportional to the transform of the Neumann function, $Y_0(kz)$. The latter contains a singular part which is proportional to $\ln kz$.

If the above arguments in favor of choosing (3.16) for the form of the singularity are acceptable, we can proceed with an estimate of the range over which this expression is a good approximation to antenna current. For this purpose we require an estimate of $I(z)$ outside the range in which the logarithmic function is dominant. It is difficult to obtain such an estimate from (3.10). However, an alternative argument can be constructed. It is known that an expression of the form $I_m \sin k(h-|z|)$ is a fair approximation to current on a finite antenna over most of its length. It is convenient, rather than necessary, to use knowledge of the finite length antenna in estimating the range of the singularity. We now arbitrarily establish the criterion that the logarithmic function is to be used in the range $|z| < \eta$ where η is given by

$$-\frac{4kaV}{Z_0} \ln k\eta \sim |I_m|. \quad (3.18)$$

$|I_m|$ is of the order of 0.01 when $V=1$. Z_0 is of the order of 400. An order of magnitude estimate for η is

$$\eta \sim \frac{\lambda}{2\pi} e^{-1/ka}. \quad (3.19)$$

This is a small fraction of a wavelength even for quite thick antennas. Moderately large changes in

$|I_m|$ do not affect this conclusion appreciably.

Further examination of this question would require analytic or numerical inversion of (3.10). Either approach is apparently formidable.

4. Iterative Solutions for Finite Antennas

A brief discussion of iterative solutions is provided here as background for the general reader. We are primarily interested in presenting a critique of the approach rather than compiling a report on the voluminous literature of the cylindrical antenna problem. Consequently, the presentation omits many points which are essential to a detailed understanding of the iterative method. It does present a few features which require comment by way of justifying additional consideration of finite antenna theory.

The first task is to cast eq (2.17) into a form suitable for iteration. To that end the quantity

$$f(z)\psi(z) = \int_{-h}^h f(z)w(z, \xi) d\xi \quad (4.1)$$

is added and subtracted to the left hand side of (2.17). It is convenient to abbreviate by letting

$$C \cos kz + \frac{1}{2} \sin k|z| = P(z). \quad (4.2)$$

With these changes and some elementary transpositions, (2.17) can be written

$$f(z) = \frac{1}{\psi(z)} \left\{ P(z) - \int_{-h}^h [f(\xi)g(z-\xi) - f(z)w(z, \xi)] d\xi \right\}. \quad (4.3)$$

Assuming that $w(z, \xi)$ has been selected, a program for obtaining a solution is:

1. Substitute an approximation to $f(z)$ under the integral on the right hand side of (4.3). Denote this zeroth order approximation by $f_0(z)$. Carry out the indicated integrations to obtain $f_1(z)$ and adjust C so that $f_1(+h) = 0$.

2. Repeat, using $f_1(z)$ to generate $f_2(z)$. Readjust C so that $f_2(+h) = 0$.

In principle this process may be continued indefinitely with the formula for the N th approximation being

$$f_N(z) = \frac{1}{\psi(z)} \left\{ P(z) - \int_{-h}^h [f_{N-1}(\xi)g(z-\xi) - f_{N-1}(z)w(z, \xi)] d\xi \right\} \quad (4.4)$$

subject to $f_N(+h) = 0$, which defines C_N , the N th approximation to C .

Equation (4.4) is formally true for any $w(z, \xi)$. However, it will clearly be to the advantage of the investigator to make a choice which results in rapid convergence of the iterative process. This matter is the *raison d'être* of much of the literature of

linear antenna theory. A choice which leads to manageable integrals is

$$w_H(z, \xi) = \frac{1}{[a^2 + (z - \xi)^2]^{1/2}}. \quad (4.5)$$

Then

$$\psi_H(z) = \int_{-h}^{+h} \frac{d\xi}{[a^2 + (z - \xi)^2]^{1/2}}. \quad (4.6)$$

The kernel $g(z - \xi)$ as given by (2.14) and (2.15) is difficult to handle. A manageable but crude approximation is

$$g(z - \xi) = \frac{e^{-jk|z - \xi|}}{|z - \xi|}. \quad (4.7)$$

If $g(z - \xi)$ is approximated to this order it is appropriate to approximate $w_H(z - \xi)$ to the same order when it is used in the integrals on the right hand side of (4.4), but not in the calculation of $\psi_H(z)$. Then

$$f_N(z) = \frac{1}{\psi_H(z)} \left\{ P(z) - \int_{-h}^h \frac{f_{N-1}(\xi)e^{-jk|z - \xi|} - f_{N-1}(z)}{|z - \xi|} d\xi \right\} \quad (4.8)$$

becomes the fundamental equation of the iterative program. Equation (4.8) has been used by Hallén in the investigation of linear antenna theory [6].

Equation (4.8) can be criticized on two counts. First, the approximation involved in replacing k by simply $|z - \xi|$ is quite severe. Secondly, $w(z, \xi)$ was chosen for its simplicity rather than according to the requirement that the iterative program produce good results in low order. King and Middleton improved the iterative procedure outlined above in that they used a kernel distance

$$R_1 = [a^2 + (z - \xi)^2]^{1/2}. \quad (4.9)$$

This is a better approximation to R than is the quantity $|z - \xi|$.

The second modification introduced by King and Middleton comes from considering the combination of integrals on the right hand side of (4.3). Denote these by

$$Q(z) = \int_{-h}^h [f(\xi)g(z - \xi) - f(z)w(z, \xi)] d\xi. \quad (4.10)$$

$Q(z)$ can be rewritten as

$$Q(z) = \int_{-h}^h [f(\xi) - f(z)W(z, \xi)] g(z - \xi) d\xi. \quad (4.11)$$

A $W(z, \xi)$ which makes the integrand of (4.11) vanish is

$$W(z, \xi) = f(\xi)/f(z). \quad (4.12)$$

Of course, one cannot know the desired $W(z, \xi)$ because $f(z)$ is not yet known. One can, however, approximate $W(z, \xi)$ by making use of a fair low order approximation to $f(z)$. A suitable choice of $f(z)$ in this case is the sinusoidal approximation to antenna current.³

Instead of $W(z, \xi)$ King and Middleton introduce

$$W_K(z, \xi) = \frac{\sin k(h - |\xi|)}{\sin k(h - |z|)}, \quad (4.13)$$

with the attendant

$$\psi_K(z) = \int_{-h}^h W_K(z, \xi) \frac{e^{-jkR_1}}{R_1} d\xi. \quad (4.14)$$

Using these definitions the iterative program is based on

$$f_N(z) = \frac{1}{\psi_K(z)} \left\{ P(z) - \int_{-h}^h [f_{N-1}(\xi) - f_{N-1}(z)W_K(z, \xi)] \frac{e^{-jkR_1}}{R_1} d\xi \right\}. \quad (4.15)$$

Equations (4.8) and (4.15) are not quite the forms used by Hallén and King-Middleton in their computational programs. To appreciate the need for some improvement consider the boundary condition $f(+h) = 0$ applied to (4.4) from which (4.8) and (4.15) were developed. The result of applying the boundary condition is

$$0 = P(h) - \int_{-h}^h f_{N-1}(\xi) g(h - \xi) d\xi. \quad (4.16)$$

(The term involving $f_{N-1}(z)$ drops out because the boundary condition is applied at each iteration.) Now, $P(h)$ contains $C \cos kh$ and if $kh = \pi/2$, the constant C disappears completely and (4.16) cannot be satisfied. A revision of the theory to overcome this defect can be made by subtracting (4.16) from (4.4) to obtain

$$f_N(z) = \frac{1}{\psi(z)} \left\{ P(z) - P(h) + \int_{-h}^h f_{N-1}(\xi) g(h - \xi) d\xi - \int_{-h}^h [f_{N-1}(\xi) g(z - \xi) - f_{N-1}(z) w(z, \xi)] d\xi \right\}. \quad (4.17)$$

The condition $f_N(+h) = 0$ is always automatically satisfied by (4.17). Equation (4.16) is forced to hold for all N so that C is determined by

$$0 = P(h) - \int_{-h}^h f_N(\xi) g(h - \xi) d\xi. \quad (4.18)$$

A zeroth order approximation which satisfies boundary conditions can be obtained directly from

(4.17) by omitting the integrals. Then

$$f_0(z) = \frac{P(z) - P(h)}{\psi(z)}. \quad (4.19)$$

Additional notation and definitions may be invented so that the result of the iterative process can be cast into series form. The series can be designed to lead off with $f_0(z)$ as given by (4.19). A sufficient basis for the remaining part of our discussion has been displayed at this point.

A noteworthy criticism of the use of R_1 has been present by Gans [7]. Gans correctly points out that

$$\int_{-h}^h f(\xi) \frac{e^{-jkR_1}}{R_1} d\xi = C \cos kz + \frac{1}{2} \sin k|z| \quad (4.20)$$

is not a true equation because the right hand side has discontinuous derivatives in z whereas the derivatives of the left hand side are continuous.

Hallén claims immunity from Gans' criticism on the grounds that he uses the distance $|z - \xi|$. It seems to us that this practice raises another difficulty. A development similar to that used in examining the singularity in $f(\xi)$ shows that $g(z - \xi)$ is logarithmic near $z - \xi = 0$. The approximate kernel $|z - \xi|^{-1} \exp(-jk|z - \xi|)$ has an entirely different kind of singularity. It is extremely doubtful if the Hallén theory develops a solution to the original integral equation.

These considerations lead to a definite statement that

$$f(z) \neq \lim_{N \rightarrow \infty} f_N(z) \quad (4.21)$$

where $f_N(z)$ is taken from either the Hallén or King Middleton form of the theory and $f(z)$ is the correct solution of (4.3). Even though one is compelled to this conclusion, it is completely irrelevant because it is entirely possible for

$$f(z) \simeq f_N(z) \quad (4.22)$$

in low order. If any confusion exists about this matter it is because many writers (including some authors of senior and graduate level texts) begin their discussion directly with eq (4.20). The only correct procedure is to formulate a problem which is soluble in principle and to introduce judicious approximations as needed during the course of solution.

Iterative solutions have the disadvantage that they become tedious in second and third order even if approximations are made. High-order solutions with approximate kernels are not even desirable as they may have nothing to do with the original problem. When all is considered, one needs to know over what range of antenna parameters such solutions can be used with confidence. Obviously, the kernels used in Hallén and King-Middleton theory approximate $g(z - \xi)$ over a range comparable to antenna length only if h/a is large. The point at which these theories

³ A choice of $f(z)$ to serve in constructing $W(z, \xi)$ and $\psi(z)$ need not influence the choice of $f_N(z)$ which is used to start the iterative process.

break down is somewhat arbitrary since it must depend upon an arbitrarily selected amount of tolerable error.

5. Fourier Series Solutions of Storm and Zuhrt

One disadvantage of the iterative solutions discussed in section 1 is that they become extremely tedious beyond second or third order. Storm attempted to invent a theory which could be extended to higher order [8]. Unfortunately, he introduced the kernel distance $R_1 = [a^2 + (z - \zeta)^2]^{1/2}$ and studied

$$\int_{-h}^h f(\zeta) \frac{e^{-jkR_1}}{R_1} d\zeta = C \cos kz + \frac{1}{2} \sin k|z| \quad (5.1)$$

which has, in fact, no solution at all. "Solutions" to (5.1) are physically meaningful only if they apply to sufficiently thin antennas and if they are restricted to low order. In addition, Storm's theory contains fundamental errors which invalidate his solution no matter what kernel distance is used.

Storm expands the unknown function in the form

$$f(\zeta) = B \sin k(h - |\zeta|) + \sum_{n=0}^{n=N} F_n \cos(2n+1)\pi\zeta/2h. \quad (5.2)$$

Since $f(\zeta)$ is an even function the expansion also represents $f(\zeta)$ in the range $-h \leq \zeta \leq 0$.

Following Storm, we seek to determine the coefficients B and F_n of the above expansion. The result of substituting (5.2) into (5.1) is

$$M_0(z)B + \sum_{n=0}^{n=N} S_n(z)F_n = C \cos kz + \frac{1}{2} \sin k|z|, \quad (5.3)$$

where

$$M_0(z) = \int_{-h}^h \sin k(h - |\zeta|) \frac{e^{-jkR_1}}{R_1} d\zeta, \quad (5.4)$$

$$S_n(z) = \int_{-h}^h \cos \frac{(2n+1)\pi\zeta}{2h} \frac{e^{-jkR_1}}{R_1} d\zeta. \quad (5.5)$$

The integrals in (5.4) and (5.5) are somewhat difficult to evaluate unless approximations are made. Storm replaces the kernel with $|z - \zeta|^{-1} \exp(-jk|z - \zeta|)$ outside the range $z - 5a < \zeta < z + 5a$. Inside this range he replaces the kernel by $[a^2 + (z - \zeta)^2]^{-1/2}$. These ranges are ambiguous if z is within $5a$ of the ends of the antenna since ζ must also be restricted to the range $-h \leq \zeta \leq h$. Presumably we are not to consider values of z too close to the ends of the antenna in what follows. Once the approximations are made, the integrations required in (5.4) and (5.5) can be performed in terms of elementary functions. We shall omit the details and return to consideration of (5.3).

Storm explicitly satisfies (5.3) at $N+2$ points and obtains $N+2$ equations in $N+2$ unknowns which

TABLE 1

kh	Storm: 5 point calculation	King-Middleton
$\pi/2$	$Z_s = 81.5 + j 44.5$ $Z_i = 1162 - j 1354$	$Z_{KM} = 81.5 + j 43.4$ $Z_{KM} = 1000 - j 1350$

are B , C , and N of the F_n . He has performed calculations with $N=0, 1, 2$, and 3 for both full and half wavelength antennas with $h/a=904$. The agreement with King-Middleton iterative theory is remarkable. A comparison between the impedances from the latter theory with those from Storm's five-point calculation is made in table 1. King-Middleton data used in this comparison are second order except for the resistance in the half wavelength case which is third order.

In spite of the success of Storm's calculation, his theory breaks down in higher order or for smaller h/a ratios. The difficulties are made more evident if we specify the unknown function by the expansion

$$f(\zeta) = B \sum_{n=0}^{n=N} A_n \cos \frac{(2n+1)\pi\zeta}{2h} + \sum_{n=0}^{n=N} F_n \cos \frac{(2n+1)\pi\zeta}{2h}, \quad (5.6)$$

where the A_n are the first N terms of an expansion of $\sin k(h - |\zeta|)$. As such the A_n are known explicitly. It is clear that (5.6) approaches (5.2) as N becomes large. If (5.6) is used for $f(\zeta)$, (5.4) must be changed to

$$M'_0(z) = B \int_{-h}^h \frac{e^{-jkR_1}}{R_1} \left\{ \sum_{n=0}^{n=N} A_n \cos \frac{(2n+1)\pi\zeta}{2h} \right\} d\zeta. \quad (5.7)$$

The definition of $S_n(z)$ does not change. The new equation to be satisfied is

$$M'_0(z)B + \sum_{n=0}^{n=N} S_n(z)F_n = C \cos kz + \frac{1}{2} \sin k|z|. \quad (5.8)$$

Set aside, for the moment, the question of how C is to be determined and consider the solution in terms of C . A set of linear simultaneous equations for the unknowns B, F_0, F_1, \dots, F_N is obtained by satisfying (5.8) at $(N+1)$ values of z . The matrix of coefficients is

$$\begin{vmatrix} M'_0(z_1) & S_0(z_1) & S_1(z_1) & \dots & S_N(z_1) \\ M'_0(z_2) & S_0(z_2) & S_1(z_2) & \dots & S_N(z_2) \\ \vdots & \vdots & \vdots & \ddots & \vdots \\ M'_0(z_N) & S_0(z_N) & S_1(z_N) & \dots & S_N(z_N) \end{vmatrix}$$

By comparing (5.5) and (5.7), one sees that the $M_0(z_m)$ are linear combinations of the $S_n(z_m)$. The determinant of the above matrix is identically zero for any N . If the left hand column is replaced by $M_0(z_m)$ so that all of $B \sin k(h-|z|)$ is used, the determinant of the matrix must approach zero as N becomes large. No high order solution can be obtained unless one of the unknowns is assigned an arbitrary value. A likely candidate for the assignment is B which can be selected from the elementary induced emf theory according to $B = (jZ_0/4\pi)I_m$.

Evidently, Storm did not become aware of these difficulties because he included C among the unknowns. If this is done and the matrix is augmented by appropriate bordering elements, a system of equations with a unique solution for every N results. However, the value of C which is obtained may not be the correct one. Storm's expansion for $f(z)$ is identically zero at the boundaries. If the coefficients, F_n , of that expansion are calculated in terms of a spurious C it may happen that the expansion (for large N) does not approach zero at the boundaries even though it is identically zero at $z = \pm h$. The only way out of this dilemma is to expand the current in functions which are not identically zero at $z = \pm h$ and then use the boundary condition $f(\pm h) = 0$ to determine C .

An actual calculation to support these criticisms is worthwhile. In performing the calculation we used the theory of the next section which is equivalent to a corrected version of Storm's theory even though several of the technical details are quite different. Storm was followed to the extent that $f(\xi)$ was expanded in the set $\{\cos(2n+1)\pi\xi/2h\}$, and C was treated as an independent unknown. A structure with $h/a = 60$ was selected for study. The results are shown in figure 2 which displays the real and

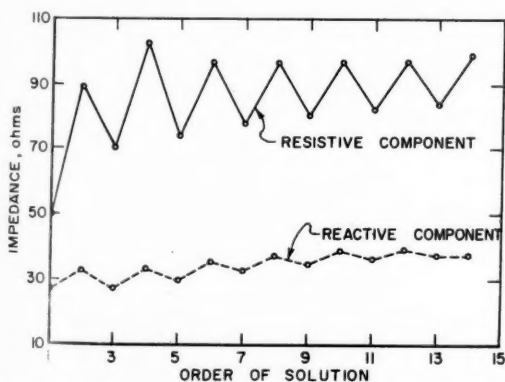


FIGURE 2. Impedance versus order of solution (Storm's procedure).

imaginary parts of antenna impedance as a function of the order of solution. Corresponding values of C are shown in figure 3. The result of mistreating the parameter C is easily observed from these curves. We have conjectured that the amplitude of oscillation in the results may decrease with increasing h/a .

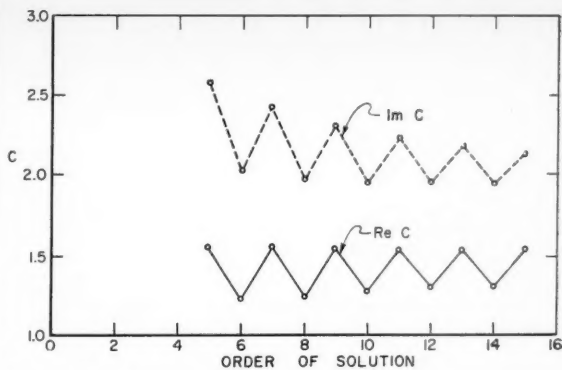


FIGURE 3. The parameter C versus order of solution (Storm's procedure).

If this is so it explains why Storm obtained good results with a defective theory.

Zuhrt considered the problem of developing $f(z)$ in a Fourier series from a somewhat different point of view [9]. Instead of considering a single isolated antenna, he formulated a boundary value problem for an infinite collinear array of such antennas spaced along the z -axis with centers at $z = \pm nd$, where $d > h$. Each unit is center-driven by a potential $V_n = (-1)^n V_0$ impressed across a gap of finite width. Ultimately he allows d to approach infinity and the gap width to become small. In this limit only the center unit remains and his theory represents the simple tubular model. This approach is unnecessarily intricate. Zuhrt's final equation can be derived directly from the Hallén integral equation. Equation (3.3) may be written

$$g(z-\xi) = -j \int_0^\infty J_0(\beta a) H_0^{(2)}(\beta a) \cos \alpha(z-\xi) d\alpha. \quad (5.9)$$

The term $\cos \alpha(z-\xi)$ in the integrand can be expanded and the term $\sin \alpha z \sin \alpha \xi$ omitted since $f(\xi)$ is even for a center-fed antenna. Therefore, we can consider

$$\int_{-h}^h f(\xi) K(z, \xi) d\xi = C \cos kz + \frac{1}{2} \sin k|z|, \quad (5.10)$$

where

$$K(z, \xi) = -j \int_0^\infty J_0(\beta a) H_0^{(2)}(\beta a) \cos \alpha z \cos \alpha \xi d\alpha. \quad (5.11)$$

Applying the operator $L_z = \partial^2 / \partial z^2 + k^2$ to both sides of (5.10), one obtains

$$\int_{-h}^h f(\xi) L_z K(z, \xi) d\xi = k \delta(z). \quad (5.12)$$

Now expand $f(\zeta)$ as

$$f(\zeta) = \sum_{n=0}^{n=N} F_n \cos H_n \zeta, \quad (5.13)$$

where

$$\frac{(2n+1)\pi}{2h} = H_n. \quad (5.14)$$

Substituting the assumed current expansion into (5.12), one obtains

$$\sum_{n=0}^{n=N} \left\{ \int_{-h}^h \cos H_n \zeta L_z K(z, \zeta) d\zeta \right\} F_n = k\delta(z). \quad (5.15)$$

Now multiply both sides of (5.15) by $\cos H_p z$, and integrate on z over the range $-h \leq z \leq h$ to obtain

$$\sum_{n=0}^{n=N} \left\{ \frac{1}{k} \int_{-h}^h \cos H_p z dz \int_{-h}^h \cos H_n \zeta L_z K(z, \zeta) d\zeta \right\} F_n = 1. \quad (5.16)$$

Equation (5.16) generates an infinite set of linear simultaneous equations as the indexing parameter, p , is allowed to range from zero to infinity. The coefficients are given by

$$Z_{pn} = \frac{1}{k} \int_{-h}^h \cos H_p z dz \int_{-h}^h \cos H_n \zeta L_z K(z, \zeta) d\zeta. \quad (5.17)$$

Further reduction is accomplished by substituting (5.11) for $K(z, \zeta)$ and carrying out the indicated operations. When this is done,

$$Z_{pn} = -4j(-1)^{p+n} H_p H_n \int_0^\infty \frac{J_0(\beta a) H_0^{(2)}(\beta a) (k^2 - \alpha^2) \cos^2 \alpha k}{(H_p^2 - \alpha^2)(H_n^2 - \alpha^2)} d\alpha. \quad (5.18)$$

This is the same as Zuhrt's formula except for trivial differences in notation.

Zuhrt obtains an N th order theory by truncating the infinite scheme at N th order. The integral which defines the matrix elements is difficult to evaluate. Zuhrt resolves this difficulty by resorting to graphical integration. Each coefficient has a real and an imaginary part, so that an N th order theory requires $2N^2$ graphical integrations, a formidable amount of labor even for small N .

6. Further Development of Fourier Series Solutions

The kernel of Hallén's integral equation,

$$g(z - \zeta) = \frac{1}{2\pi} \int_{-\pi}^{\pi} \frac{e^{-jkR}}{R} d\phi, \quad (6.1)$$

where

$$R = [4a^2 \sin^2 \phi / 2 + (z - \zeta)^2]^{1/2}, \quad (6.2)$$

represents the radiation at any value of z on a

cylinder of radius a from a ring source of radius a located at ζ . As such it is meaningful in the entire domain $-\infty < z < +\infty$. However, the integral equation is valid only on the range $-h \leq z \leq +h$ and operations on the source coordinate, ζ , are restricted to the same range. Hence, a special expansion of $g(z - \zeta)$ for $-h \leq z, \zeta \leq +h$ is desirable. A frontal attack on the problem of obtaining such an expansion has been made by Bohn in an investigation of a theoretical model which is quite different from the one used here [10]. The point of interest at present is his method of handling $g(z - \zeta)$ which is the kernel of an integral equation occurring in his theory.

In our notation Bohn's expansion is

$$g(z - \zeta) = \sum_{n=-\infty}^{n=\infty} \sum_{m=-\infty}^{m=\infty} G_{nm} e^{j(n\pi z/h - m\pi \zeta/h)} \quad (6.3)$$

for $-h \leq z, \zeta \leq +h$, where the coefficients of the Fourier series are given by

$$G_{nm} = \frac{1}{4h^2} \int_{-h}^h \int_{-h}^h g(z - \zeta) e^{-j(n\pi z/h - m\pi \zeta/h)} dz d\zeta. \quad (6.4)$$

Substituting (5.9) for $g(z - \zeta)$, (6.4) becomes

$$G_{nm} = -2jh^2 \int_{-\infty}^{+\infty} \frac{J_0(\beta a) H_0^{(2)}(\beta a) \sin(n\pi - \alpha h) \sin(m\pi - \alpha h) d\alpha}{(n\pi - \alpha h)(m\pi - \alpha h)}. \quad (6.5)$$

This expression exhibits the difficulties involved in a direct attack. The reader will appreciate that the integration is not trivial. Bohn evaluates (6.5) approximately by means of ingenious distortions of the contour of integration. Details will be omitted here, it being sufficient for our purpose to note that no investigator to date has been able to obtain the exact coefficients of a double Fourier series representation of $g(z - \zeta)$.

Fortunately, it is possible to avoid the double Fourier series representation entirely. It is only necessary to make use of the fact that z and ζ enter only as the square of their difference. Thus, $g(z - \zeta)$ is not a general function of (z, ζ) . To proceed, let

$$\xi = (z - \zeta). \quad (6.6)$$

If z and ζ are separately in the range $-h \leq z, \zeta \leq h$, then ξ is in the range $-2h \leq \xi \leq 2h$. Since $g(\xi)$ contains only ξ^2 , a cosine series in the range 0 to $2h$ will suffice. Thus, we seek an expansion of the form

$$g(\xi) = \frac{D_0}{2} + \sum_{m=1}^{m=\infty} D_m \cos m\pi \xi / 2h, \text{ for } 0 \leq \xi \leq 2h. \quad (6.7)$$

The fundamental formula for any coefficient is

$$D_m = \frac{1}{2h} \int_0^{2h} g(\xi) \cos m\pi \xi / 2h d\xi. \quad (6.8)$$

Direct integration of (6.8) is difficult. An indirect method can be constructed by writing

$$g(\xi) = g_1(\xi) + g_2(\xi), \quad (6.9)$$

where $g_1(\xi) = g(\xi)$ in the range $0 \leq \xi \leq 2h$, and is zero outside this range, $g_2(\xi)$ is equal to zero in the range $0 \leq \xi \leq 2h$, and is identical to $g(\xi)$ in the range $2h \leq \xi \leq \infty$. Transposition of (6.9) gives

$$g_1(\xi) = g(\xi) - g_2(\xi). \quad (6.10)$$

The symbolic cosine transform of (6.10) is

$$G_1(\alpha) = G(\alpha) - G_2(\alpha). \quad (6.11)$$

The transform of $g_1(\xi)$ and its inverse are given by

$$G_1(\alpha) = \sqrt{\frac{2}{\pi}} \int_0^{2h} g_1(\xi) \cos \alpha \xi d\xi, \quad (6.12)$$

and

$$g_1(\xi) = \sqrt{\frac{2}{\pi}} \int_0^\infty G_1(\alpha) \cos \alpha \xi d\alpha. \quad (6.13)$$

Comparison of (6.12) and (6.8) shows that the coefficients of the cosine series expansion for $g_1(\xi)$ are simply proportional to sample values of its cosine transform, $G_1(\alpha)$. Thus,

$$D_m = \frac{1}{h} \sqrt{\frac{\pi}{2}} \left[G\left(\frac{m\pi}{2h}\right) - G_2\left(\frac{m\pi}{2h}\right) \right]. \quad (6.14)$$

$G(\alpha)$ can be immediately identified from (5.9) as

$$G(\alpha) = -j \sqrt{\frac{\pi}{2}} J_0(\beta \alpha) H_0^{(2)}(\beta \alpha). \quad (6.15)$$

Incidentally, an asymptotic expansion of $G(\alpha)$ shows that, for small ξ , $g(\xi) \sim \ln \xi$. Since the singularity in $g(\xi)$ is no worse than logarithmic, the integrals defining the D_m exist.

Determination of $G_2(\alpha)$ is tedious but not difficult. The definition of $G_2(\alpha)$ is

$$G_2(\alpha) = \sqrt{\frac{2}{\pi}} \int_{2h}^\infty g(\xi) \cos \alpha \xi d\xi, \quad (6.16)$$

which can be expanded in a highly convergent infinite series. If, for convenience, we set

$$y^2 = 4a^2 \sin^2 \phi / 2 \quad (6.17)$$

and

$$u^2 = y^2 / \xi^2, \quad (6.18)$$

(6.1) becomes

$$g(\xi^2 > y^2) = \frac{1}{2\pi} \int_{-\pi}^{\pi} \frac{e^{-jk\xi\sqrt{1+u^2}}}{\xi} (1+u^2)^{-1/2} d\phi. \quad (6.19)$$

When appropriate expansions of the integrand are made and the ϕ -integration is performed, there

results

$$g(\xi^2 > y^2) = \frac{e^{-jk\xi}}{\xi} \left[1 - \frac{jka^2}{\xi} \frac{a^2}{\xi^2} \dots \right]. \quad (6.20)$$

The above expression is to be used when $\xi \geq 2h$. The parameter k is of the same order as $1/h$. Therefore the terms retained in the square bracket are of order $(a/h)^2$. The first omitted term is of order $(a/h)^4$. We shall now omit all of (6.20) except the first term. It is not difficult to restore the small correction terms later.

With this omission, (6.16) becomes

$$G_2(\alpha) \simeq \sqrt{\frac{2}{\pi}} \int_{2h}^\infty \frac{e^{-jk\xi} \cos \alpha \xi}{\xi} d\xi. \quad (6.21)$$

Sine and cosine integral functions are defined by

$$Si(x) = \int_0^x \frac{\sin x}{x} dx = \frac{\pi}{2} - \int_x^\infty \frac{\sin x}{x} dx; \quad (6.22)$$

$$Ci(x) = - \int_x^\infty \frac{\cos x}{x} dx.$$

With the above, a few trigonometric identities, and a few elementary changes of variable, the integration of (6.21) follows almost by definition, it being only necessary to exercise a little care depending on whether $\alpha < k$ or $\alpha > k$. The case of $\alpha = k$ will require special attention. We have

$$G_2(\alpha < k) \simeq - \sqrt{\frac{1}{2\pi}} \{ Ci[(k+) \alpha 2h] + Ci[(k-\alpha) 2h] + j\pi - jSi[(k+\alpha) 2h] - jSi[(k-\alpha) 2h] \}. \quad (6.23)$$

$$G_2(\alpha > k) \simeq - \sqrt{\frac{1}{2\pi}} \{ Ci[(\alpha+k) 2h] + Ci[(\alpha-k) 2h] - jSi[(\alpha+k) 2h] + jSi[(\alpha-k) 2h] \}. \quad (6.24)$$

It is convenient to rewrite $G(\alpha)$ from (6.15) separately for the cases $\alpha < k$ and $\alpha > k$. Let $|\beta| = b$. The phase of β has been defined so that $\beta = b$ if $\alpha < k$ and $\beta = -jb$ if $\alpha > k$. Then

$$G(\alpha < k) = -j \sqrt{\frac{\pi}{2}} J_0(ba) H_0^{(2)}(ba), \quad (6.25)$$

and

$$G(\alpha > k) = \sqrt{\frac{2}{\pi}} I_0(ba) K_0(ba). \quad (6.26)$$

Now $G_2(\alpha < k)$, $G_2(\alpha > k)$, $G(\alpha < k)$, $G(\alpha > k)$ are all singular at $\alpha = k$. In the first two functions the singularity comes from the cosine integral function, in the last two $H_0^{(2)}(ba)$ and $K_0(ba)$ become singular. Since these functions are to be sampled at the points

$m\pi/2h$, the singularities apparently give trouble if $h=m\lambda/4$. Actually we are concerned only with the difference $G(\alpha)-G_2(\alpha)$ and this turns out to be finite and independent of whether α approaches k from above or below. The special formula required for the $\alpha=k$ case is found from combining (6.23), (6.25) and making use of small argument formulas for the various functions involved. The latter are tabulated for the reader's convenience.

For small x ,

$$J_0(x) \simeq 1, \quad Si(x) \simeq 0, \\ H_0^{(2)}(x) \simeq 1 + j \frac{2}{\pi} \ln \frac{2}{\gamma x}, \quad Ci(x) \simeq \ln \gamma x. \quad (6.27)$$

The logarithmic singularities subtract off in $G(\alpha)-G_2(\alpha)$ and one obtains

$$G_1(\alpha=k) \simeq \frac{1}{\sqrt{2\pi}} \left\{ \ln \frac{4h}{\gamma k a^2} + Ci(4kh) - jSi(4kh) \right\}. \quad (6.28)$$

The same result can be obtained by using (6.24), (6.26), and the small argument formulas for $I_0(ba)$ and $K_0(ba)$.

The degree of approximation in the above formulas may be improved by calculating the cosine transforms of the correction terms in (6.20). The next term to be included is

$$T_1(\alpha) = -jka^2 \sqrt{\frac{2}{\pi}} \int_{2h}^{\infty} \frac{e^{-jk\xi}}{\xi^2} \cos \alpha \xi d\xi, \quad (6.29)$$

which reduces to trigonometric functions, sine integral functions and cosine integral functions. All higher order correction terms may be similarly treated.

Thus, an expansion of $g(z-\zeta)$ in the form (6.7) can be achieved and the coefficients can be calculated with any desired degree of accuracy. It will be convenient in what follows to re-define D_0 so that the leading term can be included under the summation sign. If this is done

$$g(z-\zeta) = \sum_{m=0}^{m=\infty} D_m [\cos m\pi z/2h \cos m\pi \zeta/2h \\ + \sin m\pi z/2h \sin m\pi \zeta/2h]. \quad (6.30)$$

The sine terms are not needed in the treatment of a center-fed antenna. We are then led to consider

$$\int_{-h}^h f(\zeta) K(z, \zeta) d\zeta = C \cos kz + \frac{1}{2} \sin k|z|, \quad (6.31)$$

where

$$K(z, \zeta) = \sum_{m=0}^{m=\infty} D_m \cos m\pi z/2h \cos m\pi \zeta/2h, \quad (6.32)$$

subject to $f(\pm h) = 0$.

We now expand $f(\zeta)$ as

$$f(\zeta) = \sum_{n=0}^{n=\infty} F_n \cos n\pi \zeta/h \quad (6.33)$$

and substitute into (6.31). After the ζ integration,

$$\sum_{n=0}^{n=\infty} \sum_{m=0}^{m=\infty} F_n D_m \gamma_{nm} \cos m\pi z/2h = C \cos kz + \frac{1}{2} \sin k|z|, \quad (6.34)$$

$$\gamma_{nm} = 2 \int_0^h \cos n\pi \zeta/h \cos m\pi \zeta/2h d\zeta. \quad (6.35)$$

An infinite set of linear simultaneous equations is obtained by multiplying both sides of (6.34) by $\{\cos(2p+1)\pi z/2h\}$ and integrating on z from $-h$ to $+h$. The result is

$$\sum_{n=0}^{n=\infty} \sum_{m=0}^{m=\infty} F_n D_m \gamma_{nm} \beta_{pm} = C r_p + v_p, \quad (6.36)$$

where

$$\beta_{pm} = 2 \int_0^h \cos [(2p+1)\pi z/2h] \cos [m\pi z/2h] dz, \quad (6.37)$$

$$r_p = 2 \int_0^h \cos kz \cos [(2p+1)\pi z/2h] dz, \quad (6.38)$$

and

$$v_p = 2 \int_0^h \sin kz \cos [(2p+1)\pi z/2h] dz. \quad (6.39)$$

Equation (6.36) can be written

$$\sum_{n=0}^{n=\infty} \Gamma_{pn} F_n = C r_p + v_p, \quad (6.40)$$

where

$$\Gamma_{pn} = \sum_{m=0}^{m=\infty} D_m \gamma_{nm} \beta_{pm}. \quad (6.41)$$

If (6.41) were actually an infinite sum, many terms would be required to satisfactorily approximate each Γ_{pn} and the theory would be laborious except in low order. However, (6.41) contains only two nonzero terms! To appreciate this fact consider the set of functions $\{\cos(m\pi z/2h)\}$ which appear in the expansion of $K(z, \zeta)$. These functions are complete on $0 \leq z \leq 2h$. They appeared in the theory because we expanded a function of $(z-\zeta)$. Clearly since m is either even or odd, this basic set of functions can be divided into two subsets $\{\cos m\pi z/h\}$ and $\{\cos(2m+1)\pi z/2h\}$. Both of the subsets are complete and orthogonal on the range where they are actually used. In a sense we can refer to (6.32) as an over-complete expansion of $K(z, \zeta)$. Therefore, the summation in (6.41) can be broken into two parts, one for m even, the other for m odd, and reduced to

$$\Gamma_{pn} = h[\beta_{p,2n} D_{2n} + \gamma_{n,2p+1} D_{2p+1}]. \quad (6.42)$$

The set of equations generated by (6.40) as p ranges from zero to infinity can be cast in matrix form as

$$\Gamma F = Cr + v, \quad (6.43)$$

where Γ is a matrix of the Γ_{pn} ; F , r , and v are column vectors.

The method of obtaining simultaneous equations from (6.34) used here is formally equivalent to any other method which might be used. Consider multiplying (6.34) by $X_p(z)$ and integrating on z from $-h$ to h , where $X_p(z)$ is arbitrary. Now $X_p(z)$ can be expanded in the set $\{\cos(2p+1)\pi z/2h\}$ so that the set of equations obtained by using $X_p(z)$ is a linear combination of the equations represented by (6.43). An N th order collocation scheme is equivalent to choosing $X_p(z)$ from a set of N delta functions, $\delta(z-z_p)$ with $p=1, 2, 3, \dots, N$.

The formal solution of (6.43) in terms of Γ^{-1} is simply

$$F = C\Gamma^{-1}r + \Gamma^{-1}v. \quad (6.44)$$

We have not been able to discover a general form for Γ^{-1} . Consequently, it has been necessary to truncate the system of equations to finite order and invert finite matrices using digital computer methods.⁴ This procedure is a cause of some concern in that there are apparently no mathematical theorems which justify the assumption that a sequence of such inverses converges to the inverse of the infinite matrix. However, there is evidence that the procedure being used here produces the correct solution of Hallén's integral equation. First of all, we have examined sequences of finite inverses up to 25th order for $h/a=60$ and $kh=\pi/2$. These are well-behaved and stable. For a rough definition of stability, we shall say that a stable N th order inverse has been found if the elements of an N th order matrix formed by truncating the inverse matrix of an $(N+M)$ th order solution do not change appreciably as M is increased. M will be referred to as the stability margin. For the problem at hand our work indicates that $M \sim 3$.

The results obtained for finite antennas are thoroughly reasonable when compared to results obtained by other methods. From a pragmatic point of view there seems to be sufficient evidence that the matrix inversion procedure does indeed produce a finite number of terms of the correct solution to the original integral equation.

If the elements of the inverse of an N th order truncation of Γ are designated as H_{np}^N the numerical solution is

$$F_n(C) = \sum_{p=0}^{p=N} H_{np}^N (Cr_p + v_p). \quad (6.45)$$

⁴ Numerical inversion of the required matrices was accomplished on the IBM 650, using a library program furnished by IBM Corporation.

The N th approximation to $f(z)$ given by the computational program is

$$f_N(z) = \sum_{n=0}^{n=N} F_n(C) \cos(n\pi z/h). \quad (6.46)$$

The leading terms of (6.46) are not a good approximation to antenna current. Consequently, this representation is slowly convergent. To improve convergence a good low order approximation to $f(z)$ was chosen, and expanded in a series

$$x(z) = \sum_{n=0}^{n=N} X_n \cos(n\pi z/h). \quad (6.47)$$

Candidates for the role of $x(z)$ are the classical sinusoidal distribution, the zeroth order approximation from an iterative solution, the King-Middleton modified zeroth order approximation, or a new low order approximation by R. W. P. King referred to by its author as the "quasi-zeroth order approximation" [11]. We have used the latter. Once the choice has been made and X_n have been calculated, (6.46) is modified to read

$$f_N(z) = x(z) + \sum_{n=0}^{n=N} [F_n(C) - X_n] \cos(n\pi z/h). \quad (6.48)$$

When the boundary condition $f(h)=0$ is imposed, one obtains an N th order approximation to C from

$$\sum_{n=0}^{n=N} [F_n(C) - X_n] (-1)^n = 0. \quad (6.49)$$

By letting $N=0, 1, 2, \dots, N$, (6.49) can be used to generate a sequence,

$$C_0, C_1, C_2, \dots, C_N \quad (6.50)$$

Now an N th order solution should be regarded as the first N terms of a solution of infinite order, only the latter solution involves the Fourier series for $f(z)$. The Fourier series is unique and logically it must be in terms of C_∞ . The most direct method of determining C_∞ is to plot the above sequence versus $1/n$ and extrapolate. Unfortunately, the sequence of C values obtained from the boundary condition oscillates and the extrapolation is subject to large error. This difficulty can be overcome by applying a Cesaro transformation to the sequence of C values to form a new sequence which converges to the same limit. The transformed sequence plots a smooth curve against $1/n$, the extrapolated limit of which is taken to be C_∞ . A graph of a typical treatment of C is shown in figure 4.

Our final expression for $f(z)$ is

$$f_N(z) = x(z) + \sum_{n=0}^{n=N} [F_n(C_\infty) - X_n] \cos(n\pi z/h). \quad (6.51)$$

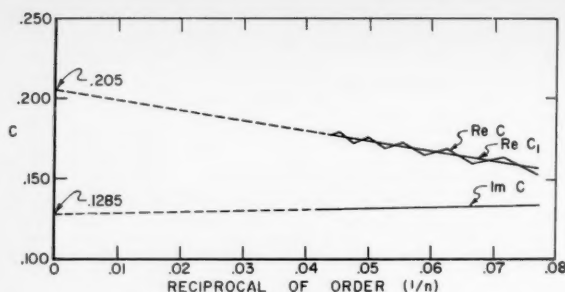


FIGURE 4. Determination of parameter C .

This expression does not quite satisfy the boundary condition $f(+h)=0$. However, except for truncation errors which affect only the last two or three of the F_n appreciably, it represents an estimate of the first N terms of a solution of infinite order. Readers who may prefer an expression which satisfies the boundary condition exactly in N th order should be reminded once again that a finite number of terms of a Fourier series provides a least squares best fit over the entire range of the function being represented. This type of fit is to be preferred over one which is identically equal to the function at one point.

The admittance of the antenna is now simply

$$Y_N = \frac{4\pi}{jZ_0} \left\{ x(0) + \sum_{n=0}^{n=N} [F_n(C_\infty) - X_n] \right\}. \quad (6.52)$$

The function $f(\xi)$ is proportional to the sum of the currents on both the inner and outer surfaces of the tubular conductor. It was pointed out earlier that only the current on the outer surface and not the tube current is to be associated with the experimental admittance of the antenna.

The generic expression for the vector potential at a field point (ρ, ϕ, z) when $\rho_0 = a$ is

$$A_z = \frac{\mu}{4\pi} \int_{-h}^h I(\xi) g(\rho, z; a, \xi) d\xi, \quad (6.53)$$

where $g(\rho, z; a, \xi)$ is given by either

$$g(\rho, z; a, \xi) = \frac{1}{2\pi} \int_{-\pi}^{\pi} \frac{e^{-jkR}}{R} d\phi \quad (6.54)$$

with

$$R = [\rho^2 + a^2 - 2\rho a \cos \phi + (z - \xi)^2]^{1/2} \quad (6.55)$$

or

$$g(\rho, z; a, \xi) = -j \int_0^\infty J_0(\beta a) H_0^{(2)}(\beta \rho) \cos \alpha(z - \xi) d\alpha. \quad (6.56)$$

As a consequence of the ϕ -symmetry, only the ϕ -component of \vec{H} is different from zero, and is given by

$$H_\phi = -\frac{1}{\mu} \partial A_z / \partial \rho. \quad (6.57)$$

The surface current density on the outer surface of the tube is obtained from the boundary condition $\vec{n} \times \vec{H} = \vec{K}$, and the current distribution along the outer surface is

$$I^0(z) = \frac{1}{4\pi} \int_{-h}^h I(\xi) g^0(\rho, z; a, \xi) d\xi \quad (6.58)$$

where

$$g^0(\rho, z; a, \xi) = -2\pi a \left[\frac{\partial}{\partial \rho} g(\rho, z; a, \xi) \right]_{\rho=a+}. \quad (6.59)$$

If $g(\rho, z; a, \xi)$ is expanded in the Fourier series

$$g^0(\rho, z; a, \xi) = \sum_{m=0}^{m=\infty} D_m^0 \cos \frac{m\pi(z - \xi)}{2h}, \quad 0 \leq |z - \xi| \leq h, \quad (6.60)$$

the coefficients D_m^0 may be determined by the same procedure used in expanding the kernel of Hallén's equation. Omitting details, the D_m^0 are given by sample values of

$$G_1^0(\alpha) = -j\beta a J_0(\beta a) H_1^{(2)}(\beta a) + \left\{ \frac{\partial}{\partial \rho} \int_{2h}^\infty \int_{-\pi}^\pi \frac{e^{-jkR}}{R} \cos \alpha(z - \xi) d\phi d(z - \xi) \right\}_{\rho=a+}, \quad (6.61)$$

where R is given by (6.55).

This leads to the following expression for Fourier coefficients of the exterior current:

$$I_m^0 = \frac{4\pi}{jZ_0} D_m^0 \left\{ \int_{-h}^h x(\xi) \cos(m\pi\xi/2h) d\xi + \sum_{n=0}^{n=N} [F_n - X_n] \int_{-h}^h \cos(n\pi\xi/h) \cos(m\pi\xi/2h) d\xi \right\}. \quad (6.62)$$

7. Results

We have applied the theory to half and full wavelength antennas with $h/a=60$ and 500π , respectively. In each case the calculations were performed at 25th order. Correction terms from (6.30) were included in the calculation so that each matrix element is accurate to one part in 10^5 . Graphs of total current and plots of total admittance versus order are shown (figs. 5 to 12). In the latter graphs, an n th order admittance is obtained by using the first n terms of a 25th order solution.

Comparison of these results with those of the King-Middleton theory in terms of impedance are shown in table 2.

King-Middleton impedances in table 2 were obtained by graphical interpolation of tables given in reference [2]. Resistances of the half wavelength structures are from third order solutions. Other quantities from King-Middleton theory are second order. Our own Z_T for the full wavelength antenna

with $h/a=60$ is obtained by extrapolating the current graph to $z=0$. The current distribution on a full wavelength structure does not have zero slope at the origin as do the cosine terms used to describe it. Consequently, many cosine terms are required for high accuracy, especially in the treatment of a thick structure. The inner current correction is entirely negligible for structures with $h/a=500\pi$; it is still small for $h/a=60$.

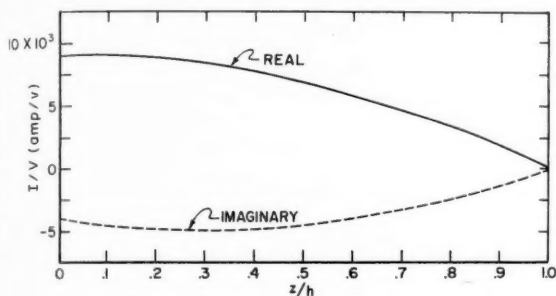


FIGURE 5. Current distribution: $kh=\pi/2$, $h/a=60$.

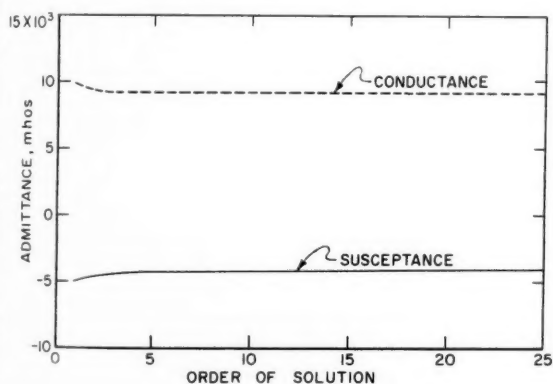


FIGURE 6. Admittance versus order of solution: $kh=\pi/2$, $h/a=60$.

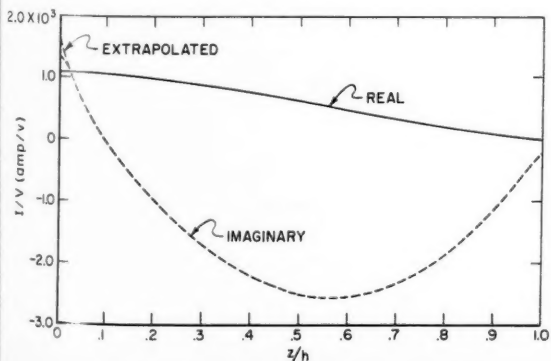


FIGURE 7. Current distribution: $kh=\pi$, $h/a=60$.

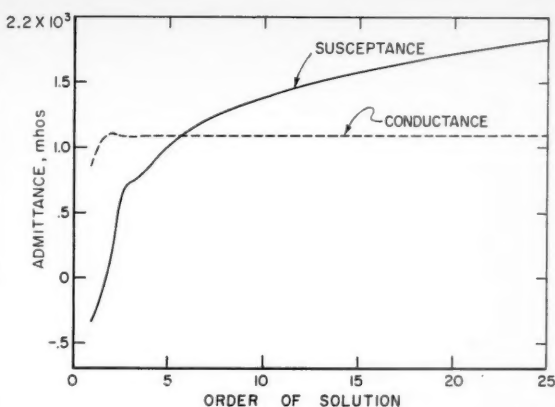


FIGURE 8. Admittance versus order of solution: $kh=\pi$, $h/a=60$.

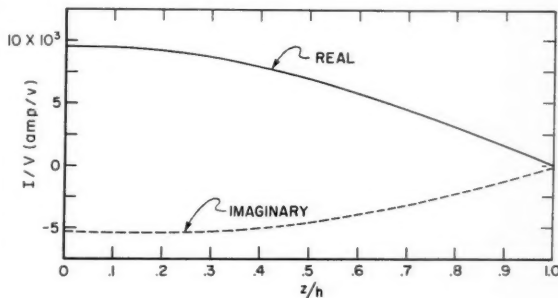


FIGURE 9. Current distribution: $kh=\pi/2$, $h/a=500\pi$.

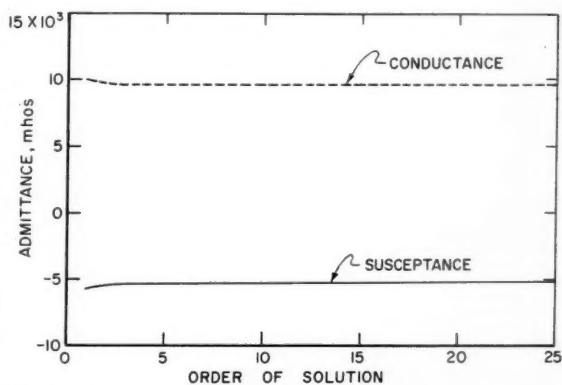


FIGURE 10. Admittance versus order of solution: $kh=\pi/2$, $h/a=500\pi$.

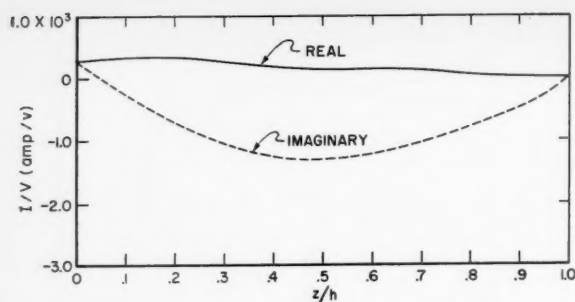


FIGURE 11. Current distribution: $kh=\pi$, $h/a=500\pi$.

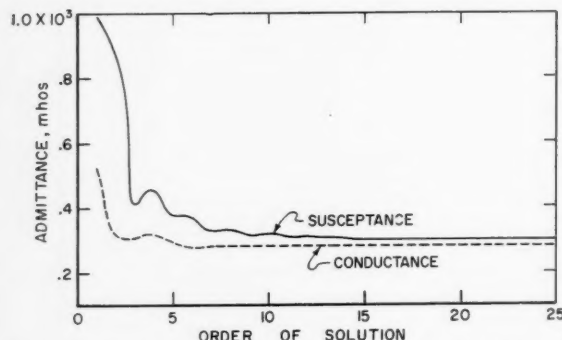


FIGURE 12. Admittance versus order of solution: $kh=\pi$, $h/a=500\pi$.

It can be seen from table 2 that the amount of disagreement between this theory and the King-Middleton theory is only about two percent. One may expect disagreement of this order or less over the entire range of $h/a > 60$.

TABLE 2

kh	h/a	Z_T	Z^0	Z_{KM}
$\pi/2$	60	91.4+j 38.6	92.5+j 40.6	91.4+j 41.5
π	60	205 -j 382	205 -j 380	206 -j 380
$\pi/2$	500 π	79.7-j 42.9		80.3-j 43.4
π	500 π	1646 -j 1768		1625 -j 1744

It can be seen from the graphs of admittance versus order that, except for thick full wavelength structures, 25 terms are excessive for $h/a > 60$. Thus, a great deal of margin for the study of thicker antennas is inherent in 25th order solutions. Studies of full wavelength antennas with $h/a < 60$ will require more than 25 terms or further modification of some of the technical details of the theory.

The authors express their appreciation to T. R. Ferguson for his assistance in the calculations, to Walter Haas for the computer programs and to R. M. Conkling for fruitful discussions during the preparation of this paper.

8. References

- [1] S. A. Schelkunoff and H. T. Friis, Antennas, theory and practice, chap. 8 (John Wiley and Sons, New York, N.Y., 1952).
- [2] R. W. P. King, The theory of linear antennas (Harvard University Press, Cambridge, Mass., 1956).
- [3] T. Wu and R. W. P. King, Driving point and input admittance of linear antennas, J. A. P., **30**, 1, 74 (1959).
- [4] N. Marcuvitz, Waveguide Handbook, p. 66, (McGraw-Hill Book Co., New York, N.Y., 1951).
- [5] A. Erdélyi, et al., Tables of integral transforms, Vol. I (McGraw-Hill Book Co., New York, N.Y., 1953).
- [6] Erik Hallén, Exact Treatment of Antenna Current Wave Reflection at the End of a Tube Shaped Cylindrical Antenna, IRE Trans. on Ant. and Prop., **AP-4**, 3, 479, (1956).
- [7] R. Gans, Zur Theorie der Geradlinigen Antenna, Arch. Electr. Übertragung, **7**, 169, (1953).
- [8] B. Storm, Investigations into modern aerial theory and a new solution of Hallén's integral equation for a cylindrical aerial, dissertation, Imperial College, London, 1953; Summary in wireless engineer (July 1953).
- [9] H. Zuhrt, Eine Strenge Berechnung der Dipolantennen mit Röhrenförmigen Querschnitt, Frequenz **4**, 135 (1950).
- [10] E. V. Bohn, The current distribution and input impedance of cylindrical antennas, IRE Trans. on Ant. and Prop. **AP-5**, 4, 343 (1957).
- [11] R. W. P. King, Linear Arrays: Currents, Impedance and Fields, U.R.S.I. Symposium on electromagnetic theory, University of Toronto (June 1959).

Publications of the staff of the National Bureau of Standards *

Selected Abstracts

Half-round inductive obstacles in rectangular waveguide, D. M. Kerns, *J. Research NBS* **64B**, 113 (1960).

Formulas are derived for the accurate calculation of the lowest-mode, lumped-element representation of perfectly conducting half-round inductive obstacles in rectangular waveguide. These obstacles consist of either one or two opposed semicircular cylindrical indentations extending across the narrow sides of the waveguide. They seem especially suitable for use as precise calculable standards of reflection or impedance in waveguide. Schwinger's integral equation approach is used to obtain stationary expressions for the desired parameters as functionals of the surface currents on the obstacles. Upper bounds are obtained for one of the two parameters. Explicit formulas are derived for the values of the parameters under the assumption of n -term Fourier sine-series expansions for the obstacle currents. Rapid convergence is indicated by numerical evaluations for $n=1, 2$, and 3 . In the process of obtaining expressions suitable for numerical calculation, an expansion (believed to be new) of the Green's function of the problem is obtained and the sums of certain infinite series of Bessel's functions occurring in this expansion are expressed in terms of definite integrals. A brief numerical table of these sums, sufficient for the evaluation of the $n=1$ approximation, is included.

Mean electron density variations of the quiet ionosphere, 2 April 1959, J. W. Wright and L. A. Fine, *NBS Tech. Note* 40-2 (PB151399-1) (1960) \$1.25.

The CRPL has initiated a program for large-scale computation of electron density profiles from ionospheric vertical soundings. Scaling is performed at field stations permitting computation of hourly profiles at the central laboratory. These profiles are combined to form hourly mean quiet profiles for each station and month. The results of this program for the month of April are illustrated graphically. This report is the second of a series illustrating the electron density variations in the mean quiet ionosphere between latitudes 15° N and 50° N along the 75° W meridian.

A summary of VHF and UHF tropospheric transmission loss data and their long-term variability, D. A. Williamson, V. L. Fuller, A. G. Longley, and P. L. Rice, *NBS Tech. Note* 43 (PB151402) (1960) \$2.25.

Cumulative distributions of hourly median basic transmission loss are presented for 135 beyond-line-of-sight radio paths in the United States. In order to allow for seasonal trends of transmission loss, the year is divided into a summer period, May through October, and a winter period, November through April.

The long-term variability of observed hourly medians is compared with predicted variability based on empirical curves by Rice, Longley, and Norton.

Tables for the statistical prediction of radio ray bending and elevation angle error using surface values of the refractive index, B. R. Bean, B. A. Cahoon, and G. D. Thayer, *NBS Tech. Note* 44 (PB151403) (1960) 50 cents.

Using geometrical-optical formulas, radio ray bending, τ , and elevation angle error, ϵ , have been calculated for a wide range of meteorological conditions at 13 climatically diverse U.S. radiosonde stations. The parameters in the observed linear regression equations of τ and ϵ upon the surface value of the refractive index are given for heights of 0.1 to 70 kilometers and initial elevation angles of the ray from 0 to 900 milliradians.

Field strength calculations for ELF radio waves, J. R. Wait and N. F. Carter, *NBS Tech. Note* 52 (PB 151411) (1960) 50 cents.

The mode theory of propagation of electromagnetic waves at extremely low frequencies (1.0 to 3000 c/s) is briefly reviewed in this paper. Starting with the representation of the field

as a sum of modes, approximate formulas are presented for the attenuation and phase constants. At the shorter distances, where the range is comparable to the wavelength, the spherical-earth mode series is best transformed to a series involving cylindrical wave functions. This latter form is used to evaluate the near field behavior of the various field components. The effect of the earth's magnetic field is also evaluated using a quasi-longitudinal approximation which is particularly appropriate for propagation in the magnetic meridian. In general it is indicated that if the gyrofrequency is comparable or greater than the effective value of the collision frequency, the presence of the earth's magnetic field may be important for ELF. In this case the attenuation may be increased somewhat. The influence of a purely transverse magnetic field is also considered.

This technical note is actually a numerical supplement to the paper "Mode Theory and the Propagation of ELF Radio Waves," by J. R. Wait, *J. Research NBS* **64D**, 387 July-Aug. 1960; however, for sake of completeness the relevant theory is briefly presented.

Measured distributions of the instantaneous envelope amplitude and instantaneous frequency of carriers plus thermal and atmospheric noise, A. D. Watt and R. W. Plush, *Statistical Methods in Radio Wave Propagation*, edited by W. C. Hoffman, p. 233 (Pergamon Press, Inc., New York, N.Y., 1960).

Distributions of the instantaneous envelope amplitude and instantaneous frequency as a function of radio of carrier-to-noise level have been obtained for both thermal and atmospheric noise conditions. The envelope amplitude distribution of carrier plus thermal noise is found to agree well with that predicted by mathematical analysis, and the carrier-to-atmospheric noise distributions are observed to differ appreciably from the thermal noise conditions as might be anticipated from the distributions of the atmospheric noise envelope by itself.

The instantaneous frequency distributions are observed to depart appreciably from the normal distribution. Under carrier plus atmospheric noise conditions, the shape of the instantaneous frequency distribution is found to be rather similar to that obtained with carrier plus thermal noise.

A phenomenological theory of overvoltage for metallic particles, James R. Wait, *Ch. 3 of Overvoltage Research and Geophysical Applications*, edited by James R. Wait (Pergamon Press, Inc., New York, N.Y., 1960).

A brief theoretical derivation is presented for the effective conductivity and dielectric constant of a homogeneous medium loaded with a uniform distribution of spherical conducting particles. To account for the effect of induced polarization, the particles are taken to have a concentric membrane or film which has a blocking action to the current flow into the particle.

The variable-frequency method, J. R. Wait, *Ch. 4 of Overvoltage Research and Geophysical Applications* (Pergamon Press, Inc., New York, N.Y., 1959).

It has been found that the complex conductivity of rocks is a function of frequency. These dispersion or overvoltage effects, which are very pronounced in mineralized media, can be attributed mainly to interfacial polarization at the boundaries of the metallic ore particles and the electrolyte in the pores of the host rock. In the first part of this paper, the variation of the magnitude and the phase of the conductivity for mineralized and non-mineralized samples is reported for frequencies in the range from 0.1 to 10^5 c/s. The mathematical relation between a frequency dependent conductivity and the transient build up of the field for a step function current is then derived. The interrelation is demonstrated by an actual example which is verified experimentally for a mineralized sample.

In the second part, electromagnetic propagation and interwire coupling effects are discussed briefly from the standpoint of their masking effect on the overvoltage measurement when a four electrode array is employed. In the third part, results from a preliminary field trial of the frequency variation method carried out in the summer of 1950 in the vicinity of Jerome, Arizona are described.

Laboratory investigation of overvoltage, L. S. Collett, A. A. Brant, W. E. Bell, K. A. Ruddock, H. O. Siegel, and J. R. Wait, *Ch. 5 of Overvoltage Research and Geophysical Applications* (Pergamon Press, Inc., New York, N.Y., 1959).

A technique for the laboratory studies of induced polarization in mineralized and nonmineralized rock specimens is discussed. The equipment for both the transient and the frequency variation procedures is described in outline. Some typical results are presented for various metallic and non-metallic minerals.

Criteria from the transient decay curves, J. R. Wait and L. S. Collett, *Ch. 6a of Overvoltage Research and Geophysical Applications* (Pergamon Press, Inc., New York, N.Y., 1959).

In this chapter, the progress in the analysis of induced polarization decay curves on rock specimens is described. The curves analyzed are those taken by Collett with the standard accepted technique including the electro-osmosis treatment described in Chapter 5. Particular attention is paid to the examination of the curve shape. For this purpose the first, second and third derivatives are evaluated and shown plotted against the magnitude of the response in each case. Several other interesting properties of the decay curves are also investigated. The descriptions in the text of this chapter are brief since most of the information is listed on the illustrations.

The error in prediction of F2 maximum usable frequencies by world maps based on sunspot number, E. L. Crow and D. H. Zacharisen, *Statistical Methods in Radio Wave Propagation*, edited by W. C. Hoffman, p. 248 (Pergamon Press, Inc., New York, N.Y., 1960).

The feasibility of preparing semi-permanent world maps for predicting F2 maximum usable frequencies based on sunspot number is studied. The components of variance of the prediction are estimated; they arise from the following four major sources of error: determining regressions of F2 characteristics on sunspot number with limited years of data, the scatter of points about these regressions, drawing world contour maps with limited numbers of stations, predicting the future sunspot number. All four sources are found to contribute about equally to a total standard deviation of monthly median maximum usable frequency predicted five months in advance of about 1 and 3 Mc for 0 and 4000 km, respectively. Hence the proposed maps are concluded to be feasible.

The components of power appearing in the harmonic analysis of a stationary process, M. M. Siddiqui, *Statistical Methods in Radio Wave Propagation*, edited by W. C. Hoffman, p. 112 (Pergamon Press, Inc., New York, N.Y., 1960).

Suppose that from a continuous record of a stationary process over a time interval T seconds, $2n+1$ equally spaced readings are taken and the usual harmonic analysis is performed. Assuming the true frequencies present in the process to be $\dots, 1/(3T), 1/(2T), 1/T, 2/T, \dots$, cycles per second, it is shown that the power ascribed to the frequency j/T c/s consists of three components: (1) the true power in the frequency j/T c/s; (2) the powers in the frequencies $(2kn \pm j)/T$ c/s, $k=1, 2, \dots$; (3) a part of the powers in the frequencies $1/(mT)$ c/s, $m=2, 3, \dots$

Refraction of radio waves at low angles within various air masses, B. R. Bean, J. D. Horn, and L. P. Riggs, *J. Geophys. Research* **65**, 1183 (1960).

The refractive index structure and bending of radio rays within air masses of nonexponential refractive index height structure is treated in terms of the value expected in an average atmosphere of exponential form. It is demonstrated that refraction differences between air masses arise from

departures of refractive index structure from the normal exponential decrease with height. The effect upon radio ray refraction of these departures from the normal exponential refractive index structure is most pronounced for small initial elevation angles of the radio ray.

Peculiarities of the ionosphere in the Far East: A report on IGY observations of sporadic E and F-region scatter, E. K. Smith, Jr., and J. W. Finney, *J. Geophys. Research* **65**: 885 (1960).

This paper considers the results for the period October 1, 1957, to October 1, 1958, from the IGY 'VHF oblique-incidence sporadic-E measurements' program which operated circuits at 50 Mc/s in the Far East and the Caribbean. Sporadic E is found to be three to five times more frequent in the Far East than in the Caribbean for reflection coefficients of -20 to -80 db relative to inverse distance. Negligible dependence of magnetic activity is observed in either area, but diurnal and seasonal variations are more regular in the Far East. It is suggested that this longitudinal difference may be due either to the influence of the East Asiatic monsoon, perhaps through the mechanism proposed by Martyn, or to the difference in the relationship of magnetic dip to geographic latitude in these two areas.

A peculiar evening signal enhancement, referred to as the 'Far Eastern anomaly' or the 'evening signal anomaly', appeared quite regularly in the Far East, and pulse-delay measurements indicate the probable source of the reflection to the F region. The corresponding effect in the Caribbean is about 100 times less frequent, if it exists at all. The F_2 (layer tilt) reflection mechanism proposed by workers at Stanford does not appear too promising in this case, owing to the pulse broadening of the order of 1 millisecond which is normally encountered in the evening signal anomaly. A mechanism that would explain the structure of the observed signal involves reflection from field-aligned ionization similar to the mechanism invoked to explain the 'low-latitude auroral echoes' observed at Stanford.

The effect of multipath distortion on the choice of operating frequencies for high-frequency communication circuits, D. K. Bailey, *IRE Trans. AP-7*, 397 (1959).

Harmful multipath distortion on high-frequency facsimile services and telegraphic services operating at high speeds occurs when the received signal is composed of two or more components arriving by different modes over the same great-circle path with comparable intensities, but having travel times which differ by an amount equal to an appreciable fraction of the duration of a signal element. The dependence of multipath distortion on the relationship of the operating frequency to the MUF is discussed and a new term, the multipath reduction factor (MRF), is introduced which permits calculation in terms of the MUF of the lowest frequency which can be used to provide a specified measure of protection against multipath distortion. The MRF has a marked path-length dependence and is calculated as a function of path length for representative values of the other parameters involved by making use of an ionospheric model. It is then shown how the MRF can be used in connection with worldwide MUF prediction material to determine the minimum number of frequencies which must be assigned to a high-frequency communication service of continuous availability operating at high speed. Some comparisons with observations are discussed, and finally conclusions are drawn concerning manner of operation and choice of operating frequencies to reduce or to eliminate harmful multipath distortion.

The effect of the earth's magnetic field on m.u.f. calculations, K. Davies, *Research note, J. Atmospheric and Terrest. Phys.* **16**, 187 (1959).

Practically all of the methods at present used in the determination of maximum usable frequencies for ionospheric propagation neglect the effects of the earth's magnetic field. Thomson and Robbins (1958) have pointed out, however, that the inclusion of the magnetic field can appreciably affect the determinations of the electron density distribution and

therefore the calculated m.u.f. It is the purpose of this note to draw attention to the influence of the earth's magnetic field on m.u.f. calculations using the transmission slider technique.

VLF phase characteristics deduced from atmospheric wave forms. A. G. Jean, W. L. Taylor, and J. R. Wait, *J. Geophys. Research* **65**, 907 (1960).

The wave forms of the electric field of atmospherics recorded at four widely separated stations are analyzed to yield the phase characteristics of radio waves at very low frequencies. It is indicated that the relative phase velocity for propagation to great distances is about 3 per cent greater than c (velocity of light in a vacuum) at 4 kc/s. Above this frequency, it gradually decreases, being about 1 per cent greater than c at 8 kc/s. The form of the dispersion curve is very close to that predicted by the mode theory.

Photometric observations of the twilight glow [OI] 5577 and [OI] 6300. L. R. Megill, *J. Atmospheric and Terrest. Phys.* **17**, 276 (1960).

The enhancement of both the [OI] 5577 and the [OI] 6300 atmospheric emission lines has been measured in detail for the night of 6/7 January 1958 at Rapid City, South Dakota. The enhancement of the 5577 emission cannot be explained on the basis of photo excitation alone. The 6300 emission is compared with recent theory. Fair agreement is noted between theory and observation.

Thermal and gravitational atmospheric oscillations—ionospheric dynamo effects included. M. L. White, *J. Atmospheric and Terrest. Phys.* **17**, 220 (1960).

The resonance theory of gravitational and thermal oscillations in a rotating atmosphere composed of a neutral gas is extended to include an electron and positive ion gas with a permanent magnetic field superposed (so-called dynamo effect).

Other NBS Publications

Journal of Research, Vol. 64A, No. 4, July–August 1960. 70 cents.

Gamma irradiation of hexafluorobenzene. R. E. Florin, L. A. Wall, and D. W. Brown.

Behavior of isolated disturbances superimposed on laminar flow in a rectangular pipe. Grover C. Sherlin.

Standard of spectral radiance for the region of 0.25 to 2.6 microns. Ralph Stair, Russell G. Johnston, and E. W. Halbach.

Photovoltaic effect produced in silicon solar cells by X- and gamma rays. Karl Scharf.

Phase equilibria in systems involving the rare-earth oxides. Part I. Polymorphism of the oxides of the trivalent rare-earth ions. R. S. Roth and S. J. Schneider.

Phase equilibria in systems involving the rare-earth oxides. Part II. Solid state reactions in trivalent rare-earth oxide systems. S. J. Schneider and R. S. Roth.

Some observations on the calcium aluminate carbonate hydrates. Elmer T. Carlson and Horace A. Berman.

Acid dissociation constant and related thermodynamic quantities for triethanolammonium ion in water from 0° to 50° C. Roger G. Bates and Guy F. Allen.

Ionization constants of four dinitrophenols in water at 25° C. Robert A. Robinson, Marion Maclean Davis, Maya Paabo, and Vincent E. Bower.

Dissociation constant of anisic (*p*-methoxybenzoic) acid in the system ethanol-water at 25° C. Elizabeth E. Sager and Vincent E. Bower.

Preparation of sulfur of high purity. Thomas J. Murphy, W. Stanley Clabaugh, and Raleigh Gilchrist.

Tritium-labeled compounds IV. D-Glucose-6- β -L, D-Xylose-5- β -L, and D-mannitol-1- β -L. Horace S. Isbell, Harriet L. Frush, and Joseph D. Moyer.

Tritium-labeled compounds V. Radioassay of both carbon-14 and tritium in films, with a proportional counter. Horace S. Isbell, Harriet L. Frush, and Nancy B. Holt.

High-altitude observation techniques, D. M. Gates, *Letter Sci.* **131**, 266 (1960).

The relation between confidence intervals and tests of significance—a teaching aid, M. G. Natrella, *Am. Stat.* **14**, No. 1, 20 (1960).

Electrophoretic deposition of metals, metalloids, and refractory oxides, V. A. Lamb and W. R. Reid, *Plating* **47**, No. 3, 291 (1960).

Fusion of polymer networks formed from linear polyethylene: Effect of intermolecular order, L. Mandelkern, D. E. Roberts, J. C. Halpin, and F. P. Price, *J. Am. Chem. Soc.* **82**, 46 (1960).

Determination of the recording performance of a tape from its magnetic properties, E. D. Daniel and I. Levine, *J. Acoust. Soc. Am.* **32**, No. 2, 258 (1960).

Sauter theory of the photoelectric effect, U. Fano, K. W. McVoy and J. R. Albers, *Phys. Rev.* **116**, No. 5, 1147 (1959).

Bremsstrahlung and the photoelectric effect as inverse processes, K. W. McVoy and U. Fano, *Phys. Rev.* **116**, No. 5, 1168 (1959).

Surface area and exchange capacity relation in a Florida kaolinite, W. C. Ormsby and J. M. Shartsis, *J. Am. Ceram. Soc.* **43**, No. 1, 44 (1960).

Balmer decrements: the diffuse nebulae, S. R. Pottasch, *Astrophys. J.* **131**, No. 1, 202 (1960).

Standard frequency transmission and time signals, W. D. George, *Proc. 2d all-IRIG Symp.*, prepared by Secretariat, Inter-Range Instrumentation Group, October 1958, p. 141, IRIG Document No. 107-58.

Atomistic approach to the rheology of sand-water and clay-water mixtures, W. A. Weyl and W. C. Ormsby, ch. 7, vol. III, *Rheology—Theory and applications*, edited by F. R. Eirich, p. 249 (Academic Press Inc., New York, N. Y., 1960).

Diffusion of particles in turbulent flow, C. M. Tchen, *Adv. Geophys. 6: Atmospheric diffusion and air pollution* p. 165, *Proc. Symp. Oxford, England, Aug. 1958* (Academic Press Inc., New York, N. Y., 1959).

Atmospheric tides and ionospheric electrodynamics, M. L. White, *J. Geophys. Research* **65**, 153 (1960).

Some evidence for structural anomalies in pure cristobalite, R. F. Walker, S. J. Schneider, and R. S. Roth, *J. Am. Ceram. Soc.* **42**, No. 12, 642 (1959).

La Recherche sur les radicaux libres au National Bureau of Standards, H. P. Broida, *J. chim. phys.* **56**, No. 2392, 813 (1959).

Isotope exchange processes in solid nitrogen under electron bombardment, R. Klein and E. M. Horl, *J. Chem. Phys.* **32**, No. 1, 307 (1960).

Are life testing procedures robust? M. Zelen and M. C. Dannemiller, *Proc. 6th Natl. Symp. Reliability and Quality Control in Electronics*, Jan. 11–13, 1960, Inst. Radio Engrs. Inc., p. 185 (1960).

Relative measurement of the photodetachment cross section for H⁺, S. J. Smith and D. S. Burch, *Phys. Rev.* **116**, No. 5, 1125 (1959).

Interference of orbital and spin currents on bremsstrahlung and photoelectric effect, U. Fano, K. W. McVoy, and J. R. Albers, *Phys. Rev.* **116**, No. 5, 1159 (1959).

Use of the equation of hydrostatic equilibrium in determining the temperature distribution in the outer solar atmosphere, S. R. Pottasch, *Astrophys. J.* **131**, No. 1, 68 (1960).

Reception of space diversity transmitters, J. W. Koch, *Wireless World (England)* **65**, No. 10, 512 (1959).

Improved NBS abrasive jet method for measuring abrasion resistance of coatings, A. G. Roberts, *ASTM Bull.* No. 244, 48 (TP52) (1960).

Flame-spread measurements by the radiant panel flame-spread method, D. Gross, *Forest Products J.* **X**, No. 1, 33 (1960).

Reactions en chaîne de radicaux geles, J. L. Jackson, *J. chim. phys.* **56**, No. 2392, 771 (1959).

Etude spectroscopique des produits de la décharge électrique dans l'Azote condensé à l'état solide à très basse température, prévues en faveur de l'existence d'Azote triatomique dans le solide, M. Peyron, E. M. Horl, H. W. Brown, and H. P. Broida, *J. chim. phys.* **56**, No. 2392, 736 (1959).

Apparent temperatures measured at melting points of some metal oxides in a solar furnace, J. J. Diamond and S. J. Schneider, *J. Am. Ceram. Soc.* **43**, No. 1, 1 (1960).

- What price accurate text methods? A. T. McPherson, *ASTM Bull.* (ACR Notes Column) No. 244, 7 (1960).
- Perovskite-type compounds in binary rare earth oxide systems, S. J. Schneider and R. S. Roth, *J. Am. Ceram. Soc.* **43**, No. 2, 115 (1960).
- Use of disodium *m*-benzenedisulfonate as a hardening agent in Watts nickel bath, W. H. Metzger, P. A. Krasley, and F. Ogburn, *Plating* **47**, No. 3, 285 (1960).
- On the convergence of the Rayleigh quotient iteration for the computation of characteristic roots and vectors, VI. (Usual Rayleigh quotient for nonlinear elementary divisors), A. M. Ostrowski, *Arch. Rat. Mech. Anal.* **4**, No. 2, 153 (1959).
- An analysis of time variations in tropospheric refractive index and apparent radio path length, M. C. Thompson, H. B. James, and A. W. Kirkpatrick, *J. Geophys. Research* **65**, 193 (1960).
- Neutron detection by reactions induced in scintillators, C. O. Muehlhaue, pt. I, *Fast neutron physics*, sec. III, pt. III. B, p. 387 (Interscience Publ., New York, N.Y., 1960).
- A relationship between the lower ionosphere and the [OI] 5577 nightglow emission, J. W. McCaulley and W. S. Hough, *J. Geophys. Research* **64**, No. 12, 2307 (1959).
- Many changes reflected in new dry cell standard, W. J. Hamer, *Mag. of Standards* **31**, No. 3, 81 (1960).
- Etude aux infrarouges de certains solides condensés à partir de décharges en phase gazeuse, K. B. Harvey and H. W. Brown, *J. chim. phys.* **56**, No. 2392, 745 (1959).
- Water penetration testing machine for sole leather, T. J. Carter, *J. Am. Leather Chemists' Assoc.* **LV**, No. 3, 139 (1960).
- Theory of flame propagation in solid nitrogen at low temperatures, S. G. Reed and C. M. Herzfeld, *J. Chem. Phys.* **32**, No. 1, 1 (1960).
- A note regarding the mechanism of UHF propagation beyond the horizon, A. D. Watt, E. F. Florman, and R. W. Plush, *Letter Proc. IRE* **48**, 252 (1960).
- High-frequency limit of bremsstrahlung in the Sauter approximation, U. Fano, *Phys. Rev.* **116**, No. 5, 1156 (1959).
- The weighted compounding of two independent significance tests, M. Zelen and L. S. Joel, *Ann. Math. Stat.* **30**, No. 4, 885 (1959).
- A model of the *F* region above $h_{\text{max}}F2$, J. W. Wright, *J. Geophys. Research* **65**, 185 (1960).
- Interference of antioxidant in the determination of low polymer in SBR synthetic rubber, L. T. Milliken and F. J. Linnig, *J. Polymer Sci.* **XLI**, No. 138, 544 (1959).
- Physical properties of synthetic-rubber-base dental impression materials, W. A. C. Miller, Jr., W. C. Hansen, G. Dickson, and W. T. Sweeney, *J. Am. Dental Assoc.* **60**, 211 (1960).
- Microwave absorption in compressed oxygen, A. A. Maryott and G. Birnbaum, *J. Chem. Phys.* **32**, No. 3, 686 (1960).
- Liquid hydrogen from chemical and nuclear rockets, R. B. Scott, *Discovery* **XXI**, No. 2, 74 (1960).
- Studies of infrared absorption spectra of solids at high pressures, E. R. Lippincott, C. E. Weir, A. Van Valkenburg, and E. N. Bunting, *Spectrochim. Acta* **16**, p. 58 (1960).
- Phosphorescence of nitrogen and nitrogen-argon deposited films at 4.2° K, H. P. Broida and R. W. Nicholls, *J. Chem. Phys.* **32**, No. 2, 623 (1960).
- Nickel-aluminum alloy coatings produced by electrodeposition and diffusion, D. E. Couch and J. H. Connor, *J. Electrochem. Soc.* **107**, No. 4, 272 (1960).
- Energy requirements of mechanical shear degradation in concentrated polymer solutions, A. B. Bestul, *J. Chem. Phys.* **32**, No. 2, 350 (1960).
- Detecting radiation, L. Costrell, *Chem. Eng. News*, p. 132 (1960).
- Several new methods to measure the thermal diffusivity of semiconductors, J. H. Becker, *J. Appl. Phys.* **31**, No. 3, 612 (1960).
- Opportunities in dental research, G. C. Paffenbarger, *J. Am. Dental Assoc.* **60**, 413 (1960).
- Departures of hydrogen from L. T. E. in a stellar atmosphere and the consequent structure of the solar chromosphere, S. R. Pottasch, *Commun. Observatoire Roy. Belgique* No. 157, entitled The empirical determination of the stellar photospheric structure, Paper 11, 67 (1959).
- Low-temperature transport properties of commercial metals and alloys. III. Gold-cobalt, R. L. Powell, M. D. Bunch, and E. F. Gibson, *J. Appl. Phys.* **3**, 504 (1960).
- Pilot plant data for hydrogen isotope distillation, T. M. Flynn, *Chem. Eng. Progr.* **56**, No. 3, 37 (1960).
- Correlation effects in impurity diffusion, J. R. Manning, *Phys. Rev.* **116**, No. 4, 819 (1959).
- Short-wave fadeouts without reported flares, H. DeMastus and M. Wood, *J. Geophys. Research* **65**, No. 2, 609 (1960).
- On the propagation of ELF radio waves and the influence of a nonhomogeneous ionosphere, J. R. Wait, *J. Geophys. Research* **65**, No. 2, 597 (1960).
- Precision Zeeman modulation microwave spectrometer, R. W. Zimmerman, *Rev. Sci. Instr.* **31**, 106 (1960).
- Chemistry, food, and civilization, A. T. McPherson, *J. Wash. Acad. Sci.* **50**, No. 3, 1 (1960).
- World maps of *F2* critical frequencies and maximum usable frequency factors for use in making ionospheric radio predictions, D. H. Zacharisen and V. Agy, *J. Geophys. Research* **65**, 593 (1960).
- Recent experimental evidence favouring the $pK(p)$ correlation function for describing the turbulence of refractivity in the troposphere and stratosphere, K. A. Norton, *J. Atmospheric and Terrest. Phys.* **15**, 206 (1959).
- Cavity resonator dielectric measurements on rod samples, H. Bussey, *Insulation*, p. 26 (1959).
- Low-temperature transport properties of commercial metals and alloys. II. Aluminums, R. L. Powell, W. J. Hall, and H. M. Roder, *J. Appl. Phys.* **31**, 496 (1960).
- Prediction of sunspot numbers for cycle 20, W. B. Chadwick, *Nature*, p. 1787 (1959).
- The melting of crystalline polymers, L. Mandelkern, *Rubber Chem. and Technol.* **XXXII**, No. 5, 1392 (1959).
- Sampling of leather, J. Mandel and C. W. Mann, *J. Sci. and Ind. Research* **18A**, No. 12, 575 (1959).
- Infrared studies of dense forms of ice, E. R. Lippincott, C. E. Weir, and A. Van Valkenburg, *Commun. to Editor, J. Chem. Phys.* **32**, No. 3, 612 (1960).
- A technique for reducing errors in permeability measurements with coils, B. L. Danielson and R. D. Harrington, *Proc. IRE* **48**, No. 3, 365 (1960).
- Atmospheric limitations on electronic distance measuring equipment, M. C. Thompson, Jr., H. B. Janes, and F. E. Freethy, *J. Geophys. Research* **65**, 389 (1960).
- Weighted restricted partitions, M. Newman, *Acta Arith.* **V**, 371 (1959).
- A continuous poker game, A. J. Goldman and J. J. Stone, *Duke Math. J.* **27**, No. 1, 41 (1960).
- Proposed specification for impression material: synthetic rubber base, dental, W. A. C. Miller, Jr., W. C. Hansen, G. Dickson, and W. T. Sweeney, *J. Am. Dental Assoc.* **60**, 224 (1960).
- Some results on the cross-capacitances per unit length of cylindrical three-terminal capacitors with thin dielectric films on their electrodes, D. G. Lampard and R. D. Cutkosky, *Inst. Elec. Engrs. (London, England) Monograph No. 351M*, 1 (1960).
- Low temperature phase transition of colemanite, A. Perloff and S. Block, *Letter to Editor, Am. Mineralogist*, p. 229 (1960).
- A class of non-linear dielectric materials, P. H. Fang, R. S. Roth, and H. Johnson, *J. Am. Ceram. Soc.* **43**, p. 169 (1960).

*Publications for which a price is indicated (except for NBS Technical Notes) are available only from the Superintendent of Documents, U.S. Government Printing Office, Washington 25, D.C. (foreign postage, one-fourth additional). Technical Notes are available only from the Office of Technical Service, U.S. Department of Commerce, Washington 25, D.C. (Order by PB number.) Reprints from outside journals and the NBS Journal of Research may often be obtained directly from the authors.

ERRATA

Corrections should be made to recent papers in the Journal of Research,
Section D, as follows:

Vol. 63D, No. 2, September–October 1959

p. 183, eq (5); the quantities $\frac{\pi}{2} - \phi' + 2\pi m$ and $\phi' + \frac{\pi}{2} + \pi m$ in the large brackets
should be enclosed by parentheses.

p. 184, eqs (9b) and (9c); X_1 and X_2 are defined by $X_1 = \left(\frac{ka}{2}\right)^{1/3} \left(\frac{\pi}{2} + \phi'\right)$ and
 $X_2 = \left(\frac{ka}{2}\right)^{1/3} \left(\frac{\pi}{2} - \phi'\right)$.

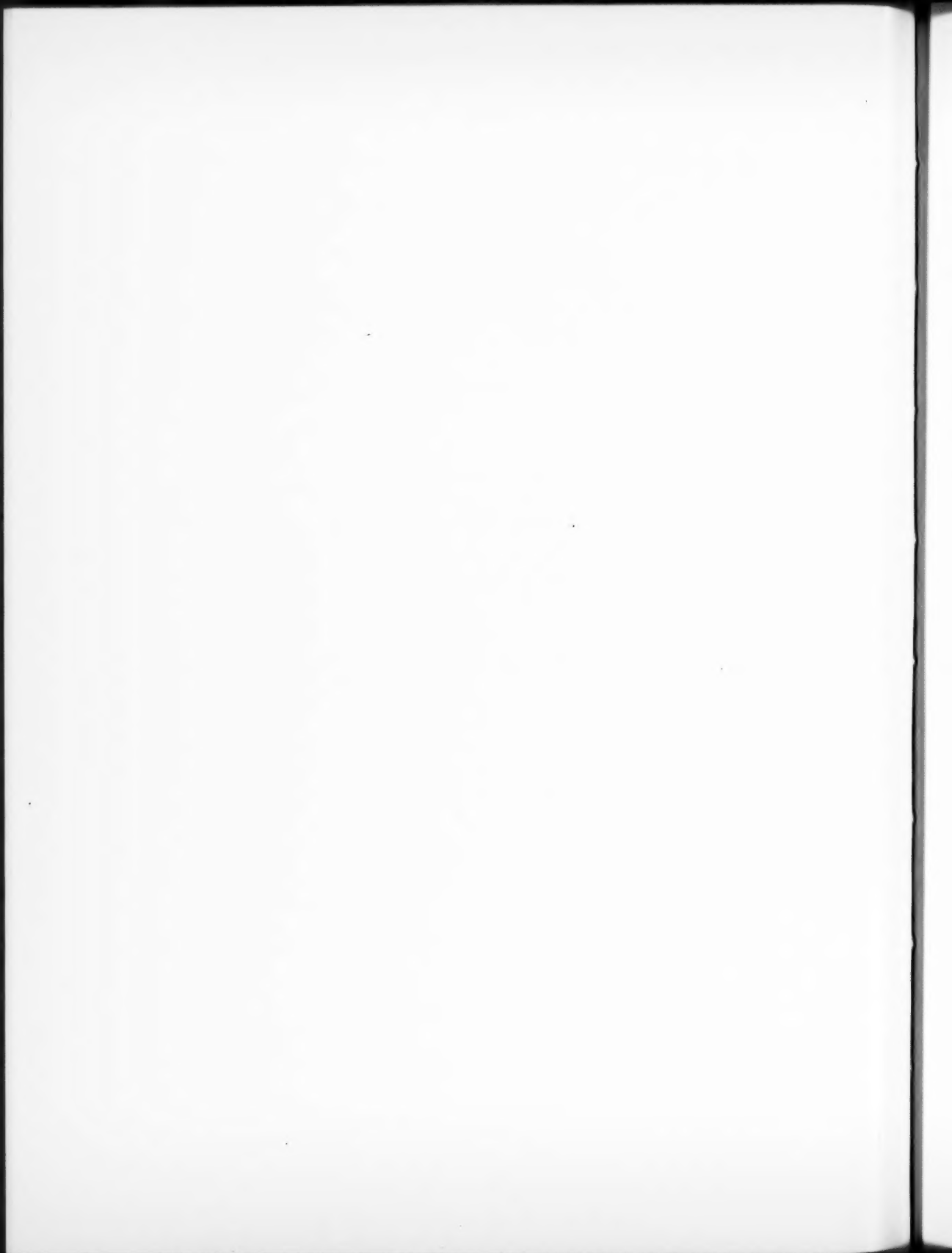
p. 184, eqs (10a) and (10b); the arguments of the functions \hat{G} are $\left(\frac{ka}{2}\right)^{1/3}$
 $(2\pi m + \phi)$ and $\left(\frac{ka}{2}\right)^{1/3} (2\pi m - \phi)$.

Vol. 64D, No. 4, July–August 1960

p. 324, line 10; "the distance" should read "the distances."

p. 325, at the end of line introducing eq (30) insert footnote reference 5, and
add footnote 5, reading:

$\delta\xi^2$ is the distance along straight line OV , of the point of integration
from the point of stationary phase.



Report of the United States of America National
Committee to the XIII General Assembly of the In-
ternational Scientific Radio Union, London, England,
September 5 to 15, 1960.

Foreword

The U.S.A. National Committee Report for the period 1957-1960 represents a departure from previous reports in scope and form. The Committee decided that a concerted effort should be made by the Commissions to review the work in their fields more critically than was done heretofore. The evaluation of progress rather than a bibliographical summary and a résumé that places the status of the field in its proper perspective were set as major objectives. The members of the Commissions responded enthusiastically to the call for contributions and the objectives have been met in a large measure. We hope that the National Committee Report will itself furnish a basis for discussions at the General Assembly and it represents a step forward in the activity of the National Committee.

The National Bureau of Standards has given inestimable aid to the preparation of the report for presentation to the General Assembly. An editorial group under Mr. Bradford Bean undertook the enormous task of uniformizing the method of referencing and of checking the references and preparing the manuscript for final printing. Time was too limited to allow for extensive editing of the manuscripts and in some cases the reports are more than coverages of the period 1957-1960. However, such deviations and expansions are not without value in a first presentation of this type.

U.S.A. National Committee

Table of Contents

Commission 1. Radio Measurement Methods and Standards:	Page
Review of developments	591
1. Frequency and time interval	E. A. Gerber 592
1.1. Quartz crystal standards	592
1.2. Atomic frequency and time standards	592
1.3. Frequency and time measurement and comparison	593
1.4. References	594
2. RF and microwave power measurements	G. F. Engen 596
References	596
3. Impedance measurements and standards	G. S. Deschamps 598
References	598
4. Development in attenuation measurements and standards	Bruno O. Weinschel 599
4.1. Definition of attenuation	599
4.2. Techniques for insertion loss or attenuation measurements	599
4.3. Self-calibrating techniques	600
References	600
5. Noise measurements and standards	B. M. Oliver 601
References	601
6. Field strength measurements	M. C. Selby 603
References	603
7. Measurements of physical quantities by radio techniques	M. C. Thompson, Jr. 605
References	605
Commission 2. Tropospheric Radio Propagation:	
National Committee Report	607
1. Physical characteristics of the troposphere	607
1.1. Synoptic scale	607
1.2. Refractive irregularities	608
1.3. Absorption in the troposphere	609
2. Tropospheric propagation (theories)	612
2.1. Ground wave propagation	612
2.2. Back scattering from rough surfaces	612
2.3. Theory of propagation through a stratified atmosphere	613
2.4. Line-of-sight scintillation	613
2.5. Scatter propagation	614
a. Layers	614
b. Blobs	614
3. Experimental results from investigations of tropospheric propagation	615
3.1. Attenuation with distance	615
Data sources for report and chart	615
3.2. Effects of rough terrain	616
a. Forward scattering	616
b. Backscattering	618
3.3. Angular diversity	618
3.4. Frequency diversity	619
3.5. Diversity improvement	619
3.6. Phase stability	620
4. Radio meteorology	621
4.1. Climatic investigations	621
4.2. Refractometer investigations	621
4.3. Refraction	621
4.4. Radar meteorology	621
5. References	622
Commission 3. Ionospheric Radio Propagation:	
Review of U.S.A. activity, 1957-59	629
1. Structure of the upper atmosphere	629
2. Ionizing radiations	630
3. Electron densities	630
4. Satellite beacon studies	630
5. Ionospheric processes	630
6. Ionospheric disturbances	631
7. Sporadic E and spread F	631
8. Studies of the lower ionosphere	631
9. Radar studies of auroral ionization	631
10. Refraction in the ionosphere	632
11. Ionospheric propagation studies—general	632
12. Ionospheric scatter transmission	632
13. Radio reflection from meteor ionization	632
13.1. The reflection properties of individual trails	632
13.2. Computation and measurement of the gross propagation characteristics of ensembles of trails	632
13.3. The study of ionospheric motions through the use of meteor trails as indicators	633
14. Ionospheric propagation research with communication systems applications	633
14.1. Multipath effects	633
14.2. Fading	633
14.3. Arctic propagation	633
14.4. General	634
References	634

Commission 4. Radio Noise of Terrestrial Origin:	Page
Report of U.S. Commission 4, URSI (1957-1960).....	637
1. Radiofrequency radiation from lightning discharges..... A. Glen Jean	638
2. Properties of atmospheric noise at various receiving locations..... William Q. Crichlow	640
3. Summary of research on whistlers and related phenomena.....	642
3.1. Stanford University..... R. A. Helliwell	642
a. Methods of whistler analysis.....	642
b. IGY-IGC synoptic whistler results.....	642
c. Whistler sources.....	643
d. Association between aurorae and VLF hiss observed at Byrd Station, Antarctica.....	643
e. Duct theory.....	643
f. Ray path calculations.....	643
g. Electron density of the outer ionosphere.....	644
h. Theory of VLF emissions.....	644
i. Controlled whistler—mode experiments.....	644
j. Satellite measurements.....	644
k. Geocyclotron.....	644
3.2. Dartmouth College..... M. G. Morgan	644
a. Whistlers—East.....	644
(1) Whistlers.....	645
(2) Ionospherics.....	645
b. E 4° (Geomagnetic) stations: successor to whistler—East.....	646
c. Post—IGY results.....	646
d. E 94° (Geomagnetic) stations.....	646
e. Angle of arrival measurements.....	646
f. Acknowledgment.....	646
4. A summary of VLF and ELF propagation research..... James R. Wait	647
4.1. Introduction.....	647
4.2. Theoretical studies.....	647
4.3. Experimental studies.....	648
4.4. Recent applications of VLF propagation.....	648
5. Hydromagnetic waves and ELF oscillations in the ionosphere..... James M. Watts	650
6. The exosphere..... James M. Watts	651
6.1. Introduction.....	651
6.2. Theories of the exosphere.....	651
a. Magnetic storm effects.....	651
b. Radiation belt theory.....	651
c. Composition of the exosphere.....	651
6.3. Experiments in the exosphere.....	651
7. References.....	652
Commission 5. Radio Astronomy:	
Review of developments.....	655
1. University of Alabama.....	655
2. Air Force Cambridge Research Center.....	655
3. U.S. Army Signal Research and Development Laboratory.....	656
4. California Institute of Technology.....	656
5. Carnegie Institution of Washington.....	656
6. Cornell University.....	657
7. Collins Radio Company.....	657
8. University of Colorado.....	658
9. Harvard University.....	659
10. Hayden Planetarium.....	659
11. University of Illinois.....	659
12. U.S. Naval Research Laboratory.....	660
12.1. Planets:	
Venus.....	660
Jupiter.....	661
Mars.....	661
12.2. Cosmic radio sources.....	661
12.3. Sun.....	662
12.4. Moon.....	663
12.5. Atmospheric attenuation.....	663
13. The National Aeronautics and Space Administration.....	663
14. National Bureau of Standards, Boulder Laboratories.....	664
15. National Radio Astronomy Observatory.....	664
15.1. The flux density of radiation from Cas A at 1400 Mc/s.....	664
16. Ohio State University.....	664
17. Rensselaer Polytechnic Institute.....	665
18. Stanford University.....	665
19. Yale University.....	665
20. University of Michigan.....	666
20.1. University of Michigan 85-foot radio telescope.....	666
20.2. Traveling-Wave tube receiver at 8000 Mc/s.....	666
20.3. Maser radiometer at 8700 Mc/s.....	666
20.4. Radiometer at 1.8 CM wavelength.....	666
20.5. Theoretical radio spectrum of Venus.....	666
References.....	667

Commission 6. Radio Waves and Circuits:		
Subcommission 6.1. Information Theory:		Page
Part 1. Information theory and coding	P. Elias	671
1. Foundations		671
2. Binary channels		671
3. Sequential decoding		672
4. Conclusions on coding		672
5. Other topics		672
6. References		673
Part 2. Random processes	P. Swerling	674
References		675
Part 3. Pattern recognition	Arthur Gill	676
3.1. Redundancy removal		676
3.2. Recognition programs		676
3.3. Recognition system design		676
References		677
Part 4. Detection theory	Robert Price	678
4.1. Remarks		678
4.2. Papers		678
4.3. Bibliography:		
a. Applications to radar		678
b. Applications to communications		679
c. Sequential decision		679
d. Detection of stochastic signals in noise		679
e. Parameter estimation		679
f. Loss in nonlinear devices		679
g. Attacks on the <i>a priori</i> problem		680
h. Miscellaneous		680
4.4. Books		680
Part 5. Prediction and filtering	L. A. Zadeh	681
5.1. Nonlinear filtering		681
5.2. Filtering and radiation of nonstationary, discrete-time, and mixed processes		683
5.3. Miscellaneous contributions		684
Bibliography		684
Subcommission 6.2. Circuit Theory:		
Circuit theory	Louis Weinberg	687
1. Introduction		687
2. Combinatorial topology or linear graphs		688
2.1. Future research activity and evaluation		689
3. Synthesis by pole-zero techniques		692
3.1. Future research activity		694
4. Realizability conditions and positive real matrices		696
4.1. Future research		696
5. Systems with time-varying and nonlinear reactances		698
6. Active systems		700
6.1. Active RC synthesis		700
6.2. Adaptive systems		701
6.3. Tunnel-diode networks		701
6.4. Future research activity		702
7. Concluding remarks		703
References		704
Subcommission 6.3. Antennas and Waveguides:		
Part 1. Diffraction and scattering	L. B. Felsen and K. M. Siegel	707
1. High-frequency diffraction		707
1.1. Canonical problems		708
1.2. Approximate theories		710
Summary		712
2. Rayleigh scattering		712
3. The resonance region		712
4. Future activities		713
5. References		713
Part 2. On multiple scattering of waves	V. Twersky	715
1. Purpose		715
2. General considerations		715
3. Survey		718
3.1. Fixed configurations of <i>N</i> scatterers		718
3.2. Infinite planar lattices		720
3.3. Planar random distributions		722
a. Sparse distribution (two dimensional "rare gas")		722
b. General statistical distribution		723
3.4. Periodic volume distributions		724
3.5. Random volume distributions		724
References		725
Part 3. Antennas	R. W. Bickmore and R. C. Hansen	731
1. Introduction		731
2. Broadband antennas		731
Bibliography		732

	Page
3. Dynamic antennas.....	733
Bibliography.....	735
4. Large aperture antennas.....	735
References.....	738
5. Small aperture antennas.....	739
References.....	741
A bibliography on coherence theory.....	G. B. Parrent, Jr. 742
Text.....	742
References.....	742
A bibliography of automatic antenna data processing.....	C. J. Drane 743
Text.....	743
References.....	745
Surface and leaky wave antennas.....	F. J. Zucker 746
1. Surface wave antennas.....	746
2. Leaky wave antennas.....	747
3. Assessment and predictions.....	748
References.....	748
Commission 7. Radio Electronics:	
1. Parametric amplifiers.....	P. K. Tien and H. Heffner 751
1.1. General theory and historical development.....	751
1.2. Ferromagnetic amplifier—theory and experiment.....	751
1.3. Diode amplifiers and noise figure measurements.....	752
1.4. Electron beam parametric amplifier—space-charge wave parametric amplifier and Adler's tube.....	753
References.....	753
2. Microwave properties of ferrites.....	P. K. Tien and B. Lax 755
2.1. Finite waveguide components, frequency doubler and mixer, and ferromagnetic amplifiers.....	755
2.2. Linewidth of single crystal yttrium-iron garnet surface imperfections and rare earth impurities.....	755
2.3. Instabilities and magnetostatic modes.....	756
References.....	756
3. Progress in solid-state masers.....	A. Siegman 758
3.1. Cavity-type solid-state masers: experimental results.....	758
3.2. Applications of solid-state masers.....	758
3.3. Solid-state masers: theory and analysis.....	758
3.4. Maser materials.....	759
3.5. Pulsed and two-level masers.....	759
3.6. Traveling-wave masers.....	759
3.7. Noise in masers.....	759
3.8. Infrared and optical masers.....	760
References.....	760
4. Low-noise beam-type microwave tubes.....	L. Smullin 763
4.1. Progress during the past three years.....	763
a. Design of solid-beam, low-noise guns.....	763
b. Theory of noise on beams and low-noise amplifications.....	763
c. Hollow beam low-noise guns.....	763
d. Theory of noise in multivelocity electron beams.....	764
e. Fundamental noise measurements.....	764
f. Electron beam parametric amplifiers.....	764
g. Low-noise klystrons.....	764
References.....	764
5. Interaction between plasmas and electromagnetic fields.....	L. Smullin 766
5.1. Introduction.....	766
5.2. Propagation of electromagnetic waves in unbounded plasmas—small signal theory.....	766
5.3. Plasma waveguides.....	766
5.4. Electron stimulated plasma oscillations.....	766
5.5. Large signal oscillations.....	767
References.....	767
Publications of the staff of the National Bureau of Standards.....	769
Index to volume 64D, Radio Propagation, Jan.—Dec. 1960.....	773

Figures

Commission 2, Tropospheric Radio Propagation	
Figure 1. Attenuation due at one atmosphere.....	610
Figure 2. Water vapor attenuation for 7.5 g/cm.....	611
Figure 3. Beyond horizon transmission.....	616
Figure 4. Theoretical smooth earth curves.....	617
Commission 6, Radio Waves and Circuits	
Subcommission 6.2, Circuit Theory	
Figure 1. Chain of five 1-ohm resistances realizing the given impedance matrix.....	692
Figure 2. Idealized parametric amplifier.....	699
Figure 3. Possible form for realization of any active transfer function.....	700
Figure 4. Representation of an active driving-point function.....	700
Figure 5. Signal-flow diagram of the classical method of active RC network design.....	700
Figure 6. Network realizing the given RC voltage ratio (values in ohms and farads).....	702

Report of U.S. Commission 1, URSI RADIO MEASUREMENT
METHODS AND STANDARDS

*Review of developments occurring within the United States of America in the
fields of Radio Measurement Methods and Standards, 1957-60*

The following report briefly summarizes significant developments and lists publications of the last three years. The bibliographies are fairly complete and any omissions that may occur are unintentional. The topics covered are the following.

- | | |
|--|---------------------|
| 1. Frequency and Time Interval | E. A. Gerber |
| 2. R.F. and Microwave Power | G. F. Engen |
| 3. Impedance | G. A. Deschamps |
| 4. Attenuation | B. O. Weinschel |
| 5. Noise | B. M. Oliver |
| 6. Field Strength | M. C. Selby |
| 7. Measurement of Physical Quantities by
Radio Techniques | M. C. Thompson, Jr. |

1. Progress in the United States During the Last Three Years on Frequency and Time Interval Standards and Measurements

E. A. Gerber*

1.1. Quartz Crystal Standards

A new IRE Standard on Piezoelectric Crystals defines methods for the Determination of the Elastic, Piezoelectric, and Dielectric Constants, and for the Electromechanical Coupling Factor. Additionally, it brings order and system into the hitherto confused terminology on piezoelectric crystals [Proc. IRE, 1958].

The biggest problem for precise quartz crystal standards has been the aging of resonators. It is now possible to control the environmental influences on aging to a very large extent. Attention has, therefore recently been directed mostly to the processes within the crystal lattice. The internal friction in natural and synthetic quartz has been studied as a function of temperature and frequency and the anelastic behavior has been explained from the interplay between dislocations and impurities [Granato, Lücke, 1957; Wasilik, 1957; Mason, 1958; King, 1959]. It has been demonstrated that X-ray irradiation or simultaneous exposure to high electric fields and high temperatures (electrolytic purification) produces changes in the anelastic absorption spectrum [King, 1959].

Great progress has been made in the improvement of the stability of quartz crystals standards. The aging, the Q , and other properties of quartz resonators vibrating in various modes have been studied in the temperature range from 4 to 330 °K. A Q of 50 millions has been observed on one mode at 4.2 °K [White, 1958; Warner, 1958] and the aging rate at this temperature was extremely low, its value of a few parts in 10^{11} per day probably given by the limits of instrumentation [Warner, 1958; Simpson, Morgan, 1959]. The quartz resonators, however, proved to be rather sensitive with respect to shock and vibration, and this observation might explain the fact that the short-time stability at 4 °K, as measured in comparison with an ammonia maser, is less than the stability measured over 2 hr [Morgan, Barnes, 1959]. Quartz resonators kept near room temperature still show a very low aging rate, comparable with that at 4.2 °K; the Q -values, however, are approximately one order of magnitude less [Warner, 1958]. Data on crystal standards are compiled in table 1, together with corresponding data on atomic standards. The term "accuracy"

as used in the table is defined as the relative deviation from a previously accepted frequency value; "stability" is defined as the maximum relative frequency change during a specified time interval from the value at the beginning of this interval. It must be pointed out that the data in table 1 are intended to give information on orders of magnitude only. More precise data on accuracy and stability would require a detailed description of the apparatus.

1.2. Atomic Frequency and Time Standards

Great progress in the above field has continued, especially along the lines of first, passive beam devices; secondly, ammonia masers; and thirdly, gas cell devices.

A cesium beam standard has become commercially available under the trade name "Atomichron" [McCoubrey, 1958; Mainberger, Orenberg, 1958; Mainberger, 1958]. To improve its performance the geometry of the microwave structure has been changed and the microwave source has been simplified for greater reliability and reduction of sidebands [McCoubrey, 1958]. The integrated outputs of several Atomichrons have been compared in order to observe the difference in accumulated phase over extended periods. The two best Atomichrons were found to have deviated by no more than 1 μ sec after 63 hr or 5 parts in 10^{12} of the measured time interval [Bridgham, Winkler, Reder, 1959]. Cesium beam standards of British and United States design have been compared and the principal sources of error studied [Holloway et al., 1959]. There remains an unresolved discrepancy between the standards of about 2 parts in 10^{10} . Efforts to increase the precision of atomic beam standards have been going into two directions: First, the "broken beam experiment" to increase the microwave interaction time [Kleppner, Ramsey, Fjelstadt, 1958] and secondly, studies of molecular spectra in the millimeter range [Hughes, 1959; Gallagher, 1959] to improve the Q of the quantum mechanical resonator. The described work in passive beam standards has been supported by studies of a more fundamental nature, such as molecular beam resonances for various combinations of nonuniform fixed and oscillatory fields [Ramsey, 1958].

Work on high precision ammonia maser oscillators has been continued at a high rate. The effects on the maser frequency resulting from cavity pulling,

* U.S. Army Signal Research & Development Laboratory, Fort Monmouth, N.J.

TABLE 1. Typical precision frequency standards

Device	Frequency of resonator	Accuracy†	Stability (with respect to time)	Q of resonator	Operational time of resonator	Space requirement (with freq. translating equipment)	Weight
Precision crystal oscillator (commercially available)	Mc/s 1	$\pm 1 \times 10^{-6}$ *	3×10^{-4} /mo	1×10^6	Not specified	ft ³	lb 20
Precision crystal oscillator (experimental)	2.5	$\pm 1 \times 10^{-6}$ *	2×10^{-10} /mo 2×10^{-10} /sec	5×10^6	Not specified		25
Cs-beam frequency standard (commercially available under the name "Atomichron")	9,193	$\pm 2 \times 10^{-10}$	2×10^{-11} /day however, no measurable long-term drift	60×10^6	10,000 and better	16	800 (Commercial model 1001)
						12	500 (Military model)
Ammonia maser (experimental, portable, with limited coolant supply)	23,870	$\pm 1 \times 10^{-6}$	1×10^{-11} /hr 2×10^{-10} /sec	5×10^6	8	1	40
Gas cell (rubidium 87, experimental)	6,835	$\pm 1 \times 10^{-9}$	1×10^{-10} /mo	300×10^6	Not specified	3½	30 (Estimated)

*Crystal manufacturing tolerances only.

†The accuracy in the table presumes no prior adjustment of the device against a primary frequency standard. If this were done, the accuracy of the device merely approaches the resolution of the measurement equipment at the moment of adjustment.

nonuniform radiation of the beam inside the cavity, hyperfine structure of the spectral line, thermal effects and variations in beam flux and residual pressure have been studied in great detail [Mockler et al., 1958; Vonbun, 1959; White, 1959; Barnes, 1959; Townes, 1957; Vonbun, 1958a]. The following measures, employed either single or in combination, may yield accuracies and stabilities as plotted in table 1: Symmetrical maser structure employing two beams [Mockler et al., 1958], temperature controlled cavity ($\pm 0.001^\circ \text{C}$) [Mockler et al., 1958] or quartz cavity near a temperature for which the expansion coefficient goes through zero [Vonbun, 1959], center line location by using the Zeeman effect [Vonbun, 1958a], precise control of residual pressure [White, 1959]. A small sealed-off maser for missile application maintained its frequency to better than 5 parts in 10^{10} under a static acceleration of 25G [Reder, Bickart, 1959]. Exact data on state separator construction have become available [Vonbun, 1958b]. Two-cavity masers have been studied [Higa, 1957; Wells, 1958] and it has been found that the two cascaded cavities may oscillate at different frequencies. Investigations of the noise in ammonia maser amplifiers resulted in data for the noise figure as a whole [Helmer, 1957] and for the beam temperature [Gordon, White, 1958], and suggest how signal-to-noise ratios can be improved [Beers, 1959]. Studies of the ammonia spectrum itself [Hadley, 1957; Vuylsteke, 1959] and of the interaction between the electromagnetic field and a number of similar atomic systems [Senitzky, 1959], round up the maser work in the reporting period.

A considerable amount of work on gas cells has been done in several places, employing mostly rubidium or cesium as the reference atom. In contrast to beam devices where the Boltzmann distribution of atoms or molecules among the various possible energy states is changed by means of state

separators employing electric or magnetic fields, atoms in gas cells are "optically pumped" into a desired ground state hyperfine level. The intensity of the pumping radiation absorbed or scattered by the gas cell changes when the desired microwave transition occurs. This offers a very convenient way of detecting the microwave resonance. Additionally, the introduction of a "buffer gas" into the cell is necessary to reduce the Doppler broadening of the microwave line. However, the buffer gas produces a shift of the center frequency of the hyperfine transition and this shift is a function of temperature and pressure [Beaty et al., 1959; Bender et al., 1958; Arditi, 1960; Andres, 1959; Whitehorn, 1959; Bell, 1958]. Mixtures of buffer gases have been made, however, which make both the temperature and pressure coefficient small and keep the signal-to-noise ratio moderate [Beaty et al., 1959; Arditi, 1960]. The frequency shift in the hyperfine splitting of alkalis caused by added gases has been found to be caused by exchange as well as dispersion forces [Margenau et al., 1959]. In order to obtain a strong signal for the optical detection of the ($M_F=0 \rightarrow M_F=0$, $\Delta F=\pm 1$) transition, selective hyperfine filtering of the pumping light [Bender et al., 1958; Bell et al., 1958] or pulses of rf radiation at the Zeeman frequency have been used [Alley, 1959]. With the usage of optical detection, a mixture of 12 percent neon and 88 percent argon as buffer gas, and a temperature stability of 0.1°C , data as indicated in table 1 can be obtained [Beaty et al., 1959].

1.3. Frequency and Time Measurement and Comparison

Two methods have mainly been used for high precision frequency and time measurement: The first employs multiplication of the unknown and the standard frequency to 1000 Mc/s and above, and

measurement of the beat frequency; the precision of measurement can be 1.10^{-11} for a 100-sec count [Simpson, Morgan, 1959]. The second method also employs frequency multiplication; however, the period of the beat note is measured [Simpson, Morgan, 1959; Tanzman, 1959]. The sensitivity of the latter method is, for multiplication to 100 Mc/s and for n periods $(6.10^{-10})/n$ [Tanzman, 1959]. Another method uses timing pulses at the instant the two signals to be compared are in opposition. This yields for a comparison of 100 kc/s frequencies and 10-sec beat period a timing accuracy of 1 μ sec or an accuracy of frequency comparison of 1.10^{-13} [Thompson, Archer, 1959]. Digital rate synthesis has also been used for frequency measurement [Rey, 1959]. The efficiency of frequency measurements with an atomic clock is given by the ratio: information gained/entropy increase [Peter, Strandberg, 1959]. The term "resolution" of a frequency measurement has been derived, meaning the relative error in the determination of a frequency due to phase modulation, noise, and errors in time interval measurements [Winkler, 1959].

In order to compare two frequencies, their values must be made compatible. For this purpose, and mostly in connection with atomic standards, frequency synthesizers and translators have been developed [McCoubrey, 1958; Mainberger, Orenburg, 1958; Mainberger, 1958; McCoubrey, 1959; Reder, Bickert, 1959; Saunders, 1959]. They consist of harmonic generators, mixers, and phase detectors. Usually, the atomic standard is phase locked either directly or via klystron to a harmonic of a crystal oscillator. Progress has been made in the understanding of harmonic generation with rectifiers and nonlinear reactances. The n th harmonic cannot be generated by ideal rectifiers with an efficiency exceeding $1/n^2$ [Page, 1958]. Usage of nonlinear capacitors will not enable one to greatly exceed the above limitations [Rafuse, 1959; Leeson, Weinreb, 1959]. Frequency multiplication with phase-locked oscillators has been achieved from 100 kc/s to 1000 Mc/s [McAleer, 1958], and above.

A determination of the frequency of the $(4,0 \rightarrow 3,0)$ transition in cesium in terms of the second of Ephemeris Time (E.T.) has been made [Markowitz et al., 1958; Markowitz, 1959]. The frequency is $9,192,631,770 \pm 20$ cps (of E.T.). The second of E.T. is identical with the prototype unit defined by the International Bureau of Weights and Measures in 1956. On January 1, 1959, the U.S. Naval Observatory placed in operation a system of Atomic Time, denoted A. 1, provided by cesium clocks and based on the above frequency. The WWV standard frequency transmissions of the National Bureau of Standards have been based on the U.S. Frequency Standard which is derived from atomic standards. The latter standards in turn have been brought into agreement with A. 1 beginning with January 1, 1960 [National Standards of Time and Frequency, 1960]. Corrections of the WWV transmissions with respect to the U.S. Frequency Standard are published monthly [WWV Standard Frequency Transmissions].

Several studies have been undertaken to make frequency and time comparison possible over long distances. Calculations showed that 10 to 100 kw for frequencies in the vicinity of 20 kc/s are required to provide a worldwide coverage [Watt, Plush, 1959]. Various frequency comparisons between stations in the United States and between United States and British stations controlled by atomic clocks using VLF carriers yielded standard deviations as low as 2 parts in 10^{11} [Pierce, 1958; Reder, Winkler]. Clock synchronization by transportation of atomic clocks has been achieved with an accuracy of much better than 1 μ sec for several hours flying time [Reder, Winkler].

In closing, a sort of Michelson-Morley experiment using ammonia masers is worthy of mention [Cedarholm et al., 1958]. Two masers with oppositely directed beams were compared and turned with respect to the earth's motion. It was concluded that the maximum ether drift, if any, is less than 1/1000 of the earth's orbital motion.

1.4. References (as of February 1960)

- Alley, C., Triple resonance method to achieve narrow and strong spectral lines, Proc. 13th Ann. Symp. Freq. Control, 632 (1959).
- Andres, J. M., D. J. Farmer, and G. T. Inouye, Design Studies for a rubidium gas cell frequency standard, IRE Trans. on Military Electron. **MIL-3**, 178 (1959).
- Arditi, M., A gas cell "atomic clock" as a high-stability frequency standard, IRE Trans. on Military Electron. **4**, 25 (1960).
- Barnes, F. S., Operating characteristics of an ammonia beam maser, Proc. IRE **47**, 2085 (1959).
- Beaty, E. C., P. L. Bender, and A. R. Chi, Hyperfine transitions in rubidium-87 vapor, Proc. 13th Ann. Symp. Freq. Control, 669 (1959).
- Beers, Y., Theory of the cavity microwave spectrometer and molecular frequency standard, Rev. Sci. Instr. **30**, 9 (1959).
- Bell, W., and A. L. Bloom, Optically detected field independent transition in Na vapor, Phys. Rev. **109**, 219 (1958).
- Bender, P. L., E. C. Beaty, and A. R. Chi, Optical detection of narrow Rb⁸⁷ hyperfine absorption lines, Phys. Rev. Letters **1**, 311 (1958).
- Bridgham, R., G. M. R. Winkler, and F. H. Reder, Synchronized clock experiment, Proc. 13th Ann. Symp. Freq. Control, 342 (1959).
- Cedarholm, J. P., G. F. Bland, B. L. Havens, and C. H. Townes, New experimental test of special relativity, Phys. Rev. Letters **9**, 342 (1958).
- Gallagher, J. J., Suitable molecules for utilizing millimeter wave transitions for frequency control, Proc. 13th Ann. Symp. Freq. Control, 604 (1959).
- Gordon, J. P., and L. D. White, Noise in maser amplifiers—theory and experiment, Proc. IRE **46**, 1588 (1958).
- Granato, A., and K. Lueke, On the orientation dependence of internal friction, J. Appl. Phys. **28**, 635 (1957).
- Hadley, G. F., $J=3$, $K=2$ Line in the inversion spectrum of NH_3 , Phys. Rev. **108**, 291 (1957).
- Helmer, J. C., Maser noise measurement, Phys. Rev. **107**, 902 (1957).
- Higa, W. H., Observations of non-linear maser phenomena, Rev. Sci. Instr. **28**, 726 (1957).
- Holloway, J., W. Mainberger, F. H. Reder, G. M. R. Winkler, L. Essen, and V. L. Parry, Comparison and evaluation of cesium atomic beam frequency standards, Proc. IRE **47**, 1730 (1959).
- Hughes, V. W., Considerations on the design of a molecular frequency standard based on the molecular beam electric resonance method, Rev. Sci. Instr. **30**, 689 (1959).
- King, J. C., The anelasticity of natural and synthetic quartz at low temperatures, Bell System Tech. J. **38**, 573 (1959).

- Kleppner, D., N. F. Ramsey, and P. Fjelstadt, Broken atomic beam resonance experiment, *Phys. Rev. Letters* **1**, 232 (1958).
- Leeson, D. B., and S. Weinreb, Frequency multiplication with nonlinear capacitors—A circuit analysis, *Proc. IRE* **47**, 2076 (1959).
- Mainberger, W., Primary frequency standard using resonant Cs, *Electronics* **31**, 80 (1958).
- Mainberger, W., and A. Orenburg, The atomichron-operation and performance, *IRE Natl. Conv. Record*, 14 (1958).
- Margenau, H., P. Fontana, and L. Klein, Frequency shifts in hyperfine splitting of alkalis caused by foreign gasses, *Phys. Rev.* **115**, 87 (1959).
- Markowitz, W., R. J. Hall, L. Essen, and J. V. L. Parry, Frequency of Cs in terms of ephemeris time, *Phys. Rev. Letters* **1**, 105 (1958).
- Markowitz, W., The system of atomic time, A. 1, *Proc. 13th Ann. Symp. Freq. Control*, 316 (1959).
- Mason, W. P., Use of internal friction measurements in determining the causes of frequency instabilities in mechanically vibrating frequency standards, *IRE Trans. on Instr.* **1-7**, 189 (1958).
- McAleer, H. T., Frequency multiplication with phase-locked oscillators, *Proc. 12th Ann. Symp. Freq. Control*, 420 (1958).
- McCoubrey, A. O., The atomichron-an atomic frequency standard physical foundation, *IRE Natl. Conv. Record*, 10 (1958).
- McCoubrey, A. O., National's militarized cesium beam frequency standard, *Proc. 13th Ann. Symp. Freq. Control*, 276 (1959).
- Mockler, R. C., J. Barnes, R. Beehler, H. Salazar, and L. Fey, The ammonia maser as an atomic frequency and time standard, *IRE Trans. on Instr.* **1-7**, 201 (1958).
- Morgan, A. H., and J. A. Barnes, Short-time stability of a quartz crystal oscillator as measured with an ammonia maser, *Proc. IRE* **47**, 1782 (1959).
- Page, C. H., Harmonic generation with ideal rectifiers, *Proc. IRE* **46**, 1738 (1958).
- Peter, M., and M. W. P. Strandberg, Efficiency of frequency measurements with an atomic clock, *Proc. IRE* **47**, 92 (1959).
- Pierce, J. A., Recent long-distance frequency comparisons, *IRE Trans. on Instr.* **1-7**, 207 (1958).
- Proc. of the IRE, National standards of time and frequency in the U.S. **48**, 105 (1960).
- Proc. of the IRE, Standards on piezoelectric crystals, 1958, determination of the elastic, piezoelectric and dielectric constants—the electromechanical coupling factor **46**, 764 (1958).
- Proc. of the IRE, WWV standard frequency transmissions (published monthly).
- Rafuse, R., Parametric frequency multiplication for atomic frequency standards, *Proc. 13th Ann. Symp. Freq. Control*, 350 (1959).
- Ramsey, N. F., Molecular beam resonances in oscillatory fields of nonuniform amplitudes and phases, *Phys. Rev.* **109**, 822 (1958).
- Reder, F. H., and C. J. Biebart, A missile-borne maser frequency standard, *Proc. 13th Ann. Symp. Freq. Control*, 546 (1959).
- Reder, F. H., and G. M. R. Winkler, World-wide clock synchronization (to appear in print in the *IRE Trans. on Military Electron.*).
- Rey, T. J., Digital rate synthesis for frequency measurement and control, *Proc. IRE* **47**, 2106 (1959).
- Saunders, W. K., A compact frequency translator for use with the ammonia maser, *Proc. 13th Ann. Symp. Freq. Control*, 566 (1959).
- Senitzky, I. R., Induced and spontaneous emission in a coherent field, *Phys. Rev.* **111**, 3 (1958); Induced and spontaneous emission in a coherent field, II, *Phys. Rev.* **115**, 227 (1959).
- Simpson, P. A., and A. H. Morgan, Quartz crystals at low temperatures, *Proc. 13th Ann. Symp. Freq. Control*, 207 (1959).
- Tanzen, H. D., Short-term frequency stability measurements, *Proc. 13th Ann. Symp. Freq. Control*, 384 (1959).
- Thompson, A., and R. W. Archer, A very precise short period comparator for 100 ke frequency standards, *Proc. IEEE* **106**, 61 (1959).
- Townes, C. H., Comments on frequency-pulling of maser oscillators, *J. Appl. Phys.* **28**, 920 (1957).
- Vonbun, F. O., Proposed method for tuning a maser cavity, *Rev. Sci. Instr.* **29**, 792 (1958a).
- Vonbun, F. O., Analysis of a multipole state separator and focuser for polarizable molecules, *J. Appl. Phys.* **29**, 632 (1958b).
- Vonbun, F. O., Maser laboratory frequency standard, *Proc. 13th Ann. Symp. Freq. Control*, 618 (1959).
- Vuytsteke, A. A., Maser states in ammonia-inversion, *Am. J. Phys.* **27**, 554 (1959).
- Warner, A. W., Ultra-precise quartz crystal frequency standards, *IRE Trans. on Instr.* **1-7**, 185 (1958).
- Wasilik, J. H., Anisotropic relaxation peak in the internal friction of crystalline quartz, *Phys. Rev.* **105**, 1174 (1957).
- Watt, A. D., and R. W. Plush, Power requirements and choice of an optimum frequency for a worldwide standard-frequency broadcasting station, *J. Research NBS* **63D**, 35 (1959).
- Wells, W. H., Maser oscillator with one beam through two cavities, *J. Appl. Phys.* **29**, 714 (1958).
- White, D. L., High Q quartz crystals at low temperatures, *J. Appl. Phys.* **29**, 856 (1958).
- White, L. D., Ammonia maser work, *Proc. 13th Ann. Symp. Freq. Control*, 596 (1959).
- Whitehorn, R. M., Gas cell frequency standards using buffer gases and buffer walls, *Proc. 13th Ann. Symp. Freq. Control*, 648 (1959).
- Winkler, G. M. R., Short time stability measurements on frequency standards and the notion of resolution, *Proc. IRE* **47**, 101 (1959).

Note added in proof.

The book, "Quantum Electronics, A Symposium," Columbia University Press, New York, 1960, edited by Charles H. Townes appeared shortly after the completion of this report and contains additional valuable information which should not go unmentioned. The following comments apply to passive beam devices, masers, and gas cell devices.

A cesium beam standard with an estimated accuracy of $\pm 8.5 \times 10^{-11}$ is described and the influence of the power spectra of the radiation exciting the Cs transition upon the frequency determination is discussed [Mockler et al., p. 127].

Several papers are devoted to the molecular beam maser. They furnish detailed studies and discuss new possibilities. Considerations of the influence of thermal noise on the short term frequency stability yield for the fractional phase error

due to thermal noise: $\frac{\langle \Delta \theta \rangle}{\theta} = 2 \times 10^{-13} t^{-\frac{1}{2}}$, where t is the

time of observation [Gordon, p. 3]. The advantage of new molecules and new transitions, especially in the millimeter and submillimeter range is discussed [Thaddeus et al., p. 47; Barnes, p. 57]. Higher transition frequencies together with a Fabry-Perot interferometer instead of a cavity, will make masers with stabilities of a few parts in 10^{11} feasible [Barnes, p. 57]. The dependence of the molecular beam peak intensity and beam width upon the total flow rate has been calculated [Giordmaine et al., p. 67]. The use of a parabolic focuser with a point source effuser allows reduced molecular flow for the same output in a NH_3 -maser [Helmer et al., p. 78]. Operation at very low temperatures of an atomic beam oscillator using hyperfine transitions, may yield a spectral purity of a few orders of magnitude greater than that suggested for the ammonia maser [Heer, p. 17]. Operation at 1.5° K may even make a solid state maser competitive with beam and vapor clocks if a zero-field transition in a magnetic salt is used [Bloembergen, p. 160].

Additional work on gas cells has been devoted to the explanation of the frequency shifts due to temperature and pressure, and of the line broadening. The frequency shifts can be thought of as being caused by successive small phase changes in the coefficients of the $M_F=0$ parts of the alkali wave junction and the observed line widths as statistical fluctuations in the phase shifts [Bender, p. 110].

2. Radiofrequency and Microwave Power Measurements

G. F. Engen*

In the field of radiofrequency and microwave power measurements, contributions have been made to the bolometric, calorimetric, and other miscellaneous techniques, and the National Primary Standard of power measurement is based upon a combination of refinements in these techniques which have been made at the National Bureau of Standards. These contributions will be described in the given order.

A self-balancing d-c bolometer bridge of high accuracy (0.1% in substituted power) based on a design originated at the National Bureau of Standards [Engen, 1957], and a thermistor bridge type of power meter which provides automatic temperature compensation [Aslan, 1960] have been made commercially available.

A previously unrecognized source of error in bolometric type power meters employing combinations of audio and d-c bias power has been investigated and reported [Raff, Sorger, 1960], and a study has been made of the characteristics of low-temperature bolometer detectors [Birx, Fuschillo, 1958].

A series of broadband (VSWR < 1.5 over the recommended waveguide frequency band) barretter and thermistor mounts [Kent, 1958a] have been developed by several different manufacturers and are commercially available.

The use of a rhodium-platinum alloy has permitted a reduction in the size of the bolometer (barretter) element and improved broadband performance at microwave frequencies [Kent, 1958b].

An improved method of making the impedance measurements implicit in the "impedance" method of determining bolometer mount efficiency has been developed and excellent agreement achieved with calorimetric determinations [Engen, 1958].

In the area of low-level calorimetry, a micro-calorimeter which provides a determination of the effective efficiency of microwave bolometer mounts was placed in operation at the National Bureau of Standards [Engen, 1959]. Through use of this instrument, intercomparisons of microwave power standards were made with Japan and Great Britain in accordance with the Commission I resolution.

Variants of this type of calorimeter [Sucher and Carlin, 1958; James and Sweet, 1958] are available commercially from several sources with advertised accuracies of a few percent, and in one case accessory equipment, which provides a rapid and direct read-out, has been developed for use in conjunction with these calorimeters [DiToro, Nadler, and Blanchard, 1959]. A coaxial, self-balancing, direct-reading flow calorimeter for the range 0.01 to 10 w is also commercially available [Hand, 1958].

At lower frequencies (below 300 Mc/s) a dry, static calorimeter using a thin film disk type load has been

developed at the National Bureau of Standards which covers the power range 0.1 to 20 w [Hudson and Allred, 1958]. Another version of this instrument is under development which will extend the operating range in both power level and frequency. Other techniques which are currently under additional development at the National Bureau of Standards include a 2,000 w flow calorimeter for frequencies below 1,000 Mc/s, a high-power stirred-water calorimeter for waveguide frequencies, and the electron beam technique of power measurement.

The Microwave Research Institute (Polytechnic Institute of Brooklyn) has investigated the use of a series of probes to monitor the power flow in a transmission line where standing waves are present. The optimum spacing for a series of such probes was determined. The use of ferromagnetic films and evaporated indium antimonide for the monitoring of high power through the Hall effect was also investigated [Sucher, 1959].

Finally, the impedance problems attending the intercomparison of power meters have been investigated and improved procedures developed [Engen, 1958; Hudson, 1960; Engen, 1960].

References

- *Aslan, E. E., Temperature compensated microwatt power meter, 1960 Conf. on Standards and Electronic Measurements, Boulder, Colo. (June 22 to 24, 1960).
- Birx, D. L. and N. Fuschillo, The theory of low-temperature bolometer detectors applied to the measurement of low-level RF power, IRE Trans. Instr. **1-7**, No. 3 & 4, 310 (1958).
- DiToro, M. J., L. A. Nadler, and S. J. Blanchard, Dry calorimetric power meters, P.R.D. Repts. **6**, (1959).
- Engen, G. F., A self-balancing dc bridge for accurate bolometric power measurements, J. Research NBS **59**, 101 (1957), RP2776.
- *Engen, G. F., Recent developments in the field of microwave power measurements at the National Bureau of Standards, IRE Trans. Instr. **1-7**, No. 3 & 4, 304 (1958).
- Engen, G. F., A refined X-band microwave microcalorimeter, J. Research NBS, **63C**, 77 (1959).
- *Engen, G. F., A transfer instrument for the intercomparison of microwave power meters, 1960 Conference on Standards and Electronic Measurements, Boulder, Colo. (June 22-24, 1960).
- Hand, B. P., An automatic dc to X-band power meter for the medium power range, Hewlett-Packard Journal **9**, (August 1958).
- Hudson, P. A. and C. M. Allred, A dry, static calorimeter for RF power measurement, IRE Trans. Instr. **1-7**, No. 3 & 4, 292 (1958).
- *Hudson, P. A., A precision RF power transfer standard, 1960 Conference on Standards and Electronic Measurements, Boulder, Colo. (June 22-24, 1960).
- James, A. V. and L. O. Sweet, Broad-band calorimeters for the measurement of low and medium level microwave power, II. Construction and performance, IRE Trans. MTT-**6**, 195 (1958).
- Kent, L. I., Microwave applications of thermistors. Parts 1 and 2, Electronic Design **6**, 26 (1958) and **7**, 46 (1958).
- Kent, L. I., Broadband waveguide bolometer mounts IRE Wescon Conv. Rec. **2**, Pt. 5, 114 (1958).

*National Bureau of Standards Boulder Laboratories, Boulder, Colo.

ents

standards
Hudson
instru-
and the
quency,
r addi-
Stand-
quencies
calorim-
electron

technic
se of a
trans-
The
es was
as and
ring of
investi-
ng the
investi-
Engen,

power
easure-
erature
of low-
4, 310

calori-
e bolo-
9, 101

rowave
dards,
imeter.

parison
ndards
22-24,

for the
August

imeter
7, No.

ndard,
asure-

ers for
rowave
Trans.

Parts
1958).
IRE

*Raff, S. J. and G. U. Sorger, A subtle error in RF power measurements, 1960 Conference on Standards and Electronic Measurements, Boulder, Colo. (June 22-24, 1960).
Sucher, M. and H. J. Carlin, Broad-band calorimeters for the measurement of low and medium level microwave power, I. Analysis and design, IRE Trans. **MTT-6**, 188 (1958).

Sucher, M., Final report on high power measuring techniques, Rept. R-718-59, P.I.B.-646, Microwave Research Institute (Polytechnic Institute of Brooklyn, Brooklyn, N.Y., 1959).

*The Conference Proceedings are to be published in an early issue of the IRE Transactions on Instrumentation.

3. Impedance Measurements and Standards

G. A. Deschamps*

Contributions reported in this section were published during the three-year period from January 1, 1957 to January 1, 1960. They consist mainly of refinements and extensions of known methods leading to improvements in the accuracy of measurements and to the development of better impedance standards for high frequencies and microwaves.

A new IRE standard on Waveguide and Waveguide Component Measurements was published [IRE Standards on Antennas & Waveguides, 1959]. The standard contains definition of terms and several sections on impedance measurement methods.

The method of measurement of a two-port device by observing the input impedance (or reflection coefficient) when a variable load (sliding termination or variable resistance) is connected to the output, continues to be applied in several different forms. The junction from a waveguide to a semiconductor device has been calibrated by replacing the device by known resistances and measuring the reflection coefficient in the waveguide [Waltz, 1959]. The insertion parameters of transistors (related to the scattering matrix elements) have been measured by techniques and graphical computations similar to those used for waveguide components [Follingstad, 1957]. The sliding-load method, applied for finding the scattering matrix of a two-port junction over a wide range of frequencies, has been simplified by using fixed positions of the short-circuit in the output waveguide [Deschamps, 1957].

A sliding termination that can be adjusted to produce, in a rectangular waveguide, a reflection coefficient from zero to nearly unity in magnitude and any desired phase has been described [Beatty, 1957].

The guard technique has been extended to measure the capacitance per unit length between two infinite cones of arbitrary cross section having the same apex. Thus the characteristic impedance of the corresponding transmission line is determined [Dyson, 1959].

Capacitance Standards of the order of 1 pf have been constructed and can be used in an electrostatic determination of the ohm [Thompson, 1958; McGregor & others, 1958]. They can be compared by means of a bridge with accuracies of 10^{-6} or better [McGregor and others, 1958]. Coaxial capacitors serve as a starting point in the calibration of impedances at high frequencies up to 300 Mc/s [Powell, Jickling, and Hess, 1958].

At microwave frequencies (X-band), in rectangular waveguides WR-90, nonreflecting terminations have been constructed having a return loss greater than 80 db [Beatty and Kerns, 1958].

Inductive half-round obstacles in a rectangular waveguide can be used as impedance standards. Universal tables of reflection have been computed and a number of standards have been constructed and measured. The agreement with calculated

value was to within 0.05 percent in SWR [Beatty and Kerns, 1958].

Quarter wavelength short-circuits have been constructed in WR-90 (X-band) waveguide and accurate calculation made of their reflection based upon the measured conductivity of the metal used in their construction. It is estimated that the accuracy of the result is ± 0.002 percent. They have been checked independently by measuring their power loss in the microcalorimeter [Beatty and Kerns, 1958].

References

- Beatty, R. W., An adjustable sliding termination for rectangular waveguide, IRE Trans. **MTT-5**, 192 (1957).
Beatty, R. W., and D. M. Kerns, Recently developed microwave impedance standards and methods of measurement, IRE Trans. **I-7**, 319 (1958).
Beatty, R. W., Magnified and squared VSWR responses for microwave reflection coefficient measurements, IRE Trans. **MTT-7**, 346 (1959).
Deschamps, G. A., A variant in the measurement of two-port junctions, IRE Trans. **MTT-5**, 159 (1957).
Dyson, J. D., Measuring the capacitance per unit length of two infinite cones of arbitrary cross section, IRE Trans. **AP-7**, 102 (1959).
Dropkin, H. A., Direct reading microwave phase-meter, IRE National Convention Record **6**, Pt. 1, 57 (1958).
Engen, G. F., and R. W. Beatty, Microwave reflectometer techniques, IRE Trans. **MTT-7**, 351 (1959).
Felsen, L. B., W. K. Kahn, and L. Levey, Measurement of two-mode discontinuities in a multimode waveguide by a resonance technique, IRE Trans. **MTT-7**, 102 (1959).
Follingstad, H. G., Complete linear characterization of transistors from low through very high frequencies, IRE Trans. **I-6**, 49 (1957).
Lewis, D. J., Mode couplers and multimode measurement technique, IRE Trans. **MTT-7**, 110 (1959).
Linker, J. B. Jr., and H. H. Grimm, Wide-band microwave transmission measuring system, IRE Trans. **MTT-6**, 415 (1958).
Magid, M., Precision microwave phase shift measurements, IRE Trans. **I-7**, 321 (1958).
McGregor, M. C., J. F. Hersh, R. D. Cutkosky, F. K. Harris, and F. R. Kotter, New apparatus at the National Bureau of Standards for absolute capacitance measurements, IRE Trans. **I-7**, 253 (1958).
Mittra, R., An automatic phase-measuring circuit at microwaves, IRE Trans. **PGI-6**, 238 (1957).
Powell, R. C., R. M. Jickling, and A. E. Hess, High-frequency impedance standards at the National Bureau of Standards, IRE Trans. **I-7**, 270 (1958).
Proc. of the IRE, IRE standards on antennas and waveguides: wave guide and waveguide component measurements **47**, 568 (1959).
Schafer, G. E., and R. W. Beatty, A method for measuring the directivity of directional couplers, IRE Trans. **MTT-6**, 419 (1958).
Thompson, A. M., The precise measurement of small capacitances, IRE Trans. **I-7**, 245 (1958).
Waltz, M. C., A technique for the measurement of microwave impedance in the junction region of a semiconductor device, The Microwave J. **2**, 23 (1959).
Watts, C. B., and A. Alford, An automatic impedance plotter based on a hybrid-like network with a very wide frequency range, IRE Nat. Conv. Record **5**, Part 5, 146 (1957).
Williams, E. M., and J. H. Foster, Standing-wave line for U.H.F. measurements of high-dielectric constant materials, IRE Trans. **I-6**, 210 (1957).

*University of Illinois, Urbana, Ill.

4. Development in Attenuation Measurements and Standards

Bruno O. Weinschel*

4.1. Definition of Attenuation

When dealing with the propagation of guided waves within uniform transmission lines, the term "attenuation constant" describes the relative decrease of amplitude of voltage or current in the direction of propagation in nepers per unit length [IRE Standards on Antennas and Waveguides, 1953; 1959]. This concept shows the historical origin of the term "attenuation"; however, in relation to measurement of "standard attenuators," it has limited application.

The terms "insertion loss" and "incremental attenuation above minimum insertion loss" are of greater utility. Insertion loss in its general definition [IRE Standards on Antennas and Waveguides, 1953] makes no requirements on the source and load impedance. It is "the ratio, expressed in decibels, of the power received at the load before insertion of the apparatus, to the power received at the load after insertion." However, it is also commonly used to denote the minimum attenuation of variable attenuators.

For lower frequencies, the source and load impedances are specified, but the choice of impedances is somewhat more arbitrary.

It must be realized that a source of constant incident power is in a sense the electrical equivalent of a matched source. This equivalence has practical significance, since the power consuming isolation pad frequently used with an unmatched source may be replaced by a high-directivity directional coupler, which supervises the incident power and maintains it constant by manual or automatic feedback [Engen, 1958].

In contrast to the "insertion loss" of a four terminal network, the definition of the "voltage division ratio" of a four terminal network (e.g., attenuator pad with low-output impedance) utilizes not a matched source but a source of zero impedance which is electrically equivalent to a "source of constant voltage". Voltage division ratio is then defined as "the change in load voltage, due to the insertion of a transmission line component at some point in a transmission system where the voltage in the terminal plane of insertion is held constant before and after insertion of the component, the change in load voltage is expressed as a ratio of the voltage in the terminal plane of the termination before and after the insertion of the component". This definition was used in [Sorger, Weinschel, and Hedrich, 1959].

4.2. Techniques for Insertion Loss or Attenuation Measurements

For limited range measurements (up to 20 or 30 db), high accuracy (better than 0.02 db/10 db) can be achieved by using square law detectors such as a barretter in conjunction with 100 percent square wave amplitude modulation at an audio-frequency. Sorger and Weinschel [1959] shows that the deviation from square law of typical commercial barretters used at power levels below -7 dbm can cause a maximum error in insertion loss measurement of the order of 0.01 db.

For HF and microwave measurements, a more restrictive definition requiring a matched source and a matched load is of greater value [IRE Standards on Antennas and Waveguides, 1959]. The additional restriction is that "the specified input and output waveguides connected to the component are reflectionless, looking in both directions from the component (match terminated)".

For measurements requiring a greater dynamic range, a linear heterodyne detector is more practical. Hedrich and Weinschel [1958] and Weinschel, Sorger, and Hedrich [1959] show that the deviation of a crystal mixer from linearity will not cause insertion loss errors exceeding 0.01 db if the maximum signal power is 20 db below the local oscillator power in the mixer crystal.

Heterodyne systems having greater range are of the parallel IF substitution type. In this arrangement, the piston attenuator which operates at the intermediate frequency is not in the IF channel, but in a separate path coming from a highly stable source. The mixer output is compared to this stable signal by null techniques. By this means, greater freedom from drift is achieved and the minimum loss of the piston attenuator is kept out of the signal path.

Hedrich and Weinschel [1958] and Weinschel, Sorger, and Hedrich [1959] use this method in the frequency range of 100 to 1,000 Mc/s to achieve an accuracy better than 0.02 db/10 db over a 50-db range. Weinschel, Sorger, and Hedrich [1959] also contains a careful analysis of the design of the piston attenuators for this application.

To extend the single step and total ranges of these measuring systems, it is desirable to reduce the low-level limit which is set by noise. This can most easily be done by using a small bandwidth following the first detector. For square law systems, this requires a high degree of frequency stability of the audiofrequency modulation. A bolometer preamplifier with a variable bandwidth has been

*Weinschel Engineering, Kensington, Md.

described in Hedrich [1959]. The gain is fairly constant while the bandwidth is changed from 2 to 30 c/s. While this instrument is not recommended for precise standards measurements, the principle is useful.

In order to use a small bandwidth in IF amplifiers, following a first linear detector, it is either necessary that the frequency stability of the RF source and the local oscillator be sufficiently high or that the local oscillator frequency be directly derived from the frequency of the RF source by means of single side band modulation. This latter approach requires a higher level signal, synchronous with the test signal. In this type of frequency stabilization, great care must be taken with isolation. One method for achieving single side band modulation is by phase modulation of a traveling wave tube (serrodyne) [Linkner and Grimm 1958; Mathers, 1957; Cumming, 1957]. These single sideband techniques are not in general use for precision standards measurements, but it is clear that the principle can be so applied. Mathers [1957] reports a dynamic range of 80 db, using an intermediate frequency of 1,000 c/s. Linkner & Grimm [1958] uses a 20,000/ c/s intermediate frequency and a simultaneous amplitude modulation at 1,000 c/s, and an attenuation accuracy of ± 2 percent up to 24 db is claimed. Mathers [1957] considers not only the attenuation, but also the relative phase. An accuracy of 1° in phase is claimed.

A frequency offset can also be accomplished by mechanical means (rotating phase shifter) or by a ferrite phase modulator [O'Hara and Scharfman, 1959].

Increased frequency stabilization of RF sources or single sideband modulation makes feasible lower intermediate frequencies. The use of intermediate frequencies below 100,000 c/s permits the use of accurate wirewound resistor attenuators as standards instead of the piston attenuator. At lower frequencies mixer noise is generally thought to increase inversely with frequency, however. Greene and Lyons [1959] and Andrews and Bazydlo [1959] deal with the modern mixer crystals and show that the mixer noise above 100 kc/s is rather constant and that below 100 kc/s it increases about 12 db for each factor of 10 of frequency reduction.

The method of measuring attenuation by RF substitution does not require the detector response law to be known. Very wide ranges of measurements are possible by this method. To achieve these greater ranges, two or more previously calibrated attenuators are frequently cascade-connected or the calibrated and test attenuators are cascade-connected. Errors introduced by such cascading are analyzed in [Schafer and Rumfelt, 1959].

Another method of measuring attenuation [Engen and Beatty, 1960] utilizes certain bolometric power measurement and stabilization techniques [Engen, 1957] and [Engen, 1958]. By means of these procedures a system stability and resolution of 0.0001 db

is achieved and attenuations in the range 0.01 to 50 db can be measured with accuracies of 0.0001 to 0.06 db.

Due to coaxial cable flexing effects at frequencies above 4,000 Mc/s, it is necessary to use special jigs for alignment, so that measurements can be repeated. Rumfelt and Como [1959] describes a rapid insertion device for coaxial attenuators.

4.3. Self-Calibrating Techniques

NBS Tech. News Bulletin [1957] describes a "self-calibrating" method of measuring insertion ratio. That is, it does not rely on any standard attenuator for comparison, as do the previously mentioned methods.

References

- Andrews, G. B., and H. A. Bazydlo, Crystal noise effects on zero I.F. receivers, *Proc. IRE* **47**, 2018 (1959).
- Cumming, R. C., Serrodyne frequency translator, *Proc. IRE* **45**, 175 (1957).
- Engen, G. F., A self-balancing D-C bridge for accurate bolometric power measurements, *NBS J. Research* **59**, 101 (1957), RP 2776.
- Engen, G. F., Amplitude stabilization of microwave signal source, *IRE Trans. MTT-6*, 202 (1958).
- Engen, G. F., and R. W. Beatty, Microwave attenuation measurements with accuracies from 0.0001 to 0.06 decibel over a range of 0.01 to 50 decibels, *NBS J. Research* **64C** (1960).
- Greene, J. C., and J. F. Lyons, Receiver with zero intermediate frequency, *Proc. IRE* **47**, 335 (1959).
- Hedrich, A. L., B. O. Weinschel, G. U. Sorger, and S. J. Raff, Calibration of signal generator output voltage in the range of 100 to 1,000 megacycles, *IRE Trans. Inst. I-7*, 275 (1958).
- Hedrich, A. L., A new receiver for antenna pattern ranges, *Microwave J.* **2**, 34 (1959).
- IRE Standards on antennas and waveguides: Definition of terms, 1953 Standard, 2.S1.
- IRE Standards on antennas and waveguides: Waveguide and waveguide component measurements, 1959 Standard, 2.S1.
- Linkner, J. B. Jr., and H. H. Grimm, Wide-band microwave transmission measuring system, *IRE Trans. MTT-6*, 415 (1958).
- Mathers, G. W., Homodyne generator and detection system, *IRE Wescon Conv. Rec.*, Part 1 on Microwaves, Antennas and Propagation, 194 (1957).
- O'Hara, F. J., and H. Scharfman, A ferrite serrodyne for microwave frequency translation, *IRE Trans. MTT-7*, 32 (1959).
- Rumfelt, A. Y., and R. J. Como, Rapid insertion device for coaxial attenuators, *Rev. Sci. Instr.*, **30**, 687 (1959).
- Sorger, G. U., and B. O. Weinschel, Comparison of deviations from square law for RF crystal diodes and barretters, *IRE Trans. I-8*, 103 (1959).
- Sorger, G. U., B. O. Weinschel, and A. L. Hedrich, A radio frequency voltage standard for receiver calibration in the frequency range of from 2 to 1,000 megacycles/sec., *URSI Conf.* (1959).
- Schafer, G. E., and A. Y. Rumfelt, Mismatch errors in cascade-connected variable attenuators, *IRE Trans. MTT-7*, 447 (1959).
- Tech. News Bull., N.B.S., Self-calibrating method of measuring insertion ratio **41**, 132 (1957).
- Weinschel, B. O., G. U. Sorger, and A. L. Hedrich, Relative voltmeter for VHF/UHF signal generator attenuator calibration, *IRE Trans. I-8*, 22 (1959).

5. Noise Measurements and Standards

B. M. Oliver*

Because of the rapid development of low-noise devices such as masers and parametric amplifiers, both the theory of noise, and the technique of its measurement have been extended considerably over the last three years.

Numerous papers have appeared [Pound, 1957; Weber, 1957; Weber, 1959; Senitzky, 1958; Senitzky, 1959; Mueller, 1957; Strandberg, 1957; Shimoda, Takahasi and Townes, 1957; Jones, 1959; Strum, 1958] giving quantum-mechanical analyses of the limiting noise performance to be expected from linear radiation detectors (coherent amplifiers). There is now general agreement on this matter and, while the general quantum mechanical proofs are rather complex, the results are simply stated, as follows. All low-noise coherent amplifiers avoid dissipation at signal frequencies in their input circuits and obtain their amplifying action by induced emission of photons, i.e., by transitions of the system from higher to lower quantum states. Since transitions can also be induced from the lower to the higher state at the expense of signal power (absorption) the lower state must be kept relatively depopulated, and the upper state overpopulated by some sort of pumping action. Making use of the usual Boltzmann factor $\exp(-\Delta E/kT)$ for the relative population of states in thermodynamic equilibrium, this overpopulation of the upper state with respect to the lower may be described as an effective *negative* temperature, T_a , of the amplifying medium. As the relative population of the lower state approaches zero (complete pumping), T_a approaches zero (from the negative side). There is then no absorption of signal photons, only emission. Some of the emission will be stimulated (and therefore coherent) and represents signal amplification, but some will be spontaneous and represents added noise. The total noise power spectral density referred to the input is given by

$$W(\nu) = \{h\nu / [\exp(h\nu/kT_s) - 1]\} + \{h\nu / [1 - \exp(h\nu/kT_a)]\}.$$

where ν = frequency,

h = Planck's constant,

k = Boltzmann's constant,

T_s = Absolute temperature of source.

The first term will be recognized as the ordinary expression for the thermal noise of a source at temperature T_s , while the second term represents the spontaneous emission of the amplifier. The second term is reduced as $T_a \rightarrow -0$, and approaches the limit $h\nu$. Thus for an ideal coherent detector:

$$W(\nu) = \{h\nu / [\exp(h\nu/kT_s) - 1]\} + h\nu \\ \approx k\left(T_s + \frac{h\nu}{k}\right) \quad \text{if } \frac{h\nu}{kT_s} \ll 1.$$

The second term is an effective noise temperature of the detector:

$$T_{eff} = \frac{h\nu}{k} = (4.8 \times 10^{-11})\nu.$$

For a receiver at X-band (10,000 Mc/s), $T_{eff} = 0.48^\circ \text{K}$.

Many experiments have been reported [Alsop et al., 1957; Gordon and White, 1957; 1958; Cohen, 1960] confirming these low-noise capabilities of linear receivers.

Using low-noise receivers, studies have been made of the effective temperature of the sky as a function of elevation angle [Ko, 1958; DeGrasse et al., 1959]. The measurements agree well with theory [Hogg, 1959] based upon known absorption coefficients for atmospheric gases and water vapor and known temperature as a function of altitude. Galactic noise is found to be the dominating factor in sky temperature below about 500 Mc/s at zero elevation, and below about 3 kMc/s at the zenith. The minimum sky temperature is near the zenith and galactic poles (normal to the plane of the milky way) and is about 3°K . Thus modern amplifiers of the maser type are reaching the limit of practical performance in communication and detection systems.

Standard noise sources for measurement and calibration purposes have improved over the last 3 years. For low-noise receivers, terminations at known temperature are quite satisfactory reference sources. For receivers with higher inherent noise shot noise diodes and gas discharge sources are currently used. The latter have been developed to have greater stability and more accurately known noise during recent years [Zucher, Baskin, et al., 1958; Olson, 1958].

Commercial instruments have been developed which automatically, and in some cases continuously, monitor the noise figure of receivers.

The theory of noise in linear twoports has been analyzed [Haas et al., 1960] and IRE standards for its measurement have been published [IRE standards on measuring noise in linear twoports, 1959].

The National Bureau of Standards has announced [Tech. News Bull. 1959] that its facilities for calibration of noise standards are nearly complete so that soon convenient cross checking of standards will be possible.

References

- Alsop et al., Measurement of noise in a maser amplifier, *Phys. Rev.* **107**, 1450 (1957).
- Cohen, S., Experimental determination of parametric amplifier excess noise using transformer coupling, *Proc. IRE* **48**, 109 (1960).

*Hewlett-Packard Company, Palo Alto, Calif.

- De Grasse, Hogg, Ohm, and Scovil, Ultra-low-noise measurements using a horn reflector antenna and a traveling wave maser, *J. Appl. Phys.* **30**, 2013 (1959).
- Gordon and White, Experimental determination of the noise figure of a maser amplifier, *Phys. Rev.* **107**, 1728 (1957).
- Gordon and White, Noise in maser amplifiers—theory and experiment, *Proc. IRE* **46**, 1588 (1958).
- Haas, H. A., et al., Representation of noise in linear twoports, *Proc. IRE* **48**, 68 (1960).
- Hogg, D. C., Effective antenna temperatures due to oxygen and water vapor, *J. Appl. Phys.* **30**, 1417 (1959).
- Jones, R. C., Noise in radiation detectors, *Proc. IRE* **47**, 1481 (1959).
- Ko, H. C., The distribution of cosmic background radiation, *Proc. IRE* **46**, 208 (1958).
- Muller, M. W., Noise in a molecular amplifier, *Phys. Rev.* **106**, 8 (1957).
- Olson, K. W., Reproducible gas discharge noise sources as possible microwave noise standards, *Trans. IRE, PGI*, 315 (1958).
- Pound, R. V., Spontaneous emission and the noise figure of maser amplifiers, *Annals of Physics* **1**, 24 (1957).
- Proceedings of the IRE, Standards on methods of measuring noise in linear twoports, 60 (1960).
- Senitzky, I. R., Induced and spontaneous emission in a coherent field (Part I), *Phys. Rev.* **111**, 3 (1958).
- Senitzky, I. R., Induced and spontaneous emission in a coherent field (Part II), *Phys. Rev.* **115**, 227 (1959).
- Shimoda, Takahasi, Townes, Fluctuations in the amplification of quanta with application to maser amplifiers, *J. Phys. Soc. Japan* **12**, 686 (1957).
- Strandberg, M. W. P., Inherent noise of quantum mechanical amplifiers, *Phys. Rev.* **106**, 617 (1957).
- Strum, Peter D., Considerations in high sensitivity microwave radiometry, *Proc. IRE* **43** (1958).
- Tech. News Bull. NBS, Standards and calibration in radio and electronics **43**, 226 (1959).
- Weber, J., Masers, *Rev. Mod. Phys.* **31**, 681 (1959).
- Weber, J., Maser noise considerations, *Phys. Rev.* **108**, 537 (1957).
- Zucker, Baskin, et al., Design and development of a standard White noise generator and noise indicating instrument, *Trans. IRE, PGI*, 279 (1958).

6. Field Strength Measurements

M. C. Selby*

Progress was made in the development of the art of field-strength measurements by some commercial concerns, as evidenced by products placed on the market. At least 3 m were offered for field-strength and interference measurements at frequencies to about 10 kMc/s, input levels of 20 μ v to several volts and internal accuracies (excluding antenna coefficients) of the order of 1 db. These meters were employing superheterodyne receivers, input attenuation up to 80 db, internal or external cw and impulse noise calibration, and they measured average, peak and quasi-peak values [Rosen, 1958; Borek, Rodriguez, 1959].

There were also at least two devices placed on the market to measure near fields for use as RF radiation hazard meters. The frequency and power density ranges in one case were 200 to 10,000 Mc/s at 1 mw/cm² to 1 w/cm² and in another 2,600 to 10,000 Mc/s at a fixed level of 10 mw/cm². The claimed accuracy was of the order of 1 to 3 db. [Electronics, 1958].

Work was initiated at the National Bureau of Standards to develop primary and secondary national standards of cw, field strength and antenna gain at frequencies above 300 Mc/s [NBS Research Highlights, 1958, 1959]. Immediate objectives were the improvement of the stability of an insertion loss measuring system to 0.01 db/hr, evaluation of a microwave absorbing enclosure and of effects of absorbing materials and selection of a waveguide horn as a national standard for frequencies up to 12,400 Mc/s. In line with these objectives a signal source level was stabilized to a ten-thousandths of a decibel and a phase-lock system of frequency control was developed which was capable of locking two free running reflex klystrons—all in noncontrolled environment.

Intensive work was in progress in numerous laboratories on many special problems involving incidental field measurements. These included problems on interference [Hubbard and Cateora, 1959; Albin and Pearleton, 1958; Morelli, 1958; Epstein and Schulz, 1959; Chapin, 1959; White and Ball, 1960], propagation studies [Knudsen and Larsen, 1960; Agy and Davies, 1959], antenna patterns [Morrow, et al, 1958; Kamen, 1959] and others. Instrumentation and technique in these cases were usually adapted to the particular requirements; however, occasionally one may find under these subjects information applicable to the problem of field measurements in general. Some references to these activities are therefore indicated. Work of interest at 100 to 118 kMc/s was recently conducted as a study in propagation [Tolbert and Straiton, 1959; Tolbert, Straiton and Douglas, 1958]. However, this activity was limited

to attenuation measurements and apparently did not attempt measurement of absolute field values.

Considerable information on field theory and measurements at the low end of the frequency spectrum, e.g., from 1 to 300 c/s may be found in papers presented at the 1960 Earth-Current Communications Seminar [J. Research, 1960; Wait, 1960]. An experimental and theoretical study of fields at 18.6 kc/s in a medium of fresh water to depths of 1,000 ft using monopole and loop antennas and encouraging results are described [Saran and Held, 1960].

The continuous efforts of C.C.I.R. Study Group V on measurements of field strength [CCIR Report, 1959] should be followed by those interested in this subject.

References

- Agy, V., and K. Davies, Ionospheric investigations using the sweep-frequency pulse technique at oblique incidence, J. Research NBS **63D** (1959).
- Albin, A. L., and C. B. Pearleton, Measurement of spurious radiation from missileborne electronic equipments, IRE Conv. Record **6**, 8, 155 (1958).
- Borek, A., and M. Rodriguez, Design and development of a noise and field instrument for 1,000 to 12,000 Mc/s frequency range, IRE. National Conv. Record **VII**, 9, 125 (1959).
- C.C.I.R.—Doc. 239-E, Measurement of field strength, field intensity, radiated power, available power from the receiving antenna and the transmission loss, Question no. 8 (1959).
- Chapin, E. W., Standard measurement parameters for phenomena distributed in time and frequency, IRE Conv. Record **7**, 8, 60 (1959).
- Electrons at work, power meter protects microwave workers, Electronics **31**, 43, 100 (1958).
- Epstein, M., and R. B. Schulz, Magnetic-field pickup for low-frequency radio-frequency measuring sets, IRE Conv. Record **7**, 8, 64 (1959).
- Hubbard, R. W., and J. V. Cateora, an X-band field intensity recording receiver with extremely narrow bandwidth, IRE-URSI joint meeting (Oct. 1959), San Diego, Calif.
- Journal of Research NBS, Earth-current communications seminar, NBS, Boulder, Colo., Jan. 26-27 (1960), NBS special issue.
- Kamen, Ira, Large antenna systems for propagation studies, IRE Nat. Conv. Record **7**, 1, 51 (1959).
- Knudsen, H. L., and T. Larsen, The electric field at the ground plane near a top-loaded monopole antenna with special regard to electrically small L- and T-antennas, J. Research NBS **64D** (1960).
- Morelli, M., Spurious frequency measurement in waveguide, IRE Conv. Record **6**, 8, 176 (1958).
- Morrow, C. W., P. E. Tayler, H. T. Ward, Phase and amplitude measurements of the near field of microwave lenses, IRE Conv. Record **6**, 1, 166 (1958).
- Research highlights of the National Bureau of Standards, chapter on Radio Standards (1958, 1959).
- Rosen, B., Microwave field intensity meter, Proc. of the Fourth Conference on Radio Interference Reduction and Electronic Compatibility, conducted by Armour Research Foundation of Ill. Instit. Tech., 242 (1958).
- Saran, G. S., and G. Held, Field strength measurements in fresh water, J. Research NBS **64D** (1960).

*National Bureau of Standards Boulder Laboratories, Boulder, Colo.

Tolbert, C. W., A. W. Straiton, J. M. Douglas, Studies of 2.15 Mm propagation at an elevation of 4 kms and the millimeter absorption spectrum, Electrical Engineering Research Laboratory, Univ. of Texas, Rep. no. 104 (1958).
Tolbert, C. W., A. W. Straiton, Radio propagation measurements in the 100 to 118 kMc's spectrum, IRE Wescon Conv. Record **3**, 1, 56 (1959).

Wait, J. R., Mode theory and the propagation of E.L.F. radio waves, published in the J. Research, NBS special issue, on Earth-current communications seminar, NBS, Boulder, Colo., January 26-27 (1960).
White, W. D., and C. O. Ball, Simulation tests on an interference rejection antenna system, presented at Session 4, IRE Intern. Conv., NYC (1960).

I
tech
surv
at t
to l
equ
with
deter
scie
O
dist
men
lent
prop
and
mea
thus
erro
(or
bas
the
incl
of e
dete
met
relat
tem
erro
phys
A
[The
Free
error
along
obse
cond
obse
stan
Unfo
from
estim
of th
In
meas
dista
and

* Nat

7. Measurements of Physical Quantities by Radio Techniques

M. C. Thompson, Jr.*

During the past few years the use of radio techniques for precise distance measuring in land surveying has met with notable success. Although at this time only two commercial firms are known to be engaged in the manufacture of this type of equipment: [Microdist; Tellurometer] the enthusiasm with which it has been received in the field of geodesics indicates clearly that it is an important scientific achievement.

One of the limitations on the accuracy of electronic distance measuring is the fact that the basic measurements of transit time must be converted to equivalent distance. This requires a knowledge of the propagation velocity along the path being measured and this can practically only be estimated from measurements at discrete points. The errors can, thus, be divided into two general classes: first, the errors in approximating the space average of velocity (or refractive index) along a line several miles long based on a few point measurements; and second, the errors in calculating phase velocity. The latter include: (1) Uncertainty in the value of c , (velocity of electromagnetic waves in vacuum); (2) errors in determining the constants appearing in the psychrometric equation [Smith and Weintraub, 1953] relating refractive index to measurements of pressure, temperature and water vapor content; and (3) the errors inherent in the measurement of these latter physical quantities.

A number of experiments have been examined [Thompson and Janes, 1959; Thompson and Freethy, 1958] to determine the behavior of the error introduced by interpolating velocity corrections along paths of various lengths based on psychrometric observations under various geographical and seasonal conditions. This work shows that the corrected observations using psychrometric methods have standard deviations of several parts per million. Unfortunately, the experimental errors expected from the atmospheric measurements (3 above) are estimated to be of the same order so that the extent of the interpolation error is probably obscured.

In addition to the interpolation and correction measurements errors, the accuracy of electronic distance measuring is limited by the accuracy of c and of the coefficients relating phase velocity to

atmospheric composition. Although the value of c recommended by URSI is apparently universally used, no one set of psychrometric coefficients has been adopted. Recommendations have been made, however, to the International Association of Geodesy that values be selected for international use to simplify the problems of comparing research and results of different workers. (The discussion of advances in the determination of c is to be found in other sections of this report.)

The work described above suggests that the present practical limitation on the precision of electronic distance measuring is the error in estimating the proper correction for atmospheric properties. As an aid in resolving this error, the National Bureau of Standards, since 1958, has been working to develop a microwave refractometer having sufficient long-term calibration stability to justify absolute calibration. By the use of such an instrument it should be possible to reduce the errors in electronic distance measuring to less than a part in a million.

The instrument recently developed by M. J. Vetter of the National Bureau of Standards operates on a principle distinctly different from those used by Birnbaum and by Crain. By the use of feedback techniques, the new method effectively removes electronic component (including klystron) characteristics from the performance. Preliminary tests suggest that the electronic stability is of the order of a few parts in 10 million for periods of weeks or longer. The residual errors are essentially a function of sampling cavity design and operating conditions (e.g. temperature compensation, cavity contamination and corrosion, etc.).

References

- Microdist, Cubic Corporation, San Diego, California.
- Smith, E. K. Jr., and Stanley Weintraub, The constants in the equation for atmospheric refractive index at radio frequencies; *Proc. IRE*, **41**, 8 (1953), $(n-1) \times 10^6 = (A_p/T) + (B_p/T^2)$.
- Tellurometer (Pty.) Ltd., Capetown, Union of South Africa.
- Thompson, M. C. Jr., and F. E. Freethy, Hourly correlation of radio path lengths and surface refractivity index from Maui, T. H., phase stability program, NBS Rpt. 5579 (June 1958).
- Thompson, M. C. Jr., and H. B. Janes, Measurements of phase stability over a low-level tropospheric path, *J Research NBS* **63D**, 45 (1959).

* National Bureau of Standards Boulder Laboratories, Boulder, Colo.

described in Hedrich [1959]. The gain is fairly constant while the bandwidth is changed from 2 to 30 c/s. While this instrument is not recommended for precise standards measurements, the principle is useful.

In order to use a small bandwidth in IF amplifiers, following a first linear detector, it is either necessary that the frequency stability of the RF source and the local oscillator be sufficiently high or that the local oscillator frequency be directly derived from the frequency of the RF source by means of single side band modulation. This latter approach requires a higher level signal, synchronous with the test signal. In this type of frequency stabilization, great care must be taken with isolation. One method for achieving single side band modulation is by phase modulation of a traveling wave tube (serrodyne) [Linkner and Grimm 1958; Mathers, 1957; Cumming, 1957]. These single sideband techniques are not in general use for precision standards measurements, but it is clear that the principle can be so applied. Mathers [1957] reports a dynamic range of 80 db, using an intermediate frequency of 1,000 c/s. Linkner & Grimm [1958] uses a 20,000/c/s intermediate frequency and a simultaneous amplitude modulation at 1,000 c/s, and an attenuation accuracy of ± 2 percent up to 24 db is claimed. Mathers [1957] considers not only the attenuation, but also the relative phase. An accuracy of 1° in phase is claimed.

A frequency offset can also be accomplished by mechanical means (rotating phase shifter) or by a ferrite phase modulator [O'Hara and Scharfman, 1959].

Increased frequency stabilization of RF sources or single sideband modulation makes feasible lower intermediate frequencies. The use of intermediate frequencies below 100,000 c/s permits the use of accurate wirewound resistor attenuators as standards instead of the piston attenuator. At lower frequencies mixer noise is generally thought to increase inversely with frequency, however. Greene and Lyons [1959] and Andrews and Bazydlo [1959] deal with the modern mixer crystals and show that the mixer noise above 100 kc/s is rather constant and that below 100 kc/s it increases about 12 db for each factor of 10 of frequency reduction.

The method of measuring attenuation by RF substitution does not require the detector response law to be known. Very wide ranges of measurements are possible by this method. To achieve these greater ranges, two or more previously calibrated attenuators are frequently cascade-connected or the calibrated and test attenuators are cascade-connected. Errors introduced by such cascading are analyzed in [Schafer and Rumfelt, 1959].

Another method of measuring attenuation [Engen and Beatty, 1960] utilizes certain bolometric power measurement and stabilization techniques [Engen, 1957] and [Engen, 1958]. By means of these procedures a system stability and resolution of 0.0001 db

is achieved and attenuations in the range 0.01 to 50 db can be measured with accuracies of 0.0001 to 0.06 db.

Due to coaxial cable flexing effects at frequencies above 4,000 Mc/s, it is necessary to use special jigs for alignment, so that measurements can be repeated. Rumfelt and Como [1959] describes a rapid insertion device for coaxial attenuators.

4.3. Self-Calibrating Techniques

NBS Tech. News Bulletin [1957] describes a "self-calibrating" method of measuring insertion ratio. That is, it does not rely on any standard attenuator for comparison, as do the previously mentioned methods.

References

- Andrews, G. B., and H. A. Bazydlo, Crystal noise effects on zero I.F. receivers, *Proc. IRE* **47**, 2018 (1959).
- Cumming, R. C., Serrodyne frequency translator, *Proc. IRE* **45**, 175 (1957).
- Engen, G. F., A self-balancing D-C bridge for accurate bolometric power measurements, *NBS J. Research* **59**, 101 (1957), RP 2776.
- Engen, G. F., Amplitude stabilization of microwave signal source, *IRE Trans. MTT-6*, 202 (1958).
- Engen, G. F., and R. W. Beatty, Microwave attenuation measurements with accuracies from 0.0001 to 0.06 decibel over a range of 0.01 to 50 decibels, *NBS J. Research* **64C** (1960).
- Greene, J. C., and J. F. Lyons, Receiver with zero intermediate frequency, *Proc. IRE* **47**, 335 (1959).
- Hedrich, A. L., B. O. Weinschel, G. U. Sorger, and S. J. Raff, Calibration of signal generator output voltage in the range of 100 to 1,000 megacycles, *IRE Trans. Inst.* **1-7**, 275 (1958).
- Hedrich, A. L., A new receiver for antenna pattern ranges, *Microwave J.* **2**, 34 (1959).
- IRE Standards on antennas and waveguides: Definition of terms, 1953 Standard, 2.S1.
- IRE Standards on antennas and waveguides: Waveguide and waveguide component measurements, 1959 Standard, 2.S1.
- Linkner, J. B. Jr., and H. H. Grimm, Wide-band microwave transmission measuring system, *IRE Trans. MTT-6*, 415 (1958).
- Mathers, G. W., Homodyne generator and detection system, *IRE Wescon Conv. Rec.*, Part 1 on Microwaves, Antennas and Propagation, 194 (1957).
- O'Hara, F. J., and H. Scharfman, A ferrite serrodyne for microwave frequency translation, *IRE Trans. MTT-7*, 32 (1959).
- Rumfelt, A. Y., and R. J. Como, Rapid insertion device for coaxial attenuators, *Rev. Sci. Instr.*, **30**, 687 (1959).
- Sorger, G. U., and B. O. Weinschel, Comparison of deviations from square law for RF crystal diodes and barretters, *IRE Trans. I-8*, 103 (1959).
- Sorger, G. U., B. O. Weinschel, and A. L. Hedrich, A radio frequency voltage standard for receiver calibration in the frequency range of from 2 to 1,000 megacycles/sec., *URSI Conf.* (1959).
- Schafer, G. E., and A. Y. Rumfelt, Mismatch errors in cascade-connected variable attenuators, *IRE Trans. MTT-7*, 447 (1959).
- Tech. News Bull., N.B.S., Self-calibrating method of measuring insertion ratio **41**, 132 (1957).
- Weinschel, B. O., G. U. Sorger, and A. L. Hedrich, Relative voltmeter for VHF/UHF signal generator attenuator calibration, *IRE Trans. I-8*, 22 (1959).

5. Noise Measurements and Standards

B. M. Oliver*

Because of the rapid development of low-noise devices such as masers and parametric amplifiers, both the theory of noise, and the technique of its measurement have been extended considerably over the last three years.

Numerous papers have appeared [Pound, 1957; Weber, 1957; Weber, 1959; Senitzky, 1958; Senitzky, 1959; Mueller, 1957; Strandberg, 1957; Shimoda, Takahasi and Townes, 1957; Jones, 1959; Strum, 1958] giving quantum-mechanical analyses of the limiting noise performance to be expected from linear radiation detectors (coherent amplifiers). There is now general agreement on this matter and, while the general quantum mechanical proofs are rather complex, the results are simply stated, as follows. All low-noise coherent amplifiers avoid dissipation at signal frequencies in their input circuits and obtain their amplifying action by induced emission of photons, i.e., by transitions of the system from higher to lower quantum states. Since transitions can also be induced from the lower to the higher state at the expense of signal power (absorption) the lower state must be kept relatively depopulated, and the upper state overpopulated by some sort of pumping action. Making use of the usual Boltzmann factor $\exp(-\Delta E/kT)$ for the relative population of states in thermodynamic equilibrium, this overpopulation of the upper state with respect to the lower may be described as an effective *negative* temperature, T_a , of the amplifying medium. As the relative population of the lower state approaches zero (complete pumping), T_a approaches zero (from the negative side). There is then no absorption of signal photons, only emission. Some of the emission will be stimulated (and therefore coherent) and represents signal amplification, but some will be spontaneous and represents added noise. The total noise power spectral density referred to the input is given by

$$W(\nu) = \{h\nu / [\exp(h\nu/kT_s) - 1]\} + \{h\nu / [1 - \exp(h\nu/kT_a)]\}.$$

where ν = frequency,

h = Planck's constant,

k = Boltzmann's constant,

T_s = Absolute temperature of source.

The first term will be recognized as the ordinary expression for the thermal noise of a source at temperature T_s , while the second term represents the spontaneous emission of the amplifier. The second term is reduced as $T_a \rightarrow 0$, and approaches the limit $h\nu$. Thus for an ideal coherent detector:

$$W(\nu) = \{h\nu / [\exp(h\nu/kT_s) - 1]\} + h\nu \\ \approx k\left(T_s + \frac{h\nu}{k}\right) \text{ if } \frac{h\nu}{kT_s} \ll 1.$$

The second term is an effective noise temperature of the detector:

$$T_{eff} = \frac{h\nu}{k} = (4.8 \times 10^{-11})\nu.$$

For a receiver at X-band (10,000 Mc/s), $T_{eff} = 0.48^\circ \text{K}$.

Many experiments have been reported [Alsop et al., 1957; Gordon and White, 1957; 1958; Cohen, 1960] confirming these low-noise capabilities of linear receivers.

Using low-noise receivers, studies have been made of the effective temperature of the sky as a function of elevation angle [Ko, 1958; DeGrasse et al., 1959]. The measurements agree well with theory [Hogg, 1959] based upon known absorption coefficients for atmospheric gases and water vapor and known temperature as a function of altitude. Galactic noise is found to be the dominating factor in sky temperature below about 500 Mc/s at zero elevation, and below about 3 kMc/s at the zenith. The minimum sky temperature is near the zenith and galactic poles (normal to the plane of the milky way) and is about 3°K . Thus modern amplifiers of the maser type are reaching the limit of practical performance in communication and detection systems.

Standard noise sources for measurement and calibration purposes have improved over the last 3 years. For low-noise receivers, terminations at known temperature are quite satisfactory reference sources. For receivers with higher inherent noise shot noise diodes and gas discharge sources are currently used. The latter have been developed to have greater stability and more accurately known noise during recent years [Zucher, Baskin, et al., 1958; Olson, 1958].

Commercial instruments have been developed which automatically, and in some cases continuously, monitor the noise figure of receivers.

The theory of noise in linear twoports has been analyzed [Haas et al., 1960] and IRE standards for its measurement have been published [IRE standards on measuring noise in linear twoports, 1959].

The National Bureau of Standards has announced [Tech. News Bull. 1959] that its facilities for calibration of noise standards are nearly complete so that soon convenient cross checking of standards will be possible.

References

- Alsop et al., Measurement of noise in a maser amplifier, Phys. Rev. **107**, 1450 (1957).
- Cohen, S., Experimental determination of parametric amplifier excess noise using transformer coupling, Proc. IRE **48**, 109 (1960).

*Hewlett-Packard Company, Palo Alto, Calif.

- De Grasse, Hogg, Ohm, and Scovil, Ultra-low-noise measurements using a horn reflector antenna and a traveling wave maser, *J. Appl. Phys.* **30**, 2013 (1959).
- Gordon and White, Experimental determination of the noise figure of a maser amplifier, *Phys. Rev.* **107**, 1728 (1957).
- Gordon and White, Noise in maser amplifiers—theory and experiment, *Proc. IRE* **46**, 1588 (1958).
- Haas, H. A., et al., Representation of noise in linear twoports, *Proc. IRE* **48**, 68 (1960).
- Hogg, D. C., Effective antenna temperatures due to oxygen and water vapor, *J. Appl. Phys.* **30**, 1417 (1959).
- Jones, R. C., Noise in radiation detectors, *Proc. IRE* **47**, 1481 (1959).
- Ko, H. C., The distribution of cosmic background radiation, *Proc. IRE* **46**, 208 (1958).
- Muller, M. W., Noise in a molecular amplifier, *Phys. Rev.* **106**, 8 (1957).
- Olson, K. W., Reproducible gas discharge noise sources as possible microwave noise standards, *Trans. IRE, PGI*, 315 (1958).
- Pound, R. V., Spontaneous emission and the noise figure of maser amplifiers, *Annals of Physics* **1**, 24 (1957).
- Proceedings of the IRE, Standards on methods of measuring noise in linear twoports, 60 (1960).
- Senitzky, I. R., Induced and spontaneous emission in a coherent field (Part I), *Phys. Rev.* **111**, 3 (1958).
- Senitzky, I. R., Induced and spontaneous emission in a coherent field (Part II), *Phys. Rev.* **115**, 227 (1959).
- Shimoda, Takahasi, Townes, Fluctuations in the amplification of quanta with application to maser amplifiers, *J. Phys. Soc. Japan* **12**, 686 (1957).
- Strandberg, M. W. P., Inherent noise of quantum mechanical amplifiers, *Phys. Rev.* **106**, 617 (1957).
- Strum, Peter D., Considerations in high sensitivity microwave radiometry, *Proc. IRE* **43** (1958).
- Tech. News Bull. NBS, Standards and calibration in radio and electronics **43**, 226 (1959).
- Weber, J., Masers, *Rev. Mod. Phys.* **31**, 681 (1959).
- Weber, J., Maser noise considerations, *Phys. Rev.* **108**, 537 (1957).
- Zucker, Baskin, et al., Design and development of a standard White noise generator and noise indicating instrument, *Trans. IRE, PGI*, 279 (1958).

6. Field Strength Measurements

M. C. Selby*

Progress was made in the development of the art of field-strength measurements by some commercial concerns, as evidenced by products placed on the market. At least 3 m were offered for field-strength and interference measurements at frequencies to about 10 kMc/s, input levels of 20 μ v to several volts and internal accuracies (excluding antenna coefficients) of the order of 1 db. These meters were employing superheterodyne receivers, input attenuation up to 80 db, internal or external cw and impulse noise calibration, and they measured average, peak and quasi-peak values [Rosen, 1958; Borek, Rodriguez, 1959].

There were also at least two devices placed on the market to measure near fields for use as RF radiation hazard meters. The frequency and power density ranges in one case were 200 to 10,000 Mc/s at 1 mw/cm² to 1 w/cm² and in another 2,600 to 10,000 Mc/s at a fixed level of 10 mw/cm². The claimed accuracy was of the order of 1 to 3 db. [Electronics, 1958].

Work was initiated at the National Bureau of Standards to develop primary and secondary national standards of cw, field strength and antenna gain at frequencies above 300 Mc/s [NBS Research Highlights, 1958, 1959]. Immediate objectives were the improvement of the stability of an insertion loss measuring system to 0.01 db/hr, evaluation of a microwave absorbing enclosure and of effects of absorbing materials and selection of a waveguide horn as a national standard for frequencies up to 12,400 Mc/s. In line with these objectives a signal source level was stabilized to a ten-thousandths of a decibel and a phase-lock system of frequency control was developed which was capable of locking two free running reflex klystrons—all in noncontrolled environment.

Intensive work was in progress in numerous laboratories on many special problems involving incidental field measurements. These included problems on interference [Hubbard and Cateora, 1959; Albin and Pearleton, 1958; Morelli, 1958; Epstein and Schulz, 1959; Chapin, 1959; White and Ball, 1960], propagation studies [Knudsen and Larsen, 1960; Agy and Davies, 1959], antenna patterns [Morrow, et al, 1958; Kamen, 1959] and others. Instrumentation and technique in these cases were usually adapted to the particular requirements; however, occasionally one may find under these subjects information applicable to the problem of field measurements in general. Some references to these activities are therefore indicated. Work of interest at 100 to 118 kMc/s was recently conducted as a study in propagation [Tolbert and Straiton, 1959; Tolbert, Straiton and Douglas, 1958]. However, this activity was limited

to attenuation measurements and apparently did not attempt measurement of absolute field values.

Considerable information on field theory and measurements at the low end of the frequency spectrum, e.g., from 1 to 300 c/s may be found in papers presented at the 1960 Earth-Current Communications Seminar [J. Research, 1960; Wait, 1960]. An experimental and theoretical study of fields at 18.6 kc/s in a medium of fresh water to depths of 1,000 ft using monopole and loop antennas and encouraging results are described [Saran and Held, 1960].

The continuous efforts of C.C.I.R. Study Group V on measurements of field strength [CCIR Report, 1959] should be followed by those interested in this subject.

References

- Agy, V., and K. Davies, Ionospheric investigations using the sweep-frequency pulse technique at oblique incidence, J. Research NBS **63D** (1959).
- Albin, A. L., and C. B. Pearleton, Measurement of spurious radiation from missileborne electronic equipments, IRE Conv. Record **6**, 8, 155 (1958).
- Borek, A., and M. Rodriguez, Design and development of a noise and field instrument for 1,000 to 12,000 Mc/s frequency range, IRE. National Conv. Record **VII**, 9, 125 (1959).
- C.C.I.R.—Doc. 239-E, Measurement of field strength, field intensity, radiated power, available power from the receiving antenna and the transmission loss, Question no. 8 (1959).
- Chapin, E. W., Standard measurement parameters for phenomena distributed in time and frequency, IRE Conv. Record **7**, 8, 60 (1959).
- Electrons at work, power meter protects microwave workers, Electronics **31**, 43, 100 (1958).
- Epstein, M., and R. B. Schulz, Magnetic-field pickup for low-frequency radio-frequency measuring sets, IRE Conv. Record **7**, 8, 64 (1959).
- Hubbard, R. W., and J. V. Cateora, an X-band field intensity recording receiver with extremely narrow bandwidth, IRE-URSI joint meeting (Oct. 1959), San Diego, Calif.
- Journal of Research NBS, Earth-current communications seminar, NBS, Boulder, Colo., Jan. 26-27 (1960), NBS special issue.
- Kamen, Ira, Large antenna systems for propagation studies, IRE Nat. Conv. Record **7**, 1, 51 (1959).
- Knudsen, H. L., and T. Larsen, The electric field at the ground plane near a top-loaded monopole antenna with special regard to electrically small L- and T-antennas, J. Research NBS **64D** (1960).
- Morelli, M., Spurious frequency measurement in waveguide, IRE Conv. Record **6**, 8, 176 (1958).
- Morrow, C. W., P. E. Tayler, H. T. Ward, Phase and amplitude measurements of the near field of microwave lenses, IRE Conv. Record **6**, 1, 166 (1958).
- Research highlights of the National Bureau of Standards, chapter on Radio Standards (1958, 1959).
- Rosen, B., Microwave field intensity meter, Proc. of the Fourth Conference on Radio Interference Reduction and Electronic Compatibility, conducted by Armour Research Foundation of Ill. Instit. Tech., 242 (1958).
- Saran, G. S., and G. Held, Field strength measurements in fresh water, J. Research NBS **64D** (1960).

*National Bureau of Standards Boulder Laboratories, Boulder, Colo.

- Tolbert, C. W., A. W. Straiton, J. M. Douglas, Studies of 2.15 Mm propagation at an elevation of 4 kms and the millimeter absorption spectrum, Electrical Engineering Research Laboratory, Univ. of Texas, Rep. no. 104 (1958).
- Tolbert, C. W., A. W. Straiton, Radio propagation measurements in the 100 to 118 kMc's spectrum, IRE Wescon Conv. Record **3**, 1, 56 (1959).
- Wait, J. R., Mode theory and the propagation of E.L.F. radio waves, published in the J. Research, NBS special issue, on Earth-current communications seminar, NBS, Boulder, Colo., January 26-27 (1960).
- White, W. D., and C. O. Ball, Simulation tests on an interference rejection antenna system, presented at Session 4, IRE Intern. Conv., NYC (1960).

7. Measurements of Physical Quantities by Radio Techniques

M. C. Thompson, Jr.*

During the past few years the use of radio techniques for precise distance measuring in land surveying has met with notable success. Although at this time only two commercial firms are known to be engaged in the manufacture of this type of equipment: [Microdist; Tellurometer] the enthusiasm with which it has been received in the field of geodetics indicates clearly that it is an important scientific achievement.

One of the limitations on the accuracy of electronic distance measuring is the fact that the basic measurements of transit time must be converted to equivalent distance. This requires a knowledge of the propagation velocity along the path being measured and this can practically only be estimated from measurements at discrete points. The errors can, thus, be divided into two general classes: first, the errors in approximating the space average of velocity (or refractive index) along a line several miles long based on a few point measurements; and second, the errors in calculating phase velocity. The latter include: (1) Uncertainty in the value of c , (velocity of electromagnetic waves in vacuum); (2) errors in determining the constants appearing in the psychrometric equation [Smith and Weintraub, 1953] relating refractive index to measurements of pressure, temperature and water vapor content; and (3) the errors inherent in the measurement of these latter physical quantities.

A number of experiments have been examined [Thompson and Janes, 1959; Thompson and Freethey, 1958] to determine the behavior of the error introduced by interpolating velocity corrections along paths of various lengths based on psychrometric observations under various geographical and seasonal conditions. This work shows that the corrected observations using psychrometric methods have standard deviations of several parts per million. Unfortunately, the experimental errors expected from the atmospheric measurements (3 above) are estimated to be of the same order so that the extent of the interpolation error is probably obscured.

In addition to the interpolation and correction measurements errors, the accuracy of electronic distance measuring is limited by the accuracy of c and of the coefficients relating phase velocity to

atmospheric composition. Although the value of c recommended by URSI is apparently universally used, no one set of psychrometric coefficients has been adopted. Recommendations have been made, however, to the International Association of Geodesy that values be selected for international use to simplify the problems of comparing research and results of different workers. (The discussion of advances in the determination of c is to be found in other sections of this report.)

The work described above suggests that the present practical limitation on the precision of electronic distance measuring is the error in estimating the proper correction for atmospheric properties. As an aid in resolving this error, the National Bureau of Standards, since 1958, has been working to develop a microwave refractometer having sufficient long-term calibration stability to justify absolute calibration. By the use of such an instrument it should be possible to reduce the errors in electronic distance measuring to less than a part in a million.

The instrument recently developed by M. J. Vetter of the National Bureau of Standards operates on a principle distinctly different from those used by Birnbaum and by Crain. By the use of feedback techniques, the new method effectively removes electronic component (including klystron) characteristics from the performance. Preliminary tests suggest that the electronic stability is of the order of a few parts in 10 million for periods of weeks or longer. The residual errors are essentially a function of sampling cavity design and operating conditions (e.g. temperature compensation, cavity contamination and corrosion, etc.).

References

- Microdist, Cubic Corporation, San Diego, California.
- Smith, E. K. Jr., and Stanley Weintraub, The constants in the equation for atmospheric refractive index at radio frequencies; *Proc. IRE*, **41**, 8 (1953), $(n-1) \times 10^6 = (A_p/T) + (B_e/T^2)$.
- Tellurometer (Pty.) Ltd., Capetown, Union of South Africa.
- Thompson, M. C. Jr., and F. E. Freethey, Hourly correlation of radio path lengths and surface refractivity index from Maui, T. H., phase stability program, NBS Rpt. 5579 (June 1958).
- Thompson, M. C. Jr., and H. B. Janes, Measurements of phase stability over a low-level tropospheric path, *J Research NBS* **63D**, 45 (1959).

* National Bureau of Standards Boulder Laboratories, Boulder, Colo.

Report of U.S. Commission 2, URSI TROPOSPHERIC
RADIO PROPAGATION

The USA National Committee of Commission 2 Tropospheric Radio Propagation, has been quite active since the XIIth General Assembly held in Boulder, Colo., 1957. This report contains a brief summary of the work of this Commission arranged in accordance with the topics to be discussed at the XIIIth General Assembly, London, 1960. The bibliography at the end of this report includes principally the papers published since the XIIth General Assembly. References to work that is not generally available in the published literature have not been included.

The following members of Commission 2 participated in the preparation of this report: I. H. Gerks, US Chairman, J. W. Herbstreit, coordinator, W. S. Ament, L. J. Anderson, B. R. Bean, G. Birnbaum, R. Bolgiano, Jr., H. G. Booker, K. Bullington, J. H. Chisholm, C. M. Crain, A. B. Crawford, B. M. Fannin, J. Gerhardt, W. E. Gordon, E. Gossard, I. Katz, M. Katzin, R. S. Kirby, D. Ringwalt, J. F. Roche, J. B. Smyth, H. Staras, A. W. Straiton, M. C. Thompson, L. G. Trolese, A. T. Waterman, and A. D. Wheelon.

The following, although not members of Commission 2, also participated in the preparation of this report: J. R. Bauer, D. C. Hogg, B. Y. Koo, W. H. Kummer, A. H. LaGrone, P. L. Rice, and J. R. Wait.

1. Physical Characteristics of the Troposphere

1.1. Synoptic Scale

Studies on the synoptic scale [Bean, 1959 a, b] have shown that the radio refractive index, when referenced to sea level, is a sensitive indicator of departures from average of atmospheric structure due to tropospheric storms. Indeed, since this reduced-to-sea-level index combines temperature, pressure, and humidity into one term, it appears to have much to recommend it to the meteorologist as an aid in synoptic forecasting. Encouraging correlation has been found between standard weather map information and the variations with time of 1,000 and 10,000 Mc/s beyond the horizon radio fields [Moler, 1958a].

This same reduced-to-sea-level index has facilitated the preparation of world-wide contour maps of the refractive index near the earth's surface by effectively removing altitude dependence [Bean, 1959c]. These charts showing the annual cycle of the mean refractive index may be used to indicate not only climatic comparisons between various regions but also the stability or range of weather in different geographic areas. Studies of atmospheric refraction of radio waves [Anderson, 1958; Bauer, 1958a; Bean, 1959d] have shown that an exponential decrease of refractive index with height is more representative of the true structure and yields more reliable estimates of refraction effects than the linear decrease assumed by the effective earth's radius theory. The rate of exponen-

tial decrease with height may be specified by surface conditions alone [Bean, 1959d]. Consideration of these results led the CCIR Plenary Assembly in Los Angeles in April 1959 to recommend the international adoption of a basic reference atmosphere of exponential form.

A bibliography on the physical properties of the atmosphere at radiofrequencies has been collected and published [Nupen, 1957].

Further studies of the refractive index structure of the atmosphere will be facilitated by two newly established national data centers. The Electrical Engineering Research Laboratory of the University of Texas has accumulated approximately 2,700 airborne refractometer profiles from the North American, Mediterranean, and Hawaiian areas. The Central Radio Propagation Laboratory of the National Bureau of Standards has available approximately 50,000 individual radiosonde ascents taken by military and civilian observations in 40 different locations ranging from the arctic to the tropics.

A large percentage of the earth's atmosphere, and almost all of its water vapor, is contained in the troposphere. The atmospheric gases are more or less horizontally stratified over extended areas, and the gross effect is a gradual decrease in the dielectric constant with altitude. If this gradient of the average dielectric constant is independent of distance and time then the radio propagation problem reduces to a simply stated boundary value problem which might be called mode theory with many tiers of sophistication. These range all the way from simple ray optics approximations to intricate superposition of a large number of modes [Carroll, 1955]. To describe nonoptical fields, the first

suggestion embraced the idea of replacing the problem of diffraction around the earth immersed in a nonhomogeneous atmosphere by diffraction around a sphere of different radius surrounded by a homogeneous medium. In this way, the gradual downward refraction of the radio waves would be accounted for by a larger earth's radius. This idea has been tested and it is found that the factor multiplying the earth's radius is not a simple function of the radiofrequency and the index of refraction profile.

Schelkunoff has proposed an approximate analysis of guided propagation which has been quite useful in determining the cutoff frequency for a given index of refraction profile. This method only states that frequencies above a certain value will or will not be strongly guided, the attenuation rate is not determined. Some success has been obtained in the application of this analysis to microwave propagation in the oceanic duct.

Airborne refractometer investigation [Ament, 1959a] found that the tradewind inversion between the east coast of Florida and Nassau (about 500 km), was consistently at an elevation of 1.5 km with a 50-N unit decrease across the inversion. The intensity of refractive index fluctuations within the layer were found to vary considerably with horizontal distance. Further work on refractive index structure of layers has been carried out by analysis of several thousand refractometer soundings over southwest Ohio and the west coast of Washington state [Moyer, 1958]. Both regions showed a preference for layer occurrence at a height of 1.75 km with the average vertical gradient just necessary for ducting (160 N units/km). Although the average layer thickness was of the order of 150 m in both cases, the Washington coast layers were more evenly distributed between thicknesses of 60 and 210 m. Refractometer investigations have resulted in additional knowledge of humidity structure within elevated layers and also have shown that such layers can satisfy Rayleigh's criterion for smoothness for wavelengths perhaps as small as 1 m [Bauer, 1958b]. Further investigation utilizing airborne refractometers has revealed that the turbulent structure in converging air at 1.2 km is an order of magnitude greater than that found in diverging air within a high-pressure region [Wagner, 1957]. Similar investigations have shown that the "simple" trade wind cumulus cloud is in fact of the most complicated structure from the viewpoint of the refractive index [Cunningham, 1958]. Details of the temperature, humidity and refractive index structure of the trade wind region have been studied with radiosondes [Gutnich, 1958], catalogued in climatological atlases [U.S. Navy, 1955, 1956, 1957, 1958], and examined with airborne refractometers by the Naval Research Laboratories.

1.2. Refractive Irregularities

Progress in describing the radio refractive index structure of the atmosphere has been made on the micrometeorological scale by the use of airborne

refractometers in the study of fundamental theories of turbulence. Two authors have attempted to calculate, using turbulent mixing theories, the spectrum of refractive index variations to be expected in a turbulent region possessing a mean gradient of refractive index, such as the troposphere or ionosphere. Wheelon [1957a, b, 1958a] has attempted to describe analytically the results expected from the gradient-mixing mechanism described earlier by Villars and Weisskopf. Bolgiano [1957, 1958a, b], extending the concept of isotropic-mixing theory to account for the presence of a gradient, does not modify the isotropic-mixing results in a range of interest, in contradiction with the conclusion reached by Wheelon [1958b].

Techniques similar to those employed by Heisenberg for velocity fields have been applied to an investigation of temperature fluctuations in a turbulent region [Ogura, 1958]. Also investigated theoretically was the generalization of mixing by isotropic turbulence to include the effect of a simple chemical reaction on the concentration field [Corrsin, 1958].

A marked disagreement has been expressed [Kraichnan, 1957, 1959; Munch, 1958] as to the seriousness of the error introduced by the assumption that the fourth-order moments of the two-time velocity amplitude distribution are related to second-order moments as in a normal distribution. This quasi-normal approximation has been made in order to calculate the space-time correlation in stationary isotropic turbulence [Munch, 1958].

One theory [Kraichnan, 1958a, b] of unbounded turbulence, driven by Gaussian-distributed homogeneous forces, was developed which gives a wave-number spectrum which is a function of the rms velocity, in contradiction to the Kolmogorov similarity hypothesis.

Two articles extend Chandrasekhar's results on the spectrum of turbulence, one [Blanch, 1959] giving improved numerical results and comments on the choice of equations for numerical evaluation and the other [Wentzel, 1958] working out the spectra for specific examples.

A general power-spectrum equation, basically empirical, for stationary random gusts has been obtained [Saunders, 1958].

Booker continued a discussion of a previously presented concept of a mechanism connected with ionospheric turbulence and meteor trails [Booker, 1958].

Results based on the energy transfer mechanism suggested by Kovasznay have been used to calculate solutions for the energy spectrum and the transfer function in the initial period of decay [Reid, 1959].

Other theoretical investigations have been concerned with turbulent-flow equations [Squire, 1959] and with the relation between time symmetry and reflection symmetry [Meecham, 1958].

The concept of a "locally stationary random process" has been rigorously defined and discussed [Silverman, 1957a; Ogura, 1957; Dryden, 1957].

A possible influence of the mean stability and shear on the spectrum of turbulence, and indirectly

on the spectrum of refractive index fluctuations, has been discussed by Bolgiano [1960], who has suggested that this effect may account for the variable wavelength dependence of scatter propagation [Bolgiano, 1959]. However, Norton [1960] reanalyzed the data employed by Bolgiano, and concluded that they could not be interpreted as indicating a variable frequency dependence; he found that the fixed-frequency dependence $30 \log_{10} f_{Mc/s}$ of the basic transmission loss derived from the $\rho K_1(\rho)$ correlation model for the refractive index was in agreement with the data. Norton [1959a] has published an analysis of the agreement of the $\rho K_1(\rho)$ model with three independent kinds of experimental evidence: (a) Frequency spectra of refractivity; (b) frequency spectra of the phase variations on a line-of-sight path; and (c) the frequency dependence of tropospheric forward scattered power. He concludes that all of these data are in agreement, within experimental error, with this model. In a note at the end of the paper, he calls attention to the fact that the improved data recently published by Thompson and Janes [1959a] appear to indicate that it is not safe to assume that the variations in time of the refractive index at a fixed point may be described by the assumption that a frozen structure, described by a wavenumber spectrum, is moved past this point with the mean wind.

Observations of smoke puffs [Gifford, 1957] and stack gases [Hilst, 1958] have been compared with diffusion theories. Other investigations compare spectra obtained from concurrent airplane and tower measurements [Lappe, 1959] and compare simultaneous observations of space correlations and time correlations [Panofsky, 1958].

Velocity spectra have been deduced from the average rate at which a radar signal crosses a given voltage level [Fleisher, 1959]; the effects of wind speed, lapse rate, and altitude on the velocity spectrum at low altitudes has been studied [Henry, 1959]; the power spectrum of horizontal wind speed in the frequency range from 0.0007 to 900 c/hr have been measured [Van der Hoven, 1957]; and data obtained by flight test techniques have been analyzed to determine how well the velocity variations satisfy the conditions of a stationary Gaussian process and of isotropic turbulence [Press, 1957].

Turbulence measurements have been made for general clear-air conditions [Anderson, 1957; Clem, 1957], near jet streams [Endlich, 1957], near [Ackerman, 1958] and in [Ackerman, 1959] clouds, and associated with a cold front (radar observations) [Ligda, 1958a].

Eddy sizes near the ground have been determined by measurements of temperature [Longley, 1959].

1.3. Absorption in the Troposphere

During recent years generators and components have been improved to the extent that absorption measurements of the actual atmosphere could be made in the millimeter wavelength region. Such measurements have been made by Crawford and Hogg [1956] in the 5- to 6-mm region and at 4.3 and 3.55 mm, and by E. E. R. L. of the University of Texas [Tolbert, 1959a] in the range 1.2 to 1.7 cm, at 8.6, 4.3, 3.55, 2.15 mm, and at a number of wavelengths in the range from 2.5 to 3 mm. The comparisons of the measured losses with those calculated from the Van Vleck-Weisskopf equation are shown in figures 1 and 2. It is seen that the agreement between theory and experiment is good in the case of atmospheric oxygen using the value of 0.02 cm^{-1} for the 5-mm lines. In the case of atmospheric water vapor, however, the agreement is poor, no one line width fitting the entire data. Moreover, the line width of 0.1 cm^{-1} or 0.27 cm^{-1} does not give a completely satisfactory fit for the region around 1.35 cm or the higher frequency region, respectively.

The recent advances on the determination of the line width parameters may be summarized as follows. Benedict and Kaplan [1959], using the quantum theory of Anderson, find that the line widths in $\text{H}_2\text{O}-\text{N}_2$ collisions vary from 0.111 to $0.032 \text{ cm}^{-1} \text{ atm}^{-1}$. Such values indicate that an often quoted average value of $0.1 \text{ cm}^{-1} \text{ atm}^{-1}$ may actually be on the high side. Laboratory measurements of the nonresonant absorption in pure oxygen by Maryott and Birnbaum [1955] give a value of $0.017 \text{ cm}^{-1} \text{ atm}^{-1}$. The line width parameter they found necessary to fit the resonant absorption, namely $0.05 \text{ cm}^{-1} \text{ atm}^{-1}$, is in agreement with the work of Artman [1954].

The discrepancy between theory and experiment in the case of water vapor absorption has long been the cause for examining the limits of applicability of the Van Vleck-Weisskopf theory. Gora [1956] has recently reviewed the situation and finds that no important modification of their equation is needed until the 1-mm region is reached.

Recent measurements by Maryott, Wacker, and Birnbaum [1957] have revealed absorption by the nonpolar gas CO_2 due to collision-induced dipole moments. Although such absorption in atmospheric CO_2 is far too small to play a role, it suggests a direction in which one might look for an explanation of the absorption anomaly. In this connection, Birnbaum and Maryott have found that a large part of the absorption in the microwave wings of the infrared rotational lines of HCl and DCl can be accounted for by assuming the presence of pressure-induced absorption.

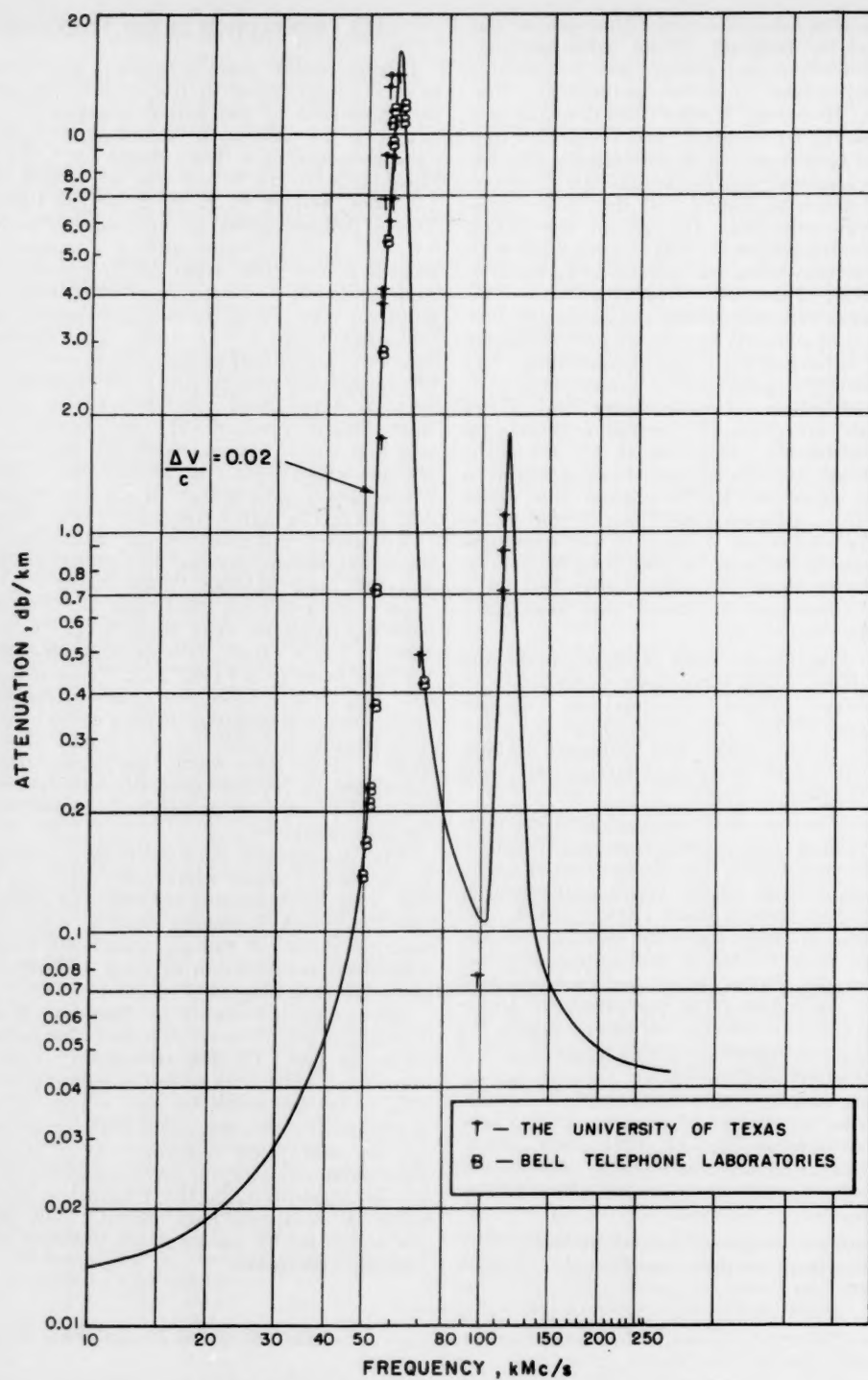


FIGURE 1. Attenuation due at one atmosphere.

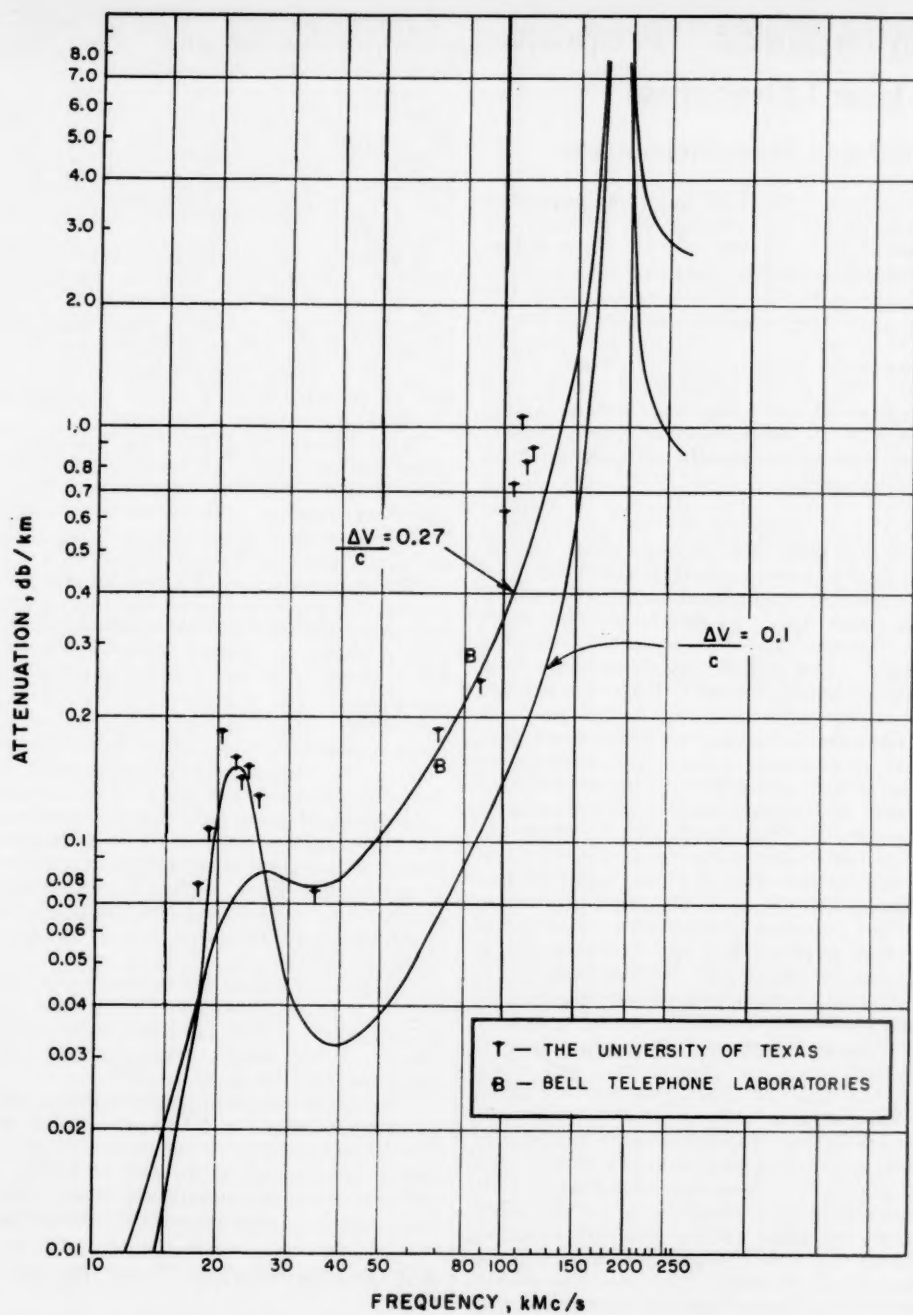


FIGURE 2. Water vapor attenuation for 7.5 grams per centimeter.

2. Tropospheric Propagation (Theories)

2.1. Ground Wave Propagation

Renewed interest in the VLF band has prompted several investigations concerning the propagation characteristics of groundwaves. In the range below 100 kc/s the groundwave may compete with and can often exceed the skywave. Furthermore, with the use of pulse type transmissions such as Cytac or Loran C, the groundwave and skywave may be observed separately [Frantz, 1957; Dean, 1957; Frank, 1957]. This is not possible, of course, in a CW system such as Decca. It is also essential to take proper account of the groundwave in the analysis of sferics which are radio signals originating from distant lightning strokes.

With the above motivation (if such is needed) several theoretical investigations of groundwave propagation have been carried out [Wait, 1958a]. Using the residue series representation as developed, graphs and tables of attenuation and phase for CW transmission have been prepared [Johler, 1956, 1959a; Wait, 1956a]. The frequency range is from 100 c/s to 500 kc/s and various ground constants and antenna heights were chosen. These curves are presented in terms of field strength and they are normalized for a dipole transmitter of fixed moment.

Theoretical groundwave investigations have included studies of methods to include variations of the refractive index of the troposphere. As mentioned under the section of this report dealing with the synoptic scale variations of the physical characteristics of the troposphere, (sec. I, 1), the usual method of accounting for the gradual downward bending of radio waves is to replace the actual earth's radius a by an effective earth's radius a_e . The ratio a_e/a is usually taken to be about 4/3. It has been shown [Wait, 1958b] that such a procedure is a mathematically adequate approximation for propagation in a standard type atmosphere if the antenna heights are not too high (i.e., less than 1 km) and if the frequency is not too low (i.e., greater than about 50 kc/s). When either of these conditions is violated, it is necessary to consider the influence of nonlinearity in the lapse rate of the refractive index with height. Theoretical studies have been carried out which indicate that the diffraction theory for a 4/3 rds earth may be simply modified for an atmosphere whose refractive index varies with height in a smooth monotonic fashion [Wait, 1958b]. The essential conclusion is that the structure of the diffraction field near and beyond line-of-sight is similar to that for a homogeneous atmosphere. Thus the available calculated results based on the 4/3 rds. earth may be simply adapted to the tapered model by simply shifting the horizon point which is calculable using geometrical or ray optics. Such a procedure had been used earlier by K. A. Norton [1958] which, at the time, was justified on physical grounds.

All the "eigenvalue" or "proper value" solutions suffer from some difficulties. The problem is centered around the determination of the complex propagation constants associated with the dominant modes. These numbers are extremely sensitive to the detailed structure of the index of refraction profile. A given experimental refractive index profile can be represented by numerous smooth curves, each yielding a different mode sum for the radio field.

In addition, the sensitivity depends upon the wave function accepted as a solution; for example, if the well-known WKB approximation is considered an appropriate wave solution, continuous index of refraction profiles with continuous first order derivatives will yield no "proper values" since there is no way to couple the field of the up-going wave with the field of the down-going wave.

The influence of a land sea boundary has been given further study. A solution has been presented for a smooth earth for a mixed path with both two and three sections. Numerical results for amplitude and phase over a frequency range of 20 to 200 kc/s are also available [Wait, 1957a].

The propagation of electromagnetic pulses over a smooth homogeneous earth has been given considerable attention from a theoretical point of view [Wait, 1956b, 1957b, c, 1959a; Johler, 1957, 1958, 1959b; Levy, 1958]. For low frequencies the dispersion of the pulse is due mainly to the influence of earth curvature. The finite conductivity of the ground plays a relatively minor role. Some thought has also been given to the influence of a coast line on the shape of a groundwave pulse [Wait, 1957d].

It was pointed out that the presentation of ground-wave propagation data in terms of transmission loss requires that the input impedances of the antennas be considered [Wait, 1959b; Norton, 1958]. Various methods of calculating transmission loss of the groundwave are reviewed in a comprehensive paper [Norton, 1959b].

The penetration of the groundwave into the earth or the sea has been considered in several recent papers [Wait, 1959c, d; Kraichman, 1960; Keilson, 1960]. Both buried transmitting and receiving antennas have been considered.

The influence of ground stratification has been given some attention [Wait, 1958c]. It is indicated that the attenuation of the groundwave may be quite low if the underlying stratum is highly conducting and located at an appropriate depth. The measurements are in accord with theory [Stanley, 1960].

2.2. Backscattering From Rough Surfaces

Katzin [1957] has continued his theoretical development of backscattering from a sea surface. He has extended to high-depression angles the statistical treatment previously made for low angles. He finds that σ_0 varies as λ^{-n} for frequencies in the region where the facets are small compared to a wavelength. As the frequency increases a region is reached where the facets are large compared with λ ; above this

region, σ_0 is constant with further increase in frequency. He also finds σ_0 is inversely proportional to wind speed and that the depression angle dependence is $\exp(-\cot^2\theta/2\sigma^2)$.

Spetner and Katz [1960] have approached radar backscattering from a statistical point of view. They calculate the normalized radar cross section, σ_0 , for two different terrain models. The first model is a distribution of independent scatterers. For this model σ_0 is independent of depression angle, θ , but has a local wavelength dependence as λ^n , where n can be -6 , -4 , or -2 . The second model is a surface of specular points where the slope distribution is Gaussian. Here, for small λ , σ_0 varies as $k\lambda^{-2} \exp(-\cot^2\theta/2\sigma_s^2)$. For large λ the relationship depends on the surface slope spectrum. For a flat spectrum, whose cutoff wave length is λ_2 , σ_0 varies as $k_1\lambda^{-6} \exp(-\lambda\cot^2\theta/2\lambda_2\sigma_s^2) + k_2\lambda^{-6}$ and for a spectrum with a single peak the σ_0 relationship is $k\lambda^{-6}$.

Moore [1957] has obtained the same angular dependence, using a model based on random distribution of heights of facets:

$$\sigma_0 = \frac{(90^\circ - \theta)a^2 \sec \theta}{4\pi\sigma^2} e^{-a^2/4\sigma^2 \cot^2 \theta}.$$

Here a is the horizontal correlation distance of height and σ is the standard deviation of height. The specular return is reduced by $e^{-2(2\pi\sigma/\lambda)^2}$ from the smooth surface value.

2.3. Theory of Propagation Through a Stratified Atmosphere

The earth-flattening approximation has been used widely in the theory of a stratified atmosphere to obtain approximate solutions for various types of refractive index distributions. In a refinement of the earth-flattening procedure, Koo and Katzin [1960] have shown that this procedure may be made exact, so that it may be applied for arbitrarily large heights and distances. Furthermore, it is found that existing solutions for the height-gain function obtained with the use of the previous earth-flattening approximation can be made to give the exact solutions for a slightly different refractive-index distribution. This method, which has been developed for spherical geometry, can be extended to other separable shapes.

In an extension of this work, Katzin has shown that mathematical approximations introduced to facilitate the solution of propagation problems can be interpreted as a change in the physical problem which is being solved. Thus, in the normal mode solution for propagation through a homogeneous atmosphere around a spherical earth, the WKB (tangent) or Hankel approximations for the eigenvalues are found to be the exact eigenvalues for a slightly inhomogeneous atmosphere, the inhomogeneity being different for the two approximations. In general, the approximations introduced represent a change in the refractive index distribution, in the geometry, or in both.

2.4. Line-of-Sight Scintillation

The electromagnetic response of a wave to a statistically irregular refractive index structure,

$$n(r,t) = n_0 + \Delta n(r,t),$$

is well approximated by the basic wave equation:

$$\{\nabla^2 + k^2[n_0 + \Delta n(r,t)]\} \vec{E} = 0, \quad (1)$$

where $k = 2\pi/\lambda$ is the free space wavenumber and $\vec{E}(r,t)$ the developing electric field. It still does not seem to be possible to solve eq (1) exactly, since $\Delta n(r,t)$ is an a priori unknown stochastic function of position and time. Hence, we can conveniently group research according to the approximate methods which have been used to solve the basic wave equation.

The ray theory or geometrical optics approximation to the solution of eq (1) has proven valuable in studying phase fluctuations in the Fresnel scattering regime, but is generally not adequate to predict amplitude variations, time and space correlation of phase records; and the appropriate correction factors for finite data sample and aperture smoothing limitations have been derived [Wheelon, 1957c] for an arbitrary model (spectrum or correlation) of tropospheric irregularities which are statistically stationary and homogeneous. Explicit expressions for finite aperture smoothing corrections were reported [Levin, 1959]. Corresponding results for angle-of-arrival variations are also given [Wheelon, 1957c]. A summary of all explicit geometrical optics calculations is presented in table 2 of Wheelon, 1959.

The single scattering or Born approximation has been widely used to study both phase and amplitude scintillations. Early calculations were based on particular models of the irregularities. However, a new approach was presented [Wheelon, 1957c] and further developed [Wheelon, 1959] which permits one to isolate the electromagnetic propagation calculations from the spectrum or correlation function. A model choice can thus be delayed until all electromagnetic calculations have been both completed. The relay-link and radio-star problems have been treated with this new method, and a technique has been devised [Wheelon, 1959] to study the complicated effects of ground reflections, aperture smoothing, and time and space correlations within the framework of a single scattering theory. Almost all of the previous calculations dealt exclusively with continuous wave transmissions, whereas Bugnolo [1959a] discusses the effect of the time variability of refractive irregularities on signal bandwidth and information capacity. Two investigations [Balser, 1957; Stein, 1958] into scattering of a vector field clarified several questions about the validity of previous scalar treatments, and discussed the effect of certain small terms which were dropped in writing eq (1).

A novel approach to the problem of stochastic propagation based on earlier astrophysical work is given [Bellman, 1958]. The basic idea is to replace the linear second order differential eq (1) by a non-linear first order (Ricatti) differential equation, whose solution is identified with the reflection or transmission coefficient directly. This technique has not yet produced explicit answers of the type previously derived with ray theory, and will bear further research.

Statistical properties of a constant vector plus a Rayleigh-distributed vector were investigated further. Such a combination is presumably a good representation of the vector voltage diagram of line-of-sight signals containing both the free space and scattered signal components. Previous papers [Wheelon, 1959] had discussed the distributions of phase and amplitude at a single time. The mean square phase and average phase of such a combination were computed explicitly [Johler, 1959c] as a function of the mean signal to rms amplitude ratio. Bremmer [1959] considers the distributions of amplitude and phase at two different times.

2.5. Scatter Propagation

a. Layers

There has been no comprehensive treatment of the theory of beyond-the-horizon propagation via stratified layers in the atmosphere during the past two years in the United States. However, several papers have been published which provide evidence supporting reflections from layers as an important mechanism in the propagation. Airborne refractometer and meteorological measurements offer direct evidence of layers with sufficiently sharp gradients over sufficiently small intervals of height to provide reflection [Bauer, 1956] while [Bauer, 1958b] offers an explanation for the occurrence of layers. Substantial propagation data [Crawford, 1959] have been interpreted in terms of the reflection theory [Friis, 1957]. Correlation between signal characteristics and gross layer characteristics has been observed [Bauer, 1956; Barsis, 1957]. Time delay measurements [Chisholm, 1957a] airborne long distance measurements, and rapid antenna scanning [Ames, 1959a] have produced results that are not inconsistent with layer reflection.

b. Blobs

Activity in the field of tropospheric scatter propagation has been less intense in the last two years than previously. This diminished endeavor probably reflects the rather thorough exploitation of the turbulent scattering model which has been achieved in previous years. For example, it appears that almost nothing has been written about coherent partial reflection in the past several years, but several papers suggesting scattering by layers [Friis, 1957] or multiple scattering by blobs [Kay, 1958; Ament, 1960] have appeared. It is worth mentioning that the formalism introduced by Staras [1955] for taking

into account anisotropy in the blob-structure bridges the gap between the spherical blobs introduced by Booker and Gordon [1950, 1957] and the layers introduced by Friis, et al. [1957].

A summary on the theoretical progress in tropospheric scatter propagation has appeared recently [Staras, 1959a]. That summary restricted its consideration to single scattering. Diffraction and ducting effects are neglected in single scattering for lack of a tractable solution. The generally stratified average atmosphere [Misme, 1958] enters only through ray bending, allowing more or less favorably situated blobs to enter in the single-scattering phenomenon. The dominant parameter in a single-scattering theory is the autocorrelation function of the random irregularities which in turn is related to the spectrum of these very same irregularities. Thus, the characteristics of over-the-horizon propagation make contact with the various models of atmospheric turbulence [Wheelon, 1957a; Bolgiano, 1958a; Paul, 1958; Silverman, 1957b]. This has already been discussed previously [Staras, 1959a]. It should be emphasized though that the fundamental role of the spectrum of refractive-index irregularities as opposed to that of the correlation function has been clearly established. This is most important since attempts at empirical determination are at best estimates over a limited range of values; and limited knowledge of one member of the Fourier transform pair cannot yield positive identification of the other. In addition, evidence both from radio investigations and meteorology indicate that atmospheric spectra vary not only in intensity, but also in shape. This emphasizes the danger of assuming a unique form for the refractive-index spectrum as has been discussed by Bolgiano [1959] who suggested that the variable form for the refractive-index spectrum may account for the variable wavelength dependence of scatter propagation. However, in a recent analysis Norton [1960] states that the wave number refractivity spectrum pertinent to the forward scatter of radio waves *cannot* be directly measured when the medium is anisotropic. He proposes a scheme for a direct measurement of the refractivity characteristics of the atmosphere leading to an anisotropic correlation function which could then be transformed into the appropriate wave number spectrum.

An aspect of single scatter theory which is receiving increased attention lately is angle diversity [Bolgiano, 1958c; Vogelmann, 1959]. This is intimately related to the concept of antenna coupling loss developed earlier [Booker, 1955; Staras, 1957, 1959b; Hartman, 1959]. Since antenna coupling loss is believed to arise from a failure to fully illuminate the effective scatter volume when the antenna becomes very large, some investigators have suggested that a multiplicity of feeds in a very large parabolic antenna could be used to illuminate the entire scattering volume and thereby cut down on the coupling loss. While this is undoubtedly true, it is indicated [Staras, 1960] that there may be easier and more standard ways of achieving the same result as would be accomplished by angle diversity.

In summary, it appears that the major development in transhorizon tropospheric propagation during the past several years in the growing body of evidence indicating that no single mechanism (scattering, reflection from layers, ducting, etc.) can account for all the experimental results. Typical of this are Crawford, Hogg, and Kummer's experiments [1959]. They appear to support a scatter model 60 to 70 percent of the time and a layer reflection model much of the remainder. From Staras' [1955] point of view, this experimental result would suggest that the anisotropy in scatter propagation is highly variable. Recent work on multiple scattering [Kay, 1958; Ament, 1960] and scattering by layers [Friis, 1957] should also prove to be useful for explaining some of these other mechanisms.

However, for that part of the time when scattering is expected, single-scattering theory has been used with essentially no adjustable parameters to provide a satisfactory explanation of forward scatter data [Nortom, 1959b; Rice, 1959].

3. Experimental Results From Investigations of Tropospheric Propagation

3.1. Attenuation With Distance

Recent experimental data on beyond horizon tropospheric transmission have provided very useful information at distances up to 1,200 km. Most of the new results are in the frequency range below 500 Mc/s. These data together with earlier information clearly establish that the decrease in signal level at the greater distances follows an exponential law at a rate of about 0.075 db/km near the surface. Airborne measurements have corroborated that the path loss depends upon the "angular" distance between the two terminals, not upon the surface distance alone.

Figure 3 shows observed median values of beyond horizon basic transmission loss plotted versus distance and coded by frequency groups for a large, heterogeneous sample of U.S. data, obtained in most cases with broad beam antennas. No normalization for the effects of frequency, antenna height, angular distance, path asymmetry, terrain, time of day or season, or climatic parameters is included. Most of the spread of the data, in addition to that caused by changes in frequency, appears to be due to the diversity of antenna heights and terrain represented by the actual propagation paths. Differences in atmospheric conditions appear to be the next most important consideration.

Some experimental data, particularly for transmission over water, show a 5- to 10-db hump in the curve in the neighborhood of 300 to 500 km. This is not clearly understood, but it may be significant that the volume of the atmosphere visible from

both transmitting and receiving antennas for this case is at elevations of 2 to 4 km where most of the visible clouds occur.

Two sets of curves are compared with the data. One is based on the assumption that basic transmission loss varies as the second power of the frequency; these curves were approved by the CCIR in April 1959, for frequencies up to 600 Mc/s and for antenna heights of 10 and 300 m. The other set of curves is calculated for a smooth earth of effective radius 9,000 km, for antenna heights each equal to 10 m, and for various frequencies, assuming an exponential decay of refractive index with height such that the refractive index is $1/e$ times the surface value at a height of 6.9 km. Frequency dependences are influenced by the nature of the terrain and atmosphere and by whether antennas are high or low; these factors determine the dominance of various propagation mechanisms. The large influence of antenna height is illustrated in figure 4 which shows theoretical smooth earth curves for a frequency of 500 Mc/s with one antenna height fixed at 10 m and the other varying from 10 to 100,000 m.

In temperate latitudes the seasonal variation of received signals shows a minimum during the winter, and the diurnal trend has its minimum in the afternoon. These minima are on the order of 10 db below the annual median value, except that diurnal trends are less pronounced at great distances. Since the signal level depends to some extent on atmospheric refraction, the median signal level in low latitudes is usually higher than in the high latitudes.

Data from the following sources have been considered in the preparation of this report and the accompanying chart:

1. Federal Communications Commission Technical Information Division Reports 2.4.6, May 1949; 2.4.10, October 1950; 2.4.13, December 1954; 2.4.16, October 1956; and private communications.

2. National Bureau of Standards Reports 1826, July 1952; 2494, May 1953; 2539, May 1953; 3536, March 1954; 3520, January 1955; 3568, February 1956; 5067, December 1956; 5072, May 1957; 5524, October 1957; 5582, June 1958; 6019, November 1958; and NBS Circ. 554, January 1955.

3. Proc. IRE, Vol. 43, No. 10, October 1955, pp. 1306-1316. Proc. IRE, Vol. 43, No. 10, October 1955, pp. 1369-1373. Proc. IRE, Vol. 43, No. 10, October 1955, pp. 1488-1526. Proc. IRE, Vol. 46, No. 7, July 1958, pp. 1401-1410.

4. IRE Summary of Technical Papers, 4th National Aero-Com Symposium, October, 1958.

5. Bell System Technical Journal, September 1959.

6. International Telephone and Telegraph Corporation, Federal Telecommunication Labs., Technical Memo 566, November 1955.

7. Air Force Cambridge Research Center AFCRC February, 1958, private communication. Air Force Cambridge Research Center AFCRC-TR-55-115, June 1955 (see also Ames, 1959a).

8. Massachusetts Institute of Technology, Lincoln Labs., private communication.

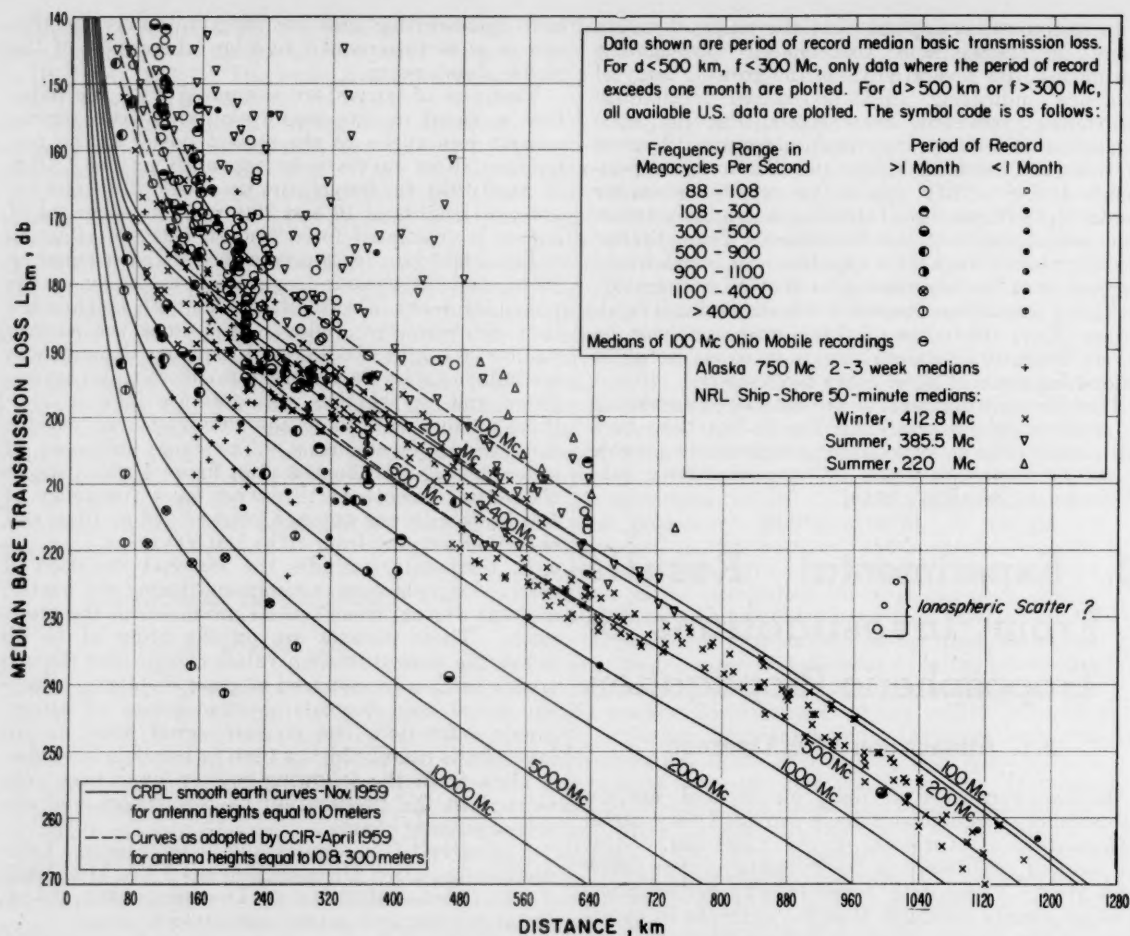


FIGURE 3. Beyond horizon transmission.

9. Radio Corporation of America, RCA Review, September 1958.

10. Page Engineers Interim Report P.C.E.-R-4378, May 1957.

11. Syracuse University Technical Reports, EE 312-5511P, Nov. 1955; EE312-5611T3, Nov. 1956; EE12-5711T4, Nov. 1957; and EE312-5810F, October, 1958.

12. Cornell University Research Reports EE229, 1 December 1954 and EE260, 10 Sept. 1955.

13. Additional unpublished data collected by CRPL.

3.2. Effects of Rough Terrain

a. Forward Scattering

Nearly all radio services employ propagation paths in which the electromagnetic waves are transmitted along an irregular, inhomogeneous ground boundary for at least part, if not all, of the transmission path. The result of this influence is manifest in spatial variations in transmission loss.

Electrical ground constants, reflection, diffraction, and absorption are all important in varying degrees. Conductivity plays the most important role in the lower frequency ranges below roughly 30 Mc/s, while reflection, diffraction, and absorption become relatively more important at higher frequencies. In any given case the transmission loss at any instant of time is a result of several causes and effects which are exceedingly complex to predict.

Since the XIIth General Assembly held in August and September 1957, most of the work in the U.S.A. involving irregular terrain propagation has dealt with the prediction of VHF and UHF broadcast service fields and the effect of large obstacles producing knife-edge diffraction on point-to-point propagation paths.

The Television Allocations Study Organization carried out studies in 1957 to 1959 of all technical phases of television broadcasting [TASO, 1959]. A large amount of propagation data was obtained representative of television signals transmitted over irregular terrain at both VHF and UHF. New

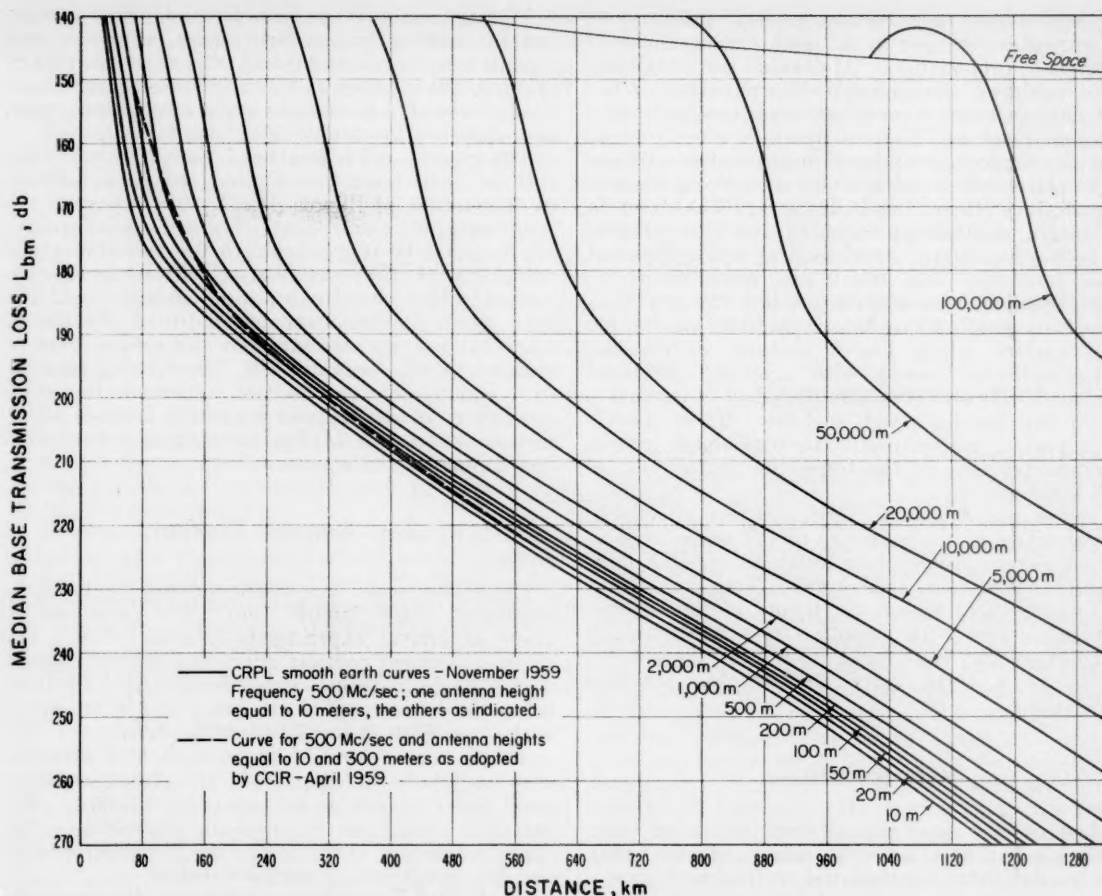


FIGURE 4. Theoretical smooth earth curves.

methods of specifying the coverage of a television station are discussed. These methods take the variability of the signal propagated over irregular terrain into account in terms of the statistical probability of receiving the signal throughout various areas surrounding the transmitter.

LaGrone [1959] has developed a new method for predicting the median transmission loss as well as departures from the median expected over irregular terrain paths typical of television transmission paths. His method is largely empirical and is based on the data collected by TASO and on diffraction theory.

Study Group 5 of CCIR [CCIR, 1959] adopted a report concerning the measurement and description of service fields for television broadcasting at the IXth Plenary Assembly held in Los Angeles in April 1959. This work gives a method for describing the coverage of broadcast services in terms of the probability of receiving service in the area surrounding the transmitting station. This paper also presents a statistically efficient method for measuring or estimating the coverage.

Egli [1957] has analyzed irregular terrain propaga-

tion data for various low- and high-transmitting and receiving-antenna heights. He has prepared curves and nomograms which should be useful in systems engineering for services affected by irregular terrain, such as land mobile and point-to-point services.

The obstacle-gain phenomenon associated with knife-edge diffraction over a large obstacle has been under further study by both U.S.A. and Canadian investigators. Neugebauer and Bachynski [1958] of Canada have developed a relatively simple method for solving the special case of diffraction over a smooth cylindrical surface. This solution is based on the assumption that the radiating aperture is illuminated by both direct rays and by rays reflected from the illuminated side of the obstacle. The subsequent radiation is also reflected from the shadow side of the obstacle. Although their procedure is not rigorous, it does lead to results which are in good agreement with observations. Wait and Conda [1959e] have developed a method for computing the fields diffracted by convex surfaces which is both rigorous and easy to apply.

A significant contribution to the problem of ground reflections has been made in the field of air-ground propagation. McGavin and Maloney [1959] made an experimental determination of the reflection coefficient over rough terrain using various terminal heights. They separated the specular from the random component and found a terminal height above which the specular component became insignificant. Beard and Katz [1957] found a qualitative relationship between the spectrum of the forward scattered total field and the apparent ocean roughness and the ocean wave spectrum. Wait [1959f] has extensively studied the reflection of electromagnetic waves from a perfectly conducting plane surface which has a uniform distribution of hemispherical bosses with arbitrary electrical constants. He also considers the effect of curvature and of two parallel rough surfaces. These models are expected to be useful in explaining certain experimental data on the terrestrial propagation of VLF radio waves.

Trolese and Anderson [1958] describe an experimental study of the influence of the shape of foreground terrain profiles near terminals of UHF links on the received field. Shkarofsky, Neugebauer, and Bachynski [1958] extend the theory of propagation over mountains with smooth crests presented by Neugebauer and Bachynski [1958] and present the results in a form more suitable for practical applications.

b. Backscattering

Most of the experimental work on radar backscattering has been achieved using airborne radar. Macdonald [1959] has reported on measurements of terrain reflectivity at 425, 1,250, 330, and 9,300 Mc/s with horizontal, vertical, and cross polarization at depression angles of 10 to 90 deg. Measurements were obtained for forest, desert, city, and water surfaces. All targets except the city were found to be "homogeneous" radarwise and the amplitude data showed approximately a Rayleigh distribution at all depression angles.

At the University of New Mexico [Edison, 1959] measurements at 415 and 3,800 Mc/s have been made at depression angles from 60 to 80 deg over farmland, forests, city areas, desert, water surfaces, and some areas with snow and ice cover. The radar return is interpreted as consisting of a scattered component and a specular component, the latter present only at normal incidence. Specular reflection is significant only for very smooth surfaces, such as water and sandy desert. Radar cross sections per unit area, σ_0 , sometimes called the scattering coefficient, range at vertical incidence from about 0.5 for forest to 18 for farmland and some city targets. They decrease rapidly with angle for smooth surfaces (for water $\sigma_0=50$ at 415 Mc/s, 200 at 3,800 Mc/s) and slowly for forests. If the ground were a lossless isotropic scatterer the radar cross section per unit area would be 2 at vertical incidence.

Measurements of return from highly uniform terrain such as grass, farm crops, concrete, and asphalt have been obtained at Ohio State University [Taylor, 1959] using 3, 1.2, and 0.86-cm radiation. The effects of polarization, surface roughness, rain, and snow on the results have been investigated.

The spectra of backscattered energy from the sea surface have been investigated experimentally at the University of Illinois [Hicks, 1958] using an airborne coherent 3-cm radar. The sea clutter spectra are found to be proportional to the probability distributions of the scatterer velocities on the sea surface. Theoretical calculations indicate that less than one-half of the average width of the clutter spectrum can be attributed to the orbital particle velocity of the waves while, presumably, surface drift and white-cap velocities contribute the other one-half or more. Higher sea states produce asymmetric spectra and also an irregular downwind broadening of the spectrum.

3.3. Angular Diversity

Experiments in beyond-the-horizon propagation conducted since August 1957 have reemphasized angle of arrival experiments [Staras, 1958]. The basic experiment consists of probing the atmosphere with a single movable beam—the principal advances being the narrowness of the beam and in the speed with which it is scanned. The results of this research can be applied to multiple-feed diversity systems where multiple feeds are placed near the focal point of one large parabolic reflector. The multiple beams can be used simultaneously. Significant research along these lines is exemplified by the five programs summarized below.

At the Bell Telephone Laboratories, Kummer conducted experiments at 4,110 Mc/s and 460 Mc/s, transmitting over a 171-mile path with relatively broad beams and receiving on various narrow beams—down to 0.3° at the higher frequency. By scanning the narrow beam, variations in angle of arrival were apparent, and an average beam broadening was observed. In employing a double-feed and simple-switching diversity, the diversity improvement expected for nearly independent Rayleigh distributed signals was realized at 4,110 Mc/s for both horizontal and vertical angular-beam separation. At 460 Mc/s, this improvement was realized for vertically displaced beams, but for horizontal it varied with fading rate.

At Stanford University, Waterman employed a phased array to receive signals from a 101-mile-distant broad-beam transmitter [Waterman, 1958a, 1960; Miller, 1958]. Rapid control of the phasing permitted a 0.5° beam to be swung in azimuth through a 4-deg sector at the rate of ten times per second—faster than most atmospheric variations. This technique provided a detailed picture of instant-to-instant angle-of-arrival changes and structure. Significant results indicated a finite number of reflecting facets, as if from a rippling

layer, that moved around rapidly, in marked contrast to the random scattering anticipated from turbulence theory. The possibility of searching for or tracking a single arriving component was suggested as an alternative to a fixed-beam diversity system.

The Avco Corp. [1958] performed rapid beam swinging experiments at 500 Mc/s over a 50-mile path. A 10-deg beam was scanned electronically at 50-cycle rate. Rapid variations and occasional multiplicities in the angle of arrival were observed.

At MIT-Lincoln Laboratory, the correlation was measured between two beams provided by a dual feed arrangement at a frequency of 2,290 Mc/s and a path length of 188 miles [Chisholm, 1959]. Observed correlations well below unity indicated a substantial diversity improvement for appropriate beam separations.

At Cornell University, Bolgiano, Bryant, and Gordon [1958c] investigated the improvements to be expected from angular diversity systems. Theoretical models were compared with previously obtained Stanford data.

At Rome Air Development Center, Vogelmann, Ryerson, and Bickelhaupt [1959] made measurements over a 200-mile path at 8,000 Mc/s of the correlation between 0.3° beams separated in azimuth and elevation. From the extremely low correlations obtained rather elaborate multiple-beam diversity systems were designed.

3.4. Frequency Diversity

The variation of the amplitude of a signal with frequency determines the bandwidth limitations imposed by the propagation mechanism. Experiments consisting of sweeping a frequency many times faster than the fading rate of the signal over a 20-Mc/s frequency band were performed to provide information concerning the "instantaneous bandwidth" of a tropospheric signal [Chisholm, 1958]. These measurements also inherently contained data applicable to frequency-diversity techniques.

Earlier frequency-sweep measurements at 2,290 Mc/s which were reported at the XIIth General Assembly in Boulder were continued [Chisholm, 1959]. These measurements, made over a 188 mile path, provided data indicating the variation of amplitude simultaneously in both time and frequency. Analysis of the results indicated that the correlation of the envelope was 0.5 at 2 Mc/s separation and less than 0.1 at 4 Mc/s. The average instantaneous bandwidth was 3.2 Mc/s.

Similar frequency-sweep measurements at 4,110 Mc/s over a 177-mile path and employing antennas ranging in diameter from 8' to 60' [Kummer, 1959] gave results which were in fair agreement with the 2,290 Mc/s measurements. These measurements, however, showed no dependence of the instantaneous frequency variation on the size of the antenna employed.

Preliminary results of reception of 900 Mc/s [Abraham, 1959] FM signals received on two separated sidebands over a 135-mile path were also

reported. These measurements indicated the correlation was about 0.5 at 2-Mc/s separation, the experimental limit.

A paper was also presented [Landauer, 1959] reporting a sweep experiment over a 500-Mc/s band, from 3,100 to 3,600 Mc/s. The results of these measurements are difficult to evaluate in the same terms as the other frequency-sweep experiment because of the resolution of the equipment and the slow-sweep rate. These measurements did indicate several peaks of amplitude across this 500-Mc/s frequency band.

The results of all these measured are applicable to modulation and to diversity techniques.

3.5. Diversity Improvement

The objective of any diversity system is to produce two or more channels for transmitting the same information so that the fading on the several channels is essentially uncorrelated. A comprehensive theoretical treatment of the various methods for combining such signals to achieve a signal-to-noise-ratio improvement has been given by Brennan [1959]. He designates the three principal diversity systems as selection, maximal ratio, and equal gain, and shows that the third is the simplest and will generally yield performance essentially equivalent to the maximum obtainable. His principal results are the average SNR improvement and the distribution curves for 2, 3, 4, 6, and 8 channels, with Rayleigh fading and equal SNR assumed for the individual channels. He shows that two signals may be considered uncorrelated when the cross-correlation coefficient $\rho \leq 0.3$, and that significant-diversity improvement results even when $\rho = 0.8$.

The most commonly used method for achieving several channels with uncorrelated fading is horizontal space diversity. Recent experimental results with dual diversity, frequency modulation, and maximal-ratio, post-detection combining have been reported by Wright [1960]. The frequency was in the 1,000-Mc/s range. Results include fade-duration distribution without diversity and with dual diversity and comparison with theoretical analysis, as well as total fade duration as a function of depth of fade. The antenna spacing was sufficient to produce cross-correlation coefficients less than 0.3. These data have important applications in the prediction of error rates as a function of median signal level in data transmission.

Recent trends toward the use of larger antennas and higher frequencies have led to the consideration of angular space diversity. With increasing aperture and frequency, the antenna beam becomes so narrow that the available scattering volume in the troposphere is poorly utilized, and "antenna-to-medium coupling loss" may become large. To offset this effect, multiple feeds may be mounted near the focus of a parabolic reflector so as to produce a multiplicity of beams, each of which illuminates a different portion of the scattering volume. In this

way, a number of channels is produced which have suitably low correlation coefficients. However, the median SNR's are no longer the same for all channels. The method leads to economy in the use of large reflectors and permits individual transmitters of moderate power to be connected to separate feeders if they operate on separate but closely spaced frequencies.

A beam-swinging experiment, in which a broad transmitting beam and a narrow receiving beam were employed, has been reported by Stanford University [Waterman, 1958b]. Experimental data and analysis of improvement obtained at UHF and higher frequencies have been reported by Bell Telephone Laboratories [Crawford, 1959] and Lincoln Laboratory. Data and computations for a multiple-feed system have been described by the Rome Air Development Center [Vogelman, 1959]. A theoretical analysis of problem has been made by Cornell University [Bolgiano, 1958c].

It is recognized that the uncorrelated channels required for diversity may also be obtained by the use of several frequencies sufficiently spaced from each other. This method seems best adapted for application at the higher frequencies, where spectrum space is currently not too critical. Offsetting extravagant use of spectrum is the fact that only a single feed is required and the several median SNR's are essentially equal.

Some information on the relation between channel spacing and cross-correlation coefficient is available as a result of swept-frequency experiments [Crawford, 1959]. Lincoln Laboratory [Chisholm, 1959] reports a correlation coefficient of 0.1 to 0.2 with a frequency spacing of 4 Mc/s. Airborne Instruments Laboratory reports an experiment in which the frequency was swept from 3,100 to 3,600 Mc/s on a 190-mile path in France, and in which there were at times privileged frequencies on which the signal was 10 db above the median for the band. General Electric Research Laboratory reports analyses of propagation at 915 Mc/s over 135-mile path showing a mean-correlation coefficient of 0.5 for a 2-Mc/s frequency spacing.

3.6. Phase Stability

The measurements of phase stability of radio signals propagated over line-of-sight tropospheric paths have been extended during the past three years. This work was originally undertaken to assist in evaluating the limitations imposed by atmospheric turbulence on direction finding and guidance systems [Herbstreit, 1955]. It has subsequently been expanded to provide basic contributions to our knowledge of turbulence [Thompson, 1960a], in general, and to include other engineering applications such as electronic distance measuring techniques [Thompson, 1958a, 1960b].

The original experiments conducted by the National Bureau of Standards in the Pike's Peak area

of Colorado (and later extended to the Maui, Hawaii area) were continued to include paths from about 600 m to 16 km in length, near Boulder, Colo. Effects of antenna size, polarization, radiofrequency and ground reflection were investigated. Measurements were also made over 8- and 15-km paths in Florida on the Atlantic Coast. In all cases the antenna heights were from 1 to 15 m above ground. Supplementary measurements were made of temperature, humidity, barometric pressure, wind velocity, solar radiation, and radio refractive index. The index variations and the phase and amplitude variations of the radio signals were recorded from essentially dc up to 10 c/s spectral components using a 12 channel analog magnetic tape system. Most of the recordings were continuous over 40 hr periods and one was uninterrupted for about 120 hr.

The terrain of the various paths included a very flat ground surface, irregular terrain, and paths over dense vegetation and water surfaces. Weather conditions included calm, clear weather, a cold front passage, snow and cold weather, high winds, heavy rainfall and fog. The experiments were conducted during all four seasons in Colorado and during late summer and fall in Florida [Thompson, 1959a].

The data were analyzed for frequency spectral distribution and for correlation between phase and refractive index measurements. Correlations as high as 0.92 were obtained using a 30-min sampling period. The refractive index-frequency spectra were extended to 10^{-5} c/s (<1 cycle per year) through the use of U.S. Weather Bureau data. In the region between about 2×10^{-5} c/s (~ 2 cycles per day) and 5 c/s the refractive index and phase variations had slopes of -1.6 and -2.6 , respectively, the former closely approximating the $-5/3$ value which has been found to describe the turbulence of horizontal wind velocities.

The power spectra of phase and refractive index were observed to converge at about 10^{-5} c/s (1 cycle per day). For components between this frequency and 3×10^{-5} c/s (1 cycle per year) the slope appears to be about 1.0.

These results are interpreted to have the following significance:

1. Phase fluctuations are significantly correlated with index variations on a time scale consistent with the path length.

2. For many purposes, the variations of both phase and index can best be described by the slope and intensity of their frequency spectra.

3. The most significant changes in these spectra with time appear to be in the intensity, the slopes remaining relatively unchanged.

4. Sufficient data have been obtained at this time to permit reasonably accurate estimates of the phase stability of line-of-sight tropospheric paths from knowledge of their general terrain characteristics and meteorology.

4. Radio Meteorology

4.1. Climatic Investigations

Radio meteorological investigations on the climatic scale involve the physical structure of the atmosphere and have been reported above under topic 1, Physical Characteristics of the Troposphere.

4.2. Refractometer Investigations

Efforts have continued since the XIIth General Assembly to expand our knowledge of the general refractive structure of the troposphere and lower stratosphere by means of direct observations with airborne microwave refractometers as reported under topic 1, 2. Additional refractometer radiometeorological studies have included microscale refractive index measurements to altitudes of about 50,000 ft [Ament, 1957; Bauer, 1958b; Ringwalt, 1957], measurements of the horizontal and time variations in refractive index profiles over distances of 10 to 200 miles and periods of 8 hr [Ament, 1959b], investigations of medium fine scale (several feet) variations in the refractive structure of horizontally stratified layers [Ament, 1959a], correlations of refractive index fluctuations with temperature-lapse rates and wind shear, development of multiple sampling units for aircraft measurements using spaced resonators along orthogonal axes, development of expendable and light-weight refractometers suitable for balloon-borne profile measurements [Deam, 1958, 1959a]. A new type refractometer operating at 400 mc/s and using the stabilized oscillator-beat-frequency principle has obtained profile data in initial balloon borne tests up to 30,000-ft altitude [Deam, 1959b, c], simultaneous measurements in the trade wind inversion of the Central Atlantic of refractive index, temperature, dew point, wind speed, and wind direction [Purves, 1959], extensive measurements of the refractive structure and other meteorological parameters of cumulus and other type clouds, miniaturization and refinement of airborne equipment [Thompson, 1958b], and the development of extremely stable cavity resonators [Crain, 1957a; Thompson, 1958c, 1959b].

4.3. Refraction

Research in this area has followed two general patterns: (a) Calculation of refraction effects from diverse observed refractive index profiles and prediction of refraction effects from statistical consideration of the results [Fannin, 1957; Bean, 1957a]; or (b) assumption of various mathematical models of refractive index structure, calculation of refraction effects in these models and comparison of these effects with those evaluated from observed refractive index distributions [Anderson, 1958; Millman, 1958a, b; Wong, 1958; Bean, 1959d]. Significant results

are: (a) The tropospheric component of elevation angle error or the total tropospheric bending of radio rays may be predicted to a high degree of certainty from the initial or ground level value of the refractive index for initial elevation angles as small as 3 deg [Fannin, 1957; Bean, 1957a] and reasonably well for elevation angles down to zero with the additional knowledge of the initial refractive index gradient [Bean, 1959d]. (b) The normal decrease of the refractive index with height in the troposphere is better described by an exponential function than by the linear decrease assumed by the effective earth's radius theory and the exponential model atmospheres yield more reliable estimates of refraction effects [Anderson, 1958; Bean, 1959d]. (c) The rate of decrease of refractive index with height in the atmosphere varies with geographic location and season of the year and the tropospheric part of this variation may be specified reasonably well from knowledge of the ground level value of the refractive index alone [Anderson, 1958; Bean, 1959d]. (d) From consideration of the above, the Plenary Assembly of the CCIR (Los Angeles, April, 1959) recommended for international use a basic reference atmosphere based upon an exponential model of the refractive index. Further, these studies have reemphasized the importance of the lowermost layers of the atmosphere since about one-third of the atmospheric bending of a ray leaving the earth tangentially, and passing completely through the troposphere and stratosphere, occurs in the first few hundred meters above the ground.

An important experimental investigation of tropospheric refraction effects utilizing radars [Anderson, 1959] indicates that refraction errors can be an order of magnitude greater than instrumental error for initial angles of 1 deg. Good agreement was obtained between observed and calculated elevation angles with the conclusion that the degree to which radar may be used with accuracy is directly dependent upon the availability of meteorological data.

Simplified methods have been developed [Weisbrod, 1959] which allow one to readily determine from routine radiosonde and ionogram data ray bending and retardation, as well as elevation angle error, Faraday rotation, and Doppler error caused by both the troposphere and by ionospheric layers.

Consideration of departures of atmospheric refractive index structure from the commonly assumed horizontally stratified condition indicates that such departures can significantly affect the refraction of radio rays [Wong, 1958; Bean, 1959e] but that significant departures do not commonly occur more than 20 percent of the time at most locations so that the majority of ray path calculation may be carried out under the normal assumption of horizontal stratification of the refractive index.

4.4. Radar Meteorology

The use of radar in weather analysis and forecasting is now on an operational basis in many

areas and new techniques are constantly being developed for its employment as a research tool. Recent and quite comprehensive bibliographies have been published on radar meteorology [Thuronyi, 1958] and on thunderstorm sferics [Thuronyi, 1959].

The largest outlets for the presentation of research in this field are the Weather Radar Conferences, the Proceedings of which have been published by the American Meteorological Society. Specific references to the Seventh Conference are included here. In a Conference on Hurricanes held at Miami Beach, the very complex radar instrumentation of hurricane reconnaissance aircraft was described [Hillary, 1958; Hurt, 1958]. Detailed studies of specific storms have shown that echoes can be obtained not only from precipitation bands but from sea and swell as well [Trupi, 1958]. A comprehensive analysis of hurricane spiral bands by radar has resulted in new data concerning their origin and growth [Senn, 1958].

In the larger scale employment of radar, efforts have been made to combine visual and radar return from clouds with the existing synoptic pattern [Boucher, 1959; Wilk, 1958] and to demonstrate the successful forecasting technique of combining the returns from several radars to give echo patterns on a synoptic scale [Ligda, 1958b]. By associating precipitation echoes with liquid water content, it has been shown that radar can be used effectively to study the distribution of three dimensional winds in the atmosphere [Kessler, 1958]. Some of the most striking applications of radar data can be found in analyses which have associated the detailed echo structure, growth and movement with the meso- and microscale pressure and wind patterns of hail producing thunderstorms, tornadoes and squall lines [Donaldson, 1958, 1959; Fujita, 1958a, b, 1959; Inman, 1958; Tepper, 1959]. A new Doppler radar has been developed which can be used to study the rotation characteristics of tornadoes [Holmes, 1958].

Recent studies have been made which show the growth and development of precipitation cells within storm areas [Douglas, 1957; Wexler, 1959], which discriminate between condensation-coalescence and ice crystal produced precipitation [MacCready, 1958], and which show the relationship between drop size distributions and the types of precipitation layer echoes observed [Hunsucker, 1958]. Other applications include analyses of the fluctuating nature of radar return to deduce properties of the field of turbulence within the illuminated atmosphere [Stackpole, 1958] and the exploration of such phenomena as sferics, lightning, and auroras [Atlas, 1958; Rumi, 1957].

The controversy relating to the explanation of angel-type echoes continues unabated. The radar ornithologists have given strong documentation to their viewpoints [Harper, 1958; Richardson, 1958], but the fact remains that echoes have been observed from convective phenomena and frontal systems [Atlas, 1959; Ligda, 1958a] whose only reasonable explanation lies in their associated variations of refractive index. Laboratory tests, on the other hand,

have shown that gradients are probably not responsible for echoes at millimeter wavelengths [Tolbert, 1958]. An excellent bibliography has been published [Plank, 1956].

Certain applications are being found for climatological aspects of radar return data, including area precipitation averages [Beckwith, 1958] and model reflectivity-altitude contours [Atlas, 1957]. The use of radar echo patterns to obtain quantitative rainfall-area amounts is well established [Hiser, 1958]. Another technique now in operational use is that of the automatic production of constant altitude PPI (CAPPI) cross sections. These have been found to be extremely useful in short range forecasting and research [Boucher, 1958].

5. References

- Abraham, L. G., Effective bandwidth of tropospheric propagation, paper presented URSI, Wash., D.C., (1959).
- Ackerman, B., Turbulence around tropical cumuli, *J. Meteorol.* **15**, 1, 69 (1958).
- Ackerman, B., The variability of the water contents of tropical cumuli, *J. Meteorol.* **16**, 2, 191 (1959).
- Ament, W. S., F. C. Macdonald, and D. L. Ringwalt, General investigation of electromagnetic wave propagation, Report of NRL Progress (1957).
- Ament, W. S., Toward a solution of the tropospheric scatter problem, *Trans. IRE, PGAP AP-6*, 3, 310 (1958).
- Ament, W. S., Airborne radiometeorological research, *Proc. IRE* **47**, 5, 756 (1959a).
- Ament, W. S., C. G. Purves, and D. L. Randall, Effects of trade-wind meteorology on radar coverage, Report of NRL Progress (1959b).
- Ament, W. S., Modification of a ray-tracer for Monte Carlo prediction of multiple-scattered radio fields, Statistical Methods in Radio Wave Propagation (Proc. Symposium Univ. of Calif., 1958) pp. 184-196 (Pergamon Press, New York, N.Y., 1960).
- Ames, L. A., E. J. Martin, and T. F. Rogers, Some characteristics of persistent VHF radiowave field strengths far beyond the radio horizon, *Proc. IRE* **47**, 5, 764 (1959a).
- Ames, L. A., and T. F. Rogers, 220 Mc radiowave reception at 700-1000 miles, *Proc. IRE* **47**, 1, 86 (1959b).
- Anderson, A. D., Free-air turbulence, *J. Meteorol.* **14**, 6, 477, (1957).
- Anderson, L. J., Tropospheric bending of radio waves, *Trans. AGU* **39**, 208 (1958).
- Anderson, W. L., N. J. Beyers, and B. M. Fannin, Comparison of computed with observed atmospheric refraction, *IRE, Trans. AP-7*, 3, 258 (1959).
- Artman, J. O., and J. P. Gordon, Absorption of microwaves by oxygen in the millimeter wavelength region, *Phys. Rev.* **96**, 1237 (1954).
- Ash, W. O., and J. E. Freund, Randomized estimates in power spectral analysis, Virginia Polytechnic Inst. Report TR-31 (1957).
- Atlas, D., and E. Kessler, III, A model atmosphere for wide-spread precipitation, *Aeronaut. Eng. Rev.* **16**, 2, 69 (1957).
- Atlas, D., Radar as a sferics detector, *Proc. 7th Weather Radar Conf.* (1958).
- Atlas, D., Meteorological angel echoes, *J. Meteorol.* **16**, 1, 6 (1959).
- Avco Corporation, Technical report on angle of arrival of scattered waves, Final Report No. EW6673 (Contract No. AF30(602)-1846) (1958).
- Balser, M., Some observations on scattering by turbulent inhomogeneities, *Trans. IRE, PGAP AP-5*, 383 (1957).
- Balser, M., Multiple scattering in one dimension, *Trans. IRE, PGAP, AP-5*, 383, (1957) also New York Univ. Inst. Math. Sci. Report EM-122 (1959).

- Barad, M. L., Project Prairie Grass, a field program in diffusion, Geophysical Research Papers, No. 59, Air Force Cambridge (in three volumes) (1958).
- Barsis, A. P., and F. M. Capps, Effect of super-refractive layers on tropospheric signal characteristics in the Pacific coast region, WESCON Conv. Record, Pt. 1, 116 (1957).
- Bauer, J. R., The suggested role of stratified elevated layers in transhorizon short-wave radio propagation, Lincoln Lab., MIT Tech. Report 124 (Library of Congress, Washington 25, D.C., 1956).
- Bauer, J. R., W. C. Mason, and F. A. Wilson, Radio refraction in a cool exponential atmosphere, Lincoln Lab., Tech. Rpt. 186 (1958a).
- Bauer, J. R., and J. H. Meyer, Microvariations of water vapor in the lower troposphere with applications to long-range radio communications, Trans. AGU **39**, 4, 624 (1958b).
- Bean, B. R., and B. A. Cahoon, Use of surface observations to predict the total bending of radiowaves at small elevation angles, Proc. IRE **45**, 11, 1545 (1957a).
- Bean, B. R., and R. Abbott, Oxygen and water vapor absorption of radio wave in the atmosphere, Geofis. pura e appl. **37**, 127 (1957b).
- Bean, B. R., and L. P. Riggs, Synoptic variation of the radio refractive index, J. Research NBS **63D**, 1, 91 (1959a).
- Bean, B. R., L. P. Riggs, and J. D. Horn, Synoptic study of the vertical distribution of the radio refractive index, J. Research NBS **63D**, 2, 249 (1959b).
- Bean, B. R., and J. D. Horn, The radio refractive index climate near the ground, J. Research NBS **63D**, 3, 259 (1959c).
- Bean, B. R., and G. D. Thayer, Models of the atmospheric radio refractive index, Proc. IRE **47**, 5, 740 (1959d).
- Bean, B. R., and B. A. Cahoon, The effect of atmospheric horizontal inhomogeneity upon ray tracing, J. Research NBS **63D**, 3, 287 (1959e).
- Bean, B. R., and G. D. Thayer, Central Radio Propagation Laboratory exponential reference atmosphere, NBS J. Research **63D**, 3, 315 (1959f).
- Beard, C. I., and I. Katz, The dependence of microwave radio signal spectra on ocean roughness and wave spectra, Trans. IRE, PGAP, **AP-5**, 183 (1957).
- Beckwith, W. B., Shower and thunderstorm echo patterns in eastern Colorado, Proc. 7th Weather Radar Conf. (1958).
- Bellman, R., and R. Kalaba, Invariant imbedding, wave propagation, and the WKB approximation, Proc. Nat. Acad. Sci. USA, **44**, 317 (1958).
- Benedict, W. S., and L. D. Kaplan, Calculation of line widths in H_2O-N_2 collisions, J. Chem. Phys. **30**, 388 (1959).
- Beran, Mark J., On the propagation of random radiation in free space, Statistical Methods in Radio Wave Propagation, Proc. Symposium Univ. of Calif. (1958) (Pergamon Press, New York, N.Y., pp. 93-98, 1960).
- Blackman, R. B., and J. W. Tukey, Measurement of power spectra from the point of view of communications engineering, Bell System Tech. J. **37**, part 1, pp. 185-281 (1958) and part 2, pp. 485-569 (1958). (Reprinted as book by Dover Publications, New York, N.Y., 1958).
- Blanch, G., and H. Ferguson, Remarks on Chandrasekhar's results relating to Heisenberg's theory of turbulence, Phys. of Fluids **2**, 1, 79 (1959).
- Bolgiano, R., Discussion of the Wheelon paper, Radio frequency and scattering angle dependence of ionospheric scatter propagation at VHF, J. Geophys. Research **62**, 639 (1957).
- Bolgiano, R., The role of turbulent mixing in scatter propagation, IRE Trans. PGAP **6**, 2, 159 (1958a).
- Bolgiano, R., On the role of convective transfer in turbulent mixing, J. Geophys. Research **63**, 851 (1958b).
- Bolgiano, R., N. H. Bryant, and W. E. Gordon, Diversity reception in scatter communications with emphasis on angle diversity, Contract AF-30(602)-1717, Final Report Pt. 1 (Cornell Univ., Ithaca, N.Y., 1958c).
- Bolgiano, R., Wavelength dependence in transhorizon propagation, Proc. IRE **47**, 331 (1959).
- Bolgiano, R., A theory of wavelength dependence in ultrahigh frequency transhorizon propagation based on meteorological considerations, J. Research NBS **64D**, 3, 231 (1960).
- Booker, H. G., and W. E. Gordon, A theory of radio scattering in the troposphere, Proc. IRE **38**, 401 (1950).
- Booker, H. G., and J. T. deBettencourt, Theory of radio transmission by tropospheric scattering using very narrow beams, Proc. IRE **43**, 281 (1955).
- Booker, H. G., and W. E. Gordon, Role of stratospheric scattering in radio communications, Proc. IRE **45**, 1223 (1957).
- Booker, H. G., Concerning ionospheric turbulence at the meteoric level, J. Geophys. Research **63**, 1, 97 (1958).
- Boucher, R. J., Some applications of the CAPPI technique in short range forecasting and research, Proc. 7th Weather Conf. (1958).
- Boucher, R. J., Synoptic-physical implications of 1.25-cm vertical beam radar echoes, J. Meteorol. **16**, 3, 312 (1959).
- Bowhill, S. A., The distribution of the fade lengths of a randomly fading radio signal, Statistical Methods in Radio Wave Propagation (Proc. Symposium at Univ. of Calif., 1958, Pergamon Press, New York, N.Y., 220, 1960).
- Bremmer, H., On the fading properties of a fluctuating signal imposed on a constant signal, NBS Circ. **599** (1959).
- Brennan, D. G., Linear diversity combining techniques, Proc. IRE **47**, 1075 (1959).
- Brennan, D. G., The extrapolation of spatial correlation functions, Statistical Methods in Radio Wave Propagation, (Proc. Symposium Univ. of Calif., 1958, 296, Pergamon Press, New York, N.Y., 1960).
- Bugnolo, D. S., Multiple scattering of electromagnetic radiation and the transport equation of diffusion, Trans. IRE, PGAP, **AP-6**, 3, 310 (1958).
- Bugnolo, D. S., Correlation function and power spectra of radio links affected by random dielectric noise, Trans. IRE **AP-7**, 2, 137 (1959a).
- Bugnolo, D. S., Mean-squared error of a band limited long line-of-sight radio link affected by atmospheric turbulence, Trans. IRE **AP-7**, 1, 105 (1959b).
- CCIR IXth Plenary Assembly, Measurement of field strength for VHF (metric) and UHF (decimetric) broadcast services, including television, Report 142 **3**, 280 (Los Angeles, Calif., 1959).
- Carroll, T. J., and R. M. Ring, Propagation of short waves in a normally stratified troposphere, Proc. IRE **43**, 1384 (1955).
- Chisholm, J. H., Experimental measurements of angular scattering and communications capacity of tropospheric propagation well beyond the horizon, L'Onde Electrique **37**, 427 (1957a).
- Chisholm, J. H., W. E. Morrow, Jr., J. F. Roche, and A. E. Teachman, Summary of tropospheric path loss measurements at 400 Mc over distances of 25 to 83 miles (WESCON Conv., San Francisco, Calif., 1957b).
- Chisholm, J. H., L. P. Rainville, J. F. Roche, and H. G. Root, Measurement of the bandwidth of radio waves propagated by the troposphere beyond the horizon, IRE Trans. PGAP, **AP-6**, 4, 377 (1958).
- Chisholm, J. H., L. P. Rainville, J. F. Roche, and H. G. Root, Angular diversity reception at 2,290 meps over a 188 mile path, (presented at Symposium on Extended Range and Space Communications, George Washington Univ., Washington, D.C.) IRE Trans. **CS-7**, 3, 195 (1959).
- Clem, L. H., Clear air turbulence over the U.S., Aero. Eng. Rev. **16**, 11, 63 (1957).
- Corrsin, S., Statistical behavior of a reacting mixture in isotropic turbulence, Phys. of Fluids **1**, 1, 42 (1958).
- Crain, C. M., and C. E. Williams, Method of obtaining pressure and temperature insensitive microwave cavity resonators, Rev. Sci. Instr. **28**, 8 (1957a).
- Crain, C. M., Refractometers and their applications to radio propagation and to other problems, L'Onde Electrique **37** (362), 441 (1957b) (in French).
- Crawford, A. B., and D. C. Hogg, Measurement of atmospheric attenuation at millimeter wavelengths, Bell System Tech. J. **35**, 4, 907 (1956).
- Crawford, A. B., D. C. Hogg, and W. H. Kummer, Studies in tropospheric propagation beyond the horizon, Bell System Tech. J. **38**, 1067 (1959).
- Cunningham, R. M., Cumulus circulation, recent advances in atmospheric electricity, 361 (Pergamon Press, New York, N.Y., 1958).

- Davenport, W. B., Jr., and W. L. Root, An introduction to the theory of random signals and noise (McGraw-Hill Book Co., New York, N.Y., 1958).
- Deam, A. P., Status report on the development of an expendable atmospheric radio refractometer, EERL Report 5-32, Univ. of Texas (1958).
- Deam, A. P., and R. C. Staley, The use of balloon borne refractometer observations in studying problems relating to telemetry propagation from space vehicles, EERL Report 5-36 (Univ. of Texas, Austin, Tex., 1959a).
- Deam, A. P., Applications and uses of the 400 MCS refractometer, EERL Report 5-37 (Univ. of Texas, Austin, Tex., 1959b).
- Deam, A. P., An expendable atmospheric radio refractometer, EERL Report 108 (Univ. of Texas, Austin, Tex., 1959c).
- Dean, W., Part II, propagation characteristics, IRE National Convention Record (1957).
- Dinger, H. E., W. E. Garner, D. H. Hamilton, Jr., and A. E. Teachman, Investigation of long distance overwater tropospheric propagation at 400 Mc, Proc. IRE **46**, 7, 1401 (1958).
- Doherty, L. H., and G. Neal, A215 mile 2720 Mc radio link, Trans. IRE **AP-7**, 2, 117 (1959).
- Donaldson, R. J., Jr., Analysis of severe convective storms observed by radar, J. Meteorol. **15**, 1, 44 (1958).
- Donaldson, R. J., Jr., Analysis of severe convective storms observed by radar, II, J. Meteorol. **16**, 3, 281 (1959).
- Douglas, R. H., K. L. S. Gunn, and J. S. Marshall, Pattern in the vertical of snow generation, J. Meteorol. **14**, 2, 95 (1957).
- Dryden, W. A., Effects of the scale of spatial averaging on the kinetic energies of smallscale turbulent motion, J. Meteorol. **14**, 4, 287 (1957).
- Edison, A. R., F. J. Janza, R. K. Moore, and B. D. Warner, Radar cross sections of terrain near vertical incidence at 415 Mc, U. of New Mexico, Report EE-15 (1959), Report EE-24 (1959).
- Edmonds, F. N., Jr., Analysis of airborne measurements of tropospheric index of refraction fluctuations, Statistical Methods in Radio Wave Propagation (Proc. Symposium Univ. of Calif. 1958, Pergamon Press, New York, N.Y., 197, 1960).
- Egli, J. J., Radio propagation above 40 Mc over irregular terrain, Proc. IRE **45**, 10, 1383 (1957).
- Endlich, R. M., and G. S. McLean, The structure of the jet stream core, J. Meteorol. **14**, 6, 543 (1957).
- Fannin, B. M., and K. H. Jehn, A study of radar elevation angle error due to atmospheric refraction, IRE Trans. **AP-5**, 1, 71 (1957).
- Finney, R. C., Short time statistics of tropospheric radio wave propagation, Proc. IRE **47**, 1, 84 (1959).
- Fleisher, A., Some spectra of turbulence in the free atmosphere, J. Meteorol. **16**, 2, 209 (1959).
- Frank, R. L., Part III, instrumentation, IRE National Convention Record (1957).
- Frantz, W. P., A precision multi-purpose radio navigation system, Part I, characteristics and applications, IRE National Convention Record (1957).
- Frenkel, F. N., and P. A. Sheppard, Atmospheric diffusion and air pollution (Academic Press, Inc., 111 5th Ave., New York 3, N.Y., 1959).
- Friis, H. T., A. B. Crawford, and D. C. Hogg, A reflection theory for propagation beyond the horizon, Bell System Tech. J. **36**, 1627 (1957).
- Fujita, T., Tornado cyclone: bearing system of tornadoes, Proc. 7th Weather Radar Conf. (1958a).
- Fujita, T., and H. Brown, A study of meso systems and their radar echoes, Bull. Am. Meteorol. Soc. **39**, 10, 538 (1958b).
- Fujita, T., Study of meso systems associated with stationary radar echoes, J. Meteorol. **16**, 1, 38 (1959).
- Ghose, R. N., Phase instability in a microwave ground link, Trans. IRE **AP-7**, 1, 106 (1959).
- Gifford, F., Jr., Relative atmospheric diffusion of smoke puffs, J. Meteorol. **14**, 5, 410 (1957).
- Gora, E. K., The present state of the theory of microwave line shapes, Providence College, Providence, R.I., Tech. Report No. 3, Prepared for Contract No. AF-19(604)-831 (1956).
- Gutnieh, M., Climatology of the trade-wind inversion in the Caribbean, Bulletin Am. Meteorol. Soc. **39**, 8, 410 (1958).
- Harper, W. G., An unusual indicator of convection, Proc. 7th Weather Radar Conference (1958).
- Hartman, W. J., and R. E. Wilkerson, Path antenna gain in an exponential atmosphere, J. Research NBS **63D**, 3, 273 (1959).
- Hartman, W. J., The limit of resolution of a refractometer, J. Research NBS **64D**, 1 (1960).
- Hausman, A. H., Dependence of the maximum range of tropospheric scatter communications on antenna and receiver noise temperatures, Trans. IRE **CS-6**, 2, 35 (1958).
- Henry, R. M., A study of the effects of wind speed, lapse rate, and altitude on the spectrum of atmospheric turbulence at low altitude, Institute of Aeronautical Sciences 27th Meeting, N.Y., Rep. 59-43 (1959).
- Herbstreit, J. W., and M. C. Thompson, Measurements of the phase of radio waves received over transmission paths with electrical lengths varying as a result of atmospheric turbulence, Proc. IRE **43**, 10 (1955).
- Hicks, B. L., H. Knable, J. J. Kovaly, G. D. Newell, and J. P. Ruina, Sea clutter spectrum studies using airborne coherent radar III, Report R-105 (Control Systems Lab., Univ. of Ill., Chicago, Ill., 1958).
- Hillary, D. T., The national hurricane research project aircraft instrumentation, Proc. Tech. Conf. on Hurricanes (1958).
- Hilst, G. R., and C. L. Simpson, Observations of vertical diffusion rates in stable atmospheres, J. Meteorol. **15**, 1, 125 (1958).
- Hines, C. A., and C. M. Crain, Overwater refraction index measurements from the sea surface to 15,000 ft., Trans. IRE **AP-5**, 161 (1957).
- Hiser, H. W., H. V. Senn, and L. F. Conover, Rainfall measurement by radar using photographic interpretation techniques, Trans. Am. Geophys. Union **39**, 6, 1043 (1958).
- Hoffman, W. C., Statistical methods in radio wave propagation, Trans. IRE **AP-7**, 1, 105 (1959).
- Hoffman, W. C., Some statistical methods of potential value in radio wave propagation, Statistical Methods in Radio Wave Propagation (Proc. Symposium Univ. of Calif., 1958, 117, Pergamon Press, New York, N.Y., 1960).
- Hogg, D. C., and L. R. Lowry, Effect of antenna beamwidth and upper air wind velocity on fading of 4 Kmc waves propagated beyond the horizon, Trans. IRE **AP-7**, 1, 107 (1959).
- Hogg, D. C., and L. R. Lowry, Comparison of short term fading at 4110 and 460 Mc in propagation beyond the horizon, Trans. IRE **AP-7**, 1, 107 (1959).
- Holmes, D. W., and R. L. Smith, Doppler radar for weather investigation, Proc. 7th Weather Radar Conf. (1958).
- Hopkins, R. V. F., Dual frequency multirange overwater measurements of beyond-the-horizon microwave scattered field strength, Trans. IRE **AP-7**, 1, 108 (1959).
- Hunsucker, R. D., and F. W. Decker, Observations of the relationship between raindrop-size distribution and the existence of radar bright layers, Proc. 7th Weather Radar Conf. (1958).
- Hurt, D. A., Jr., Weather reconnaissance capabilities of the WV type aircraft, Proc. Tech. Conf. on Hurricanes (1958).
- Janes, H. B., J. C. Stroud, and M. T. Decker, An analysis of propagation measurements made at 418 Mc well beyond the horizon, NBS Tech. Note 6, 1959, \$2.25 (order from the Offices of Technical Service, U.S. Dept. of Commerce, Washington 25, D.C.).
- Inman, R. L., and S. G. Bigler, A preliminary classification of radar precipitation echo patterns associated with midwestern tornadoes, Proc. 7th Weather Radar Conf. (1958).
- Johler, J. R., W. J. Kellar, and L. C. Walters, Phase of the low radio-frequency ground wave, NBS Circ. 573 (1956).
- Johler, J. R., Propagation of the radio frequency ground wave transient over a finitely conducting plane earth, Geofis. pura e appl. **37**, 116 (1957).
- Johler, J. R., Transient radio frequency ground waves over the surface of a finitely conducting plane earth, J. Research NBS **60**, 281 (1958) RP 2844.

- Johler, J. R., L. C. Walters, and C. M. Lilley, Low and very low-radio-frequency tables of ground wave parameters for the spherical earth theory: the roots of Riccati's differential equation (Supplementary numerical data for NBS Circ. 573), NBS Tech. Note 7 (1959a).
- Johler, J. R., and L. C. Walters, Propagation of a ground wave pulse around a finitely conducting spherical earth from a damped sinusoidal source current, IRE Trans. **AP-7**, 1, 1 (1959b).
- Johler, J. R., and L. C. Walters, The mean absolute value and standard deviation of the phase of a constant vector plus a Rayleigh-distributed vector J. Research NBS **62**, 183 (1959c) RP 2950.
- Josephson, B., and G. Carlson, Distance dependence, fading characteristics and pulse distortion of 3,000 MC trans-horizon signals, Trans. IRE **AP-6**, 2, 173 (1958).
- Katzin, M., On the mechanisms of radar sea clutter, Proc. IRE **45**, 1, 44 (1957).
- Kay, I., and R. A. Silverman, Multiple scattering by a random stack of dielectric slabs, N. 2 del Supplemento al **9**, Serie X, Nuovo Cimento 626 (1958).
- Keilson, J., and R. V. Row, Transfer of transient electromagnetic waves into a lossy medium, J. Appl. Phys. (1960) (in press).
- Kelly, E. J., and I. S. Reed, Some properties of stationary Gaussian processes, MIT Lincoln Labs. Tech. Report 157, (1957).
- Kessler, E., III, Use of radar in kinematical studies of precipitating weather systems, Proc. 7th Weather Radar Conference (1958).
- Koo, B. Y.-C., and M. Katzin, An exact earth-flattening procedure in propagation around a sphere, J. Research NBS **64D**, 3 (1960).
- Kraichman, M. B., Basic study of electromagnetic sources immersed in conducting media, J. Research NBS **64D**, 1, 21 (1960).
- Kraichman, R. H., Relationship of fourth-order to second-order moments in stationary isotropic turbulence, Phys. Rev. **107**, 6, 1485 (1957).
- Kraichman, R. H., Irreversible statistical mechanics of incompressible hydromagnetic turbulence, Phys. Rev. **109**, 5, 1407 (1958a).
- Kraichman, R. H., Higher order interaction in homogeneous turbulence theory, Phys. of Fluids **1**, 4, 358 (1958b).
- Kraichman, R. H., Comments on space-time correlations in stationary isotropic turbulence, Phys. of Fluids **2**, 3, 334 (1959).
- Kummer, W. H., Sweep frequency studies in beyond-the-horizon propagation, Trans. IRE **AP-7**, 1, 108 (1959).
- LaGrone, A. H., Report of TASO Committee 5.4 on forecasting television service fields, 1959 IRE National Conv. Record, pt. 7 (1959).
- Landauer, W. E., Experimental swept frequency tropospheric scatter link, paper presented URSI, Washington, D.C. (1959).
- Lappe, U. O., B. Davidson, and C. B. Notess, Analysis of atmospheric turbulence spectra obtained from concurrent airplane and tower measurements, Institute of Aeronautical Sciences 27th Annual Meeting, Rep. 59-44 (1959).
- Levin, E., R. B. Muchmore, and A. D. Wheelon, Aperture-to-medium coupling on line-of-sight paths: Fresnel scattering, Trans. IRE, PGAP, **AP-7**, 142 (1959).
- Levy, B. R., and J. B. Keller, Propagation of electromagnetic pulses around the earth, IRE Trans. **AP-6**, 56 (1958).
- Ligda, M. G. H., and S. G. Bigler, Radar echoes from a cloudless cold front, J. Meteorol. **15**, 6, 494 (1958a).
- Ligda, M. G. H., The use of radar network observations in synoptic-scale weather analysis and intermediate-range forecasting, Proc. 7th Weather Radar Conference (1958b).
- Long, W. C., and R. R. Weeks, Quadruple diversity tropospheric scatter systems, Trans. IRE **CS-5**, 3, 8 (1957).
- Longley, R. W., Eddy sizes as determined by the temperature fluctuations at O'Neill, Nebraska, August and September, 1953, J. Meteorol. **16**, 2, 140 (1959).
- MacCready, P. B., T. B. Smith, and C. J. Todd, Discrimination between condensation-coalescence and ice crystal produced precipitation, Proc. 7th Weather Radar Conf. (1958).
- Macdonald, F. C. (Naval Research Laboratories), Measurement of echoes at several frequencies and polarizations, paper presented at Symposium on Terrain Return (Univ. of New Mexico, Albuquerque, N. Mex., 1959).
- Maryott, A. A., and G. Birnbaum, Microwave absorption in compressed oxygen, Phys. Rev. **99**, 1886 (1955).
- Maryott, A. A., P. W. Wacker, and G. Birnbaum, Microwave absorption in compressed gases, pressure induced absorption in CO₂ and other nondipolar gases, NBS Report 5338 (1957).
- McFadden, J. A., The axis crossing interval of random functions, Trans. IRE **IT-2**, 146, 1956; **IT-4**, 14 (1958).
- McGavin, R. E., and L. J. Maloney, A study at 1046 Mc of the reflection coefficient of irregular terrain at small grazing angles, J. Research NBS **63D**, 2, 235 (1959).
- McGinn, J. W., Jr., and E. W. Pike, A study of sea clutter spectra, Statistical Methods in Radio Wave Propagation (Proc. Symposium Univ. of Calif., 1958, 49, Pergamon Press, New York, N.Y., 1960).
- Meecham, W. C., Relation between time symmetry and reflection symmetry of turbulent fluids, Phys. of Fluids **1**, 5, 408 (1958).
- Miller, R. E., G. K. Dufey, and W. H. Huntley, Jr., A rapid-scanning phased array for propagation measurements, Contract DA36(039)SC-73151, Stanford Electronics Lab. TR 461-5 (1958).
- Millman, G. H., Atmospheric effects on VHF and UHF propagation, Proc. IRE **46**, 1492 (1958a).
- Millman, G. H., Tropospheric effects on radar target measurements, Proc. 7th Weather Radar Conference, E34-E43, (1958b).
- Misme, Pierre, The correlation between the electric field at a great distance and a new radio-meteorological parameter, IRE Trans. **AP-6**, 289 (1958).
- Moler, W. F., Macro and meso-scale meteorological effects upon microwave trans-horizon fields, Proc. 7th Weather Radar Conf. E26 (1958a).
- Moler, W. F., and W. A. Arvola, Vertical motion in the atmosphere and its effect on VHF radio signal strength, Trans. Am. Geophys. Union **37**, 4, 399 (1958b).
- Moore, R. K., Resolution of vertical incidence radar return into random and specular components, Univ. N. Mex., Eng. Exper. Sta. Rpt. EE-6 (1957).
- Morrow, W. E., Jr., Study of systems of troposphere UHF radio communication at long distance, L'Onde Electrique **37** (362), 444 (1957) (in French).
- Moyer, V. E., and J. R. Gerhardt, A preliminary climatology of airborne microwave refractometer layer characteristics, Proc. 7th Weather Radar Conf., E10E8 (1958).
- Munch, G., and A. D. Wheelon, Space-time correlations in stationary isotropic turbulence, Phys. of Fluids **1**, 6, 462 (1958).
- Neugebauer, H. E. J., and M. P. Bachynski, Diffraction by smooth cylindrical mountains, Proc. IRE **46**, 9, 1619 (1958).
- Norton, K. A., Transmission loss in radio propagation II, NBS Tech. Note 12 (1958).
- Norton, K. A., Recent experimental evidence favoring the $\rho K_1(\rho)$ correlation function for describing the turbulence of refractivity in troposphere and stratosphere, J. Atmospheric and Terrest. Phys. **15**, (3, 4), 206 (1959a).
- Norton, K. A., System loss in radiowave propagation, J. Research, NBS **63D**, 1, 53 (1959b).
- Norton, K. A., Technical considerations leading to an optimum allocation of radio frequencies in the band 25 to 60 MC, NBS Tech. Note 13 (1959). May be purchased for the price of \$2.50 (order from the Office of Technical Services, U.S. Dept. of Commerce, Washington, D.C.).
- Norton, K. A., Carrier frequency dependence of the basic transmission loss in tropospheric forward scatter propagation, J. Geophys. Research **65**, 7, 2029 (1960).
- Nupen, Wilhelm, Annotated bibliography on tropospheric propagation, Meteorol. Abstracts and Bibliography **8**, 9, 1243 (1957); **8**, 10, 1374 (1957).
- Ogura, Y., The influence of finite observation intervals on the measurement of turbulent diffusion parameters, J. Meteorol. **14**, 2, 176 (1957).
- Ogura, Y., Temperature fluctuations in an isotropic turbulent flow, J. Meteorol. **15**, 6, 539 (1958).

- Ortwein, N. R., Spectral analysis of dual frequency multirange beyond-the-horizon microwave scattered fields, *Trans. IRE AP-7*, 1, 107 (1959).
- Panofsky, H. A., and A. K. Blakadar, On the theory of the formation of turbulence by horizontal wind shear, *Trans. Am. Geophys. Union* **38**, 3, 402 (1957).
- Panofsky, H. A., H. E. Cramer, and V. R. K. Rao, The relation between Eulerian time and space spectra, *Quart. J. Roy. Meteorol. Soc.*, London **84**, 361, 270 (1958).
- Parry, C. A., A formalized procedure for the prediction and analysis of multichannel tropospheric scatter circuits, *Trans. IRE CS-7*, 3, 211 (1959).
- Paul, D. L., Scattering of electromagnetic waves in beyond the horizon transmission, *Trans. IRE AP-6*, 1, 61 (1958).
- Plank, V. G., A meteorological study of radar angles, *Geophys. Research Papers No. 52*, Geophys. Research Directorate, AFRC (1956).
- Plank, V. G., Convection and refractive index inhomogeneities, *J. Atmospheric and Terrest. Phys.* **15**, 3, 4, 228 (1959).
- Potter, C. A., Tropospheric scattering of microwave, Navy Electronics Lab. Symp. of ONR 19-20, Washington, D.C. (1957).
- Press, H., Atmospheric turbulence environment with special reference to continuous turbulence, North Atlantic Treaty Organization, Advisory Group for Aeronautical Res. and Development, Rpt. 115 (1957).
- Purves, C. G., D. L. Randall, and D. L. Ringwalt, Meteorological measurements in the south Atlantic, Rpt. of NRL Progress (1959).
- Reid, W. H., On the approach to the final period of decay in isotropic turbulence according to Heisenbergs transfer theory, *Proc. Nat. Acad. Sci.* **42**, 8, 559 (1957).
- Reid, W. H., and D. L. Harris, Similarity spectra in isotropic turbulence, *Phys. of Fluids*, **2**, 2, 139 (1959).
- Rice, P. L., A. G. Longley, and K. A. Norton, Prediction of the cumulative distribution with time of ground wave and tropospheric wave transmission loss, Part-I, The prediction formula, NBS Tech. Note 15 (1959). May be purchased for the price of \$1.50 (order from the Office of Technical Services, U.S. Depart. of Commerce, Wash. 25, D.C.).
- Rice, S. O., Distribution of the duration of fades in radio transmission-Gaussian noise model, *Bell System Tech. J.* **37**, 3, 581 (1958), also Bell Monograph, 3051.
- Richardson, R. E., J. M. Stacey, H. M. Kohler, and F. R. Naka, Radar observation of birds, *Proc. 7th Weather Radar Conf.* (1958).
- Ringwalt, D. L., W. S. Ament, and F. C. Macdonald, Scatter propagation in thunderstorm conditions, Report of NRL Progress (1957).
- Ringwalt, D. L., W. S. Ament, and F. C. Macdonald, Measurements of 1250 MC scatter propagation as a function of meteorology, *Trans. IRE AP-6*, 2, 208 (1958).
- Rosenblatt, M., The multidimensional prediction problem, *Statistical Methods in Radio Wave Propagation* (Proc. Symposium Univ. of Calif., 1958, 99, Pergamon Press, New York, N.Y., 1960).
- Rumi, G., VHF radar echoes associated with atmospheric phenomena, *J. Geophys. Research* **62**, 4, 547 (1957).
- Saunders, K. D., A power-spectrum equation for stationary random gusts, including a sample problem, *J. Aeronaut. Sci.* **25**, 5, 295 (1958).
- Senn, H. V., and H. W. Hiser, The origin and behavior of hurricane spiral bands as observed on radar, *Proc. 7th Weather Radar Conf.* (1958).
- Shkarofsky, L. P., H. E. J. Neugebauer, and M. P. Bachynski, Effects of mountains with smooth crests on wave propagation, *IRE Trans. AP-6*, 4, 341 (1958).
- Siddiqui, M. M., The components of power appearing in the harmonic analysis of a stationary process, *Statistical Methods in Radio Wave Propagation* (Proc. Symposium Univ. of Calif., 1958, 112, Pergamon Press, New York, N.Y., 1960).
- Silverman, R. A., Locally stationary random processes, *IRE, Trans. PGIT*, **3**, 3, 182 (1957a).
- Silverman, R. A., Scattering of plane waves by locally homogeneous dielectric noise, *Trans. IRE, PGAP*, **AP-6**, 3, 310 (1958). Also New York Univ. Inst. Math. Sci. Div. of Electromagnetic Research Rpt. MME-9 (1957). Also Cambridge, Phy. Soc. **54**, 530 (1957b).
- Silverman, R. A., Fading of radio waves scattered by dielectric turbulence, *J. Appl. Phys.* **28**, 4, 506 (1957). Also N.Y., Univ. Inst. of Math. Sci., Electromagnetic Research Div., Research Rpt. EM101 (1957c).
- Silverman, R. A., Remarks on the fading of scattered radio waves, *Trans. IRE AP-6*, 4, 378 (1958).
- Spetner, L. M., and I. Katz, Two statistical models for radar terrain return, *Trans. IRE, PGAP*, **AP-8** (1960).
- Squire, W., A unified theory of turbulent flow. I-Formation of the theory, *Appl. Sci. Research [A]* **2**, 3, 158 (1959).
- Stackpole, J. D., Some spectra of turbulence in the free atmosphere, *Proc. 7th Weather Radar Conference* (1958).
- Stanley, G. M., Layered-earth propagation in the vicinity of point barrow, *J. Research NBS* **64D** (1960).
- Staras, H., Forward scattering of radiowaves by anisotropic turbulence, *Proc. IRE* **43**, 1374 (1955).
- Staras, H., Antenna-to-medium coupling loss, *IRE Trans. AP-5*, 228 (1957).
- Staras, H., Tropospheric scatter propagation—a summary of recent progress, *RCA Rev.* **19**, 1, 3 (1958).
- Staras, H., and A. D. Wheelon, Theoretical research on tropospheric scatter propagation in the United States, 1954-1957, *IRE Trans. AP-7*, 1, 80 (1959a).
- Staras, H., The filling-in of an antenna null by off-path scattering on a tropospheric scatter circuit, *IRE Trans. AP-7*, 277 (1959b).
- Staras, H., Some observations on angle diversity, to be published in *Proc. IRE* (1960).
- Stein, S., Some observations on scattering by turbulent inhomogeneities, *Trans. IRE, AP-6*, 3, 299 (1958).
- Stein, S., Clarification of diversity statistics in scatter propagation, *Statistical Methods in Radio Wave Propagation* (Proc. Symposium Univ. of Calif., 1958; 274, Pergamon Press, New York, N.Y., 1960).
- Stiles, K. P., Tropospheric scatter path loss tests, Florida-Bahamas, *Trans. IRE CS-7*, 3, 205 (1959).
- TASO, Engineering aspects of television allocations, Report of the Television Allocations Study Organization to the Federal Communications Commission (1959).
- Taylor, R. C., Terrain return measurements at X, Ku, Ka band, *IRE Convention Record*, Pt. I, 19 (1959).
- Tepper, M., Meso Meteorology—The link between macro-scale atmospheric motions and local weather, *Bull. Am. Meteorol. Soc.* **40**, 2, 56 (1959).
- Thompson, M. C., and M. J. Vetter, Single-path phase measuring system for three-centimeter radio waves, *Rev. Sci. Instr.* **29**, 2, 148 (1958a).
- Thompson, M. C., and M. J. Vetter, Compact microwave refractometer for use in small aircraft, *Rev. Sci. Instr.* **29**, 12, 1098 (1958b).
- Thompson, M. C., F. E. Freethy, and D. M. Waters, Fabrication techniques for ceramic X-band cavity resonators, *Rev. Sci. Instr.* **29**, 10, 865, (1958c).
- Thompson, M. C., and H. B. Janes, Measurements of phase stability over a low-level tropospheric path, *J. Research NBS* **63D**, 45 (1959a).
- Thompson, M. C., F. E. Freethy, and D. M. Waters, End plate modification of X-band TE₀₁₁ cavity resonators, *IRE Trans. MTT*, **MTT-7**, 3, 388 (1959b).
- Thompson, M. C., H. B. Janes, and A. W. Kirkpatrick, An analysis of time variations in tropospheric refractive index and apparent radio path length, *J. Geophys. Research* **65**, 193 (1960a).
- Thompson, M. C., H. B. Janes, and F. E. Freethy, Atmospheric limitations on electronic distance measuring equipment, *J. Geophys. Research* **65**, 389 (1960b).
- Thuronyi, G., Recent literature on radar meteorology, *Meteorol. Abstracts and Bibliography* **9**, 8, 1005 (1958).
- Thuronyi, G., Annotated bibliography on thunderstorm sferics, *Meteorol. Abstracts and Bibliography* **10**, 4, 588 (1959).
- Tolbert, C. W., A. W. Straiton, and C. O. Britt, Phantom radar targets at millimeter wavelengths, *IRE Trans. AP-6*, 4, 380 (1958).
- Tolbert, C. W., and A. W. Straiton, Attenuation and fluctuation of millimeter radio waves, *IRE National Convention Record*, Pt. I, 12, (1957). Radio propagation measurements in the 100 to 118 k Mcs spectrum, *IRE WESCON Convention Record* (1959a).

- Tolbert, C. W., C. O. Britt, and A. W. Straiton, Propagation characteristics of 2.15 mm radio waves, *Trans. IRE* **AP-7**, 1, 105 (1959b).
- Trolese, L. G., and L. J. Anderson, Foreground terrain effects on overland UHF transmission, *IRE Trans.* **AP-6**, 4, 330 (1958).
- Trupi, L. E., An airborne radar reconnaissance of typhoon agnes, *Proc. 7th Weather Radar Conf.* (1958).
- U.S. Navy Marine Climatic Atlas of the World, Vol. **I**, North Atlantic Ocean, NAVAER 50-1C-528 (1955).
- U.S. Navy Marine Climatic Atlas of the World, Vol. **II**, North Pacific Ocean, NAVAER 50-1C-529 (1956).
- U.S. Navy Marine Climatic Atlas of the world, Vol. **III**, Indian Ocean, NAVAER 50-1C-530 (1957).
- U.S. Navy Marine Climatic Atlas of the world, Vol. **IV**, South Atlantic Ocean, NAVAER 50-1C-531 (1958).
- Van der Hoven, I., Power spectrum of horizontal wind speed in the frequency range from 0.0007 to 900 cycles per hour, *J. Meteorol.* **14**, 2, 160 (1957).
- Vogelman, J. H., J. L. Ryerson, and M. H. Bickelhaupt, Tropospheric scatter system using angle diversity, *Proc. IRE* **47**, 688 (1959).
- Von Mises, R., Mathematical theory of compressible fluid flow (Academic Press, Inc., 111 5th Ave., New York, N.Y., 1958).
- Wagner, N. K., The occurrence of microwave index of refraction fluctuations in a converging air stream, *Bull. Am. Meteorol. Soc.* **38**, 8, 494 (1957).
- Wait, J. R., and H. H. Howe, Amplitude and phase curves for ground wave propagation in the band 200 cycles per second to 500 kilocycles, *NBS Circ.* **574** (1956a).
- Wait, J. R., Transient fields of a vertical dipole over homogeneous curved ground, *Can. J. Research* **34**, 27 (1956b).
- Wait, J. R., and James Householder, Mixed-path ground-wave propagation: 2. Larger distances, *NBS, J. Research* **59**, 1, 19 (1957a). (A similar solution has been given recently by Y. K. Kalinin and E. L. Feinberg, *Radiotech. i Electron.* **3** 1958.)
- Wait, J. R., The transient behavior of the electromagnetic ground wave over a spherical earth, *IRE Trans.* **AP-5**, 198 (1957b).
- Wait, J. R., A note on the propagation of the transient ground wave, *Can. J. Phys.* **35**, 1146 (1957c).
- Wait, J. R., Propagation of a pulse across a coast line, *Proc. IRE* **45**, 11 (1957d).
- Wait, J. R., On the theory of propagation of electromagnetic waves along a curved surface, *Can. J. Phys.* **36**, 9 (1958a).
- Wait, J. R., On radio wave propagation in an inhomogeneous atmosphere, *NBS Tech. Note* **24** (1958b). (Also see G. Millington's article in *Marconi Rev.* **21**, 143 (1958), for similar treatment and a comprehensive paper by H. Bremmer which is in preparation for *J. Research NBS*, Sec. D. The general conclusions reached in these three published works are the same.)
- Wait, J. R., Transmission and reflection of electromagnetic waves in the presence of stratified media, *J. Research NBS* **61**, 3, 205 (1958c) RP 2899.
- Wait, J. R., and A. M. Conda, On the diffraction of electromagnetic pulses by curved conducting surfaces, *Can. J. Phys.* **37**, 1384 (1959a).
- Wait, J. R., Transmission of power in radio propagation, *Electronic and Radio Engineer* **36**, 4, 146 (1959b).
- Wait, J. R., Radiation from a small loop immersed in a semi-infinite conducting medium, *Can. J. Phys.* **37**, 672 (1959c).
- Wait, J. R., The calculation of the field in a homogeneous conductor with a wavy interface, *Proc. IRE*, **47**, 6, 1155 (1959d).
- Wait, J. R., and A. M. Conda, Diffraction of electromagnetic waves by smooth obstacles for grazing angles, *NBS Memo Report DM-79-2*, J. Research NBS **63D**, 2, 181 (1959e).
- Wait, J. R., Guiding of electromagnetic waves by uniformly rough surfaces, Parts I and II, *Trans. IRE, PGAP*, **AP-7**, (Special Supplement), S154 (1959f).
- Waterman, A. T., Jr., Some generalized scattering relationships in transhorizon propagation, *Proc. IRE* **46**, 11, 1842 (1958a).
- Waterman, A. T., Jr., A rapid beam-swinging experiment in transhorizon propagation, *IRE Trans.* **AP-6**, 338 (1958b).
- Waterman, A. T., Jr., Tropospheric motions observed in rapid beam-swinging experiments, *Trans. IRE*, **AP-7**, 1, 106 (1959).
- Waterman, A. T., Jr., Transhorizon measurement techniques, *Statistical Methods in Radio Wave Propagation* (Proc. Symposium Univ. of Calif., 1958, 212, Pergamon Press, New York, N.Y. 1960).
- Watt, A. D., and R. W. Plush, Measured distributions of the instantaneous envelope amplitude and instantaneous frequency of carriers plus thermal and atmospheric noise, *Statistical Methods in Radio Wave Propagation* (Proc. Symposium Univ. of Calif., 1958, 233, Pergamon Press, New York, N.Y. 1960).
- Weiner, Norbert, Nonlinear problems in random theory, Technology Press of MIT (1958).
- Weisbrod, S., and L. J. Anderson, Simple methods for computing tropospheric and ionospheric refractive effects on radio waves, *Proc. IRE* **47**, 10 (1959).
- Wentzel, D. G., On the spectrum of turbulence, *Phys. of Fluids* **1**, 3, 213 (1958).
- Wexler, R., and D. Atlas, Precipitation generating cells, *J. Meteorol.* **16**, 327 (1959).
- Wheelon, A. D., Spectrum of turbulent fluctuations produced by convective mixing of gradients, *Phys. Rev.* **105**, 6, 1706 (1957a).
- Wheelon, A. D., Radio frequency and scattering angle dependence of ionospheric scatter propagation at VHF, *J. Geophys. Research* **62**, 93 (1957b).
- Wheelon, A. D., Relation of radio measurements to the spectrum of tropospheric dielectric fluctuations, *J. Appl. Phys.* **28**, 684 (1957c).
- Wheelon, A. D., Refractive corrections to scatter propagation, *J. Geophys. Research* **62**, 3, 343 (1957d).
- Wheelon, A. D., On the spectrum of a passive scalar mixed by turbulence, *J. Geophys. Research* **63**, 849 (1958a).
- Wheelon, A. D., A summary of the turbulent mixing dilemma, *J. Geophys. Research* **63**, 854 (1958b).
- Wheelon, A. D., Radiowave scattering by troposphere irregularities, *J. Research NBS* **63D**, 205 (1959).
- Wiesner, J. B., New methods of radio transmission, *Sci. American*, **196**, 1, 46 (1957a).
- Wiesner, J. B., and A. J. Pote, Radio communications by means of propagation by tropospheric diffusion, *L'Onde E'lectrique* **37**, 456, (1957b) (in French).
- Wiesner, J. B., W. G. Abel, L. G. Abraham, D. K. Bailey, H. H. Beverage, K. Bullington, J. H. Chisholm, H. V. Cottony, R. C. Kirby, W. E. Murrow, Jr., K. A. Norton, W. H. Radford, J. F. Roche, T. F. Rogers, R. J. Slutz, R. M. Davis, Jr., R. G. Merrill, V. R. Eshleman, and A. D. Wheelon, Radio transmission by ionospheric and tropospheric scatter, A report of the joint technical advisory committee (JTAC), *Proc. IRE*, (1960). (Reprints available from NBS, Boulder Labs. (CRPL).)
- Wilk, K. E., Synoptic interpretation with 0.86 Cm radar, *Proc. 7th Weather Radar Conf.* (1958).
- Wong, M. S., Refraction anomalies in airborne propagation, *Proc. IRE* **46**, 2, 1628 (1958).
- Wright, K. F., J. E. Cole, and J. G. Gibson, Measured distribution of the duration of fades in tropospheric scatter transmissions, *Trans. PGAP*, **AP-8**(1960).

Review of USA Activity in the Fields of Interest of URSI Commission 3 During the Triennium 1957 Through 1959

Because of the IGY, there has been an unprecedented emphasis on the geophysical aspects of the ionosphere. Rockets, satellites, moon echoes, VLF propagation in the "whistler" mode, and, most recently, incoherent scatter by the ionospheric electrons have enabled the observable ionosphere to be extended far beyond the former limit set by the maximum electron density at 300 to 500 kilometers.

During the IGY there was a considerable shift in emphasis in ionospheric investigations toward the polar regions, both arctic and antarctic. In the antarctic conventional observing techniques were used; in the north, however, extensive programs of rocket and balloon observations were brought to bear on the special effects of the auroral zone. Ground-launched rockets were fired at Ft. Churchill, Canada, and balloon-launched rockets (rockoons) were fired at various places. Balloon-borne radiation counters were also flown at various places in and near the auroral zone.

In the URSI, Commission 4 currently has the responsibility for ionospheric propagation at VLF and LF, for whistlers and whistler mode propagation, for hydromagnetic waves in the ionosphere and the extra low frequency oscillations (micropulsations) of the geomagnetic field which are thought to be associated with them, and for certain aspects of the exosphere. The reader is therefore referred to the report of USA Commission 4 for reviews of activity in these topics.

This review is confined to work published between January 1957 and December 1959. Also rather than cover the same ground in detail, reference is made to reviews of Upper Atmosphere Studies (under Meteorology and Atmospheric Physics), and work in Geomagnetism and Geoelectricity, Solar-Terrestrial Relationships, Ionosphere, Aurora, Airglow, Chemistry of the Outer Atmosphere, and Radiation Belts (under Geomagnetism and Aeronomy), in the Triennial Report of the American Geophysical Union to the UGGI (International Union of Geodesy and Geophysics) [AGU, 1960]. Another important review paper [JTAC, 1960] on radio transmission by ionospheric scatter was prepared by the Joint Technical Advisory Committee of the Institute of Radio Engineers and of the Radio and Television Manufacturers Association.

1. Structure of the Upper Atmosphere

Model atmospheres based on rocket and satellite data were derived by Champion and Minzner [1959], Kallmann [1959] and Harris and Jastrow [1959]. Studies of atmospheric density based on satellite orbits only were made by Schilling and Sterne [1959], Schilling and Whitney [1959], and Siry [1959]. Warwick [1959] used spin decay deduced from the radio signals of Sputnik I to derive a density at 220 km. All agree that densities above about 200 km are substantially higher than was previously thought, but there is still some disagreement in the interpretation of the rocket data for the lower altitudes (e.g., 90 km). Whipple [1959] reexamined the electron temperature derived from Russian measurements with Sputnik III and concluded it should be about 8,000 °K instead of 15,000 °K. Sterne [1958], discussing the reliabilities of rocket and satellite measurements, indicated that there was substantial disagreement between measurements at the same altitudes. He concluded that the satellite measurements were more reliable. LaGow and Horowitz [1958] pointed out that there was no disagreement when allowance was made for latitudinal variations.

LaGow, Horowitz, and Ainsworth [1959] discussed the arctic atmospheric structure based on rocket measurements at 59° N latitude. Summer densities between 30- and 70-km altitude were 5 to

10 percent higher than the Rocket Panel values for 33° N; * winter densities between 25 and 40 km were 10 to 20 percent lower than the summer values (i.e., 5 to 10 percent lower than the Rocket Panel values for 33° N); daytime density at 200 km, both in summer and in winter, was higher than the summer value at 33° N. Horowitz, LaGow, and Giuliani [1959] reported measurements of fall-day atmospheric structure at 59° N. Holmes and Johnson [1959] reported measurements of relative concentrations of atomic and molecular ions in the arctic ionosphere. The positive ions of O₂, NO, N₂, H₂O, O, and N were identified. O₂⁺, NO⁺, and O⁺ were by far the most abundant. NO⁺ dominated in the region below 200 km at night, and below 180 km in daylight. O₂⁺ was only a minor constituent of the lower E region at night. O⁺ appeared above 130 km and was most abundant above 200 km day and night. O₂⁺ increased above 100 km to a maximum relative concentration between 150 and 200 km day and night, but decreased rapidly above 200 km. It was the most abundant between 85 and 90 km during a daylight polar blackout.

Stroud et al. [1959] reported extremely low arctic summer temperatures at 80-km altitude in striking contrast to relatively high temperatures at this altitude in winter. Indications of atmospheric tides

*Average of all values obtained at White Sands, New Mexico, before 1952.

in satellite motions were discussed by Parkyn and Groves [1959]. Dessler [1959] proposed that upper atmosphere density variations due to hydromagnetic heating could account for irregular orbital accelerations of satellites, as well as the sudden disappearance of trapped radiation from the Argus nuclear explosion. The theory of disturbances induced in the ionospheric plasma by satellites was discussed by Kraus and Watson [1958]. Kellogg [1959] reviewed the results of rocket and satellite measurements presented at the 1958 meeting of the CSAGI in Moscow.

2. Ionizing Radiations

Considerable progress was made in the investigation and understanding of the fluxes of radiations (photons and corpuscles) which produce the ionospheric layers and cause the associated phenomena of geomagnetic and ionospheric storms, aurora, radio wave absorption, and so forth. Both rockets and balloons were used to detect soft X-rays and low-energy protons in the auroral regions, and the flux and spectrum of solar ultraviolet radiation. Peterson and Winckler [1959] reported a solar gamma-ray burst detected during a balloon flight. The gamma-ray burst was coincident with a solar flare and associated radio noise bursts, SID, earth-current disturbance, and magnetic crochet. References to other papers are given in the AGU Triennial Report [1960], together with discussion of the implications and interrelations of these phenomena.

3. Electron Densities

Kelso [1957] developed a method for converting vertical incidence records of virtual pulse-echo height versus frequency (h'-f records, also called ionograms) into profiles of electron density versus height, which is a compromise between the original method of Kelso coefficients and the later method due to Budden. Kay [1959] discussed the relationship of the precision of virtual height measurement to the pulse length and gave a precise experimental definition of group time delay. Wright [1959] gave the results of a true-height analysis of ionograms from stations along the 75th meridian in the form of contours of electron density representing a vertical cross-section of the ionosphere for this meridian.

Jackson and Seddon [1959] reported rocket measurements through an aurora. Severe electron density gradients were encountered. There was evidence of electron densities greater than $10^6/\text{cm}^3$ in the region 90 to 130 km, and indications of "filaments" with densities greater than $10^7/\text{cm}^3$. Jackson and Kane [1959] indicated a new method of measuring local electron density using an rf probe technique. Haycock, Swigart, and Baker [1959] gave a detailed development of the theory involved in the determination of electron densities from the group retardation of 6 Mc/s pulses transmitted from rocket to

ground, and discussed the results of 3 rockets fired at White Sands to a height of 137 km.

Bauer and Daniels [1959] measured the total electron content in a vertical column of the ionosphere by means of the Faraday rotation of radio waves reflected from the moon. They found that the ratio of the number of electrons above the level of maximum density to the number below was 4 to 5 during three nights in June before sunrise, dropping to about 3 after sunrise. On two days in November the ratio was about 3 both before and after sunrise. Prenatt [1959] reported that Faraday rotation measurements by rocket to 235 km agreed with measurements by an older technique on the same rocket flight.

Gordon [1958] predicted that incoherent scattering by ionospheric electrons could be detected and would enable electron densities to be measured throughout the ionosphere. Bowles [1958] obtained the first echoes, using a high power pulse transmitter at 41 Mc/s and a special high gain antenna beamed vertically.

4. Satellite Beacon Studies

Bowhill [1958] discussed the theory of the rate of Faraday rotation of the plane of polarization for a satellite signal. Daniels and Bauer [1959] developed the theory of the rotation more generally and discussed the application of its measurement to ionospheric studies using either moon echoes or satellite beacons. Arendt [1959] reported some observations of the rotation of satellite signals and discussed their interpretation on the assumption that the ionosphere had no appreciable horizontal variations in electron density. Parthasarathy and Reid [1959] reported values of the integrated electron density for four passes of Sputnik III near 600 km over College, Alaska, based on the rate of Faraday rotation. With spaced antennas receiving Sputnik III, Parthasarathy, Balser, and DeWitt [1959] used the times of abrupt weakening of the signal to deduce the height (104 km) of a discrete absorbing region during an auroral display.

Hutchinson [1959] discussed ionospheric effects on the measurement of the slant range at nearest approach. Arendt and Hutchinson [1959] discussed the problem of disentangling spin and Faraday rotation. Wells [1958] and Garriott and Villard [1958] reported signal enhancements when the satellite was near the antipode, and Dewan [1959] discussed some unusual effects in the propagation of satellite signals.

5. Ionospheric Processes

Mitra [1959] gave a theoretical discussion of the electron loss coefficient in the daytime processes in the ionosphere from 60 to 600 km at intermediate latitudes. Dalgarno [1958] pointed out the dilemma posed by rocket measurements of neutral particle density in the F2 region, which would indicate too

rapid diffusion if the usual values of the diffusion coefficient are taken, and offers some evidence that the value of the diffusion coefficient may be about $\frac{1}{4}$ the value usually assumed. Farley [1959] discussed theory of the effects of electrostatic fields in an ionosphere with a vertical magnetic field with a view toward elucidating the phenomena of spread *F* and radio star scintillation. Hoffman [1959] called attention to a possible mechanism for radiation and reflection from ionized gas clouds.

6. Ionospheric Disturbances

A study of the storm-time variations of the *F*2 layer critical frequency was carried out for 38 stations between 60° N and 60° S geomagnetic latitude by Matsushita [1959]. Tandberg-Hanssen [1958] found that in general the height of the *E* layer remained unchanged during magnetic storms, while the *F*1 layer tended to rise. Warwick and Hansen [1959] found a definite tendency for geomagnetic disturbance to follow the largest solar flares near sunspot maximum, but not near sunspot minimum. Their results indicated that the area of the flare was a more reliable index than its "importance". Maxwell, Thompson, and Garmire [1959] found that slow-drift type II solar radio bursts were 45 percent associated with subsequent aurora and magnetic storms. The mean delay was 33 hr, in good agreement with the speed of 1,000 km/sec deduced from the radio data. The geomagnetic effects were enhanced if the bursts occurred near an equinox and were accompanied by a flare of importance 2 or 3, or by continuous (type IV) radiation.

Bauer [1957, 1958a] described an apparent correlation between the variations of the critical frequency and virtual height of the *F*2 layer with frontal passages in the troposphere, and Bauer [1958b], and Mook [1958] discussed an apparent ionospheric response to the passage of hurricanes.

7. Sporadic E and Spread F

Smith [1957] published a survey of the geographic and temporal occurrence of sporadic *E*. Thomas and Smith [1959] brought Smith's survey up-to-date. Matsushita [1958] studied the association of the occurrence of blanketing *E*s and slant *E*s with magnetic bays. Penndorf and Coroniti [1958] analyzed the occurrence of sporadic *E* in the polar regions and proposed designation of two types: the Thule type which occurs primarily over the polar cap, and the auroral type. Davis, Smith, and Ellyett [1959] analyzed the occurrence of sporadic *E* as observed at 28 and 50 Mc/s over a 1,243-km path. Gerson [1959] used reports of 50 Mc/s contacts by radio amateurs to determine the annual distribution of sporadic *E* in North America. Knecht [1959] reported a lunar influence on the time of first appearance of equatorial sporadic *E* in the morning at Huancaayo.

Renau [1959] proposed a theory of spread *F* based upon specular reflection from magnetic field-aligned

irregularities near the level of reflection in the *F*2 layer. Reber [1958] discussed the behavior of spread *F* over Hawaii since the last sunspot minimum.

8. Studies of the Lower Ionosphere

Warwick and Zirin [1957] measured the diurnal variation of the absorption of cosmic noise at 18 Mc/s, and used the results in a theoretical discussion of the distribution of electron density, and the related processes in the *D*-region of the ionosphere. Houston [1958] derived an electron distribution for the *D* and *E* regions of the ionosphere based on recent theories and information concerning the atmospheric constituents, ionizing radiations, and the reactions. The results compared favorably with experimental measurements. Seddon [1958] reported a rocket measurement of the difference in the absorption of the ordinary and extraordinary wave components at 7.75 Mc/s as a function of altitude to 96 km at White Sands, N. Mex., at noon on a summer day. The absorption was inappreciable below 88 km, small from 88 to 94 km, but increased rapidly beyond 94 km.

Phelps and Pack [1959] made laboratory measurements of the collision frequency of thermal electrons in nitrogen. Under the assumption that the cross section for collision with a molecule of oxygen is no greater, the result agrees with Kane's [1959] determination of the collision frequency in the lower ionosphere. Chapman and Davies [1958] suggested that the approximate daytime constancy of the absorption of VLF radio waves would be accounted for if electrons were liberated by photodetachment from negative ions. Bourdeau, Whipple, and Clark [1959] studied the conductivity of the atmosphere between the stratosphere and the ionosphere, and Rumi [1957] found evidence of radar echoes from this region.

Gibbons and Rao [1957] developed formulas for the calculation of group refractive indices and group heights for frequencies less than the gyrofrequency, taking account of electron collisions. Watts [1958] called attention to a peculiarity of the group refractive index at frequencies below the gyrofrequency which results in retardation of the extraordinary wave at the critical frequencies of the ordinary wave, thus giving additional information about the electron density distribution. Bowhill [1957] applied diffraction theory to the analysis of the fading of low frequency waves reflected at vertical incidence from the ionosphere to deduce properties of its irregularities.

Waynick [1957], and Gibbons and Waynick [1959] reviewed the state of knowledge of the lower ionosphere. Ellyett and Watts [1959] reviewed the evidence for stratification in the lower ionosphere.

9. Radar Studies of Auroral Ionization

Echoes from irregularities in the auroral ionosphere were obtained at frequencies from HF (ionosonde frequencies) to UHF (780 Mc/s). Such echoes have

a strong tendency to be aspect sensitive relative to the earth's magnetic field, indicating that the irregularities are field-aligned. At the higher frequencies, the echo heights are confined to about 90 to 130 km (Fricker et al., 1957; Leadabrand, Dolphin and Peterson, 1959; Presnell et al., 1959). At the lowest frequencies, however, Bates [1959] showed that the heights may extend above 400 km. Stein [1958b] proposed that long-range echoes observed at HF, such as those described by Leadabrand and Peterson [1958], could be explained in terms of echoes at *E*-region heights resulting from propagation via a tilted *F* layer; but observations at 106 Mc/s by Schlobohm et al. [1959] from a geomagnetic latitude of 43° indicate that the long-range echoes at the lower frequencies may indeed have come from *F*-region heights.

Doppler shifts in echoes obtained with 400 Mc/s radar by Leadabrand, Presnell, Berg, and Dyce [1959] indicated that irregularities tended to drift from the east toward the west with a velocity of about 500 m/s, and that there was no appreciable variation with time of day or with respect to magnetic midnight. The relationship of the irregularities observed with radar techniques to magnetic disturbances was discussed by Nichols [1959].

10. Refraction in the Ionosphere

Marcou, Pfister, and Ulwick [1958] described a ray-tracing technique, taking full account of the earth's magnetic field, suitable for use with high-speed computers. Millman [1958] and Weisbrod and Anderson [1959] discussed refractive effects on radio waves traversing the troposphere and the ionosphere, and Weisbrod and Colin [1959] called attention to the fact that ionospheric bending has a maximum a few degrees above the horizon. Toman [1959] showed the effects of the spherical geometry on the absorption as well as the bending of a wave as a function of the elevation angle near the horizon. Brysk [1958a] discussed the effect of the ionosphere on signals scattered from the surface of the moon.

11. Ionospheric Propagation Studies—General

Villard, Stein, and Yeh [1957] reported observations of exceptionally long-delayed echoes with a HF backscatter sounder beamed across the equator which they interpreted as ground backscatter propagated by two or more successive reflections from the *F*-region of the ionosphere without intermediate ground reflection, caused by tilts of the reflecting layer. It is shown that tilt-supported propagation can take place at frequencies considerably above the MUF predicted in the usual way. Stein [1958a] gave a more general discussion of the effects of tilts.

Silberstein [1958a], comparing backscatter echoes with point-to-point pulse transmission over a 2,370-km path and ionograms taken at the midpoint

of the path, concluded that with suitable care the sweep-frequency backscatter technique can provide accurate information about the MUF. Silberstein [1958b] also reported the results of measuring relative pulse time delays over a 7,647-km path at 20.1 Mc/s. Greatly differing modes of propagation were observed from one day to the next indicating that the long path is very sensitive to ionospheric conditions. Agy and Davies [1959] summarized the present state of oblique incidence investigations of the ionosphere, using the sweep-frequency pulse technique, with special reference to the work of the CRPL.

12. Ionospheric Scatter Transmission

This subject was treated in detail in a recent review [JTAC, 1960]. Some additional references are Wheelon [1957a, 1957b], Leighton [1957], Bolgiano [1957a, 1957b], and Heritage et al. [1959].

13. Radio Reflection from Meteor Ionization

Increasing attention has been given to studies of meteor ionization, both as a propagation medium and as a means for observing ionospheric motions. A review paper was given by Manning and Eshleman [1959]. The work can be grouped into several categories.

13.1. The Reflection Properties of Individual Trails

The length of the ionized column produced by a meteor was computed by Eshleman [1957a] as a function of the characteristics of the meteor; this result was then extended to determine the distributions of trail lengths to be expected for shower and sporadic meteors. The length distribution for shower meteors was compared with experimental results and good agreement as found. The theory of trail formation was extended by Manning [1958] to include the effects of the high initial velocity of the particles in the trail. In a typical case, it was found that the trail would expand to a radius of about 14 mean-free-paths in about $\frac{1}{2}$ msec and from then on diffuse in the normal manner. Further considerations of the effects of normal diffusion by Flood [1957] and by Hawkins and Winter [1957] indicated that at UHF the effective scattering length of a trail may be greatly reduced and consequently the aspect sensitivity common at VHF will not be present. The analysis of oblique scattering from under-dense trails was extended by Brysk [1958b] to include the effects of the rapid initial diffusion of the trail, and the ray solution for oblique scattering from over-dense trails was obtained by Manning [1959a].

13.2. Computation and Measurement of the Gross Propagation Characteristics of Ensembles of Trails

The discovery that meteor ionization could provide a transmission medium for point-to-point communi-

cations at VHF stimulated a number of studies of the characteristics of meteor-burst propagation. These include general experimental studies by Vincent et al. [1957a], by Casey and Holladay [1957], and by Wirth and Keary [1958], analyses of the directional properties of this propagation by Meeks and James [1957, 1959] and Eshleman and Mlodnosky [1957], and examinations of its wavelength dependence by Eshleman [1957b] and by Meeks and James [1958]. The relations between meteor-burst propagation characteristics and the design of communication systems were discussed by Vincent et al. [1957b, c], Montgomery and Sugar [1957], Bliss et al. [1959], and Carpenter and Ochs [1959].

13.3. The Study of Ionospheric Motions Through the Use of Meteor Trails as Indicators

The earlier proposal, by Booker and Cohen, that small-scale turbulence in the lower ionosphere accounted for the observed decays of long-enduring meteor trails received considerable attention by Manning and Eshleman [1957, 1958] and by Booker [1958]. An alternative proposal that large-scale turbulence plays a dominant role in the decay of long-enduring trails was advanced by Manning [1959b] and substantiated by experimental results. This theory was also applied by Manning [1959c] to determine the detailed wind structure at meteoric heights. The general problems of motions in the lower ionosphere, as deduced from meteor observations, were a major topic of an International Symposium on Fluid Mechanics in the Ionosphere and are discussed in the published transactions [Bolgiano, 1959].

14. Ionospheric Propagation Research with Communication Systems Applications

Ionospheric research specifically directed towards more efficient utilization of ionospheric propagation for communications continued during the Triennium. Papers were published which reflect progress in understanding the mechanism, or at least the characteristics of signal distortion imposed by the medium.

14.1. Multipath Effects

Bailey [1958] analyzed the effect of echo on the operation of HF communication circuits. Two distinct kinds of echo are recognized. One kind of echo is observed when the great-circle path coincides with the twilight zone encircling the earth; the second kind, common only on fairly long communication paths, is most severe when the short path is intensely illuminated. While little can be done to obviate echo of the first kind, proper choice of operating frequency and mode of operation can minimize the echo interference of the second kind. In another paper [1959] Bailey considered the relationship of multipath delay times to the path length and the ratio of the operating frequency to the MUF.

The term "multipath reduction factor" (MRF) is introduced to specify operating frequencies for given multipath protection, path lengths, and ionospheric conditions. Investigation of multipath occurring within a millisecond pulse was carried out by Lutz et al. [1959] with specific attention to phase changes due to multipath occurring within separated 1-msec pulses.

Hulst [1959], suggested the use of a linear network, called an "inverse ionosphere," which would be automatically adjusted, under the control of a "probe pulse", to provide a delay function for message signals inverse to that imposed by the ionosphere. A new communication technique designed to take advantage of multipath propagation was described by Price and Green [1958]. This rather complicated system performs a continuous detailed measurement of the multipath characteristics, and then adds the various multipath components of the message signals algebraically after appropriate time delays are inserted.

14.2. Fading

Using pulses to separate the modes, Hedlund and Edwards [1958] measured the correlation of fading of horizontally and vertically polarized components of a received wave. As negative correlation was obtained most of the time, the fading was attributed to interference between the oppositely rotating magneto-ionic components. Yeh and Villard [1958], reporting on the occurrence of a HF component (near 20 c/s) of fading superimposed on the normal slow fading, surmised that the signal arrived by two entirely different modes, with the Doppler shift of one mode being much greater than that of the other. One mode was thought to be a normal two-hop transmission, and the second a long one-hop ionosphere-tilt-supported mode. Koch [1959] described a study of the fading of signals from pairs of transmitters, locked in phase, with antennas separated by 1,540 ft for one set of tests, and by 65 miles for another set of tests. In both cases the received carrier envelope fading was approximately Rayleigh distributed, and fading speed was not significantly different for the diversity transmissions. No "diversity gain" was apparent from these tests. Price and Green [1957] reported on some short-term phase perturbation observations of fading waves. Brennan et al. [1958], in a study of the effects of selective fading and signal-to-noise ratios on the performance of phase-keying (Kineplex) and FSK communication systems found that the advantage of the phase-keying system with respect to the FSK system under low signal-to-noise conditions is reduced when selective fading is rather severe.

14.3. Arctic Propagation

Coroniti and Penndorf [1959] and Penndorf and Coroniti [1959] analyzed a large number of ionospheric records to determine the geographic distribution and diurnal variations of auroral effects and

sporadic *E* occurrence. The inference is made that, by proper choice of operating paths for a particular time of day, reliability of Arctic communications can be improved. Leadabrand and Yabroff [1958] gave methods for calculating the probability of communication by means of reflections from ionized auroral columns.

14.4. General

Silberstein [1957] conducted tests to determine the effective horizontal radiation pattern of an antenna at a great distance (3,650 km) for ionosphere-propagated signals. The long distance pattern agreed very closely with that obtained by local measurements. K. Davies [1959] pointed out the error involved in the application of standard transmission curves, which neglect the earth's magnetic field, to ionograms in which the virtual height is increased by the presence of the field. The effect is to underestimate the MUF. Millman [1959] gave a method for calculating the angle of the magnetic field with the direction of propagation for any location and for transmission directed at any azimuth and elevation. Pucillo [1957] described a condensed nomographic procedure for determination of high-frequency sky-wave absorption.

References

- AGU Triennial Report to the IUGG, Trans. Am. Geophys. Union **41**, (June 1960).
- Agy, V. and K. Davies, Ionospheric investigations using the sweep-frequency technique at oblique incidence, J. Research NBS **63D**, 151 (1959).
- Arendt, P. R., On the existence of strong magneto-ionic effects topside of the *F* maximum of the Kennelly-Heaviside layer J. Appl. Phys. **30**, 793 (1959).
- Arendt, P. R. and H. P. Hutchinson, Spin variations of satellite radio emission, IRE Proc. 3d National Convention on Military Electronics, 407 (1959).
- Bailey, D. K., The effect of echo on the operation of high-frequency communication circuits, IRE Trans. **AP-6**, 325 (1958).
- Bailey, D. K., The effect of multipath distortion on the choice of operating frequencies for high frequency communication circuits, IRE Trans. **AP-7**, 397 (1959).
- Bates, H. F., The height of the *F*-layer irregularities in the Arctic ionosphere, J. Geophys. Research **64**, 1257 (1959).
- Bauer, S. J., A possible troposphere-ionosphere relationship, J. Geophys. Research **62**, 425 (1957).
- Bauer, S. J., Correlation between tropospheric and ionospheric parameters, Geophysica Pura E Applicata **40**, 235 (1958a).
- Bauer, S. J., An apparent ionospheric response to the passage of hurricanes, J. Geophys. Research **63**, 265 (1958b).
- Bauer, S. J., and F. B. Daniels, Measurements of ionospheric electron content by the lunar radio technique, J. Geophys. Research **64**, 1371 (1959).
- Bliss, W. H., R. J. Wagner, Jr., and G. S. Wickizer, Wide-band facsimile transmission over a 900-mile path utilizing meteor ionization, IRE Trans. **CS-7**, 252 (1959).
- Bolgiano, R., Spectrum of turbulent mixing, Phys. Rev. **108**, 1348 (1957a).
- Bolgiano, R., Discussion of Wheelon paper "Radio frequency and scattering angle dependence of ionospheric scatter propagation VHF, J. Geophys. Research **62**, 639 (1957b).
- Bolgiano, R. (Editor), International symposium on fluid mechanics in the ionosphere, J. Geophys. Research **64**, 2037 (1959).
- Booker, H. G., Concerning ionospheric turbulence at the meteoric level, J. Geophys. Research **63**, 97 (1958).
- Bordeau, R. E., E. C. Whipple, and J. F. Clark, Analytic and experimental electrical conductivity between the stratosphere and the ionosphere, J. Geophys. Research **64**, 1363 (1959).
- Bowhill, S. A., Ionospheric irregularities causing random fading of very low radio frequencies, J. Atmospheric and Terrest. Phys. **11**, 91 (1957).
- Bowhill, S. A., The Faraday rotation rate of a satellite radio signal, J. Atmospheric and Terrest. Phys. **13**, 175 (1958).
- Bowles, K. L., Observation of vertical incidence scatter from the ionosphere at 41 Mc/sec., Phys. Rev. Letters **1**, 454 (1958).
- Brennan, A. T., B. Goldberg, and A. Eckstein, Comparison of multichannel radioteletype systems over a 5,000 mile ionospheric path, IRE National Convention Record **6**, pt. 8, 254 (1958).
- Brysk, H., Measurement of the scattering matrix with an intervening ionosphere, Communication and Electronics, p. 611 (1958a).
- Brysk, H., Electromagnetic scattering by low-density meteor trails, J. Geophys. Research **63**, 693 (1958b).
- Carpenter, R. J., and G. R. Ochs, The NBS meteor-burst communication system, IRE Trans. **CS-7**, 263 (1959).
- Casey, J. P., and J. A. Holladay, Some airborne measurements of VHF reflections from meteor trails, Proc. IRE **45**, 1735 (1957).
- Champion, K. W., and R. A. Minzner, Atmospheric densities from satellites and rocket observations, Planet. Space Sci. **1**, 259 (1959).
- Chapman, S., and K. Davies, On the approximate daytime constancy of the absorption of radiowaves in the lower ionosphere, J. Atmospheric and Terrest. Phys. **13**, 86 (1958).
- Coroniti, S. C., and R. Penndorf, The diurnal and annual variations of foF2 over the Polar regions, J. Geophys. Research **64**, 5 (1959).
- Dalgarno, A., Ambipolar diffusion in the F2 layer, J. Atmospheric and Terrest. Phys. **12**, 219 (1958).
- Daniels, F. B., and S. J. Bauer, The ionospheric Faraday effect and its applications, J. Franklin Inst. **267**, 187 (1959).
- Davies, K., The effect of the earth's magnetic field on MUF calculations, J. Atmospheric and Terrest. Phys. **16**, 187 (1959).
- Davis, R. M., E. K. Smith, and C. D. Ellyett, Sporadic *E* at VHF in the USA, Proc. IRE **47**, 762 (1959).
- Dessler, A. J., Upper atmosphere density variations due to hydromagnetic heating, Nature **184**, 261 (1959).
- Dewan, E. M., Unusual propagation of satellite signals, Proc. IRE **47**, 2020 (1959).
- Ellyett, C., and J. M. Watts, Stratification in the lower ionosphere, J. Research NBS **63D**, 117 (1959).
- Eshleman, V. R., The theoretical length distribution of ionized meteor trails, J. Atmospheric and Terrest. Phys. **10**, 57 (1957a).
- Eshleman, V. R., On the wavelength dependence of the information capacity of meteor-burst propagation, Proc. IRE **45**, 1710 (1957b).
- Eshleman, V. R., and R. F. Mlodnosky, Directional characteristics of meteor propagation derived from radar measurements, Proc. IRE **45**, 1715 (1957).
- Farley, D. T., Jr., A theory of electrostatic fields in a horizontally stratified ionosphere subject to a vertical magnetic field, J. Geophys. Research **64**, 1225 (1959).
- Flood, W. A., Meteor echoes at ultra high frequencies, J. Geophys. Research **62**, 79 (1957).
- Fricke, S. J., R. P. Ingalls, M. L. Stone, and S. C. Wang, U. H. F. radar observations of aurora, J. Geophys. Research **62**, 527 (1957).
- Garriott, O. K., O. G. Villard, Jr., Antipodal reception of Sputnik III, Proc. IRE **12**, 1950 (1958).
- Gerson, N. C., Annual distribution of sporadic *E*, J. Atmospheric and Terrest. Phys. **16**, 189 (1959).
- Gibbons, J. J., and B. R. Rao, Calculation of group indices and group heights at low frequencies, J. Atmospheric and Terrest. Phys. **11**, 151 (1957).
- Gibbons, J. J., and A. H. Waynick, The normal D region of the ionosphere, Proc. IRE **47**, 161 (1959).

- Gordon, W. E., incoherent scattering of radio waves by free electrons with applications to space exploration by radar, *Proc. IRE* **46**, 1824 (1958).
- Harris, I., and R. Jastrow, An interim atmosphere derived from rocket and satellite data, *Planet. Space Sci.* **1**, 20 (1959).
- Hawkins, G. S., and D. F. Winter, Radio echoes from over-dense meteor trails under conditions of severe diffusion, *Proc. IRE* **45**, 1290 (1957).
- Haycock, O. C., J. I. Swigart, and D. J. Baker, Electron densities of the ionosphere utilizing high altitude rockets, *IRE Trans.* **AP-7**, 414 (1959).
- Hedlund, D. A., and L. C. Edwards, Polarization fading over an oblique incidence path, *IRE Trans.* **AP-6**, 21 (1958).
- Heritage, J. L., S. Weisbrod, and W. J. Fay, Evidence for a 200-megacycle per second ionospheric forward scatter mode associated with the earth's magnetic field, *J. Geophys. Research* **64**, 1235 (1959).
- Hoffman, W. C., A possible mechanism for radiation and reflection from ionized gas clouds, *Proc. IRE* **47**, 1274 (1959).
- Holmes, J. C., and C. Y. Johnson, Ions in the ionosphere, *Astronautics* **4**, 30 (1959).
- Horowitz, R., H. E. LaGow, and J. F. Giuliani, Fall-day auroral zone atmospheric structure measurements from 100 to 188 km, *J. Geophys. Research* **64**, 2287 (1959).
- Houston, R. E., Jr., The effect of certain solar radiations on the lower ionosphere, *J. Atmospheric and Terrest. Phys.* **12**, 225 (1958).
- Hulst, G. D., Inverse ionosphere, *IRE National Convention Record* **7**, pt. 8, 167 (1959).
- Hutchinson, H. P., Application of satellite doppler shift measurements Part II, Slant range at nearest approach, *IRE National Convention Record* **7**, pt. 5, 61 (1959).
- Jackson, J. E., and J. A. Kane, Measurement of ionospheric electron densities using an RF probe technique, *J. Geophys. Research* **64**, 1074 (1959).
- Jackson, J. E., and J. C. Seddon, Rocket measurements through an aurora, *Trans. Am. Geophys. Union* **40**, 381 (1959).
- JTAC (Joint Technical Advisory Committee), Radio transmission by ionospheric and tropospheric scatter—I. Ionospheric scatter transmission, *Proc. IRE* **48**, 5 (1960).
- Kallmann, H. K., A preliminary model atmosphere based on rocket and satellite data, *J. Geophys. Research* **64**, 615 (1959).
- Kane, J. A., Arctic measurements of electron collision frequencies in the D-region of the ionosphere, *J. Geophys. Research* **64**, 133 (1959).
- Kay, L., On the measurement of virtual height, *IRE Trans.* **AP-7**, 11 (1959).
- Kellogg, W. W., IGY rockets and satellites: A report on the Moscow Meetings, August 1958, *Planet. Space Sci.* **1**, 71 (1959).
- Kelso, J. M., The calculation of electron density distributions, *J. Atmospheric and Terrest. Phys.* **10**, 103 (1957).
- Knecht, R. W., An additional lunar influence on equatorial Es at Huancayo, *J. Atmospheric and Terrest. Phys.* **14**, 348 (1959).
- Koch, J. W., Reception of space diversity transmitters, *Wireless World* **65**, 512 (1959).
- Kraus, L., and K. M. Watson, Plasma motions induced by satellites in the ionosphere, *Physics of Fluids* **1**, 480 (1958).
- LaGow, H. E., and R. Horowitz, Comparison of high-altitude rocket and satellite density measurements, *Physics of Fluids* **1**, 478 (1958).
- LaGow, H. E., R. Horowitz, and J. Ainsworth, Arctic atmospheric structure to 250 km, *Planet. Space Sci.* **2**, 33 (1959).
- Leadabrand, R. L., L. Dolphin, and A. M. Peterson, Preliminary results of 400 Mc radar investigations of auroral echoes at College, Alaska, *IRE Trans.* **AP-7**, 127 (1959).
- Leadabrand, R. L., and A. M. Peterson, Radio echoes from auroral ionization detected at relatively low geomagnetic latitudes, *IRE Trans.* **AP-6**, 65 (1958).
- Leadabrand, R. L., R. I. Presnell, M. R. Berg, and R. B. Dyce, Doppler investigations of the radar aurora at 400 Mc, *J. Geophys. Research* **64**, 1197 (1959).
- Leadabrand, R. L. and I. Yabroff, The geometry of auroral communications, *IRE Trans.* **AP-6**, 80 (1958).
- Leighton, H. I., Field strength variations recorded on a VHF ionospheric scatter circuit during the solar event of Feb. 23, 1956, *J. Geophys. Research* **62**, 483 (1957).
- Lutz, S. G., F. A. Losee, and A. W. Ladd, Pulse phase-change signaling in the presence of ionospheric multipath distortion, *IRE Trans.* **CS-7**, 102 (1959).
- Manning, L. A., The initial radius of meteoric ionization trails, *J. Geophys. Research* **63**, 181 (1958).
- Manning, L. A., Oblique echoes from over-dense meteor trails, *J. Atmospheric and Terrest. Phys.* **14**, 82 (1959a).
- Manning, L. A., Air motions and the fading, diversity, and aspect sensitivity of meteoric echoes, *J. Geophys. Research* **64**, 1415 (1959b).
- Manning, L. A., Air motions at meteoric heights, *J. Atmospheric and Terrest. Phys.* **15**, 137 (1959c).
- Manning, L. A., and V. R. Eshleman, Discussion of the Booker and Cohen paper, "A theory of long duration meteor echoes based on atmospheric turbulence with experimental confirmation," *J. Geophys. Research* **62**, 367 (1957).
- Manning, L. A., and V. R. Eshleman, Concerning Booker's theory of meteoric reflections, *J. Geophys. Research* **63**, 737 (1958).
- Manning, L. A., and V. R. Eshleman, Meteors in the ionosphere, *Proc. IRE* **47**, 186 (1959).
- Marcou, R. J., W. Pfister, and J. C. Ulwick, Ray-tracing technique in a horizontally stratified ionosphere using vector representation, *J. Geophys. Research* **63**, 301 (1958).
- Matsushita, S., Some studies of the upper atmosphere in the auroral zone, *Annales de Geophysique* **14**, 483 (1958).
- Matsushita, S., A study of the morphology of ionospheric storms, *J. Geophys. Research* **64**, 305 (1959).
- Maxwell, A., A. R. Thompson, and G. Garmire, The association of solar radio bursts with auroral streams, *Planet. Space Sci.* **1**, 325 (1959).
- Meeks, M. L., and J. C. James, On the influence of meteor-radiant distributions in meteor-scatter communication, *Proc. IRE* **45**, 1724 (1957).
- Meeks, M. L., and J. C. James, On the choice of frequencies for meteor-burst communication, *Proc. IRE* **46**, 1871 (1958).
- Meeks, M. L., and J. C. James, Meteor radiant distributions and the radio-echo rates observed by forward scatter, *J. Atmospheric and Terrest. Phys.* **16**, 228 (1959).
- Millman, G. H., Atmospheric effects on VHF and UHF propagation, *Proc. IRE* **46**, 1492 (1958).
- Millman, G. H., The geometry of the earth's magnetic field at ionospheric heights, *J. Geophys. Research* **64**, 717 (1959).
- Mitra, A. P., Time and height variations in the daytime processes in the ionosphere. Part I: A noontime model of the ionosphere loss coefficient from 60 to 600 km over middle latitudes, *J. Geophys. Research* **64**, 733 (1959).
- Montgomery, G. F., and G. R. Sugar, The utility of meteor bursts for intermittent radio communication, *Proc. IRE* **45**, 1684 (1957).
- Mook, C. P., The apparent ionospheric response to the passage of hurricane Diane (1955) at Washington, D.C., *J. Geophys. Research* **63**, 569 (1958).
- Nichols, B., Auroral ionization and magnetic disturbances, *Proc. IRE* **47**, 245 (1959).
- Parkyn, D. G., and G. V. Groves, Atmospheric tides and earth satellite observations, *Nature* **183**, 1045 (1959).
- Parthasarathy, R., R. Basler, and R. N. DeWitt, A new method for studying the auroral ionosphere using earth satellites, *Proc. IRE* **47**, 1660 (1959).
- Parthasarathy, R., and G. C. Reid, Signal strength recordings of the satellite 1958 52 (Sputnik III) at College, Alaska, *Proc. IRE* **47**, 78 (1959).
- Penndorf, R., and S. C. Coroniti, Polar Es, *J. Geophys. Research* **63**, 789 (1958).
- Penndorf, R., and S. C. Coroniti, Propagation of HF and VHF in the Arctic region, *IRE Trans.* **CS-7**, 121 (1959).
- Peterson, L. E., and J. R. Winckler, Gamma-ray burst from a solar flare, *J. Geophys. Research* **64**, 697 (1959).
- Phelps, A. V., and J. L. Pack, Electron collision frequencies in nitrogen and in the lower ionosphere, *Phys. Rev. Ltrs.* **3**, 340 (1959).
- Prenatt, R. E., Faraday rotation measurements at Fort Churchill, *J. Geophys. Research* **64**, 1340 (1959).

- Presnell, R. I., R. L. Leadabrand, A. M. Peterson, R. B. Dyce, J. C. Schlobohm, and M. R. Berg, VHF and UHF radar observations of the aurora at College, Alaska, *J. Geophys. Research* **64**, 1179 (1959).
- Price, R., and P. E. Green, Jr., Measurement of ionospheric pathphase for oblique incidence, *Nature* **179**, 372 (1957).
- Price, R., and P. E. Green, Jr., A communication technique for multipath channels, *Proc. IRE* **46**, 555 (1958).
- Pucillo, G. L., Determination of HF skywave absorption, *IRE Trans.* **AP-5**, 314 (1957).
- Reber, G., Solar activity cycle and spread F, *J. Geophys. Research* **63**, 869 (1958).
- Renau, J., A theory of spread F based on a scattering-screen model, *J. Geophys. Research* **64**, 971 (1959).
- Rumi, G. C., VHF radar echoes associated with atmospheric phenomena, *J. Geophys. Research* **62**, 547 (1957).
- Schilling, G. F., and T. E. Sterne, Densities and temperature of the upper atmosphere inferred from satellite observations, *J. Geophys. Research* **64**, 1 (1959).
- Schilling, G. F., and C. A. Whitney, Derivation and analysis of atmospheric density from observations of satellite 1958 epsilon, *Planet. Space Sci.* **1**, 136 (1959).
- Schlobohm, J. C., R. L. Leadabrand, R. B. Dyce, L. T. Dolphin, and M. R. Berg, High-altitude 106.1-Mc radio echoes from auroral ionization detected at a geomagnetic latitude of 43°, *J. Geophys. Research* **64**, 1191 (1959).
- Seddon, J. C., Differential absorption in the D and lower-E regions, *J. Geophys. Research* **63**, 209 (1958).
- Silberstein, R., The long distance horizontal radiation pattern of a high-frequency antenna, *IRE Trans.* **AP-5**, 379 (1957).
- Silberstein, R., The use of sweep-frequency backscatter data for determining oblique incidence ionospheric characteristics, *J. Geophys. Research* **63**, 335 (1958a).
- Silberstein, R., A long-distance pulse-propagation experiment on 20.1 megacycles, *J. Geophys. Research* **63**, 445 (1958b).
- Siry, J. W., Satellite orbits and atmospheric densities at altitudes up to 750 km obtained from the Vanguard orbit determination program, *Planet. Space Sci.* **1**, 184 (1959).
- Smith, E. K., Jr., Worldwide occurrence of sporadic E, National Bureau of Standards Circular 582, United States Government Printing Office (1957).
- Stein, S., The role of ionospheric-layer tilts in long-range high-frequency radio propagation, *J. Geophys. Research* **63**, 217 (1958a).
- Stein, S., The role of F-layer tilts in detection of auroral ionization, *J. Geophys. Research* **63**, 391 (1958b).
- Sterne, T. E., High altitude atmospheric density, *Physics of Fluids* **1**, 165 (1958).
- Stroud, W. H., W. Nordberg, W. R. Bandeen, F. L. Bartman, and P. Titus, Rocket-grenade observations of atmospheric heating in the Arctic, *J. Geophys. Research* **64**, 1342 (1959).
- Tandberg-Hanssen, E., Variation in the height of ionospheric layers during magnetic storms, *J. Geophys. Research* **63**, 157 (1958).
- Thomas, J. A., and E. K. Smith, A survey of the present knowledge of sporadic-E ionization, *J. Atmospheric and Terrest. Phys.* **13**, 295 (1959).
- Toman, Kurt, New geometrical properties and their usefulness for ionospheric radio propagation, *Proc. IRE* **47**, 1381 (1959).
- Villard, O. G., Jr., S. Stein, and K. C. Yeh, Studies of transequatorial ionospheric propagation by the scatter-sounding method, *J. Geophys. Research* **62**, 399 (1957).
- Vincent, W. R., R. T. Wolfram, B. M. Sifford, W. E. Jaye, and A. M. Peterson, Analysis of oblique path meteor propagation data from the communications viewpoint, *Proc. IRE* **45**, 1701 (1957a).
- Vincent, W. R., R. T. Wolfram, B. M. Sifford, W. E. Jaye, and A. M. Peterson, VHF propagation by ionized meteor trails: Part I: Electronic Inds. Tele-tech **16**, 52 (1957b); Part II: Electronic Inds. Tele-tech **16**, 84 (1957c).
- Warwick, C. S., and R. T. Hansen, Geomagnetic activity following large solar flares, *J. Atmospheric and Terrest. Phys.* **14**, 287 (1959).
- Warwick, J. W., Decay of spin in Sputnik I, *Planet. Space Sci.* **1**, 43 (1959).
- Warwick, J. W., and H. Zirin, Diurnal absorption in the D-region, *J. Atmospheric and Terrest. Phys.* **11**, 187 (1957).
- Watts, J. M., The interpretation of nighttime low-frequency ionograms, *J. Geophys. Research* **63**, 717 (1958).
- Waynick, A. H., The present state of knowledge concerning the lower ionosphere, *Proc. IRE* **46**, 741 (1957).
- Weisbrod, S., and L. J. Anderson, Simple methods for computing tropospheric and ionospheric refractive effects on radio waves, *Proc. IRE* **47**, 1770 (1959).
- Weisbrod, S., and L. Colin, Refraction of very high frequency radio signals at ionospheric heights, *Nature* **184**, 119 (1959).
- Wells, H. W., Unusual propagation at 40 Mc from the USSR satellite, *Proc. IRE* **46**, 610 (1958).
- Wheeler, A. D., Diurnal variations of signal level and scattering heights for VHF propagation, *J. Geophys. Research* **62**, 255 (1957a).
- Wheeler, A. D., Refractive corrections to scatter propagation, *J. Geophys. Research* **62**, 343 (1957b).
- Whipple, E. C., Jr., The ion-trap results in "Exploration of the upper atmosphere with the help of the third Soviet Sputnik," *Proc. IRE* **47**, 2023 (1959).
- Wirth, H. J., and T. J. Keary, The duty cycle associated with forward-scattered echoes from meteor trails, *IRE National Convention Record* **6**, pt. 1, 127 (1958).
- Wright, J. W., Note on quite-day vertical cross sections of the ionosphere along 75° W geographic meridian, *J. Geophys. Research* **64**, 1631 (1959).
- Yeh, K. C., and O. G. Villard, Jr., A new type of fading observable on high frequency transmissions propagated over paths crossing the magnetic equator, *Proc. IRE* **46**, 1968 (1958).

Report of U.S. Commission 4, URSI

RADIO NOISE OF TERRESTRIAL ORIGIN

Edited by William Q. Crichlow*

The scope of Commission IV has expanded extensively since the XIIth General Assembly in 1957. This has largely resulted from the increased interest in the portion of the spectrum below 30 kc/s and the fact that the electromagnetic energy released by lightning discharges provides a very useful tool for investigating various modes of radio propagation.

The purpose of this report is to summarize significant research in this field that has been carried out in the United States during the past three years. Bibliographies have also been included. The topics covered are as follows:

1. Radiofrequency radiation from lightning discharges..... A. Glenn Jean.
2. Properties of atmospheric noise at various receiving locations. W. Q. Crichlow.
3. Summary of research on whistlers and related phenomena:
 - 3.1. Stanford University..... R. A. Helliwell.
 - 3.2. Dartmouth College..... M. G. Morgan.
4. A summary of VLF and ELF Propagation research. James R. Wait.
5. Hydromagnetic waves and ELF oscillations in the ionosphere. J. M. Watts.
6. The exosphere..... J. M. Watts.

*U.S. Chairman, Commission 4, URSI.

1. Radiofrequency Radiation From Lightning Discharges

A. Glenn Jean*

A number of complex discharge processes which take place in lightning strokes are responsible for the emission of radiofrequency energy. The amplitude spectrum of such emissions extends from a few cycles per second to hundreds of megacycles per second, usually attaining a peak within the VLF region. The energy radiated from a cloud-to-ground stroke is of the order of 250,000 joules and can cause serious interference to radio communications systems. These emissions have been widely used as a source of signals in radio propagation research, in locating active thunderstorms, in identifying and tracking storms, and in basic investigations of the discharge mechanisms themselves. The radio engineer, the meteorologist and the physicist are concerned with the discharge processes and the nature of the resulting electromagnetic radiation.

It is the main purpose of this note to summarize recent research pertaining to the radiofrequency radiation from lightning discharges.

The most common type of lightning discharge occurs within the cloud between the two principle areas of opposite charge [Pierce, 1957]. The breakdown process involves the advance of a pilot leader through air that has not been ionized; and there is evidence that there is no return stroke as encountered in cloud-to-ground discharges. The pilot leader may advance in steps [Schonland, 1953], as in the case of the discharge to earth, and it is likely that the steps are mainly responsible for any induction and radiation fields produced. Radiation from the rapid field changes, such as the step referred to, has been observed at very high radiofrequencies. Atlas [1958], using a 2800 Mc/s radar, reported receiving atmospherics, having durations less than 1 msec and amplitudes of about 30 $\mu\text{V/m}$ (in a 600 kc/s bandpass) from discharges which occurred within the upper regions of a thundercloud. It was postulated that these atmospherics resulted from stepped-leader type discharges in the ice crystal region of the cloud. Following the reception of these atmospherics, radar echoes lasting from 0.1 to 0.5 sec were obtained from ionized regions up to 27,000 ft tall with horizontal base diameters of 30,000 ft. It is thought that the radar signals were reflected from the ionization created by the discharges rather than from dielectric discontinuities associated with heated columns of air. There is evidence that the ionization is propagated up toward the cloud top after the discharge. Atlas [1958] estimated that partial or "soft" reflections were obtained from regions having electron densities between 10^6 and 10^9 electrons/cm³. (A density of 10^{11} electrons/cm³ is required for a unity reflection coefficient from a sharp boundary at 2800 Mc/s.) There is also evidence resulting from 3-cm radar observations that many of the discharges might have

extended through the ice crystal anvil into clear air as reported on occasions by others [Ward, 1951; Bays, 1926]. The simultaneous observations of atmospherics and radar reflections from ionization created by the discharge constitute a powerful technique in exploring the mechanism of cloud discharges.

Cloud discharges which occurred in tornadoes were described by Jones [1958]. On three occasions, rapidly recurring light patches were observed which appeared to come from discharges within the cloud. Simultaneous observations of atmospherics indicated a noticeable absence of return-stroke discharges from cloud-to-earth and an unusually high rate of occurrence of atmospheric components at 150 kc/s. The 150 kc/s observations were made using crossed-loop direction-finding equipment. The direction-finder responses were observed to be straight lines rather than ellipses, from which it was inferred that the cloud discharges were vertical. Jones [1958] reported receiving approximately 45 atmospheric components per second at 150 kc/s from a severe storm at a 25-mile range in 1957. During this interval, 10 kc/s components were not observed. These atmospherics are reported to be related to "flare type" discharges which were visually sighted as streamers which projected over the leading edge of the anvil top of the cloud.

It would be of interest to compare observations of 150 kc/s atmospheric components observed by Jones [1958] during tornadoes with emissions at similar frequencies which might result from severe Pacific storms [Kimpara, 1958].

Most of the radiofrequency energy emitted in the VLF region from lightning discharges occurs from the return stroke. Since multiple return strokes play an important part in establishing the ambient noise level at VLF, it is of value to determine the radiation properties of individual strokes and the statistics regarding the occurrence of successive discharges.

Tepley [1959] observed two classes of ELF waveforms in Hawaii. The first class consisted of a single large half-cycle sometimes followed by a second half-cycle of substantially lower amplitude and of longer duration. This type of waveform may be obtained theoretically from a Dirac current source. The other class of waveform consists of two half-cycles of comparable amplitude, the second of which is longer than the first. A possible third half-cycle is sometimes observed. The first two half-cycles are explicable in terms of a unidirectional source current of longer duration than the current responsible for the first type of waveform. Pierce [1955] found that over 90 percent of all ground-return strokes are of positive polarity, corresponding to the lowering of a negative charge-to-ground. Brook [1957] reported one ground-return stroke in 700 produced a negative field change. Hence, it

*National Bureau of Standards, Boulder, Colo.

appears that the positive-to-negative polarity ratio of the ground-return stroke should be much greater than unity. On the contrary, Tepley [1959] found that slow-tails are negative by a ratio of more than 3:1. The possibility that most of the negative slow-tails do not originate in ground-return strokes is considered. Pierce found that the ratio of slow-negative to slow-positive field changes is about 2:1 for heat storms and about 7:1 for frontal storms. Tepley's observations are in reasonable agreement with these ratios.

Wait [1960a] pointed out that lightning discharges from cloud-to-ground and cloud-to-cloud are seldom vertical or horizontal. The modification of the pulse shape of the ELF waveform, as a result of the inclination of the current channel, would appear to be an important factor in interpreting observed data. In particular, pulses with both positive and negative polarities of the first half-cycles strongly suggest (as mentioned by Tepley) that the horizontal component of the source current is important. An observed pulse having a second half-cycle can only be reconciled with an inclined source. For certain small values of horizontal source component a third half-cycle of relatively small amplitude is also produced. In view of the small dimensions of the discharge paths in terms of a wavelength, Wait replaced the source channel by superimposed vertical and horizontal electric dipoles and calculated the resultant responses of the radiation field by superposition. Various ELF waveforms were given corresponding to different horizontal and vertical electric field components at the source. These waveforms agree remarkably well with observed waveforms.

A great number of experimental and theoretical investigations have been carried out to determine the nature of the atmospheric waveform near the source. Wait [1956b] presented calculations showing the nature of the transient response of an idealized lightning discharge at short ranges where the ionospherically reflected wave can be neglected or separately accounted for. An expression was derived for the instantaneous product of the dipole current and vertical height applicable to the return-stroke discharge. Solutions were given for moments having a buildup time of about 10 μ sec and a pulse width of about 50 μ sec which is representative of observed return-stroke discharges. Solutions are given in graphical form for the field response with time, parametric in distance, for a perfectly conducting earth. The effect of the earth conductivity upon the pulse shape at 100 km was demonstrated and the effect of the earth curvature considered. Additional terms can be used in the expansion of the dipole moment to include a sustained return current.

Wait [1958d] calculated the response of the waveguide to an impulsive current source for different ranges. The pulses have the appearance of damped sinusoids as the result of the modal characteristics

of the propagation medium. The length of the first half-cycle becomes progressively shortened with increasing range while the oscillatory nature of the pulse is becoming enhanced. It is also shown that different exponential source functions produce waveforms having different quasi half-periods at a fixed distance. Thus, the quasi half-cycle of atmospherics is determined by the source pulse as well as by the propagation medium. The results of these calculations compare favorably with quasi half-periods of atmospherics observed by Hepburn [1957].

Watt [1957a] calculated a representative radiation spectrum of return-stroke discharges using waveforms recorded at short ranges. He then synthesized a radiation spectrum combining the radiation from the return-stroke discharge with radiation from stepped-leader discharges as observed by Norinder [1954]. The resultant spectrum was subsequently used in estimating ambient noise levels at distances between 1,000 and 4,000 km from thunderstorms. The predicted levels of noise, which extended over a frequency range from 1 to 100 kc/s, compared favorably with observed noise levels.

Hill [1957] formulated a theory for the generation of low-frequency radiation in the return stroke of the cloud-to-ground lightning flash. The radiated pulse is a single cycle with a field variation which varies linearly with time. The spectrum of the radiated energy is centered at 11 kc/s and the energy radiated is about 220,000 j.

Hefley et al. [1960] reported the development of equipment capable of automatically recording the directions of arrival and spectral components of atmospherics. Results of observations made at 10.5, 40, and 100 kc/s in the Northwestern part of the United States reveal the directions of arrival and the rates of reception of atmospheric components exceeding fixed amplitude levels.

Recently, observations of the radiation spectra of return-stroke lightning discharges were reported by Taylor and Jean [1959]. In this work, atmospheric waveforms were recorded at distances ranging from about 150 to 600 km. The locations of the individual lightning flashes were determined using a direction-finding network. At these ranges, it was possible to separately identify the ground and sky-wave components. The precautions taken in selecting atmospherics radiated from return-stroke discharges and in utilizing the ground-wave pulse are described. The atmospherics resulted from discharges over high terrain at altitudes of 5,000 ft or more in the Rocky Mountain area. Values of total energy were reported to be about 30,000 j compared with approximately 300,000 j reported by Lady et al. [1940] and as derived in other experiments from discharges which occurred over land of lower elevations. These results indicate the desirability to perform similar atmospheric observations at lower land elevations and over sea water.

2. Properties of Atmospheric Noise at Various Receiving Locations

William Q. Crichlow*

The properties of sferics from individual lightning flashes are dealt with in other sections of this report. On the other hand, the composite effects at the receiver resulting from simultaneous thunderstorm activity throughout the world are discussed in this section. Although extensive investigations of these phenomena have been made in the past by several agencies and predictions of worldwide atmospheric noise levels have been published [RPU Tech. Rpt. 5, 1949; NBS Circ. 462, 1948; Crichlow et al., 1955; C.C.I.R. Rpt. 65, 1957], most of the recent studies in this country of worldwide noise levels and characteristics have been made by the Central Radio Propagation Laboratory of the National Bureau of Standards.

During the International Geophysical Year, a worldwide network of 16 radio noise recording stations was established by CRPL [Crichlow, 1957] at the following locations:

Station	Latitude	Longitude
Balboa, Canal Zone	9. 0N	79. 5W
Bill, Wyo	43. 2N	105. 2W
Boulder, Colo	40. 1N	105. 1W
Byrd, Antarctica	80. 0S	122. 0W
Cook, Australia	30. 6S	130. 4E
New Delhi, India	28. 8N	77. 3E
Enkoping, Sweden	59. 5N	17. 3E
Front Royal, Va	38. 8N	78. 2W
Ibadan, Nigeria	7. 4N	3. 9E
Kekaha, Kauai, Hawaii	22. 0N	159. 7W
Ohira, Japan	35. 6N	140. 5E
Pretoria, Union of South Africa	25. 8S	28. 3E
Rabat, Morocco	33. 9N	6. 8W
São José dos Campos, Brazil	23. 3S	45. 8W
Singapore, Malaya	1. 3N	103. 8E
Thule, Greenland	76. 6N	68. 7W

Five of these stations are operated by CRPL, two by the Signal Corps Radio Propagation Agency, and the remaining nine by foreign governments.

Standardized recording equipment, which was designed and furnished by CRPL, provides measurements on eight frequencies from 13 kc/s to 20 Mc/s.

The mean received power in a 200 c/s bandwidth, averaged over a period of several minutes, is the basic parameter recorded. It is expressed as an effective antenna noise figure, which is defined as the noise power available from an equivalent lossless antenna in decibels above kTb , where k =Boltzman's constant (1.38×10^{-23} j/°), T =absolute room temperature (taken as 288 ° K), and b =bandwidth in cycles per second.

In order to obtain additional information on the character of the noise, two other statistical moments, the average envelope voltage and the average logarithm of the envelope voltage are recorded at 10 of the stations. All data from the network are processed at the NBS, Boulder Laboratories and are published quarterly [Crichlow, 1959a; Crichlow, 1959b].

The amplitude-probability distribution (APD) of the instantaneous IF envelope voltage provides a useful means of expressing the detailed characteristics of atmospheric noise. The first measurements of the APD by U.S. experimenters were made at the University of Florida [Hoff, 1952; Sullivan et al., 1955; Sullivan, no date; George, 1957] and subsequently in Colorado, Alaska, and Panama by NBS personnel. From the NBS [Watt et al., 1957b] measurements, it was found that the noise envelope at the low-amplitude levels is Rayleigh distributed, while that at the higher levels approaches a distribution having a much greater change in level for a given change in probability. The dynamic range between the value exceeded 0.0001 percent of the time and the value exceeded 90 percent of the time varied from 59 to 102 db at 22 kc/s in a bandwidth of 1 kc/s. As the bandwidth is reduced, the dynamic range approaches 21.18 db, the value expected for the Rayleigh distributed envelope of thermal noise. This occurs at a bandwidth of approximately 0.2 c/s for atmospherics at 22 kc/s. This study of the characteristics of atmospheric noise was extended to cover the frequency range from 1 to 100 kc/s [Watt et al., 1957]. The variation of level and dynamic range with frequency was examined both theoretically and experimentally.

The value of the APD in determining the performance of radio systems in the presence of atmospheric noise has been demonstrated by additional studies at NBS [Watt et al., 1958]. The expected error rates, both with manual telegraphy and FSK systems, have been calculated from the noise APD and confirmed experimentally.

*National Bureau of Standards, Boulder, Colo.

Direct measurements of the APD at a large number of locations and over a wide frequency range are prohibitive, both in equipment and personnel requirements. Since data on the statistical moments measured by the NBS noise recorder are available from the worldwide network over a wide frequency range, an investigation was made of methods for deriving the complete distribution from these moments [Crichlow et al., 1960a]. It was found that the distribution, when plotted on Rayleigh graph paper, had a characteristic shape that could be described graphically by three independent parameters. This characteristic shape was confirmed by measurements in Colorado [Watt et al., 1957b; Crichlow et al., 1960a], Alaska [Watt et al., 1957b],

Panama [Watt et al., 1957b], Florida [Sullivan et al., 1955; Sullivan, no date; George, 1957], England [Horner, 1956], and Japan [Yuhara, 1956]. Using numerical integration methods on typical distributions, a relationship was found between the three moments measured by the NBS noise recorder and the three graphical parameters, thus providing the complete distribution from the three measured moments. Families of distribution curves in terms of the moments will be published in an NBS Monograph [Crichlow et al., 1960b] for ease in evaluation.

The effects of bandwidth on the APD have been published [Fulton, 1957] and further studies are in progress at NBS to determine the effect of bandwidth on the statistical moments.

3. Summary of Research on Whistlers and Related Phenomena

3.1. Stanford University

R. A. Helliwell*

The following is a synopsis of research on whistlers and related phenomena carried out at Stanford University since the XIIth General Assembly of URSI. Many results are presented here for the first time, and will be elaborated in reports and papers in preparation. Support for this work was obtained from several agencies including the National Science Foundation, the Air Force Office of Scientific Research, the Office of Naval Research, and the National Aeronautics and Space Administration.

a. Methods of Whistler Analysis

Techniques for spectrographic analysis of whistlers have been developed [Carpenter, 1960]. Included are methods for identifying the causative sferic associated with whistlers. In many cases, three sonagrams from a single two-minute run will provide unambiguous identification of the sources of both long and short whistlers. Simultaneous data from other stations are often needed to resolve ambiguities. Methods for quantitative description of whistlers are described.

b. IGY-IGC Synoptic Whistler Results

Some tentative results from the 10-station whistler-west program are summarized in the following paragraphs. The cooperation of the several persons and groups associated with the whistlers-west program is gratefully acknowledged. Results of pre-IGY experiments and details of the synoptic program have been published elsewhere [Helliwell and Morgan, 1959; Smith et al., 1958; Helliwell, 1958c]. At the time of writing this report, about 10,000 sonagrams of whistlers and VLF emissions had been produced. Some 1,500 whistlers had been analyzed, and the causative atmospherics for roughly 1,000 of these had been identified.

The statistical results obtained from the aural data are subject to some uncertainty because of differences in the training and ability of the listeners. For this reason, many of the indicated trends of the data can not be accepted without reservation. For example, VLF hiss is sometimes mistaken for background noise. However, the following results appear to be demonstrated by the data which have been examined.

More whistlers are heard at night than during the day, probably because *D*-region absorption increases the daytime attenuation from source to the input end of the whistler path and from the output end to the receiver.

Seasonal variations of whistler activity are complicated. Stations at geomagnetic latitudes lower than roughly 52° and greater than 62° show a wintertime maximum in occurrence, whereas stations between 52° and 62° geomagnetic latitude show a summertime maximum. This curious effect may possibly be related to differences in the behavior of long and short whistlers. Theoretically, wintertime should be more favorable for the observation of whistlers, since the local noise level is low and the sources of short whistlers are relatively numerous. However, at locations where long whistlers are known to occur frequently (principally middle latitudes), strong summer thunderstorm activity could easily produce a whistler rate exceeding that in winter. At high and low latitudes long whistlers are seldom heard, and so the wintertime peak above 62° and below 52° can be understood. The over-all whistler rate reaches a maximum at approximately 50° geomagnetic latitude.

Comparison of daily whistler rate with daily average magnetic index shows little correlation. However, any effect may be masked by the large day-to-day variation in whistler rate, which is probably correlated with variations in thunderstorm occurrence.

Comparison of daily whistler rates between stations indicates that for station spacings of 1,000 km or more, the occurrence rates tend to be independent. This conclusion includes stations of similar latitude. It is interpreted to mean that either the paths of propagation are highly localized in both latitude and longitude, or that the number of whistlers is highly sensitive to thunderstorm activity in the immediate vicinity of the ends of the path of propagation.

Chorus and hiss show a peak in occurrence at about 56° to 58° geomagnetic latitude, the distribution being skewed toward the high-latitude side. It was discovered that the latitude distribution of chorus is sensitive to magnetic index. For days of average $K_p \leq 1.5$, chorus peaks at 64° , while for days of average $K_p \geq 4$, the chorus peaks at 58° . Thus, it appears that location of chorus generation, like the aurorae, moves toward the equator during the disturbed periods.

Chorus and hiss occur more frequently on days of low-background noise than on days of high noise. The effect is apparently not due to increased detectability on days of low noise, since whistler rates do not show the correlation. This conclusion is based on one year of data from six stations. On the average, there was twice as much chorus and hiss on days of low noise as on days of high noise. The reduction in background noise is believed to have been caused mainly by increased absorption of

*Stanford University, Stanford, Calif.

atmospheres of relatively distant origin. This interesting and apparently significant result is interpreted to mean that the VLF absorption is correlated with the occurrence of chorus and hiss.

The effective area of discrete VLF emissions is found to be comparable with that for whistlers (i.e., about 1,000 km across), suggesting that the paths of propagation for emissions and whistlers may be the same. No cases of the same VLF emission forms occurring at conjugate stations have been found, indicating that the generation mechanism is highly asymmetrical with respect to the geomagnetic equator.

Whistler dispersion data show an interesting and unexpected annual variation for several stations. The dispersion was determined from time delay measurements at 5 kc/s [Carpenter, 1960]. Dispersion is minimum at the June solstice and maximum at the December solstice, and shows the same variation in both hemispheres. The explanation of this remarkable circumstance is not clear, but may be related to the eccentricity of the earth's orbit about the sun or to the seasonal asymmetry in the relation between the sun-earth line and the geomagnetic equator.

A comprehensive study of nose whistler dispersions using data from both hemispheres support the annual variation of dispersion found for ordinary whistlers. Furthermore, it is deduced that the annual variation in dispersion indicated by the nose whistlers must be caused mainly by actual electron density changes in the outer ionosphere rather than path changes.

c. Whistler Sources

The spectra and locations of whistler sources are being studied. Although final results of this work are not yet available, some tentative conclusions were reached in cooperation with the Boulder Laboratories of the National Bureau of Standards [Helliwell et al., 1958b]. It was found that often the spectrum of the source peaks at roughly 5 kc/s, whereas most lightning discharges peak at higher frequencies, near 10 kc/s. A tendency was found for whistler-producing discharges to occur more often over sea than over land. It was further shown in this investigation that the predicted time of origin using the Eckersley law of dispersion was often in error by as much as 0.4 sec. This discrepancy is readily explained in terms of the theory of noise whistlers.

d. Association Between Auroras and VLF Hiss Observed at Byrd Station, Antarctica [Martin et al., 1960]

At Byrd Station, Antarctica (70.5° S Geomagnetic) detailed and remarkably interesting records of hiss, chorus and whistlers have been obtained. Various bands of hiss have been identified ranging from the lower frequency limit of the recorder (150 c/s) to the upper frequency limit (16,000 c/s). The hiss above about 4 kc/s shows a close association

with visual aurora observed at the same station. The center frequency of this hiss is about 8 kc/s and shows variations which may be related to the particular type of aurora; in particular, a center frequency of 9.6 kc/s appears to be associated with "red" aurora. The average intensity of the auroral hiss ranges from 1 to 3 mv/m.

e. Duct Theory

Multiple path whistlers are explained in terms of discrete paths of propagation in the outer ionosphere. It is postulated that such paths are created by columns of enhanced ionization aligned with the earth's magnetic field. These "ducts" of ionization act much like ordinary wave guides. Experimental evidence supporting this hypothesis has been obtained from "hybrid" whistlers. A hybrid whistler consists of both long and short components excited by the same source. The delay of the short component is exactly one-half the delay of the long component. It is concluded, therefore, that the dispersion of a whistler is independent of the location of its source and depends only on the properties of the ionosphere. Further evidence in support of the duct theory is found in whistler echo trains, in which the echo delays are always multiples of some particular component in the initial whistler. Other evidence is found in the integral relation between the delays of simultaneous long and short whistlers excited by different sources in opposite hemispheres.

f. Ray-Path Calculations

The guiding of whistlers was treated using ray path concepts [Smith, 1960b]. The maximum allowable half-angle of the ray path cone was found to decrease from 19°29' at zero frequency (deduced first by Storey) to 11° at $f=0.19f_H$, then increase to 90° at $f=f_H$.

Calculations based on the ray-path equation derived by Hazelgrove were made for various frequencies, geomagnetic latitudes, initial wave normal directions, and models of the ionosphere [Yabroff, 1959]. Generally speaking, the ray paths do not follow the earth's magnetic field when a smooth distribution is assumed. The final latitude may be either greater or less than the initial latitude depending on conditions. Under some conditions, there is spatial focusing of the energy for certain initial latitudes. There can also be time delay focusing in which wave packets entering the ionosphere over a range of latitudes arrives in the opposite hemisphere with the same total delay.

Ray theory concepts were applied to the problem of whistler propagation in ducts [Smith et al., 1960a]. It was found that total trapping of the whistler energy will occur whenever the electron density at the center of the column exceeds the background level by a certain amount. Under certain conditions the energy can be trapped in a minimum of ionization. For middle latitudes, enhancements of

the order of only 10 percent are required to completely trap the whistler. The theory explains the marked decrease in whistler occurrence with decreasing latitude.

g. Electron Density of the Outer Ionosphere

Nose whistlers from stations in both hemispheres have shown a consistent relationship between nose frequency and nose time delay. Nose frequencies vary from 3.0 to 32 kc/s. Theoretical analysis of the dispersion of nose whistlers has led to a new method for calculating the electron density of the outer ionosphere. It is found that the shape of the nose whistler trace is insensitive to the shape of allowable electron density models. Application of this theory to the data gives a model of the outer ionosphere out to five earth radii. The average distribution of electron plasma frequency in cps can be given approximately by

$$f_o = 1,200 f_H^{\frac{1}{2}}$$

where f_H is the electron gyrofrequency in cycles per second.

h. Theory of VLF Emissions

A theory of the origin of the VLF emissions was developed jointly by Gallet and Helliwell [1959a]. It accounts, in a general way, for VLF emissions and very long trains of whistler echoes.

The required magnitude of traveling wave gain was assumed in developing the theory. Further theoretical work has led to a quantitative solution for the gain along a low density stream flowing through a plasma [Bell and Helliwell, 1959]. For a particular simplified case thought to be typical of the conditions related to VLF emissions, a gain of approximately 2 db per wavelength in the medium was obtained.

i. Controlled Whistler-Mode Experiments

Observations at Cape Horn, South America, of pulses from Station NSS on 15.5 kcs, Annapolis, Md. demonstrated that the whistler-mode is open a large fraction of the time at night, but that the paths of propagation vary widely from night to night [Helliwell et al., 1958a]. Time delays from the man-made signals were in close agreement with those obtained from whistlers. Simultaneous recordings at Byrd Station (70.5° Geomagnetic) and Greenbank, W. Va. (50° Geomagnetic) showed that the Northern Hemisphere echo delays are not twice those from the Southern Hemisphere. Quantitative comparison of these results with Cape Horn NSS data and whistler data support the interpretation that the measured echo delay depends on the strongest component which in turn depends on the location of transmitter and receiver.

j. Satellite Measurements

Signal strength measurements of Station NSS and background noise were made at 15.5 kc/s in

Explorer VI. Data are currently being analyzed. Clear signals from NSS were picked up by the satellite receiver from the launching point up to the D-region. Above 70 km NSS disappeared into the background noise, presumably because of D-region absorption. No unusual sources of natural noise were discovered within the ionosphere. However, the sensitivity of the receiver was limited by interference thought to have been generated by power converters within the satellite. It appears that for frequencies below the gyrofrequency the outer ionosphere is relatively quiet, being shielded from both extra-terrestrial noise and terrestrial atmospherics.

k. Geocyclotron

A new mechanism for accelerating charged particles in the outer ionosphere is proposed [Helliwell et al., 1960]. It is based on the properties of whistler-mode propagation, and the device for performing experiments is called the "geocyclotron". A circularly polarized swept-frequency VLF transmitter located on the ground or in a satellite accelerates relativistic electrons trapped by the earth's magnetic field. Energy from a ground-based transmitter reaches the interaction region by propagating in the whistler mode. The frequency of the radiation is adjusted so as to equal the gyrofrequency of relativistic electrons circling the lines of force of the earth's field in the plane of the geomagnetic equator. The frequency is decreased with time in such a way as to impart energy to the relativistic electrons. The mechanism is roughly analogous to that which takes place in a synrocyclotron. The presence of the artificially accelerated particles, which should form a shell about the earth, could be detected with radiation counters carried in a satellite or probe.

The geocyclotron could be used in various ways to study dynamic processes in the outer ionosphere as well as whistler-mode propagation.

3.2. Dartmouth College

M. G. Morgan*

a. Whistlers-East

A meridional chain of observing stations, nominally along W75° was set up to make synoptic observations during the IGY from Thule to Florida, at Huanacayo, and from Cape Horn to Antarctica. Fifteen stations were involved, each a story unto itself. Cooperating, in order of latitude, were Danes, Canadians, Americans, Bermudians, Peruvians, Argentines, and Britons. Some results have been published by independent cooperating workers as for example the Godhavn, Greenland, results by Ungstrup [1959], and the Washington results

*Dartmouth College, Hanover, N.H.

by Dinger [1960]. Geographically comprehensive studies have been made at Dartmouth and will soon be presented for publication. The following conclusions are based on the subjective reduction of the magnetic tapes and subsequent statistical analysis. (Latitudes given are geomagnetic.)

(1) *Whistlers*. In the Northern Hemisphere, in the longitude under study, very nearly all whistlers observed are found to be "long", and in the Southern Hemisphere, very nearly all to be "short". There is a pronounced seasonal variation in activity with a large maximum in July and August and a smaller maximum in January and February. These maxima are found in the data from both hemispheres. In the northern winter months, the northern stations report more activity in long whistlers than do the southern stations in short whistlers.

The northern stations, Knob Lake (66°), Mont Joli (60°), and Dartmouth (55°), exhibit similar and consistent patterns of whistler activity, whereas, for reasons unknown, Washington (50°) and Bermuda (44°) are notably different. (A point to consider is that these two stations used long-wire antennas, whereas all others used loops.)

In the Northern Hemisphere, whistler activity reaches a peak at about 55° and falls off rapidly above and below that latitude. In the Southern Hemisphere, it can be said that activity at Port Lockroy (53.0°) is significantly greater than at Ellsworth (67°) or at Ushuaia (43.3°).

Generally speaking, there is a broad diurnal maximum of activity at each station during the nighttime hours, and a distinct minimum just before local noon. The ratio of maximum activity to minimum varies widely from station to station and seasonally.

At Battle Creek, 13° west of Dartmouth and 2° south, the pattern of behavior has been found to be similar to that at Dartmouth but at a much lower level.

At Huancayo on the geomagnetic equator, no whistlers were reported, though the station was well run throughout 1958 and all of the tapes carefully monitored. Taking a time of very high whistler activity at Dartmouth and listening to the corresponding recordings from Huancayo, it appears that very, very faint whistlers can occasionally be heard. They would never be detected without concentrating attention on a particular moment as directed by observations from higher latitudes. The noise level at Huancayo is, of course, uniformly high.

At Knob Lake (66°) only weak, long whistlers have been heard. At Frobisher Bay (75°), they are also heard but less often and even more weakly. They have not been heard at Godhavn (80°). Short whistlerlike signals having $D=40$ to 60 and a high minimum frequency have been heard at Frobisher Bay and Godhavn, but it is an unanswered question whether these are ordinary whistlers or some other form of emission.

A study has been made of meteorological conditions at 06 h Z for 1957 October, November, and December in an effort to discern a geographical pattern of

storms associated with long whistlers observed at Dartmouth. Of the 92 days involved, whistlers were observed at Dartmouth on 66 and none on 26. Storms with electrical discharges reported were located in the general area of eastern United States and the North Atlantic on 89 days. It is interesting to note that on the three days when no storms were reported, long whistlers were observed.

The incidence of whistler echoes has been studied. Although it shows a large and smooth diurnal variation, very closely repeated from 1 yr to the next, ranging from 5 periods/month at 01 h Z to 0.3/month at 14 h Z (respectively, 20 h and 09 h W 75° time); the diurnal variation of the probability that echoes will occur when whistlers are present, is only about 2:1. The maximum and minimum of the probability curve occur at approximately the same time as those of the echo curves themselves.

(2) *Ionospherics*. During the IGY, naturally occurring VLF phenomena other than whistlers, were grouped into three ill-defined categories: "chorus", "hiss", and "other". Together these were called "VLF emissions". We have now adopted the term "ionospherics" for these, as contrasted with "tropospherics" (lightning). As defined for the IGY, "hiss" was taken to mean a broad band of noise of no special bandwidth or frequency; phenomena which occurred as isolated events or "unusual" sounds were called "other"; and most everything else, "chorus." On the basis of these definitions, the following facts have been determined concerning chorus.

In the Northern Hemisphere, stations at 55° to 60° show the most activity. The activity has a sharp maximum in April and May and a minimum in November and December.

In the Southern Hemisphere, Ellsworth (67°) shows consistently greater activity than Port Lockroy (53.4°), and, remarkably, both show a pattern largely independent of the time of year. Chorus is rarely heard at Ushuaia (43.3°). At Ellsworth it is present about 40 percent of the time.

The diurnal variation of chorus activity is sharply defined at 11 h Z (6 h W 75° time), at Mont Joli (N 60°), and at Dartmouth (N 55°), whereas at Washington (N 50°) and Bermuda (N 44°), there is a maximum near 08 h Z (03 h W 75° time). Ellsworth (S 67°) and Mont Joli (N 60°) show almost identical activity but Port Lockroy (S 53.4°) shows hardly any notable diurnal variation.

The diurnal variation seems to differ but slightly with the season. At Dartmouth, the station for which most data are available, activity for May—July and for August—October have about the same diurnal variation with a peak at 10 h Z. The diurnal variations of the activity in the periods February—April and November—June are similar to each other but have a broad maximum at 09 to 12 h Z. The level of activity for the spring months is about twice that for the winter months.

As with whistlers, the pattern of chorus activity at Battle Creek has been found to be very similar to that at Dartmouth, but the level much lower.

No ionospherics were reported from Huancayo, but chorus is heard up to the very highest latitudes, including Thule (N 88°).

Very little analysis of "hiss" and "other" has been carried out so far. It can be said that more hiss has been observed at Dartmouth than at any other station.

b. E 4° (Geomagnetic) Stations: Successor to Whistlers-East

Recognizing that the three southern hemisphere points, Ushuaia, Port Lockroy, and Ellsworth are about the best that can be had for the foreseeable future, and that the northern conjugate positions of these stations line up along W 65° (E 4° geomagnetic), attention has been concentrated along that line in the Northern Hemisphere. Frobisher Bay (75°) and Knob Lake (66°) lie close to that line. Mont Joli (60°) is being moved 150 miles northeastward to Moisie (61.7°) 15 miles east of Sept Isles on the north shore of the St. Lawrence Gulf, and a station is being established in southernmost Nova Scotia. The Bermuda station has been moved to a vastly improved location. Washington and Gainesville, Fla., have been discontinued, and Huancayo has been discontinued.

c. Post-IGY Results

Commencing with all data taken after 1959 July 1, the classification of ionospherics has been greatly refined and this is producing interesting new results. For example, the chorus data from Mont Joli (60°) and Dartmouth (55°), when restricted to rising tones only, recurring faster than 2/sec, and going above 2 kc/s, have a maximum occurrence at the same local time rather than 1.5 to 3 hr later at the higher latitude when all forms of chorus are lumped together.

d. E 94° (Geomagnetic) Stations

At the instigation of Dartmouth workers, stations have been set up on Saltholmen Island in the strait between Denmark and Sweden at Copenhagen, and at Marion Island 1,400 miles southeast of Cape Town. Although in geomagnetic latitudes N 55° and S 49°, respectively, these stations are very close to conjugate positions. A station has also been set up at Naples which is close to the northern conjugate of Durban, South Africa. These stations are in geomagnetic latitudes N 42° and S 32°, respectively. The two pairs of stations lie close to the E 94° geomagnetic meridian and are, therefore, exactly 90° east of the E 4° stations. In addition to whistler observations, the 16 kc/s whistler-mode signals from GBR in Rugby will be observed at Marion Island, which is less than 400 miles from Rugby's conjugate position.

The cooperating institutions are the Royal Technical University of Denmark, the University of Naples, the University of Natal, and Dartmouth College. A graduate student from the University of Natal is spending a year at Marion Island.

e. Angle of Arrival Measurements

An experiment to measure the angle of arrival of whistlers and ionospherics by comparing the time of arrival at three stations mutually 100 km apart is in progress and results will be available for reporting to the XIIIth Assembly.

f. Acknowledgment

The portion of this work undertaken by or assisted by Dartmouth College, has been made possible by the financial assistance of the United States National Committee for the IGY, by the United States National Science Foundation, and by the United States Air Force Cambridge Research Center (GRD).

4. A Summary of VLF and ELF Propagation Research

James R. Wait*

4.1. Introduction

The renewed interest in the VLF and ELF portions of the radio spectrum has been very evident in the 3 yr since the previous General Assembly of URSI. Applications of VLF and ELF to long-distance communication, worldwide frequency standards, navigational aids, and detection of storms, are providing continuous motivation for further research in this field.**

It is the purpose of this report to summarize research activity in VLF and ELF propagation carried out in the USA since January 1, 1957. Attention is confined to published papers relating to terrestrial propagation, and thus reference to solar and exospheric phenomena is excluded. Closely related work carried out in other countries is also briefly mentioned.

4.2. Theoretical Studies

For certain applications at VLF, particularly at short ranges, it is permissible to neglect the presence of the ionosphere. In fact, at frequencies of the order of 100 kc/s the groundwave may dominate the skywave for ranges as great as 500 km. Furthermore, with the use of pulse-type transmissions, such as used in the Cytac or Loran C navigation systems, the groundwave may be distinguished from the skywave for distances as great as 2,000 km [Frantz, 1957; Dean, 1957; Frank, 1957]. With this motivation, a number of theoretical papers on groundwave propagation have appeared in the literature dealing specifically with: (a) Amplitude and phase versus distance curves [Johler et al., 1956; Wait et al., 1956a; Johler et al., 1959a]; (b) land-sea boundary effects [Wait, 1958b; Wait et al., 1957c]; and (c) propagation of electromagnetic pulses over the surface of homogeneous and inhomogeneous ground [Wait, 1956c; Johler, 1957; Wait, 1957h; Wait, 1957a; Levy et al., 1958; Johler, 1958; Johler et al., 1959b; Wait et al., 1959b; Wait, 1957d]. The penetration of groundwave fields into the earth or sea has also been considered in some detail [Wait, 1959c; Wait, 1959d; Kraichman, 1960; Keilson, 1959] and the influence of earth stratification on the attenuation rate of the groundwave has been given further attention [Stanley, 1960; Wait, 1958e].

Unfortunately, in cw systems and at distances as small as 100 km from the source, the sky wave may often interfere with the groundwave. Thus, the total field may be considered as the resultant of a groundwave and a number of ionospherically reflected waves in the VLF band at moderate ranges

(i.e., less than 1,000 km or so) [Wait et al., 1957b; Wait et al., 1957f; Johler et al., 1960; Pfister, 1953; Poverlein, 1958a; Poverlein, 1958b]. However, it appears to be more convenient to represent the total field as a sum of waveguide type modes for VLF at great distances and, for ELF, at nearly all distances. In fact, for many applications only one or two modes need be retained, since the higher modes are either "cutoff" or have severe attenuation. A number of papers on mode theory were presented at the VLF Symposium held in Boulder, Colo. January 1957 [Liebermann, 1956b; Budden, 1957; Wait, 1957g; Wait, 1957e]. In these, the ionosphere was represented by a sharply bounded and homogeneous ionized medium, and the influence of the earth's magnetic field was neglected. Also, since the frequency could be assumed to be much less than the effective collision frequency, the ionosphere was equivalent to an isotropic conductor. More recent investigations of mode theory have removed some of the earlier restrictions. For example, the influence of stratification in the *D* and *E* regions was accounted for by using layered and exponential models [Shmoys, 1956; Wait, 1958a; Wait, 1960b; Bremmer, 1959].

It is interesting to observe that Al'pert in the USSR has also pursued the mode theory of VLF propagation [Al'pert, 1956]. In his work he also neglects the earth's magnetic field and, in his initial formulation, the ionosphere is sharply bounded. He treats the effect of ionospheric stratification by using an Epstein model which is strictly valid only for horizontal polarization. In much of the work on this topic, the effect of earth curvature is neglected for purposes of computing the attenuation of the modes. Some time earlier, Budden [1952] had obtained a first-order correction for earth curvature by using an earth-flattening type of approximation, and more recently Wait [1958f] had used a similar modification in some published curves of VLF transmission loss. From this work, it appears that earth curvature has a negligible effect on the modes for frequencies less than about 15 kc/s.

Actually, for frequencies at the upper end of the VLF band (i.e., 15 to 30 kc/s), it is necessary to abandon first-order curvature corrections and to introduce higher-order approximations for the spherical-wave functions which occur in the rigorous formulation. This aspect of the problem is discussed at length by Wait in a recent paper which includes an extensive discussion of related theoretical work [Wait, 1960c].

The influence of the earth's magnetic field on the attenuation and phase of the modes is a difficult subject. However, if expressions for the plane-wave reflection coefficients for an anisotropic ionosphere can be derived, it is not too difficult to extend these to the computation of the modes [Budden, 1952; Wait, 1960c]. Thus, the results of Bremmer [1949],

*National Bureau of Standards, Boulder, Colo.

**The VLF band is here defined as the decade 3 to 30 kc/s and the ELF band covers the range 1.0 c/s to 3 kc/s.

Yabroff, [1957], and others [Wait et al., 1957b; Wait et al., 1957f; Jöhler et al., 1960] may be adapted for mode propagation between the curved earth and a doubly refracting ionosphere [Wait, 1960c]. Using such an approach, Crombie [1960] has adapted the plane-wave reflection coefficients for a *transverse* magnetic field to the case of mode propagation around the magnetic equator. The latter example clearly demonstrates nonreciprocity in VLF propagation.

While the mode theory would seem to be particularly appropriate at ELF, certain assumptions which are usually made become questionable. These longer wavelengths penetrate further into the ionosphere so that the sharply bounded model must be modified [Bremmer, 1959]. Another approach is to postulate an effective increase in the ionospheric height as the frequency decreases [Pierce, in press]. Even more important at ELF is the fact that distance from source to observer is usually comparable with the wavelength. Thus, the numerical treatment of the mode series has been considered by Wait [1960a] for unrestricted distances.

Again using the concept of modes, the propagation of both VLF and ELF pulses has also received considerable attention [Liebermann, 1956b; Wait, 1960a; Wait, 1958c]. Of some importance is the manner in which the quasi-half periods of the oscillatory waveform of the pulse vary with range and time [Wait, 1958c].

4.3. Experimental Studies

Since the observed characteristics of VLF and ELF propagation depend on so many factors, one should be careful in placing undue emphasis on any single experiment. In particular, the validity of a particular theoretical model cannot be established on a basis of experimental data obtained in a single geographical area and for restricted intervals of time. Nevertheless, certain experiments are crucial in the sense that they confirm the concept of the model. For example, if the measured dependence of VLF field strengths on distance and frequency are in general accord with theoretical predictions, one can say that, at least for those ionospheric conditions, the model is perhaps adequate in a phenomenological sense.

A crucial test of the waveguide mode concept of VLF propagation was provided by Heritage, Weisbrod, and Bickel [1957] in a series of airborne measurements of field strengths in the Pacific Ocean. They utilized transmissions in the frequency range of 16 to 20 kc/s from the United States, Hawaii, and Japan. The daytime experimental data were in good agreement with the mode theory as indicated by Wait [1957g]; however, the nighttime data were highly variable and certain nonreciprocal effects were in evidence.

The U.S. Navy is also conducting a long-range study of VLF propagation characteristics by means of measurements made over several paths selected to show the effects of various geophysical conditions

encountered (private communications from H. E. Dinger, Naval Research Laboratory).

Phase variations of the 16 kc/s carrier signal of station GBR in England have been measured by Pierce (J. A.) [1955; 1957] in Cambridge, Massachusetts. The diurnal variation of the change of the phase has been interpreted by Wait [1959a] in terms of mode theory in a satisfactory manner.

4.4. Recent Applications of VLF Propagation

Research in VLF propagation has been prompted by many important applications. In particular, the low attenuation and high-phase stability of VLF signals make it feasible to set up a worldwide frequency standard employing only one transmitter. A careful study of this problem by Watt and colleagues [Watt et al., 1959] indicates that a minimum radiated power of 10 to 100 kw for frequencies of 20 kc/s would be required. Minimum observation times of 15 to 30 min would be needed to obtain a precision of frequency of 1 part in 10^9 . Another application is to long-range navigational systems such as the Radux-Omega in which the phase difference between two widely separated transmitting stations is measured. Frequencies used in this system are in the range 10 to 18 kc/s with typical phase stabilities on a path of 8,000 km of 4 μ secs in day and 5 μ secs at night [Casselman et al., 1959].

By application of highly precise quartz oscillators coupled with the use of atomic frequency standards, it has become possible for the U.S. Navy to stabilize its existing VLF transmitters so as to provide extremely accurate frequency and time information to naval units on a worldwide basis. The Naval Radio Station (NBA) at Balboa in the Canal Zone, Panama, has been equipped by the Naval Research Laboratory for this service and is now transmitting precise time and constant frequency. The Pearl Harbor, San Francisco, Culter, and Annapolis stations will be controlled by constant frequency as soon as equipment becomes available. Thus, no additional VLF spectrum will be required to provide the entire Navy with complete synchronization of time and frequency. These transmissions should also provide an excellent tool for propagation studies at VLF (private communication from H. F. Hastings, Naval Research Laboratory).

Many studies of VLF propagation have been made using lightning strokes as a source of energy. For example, Watt and Maxwell [1957a] showed that the propagation modified the spectral content of atmospheric radio noise in a manner which again was quite compatible with mode theory. In particular, the predicted absorption band [Wait, 1957e] at frequencies around 3 kc/s was confirmed. Attenuation rates at VLF have been deduced from the spectral analyses of atmospheric waveforms observed simultaneously at widely separated stations [Taylor et al., 1959a; Taylor, 1960]. A similar technique has been developed for deducing phase characteristics of VLF propagation in a frequency range from 1 to 30 kc/s [Jean et al., 1960].

gnal of
red by
Massa-
nge of
59a] in
r.

agation

empted
ar, the
f VLF
de fre-
mitter.
d col-
nimum
cies of
vation
tain a
nother
as such
erence
ations
are in
ilities
 μ secs

llators
dards,
abilize
de ex-
nation
Radio
Pana-
search
itting
Pearl
apolis
cy as
is, no
rovide
zation
hould
udies
tings,

been
nergy.
l that
nt of
again
par-
957e]
atten-
n the
erved
aylor
e has
ics of
to 30

Experimental studies at ELF have been primarily devoted to the recording of the ELF or "slow tail" portion of the atmospheric waveforms [Liebermann, 1956a; Holzer et al., 1957; Teplov, 1959]. In many cases, it appears that this ELF part of the waveform is a highly damped pulse with seldom more than two half-cycles with periods of the order of several milliseconds. The relation of ELF wave shapes to the orientation of the lightning stroke has been recently analyzed [Wait, 1960a].

In presenting propagation data at VLF and ELF care should be used in properly separating the losses

due to propagation and those due to the antenna systems. It is important that the change of impedance of the antennas due to the ground plane be accounted for. To retain the basic idea of power transfer introduced by Norton [1953], yet separate out the influence of the antenna environment, the concept of "propagation loss" was proposed [Wait, 1959e]. It forms one component of the system loss [Norton, 1959] which is the decibel ratio of the power into the terminals of the transmitting antenna to the power available at the terminals of the receiving antenna.

5. Hydromagnetic Waves and ELF Oscillations in the Ionosphere

James M. Watts*

The hypothesis that hydromagnetic waves [Alfvén, 1942; Lundquist, 1949] occur in the ionosphere has been pursued theoretically, observationally and experimentally in the United States.

The theoretical investigations have usually taken the form of arguments for the existence of these waves, since the conditions for their propagation exist in the region [Dessler, 1958]. The theories of the consequences of the waves have then been extended to explain certain geophysical phenomena, such as the sudden commencements of magnetic storms [Francis et al., 1959; Dessler et al., 1959a] and auroras [Warwick, 1959], ionospheric heating [Dessler, 1959b], ionospheric tides [White, 1960a; 1960b], and the motion of ionized gas near the earth [Gold, 1959].

A review of the observations of geomagnetic oscillations suggests that they may be explained by waves of the Alfvén type [Maple, 1959] excited by solar disturbances since 27-day solar dependence and correlations with magnetic and ionospheric *F*-layer disturbances were evident [Campbell, 1959; Berthold et al., 1960; Campbell, 1960].

However, hydromagnetic oscillations do not seem to explain other classes of electromagnetic disturbances [Watts, 1957; Gallet, 1959b] whose frequencies are principally well above those characteristics of geomagnetic micropulsations. Therefore, emphasis has been placed on the theory of traveling wave amplification to explain those phenomena [Gallet et al., 1959a; Bell et al., 1959].

During the triennium 1957 to 1960 controlled experiments have become feasible, using rockets, artificial earth satellites, and nuclear explosives. It has been possible to create hydromagnetic waves in the ionosphere by explosions and observe them by rockets and satellites [Nat. Acad. Sci., 1959; Kellogg et al., 1959]. That the magnitude of these effects is comparable with the magnitudes of natural occurrences is evidenced by the records of conventional magnetometers and by the sighting of auroras [Matsushita, 1959; Steiger et al., 1960].

A rocket alone has shown evidence of instability in the distant geomagnetic field. Measurement of the magnetic field intensity vector at large distances from the earth indicated a complex behavior, including nearly periodic oscillations which may have been due to hydromagnetic waves [Sonett et al., 1959].

*National Bureau of Standards, Boulder, Colo.

6. The Exosphere

James M. Watts*

6.1. Introduction

The lower boundary of the exosphere may be above defined variously as the ionospheric level just about the entire F region, as the critical level above which particles encounter no collisions and are, therefore, in free flight, or as the level above which hydrogen is the predominant constituent. If the outer boundary is taken to be 6 to 8 earth radii, including most of the gas within the region of influence by the earth's magnetic and gravitational fields, the exosphere includes the entire region in which whistlers are greatly dispersed, in which VLF emissions may originate, in which geomagnetic micropulsations are supposed to originate, and in which the earth's trapped radiation lingers.

Therefore, significant understanding of the exosphere has been achieved by observing those phenomena. The reader is referred to the USA report on whistlers for the extensive observations of whistlers and VLF emissions during the IGY, and to the report on hydromagnetic waves and ELF oscillations for references giving the USA work in that region.

6.2. Theories of the Exosphere

a. Magnetic Storm Effects

During 1956, the hypothesis was developed that solar corpuscular radiation can be injected into the earth's magnetic field and trapped there [Singer, 1956]. The particles were considered to create an electric current which was held responsible for the main phase of magnetic storms [Singer, 1957]. Later, a mechanism based on Fermi accelerations for increasing the energy of some of the particles sufficiently to produce some of the auroral effects was proposed [Singer, 1958a; 1958b]. It seemed very possible that the electrons thus accelerated can be identified with the outer radiation belt while the protons injected directly from the sun are removed after a very short time by charge exchange with neutral hydrogen in the earth's exosphere, thus bringing the magnetic storm to a decline after 1 or 2 days [Singer et al., 1960].

b. Radiation Belt Theory

Some work on properties of geomagnetically trapped particles was done prior to their discovery, for example: their penetration into the auroral ionosphere [Rhodes, 1959], the behavior of trapped cosmic ray albedo [Griem et al., 1955], and an experiment for their detection was discussed [Singer, 1958d].

Following the discovery of trapped radiation in

Explorer I in May 1958, the neutron albedo theory was developed as a means of explaining the presence of hard radiation and calculated its approximate altitude distribution, noting the probable existence of a maximum close to the earth [Singer, 1958e; 1958f]. Following this, the existence of two belts was predicted explicitly, one an inner belt close to the earth's equator produced by cosmic ray neutron albedo, and another an outer belt of solar origin and connected with the aurora [Singer, 1958a]. These features were roughly verified by the Pioneer and Lunik probes.

In detail, calculations were made of the lifetime of trapped particles both for protons and for electrons [Wentworth et al., 1959]. The distribution in energy and in space of trapped protons was investigated [Singer, 1959c].

c. Composition of the Exosphere

The distribution of neutral particles in an exosphere, taking into account ballistic and escape orbits, was calculated [Opik, et al., 1959].

Some theoretical work based on knowledge of general features of the ionosphere have led to extrapolation of these features into the exosphere, in order to predict the composition [Singer, 1959b] and densities [Johnson, 1960; Wright, 1960] above the F -layer maximum. From the latter work it appears that the region of the exosphere nearest the F -layer is expected to have a profile resembling a Chapman layer with a scale height of 100 km.

6.3. Experiments in the Exosphere

Experimentally, the region has been explored in several different ways. Rockets for the first time penetrated the region [Van Allen, 1957; Harris et al., 1959] and were the forerunners of the well-known artificial satellite experiments which have delineated the high-intensity radiation belts in the exosphere [Van Allen, 1959b; Van Allen et al., 1959a; Van Allen et al., 1958a and 1958b; Stuart, 1959]. High-altitude explosion of nuclear devices has shown that the radiation belts can be modified artificially and the resulting decay studied to verify that the theory of radiation trapping provides the correct way of interpreting the natural radiation [Singer, 1959a; Nat. Acad. Sci., 1959b].

Experiments not involving satellites and rockets, however, are relatively inexpensive and are well adapted to measuring the electronic content of the exosphere.

The moon radar measurements of Faraday rotation [Bauer et al., 1958] have given an excellent picture of the total electron content of the ionosphere plus exosphere and its variation with time.

*National Bureau of Standards, Boulder, Colo.

An entirely new technique for vertical incidence sounding of the ionosphere [Bowles, 1958] has the advantage that blanketing reflections do not obscure details above the maxima of layers, since all reflections are partial for the frequencies used. This use of extra high power and sensitivity in a sounder enables true heights and electron densities to be measured directly and should be a powerful means of studying the nearer regions of the exosphere.

7. References

- Alfvén, H., Existence of electromagnetic-hydrodynamic waves, *Nature* **150**, 405 (1942).
- Alcock, G. McK., and M. G. Morgan, Solar activity and whistler dispersion, *J. Geophys. Research* **63**, 573-576 (1958).
- Alpert, Y. A., Computation of the field of LF and VLF radio waves over the earth's surface under natural conditions, *Radiotekh. i Elektron.* **1**, 281 (1956).
- Atlas, D., Radar lightning echoes and atmospherics in vertical cross-section, *Recent Adv. Atmos. Elect.*, 441 (1958).
- Bauer, S. J., and F. B. Daniels, Ionospheric parameters deduced from the faraday rotation of lunar radio reflection, *J. Geophys. Research* **63**, 439 (1958).
- Bays, C. V., Progressive lightning, *Nature* **118**, 749 (1926).
- Bell, T. F., and R. A. Helliwell, Traveling-wave amplification in the ionosphere, *Stanford Elect. Labs. Tech. Rpt.* **2** (1959).
- Berthold, W. K., and A. K. Harris, H. J. Hope, Correlated micropulsations at magnetic sudden commencements, *J. Geophys. Research* **65**, 613 (1960).
- Bowles, K. L., Observation of vertical incidence scatter from the ionosphere at 41 Mc/sec., *Phys. Rev. Letters* **1**, 12 (1958).
- Bremmer, H., *Terrestrial radio waves*, Elsevier Press (1949).
- Bremmer, H., Mode expansion in the low-frequency range for propagation through a curved stratified atmosphere, *J. Research NBS* **63D**, 75 (1959).
- Brook, M., Thunderstorm electricity, New Mexico Inst. Mining and Tech., Research and Dev. Div., Socorro, New Mexico (1957).
- Budden, K. G., The propagation of a radio-atmospheric, Pt. II, *Phil. Mag.* **43**, 1179 (1952).
- Budden, K. G., The "waveguide mode" theory of the propagation of very-low-frequency radio waves, *Proc. IRE* **45**, 772 (1957).
- Campbell, W. H., Studies of magnetic field micropulsation with periods of 5 to 30 seconds, *J. Geophys. Research* **64**, 1819 (1959).
- Campbell, W. H., Magnetic micropulsations and the pulsating aurora, *J. Geophys. Research* **65**, 784 (1960).
- Carpenter, D. L., Identification of whistler sources on visual records and a method of routine whistler analysis, *Stanford Elect. Labs. Tech. Rpt.* No. 5 (1960).
- Casselmann, C. J., and D. P. Heritage, M. L. Tibbals, VLF propagation measurements for the radux-omega navigation system, *Proc. IRE* **47**, 829 (1959).
- C.C.I.R. Rpt. 65, Revision of atmospheric radio noise data, Internat. Telecom. Union, Geneva (1957).
- Crichlow, W. Q., D. F. Smith, R. N. Morton, and W. R. Corliss, Worldwide radio noise levels expected in the frequency band 10 kilocycles to 100 megacycles, *NBS Circ.* **557** (1955).
- Crichlow, W. Q., Noise investigation at VLF by the National Bureau of Standards, *Proc. IRE* **45**, 6, 778 (1957).
- Crichlow, W. Q., C. A. Samson, R. T. Disney, and M. A. Jenkins, Radio noise data for the International Geophysical Year July 1, 1957-December 31, 1958, *NBS Tech. Note* **18** (1959a).
- Crichlow, W. Q., C. A. Samson, R. T. Disney, and M. A. Jenkins, Quarterly Radio Noise Data-March, April, May 1959, *NBS Tech. Note* **18-2** (1959b).
- Crichlow, W. Q., C. J. Roubique, A. D. Spaulding, and W. M. Beery, Determination of the amplitude-probability distribution of atmospheric radio noise from statistical moments, *J. Research NBS* **64D**, (1960a).
- Crichlow, W. Q., A. D. Spaulding, C. J. Roubique, and R. T. Disney, Handbook of amplitude-probability distributions for atmospheric radio noise, Approved for publication as an NBS Monograph (1960b).
- Crombie, D. D., On the mode theory of VLF propagation in the presence of a transverse magnetic field, *J. Research NBS* **64D**, (1960).
- Dean, W., A precision multi-purpose radio navigation system, Pt. II, Propagation characteristics, *IRE Nat. Convention Record* (1957).
- Dessler, A. J., Large amplitude hydromagnetic waves above the ionosphere, *J. Geophys. Research* **63**, 507 (1958).
- Dessler, A. J., and E. N. Parker, Hydromagnetic theory of geomagnetic storms, *J. Geophys. Research* **64**, **12**, 2232 (1959a).
- Dessler, A. J., Ionospheric heating by hydromagnetic waves, *J. Geophys. Research* **64**, 397 (1959b).
- Dinger, H. E., *J. Geophys. Research* **571** (1960).
- Francis, W. E., M. I. Green, and A. J. Dessler, Hydromagnetic propagation of sudden commencements of magnetic storms, *J. Geophys. Research* **64**, 1643 (1959).
- Frank, R. L., A precision multi-purpose radio navigation system, Pt. III, Instrumentation, *IRE Nat. Convention Record* (1957).
- Frantz, W. P., A precision multi-purpose radio navigation system, Pt. I, characteristics and applications, *IRE Nat. Convention Record* (1957).
- Fulton, F. F. Jr., The effect of receiver bandwidth on amplitude distribution of VLF atmospheric noise, *Prepublication Record, Symposium on Propagation of VLF Radio Waves*, NBS, Boulder, Colo., **III**, Paper 37 (1957)-to be published in *J. Research NBS*, Sec. D.
- Gallet, R. M., and R. A. Helliwell, Origin of 'very-low-frequency emissions', *J. Research NBS* **63D**, **1**, 21-27 (1959a).
- Gallet, R. M., The very low-frequency emissions generated in the earth's exosphere, *Proc. IRE*, **211-231** (1959b).
- George, T. S., Investigation of atmospheric radio noise (Final Report), AFRC-TR-362, Univ. of Fla., Gainesville, Fla. (1957).
- Gold, T., Motions in the magnetosphere of the earth, *J. Geophys. Research* **64**, **9**, 1219 (1959).
- Griem, H., and S. F. Singer, Geomagnetic albedo at rocket altitudes at the equator, *Phys. Rev.* **99**, 608 (1955).
- Harris, I., and R. Jastrow, Atmosphere derived from rocket and satellite data, *Planetary and Space Sci.* **1**, 20 (1959).
- Hefley, G., R. F. Linfield, and R. H. Doherty, Initial results of a new technique for investigating sferic activity, *J. Research NBS* (to be published in **64D**, Sept. 1960).
- Helliwell, R. A., and E. Gehrels, Observations of magnetospheric duct propagation using man-made signals of very low frequency, *Proc. IRE* **46**, **4**, 785-787 (1958a).
- Helliwell, R. A., A. G. Jean, and W. L. Taylor, Some properties of lightning impulses which produce whistlers, *PIRE* **46**, **10**, 1760-1762 (1958b).
- Helliwell, R. A., Whistlers and very low frequency emissions, *Geophysics and the IGY*, *Geophys. Mono.* **2**, AGU, 35-44 (1958c).
- Helliwell, R. A., and T. F. Bell, A new mechanism for accelerating electrons in the outer ionosphere, *Stanford Elect. Labs. Tech. Rpt.* **4** (1960).
- Hepburn, F., Wave-guide interpretation of atmospheric waveforms, *J. Atmospheric and Terrest. Phys.* **10**, 121 (1957).
- Heritage, J. L., S. Weisbrod, and J. E. Bickel, A study of signal versus distance data at VLF, *Symposium on the Propagation of VLF Radio Waves*, *Prepublication Record* **4**, **29**, NBS, Boulder, Colo. (1957).
- Hill, E. L., Very low-frequency radiation from lightning strokes, *Proc. IRE* **45**, **6**, 775 (1957).
- Hoff, R. S., and R. C. Johnson, A statistical approach to the measurement of atmospheric noise, *Proc. IRE* **40**, **2**, 185 (1952).
- Holzer, R. E., O. E. Deal, and S. Ruttenberg, Low audio frequency natural electromagnetic signals, *Symposium on the Propagation of VLF Radio Waves*, *Prepublication Record* **3**, **45**, NBS Boulder, Colo. (1957). See also

- R. E. Holzer, World thunderstorm activity and ELF series, *Recent Adv. in Atm. Elec.*, 559 (1959).
- Horner, F., An investigation of atmospheric radio noise at very low frequencies, *Proc. Inst. Elec. Engs.*, Pt. B **103**, 743 (1956).
- Jean, A. G., W. L. Taylor, and J. R. Wait, VLF Phase characteristics deduced from atmospheric waveforms, *J. Geophys. Research* **65**, (1960).
- Johler, J. R., W. J. Kellar, and L. C. Walters, Phase of the low radiofrequency ground wave, *NBS Circ.* **573**, (1956).
- Johler, J. R., Propagation of the radiofrequency ground-wave transient over a finitely conducting plane earth, *Geofis. pura e appl. (Milan)*, **37**, 116 (1957).
- Johler, J. R., Transient radio frequency ground waves over the surface of a finitely conducting plane earth, *J. Research NBS* **60**, 281 (1958).
- Johler, J. R., L. C. Walters, and C. M. Lilley, Low- and very-low-radiofrequency tables of ground-wave parameters for the spherical earth theory: The roots of Riccati's differential equation (supplementary numerical data for NBS Circ. **573**), *NBS Tech. Note* 7 (1959a).
- Johler, J. R., and L. C. Walters, Propagation of a ground-wave pulse around a finitely conducting spherical earth from a damped sinusoidal source current, *IRE Trans. PGAP* **AP-7**, 1 (1959b).
- Johler, J. R., and L. C. Walters, On the theory of reflection of low- and very-low radio-frequency waves from the ionosphere, *J. Research NBS* **64D** (1960).
- Johnson, F. S., The ion distribution above the F_2 maximum, *J. Geophys. Research* **65**, 577 (1960).
- Johnson, W. C., How to listen for whistlers, *QST* **44**, 50-54 (1960).
- Jones, H. L., The identification of lightning discharges by spheric characteristics, *Recent Adv. in Atm. Elec.*, 543 (1958).
- Keilson, J., and R. V. Row, Transfer of transient electromagnetic waves into a lossy medium, *J. Appl. Phys.* **30**, 1595 (1959).
- Kellogg, P. J., E. P. Ney, and J. R. Winekler, Geophysical effects associated with high-altitude explosions, *Nature* **183**, 358 (1959).
- Kimpara, A., Atmospheres in the Far East, *Recent Adv. in Atm. Elec.*, 565 (1958).
- Kraichman, M., Basic study of electromagnetic sources immersed in conducting media, *J. Research NBS* **64D**, 21 (1960).
- Laby, et al., Waveform, energy and reflection by the ionosphere of atmospheres, *Proc. Roy. Soc. London* **A174**, 145 (1940).
- Levy, B. R., and J. B. Keller, Propagation of electromagnetic pulses around the earth, *IRE Trans. PGAP* **AP-6**, 56 (1958).
- Lundquist, S., Experimental demonstration of magneto-hydrodynamic waves, *Nature* **164**, 145 (1949).
- Liebermann, L., Extremely low-frequency electromagnetic waves, Pt. I, Reception from lightning, *J. Appl. Phys.* **27**, 1473 (1956a).
- Liebermann, L., Extremely low-frequency electromagnetic waves, Pt. II, Propagation properties, *J. Appl. Phys.* **27**, 1477 (1956b).
- Maple, E., Geomagnetic oscillations at middle latitudes, *J. Geophys. Research* **64**, 1395 and 1405 (1959).
- Martin, L. H., and R. A. Helliwell, Association between aurorae and VLF hiss observed at Byrd Station, Antarctica (submitted to *Nature*, April 1960).
- Matsushita, S., On artificial geomagnetic and ionospheric storms associated with high-altitude explosions, *J. Geophys. Research* **64**, 9, 1149 (1959).
- Morgan, M. G., Whistler studies at Dartmouth College, *Geophys. and IGY, Geophys. Mono.* **2**, AGU, 31-34 (1958a).
- Morgan, M. G., Correlation of whistlers and lightning flashes by direct aural and visual observation, *Nature* **182**, 332-333 (1958b).
- Morgan, M. G., H. W. Curtis, and W. C. Johnson, Path combinations in whistler echoes, *Proc. IRE* **47**, 328-329 (1959).
- Morgan, M. G., Whistlers, *Proc. ICSU Mixed Commission on the Ionosphere, Fifth Meeting, J. Atmospheric and Terrest. Phys.* **15**, 54-57 (1959).
- National Academy of Sciences (USA), *Proc. symposium on scientific effects of artificially introduced radiation at high altitudes*, **45** (1959). Also published in *J. Geophys. Research* **64** (1959a).
- National Academy of Sciences (USA), The argus experiment, *IGY Bull.* **27** (1959b).
- National Bureau of Standards Circular **462**, Ionospheric radio propagation (1948).
- Norinder, H., The waveforms of the electric field in atmospheres recorded simultaneously by two different stations, *Arkiv Geofysik* **2**, 9, 161 (1954).
- Norton, K. A., Transmission loss in radio propagation, *Proc. IRE* **41**, 146 (1953).
- Norton, K. A., System loss in radio wave propagation, *J. Research NBS*, **63D**, 53 (1959).
- Opik, E. J., and S. F. Singer, Distribution of density in a planetary exosphere, *Phys. of Fluids* **2**, 653-655 (1959).
- Pfister, W., Magneto-ionic multiple splitting determined with the method of phase integration, *J. Geophys. Research* **58**, 29 (1953).
- Pierce, E. T., Electrostatic field changes due to lightning discharges, *Quart. J. Roy. Meteorol. Soc.* **81**, 211-228 (1955).
- Pierce, E. T., *Meteorology, Sci. Prog.* **177**, 70 (1957).
- Pierce, E. T., The propagation of radio waves at frequencies less than 1 kc/s, *Proc. IRE* (in press).
- Pierce, J. A., The diurnal carrier-phase variation of a 16-kilocycle transatlantic signal, *Proc. IRE* **43**, 584 (1955).
- Pierce, J. A., Intercontinental frequency comparison by very-low-frequency radio transmission, *Proc. IRE* **45**, 794 (1957).
- Poevlerin, H., Low-frequency reflection in the ionosphere, Pt. I, *J. Atmospheric and Terrest. Phys.* **12**, 126 (1958a).
- Poevlerin, H., Low-frequency reflection in the ionosphere, Pt. II, *J. Atmospheric and Terrest. Phys.* **12**, 240 (1958b).
- Rhodes, R. M., Penetration of charged particles into auroral zones, *Physics Section Rpt. Zph-014*, Convair, San Diego, Calif. (1959).
- RPU Technical Report 5, Minimum required field intensities for intelligible reception of radio-telephony in presence of atmospheres or receiving set noise (1949).
- Schonland, B. F. J., The pilot streamer in lightning and the long spark, *Proc. Roy. Soc. London*, **A220**, 25 (1953).
- Shmoys, J., Long-range propagation of low-frequency radio waves between the earth and the ionosphere, *Proc. IRE* **44**, 163 (1956).
- Singer, S. F., Trapped Orbits in the earth's dipole field, *Bull. Am. Phys. Soc.* **1**, 229 (1956).
- Singer, S. F., A new model of magnetic storms and aurorae, *Trans. Am. Geophys. Union* **38**, 175-190 (1957).
- Singer, S. F., Effects of environment on space vehicles, Chapter IV in *Symposium on Space-Physics and Medicine* (San Antonio, 1958a).
- Singer, S. F., Geophysical effects of solar corpuscular radiation, *Ann. geophys.* **14**, 173-177 (1958b).
- Singer, S. F., New acceleration mechanism for auroral particles, *Bull. Am. Phys. Soc.* **3**, 40 (1958c).
- Singer, S. F., Project far side, *Missiles and Rockets* **2**, 120-128 (1958d).
- Singer, S. F., Trapped albedo theory of the radiation belt, *Phys. Rev. Letters* **1**, 171-173 (1958e).
- Singer, S. F., Trapped albedo theory of the radiation belt, *Phys. Rev. Letters* **1**, 181-183 (1958f).
- Singer, S. F., Artificial modification of the earth's radiation belt, *Adv. in Astronaut. Sci.*, 336 (1959a).
- Singer, S. F., Distribution of neutral hydrogen in the earth's exosphere, *Bull. Am. Phys. Soc.*, II **4**, 222 (1959b).
- Singer, S. F., On the cause of the minimum in the earth's radiation belt, *Phys. Rev. Letters* **3**, 188 (1959c).
- Singer, S. F., and R. C. Wentworth, Aspects of the magnetic storm belt, *Proc. Symposium on Physical Processes in the Sun-Earth Environment*, 335-346, sponsored by the CDRB, July 20-21, 1959, DRTe Publication 1025 (1960).
- Smith, R. L., J. H. Crary, and W. T. Kreiss, IGY instruction manual for automatic whistler recorders, NSF Grant Y-6.10/20, Stanford Elect. Labs. (1958).
- Smith, R. L., R. A. Helliwell, and I. W. Yabroff, A theory of trapping whistlers in field-aligned columns of enhanced ionization, *JGR* **64**, 3, 815-823 (1960a).

- Smith, R. L., The guiding of whistlers in a homogeneous medium, *J. Research NBS* **64D**, 505 (1960).
- Sonett, C. P., D. L. Judge, and J. M. Kelso, Evidence concerning instabilities of the distant geomagnetic field: Pioneer I, *J. Geophys. Research* **64**, 941 (1959).
- Stanley, G. M., Layered-earth propagation in the vicinity of Point Barrow, Alaska, *J. Research NBS* **64D**, 95 (1960).
- Steiger, W. R., and S. Matsushita, Photographs of the high-altitude nuclear explosion 'Teak', *J. Geophys. Research* **65**, 545 (1960).
- Stuart, G. W., Satellite-measured radiation, *Phys. Rev. Letters*, **2**, 417 (1959).
- Sullivan, A. W., S. P. Hersperger, R. F. Brown, and J. D. Wells, Investigation of atmospheric radio noise, *Sci. Rpt. 8, Fla., Station Univ., Tallahassee, Fla.* (1955).
- Sullivan, A. W., The characteristics of atmospheric noise, *Atmos. Noise Research Lab., Engineering and Industrial Experiment Station, Univ. of Fla., Gainesville, Fla.* (no date).
- Taylor, W. L., and J. Lange, Some characteristics of VLF propagation using atmospheric waveforms, *Recent Adv. in Atm. Elec.*, 609 (1959a).
- Taylor, W. L., and A. G. Jean, VLF radiation spectra of return-stroke lightning discharges, *J. Research NBS* **63D**, 199 (1959b).
- Taylor, W. L., Attenuation characteristics of VLF propagation deduced from sferics, *J. Research NBS* **64D**, (1960).
- Tepley, L. R., A comparison of sferics as observed in the VLF and ELF bands, *J. Geophys. Research* **64**, 12, 2315 (1959).
- Ungstrup, *Nature* 806 (1959).
- Van Allen, J. A., Direct detection of auroral radiation with rocket equipment, *Proc. Nat. Acad. Sci.* **43**, 57 (1957).
- Van Allen, J. A., et al., Observations of high intensity radiation by satellites 1958 Alpha and Gamma, *IGY Bull., Trans. Am. Geophys. Union* **30**, 767 (1958a).
- Van Allen, J. A., C. E. Mellwain, and G. H. Ludwig, Radiation observations with satellite 1958b, *J. Geophys. Research* **64**, 271 (1958b).
- Van Allen, J. A., and L. A. Frank, Radiation measurements to 658, 300 km with Pioneer IV, *Nature* **184**, 219 (1959a).
- Van Allen, J. A., The geomagnetically trapped corpuscular radiation, *J. Geophys. Research* **64**, 1683 (1959b).
- Wait, J. R., and H. H. Howe, Amplitude and phase curves for ground-wave propagation in the band 200 cycles per second to 500 kilocycles, *NBS Circ.* **574** (1956a).
- Wait, J. R., On the waveform of a radio atmospheric at short ranges, *Proc. IRE* **44**, 1052 (1956b).
- Wait, J. R., Transient fields of a vertical dipole over homogeneous curved ground, *Can. J. Research* **34**, 27 (1956c).
- Wait, J. R., A note on the propagation of the transient ground wave, *Can. J. Phys.* **35**, 1146 (1957a).
- Wait, J. R., and L. B. Perry, Calculations of ionospheric reflection coefficients at very low radio frequencies, *J. Geophys. Research* **62**, 43 (1957b).
- Wait, J. R., and J. Householder, Mixed-path ground-wave propagation: 2. Larger distances, *J. Research NBS*, **59**, 19 (1957c). (A similar solution has been given recently by Y. K. Kalinin and E. L. Feinberg, *Radiotekh. i Elektron.* **3**, 1958).
- Wait, J. R., Propagation of a pulse across a coast line, *Proc. IRE* **45**, 1550 (1957d).
- Wait, J. R., The attenuation vs frequency characteristics of VLF radio waves, *Proc. IRE* **45**, 768 (1957e).
- Wait, J. R., and A. Murphy, The geometrical optics of VLF sky-wave propagation, *Proc. IRE* **45**, 754 (1957f).
- Wait, J. R., The mode theory of VLF ionospheric propagation for finite ground conductivity, *Proc. IRE* **45**, 760 (1957g).
- Wait, J. R., The transient behaviour of the electromagnetic ground wave over a spherical earth, *IRE Trans. PGAP* **AP-5**, 198 (1957h).
- Wait, J. R., An extension to the mode theory of VLF ionospheric propagation, *J. Geophys. Research* **63**, 125 (1958a).
- Wait, J. R., On the theory of propagation of electromagnetic waves along a curved surface, *Can. J. Phys.* **36**, 9 (1958b).
- Wait, J. R., Propagation of very-low-frequency pulses to great distances, *J. Research NBS* **61**, 187 (1958c).
- Wait, J. R., The propagation of VLF waves at great distances, *J. Research NBS* **61**, 187 (1958d).
- Wait, J. R., Transmission and reflection of electromagnetic waves in the presence of stratified media, *J. Research NBS* **61**, 205 (1958e).
- Wait, J. R., Transmission loss curves for propagation at very low radio frequencies, *IRE Trans.* **CS-6**, 58 (1958f).
- Wait, J. R., Diurnal change of ionospheric heights deduced from phase velocity measurements at VLF, *Proc. IRE* **47**, 998 (1959a).
- Wait, J. R., and A. M. Conda, On the diffraction of electromagnetic pulses by curved conducting surfaces, *Can. J. Phys.* **37**, 1384 (1959b).
- Wait, J. R., Radiation from a small loop immersed in a semi-infinite conducting medium, *Can. J. Phys.* **37**, 672 (1959c).
- Wait, J. R., The calculation of the field in a homogeneous conductor with a wavy interface. *Proc. IRE* **47**, 1155 (1959d).
- Wait, J. R., Transmission of power in radio propagation, *Elec. and Radio Engr.* **36**, 146 (1959e).
- Wait, J. R., Mode theory and the propagation of ELF radio waves, *J. Research NBS* (to be published in **64D**, July (1960a)).
- Wait, J. R., On the propagation of ELF radio waves and the influence of a non-homogeneous ionosphere, *J. Geophys. Research* **65** (1960b).
- Wait, J. R., Terrestrial propagation of VLF radio waves—a theoretical investigation, *J. Research NBS* **64D**, 153 (1960c).
- Ward, C. A., Unusual lightning, *Weather* **6**, 63 (1951).
- Warwick, J. W., Some remarks on the interaction of solar plasma and the geomagnetic field, *J. Geophys. Research* **64**, 389 (1959).
- Watt, A. D., and E. L. Maxwell, Characteristics of atmospheric noise from 1 to 100 kc, *Proc. IRE* **45**, 6, 787 (1957a).
- Watt, A. D., and E. L. Maxwell, Measured statistical characteristics of VLF atmospheric radio noise, *Proc. IRE* **45**, 1, 55 (1957b).
- Watt, A. D., R. M. Coon, E. L. Maxwell, and R. W. Plush, Performance of some radio systems in the presence of thermal and atmospheric noise, *Proc. IRE* **46**, 12 (1958).
- Watt, A. D., and R. W. Plush, Power requirements and choice of an optimum frequency for a world-wide broadcasting station, *J. Research NBS* **63D**, 35 (1959).
- Watts, J. M., Audio-frequency electromagnetic hiss recorded at Boulder in 1956, *Geofis. pura e appl.* **37**, 169-173 (1957).
- Wentworth, R. C., W. M. MacDonald, and S. F. Singer, Lifetimes of trapped radiation belt particles determined by coulomb scattering, *Phys. of Fluids* **2**, 499-509 (1959).
- White, M. L., Atmospheric tides and ionospheric electrodynamics, *J. Geophys. Research* **65**, 1, 153 (1960a).
- White, M. L., Thermal and gravitational atmospheric oscillations—Ionospheric dynamo effects included, *J. Atmospheric and Terrest. Phys.* (in press, 1960b).
- Wright, J. W., A model of the F region above $h_{max} F_2$, *J. Geophys. Research* **65**, 185 (1960).
- Yabroff, I. W., Reflection at a sharply-bounded ionosphere, *Proc. IRE* **45**, 750 (1957).
- Yabroff, I. W., Computation of whistler ray paths, Final Letter Report—Pt. II., AFOSR-TN-60-71, Stanford Research Inst., Prepared for Stanford Univ., Elect. Engr. Dept., SRI Proj. 2241 (1959).
- Yuhara, H., T. Ishida, and M. Higashimura, Measurement of the amplitude-probability distribution of atmospheric noise, *J. Radio Research Labs.* **3**, 101 (1956).

Review of Developments Occurring Within the United States of America in the Field of Radio Astronomy

1. University of Alabama

Measurements of radiation from the sun and moon at millimeter wavelengths have been continued. The effective temperature of the sun, averaged over the entire disk, is found to be 6,500 °K at 8.6 mm. This temperature is in agreement with the trend shown by earlier measurements in this laboratory, which indicated temperatures of 4,500 °K at 6 mm and 5,600 °K at 7.5 mm. In these figures, the antenna efficiency and the effects of atmospheric attenuation and radiation have been taken into account.

Earlier experiments on lunar radiation between 7 and 8 mm have been repeated with better precision using a 60-in. paraboloidal antenna. A variation of lunar temperature with phase has been noted. There is evidence that the temperature varies with phase in a rather complex manner. The maximum temperature, averaged over the entire disk, is about 175 °K, and it occurs some 4 days after full moon. The minimum temperature, about 125 °K, occurs near new moon.

Work in progress includes the development of a model for radio emission from the lunar surface, and a program to determine the utility of a crystal audio radiometer for solar and lunar measurements in the wavelength range between 3 and 8 mm.

Bibliography: Mitchell, Whitehurst, Weaver (1957); Mitchell, Whitehurst (1958); Tyler, Whitehurst, Mitchell (1958); and Weaver, Mitchell, Whitehurst (1958).

2. Air Force Cambridge Research Center Sagamore Hill Radio Astronomy Observatory

During the period 1957-1960, radio astronomy techniques were used on a number of occasions to make measurements of atmospheric absorption, refraction, and scintillation with both solar and stellar radiation as the source of rf energy.

In July 1957, a comparison-type radiometer was used to make such measurements at C band (4,700 Mc/s) [Castelli, Aarons, Ferioli and Casey, 1959] with the sun as a source. Previous measurements by this group [Aarons, Barron, and Castelli 1958] had been made at 3.2 cm, 8.7 mm, and 218 Mc/s. The mean absorption, based on average solar temperatures at the various elevations for the period, was 0.00348 db/km. Average refractive errors were approximately the same as in the optical region although deviations from the mean during any day were large.

At C band, atmospheric scintillations for periods ranging from 0.5 to 90 sec. were recorded. At low angles, the scintillation amplitudes ranged from 2 to 20 percent of antenna signal temperature; at high-elevation angles, they rarely reached 10 percent and were generally less than 1 percent. Although the low-angle scintillations are probably of atmospheric origin, correlation between them and many meteorological parameters at ground level was unsuccessful.

Further light was shed on these phenomena by measurements made at three different frequencies (224, 1,300, and 3,000 Mc/s) during the solar eclipse of October 2, 1959 and during a control period bracketing this date [Aarons, Castelli, Straka, and Kidd, 1960; Aarons and Castelli, 1960]. Average refraction corrections were worked out during the control period to permit accurate antenna pointing and tracking of the sun. Interferometric solar maps for this period, taken by Bracewell at 3,300 Mc/s and by Christiansen at 1,420 Mc/s, indicated the presence of plage areas on both the east and west limbs of the sun: maps at 169 Mc/s by Denisse and Simon indicated no point sources of solar activity at this frequency range. A study of the signals received at the various frequencies revealed that scintillations of the signal were recorded for those frequencies (1,300 and 3,000 Mc/s) for which constant point sources of energy existed on the sun. During the early part of the eclipse, when the larger part of the solar disk was eclipsed and only the point sources were uncovered, scintillations of very large amplitude were evident. The periods ranged from 25 to 140 secs and large scintillations were recorded mainly for observations made below 4° of elevation.

Throughout the period studied, scintillations at the 1,300- and 3,000-Mc/s frequencies were remarkably well correlated in detail despite the fact that the frequencies had a ratio of 2.3 to 1, the apertures of the two antennas on which the data were received were quite different (84 and 8 ft.), and the two antennas were separated by 80 ft. Therefore, it has been concluded that, for this frequency range, the shadow patterns generated by the radiofrequency active areas on the sun are not frequency dependent: and that, within the distance between the centers of the two antennas, a single shadow pattern exists.

In cooperation with Stanford University, further analysis of the 3,000 Mc/s eclipse measurements was made, [Straka, Swarup, 1960] by comparing them with a 3,300 Mc/s two-dimensional solar brightness distribution map experimentally obtained at Stanford University by means of their inter-

ferometric cross 14 hr. before the eclipse. When the difference between the time at which the map was made and the time of the eclipse was taken into account, the curve obtained by artificially eclipsing the 3,300-Mc/s solar map was found to agree fairly well with the experimentally obtained eclipse measurements modified to compensate for absorption. In addition, the slope of the modified eclipse curve as a function of time was calculated at 1-min. intervals and averaged over a 2-min. period to smooth out scintillation effects. Reasonable agreement was obtained between increases in these slope measurements and the uncovering of spot regions on the interferometric map during the course of the eclipse.

During the lunar eclipse of March 13, 1960, a series of measurements of lunar temperatures at 1,300 and 3,000 Mc/s were made. Drift curves were taken of the moon with the 84-ft. Sagamore Hill Radio Telescope. Short-time constants were used and an accuracy of ± 2 percent resulted. For these frequencies, lunar temperatures were constant throughout the period of the eclipse. Additional measurements and analyses are being made at these same frequencies in order to determine temperatures over a lunation.

3. U.S. Army Signal Research and Development Laboratory

A program was established for observing the neutral hydrogen emission in the Andromeda nebula with the 60-ft. dish at the Evans area of USASRDL. However, shortly after the program began, the dish was requisitioned for Project Tiros. The dish should be released from this project in a few months. There is a possibility that radio astronomy research will be resumed either with this dish or with an 85-ft. dish in the Deal area, construction of which is scheduled to begin in 3 months.

After the change in project for the 60-ft dish, the 21-cm receiver was loaned to the Yale University Observatory with the understanding that it would be available part-time to Signal Corps personnel for research. In September 1959, by mutual agreement, the receiver was transferred to the Agassiz Station of the Harvard College Observatory.

External: Contracts with Cornell University and Dr. H. G. Booker entitled "Studies on Propagation in the Ionosphere" continued throughout this period. Papers under this contract have been presented at each URSI meeting. A new contract with the University of Virginia and Dr. E. C. Stevenson entitled "Research in Stellar Scintillations" is presently being negotiated.

4. California Institute of Technology Owens Valley Radio Observatory

One of the 90-ft telescopes commenced operation in April 1959 on a frequency of 960 Mc/s and was

used principally for a "finding" program on radio stars and a survey of the Galaxy. The principal results from this unit up to January 1, 1960 were:

- (1) The discovery of a band of decimeter radiation from Jupiter—following a lead provided by NRL;
- (2) the finding of an extensive two-jet structure in NGC 5,128/Centaurus-A which is an almost perfect model for Cygnus-A;
- (3) the result that the nonthermal radio stars have a very small spread in spectral index; and
- (4) a survey of the galactic plane listing 110 galactic sources together with angular sizes and probable spectra. About half the sources can be identified with supernova remnants or emission nebulae.

The second 90-ft telescope began operation in September 1959 with a 21-cm line receiver. Absorption lines have been found in five additional galactic sources. Narrow-band self-absorption effects in a region near the anticenter suggests the presence of a considerable amount of hydrogen in dense cool clouds.

The two telescopes commenced operation as an interferometer at 960 Mc/s on January 15th. Using a spacing of 200 wavelengths, i.e. a fringe separation of 20 mins of arc, the minimum detectable signal (defined as having an amplitude equal to peak-to-peak noise fluctuations) is 4×10^{-27} watts $m^{-2}(c/s)^{-1}$.

Observations to date include:

(1) Intensity measurements of 600 radio stars for the purposes of comparison with LF measurements in order to determine spectra.

(2) Angular size measurements of 220 radio stars including observations so far at five different baselines. About 100, mainly galactic objects have been resolved. This program is continuing.

(3) Precise position measurements on 70 radio stars. The results have now made certain the identification of at least 18 galaxies or multiple galaxies as radio emitters. One position has led to the discovery of the most distant cluster of galaxies known—with a red shift of at least $c/2$ and perhaps $2c/3$.

(4) The radiation from the planet Jupiter at 960 Mc/s is 40 percent linearly polarized with the plane of polarization parallel to the equator.

Negative results have been obtained from observations of Mercury and Venus (upper limits are close to black body expectations) and on a number of planetary nebulae. For the latter it appears that earlier observations by Drake are in error.

5. Carnegie Institution of Washington Department of Terrestrial Magnetism

Since early 1957, a 340 Mc/s, 30 element Christiansen array giving 4.8' resolution on the sun has been in nearly continuous operation. The quiet sun, the slowly varying component, and active bursts have been extensively studied. In 1959 this was supplemented by a north-south array of 16 elements. A 16-element, 87-Mc/s array has also

been constructed and used to study radiation from the active sun.

Two corner reflectors each 600 ft long were constructed for use at 400 Mc/s. Used separately they give a resolution of 12' and as an interferometer 4' fringes are obtained. The arrays have been used to measure accurate radio source positions and brightness distributions of extended sources. We have demonstrated that these arrays give an absolute accuracy of 1' and a relative accuracy of 0.1' in measuring right ascension of strong sources.

With small arrays the flux intensities of the brighter sources have been measured from 18.5 to 207 Mc/s.

The 54-channel hydrogen radiometer began regular operation in 1958. The first project was a map of high latitude galactic hydrogen. This has been followed by a survey of the galactic circle between latitudes ± 20 deg. These surveys covering the entire sky visible from Washington, D.C. are now virtually complete. The equipment is now being transferred to a larger (60-ft) paraboloid.

6. Cornell University

IGY activities. A 200 Mc/s solar noise patrol and an ionospheric-radio-disturbance flare patrol were maintained. Data were sent regularly to the IGY data centers, and to the editor of the Quarterly Bulletin of Solar Activity. These patrols were maintained continuously from the beginning of the period through December 31, 1958.

Solar burst polarization studies. Polarization of radiation from the active sun was measured using a narrow band 200 Mc/s polarimeter [Cohen, 1958a, 1958b]. Early measurements showed that a few percent of Type III bursts were weakly linearly polarized [Cohen, Fokker, 1959; Cohen, 1959]. Measurements made during the Spring and Summer of 1959 showed that a larger group of Type III bursts was weakly linearly or elliptically polarized, and that the degree of polarization decreases with the analyzing bandwidth. These results are interpreted in terms of Faraday rotations in the corona, an amount 10^4 radians or more [Akabane, Cohen, in press].

Radio wave propagation in the corona. Theoretical studies are being made of magneto-ionic mode coupling by means of magnetic field gradients in the corona [Cohen, in press]. "Transition" frequencies have been computed; for a given geometry these are at the transition between weak coupling (low frequencies) and strong coupling (high frequencies). The theory explains the observation that the wide-band microwave bursts commonly have opposite rotation directions at 1,000 and 10,000 Mc/s.

7. Collins Radio Company

Research conducted by the Radio Astronomy Group of the Collins Radio Company since the 12th General Assembly has been largely devoted to 8.7 mm

and 1.9-cm solar and lunar observations, atmospheric emission, attenuation, and refraction investigations, and to the achievement of precise, all-weather navigation systems utilizing solar and lunar radio emission. Associated activities have included extensive radiometric instrumentation and structural design to achieve precision determination of solar and lunar positions, absolute antenna temperature calibration, and combined radiometric and phase-locked tracking ability for deep-space research.

The use of a combined radio sextant-radio telescope for simultaneous measurement of angle of arrival and received power has been found to be of great value in the study of atmospheric attenuation and refraction [Liff, Marner, 1960]. It has been possible to determine atmospheric attenuation constant as a function of height above the earth at 8.7 mm [Marner, 1956] and 1.9 cm [Marner, 1958a] and to determine atmospheric refraction as a function of altitude angle and surface meteorological conditions [Marner and Liff, 1958]. New high-precision measurements are in process.

Emission from the atmosphere at these wavelengths has also been observed as a function of altitude angle and weather conditions, and it appears possible to account for the observed power levels by the use of the same model atmospheres as used in the attenuation case [Marner, 1958b]. The absence of good absolute calibration facilities left some question as to whether any galactic radiation is detectable, and new efforts are being made to achieve excellent calibration relative to absolute zero. Substantial improvement in the atmospheric emission data is also anticipated.

Interesting fluctuation properties have been observed in all of these processes, and new high figure of merit receivers and combined analog-digital recorders are being placed in operation to study these atmospheric characteristics. Several daily radio-sonde observations will be used in conjunction with the emission, attenuation, and refraction observations.

An extensive study has been made of the effect of atmospheric phenomena upon precise determination of the position of the sun, the moon, and the discrete sources [Bellville, Holt, and Liff, 1958]. The attenuation and emission gradients with respect to altitude angle, as well as the refraction, cause apparent displacements of the celestial source position which, in some circumstances, can be of substantial significance. The general principles have been worked out, and numerical examples computed for the microwave region by use of the atmospheric data cited above. By employing special instrumentation techniques intended to reduce bore-sighting errors, direct observations of these effects while tracking the moon have produced experimental verification of the theory.

The same tracking equipment is currently being used to study the location of the radio symmetry center of the sun and moon. Extensive data reduction programs are now in process.

The use of the combined radio-sextant radio telescope allows excellent attenuation corrections and the new equipments will be used to make careful studies of solar and lunar temperatures as a function of time and wavelength. Extensive solar activity observations are currently being reduced.

The radio astronomy techniques have been applied to the achievement of precise all-weather marine navigation systems [Marner, 1959, 1960a]. It has been found practical to achieve such navigation by the use of solar and lunar radiation.

The past period has experienced the advent of a new class of celestial object—the man-made satellites and space probes. An extensive amount of work has been done relative to the radio observation of these sources. Major tracking facilities were constructed for the Jet Propulsion Laboratory at Goldstone, California, Cape Canaveral, Florida, and Puerto Rico [Brockman, et al, 1960]. These employ phase-locked receivers [Jaffe and Rehtin, 1954; Hamilton, 1959] to accomplish angle tracking and telemetering functions for space probe research. Successful data reception was experienced with the Pioneer IV lunar probe until battery exhaustion at 407,000 miles range. The 0.2-w transmitter would otherwise have maintained contact to a range of 1.15×10^6 miles. A worldwide network of receiving stations is currently being installed for an extension of such space research.

The use of artificial satellites for communication has been studied and extensive observing facilities are being erected for radio scattering research in this connection. Research in the use of satellites for navigation has also been under way [Marner and McCoy, 1959; Marner, 1960], and planning is being conducted for balloon and satellite-borne radio astronomy research. A considerable expansion of these areas of research is anticipated during the next period.

8. University of Colorado High-Altitude Observatory

The most important development in our radio astronomy program since the last General Assembly is a radio spectrograph covering the range 15 to 60 Mc/s. This spectrograph sweeps this range once per second, at a bandwidth of the order of 20 kc/s. It is a phase-switch interferometer in order to make possible the detection of radio stars, and to measure changes in the position of radio sources. The receiver has a detector operating on the minimum detection principle, which permits the output recorder to omit the strong pips that would be produced on the record by interfering stations, atmospherics, and other types of undesirable noise, most troublesome in this LF range.

This receiver, in operation since July 1959, has built up a considerable amount of observational material on solar and Jupiter emission, and radio star scintillations. The observations of solar emission have been partially reported in the *Astrophysical*

Journal, Vol. 131, No. 1, January 1960, pp. 61–67. The remaining observations are as yet unpublished.

One of the principle objectives of our work has been in the study of ionospheric effects on discrete sources, in the low frequency range. To provide a stable means of routinely observing the larger sources, we have constructed a pair of scaled interferometers operating at 18 and 36 Mc/s, respectively. These interferometers regularly observe the meridian transits of Cassiopeia A, Cygnus A, and Taurus A. As a byproduct of these records, we have been able to estimate the sources in the LF range, where considerable discrepancies in the reported flux densities appear in the literature. Furthermore, it has been possible to observe Taurus A fairly close to the time of its occultation by the solar corona, near the middle of June. Our observations here cover only one occultation, that of June 1959, during which the sun was quite active. There is doubt about the precise time of ingress and egress from the corona, although with some reliability we can state that we have observed the source as early as 1 July, 1959, within 2 weeks of occultation.

These interferometers also provide a stable system for measures of the fluctuations in position of solar emission sources. From day to day, there are often striking changes in position which seem much too large to be accounted for by ionospheric effects such as scintillations or traveling disturbances. In this work we have been aided considerably by our swept-frequency interferometer.

The strong period of solar emission during the last week of August 1959 produced a splendid set of records, both with the spectrograph and with the fixed-frequency interferometers. The observations that are reported by NERA and the Fraunhofer Institute in the *Information Bulletin of Solar Radio Observatories* in Europe are confirmed by our records. Especially, we have detailed positional and intensity spectra, to our lowest limit at 15 Mc/s, of the enormous fluctuations in the apparent intensity of the solar noise during 23, 24, and 25 August. We also confirm the important sunset effects and their probable origin in ionospheric scintillations. Study of these records is still proceeding, and it is premature for us to identify which component of the fluctuations of the radiation during this event is produced locally and which may be produced in interplanetary space as suggested by Fokker. If such a separation is possible, however, our records, which show larger changes in these fluctuations, as a function of frequency, should provide strong observational tests for theories of their origin.

The final important material that has become available since the last Assembly is observations of the spectrum of Jupiter radio emission from 15 to 35 Mc/s. The striking feature of this emission on two of its strongest occasions is that the gross center of gravity of the emission appears first at the low end of the frequency range, and moves slowly towards higher frequencies, at 1 octave per hour. Interpretation of these records is still in progress.

However, there seems to be some possibility of connecting the emission to the presence of a magnetic field in Jupiter's atmosphere, and of identifying the mechanism with the synchrotron effect. Much remains to be done, especially in studies of the spectrum of the polarization of Jupiter bursts, of the time variations in the decimetric radiation, and between the decimetric radiation and the decametric radiation.

9. Harvard University Radio Astronomy Station

The research program at the Harvard Radio Astronomy Station, Fort Davis, Tex., has been devoted mainly to solar radio astronomy. The station has sweep frequency equipment covering the band 25 to 580 and 2,000 to 4,000 Mc/s, that is nearly 6 octaves of the electromagnetic spectrum [Maxwell, Swarup, Thompson, 1958; Maxwell, 1958; Maxwell, 1959]. Considerable efforts have been made to ensure continuity of the observations, and the Station has now accumulated and analyzed in detail some 3 years' records covering the maximum of the solar cycle. The characteristics of the various solar radio bursts and the statistics of their occurrence have been examined [Maxwell, Howard, Garmire, 1959; Goldstein, 1959], as well as their association with flares and prominences [Swarup, Stone, and Maxwell, 1960]. It has been shown that most slow drift bursts (Type II) and large continuum outbursts (Type IV) are generally associated with flares of large area and intensity, and that the fast drift bursts (Type III) are often associated with flares of lower importance.

The slow drift bursts, which are believed to be caused by a primary disturbance moving outwards through the solar atmosphere with a velocity of about 1,000 km/sec, are about 45 percent associated with the subsequent occurrence of terrestrial geomagnetic storms. The geomagnetic effects are enhanced if the bursts occur near the equinoxes, and if they are accompanied by a flare of importance 2 or 3, or by continuum radiation [Maxwell, Thompson, Garmire, 1959]. It has also been shown that the continuum bursts frequently precede the bombardment of the upper atmosphere by solar protons with energies up to about 300 MeV (low energy solar cosmic rays). The minimum time delay between the onset of the radio burst and the arrival at the earth of solar protons is the order of 45 min [Thompson, Maxwell, 1960a, b].

10. Hayden Planetarium

The Hayden Planetarium has a phase switching interferometer operating approximately at 20 m. Each array consists of eight inline dipoles oriented north-south, the arrays spaced 590 ft east-west. The dipoles are soon to be turned 90°. The equipment is still in the development stage. Radio frequency interference is a serious factor near Hun-

tington, Long Island, and the sky can be seen only when the ionosphere is very transparent, e.g., during the recent communications blackout imposed by the sun. At that time, when WWV was barely detectable the sun itself provided a beautiful record each day during the week of March 28 to April 4, 1960, although it was in a sidelobe of the array. Another sidelobe sees Cygnus A, but weakly. Jupiter has not yet been detected.

A computing program will start soon at the Watson Labs at Columbia. This will involve R. E. Wilson's radial velocity catalogue. The coordinates will be changed to the Lund Pole, 1900.0, and the velocities to the local standard of rest, so that the stellar velocities may be compared directly with the 21-cm hydrogen velocities.

11. University of Illinois

Support has been secured from the Office of Naval Research for the construction of a large parabolic-cylindrical radio telescope at the University of Illinois. Engineering plans have been completed by the project staff and by Hanson, Collins, and Rice, consulting structural engineers. Construction commenced in October 1959, and is expected to be completed by June 1960. Extensive investigation has produced a suitable design for the line-feed system for the instrument. A noise survey of the site indicates that it is suitable from this standpoint.

The University has purchased a little over 200 acres of land about 5 miles southeast of Danville, Ill., and has appropriated funds for a building, access road, and power line.

The characteristics of the instrument are as follows: width (E-W), 400 ft; length (N-S), 600 ft; aperture-to-vertex depth, 60 ft; focal length, 160 ft; length of feed system, 425 ft; proposed frequency of operation, approximately 600 Mc/s; expected beam width, approximately 15 min of arc; beam steerable in declination by phasing of feed elements, within 30 deg of the zenith; beam shape circular at maximum zenith angle, slightly elliptical at the zenith. The purpose of this instrument is to conduct a survey of discrete sources.

Theoretical cosmological investigations have included an interpretation of the meaning of a uniform distribution in space of extra-galactic radio sources [McVittie, 1960a, b]. The assumption was made that these sources were galaxies and so shared in the redshift phenomenon and also that they were all of the same intrinsic power output. Distances can then be calculated for various limits of observed flux density. The conventional "minus-three-halves" law for the number of sources versus limiting flux-density was shown to imply that extra-galactic radio sources were more numerous per unit volume in the past than they are now. Another type of investigation [McVittie, Wyatt, 1959] concerned the background radiation, at radio and at optical wavelengths, received from all unresolved sources in the universe. The calculations were performed for Milne's model

of an expanding universe and led to estimates of the number-density of radio sources responsible for the background radiation.

Studies have been made of the scintillation of trans-ionospheric radio signals [Keh, Swenson, 1959]. Twenty- and forty-megacycle signals from earth satellites have been used, in an effort to determine diurnal, seasonal, and geographic variations in the incidence of scintillations. It is believed that nighttime scintillation arises mainly at heights below about 220 km, and that they occur north of geographic latitude 40 deg at our longitude. Daytime scintillations arise lower in the ionosphere and occur sporadically at many latitudes.

12. U.S. Naval Research Laboratory Radio Astronomy Branch

12.1. Planets

Venus

Radiation from Venus at 3.15-cm wavelength was first detected on May 2, 1956. Further detailed observations were made using the 50-ft reflector at the U.S. Naval Research Laboratory on 34 days spread over the period May 5, 1956 to June 23, 1956, a period just prior to and including inferior conjunction [Mayer, McCullough, Sloanaker, 1958a, b]. About 600 measurements of the antenna temperature due to Venus at 3.15 cm were obtained. The measured values were characteristic of steady radiation with no apparent linearly polarized component. The measured flux density approximated the inverse-square-law variation as the distance between Venus and the earth decreased but suggested a slight decrease in the radiation level during the period. The apparent blackbody temperature of Venus deduced from the measurements was about 620 ± 55 °K p.e. near the beginning of the period and about 560 ± 45 °K p.e. near the end of the period.

In 1956 an attempt was made to put rough limits on the spectrum of the radio radiation from Venus by making observations with the 50-ft reflector at 9.4 cm wavelength [Mayer, McCullough, Sloanaker, 1958a, b]. A total of 11 measurements were made on June 25, 1956 and July 27, 1956. The average of the 9.4-cm measurements of the blackbody temperature of Venus was 580 ± 160 °K estimated p.e. which compared closely with the result at 3.15-cm wavelength. Although the accuracy of the 9.4-cm results was poor, these measurements suggested that no great percentage of the radio radiation from Venus at centimeter wavelengths has a spectrum very different from that of thermal radiation.

Beginning about 2 weeks after the inferior conjunction of 1958 observations of Venus at 3.4 cm were made using the 50-ft reflector on 9 days during the period February 12 to March 5, 1958 [Mayer,

McCullough, Sloanaker, 1958c]. The measured equivalent blackbody disk temperature deduced from these measurements was 575 ± 60 °K p.e. This value agrees closely with the results determined in 1956 at 3.15 cm.

Later, about 80 days after the 1958 conjunction, Venus was again observed with the 50-ft reflector at 3.37-cm wavelength using a solid-state maser, designed and built at Columbia University [Alsop, Giordmaine, Mayer, Townes, 1958, 1959]. These observations, made on April 18 and 19, 1958, gave an apparent blackbody temperature based on the diameter of the visible disk of Venus of 575 ± 58 °K p.e.

In order to obtain more reliable measurements near 10-cm wavelength, observations of Venus were made following the inferior conjunction of September 1, 1959 at 10.2-cm wavelength using the 84-ft reflector at the Maryland Point Observatory of the U.S. Naval Research Laboratory [Mayer, McCullough, Sloanaker, 1959]. Measurements were made on 11 days over the period September 17 to October 10, 1959. The measured blackbody temperature at 10.2 cm changed from about 535 °K 16 days after inferior conjunction to about 675 °K 39 days after conjunction. The mean apparent blackbody temperature over the entire period was 600 ± 65 °K estimated p.e.

In summary, the observations near 3- and 10-cm wavelength indicate that Venus emits centimeter wavelength radiation with a spectrum of a blackbody at a temperature of about 580 °K. The most obvious interpretation of the results is that the centimeter wavelength radiation is emitted thermally at some level deep in the atmosphere, perhaps at the solid surface where the temperature is much higher than that which is inferred from infrared observations. However, in order to account for a temperature as high as 580 °K it is necessary to assume almost complete trapping of the absorbed solar radiation, or else some other source of heat. It is perhaps possible that the observed radiation is a combination of thermal and nonthermal components which by coincidence combine to give a blackbody spectrum, but a nonthermal mechanism with an appropriate spectrum has not been found. There has been no evidence of variability in the received radiation other than suggestions of possible phase effects. However, the present observations are not sufficiently accurate or complete to define a dependence of the radio emission on the phase or rotation of Venus. It is important to make further observations to establish whether such a dependence exists, both to obtain this basic information and to allow a better understanding of the origin of the radio emission.

Measurements at 8.6 mm at inferior conjunction in January 1958 [Gibson and McEwan, 1959] yielded a brightness temperature of 410 °K with a large uncertainty, and more recent observations in September 1959 support this or a somewhat smaller value for this wavelength.

Jupiter

The steady radio emission of Jupiter has been observed at wavelengths near 3, 10, and 21 cm.

During May 1956 a limited number of observations of Jupiter were made at 3.15-cm wavelength using the 50-ft reflector [Mayer, McCullough, Sloanaker, 1958b, d]. The measurements gave a blackbody temperature for Jupiter of 140 ± 38 °K p.e.

A second series of observations of Jupiter with improved accuracy was made on seven days between March 23 and April 1, 1957 at 3.15 cm using the 50-ft reflector [Mayer, McCullough, Sloanaker, 1958b, d]. The measurements gave an equivalent blackbody temperature of 145 ± 18 °K p.e. based on the mean diameter of the visible disk of Jupiter.

Another series of observations of Jupiter was made with the Columbia University maser and the 50-ft reflector. The measurements extended over the period from April 16, 1958 to February 7, 1959 and covered a range of wavelengths from 3.03 to 3.36 cm, [Giordmaine, Alsop, Townes, Mayer, 1959a, b]. The measurements gave equivalent blackbody disk temperatures of 171 ± 20 °K p.e. at 3.03 cm (August 22 to September 4, 1958); 173 ± 20 °K p.e. at 3.17 cm (May 24 to July 29, 1958; January 31 to February 7, 1959); and 189 ± 20 °K p.e. at 3.36 cm (April 16 to May 8, 1958).

The apparent blackbody disk temperatures near 3-cm wavelength measured in 1958 and 1959 were higher than those measured in 1956 and 1957 by about $1\frac{1}{2}$ times the probable error, and the apparent increase must be considered as a possible change in the emission of Jupiter. There was also some evidence that an anomalously high disk temperature of about 268 °K was observed on April 30 to May 1, 1958. No changes in the emission at wavelengths near 3 cm were noted which could be correlated with the rotation of Jupiter.

Thirty-three measurements of the apparent blackbody temperature of Jupiter were made between June 10 and August 20, 1958 at wavelengths of 10.2 and 10.3 cm using the 84-ft reflector [Sloanaker, 1959; McClain and Sloanaker, 1959]. The mean apparent blackbody temperature was 640 ± 85 °K p.e. based on the mean diameter of the visible disk. The 10-cm measurements gave a roughly normal distribution of apparent blackbody temperature with a standard deviation of 190 °K. On the basis of the estimated measurement errors, the expected standard deviation was about 145 °K which was in reasonably good agreement with the observed scatter, but did not preclude the possibility of a variable component in the intensity of the radiation. The measured blackbody temperatures at 10 cm showed no longtime trends over the 71-day observation interval, but did show a suggestion of a cyclical variation of about 30 percent correlated with a rotation rate between 40 sec and 2 min longer than the rotation period of System II.

A series of measurements of the radiation from Jupiter at a wavelength of 20.96 cm was made on 28 days during a 1-month period from May 14 to June

18, 1959 using the 84-ft reflector [McClain, 1959]. The mean blackbody temperature for all of the 20.96-cm data was 2,496 °K with a standard deviation of 450 °K. The measured blackbody temperatures were highly suggestive of a cyclical variation with time, and an attempt was made to correlate the data with the System I and System II rotation periods. No significant correlation was observed for the System I period, but in the case of System II elevated temperatures corresponding to an enhancement of about 30 percent were observed at longitudes between 175 and 225°. While rather significant when subjected to a statistical test, this correlation with rotation is considered to be tentative because of the limited amount of data. An attempt was made to correlate the measured temperatures with solar flares [suggested by Drake, 1959 and Drake and Hvatum, 1959]. No strong correlation of this sort was noted in the measurements; however, there was a slight suggestion of elevated temperatures following an important 3+ flare on May 10 and the intense aurora of May 11 and 12, 1959.

To summarize, the emission of Jupiter at wavelengths near 3 cm can probably be accounted for as thermal radiation but the radio spectrum is not that of a blackbody at a constant temperature, and some other source of emission is necessary to account for the radiation at longer wavelengths.

Observations of Jupiter during 1959 yield a brightness temperature less than 200 °K at 8.6-mm wavelength.

Mars

The radio emission of Mars has been observed at two different times. Observations made using the 50-ft reflector at the favorable opposition of September 1956 at 3.15-cm wavelength [Mayer, McCullough and Sloanaker, 1958b, d] were sensitivity limited and it was necessary to average about 70 observations to obtain a measurement of reasonable accuracy. The result of this measurement corresponds to an apparent blackbody disk temperature for Mars of 218 ± 51 °K p.e.

Mars was again observed about 6 weeks past the opposition of November 1958 using the Columbia University maser with the 50-ft reflector at 3.14-cm wavelength [Giordmaine, Alsop, Townes and Mayer, 1959a]. This measurement gave an apparent blackbody-disk temperature for Mars of 211 ± 28 °K p.e. The apparent blackbody-disk temperature derived from the radio observations is about 40° smaller than that derived from the infrared observations, and is about 15° smaller than the estimated mean annual disk temperature. Considering the uncertainties in the observations and in the emissivities at both the radio and infrared wavelengths, the observed radio emission is consistent with the thermal radiation which would be expected on the basis of previous knowledge.

12.2. Cosmic Radio Sources

The radio sources Cygnus-A and Virgo-A were observed in 1958 at wavelengths near 3 cm using the

Columbia University maser with the 50-ft reflector [Alsop, Giordmaine, Mayer and Townes, 1959; Giordmaine, Alsop, Mayer and Townes, 1959b]. For the source Cygnus-A the measured antenna temperature was 4.6°K at a wavelength of 3.2 cm which corresponds to a point source flux density of $1.24 \times 10^{-24} \text{ w m}^{-2}(\text{c/s})^{-1}$. The measured antenna temperature for the source Virgo-A was 1.25°K at 3.37-cm wavelength which would correspond to a point source flux density of $3.4 \times 10^{-25} \text{ w m}^{-2}(\text{c/s})^{-1}$.

The positions, intensities, and sizes of eight bright discrete sources were measured during January 1959 at a wavelength of 10.2 cm using the 84-ft reflector [Sloanaker and Nichols, 1960]. For six of the sources for which accurate optical positions are available, the sources Cassiopeia-A, Cygnus-A, Taurus-A, Virgo-A, Orion Nebula, and Centaurus-A, the measured radio-positions coincided with the positions of the optical centers of the sources to within the uncertainties in the radio measurements of ± 1 min of arc p.e. in both R.A. and Dec. The positions of the optical centers of these sources, with the exception of the Orion Nebula source, refer to the optical positions given by Minkowski [1959], and Baade and Minkowski [1954]. For the Orion Nebula source, M 42, the optical position refers to the position of Theta-One Orionis, the exciting stars, obtained from Strand [1958]. The 10.2 cm measured position of the Sagittarius-A source for 1959.0 was $\text{RA}=17^{\text{h}}43^{\text{m}}1.6^{\text{s}} \pm 4.5^{\text{s}}$ p.e. and $\text{Dec.}=-28^\circ57.3' \pm 1'$ p.e. The measured position of the Omega Nebula source, M 17 for 1959.0 was $\text{RA}=18^{\text{h}}18^{\text{m}}6.1^{\text{s}} \pm 4^{\text{s}}$ p.e. and $\text{Dec.}=-16^\circ11.9' \pm 1'$ p.e. At 10.2 cm the sources Cas-A, Cyg-A, Tau-A, and Vir-A appeared as unresolved point sources with upper size limits of 3' or 4' equivalent gaussian diameters. The measured equivalent gaussian diameters of the other four sources were: Orion Nebula, $7' \pm 0.5'$ p.e. in R.A. and $7' \pm 1'$ p.e. in Dec.; Omega Nebula, $7.5' \pm 0.5'$ R.A. and $8.5' \pm 1'$ Dec.; Sag-A (bright central part only), $14' \pm 0.3'$ R.A. and $16' \pm 0.5'$ Dec.; Cent-A, $8' \pm 0.5'$ R.A. and $5' \pm 1.5'$ Dec. The measured 10.2 cm antenna temperatures for the sources were: Cas-A, $89 \pm 2^\circ\text{C}$ p.e.; Cyg-A, $45 \pm 1^\circ\text{C}$; Tau-A, $48 \pm 1^\circ\text{C}$; Vir-A, $7.5 \pm 0.4^\circ\text{C}$; Orion Nebula, $25 \pm 0.5^\circ\text{C}$; Omega Nebula, $35 \pm 0.7^\circ\text{C}$; Sag-A (bright central part only), $28 \pm 0.6^\circ\text{C}$; and Cent-A, $10 \pm 0.4^\circ\text{C}$. Based on an estimated aperture efficiency of 0.385 ± 0.031 p.e. for the 84-ft reflector, the measured point source flux densities for the sources Cas-A, Cyg-A, Tau-A, and Vir-A were in units of $\text{watts m}^{-2}(\text{c/s})^{-1}$ (124 ± 11 p.e.) $\times 10^{-25}$, $(63 \pm 6) \times 10^{-25}$, $(67 \pm 6) \times 10^{-25}$, and $(10 \pm 1) \times 10^{-25}$, respectively. For the remaining four sources, Omega, Neb., Sag-A (bright central part only), and Cent-A, the measured flux densities corrected for the measured equivalent gaussian diameters listed above were: $(40 \pm 4 \text{ p.e.}) \times 10^{-25}$, $(58 \pm 5) \times 10^{-25}$, $(65 \pm 7) \times 10^{-25}$, and $(16 \pm 2) \times 10^{-25}$ respectively in units of $\text{watts m}^{-2}(\text{c/s})^{-1}$.

During 1956 and 1957 two different experiments were conducted using the 50-ft reflector at a wavelength of 3.15 cm, in an attempt to detect plane

polarization in the radiation from the Crab Nebula (Taurus-A) [Mayer, McCullough, and Sloanaker, 1957]. The first measurements in May and June 1956 indicated a polarized component in the received wave of about 10 percent of the total radiation, with a position angle near the average over the nebula from the optical measurements. In April, May, and June 1957 more accurate measurements were made with a rotating plane-polarized feed horn installed in the 50-ft reflector. These observations indicated that about 7 percent of the total radiation of the Crab Nebula was plane-polarized at 3.15 cm with a position angle of about 150° . The observed position angle of the electric vector on the Crab Nebula differs from the average position vector over the nebula determined optically [Oort and Walraven, 1956] by about 11° . A Faraday rotation along the path of propagation of this order of magnitude is not unlikely at this wavelength, as was pointed out by Oort and Walraven [1956]. Observations of the radio source Cas-A with the rotating polarization antenna did not show any measurable polarization in the received radiation.

In 1958 a search was made for linearly-polarized components of the 10.2-cm radiation from the radio sources Cas-A (IAU 23N5A), Tau-A (IAU 05N2A), Cyg-A (IAU 19N4A), Vir-A (IAU 12N1A), and M 17 (IAU 18S1A) using the 84-ft reflector [Mayer and Sloanaker, 1959]. Only the radiation from Taurus-A showed characteristics which could be interpreted as due to a plane-polarized component of the radiation. The measurements of Taurus-A gave results which could be interpreted as a linearly-polarized component of about 3 percent of the total radiation with a position angle for the electric vector of about 135° . The sources Cas-A, Cyg-A, and Tau-A were measured at two other wavelengths as well, 11.3 and 10.5 cm. The results were similar at the three wavelengths indicating that there is little Faraday rotation along the path between Taurus-A and the earth.

Several of the brighter discrete sources have been identified at 8.6-mm wavelength, and efforts are being made to determine their flux densities.

12.3. Sun

Measurements of solar radiation intensity throughout each day were made at wavelengths of 3.15 and 9.4 cm from March 1958 through April 1959 using 4- and 6-ft diam parabolic reflectors mounted on a common polar mount. These data were communicated to IGY [McCullough and Bologna, 1958 and 1959]. A plot of daily average flux of solar radiation with time shows 3.15-cm flux to be more intense than 9.4-cm flux by the expected amount and also shows the two flux values to vary in close agreement with solar activity. The bursts of radio radiation from the sun which accompany solar flares were classified according to type, time of occurrence (peak), duration, and maximum intensity.

Beginning with the International Geophysical

Year on July 1, 1957, Coates, Edelson, McCullough and Santini [1957, 1958, 1959] have conducted simultaneous observations of solar activity in the optical and radio regions. It was found that 99 percent of the 10-cm bursts were coincident with H-alpha activity. On the other hand, only 25 percent of the H-alpha events were coincident with 10-cm radio bursts. For simple 1 and simple 2 types of bursts a trend for larger peak radio flux values for larger H-alpha intensity values was evident [Coates, Edelson, McCullough, and Santini, 1958].

In March 1959 the time resolution of the H-alpha camera was increased to 6-sec intervals. Using this improved resolution flare light curves were compared directly with observed flux curves of the associated radio bursts. Measurements of time differences between the H-alpha maximum intensity and the 10-cm peak flux indicate that the events may be classified according to the 10-cm excitation level preceding the flux peak.

In the first type, the 10-cm radio flux rises rapidly to a peak from the quiet sun level in less than 2 min, and always precedes the H-alpha maxima. In 60 percent of the events of this class, the 10-cm burst peaks occur 2 to 10 sec before the H-alpha maxima; 35 percent have time differences of 10 to 20 sec; and 5-percent lead the H-alpha by 20 to 30 sec.

In the second type, 10-cm excitation exists for more than 4 min before the time of burst peak flux. Five percent of the events of this class have 10-cm peaks following the H-alpha maxima by 0 to 10 sec, while the great majority have 10-cm peaks preceding the flare maxima with the following time distribution: 30-percent lead by 0 to 10 sec, 35-percent lead by 10 to 20 sec, 25-percent lead by 20 to 30 sec, and 5-percent lead by 30 to 40 secs. There is evidence that several events of the second type may be associated with more than one source [Edelson, Coates, Santini, and McCullough, 1959].

On June 9, 1959 a burst of solar radiation was recorded at a wavelength of 4.3-mm by Coates and Edelson at the USNRL. Simultaneously, a large outburst was recorded at 10.7-cm by Covington at the National Research Council, Canada. The peak flux at 4.3 mm was $500 \times 10^{-22} \text{ wm}^{-2} \text{ cps}^{-1}$ as compared with $2,000 \times 10^{-22} \text{ wm}^{-2} \text{ cps}^{-1}$ at 10.7 cm.

The position of the radio emitting source determined by a high-resolution scan at 10.7 cm agreed with the position of a jet on the NRL H-alpha spectroheliograms. The base of the ejection appeared to be beyond the limb on the back side of the sun. This region remained active as it rotated onto the front of the sun and it was possible to determine its position on June 9. Using this position and the known heights of the radio limb of the sun of 0.0057 R_{\odot} at 4.3 mm and 0.03 R_{\odot} at 10.7 cm, the minimum height of the emitting region was determined to be $20,000 \pm 10,000$ km and $37,000 \pm 10,000$ km, respectively. These are lower limits only; the actual emitting regions may have been located at much greater heights [Coates, Covington, and Edelson, 1959].

12.4. Moon

Observations of the moon at 2.2-cm wavelength [Grebekemper, 1958] showed that the variation in brightness with lunar phase is much less than at shorter wavelengths, i.e. 8.6 and 12.5 mm, with the variation being about ± 5 percent. The apparent mean brightness temperature was found to be 200° K . The diminished brightness variation with phase is in agreement with unpublished observations of Mayer, McCullough, and Sloanaker at 3.15-cm wavelength, and is readily accounted for by an increasing depth of penetration for the longer wavelengths, which places the origin of thermal radiation at greater depths where thermal changes are less.

The total lunar eclipse of 13 March 1960 was observed at 8.6-mm and 21-cm wavelengths, and analysis of the results is incomplete at the time of preparing the present report.

Lunar radiation of 4.3-mm wavelength was measured with the aid of an equatorially mounted paraboloidal antenna 10 ft in diameter [Coates, 1959]. By making repeated television-type scans across the moon's disk, it was possible to construct crude lunar maps for different phases. Because the angular resolution was 6.7 min of arc, compared with the moon's 31-min average diameter, the larger surface features are recognizable.

Such charts show primarily the distribution of temperature over the lunar disk. In particular, it was found that the large, dark, level areas (maria) warm up more rapidly toward full moon and afterward cool more rapidly than do the "continental" parts of the moon. However, Mare Imbrium is an exception to this general rule.

12.5. Atmospheric Attenuation

Atmospheric attenuation at 4.3-mm wavelength was measured in 1956 by Coates using a 10-ft precision paraboloid and a Dicke-type radiometer. The measured attenuations at the zenith were between 1.6 and 2.2 db depending on atmospheric conditions [Coates, 1957]. These values were verified by Edelson, Grant, and Santini in March 1960 using the same radiometer and a 2-ft precision paraboloid.

13. The National Aeronautics and Space Administration

The Astronomy and Astrophysics Programs of the Office of Satellite and Sounding Rocket Programs of NASA include projects designed to make basic astronomical observations from above the terrestrial atmosphere by radio techniques. Observations of the planets, sun, radio stars, and the galactic background will be made at radio frequencies which are absorbed by the terrestrial atmosphere and ionosphere.

The work is divided into two phases. Proposed LF (0.1 to 30 Mc/s) experiments include a space probe, to detect galactic noise, monitoring of solar bursts, polarization measurements, and multiple- and

sweep-frequency measurements of the planets and galaxy. These are being done by Haddock of the University of Michigan and by the Canadian Defence Telecommunications Board as a byproduct of a top-side sounder experiment. The HF (submillimeter frequencies) will include studies and radio spectra of the atmospheres of the sun and planets and mapping the sun, moon, planets, and galaxy in the region between the infrared and the atmospheric radio window. Because of the limitations of the present state of the art, current activity in the HF phase is limited to a survey by the University of Texas of existing techniques and of areas in which development should be encouraged promptly and to basic research in sub-millimeter techniques by Ohio State University. NASA is also supporting a measurement of the solar parallax by studying the Doppler Shift in the 21-cm line.

14. National Bureau of Standards Boulder Laboratories

The solar patrol, which was started in 1947, has been continued until the end of the International Geophysical Year. Consistent calibration and scaling of hourly medians and outstanding occurrences are complete on both 167 and 460 Mc/s. Reports were submitted regularly to the I.A.U. Quarterly Bulletin of Solar Activity. Since January 1959, the patrol has been reduced to the single frequency 167 Mc/s, and scaling has been less detailed.

The National Bureau of Standards has recently completed a program of interferometric observations of Cygnus-A for the purpose of studying ionospheric effects, particularly angular and amplitude scintillations. An important feature of this program has been the frequent observation, during daytime, of irregular angular fluctuations having a period of about 20 min and a magnitude of as much as $\frac{1}{2}$ deg at 108 Mc/s [Lawrence, 1958; Lawrence and Jespersen, 1959].

15. National Radio Astronomy Observatory Green Bank, West Virginia

The National Science Foundation contracted with Associated Universities, Inc., on November 17, 1956, to proceed with the construction and operation of the National Radio Astronomy Observatory, Green Bank, W. Va. In May 1957, Associated Universities, Inc., set up a field office on the site. Ground-breaking ceremonies were held on October 17, 1957, and the Howard E. Tatel 85-ft telescope was dedicated on October 16, 1958.

In the 12 months ending May 1960, the National Radio Astronomy Observatory has completed a transition from the first phase of site acquisition, development, and construction into an operating observatory. A key factor for the future success of the Observatory was the appointment of Dr. Otto Struve as the first Director.

The buildings that have been completed are the central section of one Karl Guthe Jansky Laboratory, which houses the Astronomy and Research Equip-

ment Development Departments as well as space for the office of the Director, administration, and engineering and construction, and a residence hall and cafeteria. A small amount of additional housing is available in a few renovated farmhouses acquired with the site. A work area building, for central shops and other service purposes, was completed the previous year. A central water supply and sewer system has been installed for the complex of the principal buildings and with the cooperation of the Monongahela Power Company a new 3-mw electric power supply has been brought to the site. On the site, the distribution system is below ground; within view of the radio telescopes. The 12-kv feeder line is in shielded cable, mounted on poles to simplify maintenance.

The Howard E. Tatel 85-ft radio telescope was used for observational programs throughout the spring, summer and early fall of 1959, at which time the Blaw Knox Co. returned to make final adjustments and corrections before turning the telescope over to Observatory. The E. W. Bliss Co. shipped two sections of the polar shaft of the 140-ft telescope in August 1959; Darin and Armstrong, the subcontractor for field work at Green Bank, has welded these sections together and the shaft is now mounted on temporary horizontal bearings in anticipation of future machining operations. Work at Green Bank is now shut down pending shipment of additional telescope components, as scheduled through the last 8 months of 1960 into 1961.

In addition to the scientific contributions that have already come from the Observatory, it has attracted many nonprofessional visitors and plans are being made to accommodate an increasing flow during the summer of 1960 and the years ahead.

15.1. The Flux Density of Radiation From Cas A at 1,400 Mc/s

As a part of the program of source calibration at the National Radio Astronomy Observatory experiments have been started to measure the flux density from the Cas A source. One major experimental difficulty in such measurements is to determine exactly the effective collecting area of the antenna that is used. To minimize this difficulty a horn antenna of about 10 m² collecting area has been built. The horn is large enough to give an antenna temperature from the Cas A source of about 8° K. The gain of such a horn can be calculated from its linear dimensions to a high accuracy. The horn is fixed in position at an elevation angle of 30° and is used as a transit instrument. It is 120-ft in length and is made of sheet aluminum with all joints internally welded to ensure high electrical conductivity.

16. Ohio State University

16.1. Radio Telescopes

A design for a radio telescope which provides a large aperture at low cost is described [Kraus, 1958a].

Equations are derived from the numbers of radio sources which a radio telescope can detect and the number which it can resolve. Based on these relations curves for the number of sources which can be both detected and resolved, as a function of frequency and aperture, are presented.

Construction of a large aperture antenna at low cost is described [Kraus, 1959a]. The antenna consists of a 360- by 70-ft standing paraboloid and tiltable flat reflector. At the highest frequency of operation (15-cm wavelength) the half-power beam widths of the antenna will be 0.1° in R. A. by 0.5° in declination. The antenna is expected to be in operation by 1961.

16.2. Cosmic Radio Noise

The results of a survey of cosmic radio background radiation at 250 Mc/s are described [Ko, 1958a].

Radio maps made at other frequencies by various groups are summarized. To present an over-all picture of the radio sky at different frequencies, eight radio maps are shown for frequencies from 64 to 910 Mc/s. All maps are modified to have the same scale, coordinates and units to facilitate inter-comparison. General features of the galactic background radiation are discussed.

A radio map of the Cygnus region made at 915 Mc/s using a 40-ft dish is presented [Eaton and Kraus, 1959].

Observations are described of radio emissions from the sun and Jupiter, during 1956 and early 1957 at a wavelength of 11 m [Kraus, 1959b].

The results of amplitude scintillation of Cygnus A at 945 Mc/s are described [Ko, 1958b]. The scintillation is strongest near the horizon with a mean-fluctuation index of 20 percent and mean fluctuation rate of 2 to 6 peaks/min. The scintillation characteristics are markedly affected by the presence of aurorae.

16.3. Earth Satellite Observations

A peculiar fluctuation on Sputnik I signal at 20 Mc/s is described and a hypothesis is advanced that the fluctuations are caused by the satellite induced ionization [Kraus and Albus, 1958].

The feasibility of detecting silent earth satellites by refraction of cw signals from a high-frequency radio station is described [Kraus, 1958b]. The possible application for long-distance communication is suggested.

Observations during the last days of Sputnik I's orbiting using cw reflection technique are described [Kraus and Dreese, 1958]. Some conclusions are drawn as to the details of the actual breakup phenomenon of the satellite.

Observations of the U.S. Satellites Explorers I and III by cw reflection using WWV signals are described [Kraus, Higgy, and Albus, 1958].

A statistical study of the satellite ionization phenomenon is described and some radar observations are also reported [Kraus, Higgy, Scheer, and Crone, 1960].

16.4. Interplanetary Medium

Some observations are described which are suggestive of doppler shifted reflections of radio signals from solar corpuscular clouds in the vicinity of the earth [Kraus and Crone, 1959].

17. Rensselaer Polytechnic Institute

Radio astronomy work at Rensselaer during the past continues to be primarily in the constructional phases of our two principal projects. The 517-Mc/s swept-lobe interferometer has successfully measured positions of some solar bursts; we expect in the next few months to be able to record angular motions, and to place the equipment in its permanent location, for which site preparation is currently in progress. A second 18-Mc/s cosmic-noise recorder is being built to provide greater stability and improved rejection of station signals; the antenna is being built in a location which will allow eventual expansion to a narrower directional pattern. Records have been secured and published at 18-Mc/s, and simultaneous records are being taken of certain meteorological parameters, with some indications of unexpectedly high tropospheric absorptions of 18-Mc/s radiation.

18. Stanford University

At the Radioscience Laboratory, Stanford, R. N. Bracewell has completed the construction of a microwave spectroheliograph and obtained sequences of maps, as yet unpublished, of the brightness distribution over the sun. V. R. E. Eshleman has obtained radar echoes from the sun. He has also investigated the character of the cislunar medium using radar echoes from the moon. R. Mlodnosky has continued theoretical and observational studies of the distribution of meteor radiants.

19. Yale University

The work of the past year has continued to be concentrated almost exclusively on the Jupiter program.

Functioning equipment now includes as basic monitoring units six phase-switching interferometers working respectively at 23.0, 22.2, 20.0, 19.2, 16.15, and 13.25 Mc/s. An additional 20.0 Mc/s interferometer is located 11 miles away from the others. This monitoring equipment, running semi-automatically and continuously, to some degree covers the sun and other planets as well as Jupiter. But during all possible Jupiter reception periods an observer is on duty to achieve optimum tuning and sensitivity of the channels. Compared to last year, Jupiter is about twice as active during this observing season. Complete reduction for rotation periods, of our monitoring records plus all other available Jupiter storm data, is under way as a part of J. Douglas' thesis.

New projects completed include facilities for high-speed recording, and for spectrum analysis using 10 separate 20-kc/s channels spaced 100 kc/s apart,

the comb-filter unit centered near 22 Mc/s. Successful recordings have been obtained on four strong Jupiter storms in the last few weeks. These fail to show any recognizable spike activity of several millisecond duration of the kind previously suggested by others. However, the recordings do show excellent correlation of fine structure down to several tenths of a second duration over bandwidths normally greater than a megacycle. There is no appreciable tendency for any of the elementary pulses to drift in frequency. But a new class of Jupiter event has appeared in which the bursts composing a group are so modulated as to make the group appear to drift from HF to LF at about 1 Mc/s/min (that is, the spectral energy distribution of the successive individual bursts changes gradually, with the peak appearing at progressively lower frequencies).

Bibliography: Smith and Douglas, 1959; and Smith 1959.

20. University of Michigan

20.1. University of Michigan 85-Foot Radio Telescope

In the summer of 1958 field construction began on the University of Michigan 85-ft antenna, designed and fabricated by the Blaw Knox Company of Pittsburgh. The antenna is polar-mounted, made of galvanized steel except for the lead counterweights and the aluminum surface panels and feed supports. The telescope may be rotated about the polar and declination axes at a fixed rate of about 20 deg/min or at a variable rate between zero and 8 deg/min. In addition, the polar axis can be driven at the sidereal or solar rate.

Mechanical testing was performed during and after construction. The axes were alined to an accuracy of 30 sec of arc and surface panels were adjusted to within 1.5 mm from a paraboloid. Antenna gain and beam width measurements indicate an aerial efficiency of about 50 percent and a beam-width of 6 min of arc at a wavelength of 3.45 cm.

20.2. Traveling-Wave Tube Receiver at 8,000 Mc/s

The 85-ft radio telescope was initially instrumented at 8,000 Mc/s with a radiometer made by the Ewen-Knight Co. It is capable of detecting signals of the order of 0.1 °K or less with a 20-sec time constant. This sensitivity is obtained through its large bandwidth of 1,000 Mc/s. The receiver is composed of three traveling-wave tubes in cascade followed by conventional Dicke circuitry using a ferrite switch. The receiver is being used to study galactic and extragalactic radio sources, the planets and planetary nebulae.

20.3. Maser Radiometer at 8,700 Mc/s

A ruby maser radiometer has been constructed by the University of Michigan Willow Run Laboratories and is mounted at the focus of the 85-ft antenna.

The maser, operating at liquid helium temperature of 4.25 °K, has a gain of 20 to 23 db and a bandwidth of 20 Mc/s, however, as used in the present radiometer the bandwidth is 8 Mc/s as determined by the IF amplifiers. Continuous operation for a period of 15 hr has been obtained before adding more liquid helium. The signal frequency is 8,700 Mc/s, the "double-pump" frequency is 22,450 Mc/s, and the operating magnetic field is 3,870 gauss.

The maser radiometer is being used in attempts to observe radiation from weak radio sources. Operation began in February 1960 and preliminary results are very promising.

20.4. Radiometer at 1.8 CM-Wavelength

A Dicke radiometer operating at 16,000 Mc/s has also been installed on the 85-ft antenna. Its bandwidth is 10 Mc/s. It employs a "magic-tee" balanced crystal mixer, and is switched by an electronically controlled ferrite. The sources Cas A, Tau A, and Venus have been measured.

20.5. Theoretical Radio Spectrum of Venus

The radio results obtained at the Naval Research Laboratory of the planet Venus have been analyzed in terms of a model atmosphere in an attempt to explain the discrepancy between the radio and infrared temperatures. Although the data is still meager in the millimeter band of wavelengths, it appears that radio results afford a means of probing below the cloud cover. On the basis of an atmosphere of 75-percent CO₂, 22- to 25-percent N₂, and 0- to 3-percent H₂O, the pressure at the surface of Venus must be between 10 and 30 (terrestrial) atm to coincide with the infrared and radio temperatures. This work will be published in brief in the June issue of the *Journal of Geophysical Research* and in full in the *Astrophysical Journal*.

Since September 1957, the sun has been observed by three mechanically tuned superheterodyne receivers. A total frequency range of 100 to 600 Mc/s is observed 3 times a second. The output is displayed as an intensity-modulated line on a high-resolution cathode-ray tube and is photographed on a slowly moving 35-mm film, producing a frequency-time-intensity plot of solar emission. Each receiver is fed from a separate broadband antenna mounted at the focus of a 28-ft equatorially mounted paraboloid reflector.

We believe that we have obtained the first evidence of three harmonically related frequencies being radiated simultaneously by the sun. That is, three bands of radiation in a 1 to 2 to 3 frequency ratio. This event occurred in the first week of observation and consisted of three U-type bursts—bursts that start drifting rapidly from high to low frequencies, then reversing and drifting back to high frequencies again in a symmetrical manner.

Dr. Takakura, a Japanese radio astronomer who was with us for a year (1957–1958), analyzed a number of these U-type bursts and found a remarkable uniformity in their duration which was independent

of the reversing frequency. This fact is in discord with a popular hypothesis for the origin of U-bursts. An alternative hypothesis has been suggested that is consistent with our observations.

The dynamic spectra of a new type of radio burst has been observed for the first time. This type of burst was discovered by Drs. Boischoit and Denisse in Paris on single frequency records. They denoted it as type IV. The observed dynamic radio spectra gave strong evidence in favor of the French hypothesis that the type IV bursts were generated in the sun's atmosphere by very energetic electrons being accelerated in the sun's magnetic field.

Solar emission has been recorded since August 28, 1957 to the present time. The equipment has been in operation at least 90 percent of the time when the sun has been above the horizon.

In the summer of 1959, a new electronically sweep receiver was installed in order to record dynamic spectra of solar bursts in the frequency range of 2,000 to 4,000 Mc/s. It uses a broad-band horn located at the focus of the above 28-ft paraboloid reflector and operates simultaneously with the above equipment. The rf signal is mixed with the local oscillator signal in a broadband balanced mixer and converted directly to a videofrequency. The videofrequency is then amplified and displayed as described above for the 100 to 600 Mc/s equipment.

The local oscillator is a backward-wave oscillator electronically sweeping on a frequency range of 2,000 to 4,000 Mc/s in 0.1 sec.

Although the equipment is not operating with satisfactory reliability, at least six broadband solar bursts had been observed by April 1960. The first was July 29, 1959. These records show that the centimeter-wave emission of solar bursts is a broadband continuum radiation, similar in nature to that of type IV emission on meter waves.

A comparison is being made of the centimeter-wave bursts with different spectral types of bursts on meter waves.

Statistical studies have been made of the relation between solar radio emission and ionospheric absorption of cosmic noise in polar cap regions (PCA), which is caused by fast protons from the sun after big flares. Broadband meter-wave outbursts (BCO)—believed to be of the same nature as type IV continuum radiation on meter-waves—have been found to be closely associated with PCA events. Further, the PCA events have a tendency to start within 5 hr after intense BCO's; for the less intense BCO's the delay appears to be greater.

The duration of the PCA events is closely related to the duration of "active regions" of noise storms on the sun (which in turn are associated with BCO or type IV flares) after the occurrence of BCO (or type IV) events, but is not related to the presence of "active regions" before the onset of the BCO. The PCA start within several hours after a BCO event and last approximately as long as the "active region" is present. Our results support the suggestion that these solar cosmic rays are accelerated by the same process as the fast electrons which are

responsible for BCO or type IV radio emission near the sun and are trapped in the same region of the solar atmosphere associated with "active regions" of noise storms and are not stored in interplanetary space. The energetic electrons lose their energy rapidly by this radiation, whereas radiation damping of the protons is negligible.

Two space radio astronomy experiments in the 0.1- to 30-Mc/s band are under preparation, (1) spot-frequency measurements from high-altitude probes, and (2) sweep-frequency measurements of solar radio bursts from satellites. These will be carried out at the lowest frequencies which are stopped by, or seriously affected in their passage through, the ionosphere. The former will give information on the spectral distribution of cosmic noise and also on electron density in the outer ionosphere and possibly in interplanetary regions; the latter will examine solar outbursts and it is hoped will extend the spectrum below the currently known lower limit. In principle, both experiments can be carried out by use of sweep-frequency receivers, but the frequency range desired and the problems of accurate calibration and telemetering make spot frequency more feasible for the former measurements.

Bibliography: Haddock, 1958, 1959, 1960a, b, c; Aller, Goldberg, Haddock, and Liller, 1958; Takakura, 1959; Barrett, 1960a, b; and Kundu and Haddock, 1960.

References

- Aarons, J., W. R. Barron, and J. P. Castelli, Radio astronomy measurements at VHF and microwaves, *Proc. IRE* **46**, 325 (1958).
- Aarons, J., J. P. Castelli, R. M. Straka, and W. C. Kidd, Observations of the solar eclipse of October 2, 1959, *Nature* **185**, 230 (1960).
- Aarons, J. and J. P. Castelli, Simultaneous scintillation observations on 1300-Mc. and 3000-Mc. signals received during the solar eclipse of 2 October 1959, *URSI Conference* (1960).
- Akabane, Cohen, Polarization measurements of type III bursts and Faraday rotation in the corona, submitted for publication.
- Aller, L., L. Goldberg, F. T. Haddock, and W. Liller, Astronomical experiments proposed for earth satellites, *UMRI Report* 2783-1-F, (1958).
- Alsop, L. E., J. A. Giordmaine, C. H. Mayer, and C. H. Townes, Observations using a maser radiometer at 3-CM wavelength, *Astron. J.* **63**, 301 (1958).
- Alsop, L. E., J. A. Giordmaine, C. H. Mayer, and C. H. Townes, Observations of discrete sources at 3-CM wavelength using a maser, *Proc. IAU-URSI Paris Symposium on Radio Astronomy* (Stanford University Press, Stanford, Calif., 1959).
- Baade, W. and R. Minkowski, Identification of the radio sources in Cassiopeia, Cygnus A, and Puppis A, and on the identification of radio sources, *Astrophys. J.* **119**, 206 and 215 (1954).
- Barrett, Microwave absorption and emission in the atmosphere of Venus, to appear in *Astron. J.* (1960a).
- Barrett, Preliminary results with a maser radiometer at 3.45 cm wavelength, abstract to appear in *Astron. J.* (1960b).
- Bellville, Holt, and Iliff, Atmospheric factors affecting precision location of celestial radio sources, *URSI U.S. Annual Meeting* (1958).
- Brockman, M. H., H. R. Buchanan, R. L. Choate, and L. R. Mallin, Extra-terrestrial radio tracking and communication, *Proc. IRE* **48**, 643 (1960).
- Castelli, J. P., J. Aarons, C. Ferioli, and J. Casey, Absorp-

- tion, refraction and scintillation measurements at 4700 Mc/s with a traveling-wave tube radiometer, *Planet. Space Sci.* **1**, 50 (Pergamon Press, Inc., 122 E. 55 St., New York 22, N.Y. (Great Britain) 1959).
- Coates, R. J., The measurement of atmospheric attenuation at 4.3 mm wavelength, *NRL Report 4898* (1957).
- Coates, R. J., The lunar brightness distribution at 4.3 mm wavelength, *AAS Meeting* (1959), summary in *Sky and Telescope* **19**, 93 (1959).
- Coates, R. J., S. Edelson, T. McCullough, and N. Santini, IGY flare studies, *NRL Report 5203* (1958).
- Coates, R. J., S. Edelson, N. Santini, and Dows, IGY and IGC H-alpha solar observations of flares, surges and active prominences, *NRL Reports* (1957-1959).
- Coates, R. J., A. E. Covington, and S. Edelson, The 4.3-MM and 10.7-CM outbursts of June 9, 1959, *Astron. J.* **64**, 326 (1959).
- Cohen, M. H., Magneto-ionic mode coupling at high frequencies, *Astrophys. J.* (in press).
- Cohen, M. H., Radio astronomy polarization measurements, *Proc. IRE* **46**, 172 (1958a).
- Cohen, M. H., The Cornell radio polarimeter, *Proc. IRE* **46**, 183 (1958b).
- Cohen, M. H. and A. D. Fokker, Some remarks on the polarization of 200 Mc/s solar radio emission, *IAU-URSI Symposium on Radio Astronomy* (Stanford Univ. Press, Stanford Calif., 1959).
- Cohen, M. H., Linear polarization in type III bursts, *Astrophys. J.* **130**, 221 (1959).
- Drake, F. D., Private communication (1959).
- Drake, F. D. and S. Hvatum, Non-thermal microwave radiation from Jupiter, *Astron. J.* **64**, 329 (1959).
- Eaton, J. J. and J. D. Kraus, A map of the Cygnus region at 915 Mc per second, *Astrophys. J.* **129**, 282 (1959).
- Edelson, S., R. J. Coates, N. Santini, and T. P. McCullough, Time relations between centimeter wavelength bursts and solar H-alpha flares, *Astron. J.* **64**, 330 (1959).
- Gibson, J. E. and R. J. McEwan, Observations of Venus at 8.6 mm wavelength, *IAU-URSI Paris Symposium on Radio Astronomy* (Stanford Univ. Press, Stanford, Calif., 1959).
- Giordmaine, J. A., L. E. Alsop, C. H. Mayer, and C. H. Townes, Observations of Jupiter and Mars at 3-cm wavelength, *Astron. J.* **64**, 332 (1959a).
- Giordmaine, J. A., L. E. Alsop, C. H. Mayer, and C. H. Townes, A maser amplifier for radio astronomy at X-band, *Proc. IRE* **47**, 1062 (1959b).
- Goldstein, S. J., The angular size of short-lived solar radio disturbances, *Astrophys. J.* **130**, 393 (1959).
- Grebenkemper, C. J., Lunar radiation at a wavelength of 2.2 Cm., *NRL Report 5151* (1958).
- Haddock, F. T., Introduction to radio astronomy, *Proc. IRE* **46**, 3, (1958).
- Haddock, F. T., Some characteristics of dynamic spectra of solar bursts, *IAU-URSI Paris Symposium on Radio Astronomy*, 188 (Stanford Univ. Press 1959).
- Haddock, F. T., Radio telescope, *McGraw-Hill Encyclopedia of Science and Technology* (McGraw-Hill Book Co., Inc., N.Y., N.Y., 1960a).
- Haddock, F. T., Radio astronomy, *McGraw-Hill Encyclopedia of Science and Technology* (McGraw-Hill Book Co., Inc., N.Y., N.Y., 1960b).
- Haddock, F. T., Radio astronomy observations from space, To appear in the July 1960 issue of the *Am. Rocket Soc. J.* (1960c).
- Hamilton, A. R., Final engineering report for 960 mc phase-lock tracking receiver, *Collins Engineering Report 1125* (1959).
- Iliff, G. R. Marner, Radio-astronomical techniques in the study of tropospheric propagation, *URSI U.S. Annual Meeting* (1960).
- Jaffe, E. Reichtin, Design and performance of phase-lock loops capable of near-optimum performance over a wide range of input signal and noise levels, *JPL Progress Report 20-243* (1954).
- Keh, K. C. and G. W. Swenson, The scintillation of radio signals from satellites, *J. Geophys. Research* **64**, 2281 (1959).
- Ko, H. C., The distribution of cosmic radio background radiation, *Proc. IRE* **46**, 208 (1958a).
- Ko, H. C., Amplitude scintillation of extra-terrestrial radio waves at ultra high frequency, *Proc. IRE* **46**, 1872 (1958b).
- Kraus, J. D., Radio telescope antennas of large aperture, *Proc. IRE* **46**, 92 (1958a).
- Kraus, J. D., Detection of Sputnik I and II by CW reflection, *Proc. IRE* **46**, 611 (1958b).
- Kraus, J. D., The Ohio state university 360-foot radio telescope, *Nature* **184**, 669 (1959a).
- Kraus, J. D., Planetary and solar radio emission at 11 meters wavelength, *Proc. IRE* **46**, 266 (1959b).
- Kraus, J. D. and J. S. Albus, A note on some signal characteristics of Sputnik I, *Proc. IRE* **46**, 610 (1958).
- Kraus, J. D. and W. R. Crone, Apparent observation of solar corpuscular clouds by direct continuous-wave reflection, *Nature* **184**, 965 (1959).
- Kraus, J. D. and E. E. Dreese, Sputnik I's last days in orbit, *Proc. IRE* **46**, 1580 (1958).
- Kraus, J. D., R. C. Higgy, and J. S. Albus, Observations of the U.S. satellites Explorers I and III by CW reflection, *Proc. IRE* **46**, 1534 (1958).
- Kraus, J. D., R. C. Higgy, D. J. Scheer, and W. R. Crone, Observations of ionization induced by artificial earth satellites, *Nature* **185**, 520 (1960).
- Kundu, F. T. Haddock, A relation between solar radio emission and polar cap absorption of cosmic noise, to appear in *Nature* (London).
- Lawrence, R. S., An investigation of the perturbations imposed upon radio waves penetrating the ionosphere, *Proc. IRE* **46**, 315 (1958).
- Lawrence, R. S. and J. L. Jespersen, A preliminary analysis of amplitude scintillations of radio stars observed at Boulder, Colorado, *NBS Tech. Note* 20 (1959).
- Marner, G. R., Radiometric measurement of 8.7 mm atmospheric attenuation, *Doctoral thesis*, State University of Iowa, Collins Engineering report 479 (1956).
- Marner, G. R., New determinations of atmospheric microwave absorption by radio-astronomical methods, *URSI U.S. Annual Meeting* (1958a).
- Marner, G. R., Atmospheric radiation received by directional antennas, *URSI U.S. Annual Meeting* (1958b).
- Marner, G. R., Automatic radio-celestial navigation, *J. (British) Inst. of Navigation* **12**, 249 (1959).
- Marner, G. R., The use of radio astronomy techniques for navigation, *URSI U.S. Annual meeting* (1960a).
- Marner, G. R., Plotting the future course of marine celestial navigation, *Institute of Navigation Annual Meeting* (1960b).
- Marner, G. R., Iliff, Observed 8.7 mm refraction as a function of surface meteorological conditions, *URSI U.S. Annual Meeting*, (1958).
- Marner, G. R. and McCoy, Navigation system using the sun and artificial satellites, *Collins Engineering Report 1587* (1959).
- Maxwell, A., G. Swarup, and A. R. Thompson, The radio spectrum of solar activity, *Proc. IRE*, **46**, 142 (1958).
- Maxwell, A., Solar radio astronomy in Texas, *Sky and Telescope* **17**, 388 (1958).
- Maxwell, A., American astronomers report, *Sky and Telescope* **18**, 556 (1959).
- Maxwell, A., W. E. Howard, and G. Garmire, Solar radio interference at 125, 200, 425, 550 Mc/s, Report prepared for Rome Air Development Center; USAF 19(604)-1394 Scientific Report No. 14.
- Maxwell, A., A. R. Thompson, and G. Garmire, The association of solar radio bursts with auroral streams, *Planet. Space Sci.* **1**, 325 (1959).
- Maver, C. H., T. P. McCullough, and R. M. Sloanaker, Evidence for polarized radio radiation from the Crab Nebula, *Astrophys. J.* **126**, 468 (1957).
- Maver, C. H., T. P. McCullough, and R. M. Sloanaker, Observations of Venus at 3.15-cm wavelength, *Astrophys. J.* **127**, 1 (1958a).
- Maver, C. H., T. P. McCullough, and R. M. Sloanaker, Measurements of planetary radiation at centimeter wavelengths, *Proc. IRE* **46**, 260 (1958b).
- Mayer, C. H., T. P. McCullough, and R. M. Sloanaker, unpublished (1958c).

- Mayer, C. H., T. P. McCullough, and R. M. Sloanaker, Observations of Mars and Jupiter at a wavelength of 3.15 cm., *Astrophys. J.* **127**, 11 (1958c).
- Mayer, C. H., T. P. McCullough, and R. M. Sloanaker, unpublished (1959).
- Mayer, C. H. and R. M. Sloanaker, Polarization of the 10-cm radiation from the Crab Nebula and other sources, *Astron. J.* **64**, 339 (1959).
- McClain, E. F., A test for non-thermal radiation from Jupiter at a wavelength of 21-cm., *Astron. J.* **64**, 339 (1959).
- McClain, E. F. and R. M. Sloanaker, Preliminary observations at 10-cm wavelength using the NRL 84-foot radio telescope, *Proc. IAU-URSI Paris Symposium on Radio Astronomy* 61 (Stanford Univ. Press, Stanford, Calif., 1959).
- McCullough and Bologna, Solar radio emission data, CRPL-F Part B, Solar Geophysical Data, National Bureau of Standards (1958-1959).
- McVittie, G. C., Les theories relativites de la gravitation, *Proc. of Colloquium, Royaumont, France, June 1959* (in press) (1960a).
- McVittie, G. C., A radio-astronomy project at the University of Ill., *IRE Trans. Military Electronics MIL4* **14** (1960b).
- McVittie, G. C. and S. P. Wyatt, The background radiation in a Milne universe, *Astrophys. J.* **130**, 1 (1959).
- Mitchell, Whitehurst, A radio study of the sun and moon at millimeter wavelengths, Final Technical Report, Office of Ordnance Research, U.S. Army (1958).
- Mitchell, Whitehurst, and Weaver, Thermal radiation from the sun at 8.5 mm wavelength, Interim Technical Report No. 3, Office of Ordnance Research, U.S. Army (1957).
- Oort, J. H. and T. Walraven, Polarization and composition of the Crab Nebula, *B. A. N.* **12**, 285 (1956).
- Sloanaker, R. M., Apparent temperature of Jupiter at a wavelength of 10-cm., *Astron. J.*, **64**, 346 (1959).
- Sloanaker, R. M. and Nichols, The positions, intensities, and sizes of bright celestial sources at a wavelength of 10.2 cm., *A. J.* **65**, 109 (1960).
- Smith, H. J., Non-thermal solar system sources other than Jupiter, *Astron. J.* **64**, 41 (1959).
- Smith, H. J. and J. N. Douglas, Observations of planetary non-thermal radiation, *Proc. IAU-URSI Paris Symposium on Radio Astronomy*, 53 (Stanford Univ. Press, Stanford, Calif., 1959).
- Straka, Swarup, 10-cm total solar eclipse observations, *URSI Conference* (1960).
- Strand, K. A., Stellar motions in the Orion Nebula cluster, *Astrophys. J.* **128**, 14 (1958).
- Swarup, Stone, Maxwell, *Astrophys. J.* (in press).
- Takakura, T., Synchrotron radiation and solar radio outbursts at microwave frequencies, *IAU-URSI Paris Symposium on Radio Astronomy*, 562 (Stanford Univ. Press, Stanford, Calif., 1959).
- Thompson, A. R., and A. Maxwell, Solar radio bursts and low energy cosmic rays, *Nature (London)* **185**, 89 (1960).
- Thompson and Maxwell, *Planet. Space Sci.* (in press).
- Tyler, W. C., R. N. Whitehurst, and F. H. Mitchell, Radio observations of the moon at 7.5 mm wavelength, *Bull. Am. Phys. Soc. II*, **3**, 301 (1958).
- Weaver, R. R., F. H. Mitchell, and R. N. Whitehurst, Solar radiation at 8.6 mm wavelength, *Bull. Am. Phys. Soc.*, **II**, **3**, 301 (1958).



Part 1. Information Theory and Coding

P. Elias*

Since 1957, there has been considerable progress in the theory of coding messages for transmission over noisy channels. There have been three main directions of advance. First, there has been work on the foundations of the theory. During this time American mathematicians interested in probability have shown a serious interest in information theory, since Feinstein's work (now available in book form) [Feinstein, 1958a] and since the interest shown by Kolmogorov and Khinchin. Second, a great deal of work has been done on error-correcting block codes for noisy binary channels. This work has involved a good deal of modern algebra, and some mathematical algebraists have been joining the communications research workers in attacking these problems. Third, there has been continuing investigation of procedures in which input messages are coded and decoded sequentially rather than in long blocks. This work and the work on binary block codes both have significant practical implications for electrical communications.

1. Foundations

Shannon's original demonstration of the noisy channel coding theorem was an existence proof [Shannon, 1949]. Given a channel of capacity C bits per second and a rate of transmission R bits per second, the transmitter sends sequences of N channel input symbols. The receiver receives sequences of N channel output symbols and decides which input sequence was transmitted, making this decision incorrectly with probability P . What Shannon showed was that for $R < C$, P could be made arbitrarily small by increasing N . The proof was not constructive, and nothing quantitative was said about how rapidly P decreased as a function of N for given R and C . Feinstein [1954; 1958a] showed that P could be bounded by a decaying exponential in N . His proof covered channels with a simple kind of finite memory. While constructive in principle it could not be used in practice to construct a code with large N . In 1957, Shannon [1957] gave a remarkably concise proof based on his original random coding argument but more detailed and precise, which also gave an exponential bound to P as a function of N , and extended the proof to channels with considerably more complex memory. Blackwell, Breimann and Thomasian [1958] proved the existence theorem for channels with a finite-state memory of a still more general kind. Wolfowitz [1960] and Feinstein [1959] have also proved converse theorems—the weak converse being that for $R > C$, P cannot approach zero, and the strong converse being that for $R > C$, P must approach 1.

The kind of technique used by Shannon [1957] can be extended to obtain upper and lower bounds to the rate of exponential decay of P with N . Earlier work on binary channels had shown that for a considerable range of R less than C the upper and lower bounds essentially agreed, and best possible behavior could be uniquely specified. Similar results have been obtained by Shannon for more general channels.

This work is not yet published, but the case of a continuous channel with additive Gaussian noise has been treated in detail [Shannon, C. E., 1959].

The increasing interest of mathematicians in this field is evidenced by an article by Wolfowitz [1958]. In general the results which the mathematicians have obtained are firmer proofs under more general circumstances of theorems whose general character was not surprising to communications researchers. However a recent paper [Blackwell, Breimann, and Thomasian, 1959], has presented an interesting new problem, defining capacity and proving a coding theorem for a channel whose parameters are not known precisely, but are constrained to lie in known ranges. This work might be relevant to incompletely measured and time-varying radio channels. So might a paper by Shannon [1958] on channels in which the transmitter has side information available about the state of a channel with memory: an example would be the information obtained by measurements of the propagation medium obtained while communicating.

2. Binary Channels

Starting with the earlier work of Hamming [1950] and Slepian [1956a, 1956b], error-correcting block codes for binary channels have been investigated extensively. Peterson and Fontaine [1959] have searched for best possible error-correcting codes of short block length (up to 29), using a computer. The number of codes grows so rapidly with block length that it was necessary to use many equivalence relations and shortcut tests to eliminate codes from consideration early. A number of counterexamples were found to common conjectures about optimum codes.

The use of error-correcting codes in practice has been limited by the difficulty of implementation, and by the fact that in many applications of interest the errors in the channel are not independent, but occur in runs or bursts. In earlier work Huffman [1956] had shown a coding and decoding procedure

*Department of Electrical Engineering, M.I.T., Cambridge 39, Mass.

for the Hamming code which was simple to implement, and Green and SanSoucie [1958] have shown an easy implementation for a short multiple-error-correcting code. Hagelbarger [1959] has described codes which correct errors occurring in bursts whose implementation is not too difficult, and Abramson [1959] has described a highly efficient and easily implemented set of codes with similar properties.

Work on codes of longer block length, which can correct multiple errors, started with a decoding procedure given by Reed [1954] some time ago for the Reed-Muller family of codes. For really large block lengths these codes are not efficient, but Perry [1958] has built a coder and decoder for a Reed-Muller code which has block length of 128 digits, 64 of which are information digits and 64 check digits. This code can correct any set of 7 or fewer errors among the group of 128 and the efficiency is quite good. Using microsecond switching devices, the units can keep up with millisecond binary digits.

Calabi and Haefeli [1959] have investigated in detail the burst correcting properties of a family of codes which has been introduced earlier for correction of independent errors [Elias, P., 1954]. They also discuss the implementation of these codes.

A new family of codes discovered by Bose and Ray-Chaudhuri [1959, 1960] is much more efficient than the Reed-Muller codes for larger block lengths. Although in the limit of infinite block length these codes may also have zero efficiency, at lengths of a few thousands digits they are still quite good. Peterson [1960] has discovered an economical way to decode these codes. There is a great deal of current work on finding more properties of these codes, finding similar codes for channels which are symmetric but not binary, and so forth.

There has been a good deal of recent work on cyclic codes, including some encouraging results on step-by-step decoding due to Prange [1959]. Cyclic codes are closely related to the sequences which can be generated by shift registers with feedback connections. Recent discussions of these sequences have been given by Elspas [1959] and by Zierler [1959]. A review of the recent algebraic work on coding theory, including the Galois field theory which enters in the Bose-Chaudhuri codes, will be given by Peterson in a monograph to be published shortly [Peterson, 1960]. Most of the results in this area extend to channels which have an input alphabet of symbols whose number is not 2 but any prime to any power, the channel still being completely symmetric in the way it makes its errors. Non-binary channels have been investigated in their own right by Lee [1958] and by Ulrich [1957].

The introduction of two thresholds rather than one in a continuous channel introduces a null zone. The transmitter sends a binary signal, but the receiver makes a ternary decision, not attempting to guess the value of signals received in the null zone. Introducing the null zone may increase channel capacity, as shown by Bloom et al. [1957]. It also has the valuable effect of reducing the amount of computation required in decoding, since it is easier

to replace missing digits than to correct incorrect ones. This is especially relevant for application to channels with Rayleigh fading.

3. Sequential Decoding

Earlier work had shown that the block coding procedure could be modified (in the binary case) by constructing codes in a convolutional fashion, so that the coding and decoding of each digit was of the same character and involved the same delay [Elias, 1955]. The parameter which replaces block length in such an argument is the delay between the receipt of a digit and the attempt to decode it reliably. This simplified the coding but left the decoding procedure as complicated as ever. However Wozencraft [1957] has shown that a suitable sequential coding procedure may be followed by a sequential decoding procedure which reduces the average amount of decoding computation immensely. Like the best of the long block codes now in prospect, this procedure promises millisecond communication with microsecond switching circuitry in the decoder at very high reliability. Unlike the block codes, however, Wozencraft's procedure is statistical and not highly algebraic, and it may be expected to generalize to other discrete channels with no special symmetry properties. On the other hand the computation remains reasonable only for a range of R well below C . Epstein [1958] has studied a sequential decoding procedure for the erasure channel, and work on more general channels is under way.

4. Conclusions on Coding

The general conclusions of interest for applications of error-correcting codes are two. First, there are now several good small codes which correct bursts of errors, which could be instrumented fairly easily for use in situations in which a rate well below capacity can be tolerated so that short codes may be used. These may find early application in sending digital data over telephone lines. Second, there are now available several kinds of large block codes and sequential codes which will permit very reliable transmission over long distance scatter channels, which can also be implemented. The cost of implementation is appreciable in these cases, but current computer circuitry is fast enough to permit decoding at transmission rates of the order of 1,000 binary digits per second, coded in blocks or with sequential constraints hundreds of digits in length, and the alternative of more large antennas or greater transmitter power are also expensive. It seems likely that such systems will be in experimental use by the next international URSI meeting in 1963.

5. Other Topics

Less progress has been made in the economical coding of information sources. In part this is because such progress becomes work in speech analysis

of television systems and not information theory as such. However it might be worth noting that a scheme for coding runs of constant intensity in television has been demonstrated at full television speed by Schreiber [1958].

A relation between the bandwidth and the duration of a signal is imposed by the Heisenberg uncertainty principle, whose applicability to time functions was pointed out by Gabor many years ago. Kay and Silverman [1959] have examined this relationship more carefully, and a form of the uncertainty principle which places a lower bound on the sums of entropies rather than on the products of second moments is discussed by Leipnik [1960]. Stam [1959] also discusses this entropic inequality and closely related results.

The sampling theorem is closely related to these questions. Linden and Abramson [1960] have given a generalization which permits the closed form expression of a bandlimited function in terms of samples of the function and its first k derivatives, taken at time intervals $(k+1)$ times as far apart as is required for samples of the function value alone. This extends earlier work by Jagerman and Fogel [1956]. Results bearing both on the uncertainty principle and on approximate sampling theorems—i.e., theorems concerning functions which include all but a fraction δ_1 of their energy in bandwidth W and all but a fraction δ_2 of their energy in a time interval of duration T —are the subject of active current work.

6. References

- Abramson, N.M., A class of systematic codes for nonindependent errors, *IRE Trans.* **IT-5**, 150 (1959).
- Blackwell, Breimann, and Thomasian, Proof of Shannon's transmission theorem for finite-state indecomposable channels, *Ann. Math. Stat.* **29**, 1209 (1958).
- Blackwell, Breimann, and Thomasian, The capacity of a class of channels, *Ann. Math. Stat.* **30**, 1229 (1959).
- Bloom, Chang, Harris, Hauptschein, and Morgan, Improvement of binary transmission by null-zone reception, *Proc. IRE* **45**, 963 (1957).
- Bose and Ray-Chaudhuri, On a class of error-correcting binary group codes, *Inform. and Control* **3**, 68 (1960).
- Bose and Ray-Chaudhuri, Further results on error-correcting binary group codes (to appear in *Inform. and Control* **3**, June or September 1960).
- Calabi, L., and H. G. Haefeli, A class of binary systematic codes correcting errors occurring at random and in bursts, *IRE Trans.* **IT-5**, 79 (1959).
- Elias, P., Error-free coding, *IRE Trans.* **PGIT-4**, 29 (1954).
- Elias, P., Coding for noisy channels, 1955 *IRE Nat. Conv. Record*, Pt. **4**, 37 (1955).
- Elsas, B., The theory of autonomous linear sequential networks, *IRE Trans.* **CT-6**, 45 (1959).
- Epstein, M. A., Algebraic decoding for a binary erasure channel, 1958 *IRE Nat. Conv. Record*, Pt. **4**, 56 (1958).
- Feinstein, A., A new basic theorem in information theory, *IRE Trans.* **PGIT-4**, 2 (1954).
- Feinstein, A., Foundations of information theory (McGraw-Hill, Book Co., Inc., New York, N.Y., 1958).
- Feinstein, A., On the coding theorem and its converse for finite memory channels, *Inform. and Control* **2**, 25 (1959).
- Green and San Soucie, An error-correcting encoder and decoder of high efficiency, *Proc. IRE* **46**, 1741 (1958).
- Hagelbarger, D. W., Recurrent codes: Easily mechanized, burst-correcting, binary codes, *Bell System Tech. J.* **38**, 969 (1959).
- Hamming, R. W., Error-detecting and error-correcting codes, *Bell System Tech. J.* **29**, 147 (1950).
- Huffman, D. A., A linear circuit viewpoint on error-correcting codes, *IRE Trans.* **IT-2**, 20 (1956).
- Jagerman and Vogel, Some general aspects of the sampling theorem, *IRE Trans.* **IT-2**, 139 (1956).
- Kay and Silverman, On the uncertainty relation for real signals, *Inform. and Control* **2**, 396 (1959).
- Lee, C. Y., Some properties of nonbinary error-correcting codes, *IRE Trans.* **IT-4**, 77 (1958).
- Leipnik, R., The extended entropy uncertainty principle, *Inform. and Control* **3**, 18 (1960).
- Linden and Abramson, A generalization of the sampling theorem, *Inform. and Control* **3**, 26 (1960).
- Perry, K. E., An error-correcting encoder and decoder for phone line data, 1958 *IRE Wescon Conv. Record*, Pt. **4**, 21 (1958).
- Peterson and Fontaine, Group code equivalence and optimum codes, *IRE Trans.* **IT-5**, 60 (1959).
- Peterson, W. W., Encoding and error-correction procedures for the Bose-Chaudhuri codes (to appear in *IRE Trans.* **IT-6**, June or September 1960).
- Peterson, W. W., Error-detecting and error-correcting codes (to appear as a Technology Press Research Monograph in 1960).
- Prange, E., Coset equivalence in the analysis and decoding of group codes, Air Force Cambridge Research Center, Tech. Note AFCRC-TR-59-164 (June 1959).
- Reed, I. S., A class of multiple-error-correcting codes, *IRE Trans.* **IT-4**, 38 (1954).
- Schreiber and Knapp, TV bandwidth reduction by digital coding, 1958 *IRE Nat. Conv. Record*, Pt. **4**, 88 (1958).
- Shannon, C. E., The mathematical theory of communication (Univ. of Ill. Press, Urbana, Ill., 1949).
- Shannon, C. E., Certain results in coding theory for noisy channels, *Inform. and Control* **1**, 6 (1957).
- Shannon, C. E., Channels with side-information at the transmitter, *IBM Journal* **2**, 289 (1958).
- Shannon, C. E., Probability of error for optimal codes in a Gaussian channel, *Bell System Tech. J.* **38**, 611 (1959).
- Slepian, D., A class of binary signalling alphabets, *Bell System Tech. J.* **35**, 203 (1956).
- Slepian, D., A note on two binary signalling alphabets, *IRE Trans.* **IT-2**, 84 (1956).
- Stam, A. J., Some inequalities satisfied by the quantities of information of Fisher and Shannon, *Inform. and Control* **2**, 101 (1959).
- Ulrich, W., Nonbinary error-correcting codes, *Bell System Tech. J.* **36**, 1341 (1957).
- Wolfowitz, J., Information theory for mathematicians, *Ann. Math. Stat.* **29**, 351 (1958).
- Wolfowitz, J., Strong converse of the coding theorem, *Inform. and Control* **3**, 89 (1960).
- Wozencraft, J. M., Sequential decoding for reliable communication, MIT Research Lab. Elec. Tech. Rpt. 325 (Aug. 1957). (To appear in revised form as a Technology Press Research Monograph during 1960).
- Zierler, N., Linear recurring sequences, *J. Soc. Indust. Appl. Math.* **7**, 31 (1959).

Part 2. Random Processes

P. Swerling*

Research on random processes in the period under consideration may be conveniently summarized under three main headings: statistical properties of the output of nonlinear devices; estimation theory for random processes; and representation theory for random processes.

Under the first heading, the investigations concern the statistical properties of the output of a nonlinear device, or of a linear filter following a nonlinear device, when the input is a random process having prescribed statistics. These problems are of great interest since this is a model for many types of receivers. The period 1957 to 1960, continuing earlier work, has seen the buildup of a large inventory of results and of methods for attacking this class of problems.

One of the most comprehensive approaches is reported on in papers by Darling and Siegert [1957], and by Siegert [1957, 1958]. These papers report on work actually done earlier. The problem considered is that of finding the (first order) probability distribution function of the quantity

$$\int \phi[x(\tau), \tau] d\tau,$$

where ϕ is a prescribed function and $x(\tau)$ is a component of a stationary n -dimensional Markoff process. Many problems in the category under consideration are special cases of this. The approach is via the characteristic function of the required probability distribution; it is shown that this characteristic function must satisfy two integral equations. Under certain conditions, it can also be shown that the characteristic function must satisfy two partial differential equations.

Another type of problem in this category is the investigation of the second or higher order probability distributions of the output, and particularly of the autocorrelation function of the output or the cross-correlation between two or more such outputs. For example, Price [1958] gives a theorem which is useful in deriving such auto- and cross-correlations when the inputs are Gaussian. The theorem stated can be used in many cases to calculate the quantity

$$R = \text{Expected Value of } \left\{ \prod_{i=1}^n f_i(x_i) \right\},$$

where (x_1, \dots, x_n) is a Gaussian vector and f_i are prescribed functions.

Many other papers, for example Leipnik [1958], Pierce [1958], Kielson et al., [1959], Helstrom and Isley [1959], McFadden [1959], Campbell [1957], and

Leipnik [1959], have been written giving special results and using a number of different approaches.

Work has also continued on the problem of the distribution of zero crossings of Gaussian processes [Helstrom, 1957, and Brown, 1959].

Under the heading of estimation theory for random processes one might first mention the subject of estimating the spectral density of stationary Gaussian processes. Two references [Grenander and Rosenblatt, 1957, and Blackman and Tukey, 1959] summarize much work on this problem, a great deal of which had been done previously (but not all of which had been published previously). Blackman and Tukey discuss two types of estimates of the power spectrum, viz: estimation of the autocorrelation function, multiplication by a prescribed function of time called a "lag window," followed by Fourier transformation; or, passing the observed process through a filter of specified transfer function and calculating the average power of the output. They derive expressions for the first and second moments of such estimates, as well as of the cross-moments of estimates of the spectral density at two different frequencies. Grenander and Rosenblatt discuss similar types of spectral estimates, emphasizing and utilizing the fact that these as well as most other useful estimates of spectral density are quadratic forms in the observed data. They derive first and second order moments, as well as asymptotic probability distributions for large observed samples, of such estimates.

A recent paper of Grenander, Pollak, and Slepian [1959] discusses the small sample case, relying heavily on the fact that spectral density estimates are usually quadratic forms in the observed data.

In an interesting paper Slepian [1958] has discussed the following hypothesis-testing problem: given an observed sample of a Gaussian random process, known to be characterized by either one of two prescribed power spectra, which power spectrum does the process actually have? It turns out that in problems of this type, the measures induced by the two alternative hypotheses may be singular with respect to each other; in which case, it is possible to decide between the alternatives with arbitrarily small error probability, and with an arbitrarily small sample. Slepian gives various sufficient conditions for this. The power spectra satisfying his conditions are, moreover, standard types very frequently postulated. This emphasizes that the mathematical model one chooses must be carefully chosen to be appropriate to the problem one is trying to solve.

Another type of estimation problem for random processes is considered by Swerling [1959]. Suppose a prescribed waveform, depending on one or more unknown parameters, is observed in additive Gaussian noise having prescribed autocovariance function

*Rand Corporation, Santa Monica, Calif.

and zero mean. Expressions are derived for the greatest lower bound for the variance of estimates of the unknown parameters having prescribed bias. These greatest lower bounds are found to coincide in certain special cases with the variance, obtained by Woodward, of maximum likelihood estimates of the unknown parameters. Similar problems are investigated in Middleton [1959].

In the field of representation theory for random processes, work has continued on the subject of representation of nonlinear operations on random processes—especially for Gaussian processes. Papers by Zadeh [1957] and Bose [1959] and a book by Wiener [1958] deal with this problem. The approach followed is, first, to express the initial random process $\{x(t)\}$ as a series

$$x(t) = \sum_{n=1}^{\infty} u_n \alpha_n(t),$$

where $\{\alpha_n(t)\}$ is a set of orthonormal functions over the interval of definition of $\{x(t)\}$. If $\{x(t)\}$ is Gaussian, the u_n are Gaussian and, if $\alpha_n(t)$ are properly chosen, can be made independent. Any linear or nonlinear functional of $\{x(t)\}$ can then be regarded as a function of u_1, \dots, u_n, \dots . Second, one may choose a set of functions of the variables u_n which are orthonormal in the stochastic sense as explained, for example, in Zadeh [1957] with respect to the process $\{x(t)\}$. Then, nonlinear functionals of $\{x(t)\}$ may be expanded in a series of the orthogonal functions of the variables u_n .

Other research in the field of representation theory has treated such subjects as:

Use of bi-orthonormal expansions [Leipnik, 1959], envelopes of waveforms [Arens, 1957, and Dugundji, 1958], the sampling theorem and related topics [Balakrishnan, 1957, and Lerner, 1959], and harmonic analysis of multidimensional processes [Weiner and Masani, 1957 and 1958].

Much of this work in representation theory provides useful tools for attacking the problems discussed under the first two headings above.

References

- Arens, R., Complex processes for envelopes of normal noise, IRE Trans. **IT-3** (Sept. 1957).
 Balakrishnan, A. V., A note on the sampling principle for continuous signals, IRE Trans. **IT-3** (June 1957).
 Blackman, R. B., and J. W. Tukey, The measurement of power spectra from the point of view of communications engineering (Dover Publ., New York, N.Y., 1959).
 Bose, A. G., Nonlinear system characterization and optimization, IRE Trans. **IT-5** (Special suppl.) (May 1959).
 Brown, W. M., Some results on noise through circuits, IRE Trans. **IT-5** (Special suppl.) (May 1959).
 Campbell, L. Lorne, On the use of hermite expansions in noise problems, J. of S.I.A.M. **5** (Dec. 1957).
 Darling, D. A., and A. J. F. Siegert, A systematic approach to a class of problems in the theory of noise and other random phenomena, Pt. I, IRE Trans. **IT-3** (March 1957).
 Dugundji, J., Envelopes and pre-envelopes of real waveforms, IRE Trans. **IT-4** (March 1958).
 Grenander, U., and M. Rosenblatt, Statistical analysis of stationary time series (John Wiley & Sons, New York, N.Y., 1957).
 Grenander, U., H. O. Pollak and D. Slepian, The distribution of quadratic forms in normal variates: A small sample theory with applications to spectral analysis, J. of S.I.A.M. **7** (Dec. 1959).
 Helstrom, C. W., and C. T. Isley, Two notes on a Markoff envelope process, IRE Trans. **IT-5** (Sept. 1959).
 Helstrom, C. W., The distribution of the number of crossings of a Gaussian stochastic process, IRE Trans. **IT-3** (Dec. 1957).
 Kielson, J., N. D. Mermin, and P. Bello, A theorem on cross correlation between noisy channels, IRE Trans. **IT-5** (June 1959).
 Leipnik, Roy, The effect of instantaneous nonlinear devices on cross correlation, IRE Trans. **IT-4** (June 1958).
 Leipnik, Roy, Integral equations, biorthonormal expansions, and noise, J. of S.I.A.M. **7** (March 1959).
 Lerner, R. M., The representation of signals, IRE Trans. **IT-5** (Special suppl.) (May 1959).
 McFadden, J. A., The probability density of the output of an RC filter when the input is a binary random process, IRE Trans. **IT-5** (Dec. 1959).
 Middleton, D., A note on the estimation of signal waveform, IRE Trans. **IT-5** (June 1959).
 Pierce, J. N., A Markoff envelope process, IRE Trans. **IT-4** (Dec. 1958).
 Price, Robert, A useful theorem for nonlinear devices having Gaussian inputs, IRE Trans. **IT-4** (June 1958).
 Siegert, A. J. F., A systematic approach to a class of problems in the theory of noise and other random phenomena, Pt. II, Examples, IRE Trans. **IT-3** (March 1957).
 Siegert, A. J. F., A systematic approach to a class of problems in the theory of noise and other random phenomena, Pt. III, Examples, IRE Trans. **IT-4** (March 1958).
 Slepian, D., Some comments on the detection of Gaussian signals in Gaussian noise, IRE Trans. **IT-4** (June 1958).
 Swerling, P., Parameter estimation for waveforms in additive Gaussian noise, J. of S.I.A.M. **7** (June 1959).
 Weiner, N., Nonlinear problems in random theory (John Wiley & Sons, New York, N.Y., 1958).
 Weiner, N. and P. Masani, The prediction theory of multivariate stochastic processes, Acta Mathematica **98** (1957) and **99** (1958).
 Zadeh, L. A., On the representation of nonlinear operators, IRE Wescon Conv. Record, pt. 2 (1957).

Part 3. Pattern Recognition

Arthur Gill*

Pattern recognition, in its widest sense, cuts across many fields of engineering interest—from character sensing to learning theory, and from machine translation to decision-making techniques. Inasmuch as the problem of recognizing patterns is that of simulating human thinking processes, it is also closely related to nonengineering fields such as physiology, psychology, cryptology and linguistics. No attempt is made in this report to summarize the developments in all these areas. Rather, pattern recognition developments are reported only to the extent that they represent a direct contribution to the theory of information. The enclosed bibliography is compiled primarily from engineering journals; consequently, it will be found that the emphasis in this report is placed on the recognition of visual patterns, rather than vocal, linguistic or other patterns, which are mainly covered in nonengineering publications.

The reason for the acute engineering interest in visual patterns is the recent emergence of the following two urgent problems: (a) How can redundancy be removed from television pictures, so that video signals could be transmitted at a greatly reduced waveband; (b) How can printed documents be read automatically, so that the most serious bottleneck—the human typist or card puncher—could be eliminated from digital data-processing systems. Although these two topics are treated separately in the literature, both represent different aspects of the same general problem of pattern recognition. This problem may be divided, somewhat artificially, into three phases: (1) Redundancy removal, (2) Recognition programs, (3) Recognition system design. This division will be adopted in the following summary. Since the boundaries between three phases are not well defined, the corresponding bibliography classification should not be regarded as too rigorous.

3.1. Redundancy Removal

Both the compression of television bandwidth and the design of character recognizers, require the determination of the source redundancies, and the establishment of scanning-coding schemes which would minimize these redundancies. Considerable work has been done in the past three years on the "run-length" scheme, where lengths of pattern runs, rather than values of individual cells, constitute the transmitted information. [Capon, 1959; Michel, 1958; 1957]. The redundancies which may be eliminated under this scheme were measured for some sources of practical interest, and bounds were found for the potential bandwidth saving [Deutsch, 1957; Powers and Staras, 1957; Schreiber and Knapp, 1958]. Another scheme that was explored is one in which scanning is confined to the minimal set of cells necessary for recognition under noiseless and noisy conditions [Gill, 1959]. Progress has also been made in the techniques of measuring the autocorrelation function of two-dimensional patterns [Kovaszny and Arman, 1957].

3.2. Recognition Programs

Although the removal of redundancies from the given patterns simplifies and accelerates their recognition, the recognition itself is a result of a predetermined series of decision rules—applied sequentially or simultaneously—which is called "a recognition program." The program invariably involves a set of transformations performed on the unknown patterns, followed by a comparison of the transformed pattern with a precompiled library of reference patterns. The size of the library and the length of

the comparison process depend on the chosen set of transformations. Thus far, no universal procedure has been formulated for selecting a necessary or sufficient transformation set for a given pattern source; rather, each investigator uses intuitive or heuristic arguments to propose such a set for the specific source under investigation [Bledsoe and Browning, 1959; Dimond, 1957]. The approach which seems to be the most popular in the case of character recognition, is the association of each pattern with a distinct set of two-dimensional features ("corner," "intersection," "arc," etc.) which can be abstracted from each pattern with the aid of digital computers [Bomba, 1959; Kamentsky, 1959; Unger, 1959]. The necessary set of concepts is, again, presented heuristically. Similar situation exists in recognition programs proposed for other classes of patterns [Gold, 1959].

3.3. Recognition System Design

Once a set of transformations is selected for the recognition program, a system has to be constructed for executing the program. The intuitive basis on which the program is constructed, forces most investigators to plan a flexible system, in which transformations can be readily varied either manually or automatically as more experience is gained on the nature of the pattern source and the performance of the program (the automatic method is closely related to problems concerning "adaptive systems," which are not reviewed in this report). The majority of all recognition systems built to date are found to be still in the "learning" stage, serving as testing grounds for the various schemes devised by the respective investigators [Grenias et al., 1957; Kirsch et al., 1957; Tersoff, 1957]. A byproduct of these

*Department of Electrical Engineering, University of California, Berkeley, Calif.

circumstances are the so-called "pattern synthesis" techniques, developed for simulating various pattern sources for test purposes [Flores and Ragonese, 1958; Grenias and Hill, 1957]. These techniques are also applied to the design of optimal-style patterns, where a limited degree of freedom may be exercised over the construction of the source itself.

It seems that although a considerable progress has been made in various areas of pattern recognition, it is still minute in comparison with the problems that still remain unresolved. The scanning-coding techniques devised for transmitting visual patterns compress the currently employed bandwidth by at most a factor of 10, while a factor of a million is required in order to approach the recognition capacity of the human eye. Automatic reading of relatively standardized characters is in a relatively high development stage, but the mechanical recognition of handwriting or speech are still practically unfeasible. Further progress in this field seems to lie in three directions: (a) Deeper analysis of the redundancies inherent in the various classes of pattern sources, (b) Formulation of procedures for determining optimal sets of transformations required for recognizing given sets of patterns, (c) Simulation of learning processes with digital computers. It is hoped that the next three years will witness significant contributions to these basic problems.

References

- Bledsoe, W. W., and I. Browning, Pattern recognition and reading by machine, 1959 Proc. EJCC, 225. (Patterns are "learned" by marking states of cell-pairs randomly distributed in the pattern area.)
- Bomba, J. S., Alpha-numeric character recognition using local operations, 1959 Proc. EJCC, 218. (Geometrical features, such as horizontal, vertical and slant lines, are extracted by operations on small sections of given patterns.)
- Capon, J., A probabilistic model for run-length coding of pictures, IRE Trans. on Inform. Theory **IT-5**, 157 (Dec. 1959). (Binary patterns are represented as first-order Markoff processes, to yield bounds on the saving gained through the use of a variable-sweep scanning system.)
- Deutsch, S., A note on some statistics concerning typewritten or printed material, IRE Trans. on Inform. Theory **IT-3**, 147 (June 1957).
- Dimond, H. L., Devices for reading handwritten characters, 1957 Proc. EJCC, 232. (A device is described for real-time recognition of handwritten characters, subject to special coordinate constraints.)
- Flores, I., and F. Ragonese, A method for synthesizing the waveform generated by a character, printed in magnetic ink, in passing beneath a magnetic reading head, IRE Trans. on Electronic Computers **EC-7**, 277 (Dec. 1958). (Formulas are derived for determining the waveform from the geometry of the character and from the empirical properties of the reading apparatus.)
- Gill, A., Minimum-scan pattern recognition, IRE Trans. on Inform. Theory **IT-5**, 52 (June 1959). (Bounds to the number of essential cells in noiseless and noisy binary patterns; algorithms for locating these cells.)
- Gold, B., Machine recognition of hand-sent Morse code, IRE Trans. on Inform. Theory **IT-5**, 17 (March 1959). (The code is recognized by applying a set of fixed language rules, and statistically determined threshold tests.)
- Greenias, E. C., and Y. M. Hill, Considerations in the design of character recognition devices, 1957 IRE Nat. Conv. Record, pt. 4, 119. (Measures of character quality and style are defined to aid the design of a recognizer; a method is shown for generating synthetic test characters.)
- Greenias, E. C., C. J. Hoppel, M. Kloomok, and J. S. Osborne, Design of logic for recognition of printed characters by simulation, IBM J. of Research and Develop **1**, 8 (Jan. 1957). (Characters are recognized by the relative size and position of the scanned elements; validity of prescribed test sequences is examined by computer simulation.)
- Kamentsky, L. A., Pattern and character recognition systems, picture processing by nets of neuron-like elements, 1959 Proc. WJCC, 304. (Neuron-like nets are used to carry out parameter-extracting operations on binary patterns; recognition is viewed as a sequence of information-destroying transformations.)
- Kirsch, R. A., L. Cahn, C. Ray and G. H. Urban, Experiments in processing pictorial information with a digital computer, 1957 Proc. EJCC, 221. (Laboratory apparatus is described for performing pattern-recognition research.)
- Kovaszny, L. S. G., and A. Arman, Optical autocorrelation measurement of two-dimensional random patterns, Rev. Sci. Instr. **28**, 793 (Oct. 1957). (The entire autocorrelation function can be obtained at once in form of a light distribution on a plate.)
- Michel, W. S., Statistical encoding for text and picture communication, Commun. and Electronics **77**, 33 (March 1958). (Various coding schemes proposed for different classes of patterns are discussed and compared.)
- Michel, W. S., W. O. Fleckenstein and E. R. Kretzner, A coded facsimile system, 1957 Wescon Conv. Record, pt. 2, 84. (Variable-length coding of binary patterns scanned through a variable-sweep scanning system may result in 3-1 saving; the transmission rate may be made proportional to the complexity of the scanned material.)
- Powers, K. H., and H. Staras, Some relations between television picture redundancy and bandwidth requirements, Commun. and Electronics **32**, 492 (Sept. 1957). (Picture redundancy is separated into nonpredictive redundancy, resulting from nonoptimal first-order probability distribution, and predictive redundancy, resulting from statistical correlation between successive signals. Nonpredictive redundancy in television is essentially zero. Predictive redundancy allows at least 2 to 1 saving.)
- Schreiber, W. F., and C. F. Knapp, TV bandwidth reduction by digital coding, 1958 IRE Nat. Conv. Record, pt. 4, 88. (Picture statistics and characteristics of human vision are utilized in coding video signals and transmitting the code at a uniform rate.)
- Tersoff, A. I., Automatic registration in high-speed character-sensing equipment, 1957 Proc. EJCC, 232. (A device is described which minimizes the effects of tilt, poor registration and extraneous marks on the recognition process.)
- Unger, S. H., Pattern detection and recognition, Proc. IRE **47**, 1737 (1959). (Characters are recognized through a spatial computer, capable of detecting a specified set of geometrical properties uniquely associated with each pattern.)

Part 4. Detection Theory

Robert Price*

4.1. Remarks

The period since the XII General Assembly has seen a consolidation of the closely related concepts of Wald, Woodward, Middleton, and Van Meter, and Peterson, Birdsall, and Fox into a fairly unified theory of detection, together with the successful application of the theory to a variety of problems. Through this approach, 'optimal' detector structures for electronic systems can be synthesized provided that the designer has *a priori* knowledge of the governing statistics and error costs. At the same time, older and more standard detection techniques have continued to receive attention, the theoretical results generally being stated in terms of probability-of-error or signal-to-noise ratio at the detector output. If one must attribute the discovery of any new, guiding principles to the preceding three-year period, the most likely candidates would seem to be found in those few studies which have sought theories which can cope effectively with situations in which *a priori* knowledge is seriously lacking.

It appears that roughly half the effort of the past three years has been devoted to specific detection problems in radar and communications. In contemporary communications studies considerable heed is paid to 'optimum' detection procedures, there being less inclination to examine conventional, suboptimum detectors than in the radar analyses. The reason for this may be that the radar designer faces considerably greater *a priori* uncertainty, both with regard to the signal and the channel through which it comes. By contrast, relatively simpler channels have usually been assumed without loss of realism in communications problems, while the communications system designer also has more direct control of the signal. The appropriate optimum detectors for communications then turn out to be rather elementary, and can at present be constructed with hardly more effort than suboptimum devices require. In fact, the communications environment is generally 'clean' enough that much recent work has been concerned with determining good sets of transmitted signal waveforms, the use of an optimum receiver being taken for granted.

The bulk of the remaining effort has dealt with special topics in detection of quite general application. Further study in sequential decision has been made both theoretically and through Monte Carlo computer experimentation, in the hope of achieving significant speedup in detection over fixed-sample operation. Greater understanding of the detection of stochastic signals in noise has been sought for applications in such fields as radio astronomy and

in systems where rapidly fading channels are encountered. There has been some work on parameter estimation for a finite number of parameters, a subject which is virtually inseparable from detection theory. Detection losses in nonlinear devices have also received further examination.

Attempts to circumvent the *a priori* difficulty represent only a small fraction of the output of the past three years in detection analysis, but have perhaps the most significance for future work. Original attacks have been made through game theory, comparison of experiments, nonparametric techniques, dynamic programming, and inductive probability. It is hoped that one or more of these tools will prove effective in breaking new ground.

4.2. Papers

The following list of references has been drawn largely from the American journals concerned with statistical communication theory and information theory, but also contains a few laboratory technical reports. This selection omits papers on multiple parameter estimation, and the estimation of signal waveforms and impulse responses, since these topics verge on filtering theory. Other closely related subjects which are not covered are classical studies in hypothesis testing that do not refer to electronic systems, investigations into ambiguity functions of radar waveforms, and information-feedback systems.¹ The future pursuit of feedback studies may well lead to wider interchanges in detection notions between radar and communications.

4.3. Bibliography

a. Applications to Radar

- Busgang, J. J., P. Nesbida and Safran, A unified analysis of range performance of CW, pulse and pulse doppler radar, *Proc. IRE* **47**, 1753 (1959). (Includes a simplified analysis for sweep integrator systems containing square-law detectors.)
- Cohn, G. I., and L. C. Peach, Detection of radar signals by direct measurement of their effects on noise statistics, *Proc. Nat. Electronics Conf.* **14**, 821 (1959). (Describes equipment for measuring waveform probabilities.)
- Dilworth, R. P., and E. Ackerlind, The analysis of post detection integration systems by Monte Carlo methods, 1957 IRE Nat. Conv. Record, Pt. 2, 40. (Measurement of output probability distributions for filter-linear detector-integrator and filter-squarer-integrator combinations.)
- Galejs, J., and W. Cowan, Interchannel correlation in a bank of parallel filters, *IRE Trans. on Inform. Theory* **IT-5**, 106 (1959). (Study of first-order effects on false alarm and detection probabilities.)

*Lincoln Laboratory, M.I.T., Lexington, Mass.

¹ Also omitted are papers contained in the March, 1957, issue of the IRE Transactions on Information Theory, which have already been referenced in the U.S.A. National Commission VI Report of the XII General Assembly

- Green, B. A. Jr., Radar detection probability with logarithmic detectors, *IRE Trans. on Inform. Theory* **IT-4**, 50 (1958). (With post-detection integration, a logarithmic detector is about 1 db worse than a square-law detector.)
- Kelly, E. J., D. H. Lyons, H. M. Jones and I. S. Reed, Analysis of some detection criteria for pulse radars, Tech. Rept. 172, Lincoln Lab., M.I.T., (1958). (Evolution of a periodogram detector and its application to samples of the phase of the received signal.)
- Max, J., Mismatching filters to improve resolution in radar, Group rept. 36-32, Lincoln Lab., M.I.T., (1958). Also an M.S. thesis in E.E., M.I.T., (1958). (Integral equations whose solutions yield improved performance against clutter.)
- McCord, H. L., An estimation of the degradation in signal detection resulting from the addition of the video voltages from two radar receivers, *IRE Nat. Conv. Record*, Pt. 2, 83 (1957). (A loss of about 2 db for linear addition, only 0.2 db for peak selection.)
- Miller, K. S., and R. I. Bernstein, An analysis of coherent integration and its application to signal detection, *IRE Trans. on Inform. Theory* **IT-3**, 237 (1957). (In covering a region of doppler uncertainty, the more filters the better.)
- Pachares, J., A table of bias levels useful in radar detection problems, *IRE Trans. on Inform. Theory* **IT-4**, 38 (1958). (Values of the incomplete Gamma function.)
- Reed, I. S., E. J. Kelly, and W. L. Root, The detection of radar echoes in noise. Pt. I: Statistical preliminaries and detector design. Pt. II: The accuracy of radar measurements. Tech. Repts. 158 and 159, Lincoln Lab., M.I.T., (1957). (Derivation of optimal detectors or estimators using orthogonal expansion coordinates, followed by evaluation of how well such devices perform.)
- Siebert, W. McC., Some applications of detection theory to radar, *IRE Nat. Conv. Record*, Pt. 4, 5 (1958). (Discusses a constant-false-alarm-rate detector for use when the noise is of variable strength.)
- Stone, W. M., R. L. Brock, and K. J. Hammerle, On the first probability of detection by a radar receiver system, *IRE Trans. on Inform. Theory* **IT-5**, 9 (1959). (Probability densities for a filter-squarer-filter detector with constant and with Rayleigh-fading input signals.)
- b. Applications to Communications**
- Cahn, C. R., Performance of digital phase-modulation communication systems, *IRE Trans. on Comm. Systems* **CS-7**, 3 (1959).
- Lawton, J. G., Theoretical error rates of 'differentially coherent' binary and 'Kineplex' data transmission systems, *Proc. IRE* **47**, 333 (1959). Also C. R. Cahn and J. G. Lawton, Comparison of coherent and phase-comparison detection of a four-phase digital signal, *Proc. IRE*, 1662 (1959). (Binary phase-comparison shown to be asymptotically as good as a coherent phase-reversal system, but in four-phase modulation there is a relative asymptotic loss of 3 db.)
- Masonson, M., Binary transmission through noise and fading, *IRE Conv. Record*, Pt. 2, 69 (1957).
- Pierce, J. N., Theoretical diversity improvement in frequency-shift keying, *Proc. IRE* **46**, 903 (1958). (Derivation and performance evaluation of optimum detectors for diversity reception.)
- Reiger, S., Error rates in data transmission, *Proc. IRE* **46**, 919 (1958). (Effectiveness of simple codes shown.)
- Shannon, C. E., Probability of error for optimal codes in a Gaussian channel, *Bell System Tech. J.* **38**, 611 (1959). (Upper and lower bounds to error probability obtained for best set of waveforms for signalling through independent Gaussian noise.)
- Sunde, E. D., Ideal binary pulse transmission by AM and FM, *Bell System Tech. J.* **38**, 1357 (1959). (With a bandwidth constraint, concludes that FM is better than AM for signalling through white noise.)
- Turin, G. L., Error probabilities for binary symmetric ideal reception through nonselective slow fading and noise, *Proc. IRE* **46**, 1603 (1958). (Considers pulse signals of familiar shapes.)
- Turin, G. L., The asymptotic behavior of ideal M-ary systems, *Proc. IRE* **47**, 93 (1959). (Shows that Shannon's fundamental theorem can be realized with incoherent detection, provided signalling alphabet is orthogonal.)
- Turin, G. L., Some computations of error rates for selectively fading multipath channels, *Proc. Nat. Electronics Conf.* **15** (in press). (Even if one of two independently fading paths is relatively weak, error probability is considerably lower than if only the stronger path is present.)
- c. Sequential Decision**
- Blasbalg, H., The relation of sequential filter theory to information theory and its application to the detection of signals in noise by Bernoulli trials, *IRE Trans. on Inform. Theory* **IT-3**, 122 (1957).
- Blasbalg, H., The sequential detection of a sine-wave carrier of arbitrary duty ratio in Gaussian noise, *IRE Trans. on Inform. Theory* **IT-3**, 248 (1957).
- Blasbalg, H., Experimental results in sequential detection, *IRE Trans. on Inform. Theory* **IT-5**, 41 (1959). (A Bernoulli trial generator was used.)
- Nuese, C., Small signal detection through binomial sequential analysis, Research Rept. 766, U.S. Navy Electronics Lab. (1957).
- Simmons, R. E., and R. A. Worley, Sequential detection statistics, Research Rept. 963, U.S. Navy Electronics Lab. (to be published). (Exact solutions for Bernoulli trials, with experimental confirmation.)
- d. Detection of Stochastic Signals in Noise**
- Davis, R. C., Optimum vs. correlator methods in tracking random signals in background noise, *Quart. Appl. Math.* **15**, 123 (1957).
- Kelly, E. J., D. H. Lyons, and W. L. Root, The theory of the radiometer, Group Report 47.16, Lincoln Lab., M.I.T. (1958). (Square-law detector shown to be optimum.)
- Middleton, D., On the detection of stochastic signals in additive normal noise, Pt. I, *IRE Trans. on Inform. Theory* **IT-3**, 86 (1957). (A filter-squarer-integrator shown to be an optimum structure.)
- Rudnick, P., Likelihood detection of small signals in stationary noise, Scripps Institution of Oceanography, LaJolla, Calif. (to be published). (Proves that in general the likelihood-ratio detector yields maximum output signal-to-noise ratio, provided that ratio is suitably defined.)
- Slepian, D., Some comments on the detection of Gaussian signals in Gaussian noise, *IRE Trans. on Inform. Theory* **IT-4**, 65 (1958). (Considers some singular cases, in which perfect detection is accomplished in an infinitely short time.)
- Stone, W. M., et al. (see under Radar).
- Strum, P. D., Considerations in high-sensitivity microwave radiometry, *Proc. IRE* **46**, 43 (1958). (Mathematical analysis in appendix.)
- Swerling, P., Detection of fluctuating pulsed signals in the presence of noise, *IRE Trans. on Inform. Theory* **IT-3**, 175 (1957). (The signals have quite general fading characteristics.)
- e. Parameter Estimation**
- Davis, R. C. (see under Stochastic Signals). (Estimation of relative delay between two identical Gaussian signals masked by noise.)
- Middleton, D., Signal analysis I-estimation of signal parameters and waveform structure in noise backgrounds, Tech. Rep. AF-50, Radiation Lab., Johns Hopkins Univ. (1958).
- Swerling, P., Parameter estimation for waveforms in additive Gaussian noise, *J. Soc. Ind. and Appl. Math.* **7**, 152 (1959).
- f. Loss in Nonlinear Devices**
- Galejs, J., Signal-to-noise ratios in smooth limiters, *IRE Trans. on Inform. Theory*, **IT-5**, 79 (1959). (Behavior of loss as a function of the saturation of an error-function limiter characteristics, for various noise spectral shapes.)

Green, B. A., Jr. (see under Radar).

Manasse, R., R. Price and R. M. Lerner, Loss of signal detectability in band-pass limiters, IRE Trans. on Inform. Theory **IT-4**, 34 (1958). (Analysis at low-signal-to-noise ratios shows little detectability loss through a hard limiter.)

g. Attacks on the *A Priori* Problem

Abramson, N., The application of 'Comparison of Experiments' to detection problems, IRE Nat. Conv. Record, Pt. 4, 22 (1958). (A simple but realistic example demonstrates the possibility of showing that one system is superior to another regardless of cost assignments and *a priori* message probabilities.)

Bellman, R. and R. Kalaba, On the role of dynamic programming in statistical communication theory, IRE Trans. on Inform. Theory **IT-3**, 197 (1957). (Although not explicitly applied to detection, this "learning" technique suggests ways of obtaining the *a priori* probabilities when they are not known, or are changing.)

Capon, J., A nonparametric technique for the detection of a constant signal in additive noise, IRE Wescon Conv. Record, Pt. 4, 92 (1959). (An approach which is strongly invariant to probability distribution, based on comparisons between the received sample, and a reference sample drawn from noise-only population.)

Nilsson, N. J., An application of the theory of games to radar reception problems, IRE Nat. Conv. Record, Pt. 4, 130 (1959). (Jamming considered. Minimax solution is for both the radar and the jammer to use broad-band noiselike waveforms.)

Schwartz, L. S., B. Harris, and A. Hauptschein, Information rate from the viewpoint of inductive probability, IRE Nat. Conv. Record, Pt. 4, 102 (1959). (Carnap's philosophy invoked to estimate probabilities.)

h. Miscellaneous

Slade, J. J. Jr., L. F. Nanni, S. Fieh, and D. A. Molony, Moment detection and coding, Commun. Electronics, 275 (1957).

Bloom, F. J., S. S. L. Chang, B. Harris, A. Hauptschein, and K. C. Morgan, Improvement of binary transmission by null-zone reception, Proc. IRE **45**, 963 (1957). (Shows that introducing decision null-zones results in a higher upper limit to allowable information rate, relative to simple binary decision.)

Middleton, D., A comparison of random and periodic data sampling for the detection of signals in noise, IRE Trans. on Inform. Theory **IT-5**, 234 (1959). (Concludes that periodic sampling is better.)

Stewart, J. L., and E. C. Westerfield, A theory of active sonar detection, Proc. IRE **47**, 872 (1959). (Considers reverberation, using a pseudo-random transmission and a cross-correlator detector.)

i. Books

Recent books, available or in press at the end of 1959, in which detection analysis receives major treatment:

Middleton, D., An introduction to statistical communication theory (McGraw-Hill Book Co., Inc., New York, N.Y., 1960).

Davenport, W. B. Jr., and W. L. Root, An introduction to the theory of random signals and noise (McGraw-Hill Book Co., Inc., New York, N.Y., 1958).

Helstrom, C. W., Statistical theory of signal detection, Pergamon Press (in press).

Part 5. Prediction and Filtering

L. A. Zadeh*

Much on the research on prediction and filtering conducted in the United States during the period 1957-1960 was concerned essentially with various extensions of Wiener's theory. In particular, extensions involving nonstationary continuous time processes, vector-valued processes, stationary and nonstationary discrete-time processes, nonGaussian processes, incompletely specified processes, and nonlinear filters and predictors have received attention.

A new and very promising direction in prediction theory has been opened by the application of Bellman's dynamic programming to the determination of optimal adaptive filters and predictors. Actually, the basic work of Bellman and Kalaba [1958, 1959, 1960] and its extensions and applications by Freimer [1959], Aoki, Kalman, and Koepcke [1958], and Merriam [1959] are not concerned with prediction and filtering as such. However, the recent work of Kalman shows that, mathematically, there is a duality between the filtering problem and the control problems considered by Bellman and Kalaba, and others. Thus, these contributions are likely to have a considerable impact on the course of development of the theory of filtering and prediction in the years ahead, and point toward an increasing utilization of digital computers and the concepts and techniques of discrete-state systems both in the design of predicting and filtering schemes and in their implementation.

During the past two years four books containing in aggregate a substantial amount of material on prediction and filtering have been published. Davenport and Root [1958] present a clear exposition of Wiener's theory and some of its extensions. Wiener [1958] discusses orthogonal expansions of nonlinear functionals but stops short of applying them to prediction problems. Bendat [1958] presents a general survey of linear prediction and treats some special problems in considerable detail. Middleton [1960] contains a thorough exposition of the classical prediction theory together with a theory of reception in which the problems of prediction and filtering are formulated in the framework of decision theory. The appendix of Middleton's book includes an informative section on the solution of the Wiener-Hopf equation and some of its variants.

A more detailed discussion of the contributions to filtering and prediction theory is presented in the following pages. For convenience, the subjects of nonlinear filtering, nonstationary and discrete-time filtering, and miscellaneous contributions are dealt with separately.

5.1. Nonlinear Filtering

The contributions to nonlinear filtering and prediction have centered largely on the fundamental work of Wiener [1953] and its earlier extensions by Bose [1956] and Barrett [1955]. A discernible trend in research in this area is to consider special types of processes for which optimal nonlinear filters assume a simple form. A key work in this connection is that of Barrett and Lampard [1955], in which the class, Λ ,¹ of all second order density functions admitting a diagonal representation of the form.

$$p(x_1, x_2; \tau) = p(x_1)p(x_2) \sum_{n=0}^{\infty} A_n(\tau) \theta_n(x_1) \theta_n(x_2) \quad (1)$$

is introduced. Here $p(x_1, x_2; \tau)$ denotes the second order density of a stationary process $\{x(t)\}$, $x_1 = x(t)$, $x_2 = x(t + \tau)$, $p(x)$ is the first order density, and $\{\theta_n(x)\}$ is a family of polynomials with the orthogonality property

$$\int p(x) \theta_m(x) \theta_n(x) dx = \delta_{mn}. \quad (2)$$

In particular, Barrett and Lampard have shown that Gaussian and Rayleigh processes are of this type, with the θ_n being Hermite and Laguerre polynomials, respectively. Convergence and other aspects of the

Barrett-Lampard expansion were investigated by Leipnik [1959], while necessary and sufficient conditions under which $P(x_1, x_2; \tau)$ can be expressed in the form (1) have been given by J. L. Brown [1958]. Brown also studied [1957] a more general class of densities for which the expansion (1) is nondiagonal and the coefficients $A_{mn}(\tau)$ are restricted by the relation $A_{m1}(\tau) = d_m a_{11}(\tau)$, $m = 1, 2, \dots$, the d_m being real constants. As shown by Brown, processes with densities of this type exhibit a number of interesting properties.

One way in which the Barrett-Lampard expansion can be used in nonlinear filtering was pointed out by Zadeh [1957]. Specifically, assume that the second order density of a process with zero mean can be represented by (1), with the $\theta_n(x)$ not necessarily having the form of polynomials. Then, if an optimal (minimum variance) filter is sought in the class of filters admitting the representation

$$F(x) = \sum_{h=0}^{\infty} \int_0^{\infty} K_h(\tau) \theta_h[x(t-\tau)] d\tau, \quad (3)$$

where the $K_h(\tau)$ are undetermined kernels, and the desired output is written as

$$F^*(x) = \sum_{m \in M} \int_{-\infty}^{\infty} K_m^*(\tau) \theta_m[x(t-\tau)] d\tau, \quad (4)$$

where M is a finite index set and the $K_m^*(\tau)$ are given kernels, the determination of the $K_h(\tau)$ reduces to the solution of a finite number of Wiener-Hopf

*Department of Electrical Engineering, University of California, Berkeley, Calif.

¹In Barrett and Lampard's definition of Λ , $p(x_1, x_2; \tau)$ is not assumed to be symmetrical.

integral equations

$$\int_0^\infty K_m(\tau)A_m(t-\tau)d\tau = \int_{-\infty}^\infty K^*(\tau)A_m(t-\tau)d\tau, m \in M \quad (5)$$

with $K_n \equiv 0$ if $n \notin M$.

Another type of process—for which the problem of determining an optimal nonlinear predictor is greatly simplified—was introduced by Nuttall [1958]. Specifically, Nuttall calls a process separable² if the conditional mean of x_2 given x_1 can be represented as

$$E\{x_2|x_1\} = \int (x_2 - \mu)p(x_2; \tau|x_1)dx_2 = (x_1 - \mu)\rho(\tau) \quad (6)$$

where μ is the mean value of the process and $\rho(\tau)$ is its normalized autocorrelation function. Separable processes form a slightly broader class than that defined by Brown [1957].

Among the many interesting properties of separable processes is the following prediction property. Let $s(t)$ be a signal mixed with additive noise. Then, if $\{s(t)\}$ is a separable process, the best estimate of $s(t+\tau)$ in terms of the best estimate of $s(t)$ is given by

$$s^*(t+\tau) = s^*(t)\rho_s(\tau) + \mu_s[1 - \rho_s(\tau)], \quad (7)$$

where $\rho_s(\tau)$ and μ_s are the normalized autocorrelation and the mean value of the signal process, and starred quantities, represent optimal (minimum variance) estimates. In the absence of noise, the explicit formula for the best predictor in terms of $s(t)$ becomes

$$s^*(t+\tau) = s(t)\rho_s(\tau) + \mu_s[1 - \rho_s(\tau)]. \quad (8)$$

Still another type of process for which the prediction problem is manageable was considered by D. A. George [1958]. Here the observed signal $f(t)$ is assumed to be the output of an invertible nonlinear system N preceded by an invertible linear system L to which a white Gaussian signal $x(t)$ is applied. Thus, symbolically, $f = NLx$ and $x = L^{-1}N^{-1}f$. Then, if an optimal estimate of $f(t+\alpha)$ is denoted by $\hat{f}(t+\alpha)$, it is not difficult to find an operator H_α acting on the present and past values of $x(t)$ such that $\hat{f}(t+\alpha) = H_\alpha[x(t)]$. Once H_α has been found, $\hat{f}(t+\alpha)$ can be expressed in terms of the present and past values of $f(t)$ by the relation $\hat{f}(t+\alpha) = H_\alpha L^{-1}N^{-1}f$.

While some authors have sought to simplify the prediction problem by considering processes with special properties, others have turned to special types of nonlinear operators. In particular, the work of Bose [1956, 1959] was extended by D. A. Chesler [1958] to operators of the form $F(\sum_{n=1}^N C_n \phi_n)$, where F denotes either a linear operator with memory, or a nonlinear memoryless operator, or a more general nonlinear operator possessing an inverse; the C_n are

adjustable constants, and the ϕ_n are nonlinear operators such that the expectation $E\{\phi_n(x)\phi_m(x)\} = 0$ for $m \neq n$, x being the input to the filter. As was shown by Bose in the absence of F the optimal value of each C can be determined by measuring the mean-square error as a function of, say, C_i and assigning to C_i the value which minimizes the mean-square error. This method is shown by Chesler to be applicable also when F is a linear operator or a nonlinear operator with no memory. The extension is less straightforward when the only assumption on F is that it possesses a realizable inverse.

In all the foregoing analyses the signal process is assumed to be stationary. However, there are many situations of practical interest in which an appropriate representation for the signal is a series of the form

$$s(t) = \sum_{i=1}^n \alpha_i \phi_i(t), \quad (9)$$

in which the $\phi_i(t)$ are known functions of time and the α_i are unknown constants or random variables. In such cases, the problem of filtering or predicting $s(t)$ reduces to the estimation of the coefficients α_i .

It was shown some time ago by Laning [1951] that when (a) the noise is additive, stationary and Gaussian, (b) the joint distribution of the α_i is known, and (c) the loss function $L(\epsilon)$ is nonnegative and vanishes for $\epsilon=0$, optimal estimators for the α_i are memoryless nonlinear functions of linear combinations of values of the input over the interval of observation. In a recent paper, similar results were obtained by a different and more rigorous method by Kallianpur [1959]. More specifically, for the case where the interval of observation is $[0, T]$, and the loss function is quadratic, Kallianpur derived explicit expressions for the best estimate of $s(t)$ at time $T+T_1$ in terms of n linear functionals of the form

$$\int_0^T x(t)p_i(t)dt, i=1, 2, \dots, n,$$

where $x(t)$ is the sum of signal and noise, and the $p_i(t)$ are square integrable solutions of integral equations

$$\int_0^T R(t-\tau)p_i(\tau)d\tau = \phi_i(t), i=1, 2, \dots, n, \quad (10)$$

in which $R(\tau)$ is the correlation function of the process.

More concrete results for the same general problem were obtained by Middleton [1959] and Glaser and Park [1958]. In particular, Middleton found explicit expressions for minimum variance estimators of the α_i for the cases where (a) the α_i are jointly normally distributed, (b) the α_i are independent and Rayleigh distributed, (c) the α_i are independent and their distributions are not symmetrical, (d) the α_i are independent and their distributions are symmetrical. Of these cases, only (a) and (d) yield linear estimators for the α_i .

² It should be noted that the term "separable process" is used in the theory of stochastic processes in an altogether different sense.

The relation between maximum likelihood, minimum variance and least squares estimates of the α_i was studied in earlier papers by Mann [1954] and Mann and Moranda [1954]. A number of interesting properties of minimum variance estimates of $s(t)$ and its derivatives for the case where the $\phi_i(t)$ are polynomials in t were found by I. Kanter [1958, 1959]. A central result of Kanter is that an optimal weighting function for predicting the j^{th} derivative of n^{th} degree polynomial can be expressed uniquely and simply in terms of optimal estimators of k^{th} derivatives of k^{th} degree polynomials, with k ranging between j and n .

5.2. Filtering and Prediction of Nonstationary, Discrete-Time, and Mixed Processes

As is well known [Miller, Zadeh, 1956], extensions of Wiener's theory to nonstationary processes lead to integral equations of the general form

$$\int_a^b R(t, \tau) x(\tau) d\tau = g(t), \quad a \leq t \leq b, \quad (11)$$

in which $R(t, \tau)$ is the covariance function of the observed process. Little can be done toward the solution of this equation when $R(t, \tau)$ is an arbitrary covariance function. Thus, contributions to the theory of prediction of nonstationary continuous time processes consist essentially of methods of solving (11) in special cases.

Along these lines, Shinbrot [1957] discussed the solution of (11) for the case where $R(t, \tau)$ can be expressed in the form

$$R(t, \tau) = \sum_{n=1}^N \alpha_n(\tau) b_n(t). \quad (12)$$

Using Shinbrot's methods, the solution of (11) reduces to the solution of a system of differential equations with time-varying coefficients. There is some advantage in such a reduction when one has available a differential analyzer or an equivalent machine. Similar results are yielded by a theory due to Darlington [1958, 1959], in which many of the concepts and techniques of time-invariant networks are extended to time-varying networks. As in the paper of Miller and Zadeh [1956], a key assumption in these approaches is that the observed process may be generated by acting on white noise with a product of differential and inverse-differential operators, or equivalently, with a lumped-parameter linear time-varying network. Darlington's paper [1958] contains also a simplified technique for finding a finite memory Wiener filter for stationary signal and noise.

A special case for which explicit solution can be found has been studied by Bendat [1957]. Here the basic assumption is that the signal is of the form $s(t) = 0$ for $t < 0$, $s(t) = \sum_{n=1}^N (\alpha_n \cos n\omega t + b_n \sin n\omega t)$ for $t \geq 0$, where the α_n and b_n are random variables with

known covariance matrices, while the covariance function of the noise is of the form

$$R(t_1, t_2) = A e^{-\beta |t_1 - t_2|} \cos \gamma(t_1 - t_2) \text{ for } t_1, t_2 \geq 0 \\ = 0 \text{ for } t_1 < 0 \text{ or } t_2 < 0. \quad (13)$$

Closely related cases in which the prediction problem can be solved completely are those in which the nonstationarity of signal and noise processes is due to a truncation (e.g., multiplying the signal and noise by a step function) of stationary processes. This is true also in the case of discrete-time processes, as is demonstrated by several examples in Friedland's [1958] extension of Wiener's theory to nonstationary sampled-data processes.

Several interesting results concerning the linear prediction of filtering of stationary discrete-time processes were described by Blum [1957a, 1958, 1957b]. In particular, Blum has developed recursive formulas which express the estimate at time n in terms of a finite number of past estimates and past values of the observed process. This type of representation is especially useful in connection with so-called growing memory filters, i.e., filters which act on the entire past of the input. Thus, if the input sequence (starting at $t=0$) is denoted by x_0, x_1, \dots, x_n , and the filter output at time n is denoted by Z_n , then Z_n is expressible as $Z_n = \sum_{r=1}^n C_r X_r$, in which the C_r depend on n . A shortcoming of this representation is that as time advances the C_r have to be recomputed at each step and their number grows with n . On the other hand, a recursive relation (if it exists) is of the form

$$Z_n = \alpha_1 Z_{n-1} + \dots + \alpha_k Z_{n-k} + b_0 x_n + b_1 x_{n-1} + \dots + b_e x_{n-e}, \quad (14)$$

where α 's, b 's, k and e are constants independent of n and hence need not be recomputed. One complication in this approach to the problem is that in order to start the recursion one must know initially Z_0, Z_1, \dots, Z_k .

A somewhat related but more general approach has been formulated recently by Kalman. Specifically, Kalman assumes that the observed process is an n -dimensional vector process $\{y(t)\}$ which is generated by acting with a linear discrete-time system on a white noise $\{u(t)\}$: thus,

$$\underline{y}(t) = P(t) \underline{x}(t) \\ \underline{x}(t+1) = G(t) \underline{x}(t) + \underline{u}(t), \quad (15)$$

where the bars denote vectors and $P(t)$ and $G(t)$ are given time-varying matrices. (This assumption is analogous to the usual one in the case of nonstationary continuous-time prediction, viz, that the observed process can be generated by acting on white noise with a time-varying network.) Kalman shows that an optimal (minimum variance) estimate

of $x(t)$ is given by the recursive relation

$$\underline{x}^*(t+1) = [G(t) - A(t)P(t)]\underline{x}^*(t) + A(t)\underline{y}(t) \quad (16)$$

where

$$A(t) = G(t)M(t)P'(t)[P(t)M(t)P'(t)]^{-1} \quad (17)$$

and $M(t)$ is given by

$$M(t+1) = [G(t) - A(t)P(t)]M(t)G'(t) + Q(t) \quad (18)$$

where G' is the transpose of G and $Q(t)$ is the covariance matrix $Q(t) = E\{\underline{u}(t)\underline{u}'(t)\}$. The matrix $M(t)$ is the expectation of the matrix $\epsilon(t)\epsilon'(t)$, where $\epsilon(t)$ is the error at time t . In this formulation, to start the recursion one must know $\underline{x}^*(0)$ and $M(0)$. However, in most cases the effect of the initial choices of $\underline{x}^*(0)$ and $M(0)$ will be insignificant by the time the system reaches its steady state.

An interesting observation made by Kalman is that the prediction problem as formulated by him is dual to a problem in control theory in which the objective is to find an input which minimizes a quadratic loss function.

In addition to extensions of Wiener's theory to nonstationary continuous and discrete-time processes, extension to processes of mixed type were also reported. In particular, Robbins [1959] solved the mean-square optimization problem for the case where the filter consists of a linear time-invariant system followed by a sampler which is followed in turn by another linear time-invariant system. Janos [1959] gave a complete analysis of the case where a stationary signal is multiplied by a train of rectangular pulses, yielding a periodic pulse-modulated time series. The filter is assumed to be a time-invariant linear network. The integral equation satisfied by the impulsive response of the optimum filter is of the Wiener-Hopf type, but a multiplying factor involving trains of rectangular pulses complicates its solution. A method of solution of this equation is given by Janos for the infinite memory as well as the finite memory case.

5.3. Miscellaneous Contributions

There are several not necessarily unimportant problems in filtering and prediction which have received relatively little attention during the period under review. Contributions concerned with such problems are discussed in this section.

It has long been recognized that the use of a quadratic loss function imposes a serious limitation on the applicability of Wiener's theory. Under certain conditions, however, optimality under the mean-square-error criterion implies optimality under a wide class of criteria. Such conditions have been found by Benedict and Sondhi [1957], and, independently, by Sherman [1958]. Thus, Benedict and Sondhi have shown that in the case of a Gaussian process optimality with respect to a loss function of the form

$L = \epsilon^2$, where ϵ denotes the error, implies optimality with respect to any loss function of the form $L = \sum_n |\epsilon|^n$,

where $n > 0$ but is not restricted to integral values. In Sherman's result, $L = f(\epsilon)$ is an even function and $\epsilon_2 \geq \epsilon_1 \geq 0$ implies $f(\epsilon_2) \geq f(\epsilon_1)$. More special cases involving the design of optimal filters under nonmean-square-error criteria have been considered by Bergen [1957] and Wernikoff [1958]. A time-weighted mean-square-error criterion which can be used to reduce the settling time of an optimal linear filter was employed by Ule [1957].

An extension of Wiener's theory to random parameter systems was described by Beutler [1958]. In Beutler's formulation, the signal and noise are assumed to have passed through a time-invariant random linear system before being available for application to a filter or predictor. The linear system is assumed to be characterized by a transfer function $H(w, \gamma)$, in which γ is a random parameter with a known distribution. In effect, this amounts to modifying the statistical characteristics of the original signal and noise processes.

The multiple series prediction problem for the infinite memory case was considered by Hsieh and Leondes [1959]. In their paper, Hsieh and Leondes describe a simplified method of solving the simultaneous integral equations for the weighting functions. Their technique is not applicable, however, to the finite memory case.

The optimization of continuous-time filters and predictors is frequently carried out by discretizing time and then letting the interval between successive samples approach zero. There are many published papers in which limiting processes of this type are used without adequate justification. A careful and rigorous analysis of the problems involved in obtaining optimum continuous-time linear estimates as limits of discrete-time estimates was given by Swerling [1958].

Bibliography

- Aoki, M., Ph. D. Thesis, UCLA, Los Angeles, Calif. (to be published).
- Barrett, J., Application of the theory of functionals to communication problems, Eng. Lab. Rept., Cambridge Univ. (1955).
- Barrett, J., and D. Lampard, an expansion for some second order probability distributions and its application to noise problems, IRE Trans. on Inform. Theory **IT-1**, 10 (1955).
- Bellman, R., and R. Kalaba, On communication processes involving learning and random duration, IRE Nat. Conv. Record, Pt. 4, 16 (1958).
- Bellman, R., and R. Kalaba, On adaptive control processes, IRE Nat. Conv. Record, Pt. 4. Reprinted in IRE Trans. on Automatic Control **AC-4**, 1 (1959).
- Bellman, R., and R. Kalaba, Dynamic programming and adaptive processes: mathematical foundation, IRE Trans. on Automatic Control **AC-5**, 5 (1960).
- Bendat, J. S., Exact integral equation solutions and synthesis for a large class of optimum time variable linear filters, IRE Trans. on Inform. Theory **IT-3**, 71 (1957).
- Bendat, J. S., Principles and applications of random noise theory (John Wiley & Sons, Inc., New York, N.Y., 1958).
- Benedict, T. R., and M. M. Sondhi, On a property of Wiener filters, Proc. IRE **45**, 1021 (1957).

- Bergen, A. R., A non-mean-square-error criterion for the synthesis of optimum finite memory sampled-data filters, IRE Nat. Conv. Record, Pt. 2, 26 (1957).
- Beutler, F. J., Prediction and filtering for random parameter systems, IRE Trans. on Inform. Theory **IT-4**, 166 (1958).
- Bose, A., A theory of nonlinear systems, Tech. Rept. 309, Research Laboratory of Electronics, M.I.T. (1956).
- Bose, A., Nonlinear system characterization and optimization, Trans. Intern. Symp. on Circuit and Inform. Theory. Repr. IRE Trans. on Circuit Theory **CT-6**, 30 (1959).
- Blum, M., Fixed memory least squares filters using recursive methods, IRE Trans. on Inform. Theory **IT-3**, 178 (1957a).
- Blum, M., On the mean square noise power of an optimum linear discrete filter operating on polynomial plus white noise input, IRE Trans. on Inform. Theory **IT-3**, 225 (1957b).
- Blum, M., Recursion formulas for growing memory digital filters, IRE Trans. on Inform. Theory **IT-4**, 24 (1958).
- Brown, J. L., Jr., On a cross-correlation property for stationary random processes, IRE Trans. on Inform. Theory **IT-3**, 28 (1957).
- Brown, J. L., Jr., A criterion for the diagonal expansion of a second-order probability distribution in orthogonal polynomials, IRE Trans. on Inform. Theory **IT-4**, 172 (1958).
- Chesler, D. A., Optimum nonlinear filters with fixed-output networks, Quart. Prog. Rept., Research Lab. of Electronics, M.I.T. 118 (1958).
- Darlington, S., Linear least-squares smoothing and prediction, with applications, Bell Syst. Tech. J. **37**, 1221 (1958).
- Darlington, S., Nonstationary smoothing and prediction using network theory concepts, Trans. Intern. Symp. on Circuit and Inform. Theory. Reprinted in IRE Trans. on Circuit Theory **CT-6**, 1 (1959).
- Davenport, W. B., Jr., and W. L. Root, An introduction to the theory of random signals and noise (McGraw-Hill Book Co., New York, N.Y., 1958).
- Friedland, B., Least squares filtering and prediction of non-stationary sampled data, Inform. and Control **1**, 297 (1958).
- Freimer, M., A dynamic programming approach to adaptive control processes, IRE Nat. Conv. Record, Pt. 4. Repr. IRE Trans. on Automatic Control **AC-4**, 10 (1959).
- George, D. A., The prediction of Gaussian-derived signals, Quart. Prog. Rept. Research Lab. of Electronics, M.I.T., 107 (1958).
- Gilser, E. M., and J. H. Park, Jr., On signal parameter estimation, IRE Trans. on Inform. Theory **IT-4**, 173 (1958).
- Hsieh, H. C., and C. T. Leondes, On the optimum synthesis of multiple control systems in the Wiener sense, IRE Nat. Conv. Record, Pt. 4. Repr. IRE Trans. on Automatic Control **AC-4**, 16 (1959).
- Janos, W. A., Optimal filtering of periodic pulse-modulated time series, IRE Trans. on Inform. Theory **IT-5**, 67 (1959).
- Kallianpur, G., A problem in optimum filtering with finite data, Ann. Math. Stat. **30**, 659 (1959).
- Kalman, R., A new approach to linear filter and prediction theory, J. Basic Eng. (to be published).
- Kalman, R. E., and R. W. Koepeke, Optimal synthesis of linear sampling control systems using generalized performance indexes, Trans. ASME **80**, 1820 (1958).
- Kanter, I., The prediction of derivatives of polynomial signals in additive stationary noise, IRE Wescon Conv. Record, Pt. 4, 131 (1958).
- Kanter, I., Some new results for the prediction of derivatives of polynomial signals in additive stationary noise, IRE Wescon Conv. Record, Pt. 4, 87 (1959).
- Laning, J. H., Jr., Prediction and filtering in the presence of Gaussian interference, Rept. R-27, M.I.T. Instrumentation Lab., (1951).
- Leipnik, R., Integral equations, biorthonormal expansions, and noise, J. S.I.A.M. **7**, 6 (1959).
- Mann, H. B., A theory of estimation for the fundamental random process and the Ornstein-Uhlenbeck process, Sankhyā **13**, Pt. 4, 325 (1954).
- Mann, H. B., and P. B. Moranda, On the efficiency of the least squares estimates of parameters in the Ornstein-Uhlenbeck process, Sankhyā **13**, Pt. 4, 351 (1954).
- Merriam, C. W., A class of optimum control systems, J. Franklin Inst. **267**, 267 (1959).
- Middleton, D., A note on the estimations of signal waveform, IRE Trans. on Inform. Theory **IT-5**, 86 (1959).
- Middleton, D., An introduction to statistical communication theory (McGraw-Hill Book Co., New York, N.Y., 1960).
- Miller, K. S., and L. A. Zadeh, Solution of an integral equation occurring in the theories of prediction and detection, IRE Trans. on Inform. Theory **IT-2**, 72 (1956).
- Nuttall, A. H., Theory and application of the separable class of random properties, Tech. Rept. 343, Research Lab. of Electronics, M.I.T. (1958).
- Robbins, H. M., An extension of Wiener filter theory to partly sampled systems, IRE Trans. on Circuit Theory **CT-6**, 362 (1959).
- Sherman, S., Non-mean-square error criteria, IRE Trans. on Inform. Theory **IT-4**, 125 (1958).
- Shinbrot, M., A generalization of a method for the solution of the integral equation arising in optimization of time-varying linear systems with unstationary inputs, IRE Trans. on Inform. Theory **IT-3**, 220 (1957).
- Swierling, P., Optimum linear estimation for random processes as the limit of estimates based on sampled data, IRE WESCON Conv. Record, Pt. 4, 158 (1958).
- Ule, L. A., A theory of weighted smoothing, IRE Trans. on Inform. Theory **IT-3**, 131 (1957).
- Wernikoff, R. E., A theory of signals, Tech. Rept. 331, Research Lab. of Electronics, M.I.T. (1958).
- Wiener, N., Mathematical problems of communication theory, Summer Session Lecture Notes, M.I.T. (1953).
- Wiener, N., Nonlinear Problems in random theory (The Technology Press and John Wiley & Sons, Inc., New York, N.Y., 1958).
- Zadeh, L., On the representation of nonlinear operators, IRE Wescon Conv. Record, Pt. 2, 105 (1957).

[The text on this page is extremely faint and illegible. It appears to be a multi-paragraph document, possibly a letter or a report, with several lines of text visible across the page. The content cannot be transcribed accurately.]

Circuit Theory

Louis Weinberg*

In this paper a report is presented on the research in circuit theory in the United States during the period 1957–1960. The paper was prepared as a progress report for submission to the XIII Triennial General Assembly of URSI, held in London in September 1960. The following subdivisions of circuit theory are treated:

1. Introduction.
2. Topology or linear graphs, including associated matrix formulations.
3. Synthesis by pole-zero techniques.
4. Realizability conditions and positive real matrices.
5. Systems with time-varying and nonlinear reactances.
6. Active systems.
7. Concluding remarks.

The discussion considers problems that have been solved in these areas as well as a number of important problems for which answers are still not available.

1. Introduction

In the past decade the boundaries of circuit theory¹ have expanded explosively; as a result the present range of circuit-theory research is enormous. It is thus manifestly impossible to give a short account of this research in the United States for the past three years. This would be true even if the "old" or more conventional definition² of circuit theory were used; use of a "new" or more encompassing definition³ makes it hold *a fortiori*. The best one can do is to offer a few examples to suggest the vigor, pertinence, and extent of the present research in circuit theory. For this purpose we have chosen to concentrate on the following subdivisions of circuit theory; (2) Topology or linear graphs, including associated matrix formulations, (3) Synthesis by pole-zero techniques, (4) Realizability conditions and positive real matrices, (5) Systems with time-varying and nonlinear reactances, and (6) Active systems.

The above divisions are obviously overlapping. We subdivide them in this way merely for convenience of discussion and we shall not hesitate to point out interrelations.

In addition, we omit from detailed consideration a number of research areas that fall within the field of circuit theory and also overlap other fields. Among

them are: (a) contact networks and digital computers; (b) data processing; (c) noise theory; (d) sequential circuits; (e) synthesis of distributed-parameter systems; and (f) matched filters. However, we will not completely neglect these areas, but will briefly mention some of the outstanding work in a few of them, though without a precise formulation of the problems. It is clear that these subdivisions of the circuit theory field, e.g., the research in data processing, have great relevance to the problems of interest to URSI, and it is recommended that some provision be made for their detailed discussion in the next triennial report.

It is difficult if not impossible to discuss the research accomplishments of the past three years in the United States without reference to much antecedent work and to work done in other countries; we see farther than our predecessors only by standing on their shoulders, and it is thus essential to refer to some of the accomplishments of the giants of former days. The presentation given here should be considered more in the nature of a portrait rather than a photograph.⁴ We shall have to invoke the artist's privilege of emphasizing certain aspects of the subject to the exclusion of other aspects. To mix a metaphor, in some respects, as is true for any attempted summary of a vast subject, this report takes on the character of a personal odyssey through the present circuit-theory research in the United States.

Finally we hasten to point out that the references are intended to be merely representative, not exhaustive. Because of the fact that parallel lines of endeavor are going on at many research centers, almost an entirely different set of references could be given to illustrate the identical discussion. If we succeed in indicating the problems that have been agitating research workers and in elucidating some of those that have been solved and others that remain unsolved, we will have accomplished our purpose.

*The writer borrows this useful metaphor from his friend, Professor R. M. Foster.

*Hughes Research Laboratories, Malibu, Calif.

¹ We use this term synonymously with *network theory*.

² Such a definition was proposed by Professor B. D. H. Tellegen at the 1957 URSI General Assembly held at Boulder, Colo. He suggested that the following definition be used to guide the deliberations of Subcommission 6.2:

Circuit theory is the theory of networks composed of black boxes characterized by relations between the currents and voltages at the terminals, which relations contain only time as an independent variable, and contain neither space nor temperature coordinates.

³ In the ensuing discussion of Professor Tellegen's definition it appeared that many of the delegates of Subcommission 6.2 considered the definition too restricted. An *ad hoc* group, of which the writer was a member, proposed the following definition of circuit theory in the wide sense:

Circuit theory is the theory of networks of black boxes which are characterized by relations between the voltages, currents, or other variables at their terminals, and which are in general abstractions of physical components of electrical systems.

There appears to be slight difference between the definitions as stated. However, the discussion made clear that the proponents of the second definition wished to include areas like sequential circuits and networks with probabilistic elements (and in general such areas that overlapped the interests of Subcommission 6.1 on Communication and Information Theory), whereas those holding to the first definition would exclude these areas.

2. Combinatorial Topology or Linear Graphs

The past decade has witnessed advances in circuit theory that are expressed in different ways. Much of what is being said about these advances becomes merely a babel unless the circuit theorist is multilingual. This should be interpreted in each of two ways. First, the same problems are being considered by competent scientists in many countries of the world. Second, different mathematical languages are being used to attack and gain insight into these problems. The use in circuit theory of the languages of function theory and some elementary aspects of matrix theory is fairly well established; new languages that have been introduced in the recent past are the language of linear graphs, the language of lattice theory, the language of vector spaces, and the language of sophisticated matrix theory [Trans. IRE 1959b]. We discuss below the field of linear graphs and associated matrix formulations of circuit-theory problems.

Though the basic concepts of linear graphs and their applications to network theory were introduced by Kirchhoff himself [1847], it is only recently that their great power for both analysis and synthesis has been widely recognized. A large part of this recognition stems from attempts to solve the synthesis problem for networks without transformers. One evidence of the intense and widespread interest in this field is the issue of the IRE Transactions of the PGCT that was devoted to this field [1958b]; another is the number of letters and industrial publications that treated this subject [Nerode and Shank, 1957; Nakagawa, 1958; Weinberg, 1958c; Kim, 1958; Calabi, 1956; and Hatcher, 1958].

A good proportion of the publications on graph theory are devoted almost exclusively to a reformulation of Kirchhoff's "Third and Fourth Laws," by which laws we mean his rules for writing down a network function almost by inspection. Some, however, do give basically new material. Mason [1956; 1957], for example showed how to determine system functions of *active* networks by topological rules. This represents an important extension, since Kirchhoff's techniques were restricted to the solution of passive networks without transformers. There were also a number of others who formulated topological rules for solving active networks [Boisvert, 1958; Coates, 1957; Mayeda, 1958b].

Mason's graphs, it should be pointed out, differ from Kirchhoff's; Mason calls them *signal-flow graphs*. These graphs are similar to the block diagrams used in system analysis; thus one difference from Kirchhoff graphs is that the algebraic sum of the signals at a node of a signal-flow graph is not zero, and a second difference is that signals flow along a branch in only one direction.

Two other problems that were solved are the realization of a loop matrix or cut-set matrix by a graph and the realization of a homogeneous polynomial as the discriminant of a network. The first problem is related to the still unsolved problem of

realizing a real matrix as the resistance or conductance matrix of an n -port network containing only resistances and no ideal transformers [Slepian and Weinberg, 1958b]. Indeed, it may also be said to be a problem in any field where linear graphs are applicable, e.g., information theory and linear programming [Elias et al., 1956; Dennis, 1958, 1959; Jewell, 1958]. For a long time this problem was unsolved⁵ and then as so often happens a number of solutions appeared almost simultaneously. Two solutions were presented at the 1959 International Symposium on Circuit and Information Theory. One paper by Guillemin is motivated by problems in network theory [Guillemin, 1959]; the second by Löfgren (of Sweden) is stated in terms of contact networks and appears to be fairly simple to apply [Löfgren, 1959]. If we exclude the work of the Russians, it is probably true that Gould was the first to solve this problem [Gould, 1957, 1958];⁶ his solution appears to be complicated in its application. Subsequently Auslander and Trent gave an alternative solution (1959).⁷

We have thus gone from poverty to an embarrassment of riches with regard to this problem; we now have what could be considered a plethora of solutions.⁸ It is critically necessary at this point to consolidate our advances. All these procedures should be compared for their generality and ease of application; their merits and advantages for solving different types of problems should be illustrated. It would also be desirable that they be stated in a common simple language so that their differences and similarities become evident. Finally, if it is possible, an everyday design procedure should be formulated. Perhaps part of this task will be accomplished at the *Fifth Midwest Symposium on Circuit Theory: Topology in Circuit Theory* to be held on May 8 and 9, 1961 at the University of Illinois.

The problem of realizing a specified homogeneous polynomial that was mentioned above and the story of one of its solutions illustrate the fact that the pace at which we are finding solutions to problems of long standing is an accelerating one. An exceedingly difficult problem in the past [Foster, 1952] was the determination of the necessary and sufficient conditions for a homogeneous polynomial of n variables to be the discriminant of a realizable network—that is, the determinant of the system matrix of the loop or node equations. Some only partially successful attacks⁹ on this problem were previously made by Cohn [1950], Shannon and Hagelbarger [1956], and Melvin [1956]. Dr. Campbell of BTL had also been interested in this problem around 1917, but he is

⁵ Perhaps it would be more accurate to state that the problem was not even formulated, since an awareness of the problem became explicit only in the last few years.

⁶ The Russians have written many papers on contact networks; the writer believes there is a high probability that solutions to this and other "unsolved" problems are waiting to be exhumed from the Russian literature.

⁷ In their paper Auslander and Trent [1959] give what could be considered an abstract solution. They have subsequently written a paper (as yet unpublished) that gives a constructive procedure for realizing the graph.

⁸ The reader should not assume that we have mentioned all the solutions. There are, for examples, a solution by Harry Lee in his MIT master's thesis done under Professor Guillemin's supervision, and a solution by W. Mayeda, which he has submitted for publication to the Transactions PGCT.

⁹ The writer is indebted to Professor R. M. Foster for this discussion of the earlier attacks on the problem.

not known to have reached any significant conclusions. Only one necessary condition was put forth in the three cited papers. If we let D be the homogeneous polynomial in the n variables R_k , and further let D_k be the partial derivative of D with respect to R_k , then the expression $(D_k D_1 - D D_{k1})$ is the square of a homogeneous function of the R_k of degree one less than D and with coefficients that may be -1 as well as $+1$. Cohn's paper attempted to show that this condition was also sufficient, but a counterexample can demonstrate this to be impossible.

The problem was then mentioned by the writer in a talk he gave at Princeton. Dr. F. Harary, who was present at the talk, casually passed the problem on (during the 1959 International Symposium on Circuit and Information Theory) to Tom Crowley of BTL, who was commentator for the session on Switching Theory. Using the techniques of Löfgren's paper, Crowley announced he had solved the problem.¹⁰ Subsequently the writer discovered that Mayeda had previously solved the problem [1958a]. It also appears that another solution has now been given by Duffin [1959].

This is not the only instance of a problem's being solved at the Symposium. A different problem that arises in linear programming [Heller and Tompkins, 1956; Hoffman and Kruskal, 1956] is the specification of a set of necessary and sufficient conditions on a real matrix for it to be a unimodular matrix, where a unimodular matrix is defined as a rectangular matrix all of whose subdeterminants (including each element considered as a subdeterminant of order one and also the determinant itself, if the matrix is square) are equal to ± 1 or 0. This problem also arises in network theory and in the theory of contact networks, and generally in any discipline that can be described in graph-theoretic terms; for example, the incidence matrix introduced by Kirchhoff is a unimodular matrix and so is the loop matrix based on a fundamental set of loops. The writer mentioned that this problem was unsolved in chairing the session on Graph and Matrix Theories; the following day D. Anderson of the Hughes Aircraft Company (who, it should be mentioned, had also been introduced to this problem previously) indicated he had a solution.¹¹

The research mentioned above—that is, the realization of a loop or cut-set matrix, the complete characterization of the unimodular matrix, and the realization of a homogeneous polynomial—are all important in what the writer considers to be the crucial network problem at the present time, namely, the realization of networks containing no ideal transformers. Distinguishing classes of networks with regard to the inclusion or exclusion of ideal transformers is a fundamental method of differentiation. For example, it can be shown that the exclusion of transformers makes the realization of the n -terminal network a problem distinct from that of the n -port

network, whereas when transformers are allowed a solution to one class of problem also solves the other. It is felt, furthermore, that solution of the problem of realizing transformerless networks will throw light on the problem of equivalent networks, and on how to obtain them by linear transformations.

As Cederbaum [1958] points out, most of the synthesis procedures for n -port networks use the artifice of the ideal transformer to solve the realization problem; to use his apt simile, the ideal transformer has been used like the *deus ex machina* of classical drama. By a suitable arrangement of transformers one can get combinations of voltages and currents which otherwise would be impossible. It is clear that new types of synthesis procedures are required; instead of assuming the network configuration in advance, as is done when we use one of the presently known procedures, the configuration will be derived from the mathematical characterization of the network. The resulting structure will probably be a complex interconnection of elements, a network in the true sense of the word, rather than one of the known canonical configurations. All of this indicates to the writer that the concepts of linear graphs will become increasingly important.

To mention one result for which no derivation is known other than a graph-theoretic one, we have the necessary condition that an impedance matrix or an admittance matrix of a pure resistance n -port must be a paramount matrix, where by a paramount matrix we mean a real symmetric matrix each of whose principal minors of order p ($p=1, 2, \dots, n$) is not less than the absolute value of any p th-order minor built from the same rows. Tellegen [1952] derived this result for a three-port by use of the fact that the voltage ratio of a resistance network cannot exceed unity; he also showed the condition to be sufficient for a three-port. However, for an n port with $n>3$, this method does not suffice and Cederbaum [1958] was forced to use linear-graph concepts for his derivation. These results and others on dominant matrices for resistance networks are summarized by Slepian and Weinberg [1958a]. The latter authors also derive a sufficiency condition on dominant *residue* matrices for two-element kind networks; this result was subsequently useful in the realization of active RC networks [Kinariwala, 1959]. In the above we use the term *dominant* matrix to mean a real symmetric matrix each of whose main-diagonal elements is not less than the sum of the absolute values of the elements in the same row.

2.1. Future Research Activity and Evaluation

The writer feels that the problem of realizing an n -port resistance network will be solved before the next General Assembly; implicit in this solution there will probably be a method for realizing RLC networks without transformers. This may appear to be a rash prediction since it was way back in 1952 that Foster wrote [Foster, 1952], "There is room for much further progress in the investigation of general n -terminal pair networks, especially the delineation

¹⁰ Though the writer has a copy of the paper that Crowley wrote, he does not believe it has yet been published.

¹¹ Again this solution has not yet been published but has been studied by the writer.

of just what can be done without ideal transformers, without mutual inductance, or with only two kinds of elements. Furthermore, even the theory of the true 3-terminal network (without pairing of terminals) for two kinds of elements (without mutual inductance or ideal transformers) is almost wholly unknown." Today each of these problems is still unsolved. However, we should recall that the problem of the discriminant that Foster also mentions is now solved. Furthermore, such men of the calibre of Guillemin and Darlington are now looking at problems of this nature. Guillemin is using linear transformations of matrices [1960a; b] as his method of attack, whereas Darlington has informed the writer in informal conversation that he was using vector spaces in his analysis of the problem.

The topological approach (as presented mainly in Cederbaum's papers) is also a promising one and should not be neglected. It has led to the brink of a major breakthrough on this problem—e.g., the statement of the paramount condition on impedance or admittance matrices of n ports containing no transformers—and provides a formulation of the problem in matrix terms that is elegant. Cederbaum [1958] has shown that a necessary and sufficient condition for a given symmetric n th-order matrix Z to be the impedance matrix of an RLC n port containing no real or ideal transformers is that it is a principal submatrix of the inverse of the triple matrix product BY_bB' , where Y_b is a diagonal matrix whose main-diagonal elements are $a, bs, c/s$ with $a, b, c > 0$, s is the complex variable $s = \sigma + j\omega$, B' is the transpose of B , and B satisfies the conditions for a cut-set matrix corresponding to an adequate system of node-pair voltages—that is, B can be realized as the cut-set matrix of a graph by one of the procedures mentioned previously. A necessary condition on B is that it be a unimodular matrix. A complete statement of the necessary and sufficient condition on B for it to be such a matrix is that there exists a decomposition of B of the form

$$B = K^{-1}Q$$

where Q is a reduced incidence matrix of the desired connected network and K is a reduced incidence matrix of the tree of node-pair voltages (that is, of the tree that is formed by drawing a branch for each voltage variable). An analogous condition can of course be stated for the admittance matrix of an n port.

This necessary and sufficient condition differs from those ordinarily given in synthesis, where sufficiency is demonstrated by a synthesis procedure.¹² Here no synthesis procedure exists because no method is known for decomposing Z into a principal submatrix of the desired congruent transformation of a diagonal matrix. Solution of this matrix problem would be a contribution of the first magnitude.

¹² For this reason it has been objected that such a form of necessary and sufficient condition is not of great value, that it in effect merely restates the problem. The writer does not agree since the restatement of the problem allows other mathematical artillery to be used in the solution. As an illustration of the value we should note that it has led to a solution of the problem of realizing a resistance n -port network that has only $(n+1)$ terminals, Cederbaum [1957].

To make this statement apply to two-element kind networks—e.g., to the RC case—we merely require that the elements of Y_b be of the form a and bs . To convert it to the problem of realizing a pure resistance n port, we stipulate that the diagonal elements of Y_b be positive numbers. In this case the elements of Z are of course no longer rational functions of s but are real numbers.

Some necessary conditions on Z are known: Z must be a symmetric positive real matrix; in addition, Z must be a paramount matrix for each value of s in the range $0 < s < \infty$. However, a set of necessary and sufficient conditions is not known even for $n=2$, that is, the two-port network without transformers; it is also not known for the RC or LC case with $n=2$.

For the case of the resistance network when the n port is formed from the links pertaining to a tree, Cederbaum [1959] has furnished a solution. For the admittance case this represents a solution for the resistance network when the n port network has only $(n+1)$ terminals. The solution consists of an algorithm whereby the decomposition

$$Z = BY_bB'$$

if it is possible at all, can be carried out. Here we note the problem is simpler in that Z is not required to be a principal submatrix of the triple product but is equal to it. However, Cederbaum's techniques may be suggestive in solving the more general problem.

It should also be mentioned that a similar formulation as a triple matrix product is given by Bryant [1959a]. He shows that the necessary and sufficient condition for a real symmetric matrix Z to be the impedance matrix of a resistive n port is that Z be of the form

$$Z = S'G^{-1}S$$

where S' is the transpose of S , S is a submatrix of a reduced incidence matrix of a tree, and G is a dominant matrix with nonpositive off-diagonal elements. Again this should not be looked upon as a mere restatement of the problem. It may have an advantage over the Cederbaum formulation in that G can be recognized by inspection; however, the problem to be mentioned below of recognizing G^{-1} (the inverse of a dominant matrix with nonpositive off-diagonal elements) still remains. The transformation matrix S can also be recognized by inspection since the necessary and sufficient conditions for a matrix to be the reduced incidence matrix of a tree is that it be nonsingular, have elements ± 1 or 0, and in each column have at most two nonzero elements, specifically, one $+1$ and one -1 . Cederbaum's transformation matrix, it should be recalled, must be unimodular, a test for which is laborious; and even if it is unimodular it may still not be realizable by a graph. Of course, the unimodular test may be omitted when this is convenient and

the procedure for realizability as a graph may be applied directly. Bryant [1959b] considers additional formulations for resistance networks in his doctorate thesis.

We mention, finally, one more approach that may yield useful insights for solving the problem of realizing a resistive n -port network. We might prefer to assume that the network possesses accessible *terminals* rather than n ports—i.e., terminals paired into ports or terminal pairs—or we might find it convenient to switch between the two representations. There is a simple formula relating system functions in one representation to system functions in the other. This formula, which is given below, is not so widely known as it should be; its first appearance and proof in the literature are somewhat in doubt, and it is continually being rediscovered. One of the conceptual advantages of the $2n$ -terminal network representation is that only driving-point measurements need be made; these characterize the n port uniquely. Thus an obvious necessary condition on each measurement is that it is a non-negative number.

Consider a resistance n port with an open-circuit resistance matrix $R=[R_{ik}]$. Of course, since the n port obeys reciprocity, of the n^2 driving-point and transfer resistances only $n(n+1)/2$ are independent—that is, the matrix is symmetrical. Now consider this network as a $2n$ -terminal network with the terminals numbered from 1 to $2n$, and with the ports so numbered that port 1 comprises terminals 1 and $(n+1)$, the assigned positive direction being from terminal 1 to terminal $(n+1)$. In general port k will run from terminal k to terminal $(n+k)$.

For the representation of the $2n$ -terminal network let $S_{i,k}$ denote the measured driving-point impedance between terminals i and k , all other terminals being left free. Then we define $S_{k,k}=0$, since this measurement corresponds to both of the measuring leads connected to the same terminal. It is clear that

$$R_{kk}=S_{k,n+k}$$

The general formula for the elements of matrix R is

$$R_{ik} = \frac{1}{2} [S_{i,n+k} + S_{k,n+i} - S_{i,k} - S_{n+i,n+k}]$$

which reduces to the previous formula when $i=k$. A simple proof of this formula that uses Kirchhoff's topological rules has been given by Professor Foster in a private letter to the writer.

There are some other unsolved problems raised by graph-theoretic considerations. For example, can a simple test for a paramount matrix be devised? A direct test that follows from the definition is to check the required conditions on each principal minor of order $p \leq n-1$ and each of its corresponding non-principal minors. The evaluation of all possible minors, however, can be laborious, and the question naturally arises whether all minors must be tested. In other words can a simplification be effected as,

for example, in the test for a positive definite matrix? We recall that for an n th-order matrix to be positive definite, it is necessary that all the principal minors are positive; it is sufficient, however, to test only a subset of n principal minors. It has been shown by Slepian and Weinberg [1958] that we must test all minors of order two. It can be shown, furthermore, that not much can be done to shorten the work of testing a matrix for its paramount character.¹³

Another matrix problem is the formulation of a simple method for determining whether the inverse of a nonsingular paramount matrix is a dominant matrix with nonpositive off-diagonal terms. This would then give a set of necessary and sufficient conditions for the realization of a real matrix as the impedance matrix of a $(n+1)$ -terminal network containing only pure resistances. Also, with regard to a dominant matrix, though we know that the condition of dominance is sufficient for realization of a given matrix as the *admittance* matrix of a resistive n port, we still don't know whether this is true for realization as the *impedance* matrix.

A final problem may be mentioned for the paramount matrix. As indicated previously, it is known that paramountcy is sufficient for the realization of an n port for $n \leq 3$; though the writer conjectures that it is not sufficient for $n > 3$, this has never been demonstrated. A method that has been suggested¹⁴ for proving or disproving the sufficiency for $n=4$ is to consider the dominant admittance matrix

$$Y = \begin{bmatrix} 7 & 1 & 2 & 3 \\ 1 & 12 & 4 & 5 \\ 2 & 4 & 15 & 6 \\ 3 & 5 & 6 & 18 \end{bmatrix}$$

This is realizable by a general procedure [Slepian and Weinberg, 1958a], but (as has been shown by Cederbaum [1959]) not by a four-port with only five terminals. Now suppose that Y is reduced to the irreducible¹⁵ paramount matrix

$$Y_1 = \begin{bmatrix} 3 & 1 & 2 & 3 \\ 1 & 5 & 4 & 5 \\ 2 & 4 & 6 & 6 \\ 3 & 5 & 6 & 53/7 \end{bmatrix}$$

Now the question is whether there exists *any* four-port with Y_1 as its admittance matrix. It may be worth while to investigate this particular case and perhaps by the use of the possible geometrical configurations [Foster, 1932] for a four-port, the fact that a nonplanar network has no dual, and by the

¹³ An example to illustrate that we cannot eliminate testing minors of order $n-1$ in an n th-order matrix was furnished the author in a private letter—etc. (See letter).

¹⁴ This suggestion was made to the writer in a private letter from Professor R. M. Foster.

¹⁵ By reducing a paramount matrix we remove main-diagonal elements without destroying the paramountcy condition. Then the reduced matrix is inverted and this reduction, if it is possible, is repeated. This yields shunt and series elements in the corresponding network. When a matrix is reached for which this is no longer possible since the paramountcy condition will be violated by such a step, this matrix is called irreducible. A detailed discussion of the reduction of a third-order matrix is given in chapter 8 of the author's book, "Network Analysis and Synthesis," to be published by the McGraw-Hill Book Co.

process of complete induction, it can be demonstrated that no such network exists and consequently that paramounty is not sufficient.

Another irreducible paramount matrix suggested by Foster is

$$Y_2 = \begin{bmatrix} 3 & 2 & 1 & 3 \\ 2 & 3 & 2 & 3 \\ 1 & 2 & 3 & 3 \\ 3 & 3 & 3 & 5 \end{bmatrix}$$

Does any four-port exist with Y_2 as its admittance matrix? Not only can this example throw light on the question of paramounty, but it may also furnish an answer to an unresolved aspect of equivalent networks—specifically, do there exist matrices which are admittance matrices of networks without transformers but not impedance matrices, and vice versa? We recall that any matrix realizable as an admittance matrix can also be realized as an impedance matrix, if ideal transformers are allowed; however, this is an unanswered question for transformerless networks. For the matrix given above as Y_2 there is a simple network if this matrix of numbers is considered as an impedance matrix, namely, a chain of five one-ohm resistances, with the ports chosen as indicated in figure 1.

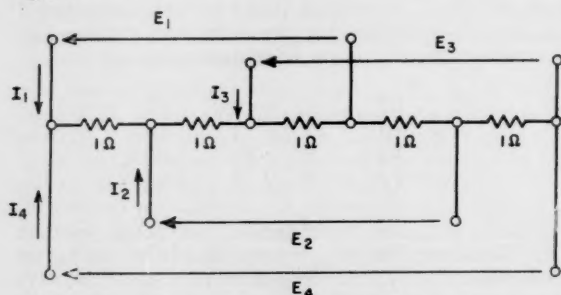


FIGURE 1. Chain of five 1-ohm resistances realizing the given impedance matrix.

Some important *analysis* problems still remain with regard to graph theory. We know that the driving-point and transfer functions of an n port may be expressed in terms of the independent driving-point functions of the network considered as a $2n$ -terminal network. Thus a simple method for determining these driving-point functions is required. This is known [Weinberg, 1958a] for those driving-point functions measured across a branch of a symmetrical graph; however, the problem of specifying the driving-point function across two nodes not connected by a branch is still unsolved. Solution of this problem is important since it would permit simple calculation of the currents and voltages of large graphs used to simulate other physical systems. For an indication of the extensive computations that are presently required the reader is referred to Branin's paper [1959].

Another aspect of graph theory that should see wider use in the future is Wang Algebra [Duffin,

1959]. This appears to be ideally suited for the application of digital computers to network investigations. One of the troublesome problems that previously held up digital-computer research on networks by use of graph-theory concepts is the direct determination of all the trees of a network without duplication [Hobbs, 1959; Mayeda, 1959]; a method has now been given by Fujisawa [1959].

It is felt that the applications of graph theory to physical systems will increase rapidly in the next few years. The rate of increase will depend on the size of the cultural lag—that is, the length of time before linear graphs is taught in the schools as a routine tool of the engineer. In the past, network theorists have assimilated mathematical disciplines like function theory, matrix theory, and Laplace transform theory, and have developed general methods for analyzing exceedingly complex networks without becoming lost in a maze of detail. Then these concepts and techniques that were developed in network theory were recognized to be of great value to the applied mathematician and physicist [Mathews, 1959], irrespective of his field of specialization. Network concepts such as input-output and others have even found their way into a recent book on pure mathematics [Kaplan, 1958]. In addition to their use in exact sciences, the input-output concept and the ubiquitous black box have yielded rich rewards in such fields as biology and economics [Leontief, 1959]. Thus network theorists have insisted that their subject had a great deal to offer other fields and hence that engineers and physicists should learn the language of network theory [Weinberg, 1960].

This situation may now be changing; the change is illustrated by the field of graph theory. Graph-theory applications are being made with great speed in other engineering fields such as linear programming, information theory, and switching circuits. It may now become necessary for engineers and physicists to use the common language of graph theory rather than redefine the concepts in a manner appropriate for their own specialty. Perhaps future teachers of electrical engineering instead of stating Kirchhoff's current law in the old form that the algebraic sum of the currents at a node is zero will teach the equivalent linear-graph statement that the 1-chain I is orthogonal to the coboundary of each point of a graph G . In any case, however it is taught, we can be fairly certain that graph theory will eventually become as established as function theory or matrix theory in the educational background of the engineer and physicist.

3. Synthesis by Pole-Zero Techniques

Though Darlington's [1939] work was done about 20 years ago his techniques are still not being used by the average engineer. Following the lead of Grossman's paper in early [1957], which attempted to make Darlington's results on elliptic function filters more readily available, Henderson published nomographs [1958], Weinberg published tables of element values for Butterworth, Chebyshev and

Bessel-polynomial networks [Weinberg, 1957a; b; c], and Henderson and Kautz presented a whole series of graphs [1958] of the transient response of such networks. The large demand for reprints of these papers with the letters of comments attest to the cultural lag between what is known about filter theory by workers in this field and the methods used to design filters by the engineers in the laboratory.

The research activity in this area for the past three years has been devoted largely to an application of the classical RLC synthesis techniques to new types of systems and secondly to the extension of synthesis procedures to include rational functions with nonreal coefficients. We shall discuss these two trends, mention a new synthesis procedure, and then briefly consider the approximation problem. Finally, we shall give a fairly thorough discussion of the problem of finding explicit formulas for the element values of ladder networks.

The design of crystal filters has generally been treated by image-parameter techniques. Kosowsky [1958] has extended these techniques in his treatment of methods for realizing such filters. O'Meara [1958a; b; c] in a series of papers has attempted to show the value of modern synthesis techniques by applying them to particular crystal-filter configurations. With the increasing stress on transformation techniques for achieving desired network configurations [Saal and Ulbrich, 1958]—e.g., the so-called *zig-zag* filter—it is felt that general synthesis procedures for crystal filters may yet be formulated.

A new RLC synthesis procedure is that of Macnee [1958]; this may be useful in frequency-multiplexing problems. The network yielded by Macnee's procedure has open-circuited inputs and paralleled outputs. He thus realizes a set of transfer impedances in contrast to Guillemin's related procedure of realizing a transfer admittance by means of ladder networks paralleled at both ends.

Lewis applied RLC synthesis techniques to the realization of pulsed networks [1958], whereas Levenstein [1958] showed that the realization of networks with linearly varying resistances—i.e., potentiometer networks—was analogous to the RC synthesis problem. This correspondence will probably be extended in the future and has already led to the analysis of positive real functions of two variables [Ozaki and Kasami, 1959].

Baum has made a significant contribution to the design of narrow-band filters [1957; 1958a]. He has extended the techniques of synthesis to apply to rational functions whose polynomials have nonreal coefficients; this requires that he consider as additional types of elements in the low-pass domain fictitious frequency-independent positive and negative reactances; when the transformation to the band-pass domain is made, the networks become physically realizable. Baum [1958b] has also shown how to use fewer elements than in the Brune procedure in the realization of driving-point functions with geometric symmetry, such as are obtained in the low-pass to band-pass reactance transformation.

The application of RLC synthesis techniques to transmission-line networks by means of Richards' transformation was considered by Grayzel [1958]. A useful summary and extension of methods for handling this problem are given by Welsh and Kuh [1958].

In considering the approximation problem we find that Kuh has presented an additional solution for approximating the ideal delay function [1957]. The solution, which is found by means of the potential analogy, yields a tandem connection of a low-pass ladder network and an all-pass bridged network. It is more efficient than the maximally flat time delay yielded by Bessel polynomials in the sense that a wider bandwidth is achieved for a prescribed number of singularities and time delay. However, the Bessel-polynomial approximation is of course much simpler.

Papoulis [1958] considered the approximation of a magnitude characteristic and found the class of polynomials that has the maximum cutoff rate under the constraint of a monotonic response. Thus his polynomials give a magnitude function that combines the monotonic property of the Butterworth polynomials and the optimum cutoff property of the Chebyshev polynomials. Again, as in the case of Kuh's approximation, some measure of simplicity is lost: the Butterworth polynomials are much simpler than the set of new polynomials.

We now come to the discussion of ladder networks and explicit formulas for their element values. This problem has tantalized research workers ever since Norton [1931], who was the first to contribute to this problem, derived the formulas for the element values of ladder networks with a Butterworth characteristic and with a resistance termination at only one end. Bennett [1932] extended Norton's work by giving the formulas for the element values for the maximally flat ladder that is terminated in resistance at both ends.¹⁶ However, Bennett's formulas are restricted to the case of equal resistance terminations. About 20 years later Belevitch [1952] derived the formulas for the Chebyshev-polynomial or equal-ripple ladder. Again, the formulas are not general: Belevitch's apply only to the matched ladder network. Orchard [1953] then extended Belevitch's formulas to the open-circuited or short-circuited Chebyshev ladder.

In 1954 a major breakthrough came when Green [1954] provided a generalization of all the preceding work; he discovered the formulas for ladders with a Butterworth or Chebyshev characteristic and with *any ratio of resistance terminations*. These formulas did not solve the complete problem since they apply only when the zeros of the reflection coefficient are chosen to lie in one half-plane. Depending on the choice of the zeros of the reflection coefficient, a number of other networks is possible. For a transfer function whose denominator is of odd degree, Wein-

¹⁶ Bosse [1951] who appeared to be unaware of Bennett's work independently solved the same problem. In addition, Bosse was the first to give complete proof of the formulas. Bennett had his proof practically complete and Norton's analysis gave general formulas for 1st, 2nd, 3rd, etc., element of ladder for any total number of elements without proving the general formula for the m th element in n -element structure.

berg [1957c] solved the case of a symmetrical distribution of the zeros of the reflection coefficient—that is, for zeros chosen to alternate in the left and right half-planes.

These formulas have led the writer and others to conclude that we are somehow “missing the boat” on the ladder network. Though in a mathematical sense the Darlington method is an elegant solution to the general problem of realizing a lossless network terminated in resistances, the computations seem unusually complicated when applied to a simple configuration like the ladder. The writer has felt for a long time that the simplest methods of analyzing and synthesizing a ladder are still to be found. The discovery (and proof) by Indjoudjian [1954] of formulas for the element values of an n -stage RC amplifier have bolstered this feeling.

One of the disconcerting aspects of most of the above results on the Chebyshev and Butterworth ladders is that they were never rigorously proved, although their correctness was universally accepted. The formulas were derived by carrying out the calculations in detail for cases of low degree and then guessing the general result. An attempt to prove the general case, in the hope that such a proof would show how to solve related problems, resulted only in a proof for the Butterworth case [Doyle, 1958]. As remarked by Doyle, his proof is a “hammer-and-tongs” one in that it gives no clue to the reason for the amazing simplicity of the final formulas. It is thus not possible to extend the proof to formulas for the Chebyshev case or for other zero distributions of the reflection coefficient or finally, to formulas for the elliptic-function filter.

The above was the state of knowledge on the ladder network at the time of the last URSI General Assembly in 1957. What followed reads almost like a detective story. At a meeting of Sub-Commission VI-2, the writer mentioned the significant problems of finding formulas for the inverse Chebyshev and the elliptic-function filters and in passing commented that the formulas given by Green for the Chebyshev-polynomial case had never been proved. One of the participants in the discussion was Dr. H. Takahasi. After the meeting the writer and Dr. Takahasi had supper at which the latter casually mentioned that he had derived and proved the formulas in 1951. It must be admitted that the reaction of the writer was disbelief; it was so hard to imagine this to be true that he felt he hadn't explained the problem clearly to Dr. Takahasi. However, the ensuing conversation showed that Dr. Takahasi was aware of all facets of the problem. He promised to send a copy of his paper [Takahasi, 1951], and some time later he did.

Thus one of the unexpected effects of this URSI meeting of scientists from different countries is the uncovering of Dr. Takahasi's paper. This gives another illustration (if any are needed) of the desirability of more such international conferences.

In this paper Takahasi derives the formulas that were later independently given by Green. The wealth of new results, the elegance of the proof, and

the implications for future work are adequately covered in the paper by Weinberg and Slepian [1960a] based on Takahasi's paper. Suffice it to say here that it is literally incredible that these results could have remained unknown to workers outside of Japan (and, it may be added, to many Japanese also) for so long a time. Perhaps the history of this problem as presented here can make some small contribution to eliminating a repetition of similar occurrences. The amount of duplication in research and calculating effort that could have been eliminated and the additional progress that could have been made in this field by widespread knowledge of Takahasi's paper are incalculable.

3.1. Future Research Activity

Though some work has been done on the realization of true RLC networks—that is, where the coupling network contains resistance elements inserted in a controlled manner—we are still in need of a general synthesis procedure. The state of knowledge even on the problem of incidental dissipation is not complete. We still don't know how to realize a network where each inductor is not restricted to the same dissipation factor. Perhaps graph theory may be useful here; some work has already been done on showing how equivalent ladder networks can be derived by the use of graph theory [Simone, 1959]. The procedures of Darlington [1939] and Bader [1942] apply to the case of nonuniform dissipation where d_c is the dissipation factor of the capacitors and d_L is the dissipation factor of the inductors. Darlington did not present his procedure in detail; as a result a generation of readers has probably had difficulty in applying it. Desoer thus performs a useful service in giving a clear interpretation of Darlington's procedure [1959]. When the network is terminated at only one end, the problem is greatly simplified. Geffe [1959] considered such a singly loaded network whose reciprocal voltage ratio is a polynomial and gave formulas for the coefficients of the polynomial after predistortion; thus the need for the Darlington or Bader procedure is eliminated in this case.^{16a} As is remarked by Bennett, in his proof appended to Geffe's letter, the fact that this closed-form solution for the coefficients is obtained should not be taken to imply that the general case can be treated similarly. However, further investigation of a possible simplification of the doubly loaded case would be worth while.

The writer also feels that formulas for the element values should exist for the uniformly predistorted Butterworth and Chebyshev cases. We know these formulas when no dissipation is introduced. One's sense of propriety is outraged when he finds that making a simple translation of the frequency variably forces him to carry out the computationally awkward continued-fraction expansion. Nature is generally not so perverse. After all, the poles of the Butterworth and Chebyshev functions still lie

^{16a} It might be added that Orchard maintains (in a letter to the Editor, Trans. PGCT, June 1960) that direct calculation of the element values is simpler than using the closed-form expression for the coefficients of the polynomial.

on a circle and ellipse, respectively, except that the figures are shifted to the right. Perhaps the deep insights of Takahasi on the properties of the continued-fraction expansion for Butterworth and Chebyshev functions should help in this problem as well as in some of the other problems mentioned below.

It appears that there is no end to the closed-form formulas that can be found for the Butterworth and Chebyshev functions. For the Butterworth transfer function given by

$$|K(j\omega)|^2 = \frac{1}{1 + \omega^{2n}}$$

the time delay $T_d = -d\beta/d\omega$ (where $K(j\omega) = |K(j\omega)|e^{j\beta}$) has been found to be

$$T_d = \sum_{m=0}^{n-1} \frac{\omega^{2m} \sin(2m+1)\pi/(2n)}{1 + \omega^{2n}}$$

For the Chebyshev function given by

$$|K(j\omega)|^2 = \frac{1}{1 + \epsilon^2 T_n^2(\omega)}$$

where $T_n(\omega)$ is the Chebyshev polynomial of the first kind (i.e., $T_n(\omega) = \cos(n \cos^{-1} \omega)$), the time delay in closed form¹⁷ is

$$T_d = \frac{\sum_{m=0}^{n-1} \frac{U_{2m}'(\omega) \sinh(2n-2m-1)\phi_2}{\epsilon^2 \sin(2m+1)\pi/(2n)}}{1 + \epsilon^2 T_n^2(\omega)}$$

In the above $U_n(\omega)$ is the Chebyshev polynomial of the second kind—i.e., $U_n(\omega) = \sin(n+1)\phi/\sin \phi$, where $\omega = \cos \phi$ —and ϕ_2 is the imaginary part of ϕ given by $\phi_2 = 1/n \sinh^{-1} 1/\epsilon$. It should now not be difficult to go further; perhaps the time delay for the inverse Chebyshev may be found in closed form, and even that of the elliptic-function filter. One of the other problems where the insights of Takahasi should be helpful is the determination of formulas for the element values of an inverse Chebyshev transfer function—that is, the function obtained by a simple transformation of a Chebyshev-polynomial function which yields a low-pass filter with a maximally flat pass band and an equal-ripple stop band. Again it should be possible to determine the effect of the transformation on the formulas for the element values of the Chebyshev transfer function. Of course, the inverse Chebyshev has finite transmission zeros so that each arm of the ladder network no longer consists of a single inductance or capacitance, but the finite zeros are known in closed form so that it should be a simple matter to add proper resonating elements to an element given by a formula. The difficulty that is introduced by the steps of the continued-fraction expansion may now be removed by the properties derived by

Takahasi. One should perhaps start with the simplest ladder network, that is a ladder with a resistance at only one end.

The problem of greatest moment with regard to the derivation of formulas for the element values is the case of the elliptic-function filter—that is, the filter with an optimum cutoff characteristic and equal ripples in both the pass and stop bands. This problem is exceedingly difficult,¹⁸ but well repays long study. Discovery of the formulas could well bring about a revolution in the applications of modern filter theory. It is suggested that some of the relationships presented by Helman [1955] may be useful here since they relate the elliptic-function filter to the Chebyshev filter (for which formulas are known) without the introduction of elliptic functions.

Most of the above could be looked upon as an attempt to achieve a general understanding of the ladder network, one aspect of which is to answer the question whether formulas for the element values can be found when the reciprocal transfer function is a polynomial many of whose properties are known analytically. For example, can such formulas be found for the transfer function with a maximally flat time delay, that is, the function yielded by use of the Bessel polynomials? The continued-fraction expansion about the origin of the ratio of the even and odd parts of the polynomial representing the reciprocal transfer function is simple, the r th coefficient of $1/s$ being given by $2r-1$; perhaps a related functional form also exists for the coefficient of s in the expansion about infinity. The transfer function corresponding to the so-called synchronously tuned amplifier, treated by Indjoudjian [1954], should be investigated for any insights it may offer. Indjoudjian derived and proved formulas for the singly loaded case; the doubly loaded case is thus still unsolved.

Finally, formulas for the element values of the network with a distribution of zeros of the reflection coefficient other than all in one half-plane are known in only one case [Weinberg, 1957c]; some effort will probably be expended in determining the formulas for other zero distributions.

Perhaps future research in this area will demonstrate that each type of function must be investigated individually, that fortuitous circumstances permitted the determination of the known formulas. At any rate, it would be desirable to establish some conclusion; such investigations will surely yield insights valuable for further research in network theory.

It appears that research on network functions expressed as functions of two complex variables may be accelerated in the next few years. Such functions arise in many different investigations. An analysis of the positive real functions of two variables that arise in potentiometer circuits has already been mentioned [Levenstein, 1958]. Reference to Takahasi's work will show that he makes elegant use of the properties of symmetrical polynomials in two

¹⁷ Both of these formulas for the time delay were sent to the writer in a private letter from H. J. Orchard.

¹⁸ One should be optimistic, however. In a private communication H. J. Orchard writes that he believes he has found the formula for the first reactance of the elliptic-function filter.

variables. Furthermore, the functions describing networks containing resistances, inductances, capacitances, and transmission lines of commensurable length are functions of two complex variables after a substitution has been made to remove the exponential terms. Such functions also arise in control theory when systems containing a transportation lag (i.e., a pure time delay) are treated.¹⁹ It has also been suggested²⁰ that the realization of networks containing inductors with unequal dissipation factors might be attacked by the use of rational functions of two variables.

The positive function introduced by Baum in his theory of narrow-band filters, as contrasted with the positive real function, will get further study and application in network theory. Already Belevitch [1959a] has used it to obtain what he feels to be a more natural derivation of the Brune cycle.

Finally, the analysis and synthesis of nonlinear networks will come in for increasing attention. A start on this problem is represented by the treatment of the piecewise linear case obtained by using networks of diodes and resistances; some work in this area is that by Stern [1956] and Dennis [1959].

4. Realizability Conditions and Positive Real Matrices

In the section on graph theory we discussed the still unsolved problem of characterizing the second-order impedance or admittance matrix of a grounded RC quadripole. Some necessary conditions have been derived using function theory rather than graph theory. It has been shown by Slepian and Weinberg [1958b] that the order relationships that hold for the numerator coefficients of the z_{tk} before cancellation of possible common factors—namely, that the coefficients of z_{21} must be positive and not greater than the corresponding coefficients of z_{11} and z_{22} —must hold even after cancellation for the z_{tk} or the y_{tk} in the case of a network with less than six nodes; in other words, for such a network it is impossible for both sets to violate the conditions. These results have been extended in a doctorate thesis by Olivares [1959]. Some additional results have been obtained in other countries [Bryant, 1959; Adams, 1958], but the general problem still remains unsolved.

For the case when only a transfer function of the RC three-terminal network is specified, some additional work has been done. Kuh [1958] has given an alternative synthesis procedure, and Kuh and Paige [1959] have determined the maximum possible multiplier for the voltage ratio of an RC ladder network.

Some recent work has been done on characterizing networks containing negative elements in addition to positive resistances, inductances, and capacitances. A general theory for the synthesis of networks con-

taining negative elements becomes more urgently needed with the widespread use of the negative-impedance converter and especially with the discovery of the tunnel diode. A basic attempt at the formulation of realizability conditions for such networks is given in Bello's doctorate thesis [Bello, 1959]. Some additional papers are scheduled for presentation at the Polytechnic Institute of Brooklyn Symposium on Active Networks and Feedback Systems to be held in April 1960. Further discussion of the synthesis aspect of this problem is given in the section on Active Systems.

The problem of characterizing the matrices of passive n ports has received much attention. The paper of Youla, Castriota, and Carlin [1959] uses the scattering matrix and attempts to derive a rigorous theory of linear, passive, time-invariant networks on an axiomatic basis. Their discussion is heavily mathematical, being replete with the concepts of Hilbert space. The papers of Weinberg and Slepian [1958; 1960b] use the impedance and admittance characterizations and thus discuss the positive real matrix. They give new realizability conditions on different types of networks; in addition, they attempt to establish simple tests for checking the realizability of specified matrices whose elements are rational functions. One of the properties of their tests is the elimination of the usually required step of solving for the roots of polynomials. Some other work on the positive real function was done by Seshu and Balabanian [1957]; they consider transformations of a positive real rational function that keep the positive real property invariant.

4.1. Future Research

Enough has been said in the graph-theory section on the unsolved problems of finding necessary and sufficient conditions for the realizability of transformerless networks, where these conditions include a synthesis procedure. We have only to add here what should be obvious, namely, that the techniques of function theory can be used to supplement those of graph theory for answering these knotty problems, and we mention one problem whose solution may give significant insight. Then we discuss positive real functions.

The problem on the RC grounded quadripole is the proving or disproving of a conjecture made by Darlington [1955]. He has stated his belief that the series-parallel network constitutes a canonical subclass for the general three-terminal RC network—that is, every second-order matrix realizable by an RC grounded quadripole may be realized in series-parallel form. Darlington has proposed the realization of the following impedance matrix to test his conjecture:

$$Z = \frac{1}{2s(s+1)} \begin{bmatrix} s^2+6s+1 & s^2-s+1 \\ s^2-s+1 & s^2+6s+1 \end{bmatrix}$$

Though this matrix satisfies all the known necessary conditions on the impedance matrix of an RC grounded network, no realization as a series-parallel

¹⁹ It should perhaps be pointed out that stability problems in this case can be treated precisely by Pontryagin's [1955] theorem. It appears that this is not known to workers in feedback control theory since a search of many of the leading books in this field reveals that complicated approximate techniques are used for determining stability.

²⁰ This suggestion was made to the writer by Prof. N. DeClaris.

structure is possible and no other type of grounded quadripole has yet been found [Olivares, 1959]. Olivares has stated his belief that the matrix is unrealizable as a three-terminal network; however the matrix is readily realizable as a symmetrical lattice.

It is inevitable that much research effort will be devoted in the future to the positive real function and the positive real matrix. The definition that is usually given [Weinberg and Slepian, 1960b] is satisfactory provided we are dealing with matrices whose elements are rational functions. However, the concept of a positive real function is important enough to be defined in general; such functions arise whenever passive systems are considered. For example, the matrices treated by Wigner and von Neumann [1954] are positive real matrices except for a trivial rotation of the axes of the complex plane. The authors show the necessary and sufficient conditions on their matrices, but these are given in a non-constructive form; in other words, no simple way of testing these matrices is given. The question arises whether tests can be devised for these matrices as was previously done for matrices of lumped-parameter electrical networks [Weinberg and Slepian, 1958; 1960b].

A general definition of a positive real function (PRF) is even needed²¹ in electrical theory, for use with distributed systems or with the limits of finite lumped systems as the number of elements increases without limit. Under such circumstances for example, the simple function \sqrt{s} should obviously be PRF; here we see that the function is real only for s real and nonnegative. Furthermore, with many transcendental functions, the definition of the function differs for s real and positive and of zero angle from s real and positive and of angle 2π . Accordingly, Professor Foster proposes that the fundamental definition of a positive real function be expressed in terms of the argument of the complex variable rather than in terms of a half-plane. The proposed definition of a PRF $F(z)$ is as follows:

- (i) $F(z)$ is an analytic function of z for $-\pi/2 < \arg z < \pi/2$
- (ii) $F(z)$ is real for $\arg z = 0$
- (iii) $\operatorname{Re}[F(z)] \geq 0$ for $-\pi/2 < \arg z < \pi/2$
- (iv) $F(z)$ to be defined by analytic continuation when possible beyond the sector in which it is defined by (i)–(iii).

Remark 1. The restriction in (i) may possibly be too strong, but at the present moment, the restriction to analyticity seems to be the only feasible assumption to make. Further study may be needed on this point.

Remark 2. If the restriction in (iii) were made stronger, that is, $\operatorname{Re}[F(z)] > 0$, the only effect would be to exclude the special case of $F(z)$ being identically

zero. From a certain point of view, this might be an advantage, since then, in quite a number of theorems, this particular case would not have to be excluded by a special statement. On the other hand, this would exclude the simple case of a short circuit (if we were talking of impedances). On the other hand, in normal mathematical procedure, we would have automatically excluded the case corresponding to $F(z)$ identically infinite. This particular impasse might perhaps be completely avoided if we defined an entirely new sort of function $W(z)$ corresponding to

$$W(z) = \frac{F(z) - 1}{F(z) + 1}.$$

This corresponds to what is accomplished by using the scattering matrix as opposed to either the short-circuit admittance matrix or open-circuit impedance matrix. More study with respect to this particular point also seems desirable.

Remark 3. Note that nothing is postulated explicitly concerning the behavior of the function on the imaginary axis. For a study of this behavior we depend entirely on analytic continuation from the sector $-\pi/2 < \arg z < \pi/2$. Also note that we do not include the suggestion of Richards that essential singularities on the imaginary axis be specifically excluded.

Remark 4. An example of a PRF:

$$F_1(z) = z^r$$

where $-1 \leq r \leq 1$. Interestingly enough, the physiologists have investigated the electrical properties of many different organic materials where the impedance over a very wide frequency range is of the form $F_1(z)$ with a constant value of r characterizing each particular kind of material, the actual numerical values somewhere in the neighborhood of -0.7 for the most part.

Remark 5. An example of a PRF with an essential singularity at the origin:

$$F_2(z) = 1 - \exp(-1/z).$$

That this function is PRF may readily be seen by noting that

$$\operatorname{Re}[F_2(x + iy)] = 1 - \exp\left(\frac{-x}{x^2 + y^2}\right) \cos \frac{y}{x^2 + y^2}.$$

Hence the positive character when x is positive.

Remark 6. Another example of PRF with an essential singularity at the origin which is not isolated, being a cluster point of poles:

$$F_3(z) = \frac{1}{1+z} + \frac{1}{2(1+2z)} + \frac{1}{4(1+4z)} + \frac{1}{8(1+8z)} + \dots$$

Here each component in the infinite series is itself a PRF, and the series is seen to be absolutely and

²¹ For the remaining discussion on positive real functions the writer is indebted to Professor R. M. Foster, who communicated these ideas in a private letter. He writes that his ideas are tentative, but the whole note is so suggestive for future research that it is used (with permission) in its entirety.

uniformly convergent in the sector $-\pi/2 < \arg z < \pi/2$ since in that sector

$$\frac{1}{N(1+Nz)} < \frac{1}{N}$$

Remark 7. An example of a PRF with all poles and zeros on the imaginary axis (i.e., i PRF to use Richards' notation [1947]:

$$F_4(z) = \tanh z.$$

That this function is PRF may readily be seen by noting that

$$\operatorname{Re}[F_4(x+iy)] = \frac{e^{4x}-1}{(e^{2x}\cos 2y+1)^2 + (e^{2x}\sin 2y)^2}$$

which is positive when x is positive.

Remark 8. An example of a PRF with a natural barrier on the imaginary axis:

$$F_5(z) = \tanh z + \frac{\tanh 2z}{2} + \frac{\tanh 4z}{4} + \frac{\tanh 8z}{8} + \dots$$

Here each component in the infinite series is itself a PRF. That the series is absolutely convergent and represents an analytic function in the sector $-\pi/2 < \arg z < \pi/2$ is seen by the following consideration:

$$\begin{aligned} |\tanh(x+iy)|^2 &= \frac{e^{4x}-2e^{2x}\cos 2y+1}{e^{4x}+2e^{2x}\cos 2y+1} \\ &\leq \frac{e^{4x}+2e^{2x}+1}{e^{4x}-2e^{2x}+1} \\ &= \operatorname{ctnh}^2 x \end{aligned}$$

and now assume that x is in the domain

$$0 < r \leq x$$

where r is some fixed positive number. Then

$$\left| \frac{\tanh N(x+iy)}{N} \right| \leq \frac{\operatorname{ctnh} Nx}{N} \leq \frac{\operatorname{ctnh} Nr}{N} \leq \frac{\operatorname{ctnh} r}{N}.$$

Thus the function is well defined.

To show the existence of a barrier, consider any value of y of the form

$$y = \frac{\pi(2m+1)}{2^{n+1}}$$

where m is any integer, positive, negative, or zero, and n is a positive integer. And then consider the term in $F_5(z)$ which is

$$\frac{\tanh Nz}{N}$$

where $N=2^n$ and for this particular value of y . The real part of this term is equal to $\frac{\operatorname{ctnh} Nx}{N}$ and becomes positively infinite as x approaches zero keeping y at this same fixed value.

It is believed that these thoughts of Professor Foster on positive real functions will stimulate future research on this important problem.

5. Systems With Time-Varying and Nonlinear Reactances²²

During the past three years networks containing nonlinear reactances have been used as amplifiers; these amplifiers have been called *parametric amplifiers*. The concept of sustained oscillations in nonlinear systems is an old one, Lord Rayleigh having described in 1877 the stability conditions for a system excited at twice the frequency of the unstable vibrations [Valdes, 1958]. Similar behavior was studied in connection with electro-mechanical systems. In addition, nonlinear reactive modulators were used in radiotelephony before 1914. It wasn't until 1957, however, that the present-day flurry of activity on parametric amplifiers started. At that time Suhl [1957] suggested using the anomalous dispersion effect in ferrites to make a variable-inductance parametric amplifier. In the succeeding three years much literature and many devices have appeared under the title of parametric amplifier. Most of the theoretical works during this period, with a few notable exceptions, are reviews, rediscoveries, and adaptations of theories already known. The device technology, however, started from zero and made startling advances. We do not discuss devices here since this will be reported on by Commission VII.

The theoretical background for parametric amplifiers can be divided into two fairly distinct categories. The first is the energy-conversion properties of nonlinear reactances, and the second is the circuit theory of linear networks with periodic time-variant parameters.

The fundamental energy-conversion property of nonlinear reactances is characterized by a set of energy relations known as the Manley-Rowe equations [1956].²³

Manley and Rowe showed that when a nonlinear capacitance imbedded in a linear fixed-parameter network is excited by sources at two frequencies ω_0 and ω_1 , the power flow $P_{m,n}$ into the capacitance at the various combination frequencies $m\omega_0 + n\omega_1$ is characterized by the equations

$$\sum_{m=1}^{\infty} \sum_{n=-\infty}^{\infty} \frac{mP_{m,n}}{m\omega_0 + n\omega_1} = 0$$

$$\sum_{m=-\infty}^{\infty} \sum_{n=1}^{\infty} \frac{nP_{m,n}}{m\omega_0 + n\omega_1} = 0.$$

²² The writer thanks Dr. B. J. Leon for his help in the preparation of this section.

²³ The so-called Manley-Rowe equations go back further than this paper. They were contained in a paper by J. M. Manley, "Some General Properties of Magnetic Amplifiers," Proc. IRE, 39, 259 (1951); this paper was based on unpublished work done by Manley much earlier, at least going back to the late 1930's.

Many subsequent papers have appeared deriving the Manley-Rowe equations in various ways. Manley and Rowe used a method of Fourier analysis. Penfield [1959] used an energy-function approach. From this he was able to extend the equations to reactive n ports with k noncommensurable exciting frequencies. Haus [1958] showed that the Manley-Rowe equations apply to the power carried by an electromagnetic field in a nonlinear lossless medium.

To see how the Manley-Rowe equations are applied to a parametric amplifier problem, let us consider the circuit of figure 2. For this circuit the powers $P_{m,n}$ are zero for $(m,n) \neq (1,0), (0,1), (1,-1)$ because the capacitance faces an open circuit at these frequencies. Thus the Manley-Rowe equations become

$$\begin{aligned} \frac{P_{1,0}}{\omega_0} + \frac{P_{1,-1}}{\omega_0 - \omega_1} &= 0 \\ -\frac{P_{1,-1}}{\omega_0 - \omega_1} + \frac{P_{0,1}}{\omega_1} &= 0. \end{aligned}$$

Since there is no source at frequency $\omega_0 - \omega_1$, $P_{1,-1}$ must be negative (flowing out of the capacitance) if at least one of the P 's is nonzero. If $\omega_0 < \omega_1$, $P_{0,1}$ is also negative and energy is converted from the frequency ω_0 to both ω_1 and $\omega_0 - \omega_1$. With this condition the "signal" at frequency ω_1 is "amplified."

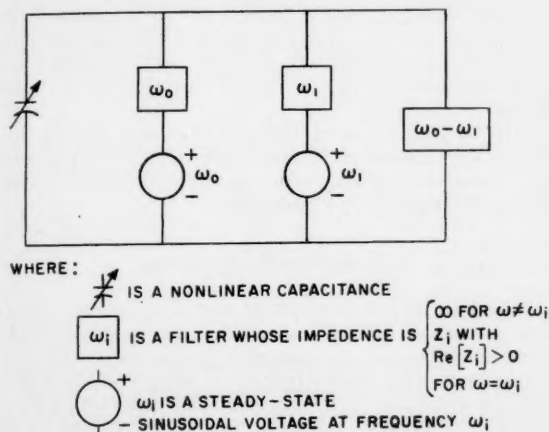


FIGURE 2. Idealized parametric amplifier.

In general the Manley-Rowe equations give an indication of feasibility for a particular amplifier with sharply tuned filters, and, in addition, they give quantitative information on the conversion efficiency. They do not give any information on the possible gain and bandwidth for a particular circuit model.

In order to get quantitative information about the performance of a parametric amplifier one must analyze a complete circuit model. No general theory exists for analyzing nonlinear circuits of the type used in parametric amplifiers. However, if the excitation at one frequency, known as the pump, is much larger than the other excitations called the

signal, a linear model characterizes this small-signal performance. The general class of circuit models which characterize the small-signal performance of parametric amplifiers are linear circuits with a few periodic time-variant parameters imbedded in a network of time-invariant parameters. The most complete proof of this statement is given by Duinker [1958]. We shall refer to networks of this type as *linear parametric networks* (LPN).

The case of linear parametric networks with limped elements (LLPN) has been studied in great detail. The time-domain equations that characterize these networks are linear differential equations with periodic coefficients. Homogeneous equations of this type have been discussed quite extensively in the mathematical literature (Starzinski, 1955; McLachlan, 1947). The techniques used on these equations are so involved that they cannot conveniently be used to obtain the general transient and steady-state solution to inhomogeneous equations. It is the latter type of equation that is of interest for the design of an amplifier. Bolle [1955] pointed out that when the excitation to an LLPN is a steady-state sinusoid, one can write down the frequencies of all the resulting currents and voltages. He discussed the case of one variable element and showed that if the element were described by a finite number of sinusoids and if the network were such that all but a finite number of the voltage and current terms were zero, then the amplitudes of the nonzero voltages and currents could be computed. Duinker [1958] extended Bolle's method to include more variable elements, but he did not eliminate the two qualifying conditions. Virtually all of the recent papers on LPN use Bolle's method [Rowe, 1958; Heffner and Wade, 1958; Seidel and Hermann, 1959].

For the case of an LLPN with a single variable element described by a finite number of sinusoids, Desoer [1959] presented a method of steady-state analysis. His method, which is exact for these circuits, consists of an algorithm for computing the amplitudes of the voltages and currents in the same manner as Bolle, but Desoer proved, in addition, that the neglected terms do not have to be zero. Desoer gave a bound for the error introduced by neglecting the higher-frequency terms, and he showed that this bound tends to zero as we increase the number of terms used.

A more general method of analysis has been presented by Leon [1959; 1960 (in press)]. He showed that the frequency-domain equations that characterize both the transient and steady-state behavior of LLPN's are linear difference equations with rational-function coefficients. The difference-equation approach yields exact computational techniques for analyzing specific circuits. It also gives formal solutions that can be discussed in general terms. Although the two papers of Leon have answered a lot of questions about the analysis of LLPN's, there are many more to be solved before a synthesis procedure for these networks can be formulated. The second paper states many of these problems in detail [Leon, in press].

For distributed LPN's Tien and Suhl [1958] showed that the approximations of Bolle's method lead to a pair of coupled equations similar to the equations for traveling-wave tubes. This has led to a number of devices of both the forward and backward traveling-wave type. For iterative LLPN's consisting of a cascade of single variable-element circuits Currie and Weglein²⁴ of the Hughes Aircraft Company have shown that Bolle's method also leads to a pair of coupled equations similar to traveling-wave tube equations. A number of other analyses of distributed LPN's has appeared [Roe and Boyd, 1959; Bell and Wade, 1959; Kurowawa and Hamasaki, 1959; Pierce, 1959; and Shafer, 1959].

The theory of LPN's is far from complete and many interesting problems exist. A bigger problem is that of obtaining a quantitative LPN approximation to a pumped nonlinear circuit. To find the model, one must analyze the nonlinear circuit with a single-frequency (pump) excitation. All solutions to date have been very approximate and apply only to very special cases.

6. Active Systems

It is well known that a passive finite lumped-parameter network can achieve all the characteristics of any stable active finite lumped-parameter network except possibly for the gain; in other words, the transfer function of the active network cannot be more complicated than a rational function. Thus figure 3 represents a possible realization of any active transfer function, where the purpose of the amplifier is merely to supply gain.

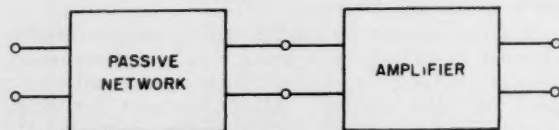


FIGURE 3. Possible form for realization of any active transfer function

It is useful to remember this fact; it saves our chasing rainbows for the proverbial pot of gold. We can add feedback loops within feedback loops almost *ad infinitum* (and often *ad nauseam*); alas, we still cannot get more than a quotient of two polynomials as the transfer function. Recognition of this fact makes us determine precisely why we are using feedback in a configuration—e.g., in the adaptive systems to be discussed below; surely not for achieving a desired transfer function that has, for example, a fast response. An open-loop configuration would do as well.

A similar simple characterization applies to an active stable driving-point function. It can always be realized by a passive driving-point function plus a negative resistance, either in series or in parallel. This is schematically illustrated in figure 4. Though

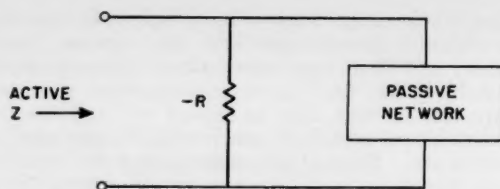


FIGURE 4. Representation of an active driving-point function.

this is not suggested as a practical means for realizing such a function, it is a feasible one.

We will not discuss systems such as those shown in figure 3, where the active element furnishes only gain (and perhaps isolation when a number of such networks are cascaded as, for example, in a flat staggered n -tuple amplifier). We will discuss two classes of active networks. In the first class the active element is used in a feedback configuration to achieve some desired result that cannot be achieved by a passive system upon which *some restriction has been placed*. Such a restriction may be the requirement of using no inductances in a network; here feedback is used as a tool in the synthesis of an RC network to achieve RLC characteristics. Another restriction can be the specification of a fixed network (called the *plant*) whose parameters vary in some manner; this network is required to yield a specified transfer function that is insensitive to the parameter variations of the fixed system. This sensitivity requirement necessitates the use of feedback; we shall discuss this in the context of the research on adaptive systems.

The second class of systems that we discuss involves negative elements that have not been achieved by a feedback circuit; more specifically, we consider networks containing tunnel diodes.

6.1. Active RC Synthesis

The use of inductances at low frequencies introduces many difficulties. Thus to achieve RLC characteristics—e.g., complex poles close to the imaginary axis—attempts have been made to use only resistances and capacitances with an active element to achieve a desired pole-zero pattern. The first active RC synthesis in the literature is due apparently to Fritzing [1938] and Scott [1938]. The principle of their method is shown by the signal-flow diagram in figure 5; this approach is now often called the classical method or the *feedback method* in distinguishing it from the approach that uses the

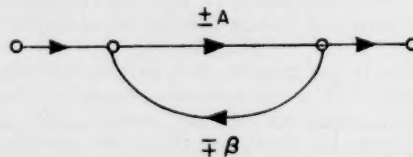


FIGURE 5. Signal-flow diagram of the classical method of active RC network design.

²⁴ A paper on these results is being prepared.

negative-impedance converter (NIC). The amplifier gain A is assumed to be a constant independent of frequency and β represents the transfer function of the RC network in the feedback path. The poles of K are the zeros of $1 + A\beta$; we can thus get complex poles that cannot be achieved with the RC network alone. The assumption of idealized properties should be noted: the active element is ideal with infinite input impedance, zero output impedance and zero reverse transmission. This field of active synthesis remained dormant for a long time—for good reasons. The passive elements, namely, the positive resistance, the positive inductance, and the positive capacitance, are rugged, long-lived and can be designed to be quite stable with respect to ambient conditions; networks containing tubes, on the contrary, are less rugged, bulkier than passive networks, and have characteristics that may deteriorate for any of a number of reasons, among them being insufficient cathode emission, the variation of an active parameter, or a change in the power-supply voltage. The concept of a negative element or a negative driving-point function is, as we've mentioned above, useful in the synthesis of active circuits. It was used by Merrill to design an NIC using vacuum tubes [1951]. This, however, possessed the disadvantages of any other vacuum-tube circuit.

The advent of the junction transistor changed this situation. It made possible a small, rugged, long-lived active package that can be used in an NIC to give the characteristics of a negative driving-point function over an operating range of frequencies. J. G. Linvill was the first to exploit the transistor in the design of an NIC [Linvill, 1953, 1954]. This brought the NIC into prominence as a tool for active network synthesis.

Linvill achieved a transfer function whose poles were not restricted to the negative real axis by the use of RC networks and an NIC. The denominator polynomial with unrestricted zeros was decomposed into the difference of two polynomials whose roots are confined to the negative real axis; the subtraction is achieved by the NIC. The zeros of the transfer function were achieved by passive networks.

Kinariwala [1959] also used the NIC to achieve RLC characteristics with RC networks. He showed how to realize any driving-point impedance by means of resistances, capacitances, and only one NIC. In his configuration the NIC could achieve the subtraction required in both the numerator and the denominator. Horowitz [1956] pursued a different course in applying the NIC: he extended the classical work of Brune, Darlington, and Dasher—i.e., synthesis by means of a cascade connection of canonical sections—to active RC synthesis. He didn't, however, solve the general problem, since he realizes only a positive real RC driving-point impedance in order to achieve an associated transfer impedance with unrestricted zeros; the network configuration is that of active RC ladders. The general problem of realizing a positive real RLC driving-point function, or even going further, a driving-point function that is not positive real, by means of a cascade of

canonical RC sections is still unsolved. In addition, Horowitz's method does not show how to realize a large gain; achieving a large constant multiplier is often an important consideration.

Horowitz [1957, 1960 (in press)] also pursued research on the classical method. Contrary to the original attacks on this problem, where as we pointed out ideal active elements were assumed, Horowitz took into account the active-element parasitics and found the limitations due to them.

6.2. Adaptive Systems

The past three years have seen a great deal of activity in plant- or process-adaptive systems. Much of the motivation appears to be due to the large and rapidly changing parameters of modern supersonic aircraft and the resulting problems imposed on the autopilot.

Nearly all workers in this field have divided up the problem into three phases:

- (1) Identification of plant or process parameters
- (2) Computation of required corrective action
- (3) Modification of system parameters or of signals to achieve corrective action.

The differences in the research have been in the methods used in one or more of these three phases. In phase (1), the following methods have been used:

- (a) correlation of noise input with plant output to obtain the plant impulse response [Anderson et al., 1958; Goodman and Hillsley, 1958];
- (b) sampling of plant input and output, and solving the difference equations relating input and output [Kalman, 1958; Mishkin and Haddad, 1959].
- (c) construction of a model of the plant and using the differences between the output of the plant and its model to vary the parameters of the model so as to minimize the differences [Margolis and Leondes, 1959].

In general the resulting systems are nonlinear and thereby difficult to analyze. Hence most of the analysis has neglected the nonlinearities. Even the linear analysis comes forth with few basic conclusions on the reasons for the adaptive systems. A critique on these adaptive systems [Horowitz, 1960] implies that there has been a singular lack of continuity between this research and fundamental feedback theory. The workers give as motivation for their work the problem of large parameter variations. Some suggest that ordinary time-invariant linear feedback is unable to cope with large parameter variations. Horowitz feels this is not true. Others suggest that ordinary feedback may be inadequate because of noise or saturation limits [Staffin and Truxal, 1958]; Horowitz feels this criticism may often be valid. It appears, however, that more analytic work is needed in this area of research.

6.3. Tunnel-Diode Networks

Except for the active RC synthesis, the field of active synthesis is largely unexplored; though some problems have been solved, there does not exist a

body of synthesis procedures comparable to that for passive networks. Some new approach is needed; it has often been felt by network theorists that the development of a pure negative resistance might stimulate such an approach. This is one reason why the discovery of the tunnel diode is exciting [Sommers et al., 1959; Lesk et al., 1959].

Much of the work on linear amplifiers using tunnel diodes has represented attempts to build a stable single-stage amplifier [Sommers et al., 1959]. According to most discussions in the literature it appears that the problems in the design of tunnel-diode amplifiers are how to achieve isolation in order to build two-stage amplifiers and how to make the tunnel diode unilateral. The writer questions whether these are the real problems. Perhaps the available synthesis procedures for passive networks can be adapted to the design of active networks.

What synthesis emphasizes is the realization of a prescribed gain-bandwidth by essentially a single process; or to be more specific, it attempts the exact realization of a prescribed function of frequency—its magnitude, its phase, and its constant multiplier. This requires a change in philosophy from that being used in present design; instead of worrying about isolating the active device, one should attempt to take advantage of its parameters in achieving a desired frequency and gain characteristic. Instead of bemoaning the fact that the tunnel diode is a two-terminal device, one should take advantage of this: our passive synthesis procedures employ two-terminal elements.

One method of adaptation of a synthesis procedure has been proposed by the writer [Weinberg, in press]. It applies to the synthesis of tunnel-diode networks, where the equivalent circuit is taken to be a parallel connection of the junction transition capacitance and a negative resistance.

This technique is an adaptation of *predistortion*. The use of the predistortion technique in reverse may be useful for realizing active networks incorporating the new devices. Instead of substituting $s=p-d$ into the given system function, we substitute $s=p+d$, where d is a positive constant, $s=\sigma+j\omega$ is the original complex variable, and p is a new complex variable.

It is recalled that in ordinary predistortion the pole of the given system function that is closest to the j axis limits the size of d that can be chosen. In reverse predistortion, however, stability considerations no longer limit the size of d , since poles of the original function, instead of moving closer to the j axis, move away from the axis. A number of other advantages are obtained by this shift of the critical frequencies to the left. For example, nonminimum-phase functions can be made minimum phase by choice of an appropriate value of d ; thus procedures that can be used only for minimum-phase functions—like Dasher's procedure for the realization of resistance-capacitance (RC) networks, or even simple ladder networks—now become applicable.

It is not true, however, that, since the shift is to the left, there are no constraints on the value of d .

As shown in [Weinberg, 1958b], for a normalized design d is the reciprocal of Q ; thus the value of the Q that can be achieved with the tunnel diode may be a limiting factor for some applications. For a negative-resistance device it is desirable that the absolute value of Q be as small as possible; for example, a small capacitance and a large absolute value of negative conductance yield a high-quality tunnel diode.

A most important effect of this procedure of reverse predistortion is that the final network, which will require negative resistances for its realization, yields what could be called a *flat gain*. This gain can be computed in a manner similar to that given in the reference [Weinberg, 1958b] for computing the flat loss.

A simple example illustrates the technique. In this example the tunnel diodes, in effect, substitute for an ideal transformer. The voltage ratio

$$K = \frac{E_2}{E_1} = \frac{H}{(s+1)(s+3)}$$

is realized by the network in figure 6 with $H=15$. The maximum possible H for a passive network without transformers is 3. Each of the RC parallel networks within the dashed lines can be replaced by a tunnel diode.

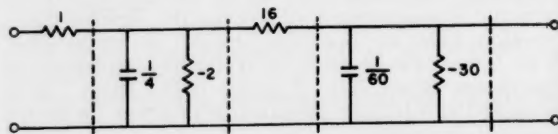


FIGURE 6. Network realizing the given RC voltage ratio. (Values in ohms and farads.)

Nonuniform predistortion can also be used to realize RLC networks containing tunnel diodes. In addition, it appears possible to control the number of tunnel diodes used in the design.

6.4. Future Research Activity

There are two approaches that have been explored in active RC synthesis using feedback techniques. One is the NIC approach exemplified by the work of Linvill [1953] and Kinariwala [1959]. Here complex poles that are unrealizable by RC networks and zeros that are inconvenient to realize by such networks are achieved by polynomial *subtraction*. The other approach, as carried forward by Horowitz [1957, 1960 (in press)], is basically the classical method; this is achieved by the *addition* of polynomials. This classification is interesting from the point of view of sensitivity. Because of the subtraction in the first approach the resulting sensitivity of the filter to the active- and passive-element variations is very large. The optimum NIC synthesis from the point of view of sensitivity to both active and passive elements was found by Horowitz [1959].

The second class of procedures leads to considerably less sensitivity to the active elements but sensitivity to passive elements is of the same order of magnitude as in the first class. While the ultimate in sensitivity in the first class has been solved,²⁵ in the second class it has been achieved only for specific configurations. Also no study has been made to determine configurations which lead to minimum sensitivity to passive-element variations. It should be mentioned, moreover, that this has not even been done in passive network synthesis.

In the matter of extending modern network synthesis to active RC systems, a significant research problem is to apply the Brune and Darlington methods to active RC realization of any input impedance by means of a cascade of canonical sections. This appears to be a very difficult problem.

With regard to active synthesis procedures using negative elements, more study should be applied to extending and applying the work of Bello [1959]. In addition, optimum tunnel-diode synthesis procedures with respect to gain-bandwidth and other criteria will probably be worked out. An inevitable problem that will arise when active synthesis becomes practicable is the sensitivity problem. Finally, it is desirable that an understanding of the deceptively simple negative resistance become more widespread; for example, one sees again and again in the literature the incorrect statement that a negative resistance cannot be both open-circuit stable and short-circuit stable.

Much basic work remains to be done in the theory of adaptive systems. Up to now the mass effort has been on building systems. This is evident from the references previously cited and a perusal of the Proceedings of the Symposium on Self Adaptive Flight Control Systems, held at Wright Air Development Center on January 13-14, 1959. To quote Lt. Gregory of the Flight Control Laboratory, Wright Air Development Center, which government organization sponsored and organized the Symposium [Gregory, 1959]: "I think there is one general statement we can make about most of our systems and that is, they work; but why do they work? In the future we intend to try to establish the basic fundamentals of why our systems work and how we can analyze them better We intend to devote more of our program to the development of the basic fundamentals." To this statement of future plans one can only say: amen. If at least a small part of government money used to support work in adaptive systems is devoted to basic research in this area, a firm analytical base will be placed under future designs.

7. Concluding Remarks

To round out our discussion of circuit theory, we make some brief comments on books, special issues of journals, and Symposia devoted to areas of circuit theory.

²⁵ H. J. Orchard in a private communication to Dr. Horowitz shows an elegant and simple method of decomposing the polynomial; this method eliminates the need of the nonlinear-equation approach used by Horowitz [1959].

Previously the student of network synthesis was forced to pick up much of his background in the field by consulting old issues of journals. This unsatisfactory situation no longer exists. The field of network synthesis has now received a wealth of documentation in book form. This will undoubtedly accelerate research in extensions of RLC synthesis techniques to active systems, to nonlinear systems, and to analogous nonelectrical systems. The driving-point problem is painstakingly treated at some length by Tuttle's book [1958], whereas Balabanian [1958] has covered both driving-point and transfer function synthesis. The book by Kuh and Pedersen [1959] attempts to introduce synthesis at the undergraduate level. These books, coupled with those of Guillemin [1957] and Storer [1957] give an adequate picture of many aspects of synthesis. At least three of the above books not only collect the significant material that could formerly be found only in technical journals, but also contain previously unpublished results or results published only as theses. Another significant event was the translation into English of Cauer's [1958] important book; this will serve as a reference and important scientific document for many years to come. It appears that there will be a continuing flow of books on the subject, now that the tap has been opened. At least two more are planned for the next year, one by Van Valkenburg [1960] and the other by Weinberg [in press]. Finally, another book that should be mentioned in this connection is the one on control systems edited by Truxal [1958]; this book contains sections on signal-flow theory, network synthesis, and sampled-data systems.

Of course, the circuit theorist will still require to read the journals in order to keep up; in fact, he will be hard put to it to keep his head above water even in his own particular area of circuit theory. The field is so fast-moving that no sooner is a new idea broached than it receives a critical comment, an extension, or a new application; an example was previously cited on Baum's introduction of the positive function and Belevitch's applying it to the realization of a Brune network. The problem of bringing circuit theorists up to date in their comprehension and application of what is now known has been a cause of some concern to the Administrative Committee of the PGCT. A number of remedies has been proposed, one of them being the sponsorship of Symposia and another being the publication of special issues of the Transactions PGCT.

Though one of the purposes of a special issue has been tutorial, most of them have in large part contained new material. The special issue on topology has already been mentioned [IRE Trans., **CT-5**, 1958b]. There have also been such issues on sequential circuits [IRE Trans., **CT-6**, 1959], active systems [IRE Trans., **CT-4**, 1957], and modern filter design techniques [IRE Trans., **CT-5**, 1958a]. Special issues are planned on the applications of electronic computers to network design and on nonlinear networks. The latter issue had Dr. B. van der Pol as Guest

Editor until his untimely death; it will be published as a memorial to the late distinguished scientist.

In the past three years the Transactions PGCT has consolidated its position as the foremost network-theory journal in the country. Under Dr. W. R. Bennett, who took over the Editor's job from Dr. W. H. Huggins, the Transactions has continued to publish the outstanding papers on the circuit-theory research that is being done in the U.S. The journal has also attracted such papers from all over the world.

The International Symposium on Circuit and Information Theory held at UCLA in June 1959, has been previously noted [IRE Trans., **CT-6**, 1959b]. In addition, an important International Symposium on the Theory of Switching was held at Harvard University on April 2-5, 1957 [Vols. XXIX and XXX, Harvard University Press, 1959]. This Symposium included three Russian papers, one of which summarizes the research on relay networks in the U.S.S.R. and gives an interesting chart comparing the numbers of articles on switching theory published in various countries [Gavrilov, 1959]. There is also a paper by Belevitch that attempts to bridge the gap between the theory of contact networks and RLC network theory by taking account of equations of current flow in contact networks [Belevitch, 1959b].

Finally, a special Transactions issue on matched (or conjugate) filters is being planned by the Professional Group on Information Theory [IRE Trans., **PGIT**, 1960]. This area appears to be one where sophisticated network design techniques are urgently needed. The TW (time-bandwidth) product for a signal or its matched filter arises in this theory; it is a most important parameter since in general a better signal requires a larger TW product. Not much has been done at the present time to realize matched filters with TW products greater than several hundred. Achieving products an order of magnitude larger by practical networks represents one of the unsolved network-theory problems. Detailed statements of the other problems in this field are given in the special issue of the Transactions PGIT.

References

- Adams, K. M., On the synthesis of three-terminal networks composed of two kinds of elements, Philips Research Rpts. **13**, 201, (1958).
- Anderson, G. W., J. A. Aseltine, A. R. Mancini and C. W. Sarture, A self-adjusting system for optimum dynamic performance, 1958 IRE Nat. Conv. Record, Pt. 4, pp. 182-190.
- Auslander, L. and M. Trent, Incidence matrices and linear graphs, J. Math. and Mech. **8**, 827 (1959).
- Bader, W., Polynomvierpole mit gegebenen Verlusten und vorgeschriebener Frequenzabhängigkeit, Arch. Elektrotech. **36**, 97 (1942).
- Balabanian, N., Network synthesis (Prentice Hall, New Jersey, 1958).
- Baum, R. F., A modification of Brune's method for narrow-band filters, IRE Trans. **CT-5**, 264 (1958a).
- Baum, R. F., Synthesis of driving point impedances with geometric symmetry, IRE Trans. **CT-5**, 359 (1958b).
- Baum, R. F., Design of unsymmetrical band-pass filters, IRE Trans. **CT-4**, 33 (1957).
- Belevitch, V., An alternative derivation of Brune's cycle, IRE Trans. **CT-6**, 389 (1959a).
- Belevitch, V., Some relations between the theory of contact networks and conventional network theory, Proc. Intern. Symp. on the Theory of Switching, Pt. II, pp. 3-12, Ann. of the Computation Lab. of Harvard Univ. **XXX** (Harvard Univ. Press, 1959b).
- Belevitch, V., Tehebyshv filters and amplifier networks, Wireless Engineer, **29**, 106 (1952).
- Bell, C. V. and G. Wade, Circuit considerations in traveling-wave parametric amplifiers, 1959 IRE Wescon Conv. Record, Pt. 2.
- Bello, P. A., Applications of linear transformation theory to the synthesis of linear active nonbilateral networks, doctorate thesis, MIT (June 1959).
- Bennett, W. R., Transmission network, U.S. Patent 1,859,656 (March 15, 1932).
- Boisvert, M., Les diagrammes de fluence de signal, Ann. Télécommun. **13**, 50 (1958).
- Bolle, A. P., Application of complex symbolism to linear variable networks, IRE Trans. **CT-2**, 32 (1955).
- Bosse, G., Siebketten ohne Dämpfungsschwankungen im Durchlassbereich (Potenzketten), Frequenz **5**, 279 (1951).
- Brannin, F. H., Jr., The relations between Kron's method and the classical methods of network analysis, 1959 IRE Wescon Conv. Record, Pt. 2, **3**, pp. 3-28.
- Bryant, P. R., Discussion on conditions for the impedance and admittance matrices of n -ports without ideal transformers, Proc. I.E.E., Pt. C, **106**, 116 (1959a).
- Bryant, P. R., Problems in electrical network theory, doctorate thesis, Univ. of Cambridge (July 1959b).
- Calabi, L., Algebraic topology of networks with application to potentiometer analog circuits, Pts. I and II, Air Force Cambridge Research Center, Air Research and Development Command, TN-56-173 and TN-56-174, Contract AF19(604)-1399 (Feb./April 1956), Parke Mathematical Labs., Concord, Mass.
- Cauer, W., Synthesis of linear communication networks, translated from the German by G. E. Knausenberger, and J. N. Warfield (McGraw-Hill Book Co., Inc., New York, N.Y., 1958).
- Cederbaum, L., Applications of matrix algebra to network theory, IRE Trans. **CT-6**, Special suppl. 127 (1959).
- Cederbaum, L., Conditions for the impedance and admittance matrices of n -ports without ideal transformers, Proc. I.E.E., Pt. C, **105**, 245 (1958); Monograph 276R (Jan. 1958).
- Coates, C. L., General topological formulas for linear network functions, Rpt. 57-RL-1746, General Electric Lab. (Aug. 1957).
- Cohn, R. M., The resistance of an electrical network, Proc. Am. Math. Soc., **1**, 316 (1950).
- Darlington, S., A survey of network realization techniques, IRE Trans. **CT-2**, 291 (1955).
- Darlington, S., Synthesis of reactance 4-poles which produce prescribed insertion loss characteristics, J. Math. Phys. **18**, 257 (1939).
- Dennis, J. B., Mathematical programming and electrical networks, Fundamental Investigations in Operations Research, MIT, Tech. Rpt. 10, (Sept. 1958) (doctorate thesis in Elec. Eng., MIT (June 1958)); also published as, Mathematical programming and electrical networks (John Wiley & Sons, New York, N.Y., 1959).
- Desoer, C. A., Notes commenting on Darlington's design procedure for networks made of uniformly dissipative coils ($d_0 + \delta$) and uniformly dissipative capacitors ($d_0 - \delta$), IRE Trans. **CT-6**, 397 (1959).
- Desoer, C. A., Steady-state transmission through a network containing a single time-varying element, IRE Trans. **CT-6**, 244 (1959).
- Doyle, W., Lossless Butterworth ladder networks operating between arbitrary resistances, J. Math. Phys. **37**, 29 (1958).
- Duffin, R. J., An analysis of the Wang algebra of networks, Trans. Am. Math. Soc. **93**, 114 (1959).
- Duinker, S., General properties of frequency converting networks, Philips Research Rpts. **13**, pp. 37-78, 101-148 (1958).
- Elias, P., A. Feinstein and C. E. Shannon, A note on the maximum flow through a network, IRE Trans. **IT-2**, 117 (1956).

- Foster, R. M., Topologic and algebraic considerations in network synthesis, BPI, Proc. Symp. on Modern Network Synthesis, pp. 8-18 (April 1952).
- Foster, R. M., Geometrical circuits of electrical networks, Trans. AIEE, **51**, 309-317, 321-328 (1932).
- Fritzinger, G., Frequency discrimination by inverse feedback, Proc. IRE **26**, 207 (1938).
- Fujisawa, T., On a problem of network topology, IRE Trans. **CT-6**, 261 (1959).
- Gavrilov, M.A., A survey of research in the theory of relay networks in the USSR, Proc. Inter. Symp. on the Theory of Switching, Pt. I, pp. 26-53, Ann. of the Computation Lab. of Harvard Univ. **XXIX** (Harvard Univ. Press, 1959).
- Geffe, P. R., A note on predistortion, IRE Trans. **CT-6**, 395 (1959) (see also Editor's Note appended to letter).
- Goodman, T. P., and R. H. Hillsley, Continuous measurement of characteristics of systems with random inputs; a step toward self-optimizing control, Am. Soc. Mech. Engrs., No. 58-IRD-5, (April 1958).
- Gould, R., Graphs and vector spaces, J. Math. Phys. **37**, 193 (1958).
- Gould, R., The application of graph theory to the synthesis of contact networks, doctorate thesis, Harvard Univ. (May 1957).
- Grayzel, A. L., A synthesis procedure for transmission line networks, IRE Trans. **CT-5**, 172 (1958).
- Green, E., Amplitude-frequency characteristics of ladder Networks, Marconi's Wireless Telegraph Co., Essex, England (1954).
- Gregory, P. C., Air Research and Development Command plans and programs, Proc. Self Adaptive Flight Control Systems Symp., WADC TR 59-49 (Jan. 13-14, 1959).
- Grossman, A. J., Synthesis of Chebyshev parameter symmetrical filters, Proc. IRE **45**, 454 (1957).
- Guillemin, E. A., An approach to the synthesis of linear networks through use of normal coordinate transformations leading to more general topological configurations, Proc. of the 1960 Intern. IRE Conv. (March 1960a).
- Guillemin, E. A., Topology and linear transformation theory in active network synthesis, Proc. of the Symp. on Active Networks and Feedback Systems (April 1960b).
- Guillemin, E. A., How to grow your own trees from given cut-set or tie-set matrices, IRE Trans. **CT-6**, Special suppl. 110 (1959).
- Guillemin, E. A., Synthesis of passive networks (John Wiley & Sons, New York, N.Y., 1957).
- Hatcher, T. R., The vertex matrix and the cut-set schedule as special cases of a more general matrix, IRE Trans. **CT-5**, 369 (1958).
- Haus, H. A., Power-flow relations in lossless nonlinear media, IRE Trans. **MTT-6**, 317 (1958).
- Heffner, H. and G. Wade, Gain-bandwidth and noise characteristics of the variable parameter amplifier, J. Appl. Phys. **29**, 1321 (1958).
- Heller, I. and C. B. Tompkins, An extension of a theorem of Dantzig's, a section in Linear inequalities and related systems, edited by H. W. Kuhn and A. W. Tucker (Princeton Univ. Press, Princeton, N.J., 1956).
- Helman, D., Chebyshev approximations for amplitude and delay with rational functions, Proc. Symp. on Modern Network Synthesis **V**, 385 BPI (April 13-15, 1955).
- Henderson, H. W., Nomographs for designing elliptic-function filters, Proc. IRE **46**, 1860 (1958).
- Henderson, K. W. and W. H. Kautz, Transient responses of conventional filters, IRE Trans. **CT-5**, 333 (1958).
- Hobbs, E. W., Topological network analysis as a computer program, IRE Trans. **CT-6**, 135 (1959).
- Hoffman, A. J. and J. B. Kruskal, Integral boundary points of convex polyhedra, a section in Linear inequalities and related systems, edited by H. W. Kuhn and A. W. Tucker (Princeton Univ. Press, 1956).
- Horowitz, I., An appraisal of a class of adaptive systems, presented at the BPI Symposium on Active Networks and Feedback Systems (April 1960).
- Horowitz, I. M., Exact design of transistor RC bandpass filters with prescribed active parameter insensitivity, accepted for publication in IRE Trans., PGCT.
- Horowitz, I. M., Optimization of negative-impedance conversion methods of active RC synthesis, IRE Trans. **CT-6**, 296 (1959).
- Horowitz, I. M., Active RC transfer function synthesis by means of cascaded RL and RC structures, 1957 IRE Wescon Conv. Record, Pt. 2.
- Horowitz, I. M., RC transistor network synthesis, Proc. Nat. Elec. Conf. **12**, 818 (1956).
- Indjoudjian, M. D., Sur certains réseaux passifs en régime transitoire, Onde Elec. pp. 441-448, 534-535 (1954).
- IRE Trans. **CT-4**, No. 3 (Sept. 1957).
- IRE Trans. **CT-5**, No. 4 (Dec. 1958a).
- IRE Trans. **CT-5**, No. 1 (March 1958b).
- IRE Trans. **CT-6**, No. 1 (March 1959a).
- IRE Trans. on Circuit Theory, Special suppl., 1959 Intern. Symp. on Circuit and Inform. Theory, **CT-6** (May 1959b).
- IRE Trans., PGIT (June 1960).
- Jewell, W. S., Optimal flow through networks, Fundamental investigations in methods of operations Research, MIT, Tech. Rpt. 8 (June 1958) (doctorate thesis in Elec. Eng., MIT (June 1958)).
- Kalman, R. E., Design of a self-optimizing control system, Trans. Am. Soc. Mech. Engrs. (Feb. 1958).
- Kaplan, W., Ordinary differential equations (Addison-Wesley Publishing Co., 1958).
- Kinariwala, B. K., Synthesis of active RC networks, Bell System Tech. J. **38**, 1269 (1959).
- Kim, W. H., Network decomposition using topological formulas, IRE Trans. **CT-5**, 373 (1958).
- Kirchhoff, G., Ueber die Auflösung der Gleichungen, auf welche man bei der Untersuchung der linearen Vertheilung Galvanischer Ströme geführt wird, Ann. Phys. Chem., **72**, 497 (1847).
- Kosowsky, D. I., High-frequency crystal filter design techniques and applications, Proc. IRE **46**, 419 (1958).
- Kuh, E. S., Synthesis of RC grounded two-ports, IRE Trans. **CT-5**, 55 (1958).
- Kuh, E. S., Synthesis of lumped parameter precision delay line, Proc. IRE **45**, 1632 (1957).
- Kuh, E. S. and A. Paige, Optimum synthesis of R.C. ladder networks, Electronics Research Lab., Ser. 60, Issue 223, Univ. of Calif. (Jan. 12, 1959).
- Kuh, E. S., and D. O. Pederson, Principles of circuit synthesis (McGraw-Hill Book Co., New York, N.Y., 1959).
- Kurowawa, K. and J. Hamasaki, Mode theory of lossless periodically distributed parametric amplifiers, IRE Trans. **MTT-7**, 360 (1959).
- Leon, B. J., A frequency domain theory for parametric networks, accepted for publication in IRE Trans., PGCT.
- Leon, B. J., A frequency domain theory of parametric amplification, Group Rept. No. 46-39, Lincoln Lab., MIT, Apr. 6, 1959 (doctorate thesis in E.E. at MIT).
- Leontief, W., On new developments in input-output analysis, presented at the Symposium on Mathematical Programming, RAND Corp. (March 16-20, 1959).
- Lesk, I. A., N. Holonyak, Jr., U. S. Davidsohn, and M. W. Aarons, Germanium and silicon tunnel diodes, 1959 IRE Wescon Conv. Record, Pt. 3, pp. 9-31.
- Levenstein, H., Theory of networks of linearly variable resistances, Proc. IRE **46**, 486 (1958).
- Lewis, P. M., II, Synthesis of sampled-signal networks, IRE Trans. **CT-5**, 74 (1958).
- Linville, J. G., Transistor negative-impedance converters, Proc. IRE **41**, 725 (1953).
- Linville, J. G., RC active filters, Proc. IRE **42**, 555 (1954).
- Löfgren, L., Irredundant and redundant boolean branch-networks, IRE Trans. **CT-6**, Special suppl. 158 (1959).
- Macnee, A. B., Synthesis of lossless networks for prescribed transfer impedances between several current sources and a single resistive load, IRE Trans. **CT-5**, 168 (1958).
- Manley, J. M. and H. E. Rowe, Some general properties of nonlinear elements—Pt. I. General energy relations, Proc. IRE **44**, 904 (1956).
- Margolis, M. and C. T. Leondes, A parameter tracking servo for adaptive control systems, 1959 IRE Wescon Conv. Record, Pt. 4, pp. 104-115.
- Mason, S., Feedback theory—further properties of signal flow graphs, Proc. IRE **44**, 920 (1956).

- Mason, S., Topological analysis of linear nonreciprocal networks, *Proc. IRE* **45**, 829 (1957).
- Mathews, J., Application of linear network analysis to Feynman diagrams, *Phys. Rev.* **113**, 381 (1959).
- Mayeda, W., Reducing computation time in the analysis of networks by digital computer, *IRE Trans. CT-6*, 136 (1959).
- Mayeda, W., The application of mathematical logic to network theory, *Interim Tech. Rpt. 9*, Elec. Eng. Research Lab., Univ. of Illinois (1958a).
- Mayeda, W., Topological formulas for active networks, *Interim Tech. Rpt. 8*, Circuit Theory Group, Elec. Eng. Research Lab., Univ. of Illinois (1958b).
- McLachlan, N. W., Theory and application of Mathieu functions (Oxford Univ. Press, Cambridge, England, 1947).
- Melvin, H. M., On concavity of resistance functions, *J. Appl. Phys.* **27**, 658 (1956).
- Merrill, J. L., Theory of the negative-impedance converter, *Bell System Tech. J.* **30**, 88 (1951).
- Mishkin, E., and R. A. Haddad, Identification and command problems in adaptive systems, 1959 IRE Wescon Conv. Record, Pt. 4, pp. 125-135.
- Nakagawa, N., On evaluation of the graph trees and the drawing point admittance, *IRE Trans. CT-5*, 122 (1958).
- Nerode, A. and H. Shank, Topological network theory, Wright Air Development Center, Tech. Rpt. 57-424 (Nov. 1957).
- Norton, E. L., Constant resistance networks with applications to filter groups, *Bell System Tech. J.* **16**, 178 (1937); first described in Filtering circuits, U.S. Patent 1,788,538 (Jan. 13, 1931).
- Olivares, J. E., Jr., Synthesis of N-port networks, doctorate thesis in Elec. Eng. Univ. of Calif. (1959).
- O'Meara, T. R., The symmetrical transfer characteristics of the narrow-bandwidth four-crystal lattice filter, *IRE Trans. CP-5*, 84 (1958a).
- O'Meara, T. R., The exact design of two types of single-crystal, wide-band crystal filters, *IRE Trans. CP-5*, 46 (1958b).
- O'Meara, T. R., On the synthesis of the crystal-capacitor lattice-filter with symmetrical insertion loss characteristics, *IRE Trans. CT-5*, 110 (1958c).
- Orchard, H. J., Formulas for ladder filters, *Wireless Engineer* **30**, 3 (1953).
- Ozaki, H. and T. Kasami, Several-variable positive real functions and their applications to variable networks (in Japanese), *J. Inst. Elec. Engrs. (Japan)* **42**, 1226 (1959).
- Papoulis, A., Optimum filters with monotonic response, *Proc. IRE* **46**, 606 (1958).
- Penfield, H., Jr., Power flow in some lossless systems, WADC Tech. Note 59-63, Wright Air Development Center (Feb. 1959); ASTIA Document AD-215, 851.
- Pierce, J. R., Use of the principles of conservation of energy and momentum in connection with the operation of wave-type parametric amplifiers, *J. Appl. Phys.* **30**, 1341 (1959).
- Pontryagin, L. S., On the zeros of some elementary transcendental functions, *Am. Math. Soc. Translations* **1**, Ser. 2, pp. 95-110, Am. Math. Soc. (1955).
- Proc. International Symposium on the Theory of Switching, Pts. I and II, Ann. of the Computation Lab. of Harvard Univ. **XXIX** and **XXX** (Harvard Univ. Press, 1959).
- Richards, P. I., A special class of functions with positive real part in a half-plane, *Duke Math. J.*, **14**, 777 (1947).
- Roe, G. M. and M. R. Boyd, Parametric energy conversion in distributed systems, *Proc. IRE* **47**, 1214 (1959).
- Rowe, H. E., Some general properties of nonlinear elements II. Small signal theory, *Proc. IRE* **46**, 850 (1958).
- Saal, R. and E. Ulbrich, On the design of filters by synthesis, *IRE Trans. CT-5*, 284 (1958).
- Scott, H. H., A new type of selective circuit and some applications, *Proc. IRE* **26**, 226 (1938).
- Seidel, H. and G. F. Hermann, Circuit aspects of parametric amplifiers 1959 IRE Wescon Conv. Record, Pt. 2, pp. 83-90.
- Seshu, S., and N. Balabanian, Transformations of positive real functions *IRE Trans. CT-4*, 306 (1957).
- Shafer, C., Noise figure for a traveling-wave parametric amplifier of the coupled-mode type, *Proc. IRE*, **47**, 2117 (1959).
- Shannon, C. E. and D. W. Hagelbarger, Concavity of resistance functions, *J. Appl. Phys.* **27**, 42 (1956).
- Simone, C. F., Equivalent ladder networks by the use of signal flow graphs, *IRE Trans. CT-6*, 75 (1959).
- Slepian, P. and L. Weinberg, Synthesis applications of paramount and dominant matrices, *Proc. Nat. Elec. Conf.* **14**, 611-630 (Oct. 12-15, 1958a).
- Slepian, P. and L. Weinberg, Necessary conditions on the matrix of an RC grounded quadripole, *IRE Trans. CT-5*, 89 (1958b).
- Sommers, H. S., Jr., K. K. N. Chang, H. Nelson, R. Steinhoff and P. Schnitzler, Tunnel diodes for low noise amplification, 1959 IRE Wescon Conv. Record, Pt. 3, pp. 3-8.
- Staffin, R. and J. G. Truxal, Executive-controlled adaptive systems, *Microwave Research Inst. Rpt. R-688-58*, BPI-616 (Sept. 9, 1958).
- Starzinski, V. M., A survey of works on the conditions of stability of the trivial solution of a system of linear differential equations with periodic coefficients, *Am. Math. Soc. Translations* **1**, Ser. 2, pp. 189-237, Am. Math. Soc. (1955).
- Stern, T. E., Piecewise-linear network theory, Research Lab. of Electronics, MIT, Tech. Rpt. 315 (June 15, 1956); (doctorate thesis, MIT, May 14, 1956).
- Storer, J. E., Passive network synthesis (McGraw-Hill Book Co., New York, N.Y., 1937).
- Suhl, H., Proposal for a ferromagnetic amplifier in the microwave range, *Phys. Rev.* **106**, 384 (1957).
- Takahasi, H., On the ladder-type filter network with Tchebysheff response (in Japanese), *J. Inst. Elec. Engrs. (Japan)*, **34** (Feb. 1951).
- Tellegen, B. D. H., Theorie der Wisselstromen (Deel III, Theorie der electrische netwerken) P. Noordhoff, N. V., Groningen, Djakarta, pp. 166-168 (1952).
- Tien, P. K. and H. Suhl, A traveling-wave ferromagnetic amplifier, *Proc. IRE* **46**, 700 (1958).
- Truxal, J. G., Control engineers' handbook (McGraw-Hill Book Co. New York, N.Y., 1958).
- Tuttle, D. F., Jr., Network synthesis (John Wiley & Sons, New York, N.Y., 1958).
- Valdes, L. B., Circuit conditions for parametric amplification, *J. Elec. Control* **5**, 129 (1958).
- Van Valkenburg, M. E., Introduction to modern network synthesis (John Wiley & Sons, New York, N.Y., 1960).
- Weinberg, L., A, B, C, D—Network design easy as pie, *Proc. Nat. Elec. Conf.*, **XIII**, 1057 (1957a).
- Weinberg, L., Tables of networks whose reflection coefficients possess alternating zeros, *IRE Trans. CT-4*, 313 (1957b).
- Weinberg, L., Explicit formulas for Tchebysheff and Butterworth ladder networks, 1957 IRE Nat. Conv. Record, Pt. 2, 200; also *J. Appl. Phys.* **28**, 1155 (1957c).
- Weinberg, L., Kirchhoff's Third and Fourth Laws, *IRE Trans. CT-5*, 21 (1958a).
- Weinberg, L., Exact ladder network design using low-Q coils, *Proc. IRE* **46**, 739 (1958b).
- Weinberg, L., Number of trees in a graph, *Proc. IRE* **46**, 1954 (1958c).
- Weinberg, L., Network analysis, *Elec. Mfg.*, **65**, 89 (1960).
- Weinberg, L., Synthesis using tunnel diodes and masers, accepted for publication in *IRE Trans.*, PGCT.
- Weinberg, L., Network analysis and synthesis (to be published by McGraw-Hill Book Co., New York, N.Y.).
- Weinberg, L. and P. Slepian, Takahasi's results on Tchebysheff and Butterworth ladder networks, *IRE Trans.*, PGCT (June 1960a).
- Weinberg, L. and P. Slepian, Positive real matrices, *J. Math. & Mech.* **9**, 71 (1960b).
- Weinberg, L. and P. Slepian, Realizability conditions on n-port networks, *IRE Trans. CT-5*, 217 (1958).
- Welsh, N. R. and E. S. Kuh, Synthesis of resistor-transmission-line networks, *Electronics Research Lab.*, Ser. 60, Issue 209, Univ. of Calif. (July 15, 1958).
- Wigner, E. P. and J. von Neumann, Significance of Loewner's theorem in the quantum theory of collisions, *Ann. of Math.* **59**, 418 (1954).
- Youla, D. C., L. J. Castriota, and H. J. Carlin, Bounded real scattering matrices and the foundations of linear passive network theory, *IRE Trans. CT-6*, 102 (1959).

Part 1. Diffraction and Scattering

L. B. Felsen and K. M. Siegel

The borderline of the diffraction and scattering field both with other fields of interest in Commission 6 and also with those of other Commissions is no longer well-defined. In order to effect a delineation, we have excluded from this report all aspects of diffraction and scattering pertaining to areas of investigation which are covered more properly under separate reports. For example, scattering from discontinuities in surface waveguides is expected to be covered in Wait's report on surface waves, while the vast area of multiple scattering and scattering by rough surfaces will be described separately by Twersky (Commission 6.3). We have also omitted any discussion of diffraction and scattering problems involving plasma media. The field of plasma physics and one of its subdivisions; namely, the transmission, scattering, and absorption of electromagnetic waves by high, low, and medium density plasmas, would appear to warrant a separate subcommission with joint membership between Commissions 3, 6, and 7. Most previous interest in plasmas has been in purely ionospheric effects and the interactions of electromagnetic waves with the ionosphere, as covered by Commission 3. However, when one considers the interaction of electromagnetic fields with plasmas caused, for example, by the motion of a high-speed vehicle through the atmosphere, problems arise which are of basic interest to the activities covered by Commission 6.3. The plasma field is growing so quickly that it would seem desirable to form at the next General Assembly a new subcommission to deal with those plasma problems of interest to several commissions.

This report will concern itself with high-frequency diffraction (involving obstacles with dimensions large compared to the wavelength), Rayleigh scattering (obstacle dimensions small compared to the wavelength), and scattering in the resonance region (obstacle dimensions comparable to the wavelength). Moreover, we mention those areas which we feel will receive attention during the next three years. The list of references appended to this report, while not presumed to be complete, is certainly representative of the current activities in the electromagnetic diffraction and scattering field in the U.S.A. through December 1959. In addition to work mentioned specifically in the body of the report we have also appended references which contain material either related to topics discussed in the text or of somewhat broader interest in diffraction theory. Additional references are to be found in recent books by Wait [1959a] and King and Wu [1959], with the latter devoted primarily to a summary of research activities in electromagnetic diffraction and scattering at Harvard University.

Primary emphasis in this report is placed on recent theoretical developments, and selected pertinent experimental results are mentioned only in conjunction with verification of certain theoretical predictions discussed in the text. The authors are well aware of the excellent experimental programs under the direction of P. Blacksmith at Air Force Cambridge Research Center, R. Kell and J. Lotsof at Cornell Aeronautical Laboratory, E. Kennaugh and L. Peters at Ohio State University, S. Silver and D. Angelakos at the University of California, Berkeley, R. King and H. Schmitt at Harvard University, and R. Hiatt at the University of Michigan. There are, of course, significant measurement programs going on at many of the major corporations. In this regard the work at Radiation Incorporated, Melbourne, Florida, should be particularly mentioned.

1. High-Frequency Diffraction

As in the preceding period, the work carried out on diffraction problems during the past 30 months can be grouped into two broad categories: (1) The solution of canonical problems, and (2) the investigation of general approximate methods of solution. By canonical problems we mean those for which exact formal mathematical solutions can be found; the asymptotic investigation of these results in the short-wavelength limit yields the rigorous asymptotic behavior of the solution. Because of the requirement of rigorous mathematical solutions, canonical problems usually involve simple configurations whose component surfaces are describable by a single coordinate in a given coordinate system.

In contrast, the aim in studying general approximate methods of solution is to provide asymptotic expressions for the scattering by objects of relatively arbitrary shape. In the limit of short wavelengths

the scattering from such objects appears to arise primarily from the vicinity of certain stationary points on its surface (at least, if the object is impenetrable). The configuration in the vicinity of these points can frequently be approximated by a canonical one, as for example, a sphere, wedge, cylinder, etc., and the total scattering can then be computed by a systematic procedure combining the effects of the various canonical contributions. Thus, a study of canonical problems is indispensable for an accurate analysis of relatively arbitrary structures. Moreover, solutions of canonical problems often provide the means for checking the results of a more general approximate procedure. It is desirable in this connection to seek an interpretation of the asymptotic solution for a canonical problem in terms of simple physically meaningful contributions, such as geometrical optics, diffraction and transition effects, with the latter arising in the vicinity of geometric optical boundaries.

1.1. Canonical Problems¹

A number of results became available during the past 30 months for the problem of diffraction by a wedge whose sides have a nonzero surface impedance. In a cylindrical coordinate representation, in terms of which this configuration is analyzed most naturally, a constant nonzero surface impedance leads to a mixed boundary condition at the wedge faces so that the usual method of separation of variables no longer applies. Following a procedure employed previously by Peters [1950] in connection with a study of water waves on a sloping beach, Senior [1959a] obtained a rigorous solution for the two-dimensional problem of diffraction by a homogeneous imperfectly conducting wedge of arbitrary angle. The method of solution is rather complicated but contains certain features which seem to indicate the feasibility of solving the wedge problem by a generalized Wiener-Hopf technique. For the special case of a right-angle wedge, Senior shows that the generally very complicated formal result reduces to a simple expression. Karp [1959a] and Karp and Karal [1958] employed an entirely different technique to solve the right-angle wedge problem for both line-source and plane-wave excitation by introducing an auxiliary problem which removes the coupling of the boundary conditions at the wedge faces. They have also employed a modification of this technique in a simple method of evaluating the diffracted far fields for a dissipative wedge with interior angle $\pi/2n$, $n=1, 2, \dots$ [Karal and Karp, 1959a]. Apart from treating the dissipative case, Karal and Karp also considered right-angle wedge configurations, one or both faces of which have a constant surface reactance which allows the propagation of a surface wave, and they have calculated the amplitude of excitation of the surface wave² [Karal and Karp, 1959a; b]. Considered in the asymptotic limit of short wavelengths, the results of Senior and Karal and Karp yield the expected decomposition of the far field into geometrical optics, diffracted (due to the presence of the edge), and, possibly surface wave contributions. The complications arising in this class of problems when an electromagnetic wave is incident obliquely have also been emphasized by the above authors [Senior, 1959b; Karal and Karp 1958].

Concerning lossless wedges, a summary of solutions for scalar steady-state and pulse excitations has been presented by Oberhettinger [1958]. Results for diffraction of pulses by a perfectly conducting wedge and by a half-plane situated on the interface between two semi-infinite dielectric media have also been obtained by Papadopoulos [1959].

As regards the numerical evaluation of the scattering from an absorbing half-plane, the formal solutions available in the literature have been suitable only for small values of surface impedance. Utilizing

previous work of Fock and Gruenberg [1944], Marcinkowski [1959] has obtained a comparatively simple far-field representation from which an evaluation for arbitrary impedance values can be carried out conveniently. He presents numerical calculations for the diffracted fields of a lossy half-plane which absorbs completely a plane wave incident at a specified angle.

Although generally mixed, the boundary conditions at the wedge faces may be uncoupled in a cylindrical coordinate representation if one chooses a surface impedance (or admittance, depending on polarization) which varies linearly with distance from the edge. This problem was solved for arbitrary wedge angles and two-dimensional excitation via the separation-of-variables technique by Felsen [1959a] who showed that if the variable impedance is reactive, the surface can support a new type of surface wave which decays exponentially away from the surface along a circular arc centered at the wedge apex. Felsen [1958] also carried out a high-frequency asymptotic evaluation of the plane wave scattering by such a wedge and found that the solution is interpretable in terms of geometrical optics and edge diffracted contributions which exhibit an explicit dependence on the rate of variation of the surface impedance. For the case where the wedge degenerates into a half-plane, Shmoys [1959] has employed a separation-of-variables analysis due to Lamb [1945] utilizing both rectangular and parabolic cylinder coordinates to obtain the solution for diffraction by a half-plane with a rather specialized impedance variation differing from the linear variation mentioned above. He has carried out an asymptotic evaluation yielding geometrical optics and diffraction effects.

Concerning diffraction by a perfectly conducting semi-infinite cone, Felsen [1959b] has obtained the expected decomposition of the rigorous far-field solution due to a radiating ring source concentric with the cone axis into geometrical optics, diffraction and transition effects. Explicit formulas are given for the geometrical optics and transition contributions, while the angular distribution of the diffracted field arising from the presence of the cone tip is represented in terms of a canonical integral (which can be evaluated approximately) [Felsen, 1957a]. Felsen [1959a] has also analyzed the two-dimensional azimuthally symmetric problem of scattering by a cone with a linearly varying surface impedance and has obtained results analogous to those described above for the similar wedge configuration.

The problem of diffraction of a scalar plane wave by a large circular aperture in an infinite plane screen was investigated by Levine and Wu [1957] via an integral equation technique. By approximating the kernel of the integral equation for the aperture in a manner which highlights the straightedge-like behavior of the aperture rim in the high-frequency limit, they solved the resulting integral equation and obtained the first few terms of an asymptotic expansion for the scattering cross section of the aperture in inverse fractional powers of ka , where k is the free-space wave number and a the aperture radius. They

¹ Although this section emphasizes the short-wavelength behavior, any formal canonical solutions apply for all wavelengths.

² The reader is also referred to their forthcoming N.Y.U., Inst. Math. Sci. Rept., Scattering of a surface wave by a discontinuity in surface reactance on a right-angled wedge.

also present a physical interpretation of the various contributions to the scattering cross section as arising from simply and multiply diffracted geometrical rays. An analogous procedure was employed by Wu and Seshadri³ for the electromagnetic problem involving a vector plane wave, and by Wu [1958] and Tang [1959] for the plane-wave and cylindrical-wave scattering, respectively, by an infinite slit.

The diffraction problems listed above give rise to asymptotic field solutions which contain geometrical optics, transition and either edge- or tip-diffraction effects. A considerable effort has also been expended on configurations which exhibit surface curvature. Suitable canonical structures in this category are the (two-dimensional) circular and elliptic cylinder and the (three-dimensional) sphere and spheroid. Emphasis has been placed on the extension and solidification of the approximate theory introduced by Fock [1946]. Wetzel,⁴ Logan,⁵ Goodrich [1958] and Wait [1959a] have reformulated the problems of diffraction by a perfectly conducting cylinder or sphere in a manner which involves directly the "canonical" functions introduced by Fock and which permits the simple asymptotic evaluation of the field on the dark side of the obstacle surface, including the transition region surrounding the light-shadow boundary. Deep in the shadow, the solution can be expressed in terms of the customary contributions from the "creeping" waves which appear to be launched at the shadow boundary, propagate along the obstacle surface into the shadow region with an exponentially decaying amplitude, and radiate energy away from the obstacle surface during their progress. In the transition region one employs the functions tabulated by Fock. Wait and Conda [1958a] have applied this technique also to formulate the scattering by imperfectly conducting cylinders and spheres and have tabulated the values of the Fock functions for this case. They treat problems with observation points situated either on the obstacle or near the light-shadow boundary off the obstacle surface. For the latter case they have exhibited a correction factor to be added to the approximate result obtained from Kirchhoff theory [Wait and Conda, 1959b]. For wave propagation between two concentric spheres, Wait [1959a] has also studied the influence of transition regions (caustics), and has calculated and plotted the correction factors to be applied to the usual geometrical optics representations in and near the caustics. The problem of the propagation around the earth of an electromagnetic pulse produced by a vertical dipole source has been analyzed by Levy and Keller [1958]. They evaluate the distortion of the pulse shape as a function of distance and material constants.

A useful technique for obtaining directly alternative representations for the solution of separable

diffraction problems is the method of characteristic Green's functions discussed by Marcuvitz [1951] and Felsen [1957b]. A refinement of this technique through the use of the Laplace transform has been carried out by Ritt [1958] and has been applied by Kazarinoff and Ritt [1959] to obtain alternative representations of the solution for the scattering of a scalar plane wave by a perfectly reflecting prolate spheroid. They have also obtained in this manner the two-dimensional Green's function for a perfectly reflecting elliptic cylinder [Ritt and Kazarinoff, 1959] and have evaluated the far field scattered in the forward direction due to an incident plane wave. The elliptic cylinder problem was also investigated via the conventional separation-of-variables technique by Levy [1958]. Upon expanding the exact solution asymptotically for small wavelengths, Levy found that the field solution on the dark side of the obstacle admits of an interpretation in terms of "creeping waves" which are launched at the shadow boundary and progress into the shadow region with an exponentially decreasing amplitude (an identical result is inferred from the solution of Kazarinoff and Ritt which corrects a different interpretation presented by Ritt [1958]). The amplitude and phase variation of the creeping waves is in agreement with that predicted by the approximate theory of Keller [1958; Keller and Levy, 1959a, c] for convex surfaces with variable curvature. Keller and Levy [1959b] have also investigated the spheroid problem and have obtained asymptotic results whose interpretation is analogous to the above. By a different procedure involving Fourier integral techniques, Clemmow [1959a] obtained integral expressions for the scattered field, and for the total scattering cross section, of a circular cylinder. Although the results obtained are not new, several novel aspects are contained in this application of Fourier techniques [Clemmow, 1959b]. Clemmow also derived an infinite Legendre integral transform defined over an infinite domain of the angular variable and has analyzed thereby the problem of diffraction by a sphere [Clemmow, 1959c].

The above-mentioned smooth objects are defined by single-coordinate surfaces in various separable coordinate systems, with surface conditions such that the associated diffraction problems can be analyzed rigorously by separation-of-variables procedures. For nonseparable configurations no comparable methods of solution are available. However, if the surface conditions on an object depart only slightly from separable ones, one can employ perturbation methods involving a small parameter which exhibits the deviation from the separable case. Such a procedure was employed by Clemmow and Weston [1959] in the approximate analysis of the plane wave scattering by a slightly noncircular, perfectly reflecting cylinder. For a sinusoidal deviation from a circular periphery, they obtained a solution to the first order in the perturbation parameter (amplitude of the deviation) and verified, from an asymptotic eval-

³ S. R. Seshadri and T. T. Wu, High-frequency diffraction of electromagnetic waves by a circular aperture in an infinite plane conducting screen, presented at URSI meeting at Penn. State Univ., Oct. 1958.

⁴ This investigation, carried out just prior to the end of the time period covered by this report, is described in detail in King and Wu (1959).

⁵ N. A. Logan, Fresnel diffraction by convex surfaces, presented at URSI meeting, Washington, D.C., May 1959.

uation of the case where the impedance varies slowly over an interval of a wavelength, that the associated creeping waves around the cylinder have a decay rate which agrees with that predicted by Keller [1958] for objects of arbitrary surface curvature. In the illuminated region the field can be constructed according to geometric optics. A perturbation method was also applied by Felsen and Marcinkowski [Felsen, 1959b] to the somewhat similar problem of diffraction by a circular cylinder with a surface impedance which varies slightly (and sinusoidally) around the periphery. A general study of diffraction by noncircular cylinders was carried out by Wu and by Wu and Seshadri.⁶

The structures considered so far have been impenetrable. Comparatively little has been done during the past 30 months on large homogeneous penetrable objects such as dielectric cylinders, spheres, etc. Work in this area has been carried out by Kodis [1959] who has studied alternative field representations for the scattering by a dielectric-coated cylinder and has obtained a formulation in terms of the perfectly conducting cylinder result plus correction terms. A somewhat greater activity has been in evidence on problems of diffraction by certain inhomogeneous structures, and by homogeneous impenetrable objects imbedded in an inhomogeneous medium. Concerning the former, Karp⁷ has obtained the (two-dimensional) solution for the reflected and transmitted waves caused by a plane wave incident nose-on on a certain curved, variable dielectric medium which occupies the region between two confocal parabolic cylinders. The variation in dielectric constant is selected so as to permit a solution by a separation-of-variables technique. Levy and Keller [1959] have analyzed the scalar problem of diffraction by a sphere with a radially varying refractive index. Flammer [1958] has calculated the electromagnetic field caused by a source at infinity in a medium whose dielectric constant varies like $1 + (c/r)$, $c = \text{constant}$, $r = \text{radial distance}$, and has obtained an asymptotic representation of the formal solution for large values of r . Diffraction by planar objects imbedded in a linearly stratified medium and by cylindrical objects imbedded in a cylindrically stratified medium was studied by Seckler and Keller [1959] who obtained asymptotic solutions by the WKB method. As expected these solutions were found to be interpretable in terms of geometrical optics and diffracted ray contributions. For a certain monotonic refractive index variation along a rectilinear coordinate, Felsen [1959c] has obtained exact solutions (and high-frequency asymptotic representations) for the diffraction of line source fields by various two-dimensional impenetrable objects including cylinders, wedges, half-planes, strips, etc. These formal solutions are obtained by showing the equivalence between a class of two-dimensional diffraction problems in a certain variable medium and a class of axially symmetric three-dimensional diffraction problems.

1.2. Approximate Theories

As predicted in the last Assembly Report, the two most actively investigated approximate theories are those due to Fock [1946] and Keller [1958]. While the theory of Fock and its extensions are concerned only with diffraction by smooth convex bodies, Keller's geometrical theory of diffraction has also been applied to objects with edge and tip singularities [Keller, 1959; Siegel, 1958] and to diffraction by objects imbedded in variable media [Seckler and Keller, 1959]. In the original formulation of his theory, Fock was concerned with the behavior of the diffracted fields near the light-shadow boundary on the surface of a smooth, convex, perfectly conducting body. His solution for the field on the dark side of the body near the light-shadow boundary involves certain functions, now called "Fock functions," which contain for their distance parameter not the actual path length from the shadow boundary on the body to the observation point, but rather the projection of that path length onto the light-shadow boundary behind the object. While the difference between these distances is small for observation points near the shadow boundary, it may be appreciable for locations of observation points deep in the shadow. Keller suggested that the correct distance parameter is the actual path length on the object as measured along the geodesic and has proposed how to calculate the amplitude and phase of a wave "creeping" along the surface of the object. Goodrich [1958] has analyzed by this modified procedure the fields diffracted into the shadow region of a perfectly conducting cone. He applied his results to the reciprocal problem of radiation into the shadow region from an infinitesimal slot on a cone, and thence to the radiation from a slot array. The good agreement between the calculated results and measurements taken at the Hughes Aircraft Company [Goodrich, et al., 1959] serves as a confirmation of the validity of the procedures of Fock and Keller⁸ for a configuration for which exact asymptotic solutions are not as yet available.

Because of its characterization of high-frequency diffraction effects in terms of various classes of geometric optical and diffracted rays, Keller's geometrical theory of diffraction highlights in a physically significant and systematic manner the mechanism of diffraction by a composite object. If the complete scattering properties of the various canonical constituents of the object, such as edges, corners, surface curvature, etc., are known (these can generally not be obtained from the geometrical theory) then the total scattered field at any point is obtained, according to Keller, by adding the contributions from the various geometric optical and diffracted rays passing through this point. The theory has been confirmed for a variety of simple canonical configurations, and also for some nonelementary structures, at least as far as the first-order contributions to the scattered

⁶ This work is described in the monograph by King and Wu (1959).

⁷ S. N. Karp, Reflection and transmission by a class of curved dielectric layers presented at URSI meeting, Washington, D.C., Apr. 1958.

⁸ Concerning diffraction by convex objects, it seems proper to credit Fock with the analysis of the transition range behavior and Keller with the formulation of the field behavior in the dark-shadow region.

field are concerned (singly diffracted ray contributions). Concerning higher order effects arising from the contributions of multiple diffracted rays, a discrepancy in some higher order terms was noted, for the case of scattering by a large circular aperture, between the scattering cross section computed by Keller [1958a] and that obtained by Levine and Wu [1957] from an asymptotic analysis based on the rigorous integral equation for the problem. This difficulty has now been resolved by Keller [Karp and Keller, 1959] through the use of a canonical solution [Buchal and Keller, 1959] for the high-frequency diffraction by a curved edge, in contrast to the single straight-edge result employed originally by Keller. However, this example would seem to demonstrate that a simple "local" analysis of diffraction problems,^{8a} while straightforward for the determination of dominant effects, must be applied with great care for the evaluation of higher order effects associated with more general configurations. Moreover, the application of a "local" analysis to scattering by objects with variable surface properties is restricted to variations which are gradual in an interval of a wavelength. For rapidly varying surface conditions, the local analysis inherent in Keller's theory must be modified and requires the solution of a new canonical problem [Felsen, 1959b; Shmoys, 1959].

As mentioned above, Keller has made some very significant extensions and systematizations of diffracted ray theory and its application to the analysis of diffraction by objects of relatively arbitrary shape, and has thereby illuminated the basic mechanism of diffraction processes. However, approximate solutions for simple composite objects have been constructed by quasi-optical techniques for some time. The treatment of diffraction by a wide slit in terms of multiple scattering from two isolated half-planes, for example, can be considered classical. More recently, Siegel [1958] has obtained by quasi-optic considerations an approximate solution for the axial plane wave back-scattering due to a finite cone. The same problem was analyzed subsequently by Keller [1959] by a purely geometric treatment. (Due to the occurrence of algebraic errors in the course of both analyses, the solutions presented by Siegel [1958] and by Keller⁹ are incorrect and differ from each other. Corrected versions of these results, in agreement, are now available [Keller, 1959; Siegel, Goodrich and Weston, 1959]^{9a}.) Karp [1959] and Karp and Zitron [1959] have employed a self-consistent field method in the analysis of the scattering by an aperture and by isolated cylinders, respectively. In this method, which can be applied to several simple obstacles or to a simple composite object, each scattering element is excited by the incident field plus the scat-

tered far fields from all the other elements. The amplitudes of the various scattered fields are then determined in a self-consistent manner. Results so obtained have been compared and agree with those available from other less direct analyses. It is also pertinent to mention in this context the work of Wu and Levine [1958] on the evaluation of the scattering cross section of a row of circular cylinders.

There is no need to dwell in detail at this time on the applications of the classical "Kirchhoff" or "physical optics" procedure to the calculation of high-frequency diffraction effects. A discussion of results obtained recently by this method was given by Siegel [1958] in a talk presented at the last General Assembly Meeting. A summary of this technique and its application to an analysis of the scattering by the tip of a perfectly conducting cone has been given by Goodrich et al. [1959]. Briefly, in the Kirchhoff procedure one assumes that the induced currents at a given point on a (perfectly conducting) body are the same as those excited on an infinite perfectly conducting plane tangent to the object at that point (i.e., the obstacle currents have a strength equal to twice that of the tangential component of the incident magnetic field). The scattered field is then computed as that arising from the radiation due to these known currents. In the asymptotic evaluation of the Kirchhoff integrals in the limit of short wavelengths, the major contribution to the scattered fields arises from certain stationary points on the object and admits an interpretation of the result in terms of geometrical optics and diffracted ray effects. The diffracted wave amplitudes computed in this manner will differ in general from those obtained by more rigorous techniques. A modification of the Kirchhoff procedure was employed recently with good results by Shkarofsky et al. [1958].

The Kirchhoff procedure can be refined by assuming in the vicinity of a stationary point not the physical optics currents but the rigorous current distribution appropriate to a canonical configuration which has the same local geometry. For example, to compute the scattering from the base of a finite cone, one can employ for the local current distribution near the curved edge the known currents for a perfectly conducting wedge. The resulting asymptotic evaluation should then yield the same result as would be obtained more directly by Keller's geometrical theory of diffraction. On the other hand, the Kirchhoff procedure can provide information about the field behavior in geometric optical transition regions which cannot be directly inferred from Keller's theory. In addition, a Kirchhoff analysis can yield approximate results for scatterer configurations whose canonical constituents have not been fully explored.

The Kirchhoff approach to determining the scattering properties of very complex shapes as, for example, of aircraft at small wavelengths, involves, in essence, a formulation in terms of physical optics currents. It is then important to use random phase

^{8a} By a "local" analysis, the field along a diffracted ray is determined by the surface properties of the scattering object "at" the point of emergence of the ray.

⁹ J. B. Keller, Diffraction by a finite cone, presented at URSI meeting Washington, D.C., Apr. 1958.

^{9a} For a detailed discussion and comparison of results, see K. M. Siegel, The resonance region, to be published in Proc. URSI XIIIth Gen. Assembly.

between the different contributors [Crispin, Goodrich, and Siegel, 1959]. This is especially true for mass-produced shapes such as aircraft and automobiles which never emerge exactly the same. For a very complicated shape like an aircraft, geometrical optics would actually be all that is required, since corrections due to edge contributions would make little change in the results.

To summarize the utility of the various approximate techniques, we note that either the Keller or Kirchhoff procedure should certainly be used in preference to simple geometrical optics for scattering problems wherein the main contributions arise from edges and corners. In these situations the geometrical optics result vanishes but the actual contribution can be quite large. When the solutions for the canonical configurations which comprise the object are available and exist in simple form, then Keller's technique is more accurate and is to be preferred over the Kirchhoff procedure. A typical example is again the finite cone. On the other hand, for problems which involve complicated shapes made up of many simple shapes, or for structures whose canonical constituents have not been investigated, the Kirchhoff procedure is more appropriate. Moreover, as pointed out before, Keller's theory does not directly yield information about the field behavior in caustic, focal, and transition regions.

Summary

Results of analyses of high-frequency scattering problems during the past 30 months involving impenetrable objects with homogeneous, or certain inhomogeneous, surface conditions have served generally to confirm the previously proposed extensions of Fock theory and also the interpretation and evaluation of diffraction phenomena via Keller's geometrical theory of diffraction, thereby strengthening the understanding of the mechanism of high-frequency scattering processes for such objects.

A number of new canonical diffraction problems have been solved. Results have been obtained for wedge-shaped surfaces whose surface impedance is constant and may have a reactive component which can support a surface wave. Other problems involve such configurations as perfectly reflecting cones, elliptic cylinders, spheroids, and imperfectly conducting cylinders and spheres. In addition to these constant impedance configurations, a variety of problems involving variable surface impedances or penetrable variable media have been treated. Asymptotic evaluations in the short-wavelength range have led to representations which can be interpreted in terms of geometrical optics, diffraction, and transition effects.

2. Rayleigh Scattering

Although no new canonical problems of diffraction at long wavelengths seem to have been solved during the past 30 months, novel integral equation

formulations for the scalar problem of diffraction by circular disks and apertures have received attention. Heins and MacCamy have treated the disk [Heins and MacCamy, 1959] while Bazer and Brown have considered the Babinet-equivalent problem of the aperture [Bazer and Brown, 1959]. Both studies depart from an integral equation formulation of Jones [1956]; the earlier work of Heins and MacCamy [1958] is also to be cited in this connection. Siegel and Senior¹⁰ have shown how higher order terms in the asymptotic expansion of the scattering amplitude for perfectly conducting bodies of certain selected shapes can be constructed at long wavelengths by an algebraic technique which is relatively straightforward. This is in contrast to other methods which require the solution of differential equations for the evaluation of higher order terms. Concerning approximate theories, Siegel [1958] discussed in some detail at the last General Assembly approximate procedures for the evaluation of diffraction effects in the Rayleigh region. One of his results implies that the scattering cross section of an axially illuminated body of revolution is independent of its detailed shape. This behavior has been verified experimentally for a finite cone by Hiatt [Brysk, Hiatt, et al., 1959]. Later Hiatt found the same scattering cross section for nose-on and rear-on illumination.¹¹ A study of the extent of the Rayleigh region in terms of the ratio of wavelength to maximum object dimensions was also carried out [Brysk, Hiatt, et al., 1959] and detailed experimental confirmation was obtained by Keys and Primich [1959].

3. The Resonance Region

Although good progress has been made recently toward the solidification of the understanding of diffraction processes in the high and low frequency ranges, many questions remain concerning the scattering in the resonance region by certain specially shaped objects whose maximum dimension is comparable to the wavelength. This is true despite the fact that for other simple shapes (such as a sphere), the inclusion of higher order quasi-optic diffraction contributions yields good agreement with exact calculation even for values of $ka \approx 1$, where k is the free-space wave number and a is the sphere radius. It is to be hoped that increased attention will be paid in the future to this interesting electromagnetic region from both the theoretical and experimental standpoints.

Concerning contributions during the past 30 months, Weston [1959] has solved exactly the problem of a pulse which is reflected by a perfectly conducting sphere. He has obtained the solution for the resonance region and has also investigated the high and low frequency behavior of the tail of

¹⁰ K. M. Siegel and T. B. A. Senior, The asymptotic expansion of electromagnetic scattering functions at long wavelengths, presented at the URSI-Toronto Symp., Univ. of Toronto, June 1959.

¹¹ R. E. Hiatt, K. M. Siegel and H. Weil, The ineffectiveness of absorbing objects illuminated by long wavelength radar, submitted to Proc. IRE.

the returned pulse as a function of sphere size and pulse length. It is found that a considerable amount of pulse lengthening can take place in the resonance region. Olte and Silver have obtained experimental results for the radar cross section of spheroids and cones in the resonance region [Olte and Silver, 1959]. The experimental work of Keys and Primich [1959] on finite cones should also be cited as well as the experimental work on cones by August and Angelakos [1957]. It might also be of interest in this connection to call attention to the recent work of Belkina [1957] on the radiation characteristics of prolate spheroids.

4. Future Activities

Concerning high-frequency scattering it appears certain that the extended theory of Fock and Keller's geometrical theory of diffraction will be applied to shapes of increased complexity. It is to be expected that the emphasis both in rigorous solutions and in the application of Keller's geometrical theory will be placed on the construction of higher order corrections (multiply diffracted ray contributions) to the asymptotic representations of the scattered field. Scattering by impenetrable objects with variable surface properties and by penetrable homogeneous or inhomogeneous objects is also likely to receive further attention.

At present, there is little evidence to expect any marked increase in activity on the study of diffraction phenomena in the Rayleigh and resonance regions, per se, although unanswered questions still remain. However, it is to be hoped that the availability of higher order diffraction contributions, as mentioned above, permitting an approach to the resonance region from the high-frequency end, will aid in the clarification of scattering phenomena in this frequency range.

One of the new problems likely to receive some attention during the next 3 years concerns the effect of model dimensions and the need for reproducing exact dimensions by precise modeling theory. Results in this area are of direct interest for electromagnetic modeling experiments for the determination of the effective mechanical tolerances required to obtain a desired scattering behavior. (The topic of surface roughness related thereto is covered separately in the report by Twersky as noted in the Introduction.) In this connection one can expect increased efforts to be devoted to the study of non-linear modeling techniques [Belyea, Low, and Siegel, 1959] which hold promise of removing some of the basic stumbling blocks associated with laboratory experiments designed on a linear modeling basis.

There is little doubt that problems involving the interaction of electromagnetic fields with anisotropic media, such as plasmas and the radiation from, or scattering by, objects embedded in a plasma medium or surrounded by a plasma sheath will receive a great deal of attention. However, as previously suggested, work in the plasma area should really be covered under a separate report.

5. References

- August, G., and D. J. Angelakos, Back scattering from cones, *Inst. Eng. Research Ser. No. 60, Issue 252, Dept. of Elec. Eng., Electron. Research Lab., Univ. Calif.* (1959).
- Bazer, J., and A. Brown, Diffraction of scalar waves by a circular aperture, *IRE Trans.* **AP-7**, S12 (1959).
- Belkina, M. G., Radiation characteristics of an elongated rotary ellipsoid; diffraction of electromagnetic waves on certain bodies of rotation, Moscow (1957).
- Belyea, J. E., R. D. Low, and K. M. Siegel, Studies in radar cross sections XXXVIII—non-linear modeling of Maxwell's equations, Rept. 2871-4-T, AFCRC-TN-60-106, Univ. Mich. Radiation Lab. (1959).
- Brysk, H., R. E. Hiatt, V. H. Weston, and K. M. Siegel, The nose-on radar cross sections of finite cones, *Can. J. Phys.* **37**, 675 (1959).
- Buchal, R. N., and J. B. Keller, Boundary layer problems in diffraction theory, Rept. EM-131, *Inst. Math. Sci., NYU* (1959).
- Clemmow, P. C., Studies in radar cross sections XXXII—on the theory of diffraction of a plane wave by a large perfectly conducting circular cylinder, Rept. 2778-3-T, Univ. Mich. Radiation Lab. (1959a).
- Clemmow, P. C., Infinite integral transforms in diffraction theory, *IRE Trans.* **AP-7**, S7 (1959).
- Clemmow, P. C., Studies in radar cross sections XXXV—on the scalar theory of diffraction of a plane wave by a large sphere, Rept. 2778-6-T, Univ. Mich. Radiation Lab. (1959c).
- Clemmow, P. C., and V. H. Weston, Studies in radar cross sections XXXVI—diffraction of a plane wave by an almost circular cylinder, Rept. 2871-3-T, AFCRC-TN-59-955, Univ. Mich. Radiation Lab. (1959).
- Crispin, J. W., Jr., R. F. Goodrich, and K. M. Siegel, A theoretical method for the calculation of the radar cross sections of aircraft and missiles, Rept. 2591-1-H, Univ. Mich. Radiation Lab. (1959).
- Felsen, L. B., Alternative field representations in regions bounded by spheres, cones and planes, *IRE Trans.* **AP-5**, 109 (1957).
- Felsen, L. B., Asymptotic expansion of the diffracted wave for a semi-infinite cone, *IRE Trans.* **AP-5** (1957a).
- Felsen, L. B., Electromagnetic properties of wedge and cone surfaces with a linearly varying surface impedance, *IRE Trans.* **AP-7**, S231 (1959).
- Felsen, L. B., Some aspects of diffraction by variable impedance and anisotropic structures, Final Rept. R-685-58, PIB-613, Sect. IIIA (1958).
- Felsen, L. B., Radiation from ring sources in the presence of a semi-infinite cone, *IRE Trans.* **AP-7**, 168 (1959b).
- Felsen, L. B., Diffraction by objects in a certain variable plasma medium, Polytech. Inst. Brooklyn, Microw. Research Inst., Electrophys. Group Memo No. 55 (July 1959c).
- Flammer C., Electromagnetic wave propagation in a medium with variable dielectric constant $1 + Kr^{-1}$, Tech. Rept. **63**, Stanford Research Inst. (1958).
- Fock, V. A., On certain integral equations in mathematical physics, *Mat. Sbornik*, **14**, 3-48 (1944) (in Russian).
- Fock, V. A., The field of a plane wave near the surface of a conducting body, *J. Phys. (USSR)* **10**, 399 (1946).
- Goodrich, R. F., Studies in radar cross sections XXVI—Fock theory, *IRE Trans.* **AP-7**, S28 (1959).
- Goodrich, R. F., R. E. Kleinman, A. F. Maffett, C. E. Schensted, K. M. Siegel, M. G. Chernin, H. E. Shanks, and R. E. Plummer, Radiation from slot arrays on cones, *IRE Trans.* **AP-7**, 213 (1959).
- Heins, A. E., and R. C. MacCamy, Axially symmetric solutions of elliptic differential equations, Tech. Rept. 41, Carnegie Inst. Technol., prepared under contract DA-36-061-ORD-490 (1958).

- Heins, A. E., and R. C. MacCamy, On the scattering of waves by a disk, Tech. Rept. **43**, Carnegie Inst. Technol., prepared under contract DA-36-061-ORD-490 (June 1959).
- Jones, D. S., A new method for calculating scattering, with particular reference to the circular disk, Comm. Pure Appl. Math. **9**, 713 (1956).
- Karal, F. C., and S. N. Karp, Diffraction of a skew plane electromagnetic wave by an absorbing right-angle wedge, Research Rept. EM-111, Inst. Math. Sci., NYU (1958).
- Karal, F. C., and S. N. Karp, A new method for the determination of far fields with applications to the problem of radiation of a line source at the tip of an absorbing wedge, IRE Trans. **AP-7**, S91 (1959a).
- Karal, F. C., and S. N. Karp, Diffraction of a plane wave by a right-angled wedge which sustains surface waves on one face, Research Rept. EM-123, Inst. Math. Sci., NYU (1959b).
- Karp, S. N., Two-dimensional Green's function for a right-angled wedge under an impedance boundary condition, Research Rept. EM-129, Inst. Math. Sci., NYU (1959a).
- Karp, S. N., and J. B. Keller, Multiple diffraction by an aperture in a hard screen, Rept. EM-143, Inst. Math. Sci., NYU (1959).
- Karp, S. N., and N. Zitron, Higher-order approximations in multiple scattering I (Two-dimensional scalar case), II (Three-dimensional scalar case), Rept. EM-126, Inst. Math. Sci., NYU (1959).
- Kazarinoff, N. D., and R. K. Ritt, On the theory of scalar diffraction and its application to the prolate spheroid, Ann. Phys., **6**, 277 (1959).
- Keller, J. B., A geometrical theory of diffraction, Calculus of variations and its applications, Proc., Symp. on Appl. Math., **8**, 27-52 (McGraw-Hill Book Co., Inc., New York, N.Y., 1958).
- Keller, J. B., Diffraction by an aperture, J. Appl. Phys. **28**, (1957). Also, J. Appl. Phys. **29**, 744 (1958a).
- Keller, J. B., Back-scattering from a finite cone, Rept. EM-127, Inst. Math. Sci., NYU (1959).
- Keller, J. B., and B. Levy, Diffraction by a smooth object, Commun. Pure and Appl. Math. **12**, (1959a).
- Keller, J. B., and B. Levy, Diffraction by a spheroid, Rept. EM-130, Inst. Math. Sci., NYU (1959b).
- Keller, J. B., and B. Levy, Decay exponents and diffraction coefficients for surface waves on surfaces of nonconstant curvature, IRE Trans. **AP-7**, S52 (1959c).
- Keys, J. E., and R. I. Primich, The nose-on radar cross sections of conducting, right circular cones, Can. J. Phys. **37** (1959).
- King, R. W. P., and T. T. Wu, The scattering and diffraction of waves, (Harvard University Press, Cambridge, Mass., 1959).
- Kodis, R. D., Back-scattering at high frequencies from a conducting cylinder with dielectric sleeve, IRE Trans. **AP-7**, S468 (1959).
- Lamb, H., Hydrodynamics, 538-541 (Dover Publications, New York, N.Y., 1945).
- Levine, H., and T. T. Wu, Diffraction by an aperture at high frequencies, Rept. 71, Appl. Math. and Stat. Lab., Stanford Univ. (1957).
- Levy, B., Diffraction by an elliptic cylinder, Rept. EM-121, Inst. Math. Sci., NYU (1958).
- Levy, B., and J. B. Keller, Diffraction of electromagnetic pulses around the earth, IRE Trans. **AP-6** (1958).
- Levy, B., and J. B. Keller, Diffraction by an inhomogeneous sphere, presented at the URSI-Toronto Symp., Univ. Toronto (June 1959).
- Marcinkowski, C. J., Diffraction by an absorbing half-plane, Rept. R-750-59, Polytech. Inst. of Brooklyn, Microw. Research Inst. (1959).
- Marcuvitz, N., Field representations in spherically stratified regions, Proc., New York Univ. Symp. on theory of electromagnetic waves, June 6-8, 1950 (Interscience Publishers, Inc., New York, N.Y., 1951).
- Oberhettinger, F., On the diffraction and reflection of waves and pulses by wedges and corners, J. Research NBS **61**, 343 (1958) RP2906.
- Olte, A., and S. Silver, New results in backscattering from cones and spheroids, IRE Trans. **AP-7**, S61 (1959).
- Papadopoulos, V. M., Diffraction and refraction of plane electromagnetic pulses, IRE Trans. **AP-7**, S78 (1959).
- Peters, A. S., The effect of a floating mat on water waves, Comm. on Pure and Appl. Math. **3**, 319 (1950).
- Ritt, R. K., Studies in radar cross sections XXX—The theory of scalar diffraction with application to the prolate spheroid (App. by N. D. Kazarinoff), Rept. 2591-4-T, AFRCR-TN-58-531, AD 160791, the Univ. Mich. Radiation Lab. (1958) and Ann. Phys. **6**, 227 (1959).
- Ritt, R. K., and N. D. Kazarinoff, Scalar diffraction by an elliptic cylinder, IRE Trans. **AP-7**, S21 (1959).
- Rumsey, V. H., Some new forms of Huygen's principle, IRE Trans. **AP-7**, S103 (1959).
- Seckler, B. D., and J. B. Keller, The geometrical theory of diffraction in inhomogeneous media, J. Acoust. Soc. Am., **31** (1959); The asymptotic theory of diffraction in inhomogeneous media, J. Acoust. Soc. Am. **31** (1959).
- Senior, T. B. A., Diffraction by an imperfectly conducting wedge, Commun. Pure and Appl. Math. **12**, 337 (1959a).
- Senior, T. B. A., Diffraction by an imperfectly conducting half-plane at oblique incidence, Appl. Sci. Research **8**, Sec. B, (1959b).
- Shkarofsky, L. P., H. E. J. Neugebauer, and P. M. Bachynski, Effects of mountains with smooth crests on wave propagation, IRE Trans. **AP-6**, (1958).
- Shmoys, J., Diffraction by a half plane with a special impedance variation, IRE Trans. **AP-7**, S88 (1959).
- Siegel, K. M., Far field scattering from bodies of revolution, Appl. Sci. Research **7**, Sec. B, 293 (1958).
- Siegel, K. M., R. F. Goodrich, and V. H. Weston, Comments on far field scattering from bodies of revolution, Appl. Sci. Research **8**, Sec. B, 8 (1959).
- Tang, C. L., High-frequency diffraction of cylindrical waves by an infinite slit in a plane screen, Rept. 297, Cruft Lab., Harvard Univ. (1959).
- Wait, J. R., and A. M. Conda, Pattern of an antenna on a curved glossy surface, IRE Trans. **AP-6**, (1958a).
- Wait, J. R., Diffractive corrections to the geometrical optics of low-frequency propagation, Proc., Symp. on Propagation of Radio Waves, Liège, Belgium, (Academic Press, Inc., London, England, 1958b).
- Wait, J. R., Electromagnetic radiation from cylindrical structures (Pergamon Press Inc., New York, N.Y., 1959a).
- Wait, J. R., and A. M. Conda, Diffraction of electromagnetic waves by smooth obstacles for grazing angles, J. Research NBS **63D**, 181 (1959b).
- Weston, V. H., Studies in radar cross sections XXXIII—Exact near-field and far-field solution for the back scattering of a pulse from a perfectly conducting sphere, Rept. 2778-4-T, Univ. Mich. Radiation Lab. (1959) and IRE Trans. **AP-7**, S43 (1959).
- Wu, T. T., High-frequency diffraction by an infinite slit, Rept. 281, Cruft Lab., Harvard Univ. (1958).
- Wu, T. T., and H. Levine, The scattering cross section of a row of circular cylinders, Rept. 73, Dept. of Math., Stanford Univ. (1958).

(Additional references are given on page 750.)

Part 2. On Multiple Scattering of Waves

V. Twersky¹

1. Purpose

The purpose of this report is to survey some of the recent analytical work on scattering of waves by many objects. It attempts to cover certain aspects of scattering by fixed configurations and by random distributions which have been dealt with in the U.S. literature in classical physics, applied mathematics, engineering, and chemistry. General analytical procedures and treatments based on distinct scatterers (as opposed to those dealing with perturbed continuous media) are emphasized.

Inasmuch as no analogous previous reports on multiple scattering are available, the literature survey is prefaced by (and interlarded with) background and introductory material intended to indicate the roots of current activity, to introduce special terms, and to delineate the restricted viewpoint and coverage of this report. This last consideration is an essential one since the survey is quite limited: no attempt is made to cover the large number of physical phenomena which involve multiple scattering (or even to list the larger number of labels by which they are referenced in the literature) or to discuss the variety of analytical and heuristic procedures used in their treatment.

2. General Considerations

The essential features of a scattering problem are the effects arising when a given obstacle, or collection of obstacles, is placed in the path of a specified wave. We assume that we are dealing with a source whose field "when isolated" is known, and seek the redistribution of radiation arising from the presence of obstacles. Physically speaking, in electromagnetics, the "primary wave" induces charges and currents in the obstacles, and these in turn give rise to the "secondary waves" that constitute the "scattered field."

If we restrict consideration to continuous wave excitation and fixed scatterers whose location, orientation, etc. are not affected by the applied field, then we formulate the problem analytically as seeking a solution of appropriate wave equations, subject to prescribed boundary conditions at the objects, and subject to conditions at large distances from the region containing the objects. The wave equations describe local properties of the media in question; the boundary conditions take account of the physical characteristics, shapes, and sizes of the objects; and the conditions at infinity specify the forms of both incident and scattered components of the solution. We may be interested in the field arising from a particular object, or from some configuration of

objects of specified shapes, etc., or in the average field and energy flux to be expected for some statistical distribution of configurations, shapes, etc.

The "single body" wave problem as it is usually formulated corresponds to the limiting case of a practical situation involving one source of radiation and one fixed obstacle, such that the effects of the scattered radiation on the source, extraneous reflections from other objects in the environment, etc., have been minimized. In general, such simple limiting cases lead to unsolvable integral equations. In a few special cases, for which the surface of a homogeneous scatterer coincides with one or more complete coordinate surfaces in one of the systems in which the wave equations are separable, solutions are obtained as infinite series of more or less tabulated special functions. Simple closed-form solutions in terms of elementary functions are rarer still. However, through analytical approximations valid for restricted values of the parameters, and through heuristic procedures motivated by the insight obtained in more elementary problems, one can now obtain explicit results which are adequate to describe many principal phenomena of physical interest. Although this subject is far from closed,² it is convenient in considering multiple scattering, to assume that solutions for the component scatterers when isolated are known, and that they may be regarded as "parameters" in the more general problem.

Thus one seeks representations for scattering by many objects in which the effects of the component scatterers are "separated" from the effects of the particular configuration (or statistical distribution of configurations) in the sense that the forms of the results are to hold independently of the type of scatterers involved. Of course, such representations can usually be obtained in the range of parameters where a single scattering approximation is valid, i.e., in which the results for a distribution of identical scatterers reduce to that for an isolated object times an "array factor". We discount this range from the start, and seek in general a functional relation for the many-body solution in terms of a single-body function. Thus if one can treat a particular spatial configuration (or statistical distribution of configurations) explicitly, and independently of the component scatterers, then the results for specific isolated objects, for particular ranges of the parameters, etc., can be inserted for detailed applications.

The above, in first regarding the single-body problem as a limiting case of that of many bodies, and then regarding the distribution as composed of objects whose solutions when isolated are known, has emphasized the view to be taken in the following.

¹ Sylvania Electronic Defense Laboratories, Mountain View, Calif.

² Recent activity on scattering by isolated objects is surveyed by L. B. Felsen and K. M. Siegel in a companion report to URSI.

Related treatments of distributions of distinct objects start essentially with Poisson's [1821; 1823] molecular model of magnetic induction, and its application to dielectrics by Faraday [1839], Kelvin [1845], Mossotti [1847], and Clausius [1897]; the work of Maxwell [1873a] on the "bulk resistivity" (essentially the reciprocal of the dielectric constant) of a distribution of resistive spheres in a medium of different resistivity, and on the permeability of a distribution of perfectly conducting spheres [Maxwell, 1873b]; the work of Lorentz [1880] and Lorenz [1880] on the index of refraction; and Rayleigh's [1892] investigation of scattering by rectangular arrays of parallel cylinders and spheres. These treatments were restricted to low frequencies, special scatterers, and limiting distributions; they range analytically from the intuitive development of Faraday to Rayleigh's detailed analysis of "packing effects" in terms of the ratio of scatterer size and spacing.

More generally, a formal representation for the solution of any given configuration of arbitrary scatterers (a configuration specified by a set of position vectors to reference points on the objects, and the scatterers specified by their shapes and boundary conditions) may be obtained as follows: We apply Green's theorem to the free-space Green's function and to the required unknown solution in the region external to all scatterers, and thereby represent the scattered field as an integral over some surface inclosing the region. Contracting the surface and breaking it up into individual portions inclosing a single object, leads to a representation of the total scattered field as a sum of surface integrals; it is the terms of this sum (the integrals over the surfaces of the individual scatterers) that we identify as the "elementary scattered waves". Then imposing the boundary conditions at each object leads to a determinate set of coupled integral equations for the fields on all scatterers, and could these values be obtained explicitly, the total field in space would follow on integration.

This analytical procedure, or similar ones applicable for relatively arbitrary scatterers, was used both for general considerations and specific applications by Ekstein [1951; 1953], Ignatowsky [1914a], Karp [1953], Lax [1952], Millar [1960], Row [1955], Storer and Sevic [1954], and Twersky [1956a, 1957a, 1958a, 1959a, 1959b]. An analogous procedure leading to sets of algebraic equations for the separable problems of arbitrary configurations of circular cylinders was used by Zavisla [1913], Ignatowsky [1914a], Row [1955], and Twersky [1953a, 1953b, 1954]; similarly Kasterin's [1897] formalism for the scalar problem of a periodic array of spheres holds for all wavelengths and for any of the usual boundary conditions. Thus, for example, for circular cylinders and homogeneous boundary conditions, the Green's functions procedure yields N coupled integral equations for the surface fields (or for their normal derivatives, or for linear combinations of fields and derivatives); equivalently, separation of variables yields an N fold infinite set of algebraic equations for the scattering coefficients.

There are essentially three different analytical procedures which may be used to obtain a representation taking into account the effects of multiple scattering, or the coupling of the radiation fields of the objects: One may seek to solve the boundary value problem for the "compound body"; one may use a self-consistent procedure based on the known response of the isolated elements (the single-scattered results) such that each object is considered as excited by the primary wave plus the resultant of the initially unknown total scattered fields of the other objects; or one may use an iterative procedure corresponding to the "successive scatterings" of the primary field. In the successive scattering approach, which is essentially an iterated form of the self-consistent one, each object is initially regarded as excited solely by the primary field and radiating in consequence its "first order of scattering"; next in response to the sum of the first orders of the others, each scatters its "second order," etc. The second and third methods differ essentially from the first in that they isolate the single-body solutions implicit in the problem. Thus they enable us to exploit known single-body results, or to seek them independently of the configuration (either analytically, or by direct measurement).

The class of many-body problems for which one may obtain a solution for the compound body is small; it comprises periodic arrays whose essential parameter is a simple sinusoid (e.g., the sinusoidal profile of a reflection grating treated by Rayleigh [1907a], or the sinusoidal refractive index of a medium considered by Bragg [1915] and Laue [1931]). More generally, however, one must consider "multiple scattering" by an infinite set of such sinusoids, i.e., by the components of the complete "spectral representation" (Fourier series or Fourier integral) of the appropriate parameters of the collection of scatterers. Thus, for example, Rayleigh [1907a] represented the grating of arbitrary periodic profile as a Fourier series; Laue [1931] represented the crystal of arbitrary periodic index as a "triple" Fourier series; Rice [1951] represented the randomly perturbed planar rough surface as a double Fourier integral; and Hoffman [1959] represented a medium whose index was a slowly varying random function of position by a triple integral. The Fourier representations treat the spectral components of the parameters of the distribution as the "individual scatterers"; they lead to rapidly convergent approximations for values of the parameters such that the field arises essentially from one sinusoid (e.g., Bragg reflections in a crystal), or when the parameters are only slightly perturbed from those of a uniform region (e.g., slightly rough plane).

A large variety of heuristic, self-consistent procedures (starting with those of Mossotti [1847], Clausius [1897], and Maxwell [1873]) have been applied to determine the macroscopic parameters of the coherent field for distributions of scatterers. Analytical self-consistent procedures for periodic structures are illustrated by Rayleigh's [1892] work on lattices of cylinders and spheres, Ignatowsky's

[1914a] treatment of the grating of arbitrary cylinders, and Ewald's [1917] analysis of the lattice of dipoles. Analogous procedures to treat the coherent field in sparse random distributions were used by Born [1933] for dipoles, and by Foldy [1947] for monopoles; dense distributions of dipoles were treated by Brown [1950] (static case) and by Mazur and Mandel [1956].

The successive orders of scattering approach (discussed by Heaviside [1893]) was used by Reiche [1916] (who also gave a self-consistent treatment) to derive the coherent field for a slab region of randomly distributed dipoles. Twersky [1950a] obtained a criterion for the range of validity of Schaefer and Reiche's [1911] single-scattering treatment of the grating of circular cylinders, and constructed a series solution for an arbitrary configuration, and series and closed form approximations for two cylinders and gratings [Twersky, 1952a, 1952b, 1952c]. Similarly Yvon [1937, 1935], Kirkwood [1936], and Jansen and Mazur [1955] averaged the scattering series for dipoles to treat the dielectric constants of dense gases.

The papers mentioned above serve to illustrate approaches for treating many-body scattering problems. Additional work will be cited in the sections on particular configurations. Thus we reserve discussion of essentially particle scattering procedures based on transport equations until the topic of "incoherent scattering" arises in its appropriate context.

The above also serves to indicate the main lines we follow. Thus we do not consider "multiple scattering treatments of single-body problems" in the following sections. However, since we mentioned single-body treatments of many scatterers, it may be appropriate to sketch the "inverse" situation. Thus a finite scatterer with sharp edges may be treated by exploiting Sommerfeld's and Macdonald's solution for the field on the semi-infinite wedge. For example, an infinite cylinder having a triangular cross section with sides large compared to wavelength may be regarded as a collection of three "infinite wedge edges" plus specularly reflecting planes. As a first approximation, each of the three edges may be treated as excited solely by the plane wave; then the "coupling effects" of the "single scattered edge waves" on each other may be developed in terms of higher order scattering processes (by regarding each edge as excited by the asymptotic forms of the waves leaving the other two in response to the primary excitation, etc.). More directly, the infinite wedge result may be used in a self-consistent procedure which treats each edge of the finite wedge as excited by the incident wave and by two cylindrical edge waves of initially unknown amplitude. The solution for the degenerate case of the wedge of zero angle (i.e., the half-plane) was first used by Schwartzchild [1902] to construct the series solution and a single scattering approximation for a wide aperture in an infinite plane screen, and higher order scattering of the edge waves was recently treated by Clemmow [1956], Karp and Russek [1956], and Keller [1958, 1957]. Similarly, Braunbek, Clemmow, Kel-

ler, and Levine treated the wide circular aperture by assuming that the edge field was approximately that on a half-plane locally coincident with the edge of the aperture, and Keller, and Siegel used the infinite wedge result to approximate the local field on the curved edge of the base of a finite cone; these treatments range from "single scattering" approximations, to Keller's detailed consideration of the "multiple scattered" edge rays. (References to these papers, and to analogous treatments of scattering by isolated objects are given in Felsen's and Siegel's URSI report, *Diffraction and Scattering*.)

Breakdown of the Many-Body Problems

In the preceding paragraphs, we more or less jumped into the literature in order to associate this general topic with such familiar names as Poisson, Faraday, Maxwell, Rayleigh, Lorentz, etc. Then, papers were cited to illustrate different procedures for taking into account the effects of multiple scattering. Since a representative selection of methods was insured at the expense of a systematic presentation of problems having physical interest, we now mention classes of problems; citations to the literature are reserved for the following sections.

We distinguish two categories of multiple scattering problems: In one, we deal with a fixed configuration; and in the other, with a statistical ensemble, or distribution of configurations. This breakdown is primarily for convenience; it serves to single out the well-defined boundary value problems of several scatterers, as well as the periodic structures for which a large variety of special analytical techniques are available. However, subsequently, we regard the fixed configuration as a limiting case of a general distribution.

Fixed configurations: Several two-body situations, general collections of N -bodies, and periodic arrays, have been treated in some detail. Explicit solutions for N -bodies have been derived for planar scatterers (e.g., infinite slabs, discontinuities on transmission lines, etc.). Explicit approximations (series and closed forms) have been obtained for completely bounded scatterers in ranges where, (1) the wavelength is large compared to the scatterer's size, and the spacing is arbitrary, and (2) for arbitrary bodies and spacing large compared to wavelength; here the literature ranges from meson-deuteron scattering in quantum mechanics to coupling effects between transmitting antennas and scatterers arising in "single body" microwave measurements.

The literature of scattering by periodic arrays covers diffraction gratings, planar lattices, dielectric constants, indices of refraction, crystal analysis, "artificial dielectrics", obstacles in rectangular waveguides, as well as the analogous antenna arrays. Single periodic layers, gratings, etc., are of interest in connection with their use as spectrum analyzers, polarizers, open-mesh reflectors, etc.; and the analysis of scattering by three-dimensional arrays facilitates studies ranging from the exploration of crystal structure by X-rays to the design of practical microwave components.

In general, the field of an infinite periodic structure consists of an infinite number of discrete plane waves; some are propagating (e.g., the usual spectral orders of a grating), and the rest are exponentially damped normal to the face planes. Analytically, one seeks to relate the amplitudes of the propagating modes of the transmitted and reflected fields to the spacings of the array, and to the single scattering characteristics of its elements. (The Fraunhofer form for a finite array is more or less a "blurred" version of the set of propagating modes.)

To a large extent, the general problems of three dimensional periodic arrays hinge on the solution for a single planar lattice; once the results for the isolated component planes are known, one can use difference equations, matrix algebra, group theoretic procedures, and other equivalent "multimode transmission line" approaches to treat the crystal. Because of this (as well as because of its intrinsic interest) the planar lattice has merited special consideration. Special attention has also been given to the essentially one-propagating-mode situations which arise when the spacings parallel to the face planes are small compared to wavelength (artificial dielectrics, obstacles in waveguides), or when the Bragg conditions are fulfilled.

Statistical distributions: The other large class of many-body problems deals with statistical distributions of scatterers. Such problems are basic in the use of scattering and propagation measurements as a diagnostic tool in discovering the fundamental properties of matter, and in various practical problems related to the transmission of information via radiation. The special distribution corresponding (more or less) to that of an "ideal gas" of elastic objects has received most extensive consideration, and some progress has been made in treating the "packing effects" in "dense gasses" and "liquid state" distributions.

The previously mentioned formal representation for the field scattered by an arbitrary fixed configuration may be applied to treat scattering by statistical distributions. One introduces an ensemble of configurations defined by an appropriate distribution function (giving the probability of occurrence of the component configurations) and seeks the expectation value of the field by averaging over all variables (positions of scatterers, scatterer sizes, etc.). One may attempt to first solve or approximate the original integral equations (e.g., by an iterative procedure), and then introduce the "statistics"; or one may average the formal solution for a single configuration over the specified ensemble, and then attempt to solve the resultant set of equations. Similarly one averages the corresponding representations for the power density (and energy flux) over the ensemble, and obtains equations for the "coherent component" (essentially the absolute square of the average wave function), and for the "incoherent" or fluctuation scattering. Although not even the simplest of such problems has been treated rigorously by these procedures, useful approximations have been obtained for various ranges of parameters. (See

Foldy's [1947] basic paper for a detailed introduction, and for a discussion of the relevance of such averages to quantities obtained by measurement.)

We may regard the periodic configuration and the ideal gas, as special cases of a general "liquid state" distribution. Thus in terms of appropriate distribution functions we may start with the limiting case of an ideal gas, and introduce "local order" in the distribution of a scatterer's neighbors to model some of the characteristics of dense gases and liquids of elastic particles. Proceeding to the limit of an appropriate parameter (essentially "compressing" the distribution) yields results corresponding to a periodic array.

The intensity pattern for the liquid lies "between" those of a gas and crystal. If we visualize a narrow beam incident on a slab region of a distribution of identical objects, then for the gas case we obtain coherent transmitted and reflected beams and a "background" of incoherent scattering (more or less resembling the single-scattered intensity pattern of a component object). As the ratio of average to minimum separation of scatterers is decreased (a minimum in general greater than the scatterer's size, and, say, of the order of several wavelengths) and the liquid state approached, the incoherent scattering becomes peaked at angles in the vicinity of those corresponding to the propagating modes of the periodic limit. With increasing local order, these additional "beams" becomes better defined, and finally go over to the propagating modes of the appropriate crystal.

Alternatively, instead of dealing with ensemble averages of configurations of distinct scatterers, one may seek to model statistically inhomogeneous regions by means of an appropriately perturbed continuum. Approximations for the coherent field may be specified in terms of the index of refraction, and corresponding approximations for the intensity depend on the autocorrelation of the values of the index at two different points. Representative papers are cited in subsequent sections.

3. Survey

3.1. Fixed Configurations of N Scatterers

The static limits for two parallel circular cylinders, a grating of N parallel cylinders, two parallel coplanar strips, and two spheres, are conveniently found in Wendt's [1958] recent review article. He has many references to the recent literature, and a bibliography of texts going back to Maxwell's. Other static problems of interest include Maxwell's [1873c] treatments of stratified conductors (N slabs with characteristics alternating as ABAB . . .), and composite dielectrics (N slabs ABC . . .).

Silver [1949] discusses coupling between transmitter and receiver antennas from a multiple scattering point of view. King [1956] treats a variety of problems involving coupling between two linear antennas (parallel, colinear, perpendicular),

between N parallel linear antennas, between three parallel antennas at the vertices of an equilateral triangle, between four at the corners of a square, etc.

Redheffer gives the solution for scattering by two parallel slabs of arbitrary physical parameters [Redheffer in Montgomery, 1947], and an elegant analytical discussion of N arbitrary parallel slabs [Redheffer, 1950, 1954]; for N slabs (arbitrary spacings, and arbitrary reflection and transmission coefficients of the isolated slabs) he uses group theory, abstract multiplication, as well as conventional matrices, and difference equations. A detailed systematic successive scattering treatment for N arbitrary parallel slabs is given by Marcus [1946]. Their closed-form solutions for N identical equally spaced slabs were obtained originally by Darwin [1914] in his basic paper on the scattering of X-rays by crystals. Redheffer [1956] also gives an exact treatment of "limit-periodic dielectric media" (the limit for $N \rightarrow \infty$ of N identical inhomogeneous slabs of thickness $1/N$), and Bazer [1959] considers the conditions for which an arbitrary configuration of N identical slabs may be analytically approximated by an appropriate continuum.

The above papers on collections of planar scatterers are but a few among the many to be found in the literature; see Hartree [1929], Luneberg [1947a, b], Lurye [1951], Russek [1951], Keller [1953], Keller and Keller [1951], Schelkunoff [1951], Bremmer [1951], Landauer [1951], and Kay [1958]. The limiting case of the arbitrary stratified region is that of an inhomogeneous medium: recent work includes that of Kay [1955], Kay and Moses [1956, 1955a, 1955b, 1955c, 1957], Saxon [1957; 1959], Schiff [1956], Saxon and Schiff [1957], Seckler and Keller [1959], and Hall [1958]. Additional references to the recent literature and discussions of procedures for treating such problems are given in Bremmer's [1958] Handbuch review of radio wave propagation; and in the same volume (Electric Fields and Waves), King's [1958] review of electric circuits, and the review of Borgnis and Papas [1958] on waveguides, include germane transmission line procedures for treating collections of planar scatterers.

Turning to arbitrary collections of arbitrary, parallel circular cylinders, the separations of variables procedure of Zaviska [1913], Ignatowsky [1914a], Row [1955], and Twersky [1953a] gives infinite sets of linear algebraic equations which relate the multiple scattered coefficients of a cylinder to known single scattered values and to Hankel functions of the spacings. A Neumann iteration of these "self-consistent" equations leads to the "orders of scattering" series whose successive terms involve higher products of single scattered coefficients; Twersky [1952a] also obtained this series by successive application of the boundary conditions.

For radii small compared to wavelength, Zaviska [1913] gives closed form approximations for two and three (equally spaced, coplanar) cylinders, such that E is parallel to their axes (henceforth E parallel), and the direction of propagation is perpendicular to the plane of their axes (henceforth k perpendicular);

for this polarization, he also considers two cylinders and k parallel (i.e., E , k , and the axes all coplanar). In these approximations, the isolated scatterers are treated essentially as monopoles (isotropic scatterers), and all orders of scattering are taken into account; e.g., Zaviska's multiple scattered coefficients for one of the two identical cylinders for E parallel and k perpendicular may be written as $A = a/(1 - aH)$, where a is the single-scattered value, and $H = H_0(kb)$ (the "configuration factor") equals the zeroth order Hankel function of spacing b and wavenumber k . [This elementary multiple scattering solution (in fact, the most elementary) serves to illustrate the terminology used previously. Thus the "self-consistent" equation leading to the closed form may be written $A = a + aH_0(kb)A$: the first term on the right is the response of the cylinder to the incident plane wave (the single scattered value a), and the second is its response to the field of its neighbor (i.e., to a cylindrical wave of strength A originating from a source at distance b). Iterating the self-consistent equation, or expanding the closed form, gives the "orders of scattering" series $A = a + a^2H + a^3H^2 + \dots$, which one would obtain directly from considerations of successive scattering processes. Also note that the single scattered coefficient a is essentially a "parameter" of the multiple scattered value A : the closed form holds for one element of all symmetrically excited pairs of identical monopoles. (Differences between results for various pairs arise from different single scattered coefficients; e.g., for perfect conductors in two dimensions, the circle involves the logarithm of the radius, and the ellipse, of the arithmetical mean of the major and minor axes.) Zaviska [1913] also considers two identical cylinders for E perpendicular and k perpendicular and gives the first two orders of scattering for the monopole and dipole terms. He also shows that if two arbitrary sized cylinders are in each other's far fields, then the problem reduces essentially to that of one cylinder excited by two plane waves (the incident wave, and a wave traveling in the plane of the axes); however, he fails to notice that this can be exploited to obtain closed forms.

Twersky [1952b, c] obtains closed forms for several cases by retaining only the largest terms involving the separation b in each order of scattering; e.g., a generalization of the above A for two different isotropic scatterers (not necessarily cylindrical) for arbitrary angle of incidence; closed forms for two scatterers with radii and spacing small compared to wave length; closed forms for two arbitrary cylinders each in the far field of the other (call this "far-multiple-scattering"), and an analogous result that holds for N equispaced coplanar cylinders (a finite grating) when end effects are neglected. He also applies an image technique to these results to consider the analogous multiple scattering problems for semicylindrical protuberances on a ground plane; he shows that for E parallel, there are no far-multiple-scattering contributions for an arbitrary configuration of arbitrary semicylindrical protuberances, and derives the first nonvanishing terms for special cases.

Row [1955] applies his general results to two identical perfect conductors for E parallel and k perpendicular. He obtains numerical values by several methods (including truncating the system of algebraic equations, and a diagonal approximation of their matrix). Comparisons with experiments are made for several wavelengths less than or equal to the diameter, for fixed spacing and a varying field point, and vice versa. In particular, he finds detailed agreement for a truncation procedure which keeps as many multiple scattered coefficients as single scattered coefficients called for by the analogous isolated cylinder problem.

Storer and Sevvick [1954] apply the variational procedure of Levine and Schwinger to their integral representation for N scatterers, and obtain a stationary form for the far-field scattering amplitude. They specialize their results to treat two finite identical, parallel circular cylinders (radius small compared to spacing and to length) for E parallel. Using a "shifted cosine" trial function, they find good agreement between theory and experiment for backscattering and k perpendicular to half-wave and full-wavelength scatterers. Minkowski and Cassey [1956] use the analogous procedure to treat the case of collinear cylinders.

Karp [1959] gives a general discussion of the integral representation for N arbitrary scatterers, and considers the conditions for convergence of the orders of scattering series. Subject to far-multiple-scattering, the integral representation for an arbitrary configuration of N arbitrary cylinders yields N simultaneous equations for the multiple scattered amplitudes in terms of their single scattered values; in particular, Karp [1959] gives the closed form for two arbitrary cylinders (the generalization of a result in Twersky's [1952b] result for two circular cylinders).

As discussed by Twersky [1952b], the closed forms that hold for far-multiple-scattering retain only the largest terms in $kb \gg 1$ of each order or scattering. Thus the series in powers of $1/\sqrt{kb}$ obtained on expanding the closed form for the multiple scattering amplitude is not the rigorous expansion of the function. Zitron and Karp [1959] show that for two cylinders, the "far-multiple-scattering, orders of scattering" series is correct in its three leading terms (i.e., to $1/kb$), and obtain the next term of the series for two arbitrary cylinders: in distinction to the leading terms, which involve only the far-field scattering amplitudes of the isolated cylinders (say f), the new term also involves derivatives of f . They specialize their result to the case of arbitrary circular cylinders, and show it agrees to appropriate order with the result obtained on approximating the complete series derived by separation of variables in Twersky [1952a]. They also obtain the corresponding number of terms of the analogous series arising for the scalar problems of two arbitrary scatterers in three dimensions.

Wu and Levine [1958] consider a row of large circular cylinders for k parallel, and obtain multiple-scattering corrections to the geometrical optics value of the total scattering cross section.

Millar [1960] considers the N simultaneous integral equations obtained for the two cases of E parallel and E perpendicular to a row of perfectly conducting cylinders of arbitrary shape. For elliptic cylinders with major axis small compared to wavelength, and arbitrary separation, he reduces the integral equations to linear algebraic equations (using a procedure similar to Bouwkamp's for the single strip). For two cylinders and E parallel, his closed form approximations for the multiple-scattered coefficients are identical with the forms for two arbitrary isotropic scatterers given in Twersky [1952b]. His plots of the real and imaginary parts of one coefficient as a function of kb , for three directions of incidence (k perpendicular, and k parallel, say, from the right, and from the left) show the effects of multiple scattering and "shielding."

The scattering of waves by two objects has also been recently considered in the literature of quantum mechanics. Thus Brueckner's [1953] closed form for the impulse approximation for S -state scattering from a two-body system, is a result for two monopoles in three dimensions (identical with the form for two isotropic scatterers given in Twersky [1952b]); and his result for P -state meson scattering, is that for the scalar problem of two dipoles in three dimensions. Representative related papers are those of Watson [1953], Takeda and Watson [1955], Brueckner [1955], and Drell and Verlet [1955]. More complex systems are discussed by Gerjuoy [1958], and in the proceedings of the recent Grenoble lecture series on many-body problems edited by Dewitt [1959].

3.2. Infinite Planar Lattices

Here we begin with the more general treatments, and then consider special procedures.

As is well known, the field of an infinite grating of arbitrary identical cylinders excited by a monochromatic plane wave consists of an infinite discrete set of plane waves; some of these waves are "propagating modes" (the usual spectral orders) and these carry energy in specific directions determined by the wavelength, the spacing, and the angle of incidence; the remaining are "surface waves" (or "evanescent modes") which are exponentially damped normal to the plane of the grating. The existence of these waves follows directly from the periodicity of the structure; i.e., the field must be representable as a Fourier series, and this has been the starting point of most rigorous approaches to the problem. But this is merely the starting point: it is the amplitudes of these waves which must be determined. Thus Rayleigh [1907a] represents the mode amplitudes in terms of an algebraic set of equations involving the Fourier components of the grating's profile, and Ignatowsky [1914a] expresses them in terms of an integral equation for the current distribution on one element; and most expansion procedures in the literature are based on one of these two classic representations. However, alternative representations prove more tractable when strong coupling

occurs. Thus Twersky [1956a] starts with the set of multiple scattering surface integrals for the elements of the array, and proceeding initially in analogy with Ewald's [1917] treatment of a lattice of dipoles, derives a "mixed representation." The mode amplitudes are expressed in terms of the multiple scattered amplitude of a cylinder in the grating, and specified through a new functional equation involving its single scattered value (as the inhomogeneous term, and in the kernel of the operator). Differing from both Ignatowsky's integral equation and Rayleigh's "sum equation" (i.e., the set of algebraic equations), the operator in the new equation equals an integral minus the analogous sum (a relatively rapidly convergent representation). The new formalism is applied [Twersky, 1956a, 1957b] to treat the grating resonances investigated experimentally by Wood and Strong; and the enhancement of one spectral order, or the diminution of another, as well as other "anomalies" with respect to single scattering theory, are interpreted in terms of surface wave coupling between the propagating spectral orders. Multiple scattering effects are significant for such resonances (which for normal incidence occur when the grating spacing is nearly an integral number of wavelengths), for near grazing incidence, and for relatively closely packed scatterers; for other situations, the multiple-scattered amplitude reduces to its single scattered value (the inhomogeneous term of the equation). Twersky [1958b] applies the general theory to circular cylinders (and obtains, for example, simple explicit results for the "packing effects" at low frequencies up to multipoles of order 2⁵), and Burke and Twersky [1960] apply it to elliptic cylinders. Analysis of such grating problems is facilitated by Ignatowsky's [1914b] elementary function representations for the Schlömilch series that arise for normal incidence, and by the analogous forms for the more general series arising for arbitrary angle of incidence derived by Twersky [1958c].

The procedure discussed above is one of the few multiple scattering treatments of a grating of general elements which expresses the field in terms of the behavior of the elements when isolated. The first of this kind was Ignatowsky's [1914a]. In addition, the variational procedure discussed by Marcuvitz [1951], and applied to circular and elliptical elements with spacing and cross-sectional dimensions small compared to wavelength, is also quite general. Another initially general procedure is Karp's [1955], which was applied by Karp and Radlow [1956] to grating resonances subject to "far-multiple-scattering" (i.e., each scatterer in the far field of all others).

The principal anomalies with the single scattering approximation for the grating (an approximation obtained originally by Schwerd [1835]) indicated by the experiments of Wood [1902], Ingersoll [1921], Strong [1936], Palmer [1952], and others, are the "resonances" mentioned previously. With reference to these, Rayleigh [1907a] treats a perfectly conducting grating, and finds that his repre-

sentation of the perpendicular polarized amplitudes diverges if there is a grazing mode. Fano [1938] considers the same range for a grating of finite conductivity. Artmann [1942] begins with Rayleigh's model (Fourier series expansion of the profile), but derives an alternative, convergent series representation for near grazing modes. Artmann's expressions for the maxima correspond to the maxima of the usual Wood anomalies; and although he does not consider the associated minima (lying between the Rayleigh wavelength and the maxima), these may also be treated using this model. Fano [1938] also presents a general expression (suggested by a quantum mechanical analogy) which can be adjusted to describe the anomalies, and he is the first to stress the role of the surface waves. Karp and Radlow [1956], and Lippmann and Oppenheim [1942] consider the anomalies, and a relatively detailed discussion is given by Twersky [1956a, 1957b, 1958b].

A perhaps more intuitive approach may also be applied to consider the grating anomalies. Thus Twersky [1952c] gives an "orders of scattering" treatment of the anomalies for a finite grating (perfectly conducting semicylinders on a plane, end-effects neglected): the extrema are interpreted as occurring at wavelengths which optimally fulfill the conditions that each order of scattering is a maximum, and that successive orders are either in or out of phase. Here a suggestion made by Wood [1902], and originally elaborated by Artmann [1942], is developed into a "vibration curve" method based on a discrete analog of the Fresnel integral [Russek and Twersky, 1953].

The method of images provides a convenient means for obtaining solutions for reflection gratings from results for analogous transmission problems. The first treatments of the reflection grating based on this approach originally took into account single scattering [Twersky, 1950a, b, c], and then analogous multiple scattering results [Twersky, 1956a, 1957b, 1958b] were obtained. The image technique itself (for wave problems) was first used by Rayleigh [1907b], who applies the results for a perfectly conducting cylinder with radius small compared to wavelength to obtain the analogous functions for a semicylinder on a perfectly conducting plane.

In addition to papers mentioned above, there are a large number of treatments of transmission gratings of specific scatterers: For example, strips are treated by Vainshtein [1955], Heins [1954], and Miles [1949]; circles are treated by Shmoys [1951], Shmoys and Sollfrey [1952], and Reiche [1953]; and fine wires are treated by Wessel [1939], Honerjager [1948] and Franz [1949]. Fine wires, closely spaced, are also treated by Lamb [1945], and Gans [1920] (both giving incorrect results for polarization perpendicular to the axis—see Twersky [1958b] for details), and by Lewin [1951], and Marcuvitz [1951]. The most detailed treatment of circular cylinders appears to be that of Twersky [1958b], which also gives comparisons with previous work.

Additional treatments of gratings included those of

Voigt [1911] (who extended Rayleigh's [1907a] procedure to a lossy interface), Tai [1948], Lippmann [1953], Meecham [1957, 1956a, b], Snow [1956], Primich [1957], Heaps [1957], Proud [1957], Parker [1957], Theissing and Caplan [1956], Hatcher and Rohrbaugh [1958, 1956], Palmer [1956], Rohrbaugh and others [1958], Wait [1958, 1955, 1959], Senior [1959], and Felsen [1959].

As for other two-dimensional planar lattices, Marcuvitz [1956] has given a general formulation for the planar lattice of arbitrary scatterers in terms of the periodicity factors of the array, and in terms of the amplitude of one element. Low frequency results for planar lattices of spheres, disks, etc., have been derived in connection with artificial dielectrics, and in connection with the related problems of obstacles in rectangular waveguides: see the recent review by Cohn [1960] for the literature of the first, and the texts by Marcuvitz [1951], and Lewin [1951] and others for the second. General scattering theorems for such structures are given by Schwinger, Dicke [1948], Redheffer [1950], Friedrichs [1949], and Twersky [1956b].

Additional papers dealing with planar periodic arrays are cited in recent reviews by Harvey [1959] and by Lysanov [1958].

3.3. Planar Random Distributions

As in the previous section, we begin with the most general treatment of the problem; this minimizes repetition.

a. Sparse Distribution (Two-Dimensional "Rare Gas")

The scattering of a plane wave by a planar random distribution of arbitrary objects may be treated by averaging the set of multiple-scattering surface integrals for one configuration over an appropriate distribution. In particular, for identical scatterers whose average separation is large compared to their minimum separation, we may assume that the one-particle and two-particle distribution functions are constant (as for a rare gas).

For such sparse planar distributions of arbitrary scatterers, Twersky [1957a, 1955], using a procedure analogous to Foldy's [1947], shows that the coherent scattered field consists of two plane waves—one in the direction of incidence, and one in the direction of specular reflection (with respect to the plane of the distribution). The amplitudes of these waves are proportional to corresponding values of the average multiple scattering amplitude of a scatterer fixed in the distribution; i.e., to the response of one fixed object to the incident field plus the fields of all other objects averaged over the configurations these other objects may assume. The average with one fixed scatterer is given [Twersky, 1957a] by an integral relation whose kernel involves the same function averaged with two scatterers held fixed; approximating one by the other (as first done explicitly for a volume of monopoles by Foldy [1947], and as done "instinctively" in earlier less analytical treatments of dielectric constants, etc.) leads to a simple expression for the unknown amplitudes in terms of their single-scattered values. (The validity of this approxima-

tion requires that the number of scatterers be large; see Foldy [1947] for discussion, and Bazer [1959] for an analytical treatment of the one-dimensional case.)

To this approximation, the total excitation of a scatterer within the distribution is proportional to the average of the coherent transmitted and reflected plane waves; and since the response of an isolated scatterer to a plane wave is known, one obtains two algebraic equations which can be solved directly. This gives simple expressions for the multiple-scattered amplitudes in terms of their presumably known single-scattered values. The final transmission and reflection coefficients take into account the major effects of coherent multiple scattering; in particular, whereas their single-scattered values would become infinite as grazing incidence is approached, the total scattered field approaches the negative of the incident wave (which merely means that only surface wave, or inhomogeneous plane wave, solutions exist in the limit), i.e., the coherent field of the distribution becomes that of a perfect reflector.

The value for the multiple scattering amplitude obtained by taking into account the coherent effects is also used [Twersky, 1957a, 1955] in the corresponding incoherent scattering (i.e., excitations arising from multiple incoherent scattering are neglected); this leads to an approximation for the total scattered field which explicitly fulfills the energy theorem. Thus, the final results (expressed solely in terms of the known single scattered amplitude, the number of scatterers per unit area, the angles of incidence and observation, and the wavelength) state simply that the average power reflected, transmitted, absorbed, and scattered by the area of distribution illuminated by unit area of incident wave is equal to the incident power density.

The multiple-scattering amplitude of the "random screen" (for the case of scatterers symmetrical to the plane of the distribution) is also imaged [Twersky, 1957a, 1955] to obtain the corresponding function for the analogous distribution of arbitrary protuberances on a ground plane; this amplitude gives directly the reflection coefficients and differential scattering cross sections per unit area for a relatively general model of "rough surfaces". It is shown that for such surfaces the coherent field fulfills an "impedance boundary condition" on the plane of the distribution (i.e., the scalar field is proportional to its normal derivative, or, equivalently, the tangential component of E is proportional to the tangential component of H), and the impedance is expressed simply in terms of the scattering amplitude of an isolated protuberance. For both "vertical" and "horizontal" polarizations, the ratios of reflected to incident fields approach minus one as grazing incidence is approached; the corresponding coherent intensity reflection coefficients approach unity, and the incoherent backscattering cross sections approach zero. More explicitly, for arbitrary protuberances on a ground plane, if the "horizon angle" (or grazing angle) approaches zero, then the reflection coefficients approach unity linearly and the backscattering for polarization perpendicular/or par-

allel to the plane of incidence vanishes like the fourth/or second power of the angle respectively.

This model for reflection and scattering from rough surfaces appears to be the only one which treats both coherent and incoherent scattering phenomena in parallel, and which relates them explicitly to each other through the energy principle. Theorems are derived to show that the sum of average powers coherently reflected, incoherently scattered, and absorbed by the area of distribution "illuminated" by unit area of incident wave equals the incident power density; and (using a general theorem for an isolated protuberance [Twersky, 1954b]), it is shown that the forms for reflection coefficient and scattering cross section (in terms of single scatterer results) explicitly fulfill the required theorems. Illustrative examples are obtained by specializing the general results to arbitrary hemispheres, and semicylinders, and explicit approximations in terms of elementary functions are given for scatterers very small or very large compared to wavelength [Twersky, 1957a, 1955].

The above model is a generalization of the one introduced by Rayleigh [1907b] to consider incoherent scattering from a striated surface; his paper gives a single-scattering treatment based on the field of a fine semicylindrical protuberance. Rayleigh's work was initially extended to obtain single-scattered coherent and incoherent intensities for distributions of small semicylinders and hemispheres [Twersky, 1950a, b, c, 1953c], and of large semicylinders [Twersky, 1952d]; then multiple-scattering effects for separations large compared to wavelength were taken into account for semicylinders [Twersky, 1953a, d]. These special scatterers are considered as illustrations in the more general treatment mentioned previously [Twersky, 1957a, 1955].

The phase of the coherent reflected wave for the special case of small hemispheres on a plane is also considered by Biot [1958]. Neglecting incoherent scattering, Biot [1957] considers a monopole source, and Wait [1959] a dipole source exciting small hemispheres on a ground plane. In particular, Wait [1959] considers surface wave effects for lossy bosses and shows that the first approximation for the coherent effects may be described by a plane having an inductive surface reactance; he also considers the analogous problems for a curved ground plane, and for parallel (plane, and curved) guides.

A variety of other models for random screens and rough surfaces exist in the literature. However, it is not the purpose of the report to consider these topics, except as they relate to multiple-scattering problems of distinct objects. The reader is referred to the works of Rice [1951], Booker, Ratcliffe, and Shinn [1950], Beckman [1957], Miles [1954], Magnus [1952], Schouten and De Hoop [1957], Ament [1956], Hoffman [1955], Lysanov [1958], Senior and Siegel [1959], Beard, Katz, and Spetner [1956], Beard and Katz [1957], Spetner [1958], LaCasce and Tarmarkin [1956], LaCasce [1958], Berning [1957], Meecham [1956], Heaps [1956], Parker [1956], Jones and Barton [1958], Katzin [1957], Pollak [1958].

Additional papers are cited by Lysanov [1958] and by Twersky [1957a].

b. General Statistical Distribution

The grating and the random screen of arbitrary cylinders are essentially the "crystalline" and "rare gas" limits of a one-dimensional "liquid" of perfectly elastic scatterers. To treat this general statistical distribution, Zernike and Prins [1927] take the one-particle distribution to be constant and use probability considerations to derive a pair distribution function; the pair-function is expressed essentially in terms of an "elbow room parameter" (L) equal to the ratio of average to minimum separation of scatterer centers, a minimum generally greater than a scatterer's width. They obtain a single scattering approximation for a large number of scatterers on a line, and show numerically that for $L \rightarrow 1$, both pair-function and intensity become sharply peaked; and that for $L \gg 1$, both become relatively smooth. (Their basic paper introduces the now standard "inversion procedure" used in X-ray scattering by liquids. Inverting a corresponding approximation for the three-dimensional case, enables one to construct approximations for the "radial distribution function" in terms of scattered intensity measurements; see Gingrich's [1943] review.)

Twersky [1959b] considers the scattering of waves by a one-dimensional liquid of coplanar, parallel, arbitrary cylinders; he obtains a continuous transitional formalism from the rare gas limit [Twersky, 1957a] to the periodic one [Twersky, 1956a]. The analysis is based on a Poisson one-particle distribution function, and on a more convergent transform of the pair-function introduced by Zernike and Prins [1927]. Representing the field of one configuration as a sum of surface integrals, and averaging over the distribution, gives an integral relation between the average fields with one and two particles held fixed; equating these to each other yields an integral equation involving the known distribution functions and the presumably known scattering amplitude of an isolated cylinder. The absolute square of the average field specifies the "coherent intensity." A corresponding approximation is constructed for the "incoherent" differential scattering cross section by taking the average field with one scatterer held fixed as the excitation of a scatterer within the distribution.

The total average intensity for this distribution depends critically on L , the relative "elbow room" per scatterer. As $L \rightarrow 1$, the "local order" increases; in the limit, it is shown [Twersky, 1959b] that the one and two particle distributions go over to δ functions, and that the scattered field reduces to the solution for the grating of equispaced arbitrary elements [Twersky, 1956a]. For this "crystalline" case, the field is all coherent and consists of the transmitted and reflected propagating spectral orders plus the infinite set of evanescent surface waves. At the other limit $L \rightarrow \infty$, the local order disappears; the distribution functions become constants, and the results reduce to those of the analogous "rare

gas" [Twersky, 1957a]. For this case, the coherent field consists of the directly transmitted and specularly reflected plane waves, and the differential cross section is relatively smoothly varying (as determined by choice of scatterers). The coherent field for the general case of the "liquid" (of infinite "length") has the same form as for the gas, but the incoherent intensity is more or less a smudged version of the intensity pattern for the periodic case: it is peaked in the vicinity of the parameters corresponding to the noncentral spectral orders of the grating, and these maxima broaden and decrease away from the directly transmitted and specular directions.

The results for scatterers symmetrical to the plane of the distribution are also imaged [Twersky, 1959b] to obtain corresponding functions for the general striated surface of arbitrary protuberances on a ground plane. Applications are given to illustrate multiple-scattering effects in certain resonance phenomena ("near-grating" anomalies), in the behavior near grazing incidence, and in the effects of packing for small scatterers.

3.4. Periodic Volume Distributions

The main lines for treating scattering of X-rays by crystals follow the works of Ewald [1917], Darwin [1914], Bragg [1915], and Laue [1931]. Ewald [1917] obtains a multiple-scattering solution for the lattice of dipoles. Laue [1931, 1935] works with a Fourier series representation for a general periodic index of refraction. Darwin [1914] uses a single-scattering approximation for the fields of the planar lattices parallel to the interface of a semi-infinite lattice, and takes into account multiple scattering between planes. He introduces the "transmission line" procedure for treating such problems; and, for the situation corresponding to Bragg [1913] and Laue [1913] resonances, Darwin's 1914 paper gives the associated pair of coupled difference equations, since rediscovered many times in connection with one-mode propagation in periodically loaded lines, guides, and artificial dielectrics. Prins [1930] applies Darwin's procedure to take into account absorption.

Laue's procedure is applied by Kohler [1933] to treat the one-mode case for the bounded periodically perturbed medium, and Mayer [1928] and Lamla [1939] consider the case of three strong modes. Essentially Darwin's procedure (but taking into account some multiple-scattering effects in the component planes) is used by Twersky [1954a] to treat the lattice of circular cylinders; and the general case is treated by this means by Marcuvitz [1956], whose results are applied to special problems by Barone and Schneider [1956].

A broad, relatively elementary survey of analytical techniques for treating scattering by periodic structures (methods introduced for scattering of X-rays by crystals) is given by James [1950], and some additional results are included in Partington's [1951] comprehensive treatise on physical chemistry (particularly vol. 3). Fourier methods for treating scattering (of anything) by periodic structures are reviewed by Slater [1958].

The lattice of spheres is treated by separating variables in the static limit by Rayleigh [1892], and for arbitrary wavelengths, by Kasterin [1897], and by Morse [1956]. Various approximations also exist in the literature of artificial dielectrics, a subject whose modern aspects start essentially with the work of Kock [1948]. The literature to 1952 is surveyed in Brown's [1953] monograph on microwave lenses, to 1957 in Cohn's [1960] review chapter of the Antenna Engineering Handbook, and to 1958 in Harvey's [1959] survey article on optical techniques at microwave frequencies. Recent papers in the U.S. literature include those of Lippmann and Oppenheim [1954], Storer [1952], Jones, Morita, and Cohn [1956], Morita and Cohn [1956], Collin [1959], Ward, Puro, and Bowie [1956], Kaprielian [1956a, 1956b, 1956c], Cohn [1956], and Hickman, Risty, and Stewart [1957].

3.5. Random Volume Distributions

The earliest analytical treatment of the scattering of waves by random distributions of objects (or potentials) is essentially Rayleigh's theory of the color of the sky [Rayleigh, 1899]. The subject has since received much attention in the literature, but much of the work has been heuristic.

Foldy's [1947] treatment of scattering by monopoles serves as a model for those seeking to treat more arbitrary scatterers. Thus Lax [1952], and Twersky [1958a, 1959a] give different generalizations for the coherent field. Foldy's self-consistent treatment of monopoles is extended essentially three different ways to obtain the propagation coefficient (say K) of the coherent field for a random distribution of relatively arbitrary scatterers excited by a wave having propagation coefficient k . Each procedure expresses K in terms of an isolated object's scattering amplitude, say f ; but Twersky [1958a] uses $f(k \rightarrow k)$, the amplitude of the object in free space; Lax [1952] uses $f(K \rightarrow K)$, the amplitude in the new medium associated with the coherent field; and later Twersky [1959a] uses $f(K \rightarrow k)$, the amplitude of an object excited in K -space but radiating into k -space. Twersky [1958d] obtains $f(K \rightarrow k)$ by introducing a new class of single-body scattering problems, in which the source and radiated terms of the solution satisfy different wave equations. [This type of scatterer may be more palatable if its limiting form for a monopole is recognized in the usual volume integral representation for the field scattered by a constant potential $k^2 - K^2$, i.e., in the integral whose kernel comprises a monopole (the free k -space Green's function) weighted by the local field: since the local field travels in K -space, these monopoles radiating into k -space are elementary forms of the "schizoid scatterer" characterized by $f(K \rightarrow k)$.]

The new formalism is applied [Twersky, 1959a] to a slab region of large tenuous scatterers, and simple explicit forms are obtained for the coherent and incoherent intensities, and for the average phase. Theoretical results are compared with a series of detailed experiments by Beard and Twersky [1958,

1960a, 1960b] on a large scale dynamical model of a "compressible gas" of spheres. Measurements were made from a relatively rare gas (average separation of centers 10 times scatterer diameter) to practically a "liquid state" case (average separation about one-eighth larger than diameter). [Here the "molecules" were 1½-in. styrofoam spheres and the measurements were made with ½-cm radiation; a system of blowers and turbulence-creating wedges produced the distribution, and the required statistical functions were measured separately by optical methods.] The recent computed and measured intensities are in accord over the full range investigated.

The three extensions [Lax, 1952; Twersky, 1958a, 1959a] of Foldy's [1947] procedure are among the more recent extensions of Rayleigh's original model. For a volume distribution of small scatterers, Rayleigh [1899] gives a leading term approximation involving $f(k \rightarrow k)$. Other results for wave scattering in terms of forms of $f(k \rightarrow k)$ appropriate for special objects, are given in Reiche [1916] (slab region of dipoles), Urlick and Ament [1949] (slab of small spheres), and Twersky [1953b] (slab region of cylinders). Similarly, expansions in terms of $f(k \rightarrow k)$ are used in the work on dense distributions of dipoles by Yvon [1937], Kirkwood [1936], Brown [1950], Mazur and Mandel [1956], Green [1952], Jansen and Mazur [1955], Jansen [1955], Fixman [1955], Born and Green [1946], and Green [1957]; these papers are particularly noteworthy for their care with the probabilistic aspects of the problem. Alternative approaches, still based on well-defined elementary scatterers, are discussed by Onsager [1936], Böttcher [1952], De Loor [1956], and others.

Brief, relatively comprehensive, introductions to various aspects of the subjects involved in the above, and additional references, are given in several articles of the Handbook of Physics edited by Condon and Odishaw [1958]: see "Dielectrics" by von Hippel; "Molecular Optics" by Condon; "Principles of Statistical Mechanics and Kinetic Theory of Gases," and "Vibrations of Crystal Lattices and Thermodynamic Properties of a Solid" by Montroll; and "The Equations of State and Transport Properties of Gases and Liquids" by Bird, Hirschfelder, and Curtiss. A detailed review of the literature of dielectrics is given by Partington [1951-1955], vol. 4 and 5. See also Frenkel [1956], Debye [1945], Hartshorn and Saxton [1958], Van Vleck [1932], Von Hippel [1954], and, in particular, the excellent recent review by Brown [1956]. Fournet [1957] gives the latest review on the structure of liquids; and the recent article by Montroll and Ward [1958] on the statistical mechanics of interacting particles, and the references it gives to the classical statistics literature, indicate the more fundamental models of matter now under study.

Much work on multiple scattering of incoherent radiation has been done from essentially a particle scattering viewpoint. Instead of the wave equation, one works with the Boltzman integro-differential equation for transport processes. See Hopf [1934],

Chandrasekhar [1950], Case [1957], Woolley and Stibbs [1953], Fano, Spencer, and Berger [1959], and Goldstein [1959] for fundamentals, applications, and reviews of computational procedures.

An alternative approach to problems of scattering and propagation in random media is to work with a perturbed continuum—see papers of Einstein [1910], Smoluchowski [1908], Pekeris [1947], Debye [1954], Booker and Gordon [1950], Villars and Weisskopf [1954], Silverman [1957, 1958], Staras [1955], Wheelon [1957], the scatter-propagation issue of the Proceedings of the IRE [1959], Bremmer's Handbuch article [1958], and the recent review of tropospheric propagation by Staras and Wheelon [1959]. References to the literature of physical chemistry involving this approach are cited by Fishman [1957] and Stacey [1956].

Recent papers on the topic of this section include Booker [1956], Kraichman [1956], Chu and Churchill [1956, 1955], Gordon [1958], Zink and Delsasso [1958], Skydzyk [1957], Silverman [1956, 1957, 1958], Stein [1958], Phillips [1959], Smith [1956], Zweig [1956], Buckingham [1956], Buckingham and Stephen [1957], Yvon [1958], Prins and Prins [1957], Longuet-Higgins and Pople [1956], Goldstein and Michalik [1955], Fixman [1955], Jefferies [1955], Megaw [1957], Peterlin [1957], Nakagaki and Heller [1956], Stevenson [1957], Richards [1955], Sekera [1957], Richards [1956], Ament [1952], Meeron [1960], Digest of Literature of Dielectrics, Conference on Electrical Insulation, National Academy of Sciences—National Research Council, Vols. 20, 21, 22 [1956, 1957, 1958].

Additional categories of phenomena involving "multiple scattering", and additional references (particularly to the literature of quantum mechanics), are given by Lax [1951, 1952].

References

- Ament, W. S., Wave propagation in suspensions, Rept. 5307, U.S. Naval Research Lab. (1952).
- Ament, W. S. Forward and backscattering from certain rough surfaces, IRE Trans. **AP-4**, 369 (1956).
- Artman, K., On the theory of the anomalous reflection at diffraction gratings, Z. Physik **119**, 529 (1942).
- Barone, S. and S. Schneider, Analysis of periodic structures, Series of Repts., Electrophys. Group. Polytech. Inst. Brooklyn (1956).
- Bazer, J., Multiple scattering in one dimension, Research Rept. EM-122, Inst. Math. Sci., NYU (1959).
- Beard, C. I. and I. Katz, The dependence of microwave radio signal spectra on ocean roughness and wave spectra, IRE Trans. **AP-5**, 183 (1957).
- Beard, C. I., I. Katz, and L. M. Spetner, Phenomenological vector model of microwave reflection from the ocean, IRE Trans. **AP-4**, 162 (1956).
- Beard, C. I. and V. Twersky, Propagation through random distributions of spheres, 1958 WESCON Conf. Record, pt. 1, Rept. EDL-M156, Sylvania Electron. Defense Labs. (1958).
- Beard, C. I. and V. Twersky, Forward coherent and incoherent scattering from random volume distributions of spheres, Rept. EDL-E46, Sylvania Electron. Defense Labs. (1960a).
- Beard, C. I. and V. Twersky, Angular scattering from random volume distributions of spheres, Rept. EDL-E47, Sylvania Electron. Defense Labs. (1960b).

- Beckmann, P., A new approach to the problem of reflection from a rough surface, *Acta Tech. CSAV* **2**, 311 (1957).
- Berning, J. A., Performance of diffraction gratings with random errors in the positions of the grating grooves, *J. Opt. Soc. Am.* **47**, 339 (1957).
- Biot, M. A., Reflection on a rough surface from an acoustic point source, *J. Acoust. Soc. Am.* **29**, 1193 (1957).
- Biot, M. A., On the reflection of electromagnetic waves on a rough surface, *J. Appl. Phys.* **28**, 1455 (1957); **29**, 998 (1958).
- Booker, H. G., A theory of scattering by nonisotropic irregularities with applications to radar reflections from the aurora, *J. Atmospheric and Terrest. Phys.* **8**, 204 (1956).
- Booker, H. G. and W. E. Gordon, A theory of radio scattering in the troposphere, *Proc. IRE* **38**, 401 (1950).
- Booker, H. G., J. A. Ratcliffe, and D. H. Shinn, Diffraction from an irregular screen with applications to ionospheric problems, *Phil. Trans. Roy. Soc. (London)* [A], **856**, 579 (1950).
- Born, F. E. and C. H. Papas, Electromagnetic waveguides and resonators, *Handbuch der Phys.* **16**, 285 (Springer, Berlin, Germany, 1958).
- Born, M. and H. S. Green, A general kinetic theory of liquids, I. The molecular distribution functions, *Proc. Roy. Soc. (London)* [A] **188**, 10 (1946).
- Born, M., *Optik*, p. 313 (Springer, Berlin, Germany, 1933).
- Botcher, C. J. F., Theory of electric polarization (Elsevier, New York, 1952).
- Bragg, W. H., X-rays and crystal structure, *Phil. Trans. Roy. Soc. (London)* [A] **215**, 253 (1915).
- Bragg, W. L., Diffraction of short electromagnetic waves by a crystal, *Proc. Cambridge Phil. Soc.* **17**, 43 (1913).
- Bremmer, H., The WKB approximation as the first term of a geometrical-optical series, *NYU Symp. on the theory of Electromagnetic Waves*, 169 (Interscience Publishers, Inc., New York, N.Y., 1951).
- Bremmer, H., Propagation of electromagnetic waves, *Handbuch der Phys.* **16**, 423 (Springer, Berlin, Germany, 1958).
- Brown, J., Microwave lenses (Methuen and Co., London, England, 1953).
- Brown, W. F., Jr., Dielectric constants of non-polar fluids, I and II, *J. Chem. Phys.* **18**, 1193 (1950).
- Brown, W. F., Jr., Dielectrics, *Handbuch der Phys.* **17**, 1-154 (Springer, Berlin, Germany, 1956).
- Brueckner, K. A., Multiple scattering corrections to the impulse approximation in the two-body system, *Phys. Rev.* **89**, 834 (1953).
- Brueckner, K. A., Two-body forces and nuclear saturation, *Phys. Rev.* **97**, 1353 (1955).
- Buckingham, A. D., The molecular refraction of an imperfect gas, *Trans. Faraday Soc.* **52**, 747 (1956).
- Buckingham, A. D. and M. J. Stephen, A theory of the depolarization of light scattered by a dense medium, *Trans. Faraday Soc.* **53**, 884 (1957).
- Burke, J. E. and V. Twersky, On scattering of waves by the grating of elliptic cylinders, *Rept. EDL-E44*, Sylvania Electron. Defense Labs. (1960).
- Case, K. M., Transfer problems and the reciprocity principle, *Rev. Mod. Phys.* **29**, 651 (1957).
- Chandrasekar, S., Radiative transfer, (Oxford Univ. Press, London, England, 1950).
- Chu, C. M. and S. W. Churchill, Numerical solution of problems in multiple scattering of electromagnetic radiation, *J. Phys. Chem.* **59**, 855 (1955).
- Chu, C. and S. W. Churchill, Multiple scattering by randomly distributed obstacles—Methods of solution, *IRE Trans. AP-4*, 581 (1956).
- Clausius, R., Die mechanische wärmetheorie **2**, p. 70 (Vieweg, Braunschweig, 1897).
- Clemmow, P. C., Edge currents in diffraction, *Trans. IRE AP-4*, 282 (1956).
- Cohn, S. B., Dielectric properties of a lattice of anisotropic particles, *J. Appl. Phys.* **27**, 1106 (1956).
- Cohn, S. B., Lens-type radiators, *Antenna Engineering Handbook* (McGraw-Hill Book Co., Inc., New York, N.Y., 1960).
- Collin, R. E., Properties of slotted dielectric interfaces, *IRE Trans. AP-7*, 62 (1959).
- Condon, E. V. and H. Odeshaw, *Handbook of Phys.* (McGraw-Hill Book Co., Inc. New York, N.Y., 1958).
- Darwin, C. G., The theory of X-ray reflection, *Phil. Mag.* **27**, pt. I, 315; Pt. II, 675 (1914).
- Debye, P., Polar molecules (Dover Publications, New York, N.Y., 1945).
- Debye, P. J. W., The collected papers of P. J. W. Debye (Interscience Publishers, Inc., New York, N.Y., 1954).
- deLoor, G. P., Dielectric properties of heterogeneous mixtures, Thesis Monograph (Lab. Phys. RVO-TNO, The Hague, 1956).
- Dewitt, C., The many body problem (John Wiley & Sons, Inc., New York, N.Y., 1959).
- Dieke, R. H., Principles of microwave circuits, ch. 5 (McGraw-Hill Book Co., Inc., New York, N.Y., 1948).
- Drell, S. D., and L. Verlet, Multiple scattering corrections in π -deuteron scattering, *Phys. Rev.* **99**, 849 (1955).
- Einstein, A., Theorie der Opaleszenz von homogenen Flüssigkeiten und Flüssigkeitsgemischen in der Nähe des kritischen Zustandes, *Ann. Phys.* **33**, 1275 (1910).
- Ekstein, H., Multiple elastic scattering and radiation damping, Pt. I, *Phys. Rev.* **83**, 721 (1951); Pt. II, **89**, 490 (1953).
- Ewald, P. P., Optics of crystals, *Ann. Phys.* **49**, 1, 117 (1916); Foundations of the optics of crystals **54**, 519 (1917).
- Fano, U., Theory of intensity anomalies in diffraction, *Ann. Phys.* **32**, 393 (1958).
- Fano, U., L. V. Spencer, and M. Berger, Penetration and diffusion of X-rays, *Handbuch der Phys.* **38/2**, 660 (Springer, Berlin, Germany, 1959).
- Faraday, M., Experimental researches in electricity **1**, 409, 418, 534 (1839).
- Felsen, L. B., The scattering of electromagnetic waves by a corrugated sheet, *Can. J. Phys.* **37**, 1565 (1959).
- Fishman, M. M., Light scattering by colloidal systems—An annotated bibliography, Tech. Service Labs., River Edge, N.Y. (1957).
- Fixman, M., Molecular theory of light scattering, *J. Chem. Phys.* **23**, 2074 (1955).
- Foldy, L. L., The multiple scattering of waves, *Phys. Rev.* **67**, 107 (1945); E. I. Carstensten and L. L. Foldy, Propagation of sound through a liquid containing bubbles, *J. Acoust. Soc. Am.* **19**, 481 (1947).
- Fournet, G., Etude de la structure des fluides de la substances amorphes au moyen de la diffusion des rayons X, *Handbuch der Phys.* **32**, 239 (Springer, Berlin, Germany, 1957).
- Franz, W., Durchlässigkeit von Drahtgittern für elektrische Wellen, *Z. Angew. Phys.* **9**, 416 (1949).
- Frenkel, J., Kinetic theory of liquids (Oxford Univ. Press, London, England, 1946).
- Friedrichs, K. O., Recent developments in the theory of wave propagation, sec. III b, *Inst. Math. Sci. NYU* (1949).
- Gans, R., Dasverhalten Hertzscher Gitter, *Ann. Phys.* **61**, 447 (1920).
- Gingrich, N. S., Diffraction of X-rays by liquid elements, *Rev. Mod. Phys.* **15**, 90 (1943).
- Gerjuoy, E., Time-independent nonrelativistic collision theory, *Ann. Phys.* **5**, 58 (1958).
- Goldstein, H., Fundamental aspects of reactor shielding (Addison-Wesley Publishing Co., Inc., Reading, Mass., 1959).
- Goldstein, M. and E. R. Michalik, Theory of scattering by an inhomogeneous solid possessing fluctuations in density and anisotropy, *J. Appl. Phys.* **26**, 1450 (1955).
- Gordon, W. E., Incoherent scattering of radio waves by free electrons with applications to space exploration by radar, *Proc. IRE* **46**, 1824 (1958).
- Green, H. S., The molecular theory of fluids (Interscience Publishers, Inc., New York, N.Y., 1952).
- Hall, J. F., Jr., Reflection coefficient of optically inhomogeneous layers, *J. Opt. Soc. Am.* **48**, 654 (1958).
- Hart, J. and R. A. Soderman, Digest of literature on dielectrics, Conf. on Elec. Insulation, Nat. Acad. Sci.—Nat. Research Council **22** (1958); **21** (1957).
- Hartree, D. R., The propagation of electromagnetic waves in a stratified medium, *Cambridge Phil. Soc. Proc.* **25**, 97 (1929).
- Hartshorn, L. and J. A. Saxton, The dispersion and absorption of electromagnetic waves, *Handbuch der Phys.* **16**, 640 (Springer, Berlin, Germany, 1958).

Harvey, A. F., Optical techniques at microwave frequencies, *Proc. IRE* **196B**, 141 (1959).

Hatcher, R. D., and J. H. Rohrbaugh, Theory of the echelette grating, *J. Opt. Soc. Am.* **46**, 104 (1956).

Hatcher, R. D., and J. H. Rohrbaugh, Theory of the echelette grating II, *J. Opt. Soc. Am.* **48**, 704 (1958).

Heaps, H. S., Reflection of a plane acoustic wave from a surface of non-uniform impedance, *J. Acoust. Soc. Am.* **28**, 666 (1956).

Heaps, H. S., Reflection of plane waves of sound from a sinusoidal surface, *J. Appl. Phys.* **28**, 815 (1957).

Heaviside, O., *Electromagnetic theory*, Sec. 182 (Dover Reprint, New York, N.Y. 1950) (originally published in *Electrician*, 1893).

Heins, A. E. and G. L. Baldwin, On the diffraction of a plane wave by an infinite plane grating, *Math. Scand.* **2**, 103 (1954).

Hickman, J. S., Donald E. Risty, and E. S. Stewart, Properties of sandwich-type structures as acoustic windows, *J. Acoust. Soc. Am.* **29**, 858 (1957).

Hoffman, J. D. and J. Hart, Digest of literature on dielectrics, *Conf. Elec. Insulation, Natl. Acad. Sci.—Natl. Research Council* **20** (1956).

Hoffman, W. C., The electromagnetic field in a randomly inhomogeneous medium, *IRE Trans.* **AP-7**, S301 (1959).

Hoffman, W. C., Scattering of electromagnetic waves from a random surface, *Quart. Appl. Math.* **13**, 291 (1956); and *IRE Trans.* **AP-3**, 96 (1955).

Honerjager, R., On the diffraction of electromagnetic waves by a wire grating, *Ann. Phys.* **4**, 6th Ser., 25 (1948).

Hopf, E., *Mathematical problems of radiative equilibrium* (Cambridge Univ. Press, London, England, 1934).

Ignatowsky, W. v., Zur Theorie der Gitter, *Ann. Phys.* **44**, 23, 369 (1914a).

Ignatowsky, W. v., Über Reihen mit zylinder funktion nach dem vielfachen des argumentes, *Arch. Math. und Phys.* **23**, 193 (1914b).

Ingersoll, L. R., Polarization of radiation by gratings, *J. Astrophys.* **51**, 129 (1920); Some peculiarities of polarization and energy distribution by specular gratings, *Phys. Rev.* **17**, 493 (1921).

James, R. W., *The optical principles of the diffraction of X-rays* (G. Bell & Sons, Ltd., London, England, 1950).

Jansen, L., Some aspects of molecular interactions in dense media, *Monograph* (Martines Nijhoff, The Hague, 1955).

Jansen, L. and P. Mazur, On the theory of molecular polarization in gases, *Physica* **21**, 193 (1955).

Jeffries, J. T., Radiative transfer in two dimensions, *Optica Acta* (Paris) **2**, 163 (1955).

Jones, J. L. and L. E. Barton, Acoustic characteristics of a lake bottom, *J. Acoust. Soc. Am.* **30**, 142 (1958).

Jones, E. M. T., T. Morita, and S. B. Cohn, Measured performance of matched dielectric lenses, *IRE Trans.* **AP-4**, 31 (1956).

Kaprielian, Z. A., Anisotropic effects in geometrically isotropic lattices, *J. Appl. Phys.* **29**, 1952 (1958).

Kaprielian, Z. A., Dielectric properties of a lattice of anisotropic particles, *J. Appl. Phys.* **27**, 24 (1956).

Kaprielian, Z. A., Electromagnetic transmission characteristics of a lattice of infinitely long conducting cylinders, *J. Appl. Phys.* **27**, 1491 (1956).

Karp, S. N., Diffraction by an infinite grating of cylinders, *Research Rept. EM-85*, Inst. Math. Sci., NYU (1955).

Karp, S. N., Diffraction by combinations of obstacles, *Proc. McGill Symp. Microw. Opt.* **198** (1953) (*Electron. Research Directorate, AFRC* (1959)).

Karp, S. N. and A. Russek, Diffraction by a wide slit, *J. Appl. Phys.* **27**, 886 (1956).

Karp, S. N. and N. Zitron, Higher order approximations in multiple scattering, *Research Rept. EM-126*, Inst. Math. Sci., NYU (1959).

Karp, S. N. and J. Radlow, On resonance in infinite gratings of cylinders, *IRE Trans.* **AP-4**, 654 (1956).

Kasterin, N., Über die dispersion der akustischen wellen in einem nichthomogenen medium, *König. Akd. Wentens VI*, 460 (1897).

Katzin, M., On the mechanism of radar sea clutter, *Proc. IRE* **45**, 44 (1957).

Kay, I., Reflection from inhomogeneous plane stratified media, *Research Rept. WP-1*, Inst. Math. Sci., NYU (1958).

Kay, I., The inverse scattering problem, *Research Rept. EM-74*, Inst. Math. Sci., NYU (1955).

Kay, I. and H. E. Moses, Reflectionless transmission through dielectrics and scattering potentials, *Research Rept. EM-91*, Inst. Math. Sci., NYU (1956).

Kay, I. and H. E. Moses, The determination of the scattering potential from the spectral measure function, *Research Rept. CX-18*, Inst. Math. Sci., NYU (1955a).

Kay, I. and H. E. Moses, The determination of the scattering potential from the spectral measure function, Part II: Point Eigenvalues and proper Eigenfunctions, *Research Rept. CX-19*, Inst. Math. Sci., NYU (1955b).

Kay, I. and H. E. Moses, The determination of the scattering potential from the spectral measure function, Part III: Calculation of the scattering potential from the scattering operator for the one-dimensional Schrödinger equation, *Research Rept. CX-20*, Inst. Math. Sci., NYU (1955c).

Kay, I. and H. E. Moses, The determination of the scattering potential from the spectral measure function, Part IV: Pathological scattering problems in one dimension, *Research Rept. CX-32*, Inst. Math. Sci., NYU (1957).

Keller, H. B. and J. B. Keller, On systems of linear ordinary differential equations, *Research Report EM-33*, Inst. Math. Sci., NYU (1951).

Keller, H. B., Ionosphere propagation of plane waves, *Research Report EM-56*, Inst. Math., NYU (1953).

Keller, J. B., A geometrical theory of diffraction, in *calculus of variations and its applications* edited by L. M. Graves (McGraw-Hill Book Co., Inc., New York, N.Y., 1958), and also as *Research Rept. EM-115*, Inst. of Math. Sci., N.Y. (1958). See also *Diffraction by an aperture*, *J. Appl. Phys.* **28**, 426 (1957), and other references cited in first paper.

Kelvin, Lord, On the mathematical theory of electricity in equilibrium, *Cambridge and Dub. Math. J.* **1**, 75 (Nov. 1845).

King, R. W. P., Quasi-stationary and non-stationary currents in electric circuits, *Handbuch der Phys.*, **16**, 165 (Springer, Berlin, Germany, 1958).

King, R. W. P., *Linear antennas*, ch. 3 (Harvard Univ. Press, Cambridge, England, 1956).

Kirkwood, J. G., On the theory of dielectric polarization, *J. Chem. Phys.* **4**, 592 (1936).

Kock, W. E., Metallic delay lenses, *Bell System Tech. J.* **27**, 58 (1948).

Kohler, M., Reflection of X-rays by absorbing crystals, *Ann. Phys.* **18**, 265 (1933).

Kraichnan, Scattering of sound in a turbulent medium, *J. Acoust. Soc. Am.* **28**, 314 (1956).

LaCasce, E. O., Jr., Note on the backscattering of sound from the sea surface, *J. Acoust. Soc. Am.* **30**, 578 (1958).

LaCasce, E. O., Jr. and P. Tamarkin, Underwater sound reflection from a corrugated surface, *J. Appl. Phys.* **27**, 138 (1956).

Lamb, H., *Hydrodynamics*, p. 357 (Dover Publications, New York, N.Y., 1945).

Lamla, E., Indirect excitation of X-ray interferences, *Ann. Phys.* **36**, 194 (1939).

Landauer, R., Reflections in one dimensional wave mechanics, *Phys. Rev.* **82**, 80 (1951).

Laue, M. v., Interferenzerscheinungen bei röntgenstrahlen, *Ann. Phys.* **41**, 971 (1913).

Laue, M. v., *Röntgenstrahl-Interferenzen* (Geest und Portig, Leipzig, 1948); *Ergeb. der exact Naturwiss* **10**, 133 (1931); *Ann. Phys.* **23**, 705 (1935).

Lax, M., Multiple scattering of waves, pt. I, *Rev. Mod. Phys.* **23**, 287 (1951); pt. II, The effective field in dense systems, *Phys. Rev.* **80**, 621 (1952).

Lewin, L., *Advance theory of waveguides*, ch. 7 (Iliffe and Sons, London, England, 1951).

Lippmann, B. A., Reflection from a periodic surface, *Nuclear Development Associates, Inc., Rept. 18-8*, (1953); also *Note on the theory of gratings*, *J. Opt. Soc. Am.* **43**, 408 (1953).

- Lippmann, B. A. and A. Oppenheim, Equivalent circuit approach to radome problems (series of reports) Tech. Research Group N.Y. (1954).
- Lippmann, B. A. and A. Oppenheim, Towards a theory of Wood's anomalies, Tech. Research Group (N.Y., 1954).
- Longuet-Higgins, H. C. and J. A. Pople, Transport properties of a dense fluid of hard spheres, *J. Chem. Phys.* **25**, 884 (1956).
- Lorentz, H. A., *Wied. Ann.* **9**, 641 (1880); Theory of electrons, p. 137 ff. (Tuebner, Leipzig, 1909).
- Lorenz, L., Über die refractionconstante, *Ann. Phys. Chem.* **11**, 70 (1890).
- Luneberg, R. K., Propagation of electromagnetic waves from an arbitrary source through inhomogeneous stratified atmospheres, Research Rept. 172-6, Inst. Math. Sci., NYU (1947a).
- Luneberg, R. K., The propagation of electromagnetic plane waves in parallel layers, Research Rept. 172-3, Inst. Math. Sci., NYU (1947b).
- Lurye, J. R., Electromagnetic scattering matrices of stratified anisotropic media, Research Rept. EM-31, Inst. Math. Sci., NYU (1951).
- Lysanov, I. P., Theory of the scattering of waves at periodically uneven surfaces, A review, *Soviet Phys. Acoust.* **4**, 3 (1958).
- Magnus, W., On the scattering effect of a rough plane surface, Research Rept. EM-40, Inst. Math. Sci., NYU (1952).
- Marcus, P. M., The interactions of discontinuities on a transmission line, Mass. Inst. Technol., Rad. Lab. Rept., 930 (1946).
- Marcuvitz, N., On the calculation of the band properties of electrons in crystals, Memo No. 9, Electrophys. Group, Polytech. Inst. of Brooklyn (1956).
- Marcuvitz, N., Waveguide handbook 268ff, 286ff (McGraw-Hill Book Co., Inc., New York, N.Y., 1951).
- Maxwell, J. C., A treatise on electricity and magnetism, Third ed. (Dover Publications, New York, N.Y., 1954) (first ed. published in 1873); a, sec. 314; b, sec. 841; c, secs. 319-321 (Stratified conductor) and secs. 328-330 (stratified dielectric).
- Mayer, G. Z., Über Anheftungen in Röntgenspektrogrammen, *Kristallogr* **66**, 585 (1928).
- Mazur, P. and M. Mandel, On the theory of the refractive index of non-polar gases, *Physica* **22**, 289 (1956).
- Meecham, W. C., A method for the calculation of the distribution of energy reflected from a periodic surface, *IRE Trans.* **AP-4**, 581 (1956).
- Meecham, W. C., Fourier transform method for the treatment of the problem of the reflection of radiation from irregular surfaces, *J. Acoust. Soc. Am.* **28**, 370 (1956).
- Meecham, W. C., Variational method for the calculation of the distribution of energy reflected from a periodic surface, *J. Appl. Phys.* **27**, 361 (1956).
- Meecham, W. C. and C. W. Peters, Reflection of plane-polarized, electromagnetic radiation from an echelette diffraction grating, *J. Appl. Phys.* **28**, 216 (1957).
- Meeron, E., Exact integral equations for particle correlation functions, Rept. 22, Boeing Scientific Research Labs. (1960).
- Megaw, E. C. S., Fundamental radio scatter propagation theory, *Proc. IRE*, Monograph 236 R, 441-445 (1957).
- Miles, J. W., The diffraction of a plane wave through a grating, *Quart. Appl. Math.* **7**, 45 (1949).
- Miles, J. W., On non-specular reflection at a sea surface, *J. Acoust. Soc. Am.* **26**, 191 (1954).
- Millar, R. F., The scattering of a plane wave by a row of small cylinders, *Can. J. Phys.* **38**, 272 (1960).
- Minkowsky, J. M. and E. S. Cassedy, Cross section of colinear arrays at normal incidence, *J. Appl. Phys.* **27**, 313 (1956).
- Montroll, E. W. and J. C. Ward, Quantum statistics of interacting particles; general theory and some remarks on properties of an electron gas, *Phys. of Fluids* **1**, 55 (1958).
- Morita, T. and S. B. Cohn, Microwave lens matching by simulated quarter wave transformers, *IRE Trans.* **AP-4**, 33 (1956).
- Morse, P. M., Waves in a lattice of spherical particles, *Proc. Nat. Acad. Sci.* **42**, 276 (1956).
- Mossotti, O. F., Recherches théoriques sur l'induction électrostatique, envisagée d'après les idées de Faraday, *Bibl. Univ. Arch.* **6**, 193 (1847). Discussione analitica sull'influenza che l'azione di un mezzo dielettrico ha sulla distribuzione dell'elettricità alla superficie di più corpi elettrici disseminati in esso, *Mem. Mat. Fis. Soc. Ital. Sci. Modena* **14**, 49 (1850).
- Nakagaki, M. and W. Heller, Effect of light scattering upon the refractive index of dispersed colloidal spheres, *J. Appl. Phys.* **27**, 975 (1956).
- Onsager, L., Electric moments of molecules in liquids, *J. Am. Chem. Soc.* **58**, 1486 (1936).
- Palmer, C. H., Parallel diffraction grating anomalies, *J. Opt. Soc. Am.* **42**, 269 (1952).
- Palmer, H. C., Jr., Diffraction grating anomalies. II. Coarse gratings, *J. Opt. Soc. Am.* **46**, 50 (1956).
- Parker, J. G., Reflection of plane sound waves from an irregular surface, *J. Acoust. Soc. Am.* **28**, 672 (1956).
- Parker, J. G., Reflection of plane sound waves from a sinusoidal surface, *J. Acoust. Soc. Am.* **29**, 377 (1957).
- Partington, J. R., An advanced treatise on physical chemistry 5 volumes (Longmann's Green, London, England, 1951-1955).
- Pekeris, C. L., Note on the scattering of radiation in an inhomogeneous medium, *Phys. Rev.* **71**, 268 (1947).
- Peterlin, A., W. Heller, and M. Nakagaki, Light scattering and statistical shape of streaming freely flexible linear macromolecules, *J. Chem. Phys.* **28**, 470 (1957).
- Phillips, C. E., Microwave scattering by turbulent air, *IRE Trans.* **AP-7**, 245 (1959).
- Pits, E. and A. Marriage, Relation between granularity and autocorrelation, *J. Opt. Soc. Am.* **47**, 321 (1957).
- Poisson, S. D., Deux mémoires sur la théorie du magnétisme, *Mem. Acad. Sci.* **5**, 247 (1821); Mémoire sur la théorie du magnétisme en mouvement **6**, 441 (1823).
- Pollak, M. J., Surface reflection of sound at 100 kc, *J. Acoust. Soc. Am.* **30**, 343 (1958).
- Primich, R. I., Some electromagnetic transmission and reflection properties of a strip grating, *IRE Trans.* **AP-5**, 176 (1957).
- Prins, J. A., Die reflexion von röntgenstrahlen an absorbierenden idealen kristallen, *Z. Phys.* **63**, 477 (1930).
- Prins, J. A., and W. Prins, Influence of molecular orientation on X-ray and optical scattering by liquids, *Physica* **23**, 253 (1957).
- Proud, J., Jr., Reflection of sound from a surface of saw-tooth profile, *J. Appl. Phys.* **28**, 1298 (1957).
- Rayleigh, Lord, On the influence of obstacles arranged in rectangular order upon the properties of a medium, *Phil. Mag.* **34**, 481 (1892) (Collected works, Cambridge Univ. Press, Cambridge, England **4**, 19 (1903)).
- Rayleigh, Lord, Transmission of light through an atmosphere containing small particles in suspension, *Phil. Mag.* **47**, 375 (1899).
- Rayleigh, Lord, Dynamical theory of the grating, *Proc. Roy. Soc. (London)* **[A]79**, 399 (1907a).
- Rayleigh, Lord, Light dispersed from fine lines ruled upon reflecting surfaces or transmitted by very narrow slits, *Phil. Mag.* **14**, 350 (1907b).
- Redheffer, R. M., In C. G. Montgomery's Technique of Microwave Measurements, Rad. Lab. **11**, 564 ff. (McGraw-Hill, Book Co., Inc., New York, N.Y., 1947).
- Redheffer, R. M., Remarks on the basis of network theory *J. Math. and Phys.* **28**, 237 (1950).
- Redheffer, R. M., Novel uses of functional equations, *J. Rat. Mech. and Ann.* **3**, 271 (1954); the Riccati equation: Initial values and inequalities, *Math. Ann.* **133**, 235 (1957).
- Redheffer, R. M., Limit periodic dielectric media, *J. Appl. Phys.* **27**, 1136 (1956); **28**, 820 (1957).
- Reiche, F., On diffraction by an infinite grating, Research Rept. EM-61, Inst. Math. Sci., NYU (1953).
- Reiche, F., Zur Theorie der Dispersion in Gasen und Dämpfen, *Ann. Phys.* **50**, 1, 121 (1916).

- Rice, S. O., Reflection of electromagnetic waves from slightly rough surfaces, *Commun. Pure and Appl. Math.* **4**, 351 (1951).
- Richards, P. I., Multiple isotropic scattering, *Phys. Rev.* **100**, 517 (1955).
- Richards, P. I., Scattering from a point source in plane clouds, *J. Opt. Soc. Am.* **46**, 927 (1956).
- Rohrbaugh, J. H., C. Pine, W. G. Zoellner, and R. D. Hatcher, Theory of the echelette grating III, *J. Opt. Soc. Am.* **48**, 410 (1958).
- Row, R. V., Theoretical and experimental study of electromagnetic scattering by two identical conducting cylinders, *J. Appl. Phys.* **26**, 666 (1955).
- Russek, A., Scattering matrices for ionosphere models, Research Rept. EM-38, Inst. Math. Sci., NYU (1951).
- Russek, J. and Twersky, V., Graphs of the function $E(N, \delta) = \sum_{n=1}^N e^{i\delta n} / \sqrt{n}$, Research Rept. EM-49, Inst. Math. Sci., NYU (1953).
- Saxon, D. S. and L. I. Schiff, High energy potential scattering, *Nuovo cimento* **6**, 614 (1957).
- Saxon, D. S., Modified WKB methods for the propagation and scattering of electromagnetic waves, *IRE Trans.* **AP-7**, 8-320 (1959).
- Saxon, D. S., Formulation of high-energy potential scattering problems, *Phys. Rev.* **107**, 871 (1957).
- Schaefer, C. and F. Reiche, Zur Theorie des beugungsgitters, *Ann. Phys.* **35**, 817 (1911).
- Schelkunoff, S. A., Remarks concerning wave propagation in stratified media, NYU Symp. on the Theory of Electromagnetic Waves, p. 181 (Interscience Publishers, Inc., New York, N.Y., 1951).
- Schiff, L. I., Approximation method for short wavelength or high energy scattering, *Phys. Rev.* **104**, 1481 (1956).
- Schouten, J. P., and A. T. deHoop, On the reflection of an electromagnetic plane wave by a perfectly conducting rough surface, *Ann. Telecomm.* **12**, 211 (1957).
- Schwarzschild, K., Die Beugung und Polarization des Lichts durch einen Spalt, *Math. Ann.* **55**, 177 (1902).
- Schwerd, F. M.; Die Beugungserscheinungen aus den Fundamental-Gesetzen der Undulations theorie analytisch entwickelt, Mannheim (1835).
- Schwinger, J., Harvard lectures on scattering.
- Seckler, B. D. and J. B. Keller, Geometrical theory of diffraction in inhomogeneous media, *J. Acoust. Soc. Am.* **31**, 192 (1959a).
- Seckler, B. D. and J. B. Keller, Asymptotic theory of diffraction in inhomogeneous media, *J. Acoust. Soc. Am.* **31**, 206 (1959b).
- Sekera, Z., Light scattering in the atmosphere and the polarization of sky light, *J. Opt. Soc. Am.* **47**, 484 (1957).
- Senior, T. B. A., The scattering of electromagnetic waves by a corrugated sheet, *Can. J. Phys.* **37**, 787, 1563 (1959).
- Senior, T. B. A. and K. M. Siegel, Radar reflection characteristics of the moon, in *Paris Symposium on Radio Astronomy*, pp. 29-45, edited by R. N. Bracewell (Stanford Univ. Press, Stanford, Calif., 1959).
- Shmoys, J., Diffraction of electromagnetic waves by a plane wire grating, *J. Opt. Soc. Am.* **41**, 324 (1951).
- Silver, S., Microwave antenna theory and design, *Rad. Lab.* **12**, p. 45 ff., p. 587 ff. (McGraw-Hill Book Co., Inc., New York, N.Y., 1949).
- Silverman, R. A., Scattering of plane waves by locally homogeneous dielectric noise, *IRE Trans.* **IT-3**, 182 (1957); *Proc. Cambridge Phil. Soc.* **54**, 530 (1958).
- Silverman, R. A., Fading of radio waves scattered by dielectric turbulence, *J. Appl. Phys.* **28**, 506 (1957).
- Silverman, R. A., Turbulent mixing theory applied to radio scattering, *J. Appl. Phys.* **27**, 699 (1956).
- Skudrzyk, E., Scattering in an inhomogeneous medium, *J. Acoust. Soc. Am.* **29**, 50 (1957).
- Slater, J. C., Interaction of waves in crystals, *Rev. Mod. Phys.* **30**, 197 (1958).
- Smith, R. E., Effective dielectric constant of heterogeneous media, *J. Appl. Phys.* **27**, 824 (1956).
- Smoluchowski, M., Molekular-kinetische, Theorie der Opaleszenz von Gasen im kritischen Zustande, sowie einiger verwandter Erscheinungen, *Ann. Phys.* **25**, 205 (1908).
- Snow, O. J., Transmission characteristics of inclined wire gratings, *IRE Trans.* **AP-4**, 650 (1956).
- Soderman, R. A. and L. J. Fresco, Digest of literature on dielectrics, Conference on Electrical Insulation, Natl. Acad. Sci.-Natl. Research Council **22** (1958).
- Sollfrey, W. and J. Shmoys, Gratings of circular cylinders, Research Rept. EM-41, Inst. Math. Sci., NYU (1952).
- Spetner, L. M., A statistical model for forward scattering of waves off a rough surface, *IRE Trans.* **AP-6**, 88 (1958).
- Stacey, K. A., Light-scattering in physical chemistry (Butterworth's Scientific Publications, London, England, 1956).
- Staras, H., Forward scattering of radio waves by anisotropic turbulence, *Proc. IRE* **43**, 1374 (1955).
- Staras, H. and A. D. Wheelon, Theoretical research on tropospheric scatter propagation in the United States, 1954-1957, *IRE Trans.* **AP-7**, 80 (1959).
- Stein, S., Some observations on scattering by turbulent inhomogeneities, *IRE Trans.* **AP-6**, 299 (1958).
- Stevenson, A. F., Note on Krishnan's reciprocity relation in light scattering, *J. Appl. Phys.* **28**, 1015 (1957).
- Stokes, A. R., The theory of light scattered by suspensions of randomly oriented long prisms, *Proc. Phys. Soc. (London)* **[B] 70**, 379 (1957).
- Strong, J., Effect of evaporated films on energy distribution in grating spectra, *Phys. Rev.* **49**, 291 (1936).
- Storer, J. E., Wave propagation in a two-dimensional periodic medium, Rept. 152, Cruft Lab., Harvard, Mass. (1952).
- Storer, J. E. and J. Sevic, General theory of plane wave scattering from finite, conducting obstacles with application to the two antenna problem, *J. Appl. Phys.* **25**, 269 (1954).
- Tai, C. T., Reflection and refraction of a plane electromagnetic wave at a periodical surface, Tech. Rept. 28, Cruft Lab., Harvard, Mass. (1948).
- Takeda, G. and K. M. Watson, Scattering of fast neutrons and protons by atomic nuclei, *Phys. Rev.* **97**, 1136 (1955).
- Theissing, H. H. and P. J. Caplan, Measurement of the solar millimeter spectrum, *J. Opt. Soc. Am.* **46**, 971 (1956).
- Twersky, V., On the nonspecular reflection of plane waves of sound, *J. Acoust. Soc. Am.* **22**, 539 (1950a).
- Twersky, V., On the nonspecular reflection of sound from planes with absorbent bosses, *J. Acoust. Soc. Am.* **23**, 336 (1951) (part of Research Rept. EM-22, Inst. Math. Sci., NYU, 1950b).
- Twersky, V., On the nonspecular reflection of electromagnetic waves, *J. Appl. Phys.* **22**, 825 (1951) (part of Research Rept. EM-26, Inst. Math. Sci., NYU, 1950c).
- Twersky, V., Multiple scattering of radiation by an arbitrary configuration of parallel cylinders, *J. Acoust. Soc. Am.* **24**, 42 (1952a).
- Twersky, V., Multiple scattering of radiation by an arbitrary planar configuration of parallel cylinders and by two parallel cylinders, *J. Appl. Phys.* **23**, 407 (1952b); additional results are given in Research Rept. EM-34, Inst. Math. Sci., NYU (1951).
- Twersky, V., On a multiple scattering theory of the finite grating and the Wood anomalies, *J. Appl. Phys.* **23**, 1099 (1952c). Remarks on the theory of grating anomalies, *J. Opt. Soc. Am.* **42**, 855 (1952).
- Twersky, V., On the reflection of waves from planar distributions of parallel cylindrical mirrors, Rept. NDA 18-3, Nuclear Develop. Assoc. (1952d).
- Twersky, V., Multiple scattering of waves by planar random distributions of parallel cylinders and bosses, Research Rept. EM-58, Inst. Math. Sci., NYU (1953a).
- Twersky, V., Multiple scattering of waves by a volume distribution of parallel cylinders, Research Rept. EM-59, Inst. Math. Sci., NYU (1953b).
- Twersky, V., Reflection coefficients for certain rough surfaces, *J. Appl. Phys.* **24**, 659 (1953c).
- Twersky, V., Reflection from semicylindrical mirrors on a plane; shadow forming beams and multiple scattering, Rept. NDA 18-10, Nuclear Develop. Assoc. (1953d).
- Twersky, V., On the scattering of electromagnetic waves by a bounded lattice of parallel cylinders, Rept. EDL-EL, Sylvania Electron. Defense Labs. (1954a).
- Twersky, V., Certain transmission and reflection theorems, *J. Appl. Phys.* **25**, 859 (1954b).

- Twersky, V., On scattering and reflection of electromagnetic waves by rough surfaces, *IRE Trans. AP-5*, 81 (1957) (part of EDL-E9, Sylvania Electron. Defense Labs., 1955).
- Twersky, V., On the scattering of waves by an infinite grating, *IRE Trans. AP-4*, 330 (1956a).
- Twersky, V., Scattering theorems for bounded periodic structures, *J. Appl. Phys.* **27**, 1118 (1956b).
- Twersky, V., On scattering and reflection of sound by rough surfaces, *J. Acoust. Soc. Am.* **29**, 209 (1957a).
- Twersky, V., Notes on scattering by gratings, Rept. EDL-M105, Sylvania Electron. Defense Labs. (1957b).
- Twersky, V., On scattering of waves by a slab region of randomly distributed objects, Rept. EDL-E26, Sylvania Electron. Defense Labs. (1958a).
- Twersky, V., On scattering of waves by the infinite grating of circular cylinders, Rept. EDL-E28, Sylvania Electron. Defense Laboratories (1958b).
- Twersky, V., Elementary function representations of Schlömilch series, Rept. EDL-E24, Sylvania Electron. Defense Labs. (1958c).
- Twersky, V., On a new class of boundary value problems of the wave equations, Rept. EDL-E32, Sylvania Electron. Defense Labs. (1958d).
- Twersky, V., On a new scattering formalism for the macroscopic electromagnetic parameters, Rept. EDL-E36, Sylvania Electron. Defense Labs. (1959a).
- Twersky, V., On scattering by quasi-periodic and quasi-random distributions, *IRE Trans. AP-7*, (special supplement) S5307-319 (1959b).
- Urick, R. J. and W. S. Ament, Propagation of sound in composite media, *J. Acoust. Soc. Am.* **21**, 115 (1949).
- Vainshtein, L. A., The diffraction of electromagnetic waves by a grid which consists of parallel conducting strips, *J. Tech. Phys.* **25**, 847 (1955) (AF-34 Translation).
- Van Vleck, J. H., The theory of electric and magnetic susceptibilities (Oxford Univ. Press, London, England, 1932).
- Villars, F., and V. F. Weisskopf, The scattering of electromagnetic waves by turbulent atmospheric fluctuations, *Phys. Rev.* **94**, 232 (1954); On scattering of radio waves by turbulent fluctuations of the atmosphere, *Proc. IRE* **43**, 1232 (1955).
- Voigt, W., Grating diffraction, *Göttinger Nachrichten*, p. 40 (1911).
- von Hippel, A. R., Dielectrics and waves (John Wiley & Sons, Inc., New York, N.Y., 1954).
- Wait, J. R., Reflection at arbitrary incidence from a parallel wire grid, *Appl. Sci. Research B* **4**, 393 (1955).
- Wait, J. R., On the theory of reflection from a wire grid parallel to an interface between homogeneous media (II), *Appl. Sci. Research B*, **7**, 355 (1958).
- Wait, J. R., The calculation of the field in a homogeneous conductor with a wavy interface, *Proc. IRE* **47**, 1155 (1959a).
- Wait, J. R., Guiding of electromagnetic waves by uniformly rough surfaces, *IRE Trans. AP-7*, pt. I, S154; pt. II, S163 (1959b).
- Ward, H. T., W. O. Puro, and D. M. Bowie, Artificial dielectrics utilizing cylindrical and spherical voids, *Proc. IRE* **44**, 71 (1956).
- Watson, K. M., Multiple scattering and the many-body problem—Applications to photomeson production in complex media, *Phys. Rev.* **87**, 575 (1953).
- Wendt, G., Statische Felder und Stationäre Ströme, *Handbuch der Phys.* **16**, p. 1-164 (Springer, Berlin, Germany, 1958).
- Wessel, W., Über den Durchgang Elektrischer Wellen durch Drahtgitter, *Hochfreq. und Elektroak* **54**, 62 (1939).
- Wheelon, A. D., Relation of radio measurements to the spectrum of tropospheric dielectric fluctuations, *J. Appl. Phys.* **28**, 684 (1957).
- Wood, R. W., Anomalous diffractive gratings, *Phys. Rev.* **48**, 928 (1935); On a remarkable case of uneven distribution of light in a diffraction grating spectrum, *Phil. Mag.* **4**, 396 (1902); Diffraction gratings with controlled groove form with abnormal distribution of intensity, *Phil. Mag.* **23**, 310 (1912).
- Woolley, R. v. d. R., and D. W. N. Stibbs, The outer layers of a star (Oxford Univ. Press, London, England, 1953).
- Wu, T. T., and H. Levine, The scattering cross section of a row of circular cylinders, Rept. 73, Dept. of Math. (Stanford Univ. Press, Stanford, Calif., 1958).
- Yvon, J., The scattering of a particle by a complex bound system, *Nuclear Phys.* **5**, 150 (1958).
- Yvon, J., Recherches sur la theories cinetique des liquides. I. Fluctuations en densite; II. La propagation et la diffusion de la lumiere, *Actualites Sci. et Ind.*, Nos. 542 and 543 (Hermann et Cie, Paris, France, 1937); *Compt. Rend.* **202**, 35 (1936). La theories statistique des fluides et l'equation d'etat, *Act. Sci. Ind.*, No. 203 (1935).
- Zaviska, F., Über die Beugung Elektromagnetischer Wellen an paralleln Unendlich langen Kreiszyllindern, *Ann. Phys.* **40**, 1023 (1913).
- Zernike, F. and J. A. Prins, Die Beugung von Röntgen-Strahlen in Flüssigkeiten als Effekt der Molekulanordnung, *Physik* **41**, 184 (1927).
- Zink, J. W. and L. P. Delsasso, Attenuation and dispersion of sound by solid particles suspended in a gas, *J. Acoust. Soc. Am.* **30**, 765 (1958).
- Zweig, H. J., Autocorrelation and granularity, Part I. Theory; Part II. Results on flashed black and white emulsions. *J. Opt. Soc. Am.* **46**, 805, 812 (1956).

Part 3. Antennas 1957-59

R. W. Bickmore* and R. C. Hansen**

Developments in antenna theory during 1957 to 1959 are summarized, with emphasis on the definitive papers. Work of U.S. authors published in United States and English language foreign journals is included. The survey is divided into four sections: Broadband antennas, dynamic antennas, large aperture antennas, and small aperture antennas. Surface wave antennas are not included in this paper.

Major progress has been made in the broadband antenna field with the appearance of log-periodic structures and unidirectional spirals. Pattern bandwidths of 10:1 have been achieved with the former.

Newest in the field are the developments arising from application of communication theory to antennas, treating the antenna as a spatial filter. Developments include: Exchange of bandwidth for aperture size or density, time modulation of certain antenna parameters to obtain multiple simultaneous modes of operation or to obtain enhanced performance, and time processing of multiple antenna outputs to obtain increased resolution or decreased array density. Thus the antenna is in general a multiterminal time varying (dynamic) device which must be considered as an integral part of the system.

Important advances in large antennas include: Application of array and electronic scanning techniques to conical geometries; electronically scanned two-dimensional arrays using frequency shift or ferrite phase shifters; use of unequal spacing between elements in an array to obtain depressed secondary responses and to utilize lower array density; annual slot arrays consisting of annuli of half-wave slots, with the advantage of a simple mechanical structure; a UHF dipole array coupled electromagnetically to a two-wire transmission line; focusing and control of radiation in the Fresnel region; determination of the constituents of antenna noise temperature.

Another important accomplishment has been the evaluation of HF aircraft antennas considering pattern, efficiency, and bandwidth.

1. Introduction

The three-year period between the 12th and 13th General Assemblies has seen substantial progress in many of the fields recommended for study in the "Resolutions and Recommendations" of the URSI Proceedings. In addition to surveying these topics, this report endeavors to cover those aspects of antenna research and development which are of primary interest to URSI and on which significant progress has been made.

The progress in the U.S.A. during 1957, 1958, and 1959 on antennas is broken down into the following topics: Broadband antennas; dynamic antennas, including data processing arrays and modulated antennas; large aperture antennas, including radio astronomy, array, and scanning antennas; and small aperture antennas, including those for space vehicles. Surface and leaky wave antennas and scattering and diffraction are covered in separate reports. The survey is based mainly on the definitive papers and reports in the field with a bibliography of supporting developments, and is not a catalog of all antenna papers. All important U.S. journals have been covered, but only papers with U.S. authors are included herein. In addition, papers by U.S. authors in certain English language foreign journals have been included, along with unclassified technical reports from major antenna establishments in the United States.

*American Systems, Inc., Los Angeles, Calif.

2. Broadband Antennas

Introduction. The term "broadband antenna," by definition, denotes an antenna having essentially constant pattern characteristics, as well as input standing wave ratio, over at least an octave of frequencies and usually several octaves. Intrinsic in this definition is the assumption that the efficiency of the antenna remains above some specific value, for efficiency is as pertinent a characteristic of broadband antennas as impedance and directivity. Often the term "broadband antenna" also carries a connotation of omnidirectionality, since it is an order of magnitude more difficult to design a broadband array of broadband elements than the broadband element alone. Thus, as is evident from Proceedings of the 12th General Assembly, early work tended to concentrate on the easier of the two problems; namely, single element broadband antennas of limited directivity. It is encouraging to note that some headway is being made on the problem of more directive broadband antennas.

Spiral antennas. The infinite equiangular spiral antenna is a device which is specified entirely by angles and is obviously frequency independent in its ideal state. Rumsey [1957] has reviewed frequency independent antennas of which the plane spiral and conical spiral represent particularly useful specializations. These antennas have been investigated on a continuing basis during the past three years primarily

**Space Tech. Labs., Inc., Los Angeles, Calif.

by Rumsey¹ and Dyson [1959a]. The necessity of having an antenna of finite size, of course, requires the specification of at least one length. Thus there is a rather definite "cut-off" frequency below which the antenna functions either with very low efficiency or not at all. The effective size of the antenna at higher frequencies is apparently bounded quite effectively by radiation damping, since excellent pattern constancy is obtained (as well as low standing wave ratio) over bandwidths of 20 or 30 to 1.

Dyson [1959b] has also shown that by extending the planar equiangular spiral into a conical spiral, the usual disadvantage of bidirectional radiation can be effectively overcome. Using this technique, bandwidths of the order of 12 to 1 have been obtained with 20 or 30 to 1 probable in the future. If flush mounting is required, some sacrifice in bandwidth or efficiency is necessary, at least with the current state of the art.

Log periodic antennas. The previous section dealt with circularly polarized radiating elements which are, theoretically, made independent of frequency through the application of the "angle concept" and the "self-complementary principle." The practical antenna, however, is frequency sensitive by virtue of the inability to construct an ideal model. If one starts with a mathematical model which is not quite frequency independent, the practical approximation can sometimes produce results superior to those of the practical approximation to the theoretically perfect antenna. Such a device is the log periodic antenna which is defined as a radiator having characteristics which vary periodically as the logarithm of the frequency [DuHamel, Isbell, 1957]. The basic log periodic antenna can be obtained by a simple modification of the angular antenna and the result is a predominantly linearly polarized antenna (although circularly polarized versions are available) having reduced end effects caused by the necessary finite size.

While there are an unlimited variety of log periodic antenna configurations, the class which has received the greatest amount of attention is the self-complementary "bow-tie" structure having tooth-like discontinuities along its radial edges. DuHamel and Isbell [1957] and DuHamel and Ore [1958] have obtained bandwidths of over 10 to 1 with such antennas, and in addition have found that the beamwidth could be controlled over a considerable range by varying the periodicity of the teeth. In general, however, the latter effect is also accompanied by a change in the low frequency "cut-off" wavelength. DuHamel and Berry [1958, 1959] have started investigation of several other designs including three dimensional versions and trapezoidal toothed structures which have promise for antennas of higher gain.

High gain broadband antennas. Two approaches to highly directive broadband antennas have recently been used. These are expansion of the effective aperture size of conventional antennas and the forming of a broadband array of broadband elements.

¹ Cheo, Rumsey, and Welch, A solution to the equiangular spiral antenna problem, paper presented at the 1959 Fall IRE-URSI Meeting, San Diego, Calif.

An example of the use of a resonance mechanism to control the effective aperture is the "Pin Wall Horn" of Parker and Anderson [1957] wherein two walls of a horn radiator are serrated with rectangular holes of ever increasing size as one proceeds from the throat to the mouth. Constant patterns in both principal planes have been obtained over a 4 to 1 bandwidth.

DuHamel and Ore [1959] and Isbell [1959] have shown that the effective aperture of a log periodic antenna can be increased by optical magnification. Log periodic feeds were constructed for paraboloidal reflectors, giving bandwidths between 10 and 20 to 1 and a VSWR of 2. Gains up to 30 db were obtained.

DuHamel and Berry [1958] have also investigated arrays of log periodic antennas of trapezoidal type which have gains of 15 to 20 db. These arrays are ingeniously designed so that the element spacing is given in terms of angles rather than distances. As a result, excellent patterns and VSWR of the order of 2 are obtained over a bandwidth approaching 10 to 1. The typical very narrow bandwidth of an array of many elements has been greatly exceeded by McCoy et al. [1958]; they have obtained a 35-percent bandwidth with a linear array of 80 waveguide horns with corporate feed structure. Sidelobe ratios near 25 db and VSWR of the order of 1.3 are maintained throughout the band (S-band). Hybrid junctions are not used for power division, hence the efficiency is high.

It is encouraging to see that someone has finally realized the advantages of an array of unequally spaced elements. D. D. King [1959] has shown analytically that a linear array, capable of being steered $\pm 90^\circ$ with respect to broadside over a 2 to 1 frequency band, can be designed to maintain its collimate characteristics with no sidelobe higher than -7 db. Also, fewer elements are needed than with an array of equally spaced elements.

Summary. In reviewing the progress represented by the above mentioned reports, several conclusions seem evident. In spite of some recent attempts, a satisfactory theory describing the operation of the newer types of broadband antennas is still lacking. At the moment it is impossible to choose between the infinite number of theoretical broadband configurations except from a constructional viewpoint.

The most important area for further work, however, would appear to be in really broadband, electrically scannable, two dimensional arrays for such applications as radio astronomy and space communications.

Bibliography

- Dyson, J., Equiangular spiral antenna, IRE, Trans. **AP-7**, 181 (1959a).
- Dyson, J., The unidirectional equiangular spiral antenna, IRE, Trans. **AP-7**, 329 (1959b).
- DuHamel, R. H., and D. G. Berry, Logarithmically periodic antenna arrays, IRE Wescon Record, pt. 1, 161 (1958).
- DuHamel, R. H., and D. G. Berry, A new concept in high frequency antenna design, IRE Conv. Record, pt. 1, 42 (1959).
- DuHamel, R. H., and D. E. Isbell, Broadband logarithmically periodic antenna structures, IRE Conv. Record, pt. 1, 119 (1957).

- DuHamel, R. H., and F. R. Ore, Logarithmically periodic antenna designs, IRE Conv. Record, pt. 1, 139 (1958).
 DuHamel, R. H., and F. R. Ore, Log periodic feeds for lenses and reflectors, IRE Conv. Record, pt. 1, 128 (1959).
 Isbell, D. E., A log-periodic reflector feed, Proc. IRE, 47, 1152 (1959).
 King, D. D., R. F. Packard, and R. K. Thomas, Broadband steerable linear arrays, Scientific Rept. No. 1 on Contract AF19(604)-5234, Oct. 7, 1959, Electron. Comm. Inc.
 McCoy, A. M., J. E. Walsh, and C. F. Winter, A broadband, low sidelobe, radar antenna, IRE Wescon Record, pt. 1, 243 (1958).
 Parker, C. F., and R. J. Anderson, Constant beamwidth broadband antennas, IRE Conv. Record, pt. 1, 87 (1957).
 Rumsey, V. H., Frequency independent antennas, IRE Conv. Record, pt. 1, 114 (1957).

3. Dynamic Antennas

Introduction. The past three years have seen a modest but concerted effort throughout the country to adapt many of the successful techniques of circuit theory to antenna design. Of particular interest have been attempts to incorporate the concepts and formulations of communications theory to the analysis of antenna performance. Under this philosophy an antenna is considered to be a spatial filter whose characteristics are completely defined in terms of a transfer function which is identical in form to that used in conventional circuit theory. The objective of the communication theory approach is to optimize the transfer function in terms of criteria which are determined on the basis of the operating antenna environment. For example, terms are introduced such as the "fidelity defect," which is a root mean square measure of the ability of a mapping or scanning antenna to provide an output signal which is an accurate reproduction of the target distribution. Unfortunately, many of the error criteria which are based on circuit theory concepts are not pertinent in applications to antenna design. The "fidelity defect" as an illustration is much too restrictive in some cases since it doesn't weigh the parameters which are important in system operation. As a result, the fundamental system concepts are often lost sight of because of the mathematical formulation. There is an urgent need, then, to reformulate the communication theory concepts in a way that takes into account the inherently different characteristics of antennas and their associated systems. In addition, care should be taken to keep from utilizing communication theory techniques in areas where conventional methods are clearer and simpler.

In addition to the use of communication theory as a tool in the rating of antenna performance, the basic concepts have been utilized to achieve *new operating techniques* which are capable of considerably improving the information gathering efficiency of an antenna system. This achievement has come about through the recognition that the antenna, viewed as a spatial filter, may be made nonstationary by the process of time modulation of the transfer function, in such a way that a direct correlation is obtained between spatially dependent and time dependent signals. More accurately, a series of orthogonal time dependent signals is generated, each one of which is modu-

lated in accordance with a different spatial pattern. Time domain processing of these signals then produces a multitude of spatial patterns which can be used in the conventional way. These techniques result in a considerably greater quantity of spatial information than would be obtained with conventional antenna operation, and it is felt that future antenna systems will place a greater reliance on these techniques.

Unfortunately, in reporting on this exciting new field of antenna theory, the authors must be content with giving merely a blanket acknowledgement to a substantial amount of work done in connection with various military projects which, obviously, is unavailable as reference material.

Communication theory applied to antennas. One of the earliest attempts to utilize the concepts of communication theory in the analysis of antenna performance was by White [1957]. The objective of this work was the determination of the fundamental limits on the information available from antenna systems. White demonstrated that an antenna (a linear array in particular) viewed as a spatial filter has a bandwidth which is determined by the aperture extent and that, therefore, it will reproduce only a finite number of the space harmonics representing a desired spatial pattern. By the same reasoning, in a two-way radar situation, the received voltage $G(\theta)$ will not exactly reproduce the target distribution $F(\theta)$ because of the finite spatial bandwidth of the antenna system. Thus from a basic standpoint, the antenna resolution is limited by the highest space harmonic within the bandwidth of the spatial filter; this bandwidth is in turn determined by the aperture size. It should be pointed out, as White has neglected to mention, that antenna resolution can be increased theoretically without limit, by the use of supergain techniques. This is equivalent to artificially increasing the space bandwidth of the antenna by producing additional spatial harmonics which contribute large amounts of reactive power. Although this technique is of little practical value for well-known reasons, it is of interest with respect to the concept of spatial filtering. Additionally, this well-known limitation on antenna resolution may be overcome by the use of correlation type processing of the antenna signals. For radar operation, White points out that improved resolution may be accomplished by correlating the signal returns with any a priori information that is available about the target distribution. In other applications, such as radio astronomy, the interferometer antenna structures are utilized in conjunction with correlation processing to achieve high resolution with low gain. Unfortunately, in addition to their low-gain characteristics, interferometric-correlation schemes are unreliable in radar operation because of the three-dimensional type of target distribution which permits the possibility of false correlations.

Raabe [1958] has also considered the antenna as a spatial filter, and he has utilized this concept in a discussion of antenna pattern synthesis. His ideas are based on the recognition that the finite spatial bandwidth of an antenna limits the highest harmonic

variation which can be contained in the radiation pattern. It is thus proposed that the bandwidth limited pattern be utilized as the desired waveform rather than the pattern of infinite harmonic content. The sampling theorem is then used to determine the optimum sample characteristics; the samples are taken as properly spaced "sinc" beams which are weighted according to the desired waveform. The spectrum represented by these samples is then said to be matched to the filter (antenna) characteristics, and the desired waveform is reproduced. This technique is very similar to Woodward's method of synthesis and Raabe presents an analysis of the similarity. Unfortunately, detailed numerical examples of actual synthesized patterns are not presented for comparison. Nevertheless, Raabe's ideas are fundamentally correct and represent an interesting application of communication theory to one of the more familiar aspects of antenna theory.

Two attempts to utilize the communication theory concepts of processing and filtering in the actual design of antennas for special application have been reported by Anderson [1958] and Dausin et al. [1959]. Essentially, Anderson considers a displaced-phase-center antenna with correlation type processing to reduce platform and scanning noise in airborne moving target radar. The work of Dausin, et al., deserves a more detailed discussion since it presents concepts which have not been mentioned previously. In this work, the spatial frequency bandwidth (and hence the angular resolution) of an antenna system is shown to depend not only on the aperture extent but also on the time frequency bandwidth of the received signal. This is not too strange, however, since the aperture extent is only uniquely defined in terms of wavelengths and, hence, the signal bandwidth should play a part in determining the spatial filter characteristics. The major conclusion from this work, then, is that signal bandwidth can be utilized in place of aperture size or density of sources to produce equivalent radiation patterns. Operationally, this is achieved by summing the autocorrelated spectral outputs from each element, weighted according to a given aperture illumination. Formulas are derived which permit the determination of the required aperture and source distribution for a given signal bandwidth characteristic. An illustrative example of this technique is presented in which a 10-percent signal bandwidth is sufficient to produce a normal 200-element pattern from a 66-element array—a 65-percent reduction in the number of elements! Obviously, the same percentage reduction will not hold for arrays with a few number of elements.

Time domain antennas. Shanks and Bickmore [1959] have presented an excellent tutorial discussion of the use of time modulation techniques in advanced antenna design. The basic concept introduced in this presentation is that of periodic time modulation of selected antenna parameters to improve the operating characteristics of an antenna system. This modulation technique produces a correlation

signals which permits time-domain processing to provide increased spatial information. Not only does this concept provide improved pattern control, as in sidelobe suppression, but it also indicates new operating techniques which are shown to have application to electronic scanning and multipattern operations. In addition, Shanks and Bickmore consider possible physical configurations which are capable of producing this type of operation and present some of the system problems of detection and processing which must be studied. Finally, an elementary experimental demonstration of the basic concepts is reported.

In an elaboration of the above work, Shanks² has discussed in detail the application of time modulation techniques to electronic scanning. It is shown that with the proper aperture modulation applied to a linear array, a series of directive-beam patterns is generated, and that the information from each may be separated by time domain processing of the received signals. The required aperture excitation is equivalent to a coherent pulse, of length much shorter than the antenna length, sweeping across the aperture. In practice this is achieved by on-off devices which are switched progressively. This technique promises to overcome many of the disadvantages which are normally associated with the conventional control devices used in electronic scanning operations.

The concept of modulated antennas has been utilized in a more restricted sense by other researchers in the field. Drane [1959] has applied periodic modulation to the relative phases of a multiple antenna system to achieve improved resolution. In particular, he considers a system comprising a number of 2-element interferometers aligned colinearly with a single linear array; the overall length of this system is many times the length of the single linear array. When the output signals from each interferometer are phase modulated and added (in a nonlinear detector) to the array output, simple time domain processing produces a pattern having no angle ambiguities and a resolution which is equivalent to that obtained from a continuous linear array with a length of the entire system. Drane also demonstrates that correlation type devices can be used in place of modulation and time domain processing to achieve the same type of results. In this case, a direct multiplication of the various element outputs is performed and this allows the addition of as many interferometer elements as desired. The major advantages in Drane's type of system is the large saving in the number of elements which are required to achieve a given angular resolution. However, two disadvantages are apparent which limit the range of application of this technique. First, the system is inherently low-gain, thereby restricting its use to applications such as radio astronomy, where long integration times can be used. Secondly, the system is unilateral because of the processing methods which are used.

² H. E. Shanks, A new technique for electronic scanning, paper presented at 1959 URSI Fall Meeting, San Diego, Calif.

Bracewell³ has presented an interesting review of switched interferometer techniques which have long been used in the field of radio astronomy. This presentation was largely an attempt to provide a better physical understanding among antenna people of the concepts which are common in the astronomy field. Of particular interest is his graphical method of constructing a spectral sensitivity diagram for interferometer-type structures. This technique provides a simple method of visualizing the effectiveness of these systems.

A study of correlation techniques in antenna pattern control has been reported by Band and Walsh⁴ in what is actually a companion paper to Drane's work. No new operating principles are introduced, but rather a description of several practical correlation and multiplication devices is presented. The work of Band and Walsh represents the first known effort to develop correlation devices which are specifically suited for the special signal output characteristics found in antenna applications; other work is by Smythe.⁵

Summary. Based on the above survey of the past three years of work in the field of dynamic antennas, it may be concluded that antennas are acquiring a "new look." The conventional concepts of antennas are gradually being pushed aside to make way for the new philosophy of integrated antenna systems. Whereas the processes of correlation, filtering, and integration have in the past been associated with systems design, these same ideas are now rightfully within the province of the antenna art. This new philosophy has important implications to antenna people, in that they can no longer rely on supporting personnel for systems inputs, but must adopt an integrated antenna-systems approach to their problems.

Bibliography

- Anderson, D. B., A microwave technique to reduce platform motion and scanning noise in airborne moving target radar, IRE Wescon Record, pt. 1, 202 (1958).
 Dausin, L. R., K. E. Niebuhr, and N. J. Nilsson, The effects of wideband signals on radar antenna design, IRE Wescon Record, pt. 1, 40 (1959).
 Drane, C. J., Phase-modulated antennas, Rept. TR-59-138, AFCRC, (Apr. 1959).
 Raabe, H. P., Antenna pattern synthesis of the most truthful approximation, IRE Wescon Record, pt. 1, 178 (1958).
 Shanks, H. E., and R. W. Bickmore, Four-dimensional electromagnetic radiators, Can. J. Phys. (March 1959).
 White, W. D., Limits on the information available from antenna systems, IRE Conv. Record, pt. 1, 57 (1957).

4. Large Aperture Antennas

Radio astronomy and large antennas. Emberson and Ashton [1958] have reviewed in detail the design of a 140-ft paraboloidal antenna for the telescope program of the National Radio Astronomy Observa-

tory; the paper presages the design of a 600-ft dish. Another large radio telescope antenna is the fixed standing parabolic reflector and tiltable flat sheet reflector which has been designed by Kraus [1958]. This antenna allows elevation scanning through tilting of the sheet reflector on an E.-W. axis and azimuth scanning through primary feed rotation. Scale model tests have been completed and are summarized [Kraus, 1958].

Bracewell [1958], in an important paper on radio interferometry, derives the relation between spacing of ground observation points and resolution of discrete sources as a function of frequency. His conclusions are that in the case of the sun, independent data are available only at points on the ground separated by at least 100λ . Bracewell [1957] has also considered the design problems of cross interferometers using dishes as elements. Swarup and Yang [1959] have also studied phasing problems for cross interferometers at microwave frequencies. A general theory in which switching antennas, such as cross-arm types, may be included is covered under Dynamic Antennas. An interesting scanning technique reported by Miller et al. [1958] uses a linear array of dishes, each of which is fed by a helix. Rotation of the helices produces phase shift and consequent scanning of the beam. Scans of the order of ± 4 beamwidths have been obtained. Another array for radio astronomy purposes consists of two parallel line sources with Yagi elements [Gallagher, 1958].

Sletten et al. [1958a] have developed shunt slot arrays for use as corrective line source feeds for paraboloids. These feeds allow an elevation fan beam yet maintain well-focused narrow beam azimuth patterns over the entire elevation interval. Another use of a line source feed is for the 1000 ft diam spherical reflector to be erected in Puerto Rico for radar astronomy studies. This fixed bowl with movable feed will allow wide angle scanning and is being designed by AFCRC and Cornell. The bowl should be useful at 21 cm, and if the tolerances can be achieved, this bowl will have at 21 cm the highest gain of any antenna, over 68 db, allowing 2 db for gain loss due to spherical aperture. Also to be mentioned is the very low sidelobe parabolic horn developed at Bell Laboratories [Friis, May, 1958], with first sidelobes below -40 db and back lobes below -70 db.

Array antennas. The previous triennium (1954 to 1956) saw completion of a very extensive program on the properties and design of array antennas, particularly waveguide slot arrays. This work is reported in the 1957 Commission 6.3 report [Cotton et al., 1959]. Efforts in the triennium 1957 to 1959 have been concentrated on extending both the theory and practice to shapes other than planar, and on new configurations, e.g., annular slot arrays and arrays of unequally spaced elements. Goodrich, Siegel, Chernin, et al. [1959] have summarized the work by University of Michigan and Hughes Aircraft Company authors on producing a pencil beam from an array on a conical surface. Although this is also

³ R. N. Bracewell, Switched interferometers, paper presented at 1959 URSI Fall Meeting, San Diego, Calif.

⁴ H. E. Band, and J. E. Walsh, Correlation techniques applied to antenna pattern control, paper presented at 1959 URSI Fall Meeting, San Diego, Calif.

⁵ J. B. Smythe and S. Weisbrod, Utilization of space frequency filters in antenna design, paper presented at 1959 URSI fall meeting, San Diego, Calif.

an electronic scanning problem, the conical surface is the unique feature of the problem. The theoretical analysis of radiation from current distributions on a cone used Geometrical Optics and Fock theory, the latter being used in the shadow region. Physical Optics was used to account for tip diffraction. A more complete discussion of the analysis problem is a paper by Goodrich et al. [1957]. A multiplicity of array configurations were studied: axial, circumferential, spiral, etc. The final design [Goodrich et al., 1959] consisted of a stack of parallel plate transmission lines, all coaxial with the cone and terminating on the conical surface. Excitation of the stacked parallel plates was provided by a central slot array, arranged to be sufficiently dispersive as to allow elevation frequency scan. Azimuth scan was accomplished by a rotation of the central waveguide feed structure. Other work on conical surface elements near the tip is by Held et al. [1958]. A paper which concerns synthesis over a conical surface is by Unz [1958]. Also investigated is the equivalence of a slot array and a continuous current distribution with particular application to a conical surface [Mayes, James, 1958]. Other papers on synthesis include a technique which uses multiple sets of elements in an interference or supergain fashion [Sletten et al., 1957a] and strip sources [Mittra, 1959]. Wait and Householder have extended the Tschebyscheff array design of Dolph to an array of axial slots disposed circumferentially about a circular cylinder [Wait, Householder, 1959].

Secondary main beams of two-dimensional slot arrays due to alternating inclination or displacement of elements have been studied by Kurtz and Yee [1957]. They treated the array as having virtual elements consisting of a pair of adjacent elements; all virtual elements were then alike. Also covered in this paper is the successful use of baffles to reduce the secondary beams.

As mentioned earlier, arrays of unequally spaced elements constitute a promising configuration. D. D. King and others⁶ have demonstrated that such effects as amplitude taper (in an equally spaced array) can be simulated with proper spacing. Irregular spacing suppresses undesirable effects such as secondary beams (usually caused by regular spacing) and may reduce the number of elements needed. This work is a continuation of earlier work of Unz.

A novel departure from the conventional array of half-wave elements wherein the element and array factors can be separated is given by Ronold King [1959]. Here, an array of full-wave dipoles is considered and the pattern derived from an integral equation of dipole current distributions. King shows that the assumption of equal, sinusoidal current distributions may produce appreciable errors in the region of minor lobes. However, the extreme difficulty of synthesizing patterns will probably severely restrict use of the analysis.

Constructional advantages over the rectangular array are offered by the annular slot arrays developed

by Kelly [1957]. Several rings of discrete slots are fed by a single radial line, offering an extremely simple yet flexible design. Excitation of the $n=1$ circumferential mode produces a beam in the normal direction; the modes for $n=0$ and higher than $n=1$ produce nulls on the axis. Schell and Bouche [1958] have developed a concentric loop array in which the loops are large in wavelengths and in which two feeds are used, allowing rotation of the pattern.

Some interesting developments have appeared in arbitrarily polarized slot arrays. Hougardy and Shanks [1958] have developed a linear array consisting of crossed slots in a square waveguide fed with two dominant orthogonal modes. Appropriate microwave plumbing allows the relative phase and amplitude and hence radiated polarizations to be adjusted. The annular arrays of Kelly [1959] above can also be excited with two modes for variable polarization. Hines and Upson [1958] have developed an interesting concept wherein a parallel plate pillbox is fed with a line source guide containing 45° inclined slots. The spacing between guide and mouth controls the polarization since the two modes have different phase velocities.

Although the emphasis has been on slot arrays, one important development has arisen in the field of dipole arrays. Sletten et al. [1957b] developed a dipole array wherein the dipoles are coupled electromagnetically to a two-wire transmission line. The shorted folded dipoles are in a plane parallel to the line and are spaced as in an array. Coupling is controlled by the angle and spacing between the dipole and the line; an analysis of the coupling is given by Seshadri and Iizuka [1959]. This array offers simplicity of construction in the UHF region comparable to that of microwave slot arrays. Cottony and others [1959] at the National Bureau of Standards have fed a large corner reflector by a collinear dipole line source, obtaining 40-db first side lobes, with a narrow azimuth beam and a broad elevation beam. The collinear array allows close realization of the design values; the 40 db is better than that obtained with waveguide slot arrays.

Electronic scanning. Electronic scanning of two-dimensional slot arrays has been achieved in practice by several means including frequency shift scanning and dielectric and ferrite phase shifters. An array which is scanned by frequency in one plane and by dielectric stub phase shifters in the other plane is described by Spradley [1958]. A serpentine (snake) main feed guide couples energy to the branch guides, allowing a small frequency swing to produce the large phase progression needed for large scan angles. Goodwin and Senf [1959] have developed a prototype 10,000-Mc/s ferrite phase shifter scanning array where a set of main line phase shifters produce elevation scanning and a set of phase shifters, one at each element, is used for azimuth scanning. All phase shifters are relay programed, with a TV-type raster scan. The term "volumetric scanning" has been used to describe these arrays, and means that

⁶ Steerable antenna focusing techniques, Electron. Comm., Inc., reports during 1959 to Rome Air Development Center.

the beam can be scanned in two planes so as to sweep out a volume. Gabriel et al [1957, 1958] have developed an "organ pipe scanner" in which a large lens is fed by a two-dimensional array of horns which in turn is excited by a feed moving across the matrix of waveguide ends. An improvement on the use of ferrite phase shifters with attendant nonlinearities is to use quadrature coils and progressive frequency harmonics to produce linear progressive phase shifts [Clavin, 1959].

Another phase shifting device is the helical trombone phase shifter of Stark [1957] where movable double coupling loops are used. This device has been very successful in the UHF region. A general investigation of beam scanning for large antennas has been conducted at Stanford Research Institute [1958]. A technique which allows scanning to be accomplished through amplitude variations rather than through the usual phase front adjustments has been proposed [Sletten et al., 1958b]. However, amplitude scanning is similar to a supergain phenomenon in that adjacent elements operate with fixed phase in an interferometric fashion to produce a net small radiating current in the proper direction, except exactly at broadside and end fire.

One of the most promising developments in the electronic scanning field is the ferrite excited slot developed by Shanks [1959]. This is a radiating element suitable for inclusion into two-dimensional arrays, in which the phase and amplitude of the element can be controlled. Slot coupling changes result from a shifting and rotation of the field inside the waveguide by means of two ferrite post irises. This is an extension of the slot developed by Tang which uses movable mechanical irises. Individual control of each element will allow maximum flexibility for both scanning and data processing type antennas. Although nonlinearity is a severe programming problem, this development offers great promise. The end-fed array appears to incur serious mutual impedance changes for large scan angles. Blasi and Elliott [1959] show that the changes of mutual impedance for uniform amplitude linear phase arrays make end feeding unsuitable due to the change in coupling as the wave proceeds down the feed line. However, corporate feeding does not suffer from this disability. Another investigation has shown that the popular $\cos \theta$ approximation for effective aperture must be modified for large scan angles. Bickmore [1958] has derived the correct result which yields the end fire value in the limit as it must. The $\cos \theta$ result is very good to a point (typically 60°), beyond which the value drops rapidly before entering the end fire region. Tolerances continue to be an important subject in antenna array design. Elliott [1958] has summarized the quantitative effects of mechanical and electrical tolerances. Of these, translation errors in element position are most important. The effect of random errors on beam pointing has also been investigated [Rondinelli, 1959]. A quality factor has been derived for evaluating the system performance of search scan-

ning antennas, taking into account such things as scan rate and hits per scan [Gardiner, 1957].

Considerable progress has been made in the reflector field. One of the most notable examples is the parabolic torus antenna [Mavroides, Provencher, 1958]. A particularly interesting version of the torus, developed by Barab et al. [1958] of Melpar, and Flaherty, and Kadak [1958] of Westinghouse, is made of wires inclined at 45° so that an internal rotating horn affords 360° scan. Another version uses a ring array of dipoles outside the torus [Fullilove et al., 1959]. These devices should be applicable to astronomy.

Li [1959] has shown that a spherical reflector can be used for wide angle scanning with good side lobes at a cost of gain. A typical gain loss for wide angle scanning is 9 db. This can be reduced below 2 db using a corrective line source feed as mentioned earlier. Another development in optical scanning devices is the double-layer pillbox of Rotman [1958]. The feed is placed in one layer with the mouth in the other, with a consequent reduction of shadowing and reflection, which in a single-layer pillbox is due to energy reflected back into the feed. Also, aberrations can be corrected either in object or image space. Zoned mirrors can be corrected to be coma-free according to Geometrical Optics. This conclusion has been refined on the basis of diffraction theory [Dasgupta, Lo, 1959]. Additional work on mirror lenses for scanning has been done at the Naval Research Laboratory [Marston, Brown, 1958].

An important generalization of symmetric lens design has been made by Morgan [1959] of BTL. He has given a general solution for the spherically symmetric lens with variable index of refraction which includes Luneberg and Eaton lenses. Proctor has given a design technique for constrained scanning lenses, i.e., lenses in which the wave propagation direction is constrained to be parallel to the beam axis [Proctor, Rees, 1957].

Near zone studies. A focusing concept developed by Bickmore has led to some interesting applications. This allows optimum transfer of energy between two unequal size apertures [Bickmore, 1957a]. Furthermore, it allows measurements with a narrow beam antenna inside the Fresnel region with the same resolution obtained in the far field region [Bickmore, 1957b]. This is accomplished in a linear array simply by introducing a slight spherical curvature of the appropriate amount into the array. In two-dimensional arrays, the requisite phase change can be introduced into the phase shifter or feed devices. With this technique, it has been possible to measure far field patterns as near as 2 percent of the normal distance $2D^2/\lambda$. Another technique for measurement of far field patterns in the Fresnel region is that of Cheng [1957]; this uses a defocused primary source. Goodrich and Hiatt [1959] have considered the transfer of energy from a point source to a point sink using an ellipsoidal reflector. A complete ellipsoid would yield according to scalar theory 100 percent transfer. The focusing properties of the ellipsoid are concomitantly studied. Harring-

ton, Villeneuve and Hu [1959] and Harrington [1958] investigated near field gain and derived a near field synthesis technique. The near field gain study obtained the widely used physical limitations on antenna gain and Q , originally derived by Chu, in a different fashion. This interesting method expands the antenna pattern in spherical harmonics and relates the maximum gain to the number of harmonics used. This is then heuristically related to physical aperture size. For the synthesis problem, the transform of the Fourier series for the aperture field is matched point by point to the pattern transform, over a surface in the near field; this is similar to Woodward's method. Both the Michigan work (Goodrich) and the Syracuse University work (Harrington et al) were supported by subcontract from General Electric Company.

Although the subject of Fresnel diffraction dates to the nineteenth century, several interesting analytical techniques have appeared. Barrar and Wilcox [1958] used the Sommerfeld $1/r^n$ expansion with success in the Fresnel region. Hu [1957] has applied Fresnel approximations to the problem of coupling between circular aperture antennas with tapered illuminations. Hansen and Bailin [1959] have computed circular aperture near field data by a computer evaluation of a series derived from the exact field formulation. This formulation produces angular integrals independent of illumination and radial integrals independent of source attitude. Results are compared with various Fresnel formulas and side lobe behavior in the Fresnel region. The side lobe ratio may actually increase over the far field value in some regions, as the side lobes decay more rapidly than the main beam amplitude. How to calculate safe radiation regions (safe against irreversible tissue damage) in the Fresnel region of high power antennas has been shown by Bickmore and Hansen [1959]. On-axis power density and defocusing factors are given.

Antenna noise and breakdown. The advent of low noise preamplifiers such as parametric amplifiers and Masers has made the evaluation of antenna or radiation noise temperature essential. Hansen [1959] has made a survey of methods for finding the effective noise temperature of a microwave antenna. Hogg [1959] gives the effect of oxygen and water vapor absorption upon antenna temperature. De Grasse et al. [1959] report very careful measurements of antenna effective noise temperature at 5,600 Mc/s using a parabolic horn antenna with very low side and back lobes (see Friis, May, 1958). A zenith temperature as low as 18 °K has been achieved. At the other end of the frequency spectrum, the precipitation particle noise mechanism for dielectric covered antennas has been shown by Tanner [1957] to be an acquisition of charge upon impact by individual precipitation particles. This has resulted in the development of successful static reduction devices. The space age has necessitated a more careful study of antenna breakdown due to high power and high altitudes. Chown et al. [1959] report on the effects of breakdown upon VSWR,

pulse shape, power, and pattern. Linder and Steele [1959] provide data for calculating breakdown for various antenna configurations as a function of frequency. An additional paper surveys the earlier state of the art [Ashwell et al., 1957].

Summary. Antennas for radio astronomy are advancing along two fronts: Mechanical design improvements allowing construction of larger single aperture dish-type antennas; and switching or data processing antenna systems wherein multiple antennas are used to obtain some performance parameters of a larger single aperture. The advance obtained by the Mill's Cross should be furthered by more sophisticated systems. These are discussed further in *Dynamic Antennas*. The quasi-optical fixed reflector scanning devices such as the parabolic torus should find use in the astronomy field.

In the array field, new techniques are needed for feeding and constructing millimeter wavelength arrays. Effort on nonconventional slot arrays such as the radial line annular slot arrays should be extended to other configurations.

The largest problems remaining in electronic scanning arrays are how to obtain the requisite phase shift, for arrays with all elements coupled together, and how to simplify the components in data processing arrays. The individually controlled element, of which the ferrite slot is a prototype, appears to offer most promise and should be broadly investigated. Application of solid state circuitry to data processing arrays, where various mixing or amplifying functions could take place at each element without severe space and weight penalties, represents another promising area.

Focusing of antennas is most easily done in data processing antennas, especially those of the time-processing type.

References

- Ashwell, J., et al., High altitude breakdown phenomena, IRE Conv. Record, pt. 1, 72 (1957).
- Barab, J. D., et al., The parabolic dome antenna: A large aperture, 360 degree, rapid scan antenna, IRE Wescon Record, pt. 1, 272 (1958).
- Barrar, R. B., and C. H. Wilcox, On the Fresnel approximation, IRE Trans. **AP-6**, 43 (1958).
- Bickmore, R. W., A note on the effective aperture of electrically scanned arrays, IRE Trans. **AP-6**, 194 (1958).
- Bickmore, R. W., On focusing electromagnetic radiators, Can. J. Phys. **35**, 1292 (1957a).
- Bickmore, R. W., Fraunhofer pattern measurement in the Fresnel region, Can. J. Phys. **35**, 1299 (1957b).
- Bickmore, R. W., and R. C. Hansen, Antenna power densities in the Fresnel region, Proc. IRE **47**, 2119 (1959).
- Blasi, E. A., and R. S. Elliott, Scanning antenna arrays of discrete elements, IRE Trans. **AP-7**, 435 (1959).
- Bracewell, R. N., Antenna problems in radio astronomy, IRE Conv. Record, pt. 1, 68 (1957).
- Bracewell, R. N., Radio interferometry of discrete sources, Proc. IRE **46**, 97 (1958).
- Cheng, D. K., On the simulation of Fraunhofer radiation patterns in the Fresnel region, IRE Trans. **AP-5**, 399 (1957).
- Chown, J. B., et al., Voltage breakdown characteristics of microwave antennas, Proc. IRE **47**, 1331 (1959).
- Clavin, A., et al., Electronically scanned microwave arrays employing synchronous ferrite phaseshifters, IRE Wescon Record, pt. 1, 25 (1959).

- Cottony, H. V., et al., URSI report on antennas and waveguides, and annotated bibliography, IRE Trans. **AP-7**, 87 (1959).
- Dasgupta, S., and Y. T. Lo, A study of the coma-corrected zoned mirror by diffraction theory, Univ. Ill., Rept. TR40 (July 1959).
- De Grasse, R. W., et al., Ultra-low-noise measurement using a horn reflector antenna and a traveling-wave maser, J. Appl. Phys., **30**, 2013 (1959).
- Elliott, R. S., Mechanical and electrical tolerances for two-dimensional scanning antenna arrays, IRE Trans. **AP-6**, 114 (1958).
- Emberson, R. M., and N. L. Ashton, The telescope program for the National Radio Astronomy Observatory at Green Bank, West Virginia, Proc. IRE **46**, 23 (1958).
- Flaherty, J. M., and E. Kadak, Early warning radar antennas, IRE Conv. Record, pt. 1, 158 (1958).
- Fris, R. W., and A. S. May, A new microwave antenna system, Elec. Engr. **77**, 502 (1958).
- Fullilove, M. N., et al., The hourglass scanner—A new rapid scan large aperture antenna, IRE Conv. Record, pt. 1, 190 (1959).
- Gabriel, W. F., et al., Volumetric scanning GCA antenna design, Rept. 5019, Nav. Res. Lab. (Nov. 1957).
- Gabriel, W. F., Volumetric scanning GCA antenna prototype, Rept. 5195, Naval Research Lab. (Oct. 1958).
- Gallagher, P. B., An antenna array for studies in meteor and radio astronomy at 13 meters, Proc. IRE **46**, 89 (1958).
- Gardiner, F. J., Note on a technique for optimizing the system performance of three-dimensional search scanning antennas, IRE Wescon Record, pt. 1, 180 (1957).
- Goebels, F. J., and K. C. Kelly, Arbitrarily polarized planar antennas, IRE Conv. Record, pt. 1, 119 (1959).
- Goodrich, R. F., et al., Radiation and scattering from simple shapes, I and II, Congr. Intern. Circuits et Antennas Hyperfréquences, Paris (Oct. 21-28, 1957).
- Goodrich, R. F., et al., Radiation from slot arrays on cones, IRE Trans. **AP-7**, 213 (1959).
- Goodrich, R. F., and R. E. Hiatt, On near zone antennas, Rept. 2861-1-F, Radiation Lab., Univ. Mich. (June 1959).
- Goodwin, F. E., and H. R. Senf, Volumetric scanning of a radar with ferrite phase shifters, Proc. IRE **47**, 453 (1959).
- Hansen, R. C., Low noise antennas, Microwave J. **2**, 19 (1959).
- Hansen, R. C., and L. L. Bailin, A new method of near field analysis, Trans. IRE **AP-7**, S458 (1959).
- Harrington, R. F., On the gain and beamwidth of directional antennas, IRE Trans. **AP-6**, 219 (1958).
- Harrington, R. F., A. T. Villeneuve, and M. K. Hu, Antenna research reports, Nos. EE 619-5812P1, Dec. 1958; EE 619-593P2, March 1959; and EE 619-597F, Sept. 1959; Syracuse Univ. on GE subcontract.
- Held, G., et al., Conical surface studies—Final report, Univ. Wash., AFCRC-TR-58-147 (July 1958).
- Hines, J. N., and J. Upson, A line source with variable polarization, IRE Trans. **AP-6**, 152 (1958).
- Hogg, D. C., Effective antenna temperatures due to oxygen and water vapor in the atmosphere, J. Appl. Phys. **30**, 1417 (1959).
- Honda, J. S., et al., Investigation of methods of scanning the beam of large antennas, Stanford Research Inst., Rept. AFCRC-TN-58-116, 117 (1958).
- Hougardy, H. H., and H. E. Shanks, Arbitrarily polarized slot array, IRE Wescon Record, pt. 1, 157 (1958).
- Hu, Ming-Kuei, Study of near-zone fields of large aperture antennas, Syracuse Univ., Final Rept. RADC-TR-57-126A and B (Apr. 1957).
- Kelly, K. C., Recent annular slot array experiments, IRE Conv. Record, pt. 1, 144 (1957).
- King, R. W. P., Linear arrays: Currents, impedances, and fields, I, IRE Trans. **AP-7**, S440 (1959).
- Kraus, J. D., Radio telescope antennas of large aperture, Proc. IRE **46**, 92 (1958).
- Kurtz, L. A., and J. S. Yee, Second-order beams of two-dimensional slot arrays, IRE Trans. **AP-5**, 356 (1957).
- Li, Tingye, A study of spherical reflectors as wide-angle scanning antennas, IRE Trans. **AP-7**, 223 (1959).
- Linder, W. J., and H. L. Steele, Estimating voltage breakdown performance of high altitude antennas, IRE Wescon Record, pt. 1, 9 (1959).
- Marston, A. E., and R. M. Brown, Jr., The design of mirror-lenses for scanning, Naval Research Lab., Rept. 5173 (Aug. 1958).
- Mavroides, W. G., and J. H. Provencher, Side lobe reduction on the torus, AFCRC, Rept. TM-58-107 (Apr. 1958).
- Mayes, P. E., and W. D. James, Pattern synthesis with small radiating slots in a prescribed conducting surface, Univ. Ill. on subcontract to Univ. of Mich., PO 154216 under Hughes Aircraft Co. Contract AF33 (038) 28634 (Feb. 1958).
- Miller, R. E., et al., A rapid scanning phased array for propagation measurements, IRE Wescon Record, pt. 1, 184 (1958).
- Mitra, Raj., On the synthesis of strip sources, Ant. Lab., Univ. Ill. TR44 (Dec. 1959).
- Morgan, S. P., Generalizations of spherically symmetric lenses, IRE Trans. **AP-7**, 342 (1959).
- Proctor, E. K., and M. H. Rees, Scanning lens design for minimum mean-square phase error, IRE Trans. **AP-5**, 348 (1957).
- Rondinelli, L. A., Effects of random errors on the performance of antenna arrays of many elements, IRE Conv. Record, pt. 1, 174 (1959).
- Rotman, W., Wide-angle scanning with microwave double-layer pillboxes, IRE Trans. **AP-6**, 96 (1958).
- Schell, A. C., and E. L. Bouche, A concentric loop array, IRE Wescon Record, pt. 1, 212 (1958).
- Seshadri, S. R., and K. Iizuka, A dipole antenna coupled electromagnetically to a two-wire transmission line, IRE Trans. **AP-7**, 386 (1959).
- Shanks, H. E., and V. Galindo, Ferrite excited slots with controllable amplitude and phase, IRE Conv. Record, pt. 1, 88 (1959).
- Sletten, C. J., et al., New method of antenna array synthesis applied to generation of double-step patterns, IRE Trans. **AP-5**, 369 (1957).
- Sletten, C. J., et al., A new satellite tracking antenna, IRE Wescon Record, pt. 1, 244 (1957).
- Sletten, C. J., et al., Amplitude scanning of antenna arrays, AFCRC, Rept. TR-58-124, (Mar. 1958).
- Sletten, C. J., et al., Corrective line sources for paraboloids, IRE Trans. **AP-6**, 239 (1958).
- Spradley, J. L., A volumetric electrically scanned two-dimensional microwave antenna array, IRE Conv. Record, pt. 1, 204 (1958).
- Stark, Louis, A helical line scanner for beam steering a linear array, IRE Trans. **AP-5**, 211 (1957).
- Swarup, G., and K. S. Yang, Interferometer phasing problems at microwave frequencies, IRE Wescon Record, pt. 1, 17 (1959).
- Tang, Raymond, A slot with variable coupling and its application to a linear array, Rept. RLM(M)56-15, Hughes Aircraft Co.
- Tanner, R. L., Precipitation particle impact noise in aircraft antennas, IRE Trans. **AP-5**, 232 (1957).
- Unz, H., Determination of a current distribution over a cone surface which will produce a prescribed radiation pattern, IRE Trans. **AP-6**, 182 (1958).
- Wait, J. R., and James Householder, Pattern synthesis for slotted-cylinder antennas, J. Research NBS **63D**, 303 (1959).
- Wilson, A. C., High gain, very low side-lobe antenna with capability for beam slewing, private communication (May 1959).

5. Small Aperture Antennas

Low gain antennas for air and space vehicles. Antennas discussed in this section are primarily simple element types such as loops, dipoles, and slots. In general, boundary value problems, such as dipoles over reactive surfaces, are covered in the companion paper on Surface Waves. Ronold King and others at Cruft Lab. have investigated loop antennas carefully and have shown that the small loop contains small electric multipoles as well as the

magnetic dipole and that the loop equations reduce to those for the folded dipole as the length approaches zero [King, 1959; Prasad, 1959]. Small antennas of both loop and dipole type have been treated by Wheeler [1959, 1958a]. For small coils or small loaded dipoles, the performance available is essentially dependent upon length and volume and independent of configuration within the two types. Oliner [1957] has obtained an improved formulation for series and shunt waveguide slots using a variational technique. Wall thickness is taken into account by a microwave network. Shape of the slot end is also considered. Radiation from the end of a waveguide loaded with ferrite has been attacked [Tyras, Held, 1958] in a manner similar to an earlier paper of Angelakos.

Radiation from many types of cylindrical structures including wedges, cylinders, half planes, and sheets has been covered in a book by Wait [1959a]. This work is an excellent compendium of the state of the art and describes in detail the mathematical techniques and solutions. Other papers include slots on spheres [Mushiake, Webster, 1957], spheroidal dipoles [Weeks, 1958; Flammer, 1957], and radial dipoles on a circular cylinder [Levis, 1959]. Wait and collaborators have studied slotted circular [Wait, 1957], elliptic [Wait, Mientka, 1959], and dielectric coated [Wait, Conda, 1959] cylinders. The circularly polarized element consisting of crossed slots on a waveguide broad wall has been investigated by Simmons [1957]. The way in which a curved and/or lossy surface effects an antenna pattern has been studied by Wait and Conda [1958], using a combination of residue series, Fock functions, and geometrical optics. An electric monopole exciting a finite cone has been studied by Adachi and Kouyoumjian [1959]. Cruzan [1959] and Weeks [1957] have treated the receiving loop antenna with a ferrite core. The important parameters for the receiving loop are the area, number of turns, and effective permeability [Wheeler, 1958b]. Polk [1959] has studied ferrite loaded biconical dipole antennas and shows, as predicted by Schelkunoff and Friis [1952], that in general, effective length is decreased by the addition of ferrite or dielectric loading except for high loss supergain conditions which are undesirable. Grimes [1958] reaches similar conclusions. A closely related subject is that of an antenna immersed in a lossy medium. Wait [1959b, 1958] shows that the field of a buried loop is essentially that of a loop on the surface plus an exponential attenuation with depth.

Air frame antennas using shunt or notch feeding have been put on a sound engineering basis by Tanner [1958]. This is a definitive paper and summarizes these types of antennas. An investigation similar to that by Infeld [1947] of a few years back on the input admittance singularity of a dipole antenna due to the delta function generator has appeared [Wu, King, 1959]. In this paper, as in Infeld, the admittance is separated into a gap capacity term and a bounded term.

In the larger realm of antenna systems,

a paper by Turner [1959] summarizes several types of submarine communication antenna systems. Antenna multicoupler systems, so important in LF and HF ranges where antenna efficiencies are typically very low, have been extensively studied in a series of reports from Stanford Research Institute [Cline]. This series is an excellent summary of the state of the art in exciting HF airframe or satellite antennas.

Medium gain antennas. Klopfenstein [1957] and Woodward [1957] have carefully reinvestigated corner reflectors with various dipole and apex angles both from the sophisticated dyadic Green's function and from the image point of view. Cottony and Wilson [1958] present excellent design curves; other limited data also are available [Neff, Tillman, 1959]. Rhombic antennas of large size have also been investigated in a paper by Decker [1959], which gives design for maximum gain. Design data for helical antennas for lengths up to 10λ has been augmented by Maclean and Kouyoumjian [1959]. They applied Sensiper's infinite helix solution and obtained results valid up to a length of 10λ . A new and very interesting antenna configuration is the trough waveguide invented by Rotman and Oliner [1958]. A continuous trough waveguide is suitable for end fire radiation and a periodic asymmetrical design covers a number of radiation directions including broadside [Rotman, Oliner, 1959]. Although the transverse resonance method is best applied to nonleaky structures, it has yielded good values for propagation characteristics in this case.

An excellent survey of the printed technique is given by McDonough et al. [1957]. They cover such different types as ladders, rhombics, cigars, and capacity-coupled collinear arrays. Another type of printed antenna is the sandwich wire antenna of Rotman and Karas [1957, 1959]. This is an array of undulating wire strips wherein each wire acts as a quasi-discrete leaky radiator.

Evaluation. A most important paper on the effect of satellite spin on radiation performance has been contributed by Bolljahn [1958]. He shows that when the satellite spin axis and the antenna axis are not aligned, the ground-received signal (with a CW signal radiated) splits into three spectral components. The variation of these with the geometry of the configuration is derived.

The evaluation of aircraft and satellite antennas has always been difficult, especially the comparison of different types of antennas, since impedance, pattern, and gain performance vary widely among types and even among variations within each type. This evaluation problem has now been satisfactorily solved by a series of papers. Lucke [1958] uses a channel capacity formula to weight patterns and impedances over frequency and space. Moore [1958] compares the various rating schemes, the three most important of which are the average channel capacity method of Lucke, the radiation pattern distribution function of Ellis, and the radiation pattern efficiency method of Granger. He shows that if carefully applied, all methods give

essentially similar results, and he therefore recommends use of the simplest method, that is, the radiation pattern efficiency technique. This defines the quality in terms of the fraction of power radiated in useful directions. Impedance compensation or broadbanding of HF antennas has long been an art without suitable boundaries. However, the broadbanding potential of such antennas has now been bounded by two important papers. Vassiliadis and Tanner [1957] have approximated the impedance by a rational algebraic function from which the broadbanding capability is readily determined. Levis [1957] has used a different approach, that of relating the impedance bandwidth to the far field polarization characteristics and to the stored energy. These papers allow determination of the best broadbanding available so that a bound can be placed on attempts to realize this performance physically. A final paper gives numerical integration computer techniques for antenna pattern calculations [Allen, 1959].

Summary. As the effect of the counterpoise shape and size upon antenna radiation pattern and impedance becomes better understood, it should be possible to devise quasi-empirical synthesis techniques which would allow optimum advantage to be taken of this effect. The search for new and advantageous radiator configurations, e.g., the sandwich-wire, should continue.

The authors thank Mary Lee Buschkotter for diligent effort in correcting and typing the manuscript.

References

- Adachi, S., et al., The finite conical antenna, IRE Trans. **AP-7**, S406 (1959).
- Allen, C. C., Numerical integration methods for antenna pattern calculations, IRE Trans. **AP-7**, S387 (1959).
- Bolljahn, J. T., Effects of satellite spin on ground-received signal, IRE Trans. **AP-6**, 261 (1958).
- Cline, J. F., et al., Design data for antenna-multicoupler systems, Stanford Research Inst., series of Sci. Rept. on AF 19(604)2247, AFCRC.
- Cottony, H. V., and A. C. Wilson, Gains of finite-size corner-reflector antennas, IRE Trans. **AP-6**, 366 (1958).
- Cruzan, O. R., Radiation properties of a thin wire loop antenna embedded in a spherical medium, IRE Trans. **AP-7**, 345 (1959).
- Decker, R. P., The influence of gain and current attenuation on the design of the rhombic antenna, IRE Trans. **AP-7**, 188 (1959).
- Flammer, C., The prolate spheroidal monopole antenna, Stanford Research Inst., Rept. AFCRC-TN-57-581 (June 1957).
- Grimes, D. M., Miniaturized resonant antenna using ferrites, J. Appl. Phys. **29**, 401 (1958).
- Infeld, L., The influence of the width of the gap upon the theory of antennas, Quart. Appl. Math. **5**, 113 (1947).
- King, R. W. P., The rectangular loop antenna as a dipole, IRE Trans. **AP-7**, 53 (1959).
- Klopfenstein, R. W., Corner reflector antennas with arbitrary dipole orientation and apex angle, IRE Trans. **AP-5**, 297 (1957).
- Levis, C. A., A reactance theorem for antennas, Proc. IRE **45**, 1128 (1957).
- Levis, C. A., Patterns of a radial dipole on an infinite circular cylinder: Numerical values, Ohio State Univ., Rept. 667-51 (Feb. 1959).
- Lucke, W. S., Antenna evaluation methods, IRE Trans. **AP-6**, 251 (1958).
- Maclean, T. S. M., and R. G. Kouyoumjian, Bandwidth of the uniform helical antenna, IRE Trans. **AP-7**, S379 (1959).
- McDonough, J. A., et al., Recent developments in the study of printed antennas, IRE Conv. Record, pt. 1, 173 (1957).
- Moore, E. J., Performance evaluation of HF aircraft antenna systems, IRE Trans. **AP-6**, 254 (1958).
- Mushiake, Y., and R. E. Webster, Radiation characteristics with power gain for slots on a sphere, IRE Trans. **AP-5**, 47 (1957).
- Neff, H. P., and J. D. Tillman, The design of the corner-reflector antenna, AIEE Trans. Comm. and Elect., **293** (July 1959).
- Oliner, A. A., The impedance properties of narrow radiating slots in the broad face of rectangular waveguide: theory and measurements, IRE Trans. **AP-5**, 4 (1957).
- Oliner, A. A., and W. Rotman, Periodic structures in trough waveguide, Polytech. Inst. Brooklyn, Rept. AFCRC-TN-58-195 (July 1958).
- Polk, C., Resonance and super-gain effects in small ferromagnetically or dielectrically loaded biconical antennas, IRE Trans. **AP-7**, S414 (1959).
- Prasad, S., Theory of corner-driven coupled square loop antennas, Cruft Lab., Rept. NR-371-016 (Feb. 1959).
- Rotman, W., and N. Karas, Printed circuit radiators: The sandwich wire antenna, Microw. J. **2**, 29 (1959).
- Rotman, W., N. Karas, The sandwich wire antenna: A new type of microwave line source radiator, IRE Conv. Record, pt. 1, 166 (1957).
- Rotman, W., A. A. Oliner, Asymmetrical trough waveguide antennas, IRE Trans. **AP-7**, 153 (1959).
- Schellkunoff, S. A., and H. T. Friis, Antennas theory and practice, p. 325 (John Wiley and Sons, Inc., New York, N.Y., 1952).
- Simmons, A. J., Circularly polarized slot radiators, IRE Trans. **AP-5**, 31 (1957).
- Tanner, R. L., Shunt and notch-fed HF aircraft antennas, IRE Trans. **AP-6**, 35 (1958).
- Turner, R. W., Submarine communication antenna systems, Proc. IRE **47**, 735 (1959).
- Tyras, G., G. Held, Radiation from a rectangular waveguide filled with ferrite, IRE Trans. **MTT-6**, 268 (1958).
- Vassiliadis, A., R. L. Tanner, Evaluating the impedance broadbanding potential of antennas, IRE Conv. Record, pt. 1, 108 (1957).
- Wait, J. R., A low-frequency annular-slot antenna, J. Research NBS, **60**, 59 (1958) RP2822.
- Wait, J. R., Electromagnetic radiation from cylindrical structures (Pergamon Press Inc., New York, N.Y., 1959a).
- Wait, J. R., Pattern of a flush-mounted microwave antenna, J. Research NBS, **59**, 255 (1957) RP2796.
- Wait, J. R., Radiation from a small loop immersed in a semi-infinite conducting medium, Can. J. Phys. **37**, 672 (1959b).
- Wait, J. R., A. M. Conda, Pattern of an antenna on a curved lossy surface, IRE Trans. **AP-6**, 348 (1958).
- Wait, J. R., and A. M. Conda, Radiation from slots on dielectric-clad and corrugated cylinders, J. Research NBS, **59**, 307 (1959) RP2802.
- Wait, J. R., and W. E. Mientka, Calculated patterns of slotted elliptic-cylinder antennae, Appl. Sci. Research **7**, sec. B, 449 (1959).
- Weeks, W. L., Dielectric coated spheroidal radiators, Univ. Ill., Rept. TR34 (Sept. 1958).
- Weeks, W. L., On the estimation of ferrite loop antenna impedance, Univ. Ill., Rept. TR17 (Apr. 1957).
- Wheeler, H. A., Fundamental limitations of a small VLF antenna for submarines, IRE Trans. **AP-6**, 123 (1958b).
- Wheeler, H. A., The radiansphere around a small antenna, Proc. IRE **47**, 1325 (1959).
- Wheeler, H. A., The spherical coil as an inductor, shield, or antenna, Proc. IRE **46**, 1595 (1958a).
- Woodward, O. M., A circularly-polarized corner reflector antenna, IRE Trans. **AP-5**, 290 (1957).
- Wu, T. T., and R. W. P. King, Driving point and input admittance of linear antennas, J. Appl. Phys. **30**, 74 (1959).

A Bibliography on Coherence Theory

G. B. Parrent, Jr.*

The inadequacy of the concepts of complete coherence and complete incoherence for the description of physically interesting phenomena was recognized by Verdet in 1869 when he showed that sunlight could produce fringes in a Young's interference experiment. After Verdet the development of coherence theory before 1940 was associated with the names of Von Laue [1907], Van Cittert [1935], and F. Zernike [1937]. Each of these investigators introduced his own, apparently different, formulation of the theory—each formulation being well suited to the problems considered by the particular investigator. In [1951], H. H. Hopkins again reformulated the theory in a manner which was particularly suited to the treatment of imaging problems. While each of these theories took account of intermediate states (partial coherence), they each suffered from one or more of the following restrictions: (1) They were applicable only to fields created by incoherent sources; (2) they were applicable only to nearly monochromatic fields; (3) they were formulated in terms of undefined complex functions.

These shortcomings were all removed in the new formulations of the theory of partial coherence introduced independently by Wolf [1955], and by Blanc-Lapierre and Dumontet [1955]. While these formulations are equivalent, it is much more convenient to work with the definitions introduced by Wolf. Working with the Wolf theory of partial coherence, Parrent [1958-1960] has extended the theory by finding several of the implications of the formulation and existence theorems for the basic functions of the theory and by showing how the approximate propagation laws of earlier theories are related to the solution of the wave equations that describe the propagation of partially coherent radiation. Using these theorems it was possible to formulate the imaging or mapping problem in a general and rigorous way for partially coherent illumination of arbitrary spectral width.

Thus, finally, the formulation and structure of a rigorous theory of partial coherence for scalar fields is complete enough to be considered as an available tool for the solution of problems involving statistical radiation. Part A of this bibliography provides a reasonably complete survey of the principal works on the subject.

The problem of discussing the behavior of, and formulating a calculus for, the description of vector fields is considerably more complex than the corresponding scalar problem. Consequently in this area very little has been accomplished by comparison. The general problem of discussing statistical vector fields consists in two essential concepts: Partial co-

herence (the correlation between the disturbance at two different points), and partial polarization (the correlation of the various components at the same point). Limiting our attention to a plane wave eliminates coherence problems and isolates partial polarization effects. Wolf has treated this class of problems at some length in the last few years, and recently Parrent and Roman have used the results of Wolf's work as a basis for constructing a matrix calculus for the study of partial polarization effects. Nonplane waves have not been extensively discussed as yet; however, Roman has succeeded in generalizing the Stokes parameters to a set applicable to nonplane waves. This is, of course, an important first step in the understanding of this field. Part B of this bibliography is an attempt to list the most important papers related to the description of statistical vector fields.

References

- Beran, M. J., *Optica Acta* (Paris) **5**, 88 (1958).
- Blanc-Lapierre, A., and P. Dumontet, The concept of coherence in optics, *Rev. opt.* **34**, 1 (1955).
- Born, M., and E. Wolf, *Principles of optics*, in particular ch. X (Pergamon Press, Inc., New York, N.Y., 1959).
- Dumontet, P. M., *Compt. rend. acad. sci.* (Paris) **238**, 1109 (1954).
- Dumontet, P. M., An object image correspondence in optics, *Optica Acta* (Paris) **2**, No. 2, 53 (1955).
- Fano, U., *Phys. Rev.* **93**, 121 (1954).
- Forrester, A. T., *Am. J. Phys.* **24**, 192 (1956).
- Hopkins, H. H., The concept of partial coherence in optics, *Proc. Roy. Soc. [A]* **208**, 263 (1951).
- Hopkins, H. H., Applications of coherence theory in optics, *J. Opt. Soc. Am.* **47**, No. 6, 508 (1957).
- Hopkins, H. H., *Proc. Roy. Soc. [A]* **217**, 408 (1953).
- Hopkins, H. H., *Proc. Roy. Soc. [A]* **231**, 91 (1955).
- Parrent, G. B., Jr., On the propagation of mutual coherence, *J. Opt. Soc. Am.* **49**, No. 8, 787 (1959).
- Parrent, G. B., Jr., Studies in the theory of partial coherence, *Optica Acta* (Paris) **6**, 285 (1959).
- Parrent and Roman, *Nuovo Cimento*, in press (1959).
- Steel, W. H., Scalar diffraction in terms of coherence, *Proc. Roy. Soc.* **574**, (1959).
- von Laue, M., *Ann. Phys. (Lipzig)* **23**, 1 (1907).
- Wolf, E., Coherence properties of partially polarized electromagnetic radiation, *Nuovo Cimento* **12**, 884 (1954).
- Wolf, E., A macroscopic theory of interference and diffraction of light from finite sources, I, *Proc. Roy. Soc. [A]* **225**, 96 (1954).
- Wolf, E., A macroscopic theory of interference and diffraction of light from finite sources, II, *Proc. Roy. Soc. [A]* **230**, 246 (1955).
- Wolf, E., *Nuovo Cimento* **10**, 1165 (1959).
- Wolf, E., Partially coherent optical fields, *Proc. Astro Opt.*, 59 (North Holland Publ. Co., Amsterdam, Netherlands, 1956).
- Wolf, E., Reciprocity inequalities, coherence time and bandwidth in signal analysis and optics, *Proc. Phys. Soc. (London)* **71**, 257 (1958).
- Zernike, F., *Physica* **5**, 785 (1938).

*Air Force Cambridge Research Center.

A Bibliography of Automatic Antenna Data Processing

C. J. Drane*

Many source detection applications have required ever higher antenna resolving power to distinguish distant sources from adjacent sources. In the optical region, the limitation to the increase of resolution has been the fluctuations existing in the earth's atmosphere. In the radio region, on the other hand, the most immediately apparent limitation to high resolution has been largely an economic one, the high cost of materials, as well as the difficult problem of construction tolerance. Additionally, recent work by [Skinner, 1960] has brought to light certain limitations on the gain and resolving power of antennas used for the reception of randomly varying signals due to statistical fluctuations of the source distribution and/or of the intervening medium characteristics.

In both the optical and radio regions interferometric techniques of one sort or another have yielded greater resolution than obtainable with equal size dishes or mattress arrays. Conventional interferometry suffers from pattern ambiguity, but diverse methods of data processing can be used to overcome this ambiguity, and to optimize different aspects of the antenna systems performance.

In view of the fact that the resolving power of an interferometer is generally proportional to l/λ , where l is the separation of interferometer elements while λ is the wavelength of radiation, it would seem that one should either increase the separation (baseline) or the frequency or both. To increase the frequency without limit would be impractical, first because of the decrease in source intensity with wavelength, then because the construction of large antennas and sensitive receivers is more difficult as the wavelength decreases, and finally because one sometimes wishes to study the diameter of a source as a function of frequency. All of these reasons favor increasing the interferometer baseline.

Mills [1952] describes a radio transmission link as a means of increasing the baseline of the interferometer—and thus the resolution of this instrument—with phase preserved in the following manner. The received signal frequency at one element of the interferometer is converted to a radiofrequency which is transmitted along with the local oscillator frequency over the same path to a receiver located near the other element. This signal is then reconverted to the original frequency and combined with the signal from the other antenna, the latter signal having been delayed by an amount equivalent to the propagation time across the radio link. There is, however, a limitation on the length of this radio link, which is introduced by the effect of turbulence of the intervening medium on the phase stability of the transmitted signal. When converting the

radio frequency signals at each antenna element of the interferometer to a low frequency, transmitting by a radio link one of these low-frequency signals as an amplitude modulation of a radiofrequency carrier, and cross-correlating the two low-frequency signals, it has been shown [Brown & Twiss, 1954; Brown et al., 1952] that several advantages arise. The relative phase of the two low-frequency signals is more easily preserved than that of the radio frequency signals, and it is equal to the latter in this particular arrangement. In view of this, the baseline of this interferometer can be made much larger, possibly indefinitely so by recording the interferometer element signals separately on magnetic tape and cross-correlating later. The system also happens to be less sensitive to ionospheric disturbances. One disadvantage is that the antenna yields information only about the amplitude distribution across the source. It is also relatively insensitive to weak sources inasmuch as the signal-to-noise ratio is proportional $(P_s/(P_r+P_c))^2$, whereas for the usual interferometer it is proportional to just $P_s/(P_r+P_c)$, where P_s =power in source signal, P_r =receiver noise power, P_c =cosmic noise power.

To improve the detection of weak "point" sources in the presence of much more intense extended sources or continuous background radiation, Ryle [1952] suggested the periodic introduction of a half wavelength of cable into one of the antenna lines of an interferometer. The interference pattern has an alternating component in addition to a steady component as a result of the alternately in-phase and out-of-phase relationship between the two antennas. Upon separating the alternating term from the steady one by means of a phase-sensitive detector, one can separate the background radiation from the "point" sources. Additionally, this system provides a means of more accurate determination of the position of radio sources in such a way as to be reasonably independent of rapid variations in the intensity of the radiation. The improvement of the ability to detect and localize weak signals by using correlators has been investigated by Faran and Hills [1952]. They have pointed out that in some instances signal-to-noise ratios can be improved in some interferometers, but by no more than 3 db, while in others a decrease in this ratio is seen, compared to a conventional antenna system. Any disadvantage here may be offset in part at least by the opportunity to use much higher gain recording instruments after the correlator in view of the fact that the amount of background noise does not contribute largely to the average output of the correlator. They also suggest the possibility of trading signal-processing time for physical antenna size.

*Air Force Cambridge Research Center.

These systems previously described possess multiple principal lobes and are, hence, ambiguous when several sources are present. By considering interferometer elements whose patterns differ essentially from one another, unidirectional interferometer patterns can be obtained. Ryle suggested that a decrease in the solid angle of the principal lobe of the reception pattern could be obtained without necessarily increasing the total antenna area thus permitting an increase in the number of detectable sources. Mills and Little [1953] have emphasized that the number of discrete sources with intensities above the detectable threshold will normally greatly exceed the number which may be separately resolved, so that one may attempt to design antennas of increased resolving power but relatively low gain that may lack very little of the usefulness of conventional antennas, and cost a great deal less. They have introduced a system consisting of two linear arrays mutually perpendicular in the form of a cross, such that phase centers are coincident. When the technique of phase switching of the signal in one antenna channel is coupled with synchronous detection of the product of the fan-shaped patterns of the two antennas, a pencil-shaped single-lobed pattern is produced. Covington and Broten [1957] have investigated an interferometer similarly composed of two dissimilar linear antenna elements; however, these are arranged along the same axis end-to-end. The two elements, one a nonresonant slotted waveguide array, the other a two-element interferometer, are coupled by a rotary phase shifter, to produce upon synchronous detection of the alternating component in the radiation pattern a single-lobed fan-shaped beam with a twofold increase in resolving power in one plane over that of a uniform array of equal dimension. To produce a nonambiguous radiation pattern, also with an economy of the number of antenna elements, Band and Walsh [1959] have used two linear additive arrays of uniformly spaced nondirectional elements—the common spacing being different in each and greater than a wavelength—as inputs to a correlator. Nonambiguity was also achieved by them when they replaced one of the linear arrays by a closely spaced or continuous aperture antenna. These techniques have resulted in the use of fewer elements, as well as an improvement in signal-to-noise ratio over an equivalent additive array. For reasons of stability of the multiplication process, amplitude modulation is imposed on the radio frequency signal. The desired correlation signal is the output of an audio-filter tuned to the modulation frequency and following the multiplier.

Berman and Clay [1957] have considered non-uniformly-spaced omnidirectional detectors whose outputs are selectively multiplied together and time averaged according to a prescribed plan, such that a directional pattern results that is equivalent to that of a linear additive array of a larger number of elements. Here, too, the length of the multiplicative array often turns out to be half that of the equivalent one.

A comparison between the arrays of Faran and Hill and those of Berman and Clay has been made by Fakley [1959] for three applications: (a) The detection of a "point" source in a noisy background; (b) the resolution of two closely spaced point sources; and (c) the measurement of intensity distribution across an extended source. It was shown that the type of arrays described by Berman and Clay for four receiving elements, under idealized conditions, has no particular advantage over the other for the applications mentioned. It was also suggested that this conclusion could be extended to arrays consisting of more than four elements.

Drane [1959] has studied the coupling of a directional array with nonuniformly spaced omnidirectional elements after the fashion of Berman and Clay, but modified by the addition of continuously rotating phase shifters selectively used in conjunction with synchronous detection to yield nonambiguous radiation patterns. The suggested application has been to the tracking of moving targets which can be considered essentially "point" sources. Walsh and Band [1960] have also investigated such systems.

Time can be used as a degree of freedom supplementary to the three dimensions of space to achieve greater flexibility in the design of antennas. For example, it has been shown by Shanks and Bickmore [1959] that, in general, by periodic modulation of one or more of the antenna parameters (phase distribution, physical size, frequency, etc.) one obtains a temporally fluctuating radiation pattern. This pattern can be analyzed as an infinite sum of harmonics, and associated with each such frequency channel is a characteristic spatial distribution. They have applied such techniques to multipattern operation, simultaneous scanning [Shanks, 1959a], and sidelobe suppression [Shanks, 1959b].

Barber [1958] points out that on interpreting the "compound interferometer" of Covington and Broten as an array of essentially omnidirectional elementary detectors, two widely spaced ones forming the simple interferometer with several closely and uniformly spaced elements comprising the slotted waveguide, the receiving pattern can be considered the sum of all possible mean products of one element of the interferometer and one element of the long array. He suggests that one can also obtain the same members of the sum with several other configurations, all consisting essentially of two arrays in a line each having uniformly spaced elements of common spacing different from the other array of the configuration. The system with the fewest number of elements (for constant overall length) is that in which the number of detectors of one array differs from that of the other by at most unity. Covington and Broten [1958] have extended their system in just this fashion by adding two elements separated from each other and the extreme element of the simple interferometer by a distance equal to the length of the long array, i.e., by the separation of the interferometer elements. To ensure that all necessary signal products are obtained appropriate switches are used. It is to be noted that since the length of the long array remained

the same, the resolving power was doubled, but the analytical properties of the radiation pattern remained unchanged. In the system discussed by Drane the overall length is extended not by producing two different but uniformly spaced arrays, but by using a uniformly and closely spaced array (to simulate the continuous array), another array whose interelement spacing increases in accordance with a geometric progression, as well as appropriately placed frequency shifters. Dausin, Niebuhr, and Nilsson [1959] while examining the problem of the reception of wideband signals have arrived at just such an "optimum" spacing on considering elemental arrays of variable spacing with the elements coupled by matched filters.

The work of Kock and Stone [1958] on the equivalence between dimensional properties of antennas and frequency content of signal in the production of a given response is in essential agreement with the results of Dausin, Niebuhr, and Nilsson for multi-element arrays, wide-band sources, and with those of Covington and Broten, Drane, Walsh, and Band for complex interferometric arrays and monochromatic sources (artificially made multifrequency). They have shown that in a detection system antenna size and space complexity can be reduced for the detection of wide-band (continuous or discrete spectrum) signals by using a two-receiver cross-correlation antenna system. With such a system directional patterns equivalent to those characteristic of multielement, additive, narrow-band arrays are obtainable. Here, there exists the limitation imposed by the requirement that the antennas used in the interferometer complex be fairly broadband.

White, Ball, and Deckett [1959] have made a comprehensive study of nonlinear antennas of the various types considered above, comparing each one with linear antennas. They have found that the performance of any nonlinear antenna in the presence of continuous interference is inferior to a linear one in the same environment. Power gain and directivity of the nonlinear antenna are likewise generally inferior to those of the linear antenna. By artificially broadbanding the transmitted signal or confining the application to low-duty-cycle transmission these disadvantages may be made less significant. However, a nonlinear antenna of the space-coincidence type is described to provide a spatial selectivity not obtainable with a linear antenna.

We have been talking about situations in which it may be said that the data processing is done essentially automatically by the antenna system. Much work has been done and thoroughly discussed in the literature [Astia AD117067, 1957; Bracewell & Robert, 1954; Arsac, 1957] on the subject of the extraction of information about and reconstruction of the source intensity distribution from a knowledge of the information actually received by a conventional antenna, as well as of the properties (shape and aperture field distribution) peculiar to the antenna itself. Here, the term space-frequency—periodic spatial intensity distribution—is introduced. In both the optical and radio regions the receptor

acts effectively as a low pass space frequency filter whose cutoff frequency is proportional to the physical extent of the receptor's aperture. This provides a distinct limitation to the extent to which the source characteristics may be reconstructed from the signal distribution actually observed.

References

- Arsac, J., Application of mathematical theories of approximation to aerial smoothing in radio astronomy, *Australian J. Phys.* **10**, 16 (1957).
- Band, H. E., and J. E. Walsh, Correlation techniques applied to antenna pattern control, Pickard & Burns, Inc. (paper presented at URSI-IRE Meeting, San Diego, Calif., Oct. 1959).
- Barber, N. F., Compound interferometers, *Proc. IRE* (correspondence) **46** (1951) (1958).
- Berman, A., and C. S. Clay, Theory of time-averaged product arrays, *J. Acoust. Soc. Am.* **29**, 805 (1957).
- Bracewell, R. N., and J. A. Roberts, Aerial smoothing in radio astronomy, *Australian J. Phys.* **7**, 615 (1954).
- Brown, R. H., R. C. Jennison, and M. K. DasGupta, Apparent angular sizes of discrete radio sources, *Nature* **170**, 1061 (1952).
- Brown, R. H., and R. Q. Twiss, A new type of interferometer for use in radio astronomy, *Phil. Mag.* **45**, 663 (1954).
- Covington, A. E., and N. W. Broten, An interferometer for radio astronomy with a single-lobed radiation pattern, *IRE Trans.* **AP-5**, 247 (1957).
- Covington, A. E., and N. W. Broten, Compound interferometers, (author's comment), *Proc. IRE* (correspondence) **46** (1951) (1958).
- Dausin, L. R., K. E. Niebuhr, and N. J. Nilsson, The effects of wide-band signals on radar antenna design, Rome Air Development Center (Paper presented at WESCON, San Francisco, Calif., Aug. 1959).
- Drane, C. J., Jr., Phase-modulated antennas, Air Force Cambridge Research Center Tech. Rept. No. AFCRC-TR-59-138 (AD215374) (Apr. 1959).
- Fakley, D. C., Comparison between the performances of a time-averaged product array and an intraclass correlator, *J. Acoust. Soc. Am.* **31**, 1352 (1959).
- Faran, J. J., and R. Hills, The application of correlation techniques to acoustic receiving systems, Acoustics Research Lab. Harvard Univ., Tech. Memo. No. 28 (Nov. 1952).
- Kock, W. E., and J. L. Stone, Space-frequency equivalence, *Proc. IRE* (correspondence) **46**, 499 (1958).
- Mills, B. Y., Apparent angular sizes of discrete radio sources, *Nature* **170**, 1063 (1952).
- Mills, B. Y., and A. G. Little, A high-resolution aerial system of a new type, *Australian J. Phys.* **6**, 272 (1953).
- Proc. symp. communication theory and antenna design, Air Force Cambridge Research Center—Boston Univ., AFCRC-TR-57-105 Astia No. AD117067 (Jan. 1957).
- Ryle, M., A new radio interferometer and its application to the observation of weak radio stars, *Proc. Roy. Soc. (London)* **[A]** **211**, 351 (1952).
- Shanks, H. E., A new technique for electronic scanning, Hughes Aircraft Co. (Paper presented at URSI-IRE Meeting, 1959a San Diego, Calif., Oct. 1959a.)
- Shanks, H. E., Time domain sidelobe suppression, *Quarterly Rept., Air Force Contract No. AF30(602)-2021, RADC-TN-59-339*, 1959b (Sept. 1959b).
- Shanks, H. E., and R. W. Bickmore, Four-dimensional electromagnetic radiators, *Can. J. Phys.* **37**, 263 (1959).
- Skinner, T. J., The effect of partially coherent radiation on antenna gain and beamwidth, Air Force Cambridge Research Center (paper to be presented at URSI-IRE Meeting, Washington, D.C., May 1960).
- Walsh, J. E., and H. E. Band, Final report on interferometer development, Air Force Contract No. AF19(604)-4535, AFCRC TR-60-120 (Feb. 1960).
- White, W. D., C. O. Ball, and M. Deckett, Final report on nonlinear antenna study, Contract No. AF30(602)-1873, RADC-TR-59-179 (Sept. 1959).

Progress During the Past Three Years In Surface and Leaky Wave Antennas

F. J. Zucker*

This summary report begins where the previous URSI report on traveling wave antennas [Cottony and others, 1959] left off. The bibliography partially overlaps that in the previous reference: papers that were previously listed as reports, but have since appeared in the open literature, are listed here again with their journal references [Pease, 1958; Plummer, 1958; Hansen, 1957; Hougardy and Hansen, 1958; Plummer and Hansen, 1957; Friedman and Williams, 1958; Weeks, 1957; Goldstone and Oliner, 1959; Elliott, 1957; Kelley and Elliot, 1957; Hines and Upson, 1958].

Though both surface and leaky wave antennas belong to the general class of traveling wave radiators, they differ essentially in radiation mechanism, design principles, and performance characteristics. Surface waves are guided by the real or artificial dielectric structure along which they travel, and radiate only at discontinuities; usually there is just one of these, the termination. The total antenna pattern, which is endfire, is formed by superposition of terminal radiation and direct radiation from the feed. Beam shaping possibilities are limited. This type of radiator is nevertheless important whenever antenna height (as of a dish) must be traded for length. Leaky waves, by contrast, radiate continuously as they travel along the aperture, and very precise pattern control can be achieved. The beam is non-endfire and can be scanned over wide angles with negligible pattern deterioration.

1. Surface Wave Antennas

The *excitation* of surface waves, a problem that received considerable attention in the period before 1957 [Cottony and others, 1959; Friedman and Williams, 1958], was further examined. Wait [1957; 1958] gave a unified treatment of surface wave excitation by a dipole over diversely modified interfaces. While it had been known previously that efficiency of excitation depends on endfire directivity of the feed [Kay and Zucker, 1959], Brown now shows [1959] in a paper with interesting design implications that in the absence of supergaining, the efficiency of a source is limited to a maximum value that is a function of its physical size. In continuation of earlier work, Reynolds and Sigelman [1959] report that very clean $\sin \xi/\xi$ patterns are obtainable by using feeds that are distributed over the first third of the antenna length. Turning our attention to more specific structures, we find a precise analysis, using Wiener-Hopf techniques, of the launching of TM surface waves by a parallel plate waveguide (Angulo and Chang [1959a]). Duncan [1958] gives a Sommerfeld-type treatment of the excitation of dielectric rods; the mode he considers (lowest TM) is not that used in antenna applications, but this is the first time that the excitation problem on a rod has been tackled at all. In a paper of considerable practical interest, DuHamel and Duncan [1958] measure the efficiency with which diverse slot and wire feeds excite the HE_{11} mode on a rod.

The terminal discontinuity of a dielectric slab was examined in detail by Angulo [1957], who used variational techniques to find the terminal impedance and stationary phase methods for the radiation pattern. Angulo and Chang [1959b] calculated the terminal impedance of the lowest TM mode on a dielectric rod, Arbel [1959] analyzed the terminated

dielectric disk, and Kay [1959] gave a detailed description using Wiener-Hopf methods, of discontinuities on reactive surfaces, including the terminal discontinuity. He calculated and plotted radiation fields and the surface wave reflection and transmission coefficients.

The radiation mechanism of surface wave antennas can be viewed in two ways: As the superposition of radiation from two quasi-point sources—the feed and the terminal discontinuity—or as the Fourier integral over the current distribution along the antenna structure. As one finds them discussed in the literature, these two approaches lead to pattern calculations and design recommendations that partly contradict each other. Zucker [1958] showed, for a simple case, what approximations are involved in deriving each from the rigorous Green's function formulation and indicated how the two approaches are reconciled by taking these approximations into account. Schlesinger and Vigants [1959] improved the conventional aperture integration approach and were able to predict the pattern of dielectric rods with higher accuracy than before. Kay [1960] examined the near field of Yagis experimentally and gave physical details that connect the two approaches.

Optimum design principles of surface wave antennas are still largely based on cut-and-try methods. Ehrenspeck and Poehler [1959] showed how the Hansen-Woodyard condition for optimum gain must be modified for surface wave antennas, and Ehrenspeck and Kearns [1957] used parasitic side rows to suppress the sidelobe level of a Yagi to 30 db. Bandwidths of 2:1 were achieved with polyrods by Parker and Anderson [1957]. Optimum design principles based on this and earlier work were collected for systematic presentation in the Handbook of Antenna Engineering [Zucker, 1960].

One approach to *pattern control* is to place radiating discontinuities at discrete intervals along a surface wave antenna, for example by spiking a polyrod with

*Air Force Cambridge Research Center.

short pieces of wire, coupling being controlled by the depth and angle of insertion [Duncan and DuHamel, 1957]. A Goubau wire was similarly spiked [Scheibe, 1958]. A two-dimensional slot array excited by the surface wave on a dielectric image line, was shown by Cooper et al. [1958] to be capable of producing a broadside, endfire, or sidefire pattern, depending on the arrangement of the slots.

A second approach to pattern control consists in the use of variable impedance surfaces. Felsen [1957; 1959] gave the first rigorous solution to a problem of this type: he showed that on a surface with linearly increasing admittance (impedance) a TM (TE) surface wave propagates at the velocity of light with cylindrically spreading phase front, and without loss in total energy. This result is a key to the understanding of long tapered sections on surface wave antennas. Oliner and Hessel [1957] performed a detailed modal analysis of sinusoidally varying impedance sheets, showing that for periods shorter than about half a wavelength the surface supports a wave that is wholly trapped, while longer periods produce a leaky wave. An exact procedure for the design of an interface that supports a prescribed spectrum of waves (a "modulated" surface wave) has been given by Bolljahn [1959]. This important group of papers is the bridge between earlier work on surface wave modulation [Cottony and others, 1959], which did not concern itself with physical realizability, and the ultimate goal, which is pattern control—including the generation of non-endfire beams—with parasitically excited antenna structures.

A third approach to pattern control employs a distributed feed that is coupled to the antenna along its entire length. In continuation of earlier work Cottony and others [1959], Weeks [1957], and Giarola [1959] analyzed this problem in terms of coupled waveguide theory and obtained experimental results on a 40λ long Yagi coupled to a two-wire line. It is, however, doubtful whether practically useful means for independently controlling phase and amplitude along the structure can ever be found in this way.

Turning now to more specific structures, we find that the *dielectric rod* continues receiving attention. Kornhauser [1959] gives general results on the modal characteristics of rods of very general cross sections, and Mickey and Chadwick [1958] worked with rods of dielectric constants up to 165, which are very much thinner than polyrods (though just as long, for equal pattern performance). Reggia, Spencer, et al. [1957] excited arrays of ferrimagnetic rods inserted in a cavity or the narrow wall of a waveguide, and show diverse arrangements for rapid switching, turning the plane of polarization, lobing, etc. Work on broadband polyrods [Parker and Anderson, 1957] has already been mentioned.

The relation between the phase velocity of a surface wave on a Yagi and the height, diameter, and spacing of the elements was found experimentally in [Ehrenspeck and Poehler, 1959], supplementary data being furnished by Frost [1957] and Spector [1958]. Sengupta [1959], using a loaded transmission line

model, and Serracchioli and Levis [1959], using an approximate coupled element approach, calculated these relations theoretically; their results agree quite well with the experimental data. Very long Yagis are treated in Kay, [1960], and twisted Yagis (for circular polarization) in Reynolds and Sigelman, [1959].

A number of *new structures* were examined. Hyne-man and Hougardy [1958] invented an array of contiguous below-cutoff waveguides with closely-spaced, nonresonant, transverse slots. Sengupta [1958] discussed a zigzag antenna, and Querido [1958] gave an approximate treatment of the fakir's bed antenna (array of pins).

Area sources permit scanning in azimuth. Goldstone and Oliner [1959b] pointed out a general relation for surface waves that travel obliquely across a corrugated surface, supplementing earlier work [Hougardy and Hansen, 1958] on the scanning of such an antenna. Walter [1957] obtains 360° scan from a dielectric sheet Luneberg lens whose elevation pattern is shaped by the surface wave.

Volume arrays of endfire line sources have diverse applications. Ehrenspeck and Kearns [1959] used a Yagi-Adcock arrangement for satellite tracking. Kamen and Bogner [1959] are interested in the advantages, under certain circumstances, of arrays of cigar or Yagi antennas over dishes and have built several satellite tracking and communication arrays of this type. An interesting new structure, called the *backfire* antenna [Ehrenspeck, 1960], looks like a Yagi with a large flat reflector at the end opposite the feed, and produces gains up to 6 db above that of an equal-length surface wave line source.

The influence of a *finite ground plane* on the pattern of an endfire surface-wave antenna has been considered by Wait and Conda. The model they used was a conducting half-plane which itself could be located in the interface of an imperfectly conducting half-space [Wait and Conda, 1958]. The main effect of the truncation is to tilt the beam upward and to degrade the side lobe level.

Another related problem, treated by Cullen [1960], is the excitation of a corrugated cylinder by an axial slot. He showed for certain combinations of cylinder dimensions and surface impedance that a very pure $\cos m\phi$ pattern may be produced. This work has been extended by Wait and Conda [1960] who also treated elliptic cylinders with a nonuniform distribution of surface impedance.

2. Leaky Wave Antennas

Earlier work by Marcuvitz [IRE Trans., 1959] and Barone [IRE Trans., 1959] has clarified the manner in which leaky waves, in spite of their nonspectral nature, enter in the description of the total field of a source above an interface. Barone and Hessel [1958] continue this work for the case of an electric line source over a dielectric slab.

To calculate the parameters of leaky waves, Goldstone and Oliner [1959a; 1958] introduce a

perturbation procedure that is very much simpler than solving directly the complicated transcendental equations that arise in these problems.

Attention has focused principally on four groups of leaky wave structures. The *asymmetric trough waveguide* was analyzed by Rotman and Oliner [1959], and applications were made by Rotman and Naumann [1958] that include positioning the beam in the broadside region by periodically reversing the deep and shallow side of the trough. Unlike conventional slot antennas, the periodically asymmetric trough guide can be scanned through broadside.

The *transverse wire grid* antenna developed by Honey [1959] has excellent frequency scanning properties (no beam deterioration from 30° to 70° off endfire), and allows precise pattern control. It has been used as an X-band area source [Honey, 1959], as a millimeter waveline source [Honey, 1960], as an area source curved on a cylindrical surface [Shimizu and Honey, 1960], and as a flat center-fed disk [Hill and Held, 1958].

Jones and Shimizu [1959] designed an area array of thick *transverse slots* which, in contrast to the wire grid, is vertically polarized. Hyneman [1959] gave a careful treatment of closely-spaced transverse slots in thin-walled rectangular waveguide. Earlier work on the "serrated" waveguide [Elliot, 1957; Kelly and Elliot, 1957] had treated the thick-walled case.

The longslot in waveguide, which had received much attention in Cottony and others [1959], was examined by Nishida [1959a] for the case when it is covered by a thin dielectric sheet. Nishida also analyzed the effect on leaky wave phase velocity and attenuation of coupling two parallel long slots in a plane [Nishida, 1959b] or on a cylinder [Nishida, 1959c].

As in the case of surface wave antennas, feeds can be designed for leaky waves that couple along the entire length of structure. The advantage in this instance is that the initial section of the leaky wave antenna would not have to carry as much power as it must when fed from one end. Barkson [1957], with this goal in mind though confining himself to a shielded case, analyzed the coupling of rectangular waveguides through a common broad wall with non-resonant transverse slots. MacPhie [1959] examined a radiating coupled structure, and by varying the coupling region achieved mechanical beam scanning.

3. Assessment and Predictions

Although the launching of surface waves, and their radiation from the terminal discontinuity, have each been separately analyzed in considerable detail, the combined and much more difficult problem of a source exciting an impedance structure of finite length has not yet been tackled. This ought to be done.

Attempts will probably be made to place the optimum design of surface wave antennas on a firm theoretical basis. Now that rigorous results are available on tapered impedance surfaces, for example, there is hope that an explanation can be found for the

cut-and-dry rule that, for maximum gain, the taper should be short, for minimum sidelobes longer, and for wide bandwidth as long as the antenna itself.

Antenna structures that combine broadside aperture and endfire line source features (such as the backfire antenna) will receive attention. An effort should be made to synthesize artificial or natural dielectrics with more broadband dispersion characteristics than those of present structures.

Variable impedance surfaces will be used in attempts to diversify the pattern potentialities of surface wave antennas. Structures that permit independent control of amplitude and phase along the aperture are especially needed if modulation techniques are to become a practical reality.

The principal item of unfinished business in the theory of leaky wave antennas is the solution of a source problem over a complex impedance interface, on which the leaky wave—unlike in the case of the dielectric slab previously considered—is the dominant part of the total field.

An interesting problem that could be examined is the synthesis of complex impedance interfaces whose dispersion is such as to result in some prescribed variation of scan angle with frequency. Alternatively, the dispersion could perhaps be controlled (ferroelectrically or mechanically) to allow programed scanning. Scanning through broadside with periodically asymmetric structures will no doubt be fully exploited.

References

- Angulo, C. M., Diffraction of surface waves by a semi-infinite dielectric slab, *IRE Trans.* **AP-5**, 100 (1957).
- Angulo, C. M., and W. S. Chang, The launching of surface waves by a parallel plate waveguide, *IRE Trans.* **AP-7**, 359 (1959a).
- Angulo, C. M., and W. S. Chang, A variational expression for the terminal admittance of a semi-infinite dielectric rod, *IRE Trans.* **AP-7**, 207 (1959b).
- Arbel, E., Diffraction of surface waves by a dielectric disc, *MRI Rept. R-734-59*, PIB-662, Polytech. Inst. Brooklyn (1959).
- Barkson, J. A., Coupling of rectangular wave guides having a common broad wall which contains uniform transverse slots, *IRE 1957 WESCON Conv. Record*, pt. 1, 30 (1957).
- Barone, S., and A. Hessel, Leaky wave contributions to the field of a line source above a dielectric slab—Part II, *MRI Rept. R-698-59*, PIB-626, Polytech. Inst. Brooklyn (1958).
- Bolljahn, J. T., Synthesis of modulated corrugated surface-wave structures AFCRC-TN-59-973, Stanford Research Inst., Menlo Park, Calif. (1959).
- Brown, J., Some theoretical results for surface wave launchers, *IRE Trans.* **AP-7** (special supplement) S169 (1959).
- Cooper, H. W., M. Hoffman, and S. Isaacson, Image line surface wave antenna, 1958 *IRE Natl. Conv. Record*, pt 1, 230 (1958).
- Cottony, H. V., R. S. Elliot, E. C. Jordon, V. H. Rumsey, K. M. Siegel, J. R. Wait, and O. C. Woodyard, *USA Natl. Comm. Rept. URSI Subcomm. 6.3 Antennas and Waveguides*, and Annotated Bibliography, *IRE Trans.* **AP-7**, 87 (1959).
- Cullen, A. L., Surface-wave resonance effect in a reactive cylindrical structure excited by an axial line source, *J. Research NBS* **64D**, 13 (1960).
- DuHamel, R. H., and J. W. Duncan, Launching efficiency of wires and slots for a dielectric rod waveguide, *IRE Trans.* **MTT-6**, 277 (1958).
- Duncan, J. W., and R. H. DuHamel, A technique for controlling the radiation from dielectric rod waveguides, *IRE Trans.* **AP-5**, 284 (1957).

- Duncan, J. W., The efficiency of excitation of a surface wave on a dielectric cylinder, Technical Report No. 32, Antenna Laboratory, Univ. of Illinois, Urbana, Ill. (1958).
- Ehrenspeck, H. W., and W. Kearns, Two-dimensional endfire array with increased gain and side lobe suppression, 1957 IRE WESCON Conv. Record, pt. 1, 217 (1957).
- Ehrenspeck, H. W., and H. Poehler, A new method for obtaining maximum gain from Yagi antennas, IRE Trans. **AP-7**, 379 (1959).
- Ehrenspeck, H. W., The backfire antenna, a new type of directional line source, Proc. IRE **48**, 109 (1960).
- Ehrenspeck, H. W., and W. J. Kearns, A Yagi-Adcock system for satellite-tracking, AFCRC-TR-59-374, Air Force Cambridge Research Center, Bedford, Mass. (1959).
- Elliot, R. S., Serrated waveguide—Part I: Theory, IRE Trans. **AP-5**, 270 (1957).
- Felsen, L. B., Field solutions for a class of corrugated wedge and cone surfaces, MRI Electrophys. Group Memo No. 32, Polytech. Inst. Brooklyn (1957).
- Felsen, L. B., Electromagnetic properties of wedge and cone surfaces with a linearly varying surface impedance, IRE Trans. **AP-7**, (special supplement), S231 (1959).
- Friedman, B., and W. E. Williams, Excitation of surface waves, Proc. IEE, pt. C, Monograph No. 277R (1958).
- Frost, A. D., Surface waves in Yagi antennas and dielectric waveguides, AFCRC-TR-57-368, Tufts Univ., Medford, Mass. (1957).
- Giarola, A. J., Continuously excited traveling wave antennas, AFCRC-TN-59-369, Seattle Univ., Seattle, Wash. (1959).
- Goldstone, L. O., and A. A. Oliner, Leaky wave antennas II: Circular waveguides, MRI Rept. R-629-57, PIB-557, Polytech. Inst. Brooklyn (1958).
- Goldstone, L. O., and A. A. Oliner, Leaky wave antennas I: Rectangular waveguides, IRE Trans. **AP-7**, 307 (1959a).
- Goldstone, L. O., and A. A. Oliner, A note on surface waves along corrugated structures, IRE Trans. **AP-7**, 274 (1959b).
- Hansen, R. C., Single slab arbitrary polarization surface wave structure, IRE Trans. **MTT-5**, 115 (1957).
- Hill, R. V., and G. Held, A radial surface wave antenna, TR-No. 27, Univ. Washington, Seattle, Wash. (1958).
- Hines, J. N., and J. Upson, A line source with variable polarization, IRE Trans. **AP-6**, 152 (1958).
- Honey, R. C., A flush-mounted leaky-wave antenna with predictable patterns, IRE Trans. **AP-7**, 320 (1959).
- Honey, R. C., L. A. Robinson, and J. K. Shimizu, Third annual report, project 1954, Stanford Research Inst., Menlo Park, Calif. (1960).
- Hougardy, R. W., and R. C. Hansen, Scanning surface wave antennas, IRE Trans. **AP-6**, 370 (1958).
- Hyneman, R. F., and R. W. Hougardy, Waveguide loaded surface wave antenna, 1958 Natl. Conv. Record, pt. 1, 225 (1958).
- Hyneman, R. F., Closely-spaced transverse slots in waveguide, IRE Trans. **AP-7**, 335 (1959).
- Jones, E. M. T., and J. K. Shimizu, A wide-band transverse-slot flush-mounted array, AFCRC-TN-59-975, Stanford Research Inst., Menlo Park, Calif. (1959).
- Kamen, I., and R. Bogner, Antenna array for satellite tracking and communication, GB Electron. Corp., Garden City, N.Y. (1959).
- Kay, A. F., Scattering of a surface wave by a discontinuity in reactance, IRE Trans. **AP-7**, 22 (1959).
- Kay, A. F., Yagi antenna study, TRG-SR-121-1, Tech. Research Group, Inc., Somerville, Mass. (1960).
- Kelly, K. C., and R. S. Elliot, Serrated waveguide—Part II: Experiment, IRE Trans. **AP-5**, 276 (1957).
- Kornhauser, E. T., On the discrete spectrum for dielectric rods of arbitrary cross section, AFCRC-TN-59-146, Sci. Rept. AF-4561/3, Brown Univ., Providence, R. I. (1959).
- MacPhie, R. H., Use of coupled waveguides in a traveling wave scanning antenna, Antenna Lab. Rept. No. 36, Univ. Illinois, Urbana, Ill. (1959).
- Mickey, L. W., and G. G. Chadwick, Closely spaced high dielectric constant polyrod arrays, 1958 IRE Natl. Conv. Record, pt. 1, 213 (1958).
- Nishida, S., Theory of thin dielectric cover on slitted rectangular waveguide antenna, MRI Rept. R-754-59, PIB-682, Polytech. Inst. Brooklyn (1959a).
- Nishida, S., Coupled leaky waveguides, I: Two parallel slits in a plane, MRI Rept. R-732-59, PIB-660, Polytech. Inst. Brooklyn (1959b).
- Nishida, S., Coupled leaky waveguides, II: Two parallel slits in a cylinder, MRI Rept. R-746-59, PIB-674, Polytech. Inst. Brooklyn, (1959c).
- Oliner, A. A., and A. Hessel, Guided waves on sinusoidally-modulated reactance surfaces, IRE Trans. **AP-7**, (special supplement) S 201 (1957).
- Parker, C. F., and R. J. Anderson, Constant beamwidth antennas, 1957 IRE Natl. Conv. Record, pt. 1, 87 (1957).
- Pease, R. L., On the propagation of surface waves over an infinite grounded ferrite slab, IRE Trans. **AP-6**, 13 (1958).
- Plummer, R. E., Surface-wave beacon antennas, IRE Trans. **AP-6**, 105 (1958).
- Plummer, R. E., and R. C. Hansen, Double-slab arbitrary-polarization surface-wave structure, Proc. IEE, pt. C, Monograph 238R (1957).
- Querido, H. B., Surface wave fields and phase velocity variation of grounded dielectric sheets and of periodic structures of metal posts on a ground plane, Antenna Lab. Rept. No. 667-46, Ohio State Univ. Research Foundation, Columbus, Ohio (1958).
- Reggia, F., E. G. Spencer, R. D. Hatcher, and J. E. Tompkins, Ferrod radiator system, Proc. IRE **45**, 344 (1957).
- Reynolds, D. K., and R. A. Sigelman, Research on traveling wave antennas, AFCRC-TR-59-160, Seattle Univ., Seattle, Wash. (1959).
- Rotman, W., and S. J. Naumann, The design of trough waveguide antenna arrays, AFCRC-TR-58-154, Air Force Cambridge Research Center, Bedford, Mass. (1958).
- Rotman, W., and A. A. Oliner, Asymmetrical trough waveguide antennas, IRE Trans. **AP-7**, 153 (1959).
- Scheibe, E. H., Final Report, Contract No. DA 36-039-sc-71158, Univ. Wisconsin, Madison, Wisc. (1958).
- Schlesinger, S. P., and A. Vigants, HE₁₁ excited dielectric surface wave radiators, AFCRC-TN-59-573, School of Engineering, Columbia Univ., New York, N.Y. (1959).
- Sengupta, D. L., The radiation characteristics of a zig-zag antenna, IRE Trans. **AP-6**, 191 (1958).
- Sengupta, D. L., On the phase velocity of wave propagation along an infinite Yagi structure, IRE Trans. **AP-7**, 234 (1959).
- Serrachioli, F., and C. A. Levis, The calculated phase velocity of long end-fire uniform dipole arrays, IRE Trans. **AP-7** (special supplement), S 424 (1959).
- Shimizu, J. K., and R. C. Honey, Stanford Research Inst., Menlo Park, Calif. (to be published in 1960).
- Spector, J. O., An investigation of periodic rod structures for Yagi aerials, Proc. ICC, pt. B, 105, 38 (1958).
- Walter, C. H., Surface wave Luneberg lens antenna, Antenna Lab. Rept. No. 667-32, Ohio State Univ. Research Foundation, Columbus, Ohio (1957).
- Wait, J. R., Excitation of surface waves on conducting, stratified, dielectric-clad, and corrugated surfaces, J. Research NBS **59**, 365 (1957) RP2807.
- Wait, J. R., Guiding of electromagnetic waves by uniformly rough surfaces, IRE Trans. **AP-7** (special supplement), S 154 (1959).
- Wait, J. R., and A. M. Conda, The patterns of a slot-array antenna on a finite imperfect ground plane, Proc. Intern. Congr. UHF Circuits and Antennas, Oct. 1957 (in special issue of L'onde Elec., No. 376, Bis, 1958).
- Wait, J. R., and A. M. Conda, On the resonance excitation of a corrugated cylinder antenna, Sci. Rept. No. 7, Nov. 1959 (AFCRC-TN-59-969) (to be published Proc. Inst. Elect. Engrs., sec. C, 1960).
- Weeks, W. L., Coupled waveguide excitation of traveling wave antennas, 1957 IRE WESCON Conv. Record, pt. 1, 236 (1957).
- Zucker, F. J., A surface wave antenna paradox, presented at URSI Fall Meeting, Penn. State Univ. (1958) (to be published in 1960).
- Zucker, F. J., Surface and leaky wave antennas, ch. 16, Handbook of Antenna Engineering, H. Jasik, ed. (McGraw-Hill Book Co., Inc., New York, N.Y., 1960).

- Mitra, R., The finite range Wiener-Hopf integral equation and a boundary value problem in a waveguide, IRE Trans. **AP-7** (1959).
- Kay, I., Fields in the neighborhood of a caustic, New York Univ., Inst. Math. Sci., Rept. EM-138 (Sept. 1959).
- Felsen, L.B., and S.N. Karp, Relation between a class of two-dimensional and three-dimensional problems, Polytech. Inst. Brooklyn, Microw. Research Inst., Rept. R-694-58, PIB-622 (Jan. 1959).
- Noble, B., The potential and charge distribution near the tip of a flat angular sector, New York Univ., Inst. Math. Sci., Rept. EM-135 (May 1959).
- Hochstadt, H., Some diffraction by convex bodies, Arch. Rat. Mech. Anal. **3**, No. 5 (1959).
- Felsen, L. B., Radiation of sound from a vibrating wedge, Polytech. Inst. Brooklyn, Microw. Research Inst., Rept. R-613-57, PIB-541 (Oct. 1957).
- Unz, H., Diffraction of electromagnetic waves by an aperture in a plane screen, Univ. Kansas, Dept. Elec. Eng. (Dec. 1957).
- Wait, J. R., The transient behavior of the electromagnetic ground wave on the earth, IRE Trans. PGAP **AP-5** (Apr. 1957).
- Karp, S. N., Diffraction of a plane wave by a unidirectionally conducting half plane, New York Univ., Inst. Math. Sci., Rept. EM-108 (Aug. 1957).
- Tang, C. L., Backscattering from dielectric coated infinite cylindrical obstacles, J. Appl. Phys. **28**, No. 5, pp. 628-633 (May 1957).
- Adey, A. W., Field of a dielectric-loaded infinite corner reflector, Can. J. Phys. **36**, No. 4, pp. 438-495 (Apr. 1958).
- Heins, A. E., and S. Silver, Comments on the treatment of diffraction of plane waves: addendum to The edge condition and field representation theorems in the theory of electromagnetic diffraction, Proc. Cambridge Phil. Soc. **54**, pt. 1, pp. 131-133 (Jan. 1958).
- Kear, G., The scattering of waves by a large sphere for impedance boundary conditions, Ann. Phys. (New York) **6**, No. 1, pp. 102-113 (Jan. 1959).
- Radlow, J., Diffraction of a dipole field by a unidirectionally conducting semi-infinite plane screen, Quart. Appl. Math. **17**, No. 2 (July 1959).
- Keller, J. D., and B. Levy, Decay exponents and diffractions coefficients for surface waves on surfaces of non-constant curvature, New York Univ., Inst. Math. Sci., Rept. EM-147 (Oct. 1959).
- Kodis, R. D., On the Green's function for a cylinder, Brown Univ., Div. Eng., Sci. Rept. 1391-A (Oct. 1957).
- Yang, C. H., On some Fredholm integral equations arising in diffraction theory, New York Univ., Inst. Math. Sci., Research Rept. BR-31 (Aug. 1959).
- Rubinow, S. I., and J. B. Keller, Asymptotic solution of eigenvalue problem, New York Univ., Research Rept. CX-38 (Feb. 1959).
- Keller, J. B., How dark is the shadow of a round-ended screen?, New York Univ., Rept. EM-119 (Oct. 1958).

1. Parametric Amplifiers

P. K. Tien and H. Heffner

1.1. General Theory and Historical Development

The parametric amplifier was first introduced to the microwave field in 1957 by Suhl. In his first paper [Suhl, 1957a], he proposed an equivalent circuit for a cavity type of parametric amplifier. It consists of two resonant circuits coupled to each other through a time-varying capacitor or inductor. The use of a ferromagnetic sample as a time-varying element was discussed. In his second paper [Suhl, 1957b], he theorizes in great detail on three different possible operations of a ferromagnetic amplifier; namely

- (a) Electromagnetic,
- (b) semielectromagnetic, and
- (c) magnetostatic.

Tien and Suhl [1958] then worked out the traveling wave version of the parametric amplifier. In their paper a propagating circuit loaded with time-varying reactor was studied. They found that, for optimum gain and bandwidth, the following conditions must be satisfied

$$(a) \omega = \omega_1 + \omega_2, (b) \beta = \beta_1 + \beta_2$$

and

$$(c) \frac{(d\omega)}{(d\beta)_1} = \frac{(d\omega)}{(d\beta)_2}$$

where ω_1 , ω_2 , and ω are, respectively, the signal, idler, and pump frequencies, and β_1 , β_2 , and β are their phase velocities. In a later paper, Tien [1958] investigated amplification and frequency conversion of propagating circuits including bandwidth, noise figure, and circuits of opposite group velocities. An alternative derivation of Tien's gain expression was derived by Chang [1959a].

The basic principles of parametric interaction are the Manley and Rowe relations. They were discussed in a paper [Manley, 1956] published in 1956, actually earlier than Suhl's invention. It stated that power at different frequencies measured at the terminals of a nonlinear reactance must obey certain relations which bear the names of the authors. Rowe [1958; Manley and Rowe, 1959] later published two papers discussing, respectively, the small signal theory and general properties of a nonlinear element. Pantell [1958] also studied the energy relations of a nonlinear resistive element. Some extensions of the

Manley-Rowe relations have been made by Yeh [1960] and by P. A. Sturrock [1959], and alternative derivations have been presented by Salzberg [1957] and Weiss [1957a].

An important calculation was carried out [Heffner and Wade, 1958] concerning noise of the parametric amplifiers. They found that noise generated in the idler circuit adds to the noise generated in the signal circuit. Under usual operating conditions, the noise figure of the parametric amplifier is

$$1 + \frac{\omega_1}{\omega_2}$$

instead of 1 for a noiseless amplifier. Here ω_1 is the signal frequency and ω_2 , the idler frequency. The signal and the idler circuits are assumed at the same temperature.

The parametric amplifiers so far described require a pump source at a frequency higher than that of the signal. A scheme was described by Bloom and Chang [1958] in which an effective pump of frequency 2ω is obtained by actually pumping at frequency ω , without providing any resonant circuit at 2ω . Another low-frequency pumping scheme was proposed by Hogan et al. [1958] and also independently by Heffner. In the latter scheme, the parametric amplifier involves four frequencies, and is sort of a modulator internally coupled with a basic amplifying unit. Those schemes are very interesting but are rather limited in practical applications.

A dispersionless parametric propagating circuit which carries an infinite number of mixed frequencies was analyzed by Roe and Boyd [1959]. They showed that when a sinusoidal signal is applied to the input end of such a circuit, the signal will contain more and more harmonics as it travels down the circuit and eventually becomes a chain of sharp pulses. Landauer [1960] also theorizes that such a dispersionless nonlinear transmission line may produce electromagnetic shock waves.

1.2. Ferromagnetic Amplifier—Theory and Experiment

A few months after Suhl's invention, Weiss [1957b] experimentally demonstrated the electromagnetic operation of the ferromagnetic amplifier. In the next year, Poole and Tien [1958] reported a ferromagnetic resonance frequency converter and obtained a fair agreement between the theory and the measurement.

Berk et al. [1958] reported a modified operation of ferromagnetic amplifiers. In their experiment, the ferromagnetic resonance is positioned at the idler frequency instead of the pump frequency as originally proposed by Suhl.

Ferromagnetic amplifier has not been very successful in the past because of excess loss at the ferromagnetic resonance. Both Weiss and Berk have reported a pump power in the kilowatt range which is much too large for practical applications. The situation is, however, being improved lately as new techniques are developed in reducing the linewidth of yttrium iron garnet. A linewidth of less than 1 oersted has been reported up to 59 kMc/s.

Very recently, Denton [1960] has constructed a c.w. ferromagnetic amplifier which is operated in magnetostatic modes. The amplifier requires only 500 mw of pump power. The pump frequency is 9196 Mc/s and the pump field is in parallel with the d-c biasing field. The signal and idler frequencies are respectively 4626 and 4570 Mc and are the resonance frequencies of the 310 and the 310 modes (Walker's magnetostatic modes). The sample is a single crystal yttrium iron garnet sphere of 0.043 in. in diameter and has a linewidth of 0.40 oersteds. A gain of 25 db is measured and the noise figure is below 12 db. Some additional considerations of the limitations on ferromagnetic amplifier performance has been given by Damon and Eshbach [1960].

1.3. Diode Amplifiers and Noise Figure Measurements

Early in 1956, Uhlir [1956] investigated the use of *p-n* junction devices for frequency conversion in communication systems. The first semiconductor parametric amplifier was, however, demonstrated by Hines [1957] after Suhl's invention. In 1958, a traveling wave parametric diode amplifier was constructed by Engelbrecht [1958]. Since then, the diode amplifier has attracted much attention in the field of low-noise devices.

Most of the noise figure measurements were made on the cavity type of diode amplifier, and may be outlined briefly below: A noise figure of about 3 db (double side-band operation) was reported by Herrmann, Uenohara, and Uhlir [1958] using silicon and germanium diffused *p-n* junction diodes and also gold bond germanium diodes. They also reported a noise figure of 2.5 db for up-frequency conversion from 460 to 9375 Mc/s. At the same time, Heffner and Kotzebue [1958] reported a noise figure of less than 4.8 db about 2 kMc/s using Western Electric 427A diodes. Salzberg and Sard [1958] reported an excess noise temperature of 30°K for up-frequency conversion from 1 to 21 Mc/s using Hoffman 1N470 silicon diodes. In 1959, Knechtli and Weglein [1959] reported an excess noise temperature of 50 °K (double side-band operation) at 3 kMc/s using gold bond germanium diodes refrigerated to liquid nitrogen temperature (78 °K). Lately, a noise figure of 0.6 db (or an excess noise temperature of 44 °K)

was reported by Uenohara and Bakanowski [1959] at 6 kMc/s using germanium diffused mesa-type *p-n* junction diodes refrigerated to 87 °K. The best noise figure so far measured is 0.3 db or 21 °K excess noise temperature for double side-band operation. This was obtained by Uenohara and Sharpless [1959] at 6 kMc/s using Ga-As point contact diodes refrigerated to 90 °K. Gallium arsenide diodes have many good features [Sharpless, 1959] including higher energy gap, larger electron mobility, and lower dielectric constant.

Other work on diode parametric amplifiers at various frequencies and with various noise figures have been reported by Brand et al. [1959], by Chang [1959], by Hsu [1959], by De Loach and Sharpless [1959a], by Lombardo [1959], by Lombardo and Sard [1959], and Kibler [1960]. The highest frequency amplifier reported up to now also used a Ga-As diode operated in a degenerate mode at a signal frequency of 11.55 kMc/s with a gain of 10 db, a bandwidth of 53 Mc/s and a measured double channel noise figure of 3.2 db. This was reported by De Loach and Sharpless [1959b].

The major noise in diode comes from the spreading resistance. With a spreading resistance, R_s , and an average shunt capacitance across the diode, C_0 , the figure of merit of the diode as a parametric amplifier element is

$$Q_d = \frac{1}{\omega_1 C_0 R_s}$$

Here ω_1 is the signal frequency. Uenohara in a recent paper [1960] has shown experimentally and theoretically that larger gains and lower noise figures are obtained with diodes of larger Q_d 's. From the definition of Q_d we may easily see that, for a particular diode, the noise figure of the amplifier increases linearly with the frequency. It may, therefore, take years of research in material and fabrication technique before diode amplifiers may be used in millimeter wave regions as low-noise devices.

Several papers have investigated certain interesting relaxation oscillations which occur in diode amplifiers at very high pump powers. These oscillations make possible their operation as self-quenched superregenerative amplifiers. These properties have been discussed in papers by Bossard [1959], by Younger et al. [1959a; b], and by Endler et al. [1959]. There has also been an investigation of the saturation characteristics of cavity-type diode amplifiers with possible applications for phase distortionless limiting by Olson et al. [1959].

In addition to this work on various ways of using diodes in amplifiers, there has also been considerable effort devoted to investigating the properties of diodes as parametric elements and the design and characteristics which optimize the performance of these diodes [Giacoletto and O'Connell, 1956; Mortenson, 1959; Jorsboe, 1959; Spector, 1959; Firlie and Hayes, 1959; Bakanowski, 1959]. Along with this work should be mentioned the development of two new types of variable capacitance diodes. One of these

employs a $p-n-p$ configuration which gives a symmetrical capacity voltage characteristic and hence can produce capacity changes at a frequency twice that of the pump. This was developed by Gibbons and Pearson [1960]. The second type involves a thin nonconducting layer of oxide sandwiched between a metal on one side and a thin layer of lightly doped semiconductor on the other side. These devices can give extremely large changes of capacity with bias though they are somewhat more lossy than the normal junction diodes. The invention seems to have been made independently by Moll [1959] and by Pfann and Garrett [1959].

Among other investigations involving diode parametric amplifiers might be mentioned a significant improvement in the bandwidth of the cavity-type amplifier which was obtained by use of a filter structure as a signal and idle frequency circuit instead of single-tuned resonant cavities. This technique is described by Seidel and Herrmann [1959]. With this technique the authors have constructed a diode amplifier at UHF with a 40 percent bandwidth. Another interesting application involves using the parametric principle for a limiter. This is described by Siegman [1959]. If the parametric element is ideal, the limiting is phase distortionless. Experimental results on a limiter of this type are presented by Wolf and Pippin [1960].

1.4. Electron Beam Parametric Amplifier—Space-Charge Wave Parametric Amplifier and Adler's Tube

The first electron-beam parametric amplifier was demonstrated by Bridges [1958]. The beam is premodulated by a pump and then exposed to signal field of a double gap cavity specially designed to reduce noise. Later, Louisell and Quate [1958] suggested the use of space-charge waves in an electron beam as a variable reactance element. Such tubes have been constructed by Ashkin [1958] and show large amplification both at the lower and upper sidebands. Since the phase velocities of space-charge waves vary slowly with frequency, many sidebands are generated in the electron beam. As each sideband may be considered as separate idler circuit and all the idlers introduce additional noise, those tubes are relatively noisy. The problem has also been studied by many others [Cook and Louisell, 1958; Louisell, 1959; Haus, 1958; Wade and Adler, 1959; Wade and Heffner, 1958].

A much better noise figure is obtained from a tube which utilizes cyclotron motion of electrons. This type of tube was first proposed by Adler et al. [1958, 1959] and has been extensively studied by many others [Johnson, 1959; Siegman, 1959].

The Adler tube consists of three sections. The first section is a fast wave coupler which has been studied by Cuccia [1949], Ashkin, Louisell, and Quate [1960], and Gould [1959]. In the coupler, a signal fast cyclotron wave is excited and noise of the same wave in the electron beam is stripped. The electron beam then enters the next section known as the pump

cavity in which a quadrupolar electric field is excited by a local oscillator of the pump frequency. As the signal is amplified after the electron beam passes through the pump cavity, it finally reaches another coupler (the third section of the tube) where the electromagnetic power of the amplified signal is extracted.

A noise figure of 1.4 db has been obtained by Adler et al. [1959] in the 400 and 800 Mc/s region. A microwave version of the Adler tube was constructed by Bridges and Ashkin [1960], and a noise figure of 2.5 db was measured at 4 kMc/s.

References

- Adler, R., G. Hrbek, and G. Wade, A low-noise electron beam parametric amplifier, *Proc. IRE* **46**, 1756 (1958).
- Adler, R., G. Hrbek, and G. Wade, The quadruple amplifier, a low-noise parametric device, *Proc. IRE* **47**, 1713 (1959).
- Ashkin, A., Parametric amplification of space-charge waves, *J. Appl. Phys.* **29**, 1646 (1958).
- Ashkin, A., W. H. Louisell, and C. F. Quate, Fast wave couplers for longitudinal beam parametric amplifiers (to be published in *J. Electronics and Control*).
- Bakanowski, A. E., N. G. Cranna, and A. Uhler, Jr., Diffused silicon nonlinear capacitors, *IRE Trans. PGED-6*, 384 (1959).
- Berk, A. D., L. Kleinman, and C. E. Nelson, Modified semi-state ferrite amplifier, *WESCON Conv. Record* 2, pt. III, 9 (1958).
- Bloom, S., and K. K. N. Chang, Parametric amplifiers using low-frequency pumping, *J. Appl. Phys.* **29**, 594 (1958).
- Bossard, B. B., Superregenerative reactance amplifiers, *Proc. IRE* **47**, 1269 (1959).
- Brand, F. A., W. G. Matthei, and T. Saad, The reactatron—low noise, semiconductor diode, microwave amplifier, *Proc. IRE* **47**, 42 (1959).
- Bridges, T. J., and A. Ashkin, A microwave adler tube (to be published).
- Bridges, T. J., An electron beam parametric amplifier, *Proc. IRE* **46**, 494 (1958).
- Chang, N. C., Parametric amplification and conversion in propagating circuits using nonlinear reactances, *Proc. IRE* **47**, 2117 (1959a).
- Chang, K. K. N., and S. Bloom, Parametric amplifiers using low-frequency pumping, *Proc. IRE* **46**, 1383 (1958).
- Chang, K. K. N., Four terminal parametric amplifier, *Proc. IRE* **47**, 81 (1959b).
- Cook, J. S., and W. H. Louisell, Traveling-wave tube equations including the effect of parametric pumping.
- Cuccia, C. L., The electron coupler, *RCA Rev.* **10**, 270 (1949).
- Damon, R. W., and J. R. Eshbach, Theoretical limitations to ferromagnetic parametric amplifier performance, *IRE Trans. MTT-8*, 4 (1960).
- De Loach, B. C., and W. M. Sharpless, An X-band parametric amplifier, *Proc. IRE* **47**, 1664 (1959a).
- De Loach, B. C., and W. M. Sharpless, X-band parametric amplifier noise figures, *Proc. IRE* **47**, 2115 (1959b).
- Denton, R. T., A ferromagnetic amplifier using longitudinal pumping, *Proc. IRE* **48**, 937 (1960).
- Endler, H., A. D. Berk, and W. L. Whirry, Relaxation phenomena in diode parametric amplifiers, *Proc. IRE* **47**, 1375 (1959).
- Englebrecht, R. S., A low-noise nonlinear reactance traveling-wave amplifier, *Proc. IRE* **46**, 1655 (1958).
- Farle, T. E., and O. E. Hayes, Some reactive effects in forward biased junctions, *IRE Trans. PGED-6*, 330 (1959).
- Giacoletto, L. J., and J. O'Connell, A variable-capacitance germanium junction diode for UHF, *RCA Rev.* **17**, 68 (1956).
- Gibbons, J. F., and G. L. Pearson, P-N-P variable capacitance diodes, *Proc. IRE* **48**, 253 (1960).
- Gould, R. W., Traveling-wave couplers for longitudinal beam type amplifiers, *Proc. IRE* **47**, 419 (1959).

- Haus, H. A., The kinetic power theorem for parametric longitudinal electron beam amplifiers, *IRE Trans. PGED-5*, 225 (1958).
- Heffner, H., Stanford Univ.
- Heffner, H., and K. Kotzebue, Experimental characteristics of a microwave parametric amplifier using a semiconductor diode, *Proc. IRE* **46**, 1301 (1958).
- Heffner, H., and G. Wade, Gain, bandwidth, and noise characteristics of the variable-parameter amplifier, *J. Appl. Phys.* **29**, 1321 (1958).
- Herrmann, G. F., M. Uenohara, and A. Uhlir, Jr., Noise figure measurements on two types of variable reactance amplifiers using semiconductor diodes, *Proc. IRE* **46**, 1301 (1958).
- Hines, M. E., Amplification with nonlinear modulators, presented at Electron Tube Research Conf., Univ. Calif., Berkeley, Calif. (June 1957).
- Hogan, C. L., R. L. Jepsen, and P. H. Vartanian, A new type of parametric amplifier, *J. Appl. Phys.* **29**, 422 (1958).
- Hsu, H., Multiple frequency parametric devices, *Dig. Tech. Papers, 1959 Solid-State Circuits Conf.*, 12 (1959).
- Johnson, C. C., Theory of fast wave parametric amplification, *Tech. Memo. Hughes Aircraft Co.* (1959).
- Jorsboe, Helge, Space-charge capacitance of a P-N junction, *Proc. IRE* **47**, 591 (1959).
- Kibler, L. U., Parametric oscillations with point-contact diodes at frequencies higher than pumping frequencies, *Proc. IRE* **48**, 239 (1960).
- Knechtli, R. C., and R. D. Weglein, Low-noise parametric amplifier, *Proc. IRE* **47**, 585 (1959).
- Landauer, Rolf., Parametric amplification along nonlinear transmission lines, *J. Appl. Phys.* **31**, 479 (1959).
- Lombardo, P. P., Low-noise 400 Mc reactance amplifiers, *Dig. Tech. Papers, 1959 Solid-State Circuits Conf.*, 6 (1959).
- Lombardo, P. P., and E. W. Sard, Low-noise microwave reactance amplifiers with large gain bandwidth products, *IRE WESCON Conv. Record*, pt. 1, 83 (1959).
- Louisell, W. H., and C. F. Quate, Parametric amplification of space-charge waves, *Proc. IRE* **46**, 707 (1958).
- Louisell, W. H., A three frequency electron beam parametric amplifier, *J. Electronics and Control* **6**, 1 (1959), *Proc. IRE* **47**, 2016 (1959).
- Manley, J. M., and H. E. Rowe, Some general properties of nonlinear elements, I. General energy relations, *Proc. IRE* **44**, 904 (1956).
- Manley, J. M., and H. E. Rowe, General energy relation in nonlinear reactance, *Proc. IRE* **47**, 2115 (1959).
- Moll, J., Variable capacitance with large capacity change, *1959 IRE WESCON Conv. Record*, Pt. III (1959).
- Mortenson, K. E., Alloyed, thin-base diode capacitors for parametric amplification, *J. Appl. Phys.* **30**, 1542 (1959).
- Olson, F. A., C. P. Wang, and G. Wade, Parametric devices tested for phase distortionless limiting, *Proc. IRE* **47**, 587 (1959).
- Pantell, R. H., General power relationships for positive and negative nonlinear resistive elements, *Proc. IRE* **46**, 1910 (1958).
- Pfann, W. G., and C. G. B. Garrett, Semiconductor varactors using surface space-charge layers, *Proc. IRE* **47**, 2011 (1959).
- Poole, K. M., and P. K. Tien, A ferromagnetic resonance frequency converter, *Proc. IRE* **46**, 1387 (1958).
- Roe, G. M., and M. R. Boyd, Parametric energy conversion in distributed systems, *Proc. IRE* **47**, 1213 (1959).
- Rowe, H. E., Some general properties of nonlinear elements. II. Small signal theory, *Proc. IRE* **46**, 850 (1958).
- Salzberg, B., Masers and reactance amplifier—basic power relations, *Proc. IRE* **45**, 1544 (1957).
- Salzberg, B., and W. E. Sard, A low-noise wide-band reactance amplifier, *Proc. IRE* **46**, 1303 (1958).
- Seidel, H., and G. F. Herrmann, Circuit aspects of parametric amplifiers, *IRE WESCON Conv. Record*, Pt. II, 83 (1959).
- Sharpless, W. M., High frequency gallium arsenide point-contact rectifiers, *BSTJ* **38**, 259 (1959).
- Siegmán, A. E., Phase-distortionless limiting by a parametric method, *Proc. IRE* **47**, 447 (1959).
- Siegmán, A. E., The waves on a filamentary electron beam in a transverse field slow wave circuit, *Stanford Electron. Lab. Tech. Rept.* (1959).
- Spector, C. J., A design theory for the high-frequency P-N junction variable capacitor, *IRE Trans. PGED-6*, 347 (1959).
- Sturrock, P. A., Action-transfer and frequency-shift relations in the nonlinear theory of waves and oscillations, *Tech. Note, Stanford Univ. Microw. Lab. Rept.* 625 (1959).
- Suhl, H., A proposal for a ferromagnetic amplifier in the microwave range, *Phys. Rev.* **106**, 384 (1957a).
- Suhl, H., Theory of the ferromagnetic microwave amplifier, *J. Appl. Phys.* **28**, 1225 (1957b).
- Tien, P. K., Parametric amplification and frequency mixing in propagating circuits, *J. Appl. Phys.* **29**, 1347 (1958).
- Tien, P. K., and H. Suhl, A traveling-wave ferromagnetic amplifier, *Proc. IRE* **46**, 700 (1958).
- Uenohara, M., and A. E. Bakanowski, Low-noise parametric amplifier using GE P-N junction diode at 6 kmc, *Proc. IRE* **47**, 2113 (1959).
- Uenohara, M., and N. M. Sharpless, An extremely low-noise 6 kmc parametric amplifier using gallium arsenide point-contact diodes, *Proc. IRE* **47**, 2114 (1959).
- Uenohara, M., Noise consideration of the variable capacitance parametric amplifier, *Proc. IRE* **48**, 169 (1960).
- Uhlir, A., Jr., Two terminal p-n junction devices for frequency conversion and computation, *Proc. IRE* **44**, 1183 (1956).
- Wade, G., and R. Adler, A new method for pumping a fast space-charge wave, *Proc. IRE* **47**, 79 (1959).
- Wade, G., and H. Heffner, Gain, bandwidth and noise in a cavity-type parametric amplifier using an electron beam, *J. Electron. Control* **5**, 497 (1958).
- Weiss, M. T., Quantum derivation of energy relations analogous to those for nonlinear reactances, *Proc. IRE* **45**, 1012 (1957a).
- Weiss, M. T., Solid-state microwave amplifier and oscillator using ferrites, *Phys. Rev.* **107**, 317 (1957b).
- Wolf, A. A., and J. E. Pippin, A passive parametric limiter, *Dig. Tech. Papers, 1960 Solid-State Circuits Conf.*, 90 (1960).
- Yeh, Chai, Generalized energy relation of nonlinear reactive elements, *Proc. IRE* **48**, 253 (1960).
- Younger, J. J., A. G. Little, H. Heffner, and G. Wade, Superregenerative operation of parametric amplifiers and detectors, *IRE WESCON Conv. Record*, Pt. 1, 108 (1959b).
- Younger, J. J., A. G. Little, H. Heffner, and G. Wade, Parametric amplifiers as superregenerative detectors, *Proc. IRE* **47**, 1271 (1959a).

2. Microwave Properties of Ferrites

P. K. Tien and B. Lax

2.1. Finite Waveguide Components, Frequency Doubler and Mixer, and Ferromagnetic Amplifiers

Ferrite waveguide components have attracted much attention in the past. They may be classified in four groups:

- a. Devices using Faraday relation phenomenon,
- b. the nonreciprocal phase shifter in rectangular waveguide,
- c. the resonance isolator,
- d. the field-displacement isolator.

Major advancements in those devices were made between 1952-1956 and have been reviewed by many authors [Hogan, 1953; Rowan, 1953; Kales, 1954; Lax, 1954; Fox et al., 1955; Hogan, 1956; Lax, 1956; Clarricoats et al., 1956; Lax, 1958].

One of the important developments in nonreciprocal devices after 1956 is the coaxial line resonance isolator reported by Duncan et al. [1957]. They obtained more than 10.5-db isolation over 2-4 kMc/s with a forward loss of less than 0.8 db. In addition to broad banding, the coaxial configuration permits the construction of very compact devices. Usually ferrite effects in TEM propagating waves are reciprocal. Here a section of coaxial line is partially filled with dielectric. An almost true sense of circular polarization is created at the air-dielectric interface where two transversely magnetized ferrite rods provide nonreciprocal resonant elements. Obviously this new device offers many possibilities. A coaxial line nonreciprocal phase shifter is discussed by Sucher and Carlin [1957] and also by Button [1958]. Nonreciprocity in dielectric loaded strip line is investigated by Fleri and Hanley [1959].

There have been further investigations of phase shifters and isolators by various investigators [Boyet et al., 1959; Kravitz and Heller, 1959; Clavin, 1958; Seidel, 1957].

Another important development is the Y circulator reported by Chait and Curry [1959]. Such circulators are simple in construction and require little d-c magnetic field. They obtained 0.75-db insertion loss and more than 18-db isolation between 9200-9500 Mc/s. The circulator has been operated at 50 kMc/s peak power without breakdown. Y circulators in the millimeter wave range have been constructed by Thaxter and Heller [1960]. The 70-kMc/s circulator has an insertion loss about 1 db with a maximum isolation more than 40 db. The 140 kMc/s circulator has the insertion loss less than $\frac{1}{2}$ db with isolation about 20 db. The applied magnetic field in both cases is about 20 gauss.

There has been an application to strip line by Davis et al. [1960]. There have also been a series of investigations on the nature of the various modes in

a ferrite filled or partially filled waveguide [Angelakas 1959; Button, 1958; to Taichen, 1960]. A particularly interesting set of problems have arisen in connection with anomalous modes of propagation which apparently can exist in ferrite filled waveguides of arbitrarily small cross section [Seidel, 1957, 1956; Seidel and Fletcher, 1959; Fletcher and Seidel, 1959].

Beside waveguide components, the nonlinear property of the ferrites has been used for frequency doubling and mixing. The phenomenon can easily be analyzed from the equation of motion of the magnetization vector and has been investigated by Pippin [1956] and Stern and Persham [1957]. For the frequency doubler, the conversion efficiency is about -30 db at relatively low power levels. With a 30-kMc/s peak power at 9 kMc/s, Melcher, Ayres, and Vartanian [1957] were able to obtain 8-kw output at 18 kMc/s with an impressive conversion-efficiency of -6 db. A millimeter wave frequency doubler is reported by Ayres [1959]. He obtained more than 10-w output peak power at 2 mm.

Some work on generation of the third harmonic has also been reported [Skomal and Medins, 1959].

The ferromagnetic amplifiers are discussed under the topic "Parametric Amplifiers" and will not be repeated here.

2.2. Linewidth of Single Crystal Yttrium-Iron Garnet-Surface Imperfections and Rare Earth Impurities

The loss of a magnetized ferrite sample is measured by the linewidth at the resonance. It is therefore essential to have ferrites of narrow linewidths in order to reduce loss in devices. The linewidths of usual spinel ferrites are more than 25 oersted. The search for materials of better linewidths had not been successful until the discovery of a new class of magnetic oxides of cubic symmetry-yttrium-iron and rare earth iron garnets.

Yttrium-iron and rare earth iron garnets were discovered by Bertant and Forrat [1956] [Bertant and Pauthenet, 1956], and also independently though somewhat later by Geller and Gilleo [1957]. As first reported by Dillion [1957], this material has the following general properties:

- (a) Saturation magnetization $4\pi M_s \approx 1700$ gauss
- (b) resistivity in the order of 10^6 ohm-cm,
- (c) anisotropy at room temperature ≈ 90 oersteds,
- (d) linewidths at room temperature less than 10 oersteds, and
- (e) spectroscopic splitting factor $= 2.005 \pm 0.002$ at the room temperature.

Data reported by Dillion were taken at two frequencies, 9300 and 2400 Mc/s, and at various temperatures from 2.85 to about 540 °K. He found

that the linewidth increases as temperature decreases from the room temperature and reaches to a peak between 20 and 65 °K. The linewidth then decreases to about 5 oersteds at 2.85 °K. The behavior of the magnetocrystalline anisotropy is also very complex at low temperature. A more detailed report was given in one of his later papers [Dillion, 1958].

A major advance in linewidth of yttrium-iron garnet was achieved by LeCraw, Spencer, and Porter [1958a, b]. They polished the surfaces of single crystal garnet spheres, using polishing papers of different mean grit sizes. They found that the linewidth in spherical samples decreases by over a factor of 20, as the samples are polished by successively finer grit sizes. They finally obtained a linewidth of about $\frac{1}{2}$ oersted using a mean grit size in the order of 1 μ . The measurement was made at 9300 Mc/s.

The question now is, "What is the intrinsic linewidth of the garnet?" There were at that time several papers discussing the sources of the linewidth. The linewidth was calculated by studying the rate at which the uniform precession is dissipated into disturbances of shorter wavelengths by scattering due to various mechanisms. For example, the scattering perturbation has been taken to be magnetic ion randomness of interatomic wavelengths by Clogston et al. [1956], to be inhomogeneities of M or H of long wavelengths by Geschwind et al. [1957], and to be microcrystal effects in polycrystalline materials by Schlomann [1958]. Those theories appear to explain satisfactorily the order of magnitude of linewidth more than 25 oersteds found in spinel ferrites, but obviously not the kind of linewidth obtained in polished garnet spheres.

In 1959, Dillion and Nielson [1960] discovered that the peak of the linewidth and the anomalous anisotropy reported previously by Dillion at low temperature, are the effects of the rare earth impurities contained in the crystal. He found that the linewidth peak at about 90 °K becomes much more prominent with the crystals doped with terbium. Spencer, LeCraw, and Clogston [1960] also found that with a specially purified crystal (the rare earth impurities less than 0.1 ppm), the maximum linewidth is reduced from 6 oersteds (normal crystal) to slightly over 0.1 oersted (purified crystal), a factor of 50:1. Kittel [1960] has forwarded a possible mechanism for such anomalous effects.

Other contributions to the theory of ferromagnetic resonance in garnets and to the relaxation mechanism have been made by Spencer and LeCraw [1960], and by Kittel and various co-workers [Sparks and Kittel, 1960; Kittel, 1959; de Gennes et al., 1959].

Recently, Turner reported linewidth measurements in a range from 9 kMc/s up to 59 kMc/s. The linewidth varies almost linearly with frequency, from about 0.3 oersted at 9 kMc/s to slightly less than 1 oersted at 59 kMc/s. The linewidth therefore varies little with frequency; the future applications of ferrite in millimeter wave region seem to be unlimited.

2.3. Instabilities and Magnetostatic Modes

It was first reported by Bloembergen and Wang [1954] that the linewidth of a ferrite sample broadens at high microwave signal levels and in some cases subsidiary absorption peaks are observed. Such instabilities were later analyzed by Suhl [1956a, b, 1957] and his theory agrees quite well with the experiments.

Suhl found two types of instability:

(a) Spin waves directed in parallel with the magnetizing field,

(b) Spin waves not directed in parallel with the magnetizing field. In this case, subsidiary absorption peak appears at a magnetizing field lower than that required for the resonance.

In both cases, the spin waves are coupled to the uniform precession and instabilities are produced by the second order small quantities in the equation of the motion of magnetization. In the latter case, however, when the subsidiary absorption peak coincides with the main resonance line, the instability involves first order small quantities and the critical field for the onset of the instability is very low.

According to Suhl's theory, the critical field at which the instability starts, depends on the line width associated with the spin waves. Attempts have been made by LeCraw, Spencer, and Porter [1958a, b; LeCraw and Spencer, 1959] to determine the intrinsic line width by measuring the critical field. They indeed found that the line width thus determined is independent of the surface conditions of the sample, and is of a magnitude comparable to the spin-lattice relaxation time measured by Farrar by a different method [Farrar, 1959].

Instability at a power level much higher than Suhl's threshold has recently been studied by Seiden and Shaw [1960].

At the bottom of the spin-wave spectrum, the wavelength becomes so long that the effect of exchange force may be neglected. The electromagnetic fields satisfying proper boundary conditions are then the magnetostatic modes.

There have been some experimental studies of these modes made back in 1956 by White, Solt, and Mercereau and also by Dillion. An excellent theory was given by Walker [1957, 1958]. Coupling of the magnetostatic modes have been studied by Fletcher and Solt [1959].

Additional studies on behavior of spin waves have been published by Buffler [1959], Solt, White, and Mercereau [1958]. Van Uiter et al. [1959] have proposed a method for varying the composition of a ferromagnetic material so as to increase the spin wave linewidth.

References

- Angelakos, D. J., Transverse electric field distributions in ferrite loaded waveguide, IRE Trans. PGMTT **7**, 390 (1959).
- Bertant, F., and F. Forrat, Structure des ferrites ferrimagnétiques des terres rares, Compt. Rend. **242**, 382 (1956).

- Bertant, F., and R. Pauthenet, Crystalline structure and magnetic properties of ferrites having the general formula $5\text{Fe}_2\text{O}_3\cdot 3\text{M}_2\text{O}_3$, *Proc. IRE* **104B**, 261 (1956).
- Bloembergen, N., and S. Wang, Relaxation effects in para- and ferromagnetic resonances, *Phys. Rev.* **93**, 72 (1954).
- Boyett, H., S. Weisbaum, and I. Gerst, Design calculations for UHF ferrite circulators, *IRE Trans. PGMTT* **7**, 4 (1959).
- Buffer, C. R., Ferromagnetic resonance near the upper limit of the spin wave manifold, *J. Appl. Phys. Supp.* **30** (1959).
- Button, K. J., Theoretical analysis of the operation of the field-displacement ferrite isolator, *IRE Trans. PGMTT* **6**, 303 (1958a).
- Button, K. J., Theory of nonreciprocal ferrite phase shifter in dielectric loaded coaxial line, *J. Appl. Phys.* **29**, 998 (1958b).
- Claricoats, P. J. B., A. G. Hayes, and A. T. Harvey, A survey of the theory and applications of ferrite at microwave frequencies, *Proc. IRE* **104B**, 267 (1956).
- Clavin, A., Reciprocal ferrite phase shifters in rectangular waveguide, *IRE Trans. PGMTT* **6**, 3 (1958).
- Clogston, A. M., N. Suhl, L. R. Walker, and P. W. Anderson, Possible source of linewidth in ferromagnetic resonance, *Phys. Rev.* **101**, 903 (1956).
- Davis, L., U. Milano, and J. Saunders, A strip line L-band compact circulator, *Proc. IRE* **48**, 115 (1960).
- deGennes, P. G., C. Kittel, and A. M. Portis, Theory of ferromagnetic resonance in rare earth garnets II. Line widths, *Phys. Rev.* **116**, 323 (1959).
- Dillion, J. F., Jr., Ferromagnetic resonance in yttrium-iron at liquid helium temperatures, *Phys. Rev.* **111**, 1476 (1958).
- Dillion, J. F., Jr., Ferromagnetic resonance in yttrium-iron garnet, *Phys. Rev.* **105**, 759 (1957).
- Dillion, J. F., and J. W. Nielson, Effects of rare earth impurities on ferromagnetic resonance in yttrium-iron garnet, *Phys. Rev. Letters* **3**, 30 (1960).
- Duncan, B. J., L. Swern, and K. Tonisvasu, Design considerations for broadband ferrite coaxial line isolators, *Proc. IRE* **45**, 483 (1957).
- Farrar, R. T., Spin-lattice relaxation time in yttrium-iron garnet, *J. Appl. Phys.* **30**, 425 (1959).
- Fleri, D., and G. Hanley, Nonreciprocity in dielectric loaded TEM mode transmission lines, *Trans. IRE PGMTT* **7**, 23 (1959).
- Fletcher, R. C., and H. Seidel, Limitations of elementary mode considerations in ferrite loaded waveguide, *J. Appl. Phys.* **30**, 1475 (1959).
- Fletcher, P. C., and I. H. Solt, Coupling of magnetostatic modes, *J. Appl. Phys.* **30**, 1815 (1959).
- Fox, A. G., S. E. Miller, and M. T. Weiss, Behavior and application of ferrites in the microwave region, *BSTJ* **34** (1955).
- Geller, S., and M. A. Gilleo, Structure and ferromagnetism of yttrium and rare earth iron garnets, *Acta Cryst.* **10**, 239 (1957).
- Geller, S., and M. A. Gilleo, *J. Phys. Chem. Solids* **3**, 20 (1957).
- Geschwind, S., and A. M. Clogston, *Phys. Rev.* **108**, 49 (1957).
- Hogan, C. L., The ferromagnetic faraday effect at microwave frequencies and its applications, *Rev. Mod. Phys.* **25**, 253 (1953).
- Hogan, C. L., The elements of nonreciprocal microwave devices, *Proc. IRE* **44**, 1368 (1956).
- Kales, M. L., Propagation of fields through ferrite loaded waveguides, *Proc. Symp. Mod. Adv. Microw. Tech. Polytech. Inst. of Brooklyn, Brooklyn, N.Y.*, 215 (1954).
- Kittel, C., Theory of ferromagnetic resonance in rare earth garnets, I. g-values, *Phys. Rev.* **115**, 1587 (1959).
- Kravitz, L. C., and G. S. Heller, Resonance isolator at 70 kmc, *Proc. IRE* **47**, 2 (1959).
- Lax, B., Fundamental design principles of ferrite devices, *Proc. Symp. Mod. Adv. Microw. Tech. Polytech. Inst. of Brooklyn, Brooklyn, N.Y.*, 229 (1954).
- Lax, B., Frequency and ton characteristics of microwave ferrite devices, *Proc. IRE* **44**, 1368 (1956).
- Lax, B., The status of microwave application of ferrites and semiconductors, *Trans. IRE PGMTT* **6**, 5 (1958).
- LeCraw, R. C., E. G. Spencer, and C. S. Porter, Ferromagnetic resonance and nonlinear effects in yttrium-iron garnet, *J. Appl. Phys.* **29**, 326 (1958a).
- LeCraw, R. C., E. G. Spencer, and C. S. Porter, Ferromagnetic resonance linewidth in yttrium-iron garnet single crystals, *Phys. Rev.* **110**, 1131 (1958b).
- LeCraw, R. C., and E. G. Spencer, Surface independent spin-wave relaxation in ferromagnetic resonance of yttrium-iron garnet, *J. Appl. Phys.* **30**, 1855 (1959).
- Melcher, J. L., W. P. Ayres, and P. H. Vartanian, Microwave frequency doubling from 9 to 18 kmc in ferrites, *Proc. IRE* **45**, (1957).
- Pippin, J. E., Frequency doubling and mixing in ferrites, *Proc. IRE* **44**, 1054 (1956).
- Rowen, J. H., Ferrites in microwave applications, *BSTJ* **32**, 1333 (1953).
- Schlomann, E., Spin wave analysis of ferromagnetic resonance in polycrystalline ferrites, *J. Phys. Chem. Solids* **6**, 242 (1958).
- Seidel, H., Anomalous propagation in ferrite-loaded waveguide, *Proc. IRE* **44**, 1410 (1956).
- Seidel, H., The character of waveguide modes in gyromagnetic media, *BSTJ* **36**, No. 2 (1957).
- Seidel, H., Ferrite slabs in transverse electric mode waveguide, *J. Appl. Phys.* **28**, 216 (1957).
- Seidel, H., and R. C. Fletcher, Gyromagnetic modes in waveguide partially loaded with ferrite, *BSTJ* **38**, 1427 (1959).
- Seiden, P. E., and H. J. Shaw, High power effects in ferromagnetic resonance, *J. Appl. Phys.* **31**, 432 (1960).
- Skomal, E. N., and M. A. Medina, Study of a microwave ferromagnetic multiple signal conversion process, *J. Appl. Phys. Supp.* **30**, no. 4, (1959).
- Solt, I. H., W. L. White, and J. E. Mercereau, Multiplicities of the uniform procession mode in ferromagnetic resonance, *J. Appl. Phys.* **29**, 324 (1958).
- Sparks, M., and C. Kittel, Ferromagnetic relaxation mechanism for M_x in yttrium-iron garnet, *Phys. Rev. Letters* **4**, 232 (1960).
- Spencer, E. G., and R. C. LeCraw, Spin-lattice relaxation in yttrium-iron garnet, *Phys. Rev. Letters* **4**, 130 (1960).
- Spencer, E. G., R. C. LeCraw, and A. M. Clogston, Low temperature linewidth maximum in yttrium-iron garnet, *Phys. Rev. Letters* **3**, 32 (1960).
- Spencer, E. G., R. C. LeCraw, and C. S. Porter, Ferromagnetic resonance in yttrium-iron garnet at low frequencies, *J. Appl. Phys.* **29**, 429 (1958).
- Stern, E., and P. Persham, Harmonic generation in ferrites, Presented at Symp. on the Role of Solid-State Phenomena in Electric Circuits, Polytech. Inst. of Brooklyn, Brooklyn, N.Y. (1957).
- Sucher, M., and H. J. Carlin, Coaxial line nonreciprocal phase shifters, *J. Appl. Phys.* **28**, 921 (1957).
- Suhl, H., The nonlinear behavior of ferrites at high microwave signal levels, *Proc. IRE* **44**, 1270 (1956).
- Suhl, H., The theory of ferromagnetic resonance at high power signal powers, *J. Phys. Chem. Solids* **1**, 209 (1957).
- To Tai Chen, Evanescent modes in a partially filled gyromagnetic rectangular waveguide, *J. Appl. Phys.* **31**, No. 1, 220 (1960).
- Thaxter, J. B., and G. S. Heller, Circulators at 70 and 140 kmc, *Proc. IRE* **48**, 110 (1960).
- Turner, E. H. (unpublished work) Bell Telephone Labs., Holmdel, N.J.
- Van Uitert, L. G., R. C. LeCraw, E. G. Spencer, and R. L. Martin, Proposed means of realizing high power stability in magnetic oxides, *J. Appl. Phys.* **30**, 1623 (1959).
- Walker, L. R., Magnetostatic modes in ferromagnetic resonance, *Phys. Rev.* **105**, 390 (1957).
- Walker, L. R., Ferromagnetic resonance: line structures, *J. Appl. Phys.* **29**, 318 (1958).

3. Progress in Solid-State Masers

A. Siegman

During the past three years an important accomplishment in masers has been the development of the solid-state maser and most of the recent work has been concerned with this device.

Although most of this review will be devoted to this work on the solid-state maser, we may mention some research concerned with ammonia beam masers [Barnes, 1959; Helmer, 1957; Wells, 1958]. There has also been some work on the so-called atomic clock. This is not really a maser device since it only involves absorption on a resonance line and not emission. However, it is a competitor of the ammonia maser as a time-keeper, and there have been a number of papers on such atomic clocks [Arditi, 1958; Bell, 1959; Mainberger and Orenberg, 1958; McCoubry, 1958].

Most of the recent work in masers is a consequence of Bloembergen's original proposal for a three-level solid-state maser [Bloembergen, 1956]. The same three-level pumping scheme had also been independently proposed earlier by the Russians in connection with gas masers, but the proposal had not been exploited. Bloembergen's proposal was very rapidly verified in every essential through the experimental work of Scovil et al. [Scovil, Feher, and Seidel, 1957]. The rapid development which ensued can be judged from the work which will be described below.

3.1. Cavity-type Solid-state Masers: Experimental Results

Three-level solid-state masers have now been operated in many laboratories mostly at helium temperatures at frequencies ranging from 350 to 35,000 Mc/s. Shortly after the initial maser operation mentioned above, definitive measurements on an S-band maser using potassium chromocyanide as the maser crystal were made by a group at Lincoln Laboratories [McWhorter and Meyer, 1958]. The maser material ruby, i.e., sapphire (Al_2O_3) containing a small amount of chromium, was soon introduced by the University of Michigan and has become probably the most widely used maser material. [Makhov, Kikuchi, Lambe, and Terhune, 1958]. A number of groups have developed masers in the UHF region and in L-band, the latter frequency band containing the important hydrogen emission line at 1420 Mc/s [Arams and Okwit, 1959; Artman, Bloembergen, and Shapiro, 1958; Autler and McAvoy, 1958; Kingston, 1958, 1959; Wessel, 1959]. An S-band maser (approximately 3000 Mc/s) with a large gain bandwidth has been reported by Stanford University and many tunable high-performance masers have been reported at X-band (about 10,000 Mc/s) [Chang, Cromack, and Siegman, 1959; Arams, 1959; Gionino and Dominick, 1960; King and Terhune, 1959; Morris, Kyhl, and Strandberg, 1959; Strandberg, Davis, Faughnan, and Kyhl, 1958]. A group at RCA has used titania (rutile) as a high-frequency maser material [Gerritsen and Lewis, 1960]. Three-level maser operation at liquid nitrogen temperature (with a considerable sacrifice in performance over helium temperature) has been achieved in England and at the Hughes Aircraft Co. [Ditchfield and Forrester, 1958; Maiman, 1960]. The principle of harmonic pumping offers considerable future promise for masers amplifying at higher than the pumped frequency. The principle has been successfully demonstrated by Arams [1960]. An ingenious and very useful practical development

has been the use of superconducting solenoids immersed in a helium bath to supply the masers' d-c magnetic field [Autler, 1959]. Fields up to 5,000 gauss were obtained with a flashlight battery as power supply or even with no power supply by setting up a persistent current in the solenoid. Other useful practical developments included techniques for orienting ruby boules and making silver-plated ruby maser cavities [Mattuck and Strandberg, 1959; Gross, 1959].

3.2. Applications of Solid-State Masers

Several important applications of the solid-state maser to radio astronomy and radar astronomy have already been made. The first use of a maser was by Lincoln Laboratories in contacting the planet Venus by radar at a frequency of 440 Mc/s [Price, 1959]. A group from Columbia and the Naval Research Laboratory have used a maser as a preamplifier for an X-band radiometer, obtaining a substantial increase in sensitivity. Thermal emission from Venus and Jupiter was detected, as well as radio emissions from several radio stars [Alsop, Giordmaine, Mayer, and Townes, 1958; Giordmaine, Alsop, Mayer, and Townes, 1959; Alsop, Giordmaine, Mayer, and Townes, 1959]. A maser has also been tested as the first-stage receiver for an X-band radar system, with again a substantial increase in performance. However, special measures were required to obtain satisfactory duplexing in the system [Forward, Goodwin, and Kiefer, 1959; Goodwin, 1960].

3.3. Solid-State Masers: Theory and Analysis

Numerous papers devoted to aspects of maser theory and analysis have appeared since Bloembergen's paper cited earlier. Detailed quantum-mechanical analyses of the solid-state maser have been carried out by several workers [Anderson, 1957;

Clogston, 1958; Javan, 1957]. Analyses of the solid-state maser at somewhat less rarefied levels can be found in several review papers and also in the following [Bergman, 1959; Burkhart, 1958; Schulz-DuBois, Scovil, and DeGrasse, 1959; Scovil, 1958; Siegman, 1957; Stitch, 1958]. More specialized problems such as the reaction field, maser efficiency, phonon effects, double-quantum transitions, and others have also been considered [Bloembergen, 1958; Feynman, Vernon, and Hellwarth, 1957; Heffner, 1957; Javan, 1958; King, Birko, and Makhov, 1959; Mims and McGee, 1959; Scovil and Schulz-DuBois, 1959; Yatsiv, 1959]. The circulator is a vital component in the reflection-type cavity maser, and one paper discussing this topic has appeared. In addition, proposals have been made for a circulatorless amplifier using two balanced maser cavities and a magic tee, and for nonreciprocal cavity masers without circulators using the non-reciprocal nature of the maser interaction process itself [Arams and Krayner, 1958; Autler, 1958; Strandberg and Kyhl]. Proposals have also been made for radiofrequency masers using nuclear spin levels, although the numerical calculations are not encouraging, particularly at lower frequencies [Braunstein, 1957; Donovan and Vuylsteke, 1960].

3.4. Maser Materials

Ruby is probably the most widely used maser material at present. The properties of ruby as a maser material have been summarized by the University of Michigan group [Kikuchi, Lambe, Makhov, and Terhune, 1959]. Extensive tabulations of the energy levels and transition probability matrix elements for ruby and potassium chromicyanide have been given in reports from Stanford University [Chang and Siegman, 1958, 1959] and from the Royal Radar Establishment in England. Garstens [1959] has also given a method for finding an operating point, given the desired pump and signal frequencies.

3.5. Pulsed and Two-Level Masers

There exists a variety of methods for obtaining population inversion in a material having only two energy levels, although nearly all of these methods permit only intermittent or pulsed amplification. The two-level maser may nonetheless have certain advantages over the three-level maser, and work on the former has been carried out in several places. The various possible two-level schemes, including one as yet untried scheme for a CW two-level maser, are summarized by Bolef and Chester [1958]. Experimental work carried on via two-level masers has included the measurement of relaxation times and the study of paramagnetic levels in irradiated crystals of various sorts [Burkhardt, 1959; Chester and Bolef, 1957; Chester, Wagner, and Castle, 1958; Feher, Gordon, Buehler, Gere, and Thurmond, 1958; Hoskins, 1959; Wagner, Castle, and Chester, 1959].

The above work all uses adiabatic fast passage to obtain the population inversion. An MIT group has successfully used the rather more difficult 180° pulse technique [Collins, Kyhl, and Standberg, 1959]. A staircase scheme involving two successive adiabatic-fast-passage inversions has been suggested as a means for generating higher frequencies [Siegman and Morris, 1959]. Two other groups have generated high microwave frequencies by a "brute force" approach; that is, by inverting a spin population at a relatively low frequency and then rapidly pulsing the magnetic field to a high value to obtain a high output frequency [Foner, 1959; Foner, Momo, and Mayer, 1959; Momo, Mayer, and Foner, 1960; Hoskins, 1959]. Momo et al., in particular, have obtained output at frequencies up to 70 kMc/s by pulsing the magnetic field up to 30 kilogauss.

Immediately after the spin population in a maser cavity is inverted, intermittent or relaxation-type oscillations are often obtained instead of a continuous oscillation. The explanation of these effects in terms of the dynamics of the spin system and the cavity fields has occupied several workers [Kemp, 1959; Senitzky, 1958; Theissing, Dieter, Caplan, 1958; Yariv, Singer, and Kemp, 1959]. Finally, the topics of electron free precession and spin echoes from electron spins are at least distantly related to masers, and some work on these topics has been reported [Gordon and Bowers, 1958; Kaplan and Browne, 1959; Norton, 1957].

3.6. Traveling Wave Masers

In the traveling wave type of maser, the active maser material is distributed along a low-group-velocity slow-wave circuit, rather than being concentrated in a resonant cavity. As a result, the traveling wave maser achieves broader bandwidth, easier frequency tuning, much better gain stability, and built-in nonreciprocity. Although the traveling wave maser would appear to hold much more promise than the cavity type, only a few groups have so far constructed traveling wave masers. At the Bell Telephone Laboratories, the comb slow-wave structure has been used with good results in a traveling wave maser at 6000 Mc/s [DeGrasse, 1958; DeGrasse, Schulz-DuBois, and Scovil, 1959]. Another slow-wave structure, the so-called meander line, has been developed at Stanford University and used in an S-band traveling wave maser [Chang, Cromack, and Siegman, 1959]. A MELabs group has also worked at 3000 Mc/s, exploring various modifications of the comb circuit [Tenney, Roberts, and Vartanian, 1959]. Various general discussions of the traveling wave maser have also been published [Siegman, Butcher, Cromack, and Chang, 1958].

3.7. Noise in Masers

So far as noise in masers is concerned, one can say in general that the inherent noise in a maser amplifier is extremely small, corresponding to a noise tem-

perature of $\sim 1^\circ \text{K}$ for typical microwave masers at helium temperature. The fundamental source of noise in masers is spontaneous emission from spins in the upper amplifying level. However, one can show by heuristic arguments that the noise generation in a maser material is given by ordinary thermal noise formulas, providing that one is willing to tolerate the idea of a negative resistance with a negative temperature (the spin temperature). This viewpoint has been used by many workers to analyze maser noise [Ewen, 1959; Gordon and White, 1958; Pound, 1957; Strandberg, 1957a, b; Weber, 1957]. The results of these analyses are in agreement with more rigorous analyses which have been carried out. [Muller, 1957; Shimoda, Takahasi, and Townes, 1957].

Because of the small noise output of masers, accurate noise measurements are quite difficult. Moreover, the inherent maser noise is generally masked by extraneous noise sources. Small losses in the input cables and connections of the maser are a particularly troublesome noise source and generally determine the overall system noise figure in practical maser amplifiers. Nonetheless, all the noise measurements which have been made are in excellent agreement with theory and give strong support to the noise analyses listed above. Measurements have been made on ammonia beam maser amplifiers by several groups [Alsop, Giordmaine, Townes, and Wang, 1957; Gordon and White, 1957; Helmer, 1957; Helmer and Muller, 1958]. The first and still one of the definitive noise measurements on a cavity-type solid-state maser was made by the Lincoln group, who achieved a system noise figure of 20°K in good agreement with theory [McWhorter, Meyer, and Strum, 1957; McWhorter and Arams, 1958]. More recent measurements at the Bell Telephone Laboratories on a traveling wave maser have shown that the noise in a carefully engineered maser system can be reduced to as low as $\sim 10^\circ \text{K}$ for the maser and associated circuitry, and to as low as $\sim 18^\circ \text{K}$ including noise contributions from the antenna and the sky noise. In addition, the accuracy of the measurement was such as to permit careful verification of the maser's intrinsic noise ($\sim 2^\circ \text{K}$ in this case) by subtracting out the known extraneous noise sources [DeGrasse and Scovil, 1960; DeGrasse, Hogg, Ohn, and Scovil, 1959].

The maser is certainly the lowest noise amplifier obtainable in practice. Is it also the lowest noise amplifier that one can conceive in principle, and is there any fundamental limitation on amplifier noise figure? These two questions have been recently considered in two very stimulating papers apparently developed simultaneously and independently [Friedburg, 1960; Serber and Townes, 1960]. The gist of the papers is that the uncertainty principle of quantum theory sets a lower limit on the noise figure of an amplifier, with an ideal maser just attaining this theoretical limit. The lower limit corresponds to an uncertainty of one quantum per resolution time. Certain devices such as the quantum counter mentioned in the next section appear to be completely

noiseless since they can detect incident photons with no inherent noise or error. However, the uncertainty principle then requires that they lose all ability to measure the phase of an incident signal. These latter devices might better be called counters or detectors than true amplifiers.

3.8. Infrared and Optical Masers

With the microwave-frequency solid-state maser now fairly well under control, considerable attention is turning to possibilities for application of the maser principle at optical and infrared frequencies. There have been a number of proposals for optical or optically pumped masers, but as yet no successful experiments. Schwalow and Townes have summarized the problems involved [Schwalow and Townes, 1958]. Several proposals involve the use of energy levels in gases, with excitation at optical frequencies, and amplification or oscillation at optical, infrared, or microwave frequencies [Bergmann, 1960; Hawkins and Dicke, 1953; Singer, 1959]. Two authors have pointed out that it may also be possible to excite or pump a gaseous optical maser by electron impact [Javan, 1959; Sanders, 1959]. Another technique, proposed in Russia, would use impact ionization to excite holes or electrons to higher levels in impurity-doped semiconductors. The possibilities of optical pumping in crystals have been discussed, and an interaction between optical and microwave radiation in ruby has been observed successfully (although no maser operation was obtained) first by Wieder and then by a Bell Laboratories group [Theissing, Caplan, Dieter, and Rabbinder, 1959; Wieder, 1959; Geschwind, Collins, and Schwalow, 1959]. As a pump source for his optical experiments in ruby, Wieder developed a very interesting narrowband high-power (~ 100 milliwatts) light source using the fluorescence of the R_1 and R_2 optical lines in a second piece of ruby [Wieder, 1959]. An alternative type of maser-like device for infrared frequencies called the quantum counter has been proposed by Bloembergen and also by Robinson [Bloembergen, 1959a, b; Robinson, 1960]. The quantum counter operates in a fashion similar to the Geiger counter or other particle detectors. As mentioned in the previous section, the quantum counter has the advantage in comparison with the maser of having no inherent noise even at high frequencies if operated at a very low temperature.

References

- Alsop, L. E., J. A. Giordmaine, C. H. Mayer, and C. H. Townes, Observations using a maser radiometer at 3 cm wavelength, *Astronom. J.* **63**, 301 (1958).
- Alsop, L. E., J. A. Giordmaine, C. H. Mayer, and C. H. Townes, Observation of discrete radio sources at 3 cm wavelength using a maser, *Paris Symp. on Radio Astron.* R. N. Bracewell (ed.), Stanford Univ. Press, Stanford, Calif., p. 69 (1959).
- Alsop, L. E., J. A. Giordmaine, C. H. Townes, and T. C. Wang, Measurement of noise in a (n ammonia) maser amplifier, *Phys. Rev.* **107**, 1450 (1957).

- Anderson, P. W., The reaction field and its use in some solid-state amplifiers, *J. Appl. Phys.* **28**, 1049 (1957).
- Arams, F. R., Low-field X-band ruby maser, *Proc. IRE* **47**, 1373 (1959).
- Arams, F. R., Maser operation with signal frequency higher than pump frequency, *Proc. IRE* **48**, 108 (1960).
- Arams, F. R., and G. Krayer, Design considerations for circulator maser systems, *Proc. IRE* **46**, 912 (1958).
- Arams, F. R., and S. Okwit, Tunable L-band ruby maser, *Proc. IRE* **47**, 992 (1959).
- Arditi, M., and T. R. Carver, A gas call 'atomic clock' using optical pumping and optical detection, 1958 IRE Natl. Conv. Rec., pt. 1, 3.
- Artman, J. O., N. Bloembergen, and S. Shapiro, Operation of a three-level solid-state maser at 21 centimeters, *Phys. Rev.* **109**, 1392 (1958).
- Autler, S. H., Proposal for a maser amplifier system without non-reciprocal elements, *Proc. IRE* **46**, 1880 (1958).
- Autler, S. H., Superconducting electromagnets, *Bull. Am. Phys. Soc.* **II** **4**, 413 (1959); *Rev. Sci. Instr.* (to be published).
- Autler, S. H., and M. McAvoy, A 21-centimeter solid-state maser, *Phys. Rev.* **110**, 280 (1958).
- Barnes, F. S., Operating characteristics of an ammonia beam maser, *Proc. IRE* **47**, 2085 (1959).
- Bell, W. E., A. Bloom, and R. Williams, A microwave frequency standard employing optically pumped sodium vapor, *IRE Trans. MIT-7*, 95 (1959).
- Bergmann, S. M., Three-level solid-state maser, *J. Appl. Phys.* **30**, 35 (1959).
- Bergmann, S. M., Submillimeter wave maser, *J. Appl. Phys.* **31**, 275 (1960).
- Bloembergen, N., Proposal for a new type solid-state maser, *Phys. Rev.* **104**, 324 (1956).
- Bloembergen, N., Electron spin and phonon equilibrium in masers, *Phys. Rev.* **109**, 2209 (1958).
- Bloembergen, N., Solid-state infrared quantum counters, *Phys. Rev. Letters* **2**, 84 (1959a).
- Bloembergen, N., Noise characteristics of infrared quantum counters, (abstract only), *Bull. Am. Phys. Soc.* **II**, **4**, 165 (1959b).
- Bolef, D. I., and P. F. Chester, Some techniques of microwave generation and amplification using electron spin states in solids, *IRE Trans. MIT-6*, 47 (1958).
- Braunstein, R., Proposal for a nuclear quadrupole maser, *Phys. Rev.* **107**, 1195 (1957).
- Burkhardt, J. L., et al., Theory of two-level masers, Final Report, ONR Contract Nonr 2254(00), Hycon Eastern, Inc. (now Hermes Electronics), Cambridge Parkway, Cambridge 42, Mass., Feb. 3, 1958.
- Burkhardt, J. K., Inversion of paramagnetic resonance lines in irradiated calcite, *Phys. Rev. Letters* **2**, 149 (1959).
- Chang, W. S. C., J. Cromack, and A. E. Siegman, Cavity and traveling-wave masers using ruby at S-band, *IRE Wescon Conv. Rec.*, pt. 1, 142 (1959a).
- Chang, W. S. C., J. Cromack, and A. E. Siegman, Cavity maser experiments using ruby at S-band, *J. Electron. Control* **6**, 508 (1959b).
- Chang, W. S., and A. E. Siegman, Characteristics of potassium Chromiyanide for Zeeman transitions, *Tech. Rep. No. 156-1*, Stanford Electronics Lab., Stanford Univ., Stanford, Calif. (May 16, 1958).
- Chang, W. S., and A. E. Siegman, Characteristics of ruby for maser applications, *Tech. Rep. No. 156-2*, Stanford Electronics Lab., Stanford Univ., Calif. (Sept. 30, 1958); also published as a special appendix to "Masers" by J. Weber, *Rev. Mod. Phys.* **31**, 681 (1959).
- Chester, P. F., and D. I. Bolef, Superregenerative masers, *Proc. IRE* **45**, 1287 (1957).
- Chester, P. F., P. E. Wagner, and J. G. Castle, Two-level solid-state maser, *Phys. Rev.* **110**, 281 (1958).
- Clogston, A. M., Susceptibility of the three-level maser, *J. Phys. Chem. Solids* **4**, 271 (1958).
- Collins, S. A., Jr., R. I. Kyhl, and M. W. P. Strandberg, Spin-lattice relaxation from state of negative susceptibility, *Phys. Rev. Letters* **2**, 88 (1959).
- DeGrasse, R. W., Slow-wave structures for unilateral solid-state maser amplifiers, *IRE Wescon Conv. Rec.* pt. 3, 29 (1958).
- DeGrasse, R. W., D. C. Hogg, E. A. Ohm, and H. E. D. Scovil, Ultra-low noise measurements using a horn reflector antenna and a traveling-wave maser, *J. Appl. Phys.* **30**, 2013 (1959).
- DeGrasse, R. W., E. O. Schulz-DuBois, and H. E. D. Scovil, The three-level solid-state traveling-wave maser, *BSTJ* **39**, 305 (1959).
- DeGrasse, R. W., and H. E. D. Scovil, Noise temperature measurement on a traveling-wave maser preamplifier, *J. Appl. Phys.* **31**, 443 (1960).
- Ditchfield, C. R., and P. A. Forrester, Maser action in the region of 60 °K, *Phys. Rev. Letters* **1**, 448 (1958).
- Donovan, R. E., and A. A. Vuylsteke, On the possibility of maser action in nuclear quadrupole systems, *J. Appl. Phys.* **31**, 614 (1960).
- Ewen, H. I., A thermodynamic analysis of maser systems, *Microw. J.* **3**, 41 (1959).
- Feher, G., J. R. Gordon, E. Buehler, E. A. Gere, and C. D. Thurmond, Spontaneous emission of radiation from electron spin system, *Phys. Rev.* **109**, 221 (1958).
- Feynman, R. P., F. L. Vernon, Jr., and R. W. Hellwarth, Geometrical representation of the Schrodinger equation for solving maser problems, *J. Appl. Phys.* **28**, 49 (1957).
- Foner, S., *J. Phys. Radium* **20**, 336 (1959).
- Foner, S., L. R. Momo, and A. Mayer, Multilevel pulsed field maser for generation of high frequencies, *Phys. Rev. Letters* **3**, 36 (1959).
- Forward, R. L., F. E. Goodwin, and J. E. Kiefer, Application of a solid-state ruby maser to an X-band radar system, *IRE Wescon Conv. Rec.* pt. 1, 119 (1959).
- Friedburg, H., General amplifier noise limit, *Quantum Electronics*, ed. by C. H. Townes, Columbia Univ. Press, to be published in 1960.
- Garstens, M. A., Method for calculating simultaneous resonance conditions in a three-level ruby maser, *J. Appl. Phys.* **30**, 976 (1959).
- Geschwind, S., R. J. Collins, and A. L. Schwalow, Optical detection of paramagnetic resonance in an excited state of Cr^{3+} in Al_2O_3 , *Phys. Rev. Letters* **3**, 545 (1959).
- Gerritsen, H. J., and H. R. Lewis, Operation of a chromium doped titania maser, *J. Appl. Phys.* **31**, 608 (1960).
- Gianino, P. D., and F. J. Dominick, A tunable X-band ruby maser, *Proc. IRE* **48**, 260 (1960).
- Giordmaine, J. A., L. E. Alsop, C. H. Mayer, and C. H. Townes, A maser amplifier for radio astronomy at X-band, *Proc. IRE* **47**, 1062 (1959).
- Goodwin, F. E., Duplexing a solid-state ruby maser in an X-band radar system, *Proc. IRE* **48**, 113 (1960).
- Gordon, J. P., and K. D. Bowers, Microwave spin echoes from donor electrons in silicon, *Phys. Rev. Letters* **1**, 368 (1958).
- Gordon, J. P., and L. D. White, Experimental determination of the noise figure of an ammonia maser, *Phys. Rev.* **107**, 1728 (1957).
- Gordon, J. P., and L. D. White, Noise in (ammonia) maser amplifiers—theory and experiment, *Proc. IRE* **46**, 1588 (1958).
- Gross, L. G., Silvered ruby maser cavity, *J. Appl. Phys.* **30**, 1459 (1959).
- Hawkins, W. B., and R. H. Dicke, The polarization of sodium atoms, *Phys. Rev.* **91**, 1008 (1953).
- Heffner, H., Maximum efficiency of the solid-state maser, *Proc. IRE* **45**, 1289 (1957).
- Helmer, J. C., Maser oscillators, *J. Appl. Phys.* **28**, 212 (1957).
- Helmer, J. C., (Ammonia) maser noise measurement, *Phys. Rev.* **107**, 902 (1957).
- Helmer, J. C., and M. W. Muller, Calculation and measurement of the noise figure of a(n ammonia) maser amplifier, *IRE Trans. MIT-6*, 210 (1958).
- Hoskins, R. H., Two-level maser materials, *J. Appl. Phys.* **30**, 797 (1959).
- Hoskins, R. H., Spin-level inversion and spin-temperature mixing in ruby, *Phys. Rev. Letters* **3**, 174 (1959).
- Javan, A., Theory of a three-level maser, *Phys. Rev.* **107**, 1579 (1957).
- Javan, A., Multiple quantum transitions and maser amplification in two-level systems (in French), *J. Phys. Radium* **19**, 802 (1958).

- Javan, A., Possibility of production of negative temperature in gas discharge, *Phys. Rev. Letters* **3**, 87 (1959).
- Kaplan, D. E., and M. E. Browne, Electron free precession in paramagnetic free radicals, *Phys. Rev. Letters* **2**, 454 (1959).
- Kemp, J. D., Theory of maser oscillation, *J. Appl. Phys.* **30**, 1451 (1959).
- Kikuchi, C., J. Lambe, G. Makhov, and R. W. Terhune, Ruby as a maser material, *J. Appl. Phys.* **30**, 1061 (1959).
- King, J. E., A. Birko, and G. Makhov, A double pumping scheme applicable to low-frequency masers, *Proc. IRE* **47**, 2025 (1959).
- King, J. E., and R. W. Terhune, Operation of a zero-field X-band maser, *J. Appl. Phys.* **30**, 1844 (1959).
- Kingston, R. H., A UHF solid-state maser, *Proc. IRE* **46**, 916 (1958).
- Kingston, R. H., A UHF solid-state maser, *IRE Trans. MIT-7*, 92 (1959).
- Maiman, T. E., Maser behavior: temperature and concentration effects, *J. Appl. Phys.* **31**, 222 (1960).
- Mainberger, M., and A. Orenberg, The atomichron—an atomic frequency standard: operation and performance, 1958 IRE Nat. Conv. Rec., pt. 1, 14.
- Makhov, G., C. Kikuchi, J. Lambe, and R. W. Terhune, Jr., Maser action in ruby, *Phys. Rev.* **109**, 1399 (1958).
- McCoubry, A. O., The atomichron—an atomic frequency standard: physical foundations, 1958 IRE Natl. Conv. Rec., pt. 1, 10.
- McWhorter, A. L., and F. E. Arams, System noise measurement of a solid-state maser, *Proc. IRE* **46**, 913 (1958).
- McWhorter, A. L., and J. W. Meyer, Solid-state maser amplifier, *Phys. Rev.* **109**, 312 (1958).
- McWhorter, A. L., J. W. Meyer, and P. D. Strum, Noise temperature measurement on a solid-state maser, *Phys. Rev.* **108**, 1642 (1957).
- Mims, W. B., and J. D. McGee, Spin-spin energy transfer and the operation of three-level masers, *Proc. IRE* **47**, 2120 (1959).
- Momo, L. R., R. A. Meyers, and S. Foner, Pulsed field millimeter wave maser, *J. Appl. Phys.* **31**, 443 (1960).
- Morris, R. J., R. I. Kyhl, and M. W. P. Strandberg, A tunable maser amplifier with large bandwidth, *Proc. IRE* **47**, 80 (1959).
- Muller, M. W., Noise in a molecular amplifier, *Phys. Rev.* **106**, 8 (1957).
- Norton, L. E., Coherent spontaneous microwave emission by pulsed resonance excitation, *IRE trans. MIT-5*, 262 (1957).
- Pound, R. V., Spontaneous emission and the noise figure of maser amplifiers, *Ann. Phys.* **1**, 24 (1957).
- Price, R., et al., Radar echoes from Venus, *Science* **129**, 751 (1959).
- Robinson, W. A., Infrared quantum converter, *Bull. Am. Phys. Soc. II*, **5**, 15 (1960).
- Sanders, J. H., Optical maser design, *Phys. Rev. Letters* **3**, 86 (1959).
- Schulz-DuBois, E. O., H. E. D. Scovil, and R. W. DeGrasse, Use of active material in three-level solid-state masers, *BSTJ* **38**, 335 (1959).
- Schwalow, A. L., and C. H. Townes, Infrared and optical masers, *Phys. Rev.* **112**, 1940 (1958).
- Scovil, H. E. D., The three-level solid-state maser, *IRE Trans. MIT-6*, 29 (1958).
- Scovil, H. E. D., G. Feher, and H. Seidel, The operation of a solid-state maser, *Phys. Rev.* **105**, 762 (1957).
- Scovil, H. E. D., and E. O. Schulz-DuBois, Three-level masers as heat engines, *Phys. Rev. Letters* **2**, 262 (1959).
- Senitzky, I. R., Behavior of a two-level solid-state maser, *Phys. Rev. Letters* **1**, 167 (1958).
- Serber, R., and C. H. Townes, Limits on electromagnetic amplification due to complementarity, *Quantum electronics*, ed. by C. H. Townes, Columbia Univ. Press, to be published in 1960.
- Shimoda, K., H. Takahasi, and C. H. Townes, Fluctuations in amplification of quanta, *J. Phys. Soc. Japan* **12**, 686 (1957).
- Siegmán, A. E., Gain-bandwidth and noise in maser amplifiers, *Proc. IRE* **45**, 1737 (1957).
- Siegmán, A. E., P. N. Butcher, J. Cromack, and W. S. C. Chang, Traveling wave solid-state masers, *Proc. Brit. IRE* **105**, pt. B, Suppl. No. 11, 711 (1958).
- Siegmán, A. E., and R. J. Morris, Proposal for a "staircase" maser, *Phys. Rev. Letters* **2**, 302 (1959).
- Singer, J. R., Proposal for a tunable millimeter wave molecular oscillator and amplifier, *IRE Trans. MIT-7*, 268 (1959).
- Stitch, M. L., Maser amplifier characteristics for transmission and reflection cavities, *J. Appl. Phys.* **29**, 782 (1958).
- Strandberg, M. W. P., Computation of noise figure for quantum mechanical amplifiers, *Phys. Rev.* **107**, 1483 (1957).
- Strandberg, M. W. P., C. F. Davis, B. W. Faughnan, R. W. Kyhl, and G. J. Wolga, Operation of a solid-state quantum mechanical amplifier, *Phys. Rev.* **109**, 1988 (1958).
- Strandberg, M. W. P., and R. L. Kyhl, Nonreciprocal cavity masers, Various unpublished technical reports, MIT.
- Tenney, H. D., R. W. Roberts, and P. H. Vartanian, An S-band traveling-wave maser, 1959 IRE Wescon Conv. Rec. pt. 1, 151.
- Theissing, H. H., P. J. Caplan, F. A. Dieter, and N. Rabbiner, Optical pumping in crystals, *Phys. Rev. Letters* **3**, 460 (1959).
- Theissing, H. H., F. A. Dieter, and P. J. Caplan, Analysis of the emissive phase of a pulsed maser, *J. Appl. Phys.* **29**, 1673 (1958).
- Wagner, P. E., J. G. Castle, Jr., and P. F. Chester, Electron spin-lattice relaxation in dilute potassium chromicyanide, *Bull. Am. Phys. Soc. II-4*, 21 (1959).
- Weber, J., Maser noise considerations, *Phys. Rev.* **108**, 537 (1957).
- Wells, W. H., Maser oscillator with one beam through two cavities, *J. Appl. Phys.* **29**, 714 (1958).
- Wessel, G. K., A UHF ruby maser, *Proc. IRE* **47**, 590 (1959).
- Wieder, I., Solid-state, high intensity, monochromatic light sources, *Rev. Sci. Instr.* **30**, 995 (1959).
- Wieder, I., Optical detection of paramagnetic resonance saturation in ruby, *Phys. Rev. Letters* **3**, 468 (1959).
- Yariv, A., J. R. Singer, and J. Kemp, Radiation damping effects in two-level maser oscillators, *J. Appl. Phys.* **30**, 265 (1959).
- Yatsiv, S., Role of double-quantum transitions in masers, *Phys. Rev.* **113**, 1538 (1959).

4. Low-Noise Beam-Type Microwave Tubes

L. Smullin

At the time of the last URSI meeting in Boulder, Colo. (September 1957), theory and experiment on low-noise, beam-type microwave amplifier had reached the following stage: Traveling wave tubes with noise figures for 4-5 db had been produced in the 3,000 megacycles per second region. The noise in an electron beam was described theoretically in terms of two basic parameters S and π/S . These parameters had been shown to be invariant under ordinary beam accelerations so long as the average beam velocity was large compared with thermal fluctuations. Thus, it was possible to predict the optimum attainable noise performance of a tube if the quantities S and π/S were specified at some point beyond the virtual cathode. Experimental studies had demonstrated the invariance of S and π/S in some 3-region guns.

Thus the outstanding theoretical problems were the determination of the ultimate values of S and π/S and thus of noise figure, and the determination of the factors that governed these two parameters.

A summary of the state of the art to about 1958 is presented in L. D. Smullin and H. A. Haus, "Noise in Electron Devices," John Wiley & Sons, MIT., Technology Press, 1958.

4.1. Progress During the Past 3 Years

a. Design of Solid-Beam, Low-Noise Guns

Further progress was made in the design of low-noise guns previously described by R. W. Peter. The analysis of noise transformation within a multi-anode gun was analyzed in terms of a tapered transmission line [Echenbaum and Peter, 1959]. The deleterious effect on noise of very rapid accelerations has been pointed out. This arises from the strong transverse focusing action accompanying such accelerations in gridless gaps [Knechtli, 1958].

The manufacturing experience with an S-band low-noise amplifier, employing a 3 region, solid-beam gun has been summarized in a recent article. Of 53 tubes, 4 had noise figures below 5 db, the mean value was about 5.5 db. Life test data and performance curves are given [Kinaman and Magid, 1958].

In an attempt to get even better control over the acceleration of the beam, a gun was built with many closely spaced anodes, whose potential could be separately adjusted. A noise figure of 6.5 db was obtained at X-band; and subsequently, S-band noise figures of 3.5 db were obtained. There is some evidence that this gun may be operating in the mode of the hollow beam, magnetron injection gun (see sec. III) [Shaw, Siegman, and Watkins, 1959].

b. Theory of Noise on Beams and Low-Noise Amplification

Theoretical studies have included an examination of the higher order azimuthal modes in Brillouin focused beams, the coupling between such modes and an external circuit, and the intercoupling between the modes in a finite beam were computed. The derived theory helps to explain some hitherto anom-

alous experiments [Rigrod and Pierce, 1959; Rigrod, 1959].

A detailed analysis of the various parameters for best noise performance of a beam type backward wave amplifier has been carried out more or less similarly to such analysis for traveling wave amplifiers [Currie and Forster, 1958].

The general theory of low-noise, linear amplifiers (noisy 4 pole networks) has received renewed attention. Optimum circuit arrangements for both positive- and negative-resistance amplifiers are described [Haus and Adler, 1958a, 1958b, 1959].

c. Hollow Beam Low-Noise Guns

An interesting new development in low-noise performance is a gun that appears to behave in a different way from the solid beam low-noise gun, and S- and C-band noise figures of 3.5 db have been achieved [Currie, 1958; Coulton and St. John, 1958].

The guns described in these two letters produced hollow beams with a system of anodes near the cathode that had potentials such as to give a strong radial field and an extended region in which the axial field was small, and the space potential also was low. The noise reducing mechanism in these guns is still not fully understood, but it may be related to the mechanism described by Siegman et al. (sec. IV). Because of the method of beam formation, they have been called "magnetron injection" guns. Best performance is achieved with a strong magnetic focusing field at the cathode. A field of about 1,100 gauss was used.

Low noise tubes incorporating such guns have been described recently. One of these was a C-band traveling-wave amplifier that had a noise figure below 4 db. The other was an X-band backward wave amplifier whose noise figure was about 4.5 db [Hammer, Laico, Holvorsen, and Olsen, 1959; Nevins, 1959].

d. Theory of Noise in Multivelocity Electron Beams

The work of H. A. Haus, F. N. Robinson, and others had predicted the invariance of two basic noise parameters S and π in an electron beam, so long as accelerations were slow and the drift velocity was large compared to thermal fluctuations. Thus it is possible to predict the best noise figure obtainable if π and S are specified for a given cathode.

In the period covered by this report, some progress has been made in the theory of the multivelocity region extending from the cathode to a point where the space potential is of the order of a volt or more [Siegman and Bloom, 1957]. This paper is an attempt to explain some of the numerical results obtained earlier by Tien and is concerned with the region between cathode and virtual cathode. A resonant peak in shot-noise is predicted in the neighborhood of the plasma frequency of the virtual cathode. There is still no experimental verification of this prediction.

The region just beyond the virtual cathode has been studied theoretically [Siegman, 1957; Siegman and Watkins, 1957]. In these two papers the analysis is carried out for the region just beyond the virtual cathodes of a parallel plane diode, and it is shown that even if the initial noise excitation at the virtual cathodes has zero correlation between density and velocity fluctuations, a finite, positive correlation ($\pi/S > 0$) is produced as the beam is accelerated through the first $\frac{1}{2}$ to 1 v, and S is simultaneously lowered.

Although the model was highly idealized, the results indicated a way of possibly controlling (reducing) the noise in the beam by extending the region in which the beam drifts at low voltage. The multianode gun previously described was built with this idea in mind [Shaw, Siegman, and Watkins, 1959].

The exact reason for the improved noise performance of the magnetron injection gun is not understood. The Siegman type of analysis, if applicable, might explain it; however, the magnetic field strength plays an important role in determining the actual noise figure, and no theory has so far completely accounted for it [Currie and Forster, 1959; Muller and Currie, 1959].

e. Fundamental Noise Measurements

Several measurements of the noise quantities S and π generated in low-noise guns of the solid-beam and of the magnetron injection type have been made [Saito, 1958; Zacharias and Smullin, 1960; Jory, 1960]. Saito and Zacharias used two cavities spaced $\lambda_g/4$ apart to separately determine the noise excitation of the fast and slow space charge waves. Saito found a positive correlation, $\pi/S \approx 0.2-0.3$ in solid beam guns. This value was essentially independent of the way in which the beam was accelerated in the gun so long as strong lens effects were avoided.

In contrast, Zacharias made similar measurements on a magnetron injection gun and found S to be a

sensitive function of the voltage applied to the first anode and to the focusing electrode; but $\pi/S \approx 0$ for all settings. If true, these data indicate a difference in the operating mode of the two types of guns.

Jory also made measurements on a magnetron injection gun; but he used a backward wave amplifier with an axially movable gun. By measuring noise figure at various settings, he was able to determine S and π/S . His values show $\pi/S \approx 0.2$. Thus there appears to be a serious discrepancy between these results and those of Zacharias and Smullin. Further experiments are in progress.

f. Electron Beam Parametric Amplifiers¹

Considerable work and some success has been achieved in the design and construction of parametrically excited, low-noise, beam-type amplifiers. Earlier attempts were based on the use of space charge waves. Although it proved possible to build tubes that amplified, little success has so far been achieved in getting low-noise performance.

The principal difficulty in making low-noise, space charge wave, parametric amplifiers lies in the small separation between the fast- and slow-waves. As a result, it has so far proven practically impossible to strip the noise from the fast-wave and then to amplify it, only, without getting major contamination from slow-wave noise.

The theoretical basis of beam-parametric amplification seems firmly established; and there are now power conservation theorems, and analysis by coupling-of-modes just as for conventional beam-type amplifiers.

The use of cyclotron waves and transverse deflection allowed a great separation in velocity between the fast and slow waves (at $\omega = \omega_c = eB/m$, the fast wave has infinite phase velocity). A UHF tube was built, using a quadrupole section excited at $2\omega_c$ for parametric amplification, and Cuccia couplers for input and output circuits. This tube has a noise figure of less than 2 db and a gain of 30 db over a 10 o/o bandwidth in the range of 400 to 800 Mc/s.

Recently, a similar type tube has been built for operation at 4 kMc/s. Its double channel noise figure was about 2.5 db with a gain of 24 db, over about a 1½ o/o bandwidth.

g. Low-Noise Klystrons

Two low-noise tubes have been built for operation at S- and C-bands. They employ "conventional" solid cylindrical beam low-noise guns. Noise figures of 6 to 7 db and gains of 11.5 were attained [Rockwell, 1959].

References

- Coulton, M., and G. E. St. John, S-band traveling wave tube with noise figure below 5 db, *Proc. IRE* **46**, No. 5 (1958).
- Currie, M. R., A new type of low-noise electron gun for microwave tubes, *Proc. IRE* **46** No. 5, (1958).

¹ Detailed references are included in a section of this report concerned with the whole class of parametric amplifiers.

- Currie, M. R., and D. C. Forster, Conditions for minimum noise generation in backward wave amplifiers, IRE Trans. **ED-5**, No. 1, 88 (1958).
- Currie, M. R., and D. C. Forster, New mechanism of noise reduction in electron beams, J. Appl. Phys. **30**, No. 1 (1959).
- Echenbaum, A. E., and R. W. Peter, The exponential gun—a low-noise gun for traveling wave tube amplifiers, RCA Rev. **XX**, No. 1 (1959).
- Hammer, J. M., J. P. Laico, H. J. Holvorsen and E. G. Olsen, Low-noise C-band traveling-wave tube, IRE, 1959 Electron Devices Meeting, Oct. 29–30, Washington, D.C.
- Haus, H. A., and R. B. Adler, Optimum noise performance of linear amplifiers, Proc. IRE **46**, 1517 (1958a).
- Haus, H. A., and R. B. Adler, Canonical form of linear noisy networks, IRE Trans. **CT-5**, No. 3, 161 (1958b).
- Haus, H. A., and R. B. Adler, Circuit theory of linear noisy networks, John Wiley and Sons, MIT Technol. Press (1959).
- Jory, H. R., Noise in backward wave amplifiers, Ph.D. Thesis in Electrical Engineering, Univ. Calif. (1960).
- Kinaman, E. W., and M. Magid, Very low-noise traveling wave amplifier, Proc. IRE **46**, No. 5 (1958).
- Knechtli, R. C., Effect of electron lenses on beam noise, IRE Trans. **PGED-5**, No. 2, 84 (1958).
- Muller, W. M., and M. R. Currie, Noise propagation in uniformly accelerated multivelocity electron beams, J. Appl. Phys. **30**, No. 12 (1959).
- Nevins, J. E., Jr., A 5 db noise figure backward wave amplifier at X-band, IRE, 1959 Electron Devices Meeting, Oct. 29–30, Washington, D.C.
- Rigrod, W. W., Space charge wave harmonics and noise propagation in rotating electron beams, BSTJ **38** No. 2 (1959).
- Rigrod, W. W., and J. R. Pierce, Space charge wave excitation in solid cylindrical Brillouin beams, BSTJ **38** No. 1 (1959).
- Rockwell, R. G., Low noise klystron amplifiers, IRE Trans. **PGED-6**, 428 (1959).
- Saito, S., New method of measuring the noise parameters of an electron beam, IRE Trans. **PGED-5** No. 4 (1958).
- Shaw, A. W., A. E. Siegman, and D. A. Watkins, Reduction of electron beam noisiness by means of a low-velocity drift region, Proc. IRE **47** 2 (1959).
- Siegman, A. E., Analysis of multivelocity electron beams by the density function method, J. Appl. Phys. **28**, No. 10 (1957).
- Siegman, A. E., and S. Bloom, An equivalent circuit for microwave noise at the potential minimum, IRE Trans. **PGED-4**, No. 4 (1957).
- Siegman, A. E., D. A. Watkins, and Hsung-Cheng Hsieh, Density function calculations of noise propagation on an accelerated multivelocity electron stream, J. Appl. Phys. **28**, No. 10 (1957).

5. Interaction Between Plasmas and Electromagnetic Fields

L. Smullin

5.1. Introduction

As a result of the intense interest in such diverse subjects as thermonuclear generation of power, ion-propulsion of rockets, and direct generation of electricity from furnace heat by MHD generators, the volume of literature on plasmas has grown enormously within the last few years.

In this review, a brief survey is made of a narrow branch of plasma physics: the interaction between plasmas and electromagnetic waves, and the coulomb interaction between interpenetrating plasma streams. As evidence of the growing interest in this field, the following books have appeared recently in the United States [Landshoff, 1957; Landshoff, 1958; *Proc. of Symposium on Electronic Waveguides, Microwave Research Institute Symposia Series, Vol. VIII, Polytechnic Press, 1958*; Brown, 1959; *Notes or MIT Summer Course, 1959*; Longmire, Tuck, and Thompson, 1959; Clauser, 1960].

5.2. Propagation of Electromagnetic Waves in Unbounded Plasmas—Small Signal Theory

The propagation of plane waves of arbitrary polarization in an ideal unbounded plasma (no collisions or thermal fluctuations) has been studied in three recent papers. Dispersion characteristics have been plotted, and the possible wave surfaces have been mapped on a chart relating applied frequency to plasma and cyclotron frequency. The wave surface contour plotted in various regions of the chart represents the phase velocity of each possible wave as a function of the angle between the d-c magnetic field and the direction of propagation. [Auer, Hurwitz, and Miller, 1958; Allis, 1959; Allis and Papa, 1959.]

The same problem has been attacked for a fully ionized plasma in which the random motion of the charged particles is included. The approach is through the Boltzmann equation [Bernstein, 1958].

5.3. Plasma Waveguides

Recently, there has been considerable interest in the study of plasma columns as electromagnetic waveguides. A number of authors have studied the problem of propagation along an ideal plasma column either in free space, or coaxial with an outer metal tube. The effect of a superimposed, axial magnetostatic field is considered. For the cases in which ω_p and ω_c are small compared to the cutoff

frequency of the outer metal tube, relatively simple, approximate solutions to the dispersion equations have been found. These predict the existence of several passbands with both positive- and negative-dispersion and phase velocity small compared with c . Experiments have confirmed the theoretical predictions and both the positive- and negative-dispersion regions have been observed [Stix, 1957; Smullin and Chorney, 1958a; Chorney, 1958; Gould and Trivelpiece, 1958; Trivelpiece, 1958; Trivelpiece and Gould, 1959; Lichtenberg, 1959].

The previous papers all confine their attention to reciprocal modes of propagation. The gyroelectric, or nonreciprocal modes, have also been studied and nonreciprocal phase shifters and polarizers have been demonstrated experimentally [Goldstein, 1958].

The scattering of electromagnetic waves from an infinitely long plasma column in a strong magnetic field has been studied [Dawson and Oberman, 1959].

Much of the theoretical work now going on is aimed at finding methods of solving the less restricted problem of plasma within a metal cylinder (cavity) of arbitrary size. The earlier works of Van Trier, Suhl and Walker, and Gamo on ferrites has laid the foundation for the solution of these problems, but much remains to be done in this area.

5.4. Electron Stimulated Plasma Oscillations

The system consisting of an electron beam drifting through a stationary plasma has been studied by several authors. This is an old problem, and in a sense, it is a direct descendent of the double-stream amplifier of A. F. Haeff. For some time the primary interest in this type of interaction, except for vacuum tubes, lay in the hope that it might explain some of the phenomena of solar flares and similar astronomical occurrences. More recently, double-stream interaction has been studied as a possible means of heating a plasma and as a possible origin of some of the experimentally observed instabilities in the various large-scale plasma machines built for thermonuclear research.

Small signal analyses have been carried out for various geometrical arrangements in which an electron beam is allowed to drift through a stationary plasma. Modes of interaction have been discovered that are similar to those of traveling wave tubes, klystrons, monotrons, backward wave oscillators, and reactive-medium amplifiers (Easytrons). Direct experimental evidence has already established

the reality of several of these modes [Jepsen, 1957; Boyd, Field, and Gould, 1958a; Smullin and Chorney, 1958; Boyd, Field, and Gould, 1958b; Sturrock, 1958; Boyd, 1959; Smullen and Getty, 1960].

A study of large signal effects in electron-stimulated plasma oscillations has been carried out for a one-dimensional system, and klystron-type "Applegate" diagrams are plotted showing the overtaking of particles and the randomization of the original coherent oscillation [Buneman, 1958, 1959].

5.5. Large Signal Oscillations

The possible parametric instabilities of a plasma confined by a strong rf field have been studied theoretically. It is shown that under certain conditions, the parametrically induced oscillations may destroy the confining action of the rf field [Haus, 1959]. The use of a plasma column as a nonlinear medium for parametric amplification has been discussed. Pumping by both electromagnetic and acoustic waves is considered [Kino, 1959, 1960].

An exact solution for one-dimensional electrostatic oscillations of a collisionless plasma has been found for arbitrary large variations of electrostatic potential. It is shown that the general solution for the traveling potential wave includes a large class of waveforms, both periodic and aperiodic [Bernstein, 1957].

References

- Allis, W. P., and R. J. Papa, MIT Research Lab. Electron Quart. Prog. Rept. No. **54**, 5 (1959).
 Allis, W. P., and R. J. Papa, MIT Research Lab. Electron. Quart. Prog. Rept. No. **55**, 19 (1959).
 Auer, P. L., H. Hurwitz, Jr., and R. D. Miller, *Phys. of Fluids*, **1**, 501 (1958).
 Bernstein, I. B., Waves in a plasma in a magnetic field, *Phys. Rev.* **109**, 10 (1958).
 Bernstein, I. B., J. M. Greene, and M. D. Kruskal, Exact nonlinear plasma oscillations, *Phys. Rev.* **108**, 546 (1957).
 Boyd, G. D., Experiments on the interaction of a modulated electron beam with a plasma, Tech. Rept. No. 11, Electron Tube and Microw. Lab., Cal.Tech. (1959).
 Boyd, G. D., L. M. Field, and R. W. Gould, interaction between an electron stream and an arc discharge plasma, *Proc. Symp. Electron. Waveguides*, 367, Polytech. Press of Polytech. Inst. of Brooklyn, Brooklyn, N.Y. (1958a).
 Boyd, G. D., L. M. Field, and R. W. Gould, Excitation of plasma oscillations in growing plasma waves, *Phys. Rev.* **109**, 1393 (1958b).
 Brown, S. C., Basic data of plasma physics, The Technology Press, Cambridge (1959).
 Buneman, O., Instability, turbulence and conductivity in current-carrying plasma, *Phys. Rev. Letters*, **1**, 8 (1958).
 Buneman, Nonlinear calculation of plasma oscillations, *Proc. Conf. Plasma Oscillations*, Speedway Research Lab., Linde Co., Indianapolis, Ind., June 8-10 (1959).
 Chorney, P., Electron-stimulated ion oscillations, Tech. Rept. 277, Research Lab. Electron., MIT (1958).
 Clauser, F. H., Plasma dynamics, Addison-Wesley, Reading, Mass. (1960).
 Dawson, J., and C. Oberman, Oscillations of a finite cold plasma in a strong magnetic field, *Phys. of Fluids* **2**, 103 (1959).
 Goldstein, L., Nonreciprocal electromagnetic wave propagation in ionized gaseous media, *IRE Trans. MIT-6*, 19 (1958).
 Gould, R. W., and A. W. Trivelpiece, A new mode of wave propagation on electron beams, *Proc. Symp. Electron. Waveguides*, 215-228, Polytech. Press of Polytech. Inst. of Brooklyn, Brooklyn, N.Y. (Apr. 1958).
 Haus, H. A., MIT, Research Lab. of Electron. Quart. Prog. Rept. 46 (1959).
 Jepsen, R. L., Ion oscillations in electron beam tubes; ion motion and energy transfer, *Proc. IRE* **45**, 1069 (1957).
 Kino, G. S., A parametric amplifier theory for plasmas and electron beams, M. L. Rept. 636, Stanford Univ. (1959).
 Kino, G. S., A proposed millimeter-wave generator, M. L. Rept. 609, Stanford Univ. (1959) (paper submitted to *Proc. Symp. Polytech. Inst. Brooklyn* (1960)).
 Landshoff, R. K. M., Magneto-hydrodynamics, A symposium, Stanford Univ. Press, Palo Alto, Calif. (1957).
 Landshoff, R. K. M., The plasma in a magnetic field, *Symp. Magneto-hydrodynam.* Stanford Univ. Press, Palo Alto, Calif. (1958).
 Lichtenberg, A. J., Plasma waveguides as high-Q structures, Univ. California, Series No. 60, Issue No. 247 (1959).
 Longmire, C., J. L. Tuck, and W. B. Thompson (editors) *Progress in nuclear energy, Ser. XI Plasma Physics and Thermonuclear Research* (Pergamon Press, Inc., New York, N.Y., 1959).
 MIT Summer Course notes on Plasma dynamics (1959) (out of print).
 Smullin, L. D., and P. Chorney, Properties of plasma-filled waveguides, *Proc. IRE* **46**, 360 (1958a).
 Smullin, L. D., and P. Chorney, Propagation in ion loaded waveguides, **229**, Polytech. Press of Polytech. Inst. of Brooklyn, N.Y. (1958b), *Proc. of Symp. Electron. Waveguides*.
 Stix, Thomas H., Oscillations of a cylindrical plasma, *Phys. Rev.* **106**, No. 6 1146 (1957).
 Sturrock, P. A., Kinematics of growing waves, *Phys. Rev.* **112**, 1488 (1958).
 Symposium on Electronic Waveguides, Electronic waveguides, *Microw. Research Inst. Symp. Ser. Vol. VIII*, Polytech. Press of Polytech. Inst. of Brooklyn (1958).
 Trivelpiece, A. W., Slow wave propagation in plasma waveguides, Tech. Rept. No. 7, Electron Tube and Microw. Lab. Calif. Inst. Technol. (1958).
 Trivelpiece, A. W., and R. W. Gould, Space charge waves in cylindrical plasma columns, *J. Appl. Phys.* **30**, 1784 (1959).
 (Paper 64D6-96)

Publications of the National Bureau of Standards*

Selected Abstracts

A comparative study of absolute zenith intensities of [OI] 5577. F. E. Roach, J. W. McCaulley, E. Marovich, and C. M. Purdy, *J. Geophys. Research* **65**, 1503 (1960).

The statistical distribution of the absolute zenith intensities of [OI] 5577 is compared for four locations at north geomagnetic latitudes 49°, 53°, 65°, and 88°. The distributions are similar in nature at all stations. The median values in rayleighs are 371 (49°), 251 (53°), 2400 (65°), and 630 (88°). The percentage occurrence of intensities greater than the visual threshold is 2.2 (49°), 1.2 (53°), 83 (65°), and 15 (88°). Evidence is presented for and against a single excitation mechanism for both auroral 5577 and airglow 5577.

The intensity of [OI] 5577 in the subauroral region as a function of magnetic activity. F. E. Roach, *J. Geophys. Research* **65**, 1495 (1960).

The intensity of [OI] 5577 at Fritz Peak, Colorado, and Rapid City, South Dakota, is found to increase with increasing planetary magnetic activity. The nature of the increase is similar to but smaller than that observed in the auroral zone.

A study of local geomagnetic influence on the [OI] 5577 nightglow emission at Fritz Peak. J. W. McCaulley, F. E. Roach, and S. Matsushita, *J. Geophys. Research* **65**, 1499 (1960).

A comparison is made of (1) the horizontal magnetic intensity at Leadville, Colorado, and (2) the absolute zenith intensity of [OI] 5577 at Fritz Peak, Colorado. The absolute zenith intensity of 5577 tends to increase as the magnetic ΔH becomes more negative.

The absolute zenith intensity of [OI] 5577 at College, Alaska. F. E. Roach and M. H. Rees, *J. Geophys. Research* **65**, 1489 (1960).

The absolute zenith intensity of [OI] 5577 was measured over College, Alaska, at 5-minute intervals during nights from January 16 to April 8, 1959. A total of 3968 individual readings was obtained. The median intensity is 2.40 kilorayleighs. Eighty percent of the observations are included within the range from 0.74 to 11.5 kR. A general increase of 5577 intensity occurs with increasing geomagnetic activity.

Tropospheric fields and their long-term variability as reported by TASO. P. L. Rice, *Proc. IRE* **48**, 1021 (1960).

This report presents data from long-term recordings of radio field strength over a large number of propagation paths, and presents curves for predicting field strength over a smooth earth for frequencies between 40 megacycles and 1000 megacycles per second. The basic data provided for the Television Allocations Study Organization during 1957 and 1958 include recordings made in several parts of the world and over various types of terrain and were supplied by numerous sources.

Radio echoes from field-aligned ionization above the magnetic equator and their resemblance to auroral echoes. K. L. Bowles, R. Cohen, G. R. Ochs, B. B. Balsley, *J. Geophys. Research* **65**, 1853 (1960).

During the International Geophysical Year, under the joint auspices of the United States National Committee for the IGY, the Voice of America, and the National Bureau of Standards, the authors operated a chain of 50 Mc/s VHF forward scatter circuits near the magnetic equator in South America. An intense mode of VHF propagation associated with equatorial sporadic E was found to occur and was demonstrated to be closely identifiable in time-variation and height with the equatorial electrojet.

A survey and bibliography of recent research in the propagation of VLF radio waves. J. R. Wait, *NBS Tech. Note 58* (PB 161559) (1960), 75 cents.

A general survey of the field is given. Attention is confined primarily to terrestrial propagation, and thus solar and exospheric phenomena are generally excluded although certain

germane references dealing with these subjects are given in the bibliography.

First a brief description of recent advances of ground wave propagation is given. This is followed by sections on ray and mode concepts of ionospheric propagation. The research dealing with the waveforms of atmospherics is also considered. Finally some recent applications of VLF propagation are described. While the emphasis is on the theoretical approaches used, reference to corroborating experimental work is included. It is hoped that the shortcomings in a brief article of this kind are partially compensated by the inclusion of an extensive bibliography on the subject arranged under subject classification. While attention is confined primarily to the triennium (1957-1959) a number of basic references prior to 1957 are included.

The VLF band is here defined as the decade 3 to 30 kc/s whereas the ELF band covers the range 1.0 c/s to 3 kc/s.

Other NBS Publications

Journal of Research, Vol. 64A, No. 5, September-October 1960. 70 cents.

Infrared spectrum of hydrobromic acid. E. K. Plyler. Determination of the value of the faraday with a silver-perchloric acid coulometer. D. N. Craig, J. I. Hoffman, C. A. Law, and W. J. Hamer.

Systems silver iodide-sodium iodide and silver iodide-potassium iodide. G. Burley and H. E. Kissinger.

Conformations of the pyranoid sugars. III. Infrared absorption spectra of some acetylated aldehydopyranosides. R. Stuart Tipson and H. S. Isbell.

Dissociation constant of 4-aminopyridinium ion in water from 0 to 50 °C and related thermodynamic quantities. R. G. Bates and H. B. Hetzer.

Tritium-labeled compounds VI. Alditols-1-*t* and alditols-2-*t*. H. L. Frush, H. S. Isbell, and A. J. Fatiadi.

Journal of Research, Vol. 64B, No. 3, July-September 1960. 75 cents.

Electric polarizability of a short right circular conducting cylinder. T. T. Taylor.

Distribution of quantiles in samples from a bivariate population. M. M. Siddiqui.

Split Runge-Kutta method for simultaneous equations. J. R. Rice.

A reduction formula for partitioned matrices. E. V. Haynsworth.

Selected bibliography of statistical literature, 1930 to 1957: III. Limit theorems. L. S. Deming.

Journal of Research, Vol. 64C, No. 3, July-September 1960. 75 cents.

A new method of measuring gage blocks. J. B. Saunders. Gage blocks of superior stability: initial developments in materials and measurement. M. R. Meyerson, T. R. Young, and W. R. Ney.

Variation of resolving power and type of test pattern. F. E. Washer and W. P. Tayman.

A multiple isolated-input network with common output. C. M. Allred and C. C. Cook.

Phase angle master standard for 400 cycles per second. J. H. Park and H. N. Cones.

Disturbances due to the motion of a cylinder in a two-layer liquid system. L. H. Carpenter and G. H. Keulegan.

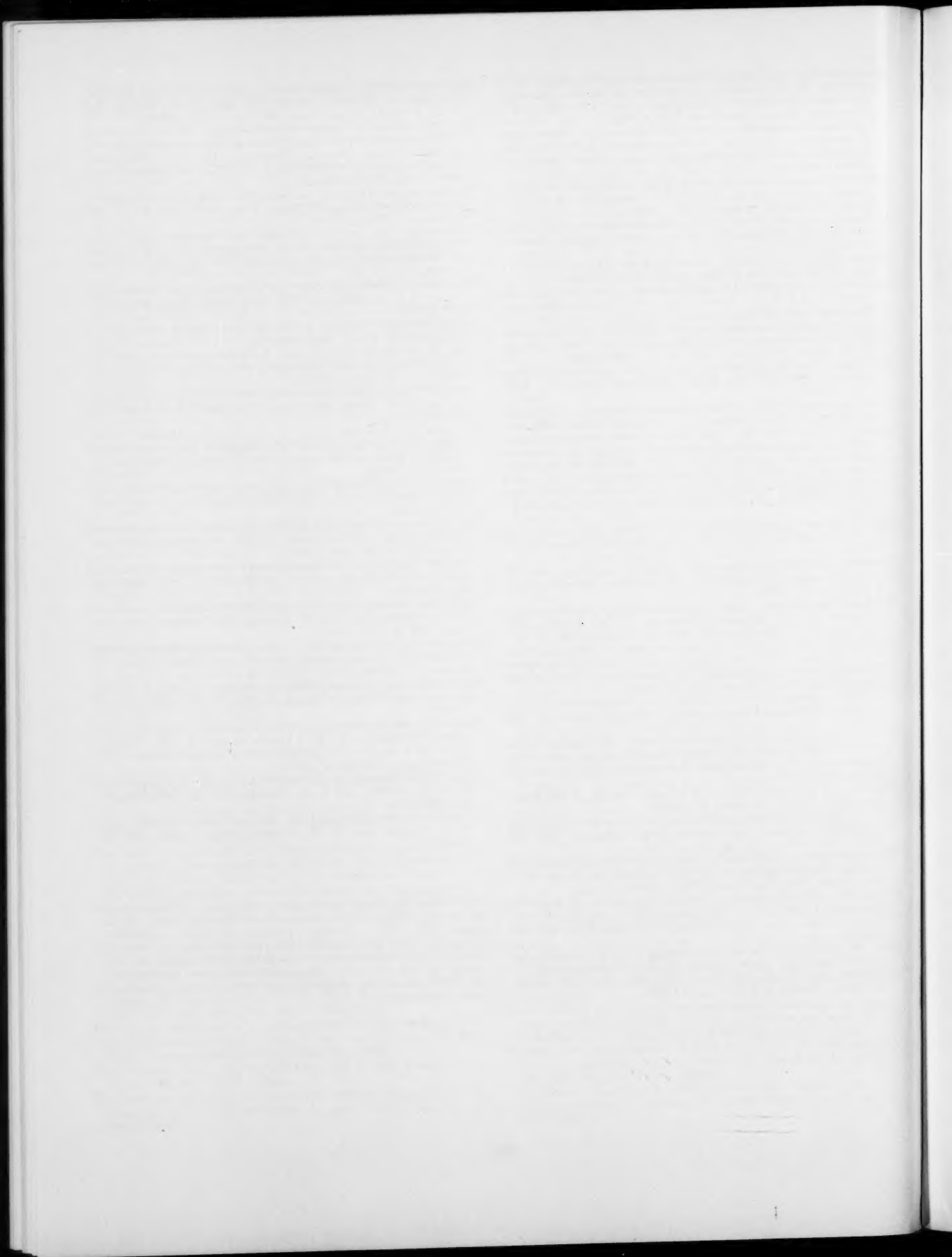
Temperature-induced stresses in solids of elementary shape. L. H. Adams and R. M. Waxler, NBS Mono. 2 (1960) 25 cents.

Table of wavenumbers, 2000 Å to 7000 Å, C. D. Coleman, W. R. Bozman, and W. F. Meggers, NBS Mono. 3, Vol. I. (1960) \$6.00.

- Table of wavenumbers, 7000 Å to 1000 μ , C. D. Coleman, W. R. Bozman, and W. F. Meggers, NBS Mono. 3, Vol. II. (1960) \$6.00.
- Mercury barometers and manometers, W. G. Brombacher, D. P. Johnson, and J. L. Cross, NBS Mono. 8 (1960) 40 cents.
- A method for the dynamic determination of the elastic, dielectric, and piezoelectric constants of quartz, S. A. Basri, NBS Mono. 9 (1960) 15 cents.
- The "1958 He⁺ Scale of Temperature," F. G. Brickwedde, H. Van Dijk, M. Durieux, J. R. Clement, and J. K. Logan, NBS Mono. 10 (1960) 20 cents.
- Mechanical properties of structural materials at low temperatures—A compilation from the literature, R. M. McClintock and H. P. Gibbons, NBS Mono. 13 (1960) \$1.50.
- Bibliography on molecular and crystal structure models, D. K. Smith, NBS Mono. 14 (1960) 15 cents.
- Vibration-rotation structure in absorption bands for the calibration of spectrometers from 2 to 16 microns, E. K. Plyler, A. Danti, L. R. Blaine, and E. D. Tidwell, NBS Mono. 16 (1960) 20 cents.
- Quarterly radio noise data—March, April, May 1959, W. Q. Crichlow, C. A. Samson, R. T. Disney, and M. A. Jenkins, NBS Tech. Note 18-2 (PB151377-2) (1960) \$1.00.
- Experimental plating of gun bores to retard erosion, V. A. Lamb and J. P. Young, NBS Tech. Note 46 (PB151405) (1960) \$2.50.
- Report on the IGY oblique-incidence sporadic-E and F-scatter program, J. W. Finney and E. K. Smith, Jr., NBS Tech. Note 48 (PB151407) (1960) \$2.50.
- Dynamic measurements of the magnetoelastic properties of ferrites, V. E. Bottom, NBS Tech. Note 49 (PB151408) (1960) \$1.00.
- Magnetic drum directory and programming system for code-sorting letter mail, P. C. Tosini, NBS Tech. Note 50 (PB151409) (1960) \$1.75.
- Isotopic abundance ratios reported for reference samples stocked by the National Bureau of Standards, F. L. Mohler, NBS Tech. Note 51 (PB161552) (1960) 50 cents.
- Field strength calculations for E. L. F. radio waves, J. R. Wait and N. F. Carter, NBS Tech. Note 52 (PB161553) (1960) 50 cents.
- Carrier frequency dependence of the basic transmission loss in tropospheric forward scatter propagation, K. A. Norton, NBS Tech. Note 53 (PB161554) (1960) \$1.00.
- Determination of a general index of effort in sorting mail by conventional methods, S. Henig, NBS Tech. Note 54 (PB161555) (1960) 50 cents.
- A bibliography of the physical equilibria and related properties of some cryogenic systems, T. M. Flynn, NBS Tech. Note 56 (PB161557) (1960) \$1.75.
- Variable capacitor calibration with an inductive voltage divider bridge, T. L. Zapf, NBS Tech. Note 57 (PB161558) (1960) 50 cents.
- A survey and bibliography of recent research in the propagation of VLF radio waves, J. R. Wait, NBS Tech. Note 58 (PB161559) (1960) 75 cents.
- The linear viscoelastic behavior of rubberlike polymers and its molecular interpretation, R. S. Marvin, *Viscoelasticity: Phenomenological aspects*, p. 27 (Academic Press, New York, N.Y., 1960).
- Low-frequency solar bursts and noise storms, A. Boischoit, R. H. Lee, J. W. Warwick, *Astrophys. J.* **131**, No. 1, 61 (1960).
- Magnetic properties of polycrystalline materials, D. M. Grimes, R. D. Harrington, and A. L. Rasmussen, *J. Phys. Chem. Solids* **12**, 28 (1959).
- Low angle X-ray diffraction of fibrous polyethylene, A. S. Posner, L. Mandelkern, C. R. Worthington, and A. F. Diorio, *J. Appl. Phys.* **31**, No. 3, 536 (1960).
- The source-function in a non-equilibrium atmosphere. IV. Evaluation and application of the net-radiative-bracket, R. N. Thomas, *Astrophys. J.* **131**, 429 (1960).
- Mass spectrometry, V. H. Dibeler and R. M. Reese, *Anal. Chem.* **32**, No. 5, 211 (1960).
- The melting temperature of natural rubber networks, D. E. Roberts and L. Mandelkern, *J. Am. Chem. Soc.* **82**, 5, 1091 (1960).
- Ionic charges of glass surfaces and other materials, and their possible role in the coagulation of blood, D. Hubbard and G. L. Lucas, *J. Appl. Physiol.* **15**, No. 2, 265 (1960).
- Emission spectra of N₂, O₂, and NO molecules trapped in solid matrices, H. P. Broida and M. Peyron, *J. Chem. Phys.* **32**, No. 4, 1068 (1960).
- The components of power appearing in the harmonic analysis of a stationary process, M. M. Siddiqui, presented at Symp. on Statistical Methods in Radio Wave Propagation, University of California, Los Angeles, June 18-20, 1958, reprinted from *Statistical methods in radio wave propagation* (Pergamon Press, New York, N.Y., 1960).
- Mechanical and electromechanical properties of indium antimonide, R. F. Potter, J. H. Wasilik, and R. B. Flippen, ch. 12, *Mechanical properties of intermetallic compounds*, p. 265 (John Wiley & Sons, Inc., New York, N.Y., 1960).
- Electrometric PH determination, R. G. Bates, *Chimia* **14**, 111 (1960).
- Measurement of radiation exposure at the walls of medical X-ray rooms for determining protective barrier requirements, S. W. Smith and J. R. Brooks, *ATOMPRAXIS* **6**, No. 3, 77 (1960).
- Introduction—Can you measure it? L. V. Judson, *Am. Soc. Tool & Mfg. Engrs. Tech. Paper* 239, Book 1, 60, 1 (1960).
- Correction for systematic wavelength shifts in atomic beam devices, R. L. Barger and K. G. Kessler, *J. Opt. Soc. Am.* **50**, No. 4, 352 (1960).
- Theory of the magnetic and spectroscopic properties of neptunium hexafluoride, J. C. Eisenstein and M. H. L. Pryce, *Proc. Roy. Soc. (London)* [A] **255**, 181 (1960).
- Some fundamentals of modern dimensional metrology, I. H. Fullmer, *Am. Soc. Tool & Mfg. Engrs. Tech. Paper* 240, Book 1, 60, 1 (1960).
- High pressure form of analcite and free energy change with pressure of analcite reactions, H. S. Yoder, Jr., and C. E. Weir, *Am. J. Sci.* **258-A**, 420 (1960).
- Class of nonlinear dielectric materials, P. H. Fang, R. S. Roth, and H. Johnson, *J. Am. Ceram. Soc.* **43**, No. 3, 169 (1960).
- The error in prediction of F2 maximum usable frequencies by world maps based on sunspot number, E. L. Crow and D. H. Zacharisen, sec. II, *Radio propagation phenomenology*, in *Statistical methods in radio wave propagation*, p. 248 (Pergamon Press, New York, N.Y., 1960).
- The use of 2,2,4,4,6,8,8-heptamethylnonane as a primary diesel fuel, T. W. Mears, R. M. David, and F. L. Howard, *ASTM Bul. No. 245*, p. 75 (1960).
- Sinn und bedeutung der strahlenschutznormen, L. S. Taylor, *Röntgen-Bl. XIII*, Heft 2, 33 (1960).
- Bremsstrahlung linear polarization, J. W. Motz and R. C. Placius, *Nuovo Cimento* **15**, Ser. X, 571 (1960).
- Geomagnetic disturbance and velocity of slow-drift solar radio bursts, M. B. Wood and C. S. Warwick, *Nature* **184**, No. 4697, 1471 (1959).
- Chemically induced vibrational excitation: hydroxyl radical emission in the 1-3 micron region produced by the H+O₂ atomic flame, D. Garvin, H. P. Broida, and H. J. Kostkowski, *J. Chem. Phys.* **32**, No. 3, 880 (1960).
- Thermoelectric effects, H. P. R. Frederikse and W. W. Scanlon, ch. 7.6 of *Methods of experimental physics*, vol. VI, p. 114 (Academic Press Inc., New York, N.Y., 1959).
- Photographs of the high-altitude nuclear explosion "Teak," W. R. Steiger and S. Matsushita, *J. Geophys. Research* **65**, No. 2, 545 (1960).
- Appraisal of Land's work on two-primary color projections, D. B. Judd, *J. Opt. Soc. Am.* **50**, No. 3, 254 (1960).
- The outlook for machine translation, F. L. Alt, *Proc. Western Joint Computer Conf.*, vol. 17, p. 203, San Francisco, Calif. (May 1960).
- Further evidence of a solar corpuscular influence on large-scale circulation at 300 Mb, N. J. MacDonald and W. O. Roberts, *J. Geophys. Research* **65**, No. 2, 529 (1960).
- Method for measurement of E'/I' in the reciprocity calibration of condenser microphones, W. Koidan, *J. Acoust. Soc. Am.* **32**, No. 5, 611 (1960).
- Microphone diaphragm null method for sound pressure measurements, W. Koidan, *J. Acoust. Soc. Am.* **32**, No. 4, 505 (1960).

- An evaluation of a cesium beam frequency standard, R. C. Mockler, R. E. Beehler, J. A. Barnes, Symp. Quantum Electron.—Resonance Phenomena, p. 127 (Columbia University Press, New York, N.Y., 1960).
- Nonresonant absorption in symmetric-top gases: Dependence of relaxation frequency on temperature, A. A. Maryott, A. Estin, and G. Birnbaum, *J. Chem. Phys.* **32**, No. 5, 1501 (1960).
- The influence of lowered permissible dose levels on atomic energy operations in the United States, L. S. Taylor, *Progr. in Nuclear Energy* **1**, 10 (1960).
- Optimum antenna height for ionospheric scatter communication, R. G. Merrill, *IRE Trans. on Commun. Systems* **CS-8**, 14 (1960).
- Forced mixing in boundary layers, G. B. Schubauer and W. G. Spangenberg, *J. Fluid Mech.* **8**, No. 1, 10 (1960).
- Statistical evaluation of interlaboratory cement tests, J. R. Crandall and R. L. Blaine, *Am. Soc. Testing Materials, Proc.* **59**, 1129 (1959).
- X-ray attenuation coefficients from 13 to 80 Mev for hydrogen, carbon, water, and aluminum, J. M. Wyckoff and H. W. Koch, *Phys. Rev.* **117**, No. 5, 1261 (1960).
- Guiding of electromagnetic waves by uniformly rough surfaces—Part II, J. R. Wait, *IRE Trans. Ant. Prop.* **AP7**, S163 (1959).
- Electron impact study of the cyanogen halides, J. T. Herron and V. H. Dibeler, *J. Am. Chem. Soc.* **82**, 1555 (1960).
- Measured distributions of the instantaneous envelope amplitude and instantaneous frequency of carriers plus thermal and atmospheric noise, A. D. Watt and R. W. Plush, in *Statistical methods of radio wave propagation: Proc. of a symp. University of California, Los Angeles, Calif., June 18-20, 1958*, p. 233 (Pergamon Press, New York, N.Y., 1960).
- Interpretation of some features of low-frequency ionograms, J. M. Watts, *J. Atmospheric and Terrest. Phys.* **15**, 73 (1959).
- Electron detachment from the negative hydrogen ion by electron impact, S. Geltman, *Proc. Phys. Soc. (London)* **LXXXV**, p. 67 (1960).
- Transactions of the Joint Commission for Spectroscopy, Minutes of the Moscow Meeting, August 12-15, 1958 (Abridged), *J. Opt. Soc. Am.* **50**, No. 4, 396 (1960).
- "Ionization" of the hydrogen negative ion, S. Geltman, *Proc. 4th Intern. Conf. on Ionization Phenomena in Gases* (North Holland Publishing Co., Amsterdam, The Netherlands), Uppsala 17-21, p. IA 19 (1960).
- Cryogenic piping system design and installation, R. B. Jacobs, *Heating, Piping and Air Conditioning*, p. 143 (1960).
- The nova outburst. V. The temperature and radius of the central exciting star and observation of elements other than hydrogen, S. Pottasch, *Ann. Astrophys. J.* **22**, No. 4, 412 (Sept.-Oct. 1959).
- Plan for the self-qualification of laboratories, A. T. McPherson, *ASTM Bull.* No. 246, 17 (1960).
- Cosmic examples of heat conduction in very rare rotating or expanding gases, S. Chapman, *Ann. Geophys.* **15**, 434 (Oct.-Dec. 1959).
- The structure of O,O'-diethyl methylphosphonothioate and conjugative properties of the P=S bond, H. Finegold, *J. Am. Chem. Soc.* **82**, No. 10, 2641 (1960).
- Effect of notch geometry on tensile properties of annealed titanium at 100°, 25°, -78° and -196° C, G. W. Geil and N. L. Carwile, *Am. Soc. Testing Materials, Proc.* **59**, 985 (1959).
- How the method of rating the cooling load for refrigerated trailers has been standardized, P. R. Achenbach, C. W. Phillips, and W. F. Goddard, *Am. Soc. Heating, Refgr. Air Cond. Engrs. J.* **2**, No. 5, 45 (1960).
- Analysis of methyl methacrylate copolymers by gas chromatography, J. Strassburger, G. M. Brauer, M. Tryon, and A. F. Forziati, *Anal. Chem.* **32**, No. 4, 454 (1960).
- The wavefront reversing interferometer, J. B. Saunders, *Colloquium on Optics and Metrology*, sponsored by Intern. Comm. Optics, Brussels, Belgium, May 8-9, 1958, published in *Optics in Metrology*, p. 227 (Pergamon Press, New York, N.Y., 1960).
- Normal modes of a lattice of oscillators with many resonances and dipolar coupling, U. Fano, *Phys. Rev.* **118**, No. 2, 451 (1960).
- Calibration for carrier operated microphones and other reversible transducers, M. D. Burkhard, E. L. R. Corliss, W. Koidan, and F. Biagi, *J. Acoust. Soc. Am.* **32**, No. 4, 501 (1960).
- Detection and estimation of low concentrations of aldehyde in air, E. E. Hughes and S. G. Lias, *Anal. Chem.* **32**, No. 6, 707 (1960).
- Magnetoresistive effects in indium antimonide and indium arsenide, H. P. R. Frederikse and W. W. Hosler, vol. 2, pt. 2, of *Solid state physics in electronics and telecommunications*, p. 651 (Academic Press, New York, N.Y., 1960).
- The NBS meteor burst communication system, R. J. Carpenter and G. R. Ochs, *IRE Trans. Commun. Systems* **CS-7**, 263 (1959).
- Characteristic energy losses of electrons, L. Marton, L. B. Leder, C. Marton, and M. D. Wagner, *Proc. 4th Intern. Conf. on Electron Microscopy*, Sept. 1958, p. 281 (Berlin, Germany, 1960).
- Guiding of electromagnetic waves by uniformly rough surfaces—Part I, J. R. Wait, *IRE Trans. Ant. Prop.* **AP7**, S154 (1959).
- Spectra emitted from rare gas-oxygen solids during electron bombardment, L. J. Schoen and H. P. Broida, *J. Chem. Phys.* **32**, No. 4, 1184 (1960).
- Accurate microwave wavemeters with convenient calibration tables, H. E. Bussey and A. J. Estin, *Rev. Sci. Instr.* **31**, 410 (1960).
- Radiation patterns of finite-size corner-reflector antennas, A. C. Wilson and H. V. Cottony, *IRE Trans. on Ant. Prop.* **AP-8**, 144 (1960).
- Kinetics of the transport of water through silicate glasses at ambient temperatures, W. Haller, *Phys. Chem. of Glass* **1**, 46 (1960).
- Flow and stress near an interface between stratified liquids, K. Lofquist, *Phys. of Fluids* **3**, No. 2, 158 (March-April 1960).
- Heat sink method for measuring the cooling loads of refrigerated structures, P. R. Achenbach and C. W. Phillips, *Proc. 10th Intern. Congress of Refrigeration*, August 1959, Copenhagen, Denmark (1959).
- A technique for gripping high-strength fabrics during physical tests, K. F. Plitt and L. A. Dunlap, *ASTM Bull.* No. 246, 33 (1960).
- Heated cell for quantitative infrared spectrophotometry, F. J. Linnig and J. E. Stewart, *Anal. Chem.* **32**, 891 (1960).

*Publications for which a price is indicated (except for NBS Technical Notes) are available only from the Superintendent of Documents, U.S. Government Printing Office, Washington 25., D.C. (foreign postage, one-fourth additional). Technical Notes are available only from the Office of Technical Services, U.S. Department of Commerce, Washington 25, D.C. (Order by PB number.) Reprints from outside journals and the NBS Journal of Research may often be obtained directly from the authors.



INDEX TO VOLUME 64D

January to December 1960

A

	Page
<i>Adachi, S.</i> , Impedance characteristics of a uniform current loop having a spherical core.....	295
Admittance and radiation of an insulated slotted-sphere antenna surrounded by a strongly ionized plasma sheath.....	525
Amplifiers, parametric.....	751
Amplitude distribution for radio signals reflected by meteor trails.....	449
Amplitude-probability distribution of atmospheric radio noise from statistical moments, determination.....	49
Analysis of propagation measurements made at 418 megacycles per second well beyond the radio horizon (a digest).....	225
Antenna data processing, automatic, bibliography.....	743
Antenna, half-wave cylindrical in a dissipative medium: current and impedance.....	365
Antenna, high gain, very low side-lobe, with capability for beam slewing.....	557
Antenna, impedance of a corner-reflector as a function of the diameter and length of the driven element.....	135
Antenna size, effect of on gain, bandwidth, and efficiency.....	1
Antennas, surface and leaky wave.....	746
Antenna surrounded by a strongly ionized plasma sheath, radiation and admittance of an insulated slotted-sphere.....	525
Antenna theory, cylindrical.....	569
Antenna, top-loaded monopole, the electric field at the ground plane with special regard to electrically small L- and T-antennas.....	139
Antenna, very-low-frequency, for investigating the ionosphere with horizontally polarized radio waves.....	27
Antennas 1957-1959.....	731
Arctic communication, conference.....	73
Astronomy, URSI, report of U.S. Commission 5.....	655
Athabasca Glacier, Alberta, Canada, electrical resistivity studies.....	439
Atmosphere, circularly stratified, focusing, defocusing, and refraction.....	287
Atmospheric bending of radio rays, methods of predicting.....	487
Atmospheric circulations and tropospheric scatter propagation.....	81
Atmospheric noise at various receiving locations, properties.....	640
Atmospheric radio noise from statistical moments, determination of the amplitude-probability distribution.....	49
Atmospherics, daytime attenuation rates in the very low frequency band.....	349
Atmospherics, very-low-frequency, measured frequency spectra.....	41
Attenuation measurements and standards, development.....	599
Aurora of October 22/23, 1958, at Rapid City, South Dakota.....	205
Automatic antenna data processing, bibliography.....	743

B

<i>Bachynski, M. P.</i> , Propagation at oblique incidence over cylindrical obstacles.....	311
—, <i>H. E. J. Neugebauer</i> , Diffraction by smooth conical obstacles.....	317
<i>Balsen, M., C. A. Wagner</i> , Measurements of the spectrum of radio noise from 50 to 100 cycles per second.....	415
Basic experimental studies of the magnetic field from electromagnetic sources immersed in a semi-infinite conducting medium.....	21
<i>Bean, B. R., E. J. Dutton</i> , On the calculation of the departures of radio wave bending from normal.....	259
—, <i>G. D. Thayer, B. A. Cahoon</i> , Methods of predicting the atmospheric bending of radio rays.....	487
Beam-type low-noise microwave tubes.....	703
<i>Berry, W. M., W. Q. Crichtow, C. J. Roubique, A. D. Spaulding</i> , Determination of the amplitude-probability distribution of atmospheric radio noise from statistical moments.....	49
Bibliography of automatic antenna data processing.....	743
Bibliography on coherence theory.....	742
<i>Bickmore, R. W., R. C. Hansen</i> , Antennas 1957-1959.....	731
<i>Bleis, B. C., J. H. Chapman</i> , Characteristics of 488 megacycles per second radio signal reflected from the moon.....	331
<i>Bolgiano, R.</i> , Theory of wavelength dependence in ultra-high frequency transhorizon propagation based on meteorological considerations.....	231
<i>Bremner, H.</i> , On the theory of wave propagation through a concentrically stratified troposphere with a smooth profile.....	467

C

Calculation of the departures of radio wave bending from normal.....	259
<i>Cahoon, B. A., B. R. Bean, G. D. Thayer</i> , Methods of predicting the atmospheric bending of radio rays.....	487
<i>Campbell, W. H.</i> , Natural electromagnetic energy below the ELF range.....	409
<i>Carpenter, R. J., G. R. Sugar, G. F. Oels</i> , Elementary considerations of the effects of multipath propagation in meteor-burst communication.....	495
Cavities, refractometer, limit of spatial resolution.....	65
Channel capacity, loss in resulting from starting delay in meteor-burst communication.....	493
<i>Chapman, J. H., B. C. Bleis</i> , Characteristics of 488 megacycles per second radio signal reflected from the moon.....	331
Characteristics of 488 megacycles per second radio signal reflected from the moon.....	331
Circuits and waves, radio, URSI, report of U.S. Commission 6.....	671
Circuit theory.....	687
Coastal deviation of high-frequency radio waves, measurements.....	57
Coding and theory, information.....	671

Page

Coherence theory, bibliography.....	742
Communication, arctic, conference.....	73
Communication, loss in channel capacity resulting from starting delay in meteor-burst.....	493
Communication, meteor-burst, elementary considerations of the effects of multipath propagation.....	495
Communication, optimum frequencies for outer space.....	105
Computation and measurement of the fading rate of moon-reflected UHF signals.....	455
Concentrically stratified troposphere with a smooth profile, on the theory of wave propagation.....	467
Conference on arctic communication.....	317
Conical obstacles, diffraction by smooth.....	317
Contribution to the theory of corrugated guides.....	533
Core, spherical, impedance characteristics of a uniform current loop.....	295
Corner-reflector antenna as a function of the diameter and length of the driven element, impedance.....	135
Corrugated guides, a contribution to the theory.....	533
<i>Crichtow, W. Q.</i> , Properties of atmospheric noise at various receiving locations.....	640
—, <i>C. J. Roubique, A. D. Spaulding, W. M. Berry</i> , Determination of the amplitude-probability distribution of atmospheric radio noise from statistical moments.....	49
<i>Crombie, D. D.</i> , On the mode theory of very-low-frequency propagation in the presence of a transverse magnetic field.....	265
<i>Cullen, A. L.</i> , Propagation of microwaves through a magneto-plasma, and a possible method for determining the electron velocity distributions.....	509
—, Surface-wave resonance effect in a reactive cylindrical structure excited by an axial line source.....	13
Current and impedance: half-wave cylindrical antenna in a dissipative medium.....	365
Cylinder of finite length, imperfectly conducting, response of a loaded electric dipole.....	289
Cylindrical antenna theory.....	569
Cylindrical obstacles, propagation at oblique incidence.....	311

D

Data processing, automatic antenna, bibliography.....	743
Daytime attenuation rates in the very low frequency band using atmospherics.....	349
<i>Decker, M. T., H. B. Janes, J. C. Stroud</i> , An analysis of propagation measurements made at 418 megacycles per second well beyond the radio horizon (a digest).....	255
Defocusing, focusing, and refraction in a circularly stratified atmosphere.....	287
Depression-angle and polarization dependence of radar terrain return.....	483
<i>Deschamps, G. A.</i> , Impedance measurements and standards.....	598
Detection theory.....	678
Determination of the amplitude-probability distribution of atmospheric radio noise from statistical moments.....	49
Development in attenuation measurements and standards.....	599
Diffraction and scattering.....	707
Diffraction by smooth conical obstacles.....	317
Dipole, loaded electric, response in an imperfectly conducting cylinder of finite length.....	289
Discharges, radiofrequency radiation from lightning.....	638
<i>Draze, G. J.</i> , A bibliography of automatic antenna data processing.....	743
<i>Duncan, P. H., P. A. Hinchey</i> , Cylindrical antenna theory.....	509
<i>Dutton, E. J., B. P. Bean</i> , On the calculation of the departures of radio wave bending from normal.....	259

E

Earth-flattening procedure in propagation around a sphere, exact.....	61
Earth propagation, layered, in the vicinity of Point Barrow, Alaska.....	95
Effect of antenna size on gain, bandwidth, and efficiency.....	1
Effects of high-altitude nuclear explosions on radio noise.....	37
Electric and magnetic fields, studies.....	405
Electric field at the ground plane near a top-loaded monopole antenna with special regard to electrically small L- and T-antennas.....	139
Electric fields, ELF, from thunderstorms.....	425
Electrical properties of snow and glacial ice, measured.....	357
Electrical resistivity studies on the Athabasca Glacier, Alberta, Canada.....	439
Electromagnetic energy, natural, below the ELF range.....	409
Electromagnetic fields and plasmas, interaction.....	766
Electromagnetic radiation in magneto-ionic media.....	515
Electromagnetic signals, shielding of by a thin conducting sheet.....	563
Electromagnetic sources immersed in a semi-infinite conducting medium, basic experimental studies of the magnetic field.....	21
Electron content and irregularities in the ionosphere, the use of polarization fading of satellite signals to study.....	335
Electron velocity distributions, propagation of microwaves through a magneto-plasma, and a possible method for determining.....	509
Electronics, radio, URSI, report of U.S. Commission 7.....	751
Elementary considerations of the effects of multipath propagation in the meteor-burst communication.....	495
ELF and VLF propagation research, a summary.....	647
ELF electric fields from thunderstorms.....	425
ELF oscillations and hydromagnetic waves in the ionosphere.....	650
ELF phenomena.....	383
ELF, possible application of the system loss concept.....	413
ELF radio waves, propagation and mode theory.....	387
ELF range, natural electromagnetic energy below.....	409
<i>Elias, P.</i> , Information theory and coding.....	671
Energy, natural electromagnetic, below the ELF range.....	409
<i>Engen, G. F.</i> , Radiofrequency and microwave power measurements.....	596
Exact earth-flattening procedure in propagation around a sphere.....	61
Exosphere.....	651
Experimental results from investigations of tropospheric propagation.....	615

	Page		Page
Fading rate of moon-reflected UHF signals, computation and measurement.....	455	Johler, J. R., I. C. Walters, On the theory of reflection of low- and very-low-radiofrequency waves from the ionosphere.....	269
Felsen, L. B., K. M. Siegel, Diffraction and scattering.....	707	Joint use of the ordinary and extraordinary virtual height curves in determining ionospheric layer profiles.....	111
Ferrites, microwave properties.....	755		
Field strength measurements.....	603	K	
Field strength measurements in fresh water.....	435	Katz, I., L. M. Spetner, Polarization and depression-angle dependence of radar terrain return.....	483
Filtering and prediction.....	681	Katzin, J. C., M. Katzin, H. Pezner, R.Y.-C. Koo, J. V. Larson, Trade wind inversion as a transoceanic duct.....	247
Florman, E. F., P. W. Plush, Measured statistical characteristics and narrow-band teletype message errors on a single-sideband 600-mile-long ultrahigh-frequency tropospheric radio link.....	125	Katzin, M., R.Y.-C. Koo, An exact earth-flattening procedure in propagation around a sphere.....	61
Focusing, defocusing, and refraction in a circularly stratified atmosphere.....	287	—, H. Pezner, R.Y.-C. Koo, J. V. Larson, J. C. Katzin, Trade wind inversion as a transoceanic duct.....	247
Frequencies, optimum, for outer space communication.....	105	Keller, G. V., F. C. Frischknecht, Electrical resistivity studies on the Athabasca Glacier, Alberta, Canada.....	439
Frequency and time interval standards and measurements, progress in the United States during the last three years.....	592	King, G. A. M., Use of logarithmic frequency spacing in ionogram analysis.....	501
Frequency spectra of very-low-frequency atmospheric, measured.....	41	King, R., C. W. Harrison, Jr., Half-wave cylindrical antenna in a dissipative medium: current and impedance.....	365
Frequency, very low, propagation in the presence of a transverse magnetic field, mode theory.....	265	—, Response of a loaded electric dipole in an imperfectly conducting cylinder of finite length.....	289
Fricker, S. J., R. P. Ingalls, W. C. Mason, M. L. Stone, D. W. Swift, Computation and measurement of the fading rate of moon-reflected UHF signals.....	455	Kirby, R. C., C. G. Little, Conference on arctic communication.....	289
Frischknecht, F. C., G. V. Keller, Electrical resistivity studies on the Athabasca Glacier, Alberta, Canada.....	439	Knudsen, H. L., T. Larsen, The electric field at the ground plane near a top-loaded monopole antenna with special regard to electrically small L- and T-antennas.....	139
G		Kogelnik, H., On electromagnetic radiation in magneto-ionic media.....	515
Garlanó, G. D., T. F. Webster, Studies of natural electric and magnetic fields.....	405	Koo, R. Y.-C., M. Katzin, An exact earth-flattening procedure in propagation around a sphere.....	61
Gautier, T. N., J. W. Wright, Note on a test of the equivalence theorem for sprad E propagation.....	347	—, H. Pezner, J. V. Larson, J. C. Katzin, Trade wind inversion as a transoceanic duct.....	247
Gerber, E. A., Progress in the United States during the last three years on frequency and time interval standards and measurements.....	592	Kraichman, M. R., Basic experimental studies of the magnetic field from electromagnetic sources immersed in a semi-infinite conducting medium.....	21
Gill, A., Pattern recognition.....	676		
Glacial ice and snow, measured electrical properties.....	357	L	
Golden, R. M., R. S. Macmillan, W. V. T. Rusch, A very-low-frequency antenna for investigating the ionosphere with horizontally polarized radio waves.....	27	Larsen, T., H. L. Knudsen, The electric field at the ground plane near a top-loaded monopole antenna with special regard to electrically small L- and T-antennas.....	139
Guides, corrugated, a contribution to the theory.....	533	Larson, J. V., M. Katzin, H. Pezner, R.Y.-C. Koo, J. C. Katzin, Trade wind inversion as a transoceanic duct.....	247
Guiding of whistlers in a homogeneous medium.....	505	Lawrence, R. S., C. G. Little, The use of polarization fading of satellite signals to study the electron content and irregularities in the ionosphere.....	335
H		Laz, B., P. K. Tien, Microwave properties of ferrites.....	755
Half-wave cylindrical antenna in a dissipative medium: current and impedance.....	365	Layered earth propagation in the vicinity of Point Barrow, Alaska.....	95
Hansen, R. C., R. W. Bickmore, Antennas 1957-1959.....	731	Leaky wave and surface antennas.....	746
Harrington, R. F., Effect of antenna size on gain, bandwidth, and efficiency.....	1	Length, response of a loaded electric dipole in an imperfectly conducting cylinder.....	289
Harrison, C. W., Jr., R. King, Half-wave cylindrical antenna in a dissipative medium: current and impedance.....	365	Lightning discharges, radiofrequency radiation.....	638
—, Response of a loaded electric dipole in an imperfectly conducting cylinder of finite length.....	289	Limit of spatial resolution of refractometer cavities.....	65
Hartman, W. J., The limit of spatial resolution of refractometer cavities.....	65	Little, C. G., R. C. Kirby, Conference on arctic communication.....	73
Haydon, G. W., Optimum frequencies for outer space communication.....	105	—, R. S. Lawrence, The use of polarization fading of satellite signals to study the electron content and irregularities in the ionosphere.....	335
Heffner, H., P. K. Tien, Parametric amplifiers.....	751	Logarithmic frequency spacing in ionogram analysis, use.....	501
Height curves, virtual, joint use of the ordinary and extraordinary in determining ionospheric layer profiles.....	111	Loop, of a uniform current having a spherical core, impedance characteristics.....	295
Held, G., G. S. Saran, Field strength measurements in fresh water.....	435	Loss in channel capacity resulting from starting delay in meteor-burst communication.....	493
Hellmuth, R. A., M. G. Morgan, Summary of research on whistlers and related phenomena.....	642	Low-noise beam-type microwave tubes.....	763
High-frequency radio waves, measurements of coastal deviation.....	57		
High-gain, very low side-lobe antenna with capability for beam slewing.....	557	M	
Hinchev, F. A., R. H. Duncan, Cylindrical antenna theory.....	569	Macmillan, R. S., W. V. T. Rusch, R. M. Golden, A very-low-frequency antenna for investigating the ionosphere with horizontally polarized radio waves.....	27
Holden, D. B., W. F. Moler, Tropospheric scatter propagation and atmospheric circulations.....	81	Magnetic and natural electric fields, studies.....	405
Homogeneous medium, guiding of whistlers.....	505	Magnetic field from electromagnetic sources immersed in a semi-infinite conducting medium, basic experimental studies.....	21
Hydromagnetic waves and ELF oscillations in the ionosphere.....	650	Magnetic field, transverse, on the mode theory of very-low-frequency propagation in the presence.....	265
I		Magneto-ionic media, on electromagnetic radiation.....	515
Ikegami, F., A preliminary study of radiometeorological effects on beyond-horizon propagation.....	239	Magneto-plasma, propagation of microwaves through, and a possible method for determining the electron velocity distributions.....	509
Impedance and current: half-wave cylindrical antenna in a dissipative medium.....	365	Marini, J. W., Radiation and admittance of an insulated slotted-sphere antenna surrounded by a strongly ionized plasma sheath.....	525
Impedance characteristics of a uniform current loop having a spherical core.....	295	Marovich, E., R. E. Foach, The aurora of October 22/23, 1958, at Rapid City, South Dakota.....	205
Impedance measurements and standards.....	598	Masers, progress in solid-state.....	758
Impedance of a corner-reflector antenna as a function of the diameter and length of the driven element.....	135	Mason, W. C., S. J. Fricker, P. P. Ingalls, M. L. Stone, D. W. Swift, Computation and measurement of the fading rate of moon-reflected UHF signals.....	455
Information theory and coding.....	671	Maxwell, E. L., A. D. Watt, Measured electrical properties of snow and glacial ice.....	357
Ingalls, R. P., S. J. Fricker, W. C. Mason, M. L. Stone, D. W. Swift, Computation and measurement of the fading rate of moon-reflected UHF signals.....	455	McLeish, C. W., Measurements of coastal deviation of high-frequency radio waves.....	57
Interaction between plasmas and electromagnetic fields.....	766	Measured electrical properties of snow and glacial ice.....	357
Investigations of tropospheric propagation, experimental results.....	615	Measured frequency spectra of very-low-frequency atmospheric.....	41
Ionized plasma sheath, radiation and admittance of an insulated slotted-sphere antenna surrounded.....	525	Measured statistical characteristics and narrow-band teletype message errors on a single-sideband 600-mile-long ultrahigh-frequency tropospheric radio link.....	125
Ionogram analysis, use of logarithmic frequency spacing.....	591	Measurement and computation of the fading rate of moon-reflected UHF signals.....	455
Ionosphere, hydromagnetic waves and ELF oscillations.....	650	Measurement methods and standards, radio, URSI, report of U.S. Commission 1.....	591
Ionosphere, theory of reflection of low- and very-low-radiofrequency waves.....	269	Measurements and standards, development in attenuation.....	599
Ionosphere, use of polarization fading of satellite signals to study the electron content and irregularities.....	335	Measurements and standards, frequency and time interval, progress in the United States during the last three years.....	592
Ionosphere with horizontally polarized radio waves, a very-low-frequency antenna for investigating.....	27	Measurements and standards, impedance.....	608
Ionospheric layer profiles, joint use of the ordinary and extraordinary virtual height curves in determining.....	111	Measurements and standards, noise.....	601
Ionospheric radio propagation, URSI, report of U.S. Commission 3.....	629	Measurements, field strength.....	608
Ionospheric scatter propagation experiments, relation of turbulence theory.....	301	Measurements in fresh water, field strength.....	435
J		Measurements of coastal deviation of high-frequency radio waves.....	57
James, H. B., J. C. Stroud, M. T. Decker, An analysis of propagation measurements made at 418 megacycles per second well beyond the radio horizon (a digest).....	255	Measurements of physical quantities by radio techniques.....	605
Jean, A. G., Radiofrequency radiation from lightning discharges.....	638		

	Page
Measurements of the spectrum of radio noise from 50 to 100 cycles per second	415
Measurements, propagation, made at 418 megacycles per second well beyond the radio horizon (a digest), analysis	255
Measurements, radiofrequency and microwave power	596
Medium, guiding of whistlers in a homogeneous	505
Megacycles per second radio signal reflected from the moon, characteristics	331
Meteor-burst communication, elementary considerations of the effects of multipath propagation	495
Meteor-burst communication, loss in channel capacity resulting from starting delay	498
Meteor trails, amplitude distribution for radio signals reflected	499
Meteorological considerations, theory of wavelength dependence in ultrahigh-frequency transhorizon propagation	231
Meteorology, radio	621
Methods and standards, radio measurement, URSL report of U.S. Commission 1	591
Methods of predicting the atmospheric bending of radio rays	487
Microwave power measurements, radiofrequency	596
Microwave properties of ferrites	755
Microwave tubes, beam-type low-noise	763
Microwaves through a magneto-plasma, and a possible method for determining the electron velocity distributions, propagation	509
Mode theory and the propagation of ELF radio waves	387
Mode theory of very-low-frequency propagation in the presence of a transverse magnetic field	265
Moler, W. F., D. R. Holden, Tropospheric scatter propagation and atmospheric circulations	81
Monopole antenna, top-loaded, the electric field at the ground plane with special regard to electrically small L- and T-antennas	139
Moon, characteristics of 488 megacycles per second radio signal reflected	331
Moon-reflected UHF signals, computation and measurement of the fading rate	455
Moon, theory of radar scattering	217
Morgan, M. G., R. A. Helliwell, Summary of research on whistlers and related phenomena	644
Multipath propagation, elementary considerations of the effects of in the meteor-burst communication	495
Multiple scattering of waves	715
N	
Natural electromagnetic energy below the ELF range	409
Neugebauer, H. E. J., M. P. Bachynski, Diffraction by smooth conical obstacles	317
Noise, atmospheric, at various receiving locations, properties	640
Noise measurements and standards	601
Norton, K. A., Possible application of the system loss concept at ELF	413
Note on a test of the equivalence theorem for sporadic E propagation	347
Nuclear, high-altitude explosions on radio noise	37
O	
Obayashi, T., Measured frequency spectra of very-low-frequency atmospheres	41
Oblique incidence, propagation at, over cylindrical obstacles	311
Obstacles, diffraction by smooth conical	317
Ochs, G. R., G. R. Sugar, R. J. Carpenter, Elementary considerations of the effects of multipath propagation in meteor-burst communication	495
Oliver, B. M., Noise measurements and standards	601
On the calculation of the departures of radio wave bending from normal	259
Optimum frequencies for outer space communication	105
Oscillations in the ionosphere, hydromagnetic waves and ELF	650
P	
Parametric amplifiers	751
Parent, G. B., Jr., A bibliography on coherence theory	742
Pattern recognition	676
Pezner, H., M. Katzin, B. Y.-C. Koo, J. V. Larson, J. C. Katzin, Trade wind inversion as a transoceanic duct	247
Physical characteristics of the troposphere	607
Physical quantities, measurement of by radio techniques	605
Piefke, G., A contribution to the theory of corrugated guides	633
Pierce, E. T., Some ELF phenomena	383
Plasma sheath, radiation and admittance of an insulated slotted-sphere antenna surrounded by a strongly ionized	525
Plasmas and electromagnetic fields, interaction	766
Plush, R. W., E. F. Florman, Measured statistical characteristics and narrow-band teletype message errors on a single-sideband 600-mile-long ultrahigh-frequency tropospheric radio link	125
Point Barrow, Alaska, layered earth propagation in the vicinity	95
Polarization and depression-angle dependence of radar terrain return	483
Polarization fading of satellite signals to study the electron content and irregularities in the ionosphere, use	385
Possible application of the system loss concept at ELF	413
Prediction and filtering	681
Preliminary study of radiometeorological effects on beyond-horizon propagation	239
Price, R., Detection theory	678
Processes, random	674
Profiles, ionospheric layer, joint use of the ordinary and extraordinary virtual height curves in determining	111
Progress in solid-state masers	592
Progress in the United States during the last three years on frequency and time interval standards and measurements	592
Propagation and mode theory of ELF radio waves	387
Propagation around a sphere, an exact earth-flattening procedure	61
Propagation at oblique incidence over cylindrical obstacles	311
Propagation, beyond-horizon, preliminary study of radio-meteorological effects	239
Propagation in the vicinity of Point Barrow, Alaska, layered earth	95
Propagation, ionospheric radio, URSL report of U.S. Commission 3	629

	Page
Propagation, ionospheric scatter experiments, relation of turbulence theory	301
Propagation measurements, analysis of, made at 418 megacycles per second well beyond the radio horizon (a digest)	255
Propagation, multipath, elementary considerations of the effects of in the meteor-burst communication	495
Propagation of microwaves through a magneto-plasma, and a possible method for determining the electron velocity distributions	509
Propagation research, a summary of VLF and ELF	647
Propagation, terrestrial, of very-low-frequency radio waves—a theoretical investigation	153
Propagation, tropospheric, experimental results of investigations	615
Propagation, tropospheric radio, URSL report of U.S. Commission 2	607
Propagation, tropospheric scatter and atmospheric circulations	81
Propagation, tropospheric (theories)	612
Propagation, very-low-frequency, mode theory of in the presence of a transverse magnetic field	265
Properties of atmospheric noise at various receiving locations	640
Properties of ferrites, microwave	755

R

Radar scattering by the moon, theory	217
Radar terrain return, polarization and depression-angle dependence	483
Radiation and admittance of an insulated slotted-sphere antenna surrounded by a strongly ionized plasma sheath	525
Radiation, electromagnetic, in magneto-ionic media	515
Radiation from lightning discharges, radiofrequency	638
Radio astronomy, URSL report of U.S. Commission 5	655
Radio electronics, URSL report of U.S. Commission 7	751
Radio horizon (a digest), an analysis of propagation measurements made at 418 megacycles per second well beyond	255
Radio measurement methods and standards, URSL report of U.S. Commission 1	591
Radio meteorology	621
Radio noise, atmospheric, from statistical moments, determination of the amplitude-probability distribution	49
Radio noise, effects of high-altitude nuclear explosions	37
Radio noise from 50 to 100 cycles per second, measurements of the spectrum	415
Radio noise of terrestrial origin, URSL report of U.S. Commission 4	637
Radio propagation, ionospheric, URSL report of U.S. Commission 3	629
Radio propagation, tropospheric, URSL report of U.S. Commission 2	607
Radio rays, method of predicting the atmospheric bending	487
Radio signal reflected from the moon, characteristics of 488 megacycles per second	331
Radio signals reflected by meteor trails, amplitude distribution	449
Radio techniques, measurements of physical quantities	605
Radio wave bending from normal, calculation of the departures	259
Radio waves and circuits, URSL report of U.S. Commission 6	671
Radio waves, ELF, propagation and mode theory	387
Radio waves, high-frequency, measurements of coastal deviation	57
Radio waves horizontally polarized, a very-low-frequency antenna for investigating the ionosphere	27
Radio waves, terrestrial propagation of very-low-frequency—a theoretical investigation	153
Radiofrequency and microwave power measurements	596
Radiofrequency radiation from lightning discharges	638
Radiofrequency waves, low and very low, on the theory of reflection from the ionosphere	269
Radiometeorological effects on beyond-horizon propagation, preliminary study	239
Random processes	674
Rapid City, South Dakota, the aurora of October 22/23, 1958	205
Rates in the very low frequency band using atmospheres, daytime attenuation	349
Rays, radio, method of predicting the atmospheric bending	487
Reactive cylindrical structure excited by an axial line source, surface-wave resonance effect	13
Recognition, pattern	676
Reflection of low- and very-low-radiofrequency waves from the ionosphere, theory	269
Refraction, focusing, and defocusing in a circularly stratified atmosphere	65
Refractometer cavities, limit of spatial resolution	65
Relation of turbulence theory to ionospheric scatter propagation experiments	301
Report of U.S. Commission 1, URSL, radio measurement methods and standards	591
Report of U.S. Commission 2, URSL, tropospheric radio propagation	607
Report of U.S. Commission 3, URSL, ionospheric radio propagation	629
Report of U.S. Commission 4, URSL, radio noise of terrestrial origin	637
Report of U.S. Commission 5, URSL, radio astronomy	655
Report of U.S. Commission 6, URSL, radio waves and circuits	671
Report of U.S. Commission 7, URSL, radio electronics	751
Research, a summary of VLF and ELF propagation	647
Research on whistlers and related phenomena, summary	642
Resistivity studies, electrical, on the Athabasca Glacier, Alberta, Canada	439
Resonance effect in a reactive cylindrical structure excited by an axial line source, surface-wave	13
Response of a loaded electric dipole in an imperfectly conducting cylinder of finite length	289
Roach, R. E., E. Marovich, The aurora of October 22/23, 1958, at Rapid City, South Dakota	205
Roubique, C. J., W. O. Crichton, A. D. Spaulding, W. M. Berry, Determination of the amplitude-probability distribution of atmospheric radio noise from statistical moments	49
Rusch, W. V. T., R. S. Macmillan, R. M. Golden, A very-low-frequency antenna for investigating the ionosphere with horizontally polarized radio waves	27
S	
Samson, C. A., Effects of high-altitude nuclear explosions on radio noise	37
Saran, G. S., G. Held, Field strength measurements in fresh water	435
Satellite signals, the use of polarization fading of to study the electron content and irregularities in the ionosphere	335

ge
25
51
55
92
87
47
231
247
467
507
615
612
507
81

125
763
301
715

455
629
655
751
591
637
671
607
501
335

27
647

415
647
387
153
269
435
475
357

650
651
e
467
259
231
671
715

405
687
599
or
449
301
642
505
or
557
d
135
or
347

681
on-
563
746

**UNITED STATES
GOVERNMENT PRINTING OFFICE**

DIVISION OF PUBLIC DOCUMENTS

WASHINGTON 25, D.C.

OFFICIAL BUSINESS

**PENALTY FOR PRIVATE USE TO AVOID
PAYMENT OF POSTAGE, \$300
(GPO)**

**JOURNAL OF RESEARCH of the National Bureau of Standards
D. Radio Propagation**

Vol. 64D, No. 6

November-December 1960

Contents

	Page
URSI National Committee Report:	
Commission 1. Radio Measurement Methods and Standards	591
Commission 2. Tropospheric Radio Propagation	607
Commission 3. Ionospheric Radio Propagation	629
Commission 4. Radio Noise of Terrestrial Origin	637
Commission 5. Radio Astronomy	655
Commission 6. Radio Waves and Circuits	671
Commission 7. Radio Electronics	751
Publications of the staff of the National Bureau of Standards	769
Index to volume 64D. Radio Propagation, Jan.-Dec. 1960	773

(A detailed Table of Contents appears on page III)

**For sale by the Superintendent of Documents, U.S. Government Printing Office, Washington 25, D.C. Price 70 cents (single copy).
Subscription price: \$4.00 a year; 75 cents additional for foreign mailing.**

UNITED STATES GOVERNMENT PRINTING OFFICE, WASHINGTON : 1960

VOID

copy.